

SELECTED REFERENCE MATERIAL
UNITED STATES ATOMIC ENERGY PROGRAM

Reactor Handbook

Physics



SELECTED REFERENCE MATERIAL
ON ATOMIC ENERGY

Research Reactors

Reactor Handbook: Physics

Reactor Handbook: Engineering

Reactor Handbook: Materials

Neutron Cross Sections

Chemical Processing and Equipment

SA

Reactor Handbook

Physics

Contributors

ARGONNE NATIONAL LABORATORY BATTELLE MEMORIAL INSTITUTE
BROOKHAVEN NATIONAL LABORATORY
KNOLLS ATOMIC POWER LABORATORY NORTH AMERICAN AVIATION, INC.
NUCLEAR DEVELOPMENT ASSOCIATES
OAK RIDGE NATIONAL LABORATORY VITRO CORPORATION OF AMERICA

UNITED STATES ATOMIC ENERGY COMMISSION
McGRAW-HILL BOOK COMPANY, INC.

New York Toronto London

1955

Reviewed on behalf of the Atomic Energy Commission by a
Review Board consisting of:

HARVEY BROOKS

Harvard University

S. LAWROSKI

Argonne National Laboratory

P. F. GAST

Nucleonics Division
General Electric Company

M. C. LEVERETT

ANP Project
General Electric Company

J. P. HOWE

North American Aviation, Inc.

W. H. ZINN, Chairman

Argonne National Laboratory

ALLAMA IQBAL LIBRARY



14753

Program managed on behalf of the Division of Reactor
Development and the Technical Information Service by:

D. F. MASTICK

Division of Military Application*



Coordination and editing by:

J. F. HOGERTON and R. C. GRASS

Vitro Corporation of America

ST 01
SA ✓

539.7502
H679R

Printed in the United States of America

* Present address General Precision Equipment Corporation.


FOREWORD

With the rapid maturity of reactor technology and its growing application to industrial power reactors, there has developed an urgent need for a comprehensive and critical compilation of nuclear engineering data. At the request of Dr. L. R. Hafstad, Director of Reactor Development, and in accord with an over-all program for the organization and consolidation of AEC-developed technical information, the Commission's Technical Information Service has issued this Reactor Handbook for convenient reference use by scientists and engineers engaged on AEC reactor projects.

The material presented in this first edition of the Handbook represents the efforts of specialists in the various areas of reactor science and technology, and summarizes the accomplishments of the Commission's nuclear reactor program to date. Future editions are planned as continuing advances in this field may require.

The Commission extends its appreciation to all participants in the Reactor Program for the time and effort expended in the completion of this Handbook.

Lewis L. Strauss
Chairman
United States Atomic Energy Commission



REVIEW BOARD PREFACE

The Review Board was appointed by the Director of the Reactor Development Division in December of 1951. The Board found itself in agreement with the objective of preparing a reactor handbook at an early date, although it was recognized that this placed the effort under a considerable handicap as did the necessity of combining the efforts of numerous author groups.

The Board instituted a mechanism for review of the material as prepared by the author groups. In the work of review the members of the Board called upon many individuals in the various Laboratories for critical comments. Without this assistance the review could not have been performed in the two or three weeks usually available, and the members of the Board express their indebtedness and thanks to these reviewers.

The general format of the Handbook received consideration and the result is recognized as a compromise of what is most desirable in a handbook and what is practical under the present circumstances.

The ultimate success of the Handbook will depend a great deal upon the refinements in subject matter and presentation which will come about in subsequent revisions. It is expected that such revisions will profit enormously from suggestions from the users of the Handbook.

To the Editorial Coordinator, John F. Hogerton, to Donald F. Mastick who represented the Technical Information Service, and to William W. Galbreath who served as secretary, the Board expresses its appreciation for a cordial working relationship. Above all, thanks are due to the various author groups who made the task of review easier by their patience in receiving criticism and suggestions.

THE REVIEW BOARD

Harvey Brooks	Stephen Lawroski
Paul F. Gast	Miles C. Leverett
John P. Howe	W. H. Zinn, Chairman

EDITORIAL PREFACE

The purpose of the Reactor Handbook is to provide a condensed source of reliable data and reference information for those working in the reactor field. Work on this first edition, jointly sponsored by the Division of Reactor Development and the Technical Information Service, started in January 1952, with a fifteen-month publishing target. The authors, most of whom had heavy project commitments, had one month in which to plan their work, and three months to a year in which to survey the field and prepare their compilation. Those preparing large sections were called upon to submit their material in parts and were allowed on the average of one month for reworking a given part after review. The Review Board had the difficult task of reviewing the Handbook material in random increments, with two to three weeks in which to review a given increment. The schedule did not permit a second review following the author's reworking. The editors had from one to three weeks in which to prepare Handbook material for the publisher. To distribute the publisher's load at Oak Ridge, parts of sections were put into the publishing machinery while other parts were still in preparation by the authors.

To meet the schedule, it was necessary to make certain compromises which should be noted here:

1. A somewhat arbitrary approach has necessarily been taken on the problem of coverage, not only with respect to the subjects treated but also the data presented on a given subject. Before using a particular section for the first time, the reader should consult the author's preface which brings out any major limitations in the scope or treatment of the data presented.

2. The policy was adopted early in the program not to attempt a detailed documentation of the source of the data presented. Some specific references are given; however, source identification is restricted primarily to tables or figures which have been taken intact from project reports or the open literature.

3. It has not been possible to achieve the consistency one would like in the use of units. In general, the metric system is used where the data are considered to be of interest primarily to "scientists," and the English system is used where the data are considered to be of interest primarily to "engineers." An attempt has been made to include conversion factors in the body of tables and charts, and in some cases data are expressed in dual units.

4. To simplify page make-up and printing problems, the decision was made early in the program to eliminate the background grid from graphs. Data were to have been presented in tabular form in cases where it was considered important to retain accurate values. In actual practice some graphs have been reproduced with grid and it is felt that this practice can and should be extended in the next edition of the Handbook.

In the present edition of the Handbook, each volume is indexed separately. The organization is the same throughout. Sections are numbered consecutively within a volume; chapters consecutively within a section; and figures, tables, and formulae consecutively within a chapter.

EDITORIAL PREFACE

The first edition combines elements of a "Handbook of Chemistry and Physics," a Marks' "Mechanical Engineer's Handbook," a Mellor's "Treatise on Inorganic Chemistry," and an industrial data book. This result is in some degree inherent in a work that cuts across a number of scientific and engineering disciplines; however, greater unity of presentation should be possible in future editions.

The editors are most appreciative of the attention their problems have received from the Review Board and the author groups, and from Alberto F. Thompson and Donald F. Mastick of the AEC staff. They are most appreciative, also, of the cooperation of William W. Galbreath of ANL, W. H. Sullivan of ORNL and Dennis Puleston of BNL, who did much to advance the Handbook effort at their respective sites, and of R. L. Cummins, E. C. Schulte, and their publishing personnel in the Technical Information Service at Oak Ridge.

John F. Hogerton and Robert C. Grass
VITRO CORPORATION OF AMERICA

CONTENTS

SECTION 1 - REACTOR PHYSICS	xiii
Author's Preface	xv
Chapter 1.1 Experimental Methods	1
Chapter 1.2 Nuclear Physics	61
Chapter 1.3 Kinetic Theory of Neutrons	365
Chapter 1.4 Reactor Statics; Theory and General Results	427
Chapter 1.5 Reactor Statics; Experimental and Numerical Results	477
Chapter 1.6 Reactor Dynamics	531
SECTION 2 - RADIATION SHIELDING	617
Acknowledgments	618
Author's Preface	619
Chapter 2.1 Sources of Radiation	621
Chapter 2.2 Permissible Levels of Radiation	629
Chapter 2.3 Gamma-ray Attenuation	637
Chapter 2.4 Neutron Attenuation	667
Chapter 2.5 Geometry	677
Chapter 2.6 Ducts Through Shields	695
Chapter 2.7 Heat Generation in Shields	701
Chapter 2.8 Shield Optimization with Respect to Weight	709
Chapter 2.9 Shield Materials	715
APPENDIX 1	753
APPENDIX 2	761
INDEX	775

Section 1
REACTOR PHYSICS

Prepared by
NUCLEAR DEVELOPMENT ASSOCIATES
under the direction of
H. SOODAK

Author's Preface

This section of the Reactor Handbook has, like all other sections, been written on a brief time schedule, and it will be apparent to the reader that the present version is but a quick and incomplete rough draft. However, it is believed that the ultimate goal will be better served by publication of this material now, so that it can reach a larger group for criticisms and suggestions, rather than by a painstaking revision of the material within the smaller author group. This section is offered, therefore, as a first small contribution to a mutual effort.

Chapter 1.2, "Nuclear Physics," leans heavily on the data compilations of both the AEC Neutron Cross-section Advisory Group* under D. J. Hughes and the National Bureau of Standards group† under K. Way. It is assumed that the reader has access to the unclassified portions of these compilations. For estimating the values of cross sections in the absence of data, results of theoretical considerations are included here, particularly in the discussion of "Collision Reactions."

Chapter 1.4, "Reactor Statics—Theory and General Results," was the last chapter written and the preparation of the sub-sections "General Kernels" through "Non-uniform Media" was especially hurried.

Chapter 1.5, "Reactor Statics—Experimental and Numerical Results," is an extract of some of the most readily available project literature, but no attempt was made at comparative evaluation.

The theoretical material of Chapter 1.6, "Reactor Dynamics and Control," appears in general symbolic form in order not to restrict the validity to particular reactor models. Time did not permit the inclusion of many particular examples.

This section of the handbook was indexed lightly, the text containing more information than the index entries indicate.

Substantial contributions to this work were made by many persons outside the author group. We should like to thank particularly H. Paxton for a valuable compilation of Los Alamos critical data; K. T. Bainbridge and John Wiley and Sons, Inc., for permission to include a mass table from a forthcoming book; G. T. Seaborg for a new edition of the Table of Isotopes; D. J. Hughes of BNL for loan of the manuscript of his book on Pile Neutron Research; I. Kaplan and J. Chernick of BNL for discussions and data on lattice reactors; the Dow Chemical Company and Detroit Edison Company, and R. Ehrlich and H. B. Stewart of KAPL, for fast-reactor results; and H. Hurwitz, Jr., of KAPL for most helpful technical discussions and unpublished results which appear in many places throughout this section.

Harry Soodak
March 31, 1953

*AECU-2040, BNL-170, BNL-170A.

†NBS-499 and its supplements, now appearing in Nuclear Science Abstracts.

Note to the Declassified Edition

This section was originally prepared using data available up to about December 1952. Except for minor editorial treatment following deletion of classified material, the original presentation has not been revised in producing this declassified version.

Harry Soodak
March 7, 1955

CHAPTER 1.1

Experimental Methods

Ira Pullman

NEUTRON SOURCES

NEUTRONS FROM NATURAL ALPHA EMITTERS

Neutrons can be produced by bombarding many of the light elements with alpha particles which are emitted by some of the natural radioactive elements. This is the oldest, cheapest, easiest, most reliable, and most compact method for obtaining neutrons with energies up to 13 mev and average intensity of 10^7 neutrons/sec.¹ Neutron yields obtained from thick* targets of various elements using alpha particles of 5.3 mev from a polonium source are given in Table 1.1.1. Beryllium furnishes the highest yield; the main reaction is:



The neutron yields obtained by bombarding Be with alpha particles from U and Ra and its decay products are listed in Table 1.1.2.

Ra-Be SOURCES

The Ra- α -Be source is the most common type. A very compact form can be produced by slurring finely ground beryllium powder in an aqueous solution of radium bromide, evaporating to dryness, and compressing the residual powder into pellet form. A pressure of 10 tons/sq in. yields a density of 1.75 gm/cm³. The pellet is then sealed in a gas-tight metal container to confine the radon decay product.

Because of the slow accumulation of the alpha-emitting decay products of radium, the intensity takes a few weeks to reach a steady state. The rate of increase is given approximately by:

$$A = A_0 \frac{1 + 5 \left(1 - \exp - \frac{t}{3.8} \right)}{6} \quad (2)$$

where: A_0 = equilibrium intensity
t = time in days after sealing

It is assumed that the Ra alpha rays contribute one sixth of all the neutrons produced. At equilibrium, the source decays with the half-life of Ra²²⁶, 1600 yr.

The strength of a source as a function of its composition by weight is given approximately by:

* "Thick" means here of sufficient size to stop all α -particles.

¹References appear at end of chapter.

Table 1.1.1 — Po- α Neutron Yields from Thick Targets
(Anderson, Neutrons from Alpha Emitters, Prelim. Rep.
No. 3, Nuclear Sci. Series, Nat. Res. Council, Dec. 1948)

Element	Yield, n/10 ⁶ alphas
Li	2.6
Be	80
B	24
C	0.11
N	.01
O	.07
F	12
Na	1.5
Mg	1.4
Al	0.25
Si	.16
Cl	.11
A	.38

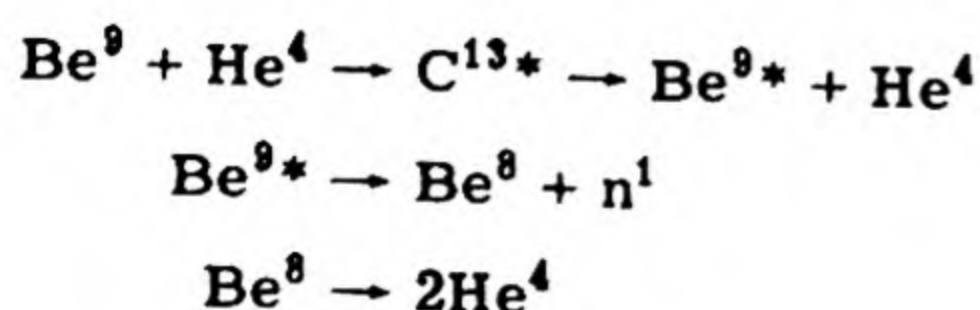
Table 1.1.2 — Neutron Yields from Thick Beryllium Targets
(Anderson, Neutrons from Alpha Emitters, Prelim. Rep. No. 3,
Nuclear Sci. Series, Nat. Res. Council, Dec. 1948)

Alpha emitter	E _{α} , mev	Yield, n/10 ⁶ alphas
U	4.18	40
Ra	4.791	55
Rn	5.486	90
RaA	5.998	120
RaC'	7.680	200
RaF (Po)	5.298	80

$$A_0 = 1.7 \times 10^7 \frac{M_{\text{Be}}}{M_{\text{Be}} + M_{\text{RaBr}_2}} = \text{neutrons}/(\text{sec})(\text{gm Ra}) \quad (3)$$

When prepared in pellet form, sources with an A of 10⁷ n/sec can be prepared in a volume of 6.5 cm³. Thus, near the surface, the neutron flux has the relatively high value of 6 × 10⁵ n/(cm²)(sec).

Because of the various alpha energies, the neutron energy spectrum is continuous up to a maximum energy of 13.2 mev. The most probable energy is about 5 mev, and the average energy is about 2.5 mev. An alpha particle of zero energy would produce a neutron with 5.4 mev, Eq. (1), but large numbers of neutrons exist with less energy. These are associated with gamma rays and are produced by excited states of C¹². Neutrons are also emitted with energies below 1 mev and sometimes only a few electron volts. They are believed to come from another reaction:



The complete reaction is:



Finally, because the product nucleus C^{12} has a low mass it attains significant velocities in the laboratory frame of reference and causes a large spread in the neutron energies.

The neutron spectrum from the Ra- α -Be source has not been measured in detail, especially at low energies. Above 1 mev, the best available spectrum is that given by Demers² and shown in Fig. 1.1.1.* The photographic plate method was used.

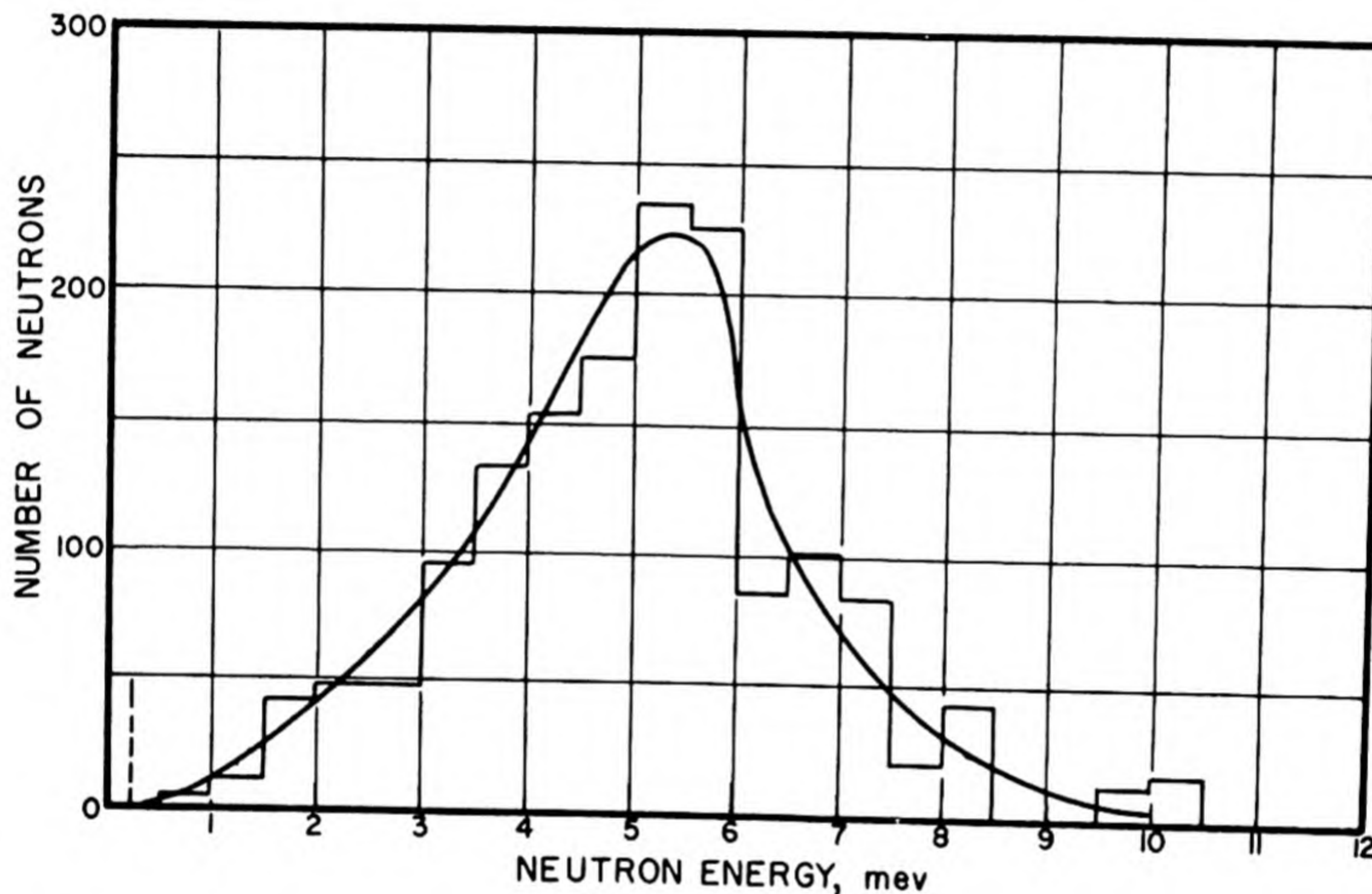


Fig. 1.1.1 — The Neutron Energy Spectrum from a Ra- α -Be Source. Reprinted from Dacey, Paine, and Goodman, Tech. Rep. No. 23, Lab. for Nuclear Sci. and Eng., M.I.T. Oct. 1949.

Besides the non-homogeneous neutron energy, an important disadvantage of the Ra- α -Be source is its high gamma ray intensity which constitutes the main health hazard. One curie of Ra will produce 0.05 roentgen in 3.5 min at a distance of 1 meter. This is the maximum allowable dose for an 8-hr day. At 1 meter, the neutron flux from a 1-gm Ra- α -Be source is not dangerous.⁴

About 7000 photons are emitted for each neutron from sources prepared as described above. The great majority of these gammas are primary radiation emitted by Ra and its decay products since only about 1 in 10^4 alphas will disintegrate the Be nucleus. The gamma spectrum of a radium source is given in Table 1.1.3. (See also footnote (§§) of Table 1.1.5.)

Po-Be SOURCES

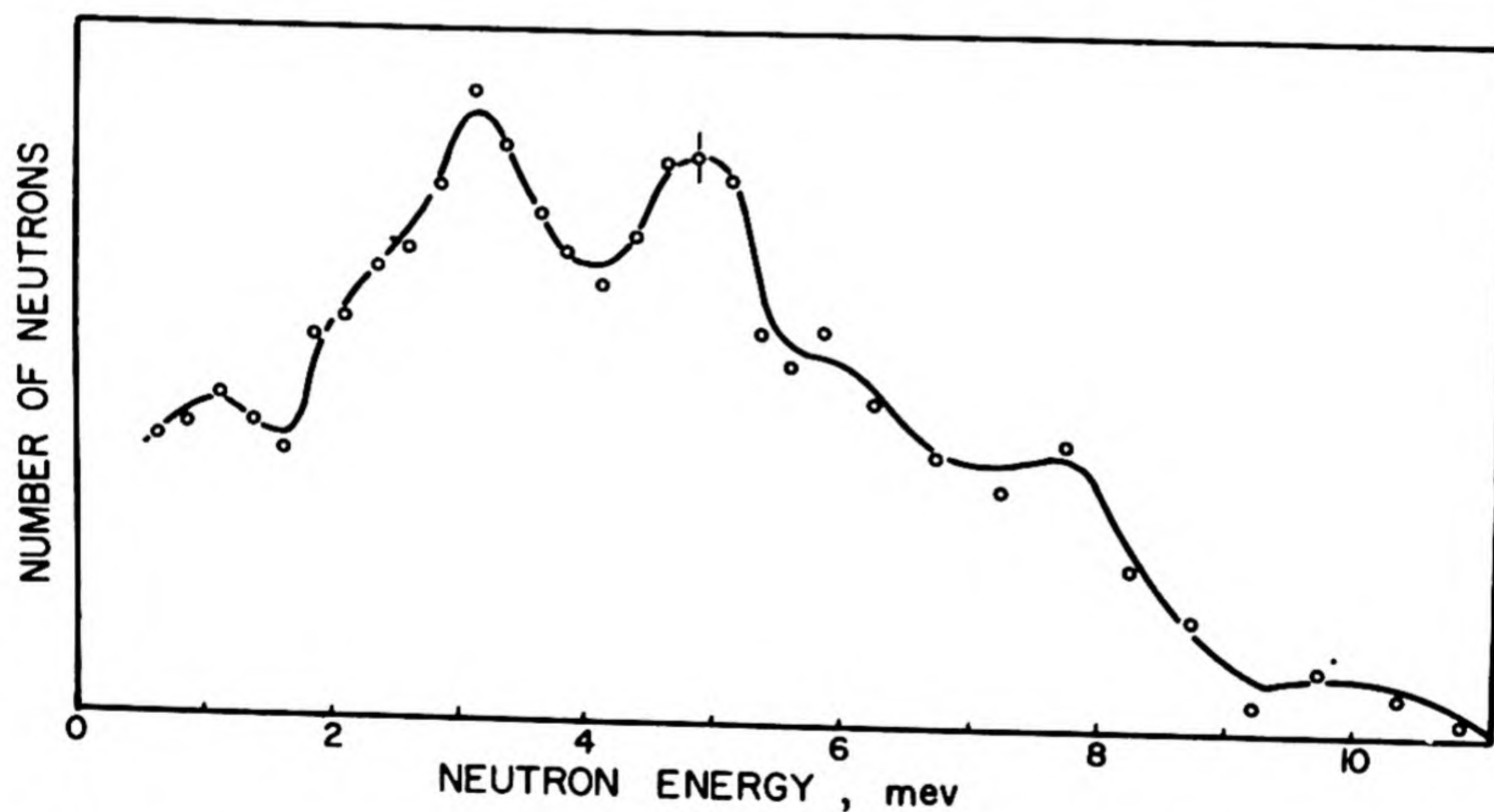
Where it is desirable to eliminate gamma activity, Po^{210} - α -Be sources may be used. One curie of Po in such a source will emit about 0.01 percent of the gamma radiation from

*Demers' experiments are discussed by Dacey, Paine, and Goodman;³ see also Anderson.¹

Table 1.1.3 — Gamma Spectrum from Radium and Its Decay Products

(R. D. Evans and R. O. Evans, Rev. Mod. Phys. 20, 1948)

Transition	Energy per photon ($h\nu$), mev	Average quanta per alpha ray of Ra (r)	Total photon energy per alpha ray (rhv), mev
Ra \rightarrow Rn	0.184	0.012	0.0022
RaB \rightarrow RaC	.241	.115	.0277
	.294	.258	.0758
	.350	.450	.1575
RaC \rightarrow RaC'	.607	.658	.4000
	.766	.065	.0498
	.933	.067	.0625
	1.120	.206	.2310
	1.238	.063	.0780
	1.379	.064	.0882
	1.761	.258	.4540
	2.198	.074	.1626
Total		2.290	1.789

Fig. 1.1.2 — The Neutron Energy Spectrum from a Po- α -Be Source. Reprinted from Whitmore and Baker, Phys. Rev., 78, 1950.

a curie of Ra.⁵ The neutron yield is about $\frac{1}{7}$ of that of Ra- α -Be. The most recent spectrum reported⁶ is shown in Fig. 1.1.2. The photographic plate method was used, putting a lower limit to the energies detectable at about 0.5 mev. Po²¹⁰ is difficult to prepare and has the great disadvantage of a relatively short half-life (140 days). Po- α -Be sources can now be purchased from Oak Ridge.

Rn-Be SOURCES

Radon, because of its availability from hospitals, has been used as an alpha source. Since it is a gas, only about 100 mg of Be is needed to realize the full efficiency of the

source. To achieve the same yield using RaBr_2 , about 13 gm of Be would be needed. However, Rn has a half-life of only 3.825 days, and therefore the neutron intensity decays rapidly.

Ra-B AND Po-B SOURCES

Boron is sometimes used as a target because the neutron energy distribution is smaller and more homogeneous. The yields, lower than those from Be, are listed in Table 1.1.4.

Table 1.1.4 — Neutron Yields from Thick Boron Targets
(Anderson, Neutrons from Alpha Emitters, Prelim. Rep. No. 3,
Nuclear Sci. Series, Nat. Res. Council, Dec. 1948)

Alpha emitter	E_α , mev	Yield, $n/10^6$ alphas
Ra	4.791	15
Rn	5.486	30
RaA	5.998	40
RaC'	7.680	100
RaF	5.298	24

$\text{Ra}-\alpha-\text{B}$ sources can be prepared in a similar manner to the $\text{Ra}-\alpha-\text{Be}$ sources described above. The intensity as a function of composition is given by:

$$A = 6.8 \times 10^6 \frac{M_B}{M_B + M_{\text{RaBr}_2}} = n/(\text{sec})(\text{gm Ra}) \quad (5)$$

Natural boron consists of two isotopes, 81.2 percent B^{11} and 18.8 percent B^{10} . The main reaction is:



Neutrons are also produced by:



but this is less favored than the reaction:



The neutron energy spectrum using Ra is similar to that using Po^{210} , and an appreciable amount of low-energy neutrons is not believed to be present. The spectrum from a $\text{Po}-\alpha-\text{B}$ source is shown in Fig. 1.1.3.⁷ The neutrons were measured in a hydrogen-filled ionization chamber. The average energy of $\text{Ra}-\alpha-\text{B}$ neutrons is about 2.9 mev.

PHOTONEUTRON SOURCES USING RADIOACTIVE NUCLEI⁸

Some artificial and natural radioactive sources emit gammas of sufficiently high energy to eject neutrons from deuterium and beryllium, which have the lowest neutron binding energies of the elements. The main advantages of such sources compared with alpha-

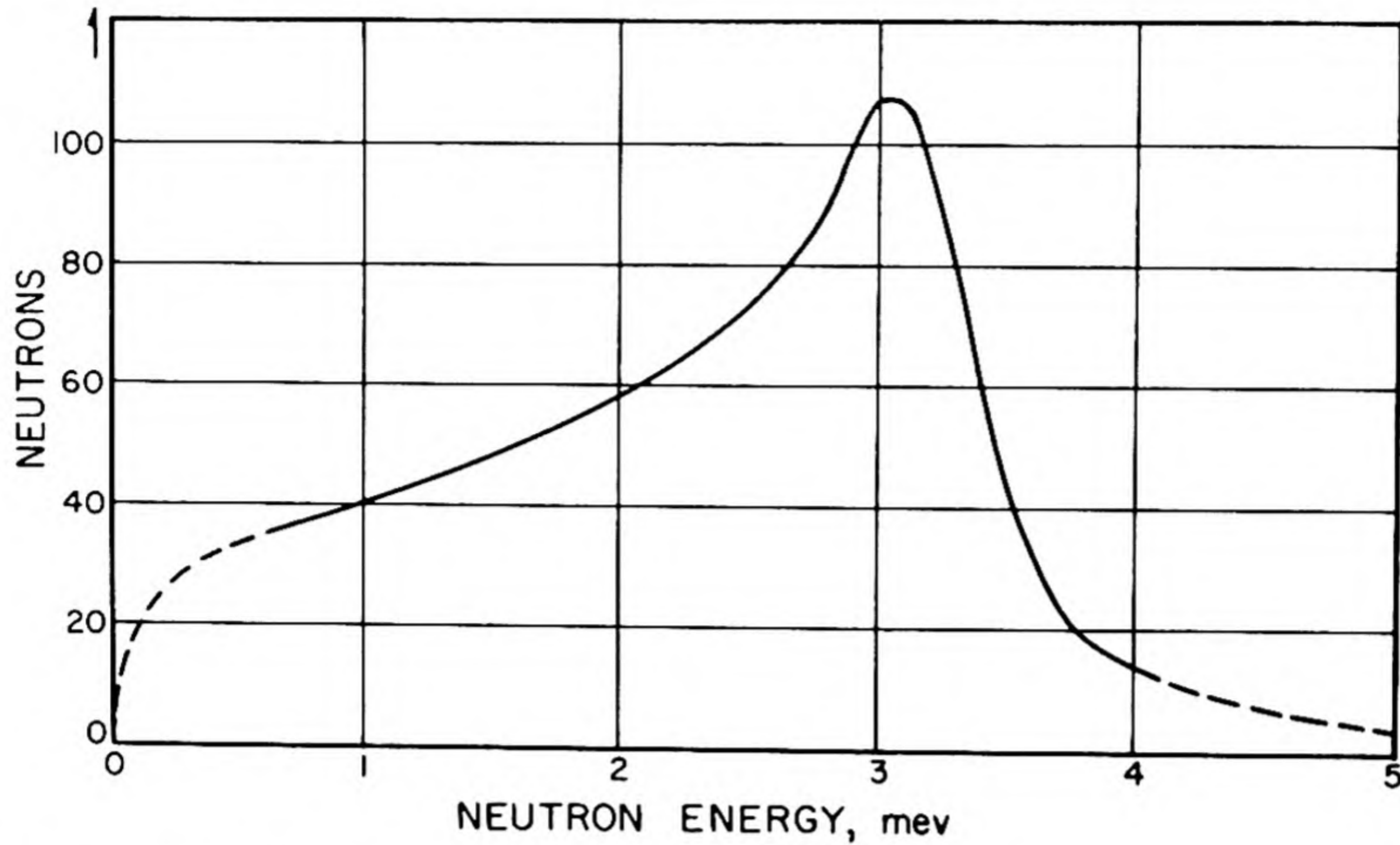


Fig. 1.1.3 — The Neutron Energy Spectrum from a Po- α -B Source. Reprinted from Anderson, Neutrons from Alpha Emitters, Prelim. Rep. No. 3, Nuclear Sci. Series, Nat. Res. Council, Dec. 1948.

neutron sources are that the emitted neutrons are monoenergetic if the gamma ray is monoenergetic and that the source strengths are easier to reproduce. However, the neutron yield is lower and the high-intensity, high-energy gamma radiation can be a health hazard and may interfere with detection of neutrons. The artificial radioisotopes have short half-lives (days or less), and sources utilizing them are not as permanent as those using natural radioactive materials.

The γ, n reactions in Be and D are:



From conservation of energy and momentum, the energy of the neutrons is given by:

$$E_n = \frac{A-1}{A} \left[E_\gamma - Q - \frac{E_\gamma^2}{1862(A-1)} \right] + \delta \quad (11)$$

where: E_n = neutron energy in mev

A = mass number of target nucleus

Q = threshold energy for reaction in mev

E_γ = gamma energy in mev

δ = a small energy spread containing the angular distribution; that is:

$$\delta \cong E_\gamma \left[\frac{2(A-1)(E_\gamma - Q)}{931A^3} \right]^{1/2} \cos \theta \quad (12)$$

where: θ = angle between gamma ray and neutron.

If the gamma rays fall upon the target in an isotropic manner, there is an inherent spread in the energy of the emitted neutrons which is given by:

$$\delta_{\max} = 2E_{\gamma} \left[\frac{2(A-1)(E_{\gamma} - Q)}{931A^3} \right]^{1/2} \quad (13)$$

The fractional spread, δ_{\max}/E_n , decreases with increasing neutron energy and is 5 to 10 times greater in deuterium than in beryllium. For 100-kev neutrons, the fractional spread is about 4 percent in Be and 25 percent in D. For 100-kev neutrons from Be, δ_{\max} is generally negligible compared to other causes of energy spread. One can lower this inherent spread by collimating the gamma rays, but this greatly reduces the neutron yield per photon.

The spectra for some photoneutron sources are shown in Fig. 1.1.4 (see footnote (†) of Table 1.1.5). The observed energy distributions (obtained with the source dimensions shown in Fig. 1.1.6) have a spread of about 20 to 30 percent full width at half-maximum, and the mean energy is 5 to 15 percent below the theoretical neutron energy. This smear-

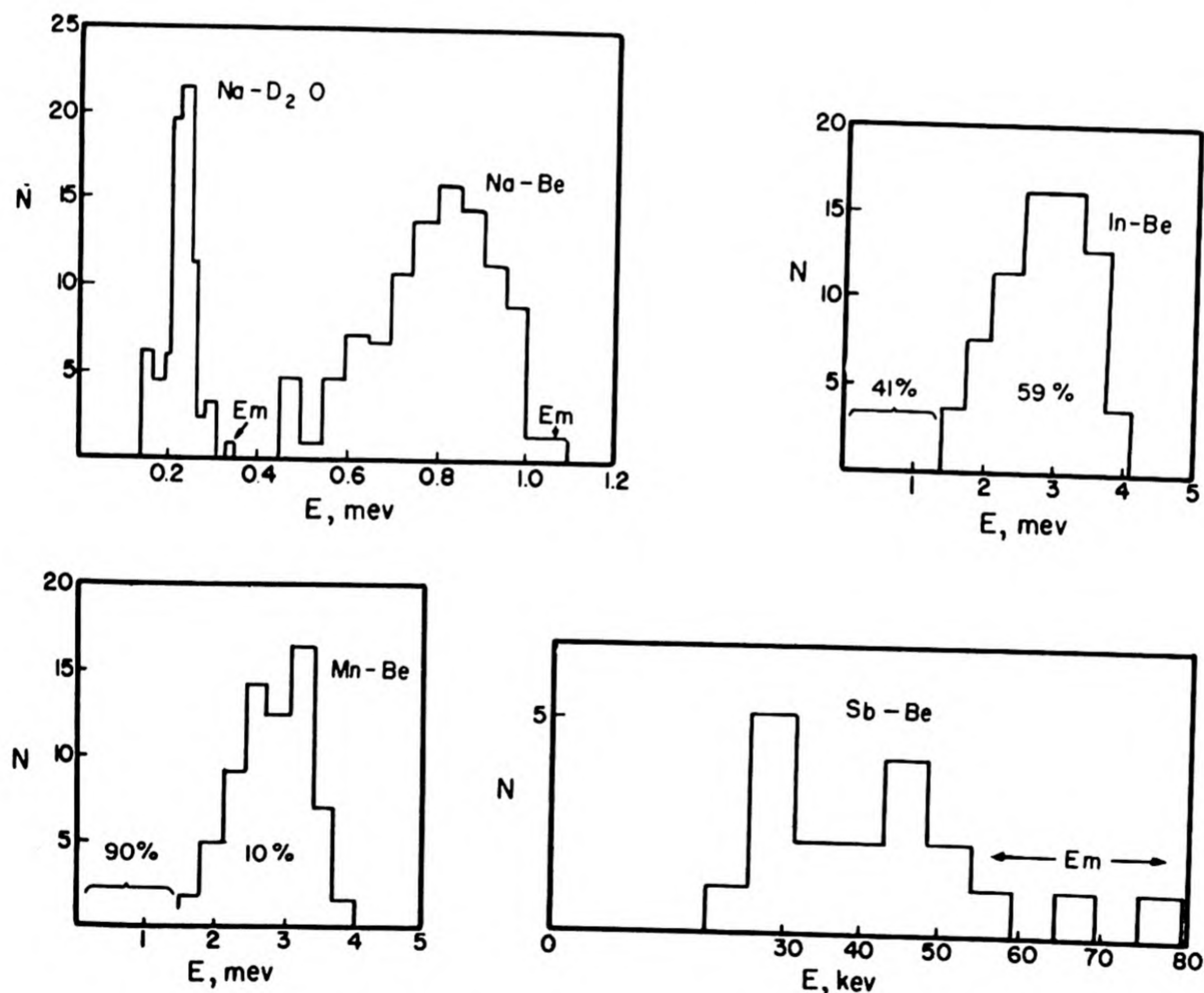


Fig. 1.1.4 — The Photoneutron Energy Spectrum from the Following Sources: Na²⁴-Be and Na²⁴-D; In¹¹⁶-Be; Mn⁵⁶-Be; and Sb¹²⁴-Be. Reprinted from Hughes and Egger, Phys. Rev. 72, 1947.

Table 1.1.5—Properties of Some Useful Photoneutron Sources

Radioisotope	Half-life	Gamma-ray energy, mev	Photons per disintegration	Target	Theoretical neutron energy, mev	Neutron yield, n/(sec)(c)	
						Observed ave. neutron energy, mev	Standard source,* $\times 10^4$ Fig. 1.1.6, ⁸³ $\times 10^6$ Source of
Na²⁴	14.8 hr	2.76	1.0	Be	0.97	0.83† .80†	14, 12 2.4
Mn⁵⁶	2.59 hr	2.76	1.0	D	.27	.22†, ‡	29, 24, 27 2.7
		1.81	0.25	Be	.14	.15†, ‡	2.9 0.5
		2.13	.15	Be	.42	.30†	
		2.7	.01	D	.25	.22†	0.3 .029
Ga⁷²	14.1 hr	1.9	.08	Be	.2	.27†	5.9, 3.7 1.04
		2.2	.33	Be	.4		
		2.5	.26	Be	.7		
		2.5	.26	D	.15		
		1.8	Low	Be	.1	.13†	6.9, 4.6 0.64
As⁷⁶	26.8 hr	2.2	Low	Be	.4	...	
Y⁸⁸	105 days	1.85	1.0	Be	.16	.158§	10
		2.76	~0.01	Be	.98	.22 ^{85, 86}	
		2.76	~.01	D	.27	...	
		1.8	<.03¶	Be	.1	<0.15†	.14
In¹¹⁶	54 min	2.1	.25	Be	.35	.30 ⁸³	0.3 .82
Sb¹²⁴	60 days	1.71	~.5	Be	.03	{.035† .024†, §	19 3.2
		2.5	~.04	Be	.7	.62†	0.23, 0.34 0.04
La¹⁴⁰	40 hr	2.5	~.04	D	.15	{.13† .15§	.68, .97 .062

Ra^{226} **	6.7 yr	2.62††	.35	Be	.86	.827§	3.5
			.35	D	.20	.197§	9.5
Ra^{226} **	1590 yr	1.761††	.258**	Be	.085	...	1.2
		2.198	.074**	Be	.382	...	
		2.42	Low	D	.10	0.12 ^{85,86}	0.1

* A standard source is defined as a gamma source of 1 curie placed 1 cm away from a target of 1 gm. The values are taken from Wattenberg.⁸ Some of the sources have more than one value, as reported by different investigators

† The neutron energies were determined by measuring the scattering cross section in hydrogen (paraffin) which is a known function of energy.¹⁰ This is an integration method, and only an average energy can be obtained. The cylindrical source of Fig. 1.1.6 was used

‡ The neutron energies were determined from observing head-on proton collisions in a hydrogen-filled cloud chamber.¹¹ A differential spectrum could be obtained (see Fig. 1.1.4). The upper tails of the peaks give a maximum energy that in most cases agrees closely with the theoretical value

§ Neutron energies were determined⁸⁴ from maximum pulse heights of recoil protons in a hydrogen-filled proportional counter. A differential spectrum could be obtained. Spherical sources were used

¶ Hughes and Egger¹¹ found the same order of intensity for low- and high-energy neutrons in In^{116} (see Fig. 1.1.4). This is in disagreement with the intensity of the 1.8-mev gamma as reported by Siätis et al.⁸⁷

** Ra^{228} (MsTh_1) and Ra^{226} are in equilibrium with their decay products. The photon and neutron yields are based on the number of disintegrations of the parent source

†† A 1.80-mev gamma (6.5% of 2.62-mev gamma intensity) and a 2.20-mev gamma (8%) also reported⁸⁸ in $\text{ThC} + \text{ThC}''$

‡‡ Latyshev⁸⁸ lists the following gamma-ray energies above 1.65 mev in RaC and their intensities relative to the 2.2-mev gamma:

2.42 mev	0.50 of 2.2-mev intensity
2.20 mev	1.00 of 2.2-mev intensity
2.09 mev	0.37 of 2.2-mev intensity
1.82 mev	.41 of 2.2-mev intensity
1.76 mev	2.42 of 2.2-mev intensity
1.69 mev	0.40 of 2.2-mev intensity

In Table 1.1.3, which was based on older measurements of Ellis and others, the distribution of the high-energy gammas is different and the 2.42-mev gamma is not reported. However, since there is some neutron emission from a $\text{Ra}-\text{D}$ source, the existence of this high-energy gamma would seem to be confirmed

ing is caused by scattering in the beryllium or deuterium which are good moderators. Reducing the target thickness unfortunately also reduces the yield. Table 1.1.5 lists the more important photoneutron sources and their neutron energies and yields. Only long-lived isotopes and only gamma-ray energies above 1.65 mev are given. The theoretical neutron energies were calculated from Eq. (11) using the latest values for threshold energies of Be and D as given in Eqs. (9) and (10).

MANUFACTURE OF PHOTONEUTRON SOURCES

To obtain a high neutron yield with minimum energy degradation in the source, the specific activity of the gamma emitter should be as high as possible. Thus, carrier-free sources with the highest possible atomic density are desirable. This generally means that the metallic form of the element should be used except in the case of sodium where fused NaF has a higher atomic density than metallic sodium. For thick sources or targets, attenuation of the gamma-ray intensity by the Compton effect may have to be considered. The Compton effect is about 10^3 times more probable than the photodisintegration process; thus, even in an infinitely thick target, one can expect only 1 neutron per 10^3 gammas.

Spherical, concentric sources in which a uniform thickness of target surrounds a sphere of the radioisotope give the highest yield in the smallest volume and will emit neutrons with spherically symmetric distribution. This is often of great value. Figure 1.1.5 shows

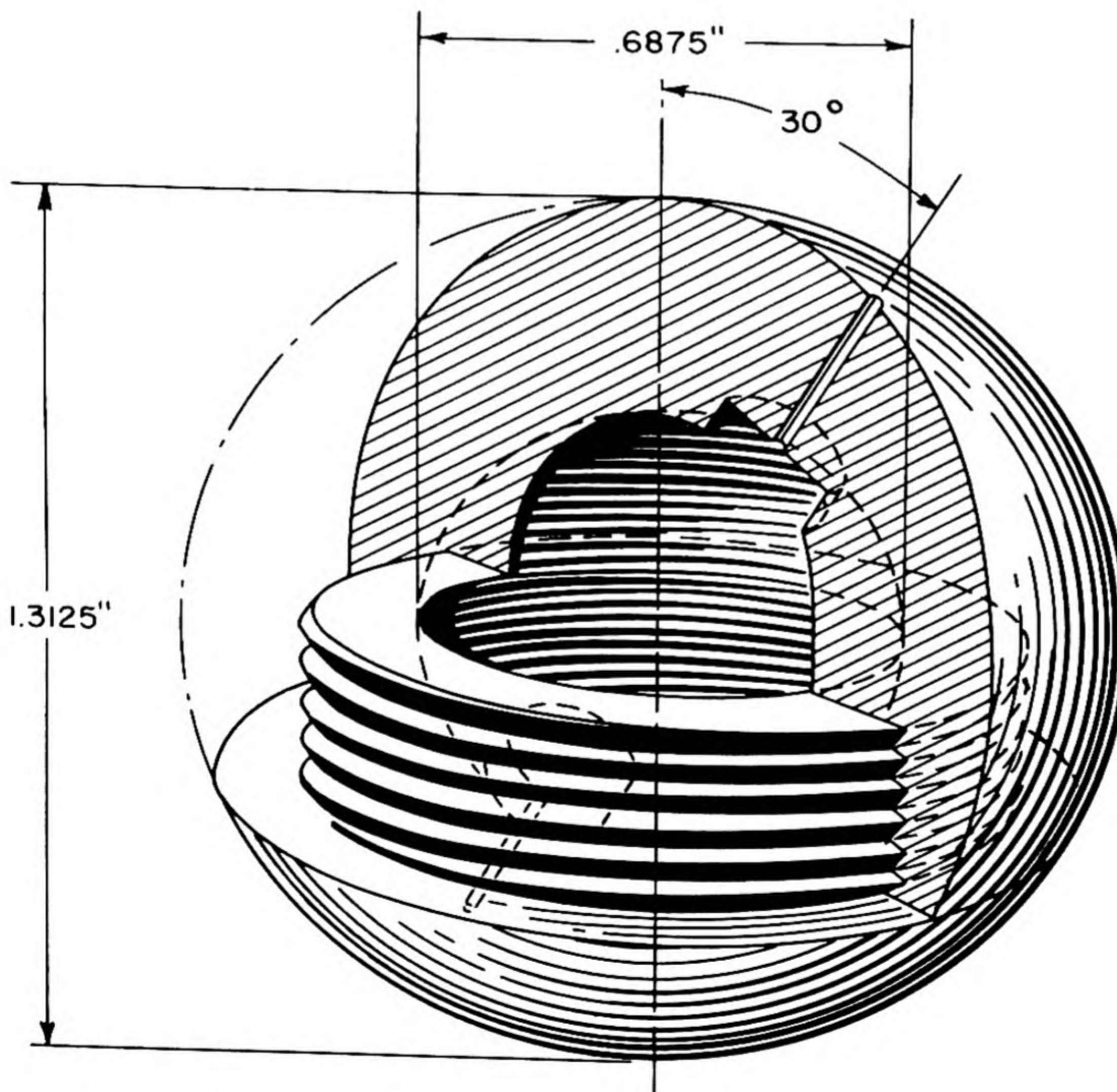


Fig. 1.1.5 — Design of a Spherical Photoneutron Source. Reprinted from A. Wattenberg, Photo-neutron Sources, Prelim. Rep. No. 6, Nuclear Sci. Series, Nat. Res. Council, July 1949. The shell is made of beryllium.

a design by the Bureau of Standards for this type of source. This shape has the disadvantage that it is difficult to change gamma emitters or remove the target material to determine effects of the gamma rays alone. A plug of beryllium may be cut out to facilitate removing the source.

A spherical source may also be made by dissolving the gamma emitter in D_2O or by preparing a homogeneous mixture of the source and Be. This method, of course, contaminates the target.

Concentric-cylinder-type sources are much easier to assemble and interchange although the yield is lower because of losses along the cylindrical axis and the neutron distribution is asymmetric. To a first approximation if the source is large, the number of neutrons will be proportional to the surface area of the target seen at the detector. Figure 1.1.6 shows the design of the cylindrical source used by Wattenberg¹⁰ and Hughes¹¹ in their measurements of neutron energies and yields.

Separating the gamma emitter from the target to collimate the gamma beam reduces the neutron energy spread and makes the geometry somewhat more reproducible. The neutron intensity drops rapidly, and the solid-angle factor becomes critical. The angular distribution of the neutron must be considered. The cross section for the photodisintegration of the deuteron is shown in Fig. 1.1.7. σ_{magnetic} is spherically symmetrical and σ_{electric} varies as $\sin^2 \theta$; above 2.5-mev gamma energy, therefore, most of the neutrons will travel off at right angles to the gamma beam.

PARTICLE ACCELERATORS

Neutrons can be produced by bombarding many of the isotopes with charged particles in accelerators. Cockcroft-Walton and electrostatic generators are used to make neutrons with carefully controlled energies up to 20 mev. Higher-energy neutrons with a much broader energy distribution can be made in cyclotrons of various types and in linear accelerators. High-energy neutrons will not be discussed here since they are not produced in reactors.

The general non-relativistic analysis of a two-body collision with a target stationary in the laboratory coordinate system yields the following results for the neutron spectrum (see Fig. 1.1.8 for schematic diagram). By definition:

$$E_2 = 0$$

$$E_3 + E_4 = E_1 + Q$$

$$E_i = \text{kinetic energy of } i\text{-th particle}$$

$$\theta_3 \text{ varies from } 0 \text{ to } \pi.$$

(14)

As a good approximation for the masses, since $Q \ll 931$ mev in all cases:

$$M_1 + M_2 = M_3 + M_4$$

(15)

The neutron energy in the laboratory coordinate system is given as a function of the incident-particle energy by the following equation which is derived from the momentum and energy conservation laws:

$$E_3 = E_1 \frac{M_1 M_3}{(M_3 + M_4)^2} \left\{ 2 \cos^2 \theta_3 + \frac{M_4(M_3 + M_4)}{M_1 M_3} \left[\frac{Q}{E_1} + \left(1 - \frac{M_1}{M_4} \right) \right] \right. \\ \left. \pm 2 \cos \theta_3 \sqrt{\cos^2 \theta_3 + \frac{M_4(M_3 + M_4)}{M_1 M_3} \left[\frac{Q}{E_1} + \left(1 - \frac{M_1}{M_4} \right) \right]} \right\} \quad (16)$$

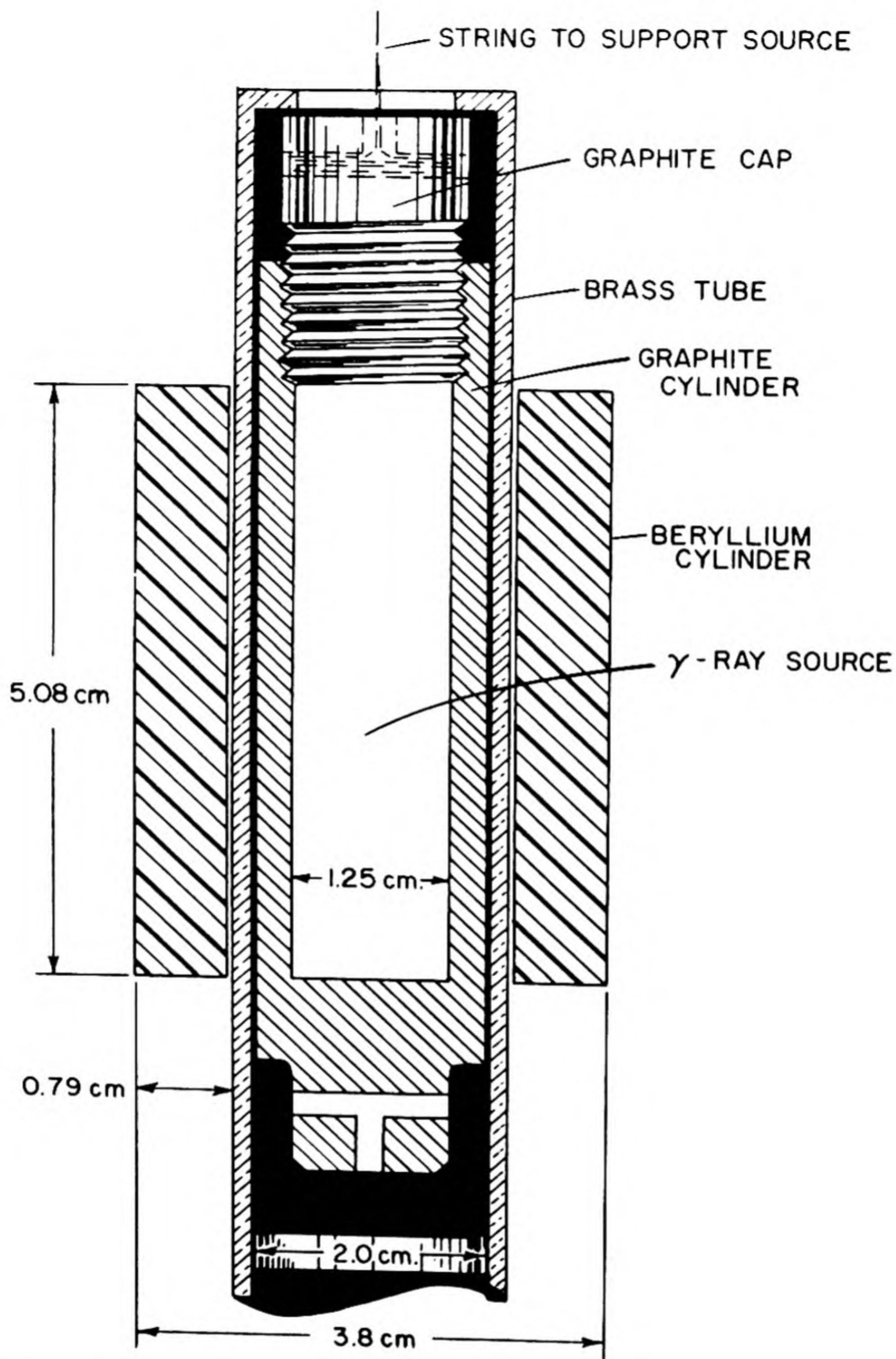


Fig. 1.1.6 — Design of a Cylindrical Photoneutron Source. Reprinted from A. Wattenberg, Photo-neutron Sources, Prelim. Rep. No. 6, Nuclear Sci. Series, Nat. Res. Council, July 1949. To use deuterium, the beryllium cylinder can be replaced by a thin-walled brass cylinder containing heavy water.

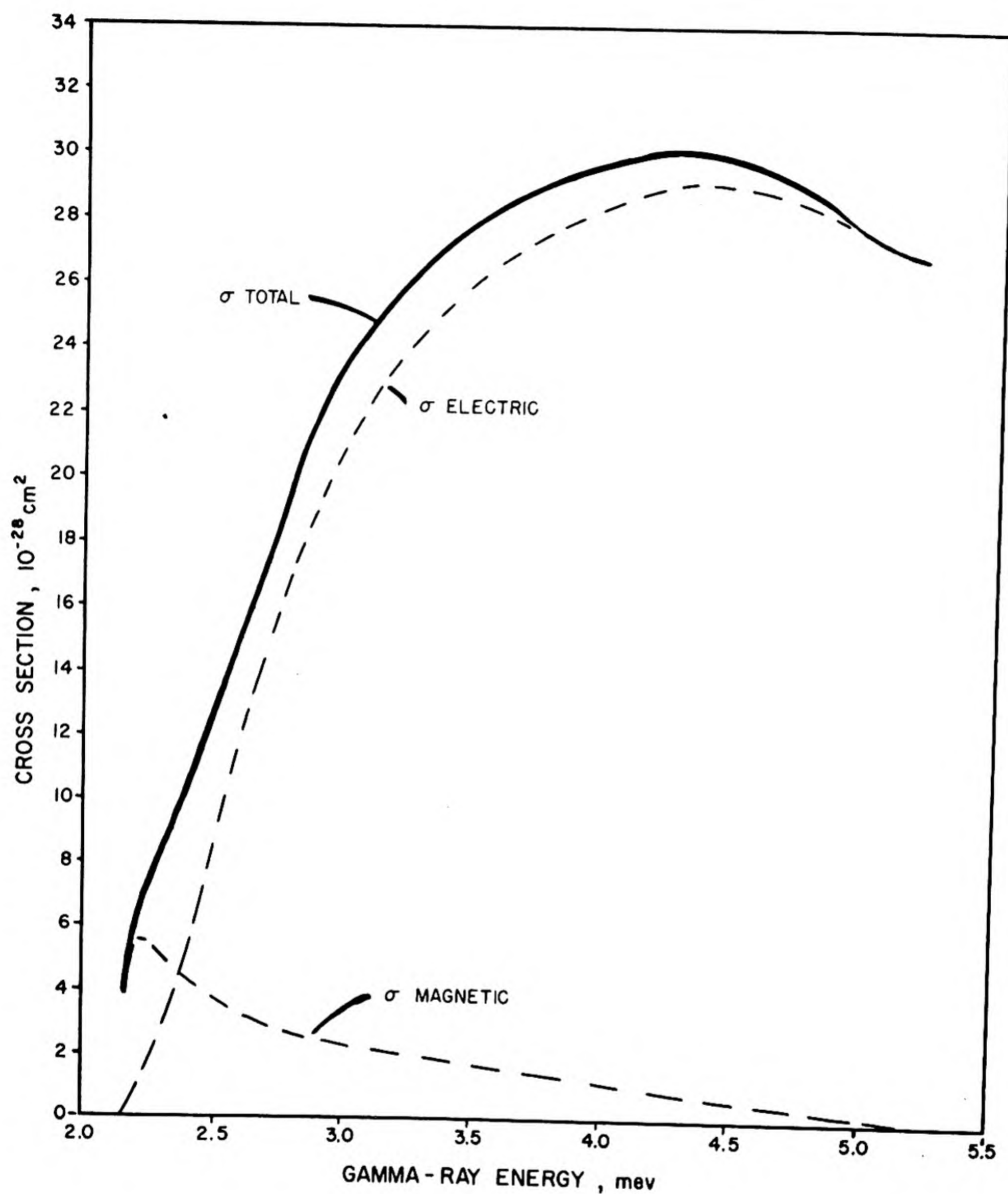


Fig. 1.1.7 — The Cross Section for the Photodisintegration of the Deuteron as a Function of Gamma-ray Energy. Reprinted from A. Wattenberg, Photoneutron Sources, Prelim. Rep. No. 6, Nuclear Sci. Series, Nat. Res. Council, July 1949.

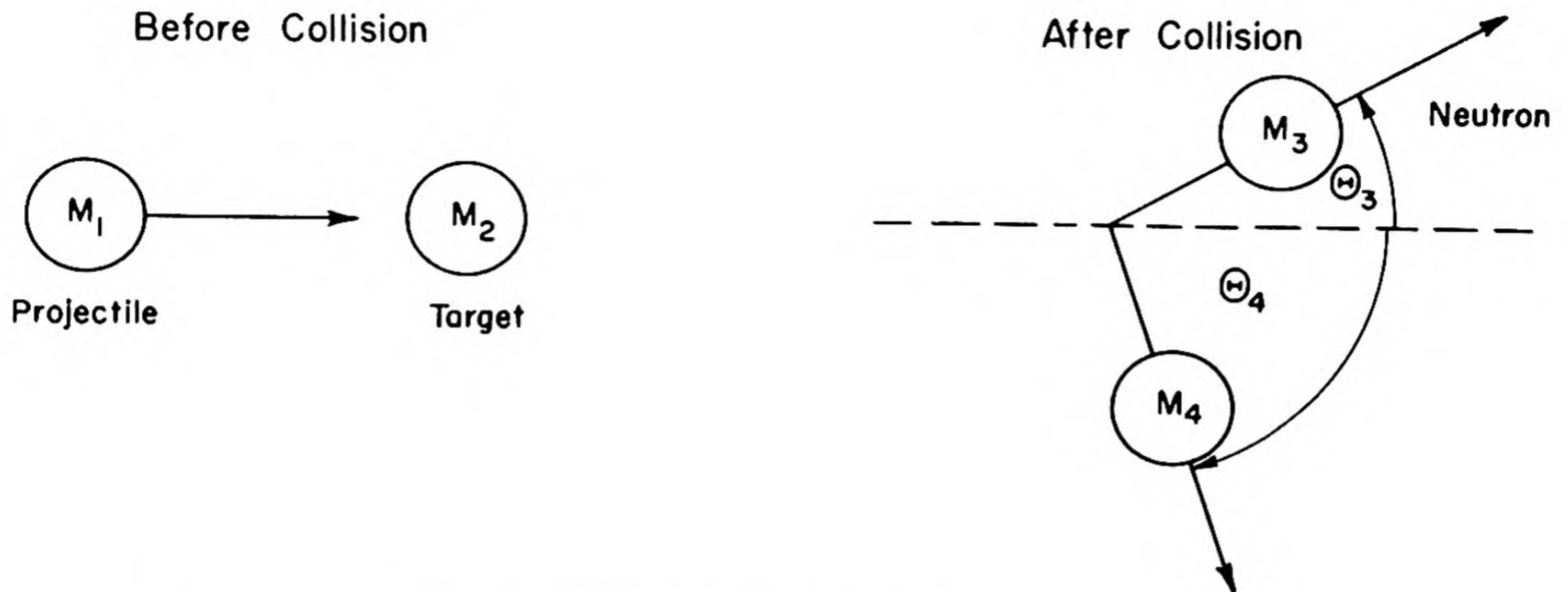


Fig. 1.1.8 — Schematic Drawing of a Two-body Collision in the Laboratory System.

It is assumed that the bombarding energy is not large enough to excite higher levels.

For exoergic reactions (positive Q), only the plus sign is used, and the neutron is monoergic at each angle θ_3 .

For endoergic reactions (negative Q), the reaction cannot proceed unless:

$$E_1 = E_{\text{threshold}} = -Q \frac{(M_1 + M_2)}{M_2} \quad (17)$$

At the threshold, the neutrons are emitted only at $\theta_3 = 0$ and travel, together with the target residue, with the velocity of the center of mass. As E_1 increases, the neutrons are emitted into a cone in the forward direction with a limiting angle given by:

$$\cos \theta_3 = \sqrt{\frac{M_4(M_3 + M_4)}{M_1 M_3} \left[\frac{M_1}{M_4} - 1 - \frac{Q}{E_1} \right]} \quad (18)$$

The energy of the neutrons at each angle θ_3 within the core is double-valued and is given by Eq. (16) with both plus and minus signs before the radical. When E_1 reaches the value:

$$E'_1 = \frac{-M_4}{M_2 - M_3} Q \quad (19)$$

the neutrons are emitted in all directions with a unique energy at each angle, as in the case of positive Q .

The most important reactions now in use¹² having high-neutron yields and requiring low bombarding energies are shown in Eqs. (20), (21), and (23) to (28).



For deuteron energies of 400 kev or less, the neutron energy will be ≈ 2.5 mev at 90° . The total cross section is of the order of 0.1 barn for E_D of 1 to 3 mev and decreases to 0.02 barn below 1 mev. As an approximate monitor for neutron intensity, the companion reaction $D(d,p)H^3$ can be used since the protons have nearly the same yield and angular distribution and have an energy of about 3 mev. The present usefulness of the D,D source

lies in its ability to provide neutrons in the energy range of 4 to 7 mev. Such neutrons are not available from $T(p,n)He^3$ and $Li^7(p,n)Be^7$ sources in existing accelerators with controlled voltages.



This reaction can produce neutrons having energies from 12 to 20 mev. Because of the large value of the cross section at a few hundred kev, large quantities of 14-mev neutrons (about 10^8 n/ μ coulomb of deuterons) can be produced utilizing thick targets. The reaction can be accurately monitored by counting the alpha particles. The total cross section is given empirically as a function of incident deuteron energy, E , in mev by:

$$\sigma(E) = \frac{58e^{-1.72/\sqrt{E}}}{E \left[1 + \left(\frac{E - 0.096}{0.174} \right)^2 \right]} \text{ barns} \quad (22)$$

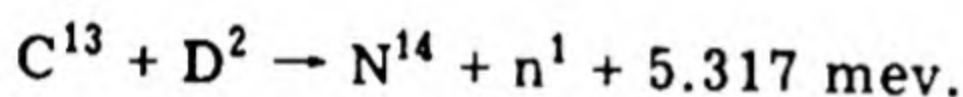
for $0 < E < 2.5$ mev



This reaction has a differential cross section ranging from $1/4$ to $1/2$ of the D-D reaction. Its usefulness will be as a monoergic neutron source filling the energy gap between the D+D and D+T reactions.



Yield is low, and there is a contamination of about 1 percent of high-energy neutrons coming from:



The source has the advantage of a low threshold.



The total cross section is about 0.2 to 0.5 barns for proton energies in the range 1.9 to 2.5 mev. To obtain usable yields of monoergic neutrons below 80 kev, it is necessary to use very large proton currents on thin targets and to observe at back angles.



Large neutron yields near threshold. Monoergic neutrons up to 5 mev. Contamination by 20-mev gammas from proton capture by T^3 can interfere with neutron detection. With the same tritium target, one can shift from low-energy neutrons to high-energy neutrons by changing from a proton beam to a deuteron beam.



Very thin targets can be easily made, and with a well defined proton beam, monoergic neutrons in the range 2 kev to 20 kev can be produced. The energy is roughly independent of angle in this region. The neutron intensity is distributed more symmetrically than in the $Li(p,n)$ reaction.

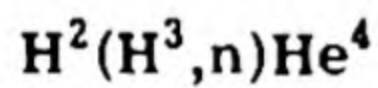
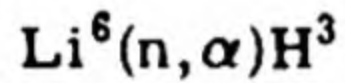


This reaction is similar to the (V,p) reaction, and the yield at threshold is about 40 times as great.

REACTOR NEUTRON SOURCES¹³

The reactor can be used as an internal source by simply placing materials to be bombarded inside the reactor or by sending them through the reactor via a pneumatic tube (rabbit).^{14,15} The latter is used when the activities produced have a short half-life (order of seconds). It was applied to the measurement of delayed neutrons in fission.¹⁵ External beams of neutrons can be obtained by piercing a hole or extending a thermal column (block of graphite) through the shielding of the reactor.

In a thermal reactor, the highest thermal flux is found inside the reactor, but the thermal column yields thermal neutrons with negligible contamination by intermediate neutrons. A material can be irradiated with the highest flux of fission neutrons by being placed inside a hollow lump of centrally located fissionable material. Thermal neutron contamination can be removed by wrapping the sample with Cd, but intermediate neutrons are still present. Fission neutrons free from intermediate neutrons are obtained by allowing thermal neutrons (from a graphite column) to fall on a plate of fissionable material. The sample or target may be wrapped in Cd and held against the converter plate. Fast neutrons (15- to 20-mev) may be obtained by placing a mixture of Li compound and D₂O inside the reactor. The neutrons are produced by the consecutive reactions:



Samples may be irradiated by neutron fluxes of varying median energies by placing them inside variously designed filter arrangements as described later under "Filters."

Since the detailed space-energy distribution of the flux depends strongly on the particulars of the reactor, the following remarks are restricted to approximate results of a general nature. Some data appear in the Appendix which lists flux values inside several reactors.

The energy integrated flux, $\Phi(r) = \int \phi(r) dE$, when averaged over the fuel-bearing regions of the reactor to give $\bar{\Phi}$, is related to the specific power and to the energy spectrum by the formula:

$$\bar{\Phi} = \frac{1.2 \times 10^{13}}{b} \frac{P}{M} \quad (29)$$

where P is the power in kilowatts, M is the mass of fissionable atoms in kilograms, and b is the fission cross section in barns per fissionable atom averaged over the energy spectrum whose average integrated flux is $\bar{\Phi}$. Thus, in a thermal reactor, b is simply the thermal cross section, and:

$$\bar{\Phi}_{\text{th}} \approx 2 \times 10^{10} \frac{P}{M}, \text{ for } b \sim 600$$

while in a very fast reactor, $b \sim 2$ and:

$$\bar{\Phi} \approx 5 \times 10^{12} \frac{P}{M}, \text{ for } b \sim 2$$

It is seen that a fast reactor has a much larger flux for the same specific power.

Equation (29) applies to the local core values of $\Phi(r)$ (as well as to the average, $\bar{\Phi}$) if P/M and b are regarded as local values. Thus, $\Phi(r)$ varies with position because of

buckling (variation in P/M) and because of variation in energy spectrum (variation in b). Bare reactor distributions for uniform loading in simple geometries are given in Table 1.4.3 and the maximum-to-average ratios, $\Phi_{\max}/\bar{\Phi}$, are listed in Table 1.1.6. The effect of a reflector is usually to lower the values of $\Phi_{\max}/\bar{\Phi}$ towards unity.

Table 1.1.6 — Maximum-to-Average Flux Ratios for Bare Reactors
with Uniform Loadings in Simple Geometries
(CL-697, Chapter IVE; MonP-147)

Geometry	ϕ_{\max}/ϕ_{av}
Infinite slab	1.57
Sphere	3.29
Circular cylinder	3.64
Rectangular parallelepiped	3.88
Hemisphere	4.38

The net leakage of neutrons into the reflector is equal to the excess of production over absorption in the core and is given by:

$$L = 3.3 \times 10^{10} \nu \frac{k-1}{k} \frac{P}{A} \quad (30)$$

where L is in neutrons per cm^2 per sec., P is the power in kilowatts, and A is the core surface area in square feet. ν and k have their usual meanings. If diffusion into the reflector is governed by a one-group theory, then the flux Φ at a distance s into the reflector is given by:

$$\Phi \approx \frac{L}{D \left(K + \frac{1}{a} \right)} \frac{e^{-Ks}}{1 + \frac{s}{a}} \quad (31)$$

where D and K are respectively the diffusion constant and inverse diffusion length of the reflector material, and " a " is the radius of the assumed spherical core.

If a hole of cross-sectional area A is pierced through the shielding and reflector terminating at the core-reflector boundary, a rough formula that gives the beam intensity at a distance r from the core-reflector boundary is:*

$$\Phi \approx \frac{LA}{4r^2} \quad (32)$$

where L is given by Eq. (30). If the hole terminates at a different position inside the reactor, the quantity L in Eq. (32) should be multiplied by the ratio of the flux at the termination position to the flux at the core reflector boundary. Also, the distance r is somewhat changed, when considering a fixed position outside the shield.

* The product LA is the total leakage from the end face; $1/2\pi r^2$ is the fraction hitting a square centimeter at r if the leakage is directed uniformly, and $\pi/2$ is the factor measuring the forwardness of the leakage. The contribution to the intensity from the reflector lateral surface of the hole is small, especially when r is large compared to the reflector thickness.

The above considerations for a beam may be adapted to yield approximate formulas for the leakage into a thermal column. Rough formulas for the transmission through the column of both thermal and fast neutrons (T_{th} and T_f) appear below:

$$T_{th} \approx e^{-Kx} \quad (33)$$

$$K^2 = \frac{1}{L^2} + \frac{2\pi^2}{A}$$

$$T_f \approx e^{-2\pi^2\tau/A} \left[1 - F\left(\frac{x}{2\sqrt{\tau}}\right) \right] \quad (34)$$

where x is the length of the column, A the cross-sectional area (assumed square), L the thermal diffusion length, τ the age of the fast neutrons entering the column, and F the error function. The fraction, $T_{f,th}$ of entering fast neutrons which emerge as thermals is:

$$T_{f,th} \approx e^{\tau/L^2} e^{-x\sqrt{1/L^2 + 2\pi^2/A}} \quad (35)$$

The above formulas for T_f and $T_{f,th}$ are based on plane-geometry age-theory* and neglect any $1/r^2$ attenuation.

The energy spectrum in a large thermal-reactor core consists of a thermal group† of flux Φ_{th} and of above-thermal neutrons of constant flux θ per unit logarithmic energy interval dE/E . Neglecting leakage, Φ_{th} and θ are related by:

$$\theta = \frac{\sigma_{a,th}}{\xi\sigma_s} \Phi_{th} \quad (36)$$

The cadmium ratio, C.R., is defined by:

$$C.R. = \frac{\text{activation of bare foil}}{\text{activation of Cd-covered foil}}$$

$$C.R. \approx \frac{\theta \int_{0.4 \text{ ev}}^{\infty} \sigma_{act} \frac{dE}{E} + \Phi_{th} \sigma_{act,th}}{\theta \int_{0.4 \text{ ev}}^{\infty} \sigma_{act} \frac{dE}{E}} \quad (37)$$

and gives:

$$\theta \approx \frac{1}{C.R. - 1} \frac{\sigma_{act,th}}{\int_{0.4 \text{ ev}}^{\infty} \sigma_{act} \frac{dE}{E}} \Phi_{th} \quad (38)$$

For a $1/v$ absorber ($\sigma_{act} = b/v$) and taking $E_{th} = 0.025 \text{ ev}$, Eq. (38) becomes:

$$\theta \approx \frac{2\Phi_{th}}{(C.R. - 1)}$$

*See Chapter 1.3 for a discussion of validity.

†In an approximate Maxwell distribution. See Chapter 1.3.

MOCK FISSION SOURCES

The U^{235} fission neutron energy spectrum (for fissions induced by thermal neutrons) can be represented approximately by the analytical expression (intensity normalized):¹⁶

$$F(E) = 0.475 \sinh \sqrt{2E} e^{-E} \quad (39)$$

This equation gives 0.72 mev for the most probable energy of a fission neutron; 2 mev for the mean energy; and 1.58 mev for the median energy.

The spectrum can be imitated¹⁷ by a source consisting of a mixture of sodium fluoroborate ($NaBF_4$) and sodium fluoroberyllate ($2NaF \cdot BeF_2$) with a mole ratio of B/Be = 96/4 impregnated with Po. By carefully mixing and compressing to a pill, a source strength of 2×10^5 /(curie)(sec) can be attained.

PRODUCING MONOENERGIC NEUTRONS BELOW 10 KEV

Above 10 kev in energy, photoneutron sources and charged particle accelerators are the best methods for obtaining monoenergetic neutrons. Below this energy, other methods are used. These include time-of-flight spectrometers, crystal monochromators, scattering filters, $1/v$ filters, and resonance filters. These methods do not produce neutrons directly but select neutrons out of a beam and then transmit them (or the remainder, in the case of absorbers) with the exception of the time of flight spectrometer. This instrument can only select neutrons. A general discussion of these methods is given by Hughes.¹³

TIME-OF-FLIGHT SPECTROMETER

The neutron energy is determined by measuring the time the neutron takes to traverse a known distance. The neutrons are produced in bursts either by pulsing a charged accelerator source^{18,19,20,21} or by rotating a mechanical chopper in front of a reactor neutron beam.^{22,23,24} The time is measured by registering only those counts from a detector which take place after a known delay with respect to the time of the burst. Many such channels with known delays are operated simultaneously. This greatly increases the relative accuracy of the spectrum as well as reducing the time needed to go through the spectrum.

The neutron energy is related to the time of flight by:

$$E = 5150/(t/m)^2 = \text{electron volts} \quad (40)$$

where: t = time in microseconds
 m = path length in meters

The customary manner for designating the resolution is the uncertainty in time measurement per unit path length (inverse velocity) with the units of microseconds per meter, $\Delta t/m$. Then the energy resolution is given by:

$$\frac{\Delta E}{E} = -2 \frac{\Delta t}{t} \quad (41)$$

and the energy spread by:

$$\Delta E = -0.028E^{3/2} \frac{\Delta t}{m} \quad (42)$$

The energy resolution drops as \sqrt{E} which ultimately sets an upper limit to the usefulness of a given instrument. Δt is determined mainly by the burst and detection widths while the

path length, m , is limited by intensity considerations. If the burst width and detection widths are rectangular, then the resulting spread in time of flight for those neutrons detected will be triangular. Actual resolution functions are roughly triangular and the spread is generally given now by the full width at half maximum. (Formerly the width of the base was used.) The most efficient operation (maximum counting rate for a given resolution) is obtained when the burst time and detector time are made equal. Table 1.1.7 lists the

Table 1.1.7—Time-of-Flight Selectors Now in Operation for the Energy Region 10 ev - 10 kev
(Hughes, Conf. on Classified Nuclear and Reactor Physics at Oak Ridge, Sept. 1952,
ORNL-52-9-9)

Machine	Sample size	Δt ,* μsec	Flight path, m	Resolution, $\mu\text{sec}/m$
Columbia cyclotron	Large	5	10	0.5
Argonne chopper	Small	5	20	.25
Oak Ridge chopper	Small	12	12	1.0
		6	40	0.15
Brookhaven cyclotron	Large	2	7	.3
GE Betatron	Large	2	10	.2
Harwell el. acc.	Large	(†)5
Brookhaven chopper	Small	2	20	.1
		1	20	.05

* Full width at half max. of resolution function, including burst width, counting channel time, detector length, and the like

† The minimum $\Delta t = 4\mu\text{secs}$, $m = 10$, giving a resolution of $0.4 \mu\text{sec}/m^{21}$

machines useful in the range 10 ev to 10 kev with their resolutions in inverse velocity and their operating status. The Brookhaven fast chopper which has the highest resolution has an energy resolution of 0.4 percent at 10 ev and 14 percent at 10 kev.

In fast choppers, the shutter is a long, rotating, steel cylinder with slits down the outside edge which permit neutrons to pass when the slits line up with similar slits in a stationary collimator. In general, the counting rate per channel is independent of rotor speed because the fractional open time of the rotor is independent of motor speed. However, the burst width is reduced by increasing the speed so the resolution can be sharpened. The upper limit is set by mechanical strength considerations as well as intensity, i.e., the counting rate decreases with sharpening of the resolution. Speeds of 10,000 to 20,000 rpm are used. To increase the counting rate, the space between the source and detector is evacuated to eliminate air scattering of the neutrons. This adds an improvement of 5 to 6 percent per meter. It has also been suggested that a scintillation counter be used in place of the usual BF_3 detector which has a low efficiency at high energies (hundreds of ev).

For examining thermal neutrons and cold neutrons (<0.01 ev), a slow chopper is used. This is of simpler design since thin cadmium can be used to stop the neutrons and longer bursts are permitted. A slow chopper of more advanced design has been built at Brookhaven using curved neutron channel paths. This selects the velocity of the neutrons to some extent as well as letting them pass so the duty cycle can be increased. The lower limit to the energy which can be measured is set by the overlap between successive bursts. It can be reduced by slowing down the chopper but this reduces the resolution

because the burst width is increased. Measurements down to 0.0004 ev have been reported using the Brookhaven slow chopper (see Neutron Cross Sections, AECU-2040).

Pulsed cyclotron techniques suffer from two disadvantages compared to the mechanical shutter reactor method: They have less intensity, and they have a beam 50 to 100 times the size of the beam which can be used with a shutter. Much smaller sources (milligrams) can be used with the shutter method.

The time-of-flight spectrometer and the crystal monochromator have the highest resolution of all the low-energy-neutron sources. The following comparison is taken from Selove.²⁴

The variation of resolution with energy is the same for the crystal and the chopper. For a given available beam size at the reactor, the crystal can give higher counting rates than the chopper by a ratio of about $50/(\Delta E/E)$, where $\Delta E/E$ is the fractional energy resolution. The crystal also has an advantage over the chopper in giving an essentially monoenergetic beam, thus making possible activation measurements, for example, as a function of energy. Since the time-of-flight spectrometer can only select neutrons of a given energy, it can only be used to measure transmission through a sample. However, there are many points in favor of the chopper. It does not suffer from the higher-order contamination present in the reflected beam from a crystal (owing to overlapping of orders). (No longer true; see below). The lower counting rate of the chopper is offset by the possibility of measuring at as many as 50 to 100 energies simultaneously; moreover, the fractional background is much smaller for the chopper, especially at higher energies. For fixed construction, the resolution of a chopper is easily adjustable; that of a crystal is not. Finally, the problems in the development and construction of a chopper spectrometer appeared to be much simpler than for a crystal spectrometer of comparable performance, the most uncertain feature of the latter being to obtain a large crystal specimen of suitable composition, mosaic structure, and curvature.

CRYSTAL MONOCHROMATOR

Neutrons can undergo Bragg reflection from a crystal lattice in the same manner as X-rays. Only those neutrons will reflect which satisfy the Bragg equation:

$$n\lambda = 2d \sin \theta \quad (43)$$

where: λ = neutron wavelength
 d = lattice spacing
 θ = glancing angle for the n^{th} order reflection

The wavelength is related to the neutron energy in electron volts by:

$$\lambda = \frac{0.2861}{\sqrt{E}} = \text{Angstroms} \quad (44)$$

Neutrons in the thermal region have wavelengths corresponding to crystal-lattice spacings (a few Å).

Because of the finite range of incident angles ($\Delta\theta$), there will be a corresponding range of reflected wavelengths ($\Delta\lambda$) centered at the wavelength given by Eq. (44).

The resolution is a function of θ only and is given by:

$$\left. \begin{aligned} \frac{\Delta\lambda}{\lambda} &= \cot \theta \Delta\theta \\ \frac{\Delta E}{E} &= 2 \frac{\Delta\lambda}{\lambda} \end{aligned} \right\} \quad (45)$$

The lowest possible order is used because the crystal reflectivity varies as $1/n^2$. The reflectivity also varies as $1/E$, and because of the high collimation needed (of the order of 0.1°), the intensity of the neutron source beam must be quite high. The method is feasible only with reactor neutron sources.

The crystals in use are LiF and, more recently, Be. The former has a d of 2.32 \AA for the (111) plane and will give a resolution of 16 percent at 10 ev for a $\Delta\theta$ of 0.1° . A Be single crystal has an unusually small d of 0.75 \AA for the (421) plane, and in the Brookhaven instrument using this crystal with a $\Delta\theta$ of 9 min, a resolution of 10 percent 50 ev and 1 percent at 1 ev is attained. Because of the loss in resolution, 10 ev is the present useful upper energy limit. The lower limit is the thermal region. Below 0.03 ev, the higher-order reflections coming from the intense thermal region cause too much interference. Recently, however, it has been shown that by taking advantage of the total reflection properties of mirrors for neutrons incident at very small glancing angles, it is possible to eliminate higher-order reflections in the beam from the crystal. In this way, the range has been extended to 0.005 ev or lower, depending on the intensity available.²⁵

Since the instrument produces a beam of monoenergetic neutrons, in contrast to the time-of-flight spectrometer, it can be used for activation and scattering experiments as well as measurements of total transmission.

To improve focussing and intensity, a bent-crystal spectrometer has been described.²⁶ A quartz crystal is bent tangent to a Rowland circle with source and detector on the circle, as in the optical case. The lower energy limit is 0.03 ev because of higher-order reflections interfering, and the upper limit is 0.7 ev because of intensity losses and rise in background. An energy resolution of 2 percent at 0.028 ev is claimed. Samples of the order of milligrams can be examined.

FILTERS

Filtration by Absorbers

Filters of various elements can be used to absorb or transmit certain sections of thermal and resonance neutrons. The method is crude but simple and does not require high-intensity neutron sources. There are three cases of practical importance, based on a study of the Breit-Wigner equation for one-level capture cross section, $\sigma(E)$:

$$\sigma(E) = \left(\frac{E_r}{E}\right)^{1/2} \frac{\sigma_0}{1 + \left(\frac{E - E_r}{\Gamma/2}\right)^2} \quad (46)$$

where: E_r = energy of resonance level

σ_0 = cross section at E_r

Γ = total width of level

Case 1: $\Gamma \gg E$

For the $B^{10}(n,\alpha)Li^7$ and $Li^6(n,\alpha)H^3$ reactions, Γ is about 10^4 ev; these absorbers will therefore be $1/v$ in nature for all neutrons below 10^3 ev. This means that such neutrons are absorbed exponentially with absorber thickness and that the effect on the neutron distribution can be calculated.

Case 2: $\Gamma \sim E_r$

For radiative neutron capture, $\Gamma \sim \Gamma_r \sim 0.1$ ev. The condition $\Gamma \sim E_r$ is equivalent to saying that a resonance occurs in or near the thermal region (examples: Cd, Gd, Sm, and Dy). Cd is the most common thermal absorber and below 0.1 ev has an average cross

section of about 3000 barns. Thus, the transmission of such neutrons through a 0.5-mm thick cadmium sheet will be less than 1 percent. The cut-off energy for cadmium is usually taken as 0.4 ev where the cross section is 300 b.

Case 3: $\Gamma \ll E_r$

This implies that $E_r > 1$ ev. Absorption is $1/v$ throughout the thermal region, and in the neighborhood of E_r , the cross section rises steeply to orders of 10^3 to 10^5 barns. The important resonance absorbers and their energies are:

Rh	1.25 ev
In	1.44 ev
Au	4.9 ev
Ag	5.1 ev

Filtration By Scatterers

The Bragg relation, Eq. (43), shows that the longest wavelength that can be reflected by a given crystal occurs when $\sin \theta = 1$:

$$\lambda_m = 2d_m \quad (47)$$

where: d_m = maximum lattice spacing in the crystal

Neutrons of wavelength greater than λ_m are essentially not scattered at all (except for incoherent scattering which is usually small) and are removed from the beam only by capture.

Since capture cross sections vary as $1/v$, filters for cold neutrons (< 0.01 ev) must have a very low capture cross section. Also wavelengths greater than λ_m should be highly scattered so that a clean break can be achieved. Only graphite and beryllium oxide have these properties. Unfortunately, they both cut off in the same wavelength range, 4 to 7 Å (0.002 – 0.005 ev).

NEUTRON DETECTION

A variety of neutron detectors have been developed although slow-neutron detectors (up to 0.1 mev), and fast-neutron detectors cannot generally be used interchangeably. If it is desired to analyze the energy spectrum, the procedure becomes more elaborate, and efficiency is usually sacrificed. Only properties of the detectors will be discussed here, but a brief summary and bibliography for work done through 1950 is available.²⁷ References for construction details will be given throughout the section.

SLOW-NEUTRON DETECTORS

Ionization chambers and proportional counters containing boron either as a coating on the walls and electrodes or as a BF_3 filling can be made into highly efficient detectors. The reactions utilized are:



The branching ratio of the two states may be strongly energy dependent.²⁸ At thermal-neutron energies, the excited state is produced 93 percent of the time. The cross section is almost pure $1/v$ up to 10-kev neutron energies. This holds if pure B^{10} is used, but if normal boron is used, scattering will limit the $1/v$ effect to 1 kev. For a $1/v$ -absorber, the counting rate is proportional to the total neutron density, ρ (neutrons/cm³), since:

$$R = NV \int n(v) v \sigma(v) dv \quad (50)$$

$$\text{but: } \sigma(v) = \sigma_0 v_0 / v$$

$$\text{therefore: } R = NV \sigma_0 v_0 \rho \text{ and } \rho = \int n(v) dv \quad (51)$$

where: R = reaction rate in counts/sec
 N = No. of B^{10} atoms per cc
 V = sensitive volume of chamber in cc
 $n(v)$ = neutron density distribution in speed, i.e.
 $n(v)dv$ = no. of neutrons per cm³ with velocities between v and $v + dv$
 v = neutron velocity
 $\sigma(v)$ = cross section in cm²
 σ_0, v_0 are at same arbitrary energy, say
 $E = 0.025$ ev where $\sigma_0 = 3960$ barns, $v_0 = 2200$ meters/sec

Ionization counters are somewhat simpler to build and operate, but proportional counters offer better pulse discrimination against gamma-ray background, better energy resolution, and are less sensitive to electrical pick-up.* Boron is easier to handle and preserve than BF_3 gas which must be carefully purified;^{30,31} however, the gas should give cleaner pulse discrimination in a proportional counter. Using separated B^{10} will, of course, increase the detection efficiency by a factor of 5. In a $B^{10}F_3$ counter, the detection efficiency can approach 100 percent if sufficiently large dimensions and high pressures are used. Typical dimensions for cylindrical BF_3 proportional counters are: diameter, 1 to 2 in.; length, 12 to 24 in.; gas pressure, 60 to 110 cm Hg; operating voltage, 2000 to 4000 v. To obtain high efficiency, the neutrons must be sent down the counter axially. An ultimate sensitivity of less than 1 neutron/sec can be attained. If the sensitive volume is accurately known, the absolute neutron density can be measured using Eq. (51).

At the other extreme in size, Lowde³² describes a 12-chamber ionization chamber that uses thin films of separated B^{10} isotope on alternate electrodes and which has an active volume of 0.4 cm³, over-all dimensions of about 1 by 2 in., and a thermal-neutron efficiency of 24 percent. The counter is filled with argon to 5 atm pressure and operated at 70 volts.

FISSION COUNTERS

If the gamma background is so high that the pile-up of electron pulses exceeds that of the alpha pulses from either B or BF_3 , then the fission process can be utilized in place of boron since the fission fragments give much larger pulses. U^{235} as enriched U_3O_8 or Pu^{239} can be placed on multiple-electrode ion chambers, and efficiencies comparable to or higher than those using boron can be attained. Rossi and Staub²⁹ describe a spirally wound electrode foil assembly which can have useful areas of several hundred square centimeters and occupies only one cubic inch. A much larger integrating type of fission ion chamber having multiple plates (also described by the above authors) is suitable for relative flux measurements in very dense slow-neutron atmospheres.

* A study of the parameters involved and many constructional details for these types of counters as well as recoil and fission counters are given in Rossi and Staub.²⁹

INDUCED RADIOACTIVITY

Elements with a large activation cross section for the (n, γ) reaction and whose products are radioactive can be used in the shape of foils to detect slow neutrons. A big advantage of such foils is their complete insensitivity to gammas of less than 6 mev energy. Another advantage is the small space they occupy (a square inch or less in area and mils in thickness). However, they are not satisfactory for continuous monitoring purposes since the foils must be removed and counted. A list of useful detectors is given in Table 1.1.8 with

Table 1.1.8—Some Useful Neutron Detectors Based on Induced Radioactivity

(Data taken from Neutron Cross Sections, AECU-2040 and Nuclear Data, NBS Circular 499)

Element or isotope	Isotope abundance, %	σ_a (thermal), barns	σ_{act} (thermal), barns	Half-life of activity*	Type of activity†	Important resonances	
						Energy, ev	Peak σ , barns
Mn ⁵⁵	100	12.6 \pm 0.6	12 \pm 2	2.6 hr	β, γ	310 2900 8200	50‡ 29 27
Rh ¹⁰³	100	150 \pm 7	12 \pm 2 140 \pm 30	4.3 min 44 sec	0.08 γ 2.6 γ	1.25	4500
Ag		60 \pm 3				5.1	7700
Ag ¹⁰⁷	51.9	30 \pm 2	44 \pm 9	2.3 min	2.8 β		
Ag ¹⁰⁹	48.1	84 \pm 7	2.8 \pm 0.5 110 \pm 20	270 days 24.5 sec	β, γ β, γ		
In		190 \pm 10				1.44 3.9 9.1	27500 460 125
In ¹¹³	4.2		56 \pm 12 2.0 \pm 0.6	50 days 72 sec	0.192 γ 2 β		
In ¹¹⁵	95.8		145 \pm 15 52 \pm 6	54 min 13 sec	β, γ ?		
Dy		1100 \pm 150				1.7 5.5	350 300
Dy ¹⁶⁴	28.2		2600 \pm 300§ < 1000§	1.3 min 2.4 hr	0.109 γ β, γ		
Dy ¹⁶⁵	(2.4 hr half-life)		5000 \pm 2000	81 hr	0.4 β		
Au ¹⁹⁷	100	94 \pm 1	96 \pm 10	2.7 days	0.97 $\beta \rightarrow$ 0.411 γ	4.9	15000
Au ¹⁹⁸	(2.7 days half-life)		18000 \pm 8000§	3.3 days	β, γ		

* Arrow means isomeric transition

† Numbers are energies in mev; β, γ means complex spectrum

‡ Mn resonances are mostly scattering

§ Reactor neutrons

their thermal-absorption and activation cross sections, the half-life of the resulting activity, the type of radiation emitted, and the more important resonances.

Indium is the most common element used for thermal (0.01 to 0.4 ev) and epithermal (>0.4 ev) neutrons. By measuring activities with and without a cadmium cover around the indium, thermal and epithermal neutrons can be separated since cadmium absorbs thermal neutrons strongly and is relatively transparent to neutrons above 0.4 ev. In using this

method, the following precautions and corrections should be made in order to interpret the counting rates correctly.^{33,34}

(1) The 54-min activity is the one measured, and the foil should be allowed to stand at least 3 min before counting to allow the 13-sec activity to die out.

(2) If the beta rays are counted, the optimum foil thickness for counting thermal neutrons is about 125 ± 25 mg/cm². With thicker foils, the counting rate drops because of internal absorption of betas and the "self-protection" of the absorber. The internal absorption effect can be reduced greatly if the gamma radiation (in a scintillation counter, for example) is counted instead of the beta rays (but see Note 4 below). The "self-protection" effect, which is the depression of the neutron flux around the absorber owing to the high absorption rate, can be corrected by Bothe's equation in the case of thermal neutrons. The factor by which the counting rate should be multiplied is:

$$F_{sp} = 1 + \frac{\alpha}{2} \left[\frac{3R}{2\lambda_{tr}} \frac{L}{R+L} - 1 \right] \text{ if } R > 2\lambda_{tr} \quad (52)$$

$$F_{sp} = 1 + \frac{0.34 \alpha R}{\lambda_{tr}} \text{ if } R \ll \lambda_{tr} \quad (53)$$

where: R = foil radius

λ_{tr} = transport mean-free-path in the medium around the foil

α = probability that a neutron will be absorbed by the foil on one transversal.

Bothe gives an expression for α as:

$$\alpha = 1 - e^{-\mu d} (1 - \mu d) + \mu^2 d^2 \text{Ei}(-\mu d) \quad (54)$$

where: μ = neutron absorption coefficient in the foil material

d = foil thickness

Ei = logarithmic integral³⁵

A plot of α vs d is given in Fig. 1.1.9; μ should be calculated at the effective energy for absorption of thermal neutrons which, for a $1/v$ absorber and a Maxwellian speed distribution, is $E_{eff} = 4/\pi$ kT or 0.032 ev at 20°C.

The neutron diffusion length (L) in the medium around the foil is given by:

$$L^2 = \frac{\lambda_{tr} \lambda_a}{3 \left(1 - \frac{2}{5} \frac{\lambda_{tr}}{\lambda_a} \right)^2}$$

where: λ_a = absorption mean-free-path = $1/N_a \sigma_a$

$\sigma_a = \sigma_{a,thermal} / 1.128$, i.e., at E_{eff}

λ_{tr} = transport mean-free-path = $\lambda_s / [1 - (\cos \theta)_{av}]$

λ_s = scattering mean-free-path

$(\cos \theta)_{av}$ = average over angles of incidence on the foil. Above 1 ev, the scattering is isotropic in the center of mass system and $(\cos \theta)_{av} = 2/3A$; A = mass no. Table 1.1.9 gives diffusion constants at thermal energies for various media.

The calculated value for F_{sp} agrees very well with experimental observations, usually to 1 percent or better. Neither equation for F_{sp} can be used for the case of a small foil in a highly absorbing medium, but fortunately, here F_{sp} is close to unity.

(3) The cadmium absorbs some of the higher-energy neutrons. The correction depends on both the cadmium and indium thicknesses. The correct counting rate can be determined experimentally by measuring the counting rate at the given indium thickness for different cadmium thicknesses and extrapolating to zero cadmium thickness. Figure 1.1.10 gives

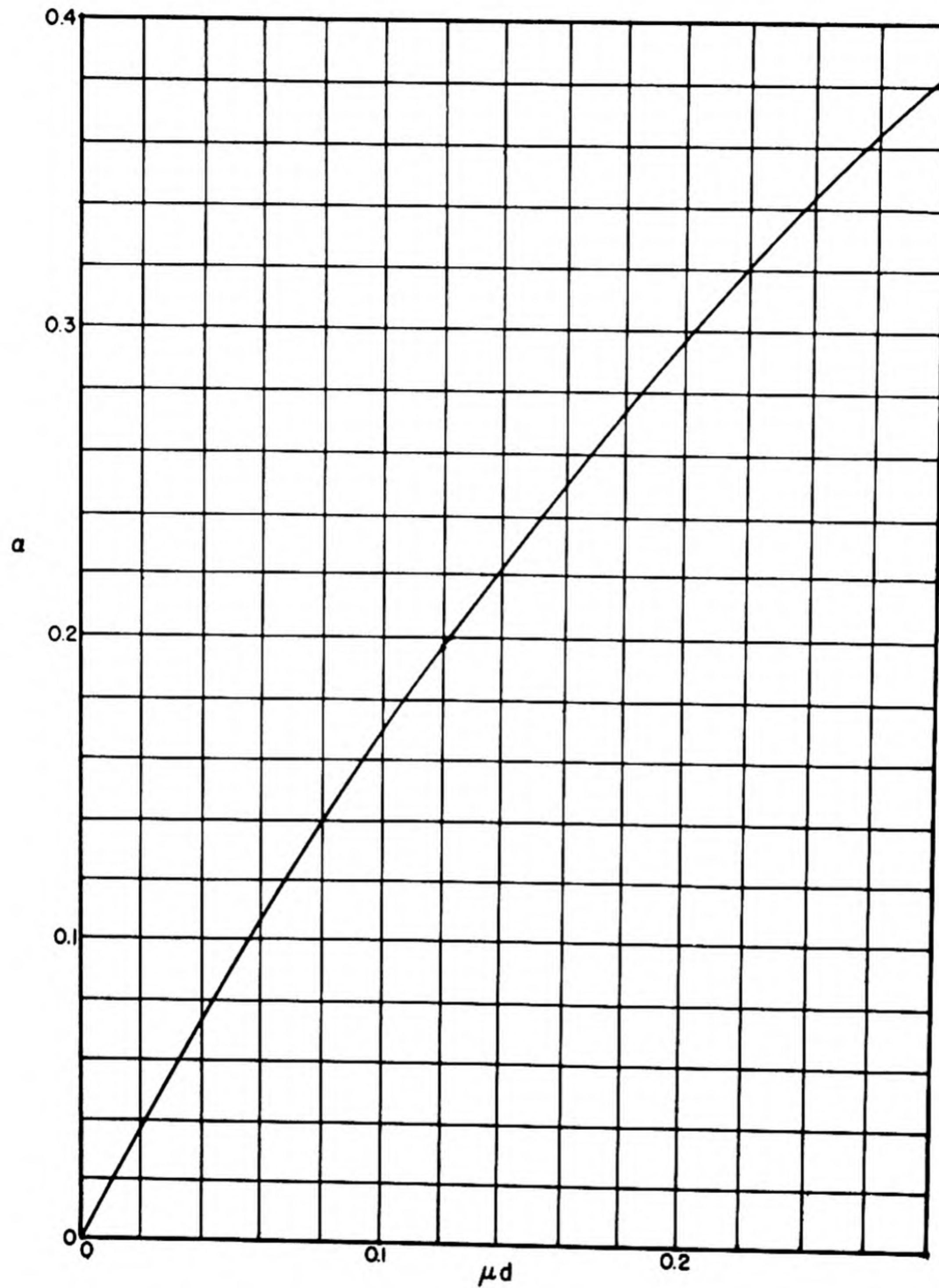


Fig. 1.1.9 — Average Probability (α) of Absorption of Neutrons in an Isotropic Flux Incident upon a Sheet of Material of Thickness d and Absorption Coefficient μ . Reprinted from Title. Nucleonics 9, No. 1, July 1951.

Table 1.1.9 — Diffusion Constants of Various Media
(Title, Nucleonics, 9, No. 1, July 1951)

Medium	Density, gm/cm ³	L, cm	λ_{tr} , cm	λ_a , cm
Paraffin	0.895*	2.42 ± 0.04	0.395 ± 0.021	44.9 ± 1.9
Water	1.00	2.76	0.425	53.8
D ₂ O	1.1	171 ± 20	2.4	37,000
Be	1.8	31	2.6	1,100
Graphite	1.62*	50.2	2.7	2,800

* Varies with the sample

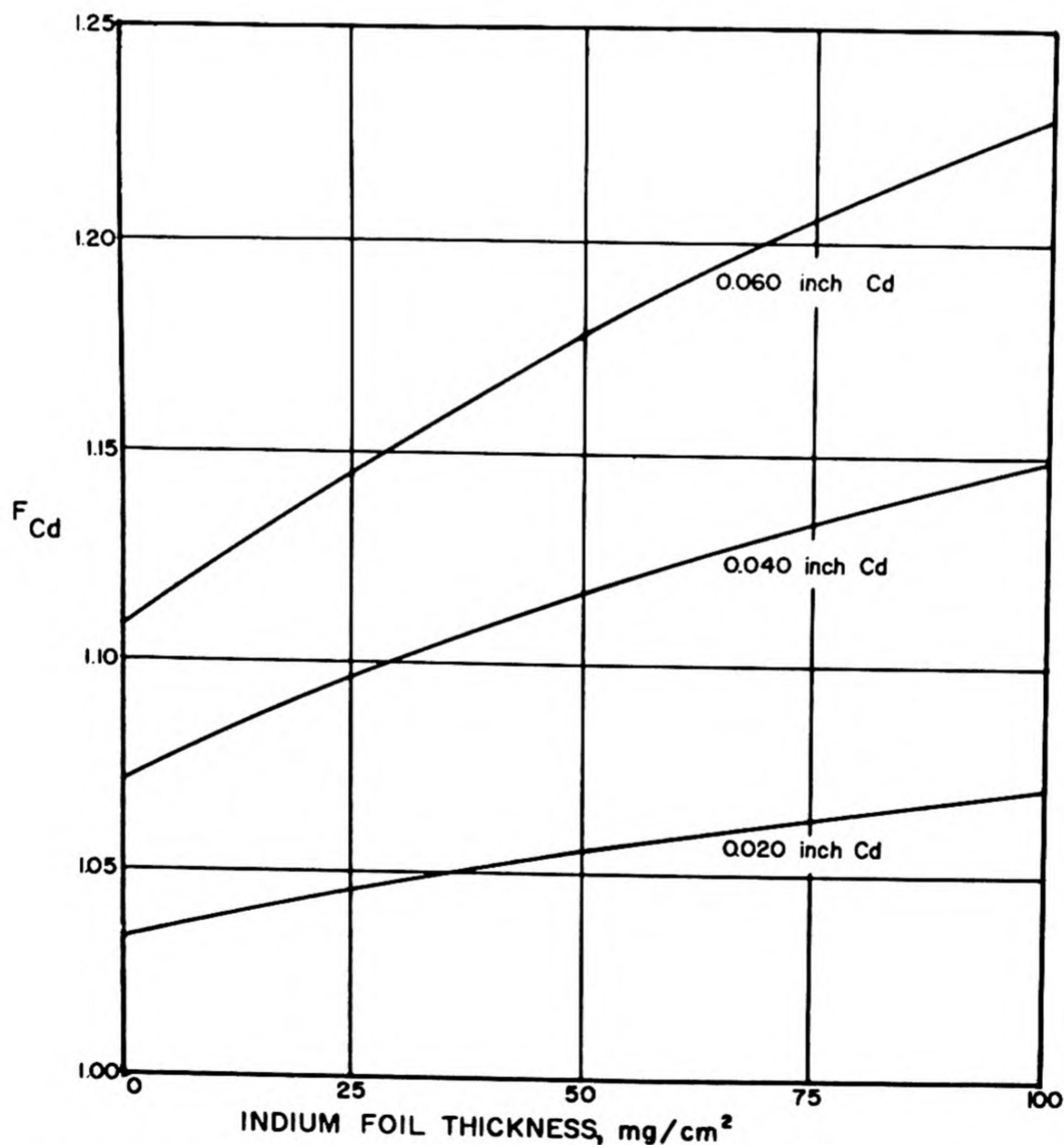


Fig. 1.1.10 — The Factor for Correcting Counting Rate of Indium Foils when Covered with Cadmium (F_{Cd}) by Which the Counting Rate is to be Multiplied, Versus Indium Foil Thickness for Various Cadmium Thicknesses. Reprinted from Title, Nucleonics, 9, No. 1, July 1951.

F_{Cd} by which the observed rate is to be multiplied for indium thicknesses from 0 to 100 mg/cm² and for 3 cadmium thicknesses, 0.02, 0.04, and 0.06 in.

(4) If fast neutrons are present, the 4.5-hr isomeric state of In^{115} can be excited by inelastic collision. The level is at 0.37 mev and emits a gamma radiation which is 50 percent internally converted. The threshold is about 1 mev, and the cross section is constant at about 0.36 barn above 2.2 mev. This activation is usually small compared to the 54-min activity if short exposure times are used. Its effect on beta counting can be reduced somewhat by using a counter that is relatively insensitive to gamma radiation, e.g., a Geiger counter or an argon ionization chamber, of which the latter can be made the more stable.

The neutron-induced activity in the foil increases as:

$$C_0 = C_{0,sat} (1 - e^{-t/\tau}) \quad (55)$$

The counting rate can be corrected for decay back to the time at the end of exposure to neutrons and also to saturation activity by the equation:

$$C_{0,sat} = \frac{N}{\tau(e^{-t_1/\tau} - e^{-t_2/\tau})(1 - e^{-t/\tau})} \quad (56)$$

where: t = length of exposure to neutrons

t_1 = start of counting, measured from end of exposure

t_2 = end of counting, measured from end of exposure

N = number of counts (background subtracted) in time $t_2 - t_1$

τ = mean lifetime of activity. For indium, $\tau = 77.8$ min

Indium foils offer a sensitive method for slow-neutron detection, and intensities as low as 1 neutron/(cm²)(sec) can be measured. The lower limit is probably set by the natural activity of In^{115} which has recently been found to be a beta emitter with a half-life of about 10^{14} yr. Another sensitive method for thermal-neutron detection is to use manganese in an aqueous solution such as calcium permanganate.³⁶ The active Mn^{56} precipitates out as MnO_2 by the Szilard-Chalmers process and can be filtered off and counted. With the source in the center of 11 liters of a 2.4 N solution of $Ca(MnO_4)_2$ surrounded by an external paraffin reflector, a detection efficiency of 8 percent and a sensitivity of about 1 neutron/sec can be obtained. This method is unaffected by gamma radiation provided the gamma energy is below the deuterium photoneutron threshold (2.23 mev). The deuterium in water limits the ultimate sensitivity.

Instead of using the Szilard-Chalmers reaction, $MnSO_4$ or CaI_2 can be dissolved in water and the active element precipitated out later. It may be easier and quicker, at the expense of sensitivity, to remove a small aliquot of the solution (after sufficient stirring) and treat this or count it directly. Although iodine has only half the activation cross section of manganese, the shorter half-life of I^{128} (25 min compared to 2.6 hr for Mn^{56}) makes iodine more convenient in some cases.

By using combinations of thermal and resonance absorbers, thermal-energy neutrons at energies of a few electron volts can be separated.

RESONANCE SCATTERERS

At higher energies of the order of a few hundred electron volts or a few kilovolts, neutrons can be detected by resonance scattering. The counter consists of BF_3 proportional counters embedded lengthwise in circles in a paraffin ring.^{37,38} The paraffin slows down the neutron and the detection efficiency is about 15 percent in the kilovolt region. The scatterer is placed in the center of the ring. Collimated neutrons must be used. For clear

interpretation, the scatter should have just one resonance or only a few widely-spaced resonances. Only a few elements satisfy this requirement. Table 1.1.10 shows three elements which may prove useful.

Table 1.1.10—Some Useful Resonance Scatterers

Element	Resonance energy, ev	Neutron width, ev	Total cross section at peak, barns	Next-nearest resonance	
				Energy, ev	Peak σ_p , barns
Co	120	2.6	1100	6000	17
Mn	345	13	50	2900	29
Na	3000	170	50	55000	10

PHOTOGRAPHIC EMULSIONS

Slow neutrons can be detected in a photographic emulsion by loading it with lithium and boron and counting the tracks of the reaction products under a microscope.^{39,40,41} The reactions which will take place in an emulsion are listed in Table 1.1.11. Loading and developing of the emulsions must be done carefully to get uniform absorption and to be able to differentiate between alpha or triton tracks and proton tracks.⁴⁰ Up to 72 mg B and 12 mg Li per cc of dry emulsion can be absorbed in 200 μ -Ilford C₂ plates from an aqueous solution of lithium tetraborate, and if separated B¹⁰ or Li⁶ is used, the detection efficiency approaches that of BF₃ counters; this is evident from the transmission curves of Fig. 1.1.11. The lithium and boron reactions can be easily distinguished by their different

Table 1.1.11—Neutron Reactions in Photographic Emulsions Loaded with Boron and Lithium Nuclei

(Kaplan and Yagoda, Rev. Sci. Inst. 23, 1952)

Reaction	E_n	σ , barns	σN , * cm ⁻¹
B ¹⁰ (n, α)Li ⁷	0.025 ev	3800 ⁸⁹	1.35
B ¹⁰ (n, p)Be ¹⁰	Thermal	< 0.2 ⁸⁹	< 7.1 $\times 10^{-5}$
B ¹¹ (n, α)Li ⁸	~1 mev	85 $\times 10^{-6}$ ⁸⁹	1.31 $\times 10^{-7}$
Li ⁶ (n, α)H ³	0.025 ev	910 ⁸⁹	6.96 $\times 10^{-2}$
Li ⁷ (n, α) α	Thermal	0.033 ⁹⁰	3.18 $\times 10^{-5}$
N ¹⁴ (n, p)C ¹⁴	Thermal	1.71 ⁹⁰	4.88 $\times 10^{-3}$
H ¹ (n, p)	E	9.42/(E + 1) ^{91, 92}	†

* Based on the composition of Ilford C-2 plates loaded from a 10-percent lithium borate solution which picked up 3.56×10^{20} atoms of B¹⁰ and 7.65×10^{19} atoms of Li⁶

† The loading process increases the normal hydrogen content of the emulsion by the addition of plasticizer and water of crystallization associated with the lithium borate compound. Measurements of neutron spectra from the ranges of proton recoil tracks are best made on a nonloaded plate

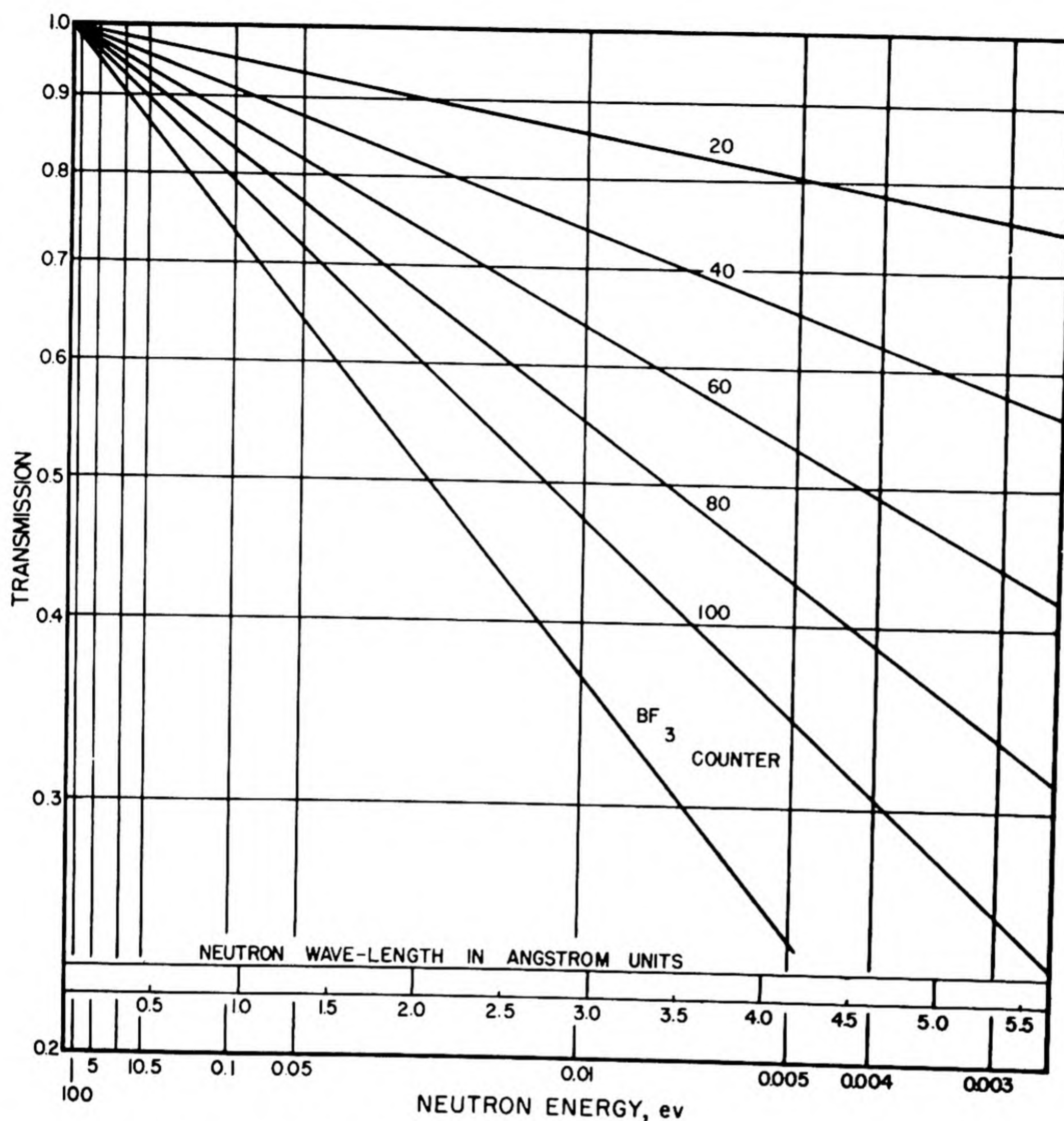


Fig. 1.1.11 — The Transmission in a Photographic Emulsion as a Function of Neutron Energy for 200-micron Ilford C2 B^{10} -loaded Plates Containing Various Amounts of B^{10} in Milligrams per cm^3 of Emulsion. Reprinted from Blau, Ruderman, and Czechowski, Rev. Sci. Inst., 21, 1950. The cross section of B^{10} was taken to be $\sigma = 627^{-1/2}$ (E in eV). The transmission of a conventional BF_3 proportional counter, 10 cm long and filled to 50 cm pressure with pure $B^{10}F_3$ is included for comparison.

lengths. The alpha and triton tracks from lithium are 180° apart and have a total length of about 44 microns while the alpha tracks from boron are 7 microns long. The proton recoils also present in the emulsion have a range of about 7 microns; therefore, tracks in a similar non-loaded emulsion must be counted and subtracted. Angular criteria, shrinkage factors (resulting from developing), and geometric escape factors are given in Kaplan and Yagoda.⁴⁰ Either set of tracks can be used to obtain the neutron flux. The internal average deviation with B^{10} is 8 to 10 percent, with Li^6 , 10 to 15 percent, and between B^{10} and Li^6 , 10 to 15 percent. At sea level, the slow-neutron flux from cosmic rays was observed to be 240 ± 30 neutrons/ $(cm^2)(day)$.

By selecting the proper emulsion, such as Ilford D₁, the sensitivity to beta and gamma radiation can be kept relatively low. After an exposure of a D₁ plate to about 80 roentgens of gamma radiation the background was still low enough to allow short alpha or proton tracks to be counted easily.

SCINTILLATION COUNTERS

Efficient scintillation crystals and liquids used in conjunction with photomultipliers for detecting slow neutrons have only been reported very recently. Hofstadter et al⁴² have grown natural LiI crystals activated with 1 percent Tl which will discriminate against gamma radiation by virtue of the much larger pulse height from the neutron reaction. Because of the large cross sections at thermal energies (910 b for Li⁶, 7.4 percent abundant, at 0.025 ev) a 1-cm-thick crystal of LiI will have almost 100 percent efficiency. By using a mixture of 7 percent Li⁶I and 93 percent NaI plus 0.1 to 1 percent Tl, the pulse height can be greatly increased without loss of counting efficiency. An energy resolution of 7 percent is claimed.⁴³ Boron has not been successfully incorporated into crystals up to the present time, but Muehlhause and Thomas⁴⁴ have mixed an alkyl borate such as tri-ethyl, tri-methyl, or tri-butyl borate with a terphenyl-phenyl-cyclohexane solution to get a scintillator which is 100 percent efficient for slow neutrons.

A combination of scintillation counter and induced activation techniques has been recently proposed by Grimeland⁴⁵ to measure absolute neutron densities. Advantage is taken of the $1/v$ capture cross section of Na²³ to activate a sodium iodide crystal mounted on a photomultiplier. The activity of Na²⁴ has a half-life of 15.06 hr while that of I¹²⁸ is only 25 min; the two activities can therefore be separated easily.

FAST-NEUTRON DETECTORS

Since the cross sections for fast neutrons are on the order of barns or fractions of a barn, fast-neutron detectors have a relatively low efficiency compared to thermal detectors, usually only a few percent or less. Most fast detectors are energy sensitive and can indicate the energy distribution to some extent. However, by surrounding the source with a moderator like water or paraffin of sufficient size, high-energy neutrons can be slowed down and detected by thermal counters or foils, or in the case of water, by dissolved manganese or iodine compounds as discussed under thermal neutrons. The efficiency in a water bath can be made to reach 100 percent, but the use of a bath is often awkward or impossible; a BF₃ proportional counter surrounded in a suitable manner is frequently used as a monitor for neutrons of all energies up to a few mev.^{46,47} Such a counter is called a "flat-response" or "long" counter because the energy response is uniform between 1 and 5 mev and decreases to only 85 percent relatively at thermal energies. The neutrons are sent in axially. The lower efficiency at thermal energies is because of the higher probability that such neutrons will be reflected back from the paraffin and away from the counter. The absolute efficiency is about 1 percent or less.

PROTON RECOIL COUNTERS

Ionization and proportional counters filled with gases containing hydrogen atoms can detect fast neutrons by the ionization produced by the recoil protons. Hydrogen gas or methane is used, the latter having the advantage of a higher hydrogen content per molecule. Instead of a gas, a solid or liquid hydrogenous radiator can be put into an argon-filled counter. Glyceryl tristearate, (C₁₇H₃₅CO₂)₃ C₃H₅, is preferred over paraffin because of its definite chemical composition. It can be evaporated to form thin, uniform layers of the order of microns. A great many types of such counters are described in Rossi and Staub, loc. cit. Skyrme et al⁴⁸ describe a cylindrical proportional counter filled with hydrogen or methane which can reproduce neutron-flux measurements to better than

5 percent in the energy range 0.1 to 1 mev. The efficiencies are of the order of tenths of a percent.

FISSION CHAMBERS

Fission chambers with coatings of pure thorium or separated U^{238} are useful for detecting energies above 1 mev.

THRESHOLD DETECTORS⁴⁹

Activation of certain elements by (n,2n) or (n,p) reactions can be used to measure neutron energies and fluxes in the range 1 to 25 mev. The (n,2n) reaction offers a sensitive method for energy measurements above 9 mev while (n,p) reactions are suitable at lower energies. The latter reaction has a low cross section at threshold and thus is not a sharp detector. Tables 1.1.12 and 1.1.13 list convenient (n,2n) and (n,p) detectors and some quantities useful in correcting the observed counting rates.

The quantity measured by a threshold detector is:

$$I = \int_B^{\infty} F(E)\sigma(E) dE \quad (57)$$

where: E = energy

B = threshold energy

F(E) = neutron flux distribution in energy

Experimentally, I is found from:

$$I = \frac{\lambda n_0}{Q[1 - \exp(-\lambda T)]} \quad (58)$$

where: λ = decay constant of activity = 0.693/half-life

T = bombarding time

n_0 = number of radioactive atoms at end of bombardment

Q = number of atoms of the reacting isotope per unit area perpendicular to the neutron beam

λn_0 is obtained from:

$$\ln\left(-\frac{dn}{dt}\right) = \ln(\lambda n_0) - \lambda t \quad (59)$$

where: $-\frac{dn}{dt}$ = rate of decrease of number of radioactive atoms

t = time after end of bombardment at which rate is measured

$-dn/dt$ is obtained from the observed counting rate R measured in some counter by correcting for the geometrical solid angle the counter sees and for various scattering and absorption effects on the radiation counted. If betas are counted, correcting for self-absorption in the detectors is usually important. The absorption of the betas can be represented in an approximate manner by an exponential relationship:

$$F = e^{-d/\alpha} \quad (60)$$

where: F = fraction transmitted per unit incident intensity

d = absorber thickness

α = 1/e thickness, a constant depending on maximum beta energy and approximately independent of the absorbing material

Table 1.1.12—Convenient (n,2n) Threshold Detectors

(Cohen, Nucleonics 8, No. 2, Feb. 1951)

Original nucleus	Threshold, mev	Half-life	Convenient material	K-capture correction*	Approximate α , † mg/cm ²	Other activities
C ¹²	20.2	20.5 min	Graphite	1.00	70	None
N ¹⁴	10.6	10.1 min	Urea	1.00	100	20.5 min carbon (n,2n)
O ¹⁶	16.5	2.1 min	Cellophane	1.00	170	20.5 min carbon (n,2n)
F ¹⁹	10.4	112 min	LiF	1.00	40	None
P ³¹	12.3	2.55 min	(NH ₄)H ₂ PO ₄	1.00	400	170 min (n,p)
Cr ⁵⁰	13.4	42 min	Cr ₂ O ₃	1.00	240	3.9 min (n,p)
Ni ⁵⁸	11.7	36 hr	Ni metal	3.0	40	2.6 hr (n, γ); 72d (n,p)
As ⁷⁵	10.3	16 days	As ₂ O ₃	1.3	85	26.8 hr (n, γ)
Ag ¹⁰⁷ †	9.6	24.5 min	Ag metal	2.3	220	2.3 min (n, γ); 13h (n,p)
Sb ¹²¹	9.25	16 min	Sb ₂ O ₃	3.0	160	2.8 days (n, γ)
I ¹²⁷	9.45	13.0 days	NH ₄ I	7.0	75	25 min (n, γ)
Pr ¹⁴¹	9.4	3.5 min	Pr ₆ O ₁₁	1.6	360	Long

* Calculated from $(F_{\beta} - F_{\alpha})/F_{\beta}$ where F_{β} and F_{α} are probabilities of β^+ emission and K-capture, respectively

† α is thickness required to reduce beta intensity by 1/e

‡ Especially convenient for most purposes

Table 1.1.13—Convenient (n,p) Threshold Detectors

(Cohen, Nucleonics 8, No. 2, Feb. 1951)

Original nucleus	Energetic threshold, mev	Effective threshold, mev	Half-life	Convenient material	Approximate α , mg/cm ²	Other activities
Mg ²⁴	2.1		14.8 hr	Mg metal	250	10.2 min (n, γ)
Al ²⁷	2.1		10.2 min	Al metal	160	2.4 min (n, γ)
P ³¹	1.1	~3.0	170 min	(NH ₄)H ₂ PO ₄	120	2.5 min (n,2n)
S ³²	1.0	~3.0	14.3 days	Flower of sulfur	160	None
Ti ⁴⁶	1.1		57 min	Ti metal powder	190	3.0 hr (n,2n); 44 hr (n,p)
Cr ⁵²	2.8		3.9 min	Cr ₂ O ₃	350	42.0 min (n,2n)
Fe ⁵⁶	2.1		2.59 hr	Fe metal	250	None

On integrating across the detector thickness, the factor by which the observed counting rate is to be divided is obtained:

$$F = \frac{\alpha}{d_0} [1 - e^{-d_0/\alpha}] \quad (61)$$

where: d_0 = detector thickness

Absorption in the counter window is corrected for by using Eq. (60). Back scattering from the pan holding the detector is usually not important unless the betas are very high in energy and the detector very thin (correction is about 10 percent for 3 mev betas and zero-thickness detector). If other radiations are emitted in cascade with the betas and the counter is sensitive to them, corrections may have to be made in order to get the true absolute intensity.

In obtaining λn_0 care must be taken that other activities are not interfering. The counting rate vs time is plotted on a semi-log scale, and the activity which has the correct half-life is extrapolated back to zero time. Longer-lived activities are also extrapolated back to zero time and subtracted to give the true λn_0 . For accurate results, the counting rates should be measured over several half-lives of the various activities.

To determine the neutron flux, the energy spectrum must be known. The total flux over 3 mev can be obtained without a knowledge of the energy spectrum by using the (n,p) reaction on P^{31} or S^{32} . For phosphorus, $\sigma = 0.14$ barn, and for sulfur, $\sigma = 0.32$ barn.

PHOTOGRAPHIC EMULSIONS

By exposing emulsions such as Ilford C₂ edge-on and counting the proton recoils in the forward direction (making an angle of less than 10° with the neutron direction), Nereson and Reines⁵⁰ were able to obtain resolution of 10 to 20 percent in the range 0.5 to 1.5 mev. The efficiency per unit cross section is independent of energy in this energy range, but from 0.5 to 0.2 mev, the efficiency decreases because of the low grain counts in the proton tracks.

Using Li⁶-loaded plates, one can use the Li⁶ (n,α)H³ reaction to measure the neutron energy, although not the flux at present.^{51,52} The energy is a double-valued function of the sum of the alpha plus triton tracks for each value of the angle θ between the alpha and triton; however, by counting only those tracks for which θ is 175° to 180°, a unique energy can be chosen, and a resolution of at least ±0.1 mev is claimed. Detection of energies from thermal up to 10 mev or more should be feasible. The method is well suited for energy measurements on monoergic neutrons within a medium where perturbations introduced by the detector must be minimized and where collimation cannot be achieved. For continuous neutron energy spectra, the capture cross section would have to be known (it is known only up to 0.7 mev) as well as the angular distribution of the reaction. Work on this is going on at present.⁵³

Scintillation Counters

Hydrogenous materials such as anthracene or stilbene crystals or the many liquid organic scintillators can be used with good efficiency. For example, Jastram et al⁵⁴ claim that a solution of 2 gm/liter of terphenyl in xylene in a cylinder 6 cm long and 4 cm in diameter has an efficiency of 50 percent for 1- to 10-mev neutrons. However, such detectors are also fairly sensitive to gamma radiation. By applying coincidence techniques in which only those recoil protons which receive almost all the energy are counted, the resolution can be considerably improved and the gamma background greatly reduced, with a corresponding sacrifice in counting efficiency.

Molding a button of lucite mixed with ZnS produces a scintillator which can be made relatively insensitive to gamma rays by proper discrimination.⁵⁵ Table 1.1.14 gives efficiencies at some energies.

Table 1.1.14—Neutron Detection Efficiencies for ZnS Scintillation Counter
(Hornyak, Rev. Sci. Inst. 23, 1952)

Background limitation	Discriminator setting	Percent efficiency for neutrons of		
		14.2 mev	~4 mev	0.50 mev
Tube noise	10	8.0	2.5	0.70
$E_\gamma < 3$ mev	15	6.8	1.7	.28
$E_\gamma < 17$ mev	30	4.0	0.86	.12

STANDARDIZATION^{13,56}

Measurement of absolute neutron source strengths and fluxes is difficult, and the accuracy is at best about 5 percent. Relative measurements can be carried out much more easily with accuracies better than 1 percent.

SOURCE STRENGTH

ABSOLUTE MEASUREMENTS

Boric Acid Bath

The source is surrounded by enough boric acid solution to absorb all the neutrons. The source strength is given by:

$$Q = 4\pi(M_B + M_H) \frac{\sigma_H}{\sigma_B} \int_0^\infty nv\sigma_B(1 + g)r^2 dr \quad (62)$$

where: Q = neutrons/sec emitted by source

M_B, M_H = moles of boron and hydrogen, respectively, per cc of solution

σ_B, σ_H = absorption cross section/mole of boron and hydrogen, respectively

$\sigma_H/\sigma_B = 2270$ (Reference 57)

$g(r)$ = neutrons absorbed/(cc)(sec) at the distance r at energies above the cadmium cut-off per neutron absorbed at thermal energies

$nv\sigma_B$ = absorption rate of slow neutrons/(cc)(mole B) at r

The fraction g is determined by measuring the counting rates of a small boron chamber at various distances in the solution with and without a cadmium cover.

The function $nv\sigma_B$ is measured in the following way. A BF_3 counter with accurately known counting volume and gas composition is placed in a thermal flux produced by some second-

ary source. The counting rate I_B of the chamber gives the neutron flux $(nv)_B$ at the counter by:

$$I_B = (nv)_B \sigma_B N_B \quad (63)$$

where: N_B = moles of boron in the counting volume

The ratio of saturated activities of In or Mn foils at a position r in the bath, A_{th} , and at the BF_3 counter in the secondary flux, A_B , is equal to the ratio of the fluxes at the points.

$$\frac{nv}{(nv)_B} = \frac{A_{th}}{A_B}$$

$$\text{Thus: } nv\sigma_B = \frac{A_{th}}{A_B} \frac{I_B}{N_B} \quad (64)$$

and the integral in Eq. (62) can be evaluated by measuring A_{th} as a function of r . The foils must be thin enough not to disturb the neutron flux distribution. In this way, the Los Alamos No. 44 Standard Ra- α -Be Source was calibrated to yield a $Q = (5.9 \pm 0.3) \times 10^6$ per sec in Oct. 1944. The Q increases by 0.54 percent per year because of the growth of PO^{210} .

Production of Helium From Boron

Since one helium atom is produced for each neutron absorbed in B^{10} , a measurement of the amount of helium produced in a bath containing a known amount of boron will give the neutron source strength. Most sources are too weak to produce enough helium to be measured; therefore, the calibration is done indirectly by measuring the amount of helium produced by reactor neutrons and then measuring the relative neutron densities of the reactor and the source by some other method, such as activation of a manganese solution. In this way, the Argonne Standard Source No. 38 (Ra- α -Be) was found to have a $Q = (5.5 \pm 0.4) \times 10^6$ per sec in Oct. 1944.

Balancing of Sub-critical Reactor With Calibrated Absorber

At Harwell, a source was calibrated by balancing the neutrons produced by the source with a sample of sodium. Determining the disintegration rate of the sample gives Q after making certain corrections, such as for the resonance capture of the fast neutrons.

RELATIVE SOURCE-STRENGTH MEASUREMENTS

If two sources are known to have similar spectra, they can be compared by setting up any suitable detector in a fixed geometry.

For sources with different spectra, all the neutrons must be captured or all slowed down to the same energy before detection. The following methods have been used.

Long Counter

The accuracy with such a counter is about 5 percent.

Infinite Medium

The sources are put into a standard graphite reactor and the slowing-down distribution is measured with indium or manganese foils. A standard reactor is a rectangular array of graphite from 5 to 7 ft on a side, 8 to 10 ft high, and covered with cadmium to keep out neutrons from the surroundings. The source is put on the center line 2 or 3 ft from one

end. The detecting foils are also placed along the center line. Such a reactor is also used for flux measurements (see below). For high accuracy, a source strength of 5×10^5 n/sec or greater is desirable:

$$\frac{Q}{Q^{\text{std}}} = \frac{\int_0^\infty q r^2 dr}{\int_0^\infty q^{\text{std}} r^2 dr} \quad (65)$$

$$\frac{q}{q^{\text{std}}} = \frac{A_{\text{res}}}{A_{\text{res}}^{\text{std}}} \quad (66)$$

where: r is the distance from the source along the center line

A_{res} is the saturated foil activity owing to neutrons above the cadmium cut-off. For indium foils, the activity is produced by 1.44-ev neutrons; for Au, 4.8-ev neutrons; and for Mn, 300-ev neutrons. An analytic form for $A_{\text{res}}(r)$ is needed to integrate the equation and is found, on the basis of Fermi age theory (see Chapter 1.3), by fitting the measured distribution to the sum of Gaussians, three usually being sufficient:

$$A_{\text{res}} = \sum_{i=1}^3 A_i e^{-r^2/r_i^2} \quad (67)$$

where A_i and r_i are empirical constants. When indium is used, corrections to the observed A_{res} have to be made for absorption in the cadmium of the 1.44-ev neutrons, for the sink effect of the indium, and for absorption in indium of higher resonances⁵⁸ (see also preceding discussion in this chapter).

If the two sources are not very different in their spectra, the relative source strengths are simply equal to the ratio of the saturated foil activities when measured at a properly chosen distance⁶⁰ in the standard reactor.

This method, while not as accurate as the integration method, is much faster and can measure weaker sources (down to 10^4 n/sec or less).

A water bath or paraffin sphere can be used to slow down the neutrons to thermal energies and the distribution measured with foils or small boron counters. The bath should be large enough to capture all the neutrons. A radius of less than 2 ft will be effectively infinite for neutrons up to fission energies. For high accuracy, a strength of 2×10^5 n/sec or more is needed. An equation similar to Eq. (65) is used with q replaced by A_{th} . The integrals are evaluated graphically until $A_{\text{th}} r^2$ becomes an exponential, and then A_{th} is fitted to the equation:

$$A_{\text{th}} = \frac{a}{r^2} e^{-r/\lambda_s} \quad (68)$$

for r up to ∞ . a and λ_s are constants.

Because of the steep distribution curve, the positions of the foil must be measured to better than a millimeter and the finite size of the foil taken into account; i.e., the root-mean-square distance from the center of the source to all parts of the foil is used. The disturbance of the neutron distribution caused by the sink effect of the foils will cancel out to a large extent in the ratio of the integrals if the same foils are used for both measurements.

A water solution of a manganese or iodine salt surrounding the source is stirred after irradiation to saturation to spread the activity uniformly throughout the solution. The ac-

tivity of an aliquot is measured. Then $Q/Q^{\text{std}} = A_s/A_s^{\text{std}}$. This method is the only one which is independent of the angular distribution of the neutrons.

Subcritical Reactor

If the reproduction factor, k , is slightly less than one, the flux of a source placed in the reactor is multiplied by $1/1 - k$. When this flux is detected by a counter in the lattice, the counting rate is closely proportional to Q because the effectiveness of fast neutrons in the reactor does not depend strongly on their energy. The reactor carries out, in effect, an integration of the neutron distribution, and only one reading is necessary. However, if the spectra are very different, corrections for differences in leakage may have to be applied. This method is rapid and has an accuracy of 1 percent.

FLUX

Standard fluxes may be obtained by measuring reaction rates of known cross sections. $1/v$ detectors such as boron or gold will actually give the neutron density (see Eq. 51) from which a thermal flux can be obtained by multiplying by 2.2×10^5 cm/sec. Such measurements can be carried out with an accuracy of 2 to 4 percent.

The standard graphite reactor with a standard source is used to produce known fluxes.⁵⁸ The distribution of resonance neutrons, A_{res} , is expressed by the semi-empirical Eq. (67). The slowing-down density is given by:

$$q_{\text{res}} = k_{\text{res}} A_{\text{res}} = \sum_{i=1}^3 \frac{F_i Q}{(\pi r_i^2)^{3/2}} e^{-r^2/r_i^2} \quad (69)$$

where: Q = source strength

F_i is the fraction of the Q n/sec emitted which are in the synthetic energy group having the range r_i :

$$F_i = \frac{k_{\text{res}} A_i \pi^{3/2} r_i^3}{Q} \quad (70)$$

k_{res} is evaluated from the relation:

$$\sum F_i = 1 = \frac{k_{\text{res}}}{Q} \pi^{3/2} \sum_i A_i r_i^3 \quad (71)$$

The thermal flux is given by:

$$(nv)_{\text{th}} = v_0 \sum n_i \quad (72)$$

where: v_0 = thermal velocity = 2.2×10^5 cm/sec

$$n_i = F_i Q \sum_{j=1}^{\infty} \sum_{k=1}^{\infty} C_{jk} \frac{b_{jk}}{2} e^{-\frac{[r_i(\text{th})]^2}{4L^2}} \left\{ \left[1 - \theta \left(\frac{z}{r_i(\text{th})} + \frac{r_i(\text{th})}{2b_{jk}} \right) \right] e^{z/b_{jk}} + \left[1 + \theta \left(\frac{z}{r_i(\text{th})} - \frac{r_i(\text{th})}{2b_{jk}} \right) \right] e^{-z/b_{jk}} \right\} \quad (73)$$

$$\text{where: } C_{jk} = \frac{6}{\lambda v_0 a^2} \cos \frac{j\pi x_s}{a} \cos \frac{k\pi y_s}{a} \cos \frac{j\pi x}{a} \cos \frac{k\pi y}{a}$$

$$\frac{1}{b_{jk}^2} = \frac{1}{L^2} + \frac{\pi^2}{a^2} (j^2 + k^2)$$

$$\theta = \theta(x) = \frac{2}{\sqrt{\pi}} \int_0^x e^{-y^2} dy$$

$$r_i^2(\text{th}) = r_i^2 + 4(\tau_{\text{th}} - \tau_{\text{In}})$$

$$4(\tau_{\text{th}} - \tau_{\text{In}}) = 268$$

τ = neutron age

L = thermal diffusion length

λ = transport mean-free-path

The reactor has its small sides of equal length with a = geometric length + 1.42λ . The origin of coordinates is taken at the center at one end of the reactor. The source is at $(x_s, y_s, 0)$ and the foils are at (x, y, z) . Since even a graphite reactor 8 to 10 ft high is not infinite in height for the thermal diffusion process for points very near the top, the observed neutron density near the top will be less than the value calculated from Eq. (73) by the factor:

$$1 - e^{-2(z_t - z)/b_{11}}$$

z_t = (z coord. at the top of the block) + 0.71λ . A reactor 5 ft wide will be effectively infinite from the sides for points along the axis ($x = y = 0$).

By measuring the thermal foil activity, A_{th} , at various points along the axis of the column and by comparing this with the calculated flux, $(nv)_{\text{th}}$, at these points, an average K_{th} such that $(nv)_{\text{th}} = K_{\text{th}} A_{\text{th}}$ may be obtained. This standardizes the foils for the measurement of thermal flux.

To convert from graphite to water:

$$K_{\text{res}}(\text{water}) = K_{\text{res}}(\text{graphite}) \frac{\lambda(\text{graphite}) \xi(\text{water})}{\lambda(\text{water}) \xi(\text{graphite})} \quad (74)$$

MEASUREMENT OF FAST NEUTRON FLUX⁶⁹

For monoenergetic neutrons, hydrogen recoil counters with known sensitive volumes can be used. Three types of counters have been described: (1) Hydrogen-filled proportional or ionization counters or counters having a thin hydrogenous radiator. The ultimate limit to the accuracy is set by the accuracy of the elastic scattering cross section, which is equal to the total cross section at high energies, capture being negligible. This is known to 2 percent up to 1.5 mev and 5 percent up to 14 mev. The lower limit to the neutron energies that can be detected is about 200 kev. (2) Integration ionization chambers in which the current is measured and is directly proportional to the flux. The accuracy is about the same as the pulse-type counters, and this counter has the advantage of being able to detect neutrons down to tens of kev. However, background effects are more difficult to eliminate. (3) Photographic plates have been used, but errors in defining the solid angle and the concentration of hydrogen atoms makes the accuracy at best 15 to 20 percent.

If the neutrons are emitted by a reaction such as $\text{H}^2(\text{H}^2, n)\text{He}^3$ or $\text{H}^2(\text{H}^3, n)\text{He}^4$, an accurate estimate of the neutrons coming off at angle θ per unit solid angle with respect to the

incident particle in the lab system can be made by counting the helium atoms at the corresponding angle ϕ :

$$\sin \phi = \sqrt{\frac{M_n E_n}{M_{He} E_{He}}} \sin \theta \quad (75)$$

This method is potentially capable of the highest accuracy (about 1 percent) for neutrons above 3 mev using the d,d reaction and for neutrons above 13 mev using the t,d reaction.

Threshold detectors with known cross sections which vary smoothly with energy are suitable secondary standards. Fission detectors are convenient because of the ease in detecting the fission fragments. NP^{237} has a threshold of 0.4 mev, and natural U has a threshold about 1 mev.

Relative fluxes can be compared using the long counter (see discussion earlier in this chapter) or the various moderating media with a detector at one point, assuming the sources are isotropic.

For polyergic sources, fluxes can be measured by the methods just described for relative fluxes. The highest accuracy is obtained with a moderating medium. Care must be taken when using the long counter because it is energy independent only over a limited energy range.

The recoil particle method is suitable for measuring polyergic sources. The energy distribution of the primary neutrons, $S(E)$, is related to the energy distribution of the recoil particles, $H(E)$, by:

$$S(E) = \frac{E_r}{N\sigma(E)} \frac{dH(E)}{dE_r} \quad (76)$$

where: E_r = energy of recoil

N = number of detecting nuclei/cm²

$\sigma(E)$ = scattering cross section

The principal difficulty is to determine dH/dE_r . The various types of hydrogen counters are most suitable. One method that has been used successfully with about 10 percent accuracy is to count the recoils from a thin radiator in a photographic plate.

CROSS-SECTION MEASUREMENTS

The atomic cross section, σ , for a reaction produced by neutrons is defined as follows:

$$\sigma = \frac{\text{Events of given type per unit time per nucleus}}{(\text{neutron density})(\text{neutron velocity})} \quad (77)$$

The neutron can be isotropic or in a beam. Dimensions are in area units. A given type means absorption, scattering, and the like or the total cross section which involves the sum of all processes that can remove neutrons from the beam.

TOTAL CROSS SECTION

The total cross section, σ_t , is found very accurately by a transmission experiment using monoergic neutron beams. The transmission is defined as the ratio of neutron flux at distance x in the material to the initial flux and is given by:

$$T = \frac{(nv)_x}{(nv)_0} = e^{-N\sigma_t x} \quad (78)$$

where N is the density of nuclei in the material. The beam intensity is measured by a detector with and without the sample in the beam. It is not necessary to know the detector efficiency because only the counting ratio is needed. The conditions for accuracy are:

- (1) Well collimated beam.
- (2) Uniform, accurately known, sample thickness.
- (3) Accurate knowledge of impurities, especially the water content and impurities with large cross sections.
- (4) Small angle subtended by detector at absorber (to avoid scattered neutrons).

The most accurate measurements of σ_t as a function of energy have been made using time-of-flight spectrometers and crystal monochromators (see previous discussion).

ABSORPTION CROSS SECTION, σ_a

TRANSMISSION METHOD

If $\sigma_t \gg \sigma_s$, then $\sigma_t = \sigma_a$. If $\sigma_t > 500$ b, the error in σ_a will be less than 5 percent. This is the case with B, Cd, U^{235} , and Pu^{249} . If $\sigma_t \approx 50 - 200$ b using a reasonable guess for σ_s will give σ_a with an error of about 10 percent.

SUBSTITUTION METHOD

This is a relative method used for $1/v$ absorbers. A source is surrounded first with the material of unknown σ_a and then with material of known σ_a , using enough material to absorb all the neutrons. The rate of neutron production will be the same in both cases, but the rate of absorption will depend on σ_a . The total number of neutrons present in each medium is found by measuring the density distribution using $1/v$ detectors. Then:

$$\frac{\left(\int_v ndv\right)_1}{\left(\int_v ndv\right)_2} = \frac{N_2\sigma_{a_2}}{N_1\sigma_{a_1}} \quad (79)$$

where: n = neutron density

N = density of absorbing atoms

For an isotropic source, it is only necessary to measure the activity, I , along one radius, plot Ir^2 vs r , and graphically integrate.

If σ_a (unknown) > 10 b, water is used for the standard, and the unknown is dissolved in water. Then:

$$\frac{\left(\int ndv\right)_{H_2O}}{\left(\int ndv\right)_{soln.}} = \frac{N_H\sigma_H + N_x\sigma_x}{N_H\sigma_H} \quad (80)$$

(The absorption of oxygen is negligible compared to hydrogen)

In this way, the ratios σ_{Li}/σ_H , σ_B/σ_H , and σ_{Mn}/σ_H have been measured.

If σ_a (unknown) ~ 10 b large volumes of concentrated solutions are usually needed. This can be avoided by the following modification of the method. Boron, because of its large cross section, is used as a standard in place of hydrogen. The source is kept at a fixed position outside the solution, the detector at a fixed position within. The concentration of boron atoms, N_B , which produces the same decrease in the slow-neutron density as is caused by a concentration, N_x , of the element x is determined. The cross section, σ_x , of this element is then given by $\sigma_B N_B = \sigma_x N_x$.

This modification is equivalent to the measurement of a single point on the activity integral curves discussed above. A basic assumption is that the fixed geometrical conditions and the low concentrations involved render negligibly any differences in the scattering properties of the elements investigated and any changes in the absorption and scattering properties of the water.

A further modification is necessary in order to study elements with $\sigma_a < 1$ b. Because σ_a of H(0.31 b) is comparable to the cross sections to be studied, water is replaced by a moderator of negligible absorption, i.e., graphite. A powdered sample of the element to be investigated is intimately mixed with graphite powder. The reduction in the neutron density by a known concentration of the element is compared with that produced by varying mixtures of boron and graphite powder.

CHANGE IN REACTOR REACTIVITY

Adding an absorber to a critical reactor will reduce the reactivity k by an amount Δk which, to a first approximation, is proportional to the absorption cross section. The method has been applied to thermal reactors in two variations; the danger-coefficient⁶⁰ method and the reactor oscillator^{61,62,63} method. It is a relative method and requires absorbers with known cross section, such as boron or gold, which are $1/v$ and thus yield the thermal cross section. The unknown must also have the same cross section spectrum or else the cross section will just be some average value over the thermal-reactor energy regions.

In the danger-coefficient method, the reactivity change is measured by the position of a control rod which has been calibrated. The reactivity, in turn, is obtained from a measurement of the reactor period as observed on a sensitive galvanometer connected to a large BF_3 chamber in the reactor.

The change in reactivity is observed for both the unknown and a standard absorber placed near the center of the reactor, and the ratio is equal to the ratio of the cross sections. Instead of using boron as a standard, it is convenient to use thin cadmium wires about 1 mm in diameter. Cd is black to neutrons up to 0.4 ev and in an isotropic flux presents a cross section of $\frac{1}{4} \pi dl$, where d = diameter and l = length. To convert a cross section measured with cadmium as a reference to a thermal cross section, it must be multiplied by the calibration ratio between cadmium and boron. The following errors may be present:

- (1) Impurities with high cross section. This is probably the most important external source of error and, according to Hughes,¹³ limits the accuracy to about 5 percent.
 - (2) Perturbation of neutron density by high absorption. This is reduced by using thin or dilute absorbers and distributing them over many graphite cells.
 - (3) Self-absorption. This effect is minimized by adjusting the thickness of the known and unknown to give the same absorption per unit area in each.
 - (4) Scattering effects. By placing the absorber in a region of zero neutron-density gradient, i.e., in the center of a moderator cell symmetrical with respect to the fuel, there will be no change in the spatial distribution. However, the absorber (as a scatterer) will increase the slowing-down power of the moderator, the resonance escape probability, and thus the reactivity. This is important for materials of low σ_a and low A but can be calculated if σ_s is known.
 - (5) In air-cooled reactors, barometric and temperature drifts and fluctuations change the amount of gas in the reactor and therefore the absorption and reactivity. Temperature drifts are slow and can be compensated for by measuring the unknown and standard in cycles. Pressure changes can be erratic and set the limit to the internal consistency of the measurements in such reactors. This is about 0.5 percent.
- The reactor oscillator is a mechanical device for oscillating a sample between positions of different flux density. The change in reactivity is observed as an a. c. signal coming

from an ion chamber placed close to the path of the moving absorber. By proper design of the ion chamber and recording circuits, the signal because of a scattering event can be made quite different from one due to absorption. The two types can be put out of phase and the scattering signal almost completely cancelled out. Corrections for scattering have to be considered when the absorption cross section becomes less than 1 percent of the scattering cross section. The main advantage of the reactor oscillator is that much smaller amounts of materials can be used, of the order of milligrams instead of the grams to kilograms required by the danger-coefficient method. The materials can be oscillated in a region of the reactor containing only graphite so that resonance effects can be greatly reduced. As an estimate of the over-all error, measurements of the indium thermal cross section showed an uncertainty of 5 percent for a 150-mg sample and a 20 percent uncertainty with a 5-mg sample.⁶²

ACTIVATION METHOD

By studying the induced radioactivity of a sample, the activation cross section can be measured. The activation may result from (n,γ) and (n,p) reactions, and thus the activation cross section may or may not be equal to the absorption cross section. If the product nucleus decays in a simple manner to a stable daughter, the activation cross section is:

$$\sigma_{\text{act}} = \frac{C_{0,\text{sat}}}{nvN_t} \quad (81)$$

where: $C_{0,\text{sat}}$ = saturation activity at end of irradiation; see Eq. (56)

nv = neutron flux

N_t = total number of atoms in beam

If the daughter of the product nucleus is also radioactive, the equation for $C_{0,\text{sat}}$ is more complicated.

If the flux is not known, relative measurements can be made. Then:

$$\sigma_x = \frac{N_{\text{std}}}{N_x} \frac{(C_{0,\text{sat}})}{(C_{0,\text{sat}})_{\text{std}}} \sigma_{\text{std}} \quad (82)$$

DEPLETION METHOD

Some of the elements have large absorption cross sections but the product nucleus is stable (Cd, Gd, Sm). The cross section can be obtained by irradiating in a reactor of known flux for a few months and analyzing the sample for initial and final nuclei concentrations in a mass spectrograph. The accuracy is poor because of uncertainties about the reactor flux. The method has also been applied to determining the cross section of Xe^{135} which has the largest absorption cross section known. Xe^{135} has a half-life of 9.2 hr and decays to the very long lived Cs^{135} (half-life $> 10^6$ yr) which can be considered stable. Two samples are put into similar counting chambers, and the ratio of activities before and after one of the chambers has been irradiated is taken. The non-irradiated sample decays according to:

$$I = I_0 e^{-\lambda t}$$

and the irradiated sample according to:

$$I = I_0 e^{-(\lambda + nv\sigma)t}$$

from which σ can be obtained.

MEASUREMENT OF DIFFUSION LENGTH

This method complements the other methods because it requires $\sigma_a \ll \sigma_s$. A rectangular reactor of the absorber is built with square cross section. A source is put at one end, and the relaxation length along the central longitudinal axis is measured. This is the length for the neutron intensity to drop by a factor e :

$$\frac{1}{\text{relaxation length}} = \sqrt{\frac{1}{L^2} + \frac{2\pi^2}{a^2}} \quad (83)$$

$$\begin{aligned} \text{where: } a &= \text{short edge length} + 1.42 \lambda_{tr} \\ L &= 1/\sqrt{3\sigma_a \sigma_{tr}} = \text{diffusion length} \\ \lambda_{tr} &= \text{transport mean-free-path} = 1/N\sigma_{tr} \\ \sigma_{tr} &= \text{transport cross section} \\ N &= \text{nuclei/cm}^3 \end{aligned} \quad (84)$$

σ_{tr} must be known. Large quantities of the absorber are needed. Measurements on D_2O , graphite, and Be have been carried out. The method has been especially useful in assaying impurities in graphite that would increase the absorption.

SCATTERING CROSS SECTION

THE DIFFERENTIAL SCATTERING CROSS SECTION

The differential scattering cross section per unit solid angle at the angle θ with respect to the incident beam is given by:

$$\frac{d\sigma_s(\theta)}{dw} = \frac{(nv)_\theta}{(nv)_0 N X \Delta w} \quad (85)$$

where: $(nv)_\theta$ = scattered flux measured by a detector at the angle θ
 $(nv)_0$ = incident beam flux
 N = density of scattering atoms
 X = thickness of scatterer
 Δw = solid angle subtended by detector at the scatterer

The thickness must be small enough to present multiple scattering. The velocity of the scattered neutron will change with angle; therefore, the change in detector sensitivity with energy must be considered. Since the scattered neutrons are distributed over 4π radians, the scattering intensities are low and the accuracy is not as great as for σ_t .

RECOIL COUNTERS FOR DIFFERENTIAL CROSS SECTION

If the scatterer is a gas, conservation laws give a relationship between the distribution in angle of the scattered neutrons and the distribution in energy of the recoils, using an incident beam of monoenergetic neutrons. The recoil energy distribution can be measured by putting the gas in an ionization chamber or proportional counter. Instead of using recoils produced in a gas it is also possible to employ a thin radiator. Elastic scattering must be the only nuclear interaction because other reactions would change the energy distribution.

The differential cross section in the center of mass system at the angle ϕ as a function of the recoil energy distribution in the lab system is given by:⁶⁴

$$\frac{d\sigma_s(\phi)}{dw} = \frac{E_n A}{\pi(A+1)^2} N(E) \quad (86)$$

where: $N(E)$ = recoil particles per unit energy interval at energy E in lab system

E_n = incident neutron energy

A = mass number of recoil particle

The relationship between the scattering angle, ϕ , of the neutron in the center of mass system and the recoil energy, E , in the lab system is:

$$E = \frac{2A}{(1+A)^2} E_n (1 - \cos \phi) \quad (87)$$

The method has been successfully applied to hydrogen, helium, and oxygen.^{65,66,67}

METHOD OF POOR GEOMETRY

A poor-geometry scattering experiment in which the scatterer is a large disk placed halfway between the (point) source and (point) detector will give the cross section for scattering through angles larger than ϕ_m , the angle the scatterer subtends at the source or detector.⁶⁸ The scattering disk must be thin, and the neutron source and detector response must be isotropic. The method is particularly useful for heavy elements and for small scattering angles of the neutrons.

The cross section is found from:

$$\frac{I}{I_0} = 1 - N \int_{\phi_m}^{\pi} \sigma(\phi) 2\pi \sin \phi d\phi \quad (88)$$

where: the integral represents the partial total cross section for ϕ from ϕ_m to π

I_0 = flux measured by detector without scatterer

I = flux measured by detector with scatterer

N = scattering nuclei per unit area

LARGE-ANGLE SCATTERING

For isotropic scattering, the amount of large-angle scattering ($> 90^\circ$) can be measured and compared with graphite whose scattering cross section is accurately known from transmission experiments.

THE TOTAL-SCATTERING CROSS SECTION

The total scattering cross section, σ_s , is obtained by integrating the differential cross section as defined by Eq. (85) over the unit sphere.

TRANSMISSION METHOD FOR TOTAL-SCATTERING CROSS SECTION

The scattering cross sections of the elements are > 1 b for thermal neutrons. If a rough absorption measurement indicates that σ_a is $\ll 1$ b, then $\sigma_t \simeq \sigma_s$. This method has been applied to H, D, Be, C, O, F, Pb, and Bi.

If $\sigma_a > \sigma_s$ and an accurate spectrum of σ_t vs E is obtained from velocity spectrometer measurements, it may be possible to analyze the curve into a constant scattering term plus a $1/v$ absorption term. The effects of crystalline structure and molecular binding on the scattering cross section are discussed in Chapter 1.2. Because of the interference effects at thermal energies, scattering cross sections of the atoms in a molecule are not additive.

INELASTIC SCATTERING CROSS SECTIONS

TRANSMISSION METHOD

The transmission is measured by putting a sphere of the scattering material round either the source or the detector. If the neutron source is not isotropic, the sphere should be put around the detector. Use of a sphere eliminates elastic scattering effects.

The detector is of the threshold type so that the experimental cross section is that for all neutrons degraded below the threshold energy, including absorption. By using detectors with different thresholds, a rough idea of the spectrum and of the contribution of absorption can be obtained.

The method gives the total inelastic cross section since the sphere has an integrating effect. To avoid geometric perturbations, the distance between source and detector should be more than three times the radius of the sphere. Errors from this effect are thereby reduced to less than one percent under the assumptions of isotropic scattering. A large plane of the scatterer may be used in place of the sphere, but the corrections are much greater.

In order to correct for scattering from the surroundings, variations in source strength, and the like, a monitor of the same detecting material is put to the side about halfway between the source and detector.

DIRECT SPECTRUM METHOD

The neutron energy spectrum is measured at different angles, and the complete inelastic scattering spectrum is thus obtained. Corrections for absorption are not necessary. This is the best method but requires sensitive detectors with known energy dependence. Results have been published for the scattering at about 90° for Fe using a photographic plate⁶⁹ and for Fe and Al using an anthracene scintillation counter.⁷⁰ The results for Fe agree within the experimental error which is about 25 percent. Measurements on the heavy elements are being performed at Los Alamos with a sphere around the source and a photographic plate for detector.⁷¹

GAMMA-RAY METHOD

The yield of gamma rays coming off as a result of inelastic scattering has been measured⁷² by means of a pair of calibrated Geiger counters in coincidence. The neutron flux was measured with a proton recoil ionization chamber. If only one level is excited, the number of gamma rays can be correlated one-to-one with the scattering events and the cross section determined. If several gamma rays are emitted in cascade, the interpretation becomes more difficult.

FISSION AND CAPTURE CROSS SECTIONS AND α

FISSION CROSS SECTION, σ_f

(1) By using a known flux, one can measure $n\sigma_f N$ by absolute counting in a fission chamber.

(2) The sample is irradiated in a reactor with known flux, and a quantitative chemical analysis of the fission products is then carried out. From this, σ_f can be calculated.

(3) The cross section is measured relative to that of U^{235} , thereby eliminating the need to know the flux.

CAPTURE CROSS SECTION, σ_c

(1) A sample with mass number A is irradiated in a known flux and analyzed for the amount of $A + 1$ isotope formed in a mass spectrograph. This is the method used for U^{235} .

(2) If the $A + 1$ nucleus is radioactive, the amount of capture can be found from the decay process. This is done for Pu^{239} by counting the spontaneous fissions in Pu^{240} .

(3) σ_c can be found by difference:

$$\sigma_c = \sigma_t - \sigma_f - \sigma_s$$

MEASUREMENT OF $\alpha = \sigma_c/\sigma_f$

σ_c and σ_f can be measured separately as described previously.

Danger Coefficient Method⁷³

The fission sample is inserted in the reactor, and the fractional change in reactivity, $(\Delta k/k)_1$, is observed:

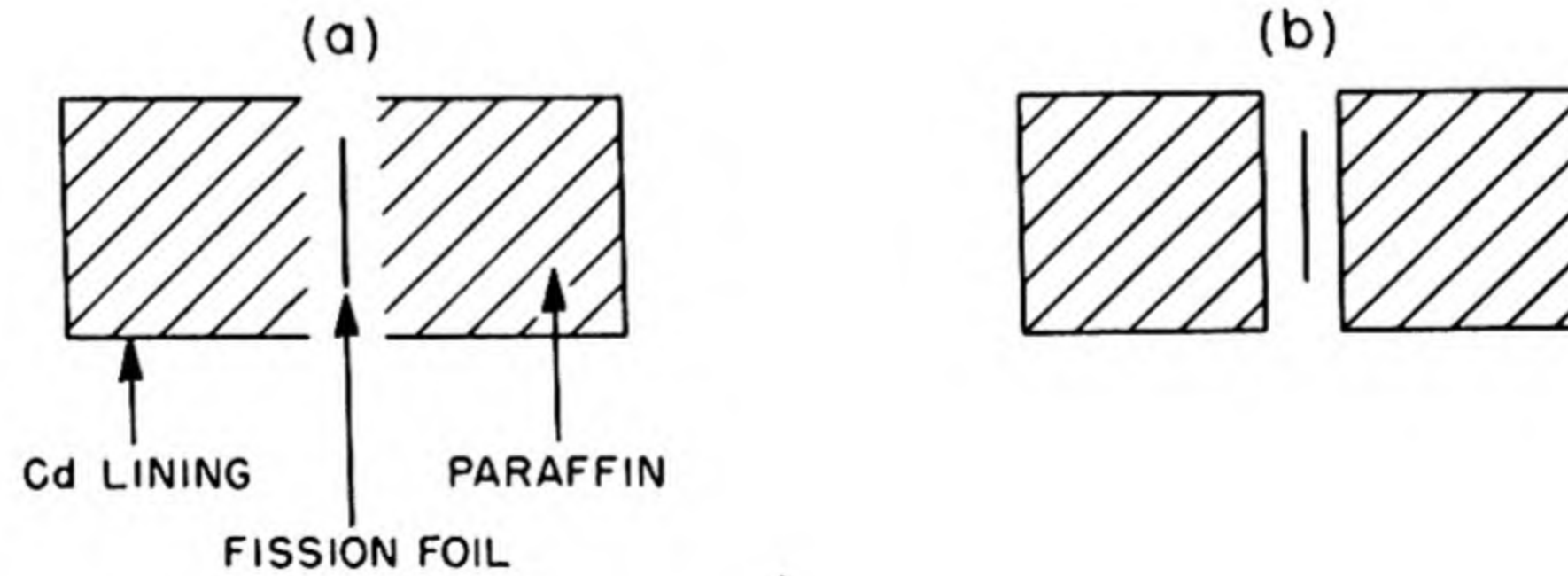
$$\left(\frac{\Delta k}{k}\right)_1 = \Delta f_1 [\nu F_H - (1 + \alpha) F_L] \quad (89)$$

where Δf_1 is the fission rate of the sample, ν the number of neutrons emitted per fission, and F_H and F_L the importance functions (see Chapter 1.4) suitably normalized. F_H and F_L are found as follows:

A non-fissionable absorber is put into the reactor at the same place, and the reactivity change and absorption rate, Δa , are determined to get F_L :

$$\left(\frac{\Delta k}{k}\right)_2 = -\Delta a F_L \quad (90)$$

F_H is obtained by two measurements. The fission sample is inserted in the reactor and is surrounded first by the cadmium-covered paraffin can shown in (a) below and then in the can shown in (b). In both (a) and (b), the over-all transmission is the same, but the inner Cd linings keep the thermal neutrons from reaching the sample in (b). The fission rates are measured for each case.



$$\left. \begin{aligned} \text{(a)} \quad \left(\frac{\Delta k}{k}\right)_3 &= \Delta f_3 [\nu F_H - (1 + \alpha) F_L] - \Delta a^1 F_L \\ \text{(b)} \quad \left(\frac{\Delta k}{k}\right)_4 &= -\Delta f_4 [(1 + \alpha) F_L] - \Delta a^1 F_L \end{aligned} \right\} \quad (91)$$

Δa^1 = absorption rate of paraffin and cadmium

The four equations can be solved for α :

$$\alpha = \frac{\left(\frac{\Delta k}{k}\right)_1}{\left(\frac{\Delta k}{k}\right)_2} \frac{\Delta a}{\Delta f_1} \frac{\Delta f_3}{\Delta f_4} + \frac{\left[\left(\frac{\Delta k}{k}\right)_4 - \left(\frac{\Delta k}{k}\right)_3\right] \Delta a}{\left(\frac{\Delta k}{k}\right)_2 \Delta f_4} - 1 \quad (92)$$

MEASUREMENTS OF REACTOR CONSTANTS

NEUTRON TEMPERATURE

The temperature, T , of neutrons is defined for thermal neutrons in a Maxwell distribution* by:

$$kT = \frac{1}{2} M v_0^2 \quad (93)$$

where v_0 is the most probable velocity. T can be found by measuring the energy distribution of the neutrons in a high resolution spectrometer, such as the crystal monochromator. T can also be found by measuring the average absorption cross section of a $1/v$ absorber using a $1/v$ detector. If:

$$\sigma_a = \frac{K}{v}$$

then:

$$\bar{\sigma}_a = \frac{2}{\sqrt{\pi}} \frac{K}{v_0} \quad (94)$$

To carry out the measurement, a transmission experiment is performed using boron as the $1/v$ absorber because the factor k in Eq. (94) is accurately known. A thin BF_3 detector is used also because of its $1/v$ nature. Such a detector will see the Maxwellian velocity distribution of the thermal neutrons, and therefore the observed cross section will be just the average cross section. Corrections have to be made for the constant scattering cross section, which is subtracted, and for the flux changes due to the finite absorber thickness ("hardening" of the beam). Temperature measurements carried out on beams inside and outside thermal columns have varied over about 100° . This variation is caused by non-equilibrium conditions as well as experimental uncertainties. The following results are quoted from Hughes.¹³

330°K for a beam from the thermal column of the Argonne deuterium reactor.

287°K—same location as above but with a slightly different graphite geometry.

255°K for beam emerging from a shallow hole in the thermal column of the Argonne graphite reactor.

285°K—deep hole in the thermal column of the Argonne graphite reactor.

MEASUREMENT OF NEUTRON AGE

The neutron age is determined in the general case by measuring \bar{r}^2 and applying the relationship:

$$\tau = \frac{\bar{r}^2}{6} \quad (95)$$

* See Chapter 1.3.

$\overline{r^2}$ is defined by:

$$\overline{r^2} = \frac{\int_0^\infty A_s r^4 dr}{\int_0^\infty A_s r^2 dr} \quad (96)$$

A_s is the activity of a resonance foil, usually cadmium-covered indium. The source is placed near* one end of the moderating medium which should be sufficiently large in volume to thermalize the neutrons. For the important practical case of measuring fission-neutron age, the neutron source usually consists of an enriched uranium disk placed in and near the end of the medium with the medium placed on top of a thermal column. A_s is measured as a function of r , the distance from the source. To extend the limit of the integral to infinity, a plot of $\ln A_s r^2$ vs r is made. At large distances from the source, the slowing-down distribution will be given to a first approximation by the distribution of first collisions. This distribution will result in the activation decreasing exponentially:

$$A_s = \frac{k e^{-r/\lambda}}{r^2} \quad (97)$$

A straight line will appear in the semi-log plot, and the constants k and λ can be determined.

The integrals can now be evaluated graphically up to some point, r_0 , which lies on the straight line and then evaluated analytically from r_0 to ∞ . The general form of the integrals is:

$$k \int_{r_0}^\infty e^{-r/\lambda} r^n dr = k\lambda e^{-r_0/\lambda} \sum_{i=0}^n [i! {}_n C_i r_0^{(n-i)} \lambda^i] \quad (98)$$

where: $n = 0, 2, 4, \dots$
 ${}_n C_i = n! / [i! (n-i)!]$

At large distances, the counting rate in Cd-covered In foils may become very low. The counting rate may be improved greatly by using bare or Al-covered In foils. Where the first collision processes predominate, the counting rate with Al-covered In will be proportional to the Cd-covered In, and the proportionality constant can be evaluated by taking overlapping points. Activation from higher-energy neutrons can be checked by measuring with In covered with enough boron to remove the 1.44-ev resonance neutrons. The error in $\overline{r^2}$ from this effect is reduced when the ratio of the integrals is taken. The correction can be quantitatively made.⁵⁸ In another technique⁷⁴ for eliminating the higher-energy activation, a single Cd-covered In foil is activated followed by a Cd-covered In sandwich consisting of three similar indium foils. The activity of the interior foil of the sandwich is subtracted from the single foil measurement, and the result is the activation of solely the 1.44-ev resonance.

To correct for the finite sizes of the source and detector, the following equation⁷⁵ may be used: Case I. Circular source of radius a' and circular detector of radius a :

$$A(r_0) = A_m(r_0) - \left(\frac{a'^2 + a^2}{4r_0} \right) \left(\frac{dA_m}{dr} \right)_{r_0} \quad (99)$$

* But not so near ($< \sqrt{\tau}$) that the effect of the boundary is felt at the positions of measurement.

Case II. Rectangular source of dimensions $2a'$ by $2b'$ and rectangular detector $2a$ by $2b$:

$$A(r_0) = A_m(r_0) - \left(\frac{a'^2 + b'^2 + a^2 + b^2}{6r_0} \right) \left(\frac{dA_m}{dr} \right)_{r_0} \quad (100)$$

Case III. Circular source of radius a' and rectangular detector of dimension $2a$ by $2b$:

$$A(r_0) = A_m(r_0) - \frac{4(a^2 + b^2 + 6a'^2)}{24r_0} \left(\frac{dA_m}{dr} \right)_{r_0} \quad (101)$$

$A_m(r_0)$ is the observed activity at the distance r_0 between the centers of the source and detector, and $A(r_0)$ is the ideal activity owing to point sources. Other combinations, such as point source and circular detector, can be obtained from the above equations by simple modifications. The assumptions used in deriving the equations require the use of foils and sources small in dimension with respect to r_0 . However, the equations have been shown to be valid for corrections up to 20 percent.

The same data used to obtain $\overline{r^2}$ can be used for higher movements:

$$\overline{r^n} = \frac{\int_0^\infty A_s r^{n+2} dr}{\int_0^\infty A_s r^2 dr} \quad n = 2, 4, 6, \dots \quad (102)$$

The accuracy decreases however with increase in n .

The above measurements give the age for the energy drop from the energy of emission to the resonance energy of the foil. The age from the resonance energy to thermal is calculated from:

$$\begin{aligned} \tau_{th} - \tau_{res} &= \int_{\ln E_{th}}^{\ln E_{res}} \frac{\overline{\lambda_{tr}^2}}{3\xi(1 - \cos \theta)} d \ln E \\ &= \frac{\overline{\lambda_{tr}^2}}{3\xi(1 - \cos \theta)} \ln \frac{E_{res}}{E_{th}} \end{aligned} \quad (103)$$

where the symbols have their usual meaning.

If the neutron source is monoergic, the log of the slowing-down density plotted against the square of the distance from the source will give a straight line the slope of which is equal to $-1/4\tau$.

THE RESONANCE ABSORPTION INTEGRAL

The resonance absorption integral, $\int \sigma dE/E$, can be measured by activation of the substance when this gives unambiguous results (i.e., all neutrons absorbed produce the same radioactive isotope) or by using the reactor oscillator (see previous discussion, "Change in Reactor Reactivity").

In the activation method,⁷⁶ the cadmium ratio for the substance, x , is determined in a reactor (dE/E) flux, and the resonance absorption integral is given by:

$$\int_{E_0}^\infty \sigma \frac{dE}{E} = \frac{K(\sigma_{th})_x}{(CdR - 1)_x} - k(\sigma_{th})_x \quad (104)$$

where: $(\sigma_{th})_x$ = thermal activation cross section for the substance (assumed known)

CdR = cadmium ratio

K = constant depending on flux only

k = constant related to epi-cadmium $1/v$ absorption

K and k are found by measuring the cadmium ratios of a substance with a standard having a known resonance absorption integral, such as gold or indium, and of a substance with pure $1/v$ absorption, such as boron:

$$K = \frac{\left(\int_{E_0}^{\infty} \sigma \, dE/E \right)_{\text{std}}}{(\sigma_{\text{th}})_{\text{std}} \left[\frac{1}{(\text{CdR} - 1)_{\text{std}}} - \frac{1}{(\text{CdR} - 1)_{1/v}} \right]} \quad (105)$$

$$k = \frac{K}{(\text{CdR} - 1)_{1/v}} \quad (106)$$

The lower limit, E_0 , to the integral will be 0.4 ev if a 0.01-in. Cd shield is used around the sample in an isotropic flux or if 0.02-in. Cd is used in a collimated neutron beam. The lower limit to the dE/E flux may be set at 0.17 ev since this energy will divide equally the intensities of the Maxwellian and dE/E distribution. The resonance integral can be calculated to 0.17 ev if the absorption cross section is known. If it is $1/v$ as is usually the case, then:

$$\int_{0.17}^{0.4} \sigma_a \frac{dE}{E} = 0.69 \, \sigma_{\text{th}} \quad (107)$$

In the activation method, it is important that the sample be as free from water as possible because H causes moderation and additional thermal absorption. To reduce self protection, very thin samples must be used. If the sample has a CdR of less than 5, indicating a strong resonance, the sample thickness will have to be 0.1 to 0.2 mg/cm² or less.

In using the reactor oscillator,¹³ the technique is similar to that described earlier under "Change in Reactor Reactivity." The samples are oscillated inside a cadmium tube and the amplitude of the reactor oscillation is calibrated with indium or gold. The advantages of the oscillator are that small samples can be investigated and that the total absorption is measured.

In measuring the resonance absorption of U^{238} , thin foils of separated U^{238} may be activated. However, in actual reactors, the amount of uranium present is so large that the dE/E spectrum is depleted at the resonance energies, the amount of depletion depending on the shape and concentration of the uranium. Thus, an effective resonance absorption integral should be measured. This is done by putting the thin U^{238} foils in a sample of the homogeneous uranium-graphite mixture which is large enough to ensure equilibrium depletion at the resonance levels—usually about a liter in volume. For unhomogeneous reactors, the uranium slugs are slotted to receive small thin U^{238} foils. The effective integral is determined for various sizes of slugs in order to get semi-empirical equations of the type of Eq. (9).

MEASUREMENTS OF DIFFUSION LENGTH

The diffusion length, L , for thermal neutrons in a substance may be obtained by measuring the space distribution of the neutrons in a rectangular block of the material. The neutrons may come from a source such as Ra- α -Be placed in the material near one end in which case the arrangement is called a sigma pile, or by locating the block adjacent to the thermal column of a reactor. The latter method gives more accurate results because of the higher intensity and more complete thermalization of the neutrons. The flux is measured with small boron counters or, more usually, with indium or dysprosium foils. The usual precautions for preventing perturbations of the flux distribution by the foils must be taken. In the case of the sigma pile, the cadmium ratio should be taken to check on the constancy of the thermalization.

To prevent scattering of thermal neutrons back into the block, it is covered with cadmium. However, this will not keep out fast neutrons, and the only way to avoid this is to place the block far from the walls of the room, the equipment, and the like. In the sigma pile, the source should not be placed too near one end.

The flux distribution along the longitudinal axis (z axis) is given by:

$$nv(z) = \frac{2S}{abD} \sum_{j,k=1}^{\infty} e^{-z/B_{jk}} \quad (j, k \text{ odd}) \quad (108)$$

where: S = source strength

a, b = extrapolated lengths of the reactor in x and y directions

D = diffusion coefficient

B_{jk} = relaxation length for (j, k) harmonic

The diffusion length is related to the relaxation lengths by:

$$\frac{1}{L^2} = \frac{1}{B_{jk}^2} - \pi^2 \left(\frac{j^2}{a^2} + \frac{k^2}{b^2} \right) \quad (109)$$

Far enough away from the source, the first harmonic, B_{11} , will predominate, leaving just one term in the equation for the flux. A plot of $\log nv$ vs z will give a straight line with slope $-1/B_{11}$. Corrections may have to be made for:

- (1) Higher harmonics
- (2) End effects
- (3) Incomplete thermalization

The side dimensions of the reactor have to be large enough so that $\pi(1/a^2 + 1/b^2)$ is small relative to B_{11}^2 . The length of the reactor must be several relaxation distances to reduce higher harmonics and end effect and to enable an accurate determination of the slope to be made.

The correction for the next higher harmonics is given by:

$$1 + \frac{1}{B_{11}} e^{z/B_{11}} [B_{13} e^{-z/B_{13}} + B_{31} e^{-z/B_{31}} + B_{33} e^{-z/B_{33}}] \quad (110)$$

The observed flux is to be divided by this factor. Since the correction is small, a trial and error method is used, the first rough measurement of B_{11} giving L from which the other harmonics are calculated by Eq. (109). The corrected values of the fluxes are then re-plotted and a better value of B_{11} thus obtained. The process is repeated until the value for L converges to the required accuracy.

At points near the end of the reactor, the flux will decrease from the straight exponential. The correction factor by which the observed flux is to be divided is approximately:

$$1 - e^{-2(C-z)/B_{11}} \quad (111)$$

where C is the extrapolated reactor length (in the z direction) measured from the source. Again an iteration method is used. For a determination of the extrapolation length, see "Measurement of Extrapolation Distance" which follows.

By using a pile with a square cross section, a by a , and by putting two sources of equal strength at the points $(\pm a/4, 0)$, the chief higher harmonics $(j, k) = (1, 3), (3, 1), (1, 5), (5, 1)$ can be suppressed. The harmonic correction was thus reduced to 0.5 percent

at 3 ft along the longitudinal axis in the Brookhaven graphite sigma pile.⁷⁷ Then, the thermal neutron flux along the z axis is given by:

$$nv(z) = \frac{3\sqrt{2} S B_{11}}{\lambda_{tr} a^2} e^{-z/B_{11}} \left[1 - \frac{1}{B_{11}} e^{z/B_{11}} \left(B_{33} e^{-z/B_{33}} + 2 B_{35} e^{-z/B_{35}} + B_{55} e^{-z/B_{55}} - 2 B_{17} e^{-z/B_{17}} \right) \right] \quad (112)$$

In actual practice at Brookhaven for measurements on the stacked moderator, the following equation was used to the neutron density:

$$n(z) = \frac{Ae^{-\sqrt{z^2+h^2}/L}}{\sqrt{z^2+h^2}} \left[1 - \sqrt{\frac{z^2+h^2}{(z+2z_0)^2+h^2}} \frac{e^{-\sqrt{(z+2z_0)^2+h^2}/L}}{e^{-\sqrt{z^2+h^2}/L}} \right] \quad (113)$$

where: h = separation between the two equal sources
 z_0 = distance from source plane to boundary

$\ln n\sqrt{z^2+h^2}$ is plotted against $\sqrt{z^2+h^2}$ to get L . The quantity in the bracket is small and can be evaluated by iteration.

If the neutrons are not completely thermalized, the neutron density will be a function of the age in a complicated manner; see Eq. (73). The correction to L is usually small (a few percent or less) and can be made a posteriori. The uncorrected L is calculated. Then, using this L together with the age as determined from the best available spectrum for the source, the neutron density is recalculated, and a more refined value of L is obtained by replotting $\ln n\sqrt{z^2+h^2}$ as described above.

MEASUREMENT OF EXTRAPOLATION DISTANCE

The extrapolation distance which is theoretically equal to $0.71\lambda_{tr}$ can be found in several ways, all basically related to the end effect in a sigma pile. Measurements of the flux are carried out in the same way as for the diffusion length. After correcting for the higher harmonics, the longitudinal flux is represented by:

$$nv \propto e^{-z/B_{11}} (1 - e^{-2(C-z)/B_{11}}) \quad (114)$$

where: C = extrapolated reactor height above the source
 $C - z$ = Extrapolated distance
 z_0 = geometric reactor lengths above source

(1) In one method, the value of C which gives the best fit of the data to a straight line plot of:

$$\ln \frac{nv}{1 - \exp\left(-\frac{2(C-z)}{B_{11}}\right)}$$

vs z is guessed by trial and error.

(2) In another method,⁷⁸ flux measurements are made throughout the interior of the reactor and near the surface. An average value for B_{11} is obtained from points in the interior, and the negative exponential intensity, $N(0)e^{-z/B_{11}}$, is plotted past the surface on a semi-

log plot as a straight line. The observed intensities, $N(z)$, near the surface are subtracted from the straight line to yield another line of opposite slope

$$N(0)e^{-z/B_{11}} - N(z) = Ke^{z/B_{11}}$$

We can assume $K = N(0)e^{-2C/B_{11}}$. The two straight lines are extrapolated to their intersection point which is at $z = C$ and $N(z) = 0$.

(3) In a third method,⁷⁹ the flux is measured at three equally spaced points along the longitudinal axis at z , $z + \epsilon$ and $z + 2\epsilon$. The observed neutron fluxes are ϕ_1 , ϕ_2 , and ϕ_3 , respectively. Then, from the equations:

$$\cosh \frac{\epsilon}{B_{11}} = \frac{\phi_1 + \phi_3}{2\phi_2} \quad (115)$$

$$\tanh \frac{C - z - \epsilon}{B_{11}} = \frac{\phi_1 + \phi_3}{\phi_1 - \phi_3} \tanh \frac{\epsilon}{B_{11}} \quad (116)$$

C can be obtained by trial and error, assuming a value for B_{11} .

THE EXPONENTIAL PILE⁸⁰

The exponential pile is a subcritical assembly built so that leakage prevents a chain reaction even if K becomes larger than 1. The pile is used to determine the optimum arrangement of the core elements once the basic constituents have been chosen. Since the pile is subcritical, it requires a neutron source such as Ra-Be or the thermal column of a full-scale reactor.

The exponential pile has the main advantage over a critical assembly in requiring less material; it also requires less shielding and fewer safety devices. However, besides having a lower flux available for activation measurements and necessitating extrapolation of many of the results to critical conditions, certain special effects in full-scale reactors cannot be simulated well in an exponential pile. These effects include reactor kinetics, reactor control, temperature effects, and poisoning by fission products.

In practice, a graphite pedestal is usually placed between the exponential pile and the neutron source. The graphite pedestal serves as a cheap method for ensuring more complete thermalization of the neutron and for damping out the higher harmonics.

The most important parameter which is measured in the exponential arrangement is the buckling. For a cylindrical shape:

$$B^2 = \frac{(2.405)^2}{R^2} - K^2 \quad (117)$$

R^2 and K^2 are determined from radial and axial flux measurements using foils. The radial measurements are fitted to the radial solution of the diffusion equation:

$$\phi = A_1 J_0 \left(\frac{2.405r}{R} \right) \quad (118)$$

which gives R . The axial measurements are fitted to:

$$\phi = A_2 \sinh K(t - z)$$

where t = extrapolated height of the system

L^2 , the thermal diffusion area, can be measured in an exponential pile by replacing the fissionable material with a non-multiplying substance having the same absorption and scattering cross sections. For example, a 2.5-percent mercury in lead alloy has Σ_a and Σ_s within 10 percent of ordinary uranium. Then, L^2 is found from:

$$\frac{1}{L^2} = K^2 - \frac{(2.405)^2}{R^2} \quad (119)$$

The multiplication factor is then calculable from:

$$K = (1 + L^2 B^2) (1 + \tau B^2)$$

where τ is the two-group neutron age. For further details see Ref. (80); the effect of gaps is discussed in Ref. (81).

MEASUREMENT OF MIGRATION AREA AND CRITICAL RADIUS

The experimental value of the migration area of a thermal reactor is best obtained from period measurements in loadings just above critical.⁸¹

The reactor period, T , is measured as a function of the loading radius, R , in a cylindrical geometry. From T , the excess reactivity, k_{ex} , is computed from the inhour equation, Eq. (36). k_{ex} is related to the loading radius and migration area, M^2 , by:

$$k_{ex} = (2.405)^2 M^2 \left(\frac{1}{R_c^2} - \frac{1}{R^2} \right) \quad (120)$$

which is a specialized form of the equation:

$$k_{ex} = M^2 B_{ex}^2 \quad (121)$$

where: $B_{ex}^2 = B_c^2 - B^2$

A plot of k_{ex} vs $1/R^2$ is linear, the intercept yielding R_c and the slope, M^2 .

The critical radius can also be determined from an exponential experiment in which the maximum flux in the pile is measured as a function of the radius.

$$\frac{1}{(nv)_{max}} = A \left(\frac{1}{R} - \frac{1}{R_c} \right) \quad (122)$$

where A is a constant.

MEASUREMENT OF MULTIPLICATION*

The multiplication, M , in the intensity of a neutron source due to a surrounding sphere of multiplying material is directly measurable as a ratio of intensities with and without the sphere. Such a measurement is useful mainly for fast assemblies, in which case corrections due to change in neutron spectrum (via fission and inelastic scattering) are not too large. The interpretation of such an experiment is very simple in a one-velocity transport approximation (see Chapter 1.4).

In this case, the multiplication is a function of σR , $\eta - 1$, and σ_{tr}/σ_a

* Further references are given by Carlson.⁸²

where: R = sphere radius

$$\sigma_a = \sigma_f + \sigma_c$$

$$\eta = \nu\sigma_f/\sigma_a$$

σ_{tr} = transport cross section

σ = total cross section

The formula for M is:

$$M = 1 + \frac{P}{Q} \frac{1 - B(1 + f)Q}{1 - B(1 + f)P} \frac{fQ}{1 - (1 + f)Q} \quad (123)$$

where:

$$f = \frac{\eta - 1}{1 + \frac{\sigma_{tr}}{\sigma_a}} \quad (124)$$

$$P = 1 - e^{-\sigma R} \quad (125)$$

$$Q = \frac{P}{K} [(1 - B) + BK] \quad (126)$$

Table 1.1.15 presents values of B and K for selected values of σR . For other values of σR , quadratic interpolation is suggested.

Table 1.1.15—Values of B and K for Selected Values of σR
(LA-1273, July 1951)

σR	B	K
0	0.3600	1.5136
0.4	.4084	1.5763
.8	.4571	1.6292
1.2	.5047	1.6729
1.6	.5509	1.7099
2.0	.5946	1.7405
2.4	.6353	1.7661
2.8	.6728	1.7872
3.2	.7069	1.8053
3.6	.7376	1.8201
4.0	.7650	1.8318
4.4	.7895	1.8422
4.8	.8111	1.8507

REFERENCES

1. Anderson, Neutrons from Alpha Emitters, Prelim. Rep. No. 3, Nuclear Sci. Series, Nat. Res. Council, Dec. 1948.
2. P. Demers, Montreal Lab. Rep. Nos. MP-74 and MP-204.
3. Dacey, Paine, and Goodman, Shielding Properties of Various Materials Against Neutrons and Gamma Rays, Tech. Rep. No. 23, Lab. for Nuclear Sci. and Eng., MIT, Oct. 20, 1949.
4. McCallun, Nucleonics 5, July 1949, p 11.
5. Spinks and Graham, Can. Jour. Res. 28A, 1950, pp 60-66.
6. Whitmore and Baker, Phys. Rev. 78, 1950, p 799.
7. H. Staub, MDDC-1490, as reported in Anderson, loc. cit.
8. A Wattenberg, Photo-neutron Sources, Prelim. Rep. No. 6, Nuclear Sci. Series, Nat. Res. Council, July 1949.
9. Mobley and Laubenstein, Phys. Rev. 80, 1950, p 309.
10. A. Wattenberg, Phys. Rev. 71, 1947, p 497.
11. D. J. Hughes and C. Egger, Phys. Rev. 72, 1947, p 902.
12. Hanson, Taschek, and Williams, Rev. Mod. Phys. 21, 1949, p 635.
13. Hughes, Pile Neutron Research, to be published.
14. Hughes, Pile Neutron Research Techniques, Nucleonics 6, No. 5, 1950, p 38.
15. Hughes, Dobbs, Cahn, and Hall, Phys. Rev. 73, 1948, p 111.
16. WAPD-45, p 26 (classified).
17. AECD-3077.
18. Havens, Rainwater et al., Phys. Rev. 70, 1946, pp 136 and 154.
19. Ibid., 71, 1947, p 65.
20. Ibid., 83, 1951, p 1123.
21. Merrison and Wiblin, Nature 167, 1951, p 346.
22. Fermi, Marshall, and Marshall, Phys. Rev. 72, 1947, p 193.
23. Brill and Lichtenberger, Phys. Rev. 72, 1947, p 585.
24. Selove, Rev. Sci. Inst. 23, 1952, p 350.
25. ORNL Quart. Prog. Rep., ORNL-1164, Phys. Div., Sept. 20, 1951.
26. Bernstein et al, Phys. Rev. 87, 1952, p 487.
27. Jordan, Detection of Nuclear Particles, Annual Rev. Nuclear Sci., Vol. 1, Annual Reviews, Inc., Stanford, Calif., 1952.
28. Blatt and Weisskopf, Theoretical Nuclear Physics, John Wiley and Sons, New York, N. Y., 1952, p 497.
29. Rossi and Staub, Ionization Chambers and Counters, McGraw-Hill Pub. Co., New York, N. Y., 1949.
30. Cocconi Tongiorgi et al, Rev. Sci. Inst. 22, 1951, p 899.
31. Fowler and Tunnicliffe, Rev. Sci. Inst. 21, 1950, p 734.
32. Lowde, Rev. Sci. Inst. 21, 1950, p 835.
33. Title, Nucleonics 8, No. 6, 1950, p 5.
34. Ibid., 9, No. 1, 1951, p 6.
35. Jahnke and Emde, Tables of Functions, Dover Press, 1945.
36. Graves and Froman, Miscellaneous Physical and Chemical Techniques of the Los Alamos Project, McGraw-Hill Pub. Co., New York, N. Y., 1952, p 135.
37. Langsdorf, Phys. Rev. 80, 1950, p 132A.
38. Hibben, Langsdorf, and Kelland, Phys. Rev. 85, 1952, p 595.
39. Yagoda, Radioactive Measurements with Nuclear Emulsions, John Wiley and Sons, New York, N. Y., 1949.
40. Kaplan and Yagoda, Rev. Sci. Inst. 23, 1952, p 155.
41. Blau, Ruderman, and Czechowski, Rev. Sci. Inst. 21, 1950, p 232.
42. Hofstadter et al., Phys. Rev. 82, 1951, p 749.
43. Schardt and Bernstein, Phys. Rev. 86, 1952, p 583A.
44. Muehlhause and Thomas (private communication to Falk and Poss), Amer. Jour. Phys. 20, 1951, p 429.
45. Grimeland, Phys. Rev. 86, 1952, p 937.
46. Rossi and Staub, loc. cit., p 192.
47. Hanson and McKibben, Phys. Rev. 72, 1947, p 673.
48. Skyrme et al, Rev. Sci. Inst. 23, 1952, p 204.
49. B. L. Cohen, Nucleonics 8, No. 2, 1951, p 29.
50. Nereson and Reines, Rev. Sci. Inst. 21, 1950, p 534.
51. Keepin and Roberts, Rev. Sci. Inst. 21, 1950, p 163.
52. Roberts, Training Manual for Microscopists, LA-1303, 1951.
53. J. H. Roberts, AECU-2007, Sept. 1951.
54. Jastram et al., Phys. Rev. 81, 1951, p 327A.
55. Hornyak, Rev. Sci. Inst. 23, 1952, p 264.
56. Clinton Laboratories Training Program, Lectures on Experimental Nuclear Physics.
57. AECU-2040.
58. Graves and Froman, loc. cit., Chapter 2.
59. Rossi and Staub, loc. cit., p 129.
60. Anderson et al, Phys. Rev. 72, 1947, p 16.
61. Weinberg and Schweinler, Phys. Rev. 74, 1948, p 851.
62. Hoover, et al, MDDC-1664.
63. Ibid., Phys. Rev. 74, 1948, p 864.

64. Rossi and Staub, loc. cit., p 135.
65. Coon and Barschall, Phys. Rev. 70, 1946, p 592.
66. Hall and Koontz, Phys. Rev. 72, 1947, p 196.
67. Baldinger, Huber, and Proctor, Phys. Rev. 84, 1951, p 1058.
68. Barschall, Rev. Mod. Phys. 24, 1952, p 120.
69. Stelson and Preston, Phys. Rev. 86, 1952, p 132.
70. Poole, Philos. Mag. 43, 1952, p 1060.
71. Rosen, Los Alamos report, to be published.
72. Grace et al, Phys. Rev. 82, 1951, p 969L.
73. H. Hurwitz, KAPL, private communication.
74. KAPL-329 (classified).
75. ORNL-181.
76. Harris et al, Phys. Rev. 79, 1950, p 11.
77. BNL-77 (classified).
78. CP-3364 (classified).
79. Glasstone and Edlund, Elements of Nuclear Reactor Theory, p 126.
80. Reactor Science and Technology, Vol. 1, No. 2, TID-72, 1951, p 39 (classified).
81. BNL-60 (classified).
82. Carlson, LA-1273 (classified).
83. Russell, Sachs, Wattenberg, and Fields, Phys. Rev. 73, 1948, p 545.
84. A. O. Hanson, Phys. Rev. 75, 1949, p 1794.
85. R. D. O'Neal, Phys. Rev. 70, 1946, p 1.
86. G. Scharff-Goldhaber, Phys. Rev. 59, 1941, p 937.
87. H. Slätis et al, Phys. Rev. 78, 1950, p 498.
88. Latyshev, Rev. Mod. Phys. 19, 1947, p 132.
89. Nuclear Data, Nat. Bur. Stand. Circ. 499, Wash., D. C., 1950.
90. Chart of the Nuclides, Gen. Elec. Res. Lab., 1950.
91. E. Bretscher and E. B. M. Murrell, Brit. Rep. No. 137, 1943.
92. P. Demers, N. R. C. Canada, Rep. No. 1571, Montreal, 1945.

CHAPTER 1.2

Nuclear Physics

Mathew M. Shapiro

PROPERTIES OF STABLE NUCLEI

This chapter is concerned with some fundamentals, definitions, and concepts which are important in the design of nuclear reactors. The nomenclature used in this chapter is defined in Table 1.2.1.

A knowledge of the size, mass, and spin of nuclei is useful in making educated guesses of cross sections and other quantities of interest in reactor design. Unfortunately, it is necessary to make such estimates since all of the pertinent data have not been gathered.

SIZE

The short-range character of nuclear forces makes it possible to ascribe dimensions (to within about 10^{-13} cm) and shape to nuclei. The very small quadrupole moments of most nuclei lead to the conclusion that the nuclei are essentially spherical. The nuclear radius is given in terms of mass number A by:

$$R = r_0 A^{1/3} \cdot 10^{-13} \text{ cm} \quad (1)$$

where r_0 is generally between 1.3 and 1.5. Table 1.2.2 gives some values of nuclear radii. These were obtained by fitting the schematic theory of Feshbach and Weisskopf¹ to neutron cross section data.* A different radius is usually required in the high- and low-energy regions.

MASS

The known masses of the neutral atoms are given in atomic mass units (amu) in Table 1.2.3. The mass of O^{16} is defined to be exactly 16 amu. From the Einstein energy-mass formula:

$$\Delta E = \Delta mc^2$$

one finds that 1 amu = 931 mev.

The binding energy is defined as:

$$\text{B.E.} = Zm_H + (A - Z)m_n - M \quad (2)$$

* Other estimates can be made from lifetimes for α -radioactivity (heavy elements), electrostatic interaction of protons in mirror nuclei (light elements), and charged particle cross sections. These are generally in agreement with Eq. (1).

¹References appear at end of chapter.

where m_H and m_n are the masses of the hydrogen atom and the neutron, respectively.

Another commonly used quantity is the packing fraction, f :

$$f = \frac{M - A}{A} \quad (3)$$

The relationship between f and B.E. is:

$$\frac{\text{B.E.}}{A} + f = 0.00853 + \left(\frac{1}{2} - \frac{Z}{A}\right) (0.00081) \text{ amu} = 7.94 + \left(\frac{1}{2} - \frac{Z}{A}\right) (0.755) \text{ mev} \quad (4)$$

An empirical formula proposed by Fermi for the isotopic mass is:

$$M_{A,Z} = 1.01464A + 0.014A^{2/3} - 0.041905 Z_A + \frac{0.041905}{Z_A} (Z - Z_A)^2 + \lambda \frac{0.036}{A^{3/4}} \quad (5)$$

where:

$$\lambda = \begin{cases} +1 & \text{if } A \text{ is even, } Z \text{ odd} \\ -1 & \text{if } A \text{ is even, } Z \text{ even} \\ 0 & \text{if } A \text{ is odd} \end{cases}$$

and:

$$Z_A = \frac{A}{1.98067 + 0.0149624 A^{2/3}} \quad (5a)$$

The binding energy of a neutron added to the target nucleus gives the excitation of the compound nucleus formed by slow-neutron bombardment. It is useful, for example, in obtaining the total energy of capture γ rays. Table 1.2.3 contains known values of the binding energy of an additional neutron, $(\text{B.E.})_{Z,A}$:

$$(\text{B.E.})_{Z,A} = M_{Z,A} + m_n - M_{Z,A+1} \quad (6)$$

For a given A , very often several isobars of different Z are stable. The values of $A-Z$ for stable nuclei are plotted vs Z in Fig. 1.2.1. The solid line is a plot obtained from Eq. (5a).

In Fig. 1.2.2, experimental packing fractions from Table 1.2.3 are plotted against A . The cusps which show up at low values of A are indicative of the special stability of α clusters. The effect of the greater stability of the so-called "magic" nuclei does not show up well on a plot of this type, but from other evidence,* it appears that nuclei with Z or $N = 2, 8, 20, 50, 82$, and 126 are particularly stable and abundant. (There is also evidence for a special effect at Z or $N = 28$.) It should be noted, however, that much of the evidence is somewhat marginal. In general, these "magic nuclei" have wider level spacings and smaller capture cross sections than their neighbors (see Fig. 1.2.16).

* For a review of this evidence see References (4) and (5) and numerous more recent articles on nuclear shell structure.

SPIN

Every nucleus possesses an intrinsic angular momentum which can interact with that of other nuclei. It is measured in units of \hbar and takes integral or half-integral values according to whether the mass number is even or odd, respectively. Known spin values for the ground state are given in Table 1.2.4.

SPONTANEOUS REACTIONS — RADIOACTIVITY

Nuclei that are unstable and decay by the emission of one or more particles (a photon is here regarded as a particle) are found in nature and can be produced artificially. Many of these have sufficiently long half-lives to be observable.

The amount of substance which decays in the very short time dt is proportional to the amount of the substance present. This is the radioactive decay law and may be mathematically expressed as follows:

$$\frac{dN(t)}{dt} = -\lambda N(t) \quad (7)$$

where $N(t)$ is the number of nuclei remaining at time t and λ is called the disintegration constant. If the number of nuclei initially present (at $t = 0$) is designated by $N(0)$, then by integration of Eq. (7), the number present at time t is:

$$N(t) = N(0)e^{-\lambda t} \quad (8)$$

The mean-life T is the reciprocal of λ :

$$T = \frac{1}{\lambda} \quad (9)$$

and is related to the half-life, the time required for half of the initial atoms to decay, by the relation:

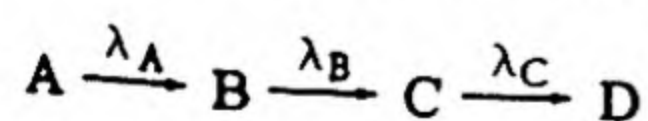
$$T_{1/2} = T \ln 2 = 0.693T \quad (9a)$$

The actual number of nuclei that will decay in a given time interval can only be given statistically. In this sense, Eqs. (7) to (9a) describe the mean behavior. If the number of disintegrations in time interval t which is small compared to the mean-life is much less than the total number of atoms present, it can be shown that the probability for m disintegrations, $p(m)$, is given by the Poisson distribution law:

$$p(m) = \frac{\bar{m}^m e^{-\bar{m}}}{m!} \quad (10)$$

where \bar{m} is the mean number to be expected in the time interval. Conversely, if m decays are observed in a given time interval, Eq. (10) is also the probability that m is the mean number to be expected.

It often happens that the residual or daughter nucleus produced by the decay of the parent nucleus is itself radioactive. Consider a decay chain of the type:



Let N_A , N_B , N_C be the number of atoms of substances A, B, C present at time t , respectively, λ_A , λ_B , λ_C be their disintegration constants (reciprocal mean-lives), and let a primary source supply A at constant rate S . Then:

$$\left. \begin{aligned} \frac{dN_A}{dt} &= S - \lambda_A N_A \\ \frac{dN_B}{dt} &= \lambda_A N_A - \lambda_B N_B \\ \frac{dN_C}{dt} &= \lambda_B N_B - \lambda_C N_C \end{aligned} \right\} \quad (11)$$

Eqs. (11) state that the rate of change of the number of nuclei of any substance in the radioactive decay chain is equal to the difference between the rate at which they are created and the rate at which they undergo decay.

Case 1: In the case where there is no primary source ($S = 0$) but where substances A, B, and C are initially present in the amounts $N_A(0)$, $N_B(0)$, and $N_C(0)$, respectively, Eqs. (11) have the solution:

$$\left. \begin{aligned} N_A(t) &= N_A(0) e^{-\lambda_A t} \\ N_B(t) &= N_B(0) e^{-\lambda_B t} + \lambda_A N_A(0) \left(\frac{e^{-\lambda_A t}}{\lambda_B - \lambda_A} + \frac{e^{-\lambda_B t}}{\lambda_A - \lambda_B} \right) \\ N_C(t) &= N_C(0) e^{-\lambda_C t} + \lambda_B N_B(0) \left(\frac{e^{-\lambda_B t}}{\lambda_C - \lambda_B} + \frac{e^{-\lambda_C t}}{\lambda_B - \lambda_C} \right) \\ &\quad + \lambda_A \lambda_B N_A(0) \left(\frac{e^{-\lambda_A t}}{(\lambda_B - \lambda_A)(\lambda_C - \lambda_A)} + \frac{e^{-\lambda_B t}}{(\lambda_A - \lambda_B)(\lambda_C - \lambda_B)} + \frac{e^{-\lambda_C t}}{(\lambda_A - \lambda_C)(\lambda_B - \lambda_C)} \right) \end{aligned} \right\} \quad (11a)$$

Case 2: In the case where there is a primary source supplying A at constant rate S but where no other radioactive substance is initially present [that is $N_A(0) = N_B(0) = N_C(0) = 0$], then Eqs. (11) have the solution:

$$\left. \begin{aligned} N_A(t) &= \frac{S}{\lambda_A} (1 - e^{-\lambda_A t}) \\ N_B(t) &= \frac{S}{(\lambda_B - \lambda_A)} \left[(1 - e^{-\lambda_A t}) - \frac{\lambda_A}{\lambda_B} (1 - e^{-\lambda_B t}) \right] \\ N_C(t) &= S \lambda_A \lambda_B \left[\frac{1 - e^{-\lambda_A t}}{\lambda_A (\lambda_B - \lambda_A) (\lambda_C - \lambda_A)} + \frac{1 - e^{-\lambda_B t}}{\lambda_B (\lambda_A - \lambda_B) (\lambda_C - \lambda_B)} \right. \\ &\quad \left. + \frac{1 - e^{-\lambda_C t}}{\lambda_C (\lambda_A - \lambda_C) (\lambda_B - \lambda_C)} \right] \end{aligned} \right\} \quad (11b)$$

These equations are valid only when B and C are produced and destroyed solely by spontaneous decay.*

More complicated problems can be solved by taking linear combinations of the solutions of the two cases presented.

*The case when A and B are removed by other processes (e.g., neutron capture) has been treated by Van Wye and J. S. Beckerley⁶ and Rubinson.⁷

Case 3: A primary source supplies A at constant rate S for time τ . The source is then removed. The amounts of A, B, and C present t units of time after the source is removed can be found by calculating $N_A(\tau)$, $N_B(\tau)$, and $N_C(\tau)$ in Case 2 and then using these values for $N_A(0)$, $N_B(0)$, and $N_C(0)$, respectively, in Case 1 to calculate $N_A(t)$, $N_B(t)$, and $N_C(t)$.

β -DECAY

Some nuclei decay by the emission of either positively or negatively charged β particles or both. In this case, the energy spectrum of the emitted particles is continuous up to a maximum energy, E. For the reaction:



the available energy is:

$$E = M_{Z,A} - M_{Z+1,A} \quad (13)$$

For the reaction $Z^A \rightarrow (Z-1)^A + \beta^+$, the available energy is:

$$E = M_{Z,A} - M_{Z-1,A} - 2m_e \quad (14)$$

where m_e is the electron mass. The energy available for capturing an atomic electron (usually from the K shell) is:

$$E = M_{Z,A} - M_{Z-1,A} \quad (15)$$

Clearly, whenever positron emission is energetically possible, electron capture is also possible. In Eqs. (13) to (15) the masses M are those of the neutral atoms.

A summary of β -decay theory has been given by Konopinski.⁸

α -DECAY

Many nuclei with $A > 208$ (and a few lighter ones) are found to emit α particles spontaneously. The α particle energy is given by:

$$E = M_{Z,A} - M_{Z-2,A-4} - M_\alpha \quad (16)$$

The mean-life of the nucleus against α -decay depends strongly on the α -particle energy. An approximate relation known as the Geiger-Nuttall law asserts that the logarithm of the disintegration energy is a linear function of the logarithm of the half-life. An empirical fit is:

$$\log E \text{ (mev)} = 0.86 - 0.013 \log T_{1/2} \text{ (sec)} \quad (17)$$

This gives the energy from the half-life quite accurately but can be wrong by several orders of magnitude when used the other way. A treatment of α -decay systematics is given by Perlman, Ghiorso, and Seaborg.⁹

Nuclei which emit α -particles from the ground state will not generally emit them from an excited state unless the excitation energy is high enough to reduce the life time against α -emission to about 10^{-13} sec, the order of magnitude of that for γ -emission.

γ -RAY EMISSION

The emission of a γ -ray signifies the transition between two states of the same nucleus. The energy of the γ -ray is, of course, the energy separation of the two levels. Since the intrinsic spin of a photon is unity (in units of \hbar) all γ -emission implies a change of spin (either in magnitude or direction) of the nucleus. Gamma-ray emission processes are

classified according to the multipole order of the transition. When the spin change is unity, we speak of a dipole transition; when it is two, of a quadrupole transition; etc. The type of transition, electric or magnetic, depends on the parity change. Dipole transitions are electric if there is a parity change and magnetic if there is not. Quadrupole transitions follow just the opposite rule. Weisskopf and Blatt¹⁰ give the following expressions for the probability of emission per unit time for electric radiation of multipole order l :

$$P_E = \frac{1}{T_E} \cong \frac{4.4 (l+1)}{l[1 \cdot 3 \dots (2l+1)]^2} \left(\frac{3}{l+3}\right)^2 \left(\frac{\hbar\omega}{197 \text{ mev}}\right)^{2l+1} \cdot (R \text{ in } 10^{-13} \text{ cm})^{2l} 10^{21} \text{ sec}^{-1} \quad (18)$$

and for magnetic radiation of multipole order l :

$$P_M = \frac{1}{T_M} \cong \frac{1.9}{4.4} P_E (R \text{ in } 10^{-13} \text{ cm})^{-2} \text{ sec}^{-1} \quad (18a)$$

where $\hbar\omega$ is the energy of the radiation in mev and R is the nuclear radius.

It should be noted that the above expressions are only very rough estimates. The actual values are likely to be smaller than these estimates by factors up to 1000 or even higher in the case where the wave functions of the initial and final states overlap only slightly.

DATA

A new table of isotopes supplied by G. T. Seaborg is reproduced here as Table 1.2.4.

RANGE-ENERGY RELATIONS

In traversing matter, charged particles lose energy by radiation, by suffering nuclear collisions, and, most important, by ionizing atoms in the medium. In air, 32.5 ev is the energy dissipated per ion pair produced.

This figure is about the same for other media. The slowing down and transport of neutrons is discussed in detail in Chapter 1.3. Photons lose energy by means of the Compton effect, the photoelectric effect, and pair production. These mechanisms are discussed in detail in Section 1.2.

For charged particles, the number of ion pairs per unit path length increases rapidly as the velocity decreases, giving rise to a well defined range.

Electron ranges are usually given in terms of an areal density, milligrams of material per square centimeter. The range of electrons in aluminum¹¹ is given to within 5 percent by:

$$412E^{(1.265 - 0.0954 \ln E)} \text{ mg/cm}^2$$

if $0.01 < E < 2.5$ mev, and by:

$$530E - 106 \text{ mg/cm}^2$$

for $E > 2.5$ mev.

Theoretically, one would expect the range to be inversely proportional to the number of atomic electrons per unit volume. The range in mg/cm^2 would then be proportional to A/Z and roughly independent of the material.

The range of α -particles in air at standard conditions is given^{12,13} to within about 10 percent by:

$$R_\alpha(\text{cm}) = 0.56E \text{ (mev) for } 0 < E < 4 \text{ mev}$$

and by:

$$R_{\alpha}(\text{cm}) = 1.24E - 2.62 \text{ for } 4 < E < 8 \text{ mev}$$

Experimentally, it is found that the range of protons in air is given quite accurately by:

$$R_p(\text{cm}) = 1.007R_{\alpha}(3.971E) - 0.20$$

where E is the proton energy in mev and R_{α} the range of α -particles in air at energy $3.971E$.

Theory predicts that for given charge Z , the range depends only on the velocity. Hence, for all helium and hydrogen isotopes:

$$R_{Z,M}(E) = \frac{M}{M_0} R_{Z,M_0}\left(\frac{M_0}{M} E\right)$$

In substances other than air, the ranges of protons and α -particles¹⁴ are given to within 15 percent over the energy range of interest here by:

$$\bar{R}(E) [\text{mg/cm}^2] = 0.56A^{1/3} R(E)_{\text{air}} [\text{cm}]$$

where A is the mass number of the stopping material.

The range energy relations for heavy particles is complicated and will not be treated here in general. A special case of interest is the range of fission products. Following neutron induced fission of U^{233} , U^{235} , or Pu^{239} , the most probable energy of the light fragment is about 92 mev and that of the heavier fragment about 60 mev.^{15,16} In about 0.2 percent of fissions, an alpha-particle with a probable energy of about 14 mev is formed. Since about 30 ev is lost per ion pair created, about 6×10^6 ion pairs will be formed by the two fragments.

Range measurements of the fission fragments show a grouping about two values corresponding to the light and heavy fragments. In air, the ranges for the light and heavy fragments¹⁷ are 2.3 and 1.8 cm, respectively. The ranges in aluminum are 3.7 and 2.8 mg/cm². Segrè and Wiegand showed that the relative stopping powers for fission fragments in collodion, aluminum, copper, silver, and gold were roughly the same as for alpha particles. Not distinguishing between fission fragments, they give for the maximum range in several materials the values in Table 1.2.5. Hence, these values are for the most energetic (light) fragments.

THE FISSION PROCESS

As used here, the term "fission" means the splitting of a nucleus into approximately equal fragments. These particles emerge in a highly excited state. This results in the almost immediate emission of neutrons and γ -rays from them. The resulting fragments still have too great a neutron-to-proton ratio to be stable against β -decay, and they undergo a series of β -disintegrations before becoming stable nuclei. Sometimes these β -decays are accompanied by γ -emission and sometimes by neutron emission. These neutrons, appearing after one or more β -disintegrations have taken place, are the so called delayed neutrons.

The average number of neutrons, delayed and prompt, which appear in fission varies according to the fissionable element and probably the incident neutron energy.

FISSION THRESHOLDS AND CROSS SECTIONS

Presumably, any nucleus will undergo fission if its excitation energy is great enough. The amount of excitation required is given directly by the threshold for γ -induced fission. In some isotopes, fission occurs spontaneously. Thresholds for γ -induced fission and data for spontaneous fission are given in Table 1.2.6 for some isotopes.

Thresholds for neutron-induced fission in these heavy elements will be smaller by the amount of the binding energy of the neutron to the target nucleus. In some cases, thermal neutrons can produce fission, and in others, a threshold exists. The known neutron fission cross sections are shown as a function of energy in Figs. 1.2.3 to 1.2.12, which are taken from the report of the AEC Neutron Cross Section Advisory Group (BNL-170 and 170A).

THE FISSION FRAGMENTS

FISSION YIELDS

The immediate product from a fission is two fragments of which the most probable mass numbers are about 95 and 139; the probability of symmetrical fission is very small. Figure 1.2.13 shows the fission yields for slow-neutron fission of U^{235} , U^{238} , and Pu^{239} plotted vs A . The fission yield is the probability of forming a nucleus of mass A . The sum of the yields equals two since there are two fragments formed. Table 1.2.7 gives the fission yield of various isotopes formed after fission.¹⁸

KINETIC ENERGY

The kinetic energy of the pair of fission fragments depends upon the way the nucleus splits. The energy distribution of fission fragments has two peaks: one for the heavy fragment around 65 mev and the other for the light fragment at about 95 mev. There is a considerable spread around the peaks when the number of fragments having a given energy are plotted vs energy. The width at half maximum around the higher energy is 12 mev and around the lower energy is 20 mev. Table 1.2.8 gives the results of Brunton and Hanna¹⁵ and of Deutsch and Ramsey¹⁶ for the kinetic energy of the fragments.

The compound nucleus occasionally splits into three particles. In one out of 250,000 fissions, the three particles have approximately equal masses; in one out of every 550 fissions, an alpha particle with a maximum energy of 26 mev and a probable energy of 14 mev is formed; in one out of 76 fissions, an as yet unidentified short-range particle of low mass number is formed. The range of the fission fragments is discussed previously in this chapter.

TIME DEPENDENCE OF THE RADIATION FROM FISSION PRODUCTS

A modification of the Wigner and Way expression for P_s/P_0 , the ratio of the rate of heat generation after shutdown to the rate of heat generation during operation, has been obtained²¹ to fit available experimental data for natural uranium. The heat production owing to U^{239} and Np^{239} after shutdown is given in Eqs. (19a) and (19b):

$$\frac{P(U^{239})}{P_0} = 0.0025 \left\{ e^{-\frac{T_s}{2040}} - e^{-\frac{(T_s + T_0)}{2040}} \right\} \quad (19a)$$

$$\frac{P(Np^{239})}{P_0} = 0.0013 \left\{ e^{-\frac{T_s}{290000}} - e^{-\frac{(T_s + T_0)}{290000}} \right\} \quad (19b)$$

where T_s = time in seconds since operation

T_0 = operation time in seconds

The authors indicate $P(\text{Np}^{239})$ as given above may be low for T_s less than the Np^{239} decay time since new data point toward a value of 0.0023 instead of 0.0013 in Eq. (19b).

The Untermeyer and Weills natural-uranium data fit is:

$$\frac{P_s}{P_0} = 0.1 \left\{ (T_s + 10)^{-0.2} - 0.87(T_s + 2 \times 10^7)^{-0.2} \right\} - 0.1 \left\{ (T_s + T_0 + 10)^{-0.2} - 0.87(T_s + T_0 + 2 \times 10^7)^{-0.2} \right\} \quad (20)$$

with the accuracy expected to be:

under 1 sec	large error
$1 - 10^2$ sec	$\pm 50\%$
$10^2 - 10^4$ sec	$\pm 30\%$
$10^4 - 10^6$ sec	$\pm 10\%$
$10^6 - 10^8$ sec	$\pm 50\%$

The heat production for U^{235} can be estimated by subtracting Eqs. (19a) and (19b) from (20). The experimental data and graphs of the results can be found in the reference.

For the time dependence of γ rays, the reader should refer to Section 1.2. The distribution of energy per fission is given in Table 1.2.11.

THE CAPTURE-TO-FISSION RATIO

When the compound nucleus has been formed by neutron bombardment, fission does not always occur because it must compete with other processes. The most important one here is γ -emission, for this process represents a loss of the absorbed neutron. In the following, the ratio of the capture cross section to the fission cross section will be denoted by α .

PROMPT NEUTRON AND GAMMA SPECTRA

Emission of prompt neutrons and γ -rays is probably completed within 10^{-15} sec after fission. The energy distribution of the prompt neutrons from thermal fission has been measured by B. E. Watt, D. Hill, T. W. Bonner, R. A. Ferrell, and M. C. Rinehart (LA-718). The neutron kinetic energy varies over a range exceeding 18 mev. The distribution is fairly well represented from 0.1 to 18 mev by the formula:

$$n(E) = \sqrt{\frac{2}{\pi e}} \sinh \sqrt{2E} e^{-E} \quad (21)$$

where $n(E)$ is normalized to one neutron and E is in mev.

The energy distribution of the γ -rays is discussed in Sect. 1.2. The total γ energy is about 5 mev/fission. It is not clear whether there are five 1-mev photons or two 2.5-mev photons.

BETA DECAY AND DELAYED NEUTRONS

The fission fragments have too large a neutron-to-proton ratio to be stable against β -decay even after emitting some neutrons and γ -rays. They have to undergo about three successive β -disintegrations before achieving stability. Some isotopes have sufficient energy following a β -disintegration to emit a neutron. This neutron appears after a mean time at least as long as the mean lifetime of the longest-lived β -emitter preceding it in the

decay chain. The β -emitters that lead to the important delayed neutrons are those in Table 1.2.9. Table 1.2.10 gives a summary of the present knowledge of delayed neutrons from fission.

SUMMARY OF ENERGY RELEASE IN FISSION

Table 1.2.11 summarizes the distribution of energy from an average fission.

The kinetic energy of the fission products and of the β -rays appears as heat very close to the place where fission took place. This can be seen from the data presented in this chapter under "Range-energy Relations." The γ -rays have, relatively, much longer mean-free-paths, and their energy is more widely distributed throughout the reactor.

The neutrino energy is not useful for the generation of heat, and therefore, the heat production capacity from fission itself is about 191 mev/fission. On the other hand, approximately half of the fission neutrons will be captured parasitically in the reactor giving rise to capture γ -rays of approximately 7 mev total energy. This brings the available energy back to about 200 mev/fission.

COLLISION REACTIONS

LABORATORY AND CENTER-OF-MASS COORDINATES

Consider a particle of mass m_1 and speed v_1 striking a particle m_2 which is initially at rest. Let E be $\frac{1}{2} m_1 v_1^2$ and $p = m_1 v_1$. The kinetic energy available for a nuclear reaction, E_0 , is E less the kinetic energy of the center of mass:

$$E_0 = \frac{1}{1 + \gamma} E \quad (22)$$

where $\gamma = m_1/m_2$.

If one defines a reduced mass as $\mu = m_1 m_2 / (m_1 + m_2)$, then $E_0 = \frac{1}{2} \mu v_1^2$. If the momentum of a particle of mass μ which has the kinetic energy E_0 is denoted by p_0 , then:

$$p_0 = \frac{1}{1 + \gamma} p \quad (23)$$

If the polar axis is taken in the direction of the incident particle and if θ_0 and θ are the angles that its velocity vector makes with this axis after the collision in the center-of-mass system and in the laboratory system, respectively, then:

$$\tan \theta = \frac{\sin \theta_0}{\gamma + \cos \theta_0} \quad (24)$$

The differential cross sections in the center-of-mass system and laboratory system are related by:

$$\sigma(\theta) = \frac{(1 + \gamma^2 + 2\gamma \cos \theta_0)^{3/2}}{|1 + \gamma \cos \theta_0|} \sigma(\theta_0) \quad (25)$$

If the reaction produces two new particles of mass m_3 and m_4 ($m_3 + m_4 = m_1 + m_2$), and an amount of energy Q is transformed from internal to kinetic energy, and if m_3 is the observed particle, Eqs. (24) and (25) still hold but with γ now being equal to:

$$\gamma = \left(\frac{m_1 m_3}{m_2 m_4} \frac{E_0}{E_0 + Q} \right)^{1/2}$$

NEUTRON CROSS SECTIONS

The interaction of neutrons with nuclei can often be explained in terms of the formation of a compound nucleus (likely exceptions are reactions involving light nuclei) which can exist only in more or less well defined energy states. When the kinetic energy of the incident neutron plus its binding energy falls within the width of an energy level of the compound nucleus, the probability of forming the compound nucleus is greatly increased. Cross sections for all processes associated with the formation of that level will exhibit a resonance behavior.

Generally speaking, the widths of nuclear levels are smaller than the spacing between levels in all nuclei at very low energies and in light nuclei even for energies of several mev. As the mass number of the nucleus increases and as the excitation energy increases, the levels become wider and more dense. Finally, for neutrons of sufficiently high energy impinging on heavy nuclei, the levels overlap and the cross sections become smooth functions of energy. In terms of this model of nuclear reactions, certain general properties of cross sections can be given. These, along with some empirical correlations, can be used as a basis for informed guesses when the desired cross section has not been measured.

In the following discussion, the neutron energy is divided into three regions: (1) less than 1 kev, (2) 1-500 kev, and (3) 0.5 to 10 mev. Neutron reactions show different qualitative behavior in these regions, but the regions are not well defined, and the transition from one into the other is of course gradual.

It is also useful to divide the target nuclei into three groups: (1) the light nuclei, $1 < A < 25$; (2) the intermediate nuclei, $25 < A < 80$; (3) the heavy nuclei, $80 < A < 240$. There is considerable overlap among these categories, and many properties of one group can be extended into the neighboring ones. This grouping, convenient for discussion, is schematically indicated in Fig. 1.2.14.

REGION A. LIGHT NUCLEI^{25, 26}

Except for the (n, α) reactions in Li^6 and B^{10} and the (n, p) reaction in He^3 , the scattering cross section is nearly equal to the total cross section and in fact differs from it only by the (n, γ) cross section until energies sufficiently high for inelastic scattering to set in are reached. Other than this, it is almost impossible to give any general rules describing nuclear reactions with these elements. Levels are few and far apart so that the cross sections in the neighborhood of these isolated resonance energies should have a dependence on energy given by the Breit-Wigner single-level formula discussed below. Some of the nuclear radii and the threshold energies are so small that charged-particle emission can occur even at energies near thermal. The first level is usually several mev above the ground state, and inelastic scattering tends to occur only at energies greater than a few mev.

REGION B. LOW AND INTERMEDIATE ENERGIES, INTERMEDIATE NUCLEI

The predominant reactions in this group are elastic scattering and radiative capture. Inelastic scattering is usually not possible since the first excited states of the compound nucleus are several hundred kev above the ground state.⁴ Reactions (n, p) and (n, α) are weak because of the coulomb barrier and threshold effects. The levels are well separated, and the capture and elastic scattering cross sections should be well represented by the Breit-Wigner one-level formula. This yields for the capture cross section:

$$\sigma_a = g_{jl} (2l + 1) \pi \chi^2 \frac{\Gamma_n \Gamma_a}{(E - E_r)^2 + \frac{\Gamma^2}{4}} \quad (26)$$

and for the scattering cross section:

$$\sigma_{sc} = (2l + 1) g_{jl} 4\pi \lambda^2 \left| \frac{\Gamma_{n/2}}{E - E_r + i\Gamma/2} + e^{i\delta_l} \sin \delta_l \right|^2 + (2l + 1) (1 - g_{jl}) 4\pi \lambda^2 \sin^2 \delta_l + \sum_{l' \neq l} (2l' + 1) 4\pi \lambda^2 \sin^2 \delta_{l'} \quad (27)$$

for a resonance formed by neutrons having orbital quantum number l .

g_{jl} is a statistical factor;* λ is the reduced wave-length of the neutron; Γ_n the width for elastic scattering of neutrons; Γ_a the absorption width; and $\Gamma = \Gamma_n + \Gamma_a$ the total width. E is the neutron energy and E_r the resonance energy. All dynamic quantities are in the center-of-mass system. The phase shifts δ_l are those which would be obtained for scattering from a "hard" sphere. The first three are given by the formulae:

$$\delta_0 = -x$$

$$\delta_1 = -x + \frac{\pi}{2} - \cot^{-1} x \quad (28)$$

$$\delta_2 = -x + \pi - \cot^{-1} \left(\frac{x^2 - 3}{3x} \right)$$

where:

$$x = R/\lambda \quad (1/\lambda = k = 0.222 \sqrt{E(\text{mev})} \cdot 10^{13} \text{ cm}^{-1})$$

In the scattering formula, the first term on the right represents the resonance scattering and the coherent part of the potential scattering;† the second, the non-interfering portion of the potential scattering; and the last is potential scattering by neutrons having l values different from the resonant one.

Neutron widths in this energy region are given approximately by:

$$\Gamma_{nl} = 0.15 \sqrt{E} \cdot 10^{-3} D T_l \quad (29)$$

where E is in ev and D is the order of the distance between levels of the same spin and parity. T_l is the transmission factor for penetration of the centrifugal barrier. The first three have the values:

$$T_0 = 1$$

$$T_1 = \frac{x^2}{1 + x^2} \quad x = R/\lambda \quad (30)$$

$$T_2 = \frac{x^4}{9 + 3x^2 + x^4}$$

* If the spin of the target nucleus is I , that of the compound nucleus j , and the orbital angular momentum of the neutron l , then:

$$g_{jl} = \frac{(2j + 1)}{2(2I + 1)(2l + 1)}$$

† Potential scattering refers to that portion of Eq. (27) which does not exhibit resonance behavior.

The capture width is generally of the order of 1 to 10 ev. If the end products have kinetic energies much greater than the incident neutron energy (as is often the case), Γ_a is relatively independent of energy. D varies very much from one nucleus to another, ranging from a few to several hundred kev. Because of the large level spacing, elastic scattering is usually the predominant process here even at thermal energies.

REGION C. HEAVY NUCLEI—LOW ENERGY

The only possible reactions in this group are those induced by $l = 0$ neutrons. These are primarily elastic scattering, radiative capture, and neutron-induced fission. The coulomb barrier precludes the probability of charged-particle emission.

The total cross section often shows very close resonances. One finds distances between resonances of the order of 10 to 100 ev; often, however, none are found in certain isotopes. There are indications that even A nuclei have resonance spacings of much more than 100 ev and that the nuclei with "magic" numbers of protons and neutrons show very large resonance spacings (many kev).

The neutron width is expected to be much smaller than the capture width which, except for fission, is primarily due to (n, γ) processes. In all measured cases, it was found that:

$$0.03 \text{ ev} < \Gamma_r < 0.15 \text{ ev} \quad (31)$$

The Doppler effect (cf., Chapter 1.6) can be important in this energy region. Because of the thermal motion of the target nuclei of mass A , the relative energy can be spread over an interval which is approximately:

$$\Delta E \sim 0.1 \sqrt{E} A^{-1/2} \text{ ev}$$

where E is in ev. This can become of the order of resonance widths at several hundred ev.

The thermal capture cross section can be very large owing to the $1/v$ law. Most elements exhibit thermal capture cross sections in excess of 5 barns with the exception of Ba, Sn, Pb, and Bi which are "magic" nuclei.

REGION D. HEAVY NUCLEI—INTERMEDIATE ENERGY

The low-energy region was characterized by the absorption width far exceeding the neutron width. The latter increases with energy as \sqrt{E} while the former is expected to be relatively constant in the intermediate energy range. For level spacings of the order of 10 ev, elastic scattering is expected to exceed capture at energies above several kev.

Since level spacings are only of the order of a few ev, one is generally interested in average values of the cross sections. The average value of the cross section for radiative capture is given by:

$$\langle \sigma(n, \gamma) \rangle_{av} = 2\pi^2 (R + \chi)^2 \frac{\Gamma_r}{D} \quad (32)$$

For heavy nuclei, Γ_r/D is found to be of the order of 10^{-2} or 10^{-3} with the exception of "magic" nuclei which may show values a few hundred times less than this.

The value of the total cross section averaged over many resonances can be estimated from Fig. 1.2.15 for neutron energies from a few kev upward for the heavy nuclei. This cross section is primarily elastic scattering and radiative capture (except for the fissionable elements), inelastic scattering and charged particle reactions being unlikely below 0.5 mev.

REGION E. HEAVY AND INTERMEDIATE NUCLEI—HIGH ENERGIES

This group is characterized by the appearance of inelastic scattering and reactions involving the emission of charged particles somewhere in this energy range. Below the energy at which this occurs, the behavior is similar to that in the intermediate energy range. For a given energy in this region, the level spacing decreases with increasing mass leading to small neutron widths and an increase in radiative capture with A . This is shown in the measurements of Hughes which are reproduced in Fig. 1.2.16.

For a given nucleus, the (n, γ) cross section decreases with increasing energy once the threshold for inelastic scattering is passed. For energies exceeding about 2 mev, the reaction cross section (total cross section minus elastic scattering cross section) is predominantly inelastic.

In regions C, D, and E, the schematic theory of Feshbach and Weisskopf should be applicable. Figure 1.2.15 shows the total cross section vs energy. Figure 1.2.17 shows the transport cross section vs R/λ , calculated by assuming the inelastic scattering to be spherically symmetrical, cf. Eq. (52).

Figures 1.2.15 and 1.2.17 should be valid at low energies if they are there interpreted as averaged over many resonances.

Figure 1.2.18 gives the reaction cross section according to the schematic theory. This curve is expected to be valid only when the compound nucleus can decay in many ways. This means that the reaction cross section is primarily the inelastic scattering cross section.

THE RECIPROCITY THEOREM²⁷

The reciprocity theorem permits the cross section of a nuclear reaction to be expressed in terms of the inverse process. Let the cross section for the reaction:



be $\sigma_{12}(E_1)$ where E_1 is the collision energy of the Be^9 and He^4 nuclei, and let the cross section for the inverse process:



be $\sigma_{21}(E_2)$. E_2 is fixed by the energy E_1 and the Q value of the reaction shown in Eq. (33a).

The reciprocal relation between these cross sections is:

$$\frac{\sigma_{12}(E_1)}{\sigma_{21}(E_2)} = \frac{g_2 p_2^2}{g_1 p_1^2} \quad (34)$$

where g_2 and g_1 are the statistical weights and p_2 and p_1 the relative momenta of the pairs $\text{C}^{12} - n$ and $\text{Be}^9 - \text{He}^4$, respectively.*

* The statistical weight is $(2I + 1)(2I' + 1)$ where I and I' are the spins of the particles of a given pair. Hence, since the spin of carbon is zero and that of the neutron is $\frac{1}{2}$, $g_2 = 2$. When all of the constituents are particles (no photons), then:

$$\frac{p_2^2}{p_1^2} = \frac{\mu_2 E_2}{\mu_1 E_1}$$

where μ is the reduced mass of the pair. All dynamic quantities are in the center-of-mass system.

The reciprocity theorem also provides a relation between the cross section for forming a compound nucleus with spin j by neutron bombardment and the width for decay of the nucleus by emitting a neutron with orbital angular momentum l . This relation is:

$$\Gamma^{(l)} = \frac{\sigma_c^{(l)} D_c^{(j)}}{(2l+1) 2\pi^2 \chi^2} \quad (35)$$

where $\sigma_c^{(l)}$ is the cross section for formation of the nucleus by neutrons of orbital angular momentum l , and $D_c^{(j)}$ is the density of levels with spin j .

LEVEL DENSITY FORMULA

In the preceding discussion, the distance between energy levels appeared quite often. The density of levels $1/D$ has been estimated by Weisskopf to be constant up to several mev above the ground state and then to rise according to the formula:

$$\frac{1}{D(E)} = C e^{\sqrt{aE}} \quad (36)$$

C and a are functions of A , and rough approximations are plotted in Fig. 1.2.19 for odd A nuclei. Little is known about level spacings for even nuclei except that they are much larger than for odd nuclei.

ELASTIC SCATTERING

COLLISION MECHANICS

Consider a neutron impinging on a nucleus of mass A . Taking the polar axis to be the initial direction of the neutron, the process of elastic scattering can be schematically represented by Fig. 1.2.20 in the laboratory system and Fig. 1.2.21 in the center-of-mass system.

The relation between θ and θ_0 is:

$$\cos \theta = \frac{A \cos \theta_0 + 1}{(A^2 + 2A \cos \theta_0 + 1)^{1/2}} \quad (37)$$

Let us define:

$$\alpha \equiv \left(\frac{A-1}{A+1} \right)^2 \quad (38)$$

Then the neutron energy in the laboratory system before collision E_1 is related to that after collision by:

$$E_2/E_1 = \frac{1}{2} [(1+\alpha) + (1-\alpha) \cos \theta_0] \quad (39)$$

The greatest energy loss occurs for $\theta = \pi$ (backward scattering) when $E_2 = \alpha E_1$. Hence, the final energies lie between E_1 and αE_1 .

A quantity of interest is the mean logarithmic energy loss, ξ , which is defined as:

$$\xi \equiv \int_{\alpha E_1}^{E_1} \ln \frac{E_1}{E_2} g(E_2, E_1) dE_2 \quad (40)$$

where $g(E_2, E_1) dE_2$ is the probability of scattering from energy E_1 into the energy interval dE_2 about E_2 .

Another quantity of interest, the average value of the cosine of the scattering angle (where the average is taken over all possible collisions), is defined as:

$$\overline{\cos \theta} = \int \cos \theta \frac{\sigma_e(\theta)}{\sigma_e} d\Omega$$

Isotropic Scattering

Isotropic scattering signifies that the differential cross section is not a function of θ_0 , i.e., that it is spherically symmetrical in the center-of-mass system. In this case, neutrons are scattered uniformly into the energy interval between E_1 and αE_1 ; i.e.:

$$\begin{aligned} g(E_2, E_1) &= \frac{1}{E_1(1-\alpha)} & \alpha E_1 \leq E_2 \leq E_1 \\ &= 0 & E_2 < \alpha E_1 \end{aligned} \quad (41)$$

and it can be shown that:

$$\xi = 1 + \frac{\alpha}{1-\alpha} \ln \alpha \quad (42)$$

For mass > 10 , an approximation accurate to 1 percent or less is:

$$\xi \approx \frac{2}{A + 2/3} \quad (43)$$

For isotropic scattering, the average value of the cosine of the scattering angle in the laboratory system is:

$$\overline{\cos \theta} = \frac{2}{3A} \quad (44)$$

Values of ξ , $1 - \alpha$, $\ln 1/\alpha$, $\overline{\cos \theta}$, and the average number of collisions required to thermalize 2-mev neutrons $[(1/\xi) \ln(2 \times 10^6/0.025)]$ are given in Table 1.2.12 for materials of interest.

Equation (41) gives the energy distribution of neutrons after one collision. The number of neutrons $N(n, E_2)$ having an energy between E_2 and $E_2 + dE_2$ after n collisions can be obtained:

$$N(n, E_2) = \frac{\left(\frac{1}{1-\alpha}\right)^n}{E_1(n-1)!} \sum_{k=0}^{\bar{k}} \binom{n}{k} (-)^k \ln \frac{\alpha^k E_1}{E_2} \quad (45)$$

where \bar{k} is the largest value of k for which the logarithm is positive. The expression is, of course, zero for $E_2 < \alpha^n E_1$.

For $E_2 \ll E_1$, this becomes:

$$N(n, E_2) \approx \frac{\left(\frac{\xi-1}{\alpha}\right)^{n-1}}{E_1(1-\alpha)} \left(\frac{6}{\pi n}\right)^{1/2} e^{-12n\chi^2} \frac{\sinh 6\chi}{6\chi}$$

where:

$$\chi = \frac{\log E_1/E_2}{n \log 1/\alpha} - 1/2 \quad (45a)$$

Results for mixtures are given in Marshak's review article.²⁸

Equation (45) is not valid when the scattering material is hydrogen ($\alpha = 0$). This case, however, admits of a closed solution. Equation (46) gives the probability that after n collisions with hydrogen nuclei, the neutron will have an energy between E_2 and $E_2 + dE_2$:

$$N(n, E_2) = \frac{1}{(n-1)! E_1} \left(\ln \frac{E_1}{E_2} \right)^{n-1} \quad (46)$$

Anisotropic Scattering

When the scattering is not isotropic in the center-of-mass system, Eq. (41) and those results which depend upon it do not hold. In general:

$$g(E_2, E_1) = 4\pi \frac{\sigma_e(\theta_0)}{\sigma_e} \frac{1}{(1-\alpha)E_1} \quad \alpha E_1 \leq E_2 \leq E_1$$

$$= 0 \quad E_2 < \alpha E_1 \quad (47)$$

where $\sigma_e(\theta_0)$ is the differential elastic scattering cross section in the center-of-mass system defined so that:

$$\sigma_e = 2\pi \int_0^\pi \sigma_e(\theta) \sin \theta \, d\theta$$

For isotropic scattering in the center-of-mass system:

$$\frac{\sigma_e(\theta_0)}{\sigma_e} = \frac{1}{4\pi}$$

The average logarithmic energy loss can still be computed from Eq. (40) in two cases of interest.* Let:

$$\sigma_e(\theta_0) = \frac{\sigma_e}{4\pi} + \frac{3}{4\pi} \sigma_1 p_1 (\cos \theta_0) + \dots$$

Then for a heavy nucleus where $(A - 1/A + 1)^2 \approx 1$ and $\theta_0 \approx \theta$:

$$\xi = \xi_0 \left(1 - \frac{\sigma_1}{\sigma_e} \right) = \xi_0 (1 - \overline{\cos \theta}) \quad (48)$$

where ξ_0 is the average loss in $\ln E$ for isotropic scattering. For arbitrary A , one can also find ξ if one restricts oneself to a $\sigma_e(\theta_0)$ containing only σ_e and σ_1 . The result in this case is:

* Mathew M. Shapiro, unpublished.

$$\xi = \xi_0 - \frac{3}{2} \left(\frac{A+1}{2A} \xi_0 - 1 \right) \frac{1 - \frac{2}{3A} - (1 - \overline{\cos \theta})}{1 - \frac{3}{5A^2}} \quad (49)$$

For large A , this reduces to:

$$\xi = \xi_0 \left[(1 - \overline{\cos \theta}) \left(1 + \frac{3}{4A} \right) - \frac{1}{12A} \right] \quad (49a)$$

CROSS SECTIONS

Thermal values of the elastic scattering cross sections are contained in Table 1.2.17. The elastic cross section is expected to equal approximately the total cross section in the middle-energy region where (n, γ) cross sections are small. Near thermal energies, where radiative capture can be dominant and above the threshold for inelastic scattering, σ_e will be noticeably less than the total cross section. At energies high enough for the schematic theory to apply, the elastic scattering cross section approaches $\pi(R + \lambda)^2$. λ is the reduced wavelength of the neutron.* This is half the asymptotic value of the total cross section. The total cross section as predicted by the schematic theory is given in Fig. 1.2.15.

Concerning the angular distribution of scattered neutrons, some experimental work on light elements has been done at Los Alamos.²⁹ Their results for the differential elastic scattering cross section are given in Figs. 1.2.22 to 1.2.28. The most probable incident neutron energy was about 1.7 mev. Table 1.2.13 gives their values of $\sigma_e(1 - \overline{\cos \theta})$.

Transport Cross Section

A derived quantity used in diffusion theory is the transport cross section, σ_{tr} . A commonly used definition of this quantity is:

$$\sigma_{tr} = 2\pi \int_0^\pi \sigma_s(\theta) (1 - \cos \theta) \sin \theta d\theta = \sigma_s(1 - \overline{\cos \theta}) \quad (50)$$

where σ_s is the scattering cross section (elastic + inelastic) other definitions are in use.

If the elastic scattering is isotropic and there is no inelastic scattering, one finds from Eq. (44):

$$\sigma_{tr} = \sigma_e \left(1 - \frac{2}{3A} \right) \quad (51)$$

By assuming the inelastic scattering to be spherically symmetric, one obtains:

$$\sigma_{tr} = \sigma_{in} + 2\pi \int_0^\pi \sigma_e(\theta) (1 - \cos \theta) \sin \theta d\theta \quad (52)$$

Table 1.2.14 contains some measured values of σ_{tr} .

CRYSTAL EFFECTS^{30,31,32} AND CHEMICAL BINDING

When the wavelength of thermal neutrons is of the same order of magnitude as the interatomic distances in crystals, the neutrons scattered from such crystals exhibit interference

* $\lambda = 4.5E^{-1/2} \cdot 10^{-13}$ cm, where E is in mev.

effects. Thus, the scattering cross sections for very-low-energy neutrons become energy dependent. The cross sections of Be and C in Figs. 1.2.29 and 1.2.30 illustrate this effect.

It is the coherent scattering cross section of the individual atoms that determines the interference properties of neutrons. (For coherent scattering, the scattered wave is capable of interfering with the incident neutron wave.) In analogy to the case of X-rays, these interference effects follow the usual Bragg law. For wavelengths larger than the Bragg cut-off wavelength (twice the largest lattice spacing), the coherent component of scattering vanishes leaving only the incoherent component.

Incoherent scattering (scattering in which the scattered wave does not interfere with the incident wave) makes up what is called "diffuse" scattering. This type of scattering does not contribute to interference effects. There are several reasons for incoherent or diffuse scattering:

(1) There may be several isotopes of an element present in the crystal. The various isotopes can give rise to different scattering cross sections. The location of the extra isotopes in the crystal will be random and hence give rise to a random variation in cross section.

(2) In nuclei with non-zero spin, another type of incoherent scattering is present. This is called "spin-dependent" incoherent scattering because it arises from variation of the cross section with the relative orientation of the neutron spin and the nuclear spin.

(3) A third reason for incoherent scattering can be found in the magnetic interaction between neutrons and the atomic magnetic moments. The atomic moments are not aligned in the majority of crystals, and since the magnetic scattering is dependent on the relative orientation of neutron moment and atomic moments, a random variation in scattering power is present, and incoherent scattering results.

(4) The coherent "crystal effects" are further decreased by another type of incoherent scattering resulting from temperature vibration of the atoms of the crystal. The magnitude of this reduction is determined by the temperature of the crystal, the wavelength of the neutrons, and the angle of scattering.

For wavelengths larger than the Bragg cut-off, the only scattering is incoherent. As the energy is increased, a large increase in cross section is observed (cf. Figs. 1.2.29 and 1.2.30) when the Bragg cut off wavelength is reached. Maxima in the cross section are observed as each new set of planes becomes active. At neutron energies above 0.1 ev, so many planes become active that the cross section varies smoothly with energy. When the neutron energy reaches several ev, the coherent scattering becomes small, but this is accompanied by a corresponding increase in the incoherent inelastic scattering so that the total scattering changes very little with energy. The inelastic scattering, where the lattice receives energy from the neutrons, increases with energy until the neutron energy is large compared to the chemical binding energy of the lattice. When this point is reached, the neutron is scattered as if the nuclei forming the lattice were free, and, barring nuclear resonances, the scattering cross section is constant with energy. This is called the free-atom cross section.

To summarize the process of a neutron losing energy in the crystal, several steps are considered.³³ A fast neutron first slows down by dislocating effectively free nuclei until its energy decreases to the order of the energy of the crystal bond. At this point, it begins to make inelastic collisions with the lattice as a whole. It continues to lose energy in this manner until its wavelength exceeds the amplitude of the temperature vibrations of the nuclei of the crystal. At this stage, further cooling takes place very slowly because elastic collisions with the lattice become the most probable process. If in some manner the neutron loses still more energy, inelastic scattering becomes important again, but, in this case, the neutron absorbs energy from the lattice.

Figures 1.2.31 and 1.2.32 illustrate another effect that is most prominent in low A elements, namely, an increase in the scattering cross section for low-energy neutrons. This effect may have more than one cause. In the case of scattering by a gas, the thermal

motion of the molecules of the gas will cause neutrons to be "bumped" from their original direction and hence give rise to an increased scattering cross section.³⁴ (This effect follows a $1/v$ law.) Superimposed on this is the so called chemical binding effect* owing to a changed reduced mass. This effect becomes important when the energy of the neutron is less than the energy of the chemical bond. In the case of a gas, this means that the mass of the neutron and molecule are used in calculating the reduced mass. In the crystalline case, it means that the mass of the neutron and crystal must be used in calculating the reduced mass (which is approximately the mass of the neutron).

If the molecule or crystal is composed of only one kind of atom, then the scattering cross section is increased over the free-atom cross section by the square of the ratio of the reduced mass of neutron and molecule (or crystal) to the reduced mass of neutron and one atom of the molecule (or crystal). Thus, for a crystal, this factor is $(A + 1)^2/A^2$. In the case of a diatomic molecule, it is $4(1 + A)^2/(1 + 2A)^2$.

$(A + 1)^2/A^2$ times the free-atom cross section is known as the "bound-atom cross section."

The discussion above relates to the effect of crystalline structure and chemical binding on the total cross section. It is clear that the chemical binding will increase the transport cross section, because with the increase in effective mass, the scattering will become more isotropic in the laboratory frame. However, the details as to how chemical binding and crystal effects influence reactor behavior are not well known at this time.

INELASTIC SCATTERING

Inelastic scattering of a neutron leaves the target nucleus in one of its excited states. The energy of the emitted neutron is less than that of the incident neutron by this excitation energy.

DATA

A summary of inelastic cross section data is presented in Table 1.2.15.

Recent measurements of the inelastic scattering of neutrons of about 1.85 mev energy on Fe show the existence of a level at 850 ± 50 kev above the ground state.⁴³ The measurements were made at 90° only. If the inelastic scattering is assumed isotropic, one is led to a cross section of 0.82 barns.

The distribution in energy of 4.3-mev neutrons inelastically scattered from tungsten is found to be practically constant in energy up to about 3.25 mev.⁴⁴ The inelastic cross section is estimated to be less than three fourths as large as the elastic cross section.

APPROXIMATE FORMULAS

When there are no data on inelastic scattering available, some crude guesses can be made provided that both the compound nucleus and the residual nucleus are sufficiently highly excited so that there are many levels lying below the level of excitation. This restricts the validity of the results to heavy nuclei. In this case, the theory predicts that the inelastically scattered neutrons are isotropically distributed.

Energy Distributions

Denote by E the energy of the incident neutron and by \bar{E} that of the inelastically scattered one. Let $D_R(x)$ be the distance between levels of the residual nucleus when excited

* G. Placzek, Phys. Rev., 86, 377, 1952, discusses the scattering of neutrons by systems of heavy nuclei. G. Breit, Phys. Rev., 71, 215, 1947, and G. Breit and P. R. Zilsel, Phys. Rev., 71, 232, 1947, discuss the scattering of slow neutrons by bound protons.

an energy x above its ground state. Finally, denote by $\sigma_c(E)$, the cross section for forming the compound nucleus by a neutron of energy E . According to the statistical theory, the number of neutrons scattered from energy E to \bar{E} is proportional to:

$$f(E, \bar{E}) = \bar{E} \sigma_c(\bar{E}) D_R^{-1}(E - \bar{E}) \quad (53)$$

A plot of $\sigma_c(E)$ as computed from statistical theory is given in Fig. 1.2.18, to be used if no data are available. D_R^{-1} is expected to be relatively constant up to a certain energy E_0 (~ 3 mev) above the ground state and then to rise exponentially:

$$D_R^{-1}(E) = D_0^{-1} \quad E \leq E_0 \quad (54)$$

$$D_R^{-1}(E) = D_0^{-1} e^{2(\sqrt{aE} - \sqrt{aE_0})} \quad E \geq E_0 \quad (55)$$

The constants D_0 , E_0 , and a are to be adjusted from experiment. Lacking evidence for a , one can use Fig. 1.2.19 to estimate it for odd nuclei. (Cf. "Level Density Formula.")

For various limiting cases, simple expressions can be found for the dependence of f on \bar{E} . When the residual nucleus is left with excitation energy greater than E_0 , then:

$$f = \bar{E} \sigma_c(\bar{E}) \exp \{2(\sqrt{a(E - \bar{E})} - \sqrt{aE_0})\} \quad E - \bar{E} > E_0 \quad (56)$$

Figs. 1.2.33 to 1.2.36 show plots of Eq. (56) for $Z = 30, 50, 70$, and 90 when $E_0 = 0$; i.e., when the exponential formula is good down to the ground state.

If only low-energy emerging neutrons are considered, then:

$$f(E, \bar{E}) = \bar{E} \sigma_c(\bar{E}) \exp \{2(\sqrt{aE} - \sqrt{aE_0})\} \exp \left\{ -\sqrt{\frac{a}{E}} \bar{E} \right\} \quad (E - \bar{E}) > E_0 \quad \bar{E} \ll E \quad (57)$$

When $E - \bar{E} < E_0$, then Eq. (54) should be used for the level density and:

$$f \propto \bar{E} \sigma_c(\bar{E}) \quad (E - \bar{E}) < E_0 \quad (58)$$

When E is close to E_0 , one must take account of the change in level density below E_0 in Eq. (53). This results in a rise in f at the high-energy end of the neutron spectrum. Figure 1.2.37 shows a typical result with $E_0 = 3$ mev.

Equations (53) through (58) are, within the limits of the theory, good approximations to the emitted neutron distribution until E becomes large enough for the $(n, 2n)$ reaction to occur. This will add more low-energy neutrons to the spectrum.

Total Inelastic Cross Sections

The cross section σ_c for compound nucleus formation can be written as the sum:

$$\sigma_c = \sigma_{in} + \sigma_{ce} + \sigma_f + \sigma_\gamma$$

of the inelastic, capture elastic,* fission, and radiative capture cross sections, from which it follows that:

$$\sigma_{in} = \frac{\sigma_{in}}{\sigma_{in} + \sigma_{ce}} (\sigma_c - \sigma_f - \sigma_\gamma) \quad (59)$$

* Scattering in which a compound nucleus is formed, a neutron emitted, and the residual nucleus left in the same state as the target nucleus is called capture elastic scattering.

The statistical theory gives:

$$\frac{\sigma_{\text{in}}}{\sigma_{\text{in}} + \sigma_{\text{ce}}} = \frac{\int_0^{E-D_0} \bar{E} \sigma_c(\bar{E}) D_R^{-1} (E - \bar{E}) d\bar{E}}{\int_0^E \bar{E} \sigma_c(\bar{E}) D_R^{-1} (E - \bar{E}) d\bar{E}} \quad (60)$$

which, together with Eq. (59) and Fig. 1.2.18 for σ_c directly determine σ_{in} in the case that the fission cross section is small (the radiative capture cross section is negligible in this case). For $E \gg D_0$, it follows that:

$$\frac{\sigma_{\text{in}}}{\sigma_{\text{in}} + \sigma_{\text{ce}}} \approx 1 \quad (61)$$

and thus that:

$$\sigma_{\text{in}}(E) \approx \sigma_c(E) \quad (61a)$$

which agrees well with 14-mev data in the absence of fission.

Deviations from Eq. (60) occur when the residual nucleus is left with excitation less than E_0 . Then:

$$\frac{\sigma_{\text{in}}}{\sigma_{\text{in}} + \sigma_{\text{ce}}} = \frac{\int_0^{E-D_0} \bar{E} \sigma_c(\bar{E}) d\bar{E}}{\int_0^E E' \sigma_c(E') dE'} = \frac{g(x')}{g(x)} \quad (62)$$

where x is the value of R/χ for neutron energy E and x' the value for energy $E - D_0$:

$$\frac{R}{\chi(E)} = 0.222 \sqrt{E(\text{mev})} R \times 10^{13}$$

The function $g(x)$ is plotted in Fig. 1.2.38 for several values of $X_0 = 10^{13} R$.

Equation (62) is a very rough approximation which neglects fluctuations due to spin differences and variations in level spacings.

In the case of light nuclei or "magic" nuclei where only a few levels are involved in the scattering process, the results depend strongly upon the spins and parities of the levels. A detailed treatment of this case and the statistical theory case is contained in Report NYO-636 and in a paper by Feshbach and Hauser.⁴⁵

(n,2n) REACTIONS

When the energy of the incident neutron exceeds the binding energy of the last neutron in the target nucleus, the (n,2n) reaction becomes energetically possible. Few measurements of (n,2n) cross sections have been made. The energy dependence has been obtained for the (n,2n) reaction in Cu^{63} by Fowler and Slye⁴⁶ and in Cu^{63} , Ni^{58} , and Tl^{203} by Martin and Diven.⁴⁷ Cross sections at 14 mev have also been measured for a few elements by Forbes,⁴⁸ whose results are included in Table 1.2.16.

The Be (n,2n) reaction is of particular interest because the threshold of 1.7 mev is the lowest known. Many measurements of this cross section have been made, usually with (α ,n) sources, but the results have not been particularly informative.

A compilation by A. H. Snell and published by Agnew⁵⁰ shows values ranging from 0.04 to 4.0 barns. The latter measurement is hardly credible, but the situation is nuclear at present.

Cohen⁵¹ has measured a large number of (n,2n) cross sections averaged over a broad spectrum of high-energy neutrons produced by the (d,n) reaction.

Most other measurements of $(n,2n)$ cross sections have been at energies of 20 mev or more.

If one assumes that after the first neutron is inelastically scattered, competition to neutron emission from other processes is small, then every inelastic scattering that leaves the nucleus sufficiently excited will lead to the emission of a second neutron.

If we denote the threshold energy by E_b , then within the limits of the statistical theory* the $(n,2n)$ cross section is given by:

$$\sigma(n,2n)_E = \sigma_{in}(E) \frac{\int_0^{E-E_b} \bar{E} \sigma_c(\bar{E}) D_R^{-1} (\bar{E} - \bar{E}) d\bar{E}}{\int_0^E \bar{E}' \sigma_c(\bar{E}') D_R^{-1} (E - \bar{E}') d\bar{E}'} \quad (63)$$

This can be simplified in several limiting cases. For $E - E_b > \sqrt{E/a}$:

$$\sigma(n,2n)_E = \sigma_{in}(E) \{1 - (1 + \gamma)e^{-\gamma}\} \quad (64)$$

For $E - E_b < \sqrt{E/a}$:

$$\sigma(n,2n)_E = \sigma_{in}(E) \frac{\sigma_c(E - E_b)}{\sigma_c(\sqrt{E/a})} \{1 - (1 + \gamma)e^{-\gamma}\} \quad (65)$$

$$\rightarrow \sigma_{in}(E) \frac{\sigma_c(E - E_b)}{\sigma_c(\sqrt{E/a})} \frac{a}{2E} (E - E_b)^2 \quad (66)$$

when:

$$E - E_b \ll \sqrt{E/a}$$

These formulae are not valid in the limit $E = E_b$. They agree with Eq. (63) to within 10 percent, however, as soon as $k'R$ is of the order of 1 or greater. Here k' is the wave number of a neutron of energy $E - E_b$ ($k' = 0.22 \sqrt{E - E_b} \times 10^{13} \text{ cm}^{-1}$, E in mev) and R is the nuclear radius.

REACTION PROCESSES

Reaction processes are those in which neutrons that are absorbed are not re-emitted. Examples discussed below are the (n,γ) , (n,α) and (n,p) processes. The (n,α) and (n,p) processes are all restricted to light nuclei at the neutron energies considered here because of the coulomb barrier and threshold effects. Thermal values of the reaction cross sections appear in Tables 1.2.17.

RADIATIVE CAPTURE (n,γ)

The general behavior of (n,γ) cross sections was discussed in some detail under "Collision Reactions." When the energy levels are far apart, the Breit-Wigner single-level formula should give a good fit to the cross section at energies near the resonance energy.

Figure 1.2.39 shows the cross section near a resonance in Cd. Parameters for a Breit-Wigner fit (the resonance energy, level width, and the maximum value of the cross section) are shown on the figure. Figures 1.2.40 and 1.2.41 show two other (n,γ) resonance cross sections. Most (n,γ) cross sections obey the $1/v$ law far from resonances in the thermal region.

* Cf. preceding discussion of "Approximate Formulas."

Radiative capture cross sections have been measured by Hughes et al,³⁰ using reactor neutrons with an effective energy of 1 mev. The cross sections are plotted vs number of neutrons in Fig. 1.2.16. Hughes notes that the energy dependence of the (n,γ) cross section in this neighborhood is approximately $1/E$. The abnormally low cross sections of some of the nuclei shown are evidence of their "magic" character.

(n,α) AND (n,p) REACTIONS

Because both the coulomb effect and threshold values for charged particle emission increase with A , these reactions are generally limited to light nuclei for neutron energies of interest in reactors. Some of these cross sections in light elements can be quite large at thermal energies. Figures 1.2.42 to 1.2.44 show the data for the (n,α) reaction in Li, B, and Be.

The (n,p) cross sections of oxygen are of interest because of the activity of the product nuclei. Table 1.2.18 gives the threshold energy and the value of the cross section averaged over the fission spectrum in the case of O^{16} , and over energies much higher than the threshold in the case of O^{17} .

Table 1.2.1 — Nomenclature

A	Atomic mass number	θ	Angle of deflection in the laboratory system
Z	Nuclear charge number	θ_0	Angle of deflection in the center of mass system
M	Mass of neutral atom	$\frac{\sigma_{tr}}{\cos \theta}$	Average value of $\cos \theta$
R	Nuclear radius	$\sigma_c(E)$	Cross section for the formation of the compound nucleus by neutrons of energy E . Also called reaction cross section
I	Nuclear spin	X_0	10^{13} R(cm)
T	Mean-life of radioactive nucleus	$f(E, \bar{E})$	Proportional to number of neutrons inelastically scattered from energy E to energy \bar{E}
$T_{1/2}$	Half-life of radioactive nucleus	ξ	Average loss in logarithm of energy
λ	$1/T$	γ	$\sqrt{\frac{a}{E}} (E - E_b)$
α	Ratio of capture cross section to fission cross section. Also, minimum ratio of final to initial energies in an elastic scattering process		
σ_e	Elastic scattering cross section		
$\sigma_e(\theta)$	Differential σ_e		
σ_{in}	Inelastic scattering cross section		
σ_s	$\sigma_e + \sigma_{in}$		

Table 1.2.2 — Nuclear Radii

Isotope	$R \times 10^{13}$, cm		Reference
	Low energy (kev)	High energy (14–25 mev)	
He ⁴	2.5	...	(2)
Li ⁷	2.7	...	(2)
Be ⁹	4.7–5.0	3.8	(2)
B ¹¹	3.5	3.4	(2)
C ¹²	4.5	3.8	(2)
O ¹⁶	5.5	4.3	(2)
F ¹⁹	5.35	...	(2)
Na ²³	5.65	...	(2)
Mg ²⁴	4.75	4.5	(2)
Al ²⁷	5.5	4.6	(2)
Si ²⁸	4.8	...	(2)
P ³¹	5.15	...	(2)
S ³²	4.2	4.1	(2)
Cl	...	4.7	(1)
K ³⁹	3.31	...	(2)
Ca ⁴⁰	3.5	...	(2)
Ti	4.75	5.0	(2)
V ⁵¹	6.5	5.3	(2)
Mn ⁵⁵	5.2	...	(2)
Fe ⁵⁶	4.0	5.6	(2)
Co ⁵⁹	5.2	...	(2)
Ni	4.7	...	(2)
Cu	5.25	5.5	(2)
Zn	5.55	5.9	(2)
Se	...	6.3	(1)
Zr	7.25	5.2	(2)
Ag	7.7	6.8–6.9	(2)
Cd	...	7.2	(1)
In ¹¹⁵	7.3	...	(2)
Sn	7.5	7.4	(2)
Sb ^{121, 123}	7.5	7.3	(2)
I ¹²⁷	7.3	...	(2)
Ta ¹⁸¹	7.9–8.0	...	(2)
W	7.7	...	(2)
Au	...	7.5	(1)
Hg	...	8.3–8.4	(1)
Pb ²⁰⁸	7.5	7.8	(2)
Pb ²⁰⁹	7.5–7.6	7.8	(2)
Bi ²⁰⁹	6.7	...	(2)
Bi	...	7.9	(1)
Th	8.7	...	(3)
U	...	8.5	

Table 1.2.3 —Isotopic Weights, Binding Energy of an Additional Neutron, and Packing Fraction

[The first five columns of the following table are taken from K. T. Bainbridge, Part V of Experimental Nuclear Physics, Volume I, edited by E. Segrè, John Wiley & Sons, Inc., New York (in press).]

Atomic number (Z)	Symbol	Mass number (A)*	Isotopic weight relative to O ¹⁶ †	Error in isotopic weight × 10 ⁶ ‡	Binding energy of additional neutron, mev§	Packing fraction × 10 ³ ¶
0	n	1	1.008982	3		8.982
1	H	<u>1</u>	1.008142	3	2.224	8.142
		<u>2</u>	2.014735	6	6.256	7.367
		3	3.016997	11		5.665
2	He	<u>3</u>	3.016977	11	20.56	5.659
		<u>4</u>	4.003873	15	-0.6601	0.968
		5	5.013564	215	1.929	2.713
		6	6.020474	27		3.412
3	Li	5				
		<u>6</u>	6.017021	22	7.243	2.837
		<u>7</u>	7.018223	26	2.036	2.603
		8	8.025018	30		3.127
4	Be	6				
		7	7.019150	26	18.88	2.736
		8	8.007850	29	1.666	0.981
		<u>9</u>	9.015043	30	6.809	1.671
		10	10.016711	28		1.671
		11				
5	B	9	9.016190	31	8.433	1.799
		<u>10</u>	10.016114	28	11.46	1.611
		<u>11</u>	11.012789	23	3.360	1.163
		<u>12</u>	12.018162	22		1.514
		13				
6	C	10	10.020605	300	13.66	2.060
		11	11.014916	24	18.71	1.356
		<u>12</u>	12.003804	17	4.946	0.317
		<u>13</u>	13.007473	14	8.168	.575
		14	14.007682	11		.549
		15				
7	N	12				
		13	13.009858	14	10.54	0.758
		<u>14</u>	14.007515	11	10.83	.537
		<u>15</u>	15.004863	12	2.891	.324
		<u>16</u>	16.010740	500	5.295	.671
		17	17.014035	500		.826
		18				
8	O	14	(14.013016)		13.25	0.930
		15	15.007768	13	15.59	.518
		<u>16</u>	16.000000	Standard	4.142	.000
		<u>17</u>	17.004533	7	8.045	.267
		<u>18</u>	18.004874	17	4.072	.271
		19	19.009482	850		.499

Table 1.2.3 — (Continued)

Atomic number (Z)	Symbol	Mass number (A)*	Isotopic weight relative to O ¹⁶ †	Error in isotopic weight × 10 ⁶ ‡	Binding energy of additional neutron, mev§	Packing fraction × 10 ³ ¶
9	F	16				
		17	17.007486	11	9.122	0.440
		18	18.006670	18	10.42	.370
		19	19.004456	15	6.597	.234
		20	20.006352	19		.318
		21				
10	Ne	18				
		19	19.007915	53	16.79	0.416
		20	19.998860	23	6.753	-.0570
		21	21.000589	21	10.52	.0280
		22	21.998270	60	5.188	-.0786
		23	23.001680	60		.0730
11	Na	21				
		22	22.001321	60	12.26	0.0600
		23	22.997139	26	6.955	-.124
		24	23.998651	28	9.165	-.0562
		25	24.997789	115		-.0884
12	Mg	22				
		23	23.001113	325	16.20	0.0484
		24	23.992696	30	7.320	-.304
		25	24.993815	33	11.10	-.247
		26	25.990871	36	6.430	-.351
		27	26.992946	36		-.261
13	Al	25				
		26	25.996194	430	14.01	-0.146
		27	26.990140	33	7.720	-.365
		28	27.990830	36	9.371	-.328
		29	28.989747	273		-.354
		30				
14	Si	27	26.995254	39	17.129	-0.176
		28	27.985837	37	8.472	-.506
		29	28.985719	45	10.60	-.492
		30	29.983313	38	6.596	-.556
		31	30.985210	41		-.477
		32				
15	P	29	28.989618	88	9.710	-0.358
		30	29.988170	107	12.60	-.394
		31	30.983622	38	7.926	-.528
		32	31.984091	36		-.497
		33				
		34				
16	S	31	30.988865	110	14.51	-0.359
		32	31.982265	35	8.645	-.554
		33	32.981961	38	11.33	-.547
		34	33.978773	44	6.890	-.624
		35	34.980354	50		-.561
		36				
		37				

Table 1.2.3 — (Continued)

Atomic number (Z)	Symbol	Mass number (A)*	Isotopic weight relative to O ¹⁶ †	Error in isotopic weight × 10 ⁶ ‡	Binding energy of additional neutron, mev§	Packing fraction × 10 ³ ¶
17	Cl	33				
		34				
		35	34.980175	50	8.559	-0.566
		36	35.979964	58	10.54	-.557
		37	36.977624	77	6.109	-.605
		38	37.980044	84		-.525
		39				
18	A	35				
		36	35.978930	58	8.764	-0.585
		37	36.978499	77	11.73	-.581
		38	37.974878	85		-.661
		39				
		40	39.975100	100	6.064	-0.622
		41	40.977569	100		-.547
19	K	37				
		38	37.981125	240	13.20	-0.497
		39	38.97593	130	7.759	-.617
		40	39.976578	130	9.984	-.586
		41	40.974836	150	7.389	-.614
		42	41.975881	150		-.574
		43				
20	Ca	39	38.983515	420	15.90	-0.423
		40	39.975420	130	8.469	-.614
		41	40.975305	160	11.41	-.602
		42	41.972036	165	8.051	-.666
		43	42.97237	100	11.31	-.642
		44	43.96920	100		-.700
		45				
		46				
		47				
		48	47.96763	120		-0.674
		49				
21	Sc	41				
		42				
		43				
		44				
		45	44.97000	60		-0.667
		46				
		47				
21	Sc	48	47.96787	190	11.70	-0.669
		49	48.96428	200		-.729
22	Ti	45				
		46				
		47	46.96700	1000	11.11	-0.702
		48	47.96405	190		-.749
		49				
		50				
		51				

Table 1.2.3 — (Continued)

Atomic number (Z)	Symbol	Mass number (A)*	Isotopic weight relative to O ¹⁶ †	Error in isotopic weight × 10 ⁶ ‡	Binding energy of additional neutron, mev§	Packing fraction × 10 ³ ¶
23	V	47				
		48	47.96840	190		−0.658
		49				
		50	49.96215	500	10.80	−0.757
		51	50.95953	150	7.273	−.794
		52	51.96070	150		−.756
24	Cr	49	48.96540	220	13.40	−0.706
		50	49.95999	90		−.800
		51				
		52	51.95693	150		−0.828
		53				
		54				
25	Mn	55				
		56				
		57				
		58				
		59				
		60				
26	Fe	54	52.96238	300	13.80	−0.710
		56	53.95654	230	8.828	−.805
		58	54.95604	140	11.32	−.799
		60	55.95286	140	7.627	−.842
		62	56.95365	140		−.813
		64				
27	Co	58	(58.95350)	170		−0.788
		60	54.95974	140	10.16	−0.732
		62	55.95781	140		−.753
		64				
		66				
		68				
28	Ni	68	58.95182	140	7.729	−0.817
		70	59.95250	140		−.792
		72				
		74				
		76				
		78				
29	Cu	63	56.95719	300	11.70	−0.751
		65	57.95360	200	9.014	−.800
		67	58.95290	200	11.55	−.798
		69	59.94948	140	8.548	−.842
		71	(60.94928)	(150)		−.831
		73				
30	Zn	64	63.94733	400		−0.823
		66				
		68				
		70				

Table 1.2.3 —(Continued)

Atomic number (Z)	Symbol	Mass number (A)*	Isotopic weight relative to O ¹⁶ †	Error in isotopic weight × 10 ⁶ ‡	Binding energy of additional neutron, mev§	Packing fraction × 10 ³ ¶
		61	60.95168	150		−0.792
		62				
		<u>63</u>	62.94862	200	7.887	−0.816
		64	63.94913	400	9.889	−.795
		<u>65</u>	64.94749	210		−.808
		66				
		67				
30	Zn	63				
		<u>64</u>	(63.94880)	400		−0.800
		65				
		<u>66</u>				
		<u>67</u>				
		<u>68</u>				
		<u>69</u>				
		<u>70</u>				
		71				
		72				
31	Ga	64				
		65				
		66				
		67				
		68				
		<u>69</u>				
		<u>70</u>				
		<u>71</u>				
		72				
		73				
32	Ge	66				
		67				
		68				
		69				
		<u>70</u>				
		<u>71</u>				
		<u>72</u>				
		<u>73</u>				
		<u>74</u>				
		<u>75</u>				
		<u>76</u>				
		77				
		78				
33	As	71				
		72				
		73				
		74				
		<u>75</u>				
		<u>76</u>				
		77				
		78				

Table 1.2.3 — (Continued)

Atomic number (Z)	Symbol	Mass number (A)*	Isotopic weight relative to O ¹⁶ †	Error in isotopic weight × 10 ⁶ ‡	Binding energy of additional neutron, mev§	Packing fraction × 10 ³ ¶
34	Se	71				
		72				
		73				
		74				
		75				
		76				
		77				
		78				
		79				
		80				
		81				
		82				
		83				
		84				
35	Br	75				
		76				
		77				
		78				
		79				
		80				
		81				
		82				
		83				
		84				
		85				
		86				
36	Kr	77				
		78				
		79				
		80				
		81				
		82				
		83				
		84				
		85				
		86				
		87				
		88				
		89				
		90				
		91				
37	Rb	81				
		82				
		83				

Table 1.2.3 —(Continued)

Atomic number (Z)	Symbol	Mass number (A)*	Isotopic weight relative to O ¹⁶ †	Error in isotopic weight × 10 ⁶ ‡	Binding energy of additional neutron, mev§	Packing fraction × 10 ³ ¶
		84				
		85	84.93100	1500	2.441	-0.812
		86	85.93736	1000	(15.680)	-.728
		87	86.9295	2000		-.810
		88				
		89				
		90				
		91				
		92				
		93				
		94				
		95				
38	Sr	84				
		85				
		86	85.9354	1000	8.548	-0.751
		87	86.9352	1000	9.852	-.745
		88	87.93360	360	8.008	-.755
		89	88.93398	420		-.742
		90				
		91				
		92				
		93				
		94				
		95				
39	Y	86				
		87				
		88	87.93758	360	8.791	-0.709
		89	88.93712	420		-.707
		90				
		91				
		92				
		93				
		94				
		95				
40	Zr	89				
		90				
		91				
		92				
		93				
		94				
		95				
		96				
		97				
41	Nb(Cb)	90				
		91				
		92				
		93				
		94				
		95				

Table 1.2.3 —(Continued)

Atomic number (Z)	Symbol	Mass number (A)*	Isotopic weight relative to O ¹⁶ †	Error in isotopic weight × 10 ⁶ ‡	Binding energy of additional neutron, mev§	Packing fraction × 10 ³ ¶
42	Mo	96				
		97				
		98				
		92				
		93				
		94	93.93522	1500		-0.689
		95				
		96	95.93558	320	7.105	-0.671
		97	96.93693	440		-.650
		98				
		99				
		100	99.93829	330		-0.617
43	Tc	101				
		102				
		92				
		93				
		94				
		95				
		96				
		97				
		98				
		99				
		100				
		101				
44	Ru	102				
		95				
		96				
		97				
		98				
		99				
		100				
		101				
		102				
		103				
		104				
		105				
45	Rh	106				
		107				
		102				
		103				
		104				
		105				
46	Pd	106				
		107				
		100				
		101				
		102				

Table 1.2.3 — (Continued)

Atomic number (Z)	Symbol	Mass number (A)*	Isotopic weight relative to O ¹⁶ †	Error in isotopic weight × 10 ⁶ ‡	Binding energy of additional neutron, mev§	Packing fraction × 10 ³ ¶
		<u>105</u>				
		<u>106</u>				
		<u>107</u>				
		<u>108</u>	107.93690	500		−0.584
		<u>109</u>				
		<u>110</u>	109.94098	620		−0.537
		<u>111</u>				
		<u>112</u>				
47	Ag	<u>102</u>				
		<u>103</u>				
		<u>104</u>				
		<u>105</u>				
		<u>106</u>				
		<u>107</u>				
		<u>108</u>				
		<u>109</u>				
		<u>110</u>	109.94218	440		−0.526
		<u>111</u>				
		<u>112</u>				
		<u>113</u>				
48	Cd	<u>106</u>				
		<u>107</u>				
		<u>108</u>				
		<u>109</u>				
		<u>110</u>	109.93911	440		−0.554
		<u>111</u>				
		<u>112</u>	111.93999	360	6.435	−0.536
		<u>113</u>	112.94206	390	10.16	−.513
		<u>114</u>	113.94013	440	5.104	−.525
		<u>115</u>	114.94363	670	9.768	−.490
		<u>116</u>	115.94212	460		−.499
		<u>117</u>				
		<u>118</u>				
49	In	<u>109</u>				
		<u>110</u>				
		<u>111</u>				
		<u>112</u>				
		<u>113</u>				
		<u>114</u>	113.94329	440	9.498	−0.497
		<u>115</u>	114.94207	670	6.584	−.504
		<u>116</u>	115.94398	700		−.483
		<u>117</u>				
50	Sn	<u>111</u>				
		<u>112</u>				
		<u>113</u>				
		<u>114</u>	113.94109	440	7.943	−0.517
		<u>115</u>	114.94154	670	11.60	−.508
		<u>116</u>	115.93806	420	4.964	−.534
		<u>117</u>	116.94171	500		−.498

Table 1.2.3 — (Continued)

Atomic number (Z)	Symbol	Mass number (A)*	Isotopic weight relative to O ¹⁶ †	Error in isotopic weight × 10 ⁶ ‡	Binding energy of additional neutron, mev§	Packing fraction × 10 ³ ¶
		<u>118</u>				
		<u>119</u>				
		<u>120</u>	119.93904	460		-0.508
		121				
		<u>122</u>	121.94260	1260		-0.470
		123				
		<u>124</u>				
		<u>125</u>				
		126				
		127				
		128				
51	Sb	117				
		118				
		119				
		120				
		<u>121</u>				
		<u>122</u>				
		<u>123</u>				
		<u>124</u>				
		125				
		126				
		127				
		128				
		129				
		130				
		131				
		132				
		133				
		134				
		135				
		136				
52	Te	118				
		119				
		<u>120</u>				
		<u>121</u>				
		<u>122</u>				
		<u>123</u>				
		<u>124</u>				
		<u>125</u>				
		<u>126</u>	125.9427	1000		-0.455
		127				
		<u>128</u>	127.9471	1000		-0.413
		129				
		<u>130</u>	129.9467	900		-0.410
		131				
		132				
		133				
		134				
		135				
		136				
		137				

Table 1.2.3 — (Continued)

Atomic number (Z)	Symbol	Mass number (A)*	Isotopic weight relative to O ¹⁶ †	Error in isotopic weight × 10 ⁶ ‡	Binding energy of additional neutron, mev§	Packing fraction × 10 ³ ¶
53	I	124				
		125				
		126				
		127	126.946	1000		-0.425
		128				
		129				
		130				
		131				
		132				
		133				
		134				
		135				
		136				
		137				
54	Xe	<u>124</u>				
		<u>125</u>				
		<u>126</u>				
		<u>127</u>				
		<u>128</u>				
		<u>129</u>	128.94533	300		-0.424
		<u>130</u>				
		<u>131</u>				
		<u>132</u>	131.94729	1000		-0.399
		133				
		<u>134</u>				
		135				
		<u>136</u>				
		137				
		138				
		139				
		140				
		141				
		142				
		143				
		144				
		145				
55	Cs	130				
		131				
		132				
		<u>133</u>				
		<u>134</u>				
		135				
		136				
		137				
		138				
		139				
		140				
		141				
		142				
		143				

Table 1.2.3 — (Continued)

Atomic number (Z)	Symbol	Mass number (A)*	Isotopic weight relative to O ¹⁶ †	Error in isotopic weight × 10 ⁶ ‡	Binding energy of additional neutron, mev§	Packing fraction × 10 ³ ¶
56	Ba	<u>130</u>				
		<u>131</u>				
		<u>132</u>				
		<u>133</u>				
		<u>134</u>				
		<u>135</u>				
		<u>136</u>				
		<u>137</u>				
		<u>138</u>				
		<u>139</u>				
		<u>140</u>				
		<u>141</u>				
		<u>142</u>				
		<u>143</u>				
		<u>144</u>				
		<u>145</u>				
57	La	<u>137</u>				
		<u>138</u>				
		<u>139</u>				
		<u>140</u>				
		<u>141</u>				
		<u>142</u>				
		<u>143</u>				
		<u>144</u>				
		<u>145</u>				
58	Ce	<u>135</u>				
		<u>136</u>				
		<u>137</u>				
		<u>138</u>				
		<u>139</u>				
		<u>140</u>				
		<u>141</u>	140.95335	1100		-0.331
		<u>142</u>				
		<u>143</u>				
		<u>146</u>				
		<u>147</u>				
59	Pr	<u>140</u>				
		<u>141</u>				
		<u>142</u>				
		<u>143</u>				
		<u>144</u>				
		<u>145</u>				
		<u>146</u>				
		<u>147</u>				
60	Nd	<u>141</u>				
		<u>142</u>				
		<u>143</u>				
		<u>144</u>	143.95607	750		-0.305
		<u>145</u>				
		<u>146</u>				

Table 1.2.3 — (Continued)

Atomic number (Z)	Symbol	Mass number (A)*	Isotopic weight relative to O ¹⁶ †	Error in isotopic weight × 10 ⁶ ‡	Binding energy of additional neutron, mev§	Packing fraction × 10 ³ ¶
		147				
		148				
		149	148.96775	800	7.403	-0.216
		150	149.96878	780		-.208
		151				
61	Pm	143				
		144				
		145				
		146				
		147				
		148				
		149				
62	Sm	144				
		145				
		146				
		147				
		148				
		149				
		150				
		151				
		152				
		153				
		154				
63	Eu	147				
		149				
		150				
		151				
		152				
		153				
		154				
		155				
		156				
		157				
		158				
64	Gd	152				
		153				
		154				
		155				
		156				
		157				
		158				
		159				
		160				
65	Tb	152				
		153				
		154				
		155				

Table 1.2.3 — (Continued)

Atomic number (Z)	Symbol	Mass number (A)*	Isotopic weight relative to O ¹⁶ †	Error in isotopic weight × 10 ⁶ ‡	Binding energy of additional neutron, mev§	Packing fraction × 10 ³ ¶
66	Dy	<u>159</u>				
		<u>160</u>				
		<u>161</u>				
		<u>156</u>				
		<u>158</u>				
		<u>159</u>				
		<u>160</u>				
		<u>161</u>				
		<u>162</u>				
		<u>163</u>				
		<u>164</u>				
		<u>165</u>				
67	Ho	<u>160</u>				
		<u>161</u>				
		<u>162</u>				
		<u>163</u>				
		<u>164</u>				
		<u>165</u>				
		<u>166</u>				
68	Er	<u>162</u>				
		<u>163</u>				
		<u>164</u>				
		<u>165</u>				
		<u>166</u>				
		<u>167</u>				
		<u>168</u>				
		<u>169</u>				
		<u>170</u>				
		<u>171</u>				
69	Tm	<u>166</u>				
		<u>167</u>				
		<u>168</u>				
		<u>169</u>				
		<u>170</u>				
70	Yb	<u>168</u>				
		<u>169</u>				
		<u>170</u>				
		<u>171</u>				
		<u>172</u>				
		<u>173</u>				
		<u>174</u>				
		<u>175</u>				
		<u>176</u>				
		<u>177</u>				
71	Lu	<u>170</u>				
		<u>171</u>				
		<u>172</u>				
		<u>175</u>				

Table 1.2.3 — (Continued)

Atomic number (Z)	Symbol	Mass number (A)*	Isotopic weight relative to O ¹⁶ †	Error in isotopic weight 10 ⁶ ‡	Binding energy of additional neutron, mev§	Packing fraction × 10 ³ ¶
72	Hf	<u>176</u>				
		<u>177</u>				
		<u>174</u>				
		<u>175</u>				
		<u>176</u>	175.99234	1000		-0.0435
		<u>177</u>				
		<u>178</u>	177.99381	1230		-0.0348
73	Ta	<u>179</u>				
		<u>180</u>	180.00440	2000		+0.0244
		<u>181</u>				
		<u>176</u>				
		<u>177</u>				
		<u>178</u>				
		<u>180</u>				
74	W	<u>181</u>				
		<u>182</u>				
		<u>179</u>				
		<u>180</u>				
		<u>181</u>				
		<u>182</u>	182.0038	2100	8.912	0.0209
		<u>183</u>	183.00321	580	5.765	.0175
75	Re	<u>184</u>	184.0060	2100		.0326
		<u>185</u>				
		<u>186</u>				
		<u>187</u>				
		<u>188</u>				
		<u>183</u>				
		<u>184</u>				
76	Os	<u>185</u>				
		<u>186</u>				
		<u>187</u>				
		<u>188</u>				
		<u>189</u>				
		<u>190</u>				
		<u>191</u>				
77	Ir	<u>192</u>				
		<u>193</u>				
		<u>190</u>				
		<u>191</u>				
		<u>192</u>				
		<u>193</u>				
		<u>194</u>	194.02637	1000		0.136
78	Pt	<u>190</u>				
		<u>191</u>				
		<u>192</u>				

Table 1.2.3—(Continued)

Atomic number (Z)	Symbol	Mass number (A)*	Isotopic weight relative to O ¹⁶ †	Error in isotopic weight × 10 ⁶ ‡	Binding energy of additional neutron, mev§	Packing fraction × 10 ³ ¶
		193				
		<u>194</u>	194.02403	1000	6.137	0.124
		<u>195</u>	195.02642	800	7.413	.135
		<u>196</u>	196.02744	600		.140
		197				
		<u>198</u>				
		<u>199</u>				
79	Au	191				
		192				
		193				
		194				
		195				
		196				
		<u>197</u>				
		198				
		199				
		200				
80	Hg	<u>196</u>				
		197				
		<u>198</u>				
		<u>199</u>				
		<u>200</u>				
		<u>201</u>				
		<u>202</u>		κ		
		203	203.03550	κ		0.175
		<u>204</u>				
		205	205.03980	κ		0.194
81	Tl	198				
		199				
		200				
		201				
		202		κ		
		<u>203</u>	203.03499	κ	6.519	0.172
		<u>204</u>	204.03697	κ	7.478	.181
		<u>205</u>	205.03792	κ	6.230	.185
		<u>206</u>	206.04021	κ	6.798	.195
	AcC''	207	207.04189	κ	3.828	.202
	ThC''	208	208.04676	κ	4.936	.225
		209	209.05044	κ	3.772	.241
	RaC''	210	210.05537	κ		.264
82	Pb	199				
		200				
		201				
		202				
		203				
		<u>204</u>	204.03612	κ	6.323	0.177
		<u>205</u>	205.03831	κ	8.102	.187
		<u>206</u>	206.03859	κ	6.733	.187
		<u>207</u>	207.04034	κ	7.375	.195

Table 1.2.3 — (Continued)

Atomic number (Z)	Symbol	Mass number (A)*	Isotopic weight relative to O ¹⁶ †	Error in isotopic weight × 10 ⁶ ‡	Binding energy of additional neutron, mev§	Packing fraction × 10 ³ ¶		
83	RaD AcB ThB RaB	208	208.04140	κ	3.866	0.199		
		209	209.04623	κ	5.243	.221		
		210	210.04958	κ	3.782	.236		
		211	211.05450	κ	5.188	.258		
		212	212.05791	κ	3.921	.273		
		213	(213.06268)		4.964	.294		
		214	214.06633	κ		.310		
	Bi	197						
		198						
		199						
		200						
		204						
		206						
		207	(207.04285)		6.817	0.207		
		208	208.04451	κ	7.441	.214		
		209	209.04550	κ	4.629	.218		
		210	210.04951	κ	5.113	.236		
		211	211.05300	κ	4.378	.251		
		212	212.05728	κ	5.160	.270		
213		213.06072	κ	4.136	.285			
214		214.06526	κ		.305			
84	Po	203						
		205						
		206						
		207						
	AcC' ThC' RaC' AcA ThA RaA	208	208.04558		6.575	0.219		
		209	209.04750	κ	7.655	.227		
		210	210.04826	κ	4.564	.230		
		211	211.05234	κ	6.007	.248		
		212	212.05487	κ	4.312	.259		
		213	213.05922	κ	5.914	.278		
		214	214.06185	κ	4.098	.289		
		215	215.06643	κ	5.793	.309		
		216	216.06919	κ	4.312	.320		
		217	(217.07354)	84	5.364	.339		
		218	218.07676	κ		.352		
		85	At	207				
				208				
				210				
				211	(211.05317)	κ	5.029	0.252
212	(212.05675)			κ	6.035	.268		
213	(213.05925)			κ	4.880	.278		
214	214.06299			κ	5.914	.294		
215	215.06562			κ	4.592	.305		
216	216.06967			κ	5.960	.323		
217	217.07225			κ	4.517	.333		
218	218.07638	κ		.350				
86	Em	212	212.05621	κ		0.265		
		215	215.06562		6.612	.306		
		216	216.06750	κ	4.592	.312		

Table 1.2.3 — (Continued)

Atomic number (Z)	Symbol	Mass number (A)*	Isotopic weight relative to O ¹⁶ †	Error in isotopic weight × 10 ⁶ ‡	Binding energy of additional neutron, mev§	Packing fraction × 10 ³ ¶	
87	An Tn	217	217.07155	κ	6.537	0.330	
		218	218.07351	κ	4.405	.337	
		219	219.07776	κ	6.342	.355	
		220	220.07993	κ	4.713	.363	
	Rn	221	(221.08385)		5.774	.379	
		222	222.08663	κ		.390	
	Fr	217	(217.07221)	κ	5.355	0.333	
		218	218.07544	κ	6.472	.346	
		219	219.07747	κ	5.206	.354	
		220	220.08086	κ	6.361	.368	
		221	221.08301	κ	4.890	.376	
		222	(222.08674)	κ	12.80	.391	
		223	(223.08197)	κ	−2.074	.368	
		224	(224.09318)	κ		.4160	
88	Ra	219	219.07824	κ	7.189	0.357	
		220	220.07950	κ	5.327	.361	
		221	221.08276	κ	6.742	.374	
		222	222.08450	κ	5.215	.381	
	AcX ThX	223	223.08788	κ	6.379	.394	
		224	224.09001	κ	5.169	.402	
	Ra	225	225.09344	κ	6.221	.415	
		226	226.09574	κ	4.564	.424	
	MsTh ₁	227	227.09982	κ	6.221	.440	
		228	228.10212	κ		.448	
89	Ac	221					
		222	222.08692	κ	6.798	0.392	
		223	223.08860	κ	5.690	.397	
		224	224.09147	κ	6.733	.408	
		225	225.09322	κ	5.299	.414	
		226	226.09651	κ	6.556	.427	
	Ac MsTh ₂	227	227.09845	κ	5.001	.434	
		228	228.10206	κ		.448	
	90	Th	223	223.09036	κ	7.617	0.405
			224	224.09116	κ	5.895	.407
225			225.09381	κ	7.022	.417	
226			226.09525	κ	5.467	.421	
RdAc RdTh		227	227.09836	κ	7.012	.433	
		228	228.09981	κ	5.588	.438	
		229	229.10279	κ	6.565	.449	
		230	230.10472	κ	5.149	.455	
		UY Th	231	231.10817	κ	6.342	.468
			232	232.11034	κ	5.122	.476
UX ₁		233	233.11382	κ	5.867	.488	
		234	234.11650	κ	4.759	.498	
		235	235.12037	κ		.512	
91		Pa	226	226.09823	κ	7.152	0.435
	227		227.09953	κ	6.063	.438	
	228		228.10200	κ	7.143	.447	
	229		229.10331	κ	5.867	.451	

Table 1.2.3 — (Continued)

Atomic number (Z)	Symbol	Mass number (A)*	Isotopic weight relative to O ¹⁶ †	Error in isotopic weight × 10 ⁶ ‡	Binding energy of additional neutron, mev§	Packing fraction × 10 ³ ¶
92	U	230	230.10599	κ	6.649	0.461
		231	231.10783	κ	5.458	.467
		232	232.11095	κ	6.919	.478
		233	233.11250	κ	5.234	.483
		234	234.11586	κ	5.867	.495
		235	235.11854	κ		.504
	U ^{III}	227	227.10166	κ	7.748	0.448
		228	228.10232	κ	6.156	.449
		229	229.10469	κ	7.580	.457
		230	230.10553	κ	5.895	.459
		231	231.10818	κ	7.161	.468
		232	232.10947	κ	6.072	.472
		233	233.11193	κ	6.631	.480
		234	234.11379	κ	5.342	.486
		235	235.11704	κ	6.426	.498
		236	236.11912		5.392	.505
	U ^I	237	237.12231	κ	5.923	.516
		238	238.12493	κ	4.862	.525
		239	239.12869	κ		.538
93	Np	231	231.11026	κ	6.407	0.477
		232	(232.11236)	κ	7.562	.484
		233	233.11322	κ	6.072	.486
		234	(234.11568)	κ	6.919	.494
		235	235.11723	κ	5.625	.499
		236	236.12017		7.050	.509
		237	237.12158	κ	5.048	.513
		238	238.12514	κ	6.351	.526
		239	239.12730	κ	5.830	.533
		240	240.13002	κ	6.053	.542
		241	241.13250	κ		.550
94	Pu	232	232.11338	κ	6.342	0.489
		233	(233.11555)	κ	7.794	.496
		234	234.11616	κ	6.240	.496
		235	235.11844	κ	7.264	.504
		236	236.11962	κ	6.221	.507
		237	(237.12192)	κ	6.724	.514
		238	238.12368	κ	5.709	.520
		239	239.12653	κ	6.416	.529
		240	240.12862		5.644	.536
		241	241.13154	κ	5.951	.546
		242	242.13413	κ	5.318	.554
		243	243.13740	κ		.565
95	Am	239	239.12740	κ	5.728	0.533
		240	(240.13023)	κ	7.171	.543
		241	241.13151	κ	5.215	.546
		242	242.13489	κ	6.528	.557
		243	243.13686	κ		.563
96	Cm	238	238.12713	κ	6.240	0.534
		239	239.12941	κ	7.403	.541

Table 1.2.3 — (Continued)

Atomic number (Z)	Symbol	Mass number (A)*	Isotopic weight relative to $O^{16}\dagger$	Error in isotopic weight $\times 10^6\dagger$	Binding energy of additional neutron, mev§	Packing fraction $\times 10^3\P$
		240	240.13044	\approx	6.696	0.544
		241	(241.13233)	\approx	6.528	.549
		242	242.13420	\approx	5.811	.555
		243	243.13694	\approx	5.960	.564
		244	244.13952	\approx		.572
97	Bk	243	243.13860	\approx	5.923	0.570
		244	(244.14122)	\approx	7.366	.579
		245	245.14229	\approx	5.402	.581
		246	246.14547	\approx		.591
98	Cf	243	(243.14131)	\approx	7.617	0.582
		244	244.14211	\approx	6.901	.582
		245	(245.14368)	\approx	6.733	.586
		246	246.14543	\approx		.591

* Numbers underlined are isotopes which occur naturally

† Figures in parentheses () indicate an uncertainty in the value since the only available input data are uncertain

‡ All errors marked \approx are ~ 1000 based on Pb^{208} error

§ See Eq. (6)

¶ See Eq. (3)

Table 1.2.4 — See page 158.

Table 1.2.5 — Maximum Ranges of Gross Fission Recoils

(Segrè and Wiegand, Phys. Rev., 70, 808, 1946)

Material	Range, mg/cm ²
Collodion	2.6
Al	3.7
Cu	5.2
U ₃ O ₈	10.0
U	12.6

Table 1.2.6—Spontaneous and Gamma-ray-induced Fission Data

(Column 2 data from LA-1010, Chapter 6, Emilio Segrè, Table 6.3-14; column 3 data from W. Koch, Phys. Rev., 77, 329, 1950)

Isotope	Spontaneous fission decay constant, fissions/(gm)(sec)	Gamma-ray-induced fission threshold, mev
Ra ²²⁶	(<0.6)	
Th ²³⁰	$< 3.8 \times 10^{-4}$	
Th ²³²	4.2×10^{-5}	5.4 ± 0.2
Pa ²³¹	5×10^{-3}	
U ²³²	16	
U ²³³	$< 2 \times 10^{-4}$	5.2 ± 0.3
U ²³⁴	$< 9 \times 10^{-3}$	
U ²³⁵	$(3.0 \pm 1.7) \times 10^{-4}$	5.3 ± 0.3
U ²³⁶	$(-6 \pm 16) \times 10^{-2}$	
U ²³⁸	$(6.90 \pm 0.24) \times 10^{-3}$	5.1 ± 0.2
Np ²³⁷	$\leq 1.4 \times 10^{-3}$	
Np ²³⁹	< 11	
Pu ²³⁸	2.14×10^3	
Pu ²³⁹	1.0×10^{-2}	5.3 ± 0.3
Pu ²⁴⁰	4.61×10^2	
95 ²⁴¹	(46)	

Table 1.2.7 — Fission Yields*

(Coryell and Sugarman, Radiochemical Studies: The Fission Products, Book 2)

Nuclide	Half-life	Slow-neutron fission			Fast-neutron fission			σ_a , b† (2200 m/sec)
		U ²³⁵	Pu ²³⁹	U ²³³	Th ²³²	U ²³⁸	Pu ²³⁹	
Zn ⁷²	49.0 hr	1.5×10^{-6}	1.1×10^{-4}		1.3×10^{-4}			
Ga ⁷³	5.0 hr	1.0×10^{-4}						
Ge ⁷⁷	12 hr	3.7×10^{-3}		0.008	0.091	4.3×10^{-3}		
As ⁷⁷	40 hr	9.1×10^{-3}		.018				
Ge ⁷⁶	2.1 hr	0.02						
As ⁷⁶	90 min	.02						
Se ⁸¹	57 min	.008						
Se ⁸¹	13.6 min	.133						
Br ⁸²	36.0 hr	3.5×10^{-5} (i)						
Se ⁸³	25 min	0.21						
Br ⁸³	2.4 hr	.48	0.080	0.70	2.4			
		.40						
Kr ⁸³	Stable	.586						
Br ⁸⁴	33 min	.65						205 ± 10
Kr ⁸⁴	Stable	1.09						
Kr ⁸⁵	4.36 hr	33% of Kr ⁸⁵						< 2
Kr ⁸⁵	9.4 yr	0.317						< 15
		.24						
Kr ⁸⁶	Stable	2.09						< 2
Rb ⁸⁶	19.5 days	3.1×10^{-5} (i)						
		1.8×10^{-4} (i)						
Kr ⁸⁷	78 min	70% of Kr ⁸⁷						
Sr ⁸⁸	53 days	4.6	1.8	5.6	6.0	3.3		
		3.2		4.1				
Sr ⁹⁰	19.9 yr				5.9			$\geq 1.0 \pm 0.6$
Sr ⁹¹	9.7 hr	5.0	2.3		5.7			
Y ⁹¹	57 days	5.9	2.8	4.1				
		4.0						

Table 1.2.7 — (Continued)

Nuclide	Half-life	Slow-neutron fission			Fast-neutron fission			σ_f , b† (2200 m/sec)
		U ²³⁵	Pu ²³⁹	U ²³³	Th ²³²	U ²³⁸	Pu ²³⁹	
Sr ⁸²	2.7 hr	5.0						
Y ⁸⁴	16.5 min	5						
Zr ⁸⁶	65 days	6.0	5.6	5.7		7.3	5.6	
		6.4; 3.2		3.9				
Zr ⁸⁷	17.0 hr	6.2	5.3		4.9		5.2	
		6.1						
Mo ⁸⁹	67 hr	6.2	6.1	4.7	2.65	5.9	5.9	
Rh ⁹²	210 days	$< 5 \times 10^{-7}$ (I)						
Ru ¹⁰³	42 days	3.7	5.5	0.85	0.18	7.4		
		0.84		.21				
Ru ¹⁰⁶	4.5 hr	.9						
Rh ¹⁰⁶	36.5 hr		3.7		0.07			
Ru ¹⁰⁶	1.0 yr	0.52	4.7	0.24	.052	2.7		
		.15		.064				
Pd ¹⁰⁹	13 hr	.028	1.0	.047	0.047		1.7	
		.017						
Ag ¹¹¹	7.6 days	.018	0.27	0.022	0.044	0.072		
		.016		.015				
Pd ¹¹²	21 hr	8.3×10^{-3}	0.10	.014	0.058			
		0.011						
Cd ¹¹³	43 days	8×10^{-4}	3×10^{-3}	0.001		6×10^{-3}		
Cd ¹¹³	2.33 days	0.011	0.045	.016	0.053	0.057		
		.020						
Cd ¹¹⁷	2.83 hr	.010						
Sn ¹²¹	26.4 hr	.014	0.041	0.018				
Sn ¹²³	130 days	1.2×10^{-3}		2.5×10^{-3}				
		8.5×10^{-4}						
Sn ¹²⁵	10.0 days	0.012	0.068	0.054				
		4.4×10^{-3}						
Sb ¹²⁵	~ 2.7 yr	0.023						
		.017						
Sn ⁽¹²⁶⁾	70 min	.1						
Sb ¹²⁷	93 hr	.094	0.37	0.092		0.12		
Te ¹²⁷	90 days	.033		.067				
		.015						
Te ¹²⁹	32 days	.19		0.22				
		.09						
Xe ¹²⁹	Stable	$< 4 \times 10^{-4}$						45 ± 15
Te ¹³¹	30 hr	0.44						
I ¹³¹	8.0 days	2.8	3.6	2.7	0.65			≥ 600 ± 300
		2.23		2.4				
Xe ¹³¹	Stable	2.80						120 ± 15
Te ¹³²	77 hr	4.4	4.9	4.9	1.6			
		4.9						
		3.4						
		2.1						
Xe ¹³²	Stable	4.17						< 5
Te ¹³³	66 min	4.5						
I ¹³³	22.4 hr	4.6	5.0					
		1.2 (I)						
Xe ¹³³	5.27 days	6.29						
Cs ¹³³	Stable	103% of Cs ¹³⁷						29.0 ± 1.5
Te ¹³⁴	44 min	6.9						
I ¹³⁴	52.5 min	5.7						
		1.0 (I)						
Xe ¹³⁴	Stable	7.41						< 5
I ¹³⁶	6.68 hr	5.6	5.5					
Xe ¹³⁶	9.2 hr	6.7‡						3.5 × 10 ⁶
		0.3 (I)						
Cs ¹³⁶	2.1 × 10 ⁶ yr	128% of Cs ¹³⁷ 110% of Cs ¹³⁷						≥ 15 ± 8
I ¹³⁶	86 sec	3.1	1.9	1.7				
Xe ¹³⁶	Stable	6.14						< 5
Cs ¹³⁶	13.7 days	6.2×10^{-3} (I)	0.09 (I)					

Table 1.2.7 — (Continued)

Nuclide	Half-life	Slow-neutron fission			Fast-neutron fission			σ_a , b† (2200 m/sec)
		U ²³⁵	Pu ²³⁹	U ²³³	Th ²³²	U ²³⁸	Pu ²³⁹	
Cs ¹³⁷	33 yr				5.8			
Ba ¹³⁹	85.0 min	6.3	5.4			5.1		$\geq 4 \pm 1$
		6.1						
Ba ¹⁴⁰	12.80 days	6.17	5.36	6.0	5.5	6.1	5.0	
		5.82		6.7		4.2		
		5.6						
La ¹⁴⁰	40.0 hr	<0.2 (I)						$\geq 3 \pm 2$
Ba ¹⁴¹	18 min	4.6						
Ce ¹⁴¹	30 days	5.7	4.9		~6			
La ¹⁴³	19 min	~3.8						
Ce ¹⁴³	33 hr	5.4	5.1					
Nd ¹⁴³	Stable	5.40						
Ce ¹⁴⁴	275 days	5.3	3.7	3.4	6.2			290 ± 30
		2.9		2.2				
Nd ¹⁴⁴	Stable	4.64						4.8 ± 0.5
Nd ¹⁴⁶	Stable	3.62						52 ± 4
Nd ¹⁴⁶	Stable	2.81						9.8 ± 0.8
Nd ¹⁴⁷	11.0 days	2.6						
Pm ¹⁴⁷	~4 yr	~0.6		0.6				$\geq 60 \pm 20$
Nd ¹⁴⁸	Stable	1.64						3.3 ± 1.0
Pm ¹⁴⁹	47 hr	1.3						
Nd ¹⁵⁰	Stable	0.658						2.9 ± 1.5
Sm ¹⁵¹	~1000 yr	.445						$\geq 7000 \pm 2000†$
Sm ¹⁵²	Stable	.279						$\geq 150 \pm 40$
Sm ¹⁵³	47 hr	.15	0.39	0.078			0.48	
Sm ¹⁵⁴	Stable	.0908						$\geq 5.5 \pm 1.1$
Sm ¹⁵⁵	25 min	0.031	0.21					
Eu ¹⁵⁶	2.0 yr	~.03						$\geq 14000 \pm 4000†$
Sm ¹⁵⁶	~10 hr	.012						
Eu ¹⁵⁶	15.4 days	.013	0.12			0.063		
		.014						
Eu ⁽¹⁵⁷⁾	15.4 hr	7.4×10^{-3}						
Gd ¹⁵⁷	Stable	0.0150						$160000 \pm 60000†$
Eu ⁽¹⁵⁸⁾	60 min	2×10^{-3}						
Gd ¹⁵⁸	Stable	0.0084						$\geq 4 \pm 2$
Gd ¹⁶⁰	Stable	.0027						$\geq 1.5 \pm 0.5$

* The independent or direct yield is designated "(I)." Other yields are total values, i.e., the independent yield plus the yield from precursors in the decay chain. Some of the yields given in the table were measured relative to 8.0-day I¹³¹. C. D. Coryell (private communication) now believes a better value for 8.0-day I¹³¹ is 3.1% (compared to the old value of 2.8%). Hence, all yields based on I¹³¹ should be increased by the factor 1.107. For detailed references, see Reference (18)

† Values of σ_a 's taken from Reference (19) unless otherwise noted

‡ The value for the total yield of Xe¹³⁶ is still somewhat in doubt. The value of 6.7% quoted here is from WAPD-RM-95

† For reactor neutrons

Table 1.2.8 — Kinetic Energy of the Fission Fragments

	U ²³⁵	U ²³⁸	Pu ²³⁹
Most probable energy of light fragment, mev	91.2	92.7	93
Most probable energy of heavy fragment, mev	55.5	59	65
Width of high energy peak, mev	14	12	12
Width of low energy peak, mev	22	20	20
Most probable total kinetic energy, mev	147.5	151.5	156
Most probable mass ratio	1.60	1.49	1.32

Table 1.2.9 — Beta-emitters Having Neutron-emitting Daughters

Isotope	Half-life, sec
Br ⁸⁷	55.6
I ¹³⁷	22.0
Br ^{(89)*}	4.51
(Te ¹³⁶)*	1.52

* Data in parentheses are uncertain

Table 1.2.10 — Delayed-neutron Data

Mean life of delayed neutrons,* sec	Energy of delayed neutrons,† kev	Yield per 10 ⁴ prompt neutrons				
		Thermal fission			Fast fission	
		U-235*	U-233‡	Pu-239§	U-238¶	Th-232**
80.2	250	2.5	1.8	1.4	10.8	43.7
31.7	570	16.6	5.8	10.5	90.3	102.0
6.51	412	21.3	8.6	12.6††	60.2	97.0
2.19	670	24.1	6.2	11.9‡‡	120.4	61.1
0.62	400	8.5	1.8		38.5	16.5
.07		2.5				
TOTAL		75.5	24.2	36.4§§	[320]¶¶	[320]¶¶

* Hughes, Dabbs, Kahn, and Hall, Phys. Rev., 73, 111, 1948

† Average of values from Hughes et al (footnote *) and Burgy, Mon S-29, 1945

‡ Hughes, Dabbs, and Kahn, CP-3147, 1945; absolute value based on U-233/U-235 = 0.33, excluding 0.07 sec mean life

§ Redman and Saxon, CK-P-2318, 1944, and Feld and de Hoffman, LA-231, 9145; absolute value based on Pu/U-235 = 0.5, excluding 0.07 sec mean life

¶ Sun et al, Phys. Rev., 79, 3, 1950; fission by neutrons of maximum energy 14 mev, absolute yield is approximate based on 0.08 ± 0.03 delayed neutron per fission and $\nu \sim 2.5$

** Based on 7.5 sec mean life

†† Based on composite 1.6 sec mean life

‡‡ Ratio of percentage yield of delayed neutrons for fast and thermal fission = $Y_F/Y_{Th} = 0.93 \pm 0.07$, ORNL-517, 1949

§§ Value uncertain

Table 1.2.11—Distribution of Energy in Slow-neutron Fission of U^{235}
(BNL-152, Jan. 1952)*

	Instantaneous, mev	Delayed, mev	Totals, mev
Localized in space	Fission-product kinetic energy = 168 ± 5	Fission product betas = 7^*	~ 175
Spread out in space	Neutron kinetic energy = 5 ± 0.5 Fission gammas = 4.6 ± 1	Fission product gammas = 6^*	~ 16
Total	~ 178	13 ± 2	~ 191
Neutrino energy, 11 mev (not available as heat source) ²⁴			~ 11
			Total ~ 202 mev

* The organization of the table was suggested by a table of John R. Stehn based on data from Old and Weil, TID 65, 1948. The division of the beta and gamma fission product is also from the latter source

Table 1.2.12 — Collision Parameters

Element	M	ξ^*	$1 - \alpha$	$\log_e 1/\alpha$	$\overline{\cos \theta}$	Number of collisions from 2 mev to thermal
H	1	1.000	1.000	∞	0.667	18
D	2	0.725	0.889	2.20	.333	25
He	4	.425	.640	1.022	.167	43
Li	7	.268	.438	0.575	.0954	67
Be	9	.209	.360	.446	.0743	86
C	12	.158	.284	.334	.0556	114
O	16	.120	.220	.250	.0417	150
Na	23	.0845	.165	.174	.0290	213
U	238	.00838	.0167	.0169	.00280	2148
Large M	A	$2/(A + \frac{2}{3})$	$4/(A + 2)$	$4/(A + 2)$	$\frac{2}{3} A$	$9A + 6$

$$*\xi = 1 + \frac{\alpha}{1 - \alpha} \ln \alpha; \alpha = \left(\frac{A - 1}{A + 1} \right)^2$$

Table 1.2.13 — $\sigma_e(1 - \overline{\cos \theta})$ for Some Light Elements
(LA-1339)

Scatterer	$\sigma_e(1 - \overline{\cos \theta}), b$
Be	1.01
C	1.47
Al	1.70
Cr	1.93
Fe	1.60
Ni	1.40
Cu	1.43

Table 1.2.14—Transport Cross Sections

(H. Feshbach, AECD-2904, The experimental work was done by Barschall, Battat, Bright, Graves, Jorgensen, and Manley at Los Alamos)

Transport cross sections, barns, for neutron energy of				
Element	0.2 mev	0.6 mev	1.5 mev	3.0 mev
Be		3.40	1.40	
B ¹⁰		3.9	2.1	
B ¹¹		2.1	2.2	
C		2.8	1.8	
Al		3.0	1.7	1.4
Fe	3	2.0	2.2	2.0
Pb	7	3.4	3.4	3.8
W	6	4.7	4.7	4.1
Au	6.4			
Ta*			3.9	
Cu*			2.2	
Ni*			2.3	
Co*			2.2	

* These data not contained in AECD-2904

Table 1.2.15 — Inelastic Cross Sections

(NYO-636, Final Report of the Fast Neutron Data Project and Byster and Carter,
private communication from Los Alamos)

Element	Incident neutron energy (E), mev	Approximate threshold energy of detector (E_t), mev	Cross section for scattering from energy E to below E_t , $\sigma_{in}(E, E_t)$, * barns	Reference
Be	14	3	0.16 ± 0.07	(35)
		11	$.82 \pm .03$	
B	14	3	$.24 \pm .04$	(35)
		11	$.69 \pm .10$	
C	2.5	2.5	< 0.006	(36)
	14	11	0.85 ± 0.02	(35)
F	2.5	2.5	$.62 \pm .01$	(36)
Mg	2.5	2.5	$1.0 \pm .15$	(36)
Al	Fission- spectrum neutrons	0.4	0.12	(37)
		.7	.37	
		~3	.73	
	14	3	0.62 ± 0.07	(35)
		11	$1.06 \pm .05$	
S	2.5	2.5	$0.44 \pm .06$	(36)
Fe	Fission- spectrum neutrons	0.4	$.265 \pm .04$	(37)
		.7	0.70	
		~3	1.30	
	1.5	0.5	0	(38)
		.9	0.6	
	3.0	.75	.3	
		1.50	.7	
		2.25	1.1	
	14	2	0.78 ± 0.03	(35)
		3	$1.21 \pm .03$	
		11	$1.45 \pm .02$	
Co	1.5	0.5	(0)	(38)
		.9	(0.2)	
		1.3	(.8)	
Ni	Fission- spectrum neutrons	0.4	.286	(37)
		.7	.72	
		~3	1.43	
	1.5	0.5	(0)	(38)
		.9	(0.1)	
		1.3	(.6)	
Cu	Fission- spectrum neutrons	0.4	.31	(37)
		.7	.91	
		~3	1.56	
	1.5	0.5	(0.3)	(38)
		.9	(.6)	
		1.3	(.9)	
	3.0	0.75	(.6)	
		1.50	(1.3)	
		2.25	(1.5)	
Zn	Fission- spectrum neutrons	0.4	0.313	(37)
		.7	.95	

Table 1.2.15 — (Continued)

Element	Incident neutron energy (E), mev	Approximate threshold energy of detector (E_t), mev	Cross section for scattering from energy E to below E_t , $\sigma_{\text{in}}(E, E_t)$, * barns	Reference
As	Fission-spectrum neutrons	0.4 .7 ~3	0.86 1.67 2.03	(37)
Zr	Fission-spectrum neutrons	~3	1.70	(37)
Cd	Fission-spectrum neutrons	0.4 .7 ~3	0.67 1.54 2.08	(37)
	14	2 3 11	1.14 ± 0.04 $1.66 \pm .07$ $1.89 \pm .06$	(35)
Sn	Fission-spectrum neutrons	0.4 .7 ~3	0.38 ± 0.05 1.15 2.07	(37)
Ta	1.5	0.5 .9 1.3	(1.4) (2.0) (2.7)	(38)
W	Fission-spectrum neutrons	0.4 .7 ~3	1.09 2.18 2.75	(37)
	1.5	0.5 .9	0.9 2.1	(38)
	3.0	.75 1.50 2.25	1.4 2.4 2.8	
Au	Fission-spectrum neutrons	0.4 .7 ~3	1.01 2.06 2.68	(37)
	3.0	0.75 1.50 2.25	(2.1) (2.8) (3.0)	(38)
	14	2 3 11	1.47 ± 0.10 $2.06 \pm .09$ $2.51 \pm .04$	(35)
Pb	Fission-spectrum neutrons	0.4 .7 ~3	$0.25 \pm .07$ 0.745 2.24	(37)
	1.5	0.5 .9	0 0.4	(38)
	3	.75 1.50 2.25	.7 1.2 1.6	
	2.5	1 2.5	0.55 1.3 ± 0.5	(39) (40)
	14	2 3 11	$0.91 \pm .06$ $2.29 \pm .04$ $2.56 \pm .04$	(35)
	14.5	3 11	$2.20 \pm .17$ $2.29 \pm .12$	

Table 1.2.15 — (Continued)

Element	Incident neutron energy (E), mev	Approximate threshold energy of detector (E_t), mev	Cross section for scattering from energy E to below E_t , $\sigma_{ln}(E, E_t)$,* barns	Reference
Bi	Fission-spectrum neutrons 2.5 14	0.4	$0.20 \pm .05$	(37)
		.7	0.743	
		~3	2.33	
		1	0.64	(39)
		2	1.03 ± 0.11	(35)
		3	$2.28 \pm .08$	
		11	$2.56 \pm .05$	

* The values in parentheses have not been corrected for the effects of multiple scattering in the target

Table 1.2.16 — (n,2n) Cross Sections at 14 Mev

Target isotope	Cross section (isotopic), barns
Cu ⁶³	0.51
Cu ⁶⁵	.97
As ¹⁰⁷	.56*
As ¹⁰⁹	1.00
U ²³⁸	0.4 ± 0.3 †

* For production of 24.5-min isomer

† See reference (49)

Table 1.2.17 — See page 351.

Table 1.2.18 — Oxygen (n,p) Cross Sections

Isotope	Threshold energy, mev	σ (n,p)	Reference
O ¹⁶	9.5	0.014 mb	(52) (53)
O ¹⁷	7.9	.010 b*	(54)

* This value is reliable only to within a factor of 10

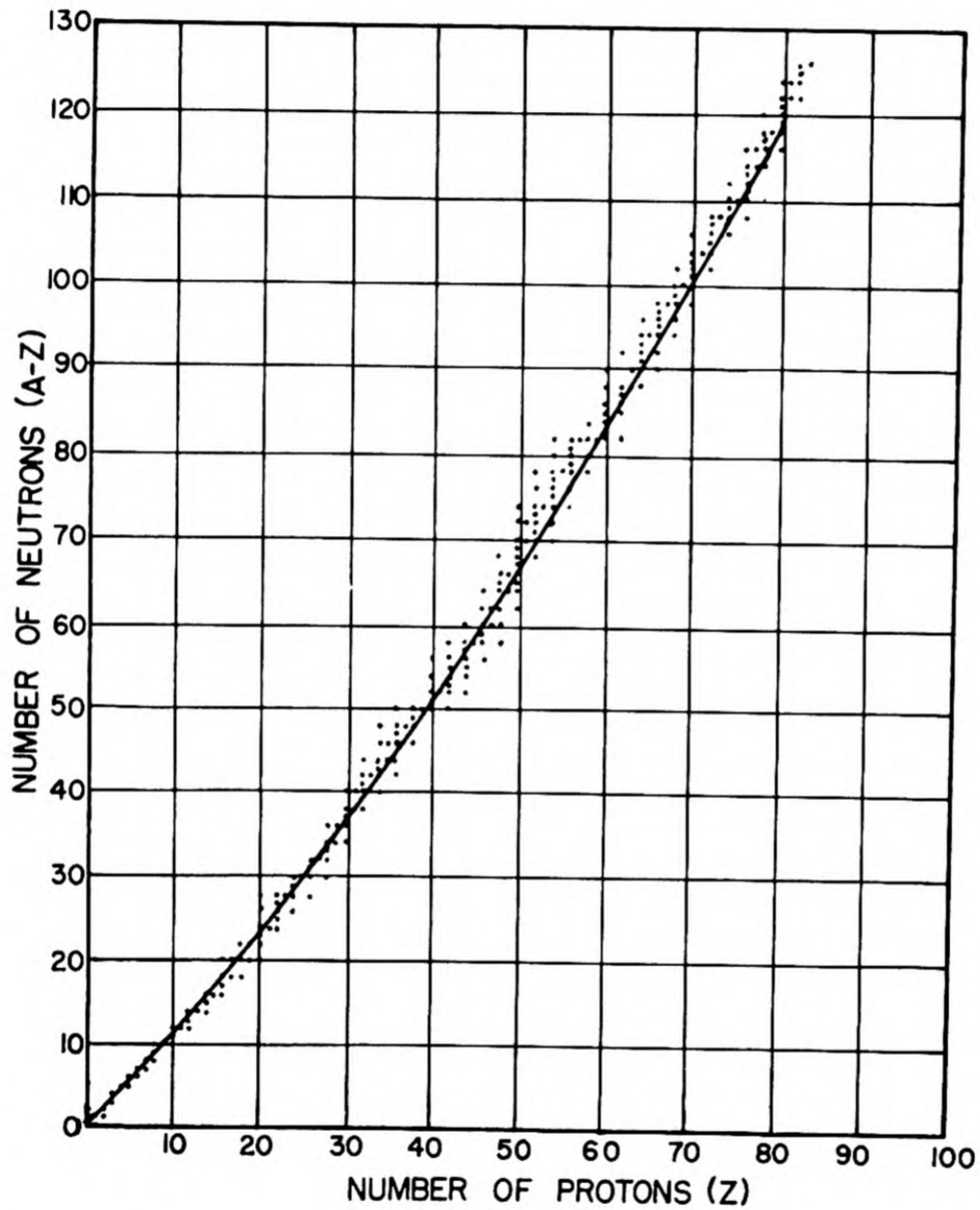


Fig. 1.2.1 — Number of Neutrons ($A-Z$) vs Number of Protons (Z) for Stable Nuclei. Solid line is a plot of Eq. (5a). Reprinted from the *Elements of Nuclear Reactor Theory*, by S. Glasstone and M. Edlund. Copyright, 1952. By permission from D. Van Nostrand Company, Inc., New York.

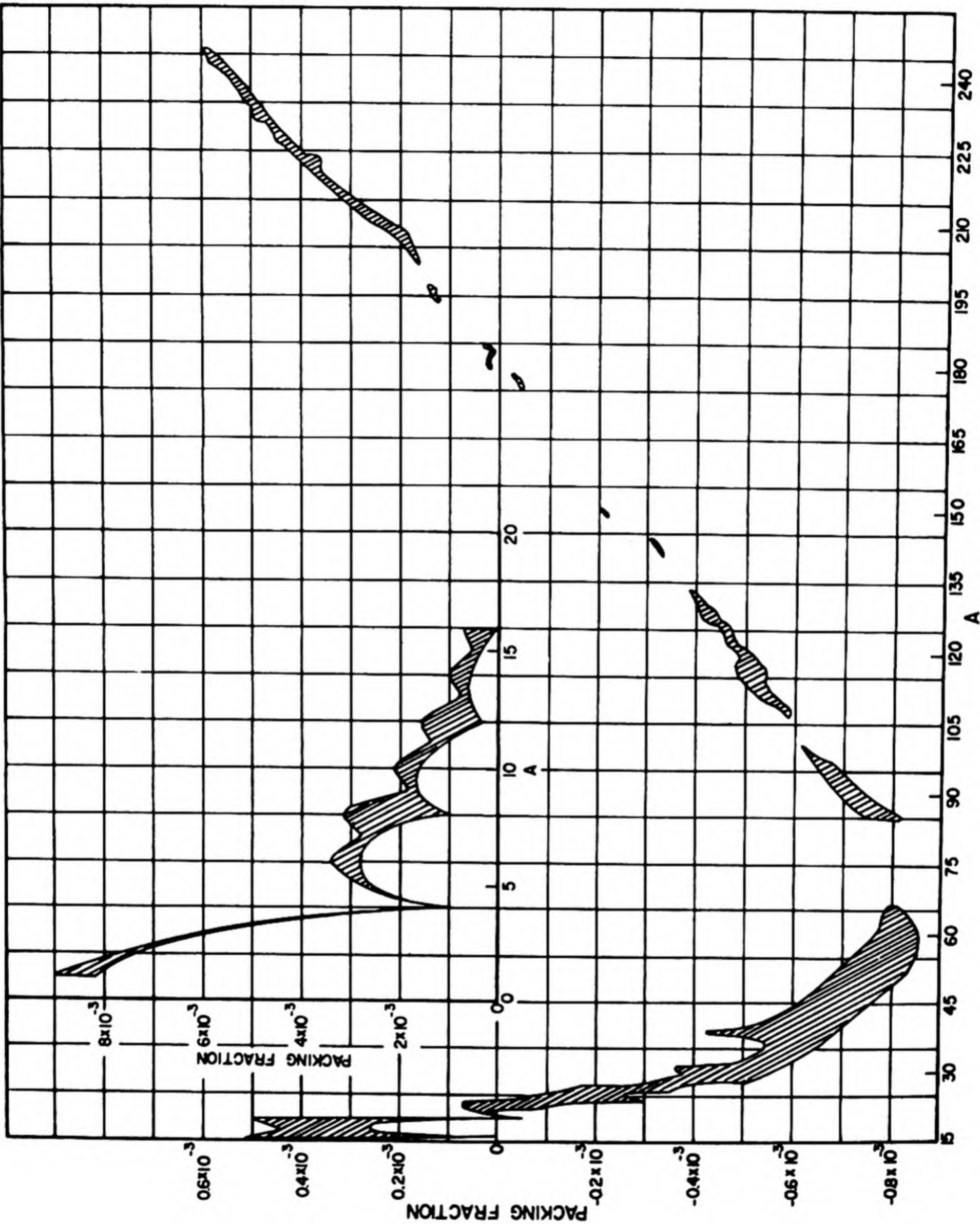


Fig. 1.2.2 — Packing Fraction Versus A. Submitted by Nuclear Development Associates, Inc., Jan. 15, 1953. The packing fractions of several isobars of a given A are available from Table 1.2.3; the spread of packing fraction values is illustrated.

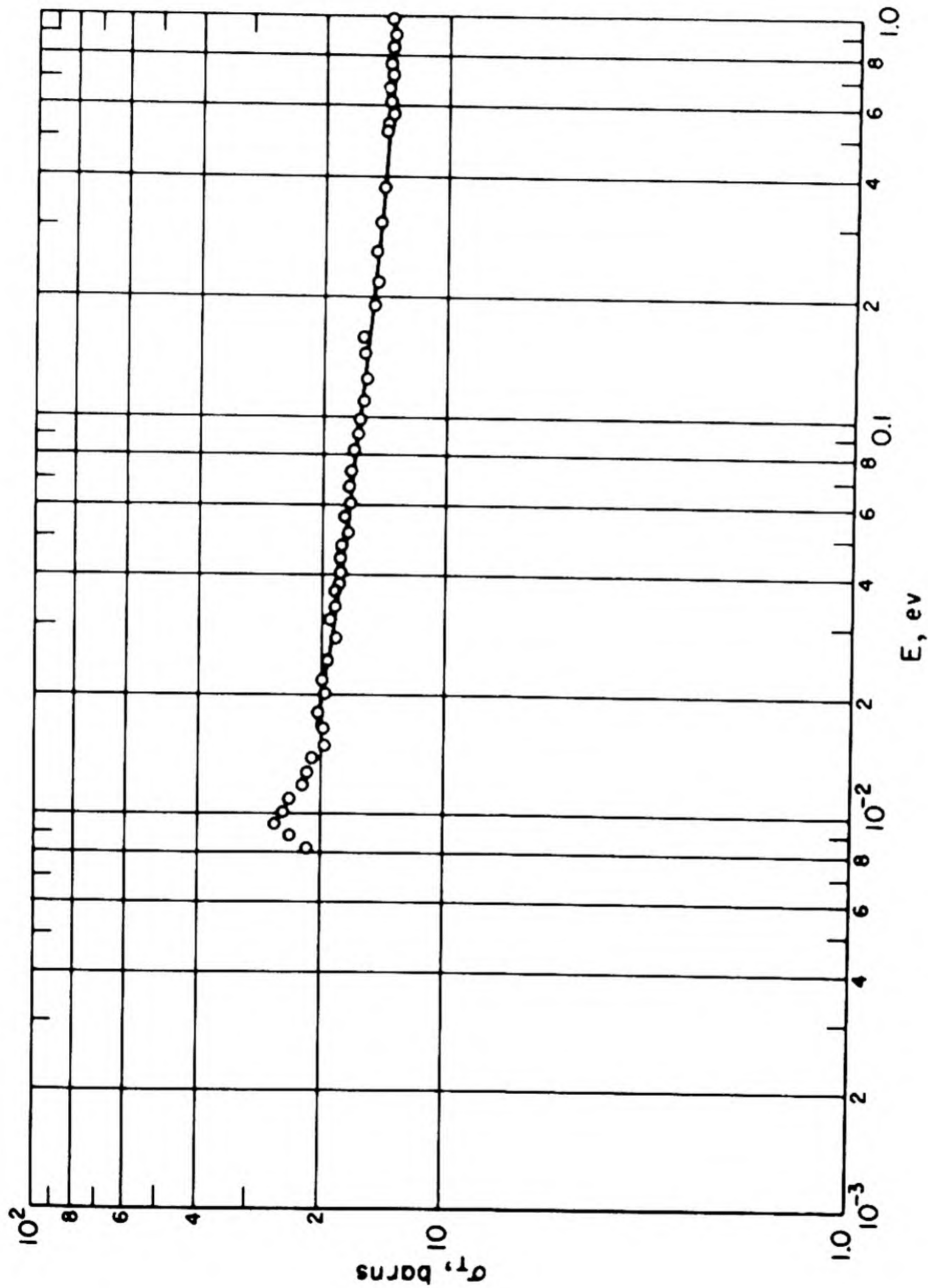


Fig. 1.2.3—Total Cross Section of ^{232}Th . Reprinted from BNL-170.

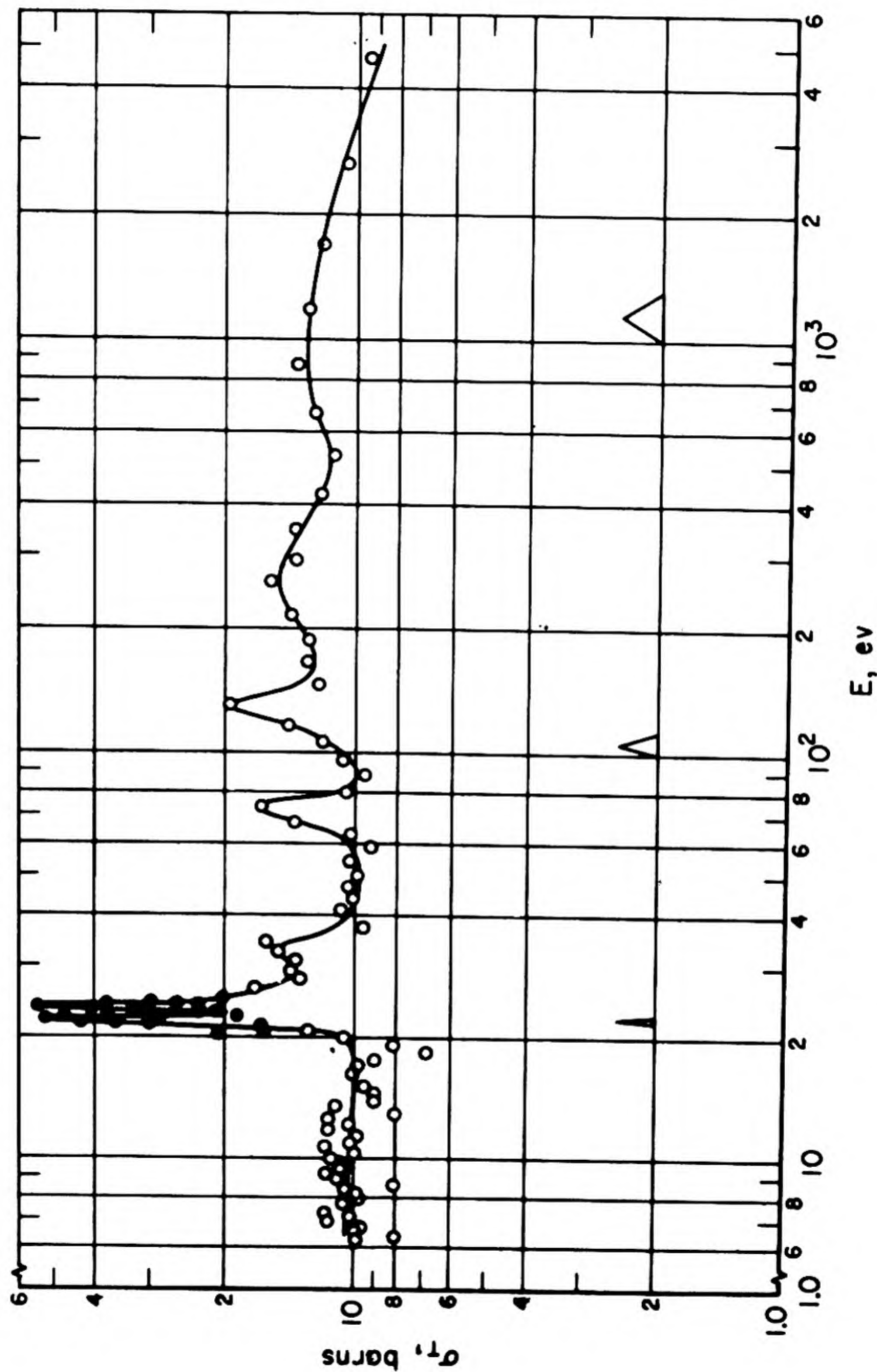


Fig. 1.2.4—Total Cross Section of ^{232}Th . Reprinted from BNL-170A.

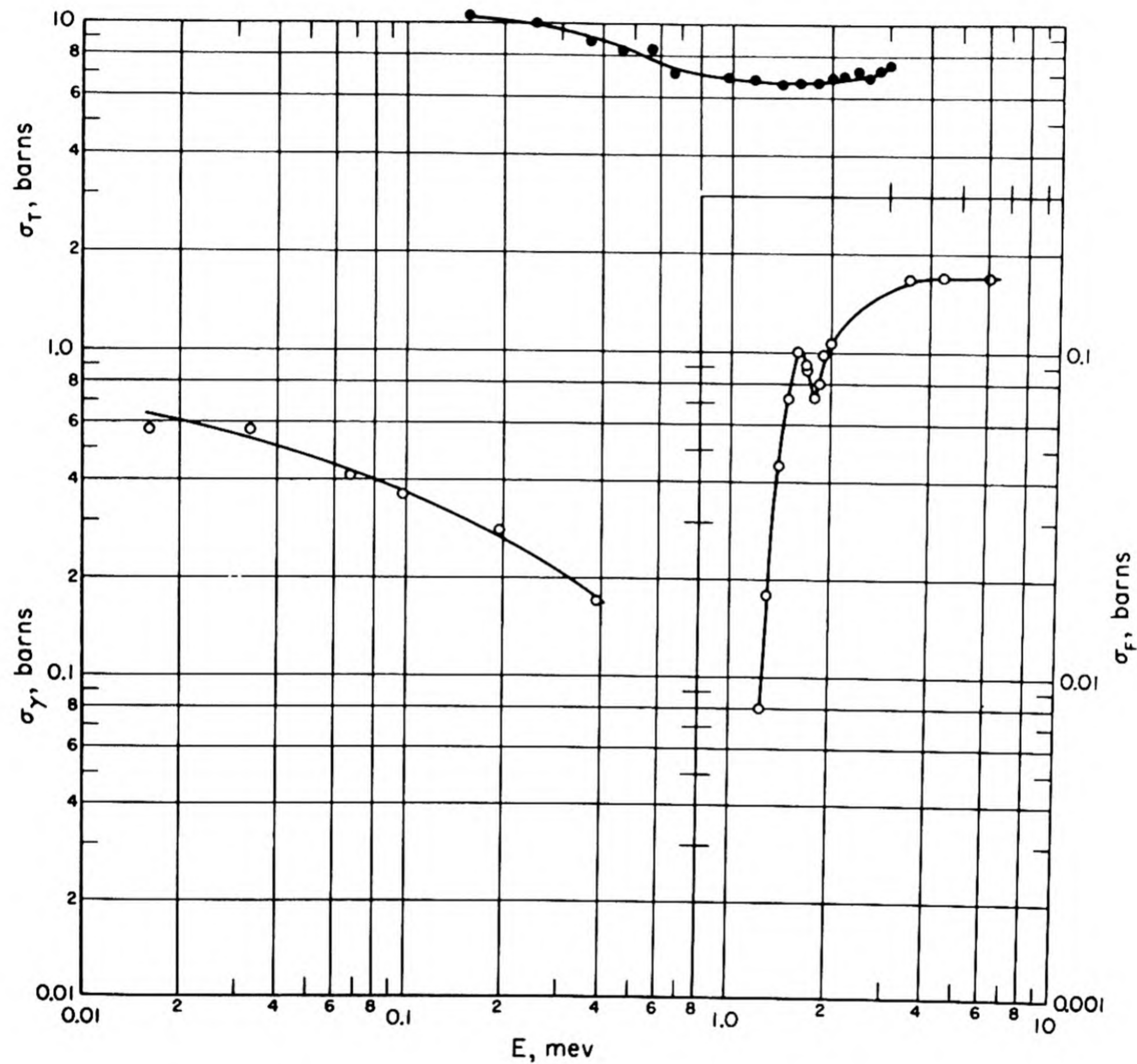


Fig. 1.2.5— Total, Capture, and Fission Cross Section of ^{232}Th . Reprinted from BNL-170.

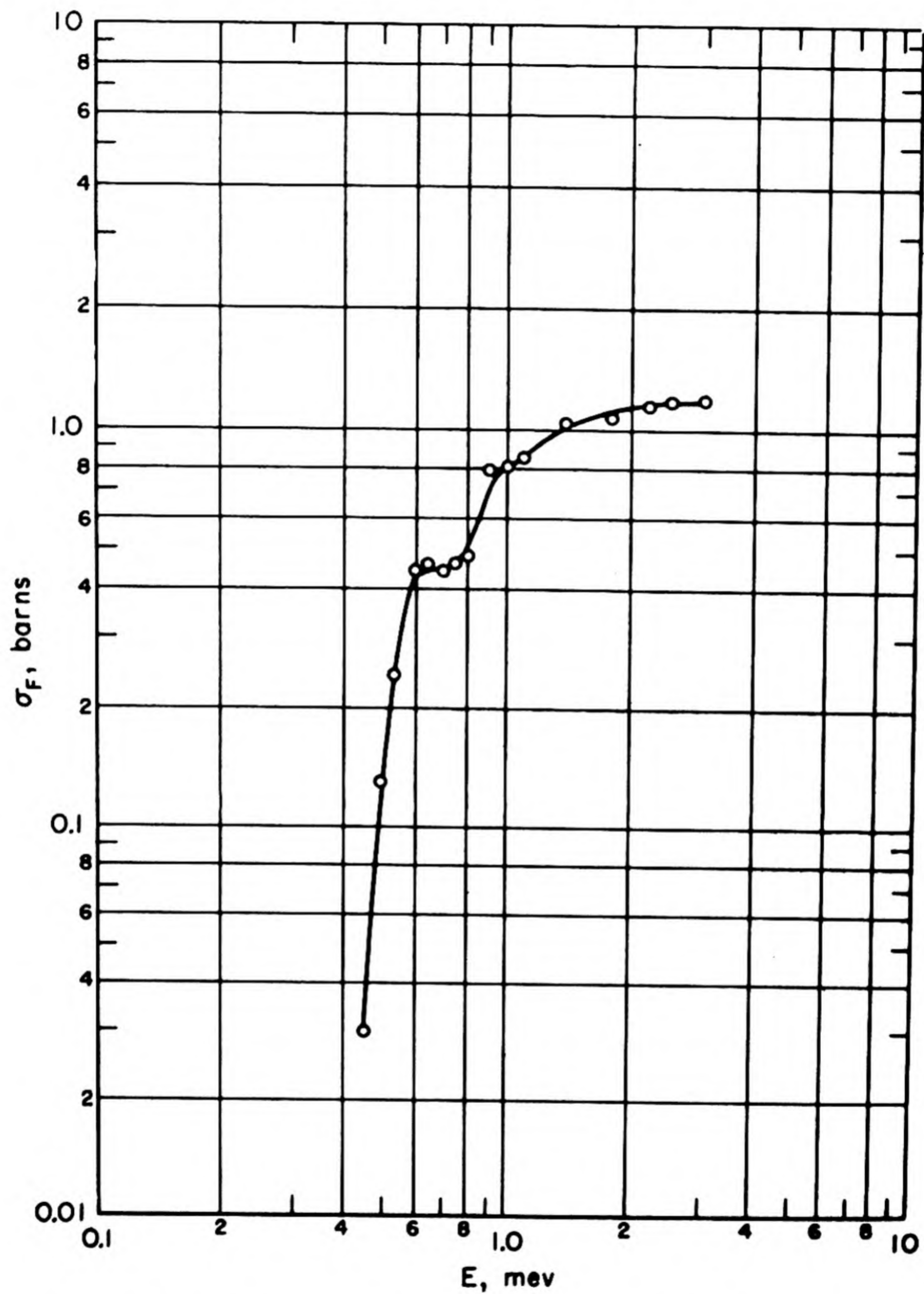


Fig. 1.2.6 — Fission Cross Section of ${}_{81}\text{Pa}^{231}$. Reprinted from BNL-170A.

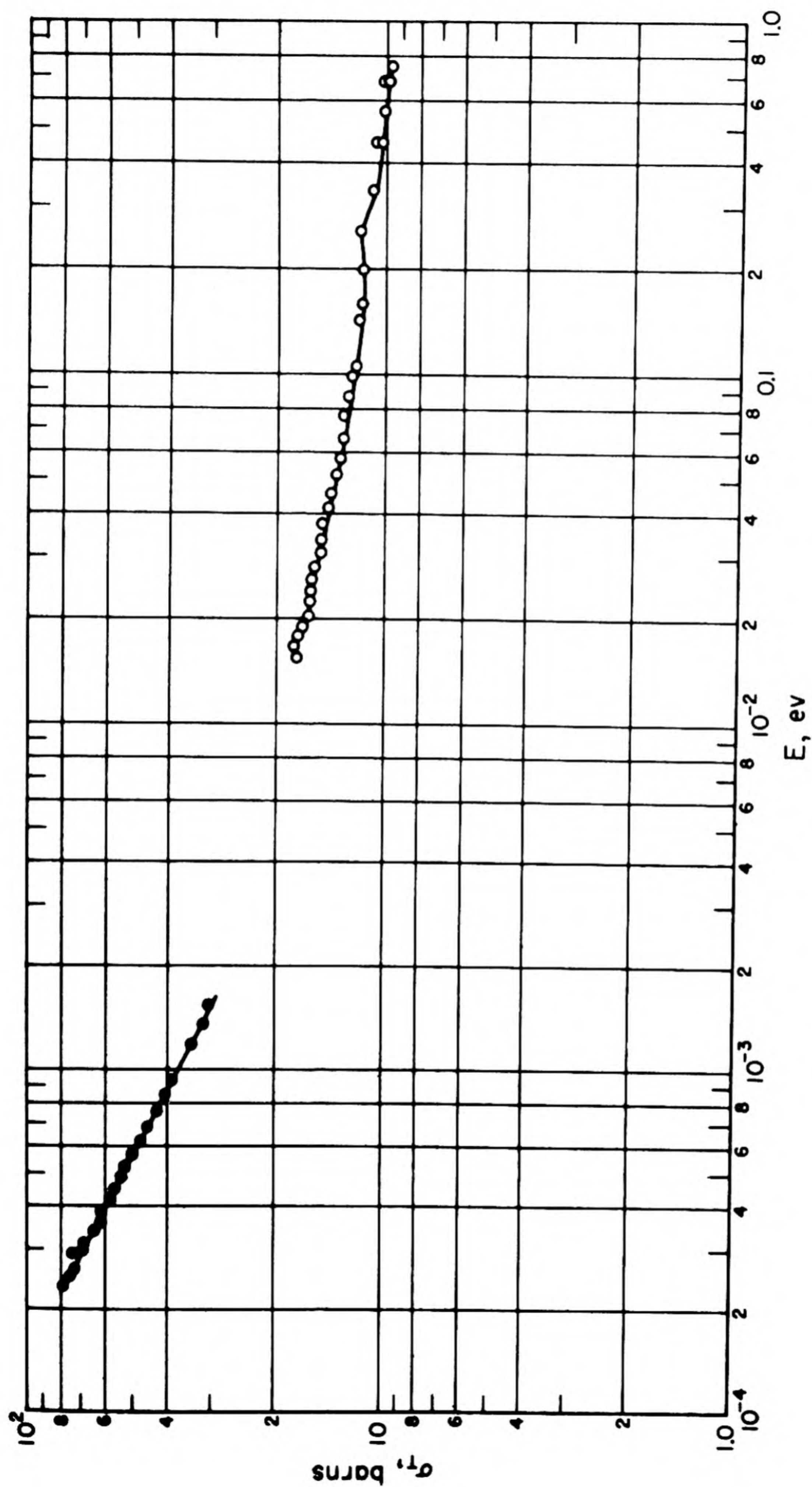


Fig. 1.2.7—Total Cross Section of Uranium. Reprinted from BNL-170.

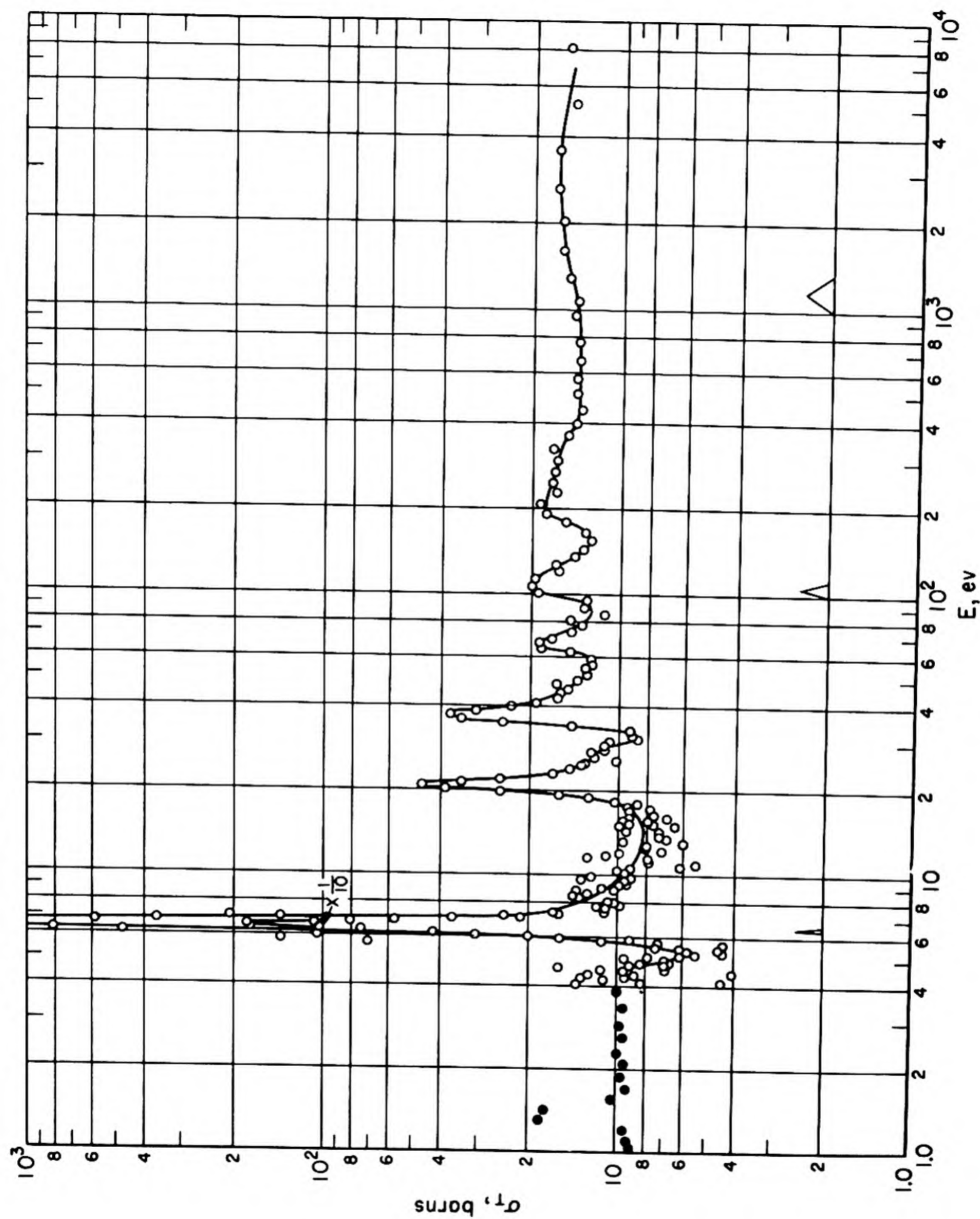


Fig. 1.2.8—Total Cross Section of Uranium. Reprinted from BNL-170A.

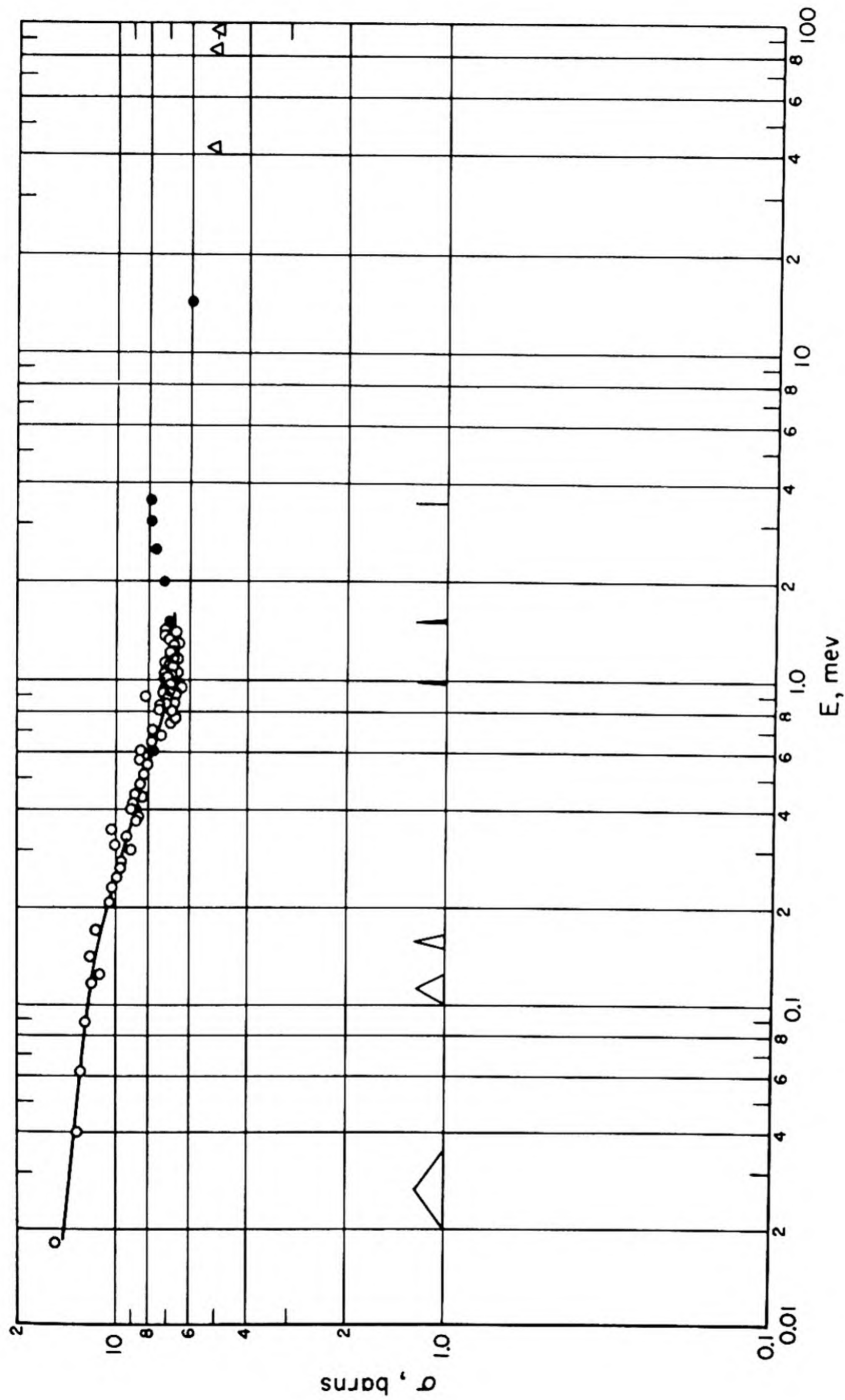


Fig. 1.2.9—Total Cross Section of Uranium. Reprinted from BNL-170.

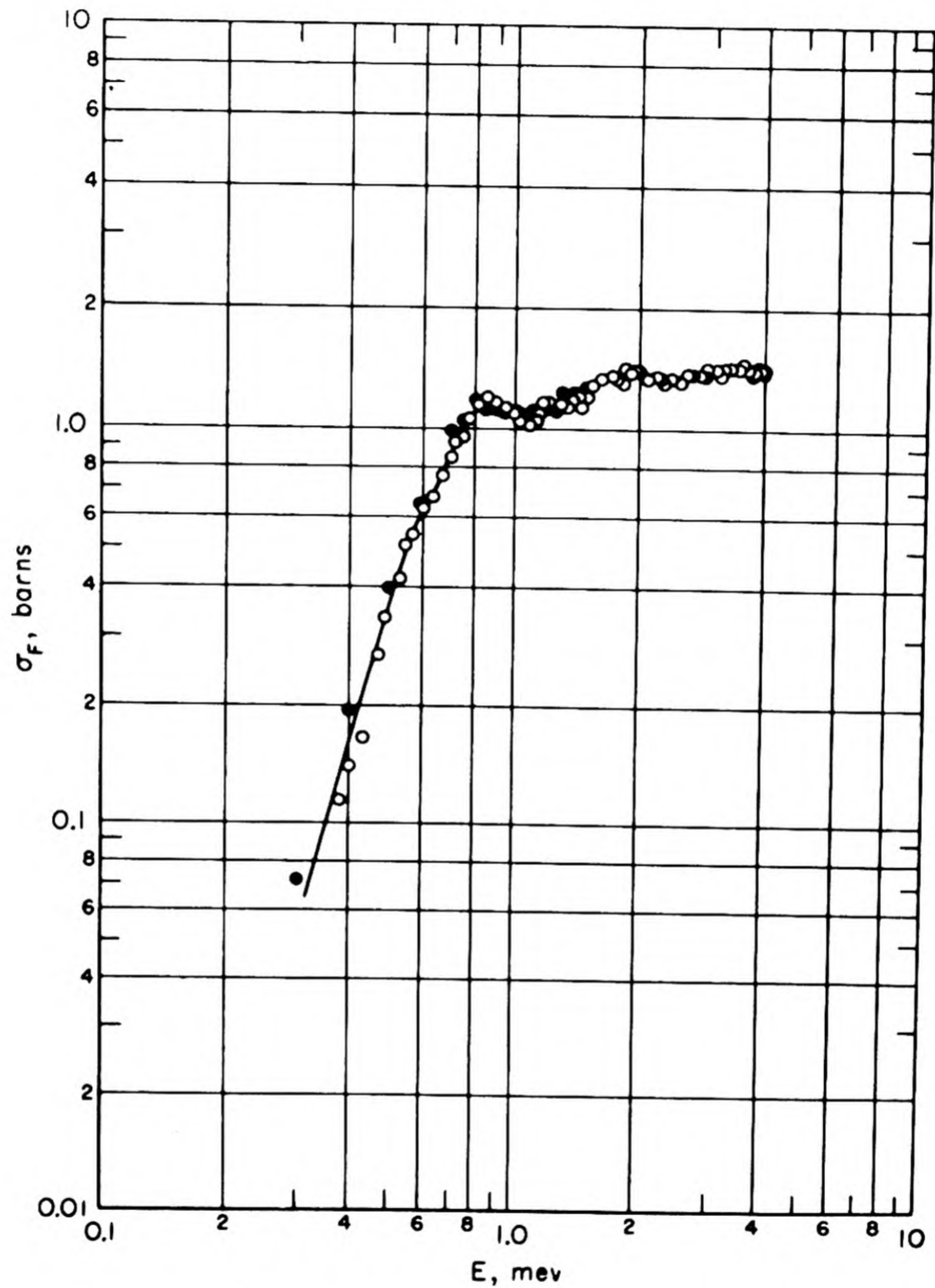


Fig. 1.2.10 — Fission Cross Section of ${}_{92}\text{U}^{235}$. Reprinted from BNL-170A.

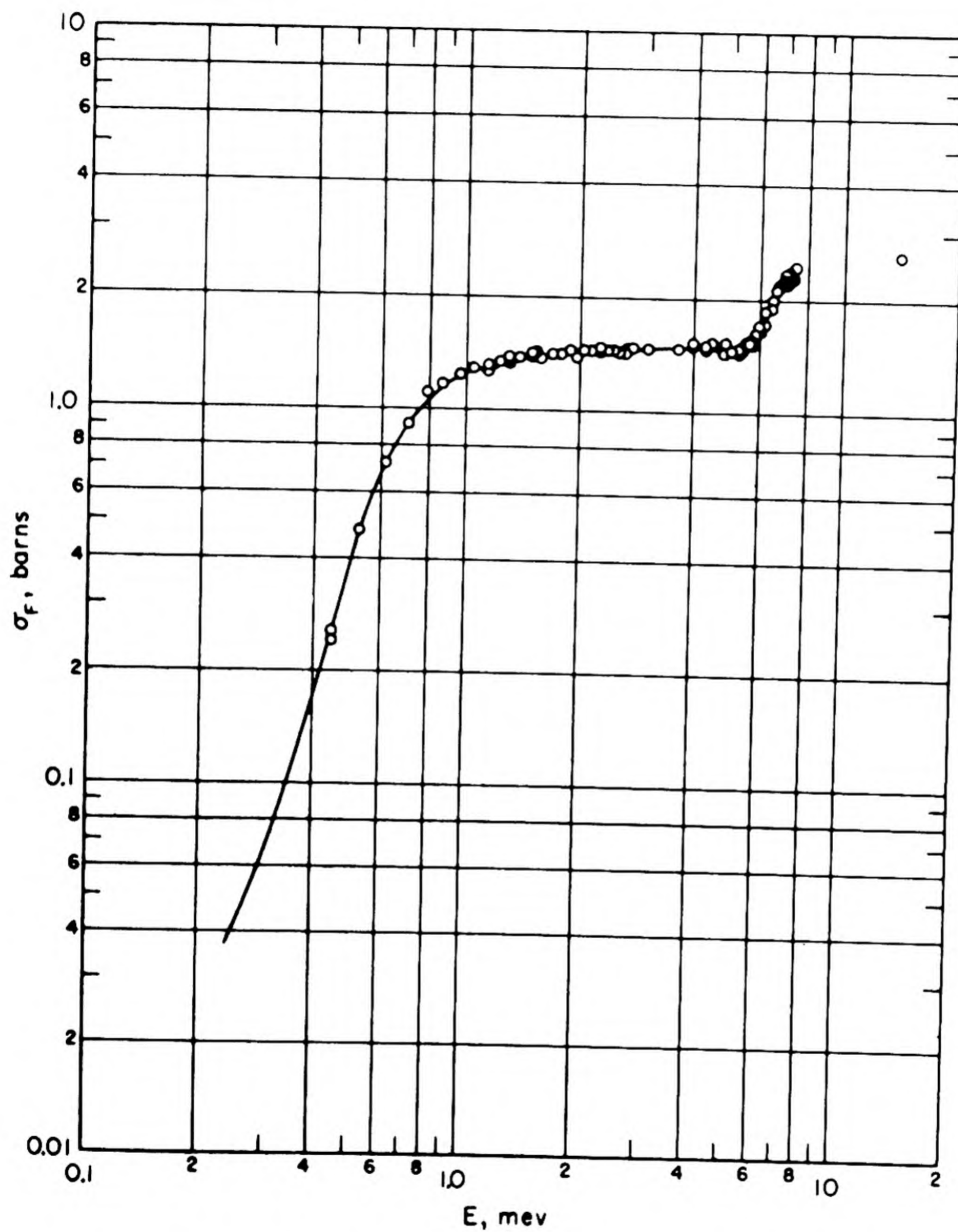


Fig. 1.2.11 — Fission Cross Section of ${}_{93}\text{Np}^{237}$. Reprinted from BNL-170A.

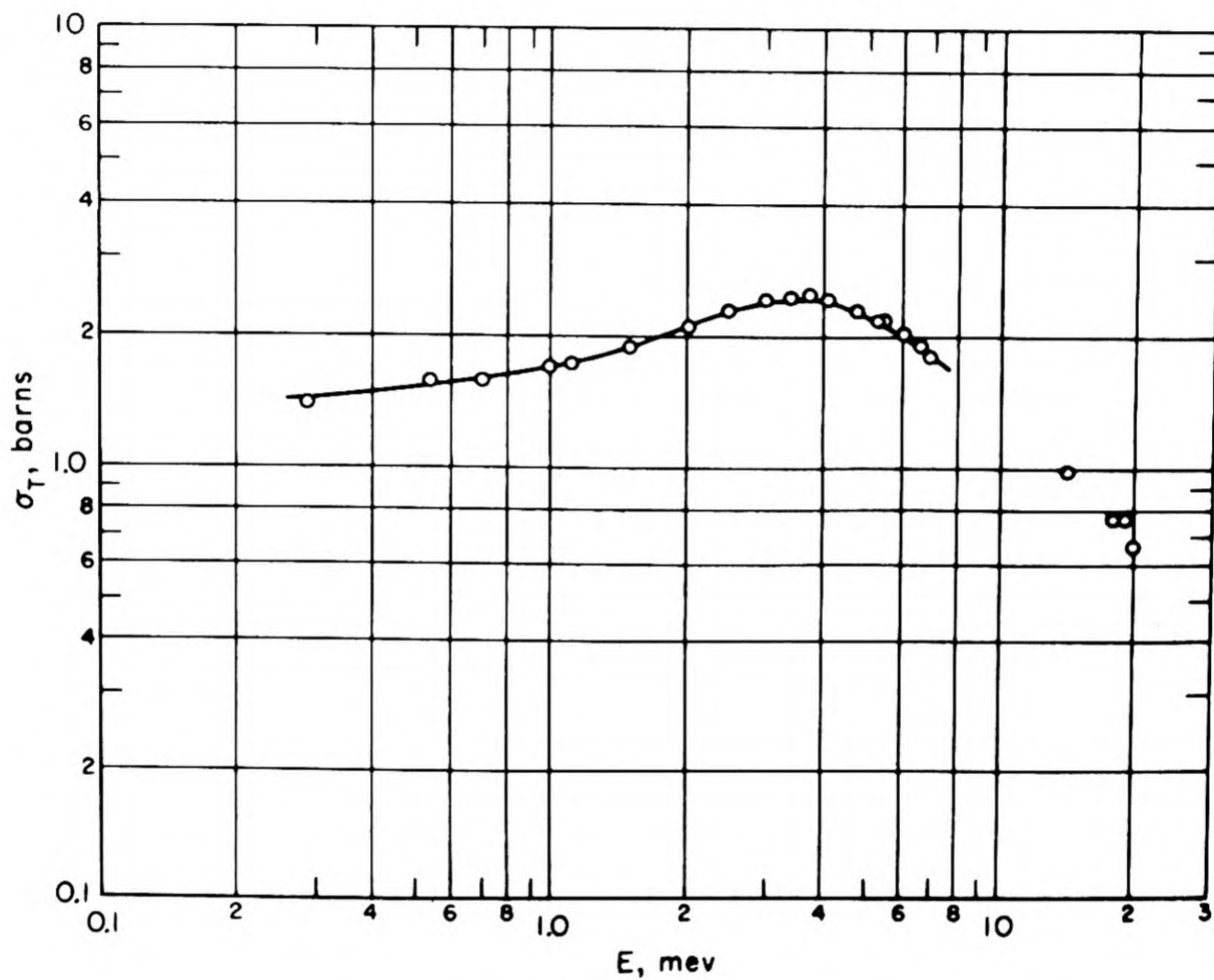


Fig. 1.2.12 — Total Cross Section of ${}^3\text{H}$. Reprinted from BNL-170A.

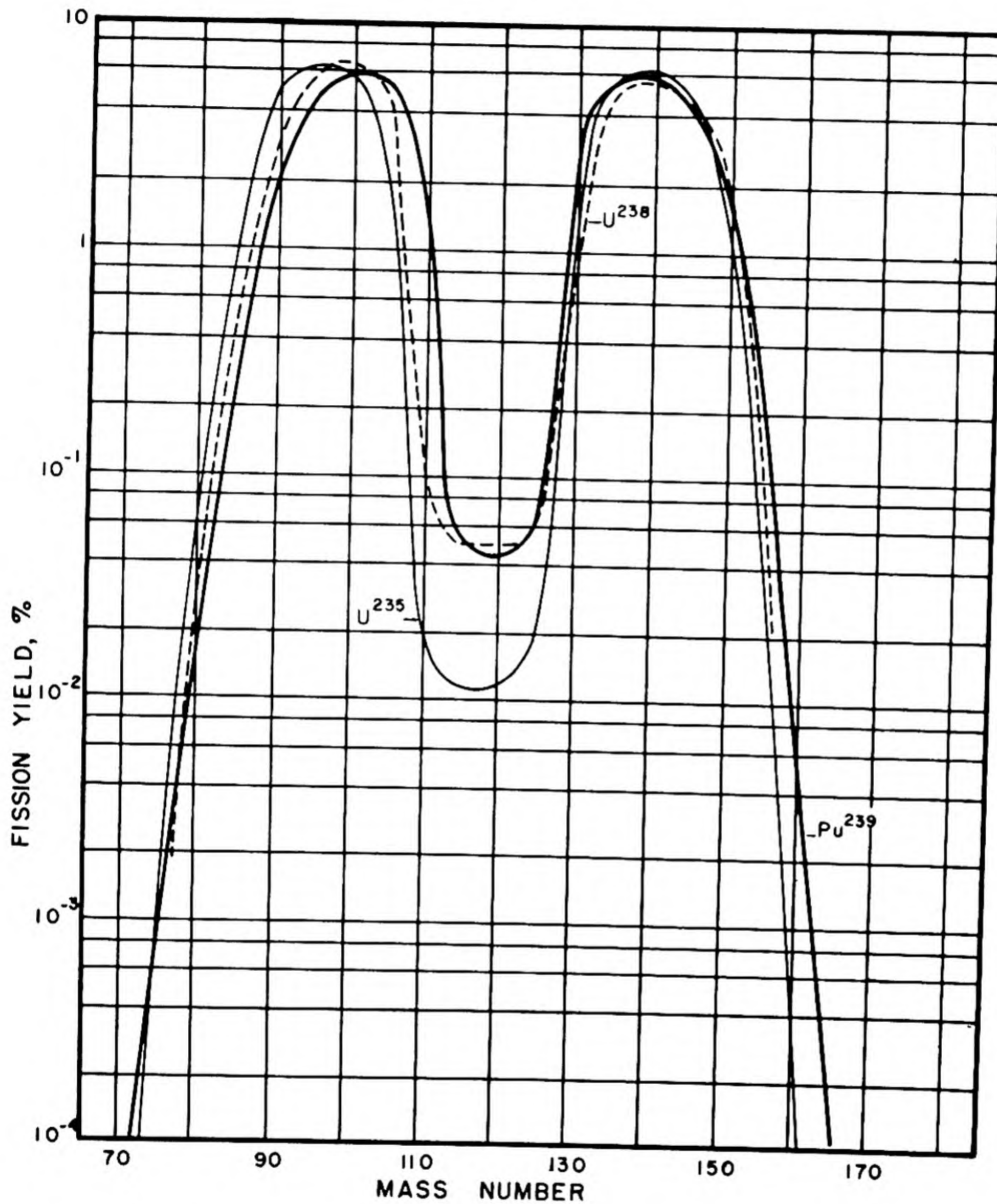


Fig. 1.2.13 — Fission Yields for Slow-neutron Fission of U^{235} , U^{238} and Pu^{239} versus A. Reprinted from Radiochemical Studies: The Fission Products, Book 3, edited by Coryell and Sugarman, McGraw Hill Book Company, Inc., New York, 1951; U^{238} from paper number 219 by Steinberg and Freedman, and U^{235} and Pu^{239} from Appendix B.

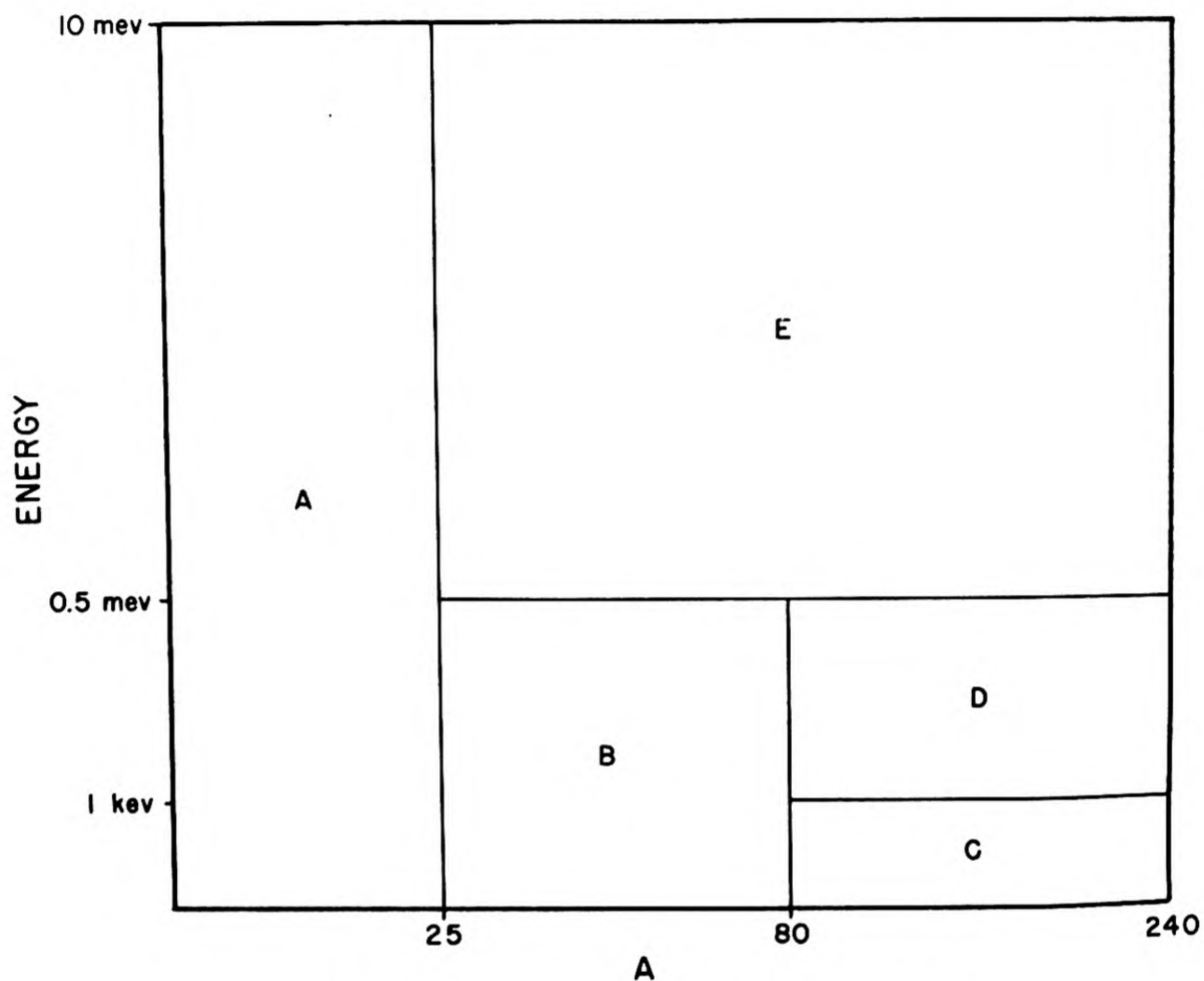


Fig. 1.2.14—Schematic Classification of Nuclear Reactions According to Energy Region and Category of Target Nucleus. Submitted by Nuclear Development Associates, Inc., Jan. 15, 1953.

- | | |
|-----------|--|
| Region A. | Light Nuclei |
| Region B. | Low and Intermediate Energies, Intermediate Nuclei |
| Region C. | Low Energy, Heavy Nuclei |
| Region D. | Intermediate Energy, Heavy Nuclei |
| Region E. | High Energies, Heavy and Intermediate Nuclei |

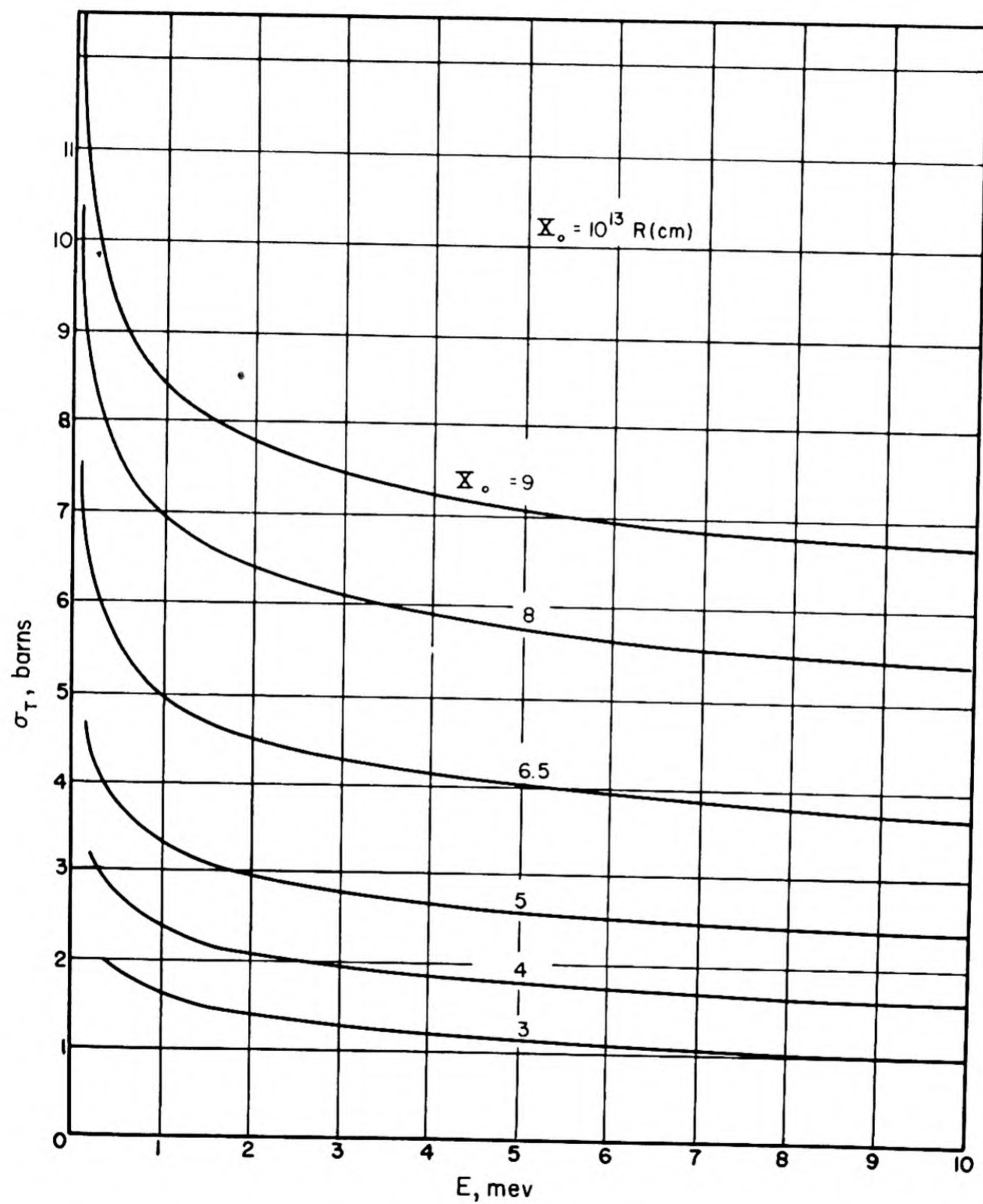


Fig. 1.2.15—Total Cross Section vs Energy for Several Values of the Nuclear Radius. Reprinted from NYO-636.

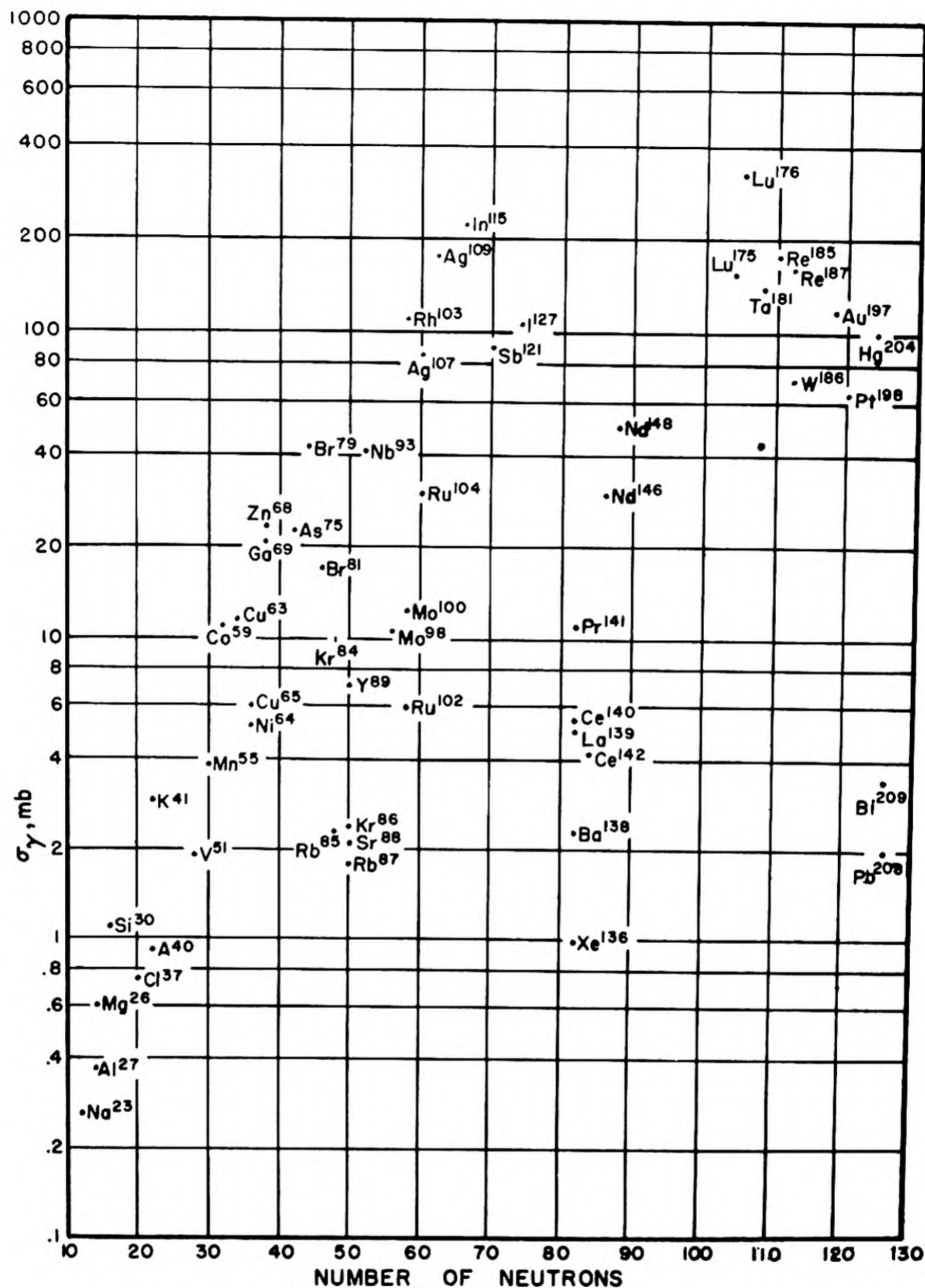


Fig. 1.2.16 — Radiative-capture Cross Sections vs Number of Neutrons. Reprinted from Pile Neutron Research, by D. S. Hughes. Copyright, 1953. By permission from Addison-Wesley Press, Inc., Cambridge.

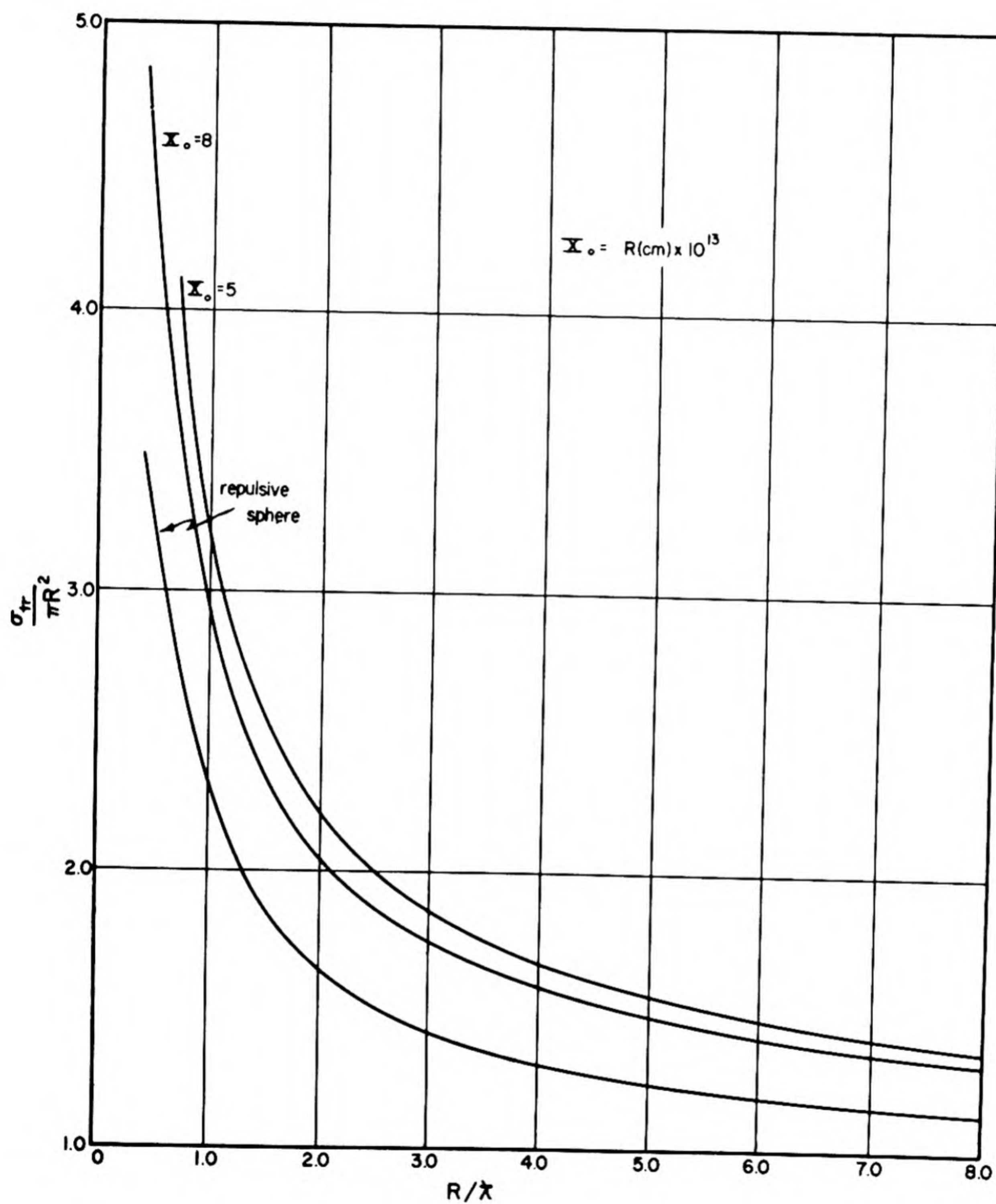


Fig. 1.2.17 — Transport Cross Section as a Function of R/λ for Various Values of the Nuclear Radius. Reprinted from ORNL-433.

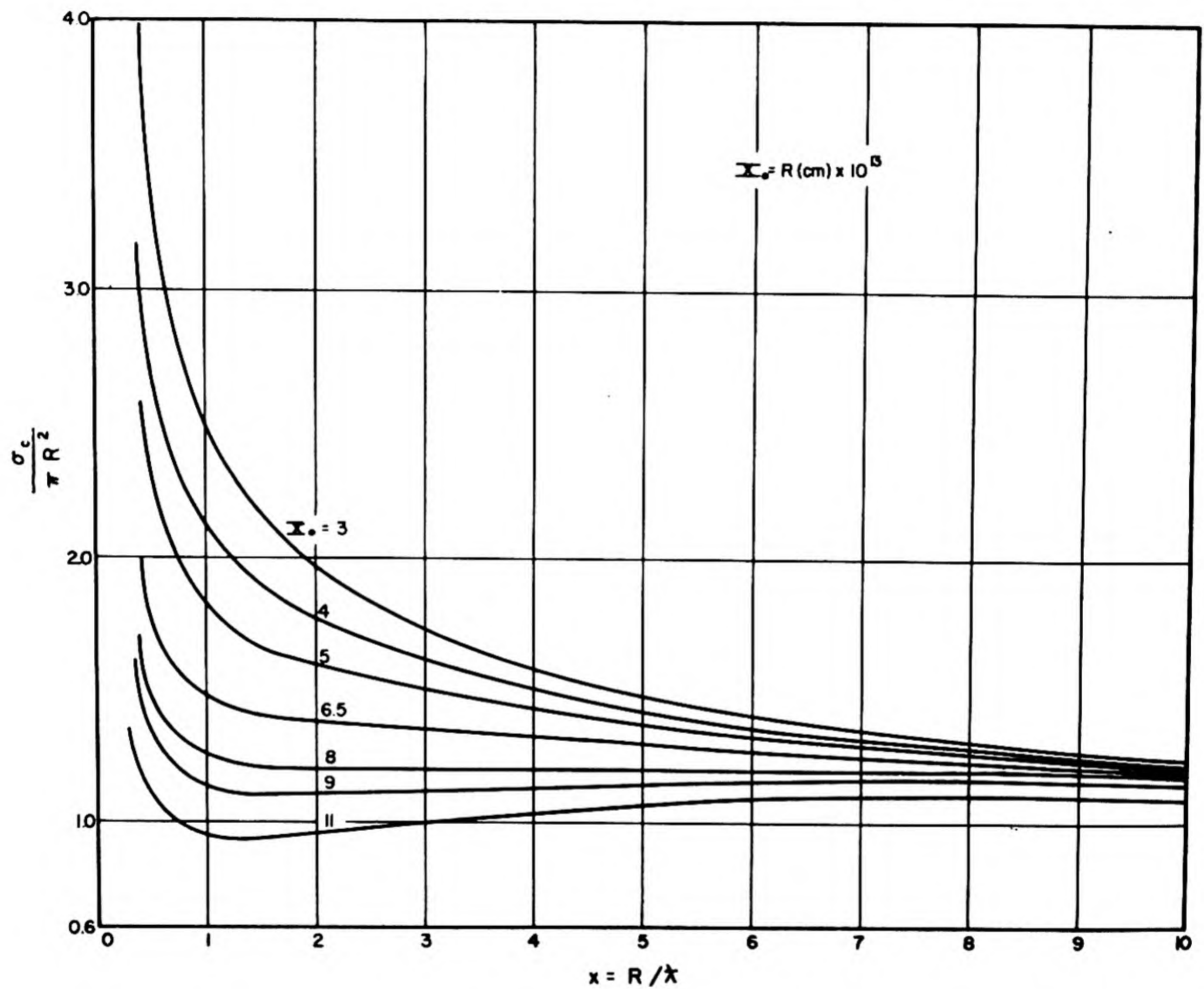


Fig. 1.2.18—Reaction Cross Section as a Function of R/λ for Various Values of the Nuclear Radius. Reprinted from NYO-636.

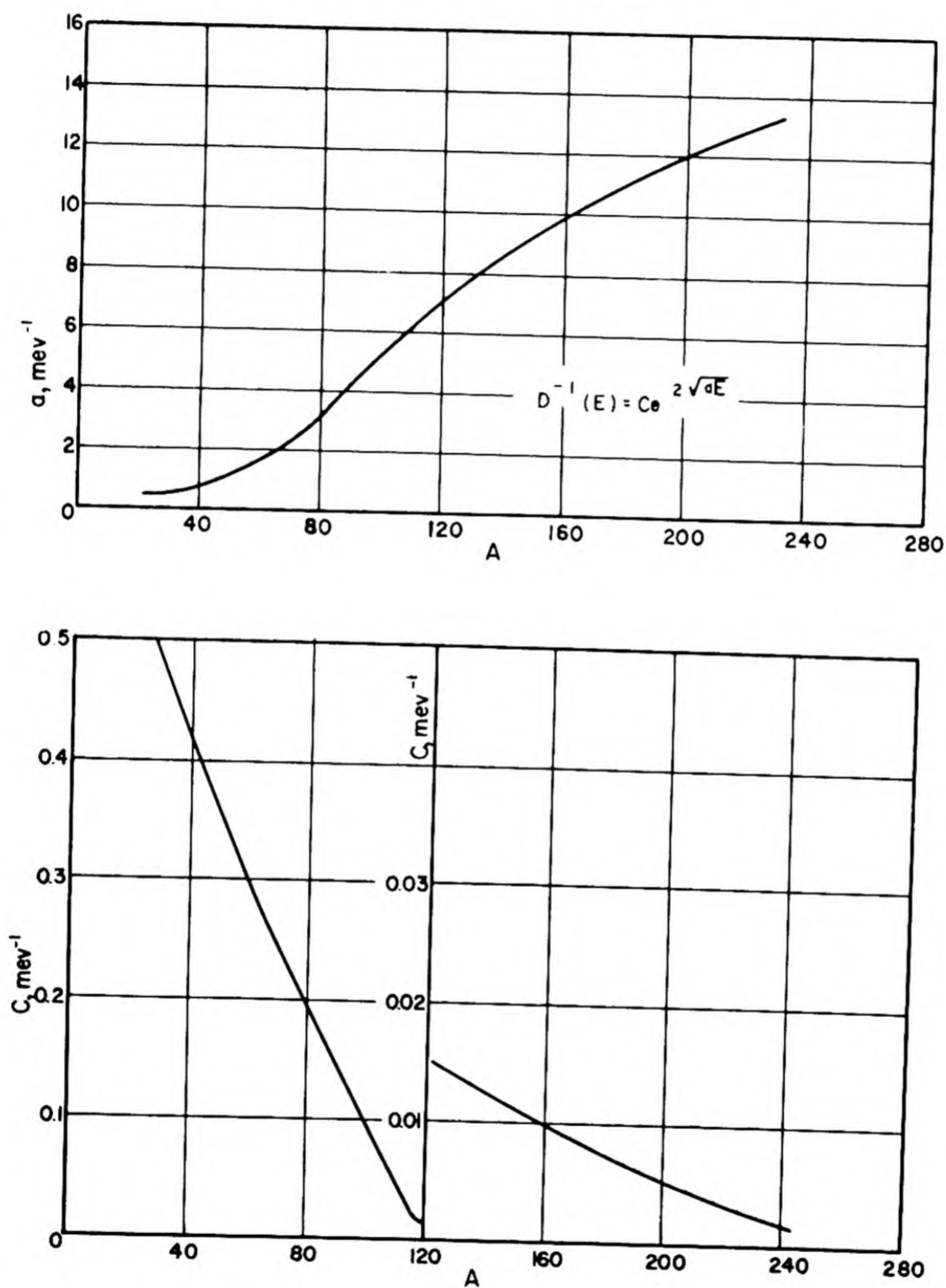


Fig. 1.2.19 — Interpolation Curves of Constants a and C for Odd A Nuclei. Reprinted from NYO-636. These constants are parameters in the formula $1/D(E) = C a^2 \sqrt{aE}$ for estimating the distance between levels $D(E)$. Even A nuclei are expected to have level separations 100 to 1000 times greater.

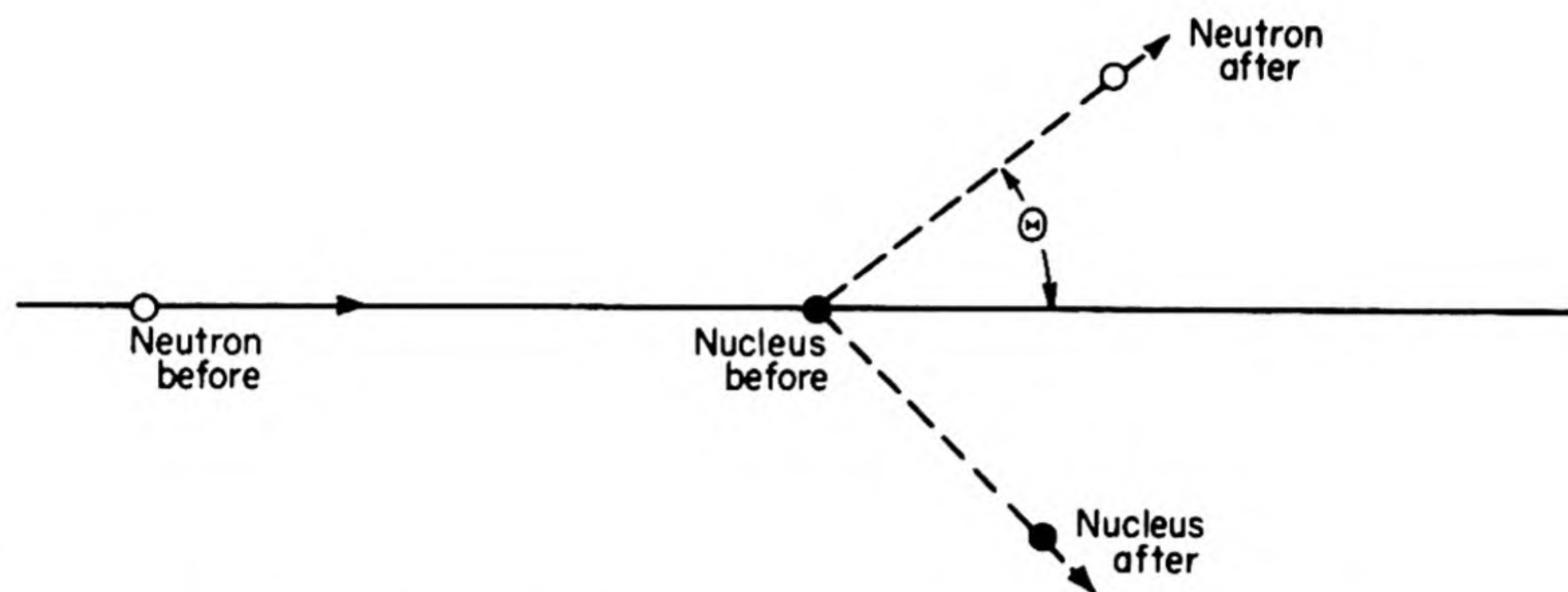


Fig. 1.2.20—Neutron Scattering in Laboratory System. Submitted by Nuclear Development Associates, Inc., Jan. 1, 1953.

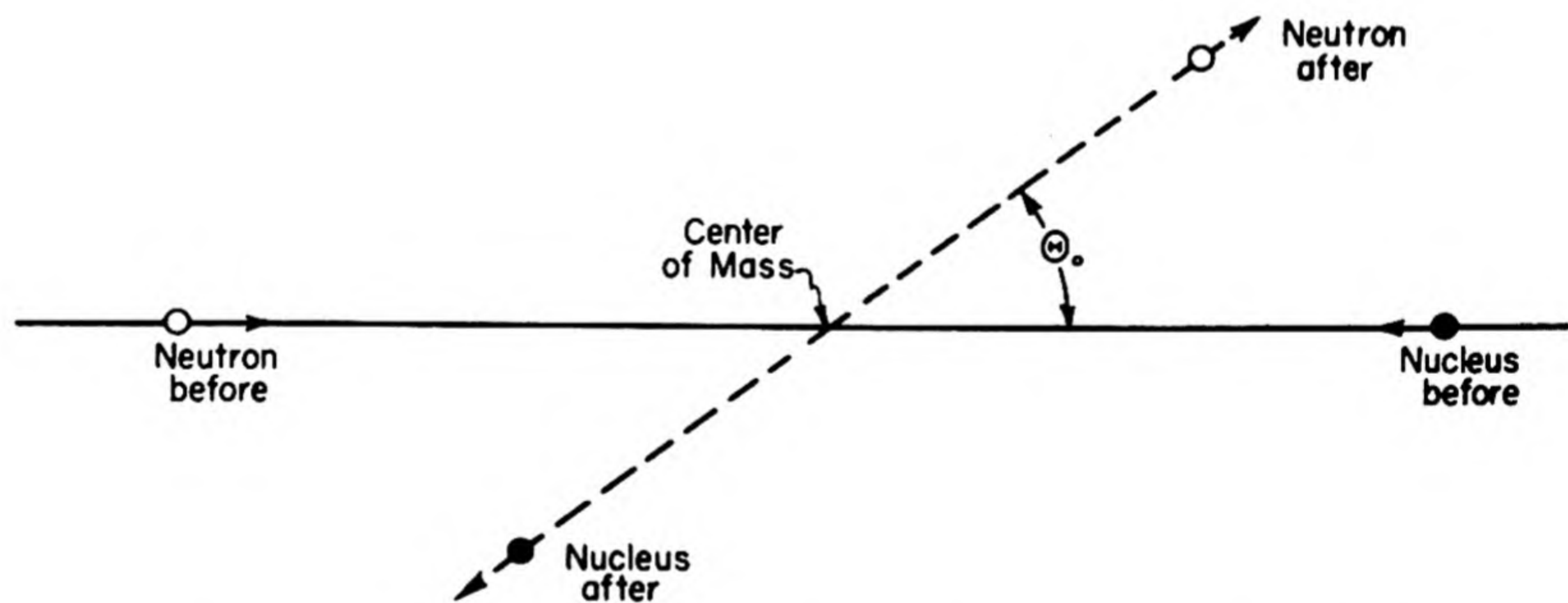


Fig. 1.2.21—Neutron Scattering in Center-of-Mass System. Submitted by Nuclear Development Associates, Inc., Jan. 1, 1953.

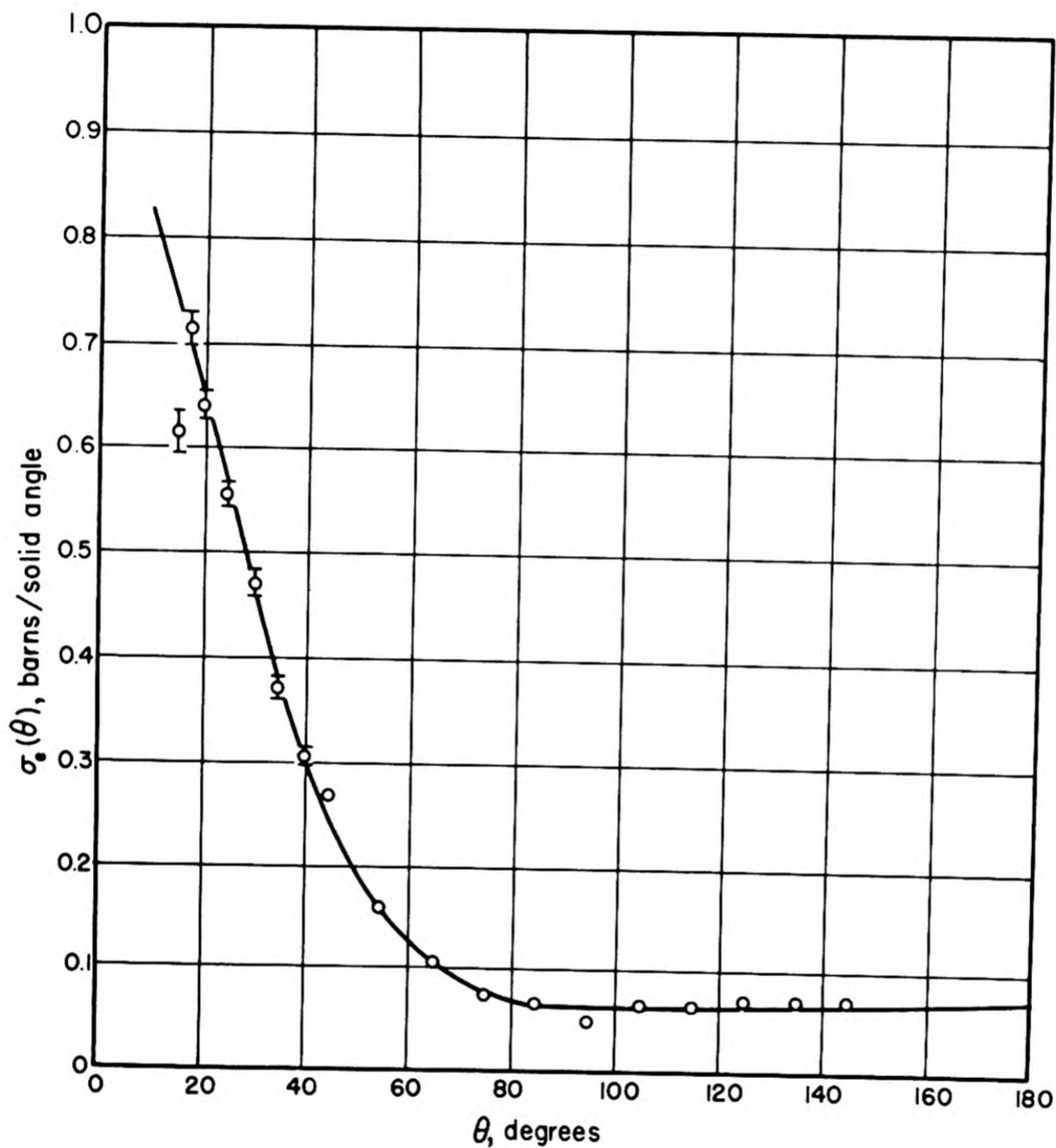


Fig. 1.2.22 —Differential Elastic Scattering Cross Section for Beryllium. Reprinted from LA-1339. Ordinate gives the differential elastic scattering cross section in barns per unit solid angle.

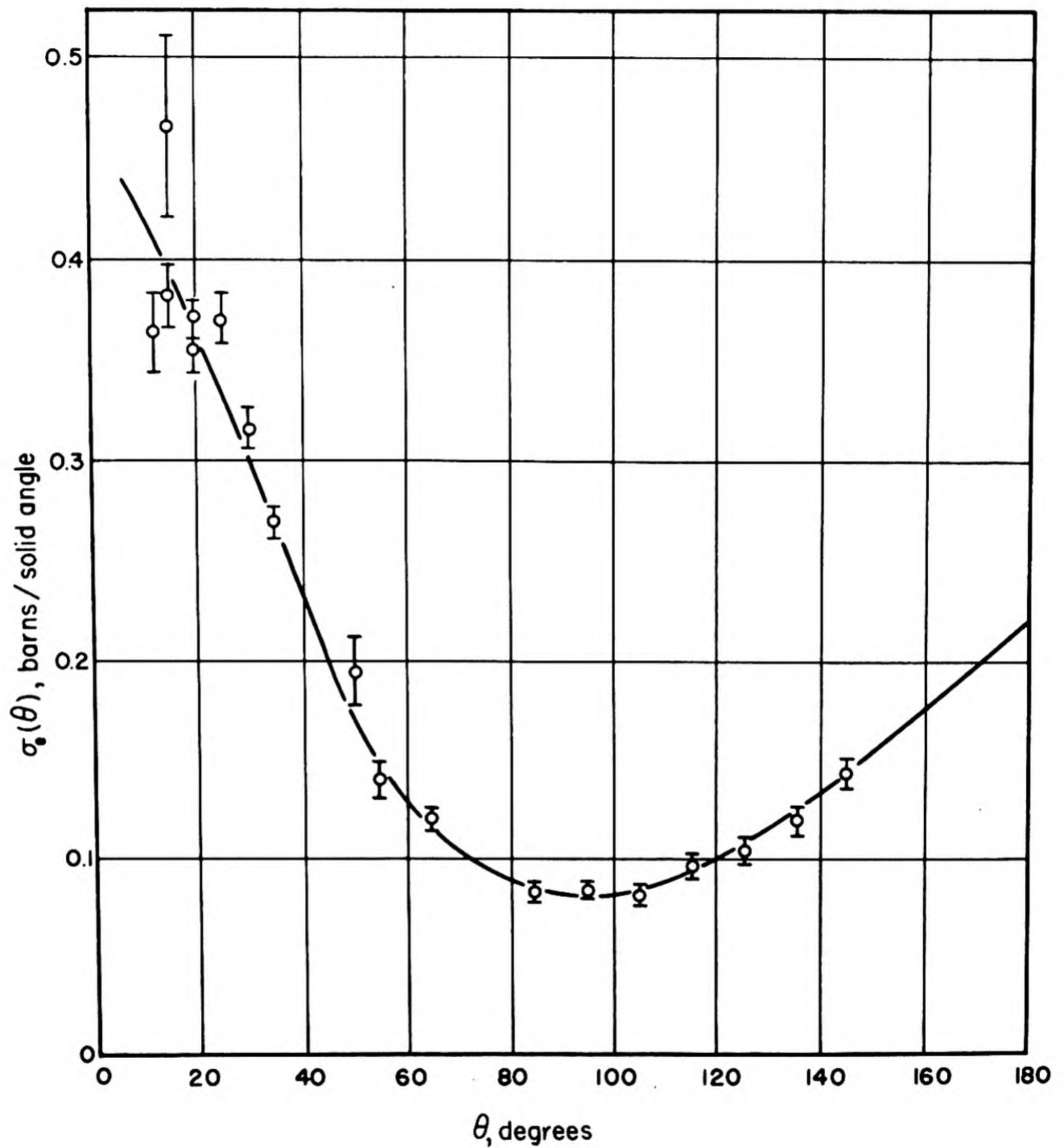


Fig. 1.2.23 —Differential Elastic Scattering Cross Section for Carbon. Reprinted from LA-1339. Ordinate gives the differential elastic scattering cross section in barns per unit solid angle.

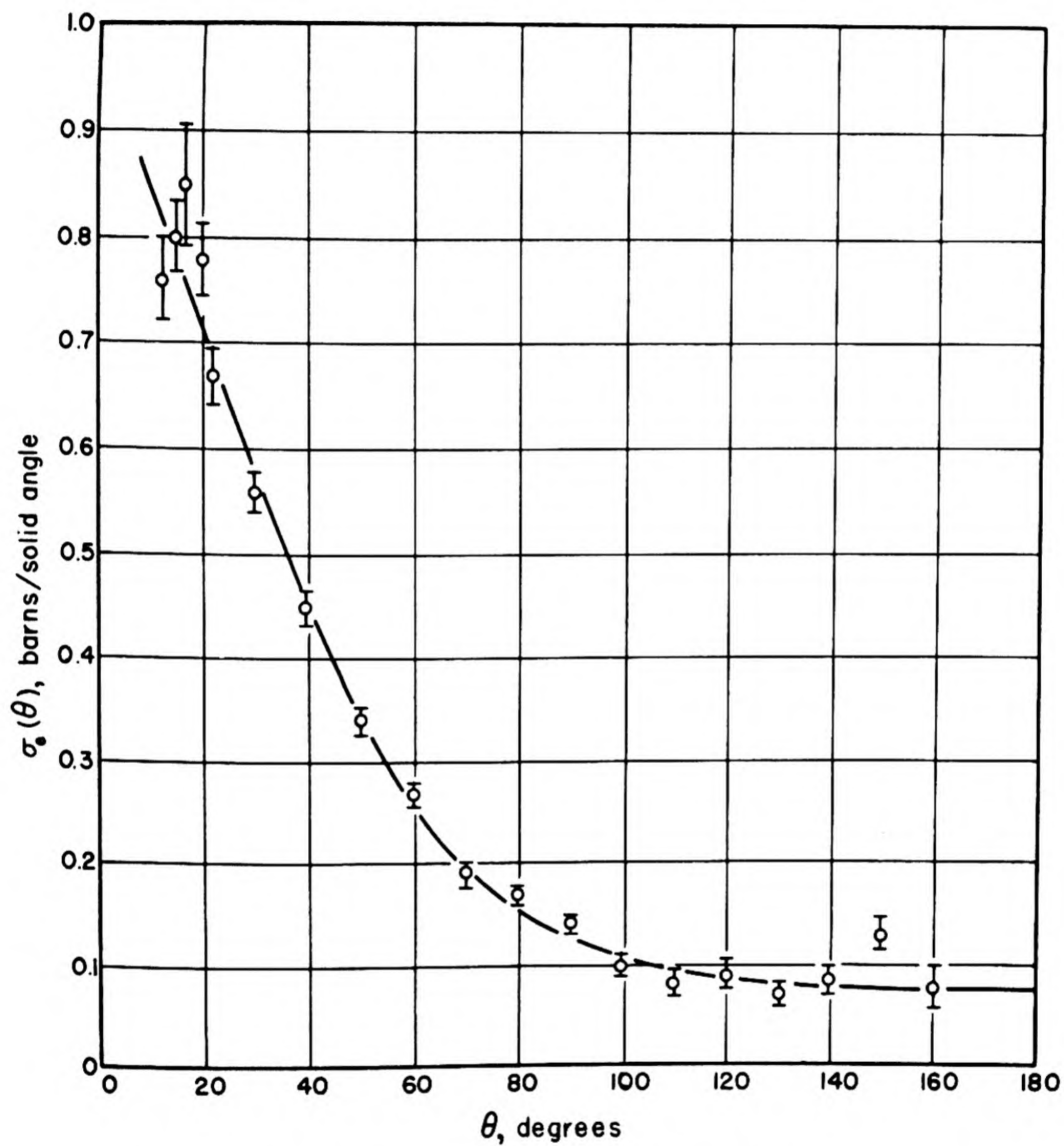


Fig. 1.2.24—Differential Elastic Scattering Cross Section for Aluminum. Reprinted from LA-1339. Ordinate gives the differential elastic scattering cross section in barns per unit solid angle.

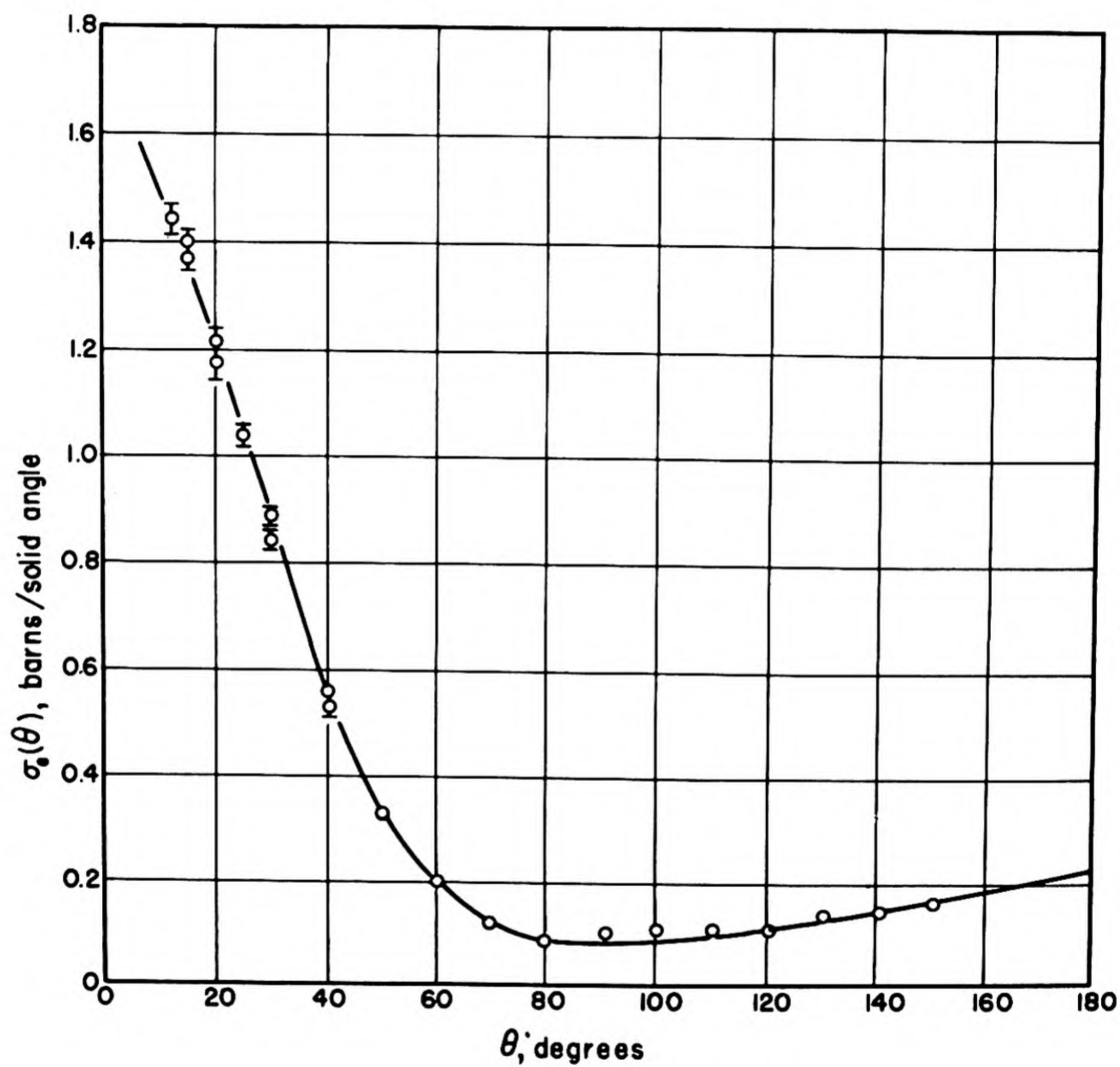


Fig. 1.2.25—Differential Elastic Scattering Cross Section for Chromium. Reprinted from LA-1339. Ordinate gives the differential elastic scattering cross section in barns per unit solid angle.

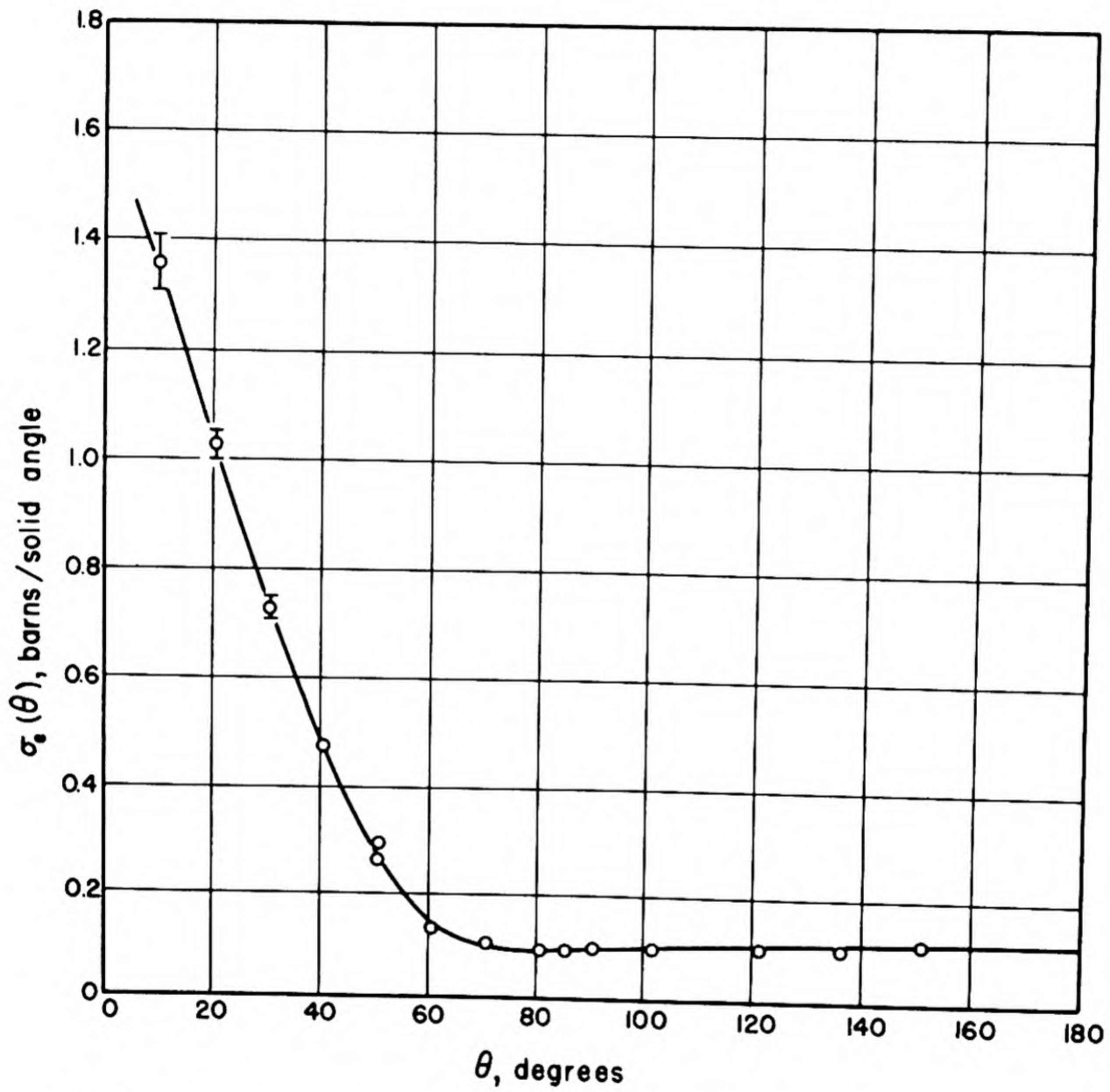


Fig. 1.2.26—Differential Elastic Scattering Cross Section for Iron. Reprinted from LA-1339. Ordinate gives the differential elastic scattering cross section in barns per unit solid angle.

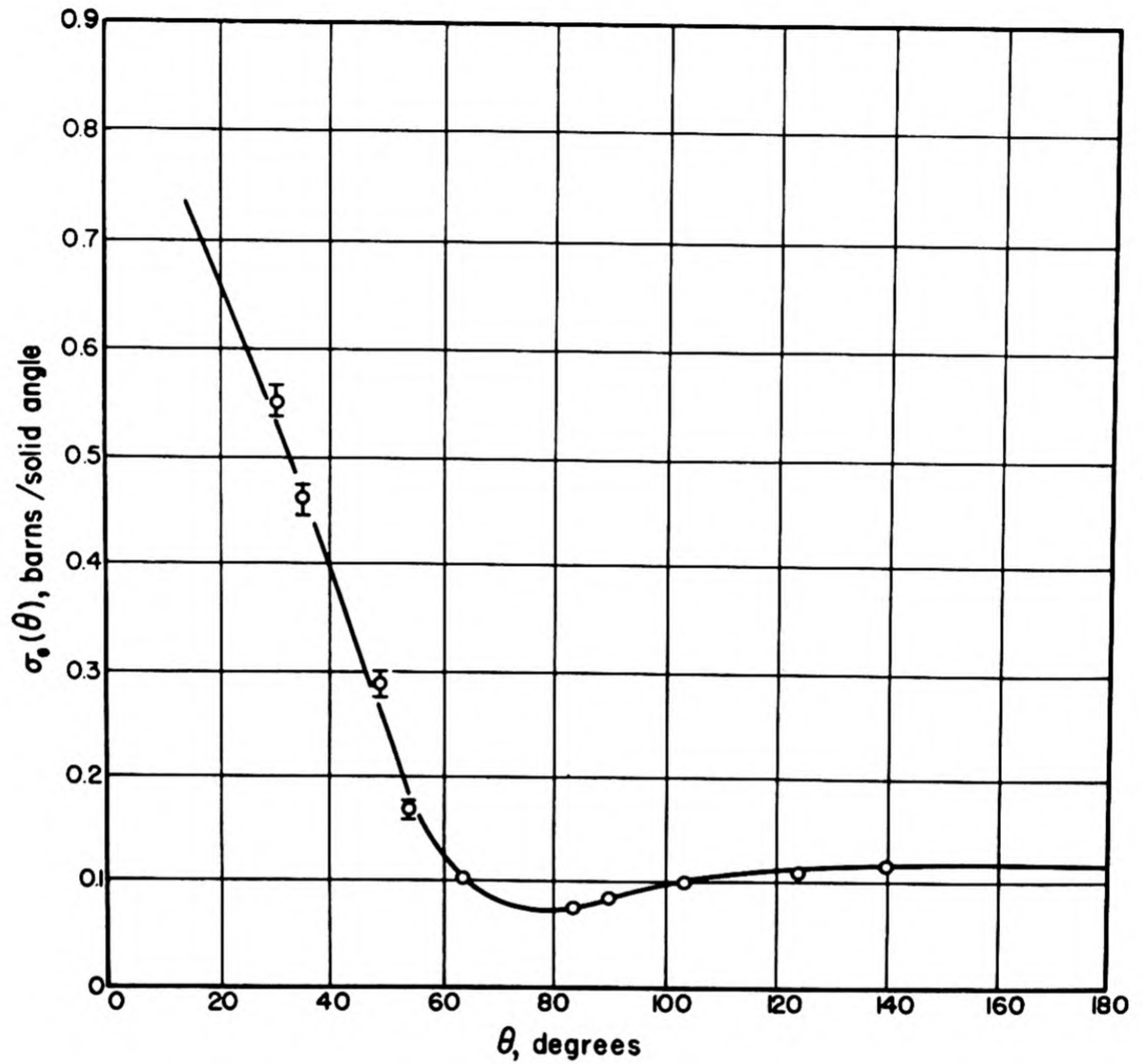


Fig. 1.2.27—Differential Elastic Scattering Cross Section for Nickel. Reprinted from LA-1339. Ordinate gives the differential elastic scattering cross section in barns per unit solid angle.

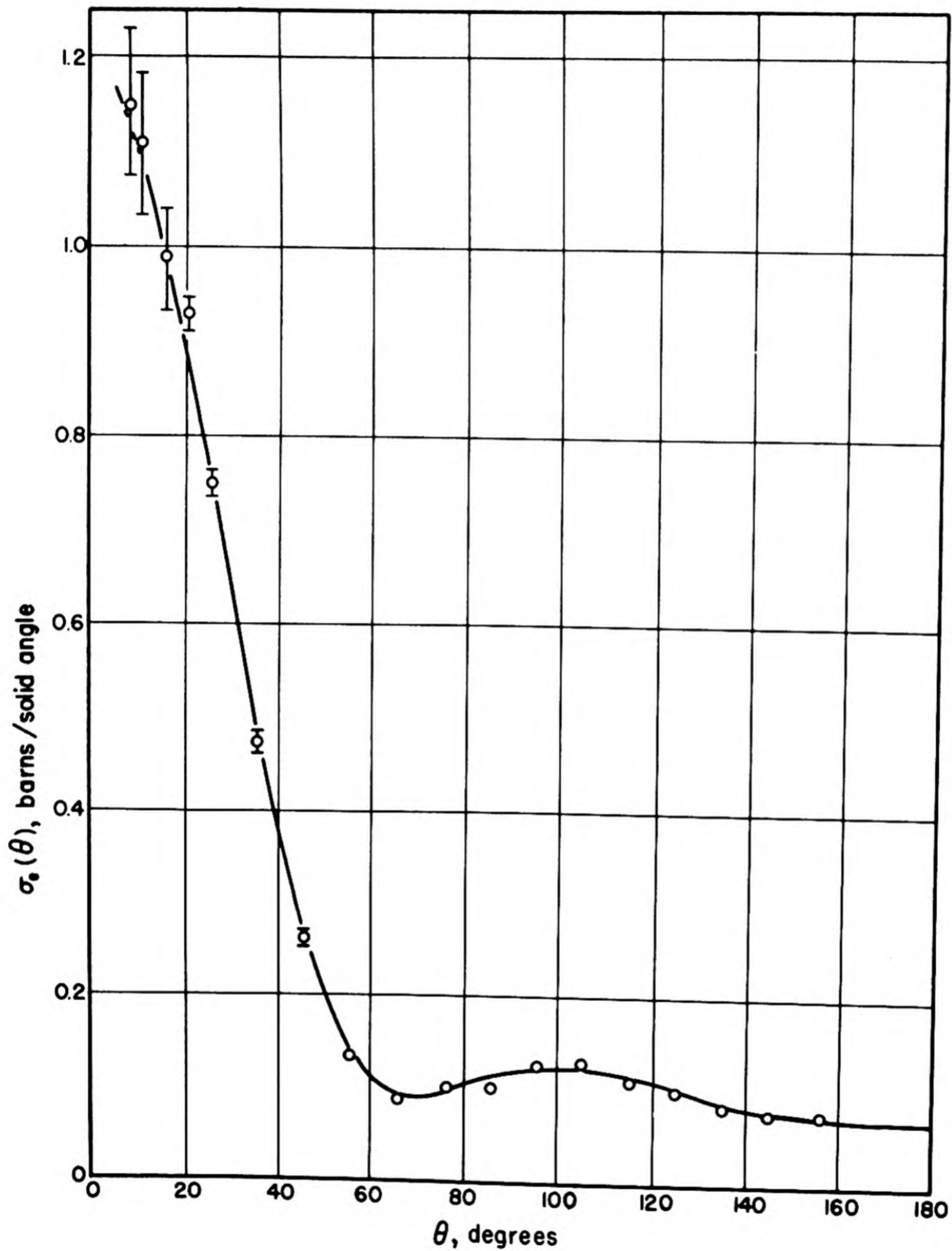


Fig. 1.2.28 — Differential Elastic Scattering Cross Section for Copper. Reprinted from LA-1339. Ordinate gives the differential elastic scattering cross section in barns per unit solid angle.

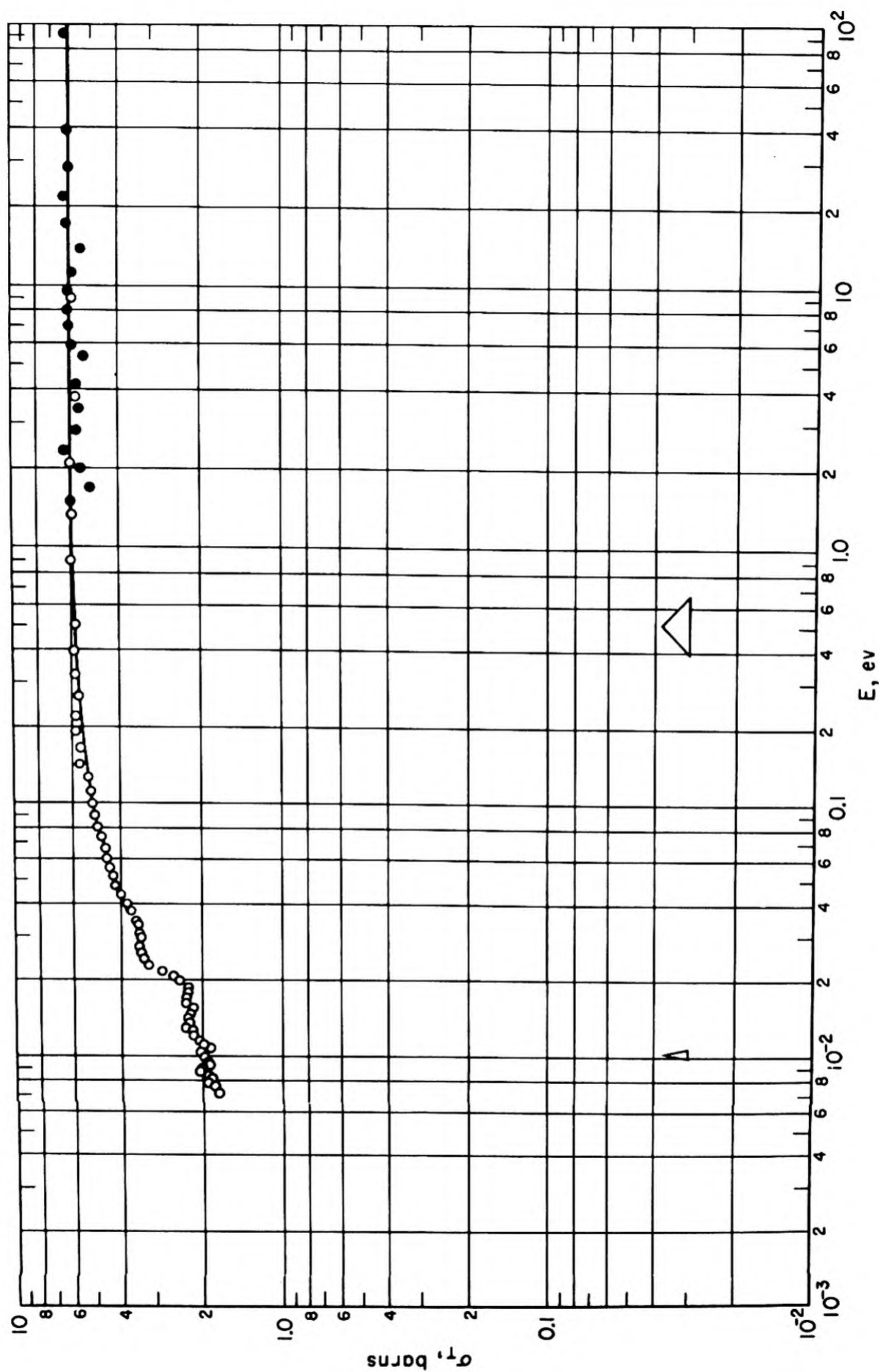


Fig. 1.2.29 — Total Cross Section of Be. Reprinted from AECU-2040.

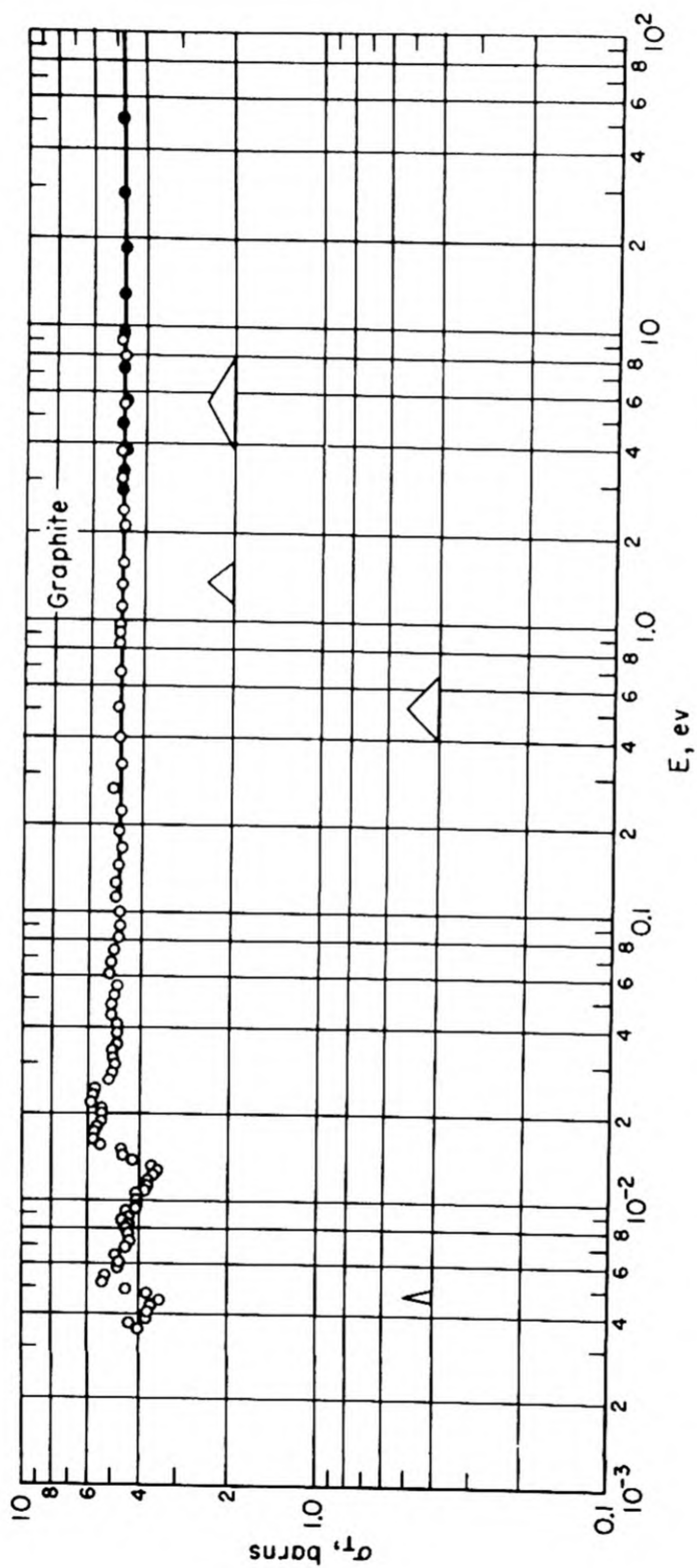


Fig. 1.2.30 — Total Cross Section of C. Reprinted from AECU-2040.

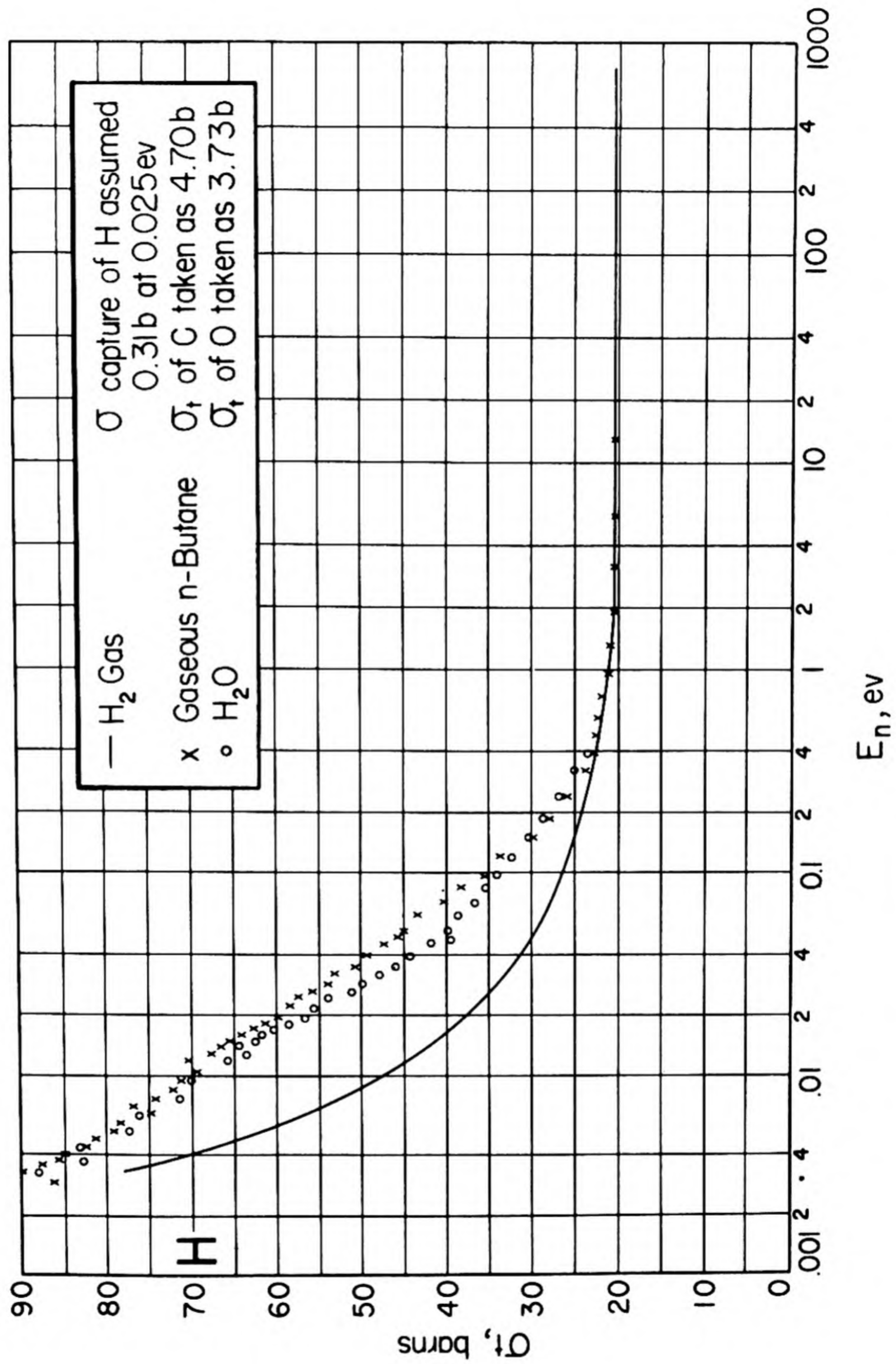


Fig. 1.2.31—Total Cross Section of Hydrogen. Reprinted from R. K. Adair, Rev. Mod. Phys., 22, 249, 1950.

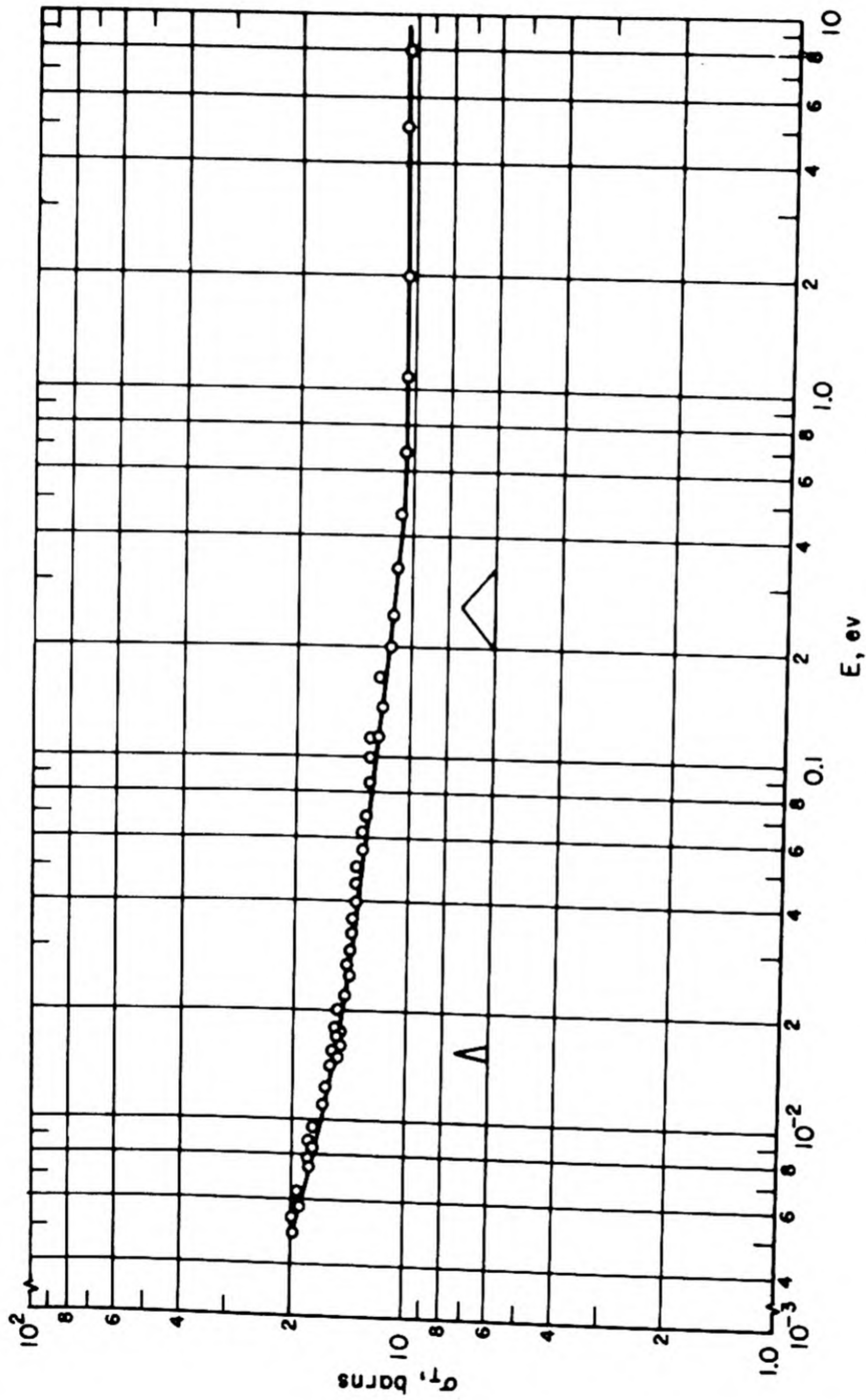


Fig. 1.2.32 — Total Cross Section of D_2O . Reprinted from AECU-2040.

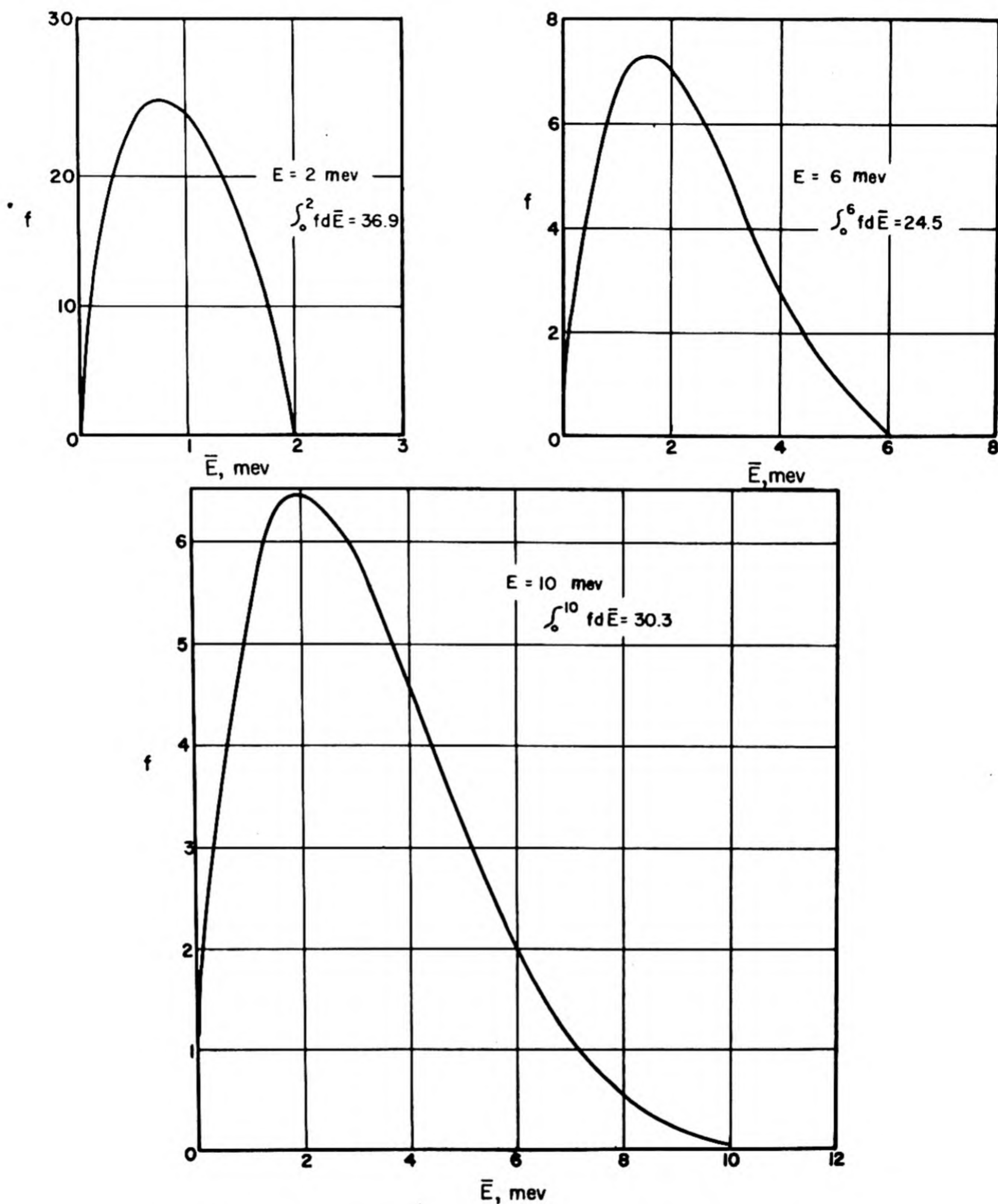


Fig. 1.2.33 —Theoretical Energy Distribution of Neutrons Inelastically Scattered by Zn. Reprinted from NYO-636. Incident neutron energy is E , and scattered neutron energy is \bar{E} . Parameters used in Eq. (56) are: ($Z = 30$, $A = 64$); $a = 1.8 \text{ MeV}^{-1}$; $r_0 = 1.5 \times 10^{-13} \text{ cm}$; $E_0 = 0$.

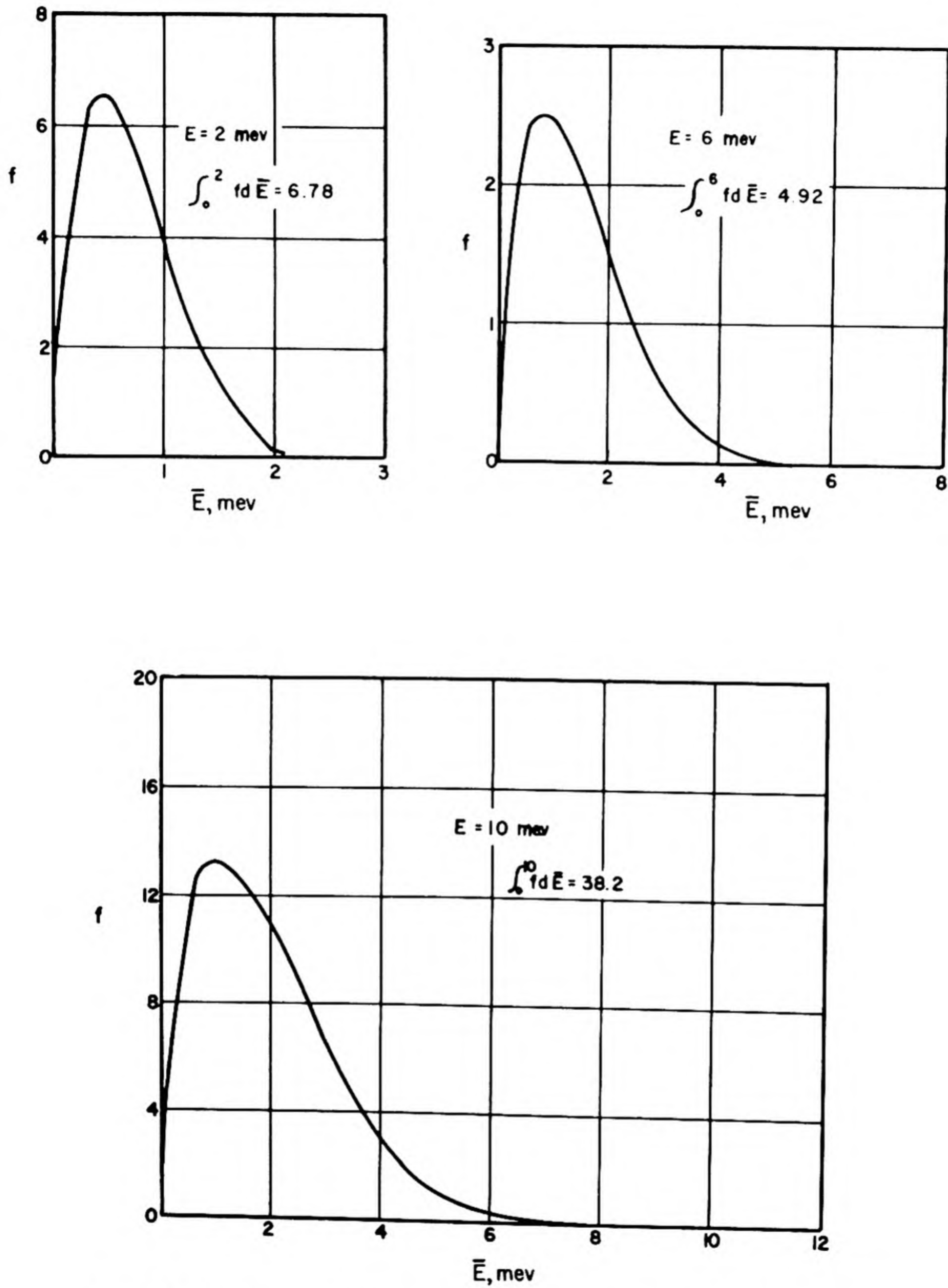


Fig. 1.2.34 — Theoretical Energy Distribution of Neutrons Inelastically Scattered by Sn. Reprinted from NYO-636. Incident neutron energy is E and scattered neutron energy is \bar{E} . Parameters used in Eq. (56) are: ($Z = 50$, $A = 120$); $a = 6.8 \text{ meV}^{-1}$; $r_0 = 1.5 \times 10^{-13} \text{ cm}$; $E_0 = 0$.

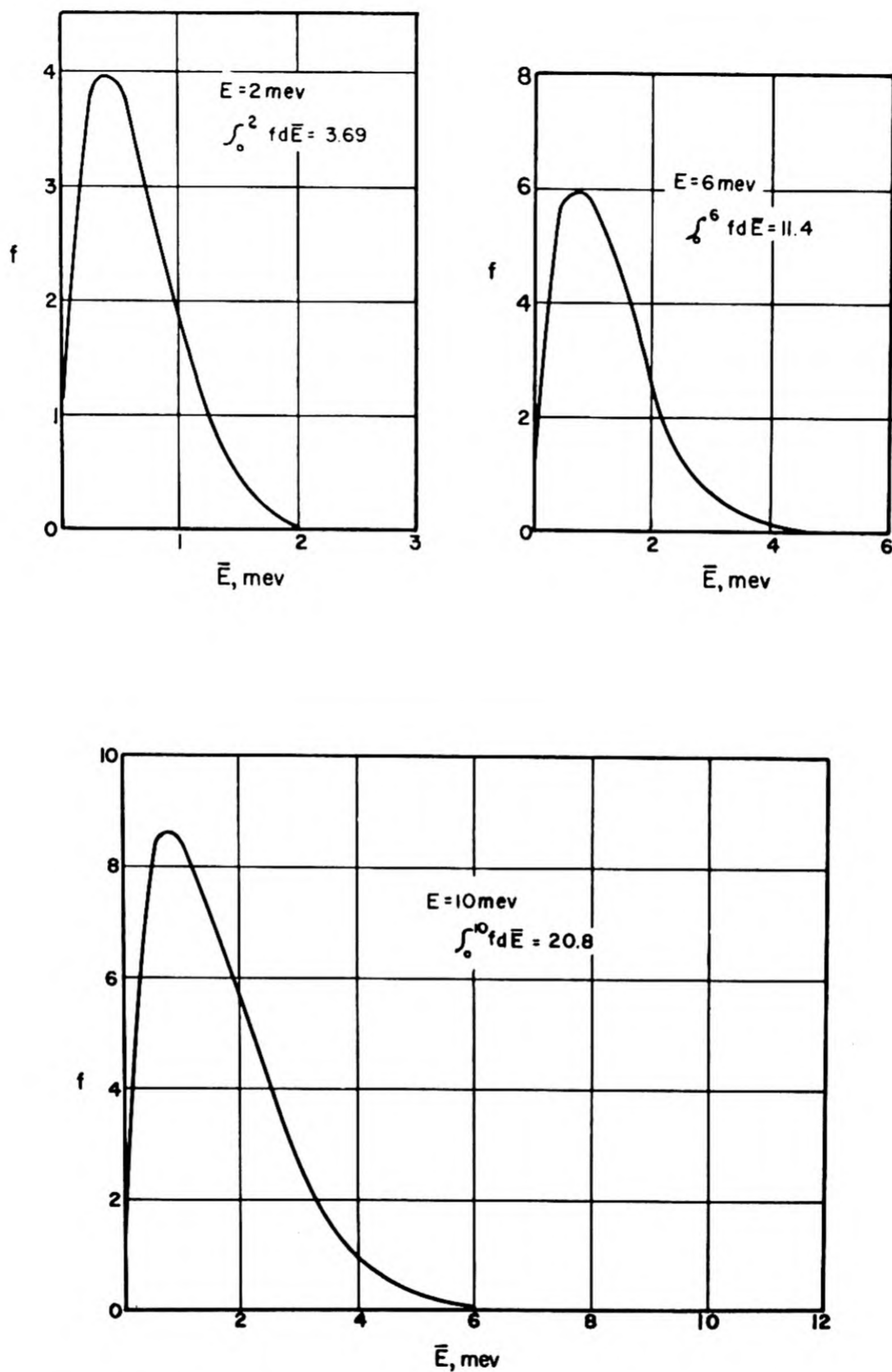


Fig. 1.2.35—Theoretical Energy Distribution of Neutrons Inelastically Scattered by Yb. Reprinted from NYO-636. Incident neutron energy is E , and scattered neutron energy is \bar{E} . Parameters used in Eq. (56) are: ($Z = 70$; $A = 174$); $a = 10.7 \text{ MeV}^{-1}$; $r_0 = 1.5 \times 10^{-13} \text{ cm}$; $E_0 = 0$.

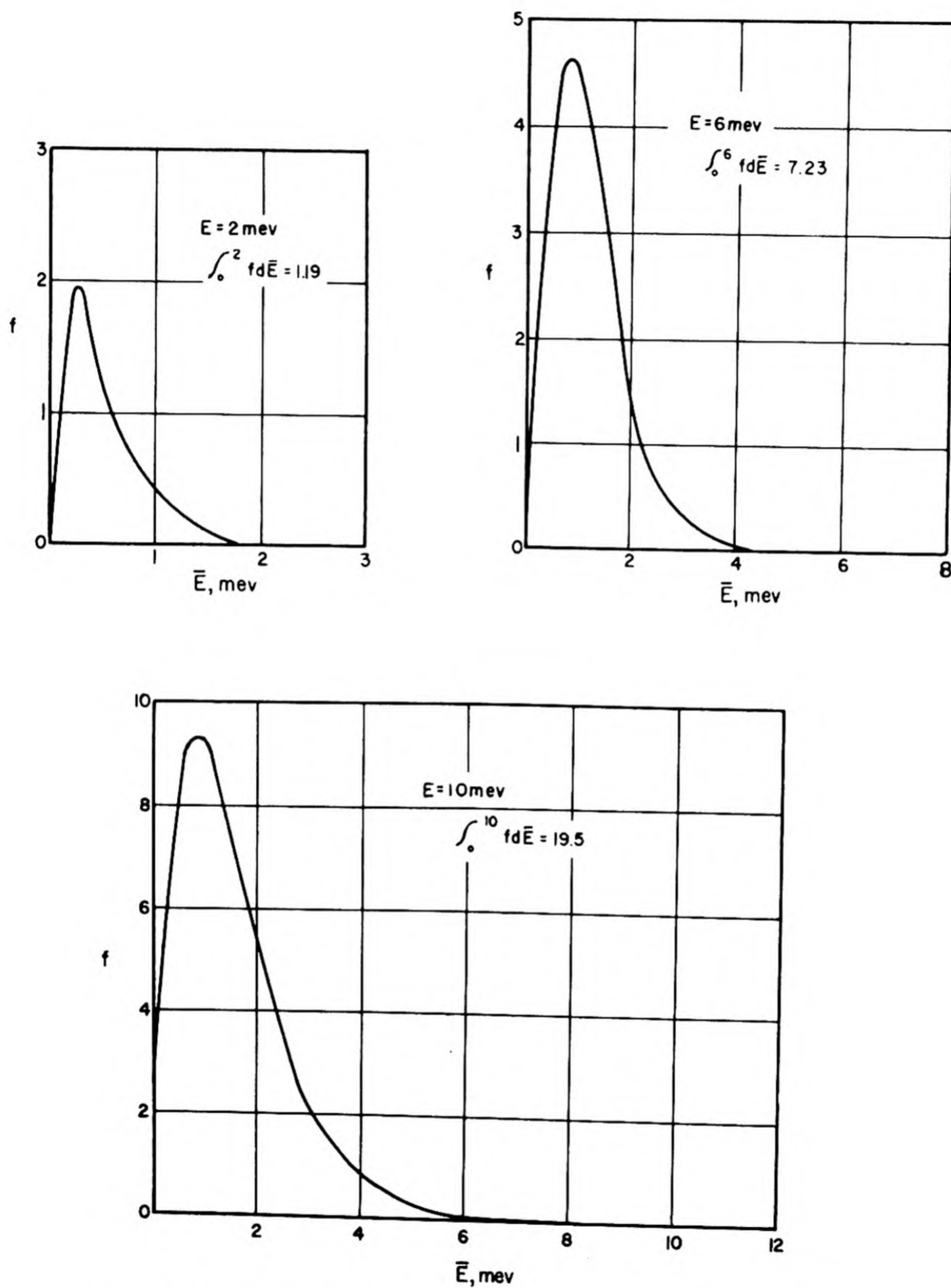


Fig. 1.2.36 — Theoretical Energy Distribution of Neutrons Inelastically Scattered by Th. Reprinted from NYO-636. Incident neutron energy is E , and scattered neutron energy is \bar{E} . Parameters used in Eq. (56) are: ($Z = 90$; $A = 232$); $a = 13.2 \text{ MeV}^{-1}$; $r_0 = 1.5 \times 10^{-13} \text{ cm}$; $E_0 = 0$.

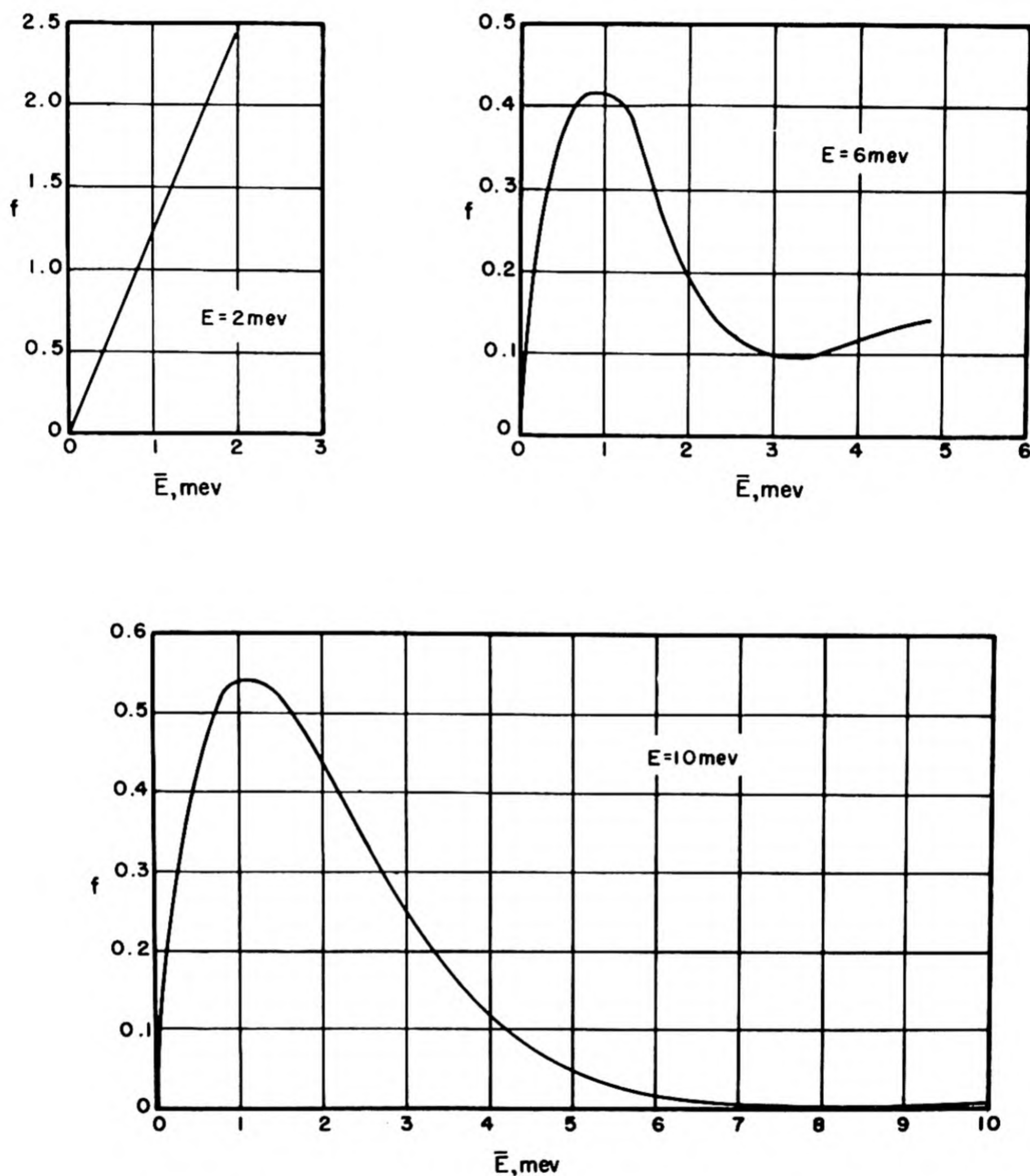


Fig. 1.2.37 — Theoretical Energy Distribution of Neutrons Inelastically Scattered from Sn for Various Incident Energies. Reprinted from NYO-636. Parameters used are: ($Z = 90$; $A = 125$); $a = 6.8 \text{ meV}^{-1}$; $r_0 = 7.5 \times 10^{-13} \text{ cm}$; $E_0 = 3 \text{ meV}$.

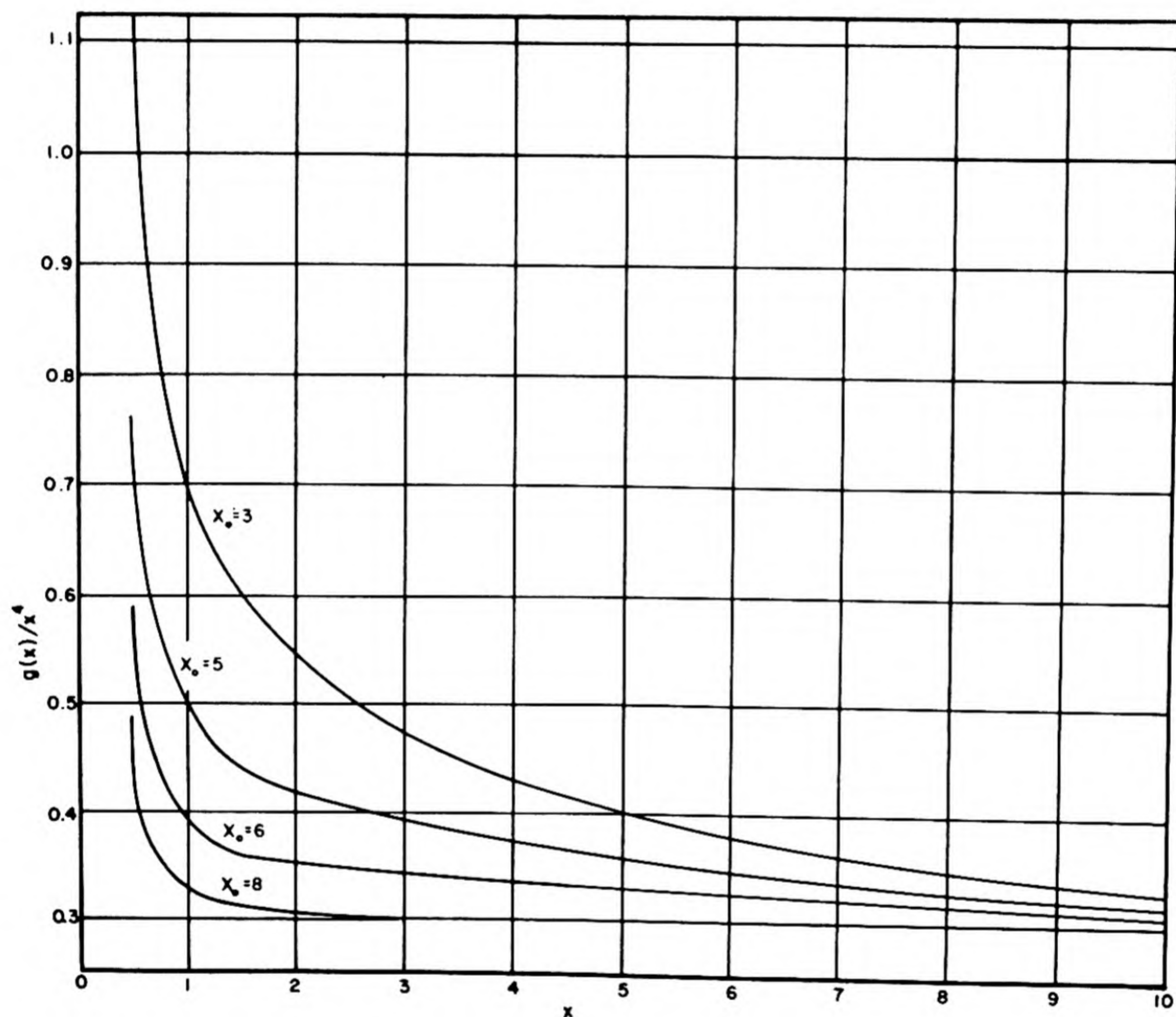


Fig. 1.2.38 — $g(x)/x^4$ vs x for Several Values of the Nuclear Radius. Reprinted from NYO-636.

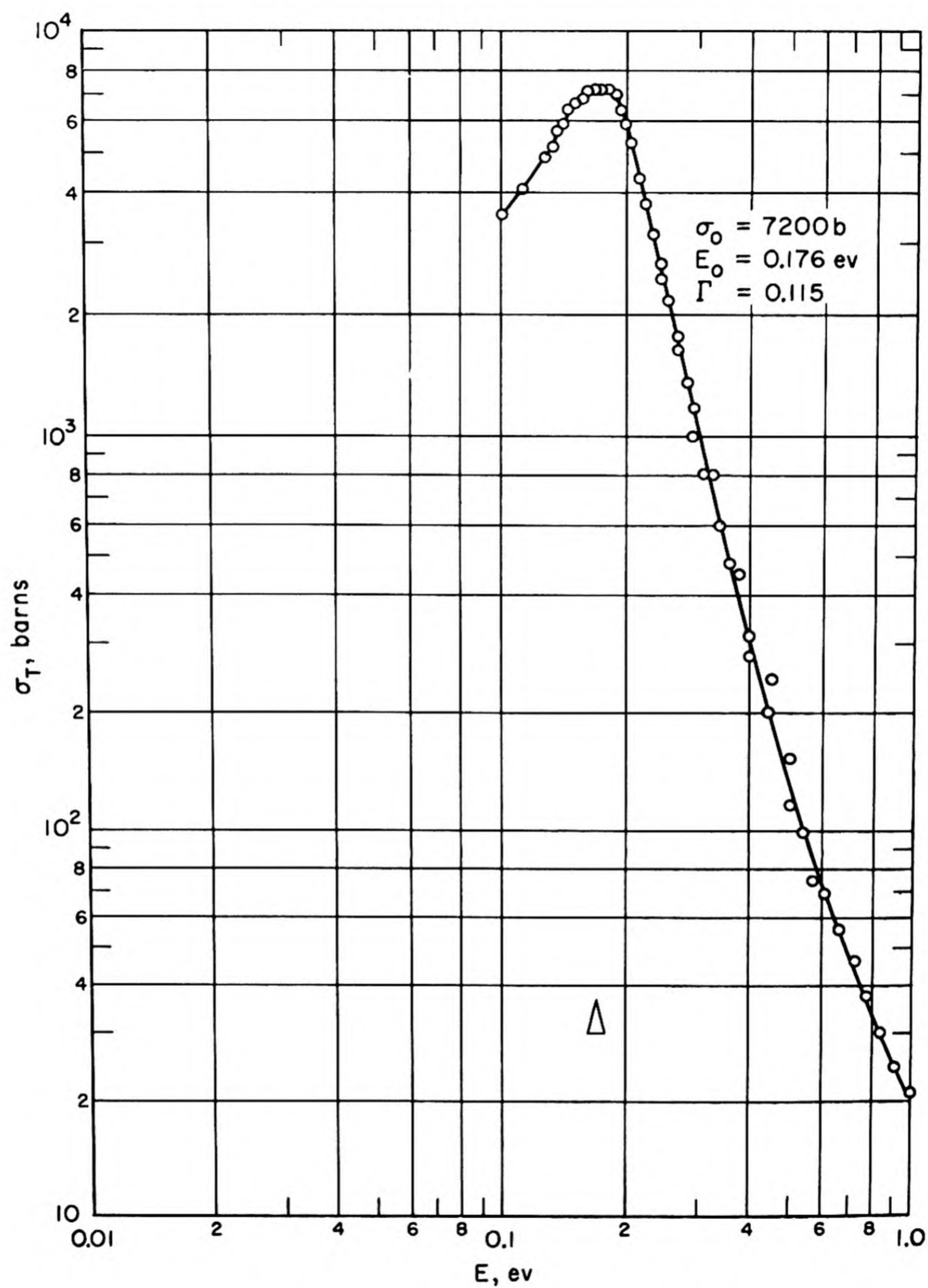


Fig. 1.2.39 — Total Cross Section of Cd. Reprinted from AECU-2040.

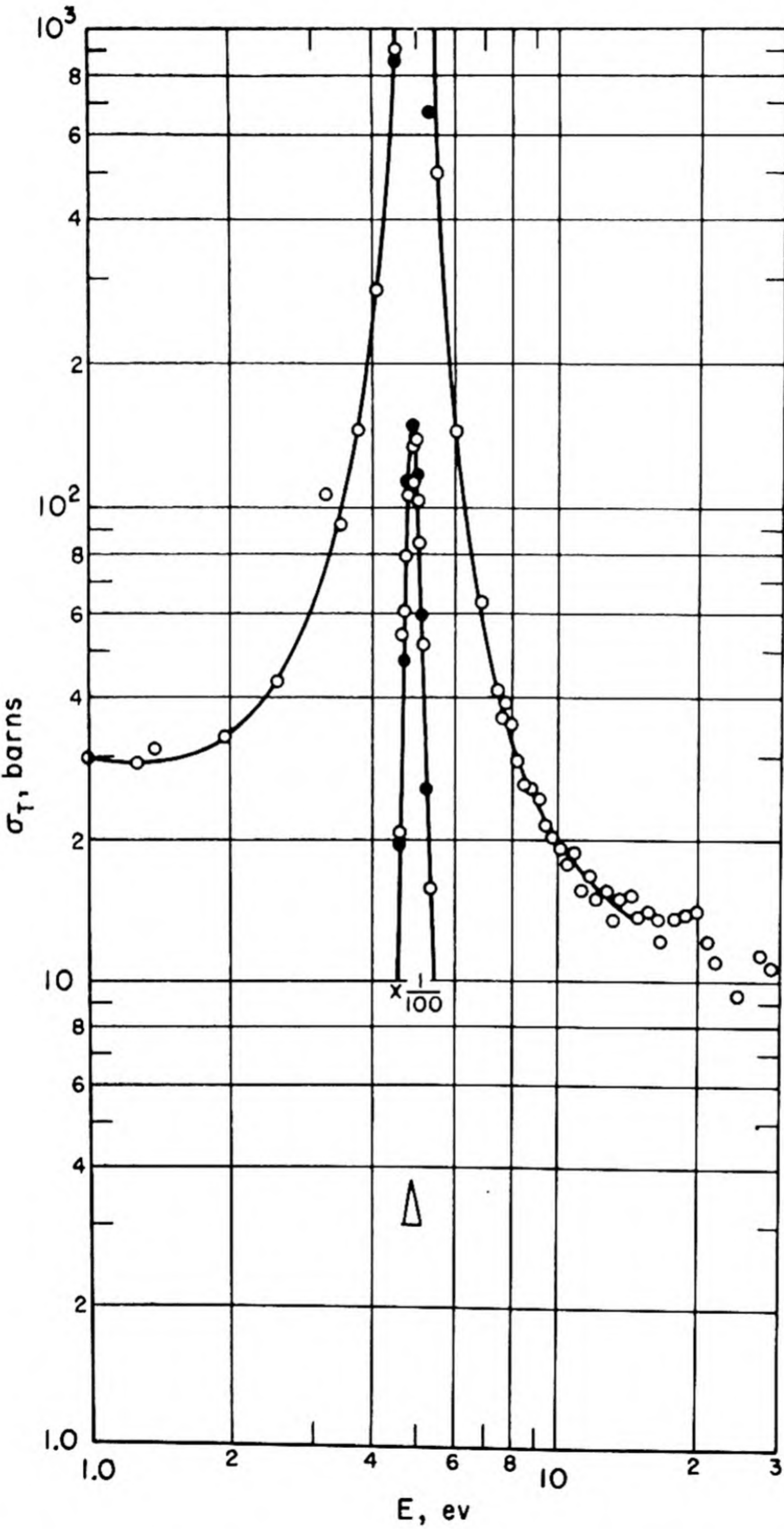


Fig. 1.2.40 —Total Cross Section of Au. Reprinted from AECU-2040.

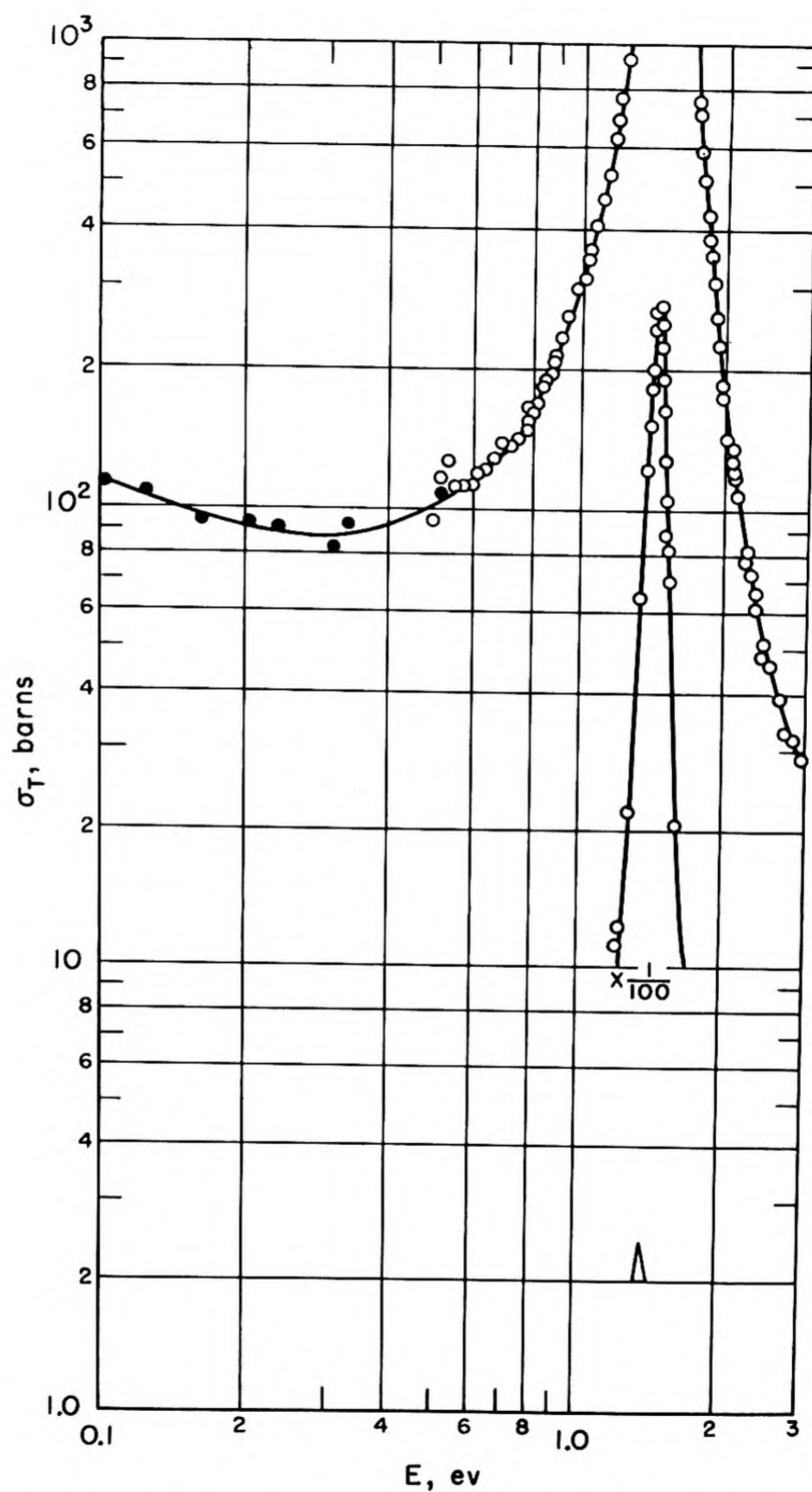


Fig. 1.2.41 — Total Cross Section of In. Reprinted from AECU-2040.

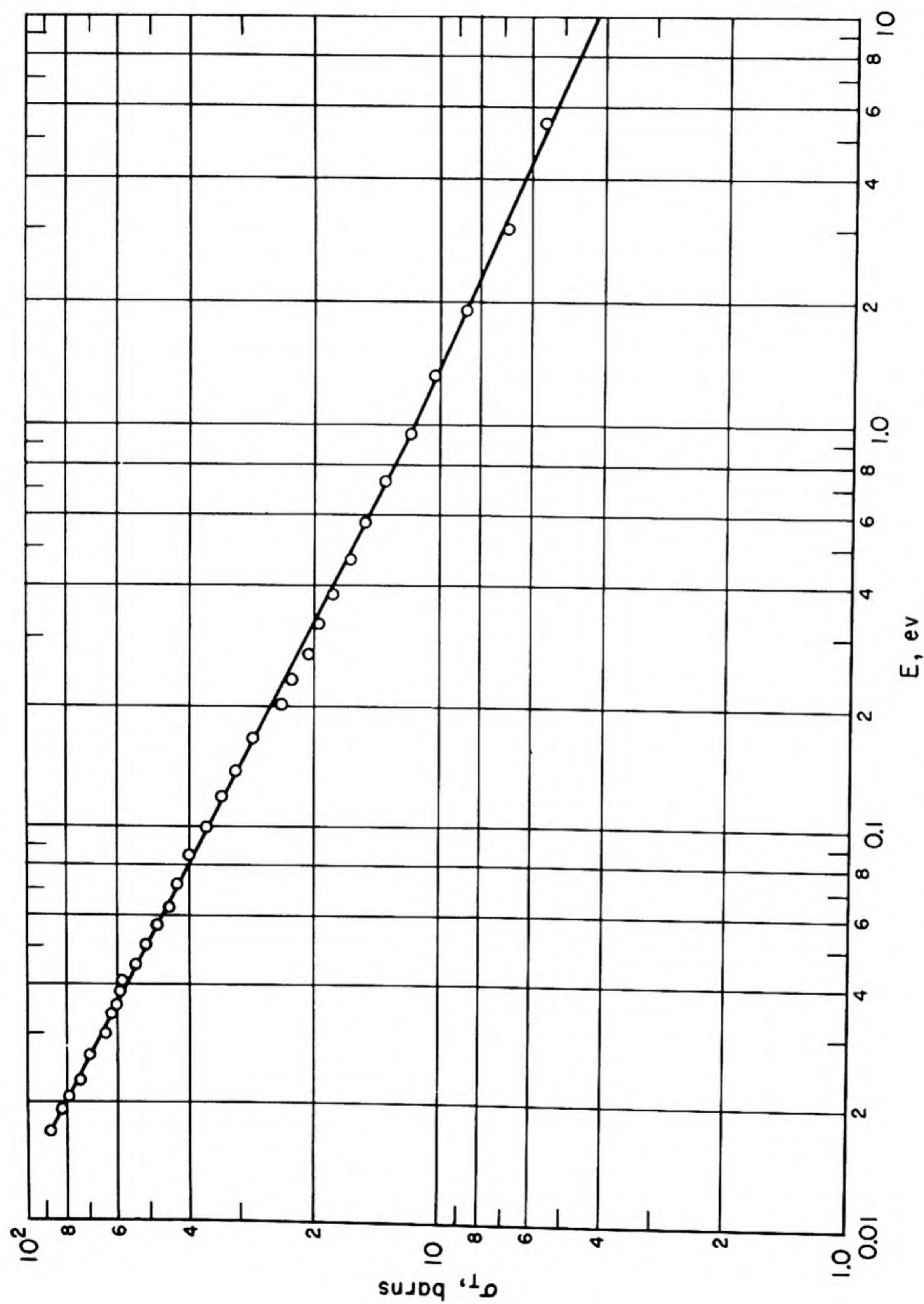


Fig. 1.2.42 — Total Cross Section of Li. Reprinted from AECU-2040.

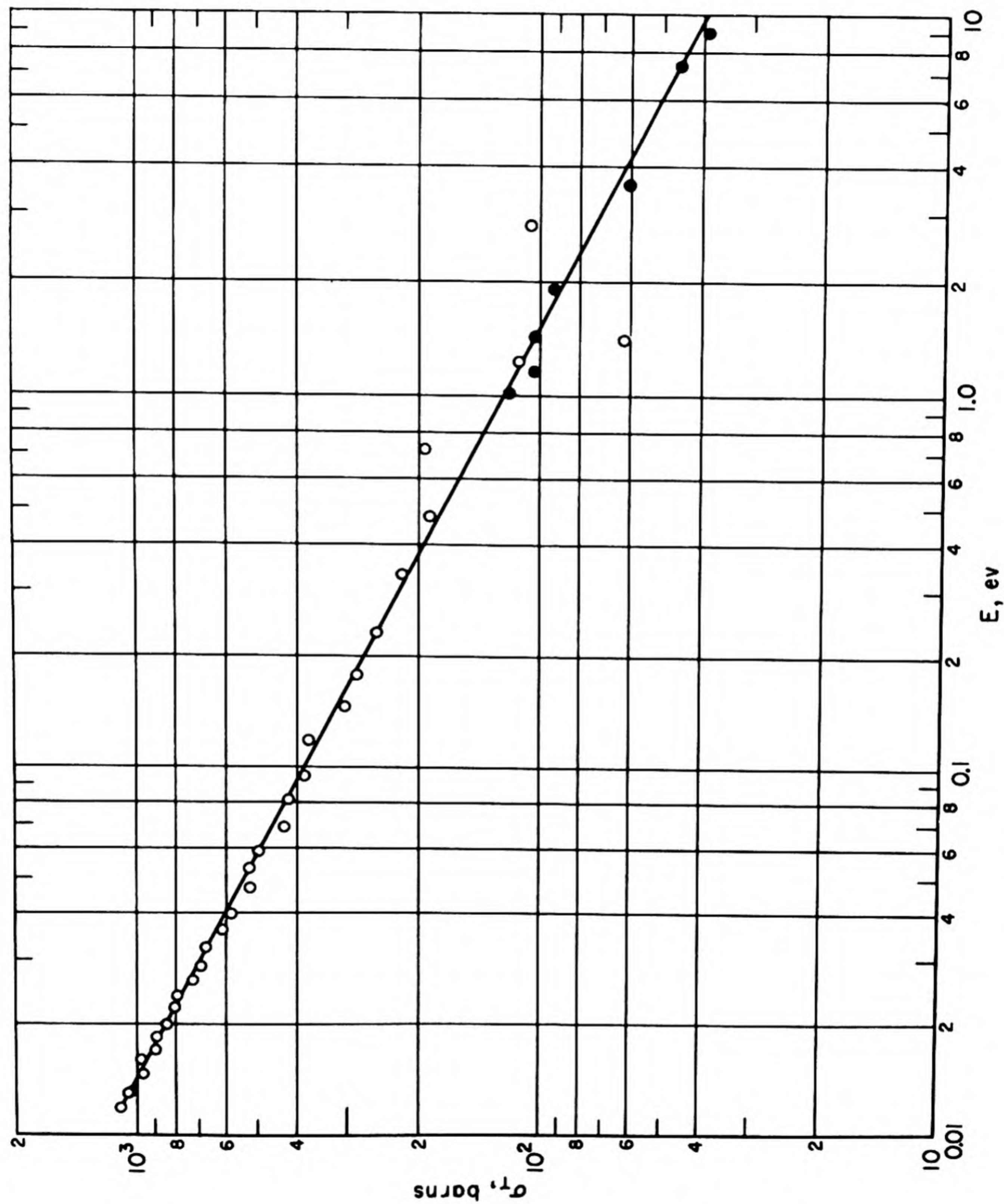


Fig. 1.2.43—Total Cross Section of B. Reprinted from AECU-2040.

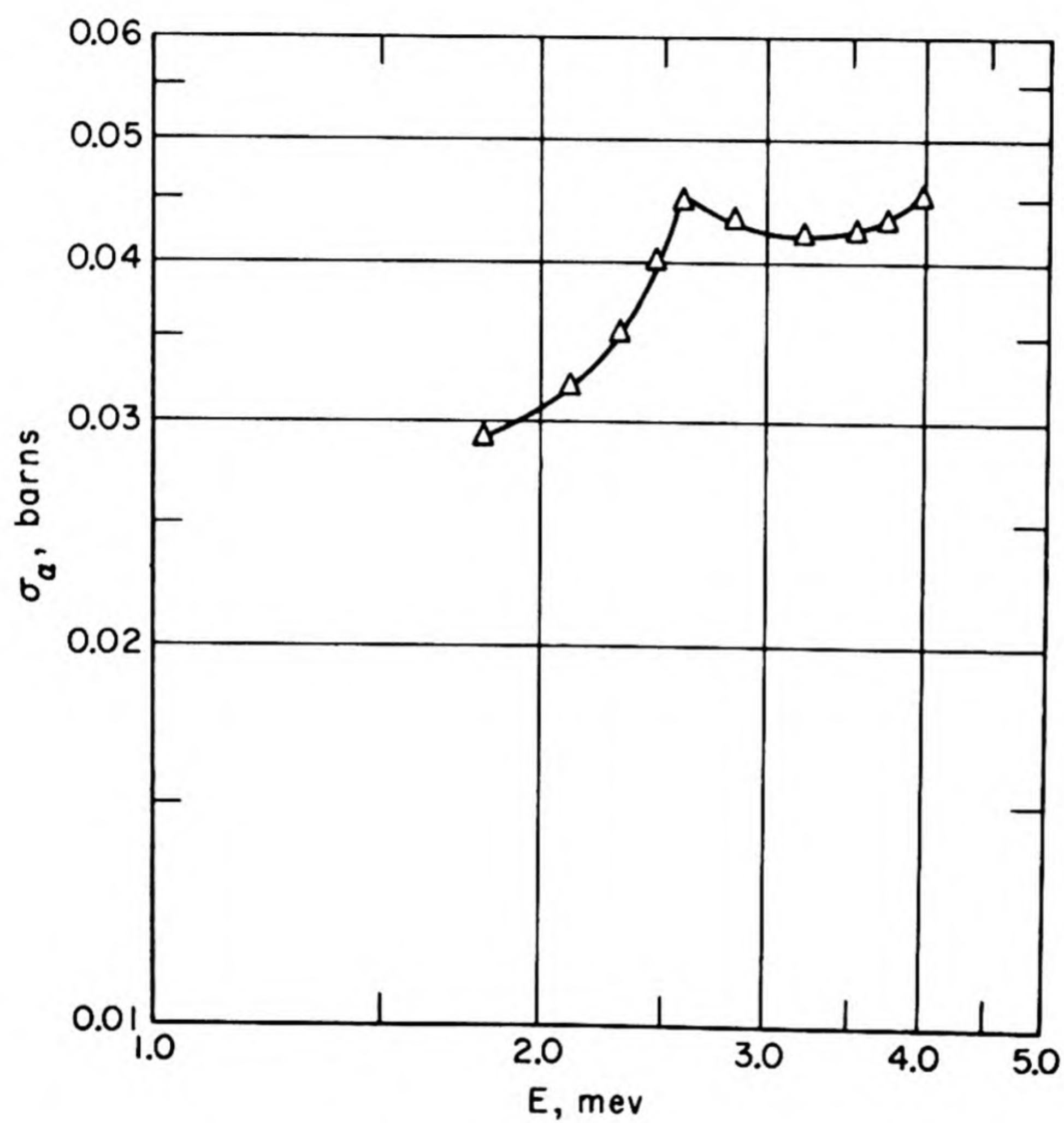


Fig. 1.2.44 — Cross Section for $\text{Be}(n, \alpha)$ Reaction. Reprinted from AECU-2040.

Table 1.2.4 — Table of Isotopes

J. M. Hollander, I. Perlman, and G. T. Seaborg
 Department of Chemistry and Radiation Laboratory
 University of California, Berkeley, California

December 1952

The following table represents a complete list of all the radioactive and stable isotopes of the elements, together with a number of their salient features, as recorded in the literature or by private communication by approximately December 1952.

A primary objective has been to retain as much of the compactness of the previous editions as is consistent with an adequate coverage of the multitudes of nuclear data presently available.

A new system of references has been employed. Each paper is represented by the code symbol of the first author, followed by the year in which the paper was published. If two or more papers by one author have appeared during a single year, these are distinguished by the small letters a, b, c, etc. following the main reference. For example, 16H is the code symbol given to O. Hahn; thus, the references 16H41, 16H41a, and 16H41b represent three papers published in 1941 of which O. Hahn is the first author. The code symbols given to the authors are arranged alphabetically only with respect to the first letter of their names.

A description of the entries in the various columns is given below, followed by a table listing some frequently used abbreviations.

ISOTOPE

The first column lists the atomic numbers, chemical symbols, and mass numbers of the nuclear species. Separate entries have been made for each nuclear state whose half-life has been experimentally determined. Metastable excited states are denoted by the superscript "m" following the mass number, and for those cases in which two or more isomeric states are known, they are distinguished by the use of the superscripts "m₁", "m₂", etc.

CLASS AND IDENTIFICATION

The degree of certainty of each isotopic assignment is indicated by a letter, according to the following code:

- A Element and mass number certain
- B Element certain and mass number probable
- C Element probable and mass number certain or probable
- D Element certain and mass number not well established
- E Element probable and mass number not well established or unknown (mass number not listed means that it is unknown)
- F Insufficient evidence
- G Assignment probably in error

Data which have been shown to be in error have in general been eliminated from the table. A few isotopes have been quoted so widely in the literature, however, that it was felt some reference

should be made to them. For these cases the G rating has been adopted, and reference made both to the original work and to that which has supplanted it.

The means by which the mass assignments were made are next tabulated. In general, several references are given here, the first of which denoted the probable discoverer of the isotope (except in the cases of the old natural radioactivities). Following this, references are given to the paper or papers which contributed most significantly toward giving the isotope its best or present rating. Some indication of the experimental methods used in making the various assignments may be had from the following symbolism:

chem	Chemical separations, establishing uniquely the chemical identity (atomic number) of the isotope
genet	Proven genetic relationships (by chemical or other means) with other isotopes whose mass assignments are presumably known
genet energy levels	Proof of isobaric relationship with an identified nuclide by observation of identical energy levels following decay of both, implying decay to the same product
excit	Loosely refers to energetic considerations which have aided in making the mass assignment. Some of these might be: <ol style="list-style-type: none"> (1) Excitation or yield experiments to establish the nuclear reaction which produces the isotope (2) Bombardments with low energy particles, in which possible products are few (3) Mass calculations, or other estimates or measurements of Q values (4) In a few cases, use of fission yield data in making assignments
cross bomb	Studies of yields of the isotope in several different types of bombardments, in which the target elements as well as the projectiles have been varied
n-capt	Cases where bombardments with slow neutrons (n- γ reactions) have provided key evidence in the mass assignments
sep isotopes	The use of target elements enriched or depleted in a certain isotope
mass spect	Identification of the mass number by means of a mass spectrograph
resonance neutron activation	Identification of a nuclear isomer by observing both isomers upon irradiation with filtered neutrons
decay charac	Identification of expected or predicted decay characteristics

PERCENT ABUNDANCE

The relative isotopic abundances for the elements are given in accordance with the "best values" listed in the report (1B50) by K. T. Bainbridge and A. O. Nier. In some of the light elements,

reference is made also to papers which discuss source variations in isotope abundances.

TYPE OF DECAY

The observed modes of decay have been listed for all radioactive nuclei. In cases of branched decay between two or more modes, the branching ratios are listed wherever they are known. Symbols used are:

β^- Negative beta particle (negatron) emission

β^+ Positive beta particle (positron) emission

α Alpha particle emission

EC Orbital electron capture. It may be assumed that x-rays have been observed or actually identified in virtually all cases of orbital electron capture listed. If the ratio of L electron capture to K electron capture has been determined, it is given here as L/K.

IT Isomeric transition (transition from upper to lower isomeric state of same nucleus)

n Neutron emission

When experimenters have searched for and failed to find a particular mode of decay, this is indicated, for example, as "no β^+ ", Experimental upper limits are frequently given, but no theoretically predicted limits have been quoted.

Among the heavy alpha emitting isotopes, calculations by means of closed radioactive decay cycles have shown that many of these isotopes are thermodynamically stable against β^- , β^+ , or EC decay. This has been indicated by the term " β stable," followed by an abbreviation for the principle of conservation of energy, which is used in the calculations.

HALF-LIFE

Half-life values are listed without qualification where the determination has been a direct measurement of decay rate. In other cases, the experimental methods have been described with the aid of the following symbols:

sp act Determination by weighing a long lived isotope of known purity

delay coinc Measurement of the time interval between two successive nuclear events (such as β^- and γ emission) thus establishing the lifetime of the state responsible for the second event. By this method, half-lives between 10^{-3} s and 10^{-10} s have been determined.

yield	Estimation of half-life from the amount of activity resulting from a nuclear reaction whose cross section (or yield) is known or estimated
genet	Measurement of the half-life of a parent activity by determining the yield of a daughter activity as a function of time, where periodic chemical separations of daughter from parent have been performed

An attempt has been made to list the best value or values first. However, in a few cases where many values of comparable precision have been reported, and no choice seemed obvious, an average value for the half-life has been listed; this is explicitly stated, and references are given to all the papers whose values contributed to that average. Also, among the natural radioactivities an average value is often used which was taken from an international committee summary report (IC31).

PARTICLE ENERGIES

The particle energies are followed by other relevant information pertaining to the decay scheme, and by a description of the experimental methods used in obtaining the data. In cases of complex alpha structure or several partial beta spectra, the relative abundances of the various groups within that mode of decay are given in parentheses.

Beta particle energies correspond to the upper limits of the spectra.

Alpha particle energies have been quoted only where the investigator has actually measured them. Where he has determined only the relative abundances of alpha groups or the energy differences between groups, this has been indicated as in the example:

$$\alpha_0 (10\%), \alpha_{50} (75\%), \alpha_{80} (15\%)$$

meaning that 75 percent of the alpha particles lead to a state 50 kev above the ground state, and that 15 percent of the alpha particles lead to a state 80 kev above the ground state.

The term "long range α " is the classical designation for alpha particle groups emitted from excited states of the listed nuclide, and the energies therefore are not included in the Q_α value, which applies to the ground state to ground state transition. These alpha groups occur in competition with gamma ray emission, following the beta decay of the parent nuclide.

Conversion electron energies are listed only when it is not known in which shell internal conversion takes place or when no attempt was made by the experimenter to relate the electrons with observed or unobservable gamma rays; in all other cases, entries are made in the column for gamma transitions.

Experimental methods are described as follows:

abs	Absorption
-----	------------

spect	Magnetic deflection (magnetic spectrograph or spectrometer or counter with magnetic field)
scint spect	Measurement of pulses produced by a scintillating crystal or solution
ion ch	Measurement of pulse sizes in ionization chamber or proportional counter
cl ch	Cloud chamber (with magnetic field in case of beta particles)
coinc abs	Beta and gamma coincidence counters with absorbers
coinc spect	Coincidence counters arranged with a spectrometer or spectrometers

GAMMA TRANSITIONS

Gamma transitions are described by the following information, insofar as reliable data permit:

Energy of the gamma quantum. When internal conversion electrons form the basis for the energy determination, the energy listed in this column is always that of the corresponding gamma ray transition.

Abundances of gamma rays. This may be given as the number of unconverted gamma rays emitted per 100 disintegrations. Where an absolute abundance has not been determined, often the relative unconverted gamma ray abundances have been measured. These are tabulated as $\gamma_1/\gamma_2/\gamma_3 \approx 2/1/5$, for example.

Internal conversion coefficients. These are given for each gamma transition as the ratio of the number of conversion electrons emitted to the number of unconverted gamma quanta emitted, and are expressed as e/γ . Where conversion coefficients for individual electron shells have been determined, they are denoted as e_K/γ , e_L/γ , etc.

Conversion coefficient ratios. Where the ratios of internal conversion coefficients in several electron shells have been measured, they are listed as K/L , L/M , $K/L+M$, $K/L/M$, $L_I/L_{II}/L_{III}$, etc.

Gamma rays associated with short lived isomers have been listed as entries both of the isomer and of its parent.

When an author states that gamma radiation is present, but reports no energy determination, this is indicated by the symbol " γ ". Conversely, when attempts to find gamma radiation have failed, this has been indicated by "no γ ".

X-rays have been mentioned only when they are the prominent radiation observed in measuring an activity, or when the observation and identification of x-rays has been crucial in the characterization of an isotope.

The symbols used to describe the methods employed for the determination of gamma ray energies or for the elucidation of decay schemes are as follows:

spect	Secondary electrons observed with magnetic spectrograph or spectrometer
spect conv	Internal conversion electrons observed with magnetic spectrograph or spectrometer
scint spect	Measurement of pulses produced by a scintillating crystal or solution
cryst spect	Direct measurement by diffraction of gamma rays with a bent crystal spectrometer
abs	Absorption of the gamma rays
abs conv	Absorption of internal conversion electrons
abs sec	Absorption of secondary electrons
coinc	Studies of coincidences or lack of coincidences (γ - γ , γ -conv, conv-conv, β - γ , etc.) with coincidence counters, and, in some cases, spectrometers
coinc abs	Coincidence studies using absorber techniques
cl ch recoil	Secondary electrons observed in cloud chamber with magnetic field
pair spect	Magnetic analysis of positron-electron pairs produced by gamma rays in a thin radiator
Be- γ -n, D- γ -n, or D- γ -p reactions Measurements of neutron or proton energies from these reactions	

DISINTEGRATION ENERGY AND SCHEME

The disintegration energy, or Q value, of a nuclear transformation is defined as the mass difference (expressed in Mev) between the initial and final systems under consideration. For radioactive decay processes, Q is equal to the sum of the particle kinetic energy, nuclear recoil energy, and the energy of any gamma rays necessary to de-excite the final nucleus to its ground state. For positron decay, the energy equivalent to $2m_0c^2$ has been included in the Q value. Where Q values have been estimated or calculated by the authors of this compilation, the special reference "HPS" is used; otherwise, reference is made to the paper from which the quoted value is taken. In most instances Q values have been obtained from decay data; where this is not the case, the method is indicated.

Energy level diagrams have been drawn in many cases; these are not necessarily complete representations of the data, but sometimes include only those features which are reasonably well established and unambiguous. Heights of the various energy levels above the ground state are indicated at the side of the drawing. Similarly, the total angular momentum (spin) and parity of the states have been included in some cases, where these quantum numbers could be inferred with some confidence from determinations of conversion coefficients, K/L ratios, ft values, etc. We have relied heavily on the interpretation of decay data by Goldhaber and Hill (18G52).

For β^- , β^+ , α , or EC decay, the percentage figures given in the decay drawings total 100% for each mode of decay, thus expressing only the relative abundances of various groups within that mode of decay. (Branching ratios between the several modes of decay are found in the "Type of Decay" column.) In the case of gamma radiation, however, the percentages given refer to the fraction of the total disintegrations of that isotope which give rise to the gamma ray and its conversion electron. This has been done because of the difficulty of assigning a gamma ray to a particular mode of decay.

Measured values for the mechanical or spin moment I of stable or long lived isotopes have also been given in this column. Except as supplemented by more recent data, the values given here are taken from the compilation by Mack (87M50).

METHOD OF PRODUCTION AND GENETIC RELATIONSHIPS

The observed nuclear reactions (giving the target element, projectile, and outgoing particle, in order) by which the radioactive isotopes are formed, and the corresponding references are listed (p - proton, n - neutron, α - alpha particle, d - deuteron, t - triton, γ - gamma ray or x-ray, e - electron, π - pi meson, C - carbon ion). In cases in which the target material is not the naturally occurring element, but one enriched or depleted in a particular isotope, the isotope responsible for the reaction is indicated. No means for identifying the source or energy of the projectile is given.

In nuclear reactions with high energy projectiles, multiple particle ejection is common. Rather than attempt to state definitely the path by which the product nucleus was reached, these spallation reactions are briefly represented by the abbreviation "spall" followed by the symbol of the target element. High energy fission reactions are similarly represented by the words "spall-fission," and thermal or low energy neutron fission simply by "fission."

The criterion for listing genetic relationships has been with few exceptions that these relationships be demonstrated experimentally; for example, by chemical "milking" of daughter activities, analysis of growth-decay curves, or in the case of short lived isomers, by delayed coincidence experiments. The listing of these parent-daughter relationships gives some warning to the reader as to what he may expect in the way of radiation from a given isotope, since a sufficiently short lived daughter's radiation will usually be observed with that of the parent.

A few further abbreviations are listed below:

NNES-PPR Volumes of the National Nuclear Energy Series, Plutonium Project Record, McGraw-Hill Book Co., Inc., New York

[] Properties listed in brackets have not been observed directly, but have been inferred from other experimental data

est, calc Estimated or calculated from theoretical or empirical considerations

HPS Refers to the authors of this compilation

lim	Experimental upper limit
emuls	Photographic emulsion

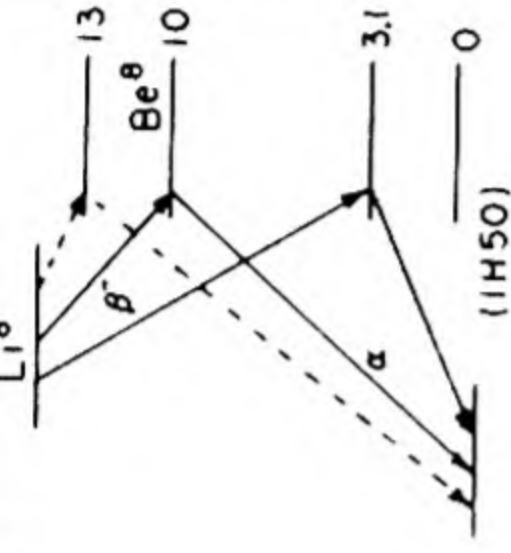
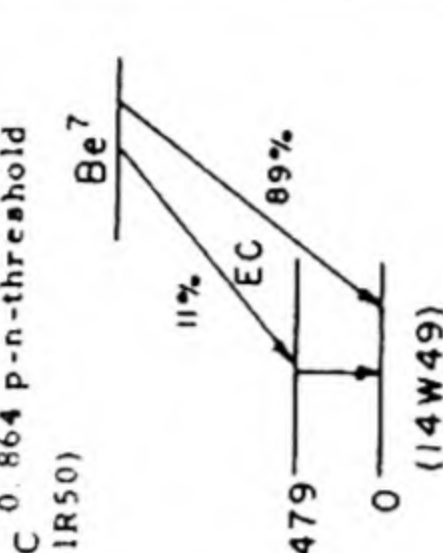
A considerable fraction of the effort necessary to produce this table consisted of abstracting the literature and organizing the data over the past few years. We are greatly indebted to Marjorie Hollander for her efficacious handling of this work, and in addition for her preparation of the drawings.

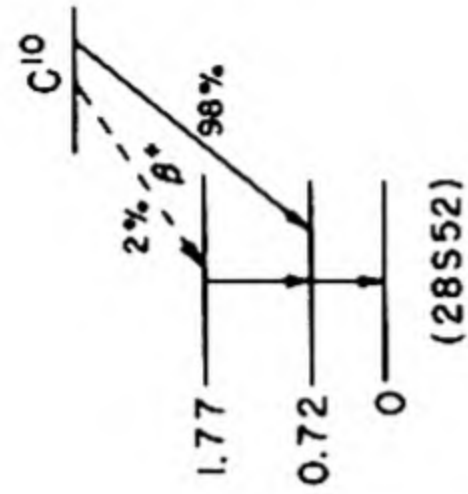
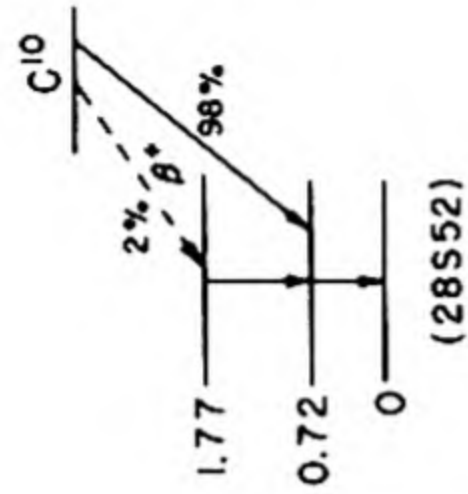
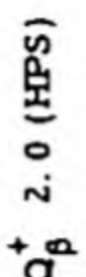
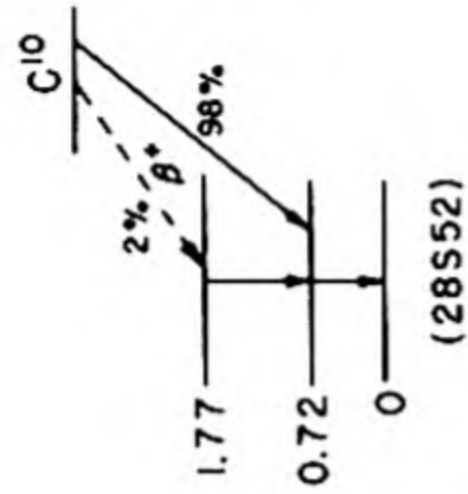
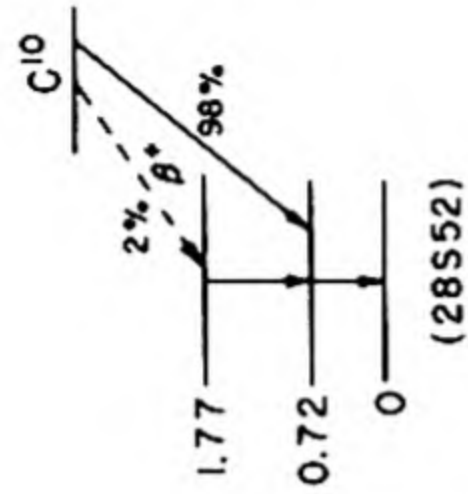
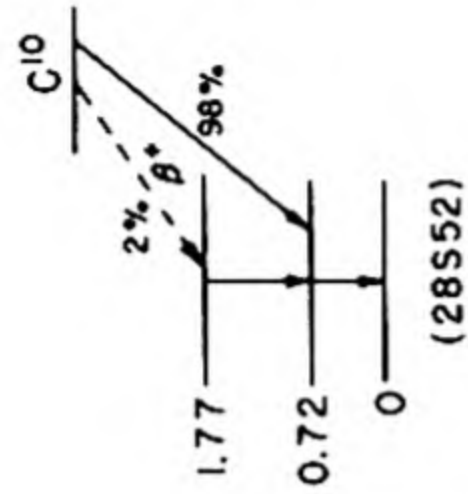
It is a pleasure to acknowledge the generous help and constructive criticism which we have received from our friends and colleagues, and to thank many of the authors whose measurements are cited for their aid in evaluating data familiar to them. We are especially grateful to Dr. Gerhart Friedlander for his invaluable assistance in checking the entire draft.

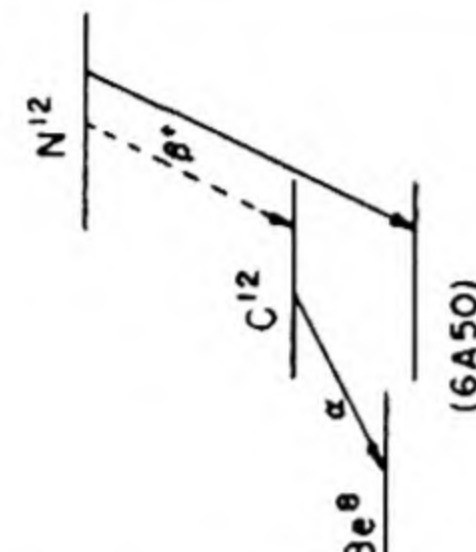
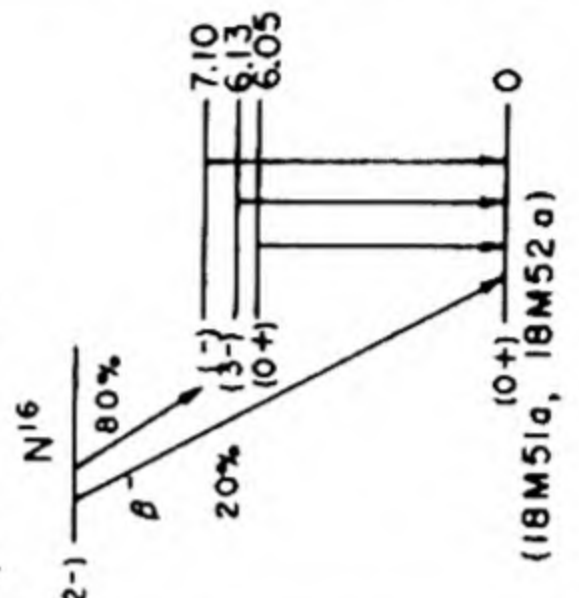
We would also like to express our appreciation to Mildred Davis for the speed and accuracy with which she prepared the manuscript.

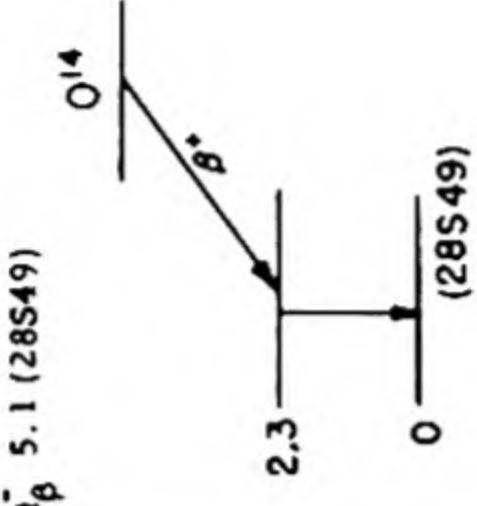
The compilation of this table was supported by the U. S. Atomic Energy Commission.

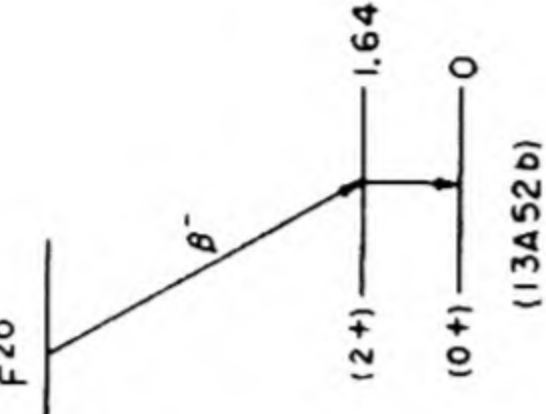
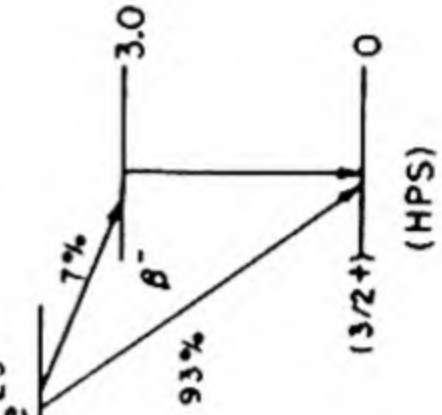
Isotope Z A	Class and identification	Percent abundance	Type of decay	Half-life	Energy of radiation in Mev		Disintegration energy and scheme	Method of production and genetic relationships
					Particles	Gamma-transitions		
${}^1_0\text{n}$	A recoil nuclei, conservation of momentum (18C32); observation of n- α reaction (4F32, 87H33)		β^- (18C35, 26S50)	12.8 m (2R51); 10-30 m (26S50)	0.78 p- β^- spect coinc (2R51)		Q_{β^-} 0.7823 (16L51) n , $I = 1/2$ (87M50)	Be- α -n (18C32); spall reactions in general; fission (92H39, 27A39, 118S39); parent H^1 (26S50, 2R50)
${}^1_1\text{H}$		99.9849 - 99.9861 (diff sources) (52K51); 99.9851 (1V38)					H^1 , $I = 1/2$ (87M50)	
${}^2_1\text{H}$		0.0139-0.0151 (diff sources) (52K51); 0.0149 (1V38)					H^2 , $I = 1$ (87M50)	
${}^3_1\text{H}$	A chem. sep isotopes, excit (6A39, 6A40a)		β^- (6A39, 6A40a)	12.46 y genet (12J50); 12.4 y sp act (11J51); 12.1 y genet (8N47)	0.01795 spect (10L52b); 0.0183 ion ch (21C49); 0.0194 spect (26H51); 0.0189 ion ch (24H49); 0.0186 (72S49a, calc from 12J49); 0.0180 abs bremsstrahlung Zr, Ta (17C49); others (22B49, 21C48, 35K51b, 51S1)	no γ (18G46)	Q_{β^-} 0.019 (HPS) H^3 , $I = 1/2$ (87M50)	D-d-p (6A39, 6A40a); D-n- γ (3Z43); He^3 -n-p (19C48, 28H48); Li-n-t (4O40); Be-d-t (4O40a, 6A40a); B-n-t, N-n-t (20C41); spall reactions (33B52)
${}^3_2\text{He}$		1.3×10^{-4} (atmos), 1.7×10^{-5} (wells) (7A46, 19C49)					He^3 , $I = 1/2$ (87M50)	
${}^4_2\text{He}$		-100					He^4 , $I = 0$ (87M50)	
${}^6_2\text{He}$	A chem (23B36, 23B36a); cross bomb, excit, chem (27S46)		β^- (23B36b)	0.823 s (9A50); 0.82 s (27H49); 0.84 s (12R49); 0.85 s (27S46)	3.50 spect (16W52); 3.2 abs (12R49); 3.5 abs (27S46); others (23B36b, 16K48, 2P50, 35A50)	no γ (16K48, 27S46)	Q_{β^-} 3.50 (16W52); Q_{β^-} 3.55 (36D52)	Be-n- α (23B36, 9P37, 27S46, 16K48, 2P50); Li- γ -p (25B47, 44S52a)
${}^6_3\text{Li}$		7.52 (17L38)					Li^6 , $I = 1$ (87M50)	
${}^7_3\text{Li}$	A excit (4E49)		IT- (4E49)	5.2×10^{-14} s Doppler broadening (4E49)		-0.48 spect (4E49)		B-n- α (4E49)
${}^7_3\text{Li}$		92.48 (17L38)					Li^7 , $I = 3/2$ (87M50)	

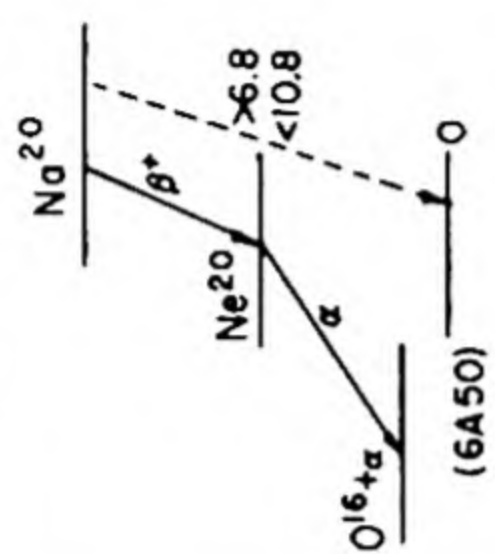
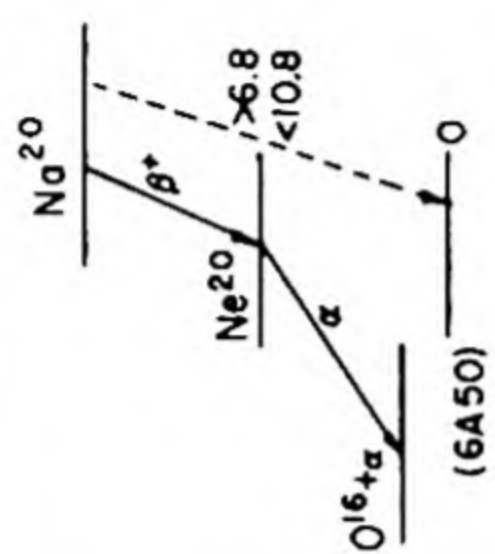
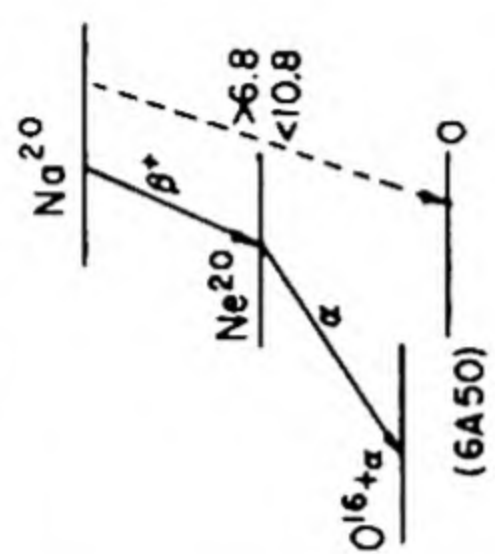
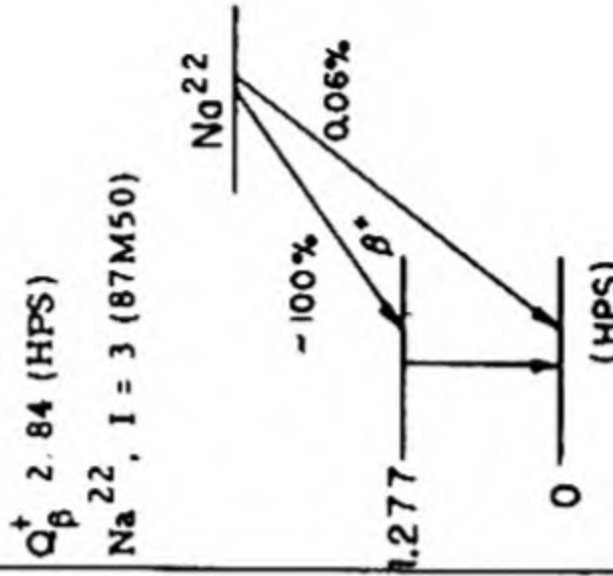
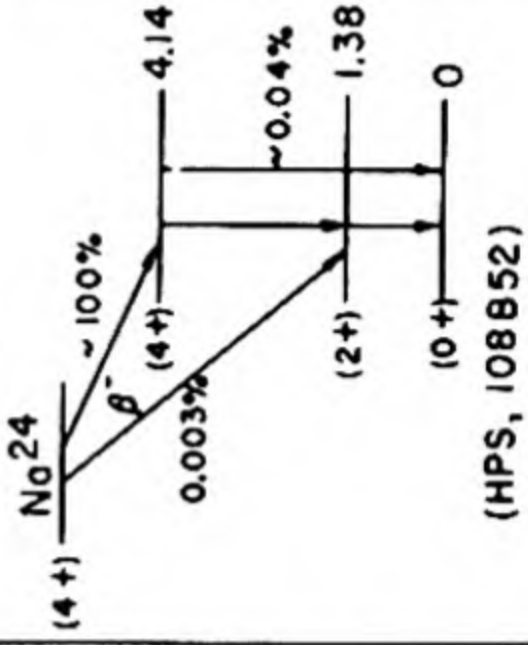
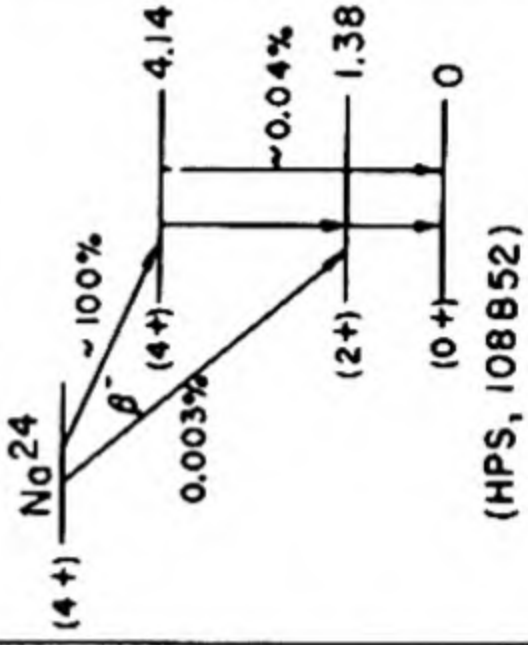
Li ⁸	A excit (22C35, 11L37); n-capt, sep isotopes, genet (28H47)	β^- , 2a (11L37)	0.825 a (11R51); 0.88 a (26B37, 3047, 10B49); 0.85 a (44S52a); 0.89 a (28H47)	β^- : 13 (-90%), -6 (-5%), -3 (-5%) spect (1H50); <13 (-2%) β - γ coinc abs (5V51a); 12.0 cl ch (26B37); abs (3047); two α 's; total energy 3.2, 7-9 cl ch (27B48)	no γ (13R37, 26B37); γ (very weak) β - γ coinc (5V51a)	Q_β^- 15.99 (9V52)		Li-n- γ (15K36, 10P46, 28H47); Li ⁷ -n- γ (28H47); Li-d-p (22C35, 5D35, 1F37, 26B37, 11L37, 1H50, 1Y50); spall C, N, Ne, A, Kr, Xe (13W50); Be- γ -p (3047, 44S52a, 40T52); B-n-a (18L39); B- γ -2p, B- γ -2pn (44S52a)
Li ⁹	B excit, cross bomb (20G51)	β^- , n (20G51, 78H52)	0.168 a (20G51); 0.170 a (78H52); 0.19 a (44S52a)			Q_β^- 0.864 p-n-threshold (51R50)		Be-d-2p (20G51); B-p-3p, B-d-3pn (20G51); B- γ -2p (44S52a); C-d-4pn, C-p-4p (20G51); C-p-4p (78H52)
⁴ Be ⁷	A chem, cross bomb, excit (13R38)	EC (13R38)	52.93 d (24S49); 53.61 d (58K52); 54.3 d (55B47); 54.5 d (29B49)		0.479 spect (4E48, 11T49); 0.478 spect (1H49); 0.485 spect (17K48); coinc abs (4Z42); 0.474 spect (5248a); γ (11%) (14W49), (10-13%) (10T49) (Be ⁷ formation yield - γ ratio); others (15R46, 7S47b)	Q_{EC} 0.864 p-n-threshold (51R50)	Li-d-n (13R38, 14R38, 14R38a, 4Z42); Li-p-n (39H39, 39H40); B-p-a (14R38a, 17M39); B-d-on (12M46); spall C (4D50, 74M51), Al, Cu, Ag, Au (74M51)	
Be ⁸	A observation of Be- γ -n reaction (18C35)	2a	<2 x 10 ⁻¹⁴ s photo-dis O16 emula (26W51); <5 x 10 ⁻¹⁴ s photo-dis O16 emula (18M52); 10-15 - 10-17 s calc (15W41)	energy of each α in center of mass system: 0.039 spect (41C51); 0.045 spect (12T49); 0.051 ion ch (40H49); 0.043 range emula (23C50)		Q_α 0.078 (41C51); Q_α 0.089 (12T49); Q_α 0.103 (40H49); Q_α 0.085 (23C50)	Be-p-d (12T49); Be- γ -n (18C35, 40H49); O- γ -2a (18M51, 53L52)	
Be ⁹					no γ (12M47, 19L47, 28H49)	Q_β^- 0.56 (HPS)	Be-d-p (12M46a, 19L47); Be-n- γ (28H47a, 13A50, 11B50a); B-n-p (9E48); C-n-a (28H46)	
Be ¹⁰	A chem (12M46a); chem, mass spect (11P46)	β^- (12M46a)	2.5 x 10 ⁶ y ap act + mass spect (12M47); 2.9 x 10 ⁶ y yield (28H47a)	0.555 spect (15F52); 0.560 spect (13A50); abs (12M46a, 12M47); 0.553 ion ch (11F49a); others (28H49, 16W49, 41H49, 11B50a)		Q_β^- 18 (calc from 6A50)	B- γ -2n, B- γ -3n (44S52a); B-p-t (6A50); Be-p-2n (6A50); C-p-na (6A50); C- γ -p3n (44S52a); spall reactions (33B52)	
⁵ B ⁸	A excit, cross bomb (6A50)	β^+ , 2a (6A50)	0.46 a (102B52a); 0.61 a (44S52a)	β^+ : 13.7 abs (6A50); spect (44S52a)		Q_β^+ 18 (calc from 6A50)		
B ¹⁰						B^{10} , I = 3 (87M50)		
B ¹¹						B^{11} , I = 3/2 (87M50)		

Isotope Z A	Class and identification	Percent abundance	Type of decay	Half-life	Energy of radiation in Mev		Disintegration energy and scheme	Method of production and genetic relationships
					Particles	Gamma-transitions		
${}^5_6\text{B}^{12}$	A excit (22C35a, 1F36)		β^- (22C35a)	0.027 s delay coinc (3J48a, 30B51); 0.022 s delay coinc (25B39)	13.43 spect (1H50); 13.3 abs (30H48); 12 cl ch (26B37); -9 (-4%) coinc abs (5V51a)	-4.5 β - γ coinc abs (5V51)		B-d-p (22C35a, 1F36, 30B51); C ¹⁴ -d-a (32H50b); N ¹⁵ -n-a (3J48a)
${}^6_6\text{C}^{10}$	A chem. sep isotopes (28S48, 28S49)		β^+ (28S49)	19.1 s (28S49)	2.2 abs (28S49)	0.72 (-100%), 1.05 (-2%) scint spect (28S52)		B-p-n, B ¹⁰ -p-n (28S48, 28S49, 28S52); C- γ -2n (44S52a)
${}^{11}_6\text{C}^{11}$	A excit (22C34, 35H34); chem. excit (33B39)		β^+ (22C34)	20.4 m (30S41); 20.5 m (29S41, 12P48, 25C50); 20.0 m (7S44a, 4D51)	0.99 spect (7S44a); 0.981 spect (14T41); 0.95 cl ch (5D40)	no γ , β - γ coinc (7S46a)		Be- α -2n (12M46b); Be-He ³ -n (1P52); B-d-n (26C35, 2Y35, 1F36); B-p- γ (22C34a, 33B39); B-p-n (33B39); C- γ -n (10B46, 12P48, 25C50, 55S51, 22E52, 44S52a); C-n-2n (1P37, 110S51, 30B52); C-d-dn (6T47); C-p-pn (27C47, 82H52); C-He ³ - α (1P52); C- α -an (12M46b, 6T47); N-p- α (33B39); N-n-p ³ n (16K47); N- γ -p ² n (10B46); N- π - ³ n (21T51a); O- γ -an (10B46, 85H52); O-n- α 2n (12M47a); O- π -p ⁴ n (21T51a); epall Cu (57G51)
${}^{12}_6\text{C}^{12}$	98.892 (limestone CO ₂)(6N50)							
${}^{13}_6\text{C}^{13}$	1.108 (limestone CO ₂)(6N50)							
${}^{14}_6\text{C}^{14}$	A chem. cross bomb. excit (16R41)		β^- (16R41)	5566 y weighted average of 3E50, 11J49, 21M50, and 20M51, all by sp act + mass spect (3L51); others (31H49, 17R46, 31H48, 10N48, 1Y48, 17W48)	0.155 spect (15F49, 18W50); 0.156 spect (28C48); 0.154 spect (2L47a), abs (29S47); 0.155 ion ch (10A49); no conv. spect (2L47a); E (average) 0.045 calorimetric (12J52)	no γ (16R41)		C-d-p (16R40, 16R41); C-n- γ (20L45); N-n-p (16R41, 20L45); O-n- α (19M47)

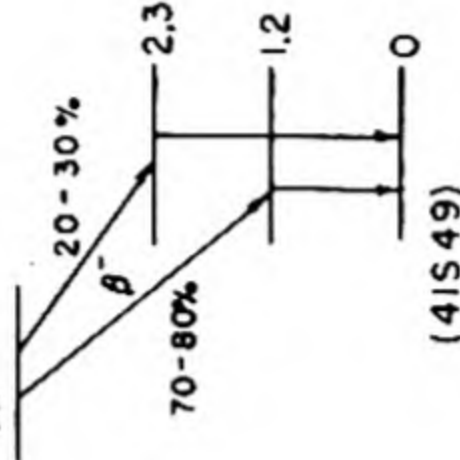
^{15}C	C excit, sep isotopes (32H50)	β^- (32H50)	2.4 s (32H50a)	8.8 abs (32H50a)	5.5 β - γ coinc abs (32H52)	^{14}C -d-p (32H50, 32H50a, 32H52); not found by: ^{14}C -n- γ (1Y50)
^{12}N	A excit, sep isotopes (6A49)	β^+ , β^+ , β^+ (6A50)	0.0125 s delay coinc (6A49)	β^+ : 16.6 abs (6A49); α : -4 total energy of three α 's (6A50)		C-p-n, ^{12}C -p-n (6A49, 6A50); N- γ -2n (33P52)
^{13}N	A excit (4C34, 22C34)	β^+ (22C34)	9.93 m (5W39a); 10.1 m (7S45); 10.2 m (28C48a)	1.24 spect (7S45); 1.25 spect (28C48a); 1.20 spect (1H48); 1.22 spect (14T41); others (21L39, 53K43)	Q_{β}^+ 2.26 (HPS)	B-n-n (4C34, 8E35, 18R37); C-d-n (22C34, 33H35, 2Y35, 26C35, 1F36); C-p- γ (33H35, 26C35); C13-p-n (11A50); N-n-2n (1P37, 34H43); N-d-t (34B42); N- γ -n (10B46, 12P48, 22E52, 44S52a); O-n-p3n (16K47); O- γ -p2n (85H52); spall Al (74M52)
^{14}N			99.635 (6N50)		^{14}N , I = 1 (87M50)	
^{15}N			0.365 (6N50)		^{15}N , I = 1/2 (87M50)	
^{16}N	A excit (22L34, 16F34)	β^- (22L34, 16F34)	7.35 s (35B47); 7.5 s (28H46a); 7.3 s (27S46)	-10.3 (-20%), -4.3 (-40%); -3.8 (-40%) cl ch (35B47); 10, 3.5 abs (27S46); 10 cl ch (28H46a)	Q_{β}^- 10.3 (35B47)	N-n- γ (28H46a, 41F52); N-d-p (1F36); O-n-p (7C37, 26S43, 35B47, 18M51a); F-n- α (22L34, 16F34, 3N36, 2N36, 9P37)
^{17}N	A chem, cross bomb (6A49a, 18K48, 27C48)	β^- , n (18K48)	4.14 s (18K48); 4.15 s (32S51)	β^- : 3.7 β -recoil coinc abs (6A49a); n: 0.9 (mean) ^{16}O recoil in ion ch (6A49a); 1.0 (mean) p recoil in cl ch (36H49)		spall O, F, Na, Mg, Al, Si, P, S, Cl, K (27C48, 18K48); C14-a-p (31S51); O-n-p (83C49); O18- γ -p (32S51); F- γ -2p (44S52a)

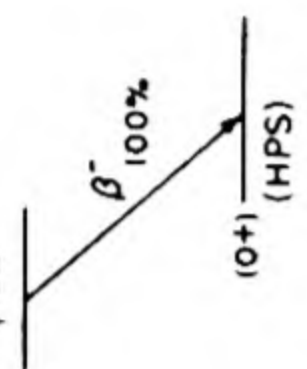
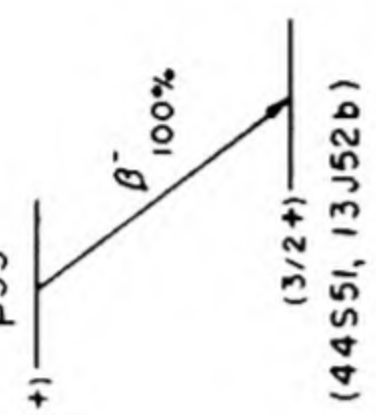
Isotope Z A	Class and identification	Percent abundance	Type of decay	Half-life	Energy of radiation in Mev		Disintegration energy and scheme	Method of production and genetic relationships
					Particles	Gamma-transitions		
8O^{14}	B chem, excit (28S49)		β^+ (28S49)	76.5 s (28S49)	1.8 abs (28S49)	2.3 coinc abs sec (28S49)	Q_{β}^- 5.1 (28S49)  Q_{β}^+ 2.70 (HPS)	N-p-n (28S49); O- γ -2n (44S52a)
8O^{15}	A chem, excit (22L34a, 12M35); excit (1F36, 19K39)		β^+ (22L34a)	118.0 s (2P49); 126 s (12M35, 37B39); 127 s (35D51)	1.683 spect (36B50); 1.68 abs (28S49)	no γ (2P50b)	Q_{β}^+ 2.70 (HPS)	C- α -n (19K39); N-d-n (22L34a, 12M35, 1F36, 36B50); N-p- γ (2D38, 35D51); O- γ -n (37B39, 34H43, 10B46, 12P48, 22E52, 44S52a); O-n-2n (1P37); O-He3- α (1P52)
8O^{16}		99.759 (air O ₂) (6N50); O ¹⁶ /O ¹⁸ variation \leq -4% (13T49, 1K46)					O ¹⁶ , I = 0 (87M50)	
8O^{17}		0.037 (air O ₂) (6N50)					O ¹⁷ , I = 5/2 (3A51)	
8O^{18}		0.204 (air O ₂) (6N50)					O ¹⁸ , I = 0 (91M51)	
8O^{19}	A excit (3N36); n-capt (22M43)		β^- (22M43)	29.4 s (11F44a); 29.5 s (28H46a); 27.0 s (35B47a)	4.5 (30%), 2.9 (70%) abs (35B47a); 4.1 abs (11F44a); -3.2 abs (34H45)	1.6 abs (11F44a)		O-n- γ (22M43, 2S46, 2S47); F-n-p (12A35, 3N36)
9F^{17}	A cross bomb (19W34, 8E34a); chem, excit (12N35, 37H35, 2D38)		β^+ (12N35)	70 s (12N35, 2P50c); 60 s (86H52); 66 s (46L51); 72 s (12P48); 74 s (2D38)	1.72 spect (2P50c); 1.7 abs (46L51); 2.1 cl ch (17K36)	no γ (2P51, 51R51)	Q_{β}^+ 2.74 (HPS)	N- α -n (19W34, 8E34a, 18R37); O-d-n (12N35, 1F36, 2P50c); O-p- γ (2D38); F- γ -2n (10B46, 12P48, 86H52)

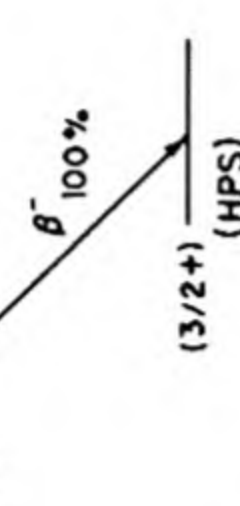

¹⁸ F	A chem (26S37); chem, sep isotopes, excit (2D38)	112 m (26S37, 12P48, 47B49); 115 m (34H43); 107 m (2D38)	0.649 spect (19R51); 0.635 spect (47B49); others (3Y38, 9K41, 20K45, 38H48)	no γ (16K48, 47B49)	Q_{β}^{+} 1.67 (19R51)	O-a-pn (2T47a); O18-p-n (2D38); O-d-n (3Y38, 3D40, 20W41); O-He3-p (1P52); O-t-n (20K45); F-n-2n (1P37); F-n-2n (9K41, 34B42); F-y-n (34H43, 10B46, 12P48, 22E52, 86H52); F-p-pn (19R51); Ne-d-a (26S37); Na-y-on (10B46, 85H52); epall Al (74M52, 74M52a), Cu (57G51, 74M52a), Cl, Ag, Au (74M52a)
¹⁹ F	100 (1A20)				F^{19} , $I = 1/2$ (87M50)	
²⁰ F	A excit (22C35, 1F36, 3N36)	10.7 s (33S50); 12 s (22C35)	5.41, no -7 β^{-} (lim 1%) spect (13A52b); 5.33 (97%), 6.7 (3%) spect (47L50); 5.0 spect, abs (3J50); others (38B40)	1.631, no 2.5 γ (lim 0.2%) spect, Be-y-n reaction (13A52b); 1.64, no 2.5 γ spect, γ - γ coinc (47L50); 1.64, 2.5 (weak) spect, abs nec (3J50); 2.2 cl ch recoil (38B40); ν (coinc with 5.0 β^{-}) β - γ coinc (21C40, 3J50)	Q_{β}^{-} 7.04 (13A52b) F20 	F-d-p (22C35, 1F36, 33S50, 3J50, 13N50, 13A52c); F-n-y (3N36, 2S47, 21K50); Na-n-a (3N36)
¹⁹ Ne	A cross bomb, excit (21W39)	18.2 s (28S49); 18.5 s (34S52); 20.3 s (21W39)	2.18 spect (34S52); 2.2 cl ch (21W39); 2.3 abs (28S49)	no γ (21W39, 34S52)	Q_{β}^{+} 3.20 (HPS)	F-p-n (21W39, 47B51a, 34S52)
²⁰ Ne	90.92 (6N50a)				Ne^{20} , $I = 0$ (87M50)	
²¹ Ne	0.257 (6N50a)				Ne^{21} , $I = 3/2$ (87M50)	
²² Ne	8.82 (6N50a)				Ne^{22} , $I = 0$ (87M50)	
²³ Ne	A excit (12A35); chem (23B37, 9P37)	40.2 s (36B50a); 40.7 s (34H44a); 40 s (12A35, 23B37)	4.21 (-93%), 1.18 (-7%) spect (36B50a); 4.3 abs (35B46a, calc from 14P40); 4.1 abs (14P40)	-3 abs (2P50a)	Q_{β}^{-} 4.21 (2P50a) Ne23 	Ne-n-y (41F52); Ne-d-p (22W40); Ne22-d-p (14P40, 36B50a, 2P50a); Na-n-p (12A35, 3N36, 9P37, 23B37); Mg-n-a (12A35)

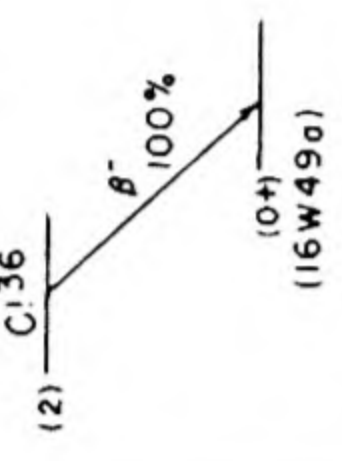
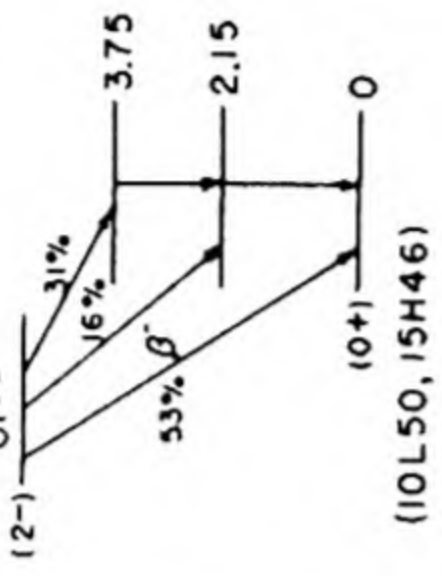
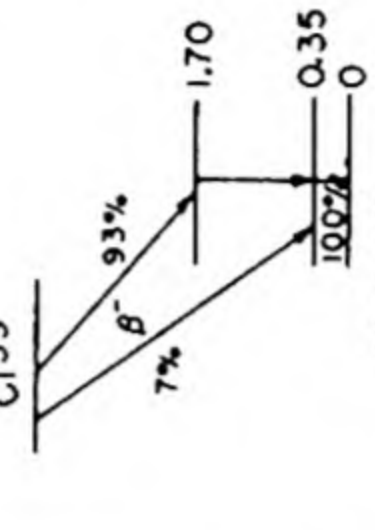
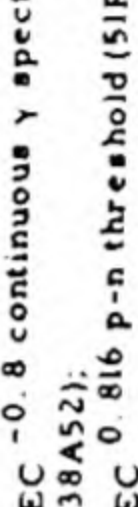
Isotope Z A	Class and identification	Percent abundance	Type of decay	Half-life	Energy of radiation in Mev		Disintegration energy and scheme	Method of production and genetic relationships
					Particles	Gamma-transitions		
¹¹ Na ²⁰	A excit (6A50)		β^+ , α (6A50, 44S51a)	0.385 s (102B52a); 0.23 s (44S51a)	$3.5 < \beta^+ < 7.3$ eat (44S51a)			Ne-p-n (6A50); Na-v-3n (44S51a, 44S52a)
²¹ Na	A excit (29C40a)		β^+ (14P40)	22.8 s (34S52); 23 s (29C40a)	2.50 spect (34S52); 2.53 spect (52B51b)	no γ (34S52)		²⁰ Ne-p- γ (40B47); Ne-p-n (29C40a); Ne-d-n (14P40); Mg-p- α (34S52); Mg ²⁴ -p- α (39B48)
²² Na	A chem, excit (17F35)		β^+ -100%, no EC (21G46)	2.60 y (23L49); 2.8 y (36S39)	0.542 spect (23M50); 0.575 spect (21G46); -1.8 (0.06%) spect (56W52); -1.8 (0.004%) cl ch (25M49); others (23L37, 2039)	1.277 spect (13A49); 1.30 (coinc with β^+) spect, β - γ coinc (21G46); 1.3 spect (2039) others (85S51)		F-o-n (17F35, 23L37, 24M37); Ne-d-n (23L37); Ne-21-p- γ (40B47); Na-n-2n (41B46, 35S47); Mg-d- α (23L37, 13A49); spall Mg, Mg ²⁵ , Mg ²⁶ (92M51), Fe (45R52), Cu (42B51a)
²³ Na		100 (37S36a)						
²⁴ Na	A chem, excit (16F34, 1L35)		β^- (1L35)	15.06 h (39S51); 15.04 h (29S50); 15.10 h (31C50); 15.0 h (38S51, 23W49)	1.390 spect, coinc (7S46b, 7S47); 1.4 spect (24L39); 4.17 (0.003%), no 5.5 β^- , spect (15T51); lim 4.15 β^- , 0.01% spect (22G50); others (42H48)	γ_1 1.3679, γ_2 2.7535 spect (12H52); γ_1 1.380, γ_2 2.758 spect (7S46b); 1.380, 2.765 spect (20R49); γ_2 (e/ γ 3×10^{-6}) (7S50b); 2.748 spect (21K50a); 2.755 spect (6W50); γ_1 (coinc with γ_2) spect, β - γ , γ - γ coinc (4E43); γ - γ coinc abs (28C46); 3.7 (0.04%) D- γ -p ion ch (101B51); -4 (0.05%) spect (15T51); others (9B50, 4141, 26M43, 41M50, 85B50a, 85S51, 55C50, 108B52)		Na-d-p (1L35, 2V36a); Na-n- γ (12A35, 2S47); Mg-d- α (35H35); Mg-n-p (12A35); Mg- γ -p (10B46, 42H47, 22E52); Al-n- α (12A35, 74M52); Al-d-pa (30C46, 30C47); Al- γ -n2p (10B46, 22E52, 42S52); Al-p-3pn (82H52); Si- γ -n3p (?) (10B46); spall Al (39F52), Fe (45R52), Cu (42B51a, 57G51), Sn (42B51); spall-fission Cu (42B51), U (6F51)
²⁵ Na	B excit (34H43a)		β^- (34H43a)	58 s (35B47a); 62 s (12P48, 10B46, 34H43a); 60 s (21R44)	3.7 (-55%), 2.7 (-45%) abs (35B47a); 3.4 abs (34H44a); 3.3 abs (21R44)	>0.5 (weak) abs (35B47a)		Mg- γ -p (34H44a, 10B46, 22E52); Mg-n-p (34H44a, 35B47a); Al- γ -2p (10B46, 12P48, 22E52, 42S52)

$^{12}\text{Mg}^{23}$	A excit, cross bomb (21W39)	β^+ (21W39)	11.9 s (34H43); 12.3 s (52B51a); 11.6 s (21W39)	2.99 scint spect (52B51a); 2.8 cl ch (21W39)	no γ (21W39)	Mg^{24} , $I = 0$ (87M50)	Na-p-n (21W39, 2D40); Mg-y-n (34H42, 34H43, 10B46, 25B47, 27M49, 22E52)
Mg^{24}	78.60 (24W48)						
Mg^{25}	10.11 (24W48)					Mg^{25} , $I = 5/2$ (87M50, 3A51a)	
Mg^{26}	11.29 (24W48)					Mg^{26} , $I = 0$ (87M50)	
Mg^{27}	A chem, excit (12A35, 35H35)	β^- (35H35)	9.45 m (3S52); 9.6 m (10E43); 10.0 m (32C39); 10.2 m (35H35)	1.80 (80%), 0.9 (20%) spect (43B48); 1.8 cl ch (10E43, 32C39); 1.7 abs (28M40); -1.8 (coinc with γ) β - γ coinc (35B47a)	γ_1 1.01, γ_2 0.84 (γ_1 coinc with γ_2) spect, γ - γ coinc (43B48); 1.02, 0.84, 0.64 spect (4141); 1.05 cl ch recoil (10E43)	Q_β^- 2.64 (43B48)	Mg-d-p (35H35); Mg-n-y (12A35, 2S47); Al-n-p (12A35, 16F34, 74M52)
Mg^{28}	A chem, genet (37L53)	β^- (37L53)	21.2 h (37L53)	0.3-0.4 abs (37L53)	<0.1 abs (37L53)		spall Cl, parent Al ²⁸ (37L53)
$^{13}\text{Al}^{24}$	A excit, decay charac (102B52)	β^+ or EC, α (p?) (102B52a)	2.3 s (102B52)				Mg-p-n (102B52)
Al^{25}	B excit, sep isotopes (39B48)	β^+ (39B48)	7.3 s (39B48)				Mg ²⁵ -p-n (39B48)
Al^{26}	A excit (17F34); cross bomb (34H43, 39B48)	β^+ (17F34)	6.5 s (30K51); 6.3 s (39B48); 7.0 s (21W39, 14A48, 12P48); 7.2 s (25W48)	2.8 abs (14A48); 3.0 cl ch (21W39); 3.4 abs (35B46a, calc from 17F34)			Na-o-n (17F34, 24M37); Mg-p-n (21W39); Mg ²⁶ -p-n (39B48); Mg-p-y (21C39, 16T46); Al-y-n (34H41, 34H42, 34H43, 10B46, 25B47, 12P48, 22E52)
Al^{27}	100 (1B50)					Al^{27} , $I = 5/2$ (87M50)	
Al^{28}	A chem, excit (4C34a, 4C34b, 16F34); chem, cross bomb (12A35)	β^- (12M35a)	2.27 m (106B52b); 2.07 m (40S48); 2.30 m (10E43)	2.865 spect (29M52); 2.75 (coinc with γ) coinc abs (35B47a); 3.01 spect (43B48); no 4.6 β^- (29M51)	1.782 spect (29M52); 1.80 spect (43B48); 1.80 abs sec (35B47a); 1.82 spect (4141)	Q_β^- 4.65 (29M52)	Mg-o-p (8E36, 18R37); Al-d-p (12M35a, 29M52); Al-n-y (12A35, 2S47, 9O49, 50H51, 29M52); Si-n-p (12A35, 35B47a); Si-y-p (10B46, 42H47); P-n-a (12A35) daughter Mg ²⁸ (37L53)

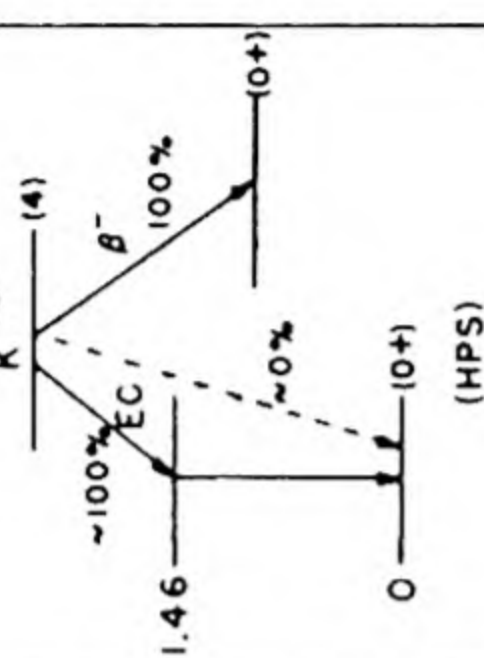
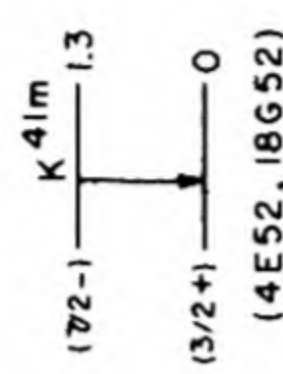
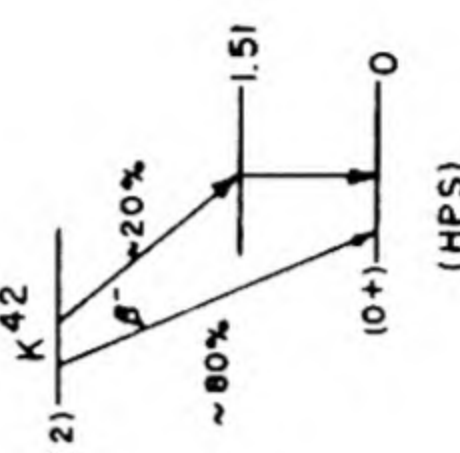
Isotope Z A	Class and identification	Percent abundance	Type of decay	Half-life	Energy of radiation in Mev		Disintegration energy and scheme	Method of production and genetic relationships
					Particles	Gamma-transitions		
¹³ Al ²⁹	A excit, cross bomb (32B39)		β^- (32B39)	6.56 m (41S49); 6.7 m (32B39)	2.5 (-70%), 1.4 (-30%) (both coinc with γ) β - γ coinc abs (41S49); -2.5 cl ch, abs (32B39)	1.2 (-80%) (coinc with 2.5 β^-), 2.3 (-20%) coinc abs sec (41S49)	 Q β^- 3.8 (41S49) Al ²⁹	Mg- α -p (8E36, 32B39, 14H39, 41S49); Al- α -2p (11Z551); Si-n-p (21F43); Si- γ -p (10B46, 42H47, 12P48); P- γ -2p (10B46, 12P48)
¹⁴ Si ²⁷	A excit (22K39)		β^+ (30M40)	4.9 s (12E41, 29C40a); 4.5 s (25W48); 5.4 s (52B51a)	3.48 scint spect (52B51a); 3.5 cl ch (33B40); 3.7 cl ch (30M40)			Mg- α -n (12E41); Al-p-n (22K39, 30M40, 29C40a, 33B40, 76C51); Si- γ -n (34H44, 25B47, 25W48)
²⁸ Si		92.27 (1B50)					Si ²⁸ , I = 0 (87M50)	
²⁹ Si		4.68 (1B50)					Si ²⁹ , I = 1/2 (87M50)	
³⁰ Si		3.05 (1B50)					Si ³⁰ , I = 0 (87M50)	
³¹ Si	A n-capt (12A35); chem, excit (12N35a)		β^- (12N35a)	2.62 h (33C38, 55W51); 2.65 h (29M52a); 2.6 h (48L50); 2.8 h (12N37, 15A40); 2.7 h (15P49)	1.471 spect (29M52a); 1.486 spect (47W52); 1.48 abs (55W51)	0.17, 0.52, -1 (weak) (?) abs (80C52); no γ (12N37)	Q β^- 1.47 (29M52a)	Si-d-p (12N35a, 12N37, 17K36); Si-n- γ (12A35, 2S47); Si-He ³ -2p (1P52); P-n-p (12A35, 1P37); S-n- α (42S36, 33C38); spall Fe (45R52)
¹⁵ P ²⁹	B excit (21W41)		β^+ (21W41)	4.57 s (30R52); 4.6 s (21W41)	3.6 cl ch (21W41)	1.28 (2.5%), 2.42 (0.5%), scint spect, γ - γ coinc (30R52)		Si-p-n (21W41); Si-d-n (14D48); P- γ -2n (?) (10B46)
³⁰ P	A excit (4C34, 17F34)		β^+ (4C34)	2.55 m (18R37); 2.18 m (33C38)	3.5 spect (24M41); 3.4 abs (35B46a, calc from 17F34); 3.0 cl ch (33B40)			Al- α -n (17F34, 4C34, 18R37); Si-p-n (33B39, 33B40); Si-He ³ -p (6A39, 1P52); P-n-2n (1P37); P- γ -n (37B39, 10B46, 12P48); S-d- α (42S36); Cl- γ -en (85H52)
³¹ P		100 (1A20)					P ³¹ , I = 1/2 (87M50)	

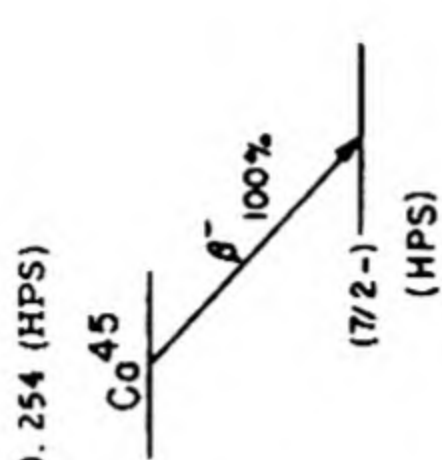
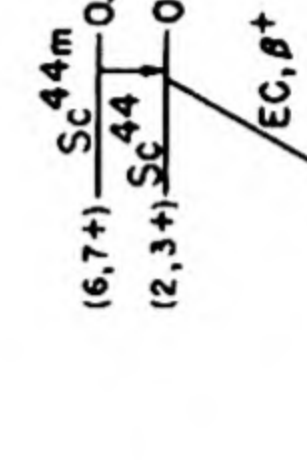
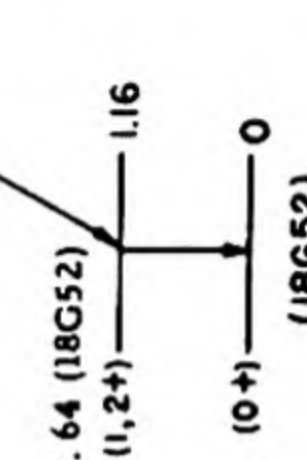
P^{32}	A chem, n-capt (12A35)	β^- (21L37)	14.30 d (12C38, 45B50); 14.35 d (23K48); 14.07 d (31M40); 14.60 d (38S51)	1.701 spect (average of 44S51, 29M52a, 13J52b, 8H51b, 16A50, 18W50a, 10L49, 7S46b); E (average) 0.70 ion ch (77C52)	no γ (17K36, 7S46b)	Q_{β}^- 1.702 (HPS)	 <p>p32</p> <p>(0+) (HPS)</p> <p>β^- 100%</p>	Si-d- γ (11Z551); Si-a-p (18F35); Si-He ³ -p (1P52); P-d-p (12N37); P-n- γ (2S47); S-n-p (12A35); S-d-a (42S36); Cl-n-a (12A35); Cl- γ -an, Cl- γ -t (85H52); Cl-d-pa (17T47); spall Fe (45R52), Cu (32M48, 42B51a)
P^{33}	A chem, cross bomb (44S51)	β^- (13J52b, 44S51)	25.4 d (58W52); 24.8 d (13J52b); 25 d (44S51)	0.27 spect (44S51); 0.26 spect (13J52b); 0.25 abs (58W52)	no γ (44S51, 58W52)	Q_{β}^- 0.27 (44S51)	 <p>p33</p> <p>(3/2+)</p> <p>(3/2+) (44S51, 13J52b)</p> <p>β^- 100%</p>	S-n-p (44S51, 13J52b, 58W52); S- γ -p (44S51, 13J52b); Cl- γ -a, Cl- γ -2p (44S51, 13J52b)
P^{34}	B excit (10C40a); chem, excit, cross bomb (35B46b)	β^- (6Z45)	12.4 a (35B46b); 12.7 a (10C40a)	5.1 (75%), 3.2 (25%) abs (35B46b)				S-n-p (10C40a, 6Z45, 35B46b); Cl-n-a (6Z45, 34H45, 35B46b)
$^{16}S^{31}$	A excit, cross bomb (21W41, 12E41)	β^+ (21W41)	3.18 a (12E41); 3.2 a (21W41, 52B51a); 2.6 a (27M49)	3.85 cl ch (21W41); 3.87 cl ch (12E41a); 4.1 acint spect (52B51a)				Si-a-n (19K40, 12E41, 12E41a); P-p-n (21W41); S- γ -n (34H41, 34H42, 34H43, 25B47, 27M49)
S^{32}	95.018 (meteoritic sulfur) (76M50a); terrestrial S ₃₂ /S ₃₄ variation ≤5% (41T50)					S^{32} , I = 0 (87M50)		
S^{33}	0.750 (meteoritic sulfur) (76M50a)					S^{33} , I = 3/2 (87M50)		
S^{34}	4.215 (meteoritic sulfur) (76M50a)					S^{34} , I = 0 (87M50)		

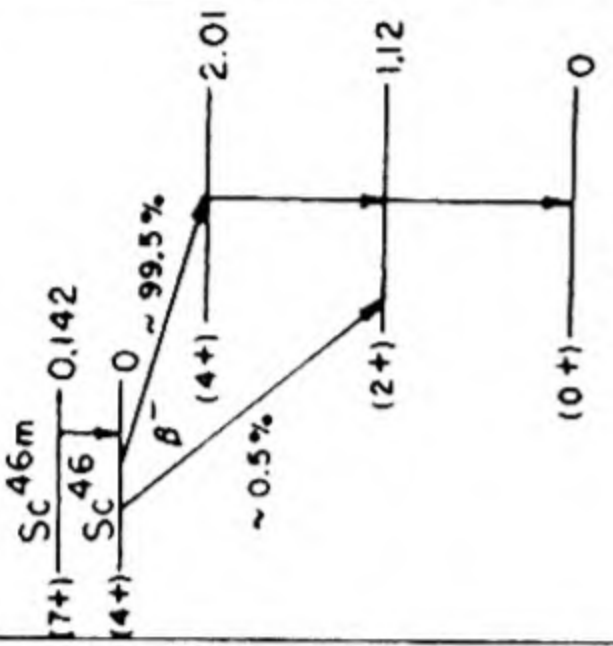
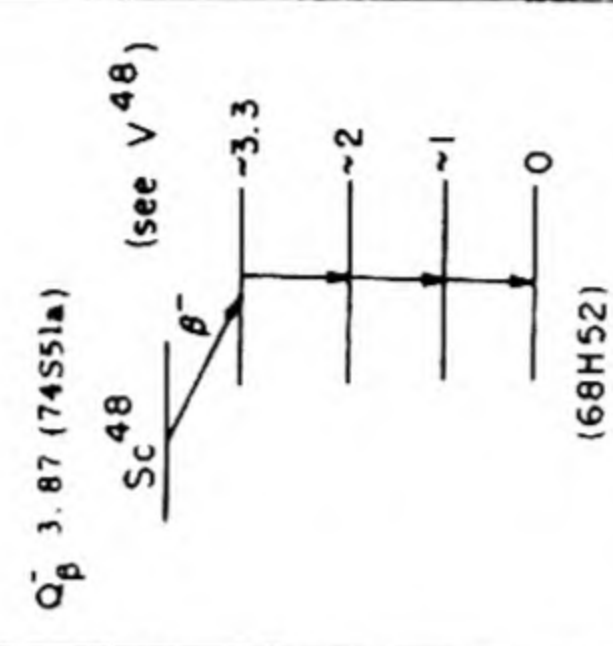
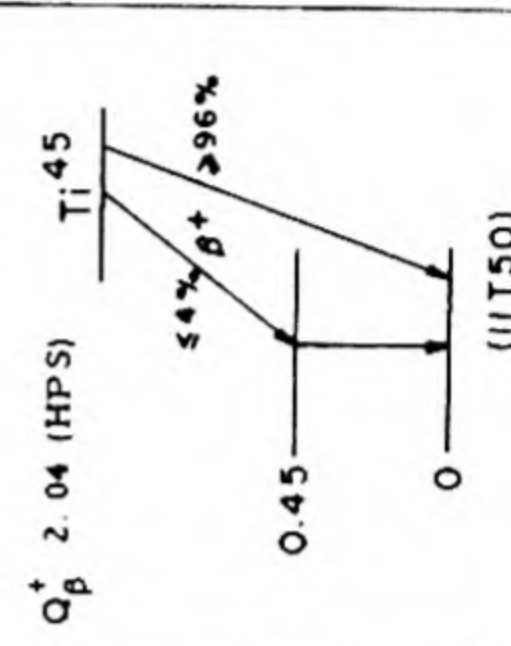
Isotope Z A	Class and identification	Percent abundance	Type of decay	Half-life	Energy of radiation in Mev		Disintegration energy and scheme	Method of production and genetic relationships
					Particles	Gamma-transitions		
³⁵ ₁₆ S	A chem, excit (17A36); chem, cross bomb, excit (1K41); sep isotopes (1K42)		β^- (3L39)	87.1 d (44H43) 88 d (26L40, 1K41)	0.1670 spect (10L50c); 0.167 spect (45H51), abs (29S47); 0.169 spect (46B48), abs (1Y48a); 0.168 spect (23G50); 0.166 spect (18A48); 0.168 ion ch (56C49)		Q_{β^-} 0.167 (HPS) S^{35} , I = 3/2 (87M50) 	S-n-γ (2S47); S-d-p (34C39, 1K41); Cl-n-p (17A36, 26L40, 1K41, 3M49); Cl35-n-p (1K42); Cl-d-α (1K41); spall Fe (45R52)
³⁶ ₁₆ S		0.017 (meteoritic sulfur) (76M50a)					S^{36} , I = 0 (87M50)	
³⁷ ₁₆ S	B chem, excit cross bomb (6Z45, 35B46b)		β^- (6Z45)	5.04 m (35B46b); 5.0 m (28H46b)	4.3 (10%), 1.6 (90%) abs (6Z45, 35B46b); 1.4, -4 abs (28H46b)	2.7 abs sec (35B46b); 2.75 abs sec (28H46b)	Q_{β^-} 4.3 (HPS) S^{37} 	S-n-γ (28H46b); Cl-n-p (6Z45, 35B46b)
³³ ₁₇ Cl	A excit (46H40); excit (21W41)		β^+ (21W41)	2.8 s (46H40, 45S48); 2.4 s (21W41); 1.8 s (52B51a)	4.13 cl ch (21W41); 4.4 scint spect (52B51a)			S-d-n (46H40, 45S48); S-p-n (21W41); Cl-γ-2n (52B51a)
³⁴ ₁₇ Cl	A chem, excit (17F34); chem, excit (42S36)		β^+ (17F34, 44B38)	33.2 m (25W48); 33.0 m (12P48); 33 m (42S36, 44B38)	4.5 (46%), 2.6 (28%), 1.3 (26%) spect (19R51); 5.1 (-80%), 2.4 (-20%) cl ch (38H46)	3.22, 2.10, 1.16 scint spect (18T51); 3.3, 2.1, 0.145 spect, spect conv (19R51); 3.4 cl ch recoil (38H46)	Q_{β^+} 5.6 (19R51)	Al-C ¹² -αn (4M50); P-α-n (17F34, 18R37, 44B38); S-d-n (42S36, 38H46); S-α, pn (28S40); S-p-n (19R51); S-t-n (20K45); Cl-n-2n (1P37); Cl-p-pn (19R51); Cl-γ-n (37B39, 34H43, 12P48, 25W48, 22E52); spall Fe (45R52), Cu (42B51a)
³⁵ ₁₇ Cl		75.4 (6N36)					Cl^{35} , I = 3/2 (87M50)	

^{36}Cl	A chem, n-capt (31G41)		β^- (31G41); no β^+ (lim 0.01%); (16W49a); (lim 0.03%); (14J49)	4.4 x 10^5 y sp act (16W49a); 3.6 x 10^5 y sp act (22R49); 2.0 x 10^5 y yield (22R49); 2 x 10^6 y yield (28H47b); -10 ⁶ y yield (10C47)	0.714 spect (15F52); 0.66 abs (10O47); 0.64 abs (31G41); others (16W49b, 16W51)	no γ (16W49a)	Q_β^- 0.714 (16W49b, 15F52) Cl ³⁶ , I = 2 (87M50, 27J51)		Cl-n- γ (31G41, 10O47, 2547); Cl-d-p (31G41)
^{37}Cl		24.6 (6N36)					^{37}Cl , I = 3/2 (87M50)		
^{38}Cl	A chem, n-capt (12A35); chem, sep isotopes (14K40)		β^- (17K36)	37.29 m (31C50); 37.5 m (47H37, 21C40a); 37.0 m (2V36a, 5S45); 38.5 m (15H46)	4.81 (53%), 2.77 (16%), 1.11 (31%) spect (10L50); 5.0, 2.8, 1.1 spect (27W39); spect, coinc abs (27W41); 5.2 (53%), 2.70 (11%), 1.19 (36%) spect (15H46)	γ_1 2.15, γ_2 1.60 ($\gamma_1/\gamma_2 = 1.3$) spect (15H46); γ_1 2.19, γ_2 1.64 (γ_1 coinc with γ_2) spect, coinc (414); 2.15, 1.65 spect (21C40a); no 3.75 γ (lim 0.03%) Be- γ -n reaction (33M49)	Q_β^- 4.81 (H ⁵ S)		Cl-d-p (17K36, 2V36a); Cl-n- γ (12A35, 14K40, 19A41, 2547); Cl ³⁷ -n- γ (14K40); K-n- α (47H37); spall Fe (45R52), Co (29W52), Cu (32M48, 42B51a); spall-fission Cu (42B51)
^{39}Cl	A chem (32M48a); chem, excit (49H49)		β^- (49H49)	55.5 m (49H49); -1 h (32M48a, 48H49)	1.65 (93%), 2.96 (7%) abs (49H50)	1.35, 0.35 (coinc with 1.65 β^-) coinc abs sec (49H50)	Q_β^- 3.3 (49H50)		A- γ -p (49H49, 49H50); spall Fe (45R52), Co (29W52), Cu (32M48a, 42B51a), As (48H49)
^{35}A	A excit (21W41, 19K40)		β^+ (12E41a, 21W41)	1.88 s (12E41a); 1.84 s (45S48)	4.38 cl ch (21W41); 4.41 cl ch (12E41a)		Q_β^+ 5.4 (HPS)		S- α -n (19K40, 45S48); Cl-p-n (21W41)
^{36}A		0.337 (6N50)					^{36}A , I = 0 (87M50)		
^{37}A	A chem, cross bomb (28W41)		EC (28W44, 46R52); EC (L/K 0.087) (17P49)	35.0 d (56M52); 34.1 d (28W44)		no γ , Cl K α - α (28W44)	Q_{EC}^- -0.8 continuous γ spectrum (38A52); Q_{EC}^- 0.816 p-n threshold (51R50)		S- α -n (28W41, 28W44); Cl-d-2n (28W41, 28W44); Cl-p-n (28W41, 28W44, 47B51a); K-d- α (28W41, 28W44); Ca-n- α (28W41, 28W44)
^{38}A		0.063 (6N50)							
^{39}A	B chem, excit (8Z52)		β^- (48B50)	-265 y sp act (8Z52)	0.565 spect (48B50)	no γ , > 0.3 (lim 0.1%) (48B50)	Q_β^- 0.57 (HPS)		A-n- γ (32K52); K-n-p (48B50, 8Z52)

Isotope Z A	Class and identification	Percent abundance	Type of decay	Half-life	Energy of radiation in Mev		Disintegration energy and scheme	Method of production and genetic relationships
					Particles	Gamma-transitions		
¹⁸ A 40		99.600 (6N50)					$A^{40}, I = 0$ (87M50)	
⁴¹ A	A chem, excit (26S36)		β^- (26S36)	109 m (35B46c); 110 m (26S36)	1.245 (~100%) spect (36B50); 1.18 (99.3%), 2.5 (0.7%) abs, coinc abs (35B46c); others (26S36, 17K36)	1.37 cl ch recoil (23R36); 1.3 (coinc with 1.2 β^-) β - γ coinc, abs sec (35B46c); γ (e/ γ -0) spect conv (36B49)	<p>$A^{41} (7/2-) \xrightarrow{\beta^- \sim 99\%} K^{41m} (7/2-) \xrightarrow{\gamma \sim 1.37} O (3/2+)$ $A^{41} (7/2-) \xrightarrow{\beta^- \sim 1\%} O (3/2+)$</p>	A-d-p (26S36, 36B49, 36B50); A-n- γ (26S36); K-n-p (47H37, 35B46c); parent K41m (4E52)
⁴² A	A chem, genet (32K52)		β^- (32K52)	33.5 y (32K52)				A-n- γ (sec order reaction) (32K52); parent K42 (32K52)
³⁷ K 19	C excit (27L48)		β^+ (52B51a)	1.3 s (27L48); 1.2 s (52B51a)	4.6 scint spect (52B51a)			K- γ -2n (27L48, 52B51a)
³⁸ K	A chem, cross bomb (47H37, 14H37)		β^+ (47H37)	7.7 m (47H37, 18R37, 58G51); 7.5 m (24R47); 7.6 m (12P48)	2.8 spect (58G51); 2.5 abs (24R47); others (18R37)	2.16 scint spect (18T51); -2.1 abs sec (24R47)	see C138	Cl-a-n (47H37, 18R37, 14H37, 24R47); K-n-2n (1P37); K-p-pn (18T51, 58G51); K- γ -n (34H42, 34H43, 12P48, 22E52); Ca-d-a (47H37)
³⁹ K		93.08 (6N50); K39/K41 variations (81C43)					$K^{39}, I = 3/2$ (87M50)	

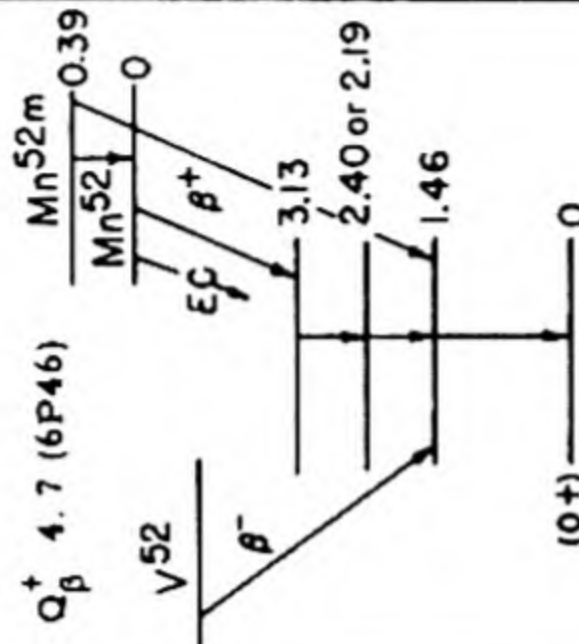
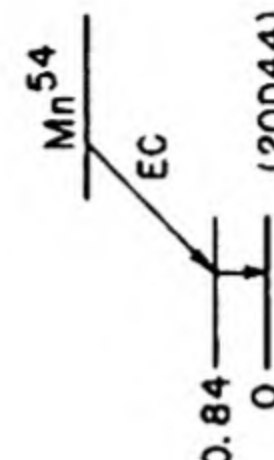
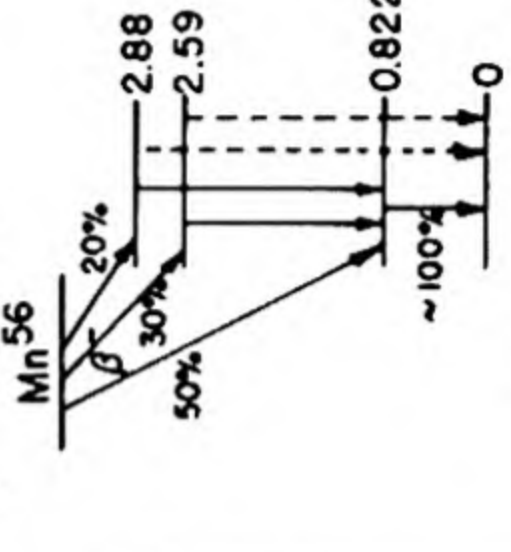
K^{40}	A chem (IT05, 54C06); chem, mass spect (15S37)	0.0119 (6N50)	β^- 89%, EC 11% (3150); β^- -88%, EC (K) -12% (46S50); β^- -93%, EC (K) -7% (36C50); assuming EC/ γ = 1, β^- 90%, EC 10% (19F50, 76H50); β^- 91%, EC 9% (48S50); β^- 89%, EC 11% (27G51); β^- 94%, EC 6% (65M52); no β^+ (lim 0.06%); (37C51); no β^+ (lim 0.002%); (11B50b); β^+ 40.1% (25G51b)	t_{β^-} spect (uncorr. for EC); 1.32 x 10 ⁹ y (47S49, 48S50); 1.26 x 10 ⁹ y (17D51, 17D51a); 1.29 x 10 ⁹ y (19F50); 1.49 x 10 ⁹ y (27G50, 76H50, 25G51); 1.42 x 10 ⁹ y (46S50); others (20A48, 20F49, 11S50); $t_{1/2}$ 1.2 x 10 ⁹ y calc from average t_{β^-} and EC/ β^- (HPS)	1.33 spect (15F52); 1.36 spect (13A50a); 1.36 scint spect (11B50c); 1.35 spect coinc (16D46); 1.41 abs (42H46, 42H48); 1.28 scint spect (25G51)	1.46 scint spect (11B50b, 25G51a); 1.48 scint spect (55H50); 1.47 scint spect (18P50); 1.54 (with EC) abs, coinc (42H46); 1.55 abs (26G47); γ (with EC) (34M47, 16P52); γ/β^- 0.12 spect (average of 19F50, 47S49, 48S50, 25G51, 20F49, 27G48, 46S49, 76H50); EC/ γ -1 (35M51, 46S50, 16P52)		natural source (IT05, 54C06)
K^{41m}	A genet (4E52)	IT (4E52)	6.7 x 10 ⁻⁹ s delay coinc (4E52)	-1.3 scint spect (4E52)			daughter A^{41} (4E52)	
K^{41}		6.91 (6N50)				K^{41} , I = 3/2 (87M50)		
K^{42}	A chem, n-capt (12A35); chem, cross bomb (71H35, 71H36)	β^- (17K36)	12.44 h (7S47c); 12.5 h (38S51, 35L52a); 12.4 h (47H37)	3.58 (75%), 2.04 (25%) spect (7S47c); 3.60, 1.9 spect (6P47); 3.5 (-70%) (not coinc with γ), -1.8 (-30%) abs, coinc (35B47a)	1.51 spect (7S47c); 1.50 spect (6P47); 1.5 (17%) scint spect (35L52a)		A-o-pn (11O49); K-d-p (47H37); K-n-y (12A35, 47H37, 2S47); Ca-n-p (71H35, 47H37); Sc-n-a (71H36, 47H37, 35B47a); spall Co (29W52), Cu (57G51); daughter A^{42} (32K52)	
K^{43}	B chem, excit (11O49)	β^- (11O49)	22.4 h (11O49)	0.81, 0.24 spect, abs (11O49)	-0.4 abs (11C49)		A-o-p (11C49)	
K^{44}	E chem, excit (30W37)	β^- (30W37)	18 m (30W37)				Ca-n-p (30W37, 30W40)	
^{39}Ca	B excit (34H43, 27M49)	β^+ (34H43)	1.06 s (34H43) 1.1 s (52B51a)	5.1 scint spect (52B51a)			Ca-y-n (34H43, 25W48, 27M49)	
Ca^{40}		96.97 (6N38a)				Ca^{40} , I = 0 (87M50)		

Isotope Z A	Class and identification	Percent abundance	Type of decay	Half-life	Energy of radiation in Mev		Disintegration energy and scheme	Method of production and genetic relationships
					Particles	Gamma-transitions		
⁴¹ Ca 20	B chem, n-capt sep isotopes (60B51)		EC (60B51)	1.1 × 10 ⁵ y yield (60B52a)		K K _a -x (60B51)		Ca-n-γ (49S51, 60B51)
⁴² Ca		0.64 (6N38a)						
⁴³ Ca		0.145 (6N38a)						
⁴⁴ Ca		2.06 (6N38a)						
⁴⁵ Ca	A chem, excit, cross bomb (30W40)		β ⁻ (30W40)	152 d (36M47); 180 d (30W40)	0.254 spect (23M50a); 0.255 scint spect (24K50); 0.260 abs (29S48); 0.26 abs (50S50); E (average) 0.075 ion ch (77C52)	no γ (29S48, 37M49, 25K46); others (52M51)	Q _β ⁻ 0.254 (HPS) 	Ca-d-p (30W40); Ca-n-γ (30W40, 25K47); Sc-n-p (30W40, 25K46); Sc-d-2p (51H48); Ti-n-α (38C48, 63H48); spall Fe (45R52), Cu (42B51a); spall-fission Bi (11G49)
⁴⁶ Ca		0.0033 (6N38a)						
⁴⁷ Ca	A (36M47); chem, genet (42B51a)		β ⁻ (36M47)	4.8 d (42B51a); 5.8 d (36M47)	1.2 abs (42B51a); 1.1 abs (36M47)			Ca-d-p (36M47); spall Fe (45R52), Cu (42B51a); parent Sc47 (42B51a)
⁴⁸ Ca		0.185 (6N38a)		t _{β⁻} > 2 × 10 ¹⁶ y sp act (28J52)				
⁴⁹ Ca	A chem, n-capt, sep isotopes (38M50)		β ⁻ (38M50)	8.5 m (38M50)	-2.7 abs (38M50)	hard (38M50)		Ca ⁴⁸ -n-γ, Ca-p-γ (38M50)
⁴¹ Sc 21	A excit (12E41)		β ⁺ (12E41a)	0.873 s (98M52); 0.87 s (12E41)	4.94 cl ch (12E41)			Ca-d-n (12E41, 12E41a); Ca-p-γ (39T52)
⁴³ Sc	A chem, excit (17F35)		β ⁺ (17F35)	3.92 h (53H45); 4 h (30W40a)	1.18 (72%), 0.77 (28%) spect (93H52); 1.12 abs, spect (53H45); 1.4 cl ch (30W37a); abs (30W40a)	0.375, no higher γ (lim 15%) spect (93H52); 1.65 abs (53H45); 1.0 abs (30W40a)		Ca-α-p (17F35, 30W40a); Ca-d-n (30W37a, 53H45); Ca-p-n (2D38, 53H45); spall Fe (45R52), Co (29W52), Cu (42B51a)
^{44m} Sc	A chem, excit cross bomb (30W37a)		IT (30W40a)	2.44 d (53H45); 2.4 d (49B50); 2.2 d (30W40a)		0.271 spect, spect conv (49B50); 0.269 spect conv (51S42); 0.26 spect conv (2H41); 0.28 abs conv (53H45)		K ⁴¹ -α-n (49B50); K-α-n (30W40a, 53H43); Ca-d-n (30W37a, 51S42, 53H43); Ca-p-n (2D38); Sc-n-2n (31B38, 53H45); Ti-d-α (30W37b); spall Fe (45R52), Co (29W52), Cu (42B51a)
⁴⁴ Sc	A chem, excit (10C38)		β ⁺ , EC (53H45)	3.92 h (53H45); 4.0 h (49B50); 4.1 h (30W40a, 51S42)	1.463 spect (49B50); 1.45 spect (51S42); 1.5 abs (39C50, 30W40a)	1.16 spect spect conv (49B50); 1.18 coince abs sec (39C50)	Q _β ⁺ 3.64 (18G52) 	K ⁴¹ -α-n (49B50); K-α-n (30W40a, 53H43); Ca-d-n (30W37a, 51S42, 53H43); Ca-p-n (2D38); Sc-n-2n (31B38, 53H43); Sc-γ-n (37B39); Ti-d-α (53H44); spall Co (29W52), Cu (42B51a); spall-fission Br (42B51)

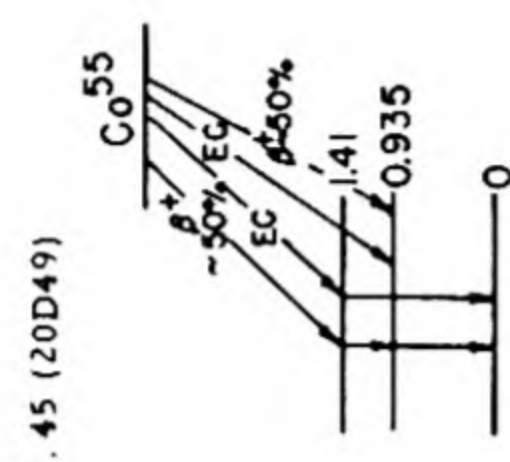
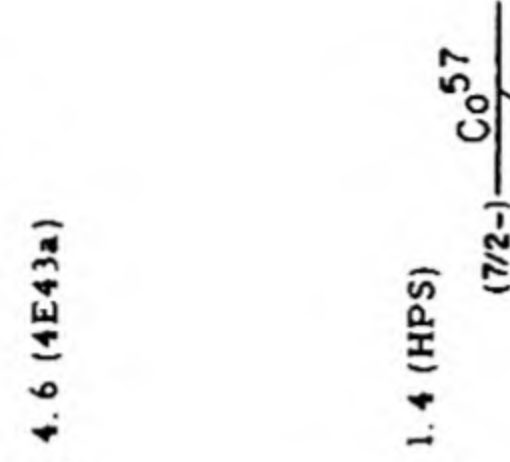
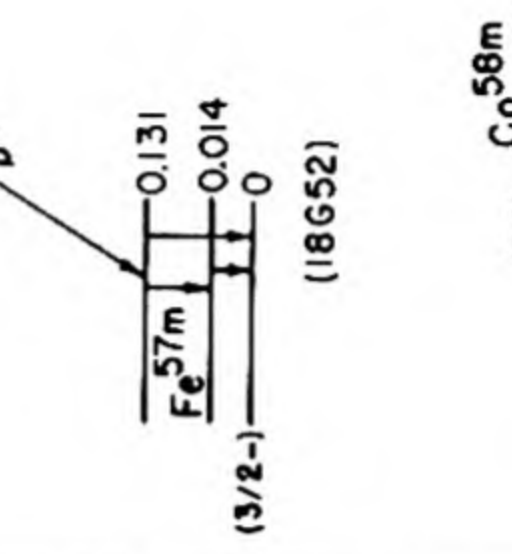
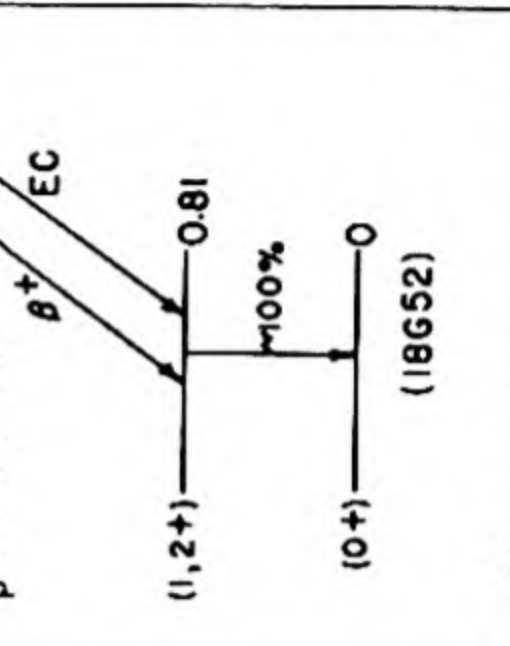
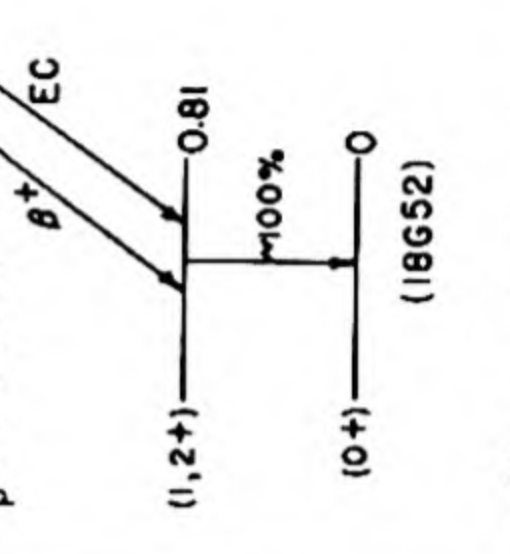
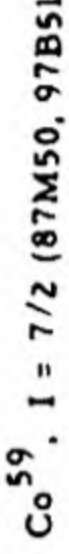
Sc ⁴⁵	100 (28L50)	IT (18G48)	19.5 s (38M51)		0.142 (K/L -10) spect conv (82B52); 0.135 scint spect (38M51)	Sc ⁴⁵ , I = 7/2 (87M50)	Sc-n-γ (18G48, 38M51)
Sc ^{46m}							
Sc ⁴⁶		p ⁺ , no EC (40M47); p ⁺ , EC (weak) (30W39); no p ⁺ (lim 0.0016%) (41M51)	85 d (30W39); 84 d (19P51)	0.36 spect (22F47, 40M47, 20P48); 0.36 abs (52S50); 0.34 abs (14N50); 1.2 (-0.5%) spect (19P51); no 1.5 p ⁺ (lim 0.05%) cl ch (52S50); no 1.5 p ⁺ (lim 0.06%) spect (39M50); 1.5 (-2%) spect (20P48); abs (14N50)	Y ₁ 0.89, Y ₂ 1.12 spect, spect conv (20P48); 0.88, 1.12 spect (22F47); 0.90, 1.12 spect (40M47); Y ₁ (e/γ 1.7 x 10 ⁻⁴), Y ₂ (e/γ 0.98 x 10 ⁻⁴) spect conv (39M50); Y ₁ (e/γ 1.4 x 10 ⁻⁴), Y ₂ (e/γ 0.61 x 10 ⁻⁴) spect conv (19P51); Y ₁ (coinc with 0.36 p ⁺ and Y ₂) p-γ; Y-γ coinc (15J48, 52S50, 26M48); Y ₁ (coinc with 1.5 p ⁺ and Y ₂) delay coinc (14N50)		Ca-α-p (30W40a); Sc-d-p (30W37c, 30W39); Sc-n-γ (71H36, 30W37c, 2547); Ti-d-α (30W37b); Ti-n-p (30W37b, 63H48); spall Fe (45R52), Cu (42B51a)
Sc ⁴⁷		p ⁻ (53H45a)	3.43 d (26K49)	0.61 abs (26K49)	γ (26K49)	$Q_{\beta}^{-} 2.37$ (18G52)	Ca-α-p (53H45a); Ca-d-n (53H45a); Ca-p-γ (53H45a); Ti-γ-p (22E52); Ti-n-p (63H48); Ti ⁴⁹ -d-α (26K49); spall Fe (45R52), Cu (42B51a); daughter Ca ⁴⁷ (42B51a)
Sc ⁴⁸		p ⁻ (30W37b)	44 h (30W40a, 26M42, 53H45a, 26K49)	0.64 spect (51S42); 0.57 abs (53H45a, 26K49)	Y ₁ 1.33, Y ₂ 0.98, Y ₃ -1.0 scint spect, γ-γ coinc (68H52); 1.32, 0.99, no 2.3 γ (lim 0.1%) scint spect (69M52); 1.33, 0.98 spect (6P46); 1.35 spect (26M42, 26M43a); 1.33 abs (53H45a)		Ca-p-n (53H43); Ca-d-2n (51S42, 26M42, 53H43, 26M43a); Ti-n-p (30W37b, 1P37, 30W40a, 26M43a); Ti ⁵⁰ -d-α (26K49); Ti-d-α (53H44); V-n-α (30W37b, 1P37, 30W40a); spall Fe (45R52)
Sc ⁴⁹		p ⁻ (30W40a)	57 m (30W40a)	1.8 abs (30W40a)	no γ (30W40a)		Ca-d-n (30W40a); Ti-n-p (30W40a); Ti-γ-p (42H47, 22E52)
2Ti ⁴³ Ti ⁴⁵		p ⁺ , EC (27K50)	0.6 s (45S48) 3.09 h (27K50); 3.05 h (11T50); 3.08 h (21A41)	1.02 (>96%), 0.57 (<4%) spect (11T50); 1.00 spect (27K50); 1.2 cl ch (21A41)	0.45 (weak), (no 0.8 γ) spect (11T50); 0.80 spect, abs (27K50)		Ca-α-n (45S48) Ca-α-n (21A41); Sc-p-n (21A41, 11T50, 27K50); Sc-d-2n (21A41, 11T50); Ti-n-2n (21A41); Ti-γ-n (34H43b, 34H44, 25W48, 22E52); spall Fe (45R52), Cu (42B51a, 74M52)

Isotope Z A	Class and identification	Percent abundance	Type of decay	Half-life	Energy of radiation in Mev		Disintegration energy and scheme	Method of production and genetic relationships
					Particles	Gamma-transitions		
⁴⁶ Ti 22		7.95 (6N38a)						
⁴⁷ Ti		7.75 (6N38a)						
⁴⁸ Ti		73.45 (6N38a)						
⁴⁹ Ti		5.51 (6N38a)						
⁵⁰ Ti		5.34 (6N38a)						
⁵¹ Ti	B n-capt (2S47)		β^- (2S47)	5.82 m (3S52); 5.75 m (2B52); 6 m (2A49a, 38M50, 2S47)	1.7, 1.35 (coinc with 0.32 γ) scint spect (38M52); 2.2 (~30%), 1.9 (~70%) abs. spect (60K52); 1.6 abs (2A49a)	0.320, 0.910 (weak) scint spect (2B52); 0.32 scint spect (38M51a, 60K52)	Ti-n- γ (2S47, 38M50)	
⁴⁶ V 23	E excit (98M52)		β^+ (98M52)	0.40 s (98M52)	>6.0 scint spect (98M52)		see Cr ⁵¹	
⁴⁷ V	A chem, excit, cross bomb (12O42); chem, sep isotopes (26K49)		β^+ (30W37b)	33 m (26K49, 12O42, 30W37b)	1.7 abs (26K49); 2.0 abs (35B46a, calc from 30W37b); -1.9 abs (12O42, 30W37b)	γ (26K49)		Ti-d-n (30W37b, 12O42); Ti-p-n (12O42); Ti ⁴⁷ -p-n (26K49) spall Fe (45R52)
⁴⁸ V	A chem, excit, cross bomb (30W37c, 30W37b)		β^+ 58%, EC 42% (21C46); β^+ , EC (30W39, 53H44)	16.0 d (30W37b)	0.69 (~95%), -0.8 (~5%) spect (43R52); 0.72 spect (6P46); 0.6 abs (53H44) 1.0 cl ch (30W37b)	γ_1 0.99, γ_2 1.32 (γ_2 coinc with γ_1), γ_3 2.29 ($\gamma_3/\gamma_2 = 0.017$) scint spect (69M52); γ_1 0.99, γ_2 1.32, γ_3 2.22 scint spect, β^+ - γ , γ - γ coinc (43R52); γ_1 0.98, γ_2 1.33 (γ_2 coinc with γ_1 , both coinc with β^+) spect, β - γ coinc (6P46); γ_1 (e/ γ 2×10^{-4}), γ_2 (e/ γ 8×10^{-5}) spect conv (7Z52); γ_3 2.22 (~2%), no 2.3 γ (lim 0.5%) scint spect (18T52); γ_1 0.99, γ_2 1.32 spect conv (20R49); γ_1 (coinc with γ_2) γ - γ coinc (34J52)	Q_β^+ 4.02 (43R52)	Sc-a-n (30W37c); Ti-d-n (30W37b); Ti-p-n (2D40, 18T52); Cr-d-a (30W37b, 6P46); spall Fe (45R52), Cu (32M48, 42B51a); daughter Cr-48 (45R52)
⁴⁹ V	D chem (30W39, 29T40); excit (43H49, est from 10C49)		EC (30W39)	635 d (10C49) -600 d (30W39)				Ti-d-n (30W39); V-n-2n (?) (10C49)
⁵⁰ V		0.24 (43H49, 28L49)					Q_β^- 1.18, Q_β^+ 2.39 (23J52); V^{50} , I = 6 (56K52)	

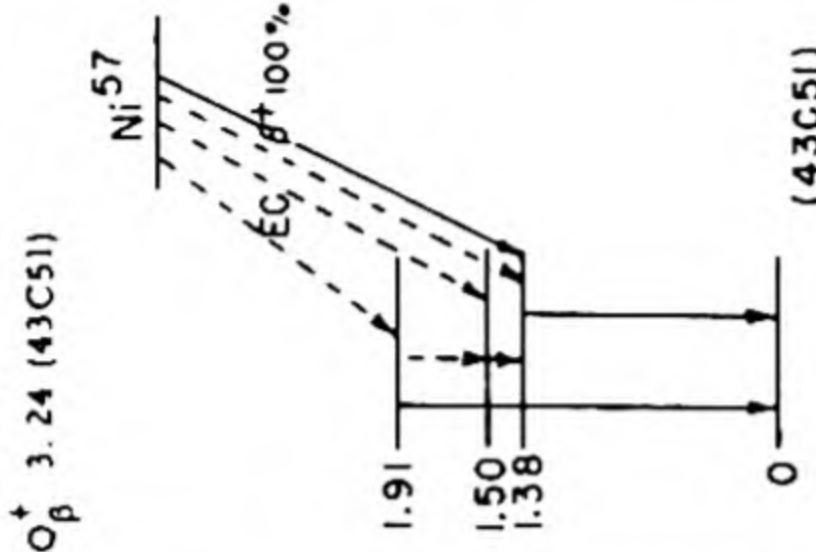
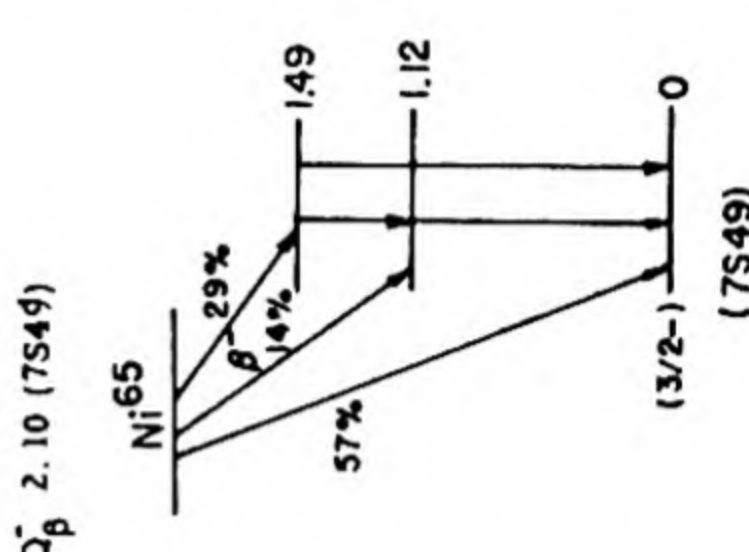
V^{51}	99.76 (43H49, 28L49)	β^- (12A35); IT (25R50)	3.76 m (3552); 3.74 m (42M47); 3.75 m (12A35)	2.1 abs (3D40a); 2.6 cl ch (4Y42); conv: 0.25, β^- with V^{52} , abs, β - γ , β -conv coinc (25R50)	1.5 abs (42M47); 1.3 abs (28G48); -1.5 γ with V^{52} (25R50)	V^{51} , I = 7/2 (87M50, 97B51c)
V^{52}	F n-capt (25R50)	β^- (25R50)	2.6 m (25R50)	2.7 cl ch (4Y42)	1.5 abs (42M47)	V-n- γ (12A35, 30W37b, 1P37, 2S47, 9O49, 25R50, 50H51); V-d-p (30W37b); Cr-n-p (30W37b, 1P37); Cr- γ -p (42H47); Cr- γ -d-a (15N50); Mn-n-a (12A35, 30W37b, 1P37) V-n- γ (25R50)
$V^{52,50m}$	F V^{52} : (10C49); V^{50m} : (43H49)		16 h (10C49)			V-n (10C49)
V^{53}	B chem, sep isotopes, excit (88H52)	β^- (88H52)	23 h (88H52)	-0.6 abs (88H52)		Cr- γ - γ -p (88H52)
$^{24}Cr^{48}$	B chem, genet (45R52)	EC (45R52)	-23 h (45R52)			spall Fe, parent V^{48} (45R52)
Cr ⁴⁹	A chem, excit, cross bomb (12O42)	β^+ (12O42)	41.9 m (12O42); 45 m (34H44)	1.45 abs, cl ch (12O42)	0.18, 1.55 abs (12O42)	Ti- α -n (12O42); Cr-n-2n (12O42); Cr- γ -n (34H44, 12P49); spall Fe (45R52), Co (29W52), Cu (32M48, 42B51a, 74M52), Ae (48H50)
Cr ⁵⁰						
Cr ⁵¹	A chem, excit, cross bomb (30W40b); chem, genet (50B50)	EC (16B45a, 30W40b); no β^+ (16B45a, 28K49, 35L52)	27.8 d (35L52); 26.5 d (30W40b)		0.330 (-3%, e γ /y-0.02), spect aspect conv (16B45a); 0.32 (8%, e/y very small) scint aspect, x- γ coinc (35L52); 0.323 spect, aspect conv (28K49); 0.320 (single γ) aspect (17K48); 0.32 spect conv (43M46); others (52M51, 28K49, 13A50b)	Ti- α -n (30W40b); V-p-n (16B45a); Cr-d-p (30W40b, 22A40); Cr-n- γ (30W40b, 2S47); Cr-n-2n (22A40); spall Fe (45R52), Cu (32M48, 42B51a), Ae (48H50); daughter Mn ⁵¹ (50B50)
Cr ⁵²						
Cr ⁵³						
Cr ⁵⁴						
Cr ⁵⁵	G not found: sep isotopes, excit, cross bomb (15N50); chem, excit (32M50)		-2 h (18D40)			Cr-n (18D40, 22A40, 2S47); Cr-d (22A40)

Isotope Z A	Class and identification	Percent abundance	Type of decay	Half-life	Energy of radiation in Mev		Disintegration energy and scheme	Method of production and genetic relationships
					Particles	Gamma-transitions		
⁴⁹ ₂₅ Mn	E excit (39T52, 98M52)		β^+ (98M52)	0.28 s (98M52); -0.5 s (39T52)	>6.3 acint spect (98M52)			Cr-p-2n (39T52); Cr-p-n (98M52)
⁵¹ _{Mn}	A chem, cross bomb (12L37, 12L38); chem, genet (50B50)		β^+ (12L37)	44.3 m (50B50); 46 m (12L38)	2.4 abs (35B46a, calc from 12L38); 2.0 abs (12L38)			Cr-d-n (12L38, 50B50); Cr-p-y (2D38, 5D39); Fe-y-p2n (42S52); spall Fe (45R52), Cu (32M48, 42B51a, 74M52); parent Cr51 (50B50)
^{52m} _{Mn}	A chem (19D37); chem, excit, cross bomb (12L37, 12L38)		β^+ 99+%, π^+ (?) -0.05% (1047)	21.3 m (40H40); 21 m (12L38, 19D37)	2.66 spect (1047); 2.2 cl ch (40H40)	1.46 (coinc with β^+) spect, β -y coinc (1047); 0.392 (0.05%) (with π^+) spect conv (1047)	Q_{β^+} 5.1 (1047)	Cr-p-n (40H40); Fe-d-a (19D37, 12L38); Fe-y-pn (22E52, 42S52); daughter Fe52 (32M48)
⁵² _{Mn}	A chem, excit, cross bomb (12L37, 12L38)		EC 65%, β^+ 35% (21G46)	6.0 d (29H50); 6.2 d (84H51); 6.5 d (12L38); 6 d (32M48)	0.58 spect (6P46); 0.75 abs (19T48); 0.77 cl ch (40H40)	γ_1 0.73, γ_2 0.94, γ_3 1.46 (γ_1 coinc with γ_2 and γ_3 , all coinc with β^+) spect, β -y coinc (6P46)	Q_{β^+} 4.7 (6P46)  (18G52, HPS)	Cr-p-n (40H40); Cr-d-2n (6P46); Fe-d-a (12L38); spall Fe (45R52), Co (29W52), Cu (32M48, 42B51a, 74M52), As (48H50); spall-fission U (6F51)
^{54m} _{Mn}	F sep isotopes (40C51)		β^- (40C51)	2.1 m (40C51)				Fe ⁵⁴ -n-p, Fe ⁵⁴ -d-2p (40C51)
⁵⁴ _{Mn}	A chem, excit, cross bomb (12L37, 12L38)		EC (6A38); no β^+ , no β^- (12L38, 20D44)	310 d (12L38)		0.84 spect, x-y coinc (20D44); 0.85 abs (12L38)	 (20D44)	V-a-n (12L38); Cr-d-n (12L38); Cr-p-n (2D40); Fe-d-a (12L38, 20D44); spall Fe (45R52), Cu (42B51a)
⁵⁵ _{Mn}		100 (37S36a)					$Mn^{55}, I = 5/2$ (97B51a)	
⁵⁶ _{Mn}	A chem, n-capt (12A35)		β^- (12A35)	2.576 h (106B52a); 2.59 h (12L38, 9B50)	2.81 (50%), 1.04 (30%), 0.65 (20%) spect (7S46c); 2.86 (60%), 1.05 (25%), 0.75 (15%) spect (4E43a); 2.88, 1.04 spect (14T41)	γ_1 0.822, γ_2 1.77, γ_3 2.06 ($\gamma_1/\gamma_2/\gamma_3 = 10/3/2$) spect (7S46c); ($\gamma_2/\gamma_3 = 1.0$) spect (5S51); γ_1 0.85, γ_2 1.81, γ_3 2.13 ($\gamma_1/\gamma_2/\gamma_3 = 10/3/2$) spect, β -y coinc (4E43a); -2.7 (-0.1%), -3.0 (-0.2%) D-y-p ion ch (9B50)	Q_{β^-} 3.63 (7S46c)  (7S46c, 4E43a)	Cr-a-p (18R37); Mn-n-y (12A35, 2S47, 9O49, 50H51); Mn-d-p (12L38); Fe-d-a (12L38); Fe-n-p (12A35); Fe-y-p (12P48, 22E52); Co-y-2pn (22E52); Co-n-a (12A35); spall Fe (45R52), Co (29W52), Cu (32M48, 42B51a, 74M52), As (48H50)
⁵⁷ _{Mn}	B chem, cross bomb (112S51)		β^- (112S51)	7 d (112S51)	1.0 spect (112S51)			Mn-a-2p, Cr-a-p (112S51)

$^{26}\text{Fe}^{52}$	A chem. genet (32M48)				no $\gamma > 0.5$ scint spect (23F51)	<p>(23F51, HPS)</p>	Cr- α -2n (23F51); Fe- γ -2n (42S52); spall Fe (45R52), Co (29W52), Cu (32M48, 51B50, 23F51, 42B51a, 74M52); parent Mn52m (32M48); not parent Mn52 (lim 5%) (23F51)
^{53}Fe	A chem (18R37); chem, excit, cross bomb (12L38a)				no γ (15N50)	<p>(23F51, HPS)</p>	^{50}Cr - α -n (15N50); Cr- α -n (18R37, 12L38a); Fe-n-2n (12L38a); Fe- γ -n (34H42, 34H44, 52B51, 22E52, 42S52); Fe54- γ -n (12P49); spall Cu (32M48, 42B51a, 74M52)
^{54}Fe		5.84 (6V41)					Mn-d-2n (51H48); Mn-p-n (2V40, 16B46b); Fe-d-p (12L39a); spall Co (93M51), Cu (42B51a, 93M51); daughter Co55 (12L41)
^{55}Fe	A chem, excit (12L39a)						
^{56}Fe		91.68 (6V41)					
^{57m}Fe	A genet (20D50)				0.014 spect (20D50)	see Co57	daughter Co57 (20D50)
^{57}Fe		2.17 (6V41)					
^{58}Fe		0.31 (6V41)					
^{59}Fe	A chem, excit, cross bomb (12L38a)					<p>(HPS)</p>	Fe-d-p (12L38a, 20D42); Fe-n- γ (26S42, 4W43, 2547); Co-n-p (12L38a, 2146); Co-d-2p (17T48); spall Cu (32M48, 51B50, 42B51a, 74M52), As (48H50); spall-fission Ta (22N52), Bi (11G49), U (6F51)
^{60}Fe	E chem (6F51)						spall-fission U (6F51)

Isotope Z A	Class and identification	Percent abundance	Type of decay	Half-life	Energy of radiation in Mev		Disintegration energy and scheme	Method of production and genetic relationships
					Particles	Gamma-transitions		
$^{54}_{27}\text{Co}$	E excit (98M52)		β^+ (98M52)	0.18 s (98M52)	>7.4 scint spect (98M52)	γ_1 0.477 (γ/β^+ 0.3, e/γ 0.0007), γ_2 0.935 (γ/β^+ 1.4, e/γ 0.0005), γ_3 1.41 (γ/β^+ 0.3, e/γ 0.0004) spect, spect conv, β - γ coinc (20D49); others (85S51)	Q_β^+ 3.45 (20D49) 	Fe-p-n (98M52) Fe-d-n (19D37, 12L41, 20D49); Fe-p-y (12L38b, 12L41); Ni-y-p2n (42S52); spall Fe (45R52), Co (29W52), Cu (32M48, 42B51a, 74M52), As (48H50); parent Fe55 (12L41)
$^{55}_{27}\text{Co}$	A chem (19D37); chem, cross bomb, genet (12L41)		β^+ -60%, EC -40% (calc from 20D49)	18.2 h (19D37)	1.50 (-50%), 1.01 (-50%) spect (20D49); 1.50 spect (24L39)			
$^{56}_{26}\text{Co}$	A chem, excit, cross bomb (12L41)		EC, β^+ (4E43a, 28C42)	72 d (12L41); 80 d (28C42)	1.50 (coinc with γ_1 and γ_2) spect (4E43a); 1.2 abs (12L41, 28C42)	γ_1 0.845, γ_2 1.26 (coinc with γ_1), γ_3 1.74, γ_4 2.01, γ_5 2.55, γ_6 3.25 ($\gamma_1/\gamma_2/\gamma_3/\gamma_4/\gamma_5/\gamma_6 =$ 1.0/0.5/0.2/0.1/0.2/0.2) spect, β - γ coinc (4E43a); others (85S51)	Q_β^+ 4.6 (4E43a) 	Fe-d-2n (12L41, 16J41, 21P42, 4E43a); Fe-a-np (12L41); Co-p-p3n (29W52); Ni-d-a (12L41, 28C42, 4E43a); Ni-y-pn (42S52); spall Fe (45R52), Cu (42B51a); daughter Ni56 (44S52, 32W52)
$^{57}_{26}\text{Co}$	A chem, excit, cross bomb (12L41)		β^+ (12L41)	270 d (12L41)	0.26 abs (12L41)	0.119, 0.131 spect (4E43a); 0.117 (e/γ large, K/L 7), 0.130 (e/γ large, K/L 7) spect, spect conv (21P42); with Fe57m: 0.014 spect (20D50)	Q_β^+ 1.4 (HPS) 	Fe-d-n (12L38b, 22P38, 54B39, 12L41); Fe-p-y (12L41); parent Fe57m (20D50); daughter Ni57 (23F52)
$^{58m}_{27}\text{Co}$	A chem, excit (55S50)		IT, no β^+ (55S50)	9.2 h (25C50); 9.0 h (37A52); 8.8 h (55S50)		0.025 (e/γ large, K/L 1.9) spect conv (55S50)		Mn-a-n, Co-d-p2n, Co-n-2n, Ni-n-p, Ni-d-2p (55S50); Fe58-p-n (37A52); Co-y-n (25C50); spall Cu (55S50, 74M52)
$^{58}_{27}\text{Co}$	A chem, excit, cross bomb (12L41)		EC 85%, β^+ 15% (21G46)	72 d (12L41)	0.47 spect (20D44); 0.4 abs (12L41)	0.81 spect, β - γ coinc (20D44); -0.81 (e/γ 0.0003) spect conv (55S50); 0.6 abs (12L41)	Q_β^+ 2.3 (18G52) 	Mn-a-n (12L38b, 12L41); Fe-d-n (12L38b, 22P38, 54B39, 12L41); Fe58-p-n (37A52); Fe-p-n (12L38b); Fe-a-np (12L41); Fe-p-y (12L41); Co-p-pn (29W52); Ni-n-p (7V38, 12L41, 20D44); spall Cu (51B50, 42B51a, 74M52), As (48H50)
$^{59}_{27}\text{Co}$		100 (45M41)					Q_β^+ 1.7 (7/2-) 	

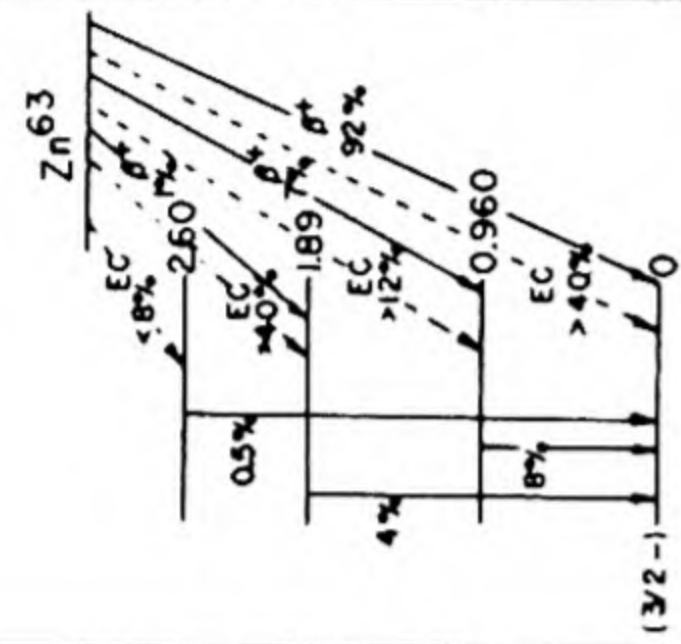
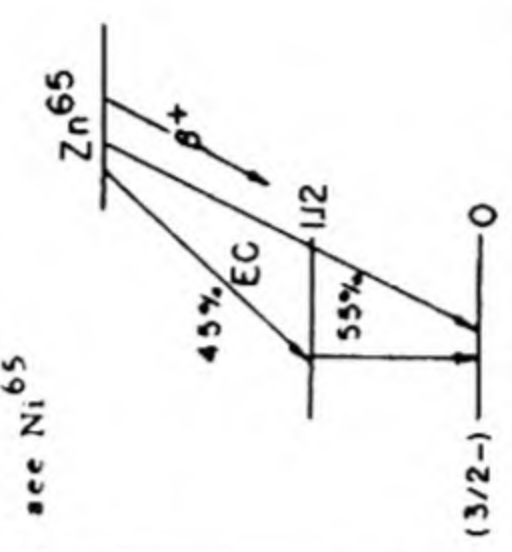
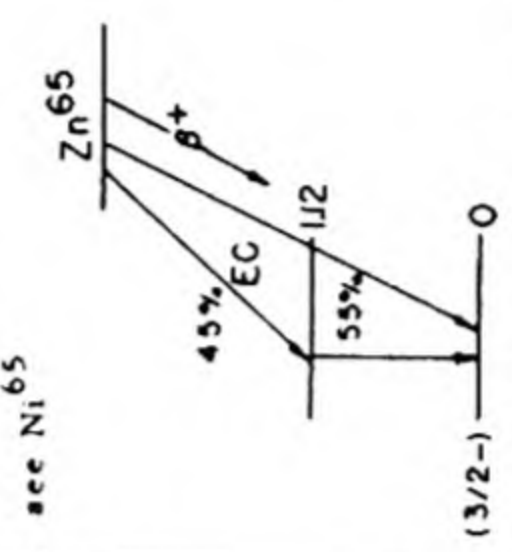
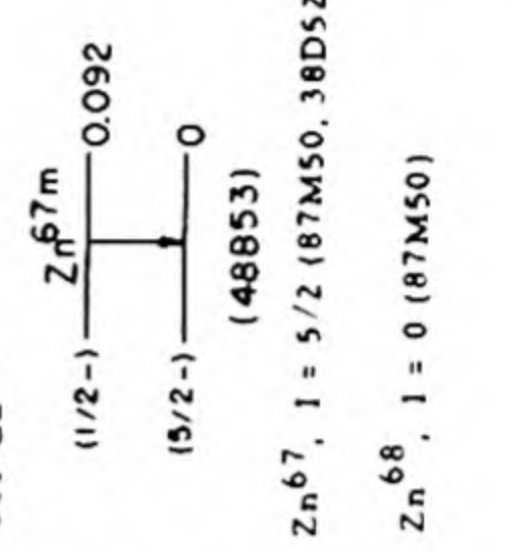
⁶⁰ Co	A n-capt (6H37a); chem, excit, cross bomb (12L41)	IT 99+%, θ^- (20D51)	10.1 m (106B52b); 10.7 m (12L41)	1.56 spect (6P47); 1.35 spect (15N42); 1.28 spect (20D45)	0.0589 (K/L 4 6) spect conv (42C50); 0.059 acint spect (31K51); 0.056 spect conv (20D45)	$Q_{\beta^-} 2.89$ (HPS)	Co-n- γ (6H37a, 12L37, 12L41, 20D42a, 2547); Co-d-p (15N42); Ni-n-p (6H37b, 12L41)
⁶⁰ Co	A n-capt (37S36); chem, excit, cross bomb (12L41)	β^- (27R37)	5.27 y (22T51); 5.3 y (12L41, 53B50, 38S51)	0.306 spect (29F52); 0.318 spect (31W50a); 0.310 spect (43M47)	γ_1 1.3316, γ_2 1.1715 spect (29L49); 1.3316, 1.1715 spect γ - γ coinc (16D51); γ_1 (e/γ 1.24 $\times 10^{-4}$), γ_2 (e/γ 1.72 $\times 10^{-4}$) spect conv (29F52); γ_1 (e/γ 1.29 $\times 10^{-4}$), γ_2 (e/γ 1.73 $\times 10^{-4}$) spect conv (31W50, 31W50a); γ_1 (e/γ 1.8 $\times 10^{-4}$), γ_2 (e/γ 2.3 $\times 10^{-4}$) spect conv (75S50); others (17B50, 44M50a, 13A49, 36A52, 37D51, 85B50a, 85S51)	$Q_{\beta^-} 2.81$ (HPS)	Co-d-p (12L38b, 54B39, 12L41, 20D42a, 15N42); Co-n- γ (27R37, 12L38b, 12L41, 2547, 1Y51); Ni-d-a (12L41); Cu-n-a (12M46c); spall-fission Bi (66B51)
⁶¹ Co	A chem, excit, cross bomb, sep isotopes, mass spect (23P47)	β^- (23P47)	99.0 m (56S51); 105 m (23P49); 110 m (48H50)	1.42 (-55%), 1.00 (-45%) abs (56S51); 1.3 abs (23P49)	-0.5 abs (56S51); no γ (23P49, 29K48)	$Q_{\beta^-} 1.4$ (HPS)	Co-a-2p (112S51); Co-t-p (29K48); Ni- γ -p (12P48, 56S51, 22E52); Ni- γ -p-a (23P47, 23P49); Ni- γ -n-p (23P47, 23P49); Ni-d-an, Cu-n-an (23P47, 23P49); Cu- γ -2p (12P48); Cu- γ -a (49H51); spall Cu (32M48, 42B51a, 74M52), As (48H50); spall-fission Ag (42B51), U (6F51)
⁶² Co	A chem, sep isotopes (23P49)	β^- (23P49)	13.9 m (23P49)	2.3 abs (23P49)	1.3 (coinc with β^-) abs, β - γ coinc (23P49)		Ni- β -n-p (23P49)
⁶² Co	E cross bomb, sep isotopes (23P49)	β^- (23P49)	1.6 m (23P49)		γ (23P49)		Ni- β -n-p, Ni- β -d-a (23P49)
⁶⁴ Co	F cross bomb, sep isotopes (23P49)		-5 m (23P49)				Ni- β -n-p (23P49)
⁵⁶ Ni	A chem (32W52); chem, sep isotopes, genet (44S52)	EC -100%, no β^+ (lim 1%) (44S52)	6.4 d (44S52); 6.0 d (32W52)		γ_1 0.17, γ_2 0.28, γ_3 0.48, γ_4 0.81, γ_5 0.96, γ_6 1.33, γ_7 1.58, γ_8 1.75 ($\gamma_1/\gamma_2/\gamma_3/\gamma_4/\gamma_5/\gamma_6/\gamma_7/\gamma_8 = 1.0/0.3/0.4/0.8/0.1/0.05/0.15/0.02$) acint spect (44S52); 0.14, 0.77, >1.4 acint spect (32W52)		Fe-a-2n (32W52); Fe- β -a-2n (44S52); spall Zn (32W52); parent Co56 (44S52, 32W52)

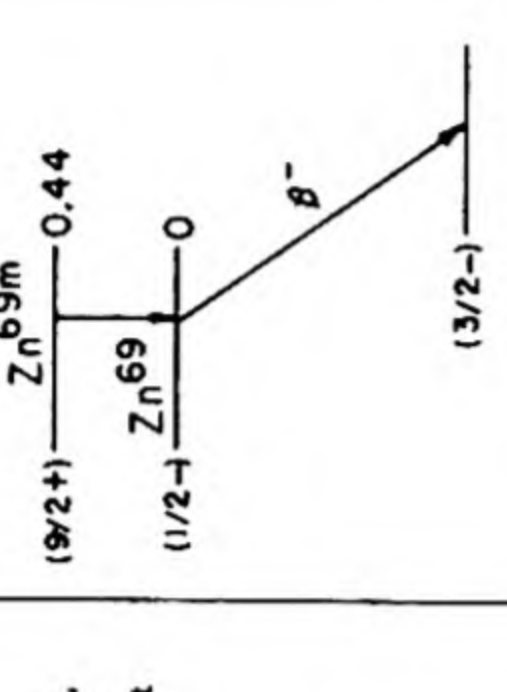
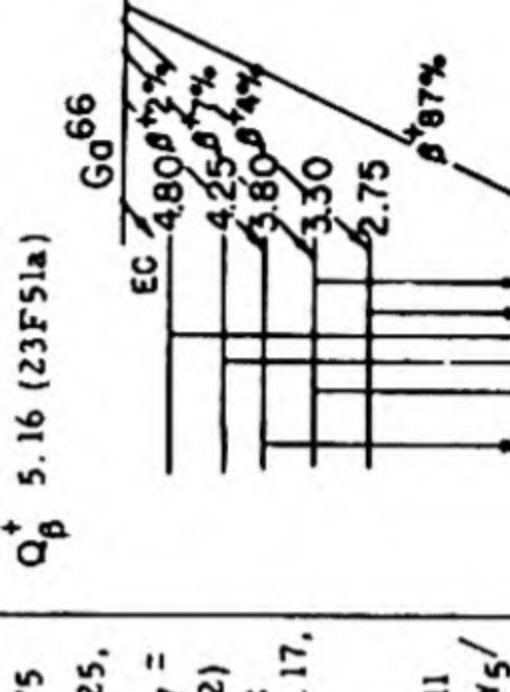
Isotope Z A	Class and identification	Percent abundance	Type of decay	Half-life	Energy of radiation in Mev		Disintegration energy and scheme	Method of production and genetic relationships
					Particles	Gamma-transitions		
⁵⁷ Ni 28	A chem, excit, cross bomb (12L38c)		β^+ 50%, EC 50% (23F50)	36 h (46M49, 12L38c)	0.835 spect (43C51); 0.845 spect (23F50)	γ_1 1.91, γ_2 1.38 ($\gamma_2/\gamma_1 = 6$) spect (43C51); γ_1 1.90, γ_2 1.39 ($\gamma_2/\gamma_1 = 5$) scint spect (44S52); 0.128 spect, spect conv (43C51); 0.120, 1.9 scint spect, spect conv, β - γ coinc (23F50)	 Q_{β^+} 3.24 (43C51) (43C51)	Fe- α -n (12L38c, 14D41, 15N42a, 46M49, 23F50, 43C51); Co-p-3n (29W52); Ni-n-2n (12L38c, 14D41, / 15N42a, 80M52); Ni-He ³ - α (1P52); Ni- γ -n (34H44, 12P48, 12P49, 22E52, 42S52); spall Cu (32M48, 42B51a, 74M52), As (48H50); parent Co57 (23F52)
⁵⁸ Ni		67.76 (24W48)						
⁵⁹ Ni	A chem, cross bomb, n-capt (44C45); chem, sep isotopes, n-capt (48B51)		EC (23F49)	8×10^4 y yield (48B51); 8×10^5 y yield (33W51); -3×10^5 y yield (23F49)		Co-K-x, no γ (33W50, 33W51); Co-K-x (48B51, 23F49)		Fe- α -n (44C45); Co-d-2n (48B51); Ni-n- γ (44C45, 33W50); Ni58-n- γ (48B51); Ni-d-p (44C45)
⁶⁰ Ni		26.16 (24W48)						
⁶¹ Ni		1.25 (24W48)						
⁶² Ni		3.66 (24W48)						
⁶³ Ni	A chem, n-capt, sep isotopes (48B51)		β^- (23F49, 48B51)	85 y yield (48B51); 61 y yield (33W51)	0.067 ion ch (48B51); 0.063 ion ch (33W49)			Ni-n- γ (23F49, 33W49, 33W50, 48B51); Ni62-n- γ (48B51)
⁶⁴ Ni		1.16 (24W48)						
⁶⁵ Ni	A n-capt (6R35); chem, sep isotopes, excit (54S46, 45C46)		β^- (6H37b)	2.564 h (57S49); 2.6 h (12L38c, 46M49)	2.10 (57%), 1.01 (14%), 0.60 (29%) spect (7S49)	1.49, 1.12, 0.37 spect, β - γ , γ - γ coinc (7S49); others (54W51)	 Q_{β^-} 2.10 (7S49) (7S49)	Ni-d-p (12L38c, 15N42a); Ni-n- γ (6H37b, 14D41, 15N42a, 2S47, 46M49); Ni64-n- γ (45C46); Cu-n-p (6H37b); Cu65-n-p (54S46); Cu65-t-He ³ (29K51); Cu-d-2p (32M48, 51B50); Zn-n- α (6H37b); spall Cu (74M52), As (48H50); spall-fission Ta (22N52); Bi (11G49), U (6O48, 6F51)

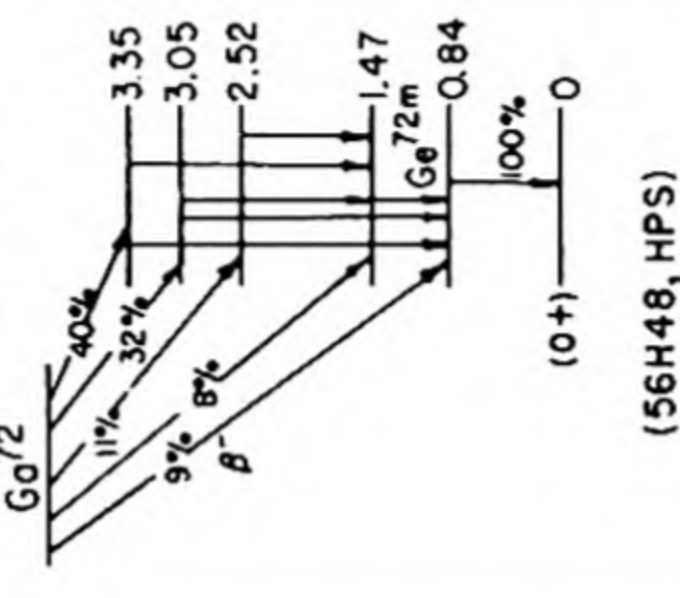
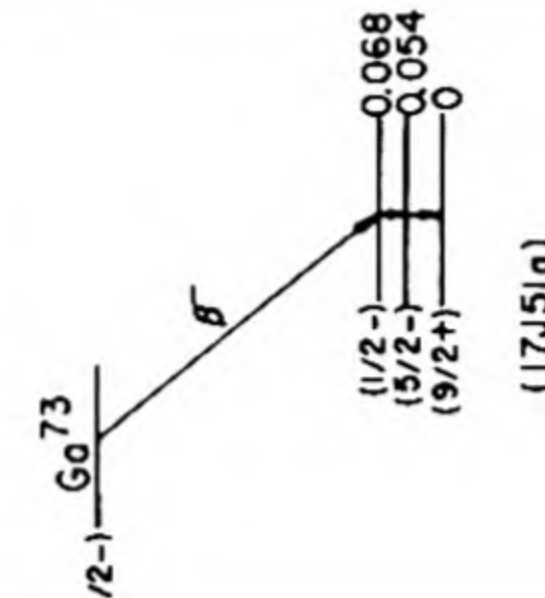
⁶⁶ Ni	A chem, genet (11G49)	β^- (11G49)	56 h (11G49, 48H50)				spall As (48H50); spall-fission Ta (22N52); Bi (11G49); U (6F51); parent Cu66 (11G49)
⁶⁸ Cu	B chem (5D39); chem, excit, sep isotopes (30L47)	β^+ (5D39)	7.9 m (5D39); 10 m (30L47)				Ni-p-n (5D39); Ni58-p-n (30L47)
⁶⁸ Cu	C excit (39T52, 98M51)	β^+ (98M51)	3.04 s (98M51); 2.6 s (39T52)	>7.5 scint spect (98M51)			Ni-p-n (39T52, 98M51)
⁶⁹ Cu	E chem (5D39); excit, sep isotopes (30L47)	β^+ (5D39)	81 s (5D39, 30L47)				Ni-p-y (5D39); Ni58-p-y (30L47)
⁶⁰ Cu	A chem, excit, sep isotopes, mass spect (30L47)	β^+ (30L47)	24.6 m (30L47)	1.8, 3.3 (<5%) abs (30L47)	1.5 abs (30L47)		Ni-p-n (30L47); Ni60-p-n, Ni60-d-2n, Ni58-a-pn (30L47); spall Cu (42B51a), As (48H48a)
⁶¹ Cu	A chem, excit (18R37a); chem, excit, sep isotopes (30L47, 29K50)	β^+ 68%, EC 32% (28C51); β^+ 72%, EC 28% (55B50); β^+ 75%, EC 25% (34H49)	3.33 h (28C48b); 3.4 h (6T37a, 18R37, 29K50); 3.3 h (48H50)	1.205 (96%), 0.55 (4%) spect (13O50); 1.23 spect (16B45b)	γ_1 0.655 (γ/β^+ 0.25, e/γ -0), γ_2 0.284 (γ/β^+ 0.05, e/γ 0.015), γ_3 0.076 (γ/β^+ 0.01, e/γ large) spect, spect conv (13O50); γ_1 (17%), γ_2 (3%), γ_3 (-0.6%) (calc from 28C51, 13O50); 0.652, 0.279, 0.070 (K/L -10) spect, spect conv (56B50)	Q_β^+ 2.23 (13O50)	Ni-d-n (6T37a); Ni-p-n, Ni-p-y (58S38, 5D39); Ni61-p-n (30L47); Ni-He3-d (1P52); Ni-a-p (18R37, 29K50); Cu-y-2n (12P48, 22E52); Zn-y-p2n (55S51, 42S52); spall Cu (32M48, 42B51a, 74M52), As (48H50); spall-fission Bi (66B51), U (6F51)
⁶² Cu	A excit (6H37a); excit, cross bomb (18R37, 58S38, 37B39); chem, sep isotopes (30L47)	β^+ (6H37a)	10.1 m (30L47); 10.0 m (18R37); 9.9 m (12P48); 10.5 m (6H37a)	2.92 spect (61H50); abs (30K50); 2.83 spect (25B49)	0.56 abs (19T47)		Co-a-n (18R37); Ni-p-n, Ni-p-y (58S38); Ni60-a-pn (48G50); Cu-n-2n (6H37b, 80M52, 30B52); Cu-p-pn (48G50); Cu-y-n (37B39, 34H43, 34H43b, 55K52, 25B49, 12P48, 22J50, 55S51, 22E52); Cu-e-e-n (59S48); Cu-d-t (9K40a, 9K41a); Zn-y-pn (55S51, 22E52, 42S52); spall Cu (32M48, 42B51a, 74M52), As (48H50); daughter Zn62 (32M48)
⁶³ Cu							

Cu⁶³, I = 3/2 (87M50)

Isotope Z A	Class and identification	Percent abundance	Type of decay	Half-life	Energy of radiation in Mev		Disintegration energy and scheme	Method of production and genetic relationships
					Particles	Gamma-transitions		
⁶⁴ ₂₈ Cu	A chem, n-capt (12A35); excit (2V36); chem, excit (5D39)		EC 42%, β^- 39%, β^+ 19% (HPS, calc from average of K/ β^+ and K/ β^-); K/ β^+ 2.2 (24P51); K/ β^+ 2.3 (28R50); K/ β^+ 1.8 (34H49); K/ β^+ 2.7 (55B50); β^-/β^+ 2.0 (55B49, 28C48c); β^-/β^+ 2.1 (16B46a); $\beta^+ + EC$ 1.62 β^- (28R50)	12.80 h (29R50); 12.74 h (53S51); 12.88 h (57S49); 12.8 h (2V36, 48H50)	β^- : 0.571 spect (28C48c, 13O49); 0.570 spect (6P47); 0.58 spect (20T39, 14T41) β^+ : 0.657 spect (28C48c, 13O49); 0.644 spect (6P47); 0.65 spect (14T41); 0.66 spect (20T39)	γ (with EC) coinc (16B46a); γ (1% of EC) (HPS, calc from 20D47, 27K50, 28R50); 1.34 (weak) spect (17K48); 1.35 (γ/β^+ 0.025) spect (20D47); 1.33 scint spect (11B50d); (γ/β^+ 0.023) abs (10V52); 1.38 (γ/β^+ 0.032) abs (27K50); -1.34 (e_K/γ -1.3 $\times 10^{-4}$) spect conv (93B52); γ (e/γ < 0.005) spect conv (47M48)	Q_{β^-} 0.57, Q_{β^+} 1.68 (HPS) (HPS)	Ni-p-n (58S38, 5D39); Ni-He ³ -p (1P52); Cu-d-p (2V36); Cu-n-y (6H37b, 2S47); Cu-n-zn (6H37b, 74M52); Cu-p-pn (23R46, 42B51a); Cu-t-d (29K51); Cu-y-n (34H43b, 34H44, 22J50, 12P49, 55S51, 22E52); Zn-n-p (12A35, 6H37b); Zn-y-pn (55S51, 22E52); spall Cu (32M48, 42B51a), Aa (48H50); spall-fission Bi (66B51), U (6F51)
⁶⁵ ₂₉ Cu								
⁶⁶ ₂₉ Cu	A n-capt (12A35); excit (7C37)	30.9 (57B47)	β^- (12A35)	5.10 m (35S2); 5.12 m (53S51); 5.17 m (30R51); 5.18 m (46C50); 5.2 m (23F51a)	2.63 (91%), 1.5 (9%) spect (23F51a); 2.7 (-94%), 1.65 (-6%) scint spect, β - γ coinc (30R51)	1.044 (γ/β^- 0.10, e/γ < 3×10^{-3}) spect, spect conv (23F51a); 1.05 scint spect (30R51, 94M51a)	 Q_{β^-} 2.63 (23F51a) Cu ⁶⁵ , I = 3/2 (87M50)	Cu-n-y (12A35, 2S47, 9O49, 50H51); Cu-d-p (31L40); Zn-n-p (6H37b); Ga-n-a (7C37); daughter Ni ⁶⁶ (11G49)
⁶⁷ ₂₉ Cu	A chem (11G49); chem, cross bomb, sep isotopes (29K50)		β^- (11G49)	58.5 h (29K50); 61.0 h (80S52); 56 h (11G49); 61 h (48H50)	0.38 (67%), 0.57 (33%) spect (80S52); 0.54 abs (29K50)	0.191 (e/γ 0.01, K/L -8), 0.096 (e/γ 0.09, K/L 7.4) scint spect, spect conv, β - γ coinc (80S52)	 see Ga ⁶⁷ (23F51a, 30R51)	Ni ⁶⁴ -a-p (29K50); Cu-a-2p (112S51); Cu-t-p (29K51); Zn ⁶⁷ -n-p (29K50); Zn-y-p (23D48, 55S51, 22E52) spall Aa (48H50); spall-fission Bi (11G49, 66B51), U (6F51)
⁶² ₃₀ Zn	A chem, genet (32M48); excit (48G50)		EC -90%, β^+ -10% (61H50)	9.33 h (61H50); 9.5 h (32M48)	0.66 spect (61H50)	0.0418 (K/L > 6) spect conv (61H50)		Ni-He ³ -n (1P52); Ni ⁶⁰ -a-2n (48G50); Cu-p-2n (48G50); Zn-y-2n (55S51, 22E52, 42S52); spall Cu (32M48, 61H50, 51B50, 42B51a), Aa (48H50); parent Cu ⁶² (32M48)

⁶³ Zn	A chem, excit (37B37, 6H37b, 18R37)	48.89 (1B50)	β^+ 93%, EC 7% (34H47)	38.3 m (34H47, 58S38); 38.5 m (5D39)	2.36 (92%), 1.40 (7%), 0.5 (-1%) spectrum (34H47); 2.32 spectrum (14T41)	0.960 (-8%, e/γ 2 $\times 10^{-4}$), 1.89 (-4%, e/γ -0), 2.60 (-0.5%, e/γ -0) spectrum, aspect conv, abs, γ - γ coinc (34H47)	Q_{β^+} 3.38 (34H47)	 (34H47)	Ni-a-n (18R37); Ni-60-a-n (48G50); Cu-p-n (58S38, 5D39, 47B, 1b, 48G50); Cu-d-2n (31L40, 14T41); Zn-n-2n (6H37b, 1P37); Zn-n- γ -n (37B39, 12P49, 55S51, 22E52, 42S52); Zn- γ -3n (55S51); spall Cu (32M48, 51B50, 42B51a) A# (48H50)
⁶⁴ Zn							$Zn^{64}, I = 0$ (87M50)	 (34H47)	Cu-d-2n (22P38); Cu-p-n (58B38, 47B51b); Cu-t-n (29K51); Zn-d-p (12L39); Zn-n- γ (42S39, 2S47); spall Cu (42B51a), A# (48H50); daughter Ga65 (12L39b)
⁶⁵ Zn	A chem (22P38); chem, excit, cross bomb (12L39)	48.89 (1B50)	EC (K) 97.5%, β^+ 2.5% (95M52, 4Y52) EC 99+%, β^+ 0.7% (calc from 30G51, 24F51, 21G46a)	250 d (12L39); 245 d (22P38)	0.325 spectrum (48M49); 0.32 spectrum (6P47)	1.120 spectrum conv (48M49); 1.125 spectrum, aspect conv (12H50); 1.114 spectrum (48M49); 1.112 (e/γ 2.3 $\times 10^{-4}$) aspect conv (31W50); 1.127 aspect spectrum (25G51a); 1.12 aspect (13J49); γ (46% of EC) x-e coinc (21G46a); γ (44% of EC) x- γ coinc (24F51); γ/β^+ = 65 γ - γ coinc (30G51); 0.21 (coinc with β^+ , e/γ -0.1) β - γ , β -conv coinc (47C50)	see Ni ⁶⁵	 (34H47)	
⁶⁶ Zn		27.81 (1B50)				0.092 (e_K/γ 0.63, K/L 7) aspect spectrum (48B53); 0.092 (e/γ 0.6) aspect spectrum (47M52)	$Zn^{66}, I = 0$ (87M50)		daughter Ga ⁶⁷ (48B53, 47M52)
^{67m} Zn	A genet (48B53, 47M52)		IT (47M52, 48B53)	8.5 $\times 10^{-6}$ s delay coinc (48B53); 9 $\times 10^{-6}$ s delay coinc (47M52)			see Ga ⁶⁷	 (34H47)	
⁶⁷ Zn		4.11 (1B50)					$Zn^{67}, I = 5/2$ (87M50, 38D52)		
⁶⁸ Zn		18.56 (1B50)					$Zn^{68}, I = 0$ (87M50)		

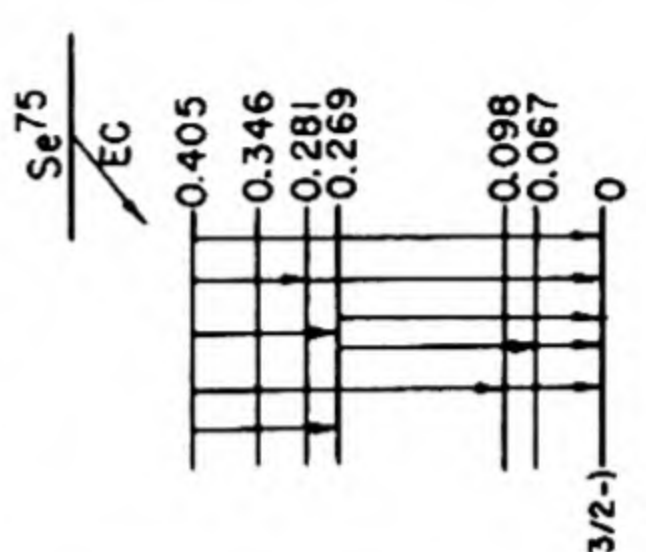
Isotope Z A	Class and identification	Percent abundance	Type of decay	Half-life	Energy of radiation in Mev		Disintegration energy and scheme	Method of production and genetic relationships
					Particles	Gamma-transitions		
⁶⁹ ₃₀ Zn	A chem, excit (6T38); chem, excit, cross bomb (12L39, 14K39)		IT (14K39)	13.8 h (12L39)		0.437 (e/γ 0.049) spect conv (9IS52b); 0.436 (e/γ -0.065) spect conv, scint spect (23D52); 0.439 (e/γ -0.04) spect, spect conv (2H41); 0.440 spect (28G41); 0.450 (e/γ -0.06) (16N44) no γ (12L39)	 Q _β 0.90 (HPS, 12L39)	Zn-d-p (12L39, 14K39, 6V39); Zn-n-γ (6T38, 12L39, 2S47); Ga-d-α (12L39); Ga-n-p (12L39); spall As (48H50); parent Zn ⁶⁹ (14K39)
⁶⁹ Zn	A chem, n-capt (6H37b); chem, excit, cross bomb (12L39, 14K39)		β ⁻ (6H37b)	57 m (12L39); 51 m (48H48b); 52 m (7H49)	0.897 spect (23D52); 0.914 spect (9IS52b); others (14K39, 12L39, 35B46a)			⁷⁰ Zn -γ-n (7H49); Zn-d-p (12L39, 14K39, 6V39); Zn-n-γ (6H36, 6T38, 2S47, 50H51, 42S39); Ga-d-α (12L39); Ga-n-p (12L39); spall As (48H48a); daughter Zn ^{69m} (14K39)
⁷⁰ Zn		0.62 (1B50)						
⁷¹ Zn	E n-capt, cross bomb (28H46b)		β ⁻ (28H46b)	2.2 m (28H46b)	2.1 abs (28H46b)			Zn-n-γ, Ge-n-α (28H46b)
⁷² Zn	A chem, genet (60S46, 60S51)		β ⁻ (60S51)	49.0 h (60S51)	-0.3 (95%), -1.6 (5%) abs (60S51)	γ (60S51)		As-p-4p (112S51); spall As (48H50); spall-fission Bi (11G49), U (6F51); fission Th (21T51), U (60S51), Pu (61S51a); parent Ga ⁷² (60S51)
⁶⁵ ₃₁ Ga	A chem, genet (12L39b)		EC (6A38); β ⁺ >50% (25A52)	15 m (6A38, 12L39b)	2.2 (25A52)	0.054, 0.117 spect conv (6V39)		Cu-He ³ -n (1P52); Zn-d-n (6A38, 12L39b); Zn-p-γ (2D40); parent Zn ⁶⁵ (12L39b)
⁶⁶ Ga	A chem, excit (50M37, 18R37a)		β ⁺ 64%, EC 36% (49M52); β ⁺ 66%, EC 34% (10L50a)	9.45 h (10L50a); 9.4 h (18R37, 59B38); 9.2 h (49M50, 50M37)	4.144 (87%), 1.4 (4%), 0.88 (7%), 0.40 (2%) spect (10L50a); 4.15 (87%), 1.38 (4%), 0.90 (7%), 0.40 (2%) spect (49M52)	 Q _β 5.16 (23F51a)	Cu-α-n (50M37, 18R37, 10L50a); Zn-p-n (59B38, 49M50); spall Cu (second order reaction) (42B51a, 29W52), spall As (48H50); spall-fission Sn, Ba (42B51); daughter Ge ⁶⁶ (48H49)	

Isotope Z A	Class and identification	Percent abundance	Type of decay	Half-life	Energy of radiation in Mev		Disintegration energy and scheme	Method of production and genetic relationships
					Particles	Gamma-transitions		
⁷² ₃₁ Ga	A chem, n-capt, excit (12L38a, 42S39)		β^- (42S39)	14.3 h (26M43a, 60S51); 14.1 h (42S39, 9B50)	3.15 (9%), 2.52 (8%), 1.5 (11%), 0.9 (32%), 0.6 (40%) spect (56H48); 3.17 (8%), 2.57 (8%), 1.7 (7) (3%), 1.5 (7) (7%), 1.00 (26%), 0.74 (23%), 0.6 (7) (25%) spect (14M48)	γ_1 2.491, γ_2 2.508 (γ_1/γ_2 0.63) spect (12H52); 2.51 (26%), 2.21 (33%), 1.87 (8%), 1.59 (5%), 1.20 (?) (<2%), 1.05 (5%), 0.84 (100%), 0.68 (<2%), 0.63 (24%) spect, spect conv (56H48); γ_1 2.50 (15%), γ_3 2.18 (33%), γ_4 1.81 (10%), γ_5 1.57, γ_6 1.47, γ_7 1.30 ($\gamma_5 + \gamma_6 + \gamma_7$ 28%), γ_8 1.05 (15%), γ_9 0.835 (100%), γ_{10} 0.691 (5%), γ_{11} 0.631 (54%) spect, spect conv (14M48); 3.4 (-0.03%), 3.1 (-0.1%) D- γ -p ion ch (9B50)	Q_{β^-} 4.0 (56H48, 14M48) see Ge 72m 	Ga-d-p (12L38a); Ga-n-p (42S39, 2S47, 60S51); Ge-n-p (42S41, 60S51); As-d-p (16C47); As- γ -He 3, As- γ -2pn (85H52); spall-fission Sn, Ba (42B51); TL (2T47b), P1 (11G49, 13P47), U (6C47, 6F51); fission Th (21T51), U (60S51); daughter Zn 72 (60S51); parent Ge 72m (28B48)
⁷³ Ga	B chem, excit (60S46, 60S51)		β^- (60S51)	5.0 h (60S51)	1.4 abn (60S51)	0.0135, 0.054 spect conv (17J51a)		Ge-n-p (60S51); Ge- γ -p (12P49); As- γ -2p (85H52); As- α -2p (11S51); spall-fission Bi (11G49); fission U (60S51)
⁶⁶ ₃₂ Ge	A chem, genet (48H49)		β^+ (?) (48H50)	-150 m (48H50)				spall Cu (second order reaction) (42B51a), spall: Ge (48H49), As (48H50); parent Ga 66 (48H49)
⁶⁷ Ge	A chem, genet (48H49)		β^+ (48H50)	21 m (48H50)				spall Cu (second order reaction) (42B51a), spall Ge (48H49), As (48H50); parent Ga 67 (48H49)
⁶⁸ Ge	A chem (50M38); chem, genet (48H48b)		EC (48H48b)	250 d (48H50)				spall Cu (second order reaction) (42B51a), spall As (48H48a, 48H50); Zn- α -Zn (50M38); parent Ga 68 (48H48a, 48H50)


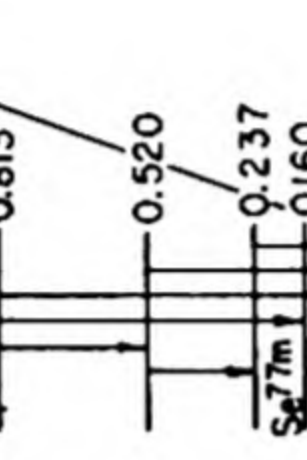
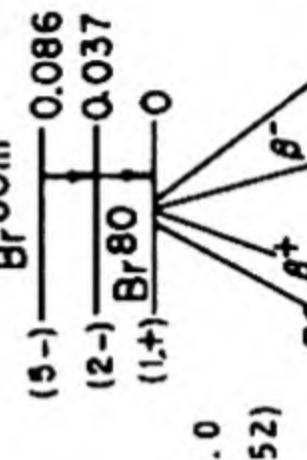
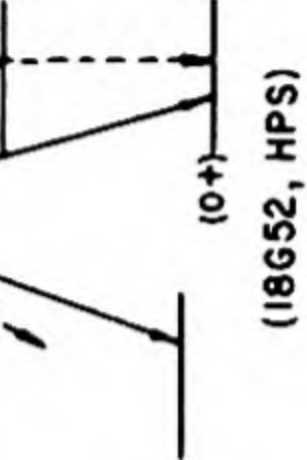
Ge ⁶⁹	A chem (50M38); chem, excit, cross bomb (51M48)	20.55 (3148a)	EC -67%, β^+ -33% (51M48); β^+ (50M38)	39.6 h (51M48); 39.7 h (12D42); 40 h (48H50); 37 h (50M38)	1.215 (88%), 0.610 (10%), 0.22 (2%) spect (10H51)	1.610, 1.340, 1.12, 0.870, 0.576, 0.388, 0.090 spect, β - γ coinc (10H51)	Q_{β}^+ 3.36 (10H51)	 Ge ⁶⁹	Zn-n-n (50M38, 51M48); Ga-d-2n (13S41a, 51M48, 10H51); Ga-p-n (12D42); Ge-n-2n (42S41, 51M48); Ge-y-n (34H44, 42S52); spall As (48H50)
Ge ⁷⁰									
Ge ⁷¹	A chem, excit, cross bomb (13S41a); sep isotopes, n-capt (22R50)		EC, no β^+ (51M48, 26M49)	11.4 d (51M48); 11.3 d (12D42); 11 d (26M49, 13S41a)	no γ (13S41a, 26M49, 51M48); Ga K-x (2547, 51M48, 26M49)			 Ge ⁷¹	Ga-d-2n (13S41a, 51M48); Ga-p-n (12D42); Ge-d-p (13S41a, 51M48); Ge-n-y (2547, 51M48, 26M49); Ge ⁷⁰ -n-y (22R50); spall As (48H50); daughter As ⁷¹ (48H49)
Ge ^{72m}	A genet (28B48)		IT (28B48)	2.9 x 10 ⁻⁷ s delay coinc (52M51); 5 x 10 ⁻⁷ s delay coinc (28B48)	0.7 (e/ γ very high) coinc abs conv (28B48, 52M51)		see Ga ⁷²		daughter Ga ⁷² (28B48); daughter As ⁷² (14S50b)
Ge ⁷²		27.37 (3148a)					Ge ⁷² , I = 0 (35T49)		
Ge ⁷³		7.67 (3148a)					Ge ⁷³ , I = 9/2 (35T49)		
Ge ⁷⁴		36.74 (3148a)					Ge ⁷⁴ , I = 0 (35T49)		
Ge ^{75m}	A excit (9F52); cross bomb, n-capt, sep isotopes (91S52c)		IT (9F52)	42 s (9F52); 48 s (91S52c)	conv. 0.14 abs (9F52)	0.175 scint spect (91S52c); -0.150 scint spect (24C52)		 Ge ⁷⁴	Ge ⁷⁴ -n-y (91S52c); Ge-n-y (9F52, 24C52); As-n-p (9F52, 91S52c)
Ge ⁷⁵	A chem, excit, cross bomb (13S41a); n-capt, sep isotopes (22R50)		β^- (13S41a)	82 m (51M48); 89 m (13S41a); 79 m (22R50)	1.137 (85%), not coinc with γ ; 0.614 (15%) spect (91S52c); 1.2 abs (13S41a); 1.3 abs (22R50)	0.265 (e/ γ very small), 0.418, 0.572, other γ 's spect, spect conv, scint spect (91S52c); 0.25 (-10%) (22R50); no γ (51M48)	Q_{β}^- 1.14 (91S52c)	 Ge ⁷⁶	Ge ⁷⁴ -n-y (22R50, 91S52c); Ge-n-y (42S39, 42S41, 2S47); Ge-d-p (42S39, 42S41, 13S41a); Ge-n-2n (42S41, 13S41a); Ge-y-n (34H44, 12P49); As-n-p (42S41, 13S41a, 51M48); Se-n-a (42S41, 13S41a)
Ge ⁷⁶		7.67 (3148a)					Ge ⁷⁶ , I = 0 (35T49)		
Ge ^m	E n-capt (24C52)		IT (24C52)	-0.35 s (24C52)	-0.06 scint spect (24C52)				Ge-n-y (24C52)

Isotope Z A	Class and identification	Percent abundance	Type of decay	Half-life	Energy of radiation in Mev		Disintegration energy and scheme	Method of production and genetic relationships
					Particles	Gamma-transitions		
⁷⁷ Ge	A cross bomb, genet, n-capt (23A47); sep isotopes (22R50)		β^- 50%, IT -50% calc (42F52); β^- , IT (14M52)	59 s (23A47); 57 s (22R50)	2.8 abs (23A47)	0.38 scint spect (14M52)		Ge-n-y, parent As ⁷⁷ (23A47, 22R50); Ge ⁷⁶ -n-y (22R50)
⁷⁶ Ge	A chem, excit, cross bomb (13S41a)		θ^- (42S41)	12 h (13S41a, 61S51, 22R50)	2.196 (42%, coinc with γ), 1.379 (35%), 0.71 (23%) spect (91S52); others (14M52, 61S51, 22R50, 26M49)	0.042, 0.073 (coinc with 0.213 and 0.264 γ), 0.213, 0.264, 0.368, 0.418, 0.564, 1.105, 1.75 spect, β^- - γ , γ - γ coinc (91S52); 0.209, 0.268, 0.300, 0.327, 0.366, 0.408, 0.425, 0.466 spect conv (91S52); 0.6, 0.3 (coinc with β^-) abs, β^- - γ coinc (22R50)		Ge ⁷⁶ -n-y (22R50); Ge-n-y (42S39, 42S41, 2S47); Ge-d-p (42S41, 13S41a, 88S52); Se-n-a (13S41a); fission Th (21T51), U (61S46, 61S51), U233 (61S48); parent As ⁷⁷ (61S46, 61S51)
⁷⁸ Ge	B chem, genet (61S46, 61S51)		β^- (61S51)	2.1 h (61S51)	-0.9 abs (61S51)	γ (61S51)		ission U, parent As ⁷⁸ (61S51)
⁷⁰ As	D chem (48H49, 48H50)		β^+ (48H50)	52 m (48H50)		0.162 spect conv (53M50)		As-d-p6n, daughter Se ⁷⁰ (48H50); not found: Ge ⁷⁰ -p (37A52)
⁷¹ As	A chem (42S41); chem, genet (48H49); mass spect (104B52)		EC (48H50); EC, β^+ (51M48a)	60 h (48H50); 50 h (51M48a)				Ca-a-2n (53M50); Ge-d-n (51M48a); As-d-p5n (48H50); parent Ge ⁷¹ (48H49)
⁷² As	A chem, excit (14M47); chem, excit, sep isotopes (51M48a)		EC, β^+ (51M48a)	26 h (51M48a, 2V40); 27 h (48H50)	3.34 (19%), 2.50 (62%), 1.84 (12%), 0.67 (5%), 0.27 (2%) spect (53M50); 2.8 abs (14M47, 51M48a)	0.835, others up to 3.0 (weak) spect (53M50)		Ca-a-n (14M47, 51M48a, 53M50); Ge-p-n (2V40); As-d-p4n (48H50); Se ⁷⁴ -d-a (51M48a); daughter Se ⁷² (48H48a)
⁷³ As	A chem (42S39b); chem, excit, cross bomb, sep isotopes (51M48a); mass spect (17J51a)		EC (4E43b); no β^+ (4E43b, 51M48a)	76 d (51M48a); 90 d (42S39b, 53M50)		0.0135 (L/M 5.4), 0.0539 (K/L+M 5.6) spect conv, conv-conv coinc (17J51a, 17J52); 0.052 spect conv (4E43b, 53M50)		Ge-d-n (42S39b, 4E43b); Ge ⁷⁰ -a-p (51M48a); Ge-a-p (51M48a, 53M50); As-d-p3n (48H50); Se ⁷⁶ -p-a (25F51)

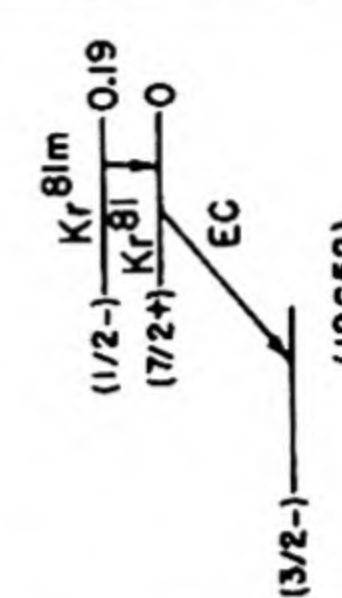
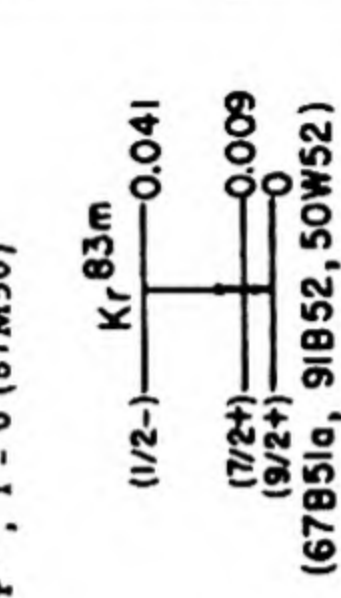
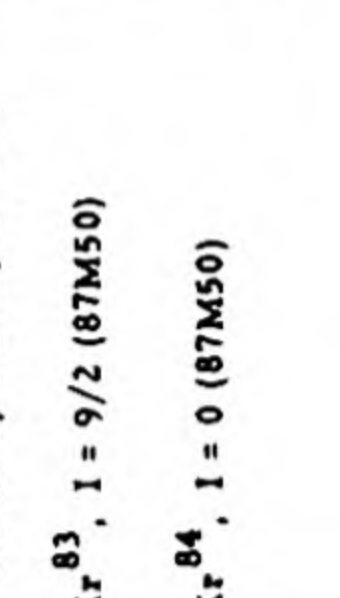
As ⁷⁴	A excit (48C38): chem, excit (42S39b)	17.5 d (51M48a); 19.0 d (48H50); 16 d (42S39b)	β^- : 1.36 (51%), 0.69 (49%) spect (17J51); 1.45 (47%), 0.82 (53%) spect (53M50) β^+ : 1.53 (11%), 0.92 (89%) spect (17J51); 0.96 spect (53M50)	γ_1 0.596, γ_2 0.635 ($\gamma_1/\gamma_2 = 4$) spect, β - γ coinc (17J51); 0.593 spect (53M50); 0.582 spect (20D41)	Q_β^- 1.36 (17J51) Q_β^+ 2.55 (17J51) As ⁷⁴ 49% 11% 51% β^- 89% β^+ 0.596 (0+)—0 (17J51)	Ge-a-n (51M48a); Ge-d-n (42S39b, 42S41, 2142) Ge-p-n (2D40); As-n-2n (48C38, 42S39b); As-d-p2n (48H50); Se-d-a (23F40); Br-y-an (85H52); spall-fission Bi (11G49)
As ⁷⁵	100 (6N37)				As ⁷⁵ , I = 3/2 (87M50, 29J52)	
As ⁷⁶	A chem, n-capt (12A35)	26.8 h (34W42); 26.3 h (14M40); 26.1 h (3P48)	β^- : no β^+ : β^+ lim 0.03% (63B47); β^+ lim 0.07% (41M51); β^+ lim 0.1% (16W48)	0.55, 1.20, 1.70 spect (7S47d); 0.557, 1.22, 1.78 (weak) spect (16W48); 0.558 (e_K/γ 0.002) spect conv (7T52); γ_1 0.57, γ_2 1.25, γ_3 1.84, γ_4 2.15 ($\gamma_1/\gamma_2/\gamma_3/\gamma_4 = 1/0.4/\text{weak}/$ weak) spect (43M46); 0.58, 1.20, 1.76, 2.02, no 2.3- 2.7 γ (lim 0.01%) acint spect, γ - γ coinc (62B51); γ_1 0.555, γ_2 0.648, γ_3 1.210, γ_4 1.410, γ_5 2.06 ($\gamma_1/\gamma_2/\gamma_3/\gamma_4/\gamma_5 =$ 1/0.1/0.25/0.02/0.06) spect (57H51); 0.568 (e/γ -0), 1.25 (e/γ -0) spect, spect conv (54M49, 54M51); others (52M51)	Q_β^- 3.1 (HPS) As ⁷⁶ 100% β^- ~20% ~20% ~50% 2.62 1.77 0.56 (2+) (0+) (HPS)	Ge-p-n (2V40); As-d-p (6T36, 48C38); As-n-y (12A35, 48C38, 9049, 50H51); Se-n-p (42S39b); Se-y-p (42H47); Se-d-a (23F40); Br-n-a (48C38); Br-y-an, Br-y-He ³ (85H52)
As ⁷⁷	A chem, genet (61S46, 61S51)	38 h (18H50, 21T51); 40 h (61S51)	β^- (61S51)	no γ (43C51a, 13J51)	Q_β^- 0.70 (43C51a) As ⁷⁷ (3/2-) β^- Se ^{77m} (7/2+) (1/2-) 0.162 (43C51a, 18G52)	Br-y-a (85H52); spall-fission Bi (11G49), Th (7N49a), U (6F51); fission Th (21T51), U (61S51); U233 (61S48); daughter Ge ⁷⁷ (61S51); daughter Ge ^{77m} (23A47, 22R50 not parent Se ^{77m} (lim 2%) (56M50a)
As ⁷⁸	B chem (26S37a): excit (48C38)	90 m (61S51, 64B51); 80 m (48C38); 65 m (26S37a, 42S39b)	β^- (26S37a)	0.27 abs (42S39b); no γ coinc with 4.1 β^- (74S51a)	Q_β^- 4.1 (74S51a)	Br-n-a (26S37a, 48C38, 42S39b, 64B51); Br-y-He ³ (85H52); Se-n-p (42S39b); fission U, daughter Ge ⁷⁸ (61S46, 61S51)

Isotope Z A	Class and identification	Percent abundance	Type of decay	Half-life	Energy of radiation in Mev		Disintegration energy and scheme	Method of production and genetic relationships
					Particles	Gamma-transitions		
⁷⁸ As 33As	F chem (64B51)			-40 m (64B51)			Q_{β}^{+} 2.70 (62S51)	Ge- α -n (49C48, 62S51); Ge-70- α -n (49C48); As-d-4n (48H50); spall-fission Bi (66B51)
⁷⁹ As 33As	D chem (65B50)		β^{-} (11V52)	9 m (65B50); 10 m (11V52)	-2.1 abs (11V52)			
⁷⁰ Se 34Se	D chem (48H49, 48H50)		β^{+} (48H50)	-44 m (48H50)				
⁷² Se 34Se	A chem, genet (48H48a)		EC (48H50)	9.7 d (48H50)				
⁷³ Se 34Se	A chem (48H48a); chem, excit, sep isotopes (49C48)		β^{+} , EC, IT 20% (?) (62S51)	7.1 h (49C48, 62S51); 6.7 h (48H50)	1.68 (1%), 1.318 (88%), 0.750 (10%), 0.25 (1%) spect (62S51)	γ_1 0.0671 (conv in Se, K/L 7.6), γ_2 0.361 (K/L 8.6), γ_3 0.860, γ_4 1.310 ($\gamma_1/\gamma_2/\gamma_3/\gamma_4 = 10/163/$ 11/8) spect, spect conv (62S51)	Q_{β}^{+} 2.70 (62S51)	Ge- α -n (49C48, 62S51); Ge-70- α -n (49C48); As-d-4n (48H50); spall-fission Bi (66B51)
⁷⁴ Se 34Se		0.87 (24W48)					Se^{74} , I = 0 (55G50)	
⁷⁵ Se 34Se	A chem, excit (2D40, 4K42); sep isotopes, n-capt (10C50)		EC, no β^{+} (26F47, 49C48, 10C50)	127 d (49C48); 128 d (10C50); 115 d (26F47); 120 d (48H50)		γ_1 0.067, γ_2 0.077, γ_3 0.098 (K/L -11, e/ γ -8), γ_4 0.124 (e/ γ -0.3), γ_5 0.138 (e/ γ -0.1), γ_6 0.203, γ_7 0.269 (e/ γ -0.09), γ_8 0.281, γ_9 0.308, γ_{10} 0.405 (e/ γ -0.001) ($\gamma_2/\gamma_3/\gamma_4/\gamma_5/\gamma_7/$ $\gamma_8/\gamma_{10} = 0.14/-0.007/-0.02/$ 0.21/0.70/-0.05/0.14) spect, spect conv, γ - γ coinc (13J52a); 0.025, 0.066, 0.081, 0.097, 0.121, 0.136, 0.199, 0.265, 0.280, 0.305, 0.402 spect conv (10C50); 0.076, 0.099 (?), 0.123, 0.137, 0.267, 0.283, 0.405 spect (11T48); 0.098 (e/ γ large), all other γ (e/ γ very small) spect, spect conv (75M51); others (52M51)	 (13J52a)	As-p-n (2D40); As-d-2n (4K42, 26F47, 49C48, 48H50); Se-n- γ (2S47, 26F47, 11T48, 13J52a); Se-74-n- γ (10C50)
⁷⁶ Se 34Se		9.02 (24W48)					Se^{76} , I = 0 (55G50)	

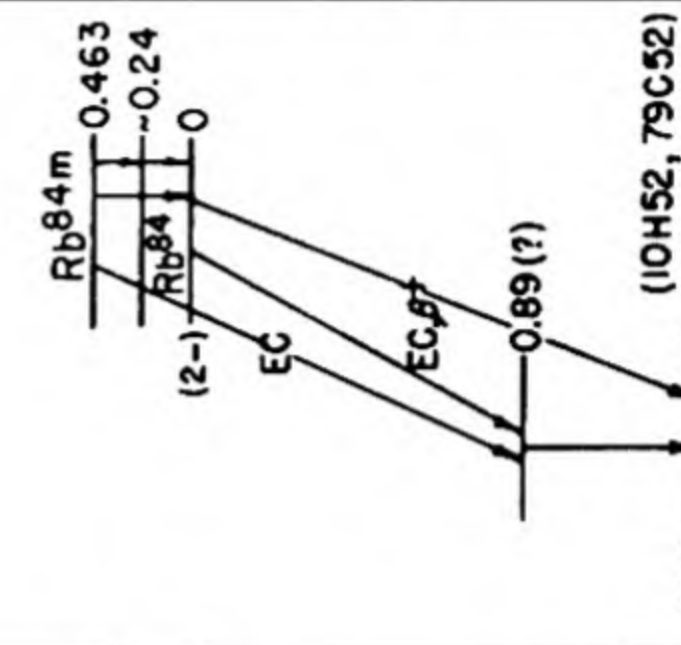
Se ^{77m}	A n-capt (23A47); sep isotopes, n-capt (18G48a); genet (43C51b)	IT (23A47)	17.5 m (23A47, 32G49, 43C51b)	0.162 (K/L 4-6) spect conv (31R52); 0.160 (e/y large) spect, spect conv (43C51b); 0.165 spect conv (19O52); abs (9F50); others (38M51, 31K51, 32G49, 23A47)	see Br ⁷⁷ (7/2+) Se ^{77m} 0.162 (1/2-) 0 (18G52)	Se-n-y (23A47); Se ⁷⁶ -n-y (18G48a); Se-x rays (32G49); daughter Br ⁷⁷ (43C51b, 43C51); not daughter As ⁷⁷ (lim 2%) (56M50a)
Se ⁷⁷			7.58 (24W48)			
Se ⁷⁸			23.52 (24W48)			
Se ^{79m}	A excit, n-capt (9F50, 9F50b); n-capt, sep isotopes (31R52)	IT (9F50b)	3.5 m (31R52); 3.9 m (9F50)	0.096 (K/L 2-9) spect conv (31R52)	Se ^{79m} (1/2-) Se ⁷⁹ 0.096 (7/2+) 0 β^- (3/2-) (18G52, HPS)	Se ⁷⁸ -n-y (31R52); Se-n-y, Se-n-2n (9F50, 9F50b); Br-n-p (9F50b)
Se ⁷⁹	B chem, spect (?) (26P49)	β^- (26P49)	$\leq 6.5 \times 10^4$ y sp act (est yield) fission (26P49)	no γ (26P49)		fission U (26P49)
Se ⁸⁰			49.82 (24W48)			
Se ^{81m}	A chem, excit, cross bomb (26S37a); sep isotopes, n-capt (32L47); mass spect (67B49)	IT (20L40)	56.5 m (25W48); 57 m (26S37a, 20L40); 59 m (33G51)	0.103 (K/L 3-0) spect conv (31R52); 0.104 (e/y very large, K/L -3-9) spect conv (67B49); 0.099 (K/L -4) spect conv (2H41)	Se ^{81m} (7/2+) Se ⁸¹ 0.103 (1/2-) 0 β^- (3/2-) (18G52)	Se-d-p (26S37a, 20L40); Se-n-y (26S37a, 6H37, 2S47); Se ⁸⁰ -n-y (32L47); Br-n-p (26S37a, 20L40); fission U (33G51); parent Se ⁸¹ (20L40)
Se ⁸¹	A chem, genet (20L40)	β^- (20L40)	17 m (33G51); 18 m (9F50); 19 m (20L40); 13.6 m (25W48)	no γ (33G51)	Q ⁻ 1.38 (67B49, 33G51) (3/2-) (18G52)	Se-d-p (26S37a, 20L40); Se-n-y (26S37a, 6H37, 2S47); Se-y-n (37B39); Br-n-p (20L40); spall-fission Bi (66B51); fission U (33G51); daughter Se ^{81m} (20L40)
Se ⁸²			9.19 (24W48)			
Se ⁸³	A chem, genet (23A47)	β^- (23A47)	67 m (23A47)	3.4 abs (23A47); no conv (31R52)	Se ⁸² , I = 0 (55G50)	Se-n-y (23A47); fission U (63S47); parent Br ⁸³ (23A47)
Se ⁸³	A chem, excit, cross bomb (26S37a); chem, genet (20L40)	β^- (26S37a)	25 m (33G51a); 26 m (31R52); 30 m (20L40)	1.5 abs (33G51a, 31R52)		Se-d-p (26S37a, 20L40); Se-n-y (26S37a, 20L40, 2S47); fission Th (72B51), U (33G51a) parent Br ⁸³ (20L40, 33G51a)
Se ⁸⁴	A chem, genet (33G46)	β^- (33G46)	-2 m (33G51b, 20E51)			fission U, parent Br ⁸⁴ (33G51b, 20E51)

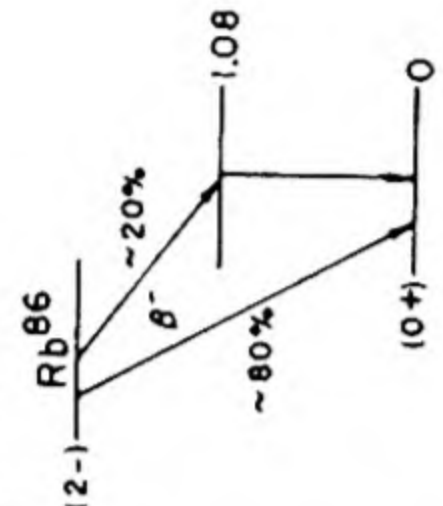
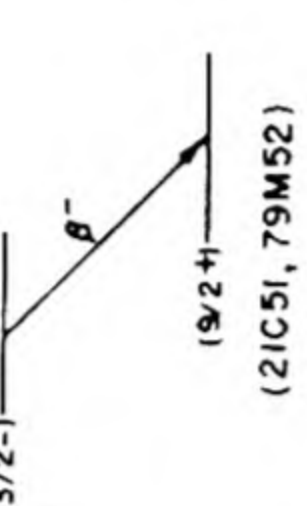
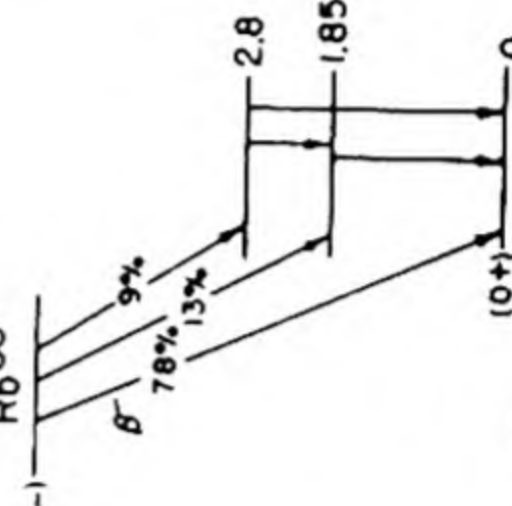


Isotope Z A	Class and identification	Percent abundance	Type of decay	Half-life	Energy of radiation in Mev		Disintegration energy and scheme	Method of production and genetic relationships
					Particles	Gamma-transitions		
⁷⁴ Br	D chem (13H51)		β^+ , EC (13H51)	~35 m (13H51)				Cu-C-3n (13H51)
⁷⁵ Br	B chem, cross bomb, sep isotopes (35W48)		β^+ , EC (35W48)	1.6 h (13H51); 1.7 h (35W48)	1.70 (46%), 0.8 (20%), 0.6 (15%), 0.3 (19%) spect (25F52); -1.8 abs (13H51)	-0.6 abs (25F52)		Cu-C-2n (13H51); Se ⁷⁴ -d-n (35W48); Se ⁷⁴ -p-y (35W48, 25F52)
⁷⁶ Br	A chem (48H48); chem, excit (13H51); chem, sep isotopes (25F52)		β^+ (48H48)	17.2 h (25F52); 16.5 h (13H51); 15.7 h (48H48)	3.57 (46%), 1.7 (10%), 1.1 (11%), 0.8 (14%), 0.6 (19%) spect (25F52); 3.5 spect (13H51)	1.2, 0.96, 0.75, 0.68, 0.42, 0.37, 0.33, 0.25 spect, spect conv (25F52); -2 abs (48H48)	$Q_{\beta}^+ 4.6$ (25F52)	As-a-3n (48H48, 13H51); Se ⁷⁶ -p-n (25F52)
⁷⁷ Br	A chem, sep isotopes (35W48)		EC 95%, β^+ 5% (35W48)	57 h (48H48, 13H51); 58 h (35W48)	0.336 spect (43C51); 0.36 spect (48H48); abs, spect (35W48)	γ_1 0.160, γ_2 0.237, γ_3 0.284, γ_4 0.298, γ_5 0.520, γ_6 0.641, γ_7 0.813 ($\gamma_1/\gamma_2/\gamma_3/\gamma_4/\gamma_5/\gamma_6/\gamma_7$ = 0.6/20/0.2/0.2/100/8.6/25) spect, spect conv (43C51); 0.160, 0.234, 0.299, 0.521 spect conv, x-y coins (25F52)		As-a-2n (48H48, 13H51, 43C51); Se ⁷⁴ -a-p (35W48); Se ⁷⁶ -d-n (35W48, 25F52); parent Se ^{77m} (43C51, 43C51b)
⁷⁸ Br	A chem, excit (26S37a)		β^+ (26S37a)	6.4 m (26S37a); 6.5 m (13H51)	2.4 abs (35B46a, calc from 26S37a); 2.3 abs (26S37a)	0.108, 0.046 spect conv (6V39)		As-a-n (26S37a, 13H51); Se-d-n (26S37a); Se-p-n (59B38, 6V39); Br-y-n (7C37, 37B39); Br-n-2n (6H37)
⁷⁹ Br		50.52 (9W46)					$Br^{79}, I = 3/2$ (87M50)	
^{80m} Br	A chem, n-capt (12A35); chem, excit, cross bomb (26S37a)		IT (24S39)	4.58 h (41M51); 4.5 h (26S37a); 4.4 h (59B38)		0.049, 0.037 (e/ γ -1.3) ion ch (32R50); 0.048, 0.036 spect conv (33L50); 0.049, 0.037 spect conv (6V39); 0.049 (L _I /L _{III} 1.0) spect conv (63M52a); 0.048 (e/ γ very large), 0.037 (e/ γ -1) abs (35G40); others (52W51)		Se-d-2n (35W48, 25F52); Se-a-p (35W48); Se-p-n (59B38, 6V39, 25F52); Br-n-y (24A36, 26S37a, 24S39, 34G46, 2547); Br-d-p (26S37a); Br-y-n (37B39); Br-n-2n (1P37); spall-fission Ta (22N52), Bi (66B51), U (6F51); fission Th (?) (9P40, 9P41)
⁸⁰ Br	A chem, n-capt (12A35); chem, excit, cross bomb (26S37a); chem, genet (24S39)		β^- -92%, β^+ -3%, EC -5% (calc from 41M51, 28R50); β^+/β^- 0.037 (41M51); $\beta^+ + EC$ 0.09 β^- (28R50); β^+/β^- 0.028 (34L51); β^+/β^- 0.03 (63B47)	18 m (26S37a, 24S39)	β^- : 1.99 (85%), 1.1 (15%) spect (34L52); 1.97 (80%), 1.1 (11%), 0.7 (9%) spect (25F52); 1.99 spect (33L50); others (34L51, 50C48, 24A36) β^+ : 0.87 spect (34L51); 1.0 spect (16D49); 0.73 abs (63B47)	$Q_{\beta}^- 2.0$ (25F52) 	Se-p-n (59B38); Br-n-y (26S37a, 34G46, 2547, 9O49); Br-d-p (26S37a); Br-y-n (37B39); Br-n-2n (1P37); daughter Br-80m (24S39, 21D40, 64S41)	

Br ⁸¹																																																																																																																																																																																																																																																																																																																																																																																																																																																																																																																																																																																																																																																																																																																																																																																																																																																																																																																																																																																																																																																																																																																																																																																																																																																																																																																																																																																																																																																																																																																																																																																																																						</
------------------	--	--	--	--	--	--	--	--	--	--	--	--	--	--	--	--	--	--	--	--	--	--	--	--	--	--	--	--	--	--	--	--	--	--	--	--	--	--	--	--	--	--	--	--	--	--	--	--	--	--	--	--	--	--	--	--	--	--	--	--	--	--	--	--	--	--	--	--	--	--	--	--	--	--	--	--	--	--	--	--	--	--	--	--	--	--	--	--	--	--	--	--	--	--	--	--	--	--	--	--	--	--	--	--	--	--	--	--	--	--	--	--	--	--	--	--	--	--	--	--	--	--	--	--	--	--	--	--	--	--	--	--	--	--	--	--	--	--	--	--	--	--	--	--	--	--	--	--	--	--	--	--	--	--	--	--	--	--	--	--	--	--	--	--	--	--	--	--	--	--	--	--	--	--	--	--	--	--	--	--	--	--	--	--	--	--	--	--	--	--	--	--	--	--	--	--	--	--	--	--	--	--	--	--	--	--	--	--	--	--	--	--	--	--	--	--	--	--	--	--	--	--	--	--	--	--	--	--	--	--	--	--	--	--	--	--	--	--	--	--	--	--	--	--	--	--	--	--	--	--	--	--	--	--	--	--	--	--	--	--	--	--	--	--	--	--	--	--	--	--	--	--	--	--	--	--	--	--	--	--	--	--	--	--	--	--	--	--	--	--	--	--	--	--	--	--	--	--	--	--	--	--	--	--	--	--	--	--	--	--	--	--	--	--	--	--	--	--	--	--	--	--	--	--	--	--	--	--	--	--	--	--	--	--	--	--	--	--	--	--	--	--	--	--	--	--	--	--	--	--	--	--	--	--	--	--	--	--	--	--	--	--	--	--	--	--	--	--	--	--	--	--	--	--	--	--	--	--	--	--	--	--	--	--	--	--	--	--	--	--	--	--	--	--	--	--	--	--	--	--	--	--	--	--	--	--	--	--	--	--	--	--	--	--	--	--	--	--	--	--	--	--	--	--	--	--	--	--	--	--	--	--	--	--	--	--	--	--	--	--	--	--	--	--	--	--	--	--	--	--	--	--	--	--	--	--	--	--	--	--	--	--	--	--	--	--	--	--	--	--	--	--	--	--	--	--	--	--	--	--	--	--	--	--	--	--	--	--	--	--	--	--	--	--	--	--	--	--	--	--	--	--	--	--	--	--	--	--	--	--	--	--	--	--	--	--	--	--	--	--	--	--	--	--	--	--	--	--	--	--	--	--	--	--	--	--	--	--	--	--	--	--	--	--	--	--	--	--	--	--	--	--	--	--	--	--	--	--	--	--	--	--	--	--	--	--	--	--	--	--	--	--	--	--	--	--	--	--	--	--	--	--	--	--	--	--	--	--	--	--	--	--	--	--	--	--	--	--	--	--	--	--	--	--	--	--	--	--	--	--	--	--	--	--	--	--	--	--	--	--	--	--	--	--	--	--	--	--	--	--	--	--	--	--	--	--	--	--	--	--	--	--	--	--	--	--	--	--	--	--	--	--	--	--	--	--	--	--	--	--	--	--	--	--	--	--	--	--	--	--	--	--	--	--	--	--	--	--	--	--	--	--	--	--	--	--	--	--	--	--	--	--	--	--	--	--	--	--	--	--	--	--	--	--	--	--	--	--	--	--	--	--	--	--	--	--	--	--	--	--	--	--	--	--	--	--	--	--	--	--	--	--	--	--	--	--	--	--	--	--	--	--	--	--	--	--	--	--	--	--	--	--	--	--	--	--	--	--	--	--	--	--	--	--	--	--	--	--	--	--	--	--	--	--	--	--	--	--	--	--	--	--	--	--	--	--	--	--	--	--	--	--	--	--	--	--	--	--	--	--	--	--	--	--	--	--	--	--	--	--	--	--	--	--	--	--	--	--	--	--	--	--	--	--	--	--	--	--	--	--	--	--	--	--	--	--	--	--	--	--	--	--	--	--	--	--	--	--	--	--	--	--	--	--	--	--	--	--	--	--	--	--	--	--	--	--	--	--	--	--	--	--	--	--	--	--	--	--	--	--	--	--	--	--	--	--	--	--	--	--	--	--	--	--	--	--	--	--	--	--	--	--	--	--	--	--	--	--	--	--	--	--	--	--	--	--	--	--	--	--	--	--	--	--	--	--	--	--	--	--	--	--	--	--	--	--	--	--	--	--	--	--	--	--	--	--	--	--	--	--	--	--	--	--	--	--	--	--	--	--	--	--	--	--	--	--	--	--	--	--	--	--	--	--	--	--	--	--	--	--	--	--	--	--	--	--	--	--	--	--	--	--	--	--	--	--	--	--	--	--	--	--	--	--	--	--	--	--	--	--	--	--	--	--	--	--	--	--	--	--	--	--	--	--	--	--	--	--	--	--	--	--	--	--	--	--	--	--	--	--	--	--	--	--	--	--	--	--	--	--	--	--	--	--	--	--	--	--	--	--	--	--	--	--	--	--	--	--	--	--	--	--	--	--	--	--	--	--	--	--	--	--	--	--	--	--	--	--	--	--	--	--	--	--	--	--	--	--	--	--	--	--	--	--	--	--	--	--	--	--	--	--	--	--	--	--	--	--	--	--	--	--	--	--	--	--	--	--	--	--	--	--	--	--	--	--	--	--	--	--	--	--	--	--	--	--	--	--	--	--	--	--	--	--	--	--	--	--	--	--	--	--	--	--	--	--	--	--	--	--	--	--	--	--	--	--	--	--	--	--	--	--	--	--	--	--	--	--	--	--	--	--	--	--	--	--	--	--	--	--	--	--	--	--	--	--	--	--	--	--	--	--	--	--	--	--	--	--	--	--	--	--	--	--	--	--	--	--	--	--	--	--	--	--	--	--	--	--	--	--	--	--	--	--	--	--	--	--	--	--	--	--	--	--	--	--	--	--	--	--	--	--	--	--	--	--	--	--	--	--	--	--	--	--	--	--	--	--	--	--	--	--	--	--	--	--	--	--	--	--	--	--	--	--	--	--	--	--	--	--	--	--	--	--	--	--	--	--	--	--	--	--	--	--	--	--	--	--	--	--	--	--	--	--	--	--	--	--	--	--	--	--	--	--	--	--	--	--	--	--	--	--	--	--	--	--	--	--	--	--	--	--	--	--	--	--	--	--	--	--	--	--	--	--	--	--	--	--	--	--	--	--	--	--	--	--	--	--	--	--	--	--	--	--	--	--	--	--	--	--	--	--	--	--	--	--	--	--	--	--	--	--	--	--	--	--	--	--	--	--	--	--	--	--	--	--	--	--	--	--	--	--	--	--	--	--	--	--	--	--	--	--	--	--	--	--	--	--	--	--	--	--	--	--	--	--	--	--	--	--	--	--	--	--	--	--	--	--	--	--	--	--	--	--	--	--	--	--	--	--	--	--	--	--	--	--	--	--	--	--	--	--	--	--	--	--	--	--	--	--	--	--	--	--	--	--	--	--	--	--	--	--	--	--	--	--	--	--	--	--	--	--	--	--	--	--	--	--	--	--	--	--	--	--	--	--	--	--	--	--	--	--	--	--	--	--	--	--	--	--	--	--	--	--	--	--	--	--	--	--	--	--	--	--	--	--	--	----

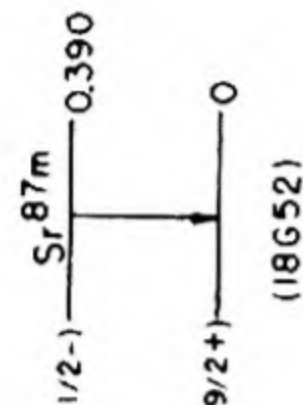
Isotope Z A	Class and identification	Percent abundance	Type of decay	Half-life	Energy of radiation in Mev		Disintegration energy and scheme	Method of production and genetic relationships
					Particles	Gamma-transitions		
⁸⁹ Br 35	D chem (63S47a)		β^- , β^-n (26S47a, 28H48a)	4.51 s (n) (28H48a); 4.45 s (n) (34R47)	n (mean): 0.43 abs paraffin (28H48a); 0.65 p recoil in cl ch (71B46)			fission U (63S47a, 26S47a, 63S49), U235 (34R47, 28H48a); parent Kr ⁸⁹ (?), parent Kr ⁸⁸ (?) (51C51)
⁷⁷ Kr 36	D chem, sep isotopes (35W48a)		EC 70%, β^+ 30% (35W48a)	1.1 h (35W48a)	1.7 abs (35W48a)	γ (35W48a)		Se-o-n, Se ⁷⁴ -o-n (35W48a)
⁷⁸ Kr		0.354 (6N50a)						
^{79m} Kr	D chem (29C40b)		IT (?), no β^+ (29C40b)	55 s (29C40b)		0.127 spect conv (29C40b)		Br-p-n (33B40a, 29C40b)
⁷⁹ Kr	A chem (29C40b); chem, sep isotopes (35W48a); mass spect (104B52)		EC 95% (L/K 0.27), β^+ 5% (12R52a, 12R52b); EC (K) -90%, β^+ -10% (67B51); EC -98%, β^+ -2% (35W48a)	34.5 h (12R52); 34 h (33B40a, 35W48a, 29C40b)	0.595 spect (67B51); 0.6 abs (58H51)	0.263 (e/ γ -0.02), 0.044 spect conv (67B51); 0.2 abs (58H51)		Se-o-n (52C41); Se ⁷⁶ -o-n (35W48a); Br-d-2n (30C44); Br-p-n (33B40a, 29C40b); Kr-d-p (26S37a, 52C41); Kr-n- γ (58H51, 67B51)
⁸⁰ Kr		2.27 (6N50a)						
^{81m} Kr	A chem (29C40b); genet (7K50)		IT, no β^+ (29C40b)	13 s (29C40b); -10 s (7K50)		0.193 spect conv (7K50); 0.187 spect conv (29C40b)		Br-p-n (33B40a, 29C40b); daughter Rb ⁸¹ (7K50)
⁸¹ Kr	A chem, mass spect (28R50a)		EC (28R50a)	2.1 x 10 ⁵ y sp act (28R50a)		0.012 abs, Br K-x (28R50a)		Kr-n- γ (28R50a)
⁸² Kr		11.56 (6N50a)						
^{83m} Kr	A chem, genet (20L40); mass spect (67B50)		IT (20L40)	114 m (67B51a, 21R46); 113 m (20L40)		0.0322 (e/ γ very large, K/L+M 0.35), 0.0093 (e/ γ very large, L/M -3) spect conv (67B51a); 0.032 (K/L 0.32), 0.009 (e/ γ -10) ion ch (91B52); 0.046, 0.029 spect conv (2H41)		Se-o-n (52C41); Kr-d-p (52C41); Kr-n- γ , Kr-x rays (37W45); fission U, daughter Br ⁸³ (20L40); daughter Rb ⁸³ (53C50)
⁸³ Kr		11.55 (6N50a)						fission U (mass spect) (13T47, 13T48a)
⁸⁴ Kr		56.90 (6N50a)						fission U (mass spect) (13T47, 13T48a)

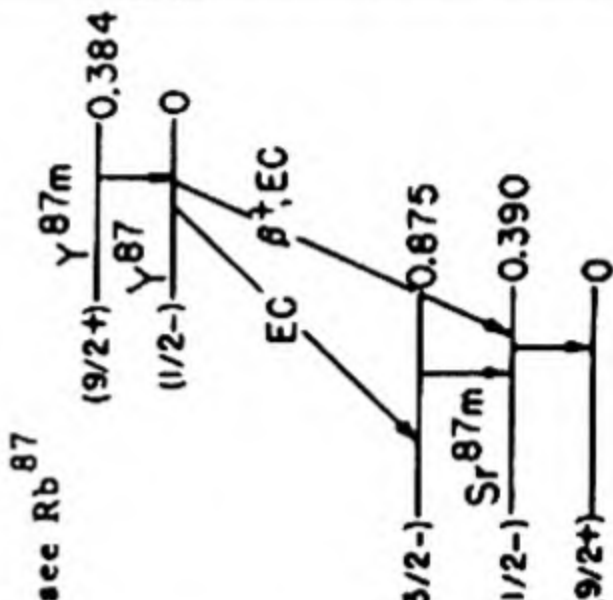
Kr^{85m}	A chem (26S37a); chem, mass spect (34K49)	β^- 77%, IT 23% (67B51d)	4.36 h (34K49); 4.4 h (35W48a); 4.5 h (58H51, 26S37a); 4.6 h (21R46, 66S43)	0.855 spect (67N51d); 0.85 abs (70B43a); 0.95 abs (58H51); 0.75 abs (34K49)	0.150 (e/y 0.057, coinc with β^-), 0.305 spect conv, β - γ coinc (67B50a, 67B51d); 0.17, 0.37 ab= (58H51)	Kr^{85m} see Sr^{85} (1/2-) Kr^{85} 0.31 (9/2+) Kr^{85} 0.54 β^- 0.695 (HPS) (3/2-) (5/2-) (8Z50, 67B50a, 18G52)	Se-a-n (35W48a); Kr-d-p (26S37a, 52C41); Kr-n-y (21R45, 58H51); Rb-n-p, Sr-n-a (70B43); fission U, daughter Br ⁸⁵ (66S43, 63S49); Kr-n-y (58H51); fission U (13T47, 58H51a)
Kr^{85}	A chem (58H51a); chem, mass spect (13T47)	β^- (58H51a)	9.4 y (13T48a); -10 y (58H51a)	0.695 (99+%), 0.15 (0.65%) spect, β - γ coinc abs (8Z50); 0.74 abs (58H51a)	0.54 (coinc with 0.15 β^-) scint spect, abs, β - γ coinc (8Z50)		
Kr^{86}		17.37 (6N50a)				Kr^{86} , I = 0 (87M50)	
Kr^{87}	A chem (26S37a); chem, mass spect (34K49)	β^- (26S37a)	78 m (34K49); 75 m (66S43, 63S49); 74 m (26S37a)	3.63 (75%), 1.27 (25%) spect (30T52a); others (34K49, 70B43a)	0.41, 1.89, -2.3 scint spect (30T52a)	Q_{β}^- 3.6 (30T52a) Kr^{87} β^- (3/2-) (30T52a)	Kr-n-y (21R46, 58H51); Kr-d-p (26S37a); Rb-n-p (70B43); fission U (70B43, 66S43); daughter Br ⁸⁷ (66S43, 70B43, 63S49)
Kr^{88}	A chem (6H39); chem, genet (20L39); chem, mass spect (34K49)	β^- (20L39)	2.77 h (34K49); 2.8 h (36G40, 63S49)	2.8 (20%), 0.9 (12%), 0.52 (68%) spect (30T52b); 2.4 (weak), -0.5 ab= (4J48, 34K49)	0.028 (coinc with 0.5 β^- , e/y -0.1, K/L+M 8) spect conv, β - γ coinc (30T52b)		fission Th (20L39, 25A39), U (6H39, 16H40a, 36G40, 16H40b); parent Rb ⁸⁸ (20L39, 25A39, 6H39, 16H40a, 36G40, 16H40b); daughter Br ⁸⁸ (63S49)
Kr^{89}	A chem, genet (36G40, 66S40); mass spect (35K51a)	β^- (36G40)	3.18 m (35K51a); 2.6 m (24D51); 2.5 m (16H43a)	4.0 abs (35K51a); 3.9 calc from average recoil energy (35K51)			fission U, parent Rb ⁸⁹ (36G40, 66S40, 16H40b, 16H43, 17B51, 35K51a); spall-fission U (11O51); fission Pu (26A51)
Kr^{90}	A chem, genet (24D51a); mass spect (35K51a)	β^- (24D51a)	33 s (35K51a, 32K46)	3.2 abs (35K51a)			fission U, ancestor Sr ⁹⁰ (24D51a, 24D51); fission Pu (26A51); parent Rb ⁹⁰ (35K51a)
Kr^{91}	A chem, genet (16H40c); mass spect (35K51a)	β^- (16H40c)	9.8 s (24D51); 10 s (35K51a); -6 s (11O51)	-3.6 abs (35K51a)			fission U, ancestor Y ⁹¹ (16H40c, 17B51, 24D51a, 24D51); spall-fission U (11O51); fission Pu (26A51); parent Rb ⁹¹ , parent Rb ^{91m} (35K51a)
Kr^{92}	B chem, genet (16H40a, 24D51)	β^- (16H40a)	3.0 s (24D51)				fission Th (16H40), U (16H40a, 16H40b, 16H43), Pu (26A51); ancestor Y ⁹² (24D51)
Kr^{93}	B chem, genet (16H42, 70S51)	β^- (16H42)	2.0 s (24D51)				fission U, ancestor Y ⁹³ (70S51); spall-fission U (11O51); fission Pu (26A51)

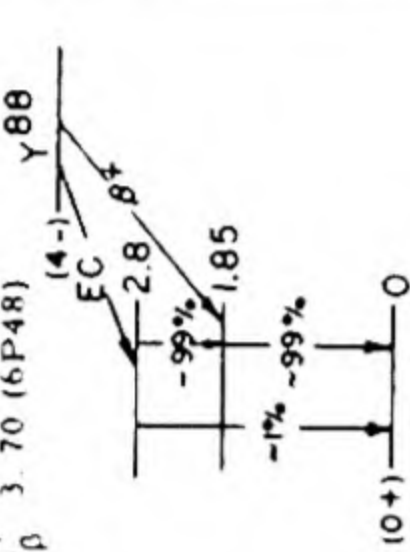
Isotope Z A	Class and identification	Percent abundance	Type of decay	Half-life	Energy of radiation in Mev		Disintegration energy and scheme	Method of production and genetic relationships
					Particles	Gamma-transitions		
⁹⁴ ₃₆ Kr	B chem, genet (16H43a, 24D51)		β^- (16H43a)	1.4 s (24D51)				fission U, ancestor Y^{94} (16H43a, 24D51)
⁹⁵ Kr	A chem, genet (24D51a)		β^- (24D51a)	short (24D51a)				fission U, ancestor Zr^{95} (24D51a)
⁹⁷ Kr	B chem, genet (26A51)		β^- (26A51)	-1 s (24D51)				fission U, ancestor Zr^{97} (26A51, 24D51); fission Pu (26A51)
⁸¹ ₃₇ Rb	A chem, mass spect (10R49)		EC 87%, β^+ 13% (7K50)	4.7 h (7K50)	0.990 spect (7K50)	0.95 abs (7K50)		Br- α -2n (10R49, 7K50); parent Kr ⁸¹ (7K50)
^{82m} Rb	B chem, genet (54L52)		β^+ (54L52)	1.25 m (54L52)	-3 abs (54L52); see Sr ⁸²			daughter Sr ⁸² (54L52)
⁸² Rb	A chem (59H40); chem, mass spect (10R49)		EC 94%, β^+ 6% (7K50)	6.3 h (7K50)	0.775 (76%), 0.175 (24%) spect (10H52); 0.670 spect (7K50)	0.188, 0.248, 0.322, 0.390, 0.423, 0.465, 0.558, 0.610, 0.690, 0.768, 0.818, 1.020, 1.314, 1.464 spect conv, spect (10H52)		Br- α -n (59H40, 10R49, 7K50); Kr-d-2n (59H40); not daughter Sr ⁸² (lim 0.01%) (54L52)
⁸³ ₃₇ Rb	A chem, mass spect (7K50)		EC (7K50)	83 d (53C50); 107 d (7K50)		-0.45, -0.15 spect conv (53C50)		Br- α -2n (7K50); daughter Sr ⁸³ (53C50); parent Kr ^{83m} (53C50)
^{84m} Rb	B chem (59H40); chem, excit (9F50a)		IT, EC (weak) (79C52); EC (9F50a)	23 m (9F50a); 20 m (59H40)		Y_1 0.463 (not coinc with Y_2 or Y_3), Y_2 0.239, Y_3 -0.239 (coinc with Y_2), Y_4 0.890 ($Y_1/Y_4 = 7$) scint spect, Y - Y coinc (79C52)		Br- α -n (59H40); Rb-n-2n (9F50a, 79C52)
⁸⁴ Rb	A chem, cross bomb (63B47); chem, mass spect (7K50)		EC, β^+ , β^- (?) (7K50, 73B50); EC/ β^+ -13 (7K50); β^+/β^- -6.2 (73B50)	34 d (7K50); 38 d (73B50)	β^+ : 1.629 (39%), 0.822 (58%), 0.373 (?) (3%) spect (10H52); 1.5 spect (7K50); 1.3 abs (73B50)	0.890 scint spect, spect conv (10H52); 0.85 abs (7K50); 0.8 abs (73B50)		Br- α -n (7K50, 73B50); Kr- α -pn, Kr-d-2n (73B50); Rb-n-2n (63B47); Sr-d- α (63B47)
^{85m} Rb	A genet (14S52)		IT (14S52)	0.9×10^{-6} s delay coinc (14S52)		0.513 spect, spect conv (11T51, 14S52)		daughter Sr ⁸⁵ (14S52)
⁸⁵ Rb		72.15 (6N50a)						fission U (mass spect) (38W52)
^{86m} Rb	B chem, excit, n-capt (9F51)		IT, no EC (12P52); EC (9F51)	0.99 m (12P52); 1.06 m (9F51)		0.57 scint spect (12P52); 0.78 abs (9F51)		Rb-n- γ , Rb-n-2n (9F51)

Rb⁸⁶	A chem, n-capt (26S37a); chem, excit (2H41a)	27.85 (6N50a)	β^- (2H41a); no β^+ (lim 0.002%); (41M51); no EC (lim 0.04%); (12P52)	19.5 d (2H41a)	β_1 1.82 (80%), β_2 0.72 (20%) spect (5Z48); β_1 1.79 spect (96M52); β_1 1.76, β_2 0.670 (coinc with γ) β - γ coinc spect (23M51); β_1 1.82 (-67%), β_2 0.56 (-33%) abs (15J48); β_2 0.72 (coinc with γ) β - γ coinc spect (55M50); β_2 0.67 scint spect (27P51); β_2 (12%) β - γ coinc (26M50)	1.076 spect (55M50); 1.081 spect (5Z48); 1.12 (coinc with β_2) coinc abs sec, β - γ coinc (15J48); others (85S51)	 <p>Rb⁸⁶ (2-) ~20% ~80% 1.08 (0+) (5Z48, HPS)</p>	Rb^{86} , $I = 2$ (98B51) Q_β^- 1.8 (5Z48) Rb-n- γ (26S37a, 69S38, 2S47); Rb- γ -n (34H44); Sr-d- α (2H41a); spall-fission Bi (11G49, 66B51), U (6F51); fission U (2F51a)
Rb⁸⁷	A chem (1T05, 54C06); chem, genet (16H37a, 8M37); chem, mass spect (40H37)	48.8 (6N50a)	β^- (1T05, 54C06)	48.8 d (2H41a)	0.275 spect (21C51); scint spect (50L52); 0.270 scint spect (11B50e); others (36K35, 34T52, 3L39, 14O41, 12S46)	no γ (21C51, 79M52, 50L52)	 <p>Rb⁸⁷ (3/2-) ~20% (9/2+) (21C51, 79M52)</p>	Rb^{87} , $I = 3/2$ (87M50) Q_β^- 0.27 (21C51) parent Sr ⁸⁷ (mass spect) (16H37a, 8M37) natural source (1T05, 54C06); fission U (mass spect) (38W52); parent Sr ⁸⁷ (mass spect) (16H37a, 8M37)
Rb⁸⁸	A chem (26S37a); chem, genet (20L39, 36G40, 16H39a)	48.8 (6N50a)	β^- (16H39a)	17.8 m (36G40, 2B51); 17.7 m (30T52b); 17.5 m (34W42); 18 m (16H40b, 26S37a)	5.30 (78%), 3.6 (13%), 2.5 (9%) spect (30T52b); 5.13 (66%), 3.29 (19%), 2.0 (15%) spect (2B51); 5.20 (-66%), 3.6 (-17%), 1.8 (-17%) abs (37G51)	2.8, 1.86, 0.90 spect (2B51); γ_1 3.0, γ_2 1.7 ($\gamma_1/\gamma_2 \sim 1/10$) abs sec, β - γ coinc (37G51)	 <p>Rb⁸⁸ (2-) 78% 13% 9% 2.8 1.85 (0+) (2B51, 30T52b, HPS)</p>	Rb^{88} , $I = 2$ (98B51) Q_β^- 5.30 (30T52b) Rb-n- γ (26S37a, 1P37, 69S38, 2S47); fission Th (25A39), Pa (2G39); fission U, daughter Kr ⁸⁸ (6H39, 20L39, 36G40, 16H40a, 16H40b)
Rb⁸⁹	A chem, genet (36G40, 66S40)	48.8 (6N50a)	β^- (36G40)	15.4 m (36G40, 16H40b); 15.5 m (16H40b)	4.5 abs (35T46a, calc from 36G40); 3.8 abs (36G40)	γ (35B46a)	 <p>Rb⁸⁹ (2-) 100% (0+) (35B46a)</p>	fission U, daughter Kr ⁸⁹ (36G40, 66S40, 16H40b, 16H43, 17B51); parent Sr ⁸⁹ (36G40, 16H40a, 16H40b, 16H43) fission U, daughter Kr ⁹⁰ parent Sr ⁹⁰ (24D51a, 24D51, 35K51a)
Rb⁹⁰	A chem, genet (35K51a)	48.8 (6N50a)	β^- (35K51a)	2.74 m (35K51a)	5.7 abs (35K51a)	γ (35K51a)	 <p>Rb⁹⁰ (2-) 100% (0+) (35K51a)</p>	fission U, daughter Kr ⁹⁰ parent Sr ⁹⁰ (24D51a, 24D51, 35K51a)

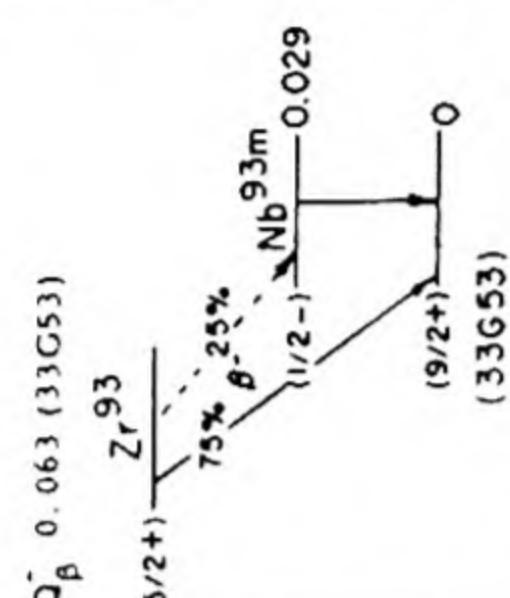
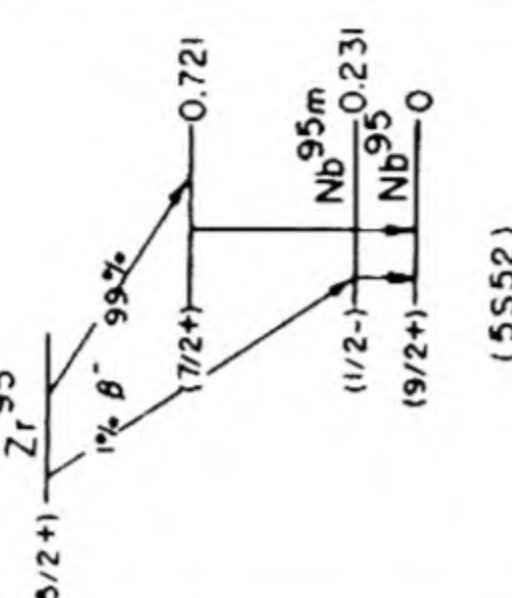
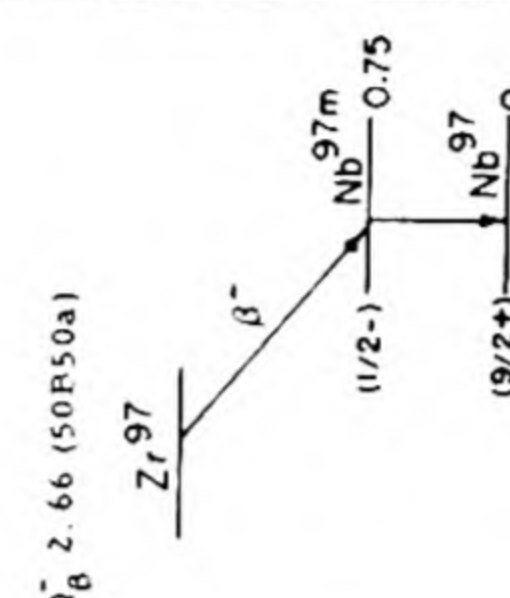
Isotope Z A	Class and identification	Percent abundance	Type of decay	Half-life	Energy of radiation in Mev		Disintegration energy and scheme	Method of production and genetic relationships
					Particles	Gamma-transitions		
⁹¹ Rb 37	A chem, genet (35K51a)		β^- (35K51a)	1.67 m (35K51a); [short] (24D51a, 17B51, 11O51, 24D51, 16H40c)	4.6 abs (35K51a)	γ (35K51a)		fission U, daughter Kr ⁹¹ , parent Sr ⁹¹ (35K51a); ancestor Y ⁹¹ (24D51a, 16H40c)
⁹¹ Rb	A chem, genet (35K51a)		β^- (35K51a)	14 m (35K51a)	3.0 abs (35K51a)	γ (35K51a)		fission U, daughter Kr ⁹¹ , parent Sr ⁹¹ (35K51a)
⁹² Rb	D chem, genet (16H40a)		β^- (16H40a)	80 s (16H40a); [short] (17B51, 24D51)				fission U, daughter Kr ⁹² , parent Sr ⁹² (16H40a, 16H40c, 16H40, 16H43, 24D51)
⁹³ Rb	[B] genet (16H42, 17B51)		$[\beta^-]$ (16H42)	[short] (17B51, 24D51, 24D51a, 16H42, 16H43)				fission U, daughter Kr ⁹³ (17B51, 24D51, 24D51a); ancestor Y ⁹³ (16H42, 16H43, 17B51)
⁹⁴ Rb	[B] genet (16H43, 16H43a)		$[\beta^-]$ (16H43, 16H43a)	[short] (24D51, 16H43, 16H43a)				fission U, daughter Kr ⁹⁴ , ancestor Y ⁹⁴ (16H43, 16H43a, 24D51)
⁹⁵ Rb	[A] genet (24D51a)		$[\beta^-]$ (24D51a)	[short] (24D51a)				fission U, daughter Kr ⁹⁵ , ancestor Zr ⁹⁵ (24D51a)
⁹⁷ Rb	[A] genet (24D51)		$[\beta^-]$ (24D51)	[short] (24D51)				fission U, daughter Kr ⁹⁷ , ancestor Zr ⁹⁷ (24D51); fission U ²³⁵ , Pu (26A51)
⁸¹ Sr 38	B chem, genet (53C50)		EC, β^+ (53C50)	29 m (53C50)	conv (53C50)			spall Rb, parent Rb ⁸¹ (53C50)
⁸² Sr	A chem, excit (53C50); mass spect (97M52)		EC, β^+ (?) (53C50)	27 d (97M52); 25 d (53C50)	β^+ with Rb ^{82m} (54L52); 3.15 spect (53C50)	0.95, -0.40, -0.15 spect conv, abs (53C50)		spall Rb (53C50); daughter Y ⁸² (78C52); parent Rb ^{82m} , not parent Rb ⁸² (lim 0.01%) (54L52)
⁸³ Sr	A chem, genet (53C50); mass spect (97M52)		EC, β^+ (53C50)	33 h (97M52); 38 h (53C50)	1.15 spect (53C50); 1.35 abs (97M52)	0.040, 0.074, 0.101, 0.151, 0.165 spect conv (53C50)		spall Rb, parent Rb ⁸³ (53C50); daughter Y ⁸³ (78C52)
⁸⁴ Sr		0.56 (6N38b)						
^{85m} Sr	A chem, excit (2D40a)		IT 86%, EC 14% (14S52)	70 m (2D40a)				

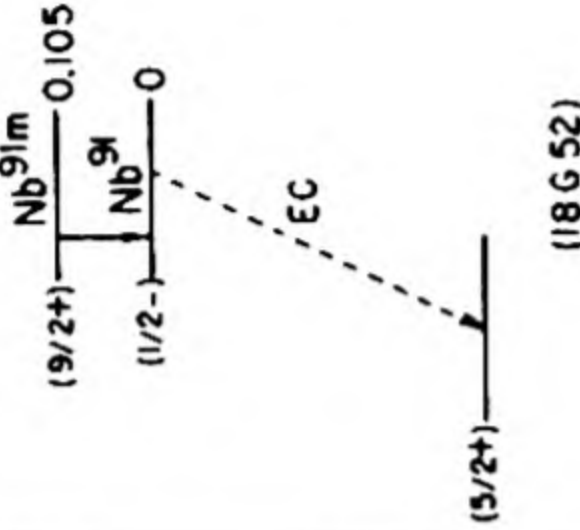
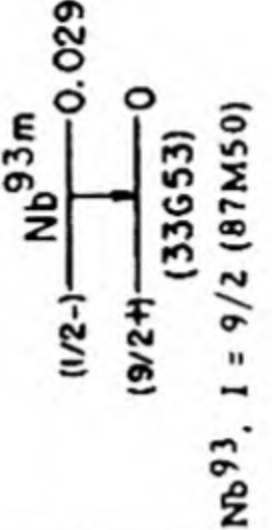
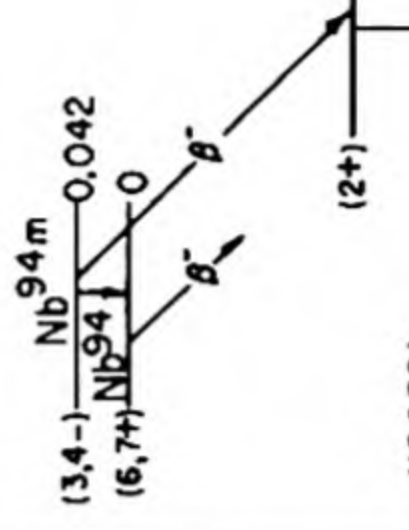
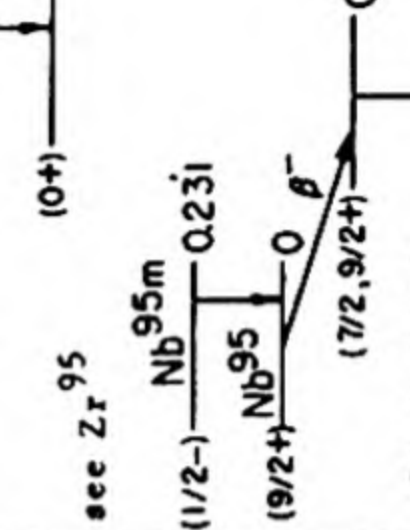
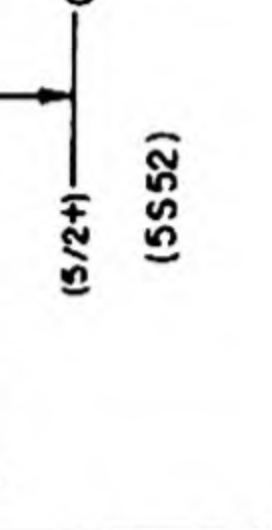
Sr ⁸⁶	9 86 (6N38b)	IT (2D40a)	2.80 h (58M5), 8H51b); 2.75 h (2D40a)	0.388 (K/L+M 5 79) spect conv (59G52); 0.390 (e/y 0 28, K/L+M 6 9) spect conv, x-conv coinc (58M51); 0.388 (K/L+M 5 5) spect conv (70E52); 0.388 spect conv (11T51); 0.394 (K/L 7 2) spect conv (8H51b); 0.386 spect conv (2H41)	Sr ⁸⁶ , I = 0 (87M50)		Rb-p-n (2D39); Sr-n-n (2D40a, 35R40, 35R40a); Sr-x rays, Sr-e-e (37W45a); Sr-d-p (71S37); Sr-n-y (71S37, 2D39, 35R40, 2547, 2547a); Sr-p-p (?) (2D40a); daughter Y87 (2D39, 2D40a, 58M50, 18H51b, 58M51); Zr-n-a (42S40)
Sr ⁸⁷	7.02 (6N38b)				Sr ⁸⁷ , I = 9/2 (87M50)		
Sr ⁸⁸	82.56 (6N38b)				Sr ⁸⁸ , I = 0 (87M50)		
Sr ⁸⁹		β^- (71S37)	53 d (1N51); 54 d (36L39); 55 d (71S39, 11G49)	no γ (1N51, 71S39, 71S37), others (52M51)	see Zr ⁸⁹ Q_β^- 1.46 (10L49)	Sr-d-p (71S37, 71S39); Sr-n-y (71S37, 71S39, 2547); Y-n-p (42S38); Zr-n-a (?) (42S40); spall-fission Pt (2T47b); Pb (13P47a), Bi (2T47b, 11G49, 66B51), Th (7N49a), U (6O48, 11O51, 6F51); fission Th (72B51, 21T51), U233 (38G48, 61S48), U235 (38G46), Pu (28F51); fission U, daughter Rb89 (36G40, 16H40a, 16H40b, 16H43, 38G46)	
Sr ⁹⁰		β^- (18N51)	19.9 y (28P50)	0.61 spect (47M48a); 0.54 spect (23L50); 0.53 spect (74B49); 0.6 abs (38G46, 33G51c)	no γ (33G51c, 39G43)	Q_β^- 0.6 (HPS) Sr ⁹⁰ (0+)	spall-fission Bi (11G49), Th (7N49a); fission Th (21T51), U233 (38G48), U235 (38G46); fission U, daughter Rb90 (24D51a, 24D51, 35K51a, 38W52); parent Y90 (16H42, 16H43, 38G46, 18N51)
Sr ⁹¹		β^- (40G41)	9.7 h (28F51a); 10 h (16H43)	2.665 (26%), 2.03 (4%), 1.36 (29%), 1.09 (33%), 0.62 (7%) spect (40A52); 3.2 (-60%), 1.3 (-40%) abs (28F51a)	0.551 (with Y91m, K/L+M 6 0), 0.64, 0.66, 0.747, 1.025, 1.413 (coinc with 0.630 γ) spect, parent spect, γ - γ coinc (40A52)	Q_β^- 2.66 (40A52) Sr ⁹¹ (5/2+)	Zr-n-a (66S43a); spall-fission Pt (2T47b), Hg (n-) (53S52), Pb (13P47a), Bi (13P47a, 13P47, 66B51), Th (7N49a), U (6F51), U (C) (13H51); fission Th (72B51, 21T51), Pu (32K48, 28F51); fission U, parent Y91m, parent Y91 (40G41, 16H43, 28F51a); daughter 1.7 m Rb91, 14 m Rb91 (35K51a)

Isotope Z A	Class and identification	Percent abundance	Type of decay	Half-life	Energy of radiation in Mev		Disintegration energy and scheme	Method of production and genetic relationships
					Particles	Gamma-transitions		
⁹² ₃₈ Sr	B chem, genet (40G41)		β^- (40G41)	2.7 h (40G41)				spall-fission Th (7N49a); fission Th (72B51), U (16H40a, 16H43, 16H43a, 32K51a, 17B51), Pu (32K48); parent Y ⁹² (40G41, 58H51b)
⁹³ _{Sr}	B chem (36L39); chem, genet (16H43)		β^- (36L39)	7 m (36L39)				fission U (36L39, 16H42, 16H43); parent Y ⁹³ (16H43, 16H43a)
⁹⁴ _{Sr}	B chem, genet (16H43, 16H43a)		β^- (16H43, 16H43a)	-2 m (16H43, 16H43a)				fission U (16H43, 16H43a, 24D51); parent Y ⁹⁴ (16H43, 16H43a)
⁹⁵ _{Sr}	[A] genet (24D51a)		β^- (24D51a)	short (24D51a)				fission U, ancestor Zr ⁹⁵ , descendant Kr ⁹⁵ (24D51a)
⁹⁷ _{Sr}	[A] genet (24D51)		β^- (24D51)	short (24D51)				fission U, ancestor Zr ⁹⁷ , descendant Kr ⁹⁷ (24D51, 26A51)
⁸² ₃₉ Y	B chem, genet (78C52)			70 m (78C52)				spall Y, parent Sr ⁸² (78C52)
⁸³ _Y	B chem, genet (78C52)			3.5 h (78C52)				spall Y, parent Sr ⁸³ (78C52)
⁸⁴ _Y	B chem, excit, sep isotopes (36R49)		β^+ , EC (36R49)	3.7 h (36R49)	2.0 abs (36R49)	γ (36R49)		Sr ⁸⁴ -d-2n, Sr ⁸⁴ -p-n (36R49)
⁸⁵ _Y	B chem, genet (78C52)			5 h (78C52)				spall Y, parent Sr ⁸⁵ (78C52)
⁸⁶ ₃₉ Y	B chem, excit, sep isotopes (53C51)		β^+ (53C51)	14.6 h (53C51, 8H51b)	1.80 (-50%), 1.19 (-50%) spect (8H51b)	1.4 abs (8H51b); -1.3 abs (53C51)		Sr-p-3n, Sr ⁸⁸ -p-3n (53C51); spall Nb, daughter Zr ⁸⁶ (8H51b)
^{87m} _Y	A chem (71S39); chem, excit, cross bomb (2D40a)		IT (2D40a); no β^+ (8H51b)	14 h (2D40a, 8H51b, 58M51)			see Rb ⁸⁷ 	Sr-d-n (71S39, 2D40a, 58M50, 58M51); Sr-p-n (2D40a, 58M51); spall Nb, daughter Zr ⁸⁷ (8H51b); parent Y ⁸⁷ (58M50, 8H51b, 58M51)
⁸⁷ _Y	A chem (71S39); chem, excit, cross bomb (2D40a)		EC 99+%, β^+ -0.3% (58M51); EC, β^+ (weak) (36R50)	80.0 h (58M51); 80 h (2D40a, 8H51b)	0.7 spect (58M51, 36R50)	0.381 (K/L+M 5.41) spect conv (59G52); 0.384 (e/ γ 0.28) spect conv, ion ch, conv-x coinc (58M51); 0.389 spect conv (8H51b); no γ >1 (58M51); conv >1 (8H51b) 0.485 (e/ γ 0.0035) spect conv, scint spect, γ -x coinc (58M51); 0.390 (with Sr ^{87m})	Sr-p-n (2D40a, 58M51); Sr-d-n (71S39, 2D40a, 58M51, 58M50) Sr ⁸⁴ -a-p (36R50); spall Nb (8H51b); Sb (37L50); daughter Y ^{87m} (58M50, 8H51b, 58M51); parent Sr ^{87m} (2D40a, 37L50, 58M50, 8H51b, 58M51) Q β^+ 2.1 (58M51)	

Y^{88}	A chem (2D40a); chem, excit (2H42); mass spect (60H48)	EC (2D40a); EC 99+%, β^+ 0.19% (6P48)	104 d (10O46); 105 d (2D40a)	0.83 spect (6P48)	0.908 (e/y 0.0003), 1.853 (e/y 0.0001), 2.76 spect conv, spect (6P48); -0.9 (e/y 0.00034), -1.85 (e/y 0.00017) spect conv (44M52b); 0.908, 1.89 spect, γ - γ coinc (25D41); 1.87 Be- γ -n reaction (17S41); 2.8 (-1%) D- γ -n reaction (41G44)	see Rb ⁸⁸ Q_{β}^+ 3.70 (6P48) 	Sr-d-2n (29P40, 2H42, 41G44, 17B50); Sr-p-n (2D40a); Y-n-2n (2H42, 10O46); daughter Zr ⁸⁸ (8H51b)
Y^{88}	G not found; chem, cross bomb, sep isotopes (36R49)	β^+ (71S37)	2.0 h (71S39)			(6P48, HPS)	Sr-d (71S37, 71S39); Sr-p (2D40b, 2D40a); Y-n (71S37)
Y^{89m}	A chem, genet (18G51)	IT (18G51)	-14 s (18G51)		0.913 spect conv (71S51); 0.917 spect conv (8H51b); -0.9 (K/L+M 7 0) spect conv (79B52); 0.92 (e/y 0.01) spect conv, scint spect (74S51, 18G51)	Y^{89m} (9/2+) — 0.913 (1/2-) — 0 (18G52)	Y-n-n, daughter Zr ⁸⁹ (18G51)
Y^{89} Y^{90}	A chem, excit, cross bomb (71S37); chem, mass spect (60H48)	β^- (71S37)	61 h (37B46, 71S37); 62 h (11G49); 65 h (18N51)	2.18 spect (10L49); 2.24 spect (23L50); 2.25 spect (74B49); 2.27 spect (96M52); 2.2 spect, abs (33G51c); E (average) 0.90 ion ch (77C52)	no γ (33G51c, 74B49, 39G43); 1.4 (0.4%) abs (11S52); others (52M51)	Y^{89} , I = 1/2 (87M50) Q_{β}^- 2.18 (10L49) Y^{90} (2-) — β^- — (0+) — 0 (74B49)	Y-d-p (71S37); Y-n- γ (71S37, 42S38, 2S47); Zr-n-p, Zr-d-a (42S40); Nb-n-a (42S38a, 42S40a); spall-fission Pt, Ti (2T47b), Bi (13P47, 11G49); fission Th (21T51); fission U, daughter Sr ⁹⁰ (16H42, 16H43, 38G46, 18N51)
Y^{91m}	A chem, genet (40G41)	IT (40G41)	51.0 m (28F51a); 50 m (40G41)		0.551 (K/L+M 6.00) scint spect (59G52); 0.61 (e/y -0.1) abs, abs conv (28F51a)	see Sr ⁹¹ Y^{91m} (9/2+) — 0.551 Y^{91} (1/2-) — β^- — 0.1% ~100% Q_{β}^- 1.537 (10L49)	Zr-n-p (66S43a); fission U, daughter Sr ⁹¹ (40G41, 16H43, 28F51a)
Y^{91}	A chem, genet (16H40c, 16H43); chem, mass spect (72B51a, 60H48)	β^- (16H40c)	61 d (38G46, 10L49); 57 d (40G41, 16H40c, 19J44)	1.537 spect (10L49); 1.54 spect (15O49); 1.55 spect (16W49c, 24K49); 1.56 spect (16A50, 96M52)	1.2, 0.2 (both <0.1%) abs, coinc abs sec, γ - γ coinc (10L49)	Q_{β}^- 1.537 (10L49) (10L49, 28F51a, 40A52)	Zr-n-p (66S43a); spall Sb (37L50); spall-fission Bi (11G49), U (11O51); fission Th (72B51), U ²³³ (38G48), Pu (28F51, 13E51); fission U, daughter (-60%) Sr ⁹¹ (40G41, 16H43, 28F51a)


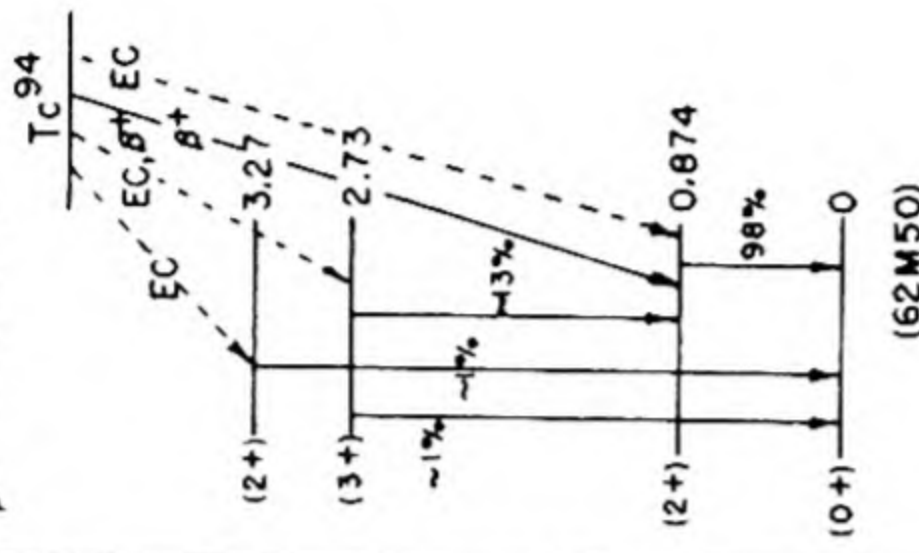
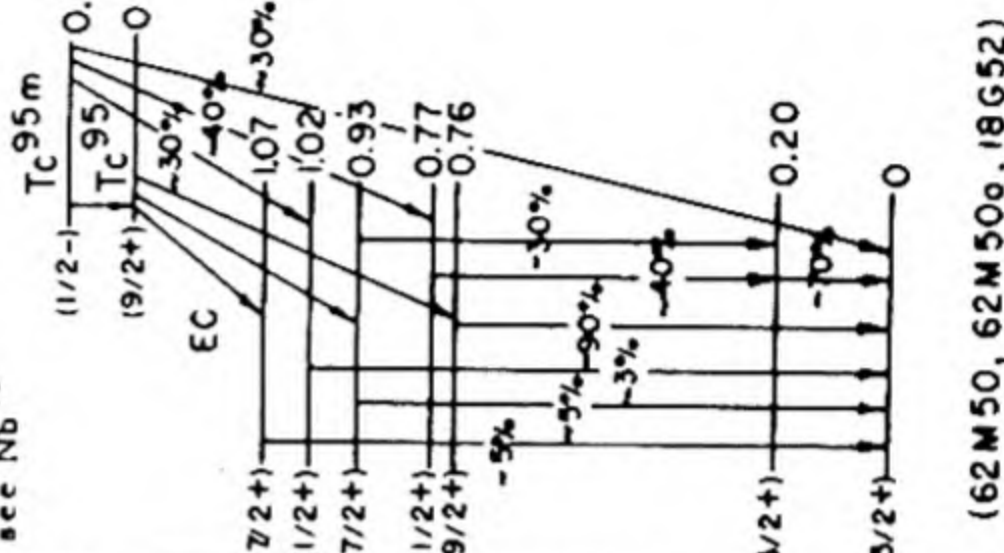
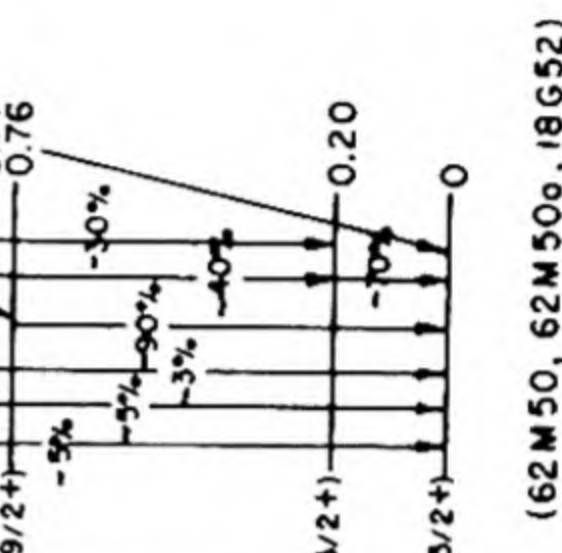
Isotope Z A	Class and identification	Percent abundance	Type of decay	Half-life	Energy of radiation in Mev		Disintegration energy and scheme	Method of production and genetic relationships
					Particles	Gamma-transitions		
⁹² Y 39 Y	B chem (36L39); fission fragment range (32K48)		β^- (36L39)	3.60 h (40A52a); 3.5 h (28A43, 16H43a, 36L39)	3.60, 2.7, 1.3 spect (40A52a); 3.5 abs (58H51b); 3.4 abs (40G41); 3.6 abs (70B43a)	0.6 abs (40G41); 0.7 - 1.1 abs (58H51b)		Zr-n-p (42S40, 66S43a, 28A43); fission Hg (π) (63S52); fission Th (72B51), Pu (32K48); fission U, daughter Sr ⁹² (40G41, 58H51b)
⁹³ Y	B chem (16H43, 72B46, 72B51b, 70S51); fission fragment range (32K48)		β^- (72B51b)	10.0 h (72B51b); 11.5 h (16H43)	3.1 abs (72B51b)	0.7 abs (72B51b)		spall-fission U (6048); fission Th (72B51), Pu (32K48); fission U, daughter Sr ⁹³ (16H43, 16H43a, 72B51b)
⁹⁴ Y	B chem (16H43, 16H43a); fission fragment range (32K48)		β^- (16H43, 16H43a)	16.5 m (75B49); 20 m (24D51b, 16H43)	5.4 abs (75B49)	1.4 abs (75B49)		Zr-n-p (66S43a); fission U (16H43, 16H43a, 24D51b), Pu (32K48); daughter Sr ⁹⁴ (16H43, 16H43a)
⁹⁵ Y	B chem, sep isotopes, excit (20K49)		β^- (20K49)	10.5 m (20K49); <1.5 h (70S51)				Zr ⁹⁶ - γ -p (20K49)
⁹⁷ Y [A] genet (24D51)			β^- (24D51)	short (24D51)				fission U, descendant Kr ⁹⁷ , parent Zr ⁹⁷ (24D51, 26A51)
⁸⁶ Zr 40 Zr	[B] chem, genet (8H51b)		EC (8H51b)	-17 h genet (8H51b)				spall Nb, parent Y ⁸⁶ (8H51b)
⁸⁷ Zr	A chem, excit, sep isotopes (36R49); chem, genet (8H51b)		β^+ , EC (36R49)	94 m (8H51b); 120 m (36R49)	2.10 spect (8H51b); 2.0 abs (36R49)	0.65, 0.35 abs (36R49)		Sr- α -n, Sr ⁸⁴ - α -n (36R49); spall Nb, parent Y ^{87m} (8H51b); Mo- γ -an (85H52)
⁸⁸ Zr	B chem, genet (8H51b)		EC (8H51b)	85 d (8H52)				spall Nb, parent Y ⁸⁸ (8H51b)
^{89m} Zr A chem, excit (2D40a)			IT, β^+ (weak) (73S51)	4.4 m (73S51); 4.5 m (2D40a)	2.5, -0.85 (both weak) (β^+ /0.59 γ = 0.004) spect, scint spect, β - γ coinc abs (73S51, 73S52)	0.586 (e/ γ 0.07, K/L4M 5.4) scint spect, spect conv (79B52, 73S51); 1.53 (-7%) scint spect (73S52)	Q_{β^+} -3.4 see Sr ⁸⁹	Y-p-n (2D40a); Zr-n-2n (?) (28A43); Zr- γ -n (73S51)
⁸⁹ Zr	A chem, excit (42S38, 2D40a)		EC -75%, β^+ -25% (18G51)	79.3 h (74S51); 77 h (8H51b); 78 h (2D40a); 80 h (11O43)	0.910 spect (8H51b); 0.905 spect (74S51); 0.890 spect (73S51)	γ (with Y ^{89m}): 0.92 (e/ γ 0.01) spect conv, scint spect (74S51, 18G51); 0.913 spect conv (73S51); 0.917 spect conv (8H51b); -0.9 (K/L+M 7.0) spect conv (79B52)	Q_{β^+} 2.84 (8H51b, 74S51) Q_{β^-} 2.84 (8H51b, 74S51) β^+ EC(2) β^+ EC 1.53 Y ^{89m} Q913 0	Y-d-2n (11O43, 18G51); Y-p-n (2D40a); Zr-n- γ -n (42S38, 42S40); Zr- γ - γ (73S51); spall, γ (8H51b); Mo-n- α (42S40); parent Y ^{89m} (18G51)
⁹⁰ Zr		51.46 (24W48)						

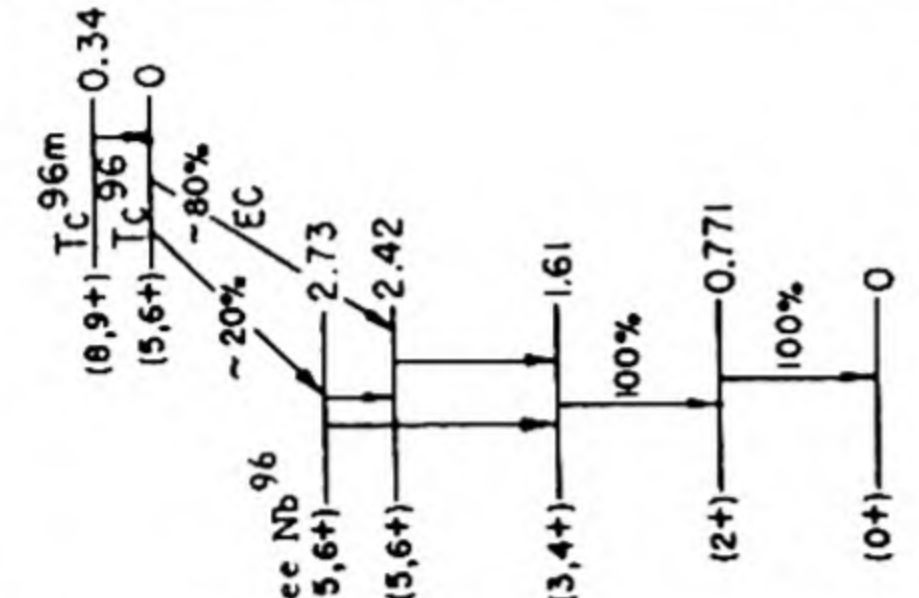

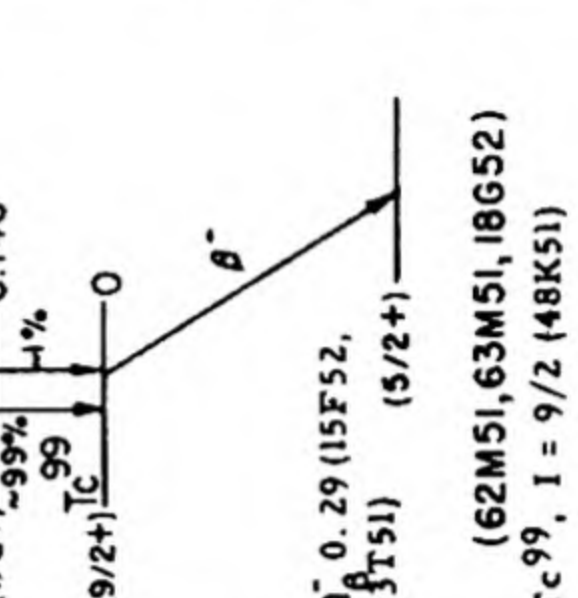

⁹¹ Zr	11.23 (24W48)	β^- (61S50)	9.5 x 10 ⁵ y ap act (33G53)	0.063 scint spect (33G53)	no γ (33G53)	Q_{β}^- 0.063 (33G53) 	fission U (61S50, 76B50); parent Nb ^{93m} (33G53)
⁹² Zr	17.11 (24W48)						
⁹³ Zr							
⁹⁴ Zr	17.40 (24W48)						
⁹⁵ Zr		β^- (42S40)	65 d (17B51a, 38G46); 66 d (2G48); 63 d (42S40)	0.371 (99%), 0.84 (1%) spect (5S52); 0.39 (98%), -1.0 (2%) spect (17N51); 0.365 (95%), -0.60 (weak), -1.1 (weak) spect (88S51b); -0.4 (98%), -1.0 (2%) abs (17B51a); 0.40 abs (26M48a); 0.40, 0.88 β - γ coinc abs. abs (14M51)	0.721 (e/ γ 0.0024), no 0.92 γ spect, spect conv (5S52); 0.73, 0.92 (γ) spect conv (17N51); 0.88 abs (17B51a); 0.91 coinc abs sec (26M48a); others (52M51)		Zr-n- γ (42S40, 2S47); Zr-d-p (42S40, 20J51); Mo-n-a (42S40); spall-fission Bi (11G49, 66B51), Th (7N49a); fission U233 (38G48, 61S48), Pu (28F51); fission U, parent (-1%) Nb ^{95m} , parent (-99%) Nb ⁹⁵ (62H49, 17B51a, 20J51, 61S51b)
⁹⁶ Zr	2.80 (24W48)						
⁹⁷ Zr		β^- (2G40)	17.0 h (50B50a, 26M52, 32K51b, 2G40)	1.91 spect (50B50a); 1.9 abs (76S49); 2.2 abs (32K51b); 2.5 abs (26M52)	with Nb ^{97m} : 0.747 (e/ γ 0.015) spect, spect conv, β - γ coinc, γ - γ coinc, β -conv coinc (50B50a)		Zr ⁹⁶ -n- γ (50B50a, 26M52); Zr-n- γ (42S40, 2S47); Mo-n-a (42S40); spall-fission Bi (66B51), Th (7N49a), U (6O47); fission Th (21T51), U (2G40, 16H41a), Pu (32K48) parent Nb ^{97m} (50B50a); descendant Kr ⁹⁷ (24D51)
^{98m} Zr		IT (24C52)	0.83 s (24C52)		-0.50 scint spect (24C52)		Zr-n (24C52)
⁹⁰ Nb		β^+ (20J51)	15.0 h (29K49); 15 h (76B49b); 18 h (20J51)	1.2 abs (29K49); -1.7 abs (76B49b)	0.14, 1.14, 2.23 scint spect (76B51d); 2.0 abs (29K49)		Zr-d-2n (20J51); Zr ⁹⁰ -d-2n (29K49); Mo-d-a (20J51); Mo ⁹² -d-a (29K49, 76B49b); Mo- γ -pn (22E52), daughter Mo ⁹⁰ (43D52)

Isotope Z A	Class and identification	Percent abundance	Type of decay	Half-life	Energy of radiation in Mev		Disintegration energy and scheme	Method of production and genetic relationships
					Particles	Gamma-transitions		
⁹¹ Nb 41	A chem, excit. (20J51); chem, sep isotopes (16O51)		IT (76B49b)	64 d (76B49b); 60 d (20J51)		0.1045 (e/y -50, K/L 2.1) spect conv, scint spect (16O51); 0.105 (K/L+M 2.1) spect conv (4P51); Nb x (76B49b, 16O51) Zr x (16O51)		⁹⁰ Zr -d-n (16O51); Zr -d-n (20J51); Mo ⁹⁴ -d-an (76B49b) [⁹⁰ Zr -d-n, daughter Nb ^{91m}] (16O51)
⁹¹ Nb	B genet (16O51)		[EC] (16O51)	long (16O51)				
⁹² Nb	B chem, excit (8J52a)		EC (8J52a)	-13 h (8J52a)		2.35 scint spect (8J52a)		Nb-p-pn (8J52a)
⁹² Nb	A chem, excit (42S38a)		EC, no β ⁻ (11m 0.05%) (4P51); EC, no β ⁻ (8J52a)	10.1 d (29K47); 9.8 d (60M48); 11 d (42S40a, 42S38a)	β ⁻ (?); 1.3 cl ch (42S40a), abs (29K47); 0.6 abs (59M44)	0.930 (with EC) spect (4P51); 0.933, 1.84 (weak) scint spect (18T52); 1.0 abs (59M44, 29K47); 1.1 abs (1P45); Zr-x (1P45)		Y-α-n (1P45); Zr-p-n (59M44); Nb-y-n (60M48, 22E52); Nb-n-2n (42S38a, 42S40a); Nb-d-t (37W46, 29K47); Mo-n-p (42S40); Mo ⁹⁴ -d-a (76B49b) Nb-d (37W46)
⁹² Nb	G not found; chem, excit (76B49b)		β ⁻ (37W46)	21.6 h (37W46)				
⁹³ Nb	B genet (33G53)	100 (37S36a)	IT (33G53)	3.65 y (33G53)		0.0292 (e/y very large, K/L 0.14) spect conv (33G53)		daughter Zr ⁹³ (33G53)
⁹⁴ Nb	A n-capt, excit (1P37, 42S38a, 18G46b, 29K46)		IT 99+%, β ⁻ -0.1% (18G46b)	6.6 m (42S40a)	1.3 abs (18G46b)	0.0415 (e/y large, K/L/M = 0.31/ 1.00/0.36) spect conv (42C50); 0.056 (e/y large) abs conv (18G46b); 0.9 (weak) scint spect (38M51a); Nb K-x (18G46a, 18G46b)		Nb-n-y (1P37, 42S38a, 42S40a, 18G46a, 18G46b, 2S47); Nb-d-p (29K46, 37W46)
⁹⁴ Nb	[A] n-capt (18G46b); chem, n-capt (63H52)		[β ⁻] (18G46b)	>5 x 10 ⁴ y yield (63H52); >>100 y yield (18G46b, 18G48a)				Nb-n-y (18G46b)
⁹⁵ Nb	A chem (13E46, 13E51a); chem, genet (61S51b)		IT (61S51b)	90 h (61S51b, 62H49); 84 h (5S52)		0.231 (e/y very large) spect conv (5S52); 0.232 (K/L+M -3.5) spect conv (4P51); 0.216 (e/y very large) spect conv (62H49); Nb K-x (61S51b)		Mo ⁹⁷ -d-a (76B49b); fission U, daughter (-1%); Zr ⁹⁵ (62H49, 17B51a, 20J51, 61S51b); spall-fission U (6F51); parent Nb ⁹⁵ (61S51b, 19L51)
⁹⁵ Nb	A chem (39G46, 39G51); chem, excit, cross bomb (20J51)		β ⁻ (39G51)	35 d (13E51b); 37 d (20J51)	0.160 spect (29F52); 0.159 spect (5S52); 0.148 spect (8S51b); 0.146 spect (62H49); 0.15 spect (17N51a); others (26M48b)	0.745 (e/y 0.0024) spect, spect conv (5S52); 0.758 (e/y 0.002) spect, spect conv (62H49); 0.77 (e/y 0.0016, K/L = 4) spect conv (29F52); 0.75 spect conv (11R47)		Mo ⁹⁷ -d-a (76B49b); Mo-d-a (20J51); spall-fission Bi (66B51); U (6F51); fission U, daughter (-99%); Zr ⁹⁵ (62H49, 17B51a, 61S51b)

⁹⁶ Nb	A chem, excit, sep isotopes (29K49a)	β^- (29K49a)	23.35 h (29K49a); 22.9 h (76B51)	0.750 (92%), 0.37 (8%) spect (4P51); 0.686 (92%), 0.37 (8%) spect (31J52); 0.75 spect (76B51)	0.216 (7%, $e/\gamma < 2.3 \times 10^{-3}$), 0.238 (10%, $e/\gamma < 1.6 \times 10^{-3}$), 0.451 (27%, $e/\gamma < 4 \times 10^{-3}$), 0.560 (61%, $e/\gamma < 1.7 \times 10^{-3}$), 0.770 (100%, $e/\gamma < 1.2 \times 10^{-3}$), 0.804 (6%, $e/\gamma < 1.3 \times 10^{-3}$), 0.840 (16%, $e/\gamma < 1.2 \times 10^{-3}$), 1.078 (52%, $e/\gamma < 0.5 \times 10^{-3}$), 1.187 (32%, $e/\gamma < 0.3 \times 10^{-3}$) spect conv, spect (4P51); 0.455, 0.545, 0.745, 0.9, 1.05, 1.1 spect, spect conv (31J52)	Q_β^- 3.16 (4P51, 74S51a) acc T_{c96} Nb ⁹⁶ β^- 92% 8% 2.79 2.57 2.41 61% 6% 1.96 1.85 1.61 52% 32% 16% 100% 0.770 (4P51)	Zr ⁹⁶ -p-n (29K49a); Mo ⁹⁸ -d-a (76B51); spall-fission Bi (66B51); fission U (68C51a)
^{97m} Nb	A chem, excit, sep isotopes, genet (50B50a)	IT (50B50a)	60 s (50B50a)				Mo ⁹⁸ -y-p (50B50a); daughter Zr ⁹⁷ (50B50a)
⁹⁷ Nb	A chem, genet (2G40)	β^- (2G40)	72.1 m (26M52); 74 m (50B50a); 75 m (2G40)	1.267 spect (50B50a); 1.35 abs (75S49); 1.4 abs (32K51b, 26M52)			Mo-n-p (42S40); Mo-y-p (42H47, 12P48, 22E52); fission U (2G40, 32K51b); Pu (32K51b); spall-fission U (6F51)
⁹⁸ Nb	E chem, sep isotopes (76B49b)	β^- (76B49b)	30 m (76B49b)				Mo ¹⁰⁰ -d-a (76B49b)
⁹⁹ Nb	B chem, excit sep isotopes (23D50)	β^- (23D50)	2.5 m (23D50)	3.2 abs (23D50)			Mo ¹⁰⁰ -y-p (23D50)
⁹⁰ Mo	B chem, genet (43D52)	β^+ , EC (43D52)	5.7 h genet (43D52)		-0.1, other γ 's abs (43D52)		spall Nb (43D52); parent Nb ⁹⁰ (43D52)
⁹¹ Mo	A excit (37B37a); chem, excit (42S38); chem, sep isotopes, excit (29K49, 23D49)	β^+ (42S38)	15.5 m (23D49, 25W48); 17 m (29K49, 37B39, 42S38)	3.7 abs (23D49); 2.7 cl ch (42S40)	no γ (23D49)		Mo-y-n (37B39, 25W48, 22E52); Mo-n-zn (6H37, 42S38, 42S40, 30B52); Mo ⁹² -n-zn (29K49); Mo ⁹² -y-n (23D49); Mo ⁹² -y-n (23D49); Mo-y-n (25W48)
⁹¹ Mo	B chem, sep isotopes (23D49)	β^+ (23D49)	75 s (23D49); 73 s (25W48)	2.6 abs (23D49)	0.3 abs (23D49)		
⁹² Mo						Mo ⁹² , $I = 0$ (87M50)	
^{93m} Mo	D chem, excit (29K46); chem, excit, cross bomb, sep isotopes (29K50a); chem, excit (76B52b); possibly Mo ^{92m} or Mo ^{94m} (HPS)	IT (29K50a)	6.95 h (76B52b); 6.75 h (29K50a)	0.262 (K/L 2.9), 0.69, 1.51 spect, spect conv (9R51); 0.256 (K/L 2.8), 0.7, 1.5 spect conv, scint spect (13A50b); 0.30 (e/γ 9), 0.70 (e/γ 0.005), 1.7 (e/γ -0) abs, abs conv, spect conv, conv-y coinc (29K50a); γ_1 0.29, γ_2 0.69, γ_3 1.46 ($\gamma_1/\gamma_2/\gamma_3 = 0.6/1/1$) scint spect (76B52b) others (85S51)			Zr ⁹⁰ -a-n (29K50a); Zr-a-n (29K46); Nb-p-n (29K46, 19R51, 76B52b); Nb-d-zn (29K46, 37W46, 29K50a); Mo ⁹⁴ -n-zn (29K50a); not found by: Mo ⁹² -n-y (76B50a); Mo ⁹⁴ -y-n (23D49); Mo ⁹² -d-p (29K50a); not daughter Tc ⁹³ (76B50a)

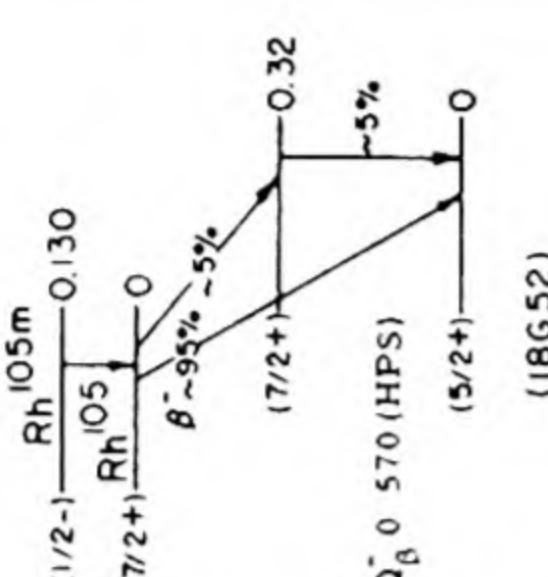
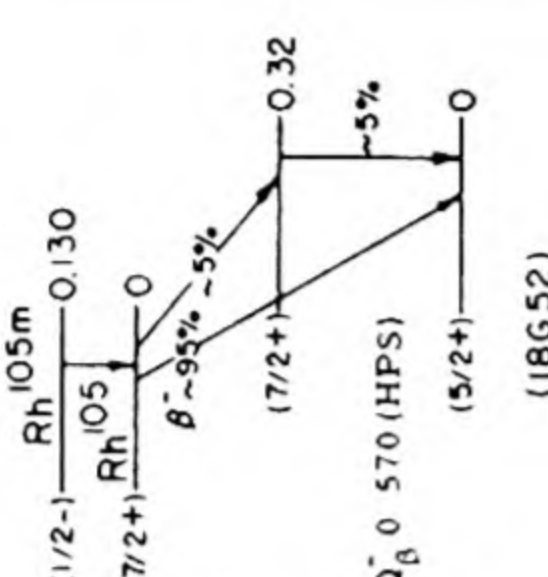
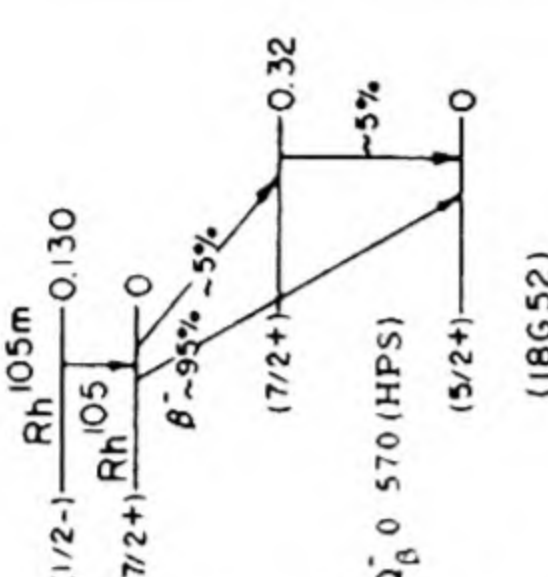
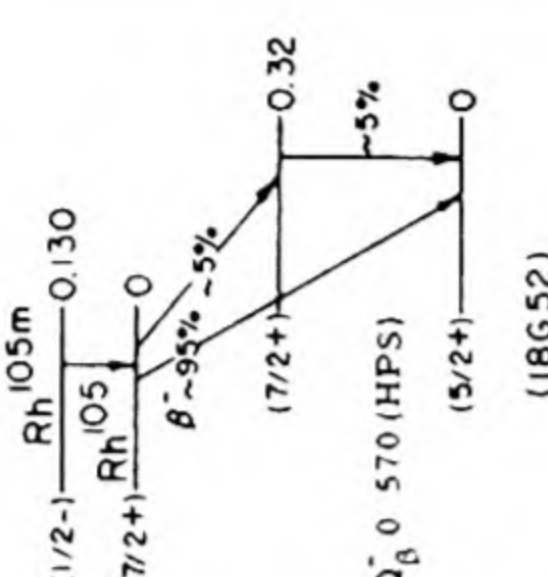
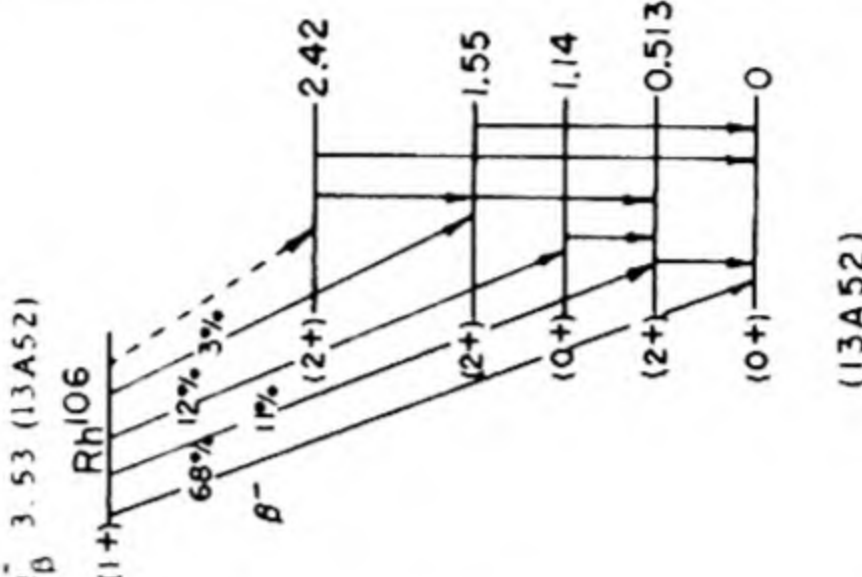
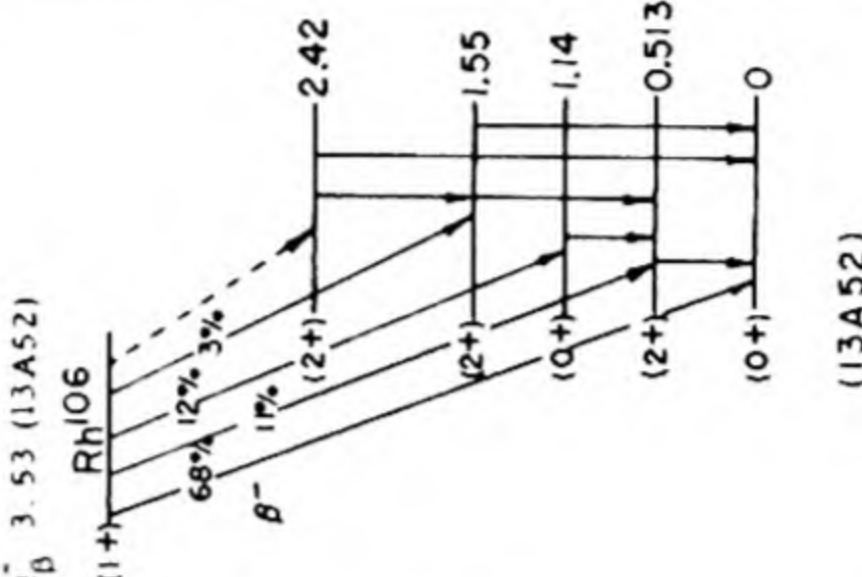
Isotope Z A	Class and identification	Percent abundance	Type of decay	Half-life	Energy of radiation in Mev		Disintegration energy and scheme	Method of production and genetic relationships
					Particles	Gamma-transitions		
⁹³ Mo 42 Mo	B chem, n-capt (76B49)		EC (76B49)	>2 y (76B49)		Nb K-x (76B49)	⁹⁴ Mo, I = 0 (87M50) ⁹⁵ Mo, I = 5/2 (87M50) ⁹⁶ Mo, I = 0 (87M50) ⁹⁷ Mo, I = 5/2 (87M50) ⁹⁸ Mo, I = 0 (87M50) ⁹⁹ Mo, I = 37 (2B50a)	Mo-n-γ (76B49)
⁹⁴ Mo		9.12 (9W46)						
⁹⁵ Mo		15.70 (9W46)						
⁹⁶ Mo		16.50 (9W46)						
⁹⁷ Mo		9.45 (9W46)						
⁹⁸ Mo		23.75 (9W46)						
⁹⁹ Mo	A chem, n-capt, excit (42S38, 42S40)		β ⁻ (42S38)	67 h (13S39); 68.3 h (10C49); 63.5 h (25W48); 64 h (42S40)	1.23 (-80%), 0.45 (-20%), -0.08 (weak) (?) spect (2B50a); 1.23 (87%), 0.54 (13%) spect (62M51); 1.25, others, spect (54M51); 1.2 abs (32K51c)	γ ₁ 0.040, γ ₂ 0.181 (K/L 5), γ ₃ 0.367, γ ₄ 0.741, γ ₅ 0.780 (γ ₃ /γ ₄ /γ ₅ = 10/100/14) spect, spect conv (2B50a); 0.728, 0.360 (weak), 0.182 (weak) spect, β-γ, γ-γ coinc (62M51); 0.179, 0.168 spect conv (10C49); γ ₄ 0.745, γ ₅ 0.780, γ ₆ 0.850 (γ ₄ /γ ₅ /γ ₆ = 100/50/30) spect (54M51); with Tc ^{99m} : 0.0018, 0.140 (62M49, 62M51); 0.142 (63M51)	Zr-α-n (14E46); Mo-d-p (13S39); Mo-n-γ (42S38, 13S39, 61M47, 2S47, 26M48c, 62M49); Mo ⁹⁸ -n-γ (61M47a); Mo-n-2n (42S40); Mo-γ-n (25W48, 22E52); spall Sb (37L50); spall-fission Pt, Ti (2T47b), Bi (13P47, 11G49, 66B51), Th (7N49a); fission Th (16H39d, 72B51, 21T51), U ²³³ (61S48), U (16H39e, 24S40, 32K51c), Pu (32K48, 28F51); parent Tc ^{99m} (13S39, 24S40, 62M49, 33G51e)	
¹⁰⁰ Mo		9.62 (9W46)					¹⁰⁰ Mo, I = 0 (87M50)	
¹⁰¹ Mo	A chem, n-capt (42S40); chem, n-capt, sep isotopes (61M47a)		β ⁻ (42S40)	14.6 m (3M41); 14 m (16H41b)	1.2, 2.1 abs (31R52); -1.0, 2.2 abs (3M41); 1.9 abs (42S40)	0.191 (K/L-6), 0.960 (coinc with 1.2 β ⁻) spect conv, scint spect, β-γ, γ-γ coinc (31R52); 0.15 scint spect (38M51a)	Mo-n-γ (42S40b, 42S40, 24S40a, 3M41, 2S47, 50H51); Mo ¹⁰⁰ -n-γ (61M47a); parent Tc ¹⁰¹ (42S40b); fission U, parent Tc ¹⁰¹ (24S40a, 37B41, 16H41, 16H41b, 3M41)	
¹⁰² Mo	D chem (16H41)		β ⁻ (16H41)	12 m (16H41); 11 m (76B49a)				fission U, parent Tc ¹⁰² (16H41, 16H41b, 76B49a)
¹⁰⁵ Mo	B chem, genet (70B43b)		β ⁻ (70B43b)	-5 m (66S47)				fission U, ancestor Ru ¹⁰⁵ (70B43b)
⁹² Tc 43 Tc	D chem, sep isotopes (61M48)		β ⁺ , EC (76B52c)	4.3 m (76B52c)	4.1 abs (76B52c)	1.3 abs (61M48)		Mo ⁹² -d-2n (61M48)
⁹² Tc	D chem, excit, sep isotopes (29K48a)		EC (29K48a)	43.5 m (62M50); 47 m (29K48a)		0.389 spect, spect conv (62M50); 1.50 abs conv (29K48a)		Mo ⁹² -d-2n, p-n (29K48a); Mo-p-n (62M50)

Tc^{93}	A chem (13S39); chem, excit, sep isotopes (29K48a)	EC 93%, β^+ 7% (29K48a, 76B51d)	2.75 h (29K48a), 2.7 h (61M48, 5D39)	0.800 spect (76B51a); 0.83 abs (29K48a)	1.34 (coinc with β^+) scint spect, β - γ coinc abs (76B51d); 2.00 abs (29K48a); 2.4 abs (61M48)	Q_{β}^+ 3.1 (76B51a)  Tc 93	Mo-92-d-n (29K48a, 61M48); Mo-d-n (13S39); Mo-p-n (5D39, 29K48a); not parent (7h) Mo-93m (76B50a)
Tc^{94}	B chem, excit (42G47); chem, excit, sep isotopes (61M48a)	β^+ -75%, EC -25% (62M50)	53 m (62M50); 50 m (61M48a)	2.41 (coinc with γ) spect, β - γ coinc (62M50); 2.5 abs (61M48a)	0.874 (e/γ -10 ⁻³), 1.85, 2.73, 3.27 spect, spect conv (62M50); 0.9 abs (61M48a)	Q_{β}^+ 4.30 (62M50)  Tc 94	Mo-p-n (42G47, 34H48, 62M50); Mo-94-d-2n (61M48a); daughter Ru-94 (12V52)
Tc^{95m}	A chem (12C37, 12C39); chem, sep isotopes (61M48b)	EC 96+%, IT -3%, β^+ 0.2-0.6% (62M50, 62M50a)	60 d (62M50); 52 d (14E47); 62 d (12C39)	0.4 cl ch (62M50)	γ_1 0.810 (e/γ 0.001), γ_2 0.201 (e/γ 0.036), γ_3 0.570 (e/γ 0.002), γ_4 1.02 ($\gamma_1/\gamma_2/\gamma_3/\gamma_4 =$ 0.3/0.7/0.4/0.03) spect, spect conv, γ - γ coinc (62M50); 0.0390 spect conv (62M50a); 0.80, 0.20, 0.58, 1.03 scint spect (76B51a); 0.8, 0.2 abs (14E47, 61M48b)	 Tc 95m	Mo-d-n (12C37, 12C39, 14E46); Mo-p-n (14E47); Mo-95-d-2n (61M48b)
Tc^{95}	A chem, sep isotopes (1E48, 61M48a)	EC (1E48); no β^+ (62M50)	20.0 h (1E48); 20 h (61M48a)		0.762 (-90%), 0.932 (-5%), 1.071 (-5%) spect conv, γ - γ coinc (62M50); 0.76, 1.07, no 0.93 γ scint spect (76B51d); 0.78 abs (1E48)	 Tc 95	Mo-a-p, Mo-p-n, Mo-92-a-p (1E48); Mo-95-d-2n (61M48a); Mo-p-n (62M50)

Isotope Z A	Class and identification	Percent abundance	Type of decay	Half-life	Energy of radiation in Mev		Disintegration energy and scheme	Method of production and genetic relationships
					Particles	Gamma-transitions		
⁹⁶ Tc 43	B chem, excit (62M50); chem, excit, sep isotopes (62M52)		IT (62M50)	51.5 m (62M50)		0.0344 (K/L 1.2) spect conv (62M50); Tc K-x (62M50)		⁹⁶ Mo -p-n (62M52); Mo -p-n (62M50)
⁹⁶ Tc	A chem (15E39); chem, excit, cross bomb (14E47); chem, excit, sep isotopes (61M48b)		EC (61M48b); no β^+ (62M50)	4.20 d (31C50); 4.35 d (62M50); 4.2 d (61M48b); 4.3 d (14E47)		γ_1 1.119 (e/ γ 3×10^{-4}), γ_2 0.842 (e/ γ 6×10^{-4}), γ_3 0.806 (e/ γ 6×10^{-4}), γ_4 0.771 (e/ γ 6×10^{-4}), γ_5 0.312 (K/L 6.4) ($\gamma_1/\gamma_2/\gamma_3/\gamma_4$ / $\gamma_5 = 0.17/1.00/0.82/1.00/0.0052$) spect, spect conv, γ - γ coinc (62M50); 1.65, 1.89, 2.39 (7) (all weak) scint spect (76B51a)	see Nb (5,6+) (5,6+) (3,4+) (2+) (0+) (62M50, 76B51a, 62M52, 18G52)	Nb-a-n (14E47); Mo-p-n (15E39, 14E47, 62M50); Mo-d-n (14E47, 13S39); Mo ⁹⁶ -d-2n (61M48b)
^{97m} Tc	A chem (22P37, 12C37); chem, genet (61M47b); excit, sep isotopes (61M48b)		IT (2H41, 14E47)	90 d (61M48b); 91 d (2H41); 95 d (14E47)		0.0958 (K'/L+M 1.6) spect conv (62M50); 0.097 (K/L -2) spect conv (2H41); 0.097 (e/ γ very large) abs conv (61M48b); 0.108 (e/ γ large) abs conv (14E47)		⁹⁷ Mo -d-2n (61M48b); Mo-d-n (12C37, 22P37, 12C39); Mo-p-n (14E47); daughter Ru ⁹⁷ (61M47b)
⁹⁷ Tc	[A] genet (76B51b)		[EC] (76B51b)	>10 ⁴ y yield (76B51b)				[daughter Tc ^{97m}] (76B51b)
^{99m} Tc	A chem, genet (13S39)		IT (13S39)	6.04 h (13S39); 5.9 h (33G51e); 6.6 h (13S39)		0.1403 (K/L 7.7), 0.1423 (-1%, K/L -2.5) spect conv (63M51); 0.1412 (e/ γ 0.11, K/L/M+N = 7.9/1/0.3), 0.0018 (e/ γ very large) spect conv (62M49, 62M51); 0.140 (K/L -9) spect, spect conv (2B50a); 0.139 (K/L -10) spect conv (54M51)		Ru-n-p (76B47); fission Th (72B51), U (24S40, 16H41, 33G51e); daughter Mo ⁹⁹ (13S39, 24S40, 62M49, 33G51e, 63M51); parent Tc ⁹⁹ (13S39, 16H41)
⁹⁹ Tc	A chem (25L46, 53S46); chem, mass spect (3147)		β^- (25L51, 53S51a)	2.12 x 10 ⁵ y sp act (30F51); 2.2 x 10 ⁵ y sp act (26P51)		no γ (61M47, 53S51a, 30F51)		fission U (3147, 25L51, 53S51a); daughter Tc ^{99m} (13S39 16H41); descendent Mo ⁹⁹ (61M47)
¹⁰⁰ Tc	A sep isotopes (64H52); sep isotopes, n-capt (76B52)		β^- (64H52)	15.8 a (76B52); 17.5 a (64H52)		0.55 scint spect (76B52c)		Mo ¹⁰⁰ -p-n (64H52); Mo-p-n (2D40); Tc ⁹⁹ -n- γ (76B52)

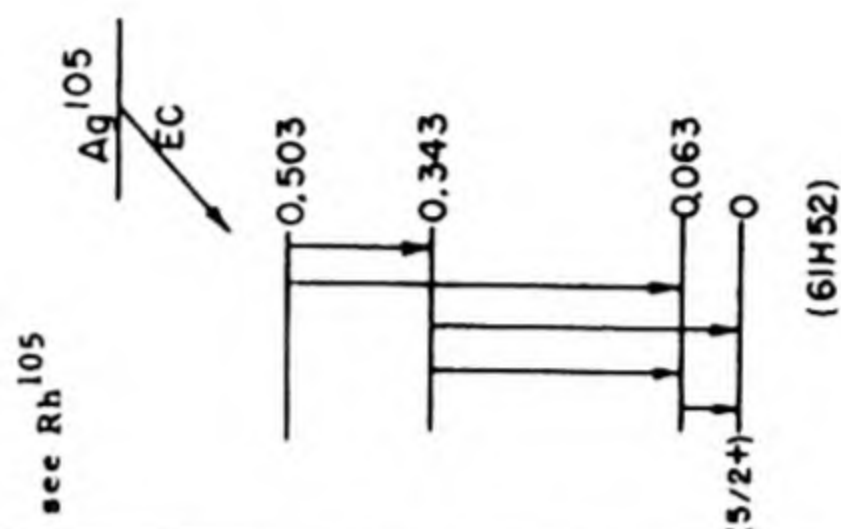
Tc^{101}	A chem, genet (42S40b)	β^- (42S40b)	14.0 m (3M41, 16H41b); 14.5 m (12P48); 16.5 m (60M48)	1.20 (>95%) abs; β - γ coinc (76B51a); 1.2 abs (42S40); 1.3 abs (3M41)	0.307 (coinc with β^- , K/L -6) spect conv, β - γ coinc, scint spect (31R52); 0.30 (coinc with β^-), 0.56 (weak) scint spect, β - γ coinc (76B51a); 0.26 scint spect (38M51a); no 0.56 γ (31R52)	Mo ¹⁰⁰ -d-n (61M48); Ru ¹⁰¹ - γ -p (12P48, 60M48); Rh ¹⁰¹ - γ -2p (22E52); fission U, daughter Mo ¹⁰¹ (24S40a, 37B41, 16H41, 16H41b, 3M41); daughter Mo ¹⁰¹ (42S40b); daughter Mo ¹⁰² (16H41, 16H41b, 76B49a); fission U, daughter Mo ¹⁰⁵ parent Ru ¹⁰⁵ (70B43b); [fission U, parent Ru ¹⁰⁷] (70B43b)
Tc^{102}	E genet (16H41)	β^- (16H41)	<25 s (76B49a); <1 m (16H41)			
Tc^{105}	B chem, genet (70B43b)	β^- (70B43b)	short (70B43b)			
Tc^{107}	[E] genet (70B43b)	[β^-] (70B43b)	<1.5 m (70B43b)			
Ru^{94}	D chem, genet (12V52)	EC (12V52)	-57 m genet (12V52)			Mo- α -2n, parent Tc ⁹⁴ (12V52)
Ru^{95}	A chem, cross bomb, sep isotopes (1E48)	EC, β^+ (1E48)	1.65 h (1E48)	1.1 abs (1E48)	1.0, 0.5 abs (1E48)	Mo- α -n, Mo ⁹² - α -n (1E48); Ru-n-2n (1E48); Ru- γ -n (60M48)
Ru^{96}						
Ru^{97}	A chem, excit (23S46); chem, cross bomb, sep isotopes (1E48)	EC (23S46)	2.8 d (23S46, 60M48)		0.217 spect (53M50a); 0.23 abs (23S46)	Mo ⁹⁴ - α -n (1E48); Ru-d-p (23S46); Ru-n- γ (23S46); Ru-n-2n (1E48); Ru- γ -n (60M48); spall Sb (37L50); parent Tc ^{97m} (61M47b)
Ru^{98}						
Ru^{99}						
Ru^{100}						
Ru^{101}						
Ru^{102}						
Ru^{103}	A excit (12L36); chem (5N42, 39G46); chem, excit (23S51, 23S51b)	β^- (5N42)	39.8 d (38K50); 42 d (23S51); 41 d (77B45, 15H48); 45 d (5N42, 60M48)	0.217 (-99%), 0.698 (-1%) spect (38K50, 38K51c); 0.222 (94%), 0.684 (6%) spect (53M50a); 0.205 (strong), 0.670 (weak) spect (79S50); 0.350 (50%), 0.665 (50%) spect (15H48); 0.2 (92%), 0.7 (8%) abs, β - γ coinc (26M50)	0.498 (coinc with 0.22 β^- , e/ γ -0.01) spect, spect conv, β - γ coinc (38K50, 38K51c); 0.498 spect (46K52); 0.494 (e/ γ 0.006, K/L 6.5) spect, spect conv (53M50a); 0.499 (K/L 8.5), 0.611 (K/L 4), 0.295 (?), 0.053 (K/L 1.0) spect conv (10C52); others (26M50, 23E52, 52M51); with Rh ^{103m} : 0.040 (38K50, 53M50a, 79S50, 37W45, 10C52)	Ru-d-p (12L36, 23S51); Ru-n- γ (23S51, 7D38); Ru- γ -n (60M48); spall Sb (37L50); spall-fission Pb (13P47a); Bi (11G49); fission Th (72B51, 21T51), U233 (38G48, 61S48), U (5N41, 5N42, 39G51a, 23S51f), Pu (28F51), parent Rh ^{103m} (23S51b)
Ru^{104}						

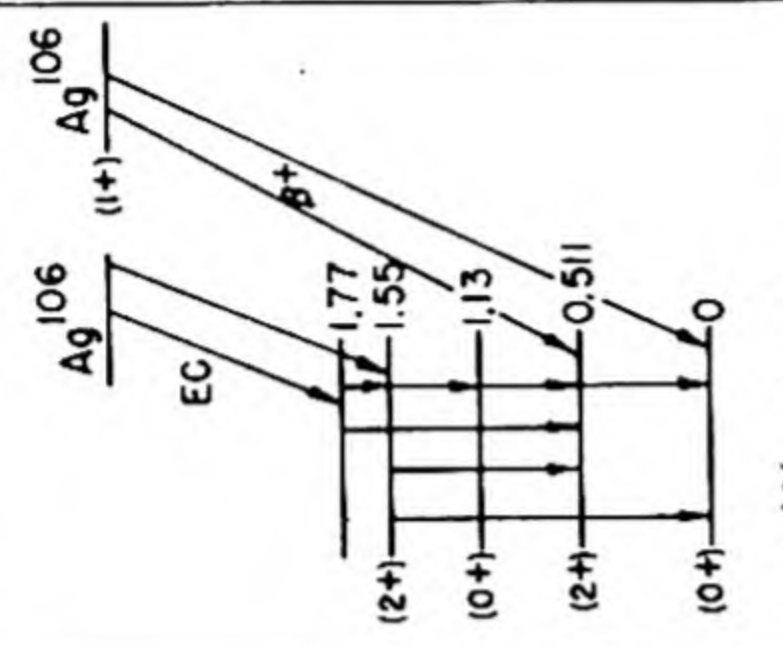
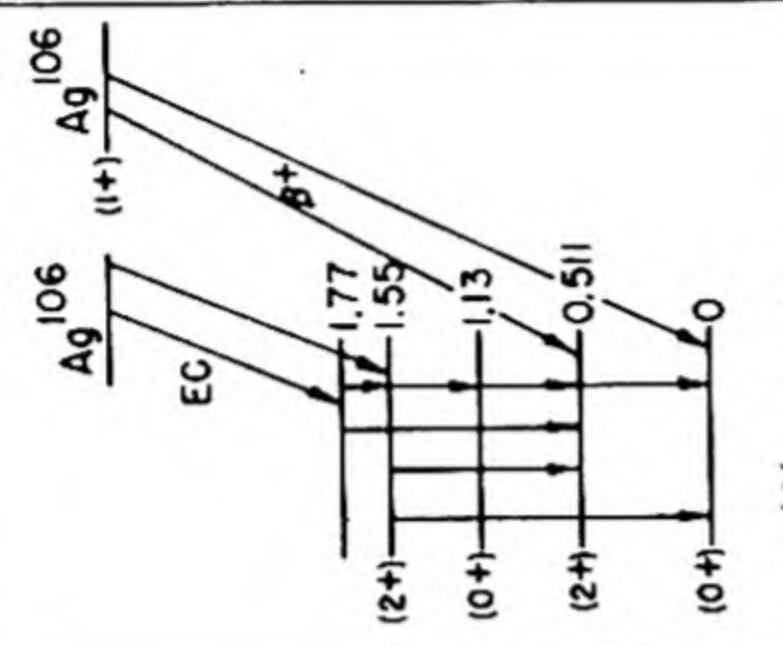
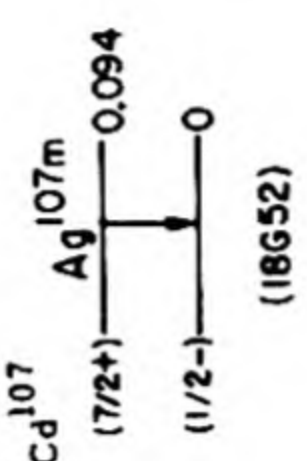


Isotope Z A	Class and identification	Percent abundance	Type of decay	Half-life	Energy of radiation in Mev		Disintegration energy and scheme	Method of production and genetic relationships
					Particles	Gamma-transitions		
¹⁰⁵ ₄₄ Ru	A chem (24S41); chem, excit (23S51c)		β^- (5N41)	4.5 h (76S51, 23S51d, 23S51a); 4.4 h (77B45)	1.150 spect (23D51); 1.15 spect (90S52); 1.3 abs (23S51d, 23S51a, 77B45)	0.726 (coinc with β^-) spect, β^- - γ coinc (23D51); 0.75 abs (23S51d); 0.7 abs (77B45); with Rh ^{105m} ; 0.130 (29A51, 23D51a, 90S52)	$Q_{\beta^-} 2.01$ (23D51) (18G52)	Ru-n- γ (7D38, 23S51c); Ru-d-p (12L36, 23S51c); spall Sb (37L50); spall-fission Pt (2T47b), Hg (π) (63S52), Tl (2T47b), Pb (13P47a), Bi (13P47, 11G49), U (6O48, 6F51); fission Th (24S41, 72B51), U (7D38, 5N41, 24S41, 70B43b, 77B45, 76S51, 23S51d); descendent Mo ¹⁰⁵ (70B43b), parent Rh ^{105m} (23D51), ancestor Rh ¹⁰⁵ (5N41, 77B45, 76S51, 23S51c)
¹⁰⁶ ₄₄ Ru	A chem (39C46, 33G46a); chem, mass spect (60H48)		β^- (39G51a, 33G51f)	1.0 y (33G51f, 66S46)	0.0392 spect (16A50); 0.038 spect (3F50b)	no γ (76S51a, 16A50)		spall Sb (37L50); spall-fission Bi (11G49), Th (7N49a), U (6F51); fission Th (72B51, 21T51), U233 (38G48, 61S48), U (33G51f), Pu (28F51); parent Rh ¹⁰⁶ (33G51f)
¹⁰⁷ ₄₄ Ru	D chem (70B43b, 33G51g)		β^- (70B43b)	4 m (33G51g, 70B43b)	-4 abs (70B43b)			fission U, parent Rh ¹⁰⁷ (33G51g, 70B43b)
⁹⁹ ₄₅ Rh	D chem (1E49)		β^+ (90S52)	4.5 h (90S52)	0.74 spect (90S52)			Ru-p-n (1E49, 90S52); Ru-d-n (1E49, 90S52)
¹⁰⁰ ₄₅ Rh	B chem (23S51e); chem, genet (37L48)		EC -95%, β^+ -5% (37L48)	19.4 h (37L48); 21 h (23S51e)	3.0 spect (37L48)	1.2 abs (37L48); 1.8 abs (23S51e)		Ru-d-n (23S51e); daughter Pd ¹⁰⁰ (37L48)
¹⁰¹ ₄₅ Rh	B chem, excit (23S51g)		EC (23S51g)	4.3 d (37L48); 5.9 d (23S51g)		0.300, 0.148 spect conv (90S52); 0.35 spect conv, abs (37L48)		Ru-p-n (90S52); Ru-d-n (23S51g, 90S52); daughter Pd ¹⁰¹ (37L48)
¹⁰² ₄₅ Rh	A chem, excit (64M41)		β^- , β^+ (64M41); EC (?) (23S51h)	210 d (64M41); 215 d (15H47)	β^- : 1.0 cl ch (15H45); 1.1 abs (64M41) β^+ : 1.1 cl ch (15H45)			Ru-d-n (23S51h); Rh-n-2n (64M41, 15H45); Rh-y-n (60M48, 22E52)
^{103m} ₄₅ Rh	A chem, excit (9F44); chem (33G46a, 33G51f); chem, genet (23S51b)		IT (9F44, 37W45)	57 m (33G51f); 56 m (53M50a); 52 m (9F47); 45 m (37W45)		0.0400 (K/L+M 0.2) spect conv, β^- - γ coinc (38K50, 38K51c); 0.0404 (e/ γ very large) spect conv (53M50a); 0.0396 (K/L 0.1) spect conv (10C52); 0.040 spect conv (79S50); abs conv (37W45); 0.042 abs conv (9F47)	 (18G52)	Rh-d-pn, Rh-p-p (15H48); Rh-n-n (9F44); Rh-e ⁻ -e ⁻ , Rh-x rays (37W45); fission U, daughter Ru ¹⁰³ (23S51b); daughter Pd ¹⁰³ (48B46, 53M50a)
¹⁰³ ₄₅ Rh		100 (57C43)					Rh ¹⁰³ , I = 1/2 (49K50)	

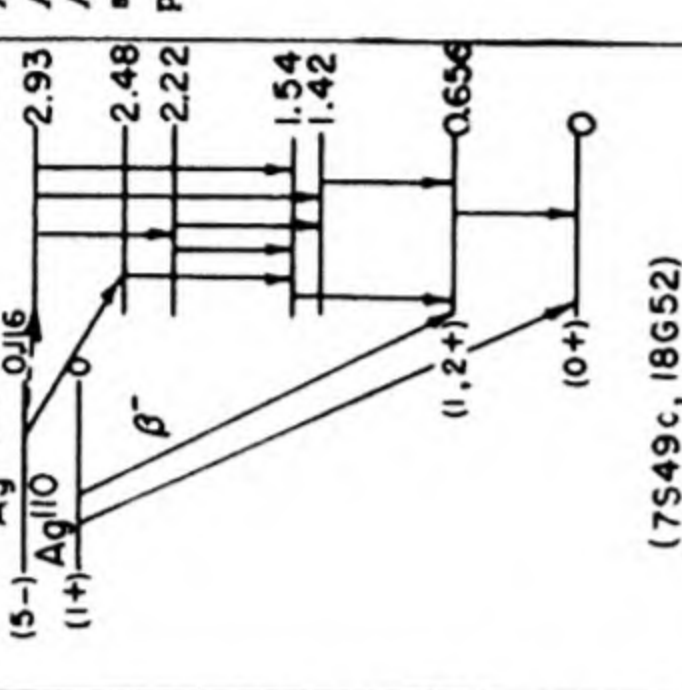
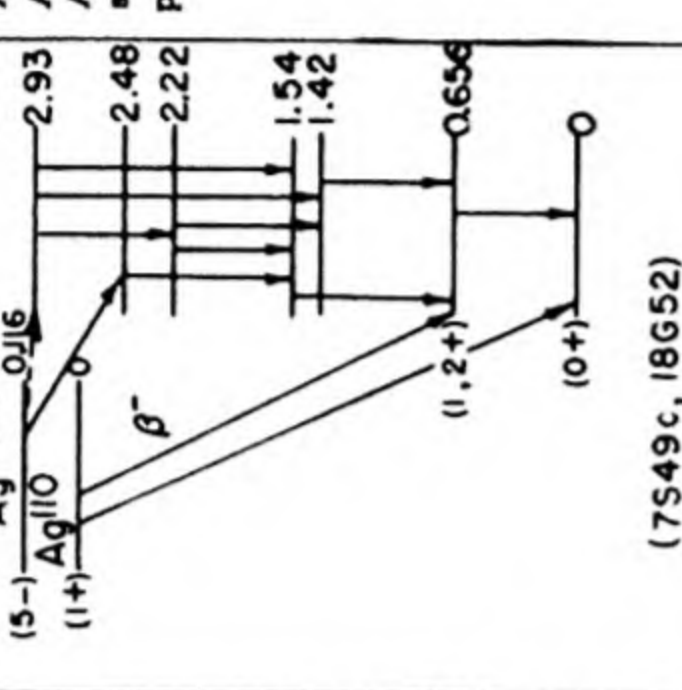
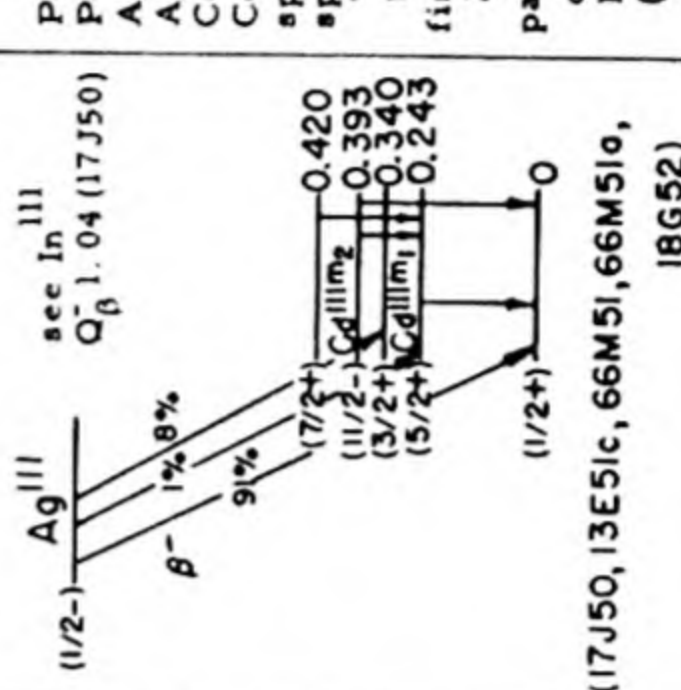
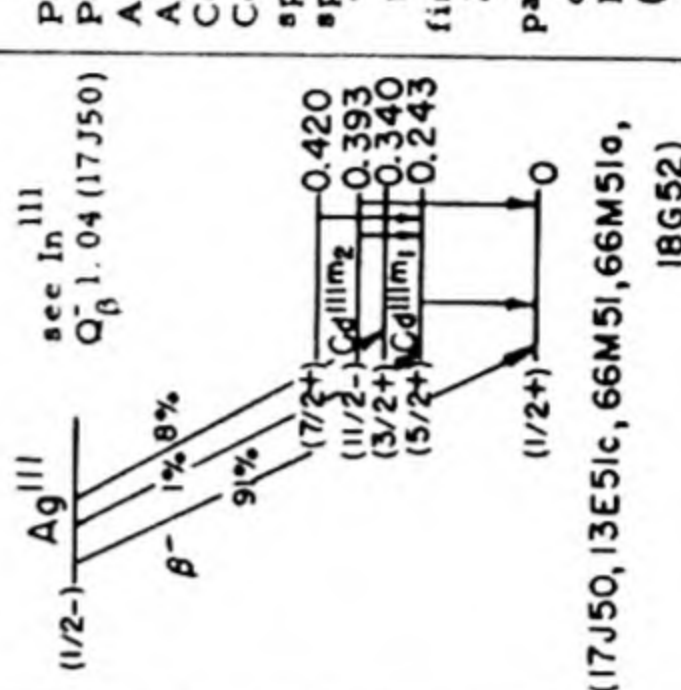
Rh ^{104m}	A n-capt (12A35)	IT (17P38, 28A43a)	4.4 m (32C39); 4.7 m (38M51, 58C47); 4.3 m (9F47)	0.052 scint spect (38M51); scint spect, ion ch (31K51); others (28A43a, 14O40, 15H47)		Ru-p-n (2D40); Rh-n-y (12A35, 1P37, 17P38, 34G46, 2S47, 50H51); Pd-y-p (42H47); parent Rh ¹⁰⁴ (17P38, 9F47)
Rh ¹⁰⁴	A n-capt (12A35); genet (17P38)	β^- (17P38)	44 s (12A35, 17P38)	0.04, 0.18, 0.95 abs, abs conv (58C47)		Rh-n-y (12A35, 17P38, 34G46); daughter Rh ^{104m} (17P38, 9F47)
Rh ^{105m}	A chem, genet (23D51)	IT (23D51)	45 s (23D51)	0.130 (e/y -3, K/L 1.5) scint spect, spect conv (29A52); 0.127 spect conv (90S52)		daughter Ru ¹⁰⁵ , parent Rh ¹⁰⁵ (23D51)
Rh ¹⁰⁵	A chem, genet (5N41); chem, genet (23S51c)	β^- (5N41)	36.5 h (23S51c); 37 h (77B45); 34 h (5N41)	0.322 (-10%, coinc with 0.26 β^-), 0.157 (very weak), 0.080 (?) scint spect, β -y coinc abs (76B52a); 0.320 (-3%) scint spect (23D51a); -0.3 (-8%, not coinc with 0.6 β^-) abs, β -y coinc (26M51); 0.33 (weak) abs (23S51)		Ru-d-n (23S51, 90S52); Rh-t-p (29K48); Pd-y-p (12P48); spall-fission U (6F51); fission Th (72B51, 21T51), U (5N41, 76S51), Pu (32K48); descendent Ru ¹⁰⁵ (5N41, 77B45, 76S51, 23S51c), daughter Rh ^{105m} (23D51)
Rh ¹⁰⁶	A chem, genet (33G46a, 33G51f)	β^- (33G51f)	30 s (33G51f); 40 s (66S46)	γ_1 0.513 (e _K /y 0.004, K/L 8), γ_2 0.624 (e _K /y 0.002), γ_3 0.87, γ_4 1.045, γ_5 1.55, γ_6 2.41 ($\gamma_1/\gamma_2/\gamma_3/\gamma_4/\gamma_5/\gamma_6 = 100/53/3/8/2.5/1$) spect, scint spect, spect conv (13A52); 0.510, 0.622 spect conv (10C52); 0.51 (17%), 0.73 (17%), 1.25 (-1%) spect, β -y, γ -y coinc (6P47a); -0.5 (e _K /y 0.005), -0.7 (e _K /y <0.003) spect conv (44M50); others (39A52)		fission U, daughter Ru ¹⁰⁶ (38G46, 33G51f); fission Pu (28F51)
Rh ¹⁰⁷	D chem, genet (70B43b)	β^- (70B43b)	26 m (33G51g); 24 m (70B43b)	1.2 abs (70B43b)		Pd-y-p (22E52); fission U, daughter Ru ¹⁰⁷ (70B43b, 33G51g)
Rh ¹⁰⁹	[A] genet (77S51)	[β^-] (77S51)	<1 h (77S51)		[fission U, parent Pd ¹⁰⁹] (77S51)	
¹⁰⁰ ₄₆ Pd	B chem, excit (37L48)	EC (37L48)	4.0 d (37L48)	0.09, 1.8 abs (37L48)	Rh-d-5n (37L48); spall Sb (37L48, 37L50); parent Rh ¹⁰⁰ (37L48)	

Isotope Z A	Class and identification	Percent abundance	Type of decay	Half-life	Energy of radiation in Mev		Disintegration energy and scheme	Method of production and genetic relationships
					Particles	Gamma-transitions		
¹⁰¹ Pd 46	B chem, genet (37L48)		EC 90%, β^+ 10% (37L48, 1E49)	8 h (37L50); 9 h (1E49)	2.3 spect (37L48); 0.5 abs (1E49)	no γ (37L48)		Ru- α -n (1E49); Rh-d-4n (37L48); spall Sb (37L48, 37L50); parent Rh ¹⁰¹ (37L48)
¹⁰² Pd								
¹⁰³ Pd	A chem, genet (48B46a); chem, excit (36M47)	0.8 (37S36a)	EC (48B46a)	17.0 d (36M47, 48B46a)		Rh K-x (36M47, 53M50a); no γ (36M47, 53M50a); with Rh ^{103m} ; 0.040 (38K50, 53M50a, 79S50, 10C52)		Rh- α -p3n (53M50a); Rh-d-2n (36M47, 37L48); Rh-p-n (36M47); Pd-n-y (48B46a, 78S50); spall Sb (37L50); parent Rh ^{103m} (48B46a, 53M50a)
¹⁰⁴ Pd								
^{105m} Pd	E excit (9F52a)	9.3 (37S36a)	IT (9F52a)	-23 s (9F52a)		0.20 (e/ γ -0.4) (9F52a)	Pd^{105} , I = 5/2 (99B51)	Pd-n-2n, Pd-n-n (9F52a)
¹⁰⁵ Pd		22.6 (37S36a)						
¹⁰⁶ Pd		27.2 (37S36a)						
¹⁰⁷ Pd	B chem (26P49a)		β^- (26P49a)	-7 x 10 ⁶ y sp act (26P49a)	-0.04 abs (26P49a)			fission U (26P49a)
¹⁰⁸ Pd		26.8 (37S36a)						
^{109m} Pd	D n-capt (31K51); excit, cross bomb, n-capt (9F52a)		IT (31K51, 9F52a)	4.8 m (9F52a)		0.173 scint spect (31K51); 0.160 (e/ γ -0.6) (9F52a)		Pd-n-2n, Pd-n-y (9F52a); Ag-n-p (9F52a)
¹⁰⁹ Pd	A n-capt (12A35); chem, excit (39K37); chem, mass spect (37R46, 67B49a)		β^- (39K37)	13.6 h (11M53); 13.1 h (25W48); 13 h (39K37, 77S51); 14.1 h (60M48)	0.961 spect (20K52); 0.95 spect (7S49b, 38K51c); others (2H46, 39K37, 77S51)	with Ag ^{109m} ; 0.087 (e/ γ \geq 11, K/L+M 1.3) spect conv (7S49b); no γ (77S51); others (52M51)	Q_{β^-} 1.05 (HPS) see Cd ¹⁰⁹ Pd ¹⁰⁹	Pd-y-n (12P48, 60M48, 25W48, 22E52); Pd-d-p (39K37); Pd-n-y (12A35, 39K37, 2547, 9O49, 50H51); Ag-d-2p (2H46, 112S51); Ag-n-p (4F38b); Ag-t-He ³ (29K47a); spall Sb (37L50), Ta (22N52); spall-fission Bi (11G49, 66B51), U (6F51); fission Th (21T51), U (77S51), U233 (61S48), Pu (32K48); parent Ag ^{109m} (24S41, 7549b, 77S51)
¹¹⁰ Pd		13.5 (37S36a)						
^{111m} Pd	B chem, genet (66M52)		IT 75%, β^- 25% (66M52)	5.5 h (66M52)		0.16, 1.77 scint spect (66M52)		Pd-d-p, parent Ag ¹¹¹ (66M52)
¹¹¹ Pd	A n-capt (12A35); chem, genet (24S41)		β^- (39K37)	22 m (66M52); 26 m (24S41)	2.13 spect (20K52); 2.15 spect (66M52); 3.5 abs (70B43b)	0.38, 0.56, 0.65, 0.73 scint spect (66M52)		Pd-d-p (12A35, 39K37); Pd-n-y (12A35, 39K37, 2547); spall Sb (37L50); spall-fission Bi (66B51); fission Th (24S41), U (24S41, 5N40a); parent Ag ¹¹¹ (39K37, 24S41)

Pd^{112}	A chem, genet (5N40a, 24S41)	β^- (5N40a)	21 h (77S51)	0.2 abs (77S51)	no γ (77S51)	In-p-4p, Pd- α -p (11Z551); spall Sb (37L50); spall-fission Bi (11G49, 66B51), Th (7N49a), U (6F51); fission Th (24S41, 21T51), U233 (61S48), Pu (32K48); fission U, parent Ag112 (5N40a, 5N40b, 24S41, 77S51)
^{102}Ag	E excit (17E39)		16 m (17E39)			Pd-p-n (17E39)
^{104}Ag	B excit (17E39); chem, excit, sep isotopes (11M52a)	β^+ , EC (37L50)	1.2 h (17E39, 11M52a)			Pd-p-n (17E39); Cd106-d- α (11M52a); spall Sb (37L50)
^{104}Ag	B chem, genet (32J52); chem, excit, sep isotopes (11M52a)	β^+ (32J52)	27 m (32J52)	2.70 spect (32J52)	0.118, 0.556, 0.148 (?), 0.179 (?) spect conv (32J52)	Cd ¹⁰⁶ -d- α (11M52a); daughter Cd104 (32J52)
^{105}Ag	A excit (17E39); chem, excit (16B47a)	EC (44G50)	40 d (44G50); 45 d (17E39)		0.0625 (e/ γ very large, K/L > 5), 0.280 (coinc with 0.063 γ , K/L 8), 0.343 (K/L 5.8), 0.440 (K/L 7), weak γ 's: 0.154, 0.181, 0.391 spect conv, spect, γ - γ coinc (61H52); 0.064, 0.220 (weak), 0.278, 0.340, 0.437 (weak) spect (53M50b); 0.281, 0.319, 0.331, 0.345, 0.393, 0.443 spect conv (32J52); others (17E39, 20D42c)	Rh- α -2n (16B47a, 44G50, 53M50b, 61H52); Pd-p-n (17E39, 44G50); Pd-d-2n (44G50, 53M50b, 61H52); Pd- α -p (44G50); spall Sb (37L50)

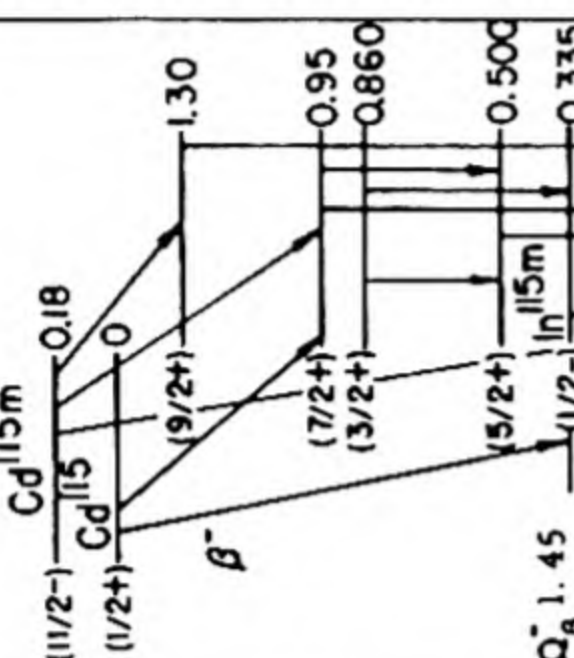


Isotope Z A	Class and identification	Percent abundance	Type of decay	Half-life	Energy of radiation in Mev		Disintegration energy and scheme	Method of production and genetic relationships
					Particles	Gamma-transitions		
¹⁰⁶ ₄₇ Ag	A excit (37B37a, 6H37); chem, excit, cross bomb (39K37, 1P38)		β^+ (39K37); β^- (?) - 2% (79B51)	24.0 m (79B51); 24.5 m (1P38); 24.4 m (2D38); 24.3 m (60M48)	β^+ : 1.95, 1.5 spect (79B51); 2.0 abn (4F38b); 1.9 cl ch (1P38) β^- (?): 0.45 spect (79B51); conv: -0.5 (weak) spect conv (79B51)	-0.5, >0.6 (weak) spect conv, scint spect, abn (79B51) no γ (4F38b, 1P38)	 see Rh ¹⁰⁶ (18G52)	Rh- α -n (1P38, 19K39, 16B47a); Pd-d-n (39K37, 1P38); Pd-p- γ (2D38); Pd-p-n (2D38, 17E39); Ag-n-2n (6H37, 1P38); Ag-d-t (29K47); Ag- γ -n (37B37a, 37B39, 60M48, 55S51, 22E52, 79B51); Ag-e ⁻ -e ⁻ n (59S48); Ag-d-p2n (9K40b); Cd-n-p (1P38)
¹⁰⁶ Ag	A chem, excit, cross bomb (39K37, 1P38)		EC (55H44)	8.2 d (1P38); 8.3 d (44G49); 7.5 d (39K37)		0.220, 0.409, 0.511 (K/L 8), 0.620, 0.717, 0.815, 1.04, 1.24, 1.55 spect conv (61H52); 0.515, 0.722, 1.04, 1.54 spect (53M50b); 0.72, 1.06, 1.63 spect (20D42c)	 see Rh ¹⁰⁶ (18G52)	Rh- α -n (1P38, 16B47a, 53M50b, 61H52); Pd-d-n (39K37, 1P38, 61H52); Pd-p-n (2D38, 17E39); Ag-n-2n (1P38, 39K37, 36S51); Cd-n-p (1P38); spall Sb (37L50)
^{107m} Ag	A chem, genet (6A40, 2H41b)		IT (6A40)	44.3 s (16B45d, 16B47); 44 s (40W51)		0.094 (e/ γ -16, K/L 0.92) spect conv (16B47); 0.093 spect conv (6V39, 2H41)	 see Cd ¹⁰⁷ (18G52)	Ag-e ⁻ -e ⁻ (37W45b); Ag-n-n (9F44); Ag- γ - γ (31F41, 37W45b, 24T45); Ag ¹⁰⁷ - γ - γ (40W51); daughter Cd ¹⁰⁷ (6A40, 2H41b, 16B45c, 2H46, 16B47)
¹⁰⁷ Ag		51.35 (24W48)					Ag ¹⁰⁷ , I = 1/2 (87M50)	
¹⁰⁸ Ag	A chem, n-capt (12A35); excit, cross bomb (1P38)		β^- 98.5%, EC 1.5% (12P52)	2.3 m (12A35, 12P48, 60M48, 37B39); 2.4 m (9F44)	1.5 scint spect (45G52)	0.45, 0.66 scint spect (12P52); 0.43, 0.60 scint spect (45G52)	 see Cd ¹⁰⁷ (18G52)	Pd-p-n (2D38, 17E39); Ag-n- γ (12A35, 9F44, 2S47, 9O49, 50H51, 36S51); Ag-e ⁻ -e ⁻ n (59S48); Ag ¹⁰⁷ -n- γ (9F44a); Ag- γ -n (37B39, 12P48, 60M48, 22E52); Ag-d-p (9K39, 9K40b); Cd-n-p (1P38)
^{109m} Ag	A chem, genet (2H41b)		IT (2H41b)	39.2 s (16B46c, 16B47); 40 s (40W51, 2H41b, 37W45b)		0.0875 spect conv (10C50b); 0.087 (e/ γ -6, K/L+M 0.75) spect conv (34H52); 0.087 (e/ γ -11, K/L+M 1.3) spect conv (75A9b); 0.087 spect conv (2H46, 16B47)	 see Cd ¹⁰⁷ (18G52)	daughter Pd ¹⁰⁹ (24S41, 7S49b); Ag-n-n (9F44); Ag- γ - γ (31F41, 37W45b, 24T45); Ag ¹⁰⁹ - γ - γ (40W51); Ag-e ⁻ -e ⁻ (37W45b); daughter Cd ¹⁰⁹ (2H41b, 16B45c, 2H46)
¹⁰⁹ Ag		48.65 (24W48)					Ag ¹⁰⁹ , I = 1/2 (87M50)	

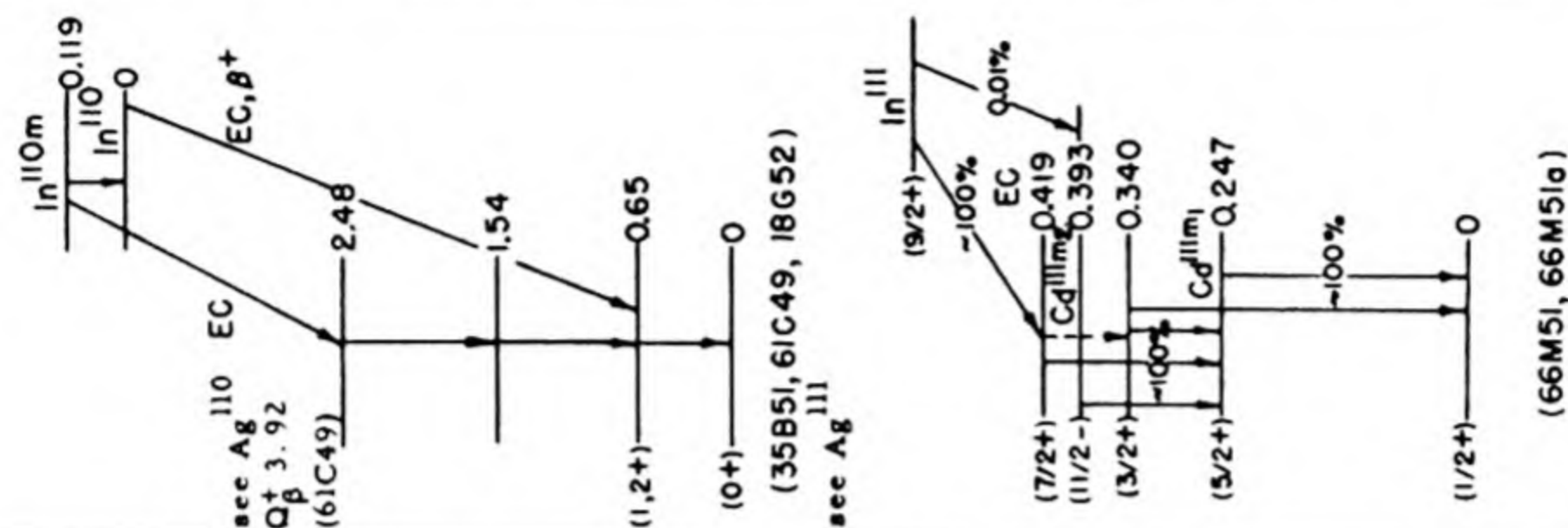
Ag^{110m}	A chem, n-capt (35R38); resonance neutron activation (18G46c); chem, sep isotopes, n-capt (18G46d); chem, mass spect (67B49a)	β^-, IT (7S49c, 56M50, 10C50a); 270 d (44G50, 10C50a); 225 d (12L38d)	with Ag ^{110m} and Ag ¹¹⁰ : 0.087 (-58%), 0.530 (-35%), 2.12 (-3%), 2.86 (-3%), others (7) spect (7S49c); 0.088 (65%), 0.520 (33%), 2.89 (-2%) spect (31A51); 0.590, 2.24, 2.91 spect (88S51a); 0.09 (coinc with γ), 0.57 (coinc with γ), 0.19 (?) abs, β - γ coinc (46M49); 0.09, 0.59 cl ch (2E49); 0.59 spect (11R47)	0.116 (e/ γ very large, K/L 1.3), 0.656 (e/ γ 0.0025), 0.676, 0.706, 0.759, 0.814, 0.885, 0.935, 1.389, 1.516 spect conv, spect, β - γ coinc, γ - γ coinc (7S49c); 0.116 (conv in Ag), 0.438, 0.446, 0.471, 0.499, 0.542, 0.575, 0.619, 0.657, 0.677, 0.705, 0.723, 0.764, 0.817, 0.884, 0.937, 1.384, 1.504 spect, spect conv (10C50a); 0.116 (K/L+M 1.8), 0.447, 0.618, 0.655 (K/L+M 4.3), 0.687, 0.706 (K/L+M 6.6), 0.740, 0.759 (K/L+M 6.5), 0.815 (K/L+M 4.1), 0.883 (K/L+M 4.2), 0.932 (K/L+M 6.5), 1.386 (K/L+M 6.5), 1.480, 1.506 (K/L+M 4.5) spect conv (31A51); 0.656 (K/L+M 14) spect conv (40K52); 0.66, 0.90, 1.40 spect conv, spect (11R47); -0.7, -0.9 (coinc with 0.7 γ) γ - γ coinc abs (5Y49); 1.7 < γ < 2.2 Be- γ -n reaction (38M50a); others (52M51)	 (7S49c, 18G52)	see 110 Q_{β}^- 3.02 (7S49c) Ag ^{110m} (5-) Ag ¹¹⁰ (1+) β^- (1.2+) (0+) (7S49c, 18G52)	Pd-d-2n (44G50); Ag-n- γ (35R38, 12L38d, 30A38, 14M38, 2S47); Ag ¹⁰⁹ -n- γ (18G46d); Ag ¹⁰⁹ -d-p (44G50); Ag-d-p (9K39, 9K40b, 65H44a); spall Sb (37L50); parent Ag ¹¹⁰ (56M50)
Ag¹¹⁰	A n-capt (12A35); sep isotopes, n-capt (9F44a); chem, genet (56M50)	β^- (1P38)	2.24 (-60%), 2.82 (-40%) scint spect (45G51a)	0.66, -0.9 (weak) scint spect (45G51a)	 (7S49c, 18G52)	Q_{β}^- 2.90 (HPS)	Ag-n- γ (12A35, 46G36, 9F44, 2S47); Ag ¹⁰⁹ -n- γ (9F44a); Cd-n-p (1P38); Cd- γ -p (42H46a, 42H47); daughter Ag ^{110m} (56M50)
Ag^{111m}	F genet (80S52)	[<5 m] (80S52)					Pd-d-n, parent Cd ^{111m2} (80S52)
Ag¹¹¹	A chem, excit (39K37); chem, excit, cross bomb (1P38)	β^- (39K37)	7.6 d (61S51c); 7.5 d (17J50, 39K37, 1P38)	γ_1 0.243 (e/ γ < 0.08), γ_2 0.340 (e/ γ -0.015) (γ_2/γ_1 -8) spect, spect conv, β - γ coinc, γ - γ coinc (17J50); 0.33 (-6.5%) abs (78S50)	 (17J50, 13E51c, 66M51, 66M51a, 18G52)	Q_{β}^- 1.04 (17J50)	Pd-d-n (39K37, 1P38, 9Z49); Pd-a-p (1P38); Ag-a-2p (66M51); Ag-t-p (29K47a); Cd-n-p (1P38); Cd- γ -p (42H47, 23D49a); spall Sb (37L50), Ta (22N52); spall-fission Bi (11G49, 66B51), Th (7N49a), U (6O48, 6F51), U (C) (13H51); fission Th (21T51), U (5N40a, 24S41, 61S51c), Pu (28F51); parent Cd ^{111m1} (13E51c), daughter Pd ¹¹¹ (39K37, 24S41, 17J50), daughter Pd ^{111m} (66M52)
Ag¹¹²	A chem, excit, cross bomb (1P38)	β^- (1P38)	3.20 h (74S51a); 3.2 h (1P38)	0.625, 1.40 (40A52b); 0.86 abs (77S51); no γ coinc with 3.5 β^- (74S51a)	 (17J50, 13E51c, 66M51, 66M51a, 18G52)		Cd-n-p (1P38); Cd- γ -p (42H47); In-n-a (1P38); spall Sb (37L50); spall-fission Bi (66B51), U (6O47, 6F51); fission Th (21T51), U233 (61S48); fission U, daughter Pd ¹¹² (5N40a, 5N40b, 24S41, 77S51)

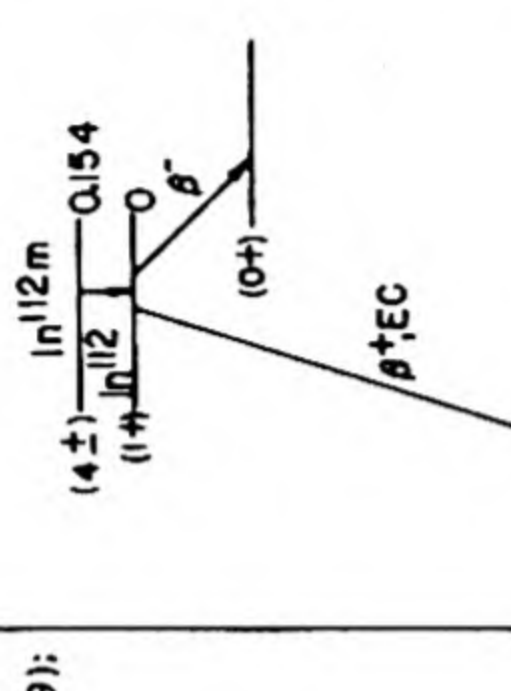

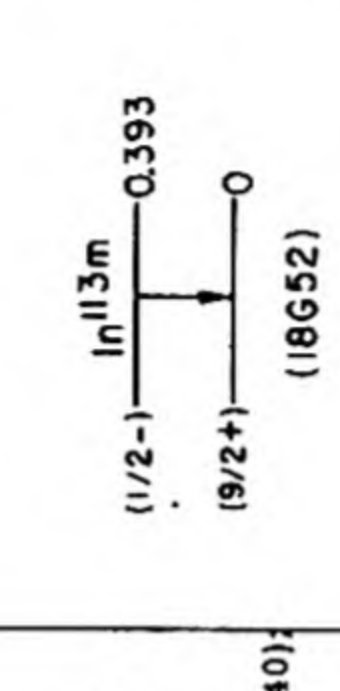
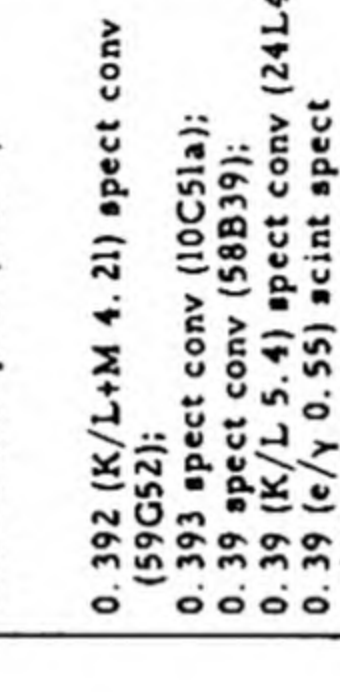
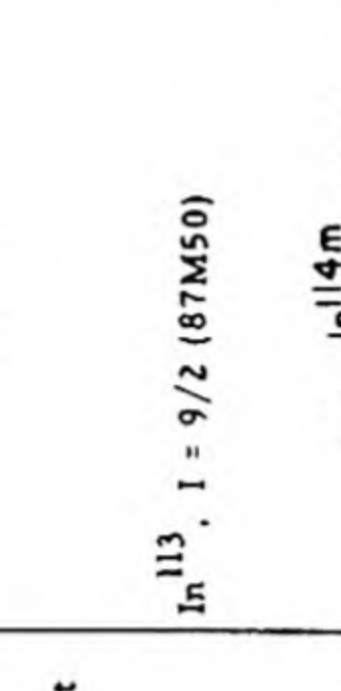
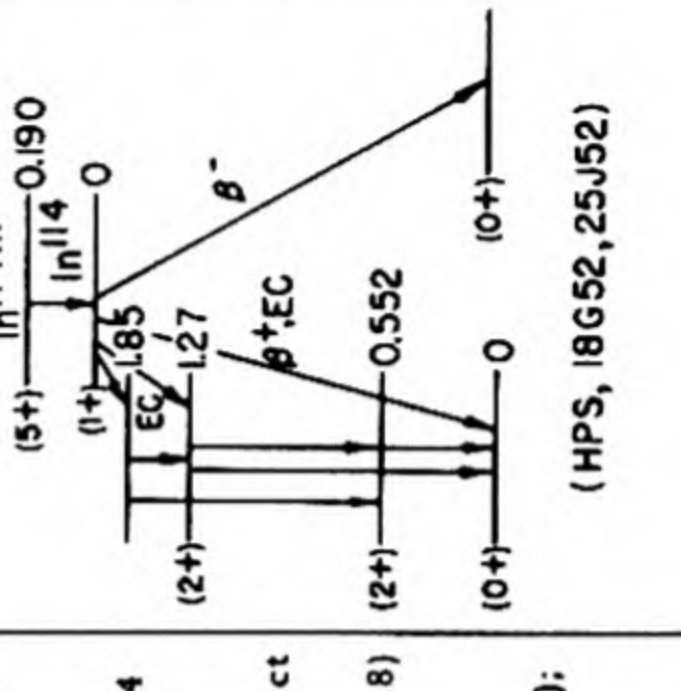
Isotope Z A	Class and identification	Percent abundance	Type of decay	Half-life	Energy of radiation in Mev		Disintegration energy and scheme	Method of production and genetic relationships
					Particles	Gamma-transitions		
¹¹³ 47Ag	A chem (21T47); chem, sep isotopes, excit (23D49a)		β^- (21T47)	5.3 h (21T47, 23D49a)	2.0 scint spect (27P51a); 2.1 abs (23D49a); 2.2 abs (21T47)	no γ (21T47, 23D49a)	$Q_{\beta}^- 2.0$ (HPS)	¹¹⁴ Cd γ -p (23D49a); Cd γ -p (23D49a); spall-fission Bi (66B51), U (6F51); fission U (21T47)
¹¹⁴ Ag	B chem (21T47, 66S47); chem, excit, sep isotopes (23D49a)		β^- (23D49a)	2 m (23D49a); 3 m (66S47)	hard β^- (23D49a)			¹¹⁴ Cd γ -p (23D49a); fission U (21T47, 66S47)
¹¹⁵ Ag	A chem (21T47, 66S47); chem, excit, sep isotopes (23D49a)		β^- (21T47)	20 m (23D49a, 66S47); 21 m genet (1W52); 22 m (21T47)	-3 abs (21T47, 23D49a)	no γ (23D49a)		Cd γ -p (23D49a); Cd γ -p (23D49a); fission U (21T47, 66S47); parent (91%) Cd ¹¹⁵ , parent (9%) Cd ^{115m} (1W52)
¹⁰⁴ 48Cd	B chem, excit (32J52)		β^+ (32J52)	59 m (32J52)	0.93 spect (32J52)	0.0666 (K/L+M -10), 0.0835 (K/L+M -15), 0.124, 0.134, other γ 's spect conv (32J52)		Ag-p-4n (32J52); parent (24 m) Ag ¹⁰⁴ (32J52)
¹⁰⁵ Cd	B cross bomb (44G50); chem, excit (32J52)		EC, β^+ (44G50)	57 m (44G50); 55 m (32J52); 65 m (54K52)	1.68 spect (32J52); 1.5 abs (44G50)	0.0255, 0.0494, 0.0525, 0.262, 0.293, 0.308, 0.312, 0.317, 0.321, 0.341, 0.347, 0.433, 2.1 spect conv, scint spect (32J52)		Pd-a-n (44G50); Ag-p-3n (32J52, 54K52); Cd-n-2n (44G50)
¹⁰⁶ Cd		1.215 (28L48)						
¹⁰⁷ Cd	A chem (5D39); chem, n-capt, sep isotopes (2H46)		EC 99+%, β^+ 0.31% (16B45d, 55B50)	6.7 h (5D39)	0.32 spect (16B45d, 16B45e)	0.846 (0.4%, e/ γ -10 ⁻³) spect, spect conv (16B45d, 16B45e); 0.7 abs (2H41); with Ag ^{107m} ; 0.094 (16B45c, 16B47, 6V39, 2H41)	$Q_{\beta}^+ 1.43$ (16B45d) (5/2, 7/2+) Cd ¹⁰⁷ EC<1% EC>99% 0.940 β^+ 0.094 (7/2+) Ag ^{107m} (1/2-) 0 (18G52)	Ag-p-n (5D39, 6V39); Ag-d-2n (9K39, 6A40, 9K40b, 2H41b); Ag-a-p-3n (2H46); Cd ¹⁰⁶ -n- γ (2H46, 18G46d); spall Sb (37L50); spall-fission U (6F51); parent Ag ^{107m} (6A40, 2H41b, 16B45c, 2H46, 16B47)
¹⁰⁸ Cd		0.875 (28L48)						
¹⁰⁹ Cd	A chem (9K40b); chem, n-capt, sep isotopes (2H46)		EC (L/K 0.28) (38M52); EC (16B46c); no β^+ (26D51)	470 d (44G50); 330 d (16B46c)		with Ag ^{109m} ; 0.0875 spect conv (10C50b); 0.087 (e γ / γ -6, K/L+M 0.75) spect conv (34H52); 0.087 (e/ γ >11, K/L+M 1.3) spect conv (7S49b)	Q_{EC} 0.16 calc (38M52) see Pd ¹⁰⁹ Cd ¹⁰⁹ EC (7/2+) Ag ^{109m} 0.087 (1/2-) 0 (18G52)	Pd-a-n (44G50); Ag-d-2n (9K40b, 2H41b, 44G50); Ag-a-pn (2H46); Cd ¹⁰⁸ -n- γ (2H46, 10C50b, 59C51); spall Sb (37L50); parent Ag ^{109m} (2H41b, 16B45c, 2H46, 16B46c)

Cd^{110}	12.39 (28L48)	IT (31F41, 37W45b)	48.6 m (66M51); 48.7 m (37W45b)	γ_1 0.150 (e/ γ -3, K/L 2.0), γ_2 0.246 (e/ γ 0.064, K/L 5.1) spect conv (66M51, 66M51a); γ_1 (e/ γ 2.3) (calc from 14S51, 66M51); γ_1 0.149, γ_2 0.247 scint spect (14S51); γ_1 0.146, γ_2 0.235 spect conv (15H48a)	see Ag^{111} and In^{111}	Cd^{110} , $I = 0$ (87M50)
Cd^{111m2}	A chem (27D38); chem, sep isotopes, n-capt (18G48a)					
Cd^{111m1}	A genet (20D49a)	IT (20D49a)	8×10^{-8} s delay coinc (20D50, 63B50, 52M51); 10×10^{-8} s delay coinc (13E51c)	0.247 scint spect (52M51)		
Cd^{111}		12.75 (28L48)				
Cd^{112}		24.07 (28L48)				
Cd^{113m}	A chem, excit (44G49); chem, excit, sep isotopes (60C50, 59C51)	β^- (60C50)	5.1 y (60C50)	0.59 scint spect (59C51); 0.5 abs (60C50)		
Cd^{113}		12.26 (28L48)				
Cd^{114}		28.86 (28L48)				

Isotope Z A	Class and identification	Percent abundance	Type of decay	Half-life	Energy of radiation in Mev		Disintegration energy and scheme	Method of production and genetic relationships
					Particles	Gamma-transitions		
Cd ^{115m} 48	A chem (10C39); chem, excit (2S47b); chem, sep isotopes, n-capt (10C50b)		β^- (10C39)	43 d (2S47b, 10C50b); 44 d (33G51h)	1.61 (-98%), 0.7 (-2%), -0.3 (weak) spect (61H52a); 1.5 abs (2S47b, 10C50b, 1W52); 1.4 abs; 0.4 (coinc with γ , ~1%) β - γ coinc abs (47G50) 1.7 abs (33G51h); -0.8 (-1.4%) abs (13E51a)	0.46, 0.50, 0.96, 1.28 scint spect, γ - γ coinc (61H52a); γ_1 0.48, γ_2 0.94 (coinc with γ_1), γ_3 1.30 (not coinc with γ_1 or γ_2) ($\gamma_1/\gamma_2/\gamma_3 \approx 13/100/40$) scint spect, γ - γ coinc (13E52), others (56G49, 52M51)	 Q β^- 1.63 (61H52a) Cd ^{115m} (11/2-) β^- Cd ¹¹⁵ (1/2+), In ^{115m} (5/2+), In ¹¹⁵ (1/2-), In ^{115g} (9/2+) (18G52)	Cd-d-p (10C39); Cd-n-y (2S47, 2S47b); Cd ¹¹⁴ -n-y (10C50b); Cd ¹¹⁶ -y-n (1W52); In-n-p (2S47b); spall Sb (37L50); spall-fission Bi (11G49), Th (7N49a), U (6O48, 6F51); fission Th (21T51), U (67M51); U233 (61S48), U235 (1W52), Pu (33G51h, 28F51); daughter (9%) Ag ¹¹⁵ (1W52)
Cd ¹¹⁵	A chem (10C37); chem, genet (18G38); chem, sep isotopes, n-capt (10C50b)		β^- (10C37)	53 h (1W52); 54 h (10C50b); 56 h (24L40, 67M51a)	1.11 (58%), 0.58 (42%) spect (10L52); 1.11 (-60%), 0.59 (-40%) spect (61H52a); -1 (-85%), -0.5 (-15%) β - γ coinc abs (1W52); others (26M49a, 10C50b, 67M51a)	0.335 (with In ^{115m}), 0.360, 0.500, 0.525 scint spect, γ - γ coinc (61H52a); 0.522 spect (28D50); 0.336, 0.344, 0.349, 0.363 (?), 0.369, 0.424, 0.452, 0.525, 0.559, 0.713 spect conv (10C50b); with In ^{115m} : 0.334 (10L52, 24L40, 61H49, 61H52a, 28D50, 20K51)	Q β^- 1.45 (61H52a) (18G52)	Cd-d-p (10C37, 10C39); Cd-n-y (18G38, 14M37, 2S47); Cd ¹¹⁴ -n-y (10C50b); Cd-n-2n (18G38); Cd-y-n (60M48); In-n-p (2S47b); spall Sb (37L50); spall-fission Th (7N49a), U (6O48, 6F51); fission Th (21T51), U233 (61S48), U235 (1W52), U (5N40a, 5N40b, 67M51a); parent In ^{115m} (18G38, 10C39, 5N40b, 67M51a, 1W52, 10L52); daughter (91%) Ag ¹¹⁵ (1W52)
Cd ¹¹⁶		7.58 (28L48)					Cd ¹¹⁶ , I = 0 (87M50)	
Cd ^{117m}	A chem, excit (10C39)		IT (51C52a)	3.0 h (51C52a); 2.9 h (25A52); 2.8 h (24L40); 2.7 h (67M51b)		with Cd ¹¹⁷ (51C52a): -1.2 abs (25A52)		Cd-d-p (10C39, 51C52a, 25A52); Cd-n-y (14M37, 18G38, 2S47, 51C52a); spall-fission U (6F51); fission U (5N40a, 5N40b, 67M51b); parent In ¹¹⁷ (18G38, 24L40, 67M51b), via Cd ¹¹⁷ (51C52a)
Cd ¹¹⁷	A chem, genet (51C52a)		β^- (51C52a)	-50 m (51C52a)	-1.6, -3.0 abs (51C52a)			Cd-n-y, Cd-d-p, parent In ¹¹⁷ parent In ^{117m} (51C52a)
In ¹⁰⁷	A chem, sep isotopes (68M49); mass spect (97M52)		β^+ (68M49)	30 m (97M52); 33 m (68M49)	-2 spect (68M49)			Cd ¹⁰⁶ -p-y, Cd ¹⁰⁶ -d-n (68M49)
In ¹⁰⁸	A chem, sep isotopes (68M49); mass spect (97M52)		β^+ (68M49)	50 m (97M52, 66M51); -55 m (68M49)	2.31 spect (66M51); 2.2 abs (37L50); -2 spect (68M49)	0.285 (<5%, K/L \approx 3) spect conv (66M51)	Q β^+ 3.3 (66M51)	Cd ¹⁰⁸ -d-2n (68M49); daughter Sn ¹⁰⁸ (68M49, 37L50, 66M51)

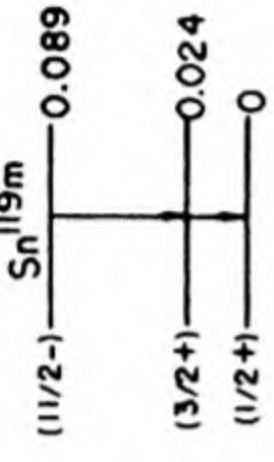
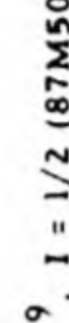
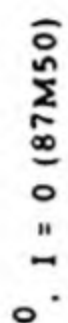



¹⁰⁹ In	A chem, excit (25T47); chem, mass spect (48G48); chem, excit, sep isotopes (68M49)	β^+ , EC (25T47, 68M49)	0.75 abs (68M49); -2 (weak) (25T47)	4.3 h (68M49); 4.2 h (66M51); 6.5 h (25T47); 5.2 h (48G48)	Ag- α -2n (25T47, 48G48, 66M51); Cd ¹⁰⁶ - α -p, Cd ¹⁰⁸ -d-n, Cd ¹⁰⁸ -p- γ (68M49)
^{110m} In	A chem (48G48); chem, genet energy levels Ag ¹¹⁰ (66M51a, 35B51)	EC 99+%, IT -0.3% (66M51)		5.0 h (66M51); 4.9 h (35B51); -5 h (48G48)	Ag- α -3n (48G48, 66M51)
¹¹⁰ In	A chem (58B39); chem, excit, mass spect (48G48)	β^+ , EC (61C49)	2.25 spect (61C49)	66 m (58B39, 35B51); 65 m (48G48)	Ag- α -n (19K39a, 25T47a, 48G48); Cd-p-n (58B39); Cd-d-2n (24L40)
¹¹¹ In	A chem (10C39); chem, excit (25T47a, 48G48); mass spect (48G48)	EC (24L40); no β^+ (lim 0.06%) (66M51); no β^+ (48G48)		2.84 d (66M51); 2.7 d (58B39, 10C39)	Ag- α - γ (112S51); Ag- α -2n (24L40, 25T47a, 48G48, 66M51); Cd-p-n (58B39); Cd- α -p (66M51); Cd-d-u (24L40); In-n-3n (10C39); spall Sb (37L50); parent (0.01%) Cd ^{111m2} (66M51a); parent Cd ^{111m1} (20D49a, 63B50)



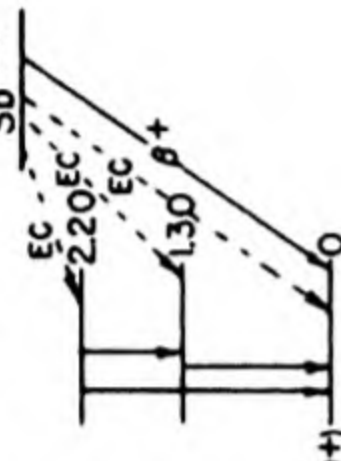
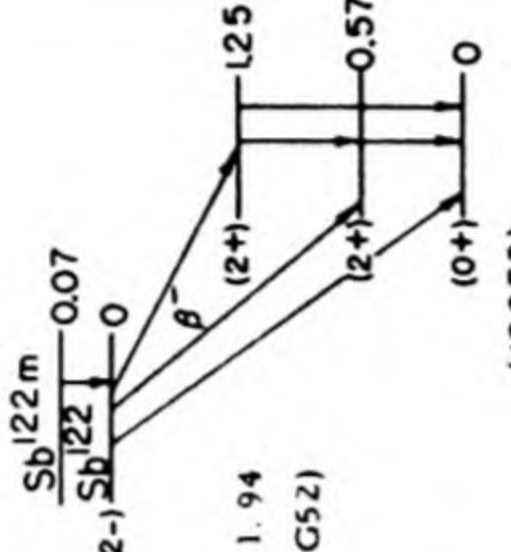
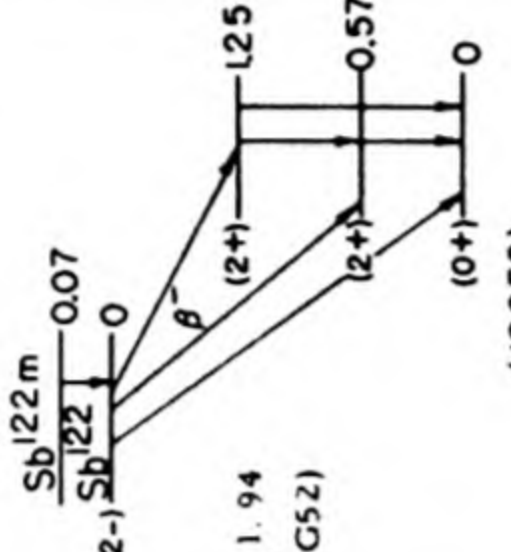
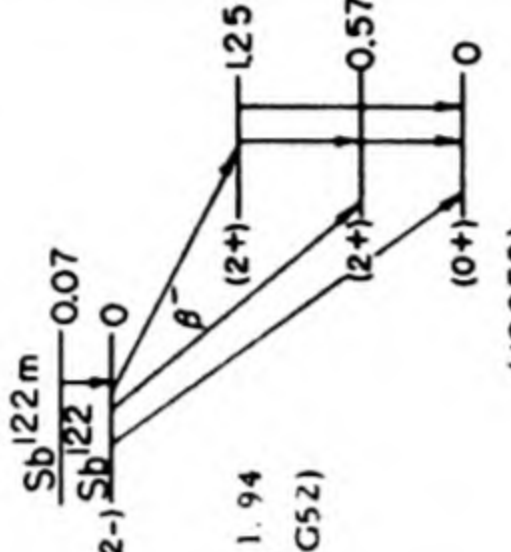
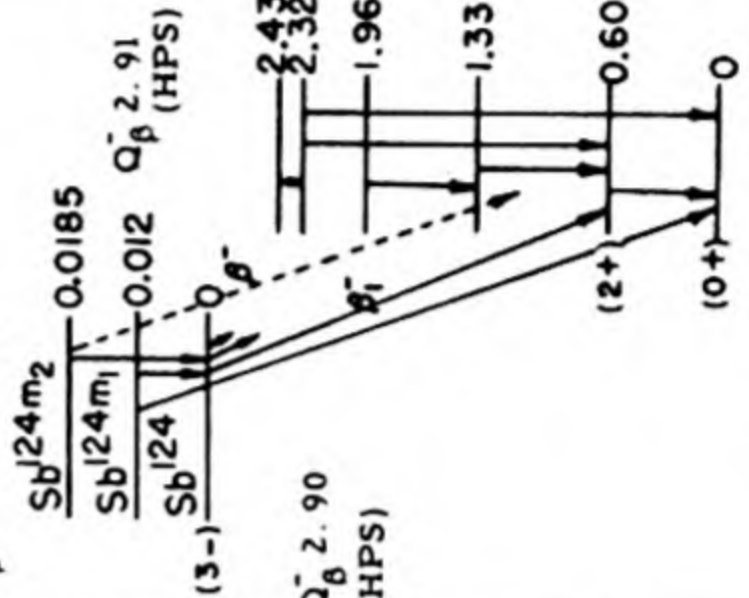
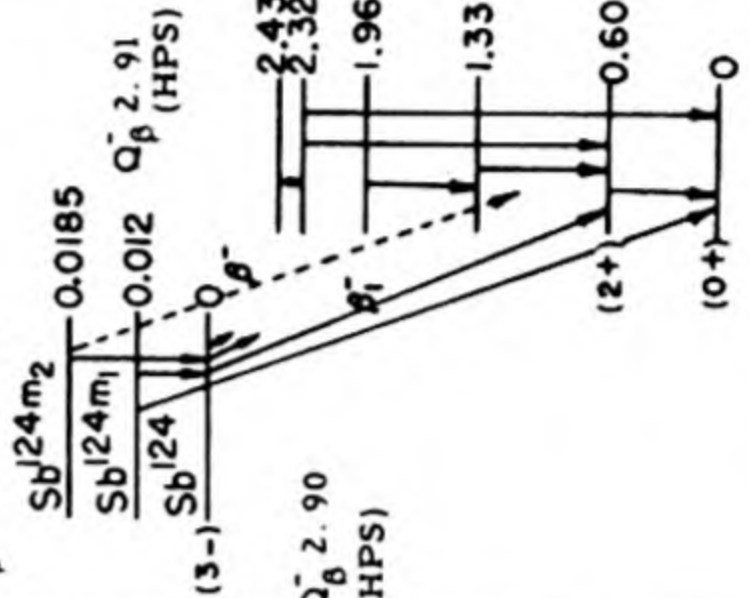
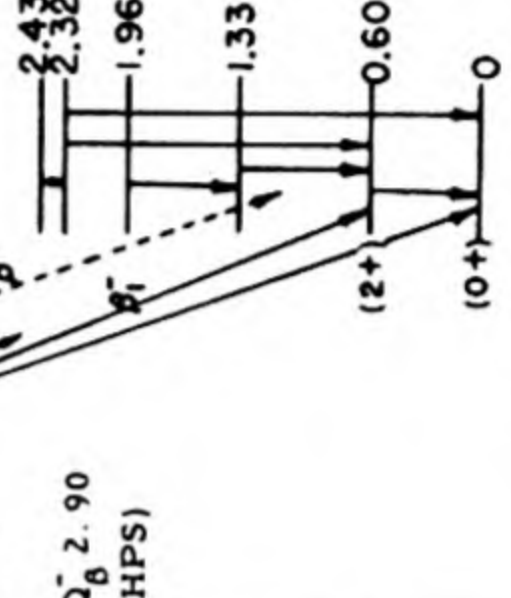
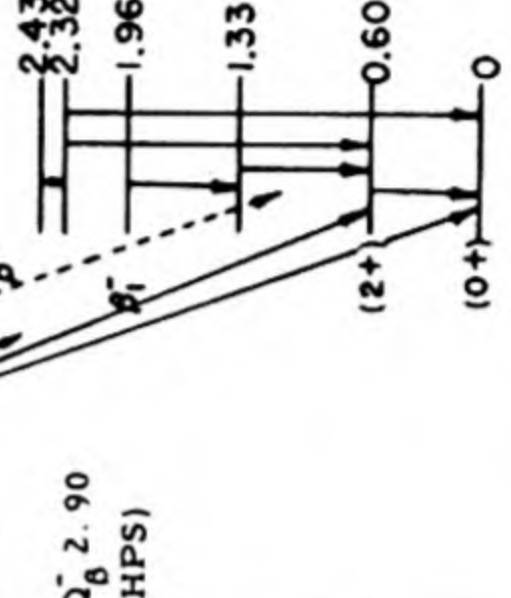
Isotope Z A	Class and identification	Percent abundance	Type of decay	Half-life	Energy of radiation in Mev		Disintegration energy and scheme	Method of production and genetic relationships
					Particles	Gamma-transitions		
¹¹² In 49	A chem (58B39); chem, cross bomb, excit (81S42); chem, excit (25T47a)		IT (81S42, 25T47a)	20.9 m (35B52); 20 m (58B39); 23 m (25T47a)		0.154 (e/γ > 4) spect conv (61C49); 0.16 spect conv (58B39); 0.16 (e/γ large) abs (25T47a)		Ag-α-n (81S42, 25T47a); Cd-d-n (24L40); Cd-p-n (58B39); In-n-2n (81S42, 25T47a); parent In ¹¹² (81S42, 25T47a, 49G50)
¹¹² In	A chem, cross bomb, excit (81S42); chem, excit (25T47a)		β ⁺ , β ⁻ , EC (25T47a, 61C49); β ⁺ /β ⁻ 2.7 (61C49)	14.5 m (35B52)	β ⁺ : 1.74 spect (61C49); 1.7 spect (24L40) β ⁻ : 0.67 spect (61C49)			Ag-α-n (81S42, 25T47a); In-n-2n (81S42, 25T47a); daughter In ^{112m} (81S42, 25T47a, 49G50)
¹¹³ In	E (31K52)		IT (31K52)	2.5 s (31K52)		0.153 scint spect (31K52)		In ¹¹³ -n (31K52)
^{113m} In	A chem, excit, genet (58B39)		IT (58B39)	104 m (24L40) 105 m (58B39)		0.392 (K/L+M 4.21) spect conv (59G52); 0.393 spect conv (10C51a); 0.39 spect conv (58B39); 0.39 (K/L 5.4) spect conv (24L40); 0.39 (e/γ 0.55) scint spect (62C52); -0.39 (e/γ 0.35, K/L 5.4) spect conv, ion ch (26T51)		Cd-p-n (58B39); Cd-d-n (24L40); In-n-n (63C48); In-γ-γ (11D47); daughter Sn ¹¹³ (58B39, 24S40a)
¹¹³ In		4.23 (24W48)						
^{114m} In	A chem, n-capt, excit (24L37, 14M38)		IT, no EC (82S52)	49 d (58B39)		γ ₁ with In ^{114m} , γ ₂ , γ ₃ , γ ₄ , γ ₅ , γ ₆ with In ¹¹⁴ ; γ ₁ 0.190, γ ₂ 0.552, γ ₃ 0.722, γ ₄ 1.27 (γ ₁ /γ ₂ /γ ₃ /γ ₄ = 100/18.6/ 18.6/1.2) spect (53M49); γ ₁ 0.192 (e/γ 4.2, K/L 1.10) spect conv, scint spect (82S51); γ ₁ 0.190 (K/L/M = 1.18/1.00/0.18) spect conv (59G52); γ ₁ 0.191 spect conv (10C48); γ ₁ (K/L 1.30) spect conv (40K52); γ ₁ 0.192 (e/γ 4, K/L 1.1), γ ₂ 0.55, γ ₃ 0.72 spect conv (56B49a); γ ₁ (e/γ 4) spect conv (10L49a); γ ₁ (K/L 1.16) spect conv (88S51a); γ ₄ /γ ₂ -0.06 scint spect, γ-γ coinc (23K52); γ ₅ 0.576, γ ₆ 1.30 (coinc with γ ₂) spect, γ-γ coinc (25J52)		Cd-p-n (58B39); Cd-d-n (24L40, 46M49); In-n-γ (24L37, 14M38, 46M49); In-d-p (24L40); In-γ-n (25W48, 22E52); In-n-2n (24L40); spall Sb (37L50); parent In ¹¹⁴ (49G50)

¹¹⁴ In	A excit (7C37, 37B37a, 24L37); n-capt, sep isotopes (18G48a)	β^- 697%, EC 23%, β^+ -0.01% (82S52); β^- 99+%, β^+ 0.015% (25J52); β^- 99+%, β^+ -0.01% (56B49a)	72 s (24L37, 58B39)	β^- : 1.984 spect (25J52); 1.98 spect (24L40); 2.01 spect (88S51a); 2.05 abs (46M49) β^+ : -1 abs (25J52); 0.65 spect (56B49a)	0.335 (e/y 0.98, K/L+M 3.76) spect conv (10L52, 59C52); 0.338 (e/y -1, K/L 5.0, K/L+M 4.0) spect conv (24L40); 0.335 (K/L 5.3) spect conv (20K51); 0.337 spect, spect conv (61H49); 0.336 spect (28D50)	Q_{β^-} 1.98 (25J52) Q_{β^+} 2.07 p-n threshold (66M51)	Cd-p-n (58B39); In-n-2n (24L37, 1F37); In-y-n (37B37a, 7C37, 25W48 22E52); In ¹¹³ -n-y (18G48a); daughter In ^{114m} (49G50)
^{115m} In	A chem, excit (18G38)	IT (24L39); β^- (11B49); IT 95%, β^- 5% (10L52)	4.50 h (11D47); 4.53 h (24L40)	0.83 spect (11B49)		Q_{β^-} 0.83 (HPS)	Cd-d-n (24L40); In-n-n (18G38, 63C48); In-p-p (58B39, 58B39a); In-a-a (38L39); In-e-e (64C40, 41W43, 41W49); In-y-y (17P38a, 64C39, 70M49, 83S51); fission Th (21T51), U (5N40a); daughter Cd ¹¹⁵ (18G38, 10C39, 5N40b, 67M51a, 1W52, 10L52) natural source (71M50)
¹¹⁵ In	A chem, sep isotopes (71M50)	β^- (71M50, 63C51)	6×10^{14} y sp act (71M50); -10 ¹⁴ y sp act (63C51)	0.63 abs (71M50)		Q_{β^-} 0.5 calc (11B49) In ¹¹⁵ , I = 9/2 (87M50) (1/2+)	
^{116m} In	A chem, n-capt (12A35); chem, excit, n-capt (24L37)	β^- (24L37)	53.93 m (57S49); 54.31 m (38R50); 54.05 m (50C47)	1.00 (51%), 0.87 (28%), 0.60 (21%) spect, β^- -y coinc (5S50); 0.85 spect (10C39); cl ch (48C40); 0.7 β^- -y coinc abs (26M48d)	2.090 (25%), 1.487 (21%), 1.274 (75%), e/y 5.7 x 10 ⁻⁴ , 1.085 (54%), e/y 8.4 x 10 ⁻⁴ , 0.406 (25%), 0.137 (3%) spect conv (5S50); 0.137, 0.171 spect conv (11K50a); others (20D42c, 48C40, 24L40, 18J45, 42W47) no y (14M38a)	Q_{β^-} 3.36 (5S50)	Cd-p-n (58B39); In-n-y (12A35, 14M38a, 34G46, 2S47, 50H51); In-d-p (24L37)
¹¹⁶ In	A n-capt (12A35); excit, n-capt (24L37)	β^- (24L37)	13 s (12A35, 10C39)	2.95 abs (35B46a, calc from 24L40); 2.8 cl ch (10C39)		Q_{β^-} 2.95 (HPS)	Cd-p-n (2D40); In-n-y (12A35, 24L37, 34G46, 2S47); In-d-p (24L37); Sn-y-p (42H47)
^{117m} In	A chem, genet (51C52a)	IT, β^- (51C52a)	-70 m (51C52a)	see In ¹¹⁷			daughter Cd ¹¹⁷ (51C52a)
¹¹⁷ In	A chem, excit (10C39)	β^- (10C39)	-2.5 h (51C52a); 1.95 h (24L40); 1.90 h (67M51b)	with In ^{117m} (7) (51C52a); 1.726 spect (20K51); 1.73 spect (10C39); 1.95 abs (67M51b) with In ¹¹⁷ ; 0.7 abs (51C52a)	0.161, 0.558 scint spect (20K51)		Cd-d-n (10C39, 24L40); Sn-y-p (42H47); fission U (5N40a, 5N40b, 67M51b), Pu (32K48); daughter Cd ^{117m} (18G38, 24L40, 67M51b); daughter Cd ¹¹⁷ (51C52a)

Isotope Z A	Class and identification	Percent abundance	Type of decay	Half-life	Energy of radiation in Mev		Disintegration energy and scheme	Method of production and genetic relationships
					Particles	Gamma-transitions		
¹¹⁸ In 49	B excit, sep isotopes (23D49b)		β^- (23D49b)	4.5 m (23D49b)	1.5 abs (23D49b)	γ (23D49b)		¹¹⁹ Sn - γ -p (23D49b)
¹¹⁹ In	B chem, excit, sep isotopes (23D49b)		β^- (23D49b)	17.5 m (23D49b)	2.7 abs (23D49b)	no γ (23D49b)		¹²⁰ Sn - γ -p (23D49b)
¹⁰⁸ Sn 50	B chem, sep isotopes (68M49)		EC (68M49)	4.0 h (66M51); 4.5 h (68M49)				¹⁰⁶ Cd - α -2n (68M49); Cd - α -2n (66M51); parent In ¹⁰⁸ (68M49, 37L50, 66M51); spall Sb (37L50)
¹¹¹ Sn	B chem, sep isotopes (66H49)		EC -71%, β^+ -29% (66M51)	35.0 m (66H49); 35 m (66M51)	1.51 spect (66M51); 1.5 abs (66H49)			Cd - α -3n (66M51); Cd ¹⁰⁸ - α -n (66H49)
¹¹² Sn		0.95 (1B50)						
¹¹³ Sn	A chem, excit (58B39, 12L39c)		EC, no β^+ (58B39); EC (L/K -0.8) (26T51)	112 d (19N50); 118 d (10C51a); 105 d (58B39)		with In ^{113m} : 0.393 (10C51a, 58B39, 24L40, 62C52, 26T51); 0.401 (weak), 0.255 (weak) spect conv (10C51a); no 0.09 γ (65C47, 26T51, 10C51a, 63M51a, 28B51)	Q_{EC} 0.43 calc (26T51) (HPS)	Cd - α -n (12L39c); In -p-n (58B39); In -d-2n (65C47); Sn -d-p (12L39c); Sn - γ -n (60M48); Sn - γ - γ (2547, 28B51); Sn ¹¹² -n- γ (19N50, 63M51a, 10C51a); spall Sb (37L50); parent In ^{113m} (58B39, 24S40a)
¹¹⁴ Sn		0.65 (1B50)						
¹¹⁵ Sn		0.34 (1B50)						
¹¹⁶ Sn		14.24 (1B50)						
^{117m} Sn	A chem (12L39c); chem, sep isotopes, cross bomb (68M50)		IT (68M50)	14.0 d (10C51a); 15 d (19N50)		0.159 (e/ γ very large, K/L 2.2), 0.162 (e/ γ 0.10) spect conv, e- γ coinc, x- γ coinc (63M50); 0.156 (e/ γ large, K/L -7), 0.159 spect conv (10C51a); 0.157 (K/L 2.2) spect conv (61H50a); 0.152 (K/L 2.4) spect conv (19N50)	 (63M50, 18G52)	Cd ¹¹⁴ - α -n (68M50); Cd - α -n (12L39c); Sn ¹¹⁶ -n- γ (63M50, 19N50); Sn ¹¹⁶ -d-p, Sn ¹¹⁸ -n-2n (68M50); Sn ¹¹⁷ -n-n (68M50, 19N50); spall Sb (37L50)
¹¹⁷ Sn		7.57 (1B50)						
¹¹⁸ Sn		24.01 (1B50)						

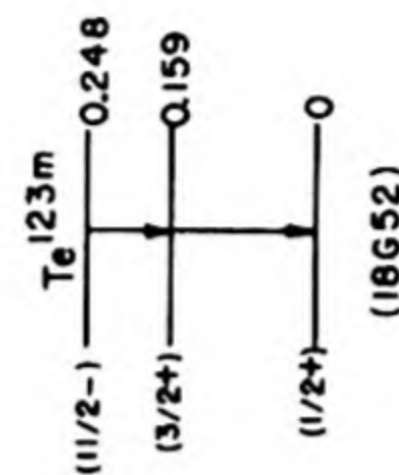
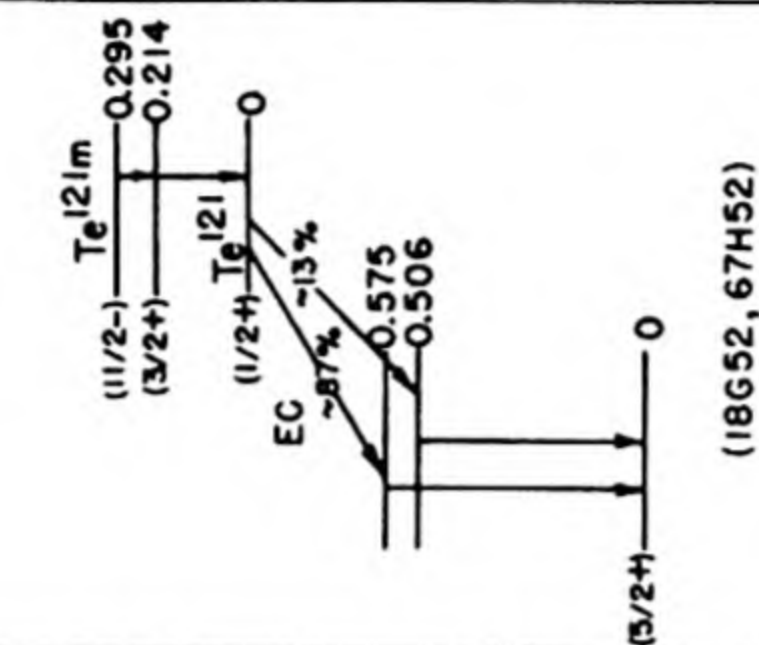
¹¹⁸ Sn	A chem, n-capt, sep isotopes (63M50)	IT (63M50)	-250 d (63M50); -245 d (19N50)	Y ₁ 0.0653 (K/L 0.51, L/M -4), Y ₂ 0.0242 (L/M -4) spect conv (67H51); Y ₂ 0.0238 (e/γ -7) scint spect, ion ch, γ-γ coinc (28B51); Y ₁ 0.065, Y ₂ 0.024 scint spect, ion ch conv (17S51b); Y ₁ 0.064 (K/L 0.82) spect conv (19N50)		Sn ¹¹⁸ -n-γ (63M50, 19V50, 17S51b, 28B51)
¹¹⁹ Sn	8.58 (1B50)					Sn ¹¹⁹ , I = 1/2 (87M50)
¹²⁰ Sn	32.97 (1B50)					Sn ¹²⁰ , I = 0 (87M50)
^{121m} Sn	E sep isotopes, n-capt (19N50)					Sn ¹²⁰ -n-γ (19N50)
¹²¹ Sn	A chem, excit (12L39c); chem, sep isotopes (37L48a)	β ⁻ (19N50) β ⁻ (12L39c)	>400 d (19N50) 27.5 h (19N50); 28 h (23D49c); -27 h (6F51)	no γ (23D49c, 37L48a, 7N49b); others (52M51)		Sn-d-p (12L39c); Sn-n-γ (12L39c, 2S47); Sn ¹²⁰ -d-p (37L48a, 39L49, 7N49b); Sn ¹²⁰ -n-γ (39L49, 23D49c, 19N50); Sn ¹²² -n-2n (39L49); Sb-d-a (37L50); spall-fission Th (7N49a), U (6O48, 6F51)
¹²² Sn	4.71 (1B50)					
¹²³ Sn	A chem (12L39c); chem, sep isotopes, excit (7N49b, 39L49, 19N50)	β ⁻ (12L39c)	39.5 m (23D49c); 40 m (12L39c, 39L49, 19N50); 41.5 m (6O48); 39 m (7N49b)	0.153 spect conv, β-e coinc (23D49c); 0.153 scint spect (76B51c); others (52M51)		Sn-d-p (12L39c); Sn-n-γ (2S47); Sn-n-2n (1P37); Sn-γ-n (6O48, 7H49); Sn ¹²⁴ -d-t (7N49b); Sn ¹²² -n-γ (23D49c, 39L49, 19N50); Sn ¹²⁴ -n-2n (39L49)
¹²³ Sn	A chem (40L46, 40L51); chem, sep isotopes, cross bomb (39L49)	β ⁻ (40L51)	136 d (38G51); 125 d (10C51a); 130 d (39L49, 7N49b, 40L51); 126 d (19N50)	no γ (39L49, 7N49b, 19N50, 10C51a, 38G51)		Sn ¹²² -n-γ (39L49, 19N50); Sn ¹²² -d-p, Sn ¹²⁴ -n-2n (39L49); Sn ¹²⁴ -d-t (7N49b); Sb-n-p (7N49b); spall-fission Th (7N49a), U (6F51); fission U (38G46, 40L51), U233 (38G48, 38G51), U235 (38G51)
¹²⁴ Sn	5.98 (1B50)					

Isotope Z A	Class and identification	Percent abundance	Type of decay	Half-life	Energy of radiation in Mev		Disintegration energy and scheme	Method of production and genetic relationships
					Particles	Gamma-transitions		
¹²⁵ ₅₀ Sn	A chem, excit, n-capt (12L39c); chem, sep isotopes (23D50a, 39L49, 19N50)		β^- (12L39c)	9.5 m (19N50); 9.8 m (39L49)	2.04, 1.17, 0.51 (7) spect (23D50a); 2.06, -0.5 abs (19N50)	0.326, others >1 (weak) spect, spect conv (23D50a); 0.38 (coinc with 2.06 β^-) abs, β - γ coinc (19N50); 1.37 (weak) scint spect (76B51c)	Q_{β}^- -2.4 (HPS)	Sn-d-p (12L39c); Sn-n-y (12L39c, 23S47, 2547); Sn ¹²⁴ -n-y (39L49, 23D50a, 19N50)
¹²⁵ ₅₀ Sn	A chem (12L39c); chem, excit, sep isotopes (39L49); chem, sep isotopes, n-capt, genet (19N50)		β^- (12L39c)	9.4 d (19N50); 10.0 d (39L49); 9.5 d (7N49b)	2.37 (-95%), 0.40 (-5%) spect (61H50b); 2.33 spect (24K50b); -0.5 (10%) β - γ coinc abs (26M52a); others (65C47, 7N49b, 39L49, 77S51a)	1.90 scint spect, abs (76B51d); 1.67 coinc abs sec (26M52a)	Q_{β}^- -2.4 (HPS)	Sn-n-y (12L39c, 2547); Sn-d-p (12L39c, 65C47); Sn ¹²⁴ -n-y (39L49, 19N50); Sn ¹²⁴ -d-p (39L49); spall-fission Th (7N49a), U (6F51); fission U ²³³ (61S48, 38G51), U (16H43b, 77S51a), U ²³⁵ (38G51); parent Sb ¹²⁵ (19N50); not parent Sb ¹²⁵ (7N49b)
¹²⁶ ₅₀ Sn	B chem, genet (80B51)		β^- (80B51)	-50 m yield (80B51)				fission U ²³⁵ , parent Sb ¹²⁶ (80B51)
¹²⁷ ₅₀ Sn	A chem, genet (80B51)		β^- (80B51)	1.5 h yield (80B51)				fission U ²³⁵ , parent Sb ¹²⁷ (80B51)
¹¹⁶ ₅₁ Sb	A chem, excit, mass spect (27T49)		β^+ (27T49)	60 m (27T49)	-1.45 spect (27T49)			In-a-3n (27T49)
¹¹⁷ ₅₁ Sb	A chem (12L39d); chem, excit, mass spect (27T49)		EC (65C47)	2.8 h (65C47, 27T49)		0.156 spect conv (27T49)		In-a-2n (27T49); Sn-d-n (12L39d, 65C47); Sn-p-n (65C47); spall I (π) (51W52)
¹¹⁸ ₅₁ Sb	B excit (27R40)		β^+ (37L48a)	3.5 m (37L48a); 3.6 m (27R40)	3.1 abs, spect (37L48a)			In-a-n (38L39, 27R40); Sn-p-n (2D40); daughter Te ¹¹⁸ (37L48a)
¹¹⁸ ₅₁ Sb	A chem, cross bomb (65C47); chem, excit, mass spect (27T49)		EC (65C47)	5.1 h (65C47, 27T49)	e -0.2 abs (65C47)	0.260 spect conv (27T49); 1.5 abs (65C47)		In-a-n (65C47, 27T49); Sn-d-n (65C47)
¹¹⁹ ₅₁ Sb	B chem, cross bomb (65C47)		EC (65C47)	39 h (65C47, 37L48a)		no γ (65C47); Sn K-x (65C47, 37L48a)		Sn-d-n, Sn-p-n (65C47); spall Sb (37L48a); daughter Te ¹¹⁹ (37L48a)
¹²⁰ ₅₁ Sb	D chem, sep isotopes (37L48a)		EC (37L48a)	6.0 d (37L48a)		-1.1 abs (37L48a)		Sb-d-p2n (37L48a); Sn ¹²⁰ -d-2n (37L48a); spall-fission Bi (11G49); not found; Sn-p, Sb-y (47B51); Sb-x rays (30K51a)

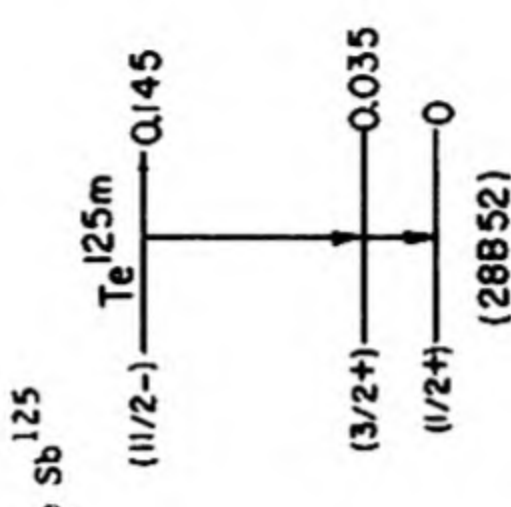
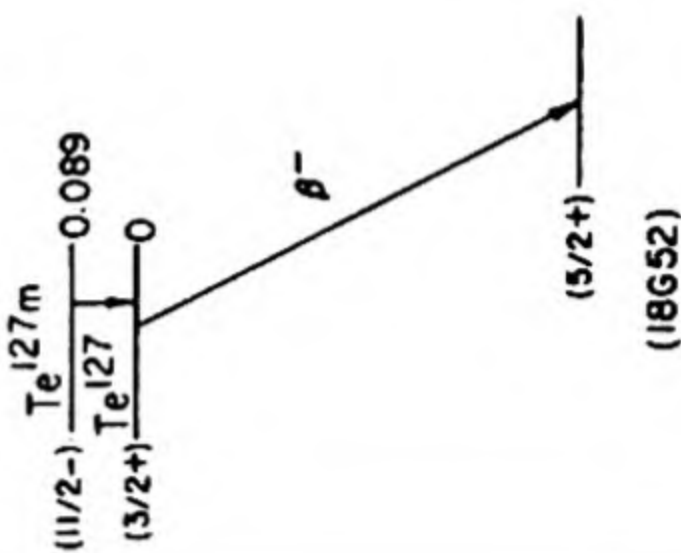

Sb^{120}	A chem, excit (37B39, 6H37, 7C37); chem, excit, cross bomb (12L37a)	57.25 (24W48)	ρ^+, EC (47B50)	16.4 m (22J50); 16.6 m (12P48); 17 m (6H37, 12L39d)	1.70 spect (47B50)	γ_1 0.90, γ_2 1.30, γ_3 2.20 ($\gamma_1/\gamma_2/\gamma_3 = 0.08/0.35/0.04$) (e/γ very small) spect (47B50)	Q_β^+ 2.7 (47B50)	 (47B50)	Sn-d-n (12L39d); Sn-p-n (47B50); Sn^{120} -d-2n (37L48a); Sb-n-2n (1P37, 6H37, 21J44, 7C37); Sb-y-n (37B39, 12P48, 27M49, 25W48, 22J50); Sb-d-t (9K41a); Sb-p-pn (23R46)
Sb^{121}							$Sb^{121}, I = 5/2$ (87M50)	 (18G52)	Sb-n-y (38M47); Sb^{121} -n-y (38M51, 31K51)
Sb^{122m}	A chem, n-capt, sep isotopes (38M47)		IT (38M47)	3.5 m (38M47)		0.068 scint spect (38M51); 0.059, 0.074 ion ch (31K51)		 (18G52)	Sn-d-2n (12L39d); Sn-p-n (47B51); Sb-d-p (12L39d); Sb-y-n (22J50, 47B51); Sb^{122m} -n-y (12A35, 12L39d, 2547, 50H51); spall Sb (37L50), I (-) (51W52); spall-fission Bi (11G49)
Sb^{122}	A chem (12A35); chem, cross bomb (12L39d)		ρ^- (12L39d)	2.80 d (47B51); 2.8 d (12L39b)	β_2 1.46 (coinc with γ) β - γ coinc spect (23M51); β_1 1.94, β_2 1.36 spect (43M46); β_1 1.8, β_2 1.2 abs, coinc abs (26M48d); β_1 1.8 abs (14M40)	0.568 spect (28C48d, 28K48); 0.57 spect conv (11R47); 0.56 (e_K/γ 0.0049), 0.68 (51G52)		 (18G52)	
Sb^{123}		42.75 (24W48)	IT, ρ^- (38M47)	21 m (38M47)		0.0185 (e/γ very large) (18G50)	$Sb^{123}, I = 7/2$ (87M50)	 (18G52, HPS)	Sb-n-y, Sb^{123} -n-y (38M47)
Sb^{124m2}	A chem, n-capt, sep isotopes (38M47)		IT, ρ^- (38M47)	1.3 m (38M47)	3.2 abs (38M47)	0.012 (e/γ very large) (18G50)		 (18G52, HPS)	Sb-n-y, Sb^{123} -n-y (38M47)
Sb^{124m1}	A chem, n-capt, sep isotopes (38M47)		ρ^- (12L39d); no ρ^+ , no EC (10L50b)	60 d (12L39d)	β_1 2.291 (21%), β_2 1.69 (7%), β_3 0.95 (7%), β_4 0.68 (26%), β_5 0.50 (39%) spect (28C48d, 10L50b); β_1 2.37 (21%), β_2 1.62 (8%), β_3 1.00 (9%), β_4 0.65 (44%), β_5 0.48 (18%) spect (28K48); β_4 0.654 spect (7J47); others (54H43, 47M47, 43M46, 14M40, 37W47)	0.121, 0.607, 0.653, 0.730, 1.708, 2.04 spect, aspect conv (28C48d, 10L50b); 0.61 γ (40-50%, e_K/γ 0.0043) spect, aspect conv (44M52a); 0.61 γ (e_K/γ 0.0036) aspect conv (94H52); 0.603 (-100%, e/γ -0.002), 0.650, 0.714, 1.708, 2.06 spect, aspect conv (28K48); 0.598, 0.645, 0.817, 1.67, 2.07 spect (13J49b); others (11R47, 14M40, 42W47, 52M51, 85S51, 89S52, 39D51, 39D51a, 42K45, 47M47)	Q_β^- 2.90 (HPS)	 (18G52, HPS)	Sn-p-n (47B51); Sn-d-2n (12L39d); Sb-d-p (12L39d, 54H43, 42K45); Sb-n-y (12L39d, 2547); spall Sb (37L50); Te-d-a (28T38); I-n-a (12L39d); spall-fission Bi (11G49)
Sb^{124}	A chem (12L37a); chem, excit, cross bomb (12L39d)							 (18G52, HPS)	

Isotope Z A	Class and identification	Percent abundance	Type of decay	Half-life	Energy of radiation in Mev		Disintegration energy and scheme	Method of production and genetic relationships
					Particles	Gamma-transitions		
¹²⁵ Sb 51	A chem (12L39d); chem, n-capt (84S51)		β^- (67C51)	-2.7 y (40L51a)	0.616 (18%), 0.299 (49%), 0.128 (33%) spect (7S49d); 0.621, 0.288, others (?) spect (28K49); others (38G46, 15J49, 26M49b, 84S51)	0.637, 0.601, 0.465, 0.425, 0.175, 0.035 spect, spect conv, coinc (7S49d); 0.646 (weak, e/y very small), 0.609 (strong), 0.466 (weak, e/y very small), 0.431 (strong), 0.174 (strong), 0.125 (weak) spect, spect conv, coinc (28K49); with ¹²⁵ Te: 0.110, 0.035 (28B52, 10C51a, 7S49d, 28K49, 67H49a)	<p>Q_{β} 0.76 (7S49d)</p> <p>Sn-d-n (12L39d); Sn-n-γ, β^- decay (7S49d, 23F48, 84S51); spall-n-fission Th (7N49a); fission ²³⁵U (38G48), ²³⁵U (67C51, 40L51a, 84S51); parent ¹²⁵Te (23F48, 28K49); daughter (9.4 d) ¹²⁵Sn (19N50); not daughter (9.4 d) ¹²⁵Sn (7N49b)</p>	
¹²⁶ Sb	B chem, excit (80B51)		β^- (80B51)	9 h (80B51)	-1 abs (80B51)	0.90, -0.4 (both coinc with β^-) scint spect, β -γ coinc (80B51)	fission ²³⁵ U, daughter ¹²⁶ Sn (80B51)	
¹²⁶ Sb	E chem (80B51)		β^- (80B51)	10 m (80B51)			fission ²³⁵ U (80B51)	
¹²⁶ Sb	D chem (38G46)		β^- (38G46)	28 d (38G46); -30 d (80B51)	1.9 (38G46)		fission ²³⁵ U (38G46), ²³⁵ U (80B51)	
¹²⁷ Sb	A chem, genet (32A39)		β^- (32A39)	93 h (76S51b); 95 h (38G46)	1.2 abs (76S51b); 0.8 abs (38G46)	0.72 abs (76S51b)	fission ²³³ U (61S48), ²³⁵ U (38G51, 80B51), ²³⁵ U (32A39, 38G46, 76S51b), Pu (32K48); parent ¹²⁷ Te (32A39, 33G51); parent (84%) ¹²⁷ Te, parent (16%) ¹²⁷ Te (78B48); daughter ¹²⁷ Sn (80B51)	
¹²⁹ Sb	A chem, genet (32A39)		β^- (32A39)	4.2 h (32A39)			fission ²³⁵ U (32A39), Pu (32K48); parent ¹²⁹ Te (32A39)	
¹³⁰ Sb	D chem, excit (fission yield) (80B52)		β^- (80B52)	40 m (80B52)			fission ²³⁵ U (80B52)	
¹³⁰ Sb	D chem, excit (fission yield) (30P52a)		β^- (80B52)	12 m (30P52a); 10 m (80B52)			fission ²³⁵ U (80B52, 30P52a)	
¹³¹ Sb	A chem, genet (30P51, 68C51)		β^- (30P51)	23.1 m (30P51); -20 m (68C51)			fission ²³⁵ U, parent ¹³¹ Te, parent ¹³¹ Te (30P51, 68C51)	
¹³² Sb	B chem, genet (32A39)		β^- (32A39)	2 m (30P51); -5 m (32A39); -2 m (68C51)			fission ²³⁵ U (32A39, 30P51, 68C51); parent ¹³² Te (32A39, 30P52a)	
¹³³ Sb	B chem, genet (30P51)		β^- (30P51)	4.4 m (30P51); 4.2 m (68C51)			fission ²³⁵ U (30P51, 68C51); parent ¹³³ Te (30P51)	

$^{134,135}\text{Sb}$	D chem (30P51)		β^- (30P51)	-50 s (30P51); 45 s (68C51)	fission U (30P51, 68C51)
$^{52}\text{Te}^{<118}$	D chem (37L48a)		β^+ (37L48b)	2.5 h (37L48a)	spall Sb (37L48a), I (w) (51W52)
^{118}Te	B chem, genet (37L48a)		EC (37L48a)	6.0 d (37L48a)	Sb-d-5n, parent (4 m) Sb ¹¹⁸ (37L48a, 37L50); spall I (w) (51W52); spall-fission Bi (11G49)
^{119}Te	B chem, genet (37L48a)		EC (37L48a)	4.5 d (37L48a)	Sb-d-4n, parent Sb ¹¹⁹ (37L48a, 37L50); spall-fission Bi (11G49)
^{120}Te		0.089 (1B50)			
$^{121\text{m}}\text{Te}$	A chem, excit, cross bomb (13S40); chem, n-capt, sep isotopes (10C51a)		IT (14E46a)	154 d (67H51d); 143 d (14E46a); 125 d (13S40); 140 d (10C51a)	Sn-a-n (13S40); Sb-d-2n (13S40, 14E46a, 43K50); Sb-p-n (13S40, 14E46a); spall Sb (37L50); Te ¹²⁰ -n- γ (10C51a); parent Te ¹²¹ (82B46)
^{121}Te	A chem, genet (14E46a, 82B46)		EC (14E46a)	17 d (14E46a); -16 d (82B46)	Sb-d-2n (14E46a); Sb-p-n (14E46a); daughter Te ^{121m} (82B46); daughter ^{121}I (74M50)
^{122}Te		2.46 (1B50)			
$^{123\text{m}}\text{Te}$	A chem, n-capt, sep isotopes (67H49)		IT (67H49)	104 d (67H51d); 121 d (10C51a)	Sb-d-2n (43K50); Te ¹²² -n- γ (67H49, 43K50, 68H51, 10C51a)
^{123}Te		0.87 (1B50)			

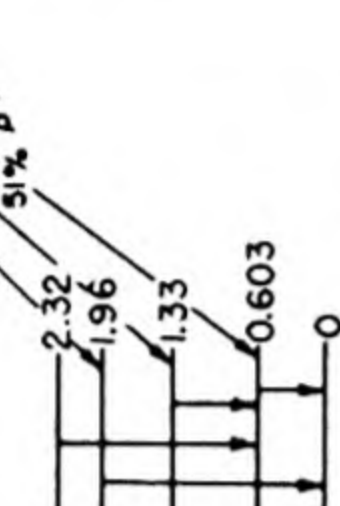
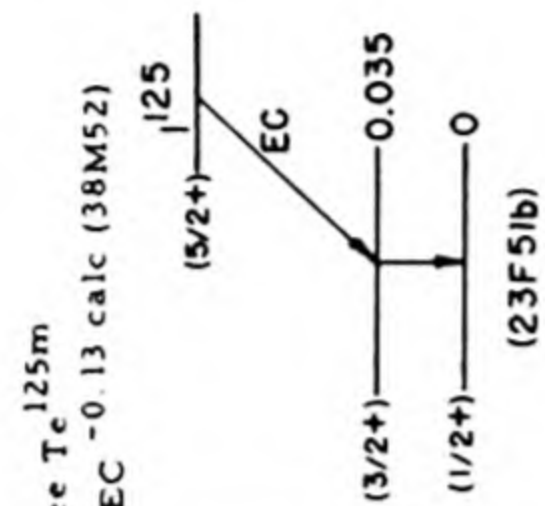
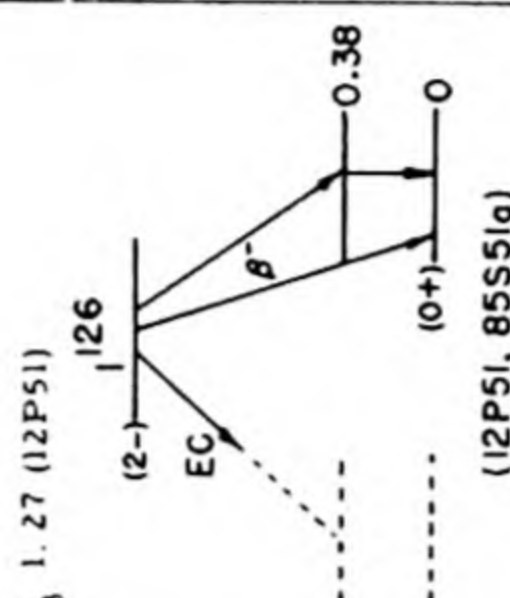
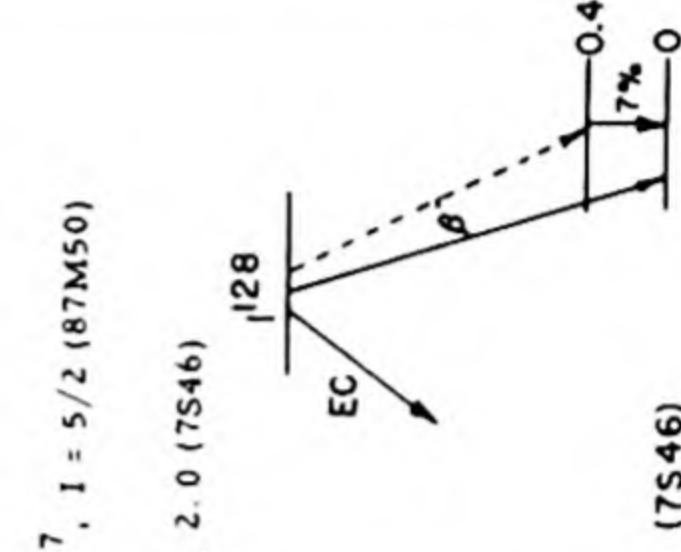
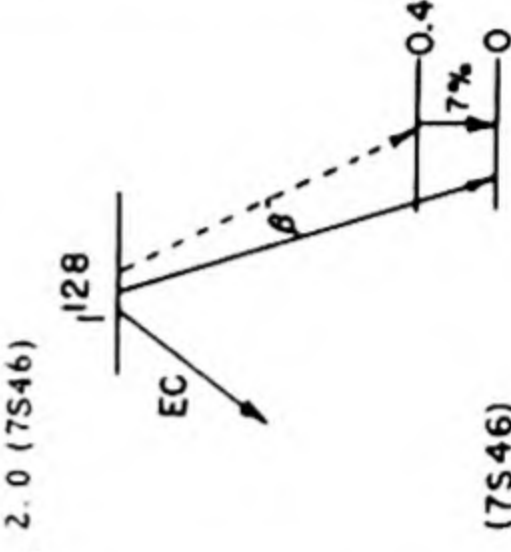


Te¹²³, I = 1/2 (87M50)

Isotope Z A	Class and identification	Percent abundance	Type of decay	Half-life	Energy of radiation in Mev		Disintegration energy and scheme	Method of production and genetic relationships
					Particles	Gamma-transitions		
¹²⁴ Te 52 125m	A chem, genet (23F48)	4.61 (1B50)	IT (23F48)	58 d (67H49a, 67H51d)		0.110 (e _K /γ -160, K/L+M 1.15), 0.0355 (e _K /γ -11.7, K/L/M = 7.3/1.0/0.18) spect conv, ion ch, scint spect, x-γ coinc, x-x coinc (28B52); 0.110, 0.0353 spect conv (10C51a); 0.110 (K/L+M 1.1), 0.035 spect conv (7S49d); 0.110 (K/L 1.2) spect conv (28K49); 0.109 (e/γ >100, K/L-1.5, L/M -3.5) spect conv (67H49a); otherm (67H49, 23F50a, 52M51, 28B49)	see Sb ¹²⁵ 	Te ¹²⁴ -n-γ (67H49); daughter Sb ¹²⁵ (23F48, 28K49); not daughter I ¹²⁵ (lim 0.05%) (23F51b)
Te ¹²⁵		6.99 (1B50)					Te ¹²⁵ , I = 1/2 (87M50)	
Te ¹²⁶		18.71 (1B50)					Te ¹²⁶ , I = 0 (87M50)	
Te ^{127m}	A chem, excit, genet (13S40)		IT (13S40)	115 d (10C51a); 90 d (13S40)		0.0885 (K/L 0.75) spect conv (67H49, 67H49a); 0.0887 spect conv (10C51a); 0.086 (e/γ very large, K/L 0.75) spect conv (2H41)		Te-n-γ (13S40, 2S47); Te-d-p (13S40); Te ¹²⁶ -n-γ (67H49); I-n-p (13S40); fission U (38G46, 33G51i, 43W48), U ²³³ (61S48, 38G48, 38G51), U ²³⁵ (38G51); parent Te ¹²⁷ (13S40, 33G51i, 43W51); daughter (16%) Sb ¹²⁷ (78B48)
Te ¹²⁷	A chem (28T38, 32A39); chem, excit, cross bomb (13S40)		β ⁻ (32A39)	9.3 h (13S40)	0.7 abs (33G51i)	no γ (33G51i)		Te-n-γ (13S40, 2S47); Te-d-p (28T38, 13S40); Te-n-2n (28T38); I-n-p (13S40); fission U (32A39, 13S40, 43W48, 33G51i), U ²³³ , U ²³⁵ (38G51); daughter Te ^{127m} (13S40, 33G51i, 43W51); daughter Sb ¹²⁷ (32A39, 33G51i), (84%) (78B48)
Te ¹²⁸		31.79 (1B50)					Te ¹²⁸ , I = 0 (87M50)	

¹²⁹ Te	A chem, genet (13S40)	IT (13S40)	33.5 d (10C51a); 32 d (13S40, 1N51a)	0.1060 spect conv (10C51a); 0.106 (K/L -1) spect conv (67H49); 0.102 (e/y very large, K/L -1) spect conv (2H41)	<p>Te^{129m} (1/2-) Te¹²⁹ (3/2+) 0.106 0.129 β⁻ (18G52, HPS)</p>	<p>Te¹²⁸ -n-γ (67H49); Te-n-γ (13S40, 2S47); Te-d-p (13S40); Te-n-2n (28T38); Te-γ-n (25W48); fission U (16H43b, 38G46, 43W48, 1N51a, 30P51a), U²³³ (38G48, 38G51), U²³⁵ (38G51); parent Te¹²⁹ (13S40, 38G46, 43W51)</p>
¹²⁹ Te	A chem, excit (37B39, 13S40)	β ⁻ (13S40)	72 m (13S40); 70 m (32A39, 33G51i); 67 m (25W48)	1.8 spect (11R47); 1.7 abs (33G51i)	<p>Te¹²⁹ (7/2+) 0.129 β⁻ (18G52, HPS)</p>	<p>Te-n-γ (13S40, 2S47); Te-d-p (13S40, 28T38); Te-γ-n (37B39, 25W48); Te-n-2n (6H37, 28T38); fission Th (72B51), U (32A39, 16H43b, 38G46, 43W48, 1N51a); daughter Te^{129m} (13S40, 38G46, 43W51); daughter Sb¹²⁹ (32A39)</p>
¹³⁰ Te			34.49 (1B50)		<p>Te¹³⁰, I = 0 (87M50)</p>	
^{131m} Te	A chem, genet (13S40)	IT (13S40)	double beta decay; -102i y Xe ratios, mass spect (3150b)	0.177 (K/L 2) spect conv (2H41)	<p>Te^{131m} (1/2-) Te¹³¹ (3/2+) 0.177 0.131 0.16 45% β⁻ 55% β⁻ (18G52, 37G52)</p>	<p>Te-n-γ (13S40, 2S47); Te-d-p (13S40); spall-fission U (6F51); fission U (32A39, 16H39a, 32K51d, 43W51, 30P51a); parent Te¹³¹ (32A39, 13S40, 43W51); daughter Sb¹³¹ (68C51)</p>
¹³¹ Te	A chem, excit (13S40)	β ⁻ (13S40)	24.8 m (37G52); 25 m (13S40)	2.0 (-55%), 1.4 (-45%) abs, β-γ coinc (37G52)	<p>Te¹³¹ (7/2+) 0.131 0.16 β⁻ (18G52, 37G52)</p>	<p>Te-d-p (13S40); Te-n-γ (13S40, 2S47, 37G52); fission U (32A39); daughter Te^{131m} (32A39, 13S40, 43W51); parent I¹³¹ (32A39, 13S40, 30P51, 68C51); daughter Sb¹³¹ (30P51, 68C51)</p>
¹³² Te	B chem (32A39); fission fragment range (32K48)	β ⁻ (32A39)	77.7 h (30P51a); 77 h (32A39)	0.231 scint spect (10L51a); 0.22 abs (1N51b)	<p>Te¹³² (7/2+) 0.131 0.16 β⁻ (18G52, 37G52)</p>	<p>Te-q-2p (11Z51); spall-fission Th (7N49a); fission Th (16H39d, 72B51, 21T51), U (32A39, 16H39e, 16H39a, 1N51b, 30P51a), Pu (32K48); daughter Sb¹³² (32A39, 30P52a); parent I¹³² (32A39, 16H39e, 16H39a, 1N51b, 44W51)</p>

Isotope Z A	Class and identification	Percent abundance	Type of decay	Half-life	Energy of radiation in Mev		Disintegration energy and scheme	Method of production and genetic relationships
					Particles	Gamma-transitions		
$^{133}_{52}\text{Te}$	A chem, genet (32A39)		IT (30P52)	63 m (30P52); 60 m (32A39, 16W40)		- 0.4 scint spect (30P52); with Te^{133} : 0.6, 1.0 abs (30P52)		fission U (32A39, 16H39a, 24S40, 16W40, 30P51), Pu (32K48); parent Te^{133} (30P52); ancestor I^{133} (32A39, 16H39a, 24S40, 16W40, 16W45, 30P51); daughter Sb^{133} (30P51) daughter Te^{133m} (30P52); parent I^{133} (30P52a)
$^{133}_{52}\text{Te}$	A chem, genet (30P52)		β^- (30P52)	2 m (30P52)	2.4 (-30%), 1.3 (-70%) abs (30P52)	0.6, 1.0 abs (30P52)		
$^{134}_{52}\text{Te}$	B chem, genet (32A39)		β^- (32A39)	44 m (30P51a); 43 m (32A39)				fission Th (9P40), U (32A39, 16H39a, 30P51a), Pu (32K48); parent I^{134} (32A39, 16H39a, 30P51a)
$^{135}_{52}\text{Te}$	[A] genet (22D40)		β^- (22D40)	<2 m (33G51j, 32K51e, 22D40)				fission U, parent I^{135} (33G51j, 32K51e)
$^{135}_{52}\text{Te}$	E chem (16H43b)		β^- (16H43b)	-1 m (16H43b)				fission U (16H43b)
$^{120}_{53}\text{I}$	D chem (74M50)		β^+ (74M50)	30 m (74M50)	4.0 abs, spect (74M50)			spall Sn (second order reaction) (74M51); Sb-a-5n (74M50)
$^{121}_{53}\text{I}$	B chem, genet (74M50)		β^+ (74M50)	1.5 h (40D52); 1.8 h (74M50)	1.2 abs, spect (74M50); 1.2, 4.0 (weak) (40D52); conv: 0.185 spect (74M50)			spall Sn (second order reaction) (74M51); Sb-a-4n, parent Te^{121} (74M50); daughter Xe^{121} (37T52, 8H52b, 40D52)
$^{122}_{53}\text{I}$	A chem, excit (74M50); sep isotopes (7Y51)		β^+ (74M50)	3.6 m (7Y51); 3.4 m (40D52); 4 m (74M50)	2.9 abs (74M50); 3.1 abs (7Y51)			Sb-a-3n (74M50); Te^{122} -p-n (7Y51); daughter Xe^{122} (37T52, 8H52b, 40D52)
$^{123}_{53}\text{I}$	A chem, excit (74M50); chem, sep isotopes (14M49)		EC (74M50)	13.0 h (14M49); 13 h (74M50)		0.159 spect, spect conv (14M49)		spall Sn (second order reaction) (74M51); Sb-a-2n (74M50); Sb121-a-2n (14M49); daughter Xe^{123} (37T52, 8H52b, 40D52)

¹²⁴ I	A chem, excit, cross bomb (12L38e)	EC -70%, β^+ -30% (74M50)	4.5 d (74M50); 4.0 d (12L38e, 2D40)	2.20 (51%), 1.50 (44%), 0.7 (5%) spect (14M49); 2.1 spect, abs (74M50)	0.603, 0.73, 1.72, 1.95 spect, spect conv (14M49); no γ coinc with 2.2 β^+ , β - γ coinc (85S51); γ - γ , β - γ coinc (37M49)	see ¹²⁴ Sb  (14M49)	spall Sn (second order reaction) (74M51); Sb- α -n (12L38e, 74M50); Sb- α -3n (74M50); Sb121- α -n (74M50); Te-p-n (2D40); spall-fission Bi (11G49, 66B51)
¹²⁵ I	A chem (17R46a); chem, excit (33G47); genet (67B51b)	EC (L/K 0.23) (38M52); EC (L/K 0.3) (23F51b); no β^+ (33G47)	60.0 d (23F51b); 56 d (17R46a)		0.035 ion ch (23F51b); 0.0355, no 0.109 γ spect conv (67B51b)	see ¹²⁵ Te  (23F51b)	Sb- α -2n (74M50); Te-d-n (17R46a, 33G47); spall-fission Bi (11G49, 66B51); daughter Xe125 (67B51b); not parent Te125m (lim 0.05%) (23F51b)
¹²⁶ I	A excit (28T38); chem, excit, cross bomb (12L38e)	EC -58%, β^- -40%, β^+ (?) -2% (12P51)	13.0 d (12L38e); 13 d (28T38)	β^- : 1.268 (27%), 0.85 (73%) spect (14M49); 1.24 (-25%), 0.85 (-75%) spect (12P51); 0.865 spect (23M51a)	with β^- : 0.382 spect conv, β - γ coinc (12P51); 0.395 spect, spect conv (14M49); with EC: 0.64 (weak) scint spect, x- γ coinc, γ - γ coinc (12P51); others (85S51)	 (12P51, 85S51a)	spall Sn (second order reaction) (74M51); Sb- α -n (12L38e, 74M50); Te-d-n (12L38e); Te-p-n (2D40); I-n-2n (12L38e, 28T38, 12P51); I- γ -n (12P49, 27M49, 30S50); spall-fission Bi (11G49, 66B51)
¹²⁷ I			100 (6N37)			 (12P51, 85S51a)	I-n- γ (12A35, 28T38, 2S47, 7S46, 9O49, 50H51); Te-d-2n (12L38e); Te-p-n (2D40)
¹²⁸ I	A chem, n-capt (12A35)	β^- 95.0%, EC + β^+ 5.0% (28R50); EC/ β^- 0.063 (41M51a)	24.99 m (69H41)	2.02 spect (7546)	0.428 (7%) spect (7546)	 (7546)	

Isotope Z A	Class and identification	Percent abundance	Type of decay	Half-life	Energy of radiation in Mev		Disintegration energy and scheme	Method of production and genetic relationships
					Particles	Gamma-transitions		
¹²⁹ ₅₃ I	A chem, n-capt (32K47)		β^- (32K47)	1.72 x 10 ⁷ y sp act (32K51f); 3 x 10 ⁷ y sp act (26P49b)	0.12 scint spect (38M52); 0.12 abs (26P49b); 0.12 ion ch (83B50); 0.13 abs (32K51f)	0.039 (coinc with β^- , e_K/γ -6, K/L-40) ion ch, β - γ coinc (83B50)	<p>I^{129}, $I = 7/2$ (87M50) $Q_\beta^- = 0.17$ (HPS) (83B50, 30T52, 18G52)</p>	fission U (32K47, 26P49b, 83B50)
¹³⁰ I	A chem, across bomb (12L38e)		β^- (12L38e)	12.6 h (12L38e)	1.03 (-60%), 0.61 (-40%) spect (33R43)	0.744 (e_K/γ 0.003), 0.667 (e_K/γ 0.004), 0.537 (e_K/γ 0.007), 0.417 (coinc with 0.6 β^- , e_K/γ 0.012) ($e_K \gg e_L$ for all γ 's) spect, spect conv, β - γ , γ - γ coinc (33R43)	<p>I^{130} (83B50, 30T52, 18G52)</p>	Te-d-2n (12L38e); Te-p-n (2D40); I^{129} -n- γ (32K47); Cs-n- α (16W40)
¹³¹ I	A chem (12L38e); chem, genet (13S40)		β^- (12L38e)	8.141 d (39S51a); 8.05 d (106B52); 8.16 d (17K51); 8.04 d (38S51)	0.815 (0.7%), 0.608 (87.2%), 0.335 (9.3%), 0.250 (2.8%) spect, β - γ coinc (8B52); 0.810, 0.606, 0.335, 0.250 spect, β - γ coinc (24K51); 0.807, 0.606, 0.339 spect (40R52); E (average) 0.189 ion ch (77C52); see also: (69C52, 11B52, 8V51, 20N51, 10C51b, 30T51, 11B51, 22F50, 28K49, 44M48, 25D42)	0.080 (2.2%, coinc with 0.284 γ , e_K/γ 1.73, K/L 7), 0.163 (coinc with Xe ^{131m2}), 0.284 (5.3%, coinc with 0.608 β^- , e_K/γ 0.047, K/L 5), 0.364 (80%, coinc with 0.608 β^- , e_K/γ 0.018, K/L 8), 0.637 (9%, coinc with 0.335 β^- , e_K/γ 0.0037, K/L 9), 0.722 (3%, coinc with 0.250 β^- , e_K/γ 0.0028, K/L 8) spect, spect conv, β - γ delay coinc, scint spect (8B52, 8B52a); γ_1 0.080133, γ_2 0.28413, γ_3 0.36418 ($\gamma_1/\gamma_2/\gamma_3 = 5/9/100$) cryst spect (29L49a); γ_2 0.284 (e_K/γ 0.052, K/L 3.3), γ_3 0.364 (e_K/γ 0.021, K/L 5.6), γ_4 0.638 (e_K/γ 0.0040), γ_5 0.723 (e_K/γ 0.0034) ($\gamma_2/\gamma_3/\gamma_4/\gamma_5 =$ 6/100/10/3) spect, spect conv (93H52a); 0.080 (4.3%, with 0.283 γ , e/γ 1.83) γ - γ , x- γ coinc, scint spect (69C52a); see also: (11B52, 48B52, 69C52, 86S52, 8V51, 30T51, 24V51, 10C51b, 22F50, 28K49, 48B49, 44M48, 13O48, 25D42, 40R52, 52V51, 24E51)	<p>I^{131} Q_β^- 0.972 (8B52)</p>	Te-d-n (12L38e, 33R41a); spall-fission Th (7N49a), U (16F41, 6O47, 6F51); fission Th (21T51), U (32A39, 16H39a, 38G46, 23S51), 32K51g), U233 (1Y47, 38G48, 61S48, 38G51), U235 (1Y47, 38G51), Pu (28F51); daughter Te ¹³¹ (12L38e, 32A39, 16H39a, 13S40, 30P51, 68C51); parent (-1%) Xe ^{131m2} (48B49, 67B50b); parent Xe ^{131m1} (14G51a)
¹³² I	B chem, genet (32A39)		β^- (32A39)	2.4 h (32A39); 2.3 h (16H39a)	2.2, 0.9 abs (1N51b); 1.5 abs (75S49); -1.4 abs (70B43a)	γ_1 0.69, γ_2 1.41, γ_3 2.0 ($\gamma_1/\gamma_2/\gamma_3$ = 37/4/1), γ_4 -0.8 (very weak) scint spect, γ - γ coinc (46M51); 0.6, 1.4 abs (1N51b)	<p>(8852, 48B52)</p>	spall-fission U (16F41, 6O47); fission Th (72B51, 21T51), U (32A39, 16H39a, 9P40, 38G46, 1N51b), U233 (38G48); daughter Te ¹³² (32A39, 16H39a, 16F39e, 1N51b, 44V51)

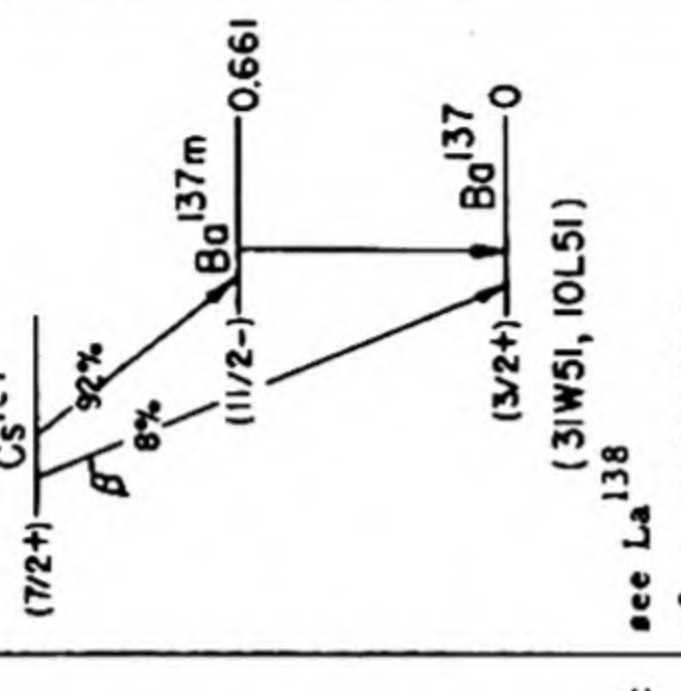
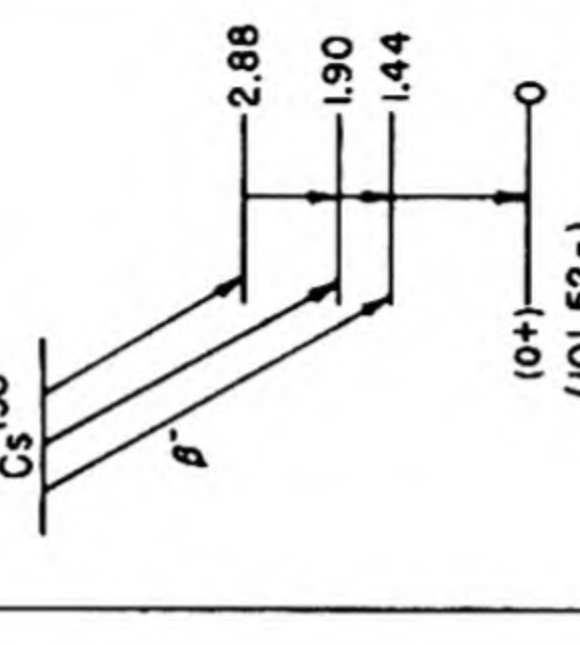



^{133}I	A chem (32A39); chem, genet (16W40)	β^- (32A39, 16H39a)	20.5 h (106B52); 22.4 h (30P51a)	1.3 (-91%), 0.4 (-9%) abs (30P52a); 1.4 (-94%), 0.5 (-6%) abs, β - γ coinc (48B49a); 1.4 abs (23S51j)	0.53 (94%), 0.85 (5%), 1.4 (1%) scint spect, γ - γ coinc (48B49a); 0.53 spect (6P47b); 0.55 abs (23S51j)	spall-fission Pb (2147b), U (16F41, 4047); fission U (32A39, 16H39a, 24S40, 16W40, 30P51, 23S51k), Pu (28F51); daughter Te^{133} (32A39, 16H39a, 24S40, 16W40, 16W45, 30P51); parent Xe^{133} (24S40, 16W40, 16W45); parent (2.4%) $\text{Xe}^{133\text{m}}$ (8Z51, 24K51a)
^{134}I	B chem (32A39); fission fragment range (32K48)	β^- (32A39)	52.5 m (30P51a); 51 m (32L49); 54 m (32A39)	1.6 (-70%), 2.8 (-30%), hard β (weak) abs (30P52a); 1.5-1.75, 3.5-4.2 abs (32L49)	>2.2 (weak) D- γ -n reaction (32L49); >1 abs (32K51h)	spall-fission U (16F41); fission Th (22D39), U ²³⁵ (1Y47, 38G51), U (16H39a, 32A39, 9P40, 9P40a, 32L49, 32K51h, 30P51a), Pu (32K48, 28F51); daughter Te^{134} (16H39a, 32A39, 30P51a)
^{135}I	A chem, genet (22D40, 24S40)	β^- (22D40, 24S40)	6.68 h (6P47b); 6.7 h (33G51j), 32K51e)	0.5 (35%), 1.0 (40%), 1.4 (25%) spect (6P47b); 1.4 abs (32K51e); 1.5 abs (23S51j)	1.8, 1.27 spect (6P47b); 1.3 abs (23S51j); 1.6 abs (32K51e); 2.4 (1.1%) abs (32L49)	spall-fission U (6O47); fission Th (72B51), U (24S40, 16W40, 22D40, 16W45, 6P47b, 33G51j, 32K51e), Pu (28F51); daughter Te^{135} (33G51j, 32K51e); parent (-30%) $\text{Xe}^{135\text{m}}$, parent (-70%) Xe^{135} (6P47b); parent $\text{Xe}^{135\text{m}}$ (40G40, 16W45); parent Xe^{135} (24S40, 22D40, 40G40, 16W45)
^{136}I	D chem (65S40)	β^- (65S40)	86 s (84S49)	6.5 abs (84S49)	1.4, 2.9 scint spect, abs (84S49, 99M52)	fission U (65S40, 66S43, 84S49), U ²³³ , Pu (84S49)
^{137}I	A chem (65S40, 26S47); chem, genet (66S43, 63S49)	β^- , β^- n (-6% of disinte- grations) (19L51a)	22.0 s (n) (28H48a); 22.5 s (n) (34R47); 19.3 s genet (63S49)	n (mean): 0.56 abs paraffin (28H48a); 0.67 p recoil in cl ch (71B46)		fission Ue (65S40, 66S43, 26S47, 34R47, 63S47a, 63S49), Pu (34R47); parent Xe^{137} (66S43, 63S49)
^{138}I	A chem, genet (63S49)	β^- (63S49)	5.9 s (63S49)			fission U, ancestor Cs^{138} (63S49)
^{139}I	A chem, genet (63S49)	β^- (63S49)	2.7 s (63S49)			fission U, parent Xe^{139} , ancestor Ba ¹³⁹ (63S49)
^{121}Xe	B chem, genet (37T52, 8H52b, 40D52)		40 m (40D52); 70 m (37T52); -60 m (8H52b)			I-p-7n (37T52, 8H52b, 40D52); parent I^{121} (37T52, 8H52b, 40D52)
^{122}Xe	A chem, genet (37T52, 8H52b, 40D52)		19.5 h (37T52); 20.0 h (40D52); 19 h (8H52b)			I-p-6n (37T52, 8H52b, 40D52); parent I^{122} (37T52, 8H52b, 40D52)
^{123}Xe	A chem, genet (37T52, 8H52b, 40D52)	β^+ (40D52)	2.1 h (37T52); 1.7 h (40D52); -2 h (8H52b)			I-p-5n (37T52, 8H52b, 40D52); parent I^{123} (37T52, 8H52b, 40D52)
^{124}Xe					0.096 (6N50a)	

Isotope Z A	Class and identification	Percent abundance	Type of decay	Half-life	Energy of radiation in Mev		Disintegration energy and scheme	Method of production and genetic relationships
					Particles	Gamma-transitions		
¹²⁵ Xe 54	A chem, sep isotopes (33A50); chem, mass spect (67B51b)		EC, no β^+ (67B51b, 33A50)	18 h (67B51b); 20 h (33A50)		0.054 (K/L-4.3), 0.096, 0.106, 0.187 (K/L-4.6), 0.243 spect conv; 0.460 scint spect (67B51b)		¹²² Te - α -n (33A50); Xe-n- γ (67B51b); parent ¹²⁵ I (67B51b)
¹²⁶ Xe		0.090 (6N50a)						I-p-n (29C40b)
¹²⁷ Xe	D chem (29C40b)		IT (?) (29C40b)	75 s (29C40b)		0.125, 0.175 spect conv (29C40b)		¹²⁴ Te - α -n (33A50); I-p-n (29C40b); I-d-2n (11O42); Xe-n- γ (44C44, 67B51c); daughter Cs ¹²⁷ (33F50)
¹²⁷ Xe	A chem (29C40b); chem, sep isotopes (33A50); mass spect (67B51c)		EC (67B51c)	34 d (29C40b); 32 d (33A50); 25 d (67B51d)		0.057, 0.145, 0.170, 0.200, 0.365 spect conv, scint spect (67B51c)		
¹²⁸ Xe		1.919 (6N50a)						
^{129m} Xe	A chem, mass spect (67B51c)		IT (67B51c)	8.0 d (67B51c)		0.196 (K/L+M 2.1) spect conv (67B51c); 0.040 (K/L+M 4.3) spect conv (30T52, 30T52c)		Xe-n- γ (67B51c)
¹²⁹ Xe		26.44 (6N50a)						
¹³⁰ Xe		4.08 (6N50a)						
^{131m2} Xe	A chem (44C44); chem, genet (48B49); mass spect (67B50b)		IT (48B49, 44C44)	12.0 d (67B50b)		0.163 (K/L+M 1.9, L/M 3.4) spect conv (67B50b, 67B51c); 0.163 (K/L+M 1.7) spect conv (8V51); 0.165 (e/ γ -20) abs conv, abs (48B49)		Xe-n-n (44C44); daughter (-1%) ¹³¹ I (48B49, 67B50b); not daughter Cs ¹³¹ (43C51c); daughter Cs ¹³¹ (70C50)
^{131m1} Xe	A genet (14G51a)		IT (14G51a)	4.8 x 10 ⁻¹⁰ s delay coinc (14G51a, 8B52a)		0.080 scint spect (14G51a, 8B52a)		daughter ¹³¹ I (14G51a, 8B52a)
¹³¹ Xe		21.18 (6N50a)						fission U (mass spect) (13T47)
¹³² Xe		26.89 (6N50a)						fission U (mass spect) (13T47)

Isotope	Half-life	Decay Mode	Parent Isotope	Decay Energy (MeV)	Decay Scheme
^{133m} Xe	2.3 d (67B51a); 2.1 d (24K51a)	IT (24K50c)			0.233 (K/L 2.9) spect conv (67B51a); 0.235 (e _K /γ 4.2) spect conv, scint spect (24K51a)
¹³³ Xe	5.270 d (76M50); 5.3 d (18E51)	β ⁻ (22D40)			0.345 spect (67B50c); 0.34 abs (18E51); 0.35 abs (13E51e)
¹³⁴ Xe	10.44 (6N50a)				
^{135m} Xe	15.6 m (21R43); 15.3 m (6P47b); 13 m (1N51c)	IT (16W45)			0.52 spect (6P47b); 0.5 (e _K /γ -0.2) abs, abs conv (16W45, 1N51c)
¹³⁵ Xe	9.13 h (60B52); 9.2 h (7N51, 58H51c); 9.1 h (30T49)	β ⁻ (24S40)			0.905 spect (67B51); 0.93 spect (6P47b); 0.95 abs (70B43a); 0.9 abs (16W45); 1.0 abs (7N51, 58H51c)
¹³⁶ Xe	8.87 (6N50a)				
¹³⁷ Xe	3.9 m (63S49); 3.8 m (66S43); 3.4 m (21R43)	β ⁻ (66S43)			-4 abs (66S43, 70B43a)
¹³⁸ Xe	17 m (36G40)	β ⁻ (16H39a)			

Isotope Z A	Class and identification	Percent abundance	Type of decay	Half-life	Energy of radiation in Mev		Disintegration energy and scheme	Method of production and genetic relationships
					Particles	Gamma-transitions		
¹³⁹ ₅₄ Xe	A chem, genet (16H39a, 6H39)		β^- (16H39a, 6H39)	41 s (24D51)				fission Th (25A39, 16H40); fission U, parent Cs ¹³⁹ (16H39a, 6H39, 16H40a); ancestor Ba ¹³⁹ (16H39a, 6H39, 24D51); daughter I ¹³⁹ (63S49)
¹⁴⁰ Xe	A chem, genet (16H40a)		β^- (16H40a)	16.0 s (24D51); 9.8 s (11O51)				fission Th (16H40); fission U, ancestor Ba ¹⁴⁰ (16H40a, 24D51a, 24D51, 11O51)
¹⁴¹ Xe	A chem, genet (17B51)		β^- (17B51)	1.7 s (32K46, 11O51); 3 s (24D51)				fission U, ancestor La ¹⁴¹ (17B51); fission U, ancestor Ce ¹⁴¹ (24D51a, 24D51, 11O51)
¹⁴³ Xe	A chem, genet (17B51)		β^- (17B51)	1.0 s (24D51)				fission U, ancestor Ce ¹⁴³ (17B51, 24D51);
¹⁴⁴ Xe	A chem, genet (24D51a)		β^- (24D51a)	-1 s (24D51)				fission U, ancestor Ce ¹⁴⁴ (24D51a, 24D51)
¹²⁵ ₅₅ Cs	A chem, mass spect (73M52)		β^+ (73M52)	45 m (73M52)	2.03 spect (73M52)			I- α -6n (73M52)
¹²⁷ Cs	A chem, mass spect (33F50)		β^+ (33F50)	5.5 h (33F50)	1.2 spect, abs (33F50)			I- α -4n (33F50); parent Xe ¹²⁷ (33F50); daughter Ba ¹²⁷ (37L52)
¹²⁸ Cs	B chem, genet (33F51)		β^+ , EC (37L52)	3.8 m (37L52); 3.1 m (33F51)	3.0 abs (33F50a, 32T50, 37L52)			daughter Ba ¹²⁸ (33F51, 37L52)
¹²⁹ Cs	A chem, mass spect (33F50)		EC, no β^+ (33F50)	31 h (33F50)	conv: -0.3 abs (33F50)	-0.5 abs (33F50)		I- α -2n (33F50); daughter Ba ¹²⁹ (33F50a, 32T5)
¹³⁰ Cs	A chem (27R48); chem, excit (91S52a); chem, mass spect (73M52)		β^+ , EC, β^- (β^+ / β^- 27.5) (91S52a)	30 m (91S52a); -30 m (27R48, 33F50)	β^+ : 1.97 spect (91S52a); β^- : 0.442 spect (91S52a)	no γ (91S52a); Xe K-x (91S52a)		I- α -n (27R48, 33F50, 91S52a)
¹³¹ Cs	A chem, genet (32K47a); chem, mass spect (7K49)		EC, no β^+ (28F47, 43C51c, 38K51d)	9.6 d (1Y49); 10.2 d (32K47a); 10.0 d (5Y47)		no γ (43C51c, 32K47a, 38K51d, 11S52); Xe K-x (43C51c, 5Y47, 1Y49, 32K47a, 28F47); -0.1 abs conv, abs (5Y47, 1Y49)		I- α - γ (11S51); daughter Ba ¹³¹ (32K47a, 5Y47, 1Y49, 43C51c); not parent Xe ^{131m2} (43C51c); parent (?) Xe ^{131m2} (70C50)
¹³² Cs	B chem, excit (44C44)		EC (44C44)	7.1 d (44C44)		0.668 scint spect (10L51a); 0.62 abs, abs conv (44C44)		Cs-n-2n (44C44, 10L51a)

^{133m} Cs	A genet (14G53)	100 (4N37)	IT (14G53)	6.0 x 10 ⁻⁹ s delay coinc (14G53)		see Xe ¹³³ ; -0.081 (e _K /γ 1.8, K/L+M 6.0) scint spect, β-γ delay coinc (14G53)	daughter Xe ¹³³ (14G53)
¹³³ Cs							
^{134m} Cs	A chem, n-capt (12A35, 77M35); chem, excit, n-capt (45K40)		IT (6P47, 18G48a, 42C50)	3.2 h (5S45); 3 h (45K40)		0.128 (K/L/M = 64.3/100/18.6) spect conv (42C50); 0.128 (e _K /γ 2.2) scint spect (14S51); 0.128 (L _{II} /L _{III} -1) spect conv (63M52a); others (6P47, 18G48a, 5S45)	Cs-n-γ (12A35, 77M35, 45K40, 2S47); Cs-d-p (45K40)
¹³⁴ Cs	A n-capt (30A38); chem, n-capt, excit (45K40)		β ⁻ (45K40); no EC (lim 4%) (31W50); no EC (lim 5%) (7S48); no β ⁺ (lim 0.009%) (41M51)	2.3 y (33G51a); 1.7 y (45K40)	0.648 (75%), 0.09 (25%) spect (20P51); 0.65 spect (31W50); 0.66 (-72%), 0.09 (-28%) spect (4E47); 0.676, 0.640, -0.08 (-24%) spect (87S52); 0.60, 0.09 abs, β-γ coinc abs (37M49); others (7S47e, 45K40, 6P47, 37W47)	0.561 (e _K /γ 0.005), 0.567 (e _K /γ 0.007), 0.601 (e/γ 0.005, K/L 6.0), 0.794 (e/γ 0.002, K/L 6.0), 1.037 (weak, K/L 4.5), 1.164 (weak, K/L 6.2), 1.365 (weak, K/L 6.1) spect conv (87S52); 0.560 (e/γ 0.008), 0.602 (e/γ 0.0053), 0.799 (e/γ 0.0025), 1.037 (weak), 1.170 (weak), 1.363 (with 0.09 β ⁻ , e/γ 0.0062) spect conv, β-γ coinc (31W50); 0.040 crit abs (47R52); Y ₁ 0.570, Y ₂ 0.601, Y ₃ 0.793, Y ₄ 1.024, Y ₅ 1.11, Y ₆ 1.35 (Y ₁ /Y ₂ / Y ₃ /Y ₆ = 0.35/0.94/1.0/0.017) spect (88S51); Y ₁ 0.57, Y ₂ 0.60, Y ₃ 0.79 (Y ₁ /Y ₂ / Y ₃ = 0.26/1.0/1.0) spect (4E47); no 1.96 γ (lim 10 ⁻⁴ %) Be-γ-n reaction (23W50); others (7S48, 20P51, 6P47, 20D50, 8B49, 45W50, 17B50, 44M50a, 85S51, 85B50, 39R51, 61K52)	Cs-n-γ (30A38, 69S38, 45K40, 2S47); Cs-d-p (45K40); Ba-d-α (51H43)
^{135m} Cs	A genet (14G53)		IT (14G53)	2.8 x 10 ⁻¹⁰ s delay coinc (14G53)		0.248 (K/L 7.0) spect conv, scint spect, β-γ delay coinc (14G53)	daughter Xe ¹³⁵ (14G53)
¹³⁵ Cs	A chem, genet (63S49a); chem, mass spect (3149a)		β ⁻ (63S49a)	3.0 x 10 ⁶ y ap act (8Z49); 2.1 x 10 ⁶ y yield (63S49a)	0.21 abs (63S49a); -0.19 abs (8Z49)	no γ (63S49a, 8Z49)	daughter Xe ¹³⁵ (63S49a); fission U (8Z49, 38W52)
¹³⁶ Cs	A chem (33G46, 33G51m); chem, excit (33G49)		β ⁻ (33G51m)	13.7 d (33G49)	0.35 abs (33G49); 0.28 β-γ coinc abs (28F51b)	-0.9 abs (33G49); 1.2 β-γ coinc abs (28F51b); two γ's (33G49)	La-n-α (44C44, 33G49); spall-fission Th (7N49a); U (6F51); fission Th (21T51), U233 (3P49a, 38G51), U235 (3P49a, 33G51m), Pu (28F51b, 33G51m)

Isotope Z A	Class and identification	Percent abundance	Type of decay	Half-life	Energy of radiation in Mev		Disintegration energy and scheme	Method of production and genetic relationships
					Particles	Gamma-transitions		
¹³⁷ 55 Ca	A chem, genet (78M41); chem, mass spect (60H46a, 3149a)		β^- (78M41)	33 y (33G51n, 38W52)	β_1 0.523 spect (16A50); β_2 0.51 (92%), β_3 1.17 (8%) spect (10L51); β_4 0.521, β_5 1.2 spect (20P49); β_6 0.518, β_7 1.18 spect (15O49); others (31W51, 10L49, 31T48)	with Ba 0.6616 cryst spect (100M52); see Ba ^{137m} : others (10L50d, 79B52, 31W51, 80H52, 40K52, 14M49a, 31T48, 20P49, 15O49)	 <p>Ca¹³⁷, I = 7/2 (87M50) Qβ 1.2 (HPS) (7/2+) Cs¹³⁷ β^- 92% β^- 8% (11/2-) Ba^{137m} 0.661 (3/2+) Ba¹³⁷ 0 (31W51, 10L51) see La¹³⁸ Qβ 4.84 (10L52a)</p>	spall-fission Th (7N49a); fission Th (21T51), U (60H48, 3149a, 33G51n, 38W52), U235 (38G51), Pu (28F51); parent Ba ^{137m} (13E48, 31T48); daughter Xe ¹³⁷ (21T51b, 33G51k)
¹³⁸ 55 Cs	A chem (16H39a, 6H39); chem, mass spect (30T49)		β^- (16H39a)	32.9 m (19E51); 33 m (25A39, 16H39a); 32 m (33G51k, 36G40)	3.40 (coinc with 1.4 γ), -2.9, -2.0 spect, β - γ coinc abs (10L52a); 2.68 spect (30T49); 2.65 abs (35B46a, calc from 36G40)	γ_1 0.463, γ_2 0.98, γ_3 1.44 (coinc with γ_1 and γ_2) spect conv, scint spect, β - γ , γ - γ coinc (10L52a); 1.2 abs (33G51k, 19E51)	 <p>Cs¹³⁸ β^- 2.88 1.90 1.44 (0+) (10L52a)</p>	Ba-n-p (66S43b); fission Th (25A39, 16H40), Pa (2G39), U (6H39, 16H40a); daughter Xe ¹³⁸ (16H40a, 36G40, 66S43b); descendent I ¹³⁸ (63S49)
¹³⁹ 55 Cs	A chem, genet (16H39a, 6H39)		β^- (16H39a)	9.5 m (63S50); 10 m (25A39, 6H39); 7 m (16H40a)			 <p>Cs¹³⁹ β^- 2.88 1.90 1.44 (0+) (10L52a)</p>	fission Th (25A39), U (16H39a, 6H39, 16H40a); daughter Xe ¹³⁹ (16H39a, 6H39, 16H40, 16H40a); descendent I ¹³⁹ (63S49); parent Ba ¹³⁹ (16H39a, 6H39, 16H40, 16H40a, 63S50)
¹⁴⁰ 55 Cs	A chem (16H40a); chem, genet (63S50)		β^- (16H40a)	66 s (63S50)			 <p>Cs¹⁴⁰ β^- 2.88 1.90 1.44 (0+) (10L52a)</p>	fission U (16H40a, 63S50); parent Ba ¹⁴⁰ (63S50)
¹⁴¹ 55 Cs	[A] genet (17B51)		[β^-] (17B51)	short (17B51, 24D51, 11O51)			 <p>Cs¹⁴¹ β^- 2.88 1.90 1.44 (0+) (10L52a)</p>	[daughter Xe ¹⁴¹] (17B51, 24D51, 11O51); [ancestor La ¹⁴¹] (17B51) fission U, parent Ba ¹⁴² (16H42a)
¹⁴² 55 Cs	D chem, genet (16H42a)		β^- (16H42a)	-1 m (16H42a)				
¹⁴³ 55 Cs	[A] genet (17B51)		[β^-] (17B51)	short (17B51, 24D51, 11O51)			<p>Cs¹⁴³ β^- 2.88 1.90 1.44 (0+) (10L52a)</p>	[daughter Xe ¹⁴³] (17B51, 24D51) [ancestor Ce ¹⁴³] (17B51, 24D51)
¹⁴⁴ 55 Cs	[A] genet (24D51a)		[β^-] (24D51a)	short (24D51a, 24D51)			<p>Cs¹⁴⁴ β^- 2.88 1.90 1.44 (0+) (10L52a)</p>	[daughter Xe ¹⁴⁴] (24D51); [ancestor Ce ¹⁴⁴] (24D51a, 24D51)

⁵⁶ Ba ¹²⁷	A chem, genet (37L52)	-12 m (37L52)			Cs-d-8n, Cs-p-7n (37L52); parent Cs ¹²⁷ (37L52)
^{Ba} ¹²⁸	B chem (33F50a, 32T50)	2.4 d (33F50a, 32T50)	EC (37L52)		Cs-d-7n (37L52); Cs-p-6n (33F50a, 32T50, 37L52); parent Cs ¹²⁸ (33F51, 37L52)
^{Ba} ¹²⁹	A chem, genet (32T50, 33F50a)	2.0 h (33F50a); 1.8 h (32T50)	β^+ (33F50a, 32T50)	hard β^+ (32T50)	Cs-p-5n (33F50a, 32T50); parent Cs ¹²⁹ (33F50a, 32T50)
^{Ba} ¹³⁰					
^{Ba} ¹³¹	A chem, n-capt, excit (32K47a)	12.0 d (32K47a); 11.7 d (5Y47)	EC (32K47a); no β^+ (5Y47, 28F47)		Ba-n-y (32K47a, 5Y47, 1Y49, 28D50a, 10Z50, 43C51c); parent Cs ¹³¹ (32K47a, 5Y47, 1Y49, 43C51c); spall-fission Bi (11G49)
^{Ba} ¹³²					
^{Ba} ^{133m}	A chem, excit (10C41, 2D40)	38.8 h (46W43a); 38.9 h (5Y48)	IT (10C41)		Cs-p-n (2D40); Cs-d-2n (10C41, 67H51a, 67H51b); Ba-y-n (60M48); Ba-n-y (5Y48); spall-fission Pb (13P47a), Bi (13P47, 11G49); parent Ba ¹³³ (5Y48)
^{Ba} ¹³³	A chem, n-capt, excit (32K47a); chem, genet (5Y48)	-9.5 y (32K52a)	EC (32K47a)		Ba-n-y (32K47a); daughter Ba ^{133m} (5Y48)
^{Ba} ¹³⁴					

Isotope Z A	Class and identification	Percent abundance	Type of decay	Half-life	Energy of radiation in Mev		Disintegration energy and scheme	Method of production and genetic relationships
					Particles	Gamma-transitions		
^{135m} Ba 56	A chem (45K40); chem, n-capt, sep isotopes (67H51a)		IT (46W43, 5Y48)	28.7 h (5Y48)		0.269 (e _K /γ -3.5, K/L -2) spect conv, scint spect (67H51a); 0.267 spect conv, spect, scint spect (39C51a)	<p>(11/2-) ^{135m}Ba — 0.269 —> (3/2+) (18G52)</p>	Ba-n-γ, Ba-n-2n (45K40); Ba-d-p (46W43, 39C51a); Ba ¹³⁴ -n-γ (67H51a); spall-fission U (6O47)
¹³⁵ Ba		6.59 (6N38b)					¹³⁵ Ba, I = 3/2 (87M50)	
¹³⁶ Ba		7.81 (6N38b)					¹³⁶ Ba, I = 0 (87M50)	
^{137m} Ba	A n-capt (12A35); chem, genet (31T48, 13E48)		IT (31T48)	2.60 m (14M49a); 2.63 m (31T48); 2.5 m (13E48)		0.6616 cryst spect (100M52); γ ₁ 0.661 (K/L+M 4.64) spect conv (10L50d, 59G52); 0.661 (K/L/M+N = 5.5/1.0/0.27) spect conv (79B52); γ ₁ (e _K /γ 0.097) spect, spect conv (31W51); γ ₁ (e _K /γ 0.095) scint spect (80H52); 0.662 (K/L+M 4.57) spect conv (40K52); 0.663 (e _K /γ 0.13, K/L 4.8) spect conv (14M49a); γ ₁ (e _K /γ 0.08, K/L 5.0) spect conv (15O49); 0.663 (e/γ 0.14) spect conv, x-conv coinc (31T48); 0.669 spect conv (20P49)	see Ca ¹³⁷	Ba-n-2n (1P37, 45K40); Ba-n-γ (12A35); daughter Ca ¹³⁷ (13E48, 31T48)
¹³⁷ Ba		11.32 (6N38b)					¹³⁷ Ba, I = 3/2 (87M50)	
¹³⁸ Ba		71.66 (6N38b)					¹³⁸ Ba, I = 0 (87M50)	
¹³⁹ Ba	A chem, n-capt (12A35); chem, excit (1P38a)		β ⁻ (1P37a)	85.0 m (24D51c); 84 m (92S48); 86 m (1P37a, 16H40a)	2.27 spect (92S48); 2.3 abs (32K51i, 70B43a)	0.163 (26%, e/γ 0.20, K/L = 6), 1.05 (0.6%) spect conv, abs, coinc (92S48); -0.163 (e _K /γ 0.28) scint spect (52M52e)		Ba-d-p (1P37a, 45K40, 92S48); Ba-n-γ (12A35, 1P37, 2S47, 1Y49a); La-n-p (1P38a); Ce-n-α (46W43); spall-fission U (γ) (42L40), U (6F51); fission Th (25A39, 16H40, 72B51), U (6H39, 16H39a, 24D51), U235 (38G51), Pu (32K48, 28F51); daughter Ca ¹³⁹ (16H39a, 6H39, 16H40, 16H40a, 63S50); descendent Xe ¹³⁹ (16H39a, 6H39, 24D51)

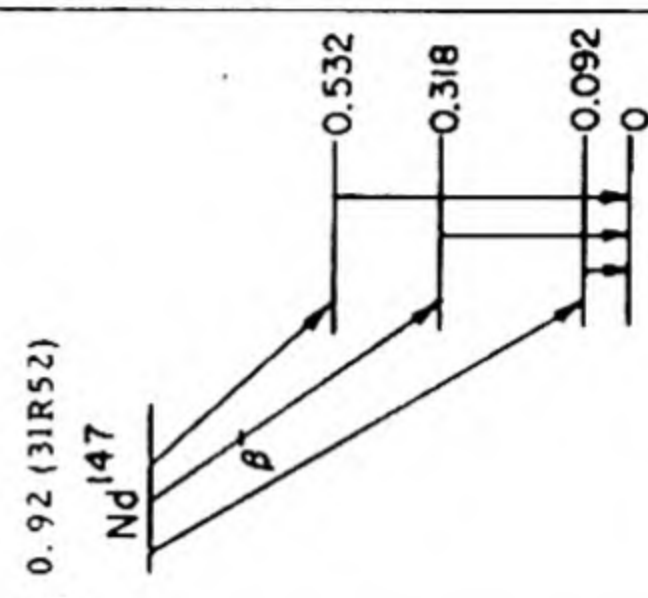
¹⁴⁰ Ba	A chem, genet (16H39, 16H39a)	β^- (16H39a)	12.80 d (13E5If, 77S47)	1.022 (60%), 0.480 spect (86B49, 43R53); 1.05 spect (4W51); 0.99, 0.47 spect (35L49); 1.0 (-75%), -0.4 (-25%) abs (13E5Ifg)	0.0296, 0.132, 0.162, 0.304, 0.537 spect conv (10C51c); 0.160, 0.310, 0.535 spect (35L49); 0.03, 0.16, 0.31, 0.54 spect, spect conv, scint spect, γ - γ coinc (86B49, 43R53); others (4W51, 26M49c)	<p>140 10+ 0.57 0.50 0.19 0.03 (2-) (3-) (43R43)</p>	Ba-n- γ (second order reaction) (32K51k); spall-fission Th (6O47, 7N49a), U (6C48, 6F51); fission Th (72B51, 21T51), U (16H39, 6H39, 16H40a, 36G40, 38G46, 63S50, 24D51, 24D51a, 17B51, 11O51, 4W51, 13E5If, 13E5Ifg), U233 (61S48, 38G51), U235 (38G51), Pu (32K48, 28F51) descendent Xe ¹⁴⁰ (16H40a, 17B51, 24D51, 24D51a, 11O51); parent La ¹⁴⁰ (16H39, 16H39a, 16H40a, 36G40, 16H42a, 38G46, 28F51c)
¹⁴¹ Ba	A chem, genet (16H42a)	β^- (16H42a)	18 m (16H42a, 52G51)	2.8 abs (32L48)	γ (52G51)	fission Th (16H39c, 16H39), U (16H42a, 52G51, 52G51a); photo-fission U (42L40); daughter Ce ¹⁴¹ (16H42a); parent La ¹⁴¹ (16H42a); descendent Xe ¹⁴¹ (17B51, 11O51, 24D51)	
¹⁴² Ba	D chem, genet (16H42a)	β^- (16H42a)	6 m (16H42a)			fission Th (16H39c, 16H39), U (16H42a); photo-fission U (42L40); daughter Ce ¹⁴² (16H42a); parent La ¹⁴² (16H42a)	
¹⁴³ Ba	B chem (16H39)	β^- (16H42a)	<0.5 m (16H42a)			fission Th (16H39c), U (16H39c, 16H39, 16H42a, 24D51, 17B51, 11O51); [descendent Xe ¹⁴³] (17B51, 24D51)	
¹⁴⁴ Ba	[A] genet (24D51)	β^- (24D51)	short (24D51, 24D51a)			[fission U, descendent Xe ¹⁴⁴ ancestor Ce ¹⁴⁴] (24D51, 24D51a)	
¹³¹ La	A chem, mass spect (53G51)	β^+ (53G51)	58 m (53G51)	1.6 abs (53G51)	1.0 abs (53G51)	spall Ba (53G51)	
¹³² La	A chem, mass spect (53G51)	β^+ (53G51)	4.5 h (53G51)	3.5 abs (53G51)		spall Ba (53G51)	
¹³³ La	A chem, mass spect (21N50)	EC, β^+ (weak) (21N50)	4.0 h (21N50)	-1.2 abs, spect (21N50); conv: 0.26 spect conv (21N50)	0.8 abs (21N50)	Ca- α -4n (21N50); daughter Ce ¹³³ (93S51)	
¹³⁴ La	B chem, genet (93S51)	β^+ -44%, EC -56% (93S51)	6.5 m (93S51)	2.7 abs, spect (93S51)	no γ (93S51)	daughter Ce ¹³⁴ (93S51)	
¹³⁵ La	A chem (81M42); chem, excit (73C48); chem, mass spect (21N50)	EC (81M42, 73C48)	19 h (21N50); 19.5 h (73C48)	0.76 (weak) abs (73C48); 0.88 abs (46W43b)		Ca- α -2n (73C48, 21N50); Ba-d-n (81M42, 46W43b); Ba-p-n (46W43b); daughter Ce ¹³⁵ (73C48)	

Isotope Z A	Class and identification	Percent abundance	Type of decay	Half-life	Energy of radiation in Mev		Disintegration energy and scheme	Method of production and genetic relationships
					Particles	Gamma-transitions		
¹³⁶ ₅₇ La	A chem (3M47); chem, excit, sep isotopes (36R50a)		EC -67%, β^+ -33% (2IN50)	9.5 m (2IN50); 9.0 m (36R50a); 10 m (3M47)	2.1 spect (2IN50); abs (3M47); 1.8 abs (36R50a)			Ce-a-n (2IN50, 36R50a); Ba-d-n (3M47); Ba ¹³⁵ -d-n, Ba ¹³⁶ -d-2n (36R50a)
¹³⁷ La	C mass spect (3148b)			>400 y yield (73C48); >30 y yield (3148b)				[daughter Ce ¹³⁷] (3148b, 73C48)
¹³⁸ La	A chem, mass spect (3147a)	0.089 (3147a)	EC (18P51); β^- -6% (85M52a)	-2.0 x 10 ¹¹ y sp act (18P51); -7 x 10 ¹⁰ y sp act (85M52a)	1.0 abs (85M52a)	γ_1 1.39, γ_2 0.81, γ_3 0.54 ($\gamma_1/\gamma_2/\gamma_3 = 1/0.65/0.3$) scint spect (18P51); 1.0, 0.54 scint spect (11B50f)		

La^{141}	A chem (16H42a); chem, genet (50B51, 23D51b)	β^- (16H42a)	3.7 h (32K51j); 3.5 h (16H42a)	2.43 (~95%), 0.9 (~5%) spect (23D51b)	1.3-1.6 (% weak) scint spect, β - γ coinc (23D51b)	<p>La-γ (second order reaction) (32K49); fission n (4C39, 7B51); U (16H42a, 32K51j); daughter Ba¹⁴¹ (16H42a); descendant Xe¹⁴¹ (17B51); parent Ce¹⁴¹ (50B51, 23D51b)</p>
La^{142}	D chem (16H42a)	β^- (32K51j)	74 m (16H42a); 77 m (32K51j)		γ (32K51j)	fission Th (16H39c), U (16H42a, 32K51j); daughter Ba ¹⁴² (16H42a)
La^{143}	A chem, genet (54G51)	β^- (54G51)	-19 m genet (54G51); -15 m (16H43b)			fission U (16H42a, 16H43b, 54G51); parent Ce ¹⁴³ (54G51)
La^{144}	[A] genet (24D51a)	[β^-] (24D51a)	short (24D51a)			[descendant Xe ¹⁴⁴ , parent Ce ¹⁴⁴] (24D51a)
$58Ce^{133}$	A chem, genet (93S51)	EC, β^+ (93S51)	6.30 h (93S51)	1.3 spect, abs (93S51)	1.8 abs (93S51)	La-p-7n (93S51); parent La ¹³³ (93S51)
Ce^{134}	B chem, excit (93S51)	EC (93S51)	72.0 h (93S51)		K- α , no γ (93S51)	La-p-6n (93S51); spall Ta (22N52); parent La ¹³⁴ (93S51)
Ce^{135}	A chem, genet (73C48)	EC, β^+ $\leq 1\%$ (93S51)	22 h (93S51)	0.81 spect (93S51)		La-d-6n (73C48); La-p-5n (93S51); spall Ta (22N52); parent La ¹³⁵ (73C48)
Ce^{136}			0.193 (3147a)			
Ce^{137}	A chem, excit (73C48); n-capt, sep isotopes (67H51c)	EC, no β^+ (73C48)	36 h (73C48)		0.257 (K/L -4) spect conv (67H51c); 0.253 (K/L -10) spect conv (11K51)	La-d-4n (73C48); La-p-3n (93S51); Ce ¹³⁶ -n- γ (67H51c, 11K51); [parent La ¹³⁷] (3148b, 73C48)
Ce^{138}			0.250 (3147a)			
Ce^{139}	A chem (1P43); chem, excit, cross bomb (1P48, 36M47); n-capt, sep isotopes (67H51c)	EC (36M47)	140 d (1P43, 1P48)		0.166 (K/L -10), 0.275 spect conv (11K51); 0.166 (K/L ≥ 4) spect conv (67H51c); -0.8 abs (1P48)	Ba-a-n (1P43, 1P48); La-d-2n (1P43, 36M47, 1P48); Ce ¹³⁸ -n- γ (67H51c, 11K51); Ce-n- γ (83M50); spall-fission Bi (11G49); daughter Pr ¹³⁹ (93S51)
Ce^{140}			88.48 (3147a)			

Isotope Z A	Class and identification	Percent abundance	Type of decay	Half-life	Energy of radiation in Mev		Disintegration energy and scheme	Method of production and generic relationships
					Particles	Gamma-transitions		
¹⁴¹ Ce 58	A chem (16H40c); chem, excit, n-capt, cross bomb (1P43, 72B51e); chem, mass spect (60H48)		β^- (16H40c)	33.1 d (49W49); 32.5 d (3F50c); 30.6 d (1P48)	0.581 (33%), 0.442 (67%) spect (3F50c); 0.58 (29%), 0.44 (71%) spect (38K51c); 0.56 (30%), 0.41 (70%) spect (92S48a); 0.56 spect, β - γ coinc abs (11T49a); others (26M49c, 94S50, 1P48, 37B46)	0.145 (e_K/γ 0.25, K/L 5.5) spect conv, spect (3F50c); -0.14 (e_K/γ 0.46) scint spect (80H52a); 0.142 (e_K/γ 0.48) scint spect (17J52a); 0.145 (K/L -7) spect conv (67H51c); 0.144 (e/γ -0.33, K/L 6.5) spect conv (38K51, 38K51c); 0.146 spect conv (11K51, 11T49a); 0.141 (coinc with β^-) spect conv, β -conv coinc (92S48a); 0.14 (coinc with β^-) scint spect, β - γ coinc (23D51b); others (94S50, 26M49c, 4B49, 42H47a, 52M51)	Q_{β^-} 0.58 (3F50c) Ba-n (1P43, 1P48); Ce-d-p (1P43, 1P48, 72B51e, 50B51); Ce-n-y (1P43, 10C48a, 72B51e); Ce-n-zn (1P43, 1P48, 72B51e); Pr-n-p (1P43); spall Ta (22N52); spall-fission Bi (11G49), U (6F51); fission Th (72B51, 21T51); U (16H40c, 50B51), U235 (38G51), Pu (28F51) daughter La141 (50B51, 23D51b); descendent Xe141 (11O51, 24D51)	
¹⁴² Ce		11.07 (3147a)						
¹⁴³ Ce	A chem (63S46, 1P43); chem, cross bomb (1P48); chem, genet (72B51e); mass spect (3148b)		β^- (63S46)	33 h (72B51e, 95S50, 37B46); 34 h (38K51c); 36 h (4B49, 1P43)	β_1 1.39, β_2 1.09, β_3 0.71 (β_1/β_2 / $\beta_3 = 1.0/1.3/1.0$) spect (50B52); β_1 1.37, β_2 1.09, β_3 0.37 (?) (β_2/β_1 1.4) spect (38K51c)	0.035, 0.126, ~0.160, 0.289, 0.356, 0.660, 0.720 spect, spect conv, scint spect (50B52) γ_1 0.057 (K/L -1), γ_2 0.283 (K/L -6), γ_3 0.649, γ_4 0.705 ($\gamma_2/\gamma_3/\gamma_4 = 4.5/1/1$) spect, spect conv, β - γ coinc (38K51, 38K51c); 0.0575 (K/L <1), 0.291 (K/L -10), 0.348 spect conv (11K51); others (95S50)	Ce-d-p (1P43, 1P48, 72B51e); Ce-n-y (1P43, 37B46, 1P48, 72B51e); Ce142-n-y (11K51); spall-fission Th (7N49a); U (6O48, 6F51); fission Th (72B51), U (17B51, 24D51, 63S51), Pu (32K48); daughter La143 (54G51); parent Pr143 (1P43, 37B46, 72B51e); descendent Xe143 (17B51, 24D51)	
¹⁴⁴ Ce	A chem (16H40c); chem, mass spect (60H48)		β^- (16H40c)	282 d (53S51); 275 d (50B51a); 290 d (19J44)	0.300 (70%), 0.170 (30%), coinc with 0.134 γ , with 0.080 γ spect, β - γ coinc (34P52); 0.304 (70%) spect (19P52); 0.17 (coinc with 0.134 γ) β - γ coinc (24K52); others (70C52, 17N51b, 6P47, 26M50a)	0.0337, 0.054, 0.0807 (e/γ large, K/L -4), 0.100, 0.134 (K/L -9) spect conv, spect (19P52); 0.034, 0.041, 0.047, 0.054 (K/L <1), 0.081 (K/L -5), 0.095, 0.101, 0.135 (K/L -10) spect conv (11K51); 0.0547, 0.079 (K/L 6.3), 0.134 (K/L 8.3), 0.231 (K/L 1.7) spect conv (70C52); -0.132 (K/L 5.3) spect conv (40K52); 0.695, 1.50, 2.18 spect (15T50); others (13A52a, 2E51)	Q_{β^-} 0.304 (19P52) spall-fission Th (7N49a); U (6O48); fission Th (21T51), U (16H40c, 70B43a, 24D51, 7N51a, 50B51a), U233 (38G48, 61S48, 38G51), U235 (38G51), Pu (28F51); parent Pr144 (16H43b, 39G43, 7N51a); descendent Xe144 (24D51, 24D51a)	
¹⁴⁵ Ce	G not found; (78C52a)			-1.8 h (72B51f)		soft γ (78C52a)		not found: fission U (78C52a); fission U (24D51, 72B51f); parent Pr145 (72P51f)
¹⁴⁶ Ce	D chem, genet (40G43)		β^- (40G43)	14.6 m (53S45); 11 m (40G46)	-0.9 abs (78C52a)			fission U, parent Pr146 (40G43, 16H43b, 53S45, 40G46)

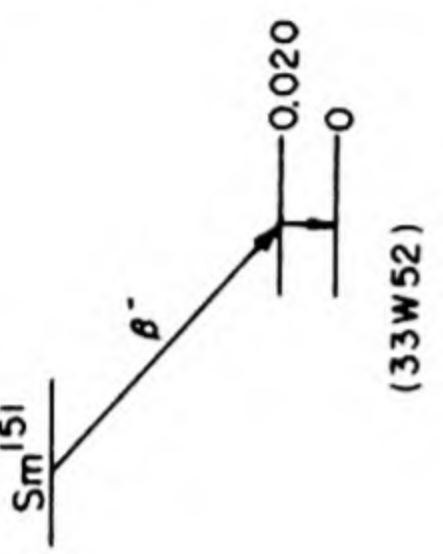
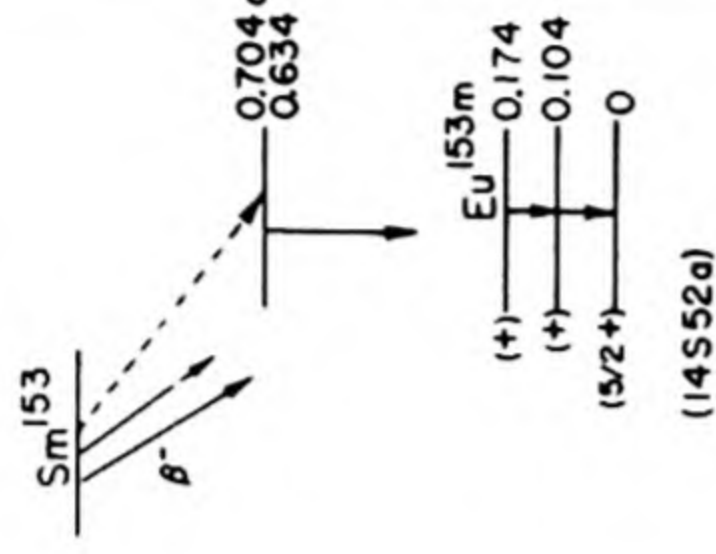
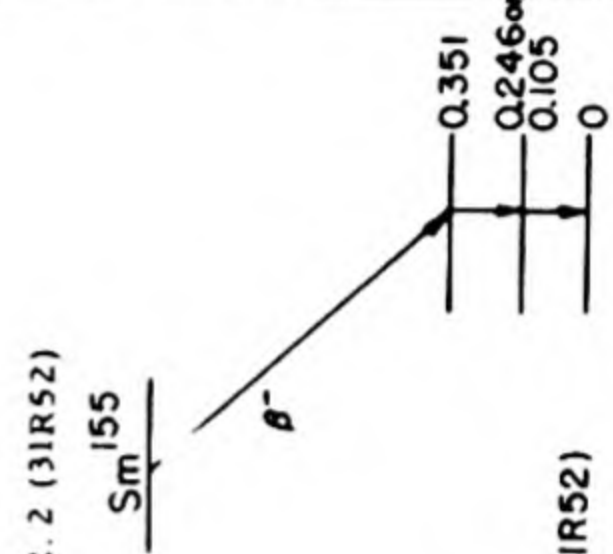
¹³⁷ Pr	B chem, mass spect (44D52)	1.8 (44D52)	1.4 h (44D52)	1.8 (44D52)	0.2, -0.5, 1.3 abs (93S51)	Ce-p-4n (44D52)
¹³⁸ Pr	A chem, excit (93S51); chem, mass spect (44D52)	EC -90%, β ⁺ -10% (93S51)	2.0 h (93S51, 44D52)	1.4 abs, spect (93S51)	1 0 abs (93S51)	Ce-p-3n (93S51, 44D52)
¹³⁹ Pr	A chem, genet (93S51); chem, mass spect (44D52)	EC -94%, β ⁺ -6% (93S51)	4.2 h (44D52); 4.5 h (93S51)	1.0 abs spect (93S51)	no γ (88B52)	Ce-p-2n (93S51, 44D52); parent Ce ¹³⁹ (93S51)
¹⁴⁰ Pr	A excit (12A35); excit (1P38a)	β ⁺ 58%, EC 42% (88B52)	3.4 m (29D42); 3.5 m (1P38a)	2.23 spect (88B52)		Ce-p-n (93S51); Pr-n-2n (12A35, 1P38a, 29D42); Pr-γ-n (34H45, 12P49); daughter Nd ¹⁴⁰ (2W49, 88B52)
¹⁴¹ Pr						
¹⁴² Pr	A n-capt (12A35, 82M35)	β ⁻ (29D42); no β ⁺ or EC (lim 0.5%) (28R50b)	19.2 h (37B46); 19.1 h (13J50); 19.3 h (29D42)	2.15 (-96%), 0.64 (-4%) spect (13J50); 2.23, 0.66 spect (41R50); 2.14 spect (96M52, 29D42); 2.23 spect (6P47); 2.22, 0.22 abs, β-γ coinc abs (26M49d); 2.5, -0.4 abs, β-γ coinc abs (15J49)	Y ₁ 0.135, Y ₂ 1.59 (Y ₁ /Y ₂ < 0.2) spect, spect conv (41R50); 1.58 spect (13J50, 13J52); 0.134, 0.329, 0.490, 0.624 spect conv; 2.1 abs (10C48); 1.5 coinc abs sec (15J49)	La-a-n (29D42); Ce-p-n (29D42); Pr-d-p (29D42); Pr-n-γ (12A35, 82M35, 1P37, 1P38a, 29D42, 2S47); Nd-n-p (1P37, 1P38a); spall-fission U (6F51)
¹⁴³ Pr	A chem (72B51g, 19J44); mass spect (60H46a)	β ⁻ (72B51g, 19J44)	13.7 d (15F49a); 13.8 d (72B51h); 13.5 d (1P48)	0.932 spect (15F49a); 0.922 spect (49B50a); 0.920 spect (11T49a); 0.92 spect (38K51); 0.84 abs (26M49c)	no γ (72B51g, 72B51h, 1P48)	Ce-d-n (1P48); spall-fission U (6F51); fission U (16H43b, 19J44, 72B51g), Pu (28F51) daughter Ce ¹⁴³ (1P43, 37B46, 72B51e)
¹⁴⁴ Pr	A chem, genet (7N51a, 16H43b, 39G43)	β ⁻ (7N51a)	17.5 m (7N51a, 77S51b); 17 m (16H43b)	2.97 (>99%), other β's (<1%) spect (19P52); 2.32 (<1%), coinc with 0.69 γ, 0.81 (<1%) spect, β-γ coinc (24K52); 2.95 (-95%), 0.87 (-5%) spect (10L52c); 2.97 (-90%), 2.3 (-5%), 0.86 (-5%) spect (13A52a); 2.99 spect (6P47); others (17N51b, 19J44, 50B51a, 70B43a, 16H43b, 26M50a, 70C52)	Y ₁ 0.0603, Y ₂ 0.696, Y ₃ 1.5, Y ₄ 2.19 (Y ₂ , Y ₃ , Y ₄ weak) scint spect, spect conv (19P52); Y ₂ 0.695, Y ₃ 1.48, Y ₄ 2.19 (Y ₂ /Y ₃ /Y ₄ = 1/0.4/1.1) spect, β-γ, γ-γ coinc (13A52a); Y ₁ 0.061 (K/L < 1) spect conv (11K51); others (17N51b, 77S51b)	fission Th (21T51), Pu (28F51); spall-fission U (6F51); daughter Ce ¹⁴⁴ (16H43b, 39G43, 7N51a)
¹⁴⁵ Pr	G not found: (78C52a)		4.5 h (72B51f)		0.490, 0.78 scint spect (20K51a); 1.4 abs (53S45a)	not found: fission U (78C52a); fission U (72B51f); daughter Ce ¹⁴⁵ (72B51f)
¹⁴⁶ Pr	D chem (40G43)	β ⁻ (40G43)	24.0 m (20K51a); 24.6 m (53S45a); 25 m (40G46)	3.8 abs (78C52a); -3 abs (53S45a)		fission U, daughter Ce ¹⁴⁶ (40G43, 16H43b, 53S45, 40G46)

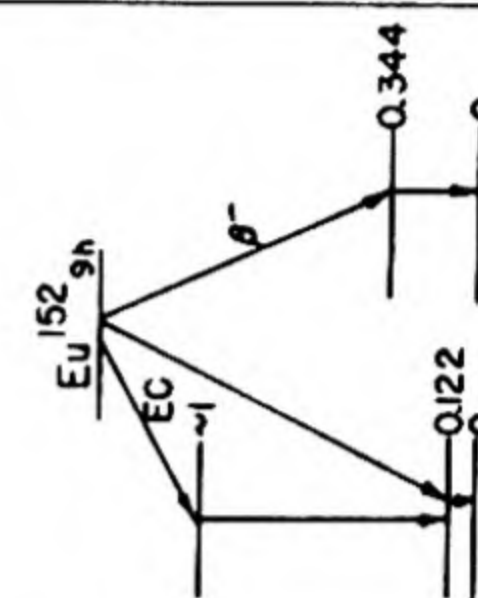
Isotope Z A	Class and identification	Percent abundance	Type of decay	Half-life	Energy of radiation in Mev		Disintegration energy and scheme	Method of production and genetic relationships
					Particles	Gamma-transitions		
¹³⁸ Nd 60	D chem, excit (93S51)		β^+ (93S51)	22 m (93S51)	-2.4 abs (93S51)			Pr-p-4n (93S51)
¹³⁹ Nd	A chem, genet (93S51)		EC -90%, β^+ -10% (93S51)	5.50 h (93S51)	3.1 abs, spect (93S51)	1.3 abs (93S51)		Pr-p-3n (93S51); ancestor Ce ¹³⁹ (93S51)
¹⁴⁰ Nd	A chem, excit, genet (2W49)		EC (88B52)	3.3 d (2W49)		Pr K-x (88B52)		Pr-p-2n (93S51); Pr-d-3n (2W49); parent Pr ¹⁴⁰ (2W49, 88B52); spall-fission U (6F51)
¹⁴¹ Nd	A excit (47K42); chem, excit (2W49)		EC -98%, β^+ -2% (2W49)	2.42 h (2W49); 2.5 h (47K42)	0.7 abs (2W49); 0.8 abs (47K42)	1.2 (weak) abs (2W49)		Pr-p-n (47K42, 2W49); Pr-d-2n (2W49); Nd-n-2n (IP38a, 47K42); Nd-y-n (47K42)
¹⁴² Nd		27.13 (3148c)						
¹⁴³ Nd		12.20 (3148c)					Nd ¹⁴³ , I = 7/2 (97B50, 88M51)	fission U ²³⁵ (mass spect) (3150a)
¹⁴⁴ Nd		23.87 (3148c)						fission U ²³⁵ (mass spect) (3150a)
¹⁴⁵ Nd		8.30 (3148c)					Nd ¹⁴⁵ , I = 7/2 (97B50, 88M51)	fission U ²³⁵ (mass spect) (3150a)
¹⁴⁶ Nd		17.18 (3148c)						fission U ²³⁵ (mass spect) (3150a)
¹⁴⁷ Nd	A chem, genet (84M47, 84M51a)		β^- (84M47, 84M51)	11.3 d (average of 31R52, 2E51a, 38K51a, 84M51, 37B46)	0.83 (-60%), 0.60 (-15%), 0.38 (-25%) spect (2E51a); 0.78 (-65%), 0.35 (-32%) spect (38K51a); 0.83, 0.60, 0.38 spect (31R52)	0.0918 (K/L ₁ = 6.4) spect conv (63M52); Y ₁ 0.0918 (e/y -0.9, K/L+M 6.5), Y ₂ 0.309, Y ₃ 0.391, Y ₄ 0.520 (Y ₁ /Y ₂ /Y ₃ /Y ₄ = 66/1/2/32) spect (38K51a); Y ₁ (K/L/M = 7.55/1/0.096) spect conv (91S52d); 0.0912 (K/L 4.9), 0.121, 0.197, 0.231, 0.260, 0.273, 0.301, 0.318, 0.398, 0.441, 0.532 (K/L -6) (all weak except 0.091 Y) spect conv, Y-Y, β -Y coinc (31R52); 0.0915 (coinc with 0.83 β^-), 0.320, 0.534 spect conv, β -conv coinc (2E51a); others (26M50b, 52M51)	Q β^- 0.92 (31R52) Nd ¹⁴⁷  (31R52, 2E51a, HPS)	Nd-d-p (47K42); Nd-n-y (37B46, 84M47, 10C48b, 84M51b); fission U (84M51); spall-fission U (6F51); parent Pm ¹⁴⁷ (84M47, 84M51a)
¹⁴⁸ Nd		5.72 (3148c)						U ²³⁵ n-fission (mass spect) (3150a)
¹⁴⁹ Nd	A excit (IP38a); chem, genet (84M51b)		β^- (IP38a)	2.0 h (37B46, IP38a); 1.8 h (31R52); 1.7 h (84M51b)	1.5, 1.1, 0.95 spect (31R52); 1.5 abs (84M51b); 1.6 abs (37B46)	0.030, 0.097 (K/L 0.9), 0.112, 0.114 (K/L -5), 0.124, 0.188, 0.198, 0.211 (K/L -7), 0.226, 0.240, 0.266 (K/L -10), 0.424, 0.538, 0.650 spect, spect conv, scint spect, coinc (31R52); others (52M51)	Q β^- 1.5 (31R52)	Nd-n-2n (IP38a); Nd-d-p (IP38a); Nd-n-y (IP38a, 37B46, 84M51b); parent Pm ¹⁴⁹ (42K52)

Nd ¹⁵⁰		5.60 (3148c)	β^- (?) (85M52, 3L34)	>2 x 10 ¹⁵ y ap act (85M52); >10 ¹³ y ap act (21C52)	1.93 spect (31R52)	0.085, 0.110, 0.117 (h/L 4), 0.421, 0.73, 1.14 spect conv, scint spect, β - γ , γ - γ coinc (31R52); Pm K-x (31R52)	fission U ²³⁵ (mass spect) (3150a)
Nd ¹⁵¹	B n-capt (84M51b); sep isotopes, n-capt, Pm K-L-M difference (31R52)	β^- (31R52)	15 m (51C52); 12 m (31R52, 84M51b)				Nd-n- γ (84M51b); Nd ¹⁵⁰ -n- γ , parent Pm ¹⁵¹ (31R52)
Pm ¹⁴¹	B chem, excit (34F52)	β^+ (34F52)	20 m (34F52)		2.4-2.8 spect (34F52)		Nd ¹⁴² -p-2n (34F52)
Pm ^{142/143}	D chem, excit (2W50a)	EC (2W50a)	250-280 d (43L52a); 285 d (2W50a)			0.95 abs (2W50a)	Pr- α -2n (2W50a, 34F52); Nd-p-n (43L52a)
Pm ^{143/144}	D chem (34F52)	EC (34F52)	200-400 d (34F52); 300-350 d (43L52a)			0.65, 0.44, 0.17 scint spect (34F52)	Pr- α -n, Pr- α -2n (34F52); Nd ¹⁴³ , ¹⁴⁴ -p-n (34F52); Nd-p-n (43L52a)
Pm ¹⁴⁵	F sep isotopes (43L52a)	β^+ (43L52a)	14-18 d (43L52a)		0.45 (43L52a)		Nd-p-n (43L52a)
Pm ¹⁴⁵	A chem, genet (65B51, 26P52)	EC (65B51)	-30 y yield (65B51)			Nd K, L-x (65B51, 26P52)	daughter Sm ¹⁴⁵ (65B51, 26P52)
Pm ¹⁴⁶	B chem, excit (34F52)	β^- (?) (34F52)	-1 y (34F52); 1-2 y (43L52a)		0.7 abs (34F52); 0.75 (43L52a)		Nd ¹⁴⁶ -p-n (34F52); Nd-p-n (43L52a)
Pm ¹⁴⁷	A chem (84M47, 84M51a); mass spect (60H48)	β^- (39G43, 72B51i)	2.6 y (53S51); 2.3 y yield (3150a)		0.223 spect (10L50c); 0.227 spect (39W52a, 33L49); 0.229 spect (16A50)		fission U (39G43, 72B51i, 77S51c, 84M51a), U233 (38G48, 38G51), U235 (3150a, 38G51); daughter Nd ¹⁴⁷ (84M47, 84M51a); parent Sm ¹⁴⁷ (42R50)
Pm ¹⁴⁸	A chem, n-capt, mass spect (26P47)	β^- (47K43)	5.3 d (47K43, 26P47)		-2.5 abs (26P47); 2 abs (47K43)	-0.8 abs (26P47)	Nd-p-n (47K43); Nd ¹⁴⁸ -p-n (43L52, 34F52); Nd-d-2n (47K42, 47K43); Nd- α -p (47K42); Pm ¹⁴⁷ -n- γ (26P47); spall-fission U (6F51)
Pm ¹⁴⁸	B excit, sep isotopes (43L52); chem (6F51)	β^- (43L52)	42 d (34F52); 43 d (6F51); 48 d (43L52)		2.4 (weak), 0.6 spect (6F51); 2.7 (weak), 0.7 abs (34F52); 1.7, 0.6 abs (43L52)	0.9 abs (6F51); 1.0 abs (34F52); 0.5 abs (43L52)	Nd ¹⁴⁸ -p-n (43L52, 34F52); spall-fission U (6F51)
Pm ¹⁴⁹	A chem (84M47, 84M51c); chem, mass spect (3147b)	β^- (84M47, 84M51c)	54 h (34F52); 55 h (3147b); 50 h (31R52, 38K51c); 47.5 h (37B46); 47 h (84M51c, 16W42, 44L41)		1.05 spect (38K51a, 31R52, 34F52); others (26M49f, 37B46, 84M51c)	0.285 (coinc with β^- , K/L 8), -1.3 (weak) spect conv, abs, β - γ coinc (31R52); no γ (38K51a); -0.2 (coinc with β^-) β - γ coinc abs (26M49f); others (52M51)	Nd ¹⁵⁰ -p-2n (34F52); Nd-d-n, Sm-n-p, Sm- γ -p (44L41); fission U (84M47, 84M51c), Pu (32K48); spall-fission U (6F51); daughter Nd ¹⁴⁹ (42K52)

 Q_β^- 0.223 (HPS)

Isotope Z A	Class and identification	Percent abundance	Type of decay	Half-life	Energy of radiation in Mev		Disintegration energy and scheme	Method of production and genetic relationships
					Particles	Gamma-transitions		
$_{61}^{150}\text{Pm}$	A excit, sep isotopes (43L52); chem, excit, sep isotopes (34F52)		β^- (43L52)	2.7 h (43L52, 34F52, 47K43)	2.01 (-70%), 3.00 (-30%) spect (34F52); 2.4 abs (43L52)	1.4, 0.3 abs (34F52)		Nd-p-n, Nd-d-2n (47K43); Nd ¹⁵⁰ -p-n (34F52, 43L52)
$_{61}^{151}\text{Pm}$	B genet, Sm K-L-M differences (31R52)		β^- (31R52)	27.5 h (31R52)	1.1 abs (31R52)	0.065 (K/L 0.3), 0.066 (K/L 0.3), 0.070 (K/L 0.3), 0.100 (K/L -5), 0.116, 0.144 (K/L -9), 0.163 (K/L -7), 0.168 (K/L -3), 0.177 (K/L -9), 0.208 (K/L -4), 0.232, 0.240, 0.275 (K/L >10), 0.340 (K/L -9), 0.715 spect conv, scint spect (31R52)		daughter Nd ¹⁵¹ (31R52); fission U (51C52)
$_{61}^{152}\text{Pm}$	E (1P38a); chem (6F51)		β^- (1P38a)	12.5 h (6F51, 1P38a)				Nd-d- (1P38a); spall-fission U (6F51)
$_{62}^{143}\text{Sm}$	E chem (65B50)			8 m (65B50)				Sm-y-n (65B50)
$_{62}^{144}\text{Sm}$		3.16 (3148d)						
$_{62}^{145}\text{Sm}$	A mass spect (3147c); chem (65B51); chem, sep isotopes, n-capt (26P52)		EC (65B51, 31R52)	-410 d (65B51); >150 d (10C48b); >72 d (3147c)		0.061 (K/L 1.0) spect conv (31R52)		¹⁴⁴ Sm -n-y (26P52); Sm-n-y (3147c, 10C48b, 65B51); parent Pm ¹⁴⁵ (65B51, 26P52)
$_{62}^{147}\text{Sm}$	A chem (71H32); sep isotopes, mass spect (48W50); chem, genet, mass spect (42R50)	15.07 (3148d)	α (71H32, 3L33)	$t_{1/2}$ corrected for abundance of Sm ¹⁴⁷ (HPS); 1.4 x 10 ¹¹ y sp act (45L47); 1.5 x 10 ¹¹ y sp act (72H35); 1 x 10 ¹¹ y sp act (31P49)	2.18 ion ch (10J50); 2.14 range emuls (74C46); 2.1 range emuls (73H49); 2.0 cl ch (72H35); others (92B49)	Sm ¹⁴⁷ , I = 7/2 (105B52); Sm ¹⁴⁷ , I = 5/2 (88M51)		natural source (71H32, 3L33, 72B48, 1D48); daughter Pm ¹⁴⁷ (42R50); fission U ²³⁵ (mass spect) (3150a)
$_{62}^{148}\text{Sm}$		11.27 (3148d)						
$_{62}^{149}\text{Sm}$		13.84 (3148d)						
$_{62}^{150}\text{Sm}$		7.47 (3148d)						
							Sm ¹⁴⁹ , I = 7/2 (105B52); Sm ¹⁴⁹ , I = 5/2 (88M51)	fission U ²³⁵ (mass spect) (3150a)

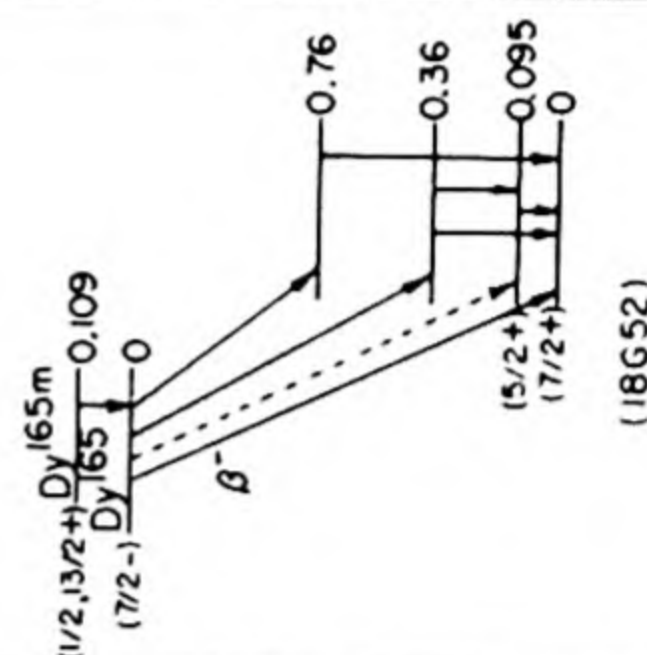
¹⁵¹ Sm	A mass spect (3147c, 3150a); chem (84M49)	β^- (3147c)	73 y (7K52); -120 y yield (3150a)	0.076 spect (16A50, 39W52b); 0.079 spect (24K49e); 0.074 spect (84M49); no conv (31R52)	0.019 (coinc with β^- ion ch, β^- y coinc (33W52); 0.021 ion ch (17S50); 0.021 scint spect (39W52b); no y (84M49, 31R52); others (52M51)		Sm-n-y (3147c); fission U (84M49); fission U235 (mass spect) (3150a)
¹⁵² Sm	26.63 (3148d)						fission U235 (mass spect) (3150a)
¹⁵³ Sm	A n-capt, excit (1P38a); mass spect (60H46, 3147b); chem (51W51)	β^- (47K42)	47 h (51W51, 37B46, 47K42, 31R52)	0.80, 0.70 (coinc with 0.101 y) scint spect, β^- -y coinc (87B52); 0.68 (-67%), 0.80 (-33%) spect (11H50); 0.70 spect (7S51); 0.82 spect (31R52); 0.78 abs (82B48); 0.73 abs (51W51)	γ_1 0.070 (e_K/γ 3.1), γ_2 0.104 (e_K/γ 1.2, coinc with γ_3 or γ_4), γ_3 0.530, γ_4 -0.60 ($\gamma_1/\gamma_2/\gamma_3/\gamma_4 = 100/425/1.0/0.3$) scint spect, γ -y coinc (14S52a); 0.069 (e_K/γ 3.8), 0.103 (e_K/γ 1.2, K/L+M 3.5) scint spect (52M52e); 0.070, 0.103 (coinc with 0.07 y, e_K/γ 0.65, K/L -6), 0.530 (weak) scint spect, spect conv, conv-conv coinc (7S51); 0.070 (weak, $e/\gamma > 10$), 0.101 ($e/\gamma < 3$), no higher y, scint spect, γ -y coinc (87B52); 0.070 (K/L 3.5, $L_I/L_{II}/L_{III} = 26/1.3/1.3$), 0.104 (K/L 6.5, $L_I/L_{II} + L_{III} = 43/2.3$) spect conv (63M52a, 63M52b); 0.070 (coinc with 0.103 y, K/L 0.29), 0.103 (K/L 3.5), 0.582 (weak) spect conv, γ -y coinc (31R52); 0.069, 0.103 spect conv (67H48a); 0.102 ($e/\gamma > 2.5$) spect conv, β^- -y, β -conv coinc (11H50); others (43M46, 82B48)		Nd- α -n (47K42); Sm-n-y (71H36, 1P38a, 44L41, 16W42, 60H46, 2S47, 51W51); Sm-n-2n (1P38a, 47K42); Sm-d-p (44L41, 47K42); Sm-y-n (44L41); spall-fission Th (7N49a), U (6F51); fission U233 (61S48), U235, Pu (51W51); parent Eu153m (52M50)
¹⁵⁴ Sm	22.53 (3148d)						fission U235 (mass spect) (3150a)
¹⁵⁵ Sm	B n-capt (12A35, 82M35); chem (51W51a)	β^- (47K42)	23.5 m (31R52); 25 m (51W51a); 21 m (1P38a)	1.8 (coinc with both γ 's) abs, β^- y coinc (31R52); 1.9 abs (51W51a); 1.8 abs (47K42)	γ_1 1.05 (K/L 3.6), γ_2 0.246 (coinc with γ_1 , K/L -8) (γ_1/γ_2 -1) spect, spect conv, γ -y coinc (31R52)		Sm-n-y (12A35, 82M35, 71H36, 1P38a, 44L41, 2S47, 3147c, 51W51a); Sm-d-p (44L41, 47K42); fission U235 (51W51a), Pu (51W51a); parent Eu155 (3147c)
¹⁵⁶ Sm	A chem, genet (51W51b)	β^- (51W51b)	-10 h (51W51b)	0.9 abs (51W51b)			fission U (51W51b); spall-fission U (6F51); parent Eu156 (51W51b)

Isotope Z A	Class and identification	Percent abundance	Type of decay	Half-life	Energy of radiation in Mev		Disintegration energy and scheme	Method of production and genetic relationships
					Particles	Gamma-transitions		
¹⁴⁴ Eu 63	C excit, sep isotopes (74H52)		β^+ (74H52)	18 m (74H52)	2.4 spect (74H52)			¹⁴⁴ Sm -p-n (74H52)
¹⁴⁵ Eu	A chem, genet, sep isotopes, excit (74H51)		EC (74H51)	5 d (74H51)	conv: 0.2 abs (74H51)			¹⁴⁷ Sm -p-3n (74H51); daughter Tb ¹⁴⁹ (74H51)
¹⁴⁶ Eu	C excit, sep isotopes (74H51)		EC (74H51)	38 h (74H51)	conv: 0.4 abs (74H51)			¹⁴⁴ Sm - α -pn, Sm ¹⁴⁷ -d-3n (74H51)
¹⁴⁷ Eu	B chem, excit, sep isotopes (74H51)		EC 99+%, α -10-3%, no β^+ (74H51)	24 d (74H51)	α : 2.88 ion ch (74H51) conv: 0.2 abs (74H51)			¹⁴⁷ Sm -p-n (74H51); Sm-d-2n, 3n (42R52)
¹⁴⁸ Eu	A chem (84M51d); excit, sep isotopes (74H51, 86M52)		EC, no β^+ (74H51)	59 d (86M52); 54 d (2W50b); 50 d (74H51); 53 d (84M51d)	conv: 0.4 abs (74H51, 2W50b)	0.57 scint spect (74H52); 1.0, 0.4 abs (84M51d, 2W50b); 0.7 abs (86M52)		¹⁴⁸ Sm -p-n (74H51, 86M52); Sm-p-n (2W50b); Sm-d-n (47K43, 84M51d)
¹⁴⁹ Eu	E sep isotopes, excit (74H52)			-120 d (74H52)		-0.4 scint spect (74H52)		¹⁴⁹ Sm -p-n (74H52)
¹⁵⁰ Eu	A chem, excit (65B50); chem, excit, sep isotopes (74H52); excit, sep isotopes (86M52)		δ^- (86M52)	15.0 h (2W50b); 15 h (65B50); 13.1 h (86M52)	1.8 spect (2W50b); 0.8, other β^+ 's (86M52)			¹⁵⁰ Sm -p-n (74H52, 86M52); Sm-p-n (2W50b); Eu-y-n (65B50)
¹⁵¹ Eu		47.77 (43H48)					¹⁵¹ Eu, I = 5/2 (87M50)	fission U (mass spect) (3150a)
¹⁵² Eu	A n-capt, mass spect (3147d); chem (84M49a)		EC, δ^- (60H49)	13 y (7K52); 5.3 y yield (60H49)	1.58, others spect (11H50); 1.58, 0.75 spect (68S48); 1.7 (-20%), 0.9 (-80%) abs (84M49a)	0.122 (conv in Sm), 0.123 (conv in Gd), 0.244, 0.344, 0.720, 0.964, 1.086 spect conv (11K51, 10C50c); 0.121, 0.244, 0.344 spect conv (43K52); 0.121 (coinc with 0.244 y), 0.123 (coinc with 0.344 y), 0.244, 0.344 (not coinc with 0.244 y) conv-conv coinc spect (35F50); others (11H50, 68S48)		Eu-n-y (3147d, 2S47)
¹⁵² Eu	A n-capt (82M35); n-capt, excit (1P38a); mass spect (60H46, 60H49)		δ^- , EC (60H49)	9.2 h (1P38a, 60H49); 9.3 h (37B46)	1.880, 0.55 (?) (weak) spect (11H50); 1.88 spect (20T39)	γ_1 0.122 (conv in Sm, K/L -4), γ_2 0.344 (conv in Gd, K/L -10) spect conv (11K51); 0.122, 0.336 (coinc with β) pair spect, β -y coinc (107S51); 0.120 (coinc with 0.9 or 0.8 y), 0.94, 0.82 (not coinc with 0.9 y) spect, spect conv, β -conv, y-y coinc (11H50); others (52W51, 20T39, 10C50c, 35F50, 23R39)		Eu-n-y (82M35, 1P38a, 71H36, 5F41b, 2S47, 60H49); Eu-n-2n (1P38a); Eu-d-p (5F39, 5F41b)

Eu ^{153m}	A genet (52M50)	52.23 (43H48)	IT (52M50)	3.0 x 10 ⁻⁹ s delay coinc (52M50)		0.069 (e _K /γ 3.8), 0.103 (e _K /γ 1.2, K/L+M 3.5) scint spect (52M52e)	(11K51, 11H50) <div><div>Eu^{153m}</div><div>0.173</div><div>0.103</div><div>(5/2+)</div><div>Eu¹⁵³, I = 5/2 (87M50)</div><div>(18G52)</div></div>	daughter Sm ¹⁵³ (52M50)
Eu ¹⁵³								fission U (mass spect) (3150a)
Eu ¹⁵⁴	A n-capt (69S38); mass spect (3147d, 60H49); chem (84M49a)		β ⁻ (60H49)	16 y (7K52); 5.4 y yield (60H49)	1.9 (-10%), 0.7 (-40%), 0.3 (-50%) abs (84M49a, calc from 60H49); -0.7 (coinc with hard γ), 0.3 abs, β-γ coinc abs (84M49a); with Eu ¹⁵⁴ and Eu ¹⁵⁵ : 1.88, 0.90, 0.59, 0.25, 0.14 spect, β-γ coinc abs (24K50d); others (37B46, 26K48, 11H50, 37W47)	0.336, 0.778, 1.116 spect conv (11K51); with Eu ¹⁵⁴ and Eu ¹⁵⁵ : 0.085, 0.101, 0.725, 1.005, 1.288 spect (24K50d); 0.122 spect conv (43K52); others (26K48, 10C48b)	Eu-n-γ (69S38, 5F39, 5F41b, 2S47); Eu-d-p (5F41b, 26K48); Eu ¹⁵³ (fission product)-n-γ (84M49a); fission U (24K50d)	
Eu ¹⁵⁵	A chem (51W51c); mass spect (60H49)		β ⁻ (51W51c)	1.7 y (31R52); yield (60H49); 2.0 y (51W51c)	0.154 (80%), 0.243 (20%) spect, β-γ, γ-γ coinc (84M49a); see Eu ¹⁵⁴ β's (24K50d)	0.060 (weak), 0.087 (K/L-8), 0.106 (K/L-8), 0.132 (weak) spect conv (31R52); 0.085, 0.099 crit abs Pb, Pt (84M49a); 0.084 crit abs Tl, Hg (51W51c); 0.015 ion ch, β-γ coinc (33W52); see Eu ¹⁵⁴ γ's (24K50d)	Sm-d-n (47K43); Eu-n-γ (second order reaction) (60H49); spall-fission Th (7N49a); fission U (51W51c, 84M49a); daughter Sm ¹⁵⁵ (3147c)	
Eu ¹⁵⁶	A chem (51W51b); mass spect (3147b, 3147c)		β ⁻ (51W51b)	15.4 d (51W51b) 3147c	-0.5 (60%), 2.4 (40%) abs (51W51b)	2.0 abs (51W51b)	Eu-n-γ (second order reaction) (3147c); spall-fission Th (7N49a), U (6048, 6F51); fission U (51W51b), Pu (28F51); daughter Sm ¹⁵⁶ (51W51b)	
Eu ¹⁵⁷	D chem (51W51d)		β ⁻ (51W51d)	15.4 h (51W51d)	-1.0 (-75%), -1.7 (-25%) abs (51W51d)	0.6, 0.2 abs (51W51d)	spall-fission Th (7N49a); fission U (51W51d), Pu (32K48)	
Eu ¹⁵⁸	D chem (51W51d)		β ⁻ (51W51d)	60 m (51W51d)	2.6 abs (51W51d)	γ (51W51d)	fission U (51W51d)	
Eu ¹⁵⁹	F excit (65B50)			20 m (65B50)			Gd-γ-p (?) (65B50)	
Gd ¹⁴⁸	B chem, excit, sep isotopes (42R52)		α, EC (?) (42R52)	>35 y (42R52)	α: 3.16 ion ch (42R52)		Sm-α-3n, Sm ¹⁴⁷ -α-3n (42R52); Eu-p-4n (42R52); spall Dy (42R52)	
Gd ¹⁴⁹	B chem, excit, sep isotopes, cross bomb (74H51)		EC 99+%, α -10-3% (42R52)	9 d (74H51)	α: 3.0 ion ch (74H51); conv: 0.35 abs (74H51)		Sm-α-2n, Sm ¹⁴⁷ -α-2n (74H51, 42R52); Eu-p-3n (74H51)	
Gd ¹⁵⁰	D chem (42R52)		α (42R52)	long (42R52)	α: 2.7 ion ch, range emuls (42R52)		Eu-d-3n (42R52)	
Gd ¹⁵¹	F chem, excit (63H50)		EC, no β ⁺ (63H50)	150 d (63H50)		0.265 (e/γ large) abs (63H50)	Eu-d-2n (5F41b, 26K48, 63H50)	
Gd ¹⁵²		0.20 (1B50)						
Gd ¹⁵³	A mass spect (3147c); chem, n-capt (63H50)		EC, no β ⁺ (63H50)	236 d (63H50); 225 d (24K49a)		0.104 (K/L 5.2) spect conv (10C52c); 0.100 spect conv, abs (24K49a); 0.106 (e/γ >0.9) abs (63H50); others (10C48b)	Eu-d-2n (63H50); Gd-n-γ (3147c, 10C48b, 24K49a, 63H50)	

Isotope Z A	Class and identification	Percent abundance	Type of decay	Half-life	Energy of radiation in Mev		Disintegration energy and scheme	Method of production and genetic relationships
					Particles	Gamma-transitions		
⁶⁴ Gd		2.15 (1B50)						
¹⁵⁵ Gd		14.73 (1B50)						
¹⁵⁶ Gd		20.47 (1B50)						
¹⁵⁷ Gd		15.68 (1B50)						
¹⁵⁸ Gd		24.87 (1B50)						
¹⁵⁹ Gd	B n-capt (2S47); chem (65B49, 63H50)		β^- (26K48)	18.0 h (65B49, 65B50, 26K48); 17.9 h (24K49b); -24 h (63H50)	0.9 abs (26K48, 65B49)	0.055, 0.38 abs (65B49); -0.3 abs (26K48); others (52M51)		Gd-n- γ (2S47, 24K49b, 65B49, 63H50); Gd-d-p (26K48); Gd- γ -n (65B50)
¹⁶⁰ Gd								
¹⁶¹ Gd	C n-capt (3146); n-capt, excit (65B49)	21.90 (1B50)	β^- (38M49)	3.6 m (65B49, 24K49b); 3.5 m (26K48); 3.3 m (38M49); 4.5 m (3146)	1.5 abs (24K49c); -2 (38M49)	0.37 abs (24K49c); -0.07 (38M49)		Gd-n- γ (3146, 26K48, 65B49, 38M49, 24K49b); parent Tb ¹⁶¹ (24K49b, 24K49c)
¹⁴⁹ Tb	A chem, mass spect (42R50)		α , EC (?) (42R52)	4.1 h (42R52)	α : 3.955 spect (42R52); 3.95 ion ch (42R52)			spall Gd, Dy (3T49, 42R52), Tb, Yb (42R52); parent Eu ¹⁴⁵ (74H51)
¹⁵¹ Tb	D chem, excit (42R52)		α , EC (?) (42R52)	19 h (42R52)	3.44 ion ch (42R52)			spall Eu (42R52), Gd, Tb, Dy (42R52)
¹⁵³ Tb	B chem, excit (2W50c)		EC (2W50c)	5.1 d (2W50c)		1.2, 0.2 abs (2W50c)		Eu- α -2n (2W50c)
¹⁵⁴ Tb	B chem, excit (2W50c)		EC 99+%, β^+ -0.5% (2W50c)	17.2 h (2W50c)	2.6 spect (2W50c)	1.3 abs (2W50c)		Eu- α -n, Eu- α -3n (2W50c); Gd-p-n (2W50c)
¹⁵⁵ Tb	D chem, excit (2W50c)		EC (2W50c)	190 d (2W50c)		1.4 abs (2W50c)		Eu- α -2n (2W50c)
¹⁵⁶ Tb	B chem, excit (2W50c)		EC >75%, β^+ <25% (2W50c)	5.0 h (2W50c)	-1.3 abs (2W50c)			Eu- α -n (2W50c); Gd-p-n (2W50c)
¹⁵⁷ Tb	B chem, excit, cross bomb (2W50c)		EC (2W50c)	4.7 d (2W50c)		1.4 abs (2W50c)		Gd-p-n (2W50c)
¹⁵⁹ Tb		100 (43H48)					Tb ¹⁵⁹ , I = 3/2 (87M50)	
¹⁶⁰ Tb	A n-capt (37B43); mass spect (3147c); chem (6F51)		β^- (37B43); no β^+ (82B50)	73.5 d (37B46); 71 d (82B50); 76 d (10C50d)	0.860 (43%), 0.521 (41%), 0.396 (16%) spect (82B50); -0.90 β^+ (coinc with 0.085 γ) scint spect, β - γ coinc (52M52)	0.962, 0.876, 0.410, 0.391, 0.375, 0.298, 0.282, 0.215, 0.196, 0.176, 0.093, 0.087 spect, spect conv (10C50d); 0.970, 0.886, 0.300, 0.200, 0.085 spect conv (82B50); with Dy ^{160m} : 0.085 (e_K/γ 1.7) scint spect (52M52a); others (10C48b)		Gd-d-2n (26K48); Tb-n- γ (37B43, 37B46, 2S47); spall-fission U (6F51); parent Dy ^{160m} (52M52, 52M52a)

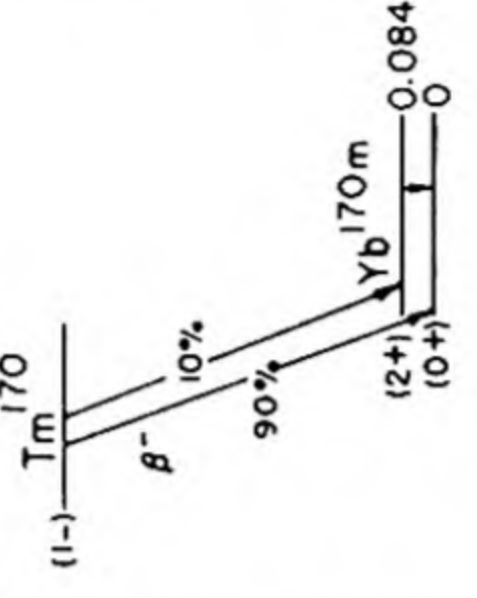
Tb ¹⁶¹	β^- excit (26K48); chem, excit (24K49c)				0.049 (L/M 3.7) spect conv (10C52c); 0.026 ion ch (17S50); 0.05 abs (65B49, 24K49a)	Gd-d-n (26K48, 65B49); spall-fission U (6 ⁻⁵); daughter Gd ¹⁶¹ (24K49b, 24K49c)
Tb ^{162,163}	E excit (65B50)					Dy-y-p (?) (65B50)
Dy ¹⁵³	E cross bomb (42R52)					Nd-C-spall, Tb-p (42R52)
Dy ¹⁵³	E cross bomb (42R52)					spall Tb, Dy (42R52)
Dy ¹⁵³	D chem (42R52)					Nd-C-spall, Tb-p (42R52)
Dy ¹⁵⁶						
Dy ¹⁵⁸						
Dy ¹⁵⁹	B chem, n-capt (24K49d); chem, cross bomb (65B51a)					Tb-d-2n (65B51a); Dy-n-y (24K49d, 65B51a)
Dy ^{160m}	A genet (52M52)					daughter Tb ¹⁶⁰ (52M52, 52M52a)
Dy ¹⁶⁰						
Dy ¹⁶¹						
Dy ¹⁶²						
Dy ¹⁶³						
Dy ¹⁶⁴						
Dy ^{165m}	A n-capt (9F44b); n-capt, sep isotopes (3147e)					Dy-n-y (9F44b, 9F46, 2S47, 18G47, 42C50); Dy ¹⁶⁴ -n-y (3147e)
Dy ¹⁶⁵	A n-capt (71H36, 82M35); n-capt, sep isotopes (3147e); mass spect (3147f)					Dy-n-y (8 ⁻¹ M35, 71H36, 1P38a, 1M40, 2S47, 24K40d); Dy ¹⁶⁴ -n-y (3147e)



(18G52)

Isotope Z A	Class and identification	Percent abundance	Type of decay	Half-life	Energy of radiation in Mev		Disintegration energy and scheme	Method of production and genetic relationships
					Particles	Gamma-transitions		
⁶⁶ Dy 66 166	A chem, genet (24K49d)		β^- (24K49d)	82 h (65B50a); 81 h (24K49d)	0.2 abs (65B50a); 0.4 abs (24K49d)			Dy-n- γ (second order reaction) (24K49d, 65B50a); spall-fission U (6F51); parent Ho ¹⁶⁶ (24K49d, 65B50a)
⁶⁷ Ho 67 166	E excit (42R52)		α (42R52)	4 m (42R52)	α : 4.2 ion ch (42R52)			Dy-p (42R52)
¹⁶⁰ Ho 68 160	C excit (2W50c)		EC 99+%, β^+ -0.5% (2W50c)	22.5 m (2W50c)	-1.3 abs (2W50c); conv: 0.2 abs (2W50c)	-1.2 abs (2W50c)		Tb- α -3n (2W50c)
¹⁶¹ Ho 68 161	B chem, excit (2W50c)		EC (2W50c)	4.6 h (2W50c)	conv: 0.1 abs (2W50c)			Tb- α -2n, Dy-p-n, Dy-d-n (2W50c)
¹⁶² Ho 68 162	B chem, excit (2W50c)		EC -85%, β^+ -15% (2W50c)	65.0 d (2W50c)	β^+ : 0.8 spect, abs (2W50c); conv: 0.1 abs (2W50c)	-1 abs (2W50c)		Tb- α -n, Dy-p-n, Dy-d-2n (2W50c)
¹⁶³ Ho 68 163	B chem, excit, cross bomb (2W50c)		EC (2W50c)	5.20 d (2W50c)	conv: 0.4 abs (2W50c)	-0.5, 1.4 abs (2W50c)		Dy-p-n, Dy-d-n, Dy-d-2n (2W50c)
¹⁶⁴ Ho 68 164	A excit (1P38a)		θ^- (2W50c)	34.0 m (2W50c); 41.5 m (25W50)	0.95 spect (2W50c)	no γ (2W50c)		Dy-p-n (2W50c); Ho-n-2n (1P38a, 25W50); Ho-y-n (25W48)
¹⁶⁵ Ho 68 165		100 (28L50)						
¹⁶⁶ Ho 68 166	A n-capt (71H36); mass spect (3147d); chem (24K49b)		β^- (71H36)	27.3 h average of (24K49b, 3147d, 37G46, 22C49, 10C49a, 31A50)	1.84 (-89%), 0.55 (-11%) spect (75S50a); 1.88 spect (22G49); 1.84 (86%), 0.66 (14%) spect (31A50); 1.85 spect (24K49); 1.90 cl ch, abs (97S50)	0.080 (e_K/γ 1.9, K/L+M 0.25), 1.38 (coinc with 0.08 γ) scint spect, γ - γ coinc (14S52a); 0.081 (K/L 0.07, $L_I/L_{II}/L_{III} =$ 0.1/0.72/1.00) spect conv (63M52); 0.080 (e_L/γ -0.4, K/L <1), 1.36 (weak) spect, spect conv, β -conv coinc (75S50a); 0.081 (e_K/γ 1.9) scint spect (52M52a); 0.081, 0.9 spect conv, abs (10C49a); 0.081, -1.5 (weak) spect conv, β - γ coinc (31A50); 0.080, 1.2 (weak) spect conv, abs (22G49)	<p>Ho¹⁶⁵, I = 7/2 (87M50)</p>	Ho-n- γ (71H36, 1P38a, 1M40, 2S47); spall-fission U (6F51); daughter Dy ¹⁶⁶ (24K49d, 65B50a); parent Er ^{166m} (57M50a, 52M52a, 63M52)
¹⁶⁶ Ho 68 166	B chem, excit (65B52)		β^- (65B52)	>30 y (65B52)	1.1 (-8%), 0.28 (-46%), 0.18 (-46%) abs (65B52)	0.212 (coinc with 1.1 β), 0.280 (coinc with 0.73 and 0.83 γ), 0.725, 0.830, 0.095 (very weak) scint spect, γ - γ , β - γ coinc (65B52)		Ho-n- γ (65B52)
^{167,169} Ho 69 167,169	E excit (65B50)			96 m (65B50)				Er-y-p (65B50)

[illegible]

Isotope Z A	Class and identification	Percent abundance	Type of decay	Half-life	Energy of radiation in Mev		Disintegration energy and scheme	Method of production and genetic relationships
					Particles	Gamma-transitions		
¹⁶⁷ Tm 69	B chem, excit (2W49a)		EC, no β^+ (2W49a)	9.6 d (2W49a)	conv: 0.21 abs (2W49a)	0.22, 0.95 abs (2W49a)		Ho- α -2n (2W49a); Er-p-n (2W49a); spall Ta (2W49a)
¹⁶⁸ Tm	A chem, excit (2W49a)		EC, β^- (?) -2% (2W49a)	85 d (2W49a)	conv: 0.16, 0.5 abs (2W49a)	0.21, 0.85 abs (2W49a)		Ho- α -n (2W49a); Er-p-n (2W49a); Tm-n-2n (2W49a)
^{169m} Tm	A genet (10D48)		IT (10D48)	all delay coinc: 0.658 x 10 ⁻⁶ s (27F50); 0.67 x 10 ⁻⁶ s (75M51a); 0.7 x 10 ⁻⁶ s (52M51); 0.60 x 10 ⁻⁶ s (14S51a)		see γ 's of Yb ¹⁶⁹		daughter Yb ¹⁶⁹ (10D48, 27F50, 52M51, 14S51a, 75M51a)
¹⁶⁹ Tm		100 (7L50)						
¹⁷⁰ Tm	A n-capt (23N36, 71H36); chem (24K48a)		β^- (37B46a); no EC (lim 0.3%), no β^+ (lim 0.01%) (14G52)	129 d (24K49b); 120 d (42C50); 127 d (37E46a)	0.968 (76%), 0.884 (24%) spect (14G52); 0.970 (~90%), 0.386 (~10%) spect (36F49); 0.970, 0.88 spect, β - γ coinc (44R52); 0.990 spect (16A50); others (14G49, 22G49a, 97S50, 9S49a)	0.0841 (3%, e γ / γ 1.6, K/L/M = 1/2.6/0.75) spect conv, β - γ coinc (14G52); γ (-3%, e γ / γ 9.4, K/L+M 0.22) x- γ coinc, scint spect (1N50); 0.085 (K/L 0.16, L _I /L _{II} /L _{III} = 0.1/0.83/1.00) spect conv (63M52); 0.085 (e γ / γ 1.5) scint spect (52M52a); 0.084 (e γ / γ 4, K/L/M -1/6.9/2.1) spect, spect conv, β - γ coinc (36F49); γ (e γ / γ >10, K/L+M 0.1) spect conv, scint spect (7S51); 0.085 spect conv (16A50, 42C50, 9S49a); others (22G50a, 4E50a, 1N50a, 10C49a, 52R52)	 <p>Tm¹⁶⁹, I = 1/2 (87M50) Qβ^- 0.970 (36F49) (1-) Tm¹⁷⁰ β^- 10% 90% Yb^{170m} (2+) 0.084 (0+) 0 (18G52)</p>	Tm-n- γ (71H36, 23N36, 2S47); Tm-d-p (24K48a); parent Yb ^{170m} (8B50, 5?M5?a, 14G52)
^{171m} Tm	B genet (10D48)		IT (10D48)	2.5 x 10 ⁻⁶ s delay coinc (10D48)				daughter Er ¹⁷¹ (10D48)
¹⁷¹ Tm	B chem, genet (24K48)		β^- (24K48)	680 d (24K49b)	0.10 spect (24K48a)			daughter Er ¹⁷¹ (24K48)
^{172(?)} Tm	E chem (6F51)		β^- (6F51)	2-3 d (6F51)				spall-fission U (6F51)
^{>171} Tm	E excit (65B50)			19 m (65B50)				Yb- γ -p (?) (65B50)
¹⁶⁶ Yb 70	D chem, genet (6F51)		EC (6F51)	62 h (6F51)				spall-fission U, parent Tm ¹⁶⁶ (6F51)
¹⁶⁸ Yb		0.140 (1B50)						

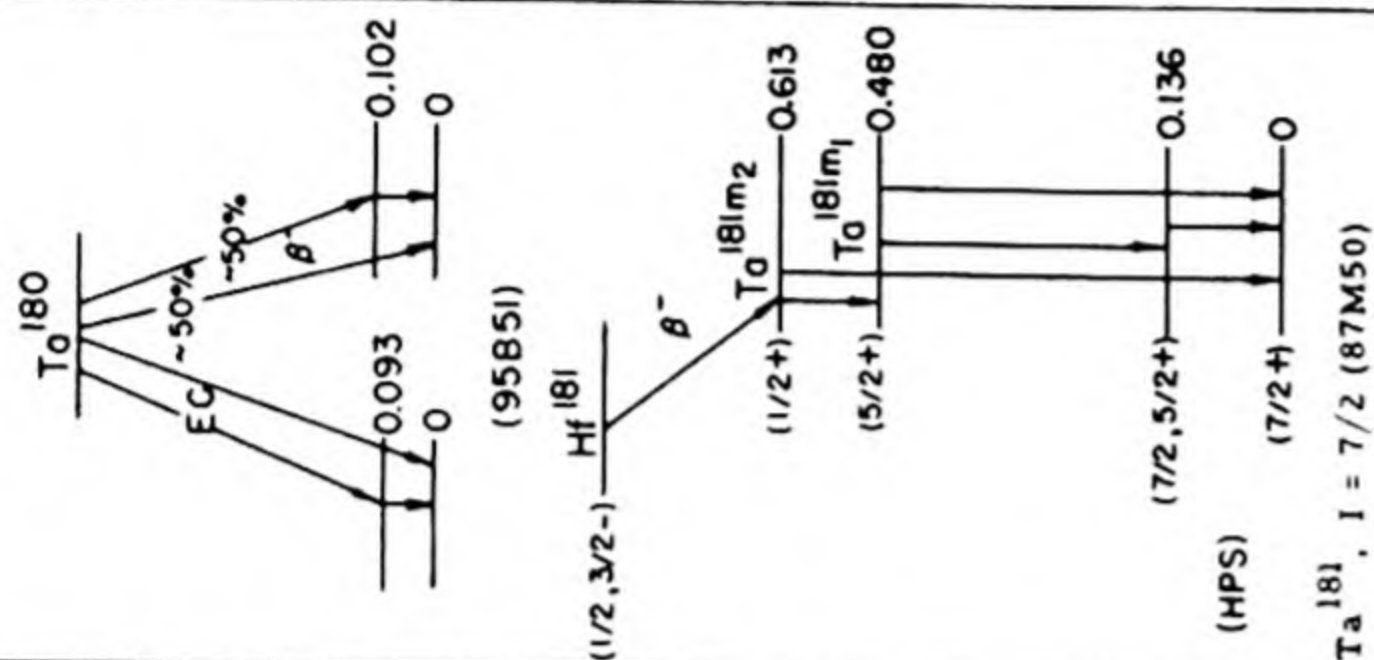
Yb^{169}	A n-capt (37B46a): chem, excit (24K48a)	31.8 d (49W49): 32.4 d (10C50e): 33 d (37B46a, 75M51a)	EC (37B46a)	Y_1 0.023, Y_2 0.064, Y_3 0.095, Y_4 0.110 (e/ γ 1.6), Y_5 0.120, Y_6 0.133 (e/ γ 0.2), Y_7 0.143, Y_8 0.160, Y_9 0.178 (e/ γ 0.8), Y_{10} 0.198 (e/ γ 0.4), Y_{11} 0.308 (e/ γ 0.04); ($\gamma_2/\gamma_4/\gamma_6/\gamma_9/\gamma_{10}/$ $\gamma_{11} = 1.3/2.1/2.0/1.0/1.7/0.6$) spect, spect conv, delay coinc (75M51a); 0.063, 0.094, 0.110, 0.131, 0.177, 0.198, 0.308 spect conv (10C50e); 0.109, 0.130, 0.177, 0.198, 0.307 scint spect, delay coinc (14S51a) 0.0841 (e γ / γ 1.6, K/L/M = 1/2.6/ 0.75) spect conv, β - γ coinc (14G52); 0.085 (e γ / γ 1.5) scint spect- (52M52a)			Tm-d-2n (24K48a): Yb -n- γ (34A45, 37B46a, 3148a): spall-fission U (6F51): parent Tm ^{169m} (10D48, 27F50, 52M51, 14S51a, 75M51a)
Yb^{170m}	A genet (8B50)	1.57 $\times 10^{-9}$ s delay coinc (14G52); 1.6 $\times 10^{-9}$ s delay coinc (52M52a)	IT (8B50)	see Tm ¹⁷⁰ (2+) Yb^{170m} 0.084 (0+) (18G52)			daughter Tm ¹⁷⁰ (8B50, 14G52, 52M52a)
Yb^{170}							
Yb^{171}							
Yb^{172}							
Yb^{173}							
Yb^{174}							
Yb^{175}	A n-capt (37B46a, 34A45): mass spect (3147f); chem (24K49b)	102 h (3147f); 99 h (37B46a): 101 h (34A45)	β^- (34A45)	0.138, 0.259, 0.283, 0.396 spect conv (10C50e); others (52M51)			Yb -n- γ (34A45, 37B46a, 3147f, 24K49b): Yb - γ -n (65B50)
Yb^{176}							
Yb^{177}	B n-capt (82M35, 71H36): chem (24K49b)	1.8 h (52M51): 1.9 h (34A45): 2.4 h (37B46a)	β^- (37B46a)	0.150 (K/L 3) spect conv, β - γ coinc (52M51)			Yb -n- γ (82M35, 71H36, 1P38a, 37B46a, 3147f): parent Lu ^{177m} (52M49, 52M51)
Yb^m	E n-capt (38M49a)	6 s (38M49a, 31K51)	IT (38M49a)	0.212, 0.104 (?) scint spect (31K51); 0.200 abs (38M49a): Yb K-x (38M49)			Yb -n- γ (38M49a, 38M49, 31K51)
Yb^m	E n-capt (38M49a)	50 s (38M49a)	IT (38M49a)	- 0.025, Yb L-x abs (38M49a)			Yb -n- γ (38M49a, 38M49)
Yb^m	E n-capt (31K51)	0.15 s (31K52)		0.455 scint spect (31K52)			Yb -n- γ (31K51)

Isotope Z A	Class and identification	Percent abundance	Type of decay	Half-life	Energy of radiation in Mev		Disintegration energy and scheme	Method of production and genetic relationships
					Particles	Gamma-transitions		
$^{170}_{71}\text{Lu}$	B chem, excit (2W51)		EC (2W51)	1.7 d (2W51)		-2.5 abs (2W51)		Tm- α - β n, spall Ta (2W51)
$^{171}_{71}\text{Lu}$	B chem, excit (2W51)		EC (2W51)	8.5 d (2W51)		-1.2 abs (2W51)		Tm- α - β n, Yb-p-n, spall Ta (2W51) daughter Hf ¹⁷¹ (2W51)
$^{171}_{71}\text{Lu}$	D chem, excit (2W51)		EC (2W51)	-600 d (2W51)		-1 abs (2W51)		Tm- α - β n (2W51)
$^{172}_{71}\text{Lu}$	B chem, excit (2W51)		EC (2W51)	6.70 d (2W51)		1.2 abs (2W51)		Tm- α -n, Yb-p-n (2W51) daughter Hf ¹⁷² (2W51)
$^{172}_{71}\text{Lu}$	B chem, excit (2W51)		β^+ , EC (?) (2W51)	4.0 h (2W51)	1.2 abs (2W51)			Tm- α -n, Yb-p-n, Lu-p-p-n (2W51)
$^{173}_{71}\text{Lu}$	B chem, excit (2W51)		EC (2W51)	-500 d (2W51)		-0.2, 0.8 abs (2W51)		Yb-p-n, Lu-p-p-n (2W51) daughter Hf ¹⁷³ (2W51)
$^{174}_{71}\text{Lu}$	A chem, excit (2W51)		EC -80%, β^- -20% (2W51)	165 d (2W51)	β^- : 0.6 abs (2W51)	-1 abs (2W51)		Lu-n- β n, Lu-d-p-n, Lu-p-p-n, Hf-d- α (2W51)
$^{175}_{71}\text{Lu}$		97.40 (60H50)						
$^{176m}_{71}\text{Lu}$	A n-capt (77M35a, 82M35); chem, excit (2W48)		β^- , no IT (17S52)	3.67 h (34A45); 3.7 h (37B46a)	1.1, 1.2 (17S52); 1.3 cl ch (34A45); 1.2 abs (9F43)	0.089 (K/L _{II} /L _{III}) = 0.24/0.71/1.00; spect conv (63M52); 0.089 (e _K /y 1.3) scint spect, β^- -y delay coinc (52M52c); 0.089 (e/y large, K/L 0.1) scint spect (17S52)		Lu-d-p (2W51, 2W48), Lu-n-y (77M35a, 82M35, 71H36, 9F43, 37B46a, 34A45, 2S47, 24K49b, 31A50a), Lu-y-y (11D47a, 65B50), parent Hf ^{176m} (52M52c) natural source (52H38, 5M39)
$^{176}_{71}\text{Lu}$	A chem (52H38); mass spect (8M39)	2.60 (60H50)	β^- , no EC (17S52a)	7.5 $\times 10^{10}$ y ap act (3L39a)	0.40 abs (9F47a, 9F43)	0.089, 0.180, 0.270 scint spect (17S52a)		
$^{177m}_{71}\text{Lu}$	B genet (52M49)		IT (52M49)	1.3 $\times 10^{-7}$ s delay coinc (52M49, 52M51)		0.150 (K/L 3) scint spect, β^- -y coinc (52M51, 52M49)		daughter Yb ¹⁷⁷ (52M49, 52M51)
$^{177}_{71}\text{Lu}$	A n-capt (71H36); mass spect (31A71); chem, excit (2W48)		β^- (37B46a)	6.8 d (37B46a, 2W48); 7.0 d (30D49); 6.6 d (9F43, 34A45)	0.495 (65%), 0.37 (17%), 0.17 (18%) spect (30D49); 0.475 spect (31A50a)	0.112 (e _K /y 0.81), 0.206 (e _K /y 0.04), 0.318 (-5%) scint spect, y-y coinc (52M52d); 0.112, 0.206, 0.317 (very weak) spect, spect conv (30D49); 0.112 (K/L/M = 1/2/0.5), 0.205 spect conv (31A50a); 0.113, 0.209 spect conv (10C49a); others (52M51)		Lu-n-y (71H36, 9F43, 34A45, 37B46a, 2S47, 24K49b, 31A50a); Lu-d-p (2W48)
$^{178,179}_{71}\text{Lu}$	D chem (65B50)			22 m (65B50)				Hf-y-p (65B50)

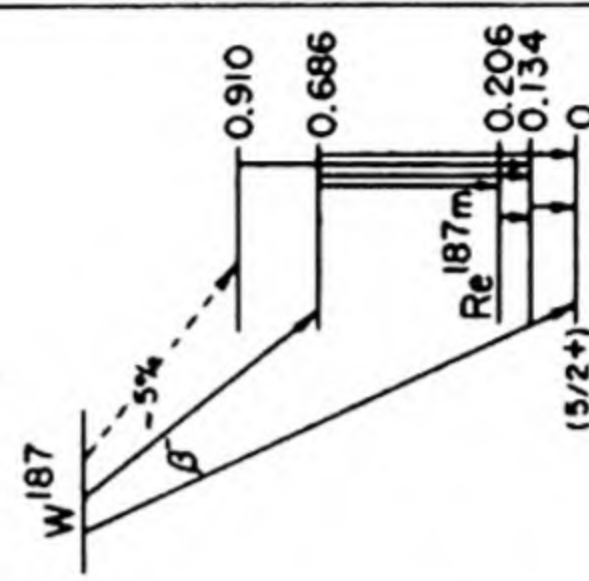
^{170}Hf	D chem (2W51)			2.4 spect (2W51)	no γ (2W51)	Lu-p-6n (2W51)
^{171}Hf	B chem, genet, excit (2W51)			112 m (2W51)	1.4 abs (2W51)	Yb-a-3n, Lu-p-5n (2W51); parent (8.5 d) Lu ¹⁷¹ (2W51)
^{172}Hf	B chem, genet (2W51)			16.0 h (2W51)	-0.28, 0.8 abs, spect conv (2W51)	Yb-a-2n, Yb-a-3n, Lu-p-4n spall Ta (2W51); parent (6.7 d) Lu ¹⁷² (2W51)
^{173}Hf	B chem, excit, genet (2W51)			-5 y (2W51)	-1 abs (2W51)	Yb-a-n, Yb-a-2n, Yb-a-3n, Lu-p-3n (2W51); parent Lu ¹⁷³ (2W51)
^{174}Hf		0.18 (75H49)		23.6 h (2W51)		
^{175}Hf	A chem, excit (2W49b); n-capt, sep isotopes (82B51); mass spect (12H51a)			70 d (2W49b)	0.089, 0.113, 0.228, 0.318, 0.342 (K/L 4.9), 0.431 spect conv (82B52); 1.5 abs (2W49b)	Lu-d-2n, Lu-p-n (2W49b); Hf-n- γ (12H51a); Hf ¹⁷⁴ -n- γ (82B51)
^{176m}Hf	A genet (52M52c)			1.35 $\times 10^{-9}$ s delay coinc (52M52c)	0.089 (e_K/γ 1.3) scint spect, β - γ coinc (52M52c)	daughter Lu ^{176m} (52M52c)
^{176}Hf		5.15 (75H49)				
^{177}Hf		18.39 (75H49)				
^{178}Hf		27.08 (75H49)				
^{179m}Hf	A n-capt (9F44b); n-capt, sep isotopes (82B51, 38M51b)			19 s (9F44b, 38M51b)	0.160, 0.217 scint spect, spect conv (82B51); -0.150, 0.215 scint spect, conv- γ coinc (38M51b); 0.150 (e/γ very large, K/L 0.9) spect conv (15H48a); 0.220 scint spect (31K51)	Hf-n- γ (9F44b, 9F46, 38M51); Hf ¹⁷⁸ -n- γ (38M51b, 82B51)
^{179}Hf		13.78 (75H49)				
^{180m}Hf	B chem, n-capt, sep isotopes (82B51)			5.5 h (82B51)	0.057, 0.093, 0.214, 0.330, 0.442 spect conv, γ -conv coinc (82B51)	Hf ¹⁷⁹ -n- γ (82B51)
^{180}Hf		35.44 (75H49)				

Isotope Z A	Class and identification	Percent abundance	Type of decay	Half-life	Energy of radiation in Mev		Disintegration energy and scheme	Method of production and genetic relationships
					Particles	Gamma-transitions		
⁷² Hf ¹⁸¹	A chem, n-capt (71H28); mass spect (12H51a); sep isotopes, n-capt (82B51)		β^- (71H38)	45 d (10C50f, 22R50); 47 d (43B48a)	0.408 spect (29F52); 0.420 spect (82B51); 0.410 spect (4E50); 0.404 spect (71C49); 0.460 spect (43B48a)	γ_1 0.133, γ_2 0.136, γ_3 0.344, γ_4 0.481, γ_5 0.611 spect conv, β -conv, conv-conv, β - γ coinc (82B51); γ_1 0.133, γ_2 0.136, γ_3 0.345, γ_4 0.481, γ_5 0.615 spect conv (4E50); γ_1 0.133 (K/L -1), γ_2 0.136 (K/L -0.2), γ_3 0.345, γ_4 0.481, γ_5 0.612 (γ_1 and γ_2 coinc with γ_3 , γ_1 coinc with γ_4 , γ_4 not coinc with γ_5) spect conv, conv- conv coinc (10C50f); γ_1 (e_K/γ 0.51), γ_4 (e_K/γ 0.034) scint spect, γ - γ coinc (52M52e); γ_1 0.130 (e/γ 0.90, K/L+M 0.6), γ_2 0.134 (e/γ -3, K/L+M -8), γ_3 0.340 (e/γ -0.1), γ_4 0.474 (e/γ 0.030, K/L+M 4.0) spect conv (29F52); γ_1 0.132, γ_2 0.135 (K/L -8), γ_3 0.345, γ_4 0.481 (γ_1/γ_2 -5, γ_4/γ_3 -8) spect, spect conv (12H51a); γ_1 0.130 (e_K/γ -1.3), γ_2 0.134, γ_3 0.337 (K/L -3.6), γ_4 0.471 (K/L -3) (γ_3/γ_4 -2.5) spect conv, β - γ , conv-conv coinc (71C49); γ_3 0.347 (K/L -5.0), γ_4 0.485 (K/L -5.2) spect, spect conv (13J49a); others (43B48a, 10C47, 24N47, 3V48, 26M49a, 49W49a, 63B50, 20D50a, 32P50, 27F50a, 35F50, 52M51, 4B48, 4B49, 14L49)	Q_β^- 1.02 (HPS) $(1/2, 3/2^-) \rightarrow (1/2^+)$ Hf ¹⁸¹ β^- To ¹⁸¹ Im ₂ (0.613) To ¹⁸¹ Im ₁ (0.480) (5/2 ⁺) (7/2, 5/2 ⁺) (7/2 ⁺) (HPS)	Hf-n- γ (71H38, 2S47); ¹⁸⁰ Lu -n- γ (82B51); Ta-n-p (24N47); spall-fission U (6F51); parent Ta ¹⁸¹ m ₁ (4E50, 63B50, 52M51); parent Ta ¹⁸¹ m ₂ (10D48, 4B48, 4E50, 63B50, 52M51)
⁷³ Hf ¹⁷⁶	E (24C52)		IT (24C52)	-3.5 s (24C52)				Hf-n (24C52)
⁷³ Ta ¹⁷⁶	B chem, excit (2W48, 2W50e)		EC (2W50e)	8.0 h (2W50e)	conv: 0.1, 0.2, -1 abs (2W50e)	-2 abs (2W50e)		Lu- α -3n (2W50e); spall Ta (2W48); daughter W ¹⁷⁶ (2W50e)
Ta ¹⁷⁷	B chem, excit (2W48, 2W50e)		EC (2W50e)	53 h (2W50e)	conv: 0.1 abs (2W50e)	-1.4 (weak) abs (2W50e)		Lu- α -2n, Lu- α -3n, Hf-p-n (2W50e); spall Ta (2W48); daughter W ¹⁷⁷ (2W50e)
Ta ¹⁷⁸	B chem, excit (2W50e)		EC -97%, β^+ -3% (2W50e)	2.1 h (2W50e)	β^+ : -1 abs (2W50e); conv: -0.1 abs (2W50e)	1.3-1.5 abs (2W50e)		Lu- α -n, Hf-p-n, Ta-p-p3n (2W50e)
Ta ¹⁷⁸	B chem, genet (2W50e)		EC -94%, β^+ -6% (2W50e)	9.35 m (2W50e)	β^+ : 1.06 spect (2W50e); conv: 0.08 spect conv (2W50e)	-1.5 abs (2W50e)		Hf-p-n (2W50e); daughter W ¹⁷⁸ (2W50e)

Ta^{179}	D chem, excit (2W50e)	EC (2W50e)	-600 d (2W50e)	conv: -0.1 abs (2W50e)	-0.7 (weak) abs (2W50e)	Lu- α -n, Hf-p-n, Ta-p-p2n (2W50e)
Ta^{180}	A chem, excit (17038)	EC -79%, β^- -21%, no β^+ (lim 0.005%) (95B51)	8.15 h (95B51); 8.00 h (2W50e); 8.2 h (17038)	0.71 (-50%), -0.61 (-50%) spect (95B51); 0.7 spect (2W50e); abs (83M51)	γ_1 0.093 (K/L -0.15), γ_2 0.102 ($\gamma_1 + \gamma_2$: e/ γ -5), γ_3 0.2, γ_4 0.4 (γ_3 and γ_4 very weak) spect conv, scint spect, β - γ , x- γ coinc (95B51); 1.3 abs (2W50e)	Ta-n-2n (1P37, 17038, 2W50e); Ta- γ -n (27M49, 55S51, 95B51); Ta-p-pn (96B49, 2W50e); W182 - γ -pn (83M51)
Ta^{181m2}	A genet (10D48)	IT (10D48)	2.2×10^{-5} s delay coinc (10D48, 4E50, 63B50); 2.0×10^{-5} s delay coinc (4B48)		see γ 's of Hf ¹⁸¹	daughter Hf ¹⁸¹ (10D48, 4B48, 4E50, 63B50, 52M51)
Ta^{181m1}	A genet (63B50)	IT (63B50)	1.2×10^{-8} s delay coinc (4E50); 1.1×10^{-8} s delay coinc (63B50); 1×10^{-8} s delay coinc (52M51)		see γ 's of Hf ¹⁸¹	daughter Hf ¹⁸¹ (4E50, 63B50, 52M51)
Ta^{181}			100 (24W48)			
Ta^m	E n-excit (24C49, 24C52)	IT (45G50)	0.33 s (24C49, 45G50, 31K51)		Ta L-x (45G50, 31K51)	Ta-n (24C49, 45G50, 31K51)
Ta^{182m}	A chem, n-capt (2S47, 15H48a)	IT (15H48a); IT -95%, β^- -5% (2W50e)	16.5 m (15H48a); 16.2 m (2S47)	β^- : 0.6 abs (2W50e)	0.180 (K/L 0.25) spect conv (15H48a); 0.180 (e _K / γ 0.8) scint spect (14S51)	Ta-n- γ (2S47, 15H48a, 2W50e)



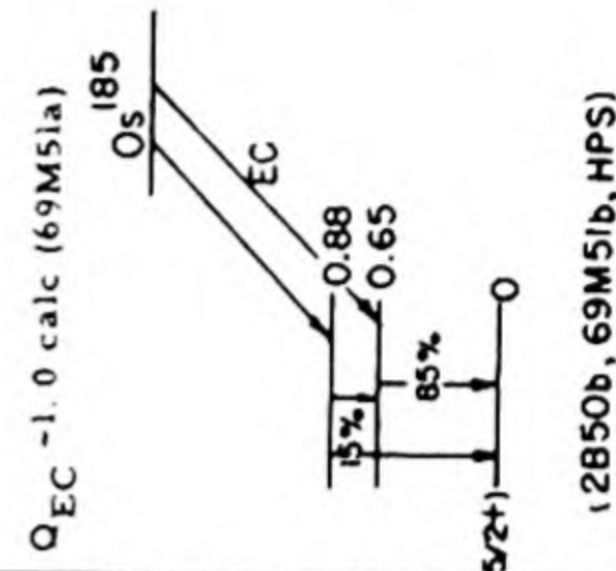
Isotope Z A	Class and identification	Percent abundance	Type of decay	Half-life	Energy of radiation in Mev		Disintegration energy and scheme	Method of production and genetic relationships
					Particles	Gamma-transitions		
¹⁸² Ta 73	A chem, n-capt (37F36, 17O38)		β^- (76H40)	111 d (21E52, 38S51); 113 d (9S49c); 117 d (2S47, 11Z43)	0.525, other β 's, spect (7J49); 0.53 spect (86B49a); others (11R47, 7J47, 24N47)	γ_1 0.065714, γ_2 0.067736, γ_3 0.084667, γ_4 0.10009, γ_5 0.11366, γ_6 0.11640, γ_7 0.15241, γ_8 0.15637, γ_9 0.17936, γ_{10} 0.19831, γ_{11} 0.22205, γ_{12} 0.22927, γ_{13} 0.26409, γ_{14} 1.121, γ_{15} 1.188, γ_{16} 1.223 (rel intens: γ_1 9, γ_2 100, γ_3 6, γ_4 46, γ_5 9, γ_6 2, γ_7 43, γ_8 14, γ_9 19, γ_{10} 9, γ_{11} 45, γ_{12} 24, γ_{13} 27, γ_{14} 352, γ_{15} 157, γ_{16} 334) cryst spect (100M52); 0.046, 0.058, 0.065, 0.067, 0.075, 0.077, 0.084, 0.100, 0.113, 0.134, 0.143, 0.152, 0.178, 0.198, 0.221, 0.228, 0.245, 0.262 spect conv (10C50e); 1.121, 1.189, 1.219 spect, spect conv (10C51e); 0.082, 0.098, 0.112, 0.122, 0.132, 0.141, 0.157, 0.165, 0.172, 0.198, 0.222, 0.243, 0.255, 0.264, 0.290 (?), 0.299 (?), 0.324, 1.133, 1.219, 1.237 spect, spect conv (86B49a); 0.224, 0.232, 0.260, 0.268, 0.280, 0.320, 0.342, 0.362, 0.392, 0.412, 0.421, 0.526, 0.565, 0.607, 0.624, 0.728, 0.763, 0.780, 0.892, 0.935, 0.993, 1.133, 1.215, 1.231 spect (18O50); others (4G49, 11R47, 10C49b, 13E50, 94S50, 98S48, 4B49, 52M51, 52W51)	Ta-n- γ (37F36, 17O38, 76H40, 2S47, 1M48); Ta-d-p (17O38, 11Z43, 31S50); W-d-a, W-n-p (33T51)	
	B chem, excit (65B50)		β^- (2W50f)	5.2 d (65P52c); 6.0 d (83M51); 6.1 d (2W50f)	0.65 scint spect (65P52c); 0.6 abs (2W50f, 83M51)	0.24 scint spect (65B52c); γ (2W50f)	W-n-p (? W50f, 65P52c); W-y-p (65E50, 83M51)	
	Ta ¹⁸⁴	B chem, excit (65P52c)		β^- (65P52c)	9.3 h (65B52c)	1.4 abs (65B52c)	0.410, 0.86, 1.10 scint spect (65B52c)	W-n-p, W ¹⁸⁴ -n-p (65P52c)
	Ta ¹⁸⁵	A chem, excit (65B50); excit, sep isotopes (23D50)		α^- (23D50)	48 m (83M51, 65B50)	1.6, 0.15 (conv?) abs (83M51); 1.7 abs (23D50)		W-y-p (65B50, 83M51); W186-y-p (23D50)
W ¹⁷⁶ 74	B chem, genet (2W50e)		EC 99+%, α^+ -0.5% (2W50e)	80 m (2W50e)	β^+ : -2 abs (2W50e); conv: -0.1, -0.2 abs (2W50e)	-1.3 abs (2W50e)	Ta-p-6n (2W50e, 22N52); parent Ta176 (2W50e)	
	B chem, genet (2W50e)		EC (2W50e)	130 m (2W50e)	conv: 0.13, -0.4 abs (2W50e)	-0.5, 1.2 abs (2W50e)	Ta-p-5n (2W50e, 22N52); parent Ta177 (2W50e)	

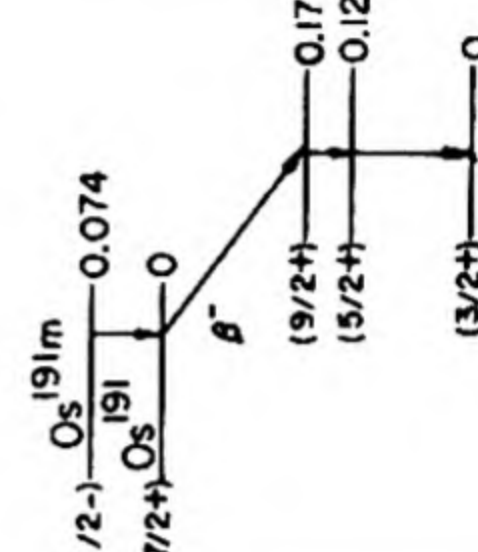
W^{178}	B chem, genet (2W50e)		EC (2W50e)	21.5 d (2W50e)	-0.3 (weak) abs (2W50e)	Ta-p-4n (2W50e, 22N52); parent 9.4 m $T_{1/2}$ (2W50e)	
W^{179}	D chem, excit (2W50e)		EC (2W50e)	30 m (2W50e)		Ta-p-3n (2W50e)	
W^{179}	D chem, excit (2W50e)		EC or IT (2W50e)	5.2 m (2W50e)		Ta-p-3n (2W50e)	
W^{180}		0.135 (9W46)					
W^{181}	A chem, excit (2W47); chem, n-capt (37L51)		EC (2W47)	140 d (2W47)	0.030, 0.600, 0.800 scint spect (13A50b); 1.8 (weak) abs (2W47)	Ta-d-2n (2W47); Ta-p-n (96B49); W-n- γ (13A50b, 37L51); not parent Ta ^{181m3} (38M51c)	
W^{182}		26.4 (9W46)					
W^{183m}	B sep isotopes, n-capt (38M49)		IT (38M49)	5.5 s (38M49, 24C52a)	0.12, 0.17 scint spect (24C52a)	W^{182} -n- γ (38M49); W-n- γ (38M49, 31K51)	
W^{183}		14.4 (9W46)					
W^{184}		30.6 (9W46)					
W^{185m}	C excit, sep isotopes (23D50)		IT (23D50)	1.85 m (23D50)		W^{186} - γ -n (23D50)	
W^{185}	A chem, excit, n-capt (64M40)		β^- (64M40)	73.2 d (9S48a); 75 d (5F40a)	no γ (10L52c, 23S45a, 65C47a); others (10C49, 4B49, 52M51)	W-n- γ (64M40, 5F40a, 2S47, 10C49); W-n-2n (64M40, 5F40a); W-d-p (5F40a); Re-d- α (5F40a)	
W^{186}		28.4 (9W46)					
W^{187}	A chem, n-capt (12A35); chem, n-capt, excit (64M40)		β^- (64M40)	24.1 h (5F40a); 24.0 h (64M40)	0.07200, 0.13425, 0.4795, 0.6189, 0.6861 cryst spect (100M52); γ_1 0.072 (coinc with γ_2 , delay coinc with γ_3), γ_2 0.134 (coinc with γ_1 , γ_4 , and γ_7 , delay coinc with γ_3), γ_3 0.480 (e_K/γ 0.022, delay coinc with γ_1 and γ_2 , not coinc with γ_4 or γ_6), γ_4 0.552 (coinc with γ_2), γ_5 0.618 (not coinc with other γ 's), γ_6 0.69, γ_7 0.775 (coinc with γ_2) ($\gamma_2/\gamma_3/\gamma_4/\gamma_5/\gamma_6/\gamma_7 = 0.45/1.00/0.31/0.42/1.48/0.23$) scint spect (14S52a); 0.133, 0.204, 0.478, 0.615, 0.680, 0.767 spect conv (2L49); 0.129, 0.462, 0.652 spect conv, 8- γ , γ - γ coinc (15H48b); 0.078, 0.138 spect conv (86B49b); others (6V41a, 72C42, 20P48, 9J51)	Q_β^- 1.33 (HPS)  W^{187} -5% 0.910 0.686 0.206 0.134 0 (5/2+) (14S52a)	W-n- γ (12A35, 77M35b, 64M40, 5F40a, 2S47, 10C49); W-d-p (5F40a, 20P48); spall U (6O48); parent Re ^{187m} (10D48, 4F49, 52M51)

Isotope Z A	Class and identification	Percent abundance	Type of decay	Half-life	Energy of radiation in Mev		Disintegration energy and scheme	Method of production and genetic relationships
					Particles	Gamma-transitions		
¹⁸⁸ ₇₄ W	A chem, genet (37L51)		β ⁻ (37L51)	65 d genet (37L51)				W-n-γ (second order reaction) (13A50c, 37L51, 37L51a); parent Re ¹⁸⁸ (37L51, 37L51a)
¹⁸² ₇₅ Re	B chem, excit (2W50g); chem, sep isotopes (31D50)		EC (2W50g)	12.7 h (2W50g); 14 h (31D50)		0.110, 0.127, 0.222, 0.250, 0.346 spect conv, spect (2W50g)		Ta-α-3n (2W50g); W-p-n (2W50g); W ¹⁸² -d-2n (31D50); daughter Os ¹⁸² (93S50)
¹⁸² _{Re}	D (182) chem, excit (2W50g); (183) chem, sep isotopes (31D50)		EC (2W50g)	64.0 h (2W50g); 67 h (31D50)		0.110, 0.127, 0.222, 0.250, 0.346 spect conv, spect (2W50g)		Ta-α-3n, W-p-n (2W50g); W ¹⁸² -d (31D50)
¹⁸³ _{Re}	B chem, excit (2W50g)		EC (2W50g)	155 d (33T51); 120 d (93S50)		0.081, 0.252 spect conv (2W50g)		Ta-α-2n, W-p-n (2W50g); W-d-n, W-α-p (33T51); daughter Os ¹⁸³ (93S50)
¹⁸⁴ _{Re}	A chem, excit (5F40a); chem, excit (2W50g)		EC (2W50g)	50 d (2W50g, 33T51)		0.159, 0.206, 0.244, 0.784, 0.89 spect conv (4W52); 0.043, 0.159, 0.205, 0.285 spect, spect conv (2W50g); 1.0 abs (33T51, 29C40)		Ta-α-n (2W50g); W-α-pn (33T51); W-p-n (2W50g); W-d-n (29C40, 5F40a, 33T51); Re-n-2n (2W50g, 5F40a)
¹⁸⁴ _{Re}	B chem, excit (2W50g)		EC or IT (2W50g)	2.2 d (2W50g)		0.043, 0.159 spect, spect conv (2W50g)		Ta-α-n (2W50g); W-p-n (2W50g)
¹⁸⁵ _{Re}		37.07 (24W48)					Re ¹⁸⁵ , ⁻ I = 5/2 (87M50)	
¹⁸⁶ _{Re}	A n-capt (8K35); n-capt, excit (99S39); chem, n-capt, excit (5F40a); mass spect (43H47)		β ⁻ -95%, EC -5%, no β ⁺ (lim 10 ⁻⁵ %) (44M51); β ⁻ -91%, EC -9% (82S51a)	92.8 h (24G47); 91 h (10C48); 90 h (99S39)	1.07 (80%), 0.93 (20%) spect (44M51); 1.070 (73%), 0.942 (27%) spect (82S51a); 1.090 (67%), 0.95 (30%), 0.64 (3%) spect (22G49a); 1.063 spect (10L49); 1.07 spect (86B49a)	with β ⁻ : γ ₁ 0.137 (e _K /γ -0.35, K/L/M = 0.6/1/0.2), 0.627, 0.764 spect, spect conv, β-γ, γ-γ coinc (44M51); γ ₁ 0.136 (e _K /γ 0.37, K/L/M = 0.6/1/0.2) spect, spect conv, β-conv, γ-γ coinc (82S51a); with EC: γ ₂ 0.123 (-2%), γ ₁ /γ ₂ = 9 (44M51); γ ₂ 0.122 (3%, e _K /γ 0.45, K/L 0.6) (82S51a); others (22G49a, 10C48, 86B49a)	<p>Re¹⁸⁶ 1.07 (44M51) Q_{β⁻} 1.07 (44M51) EC ~40% β⁻ ~60% Os¹⁸⁶ 0.123 Os^{186m} 0.137 Os¹⁸⁶ 0 Os^{186m} 0 Os¹⁸⁶ 0 Os</p>	

¹⁸⁷ Re	A genet (10D48)	IT (10D48)	5.3 x 10 ⁻⁷ s delay coinc (4B49); 5.5 x 10 ⁻⁷ s delay coinc (52M51)		0.133 (e _K /γ ≤ 3.2, K/L -5) scint spect (52M52b); see γ's of W ¹⁸⁷	see W ¹⁸⁷ (14S52a) Re ¹⁸⁷ , I = 5/2 (87M50)	daughter W ¹⁸⁷ (10D48, 4P49, 52M51)
¹⁸⁷ Re	A chem (25N48)	β ⁻ (25N48)	4 x 10 ¹² γ sp act (25N48, 63S48)	0.400 ion ch (42D52); 0.043 abs (25N48) 63S48)	no γ, no x (42D52)	natural source (25N48, 63S48)	
¹⁸⁸ Re	C n-capt, sep isotopes (63M52d, 63M52b)	IT (63M52d)	22 m (63M52d); 17 m (65B50)		0.0635, 0.092, 0.106 spect conv, scint spect (63M52b)	Re ¹⁸⁷ -n-γ (63M52b); Os-γ-p (?) (65B50)	
¹⁸⁸ Re	A chem, n-capt (12A35); n-capt, excit (99S39); chem, n-capt, excit (5F40a); mass spect (43H47)	β ⁻ (99S39)	16.9 h (37L51); 18.9 h (24G47); 18 h (1P37)	2.07 (coinc with 0.152 γ) spect, β-γ coinc (44R52a); 2.10 spect (86B49a); 2.05 abs (24G47); others (26M48b, 99S39)	0.152 (70%, e _K /γ 0.05, K/L 0.42), 0.476 (3%), 0.638 (6%), 0.933 (5%), 1.3 (5%) spect, abs, spect conv (44R52a); 0.15, 0.48, 0.64, 0.95, 1.40 spect (86B49a); 0.16, 0.48, 0.64, 0.94, 1.43 spect (43M46); 1.39 coinc abs (26M48b); 0.154 spect conv (10C48)	Re-n-γ (8K35, 12A35, 1P37, 99S39, 5F40a, 8Y40, 2S47); Re-d-p (5F40a, 24G47, 66C50); spall U (6O48); spall Re (66C50); daughter W ¹⁸⁸ (37L51, 37L51a)	
¹⁸⁹ Re	D chem (37L51, 33T51)	β ⁻ (37L51, 33T51)	150 d (37L51); 250-300 d (33T51)	0.2 abs (37L51, 33T51)	1.0 abs (33T51)	W-α-p (33T51); Re-n-γ (second order reaction) (37L51)	
Re	E chem (37L51)	β ⁻ (37L51)	≥5 y (37L51)	0.75 abs (37L51)		Re-n-γ (second order reaction) (?) (37L51)	
¹⁸² Os	B chem, genet (93S50)	EC, no β ⁺ (93S50)	24.0 h (93S50)	conv: 0.15, 0.42 spect conv (93S50)	0.3, 1.6 abs (93S50)	Re-p-4n (93S50); parent Re ¹⁸² (93S50)	
¹⁸³ Os	B chem, genet (93S50)	EC (93S50)	12.0 h (93S50)			Re-p-3n (93S50); parent Re ¹⁸³ (93S50)	
¹⁸⁴ Os							
¹⁸⁵ Os	B chem, cross bomb (24G47, 50K48)	EC (L/K -0.35) (69M51a); no β ⁺ (2B50b)	97 d (50K48, 33T51); 95 d (24G47)		γ ₁ 0.648, γ ₂ 0.878 (γ ₁ /γ ₂ -6) spect, γ-γ coinc (2B50b); γ ₁ 0.65, γ ₂ 0.88 (γ ₁ /γ ₂ 6.1) scint spect (69M51b); 0.235, 0.653 spect conv (116S52)	Q _{EC} -1.0 calc (69M51a) 185 Os EC 0.88 0.65 15% 85% 5/2+ 0	Re-α-2n (24G47, 66C50); Re-p-n (93S50); Os-n-γ (50K48)

(2B50b, 69M51b, HPS)



Isotope Z A	Class and identification	Percent abundance	Type of decay	Half-life	Energy of radiation in Mev		Disintegration energy and scheme	Method of production and genetic relationships
					Particles	Gamma-transitions		
$^{186m}_{76}\text{Os}$	A genet (52M51a)		IT (52M51a)	8×10^{-10} s delay coinc (52M51a)		0.137 scint spect (52M51a)	see Re^{186}	daughter Re^{186} (52M51a)
Os^{186}		1.59 (6N37a)		35 h (66C50)				
$^{187m}_{76}\text{Os}$	E chem (66C50)							daughter Ir^{187} (?) (66C50)
Os^{187}		1.64 (6N37a)						
Os^{188}		13.3 (6N37a)						
Os^{189}		16.1 (6N37a)					Os^{189} , $I = 1/2$ (87M50)	
$^{190m}_{76}\text{Os}$	E chem (66C50)			6 h (66C50)				daughter 12 d Ir^{190} (?) (66C50)
Os^{190m}	D chem, genet (66C50)			9.5 m (66C50)				daughter 3 h Ir^{190} (66C50)
Os^{190}		26.4 (6N37a)						
Os^{191m}	A chem, genet (116S52)		IT, no β^- (lim 5%) (116S52)	14 h (116S52)		0.0742 ($L_I/L_{II}/L_{III} = 42/24/100$) spect conv (116S52)		Os-n-y , Os-y-n , parent Os^{191} (116S52)
Os^{191}	A n-capt, (12Z40); chem, n-capt (13S41b); chem, excit (23F48a, 116S52)		β^- (13S41b)	16.0 d (66C50); 16.1 d (9S48a); 15.0 d (50K48)	0.143 spect (38K51b); 0.142 spect (9S48a); others (50K48, 13S41b, 37W47, 26M48b, 2B50b)	γ_1 0.0417 ($L_I/L_{II}/L_{III} = 32/40, e/\gamma$ large), γ_2 0.129 (coinc with γ_1 , $K/L_I/L_{II}/L_{III} = 100/30/11/6$) spect conv, conv-conv coinc (116S52); γ_1 (e_K/γ 1.36) (116S52, calc from 38K51b); 0.042 (L/M 1.8), 0.128 (e_K/γ -0.5, K/L 2.1) spect conv (38K51b, 38K51c); 0.041, 0.128 spect conv, spect (2B50b); 0.039, 0.127 spect conv (9S48a); 0.129 spect conv (10C47)	Q_{β^-} 0.313 (38K51b) (116S52, 67H53)	Os-n-y (13S41b, 12Z40, 2S47, 116S52); Os-d-p (66C50); Os-y-n (23F48a, 116S52); spall U (6O48); daughter Os^{191m} (116S52)
Os^{192}		41.0 (6N37a)						

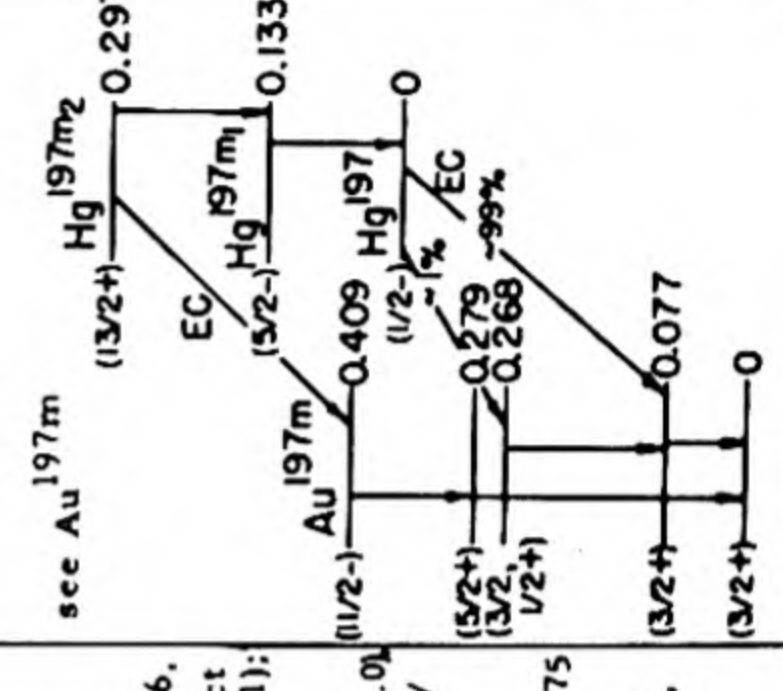
¹⁹³ Os	A n-capt (8K35, 12Z40); chem, n-capt (13S41b); chem, excit (23F48a, 116S52)	β^- (13S41b)	30.6 h (66C50); 31.9 h (24G47); 32 h (13S41b); 30 h (12Z40)	1.10 spect (2B50b); 1.05 scint spect (52M50b); 1.15 abs (66C50, 26M48b)	with ¹⁹³ Ir: 0.066 spect conv (116S52); 0.065 scint spect, β^- - γ delay coinc (52M50b); no γ (2B50b); others (24G47, 26M48b)	Q_β^- 1.17 (HPS) Os ¹⁹³ β^- >98% Ir ¹⁹³ <2% 0.065 0	Os-n- γ (8K35, 12Z40, 13S41b, 2S47); Os-d-p (24G47, 66C50); Ir-d-2p (24G47); spall U (6F51); parent Ir ^{193m} (52M50b, 52M51); not found: Os- γ -n (23F48a, 116S52)
¹⁹⁴ Os	A chem, genet (37L50a)	[β^-] (37L50a)	-700 d (37L51)				Os-n- γ (second order reaction) (37L50a, 37L51); parent Ir ¹⁹⁴ (37L50a, 37L51)
¹⁸⁷ Ir	B chem, excit, sep isotopes (66C50)	EC 99+%, β^+ -0.2% (66C50)	11.8 h (66C50)	β^+ : 2.2 spect (66C50); conv: 0.3, 1.2 spect conv (66C50)	-1.3 abs (66C50)		Re- α -2n, Re ¹⁸⁵ - α -2n (66C50); Os-d-3n (66C50); parent Os ^{187m} (?) (66C50)
¹⁸⁸ Ir	B chem, excit, sep isotopes (66C50)	EC 99+%, β^+ -0.3% (66C50)	41.5 h (66C50)	β^+ : 2.0 spect (66C50); conv: 0.2, 0.9 spect conv (66C50)	-1.8 abs (66C50)		Re- α -n, Re- α -3n, Re ¹⁸⁷ - α -3n (66C50); Os-d-2n, Os- α -3n (66C50)
¹⁹⁰ Ir	D chem, excit, sep isotopes (66C50)	β^+ , EC (?) (66C50)	3.2 h (66C50)	β^+ : 1.7 spect (66C50); conv: 0.2, 0.8 spect conv (66C50)			Re- α -n, Re ¹⁸⁷ - α -n (66C50); Os-d-n, Os- α -2n (66C50); parent 9.5 m Os ^{190m} (66C50)
¹⁹⁰ Ir	B chem, excit (24G47); chem, excit, sep isotopes (66C50)	EC (24G47)	12.6 d (66C50); 10.7 d (24G47)		0.2, 0.6 abs (66C50); 0.3 abs (24G47)		Re- α -n, Re ¹⁸⁷ - α -n (66C50); Cs-d-n (24G47, 66C50); Ir-n-2n (24G47); parent 6 h Os ^{190m} (?) (66C50)
¹⁹¹ Ir						¹⁹¹ Ir, I = 3/2 (99B50); ¹⁹¹ Ir, I = 1/2 (94B49)	
^{192m} Ir	A n-capt (12M37); resonance neutron activation (18G47a)	IT (18G47a)	1.42 m (15H48a); 1.5 m (12M37)		0.057 spect conv (42C50); 0.056 spect conv (15H48a); γ (continuum) scint spect (38M51); γ ($e_L/\gamma > 400$) ion ch (31K51)		Ir-n- γ (12M37, 18G47a, 2S47)
¹⁹² Ir	A n-capt (12A36); mass spect (37R46); chem (2W48a)	EC, β^- (10C51); no β^+ (lim 0.008%) (41M51)	74.37 d (51K51); 74.5 d (38S51); 74.7 d (66C50)	0.66 spect (88S51a); 0.67 spect (2L47); 0.68 coinc abs (37W47); 0.6 abs (26M48a, 24G47)	γ_1 0.13633, γ_2 0.20131, γ_3 0.20574, γ_4 0.29594, γ_5 0.30845, γ_6 0.31646, γ_7 0.46798, γ_8 0.4848, γ_9 0.5884, γ_{10} 0.6045, γ_{11} 0.6129 (rel abund γ_1 4, γ_2 10, γ_3 75, γ_4 380, γ_5 370, γ_6 990, γ_7 300, γ_8 11, γ_9 11, γ_{10} 14, γ_{11} 5) cryst spect (100M52); 0.136, 0.151 (or 0.156), 0.169 (or 0.173), 0.201, 0.206, 0.283, 0.295, 0.308, 0.316, 0.396 (or 0.400), 0.415, 0.434 (or 0.438), 0.467, 0.484, 0.589, 0.604, 0.611 spect conv (10C51); 0.775, 0.870 scint spect (50R52); others (10J551, 2L47, 20D50, 4B49, 67H48b, 52W51, 98S48, 56G49, 88S51a, 52M51)	Q_β^- 1.58 (50R52)	Os-d-2n (24G47, 66C50); Ir-n- γ (12A36, 12M37, 24J38, 2S47); Ir-n-2n (24G47); Ir-d-p (24G47, 2W48a); Pt-d- α (2W48a); Pt- γ -pn (25C52)

Isotope Z	Class and identification	Percent abundance	Type of decay	Half-life	Energy of radiation in Mev		Disintegration energy and scheme	Method of production and genetic relationships
					Particles	Gamma-transitions		
^{193m} 77Ir	B genet (52M50b)		IT (52M50b)	5.7 x 10 ⁻⁹ s delay coinc (52M50b)		0.065 scint spect, β-γ delay coinc (52M50b)	 ¹⁹³ Ir, I = 3/2 (99B50, 94E49)	daughter Os ¹⁹³ (52M50b, 52M51)
¹⁹³ Ir		61.5 (37S36a)						
¹⁹⁴ Ir	A n-capt (12A35); mass spect (37R46); chem (2W48a)		β ⁻ (12M37)	19.0 h (24G47); 19.5 h (53W41); 19 h (12A35, 12M37)	2.18 spect (53W41); 2.2 spect (24A36); 2.1 abs (53W41, 24G47); 0.5 β-γ coinc abs (26M48a)	γ ₁ 0.290, γ ₂ 0.326, γ ₃ 1.51 (γ ₁ /γ ₂ /γ ₃ = 1/5/1) spect (89B52); 0.328 spect conv (10C51f); 1.7-2.2 (0.14%) Be, D-γ-n reaction (23W50); others (4B49, 26M48a, 42C50, 37L51)		Ir-n-γ (12A35, 1P37, 2S47, 12M37, 24J38); Ir-d-p (24G47, 2W48a); Pt-γ-p, Pt-γ-pn (25C52)
¹⁹⁵ Ir	D chem, excit (25C52)		β ⁻ (25C52)	140 m (25C52, 65B52b)	1.8 abs (65B52b); -1 abs (25C52)	0.49, 0.84 scint spect (65B52b)		Pt-γ-p (25C52); Pt-n-p (65B52b)
¹⁹⁶ Ir	D chem, excit (65B52b)		β ⁻ (65B52b)	9 d (65B52b)	-0.08 abs (65B52b)	γ (65B52b)		Pt-n-p (65B52b)
¹⁹⁷ Ir	D chem, excit (25C52, 65B52b)		β ⁻ (65B52b)	7 m (25C52, 65B52b)	1.65, 0.6 abs (65B52b)	γ (65B52b)		Pt-γ-p (25C52); Pt-n-pn (65B52b)
¹⁹⁸ Ir	E excit (65B52b)		β ⁻ (65B52b)	45 s (65B52b)	3.6 abs (65B52b)	0.78 scint spect (65B52b)		Pt-n-p (65B52b)
¹⁹⁰ 78Pt		0.012 (28L49a)						
¹⁹¹ Pt	B chem, excit (2W48a, 90M52)		EC (2W48a)	3.00 d (2W49c, 90M52)		0.083, 0.096, 0.173 spect (116S52a); 0.6, 1.5 abs, abs conv (2W49c)		Ir-d-2n (2W48a, 2W49c); Pt-n-2n (2W48a, 2W49c); daughter Au ¹⁹¹ (2W48a, 2W49c, 90M52)
¹⁹² Pt		0.78 (3147g)						
^{193m} Pt	B chem, excit (2W48a, 90M52)		IT (116S52a); EC (2W48a)	4.33 d (2W49c); 4.6 d (90M52)		0.135 (K/L 0.28, L _I /L _{II} /L _{III} 1/0/2) spect conv (116S52a); 0.2, 1.5 abs (2W49c)		Ir-d-2n (2W49c); Pt-n-γ, Pt-n-2n, Pt-d-p (2W49c); Pt-γ-n (116S52a); daughter Au ¹⁹³ (2W49c, 90M52)
¹⁹⁴ Pt		32.8 (3147g)					Pt ¹⁹⁴ , I = 0 (87M50)	

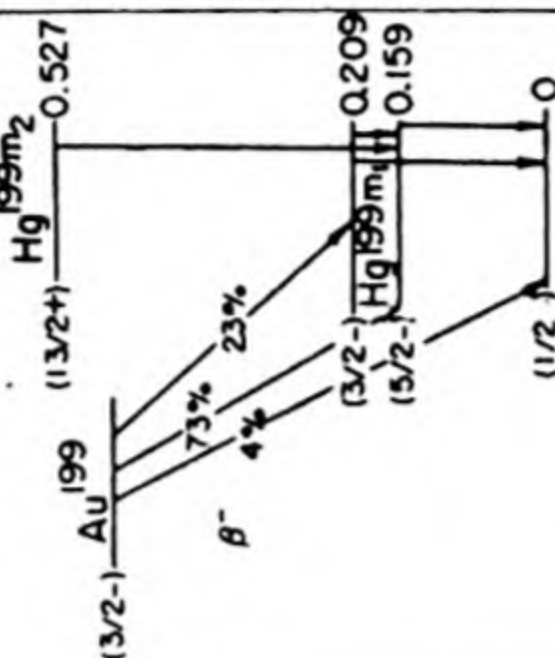
^{195m} Pt	B chem (12M37); chem, genet (104S52)	IT (104S52)	3.5 d (15H48a); 3.8 d (104S52); 4.4 d (79H52); 3.3 d (12M37)	0.029 (e/γ > 7.5), 0.097 (e/γ 9.0, K/L 5.7), 0.126, 0.129 (e/γ very large, K/L 0.26) spect, spect conv, γ-conv coinc (104S52); 0.099, 0.130 (K/L 0.1) spect conv (10C52a); 0.126 (K/L 0.23) spect conv (15H48a)	<p>Pt^{195m} (3/2+) 0.255 Pt¹⁹⁵ (5/2-) 0.126 Pt¹⁹⁵ (3/2-) 0.097 Pt¹⁹⁵ (1/2-) 0 (104S52)</p>	Pt-n-γ (26M48e, 79H52, 104S52, 12M37, 1P37, 2S47, 34H51); Pt-d-p (9K41b); Pt-γ-n (25C52); daughter Au ¹⁹⁵ (180 d) (104S52)
¹⁹⁵ Pt	33.7 (3147g)				Pt ¹⁹⁵ , I = 1/2 (87M50)	
¹⁹⁶ Pt	25.4 (3147g)				Pt ¹⁹⁶ , I = 0 (87M50)	
^{197m} Pt	B chem (28S41); chem, excit, cross bomb (25C52)	IT (15H48a)	78 m (15H48a); 80 m (28S41); 88 m (25C52)	0.337 (e/γ very large, K/L 1.3) spect conv (15H48a)	Pt-d-p (28S41); Pt-n-2n (28S41); Pt-γ-n (60M48, 25C52); Hg-n-α (28S41); Au-n-p (?) (2W50f)	
¹⁹⁷ Pt	A chem (10C36); chem, excit (12M37)	β ⁻ (12M37)	18 h (12M37); 17.4 h (10C52a)	0.077, 0.191 (K/L 6.0) spect conv (10C52a); 0.077, 0.191 spect, spect conv (105S52); others (4B49)	<p>see Au^{197m}, Hg¹⁹⁷ Q_β⁻ 0.75 (105S52) Pt¹⁹⁷ (1/2-) 0.268 Pt¹⁹⁷ (1/2-) 0.077 Pt¹⁹⁷ (1/2-) 0 (105S52)</p>	Pt-n-γ (12M37, 28S41, 2S47, 79H52); Pt-d-p (10C36, 9K41b, 28S41, 9K42, 2W48a); Pt-γ-n (25C52, 25W48); Pt-n-2n (28S41); Hg-n-α (28S41)
¹⁹⁸ Pt	7.23 (3147g)					
¹⁹⁹ Pt	A n-capt (77M35b, 12A35); chem, n-capt, excit (28S41)	β ⁻ (12M37)	31 m (12M37)	1.8 abs (9K41b, 28S41)	Pt-n-γ (12A35, 77M35b, 12M37, 28S41, 2S47, 50H51); Pt-d-p (28S41, 9K41b, 10C36) Hg-n-α (28S41)	
Pt	F n-capt (10C50g)	β ⁻ (10C50g)	82 d (10C50g)	0.5 abs (10C50g)	Pt-n-γ (10C50g)	
¹⁸³⁻⁷⁹ Au ¹⁸⁷	D chem, excit (3T49)	EC, β ⁺ , α -0.01% (3T49)	4.3 m (42R52)	α: 5.07 ion ch (42R52)	spall Pt (42R52), Au (3T49, 42R52)	
¹⁹¹ Au	B chem, genet (2W49c, 90M52)	EC (2W49c)	18 h (90M52); -1 d (2W49c)	0.053, 0.064, 0.111, 0.123, 0.166, 0.250, 0.405 spect conv (90M52)	Ir-α-4n (2W49c); Pt-d-3n (2W49c); parent Pt ¹⁹¹ (2W48a, 2W49c, 90M52); daughter Hg ¹⁹¹ (90M52)	

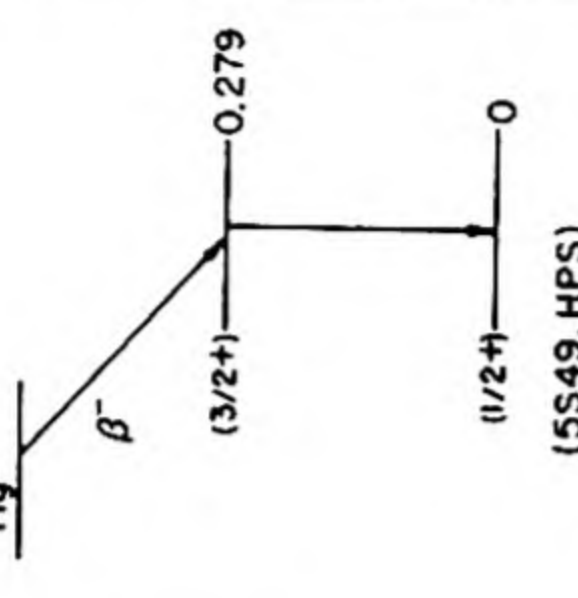
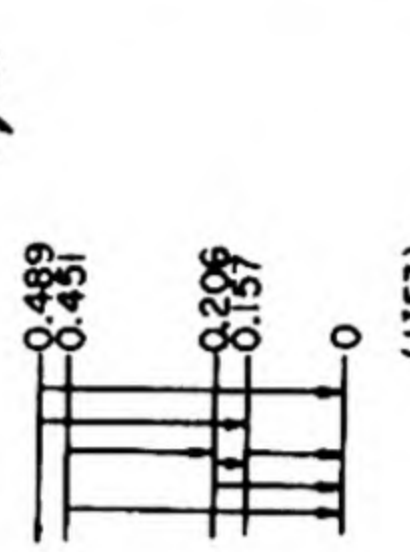
Isotope Z A	Class and identification	Percent abundance	Type of decay	Half-life	Energy of radiation in Mev		Disintegration energy and scheme	Method of production and genetic relationships
					Particles	Gamma-transitions		
¹⁹² Au 79 Au	B chem, excit (2W49c); chem, genet (42T52, 33F52)		EC, β^+ (2W49c)	5.0 h (42T52); 4.7 h (2W49c); 4.1 h (33F52)	β^+ : -1.9 abs (2W49c); conv: -0.4 abs (2W49c)	2-3 abs (2W49c)		Ir- α -3n (2W49c); Pt-d-2n (2W49c); daughter Hg ¹⁹² (33F52, 42T52)
¹⁹³ Au	B chem, genet (2W49c, 90M52)		EC (2W49c)	15.8 h (2W49c, 90M52); 15.3 h (33F52)		0.051, 0.060, 0.084, 0.093, 0.109, 0.165, 0.177, 0.235 spect conv (90M52)		Ir- α -2n (2W49c); Pt-d-n, Pt-d-3n (2W49c); parent Pt ¹⁹³ (2W49c, 90M52); daughter Hg ¹⁹³ (33F52, 90M52)
¹⁹⁴ Au	B chem, excit (2W49c)		EC -97%, β^+ -3% (2W49c)	39.5 h (2W49c); 39 h (82S49)	1.8 abs (2W49c)	0.291 (e/γ 0.054, K/L 2), 0.328 (e/γ 0.19, K/L 2), 0.466 (weak), 1.48 (e/γ 0.0026), 2.1 spect, spect conv (82S49)		Ir- α -3n (2W49c); Pt-d-2n, Pt-d-3n (2W49c); Pt-p-n (82S49)
^{195m} Au	B chem, genet (34H52a)		IT (34H52a)	0.5 m (34H52a)		0.056, 0.259 spect conv (34H52a)		daughter Hg ^{195m} (34H52a)
¹⁹⁵ Au	B chem, excit (2W49c); chem, genet (30D52)		EC (2W49c)	180 d (82S49, 30D52); 185 d (2W49c)		0.0308, 0.0990, 0.130 spect conv (30D52); 0.029 (L/M 4.6), 0.097 (K/L 5.8), 0.126 spect, spect conv, γ -conv coinc (104S52); others (34H51, 82S49)	see Pt ^{195m}	Ir- α -2n (2W49c); Pt-d-n, Pt-d-2n, Pt-d-3n (2W49c); Pt-p-n (82S49); daughter Hg ^{195m} (30D52)
¹⁹⁶ Au	B chem, excit (12M37)		EC or IT (2W49c)	14.0 h (2W49c); 13 h (12M37)		with EC: 0.332, 0.354 spect conv (106S52); 0.330 (K/L 1.7), 0.358 (K/L 1.7) spect conv (82S49); with β^- : 0.426 (e_L/γ 0.007, L/M+N 3.5), no 0.175 γ spect conv, β -conv coinc (106S52); 0.175 spect conv (82S49)		Au-n-2n (12M37, 2W49c); spall U (?) (6F51)
¹⁹⁶ Au	A chem, excit (12M37)		EC -95%, β^- -5% (82S49); EC -80%, β^- -20% (2W49c)	5.55 d (2W49c); 5.60 d (82S49)	β^- : 0.27 spect (106S52); 0.30 spect (82S49); 0.34 abs (2W49c)			Pt-d-n (9K41b, 2W49c, 106S52); Pt-p-n (82S49); Au-n-2n (12M37, 2W49c); Au- γ -n (25W48); spall U (?) (6F51)
^{197m} Au	A excit (37W45a)		IT (37W45a)	7.4 μ (40F47); 7.5 μ (37W45a)		0.130 (e_K/γ 2.0, K/L/M = 1/7.5/ 3.6), 0.279 (e_K/γ -0.3) spect conv (63M52c); 0.273 spect conv, conv-conv coinc (34H48a); 0.275 scint spect (24C52); 0.25 abs conv (37W45a)		Au- γ - γ (37W45a); Au-n-n (37W45a, 40F47); daughter 25 h Hg ¹⁹⁷ (40F47)
¹⁹⁷ Au		100 (1D35a)						

Au ¹⁹⁸	A chem, n-capt (12A35, 12M37)	β^- (12M37); no EC (lim 0.2%); (38M52); no EC (lim 0.4%); (25R49); no β^+ (lim 0.003%); (41M51)	2.69 d (57S49, 9S49b); 2.73 d (38S51, 33D46); 2.66 d (69C51)	β_1 0.963 spect (average of 9S48, 2L49a, 10L49, 82S49, 107S49, 4E51); β_2 0.290 (coinc with 0.680 γ) β - γ coinc spect (48B51a); β_3 1.37 (0.01%) spect (4E51)	γ_1 0.41177 cryst spect (100M52, 34D48); γ_1 0.4116 spect (29L51); γ_1 (ϵ_K/γ 0.031, K/L 3.1, L/M 3.3) spect conv (50S52); γ_1 (ϵ_K/γ 0.03, K/L 3, L/M 3.3) spect, spect conv (7S49e); γ_1 (ϵ_K/γ 0.029, K/L 2.1, L/M 4.3) spect conv (82S49); γ_1 (ϵ_K/γ 0.026 K/L 2.2, L/M 4) spect conv (107S49); γ_1 (ϵ_K/γ 0.03, K/L+M 2.3) spect conv (29F52); γ_1 (LII/LIII 2.5) spect conv (63M52a); γ_2 0.676 (0.5%, ϵ_K/γ 0.034, K/L 5.7), γ_3 1.088 (0.1%, ϵ_K/γ 0.005, K/L 6.3) spect, spect conv (4E51, 4E51a, 6W52); γ_2 0.680 (1%, coinc with 0.411 γ and 0.29 β^-), γ_3 1.09 (-0.2%) scint spect, β - γ coinc (48B51a); γ_2 0.673 (1.4%), γ_3 1.08 (0.3%) spect (57H51b); γ_2 0.67 (1.4%, coinc with 0.411 γ), γ_3 1.09 (0.3%) scint spect, γ - γ coinc (69C51a, 69C51); others (18P50a, 2L48, 2L49a, 9S49b, 31A50a, 12H50, 38T49, 4F44, 72C42, 7S47g, 15J48, 25R48, 52M51)	Q_β^- 1.374 (HPS)		Au-n- γ (12A35, 12M37, 1P37, 16D41, 2S47, 50H51); Au-d-p (9K41c); Hg-n-p (28S41); Pt-p-n (82S49, 82S48); spall U (6O48)
Au ¹⁹⁹	A chem, genet (12M37)	β^- (9K41b)	3.15 d (8B52b); 3.2 d (104S52); 3.3 d (12M37)	0.460, 0.297 (coinc with 0.158 γ), 0.250 (coinc with 0.207 γ) β - γ spect coinc (8B52a); -0.47 β^- (not coinc with γ) β - γ coinc (11S3); 0.47 (-4%), 0.30, 0.25 spect (108S51); 0.443 (-7%), 0.291 spect (104S52); 0.32 spect (86B49a); abs (37M49); others (26M48e, 9K41b)	γ_1 0.050 (ϵ_L/γ 6), γ_2 0.159 (ϵ_K/γ 0.19, K/L 0.6), γ_3 0.209 (ϵ_K/γ 0.54, K/L 5.4) ($\gamma_1/\gamma_2/\gamma_3 =$ 0.84/100/23.8); spect, spect conv, γ - γ coinc (108S51); γ_1 (coinc with γ_2), γ_3 (not coinc with γ_1 or γ_2) scint spect, γ - γ coinc (11S3); 0.050, 0.158 (ϵ_K/γ 0.24, K/L 0.73, L/M 3.3), 0.208 (ϵ_K/γ 0.62, K/L 5.6, L/M 4) spect, spect conv, scint spect, γ - γ , β - γ coinc (7S51); 0.0498, 0.159 (K/L 0.56, L/M 3.6), 0.208 (K/L 4.5) spect conv (10C52a); others (104S52, 86B49a, 37M49, 26M48e, 67H50, 67H50a, 63M52a, 4B49, 34H51, 10C50g)	see Tl ¹⁹⁹ , Hg ¹⁹⁹ Q_β^- 0.46 (HPS)		Pt-d-n (9K41b); Au-n- γ (second order reaction) (67H50a); Hg-n-p (28S41); daughter Pt ¹⁹⁹ (12M37, 86B49a, 37M49, 67H50); parent Hg ^{199m1} (14G51a, 8B52a)
Au ²⁰⁰	B chem (28S41); chem, sep isotopes, excit (65B52a)	β^- (28S41)	48 m (65B52a, 28S41)	2.2 abs (65B52a); -2.5 abs (28S41)	1.13, 0.39 scint spect (65B52a)			Hg-n-p (28S41, 3M42); Hg ²⁰¹ - γ -p (65B52a); Tl-n-a (3M42)
Au ²⁰¹	B chem, excit, sep isotopes (65B50, 65B52a)	β^- (65B52a)	26 m (65B52a)	1.5 abs (65B52a)	0.55 scint spect (65B52a)			Hg- γ -p (65B50); Hg ²⁰² - γ -p (65B52a)
Au ^{202,204}	E excit (65B52a)	β^- or IT (65B52a)	25 s (65B52a)					Hg-n-p (65B52a)

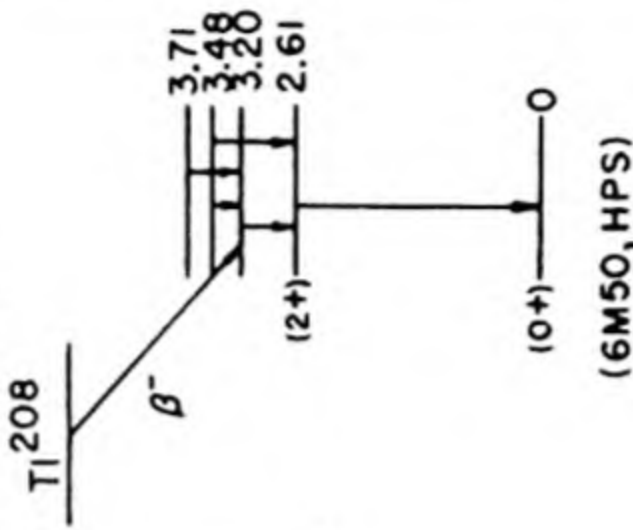
Isotope Z A	Class and identification	Percent abundance	Type of decay	Half-life	Energy of radiation in Mev		Disintegration energy and scheme	Method of production and genetic relationships
					Particles	Gamma-transitions		
²⁰³ Au 79	B chem, excit, sep isotopes (65B52a)		β^- (65B52a)	55 s (65B52a)	1.9 abs (65B52a)	0.69 acint spect (65B52a)		Hg-n-pn (65B52a); Hg ²⁰⁴ - γ -p (65B52a)
¹⁹⁵ Hg 80	E chem (3T49)		α (3T49)	0.7 m (42R52)	α : 5.60 ion ch (42R52)			spall Au (3T49)
¹⁸⁹ Hg	D chem, excit (42T52)			30 m (42T52)				spall Au (42T52)
¹⁹⁰ Hg	D chem, excit (42T52)			90 m (42T52)				spall Au (42T52)
¹⁹¹ Hg	D chem, excit (90M52)		EC (90M52)	12.4 h (90M52)				spall Au, parent Au ¹⁹¹ (90M52)
¹⁹² Hg	D chem, excit (33F52, 90M52)		EC (90M52); β^+ (33F52)	5.7 h (33F52); 8.4 h (90M52)	1.18 spect (33F52)	1.4 abs (33F52)		spall Au (90M52, 33F52); parent Au ¹⁹² (33F52, 42T52)
¹⁹³ Hg	B chem, excit (33F52, 90M52)		EC (33F52)	10.0 h (33F52); 14.5 h (?), 29.0 h (?) (90M52)				Au-p-5n (33F52, 90M52); parent Au ¹⁹³ (33F52, 90M52)
^{195m} Hg 80	B chem, excit (30D52, 33F52)		EC, IT (30D52)	38 h (30D52); -31 h (33F52); 40 h (34H52a)		0.036, 0.056 (coinc with Au ^{195m}), 0.122, 0.259 (coinc with Au ^{195m}) spect conv (34H52a); 0.037, 0.056, 0.122 (conv in Hg), 0.206, 0.261, 0.318, 0.558 spect conv (30D52)		Au-d-4n (34H52a); Au-p-3n (30D52, 33F52); parent Au ¹⁹⁵ (30D52); parent Au ^{195m} (34H52a)
¹⁹⁵ Hg	B chem, excit (30D52)		EC (30D52)	9.5 h (30D52, 34H52a)		0.061, 0.179, 0.600, 0.780 spect conv (90M52); 0.061, 0.179 spect conv (34H52a)		Au-p-3n (30D52)
¹⁹⁶ Hg								
^{197m2} Hg	A n-capt (17A36a); chem (12M37); chem, excit, cross bomb (16W41, 23F43)	0.146 (6N50a)	IT 97%, EC 3% (104S52)	23 h (23F43, 34H51); 25 h (12M37)		with IT: 0.133 (e_K/γ 0.5, K/L/M+N = 1.0/2.4/0.8), 0.164 (e_K/γ 4.6, K/L/M+N = 1.0/2.3/1.2) spect conv, γ - γ coinc (40F50, 34H51); 0.134 (K/L < 0.1), 0.165 (K/L -0.25) spect conv (10C52b); 0.134 ($L_I/L_{II}/L_{III}$ = 0.05/1.1/1.0) 0.165 ($L_I/L_{II}/L_{III}$ = 1.0/0.1/ 1.5) spect conv (63M52c); with EC: 0.191 (e_K/γ -1.7, K/L -6), 0.275 (weak, e_K/γ -0.5, K/L -5) spect conv, γ - γ coinc (40F50, 34H51); others (2H42a, 6V41b, 34H48a, 40F47, 40F50a)	see Au ^{197m} 	Pt-a-n (28S41); Au-d-2n (16W41, 9K41c, 23F43); Hg-n-2n (12M37, 23F43, 16W41); Hg-n- γ (17A36a, 16W41, 23F43); Hg-d-p (9K40); parent (3%) Au ^{197m} (40F50, 104S52); parent Hg ^{197m1} (20D50, 52M50c)

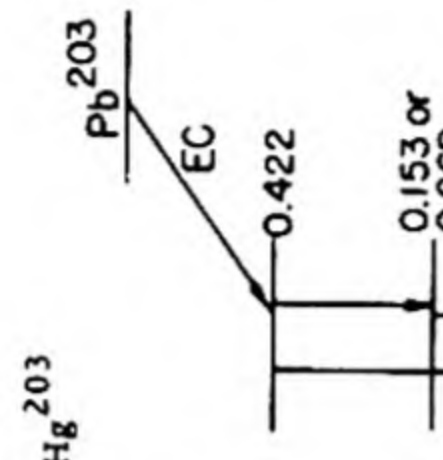
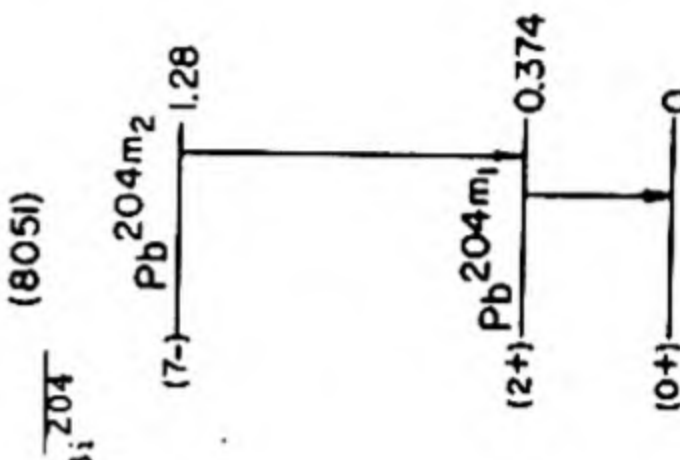
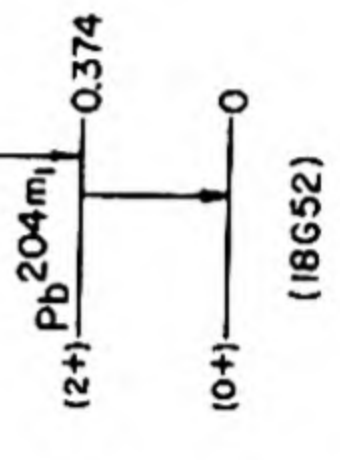
Hg^{197m1}	A genet (52M50c, 20D50)			IT (52M50c, 20D50)	7.0×10^{-9} s delay coinc (52M50c); 8×10^{-9} s delay coinc (20D50)	0.13 scint spect (20D50)	(63M52c, 104S52, HPS)	daughter Hg^{197m2} (20D50, 52M50c)
Hg^{197}	A chem, excit, cross bomb (16W41, 23F43)			EC (23F43)	65 h (34H51); 66 h (10C52b); 64 h (23F43)	0.077 (e_L/γ 2.5, L/M 3.6), 0.191 (e_K/γ -1.7, K/L -6) spect conv, γ - γ coinc (34H51, 40F50); 0.077 ($L_I/L_{II}/L_{III} = 1.0/0.45/$ 0.34) spect conv (63M52c); 0.078 (L_I/M 4), 0.191 (K/L -9) spect conv (10C52b); 0.077, 0.278 spect conv (30D52); others (2H42a, 40F47, 34H48a)		Au-d-2n (23F43, 16W41); Hg-n-2n (23F43, 16W41); Hg-n- γ (23F43, 16W41)
Hg^{198}		10.02 (6N50a)					Hg^{198} , I = 0 (87M50)	
Hg^{199m2}	A chem, excit (6H37, 12M37); mass spect (67B49b)			IT (23F43)	44 m (15H47a, 60M48); 43 m (12M37, 6H37)	0.155 (e/γ 0.25, K/L <0.4), 0.368 (e/γ >11, K/L 1.6) spect conv (15H48a); 0.159 ($L_I/L_{II}/L_{III}$ 1.6) spect conv (63M52a); 0.16 γ (coinc with 0.37 γ) scint spect, γ - γ coinc (1153); others (15H47a, 37M49)	see Au^{199} , T1 199	Pt-a-n (28541); Hg-n-2n (12M37, 1P37, 6H37, 67B49b); Hg-n-n (23F43, 16W41, 67B49b); Hg-d-p (9K40); Hg- γ -n (60M48, 37W45a); Hg- γ - γ (16W41)
Hg^{199m1}	A genet (14G51a)			IT (14G51a)	2.4×10^{-9} s delay coinc (8B52a)	0.158 spect conv, β - γ coinc (14G51a, 8B52a)		daughter Au^{199} (14G51a, 8B52a)
Hg^{199}		16.84 (6N50a)					Hg^{199} , I = 1/2 (87M50)	
Hg^{200}		23.13 (6N50a)					Hg^{200} , I = 0 (87M50)	
Hg^{201}		13.22 (6N50a)					Hg^{201} , I = 3/2 (87M50)	
Hg^{202}		29.80 (6N50a)					Hg^{202} , I = 0 (87M50)	



Isotope Z A	Class and identification	Percent abundance	Type of decay	Half-life	Energy of radiation in Mev		Disintegration energy and scheme	Method of production and genetic relationships
					Particles	Gamma-transitions		
²⁰³ Hg 80	A excit (9K40); chem, excit, n-capt (16W41, 23F43); mass spect (5S49a, 67B49a)		β^- (23F43)	47.9 d (10C52b); 45.9 d (33W51a); 46.5 d (35L51a); 43.5 d (9S48b)	0.208 β - γ coinc spect (5S49, 5S49a); 0.210 spect (33W51a); 0.205 spect (9S48b); others (37W47)	0.279 (e/ γ 0.27, K/L 3) spect, spect conv, β - γ coinc (5S49, 5S49a, 12H50); 0.278 (e/ γ 0.19, K/L+M 3.7) spect, spect conv (33W51a); -0.28 (e/ γ 0.23) scint spect (80H52); 0.279 (K/L -10) spect conv (10C52b); 0.286 (e/ γ 0.3, K/L 3) spect conv (9S48b); others (43M46, 11B50, 4B49, 100B50, 20D50, 52M51)	 <p>Qβ^- 0.487 (5S49, 5S49a) see Pb203 Hg²⁰³</p>	Hg-n- γ (23F43, 16W41, 3147h, 2S47); Hg-n-2n (16W41, 28S41, 23F43); Hg-d-p (9K40); Hg ²⁰² -n- γ (35L51a); Tl-n-p (3M42)
²⁰⁴ Hg 80		6.85 (6N50a)					Hg ²⁰⁴ , I = 0 (87M50)	Hg-d-p (9K40, 9K42); Hg-n- γ (23F43, 16W41, 2S47); Hg ²⁰⁴ -n- γ (35L51a); Tl-n-p (3M42); Pb-n-a (3M42)
²⁰⁵ Hg 80	A n-capt, excit (9K40, 9K42); sep isotopes, n-capt (35L51a)		β^- (9K40)	5.5 m (3M42, 9K40); 5.6 m (35L51a)	1.8 abs (35L51a); 1.6 abs (9K40)			
¹⁹⁸ Tl 81	B chem, excit (7O49)		EC (7O49)	1.8 h (7O49)	conv: -0.4 abs (7O49)	several γ 's, abs (7O49)		Au-a-3n (7O49); daughter Pb ¹⁹⁸ (4N50)
¹⁹⁹ Tl 81	A chem (9K40); chem, excit (7O49); genet (energy levels Hg ¹⁹⁹) (11S3)		EC (7O49); no β^+ (11S1)	7 h (7O49)		0.049, 0.078, 0.103, 0.157, 0.206, 0.245, 0.332, 0.454, 0.490 spect conv, γ - γ coinc (11S1, 11S3)	 <p>see Au¹⁹⁹, Hg¹⁹⁹ Tl¹⁹⁹ EC</p>	Au-a-2n (7O49, 11S1); Hg-d-2n (9K40); daughter Pb ¹⁹⁹ (4N50)
²⁰⁰ Tl 81	A chem, excit (7O49)		EC (7O49); no β^+ (11S1)	27 h (7O49)		0.365, 0.577, 0.622, 0.829, 1.210, 1.360 spect conv (11S1); -0.4, 1.6 abs (4N50)	(11S3)	Au-a-n (7O49, 11S1); Hg-d-2n (9K40); daughter Pb ²⁰⁰ (4N50)
²⁰¹ Tl 81	B chem, excit, cross bomb (4N50)		EC (4N50)	72 h (4N50)		0.210 spect conv, abs (4N50)		Au-a- γ (11S51); Hg-d-2n (9K40); daughter Pb ²⁰¹ (4N50)
²⁰² Tl 81	A chem, excit (9K40, 5F41)		EC (9K40, 3M42); EC (L/K -1), no β^+ or β^- (2W50)	12.5 d (80M52); 11.5 d (2W50); 11.8 d (5F41)		0.435 spect conv, abs (2W50); 0.431 scint spect (80M52)		Hg-d-2n (9K40, 2W50); Tl-n-2n (9K40, 5F41, 3M42, 80M52)

Tl ²⁰³		29.50 (1B50)				Tl ²⁰³ , I = 1/2 (87M50)	
Tl ²⁰⁴	B chem, n-capt (5F40)		β ⁻ -98%, EC -2% (33L52); β ⁻ -98.5%, EC -1.5% (38M52)	3.5 y (5F41); 2.7 y (3V45)	0.765 spect (33L52); 0.760 scint spect (38M52); 0.783 spect (9S49); 0.77 spect (6P47); others (4H47a, 5F41, 6E50)	no γ (lim 0.01%) (38M52a); no γ (lim 0.5%) (6E50); no γ (5F41); Hg K-α (33L52, 14M52a)	Tl-n-γ (5F40, 2S47); Tl-γ-n (7H49); Tl-d-p (9K40, 5F41)
Tl ²⁰⁵		70.50 (1B50)					
Tl ²⁰⁶	A n-capt (4P35); chem, genet (7B47); excit, sep isotopes (4N50a)		β ⁻ (5F40, 9K42)	4.19 m (3S52); 4.23 m (5F40); 4.3 m (13A51)	1.51 spect (13A51); 1.65 abs (5F41); 1.8 abs (9K40); no conv (13A51)	no γ (5F40, 7B47, 13A51)	Tl-n-γ (4P35, 1P37, 6H37); Tl ²⁰⁵ -n-γ (4N50a); Tl-d-p (5F40, 9K40); daughter Bi ²¹⁰ (RaE) (7B47); daughter (long-lived) Bi ²¹⁰ (4N50a)
Tl ²⁰⁷ (AcC')	A chem, genet (1C31)		β ⁻	4.79 m (3S52); 4.77 m (5F40); 4.76 m (1C31, 3S39)	1.44 abs (6E50); 1.47 abs (3S39a); 1.6 abs (6L38)	0.870 (-0.5%) (11S41)	Pb-n-p (6B40); Pb-γ-p (10B46); natural source, daughter Bi ²¹¹ (AcC)
Tl ²⁰⁸ (ThC')	A chem, genet (1C31)		β ⁻	3.1 m (1C31)	1.792 spect (6M48); 1.795 spect (14H34); 1.805 spect, β-γ coinc (4F48); 1.72 spect (7S47); 1.82 abs (3S33); β ⁻ > 1.792 (?) (<1%) spect (6M48)		natural source, daughter Bi ²¹² (ThC)



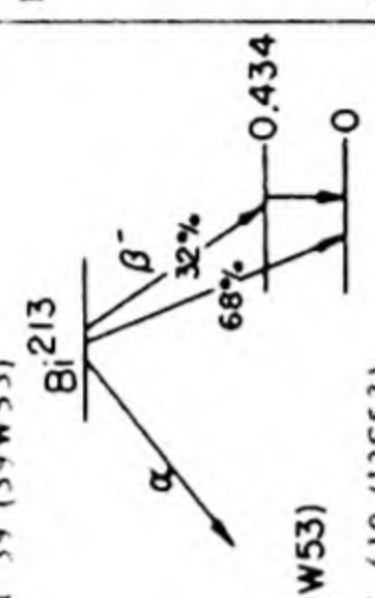
Isotope Z A	Class and identification	Percent abundance	Type of decay	Half-life	Energy of radiation in Mev		Disintegration energy and scheme	Method of production and genetic relationships
					Particles	Gamma-transitions		
^{201}Pb 82	D chem, excit (89H52)		IT (89H52)	50 s (89H52)		0.25, 0.42, 0.67 scint spect (89H52)		Tl-p-3n (89H52)
^{201}Pb	B chem (5H46); chem, genet (4N50)		EC (4N50)	8 h (4N50)				Tl-d-4n (5H46); daughter Bi^{201} , parent Tl^{201} (4N50)
^{202}Pb	E excit (89H52)		IT (89H52)	5.6 s (89H52)		0.89 scint spect (89H52)		Tl-p-2n (89H52)
^{202}Pb		$<4 \times 10^{-4}$ (9D49)		>500 y genet, yield (2T47, 4N50)				Tl-d (2T47)
^{203}Pb	B chem, excit (3M42); chem, excit, cross bomb (2T47)		EC (3M42, 8O51)	52 h (5F40, 2T47); 54 h (9K40, 12D42)		0.153, 0.269, 0.422 spect conv (8O51); 0.270, 0.420 abs conv (3M42); 0.270, -0.470 spect, spect conv (9L44)		Tl-d-2n (5F40, 9K40, 5F41, 2T47); Tl-p-n (12D42); Pb-n-2n (3M42); Pb-204 -n-2n (2T47); Pb-γ-n (10B46)
^{204}Pb	B chem (5F41); chem, excit, genet (2T47, 7K51)		IT (3M42)	68 m (3M42); 65 m (5F41)		0.905 (e/γ -0.1, K/L 1.5), 0.374 (with $\text{Pb}^{204\text{m}}$, e/γ -0.05, K/L 2.1) spect conv, abs conv, abs (14S50); 0.90 abs conv (3M42); 1.1 abs conv, abs (5F41)		Tl-d-n (5F41); Tl-d-3n (2T47); Pb-n-n (7D39, 3M42); Pb-γ-2n (10B46); daughter Bi^{204} (2T47, 14S50, 7K51), -4% (2T47); parent $\text{Pb}^{204\text{m}}$ (14S50)
$^{204\text{m}}\text{Pb}$	B genet (14S50)		IT (14S50)	3×10^{-7} s delay coinc (14S50)		0.374 (see γ's of $\text{Pb}^{204\text{m}}$)		daughter $\text{Pb}^{204\text{m}}$ (14S50); daughter Bi^{204} (14S52b)
^{204}Pb		1.48 (6N38)					Pb^{204} , I = 0 (87M50)	
^{206}Pb		23.6 (6N38)					Pb^{206} , I = 0 (87M50)	

Pb^{207m}	A excit, sep isotopes (24C51); chem, genet (23F52c)	IT (24C50)	0.84 s (24C52); 0.82 s (51L51); 0.80 s (89H52)	0.55, 1.05 scint spect (24C51); 0.5, 1.1 scint spect (23F52c)	see Bi^{207} (13/2+)- Pb^{207m} -1.60 (5/2-)-0.55 (1/2-)-0 (18G52)	Pb^{207} -n-n (24C51); Pb -n-n (51L51); daughter Bi^{207} (23F52c); not daughter Po^{211} (lim 0.005%) (23F52a)
Pb^{207}	22.6 (6N38)				Pb^{207} , $I = 1/2$ (87M50)	
Pb^{208}	52.3 (6N38)				Pb^{208} , $I = 0$ (87M50)	
Pb^{209}	A chem (6T37, 9K40); chem, sep isotopes (5F41a)	β^- (9K40, 5F41)	3.22 h (5F41); 2.75 h (9K40)	no γ , no conv (4W44, 47W52a); no γ (19L44, 39W53)	Q_{β}^- 0.64 (13S53)	Pb -d-p (6T37, 9K40, 5F41, 5F41a, 9K42, 3H50); Pb -n- γ (3M42); Bi -d-2p (11Z551); Bi -n-p (3M42); daughter Po^{213} (4H47, 11E47, 11M49); daughter Tl^{209} (11E47, 4H47)
Pb^{210} (RaD)	A chem, genet (1C31)	β^-	22 y (1C31)	γ_1 0.0465, no other γ between 0.016 and 0.060 (lim -2% of γ_1) cryst spect (26E52); γ_1 0.0467, no other γ (lim 5% of γ_1) γ_1 cryst spect (88B52a); 0.0467 (3.5%) spect conv, abs (24B30, 8S31, 19G32, 6D33); γ_1 (e_L/γ -16, $L_I/L_{II}/L_{III}/M = 1.0/0.09/0.019/0.29$) spect conv (6C50); γ_1 (e/γ -23) spect conv (33L51); γ_1 (e/γ -17, using $\gamma = 3.5\%$) spect conv (14B51); 0.032, 0.037, 0.0467 cryst spect (8F52); 0.065 (<0.2%), 0.0467 (2.8%), 0.043 (0.2%), 0.037 (0.2%), 0.032 (0.4%), 0.023 (-1%), 0.007 (-10%) cryst spect, cl ch, abs (9T46); others (9T43, 10C51, 4T52a, 63C52, 35C52)	Q_{β}^- 0.065 (51S2)	natural source, daughter Tl^{210} (RaC'), daughter Po^{214} (RaC'), parent Bi^{210} (RaE)
Pb^{211} (AcB)	A chem, genet (1C31)	β^-	36.1 m (3S39); 36.0 m (1C31)	0.065, 0.083, 0.404, 0.425, 0.487, 0.764, 0.829 spect, spect conv, abs (11S42); 0.829 (5%) (54M44); 0.8 abs (3S39a)	Q_{β}^- 1.4 (13S53)	natural source, daughter Po^{215} (AcA), parent Bi^{211} (AcC)

Isotope Z A	Class and identification	Percent abundance	Type of decay	Half-life	Energy of radiation in Mev		Disintegration energy and scheme	Method of production and genetic relationships
					Particles	Gamma-transitions		
⁸² Pb ²¹² (ThB)	A chem, genet (1C31)		β ⁻	10.6 h (1C31)	0.355, 0.589 spect, β-γ coinc (4F48); 0.331, 0.569 (~12%) spect (6M48a); 0.340 spect (6G49); 0.36 spect (3S33)	Y ₃ 0.2386 spect conv (49L51); Y ₁ 0.115, Y ₂ 0.176, Y ₃ 0.238, Y ₄ 0.249, Y ₅ 0.299 spect conv (8E32); Y ₃ 0.238 (~40%), Y ₅ 0.300 (~4%) spect (6M50); Y ₃ (L _I /L _{II} -18, M _I /M _{II} -4.3) spect conv (117S52); Y ₃ (e/γ -1), Y ₅ (e/γ -0.3) (calc from 9F39, 6M48a, 6M50); Y ₃ 0.238 spect (7S44)	 (11S46, 4F48, 6M48a)	natural source, daughter Po ²¹⁶ (ThA), parent Bi ²¹² (ThC)
⁸² Pb ²¹⁴ (RaB)	A chem, genet (1C31)		β ⁻ (3S33, 7R36)	26.8 m (1C31)	0.65 spect (3S33); 0.72 spect (8C41)	Y ₁ 0.05323, Y ₂ 0.24192, Y ₄ 0.29522, Y ₅ 0.35199 (Y ₂ /Y ₄ /Y ₅ = 0.2/0.55/1.0) cryst spect (100M52); Y ₁ 0.0528, Y ₂ 0.2410, Y ₃ 0.2578, Y ₄ 0.2942, Y ₅ 0.3509 spect (7S44); Y ₁ (1.6%) crit abs (9T43a); Y ₂ (K/L _I -6.7), Y ₄ (K/L _I -6.7), Y ₅ (K/L _I -5.9) spect conv (59K51); 0.053, 0.241, 0.257, 0.294, 0.350 spect (8E34); 0.053, 0.242, 0.295, 0.351 spect conv (10C51)	natural source, daughter Po ²¹⁸ (RaA), parent Bi ²¹⁴ (RaC)	
⁸³ Bi ^{<198}	E (2T48); chem (4N50)		α (2T48)	1.7 m (4N50)	6.2 ion ch (4N50)		spall Pb (2T48, 4N50)	
Bi ¹⁹⁸	B chem (2T48); chem, genet (4N50)		EC 99+%, α 5 × 10 ⁻² % (4N50)	7 m genet (4N50)	5.83 ion ch (4N50)		spall Pb (2T48, 4N50); parent Pb ¹⁹⁸ (4N50)	
Bi ¹⁹⁹	B chem (2T48); chem, genet (4N50)		EC 99+%, α 10 ⁻² % (4N50)	-25 m genet (4N50)	5.47 ion ch, abs mica (4N50)		spall Pb (4N50, 2T48); parent Pb ¹⁹⁹ (4N50)	
Bi ²⁰⁰	B chem, genet (4N50)		EC (4N50)	35 m genet (4N50)			spall Pb, parent Pb ²⁰⁰ (4N50)	
Bi ²⁰¹	B chem (2T48); chem, genet (4N50)		EC 99+%, α 3 × 10 ⁻³ % (4N50)	62 m (4N50)	5.15 ion ch (4N50)		spall Pb (2T48, 4N50); parent Pb ²⁰¹ (4N50)	

Bi^{201}	B chem, genet (4N50)	EC (4N50)	-2 h genet (4N50)				spall Pb, parent Pb^{201} (4N50)
Bi^{202}	B chem, genet (7K51)	EC (7K51)	95 m (7K51)				daughter Po^{202} (7K51)
Bi^{203}	B chem, genet (4N50)	EC (4N50); α -10-5% (15D52a)	12 h genet (4N50)	α : 4.85 range emuls (15D52a)			spall Pb, parent Pb^{203} (4N50); daughter Po^{203} (7K51)
Bi^{204}	B chem, sep isotopes, cross bomb (2T47)	EC, no β^+ (2T47)	12 h (2T47)	conv: -0.2, -0.8 (weak), abs, spect (2T47)	0.217 spect conv (14S50a)		Pb^{204} -d-2n (2T47); Pb^{204} -d-2n (14S50); daughter Po^{204} (7K51); Tl^{204} -3n, parent (-4%); Pb^{204m2} (2T47); parent Pb^{204m1} (14S52b)
Bi^{205}	B chem, genet, sep isotopes (7K51)	EC (7K51)	14.5 d (7K51)		0.431, 0.527, 0.550, 0.746, 1.84 spect conv (7K51)		daughter Po^{205} (7K51); daughter At^{209} (12B51)
Bi^{206}	B chem, sep isotopes (5F41a, 2T47)	EC (9L44); EC, no β^+ (13A51a)	6.4 d (9K40)		0.182, 0.234, 0.260, 0.341, 0.396, 0.470, 0.505, 0.536, 0.590, 0.803, 0.880, 0.889, 1.020, 1.097, 1.720 spect, spect conv, γ - γ coinc (13A51a); others (9K40, 5F41, 2T47a)		Tl^{206} -3n (2T47); Pb^{206} -d-2n (5F41, 5F41a, 9K40, 13A51a); Pb^{207} -d-3n (2T47); Pb^{206} -d-2n (5F41a); daughter Po^{206} (2T47a); daughter At^{210} (4N50b)
Bi^{207}	B chem, genet (4N51)	EC (5G50, 4N51)	-50 y genet (4N51)		0.56, 1.1 (coinc with 0.56 γ) scint spect, γ - γ coinc (7G51a); 0.064 or 0.137, 0.565, 1.063, 1.46, 2.05, 2.20, 2.33, 2.49 spect conv (4N51); with Pb^{207m} : 0.5, 1.1 scint spect (23F52c)		Pb^{207} -d-3n (4N51); daughter At^{211} (4N51); parent Pb^{207m} (23F52c)

Isotope Z A	Class and identification	Percent abundance	Type of decay	Half-life	Energy of radiation in Mev		Disintegration energy and scheme	Method of production and genetic relationships
					Particles	Gamma-transitions		
${}_{83}^{208}\text{Bi}$	F chem (4N51)	100 (6N38b)	EC (4N51)	long (4N51)		no γ (?) (4N51)	Q_{α} 3.2 calc (13S53)	Pb-d-Zn (4N51)
${}_{83}^{209}\text{Bi}$	G α 's not seen (91H52)		α (7F51)	$>10^{17}$ y sp act (91H52); 3×10^{17} y sp act (7F51)	-3.15 range emulsion (7F51)		${}_{\text{Bi}}^{209}$ Q_{α} 3.2 calc (13S53) ~	
${}_{83}^{210}\text{Bi}$ (RaE)	A chem, genet (1C31)		β^- 99+%, α $5 \times 10^{-5}\%$ (7B47)	5.02 d (111B52); 4.85 d (7S47f); 5.0 d (1C31); 5.1 d (15H45a)	β^- : 1.17 spect (10L37, 9F39a, 9N40, 2Z49, 10L49)	no γ (19G36, 6L47, 10C51)	Q_{β}^- 1.17, Q_{α} 5.06 calc (13S53)	
${}_{83}^{210}\text{Bi}$	A chem, genet (4N50a); chem, mass spect (52L52)		α , β^- or IT (-0.3%) (52L52)	$\sim 10^6$ y yield (52L52)	4.93 ion ch (52L52)		Q_{α} 5.03 (52L52)	natural source, daughter Pb 210 (RaD), parent Po 210 (RaF); parent Tl 206 (7B47); Pb-d- γ (112S51); Pb- α -pn (2T47); Bi-d-p (12L36, 10C40, 47H40); Bi-n- γ (7M48, 2S47); Bi-n- γ , parent Tl 206 (4N50a); parent Po 210 (52L52)
${}_{83}^{211}\text{Bi}$ (AcC)	A chem, genet (1C31)		α 99.68%, β^- 0.32% (1C31)	2.16 m (1C31)	α : 6.618 (84%), 6.272 (16%) spect (9H38, 1R31); 6.621 (82.6%), 6.274 (17.4%) spect (13V52)	0.350 abs (3S39a); -0.35 (e γ /y = 0.18, K/L 5.5) (4T52b, 10F52); 0.354 abs (16H25)	Q_{α} 6.746 (13S53) Q_{β}^- 0.61 calc (13S53)	natural source, daughter Pb 211 (AcB), parent Po 211 (AcC'), parent Tl 207 (AcC')
${}_{83}^{212}\text{Bi}$ (ThC)	A chem, genet (1C31)		β^- 66.3%, α 33.7% (6K38)	60.5 m (1C31)	α : 6.086 (27.2%), 6.047 (69.9%), 5.765 (1.7%), 5.622 (0.15%), 5.603 (1.1%), 5.481 (0.016%) spect (48R51); 6.082 (27%), 6.042 (70%), 5.760 (1.8%), 5.618 (0.2%), 5.599 (1.1%) spect (11L34); β^- : 2.250 spect (6M48a); 2.256 spect, β - γ coinc (4F48); others (7C48, 3S33)	with α : 0.040 (strong), 0.144, 0.164, 0.288, 0.328, 0.432, 0.452, 0.472, other γ 's, spect, spect conv (11S37, 11S46); 0.040 (-4%) coinc abs (21K47); (e γ /y ≥ 14 calc from 21K47, 9F39, 14B49); 0.295 spect conv (117S52); with β^- : 2.20, 1.81 (-7%), 1.61 (-7%), 1.34 (-5%), 1.03 (-6%), 0.83 (-19%), 0.72 (-19%) spect (2J47) (intensities calc from 2J47); 0.726 (-6%, e γ 0.015) spect (6M50); others (5L47)	Q_{α} 6.203, Q_{β}^- 2.25 (13S53)	natural source, daughter Pb 212 (ThB), parent Po 212 (ThC') and Tl 208 (ThC')

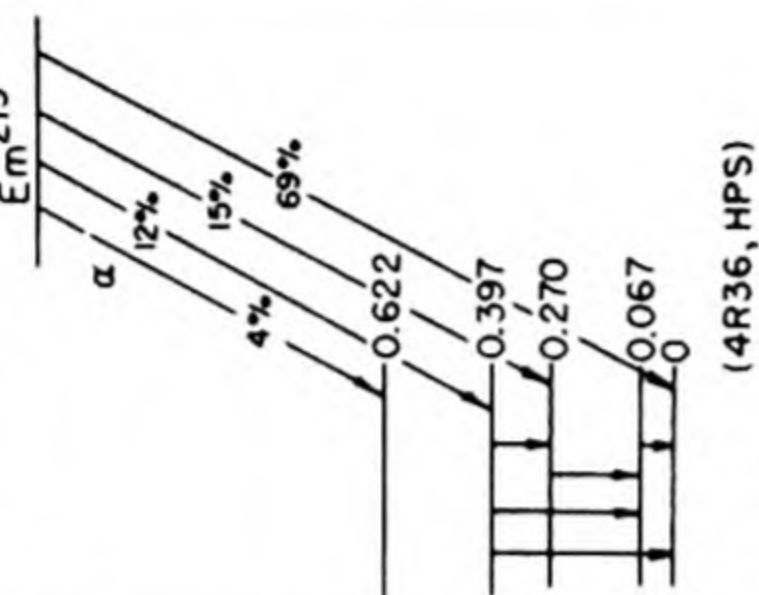
Bi ²¹³	A chem, genet (11E47, 4H47)	β ⁻ 98%, α 2% (11E47, 4H50a, 39W53)	47 m (4H47); 46 m (11E47)	β ⁻ : 1.39 (68%), 0.959 (32%) spect (39W53); -1.3 abs (4H47, 11E47); α: 5.86 ion ch (11E47); 6.0 ion ch (4H47)	0.434 spect conv, scint spect (39W53)	Q _α 5.97 (13S53) Q _β 1.39 (39W53)	 Bi ²¹³ α 68% β ⁻ 32% 0.434	daughter At ²¹⁷ , parent Po ²¹³ (4H47, 11E47, 4H50a); parent Tl ²⁰⁹ (4H50)
Bi ²¹⁴ (RaC)	A chem, genet (1C31)	β ⁻ 99+%, α 0.04% (1C31)	19.7 m (1C31)	α: 5.505 (45%), 5.444 (55%) spect (11L34); 5.52 (37%), 5.47 (46%), 5.33 (17%) spect (7C48a); β ⁻ : 3.17 (-23%), 1.65 (-77%) spect (8C41, 5L47); 3.15 spect, abs (3S33)	with β ⁻ : γ ₁ 0.6094 cryst spect (100M52); γ ₁ 0.606 (K/L 5.6), γ ₂ 0.766, γ ₃ 0.933, γ ₄ 1.120 (K/L 6.7), γ ₅ 1.238 (K/L 5.9), γ ₆ 1.379, γ ₇ 1.520, γ ₈ 1.761 (K/L 6.7), γ ₉ 1.820, γ ₁₀ 2.200, γ ₁₁ 2.420 (γ ₁ /γ ₂ /γ ₃ /γ ₄ /γ ₅ /γ ₆ /γ ₇ /γ ₈ /γ ₉ / γ ₁₀ /γ ₁₁ = 9/1.3/1.1/2.6/1.0/0.9/ 0.7/3 2/0 2/1.00/0.5) spect, spect conv (59K52, 5M50); 0.426, 0.498, 0.607, 0.766, 0.933, 1.120, 1.238, 1.379, 1.414, 1.761, 2.193 spect conv (8E34); 0.609, 0.769, 0.935, 1.122, 1.241, 1.419, 1.766 spect conv (10C51); with α: 0.0625, 0.191 spect conv (10C51); others (8E30, 8C41)	Q _α 5.610 (13S53) Q _β 3.17 (8C41)	natural source, daughter Pb ²¹⁴ (RaB), daughter At ²¹⁸ , parent Po ²¹⁴ (RaC'), parent Tl ²¹⁰ (RaC''); descendant Fr ²²² (8H51a)	
Bi ²¹⁵	A chem, genet (8H53)	β ⁻ (8H53)	8 m (8H53)			Q _β 2.01 est (60G53)	natural source, daughter At ²¹⁹ , parent Po ²¹⁵ (8H53)	
Po ²⁰⁰	B chem, genet (7K51a)	EC, α (7K51a)	11 m (7K51a)	5.84 ion ch (7K51a)			Bi-p-10n, parent Bi ²⁰⁰ (7K51a)	
Po ²⁰¹	B chem, genet (7K51a)	EC, α (7K51a)	18 m (7K51a)	5.70 ion ch (7K51a)			Bi-p-9n, parent Bi ²⁰¹ (7K51a)	
Po ²⁰²	B chem, genet, excit (7K51)	EC, α (7K51)	52 m genet (7K51)	5.59 ion ch (7K51)			Bi-p-8n, Pb-α-spall, parent Bi ²⁰² (7K51)	
Po ²⁰³	B chem, genet (7K51)	EC (7K51)	47 m genet (7K51)				Bi-p-7n, Pb-α-spall, parent Bi ²⁰³ (7K51)	
Po ²⁰⁴	B chem, genet (7K51)	EC -99%, α -1% (7K51)	3.8 h (7K51)	5.37 ion ch (7K51)			Bi-p-6n, Pb-α-spall, parent Bi ²⁰⁴ , parent Pb ²⁰⁰ (7K51)	
Po ²⁰⁵	B chem, genet, sep isotopes, excit (7K51)	EC 99+%, α 0.074% (17H51a)	1.5 h genet (7K51)	5.2 ion ch (7K51a)			Pb ²⁰⁴ -α-3n, parent Bi ²⁰⁵ , parent Pb ²⁰¹ (7K51)	
Po ²⁰⁶	B chem, genet, sep isotopes (2T47a)	EC -90%, α -10% (2T47a)	9 d (2T47a)	5.218, 5.064 spect (4R52b); 5.21 ion ch (7K51a)	0.8 abs (2T47a)	Q _α 5.321 (HPS)	Pb ²⁰⁴ -α-2n, parent Bi ²⁰⁶ (2T47a)	
Po ²⁰⁷	B chem, excit, sep isotopes (2T47a)	EC 99+%, α -10-2% (2T47a)	5.7 h (2T47a)	5.10 ion ch (7K51a)	1.3 abs (2T47a)		Pb ²⁰⁶ -α-3n (2T47a)	

Isotope Z A	Class and identification	Percent abundance	Type of decay	Half-life	Energy of radiation in Mev		Disintegration energy and scheme	Method of production and genetic relationships
					Particles	Gamma-transitions		
$^{208}_{84}\text{Po}$	A chem, excit, sep isotopes (2T47a)		α (2T47a)	2.93 y (2T50)	5.108 spect (4A52b); 5.109 spect (4R52b); 5.10 ion ch (7K51a)	no γ (2T47a, 18H51)	Q_α 5.208, Q_{EC} 1.3 calc (13S53)	Pb^{206} - α -2n (2T47a); Pb^{207} - α -3n (2T47a); Bi-d-3n (2T47a, 10K49); Bi-p-2n (4L47); daughter Em ²¹² , daughter 1.7 h At ²⁰⁸ (8H50); daughter 7.0 h At ²⁰⁸ (12B51)
$^{209}_{84}\text{Po}$	A chem, excit (10K49)		α >90%, EC <10% est (13P50)	~100 y yield (10K50)	4.877 spect (4A52b); 4.86 ion ch (7K51a)	0.87 (1%), 0.55 (0.5%), 0.2 (0.2%), 0.1 (0.07%) scint spect (18H51)	Q_α 4.972 (13S53)	Bi-d-2n (10K49)
$^{210}_{84}\text{Po}$	A chem, genet (1C31)		α : β stable (cons energy) (HPS)	138.3 d (5B49); 140 d (1C31)	5.298 spect (9H38, 16S51); 5.303 spect (7C46); -4.5 (weak) α - γ coinc, scint spect (10D52)	γ_1 0.800 (e/ γ -0.03, K/L 3.7) spect, spect conv (13A51a); γ_1 0.804 scint spect (18P52); γ_1 0.784 spect conv (10C51); γ_1 0.773 spect (7S47a); γ_1 (1.8 x 10 ⁻³ %, e/ γ -0.07), no 0.08 γ ion ch, crit abs, γ - γ coinc (7G51); γ_1 (1.6 x 10 ⁻³ %) abs (3R52); 0.77 (-10 ⁻³ %), 0.084 (-10 ⁻³ %) abs (1248); others (10D47, 49R52, 63B52)	Q_α 5.401 (13S53)	natural source, daughter Bi ²¹⁰ (RaE); Pb ²⁰⁸ - α -2n (2T47a); Bi-d-n (47H40, 10C40); Bi-p- γ (10K50); daughter At ²¹⁰ (10K49); daughter (long-lived) Bi ²¹⁰ (52L52)
$^{211}_{84}\text{Po}$ (AcC')	A genet (1C31)		α : β stable (cons energy) (HPS)	0.52 s (13L51)	7.434 spect (11L34); 6.88 (0.50%), 6.56 (0.53%), no 6.34 α (lim 0.02%) spect (74H52a); 6.90 (0.6%), 6.57 (0.5%), 6.34 (0.1%) ion ch (4N51)		Q_α 7.58 (13S53) see Bi ²⁰⁷	natural source, daughter Bi ²¹¹ (AcC); daughter At ²¹¹ (11C40, 11C40a); daughter Em ²¹⁵ (11M52); not parent Pb ^{207m} (23F52a)
$^{211}_{84}\text{Po}$	D chem, excit, sep isotopes (114S51)		α (114S51)	25 s (114S51)	7.14 ion ch (114S51)			Pb ²⁰⁸ - α -n (114S51)
$^{212}_{84}\text{Po}$ (ThC')	A genet (1C31)		α	3.04×10^{-7} s delay coinc (4B49); 3.0×10^{-7} s delay coinc (11H48); others (3J48, 4V49, 11D39, 16B43)	8.776 spect (15B36, 9H38); long range α 's: 10.536 (0.017%), 10.417 (0.002%), 9.489 (0.004%) spect (48R51)		Q_α 8.946 (13S53)	natural source, daughter Bi ²¹² (ThC); daughter Em ²¹⁶ (11M49)
$^{213}_{84}\text{Po}$	A genet (4H47, 11E47)		α (4H47, 11E47)	4.2×10^{-6} s delay coinc (3J48)	8.336 ion ch (11E47, 5C48); 8.34 ion ch (4H50a)		Q_α 8.496 (13S53)	daughter Bi ²¹³ , parent Pb ²⁰⁹ (4H47, 11E47); daughter Em ²¹⁷ (11M49)
$^{214}_{84}\text{Po}$ (RaC')	A genet (1C31)		α : β stable (cons energy) (HPS)	1.637×10^{-4} s delay coinc (13D50); -1.5 x 10 ⁻⁴ s delay coinc (11D39, 6R41, 5W42, 4J43, 14L47, 4B48); 1.4 x 10 ⁻⁴ s delay coinc (5R47)	7.680 spect (15B36, 9H38); 7.683 spect (16S51); long range α 's: 9.069 (0.002%), others 8.280-10.509 spect (11L34)		Q_α 7.826 (13S53)	natural source, daughter Bi ²¹⁴ (RaC), parent Pb ²¹⁰ (RaD); daughter Em ²¹⁸ (4S48)

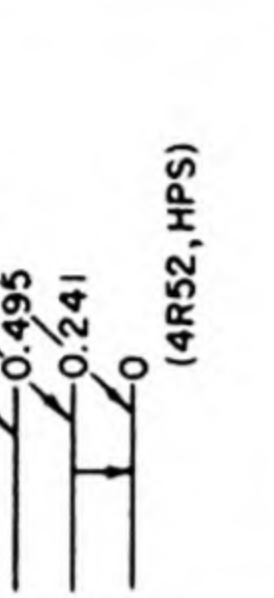
Po ²¹⁵ (AcA)	A genet (IC31)	α 99+%, β^- 5 x 10 ⁻⁴ % (5K44, 8A50)	1.83 x 10 ⁻³ s delay coinc (5W42)	7.365 spect (11L34)	Q α 7.505, Q β^- 0.8 calc (13S53)	natural source, daughter Em ²¹⁹ (An), parent Pb ²¹¹ (AcB); parent At ²¹⁵ (5K44)
Po ²¹⁶ (ThA)	A genet (IC31)	α ; β stable (cons energy) (HPS); α 99+%, β^- 0.014% (5K43)	0.158 s (5W42)	α : 6.774 spect (15B36, 9H38)	Q α 6.902 (13S53)	natural source, daughter Em ²²⁰ (Tn), parent Pb ²¹² (ThB); parent At ²¹⁶ (5K43) (?)
Po ²¹⁷	C genet (9M52b)	α (9M52b)		6.5 ion ch (9M52b)	Q α 6.7, Q β^- 1.3 est (13S53)	daughter Em ²²¹ (9M52b)
Po ²¹⁸ (RaA)	A chem, genet (IC31)	α 99+%, β^- 0.03% (5K43a)	3.05 m (IC31)	α : 5.998 spect (15B36, 9H38)	Q α 6.110, Q β^- 0.33 calc (13S53)	natural source, daughter Em ²²² (Rn), parent Pb ²¹⁴ (RaB); parent At ²¹⁸ (5K43a)
At ^{<202}	D chem, excit (12B51)	α , EC (12B51)	43 s (12B51)	6.50 ion ch (12B51)		Bi- α -spall (12B51)
At ^{<203}	D chem, excit (12B51)	α , EC (12B51)	1.7 m (12B51)	6.35 ion ch (12B51)		Bi- α -spall (12B51)
At ²⁰³	D chem, excit (12B51)	α , EC (12B51)	7 m (12B51, 13H51)	6.10 ion ch (12B51)		Bi- α -10n (12B51); Au-C-6n (13H51, 4M50)
At ²⁰⁴	B chem, excit, genet (12B51)	EC (12B51)	-25 m genet (12B51)			Bi- α -9n, parent Po ²⁰⁴ (12B51)
At ²⁰⁵	B chem, excit, genet (12B51)	α , EC (12B51)	25 m (12B51, 13H51)	5.90 ion ch (12B51)		Bi- α -8n, parent Po ²⁰⁵ (12B51); Au-C-4n (4M50, 13H51)
At ²⁰⁶	B chem, excit, genet (12B51)	EC (12B51)	2.6 h genet (12B51)			Bi- α -7n, parent Po ²⁰⁶ (12B51)
At ²⁰⁷	B chem, excit, genet (2T48a, 12B51)	EC -90%, α -10% (2T48a, 12B51)	2.0 h (12B51)	5.75 ion ch (12B51)		Bi- α -6n (2T48a, 12B51); parent Po ²⁰⁷ , parent Bi ²⁰³ (12B51)
At ²⁰⁸	B chem, excit, genet (12B51)	EC (12B51)	6.3 h genet (12B51)			Bi- α -5n, parent Po ²⁰⁸ (12B51)
At ²⁰⁸	A chem, genet (8H50)	EC 99+%, α 0.5% (8H50)	1.7 h (8H50)	5.65 ion ch (8H50)		daughter Fr ²¹² , parent Po ²⁰⁸ (8H50, 9M52a)
At ²⁰⁹	B chem, genet, excit (12B51)	EC -95%, α -5% (12B51)	5.5 h (12B51)	5.65 ion ch (12B51)		Bi- α -4n, parent Po ²⁰⁹ , parent Bi ²⁰⁵ (12B51)
At ²¹⁰	A chem, excit, genet (10K49)	EC 99+%, α 0.17% (74H52a); EC 99+%, α 0.1% (4N50b)	8.3 h (10K49)	5.519 (32%), 5.437 (31%), 5.355 (37%) spect (74H52a)		Bi- α -3n, parent Po ²¹⁰ (10K49, 12B51); parent Bi ²⁰⁶ (4N50b)
				0.2, 0.8 scint spect (89M52)		
				0.25, 1.15, 1.40 scint spect (74H52a); 1.0 abs, abs conv (10K49)		

Isotope Z A	Class and identification	Percent abundance	Type of decay	Half-life	Energy of radiation in Mev		Disintegration energy and scheme	Method of production and genetic relationships
					Particles	Gamma-transitions		
²¹¹ At 85	A chem, excit, genet (11C40, 10K49)		α 40.9%, EC 59.1% (4N51)	7.5 h (11C40, 10K49); 7.3 h (17H51)	5.862 spect (74H52a); 5.89 ion ch (2T48a, 12B51)		Q_α 5.975, Q_{EC} 0.9 est (13S53)	Bi- α -Zn (11C40, 11C40a, 10K49, 12B51); spall Th, U (20B52, 13S47)
²¹² At	E excit (7W48)		α (7W48)	0.25 s (7W48)				Bi- α -n (7W48)
²¹³ At	E genet, decay charac (57K51)		α (57K51)		9.2 range emuls (57K51)			descendent Pa ²²⁵ (57K51)
²¹⁴ At	B genet (11M49)		α (11M49)	$\sim 2 \times 10^{-6}$ s est (11M51)	8.78 ion ch (11M49, 11M51)		Q_α 8.95, Q_{EC} 1.05 calc (13S53)	daughter Fr ²¹⁸ (11M49, 11M51)
²¹⁵ At	A genet (5K44, 13G48)		α (5K44, 13G48)	$\sim 10^{-4}$ s delay coinc (13G48, 11M51); short (5K44)	8.00 ion ch (13G48, 11M51); 8.4 ion ch (5K44)		Q_α 8.15, Q_β^- 0.0 calc (13S53)	daughter Fr ²¹⁹ , parent Bi ²¹¹ (AcC) (13G48, 11M51); natural source, daughter Po ²¹⁵ (AcA), parent Bi ²¹¹ (AcC) (5K44)
²¹⁶ At	A genet (13G48)		α (5K43, 13G48)	$\sim 3 \times 10^{-4}$ s delay coinc (11M49, 11M51); short (<54 s) (5K43)	7.79 ion ch (13G48, 11M51); 7.64 ion ch (5K43)		Q_α 7.94, Q_β^- 2.03 calc, Q_{EC} 0.46 calc (13S53)	daughter Fr ²²⁰ , parent Bi ²¹² (ThC) (13G48, 11M51); natural source, parent Bi ²¹² (ThC) (5K43); daughter Po ²¹⁶ (ThA) (5K43); note Po ²¹⁶ β -stable (HPS)
²¹⁷ At	A genet (11E47, 4H47)		α (11E47, 4H47)	0.018 s delay coinc (4H47, 4H50a); 0.021 s delay coinc (11E47)	7.02 ion ch (5C48); 7.00 ion ch (4H47)		Q_α 7.15, Q_β^- 0.65 calc (13S53)	daughter Fr ²²¹ , parent Bi ²¹³ (11E47, 4H47, 4H50a)
²¹⁸ At	E genet (5K43a)		α (5K43a); α 99+%, β^- 0.1% (3W48)	1.5-2.0 s (3W48); several sec (?) (5K43a)	α : 6.63 range (5K43a); 6.7 ion ch (3W48)		Q_α 6.75, Q_β^- 2.67 calc (13S53)	natural source, daughter Po ²¹⁸ (RaA), parent Bi ²¹⁴ (RaC) (5K43a, 3W48)
²¹⁹ At	A chem, genet (8H53)		α -97%, β^- -3% (8H53)	0.9 m (8H53)	α : 6.27 ion ch (8H53)		Q_α 6.39, Q_β^- 1.45 est (13S53)	natural source, daughter Fr ²²³ (AcK), parent Em ²¹⁹ (An), parent Bi ²¹⁵ (8H53)
²⁰⁸ Em	D chem (9M52b)		EC -80%, α -20% (9M52b)	23 m (9M52b)	6.138 spect (9M52)			spall Th (9M52b)
²⁰⁹ Em	B chem, genet (9M52a)		EC -80%, α -20% (9M52a)	30 m (9M52b)	6.02 ion ch (9M52a)			Pb-C-spall, spall Th (9M52a); daughter Ra ²¹³ , parent At ²⁰⁹ (9M52a)
²¹⁰ Em	B chem, genet (9M52a)		α >95%, EC <5% (9M52b)	2.7 h (9M52a); 2.1 h (13G49)	6.036 spect (9M52); 6.02 ion ch (9M52a)		Q_α 6.153 (13S53)	spall Th (13G49, 9M52a); Pb-C-spall (9M52a); parent Po ²⁰⁶ (9M52a)
²¹¹ Em	A chem, genet (9M52a)		EC 75%, α 25% (9M52a)	16 h (9M52a)	5.847 (33%), 5.778 (67%) spect (9M52); 5.82 ion ch (9M52a)			Pb-C-spall, parent At ²¹¹ (9M52a)
²¹² Em	A chem, genet (8H50, 13G49)		α (8H50)	23 m (13G49, 8H50, 9M52a)	6.262 spect (9M52); 6.23 ion ch (9M52a)		Q_α 6.382 (13S53)	spall Th (13G49); daughter Fr ²¹² , parent Po ²⁰⁸ (8H50, 9M52a)

Em ²¹⁵	B genet (IIM52)	α (IIM52)	-10 ⁻⁶ s est (IIM52)	8.6 ion ch (IIM52)	Q _α 8.16 (13S53)	daughter Ra ²¹⁹ , parent Po ²¹¹ (AcC') (IIM52)
Em ²¹⁶	A genet (IIM49, IIM51)	α (IIM49, IIM51); β stable (cons energy) (HPS)	-10 ⁻⁴ s est (IIM51)	8.01 ion ch (7050)		daughter Ra ²²⁰ , parent Po ²¹² (ThC') (IIM49, IIM51)
Em ²¹⁷	A genet (IIM49, IIM51)	α (IIM51); β stable (cons energy) (HPS)	-10 ⁻³ s delay coinc (IIM51)	7.74 ion ch (IIM51)	Q _α 7.89 (13S53)	daughter Ra ²²¹ , parent Po ²¹³ (IIM49, IIM51)
Em ²¹⁸	A genet (4S48)	α (4S48); β stable (cons energy) (HPS)	0.019 s delay coinc (4S48)	7.12 ion ch (1J48)	Q _α 7.25 (13S53)	daughter Ra ²²² , parent Po ²¹⁴ (RaC') (4S48)
Em ²¹⁹ (An)	A chem, genet (IC31)	α	3.92 s (IC31)	6.824, 6.559, 6.434 spect (IIL34); α ₀ (69%), α ₂₇₀ (15%), α ₃₉₇ (12%), α ₆₂₂ (4%) spect (4R36)	Q _α 6.951, Q _β 0.26 calc (13S53)	natural source, daughter Ra ²²³ (AcX), parent Po ²¹⁵ (AcA); daughter At ²¹⁹ (8H53)
Em ²²⁰ (Tn)	A chem, genet (IC31)	α; β stable (cons energy) (HPS)	54.5 s (IC31)	6.282 spect (15B36, 9H38)	Q _α 6.398 (13S53)	natural source, daughter Ra ²²⁴ (ThX), parent Po ²¹⁶ (ThA)
Em ²²¹	A chem, genet (9M52a)	β ⁻ -80%, α -20% (9M52b)	25 m (9M52b)		Q _α 6.0 est, Q _β 0.9 est (13S53)	Th-p-spall, parent Fr ²²¹ (9M52a); parent Po ²¹⁷ (9M52b)
Em ²²² (Rn)	A chem, genet (IC31)	α; no β ⁻ (lim 10 ⁻⁴ %) (5K46)	3.825 d (22T51, IC31)	5.486 spect (15B36, 9H38)	Q _α 5.587 (13S53)	natural source, daughter Ra ²²⁶ , parent Po ²¹⁸ (RaA)
87Fr ²¹²	A chem, genet (8H50); chem, mass spect (9M52a)	EC 56%, α 44% (8H50)	19.3 m (8H50)	6.409 (37%), 6.387 (39%), 6.339 (24%) spect (8H52c); 6.36 ion ch (8H51)		spall Th (8H50); parent Em ²¹² (8H50, 9M52a)
Fr ²¹⁷	E genet, decay charac (57K51)	α (57K51)		8.3 range emuls (57K51)		descendent Pa ²²⁵ (57K51)

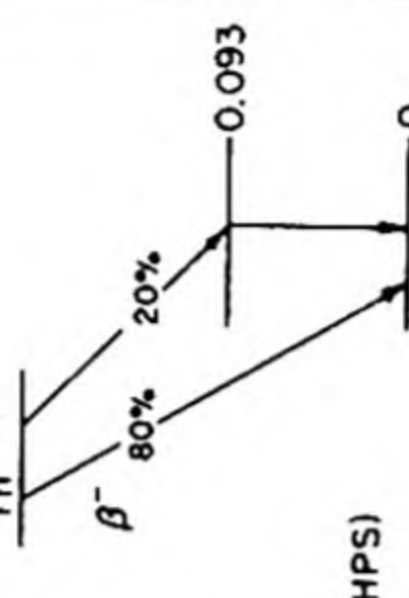


Isotope Z	Class and identification	Percent abundance	Type of decay	Half-life	Energy of radiation in Mev		Disintegration energy and scheme	Method of production and genetic relationships
					Particles	Gamma-transitions		
²¹⁸ Fr 87	B genet (11M49, 11M51)		α (11M51)	5×10^{-3} s est (11M51)	7.85 ion ch (11M51)		Q_α 8.00, Q_{EC} 1.8 calc (13S53)	daughter Ac ²²² , parent At ²¹⁴ (11M49, 11M51)
²¹⁹ Fr	A genet (13G48)		α (13G48); β stable (cons energy) (HPS)	0.02 s delay coinc (11M51)	7.30 ion ch (11M51)		Q_α 7.44 (13S53)	daughter Ac ²²³ , parent At ²¹⁵ (13G48, 11M49, 11M51)
²²⁰ Fr	A genet (13G48)		α (13G48)	27.5 s (11M51)	6.69 ion ch (11M51)		Q_α 6.81, Q_β^- 1.27 calc, Q_{EC} 0.87 calc (13S53)	daughter Ac ²²⁴ , parent At ²¹⁶ (13G48, 11M49, 11M51)
²²¹ Fr	A chem, genet (4H47, 11E47)		α (11E47, 4H47)	4.8 m (4H50a); 5 m (11E47)	6.30 ion ch (4H47, 5C48); 6.30 (-75%), 6.05 (-25%) ion ch (4H50a)	0.220 spect conv, scint spect (39W53)	Q_α 6.42, Q_β^- 0.24 calc (13S53)	daughter Ac ²²⁵ , parent At ²¹⁷ (11E47, 4H47, 5C48, 4H50a); daughter Em ²²¹ (9M52a)
²²² Fr	A chem, genet (8H50a)		β^- 99+%, α 0.01-0.1% (8H51a)	14.8 m (8H50a)			Q_α 6.00 est, Q_β^- 2.04 est, Q_{EC} 0.02 est (13S53)	spall Th, parent Ra ²²² ancestor Bi ²¹⁴ (8H50a, 8H51a)
²²³ Fr (AcK)	A chem, genet (7P39, 7P39b)		β^- (7P39a, 8G47); α $4 \times 10^{-3}\%$ (8H53)	21 m (7P39)	β^- : 1.2 cl ch (7P39a, 7P39b, 6L50)	0.09 abs (6L44, 7P46); -0.330 (6%) abs, 0.0486 (27%) crit abs (6L50)	Q_α 5.60 est, Q_β^- 1.19 calc (13S53)	natural source, daughter Ac ²²⁷ , parent Ra ²²³ (AcX) (7P39, 7P39a, 7P39b, 7P41, 7P46, 8G47, 6L50); parent At ²¹⁹ (8H53)
²¹³ Ra 88	B chem, genet (9M52a)		α (9M52a)	2.7 m (9M52c)	6.90 ion ch (9M52c)			Pb-C-spall, spall Th, parent Em ²⁰⁹ (9M52a)
²¹⁹ Ra	B genet (11M52)		α (11M52)	10^{-3} s est (11M52)	8.0 ion ch (11M52)		Q_α 8.1 (13S53)	daughter Th ²²³ , parent Em ²¹⁵ (11M52)
²²⁰ Ra	A genet (11M49, 11M51)		α (11M51)	3×10^{-2} s est (11M51)	7.43 ion ch (7O50)		Q_α 7.57 (13S53)	daughter Th ²²⁴ , parent Em ²¹⁶ (11M49, 11M51)
²²¹ Ra	A chem, genet (11M49, 11M51)		α (11M51)	30 s (11M51)	6.71 ion ch (11M51)		Q_α 6.83 (13S53)	daughter Th ²²⁵ , parent Em ²¹⁷ (11M49, 11M51)
²²² Ra	A chem, genet (4S48)		α (4S48); β stable (cons energy) (HPS)	38 s (4S48)	6.51 ion ch (1J48)		Q_α 6.63 (13S53)	daughter Th ²²⁶ , parent Em ²¹⁸ (4S48); daughter Fr ²²² (8H51a)
²²³ Ra (AcX)	A chem, genet (1C31)		α ; β stable (cons energy) (HPS)	11.2 d (1C31)	5.860 (weak), 5.730 (9%), 5.704 (53%), 5.596 (24%), 5.528 (9%), 5.487 (2%), 5.419 (3%) spect (4R52b); 5.750 (11%), 5.719 (53%), 5.607 (25%), 5.540 (9%), 5.433 (2%) spect (4A52a); no 6.0-6.1 α (lim 0.5%) (13H50); others (11L34, 4R36, 4R37)	0.144, 0.155, 0.180, 0.270, 0.340 cryst spect (8F40); 0.026, 0.064, 0.081, 0.099, 0.116, 0.154, 0.164, 0.180, 0.232, 0.268, 0.280, 0.322, 0.348, 0.444 spect conv (11S37)	Q_α 5.855 (13S53)	natural source, daughter Th ²²⁷ (RdAc), daughter Fr ²²³ (AcK), parent Em ²¹⁹ (An); daughter Ac ²²³ (11M51); spall U (13S47, 6O47, 6F51)

Ra ²²⁴ (ThX)	A chem, genet (1C31)	α : β stable (cons energy) (HPS)	3.64 d (1C31)	5.681 (95%), 5.448 (4.6%), 5.194 (0.4%) spect (4R49); 5.681 spect (15B36); 5.66 ion ch (2C45)	0.241 (e_K/γ 0.1) spect conv (4R52); no γ (1M28, 4F49)	 (4R52, HPS)	natural source, daughter Th ²²⁸ (RdTh), parent Em ²²⁰ (Tn); spall U (13S47, 6O47, 6F51)
Ra ²²⁵	A chem, genet (11E47, 4H47)	β^- (11E47, 4H47); no α (lim 0.1%) (9M52c)	14.8 d (4H50a); 14 d (11E47)	-0.31 spect (3F52a); -0.2 abs (4H50a); <0.05 abs (11E47)		daughter Th ²²⁹ , parent Ac ²²⁵ (11E47, 4H47, 4H50a); spall U (6F51)	
Ra ²²⁶	A chem, genet (1C31)	α : β stable (cons energy) (HPS)	1622 y sp act (2K49a); 1631 y sp act (3C46); 1590 y sp act (1C31)	α_0 4.777 spect (4R52b); α_0 (94.3%), α_{188} (5.7%) spect (4A52c); α_0 (95.2%), α_{186} (4.8%) ion ch (7K51a); α_0 (93.5%), α_{187} (6.5%) spect (4R49a); others (109B51)	0.186 spect conv (10C51); -0.19 (e/γ 0.88, K/L -0.5) α -conv coinc abs (14V52); 0.188 (16H24, 7R36); (e/γ -0.5) (8S43)	natural source, daughter Th ²³⁰ (Io), parent Em ²²² (Rn)	
Ra ²²⁷	A n-capt, genet (8P49)	β^- (8P49, 6F50)	41.2 m (107B52)	1.30 spect (107B52)	0.291, 0.498 scint spect (107B52)	Ra-n- γ , parent Ac ²²⁷ (8P49); spall U (6F50)	
Ra ²²⁸ (MaTh ₁)	A chem, genet (1C31)	β^-	6.7 y (1C31)	-0.012 (?) cl ch (6L48, 6L49a); 0.053 spect, abs (8L39)	-0.03 cl ch (6L48, 6L49)	natural source, daughter Th ²³² , parent Ac ²²⁸ (MaTh ₂)	
Ra ²²⁹ [B] n-capt, genet (41D52)		[β^-] (41D52)	[short] (41D52)			[Ra ²²⁸ -n- γ , parent Ac ²²⁹] (41D52)	
Ra ²³⁰	D chem (5J52)	β^- (5J52)	1 h (5J52)	1.2 abs, spect (5J52)		spall Th, parent Ac ²³⁰ (5J52)	
89Ac ²²¹	E genet, decay charac (57K51)	α (57K51)		7.6 range emuls (57K51)		descendent Pa ²²⁵ (57K51)	
Ac ²²²	B genet (11M49, 11M51)	α (11M51)	5.5 s (11M52)	6.96 ion ch (11M51)	Q_α 7.09, Q_{EC} 2.26 calc (13S53)	daughter Pa ²²⁶ , parent Fr ²¹⁸ (11M49, 11M51)	
Ac ²²³	A genet (13G48)	α 99%, EC 1% (11M51)	2.2 m (11M51)	6.64 ion ch (11M51)	Q_α 6.76, Q_{EC} 0.64 calc (13S53)	daughter Pa ²²⁷ , parent Fr ²¹⁹ parent Ra ²²³ (AcX) (13G48, 11M49, 11M51)	
Ac ²²⁴	A chem, genet (13G48)	EC -90%, α -10% (11M51)	2.9 h (11M51)	6.17 ion ch (11M51)	Q_α 6.28, Q_{EC} 1.37 calc, Q_β 0.29 calc (13S53)	daughter Pa ²²⁸ , parent Fr ²²⁰ , parent Ra ²²⁴ (ThX), (13G48, 11M49, 11M51)	
Ac ²²⁵	A chem, genet (4H47, 11E47)	α (11E47, 4H47); β stable (cons energy) (HPS)	10.0 d (4H50a, 11E47)	5.80 ion ch (4H50a, 5C48)	Q_α 5.90 (13S53)	daughter Ra ²²⁵ , parent Fr ²²¹ (4H47, 11E47, 4H50a); daughter Pa ²²⁹ (8H49a); daughter Th ²²⁵ (11M49, 11M51) spall Th (17H50), U (6O47)	

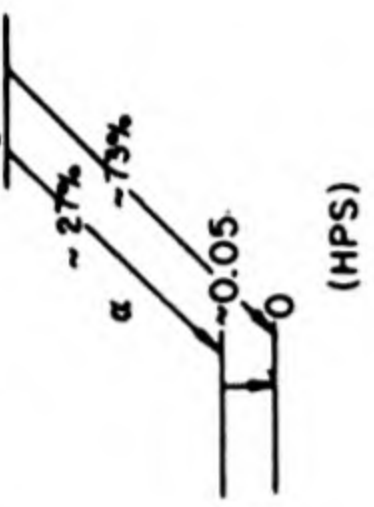
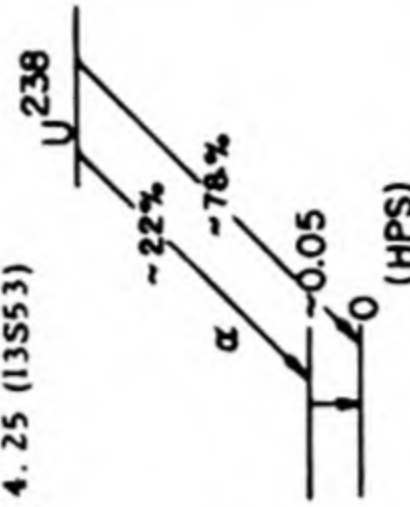
Isotope Z A	Class and identification	Percent abundance	Type of decay	Half-life	Energy of radiation in Mev		Disintegration energy and scheme	Method of production and genetic relationships
					Particles	Gamma-transitions		
²²⁶ Ac 89 A	A chem, genet (6S48)		β^- (6S48)	29 h (6S50)	1.17 abs (17H50)		Q_α 5.44 est, Q_{EC} 0.6 est, Q_β^- 1.07 est (13S53)	spall U, daughter Pa ²³⁰ , parent Th ²²⁶ (6S48, 6S50); spall Th (17H50, 11M50); daughter Pa ²³⁰ , parent Th ²²⁶ (11M50)
²²⁷ Ac	A chem, genet (1C31)		β^- -99% (7P39, 8P49a); α 1.2% (2M14, 7P39, 7P46, 8P49a)	22.0 y (13H50a); 21.7 y (4C44); 13.5 y (1C31)	α : 4.942 spect (4R52b); 4.94 (100%) ion ch (13G48a); others (3G47) β^- : 0.04 spect (3F50); -0.02 cl ch (7P46); <0.03 abs (6L44)	0.037 (weak) abs (6L43, 6L44, 7P46); (0.2%) (6L50)	Ac^{227} , $I = 3/2$ (36T51) Q_α 5.03, Q_β^- -0.08 calc (13S53)	natural source, daughter Pa ²³¹ , parent Th ²²⁷ (RdAc); parent Fr ²²³ (AcK) (7P39, 7P46); daughter Ra ²²⁷ (8P49)
²²⁸ Ac (MsTh ₂)	A chem, genet (1C31)		β^-	6.13 h (1C31)	2.18 (10%), 1.85 (9%), 1.72 (7%), 1.15 (53%), 0.66 (8%), 0.46 (13%) spect (82C52); 2.03, 1.74, 1.10 spect (5J51); others (4F38, 6L38, 3L39)	0.058, 0.129, 0.184, 0.338, 0.462, 0.914, 0.969 spect conv (13B24); 0.333, 0.462, 0.913, 0.968 spect (5T26); 0.063, 0.146, 0.186, 0.338, 0.533, 0.590, 0.905 spect conv (5J51)	Q_α 4.66 est, Q_β^- 2.18 (13S53)	natural source, daughter Ra ²²⁸ (MsTh), parent Th ²²⁸ (RdTh)
²²⁹ Ac	B chem, n-capt (41D52)		θ^- (41D52)	66 m (41D52)			Q_β^- 1.0 est (13S53)	daughter Ra ²²⁹ (41D52)
²³⁰ Ac	F genet (5J52)		β^- (5J52)	<1 m genet (5J52)	-2.2 abs, spect (5J52)			daughter Ra ²³⁰ (5J52)
²²³ Th	B genet (11M52)		α (11M52)	-0.1 s est (11M52)	7.55 ion ch (11M52)		Q_α 7.69 (13S53)	daughter U ²²⁷ , parent Ra ²¹⁹ (11M52)
²²⁴ Th	A genet (11M49, 11M51)		α (11M51); β stable (cons energy) (HPS)	-1 s est (11M51)	7.13 ion ch (7O50)		Q_α 7.26 (13S53)	daughter U ²²⁸ , parent Ra ²²⁰ (11M49, 11M51)
²²⁵ Th	A chem, genet (11M49, 11M51)		α -90%, EC -10% (11M51)	8.0 m (11M51)	6.57 ion ch (11M51)		Q_α 6.69, Q_{EC} 0.55 calc (13S53)	daughter U ²²⁹ , parent Ra ²²¹ , parent Ac ²²⁵ (11M49, 11M51)
²²⁶ Th	A chem, genet (4S48)		α (4S48); β stable (cons energy) (HPS)	30.9 m (4S48)	α_0 (78%), α_{117} (22%) spect (21S52); 6.30 ion ch (1J48)		Q_α 6.41 (13S53)	daughter U ²³⁰ , parent Ra ²²² (4S48); daughter Ac ²²⁶ (6S48, 6S50)

Th ²²⁷ (RdAc)	A chem, genet (IC31)	a: β stable (cons energy) (HPS)	18.6 d (8P49b); 18.9 d (IC31)	6.030 (19%), 6.001 (5%), 5.972 (21%), 5.952 (13%), 5.922 (-2%), 5.860 (4%), 5.796 (2%), 5.749 (17%), 5.728 (-1%), 5.704 (15%), 5.651 (-2%) spect (4R52b); 6.049 (20%), 6.017 (4%), 5.988 (25%), 5.966 (4%), 5.922 (-1%), 5.868 (2.5%), 5.815 (-1%), 5.764 (20%), 5.742 (4%), 5.717 (15%), 5.672 (2.5%) spect (11L34)	0.050, 0.057, 0.080, 0.101, 0.113, 0.129, 0.208, 0.240, 0.258 cryst spect (8F40); 0.050 (3%), 0.120 (13%), 0.280 (50%) abs (3R50); 0.050 (5%), 0.125 (10%), 0.270 (26%) abs (3B44); 0.050 (-3%), 0.125 (23%) abs (9T42)	Q _α 6.138 (13S53)	natural source, daughter Ac ²²⁷ , parent Ra ²²³ (AcX); daughter Pa ²²⁷ (13G48, 11M51); spall U (6O47)
Th ²²⁸ (RdTh)	A chem, genet (IC31)	a: β stable (cons energy) (HPS)	1.90 y (IC31)	5.423 (72%), 5.338 (28%) spect (4R49b)	0.0843 spect conv (4R52a); 0.083 (e/γ 12) a-conv coinc abs (14V52); 0.083 (2.1%, e/γ = 10) crit abs (3R53); others (1M28, 11S41a, 3R50, 103B51)	Q _α 5.520 (13S53)	natural source, daughter Ac ²²⁸ (MsTh ₂), parent Ra ²²⁴ (ThX); daughter U ²³² (9G49); daughter Pa ²²⁸ (13G48b, 11M51)
Th ²²⁹	A chem, genet (11E47, 4H47)	a: β stable (cons energy) (HPS)	7340 y genet (4H50a); -10 ⁴ y genet (11E47)	5.02 (-10%), 4.94 (-20%), 4.85 (-70%) ion ch (4H50a)		Q _α 5.11 (13S53)	daughter U ²³³ , parent Ra ²²⁵ (11E47, 4H47, 4H50a)
Th ²³⁰ (Io)	A chem, genet (IC31)	a: β stable (cons energy) (HPS)	8.0 × 10 ⁴ y sp act (8H49b); 8.2 × 10 ⁴ y genet (IC30)	4.682 (-75%), 4.613 (-25%), 4.51 (7) (weak) spect (4R48); 4.66 range air (1G22), ion ch (2C44, 2C45)	0.068, 0.228 (very weak) spect conv (4R51); 0.068 (0.85%), 0.140 (0.33%), 0.240 (0.05%) abs (4C48); -0.07 (coinc with a, e/γ -46) a-conv coinc abs (14V52, 10F51); -0.068 (0.5%), 0.190 (0.3%) abs (3R50); -0.07 (coinc with a), -0.2 (coinc with a) a-γ, a-conv coinc abs (5P51); others (6J51, 5W39)	Q _α 4.765 (13S53)	natural source, daughter U ²³⁴ (U _{II}), parent Ra ²²⁶ ; daughter Pa ²³⁰ (4S48a)
Th ²³¹ (UY)	A chem, genet (IC31)	β ⁻	25.64 h (1J51); 25.5 h (3K49); 24.6 h (IC31); 24.0 h (12G32)	0.302 (44%), 0.216 (11%), 0.094 (45%) spect (3F52); 0.39 (-20%), 0.19 (-40%), 0.10 (-40%) spect (10S51); 0.2 abs (5E37, 1J51)	Y ₁ 0.022, Y ₂ 0.059, Y ₃ 0.063, Y ₄ 0.085, Y ₅ 0.107, Y ₆ 0.122, Y ₇ 0.167, Y ₈ 0.208, Y ₉ 0.230 (Y ₂ +Y ₃ /Y ₄ +Y ₅ /Y ₆ +Y ₇ /Y ₈ +Y ₉ = 0.40/1.00/0.065/0.02/0.018/ 0.003/0.001) spect conv, scint spect (3F52); 0.059, 0.063, 0.082, 0.120 spect conv (10S51); 0.035 (>80%), 0.210 abs (3K49)	Q _α 4.19 calc (13S53) Q _β 0.324 (3F52)	natural source, daughter U ²³⁵ (AcU), parent Pa ²³¹ ; Th-n-2n (5N38, 13S52)
Th ²³²	A chem, genet (IC31)	a: β stable (cons energy) (HPS)	1.39 × 10 ¹⁰ y sp act (6K38); spont fission: 1.4 × 10 ¹⁸ y (24S52)	3.98 ion ch (2C45); 3.98 range emuls (7F51a); 4.20 ion ch (1S37)	-0.055 (coinc with 24% of a) a-conv coinc emuls (15D52); -0.075 (coinc with -20% of a) a-conv coinc emuls (5A52)	Q _α 4.05 (13S53)	natural source, parent Ra ²²¹ (MsTh ₁)

Isotope Z A	Class and identification	Percent abundance	Type of decay	Half-life	Energy of radiation in Mev		Disintegration energy and scheme	Method of production and genetic relationships
					Particles	Gamma-transitions		
⁹⁰ Th ²³³	A chem, n-capt (1M38)		β^- (13S47a)	23.3 m (2B50); 23.5 m (13S47a); 23.6 m (31R52); 23 m (2G41)	1.23 spect (2B50, 31R52); 1.24 spect (3F53); 1.2 abs (13S52)	0.098 (0.25%), 0.172 (0.03%), 0.350 (0.004%), 0.448 (0.1%), 0.662 (0.05%) scint spect (3F53); no γ (2B50, 31R52)	Q_α 3.79 est, Q_β 1.23 (13S53)	Th-n- γ (1M38, 13S47a, 13S41, 2G41); Th-d-p (9G49); parent Pa ²³³ (1M38)
⁹¹ Th ²³⁴ (UX ₁)	A chem, genet (1C31)		β^-	24.10 d (3K48); 24.1 d (3S39); 24.5 d (1C31)	0.205 (-80%), 0.111 (-20%) spect (16B46); 0.192 (56%), 0.104 (44%) spect (19H50); 0.190 spect (7J46); 0.20, 0.1 abs (4F38a)	0.090 (e/ γ -0.2) spect conv (19H50); 0.093 (-20%, e/ γ -0.34), 0.180 (4.5%) spect conv, abs (16B46); 0.092 (1M23)	Q_β 0.20 (13S53)	natural source, daughter U ²³⁸ parent Pa ²³⁴ (UX ₂)
⁹¹ Th ²³⁵	[B] n-capt, genet (20H50)		[β^-] (20H50)	<<10 m genet (20H50)				[Th ²³⁴ -n- γ , parent Pa ²³⁵] (20H50)
⁹¹ Pa ²²⁵	E excit, decay charac (57K51)		α (57K51)	2.0 s (57K51)				spall Th, ancestor Ac ²²¹ Fr ²¹⁷ , At ²¹³ (57K51)
⁹² Pa ²²⁶	B chem, genet (11M49, 11M51)		α (11M51)	1.8 m (11M51)	6.81 ion ch (11M51)		Q_α 6.93, Q_{EC} 2.8 calc (13S53)	spall Th, parent Ac ²²² (11M49, 11M51, 11M52)
⁹² Pa ²²⁷	A chem, genet (13G48)		α -85%, EC -15% (11M51)	38.3 m (11M51)	6.46 ion ch (11M51)		Q_α 6.58, Q_{EC} 1.08 calc (13S53)	spall Th, parent Ac ²²³ , parent Th ²²⁷ (RdAc) (13G48, 11M51); daughter Np ²³¹ (13G48b); spall U (6O48)
⁹² Pa ²²⁸	A chem, genet (13G48)		EC -98%, α -2% (11M51)	22 h (11M51)	6.09 (75%), 5.85 (25%) ion ch (11M51)		Q_α 6.20, Q_{EC} 2.05 calc (13S53)	spall Th, daughter U ²²⁸ , parent Ac ²²⁴ , parent Th ²²⁸ (RdTh) (13G48, 11M49, 11M51)
⁹² Pa ²²⁹	A chem, genet (8H49a)		EC 99+%, α 0.25% (21S51); EC -99%, α -1% (11M51)	1.5 d (8H48)	5.69 ion ch (11M48); 5.66 ion ch (8H48)		Q_α 5.79, Q_{EC} 0.37 calc (13S53)	Th ²³⁰ -d-3n, parent Ac ²²⁵ (8H49a); daughter U ²²⁹ (11M51)
⁹² Pa ²³⁰	A chem, genet, excit (4S48)		EC -92%, β^- -8% (4S49); α -0.003% (11M50)	17.7 d (5O49); 17.0 d (4S48)	β^- : -0.43 abs (5O49)	0.94 abs (5O49)	Q_α 5.45 est, Q_β 0.57 est, Q_{EC} 1.28 est (13S53)	Th-d-4n, Th- α -p5n, parent U ²³⁰ (4S48); Th ²³⁰ -d-2n (8H49a); Pa-d-p2n, Pa- α -on (5O49); U ²³³ -d-on (8H49); parent Th ²³⁰ (1o), parent Ac ²²⁶ (11M50)

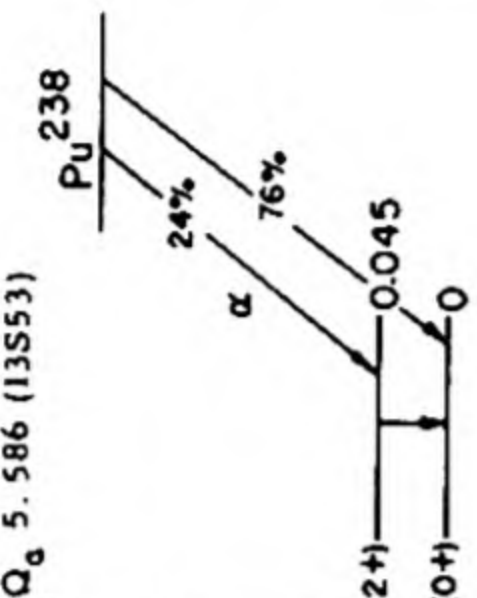
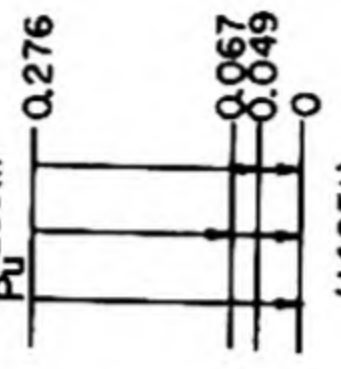
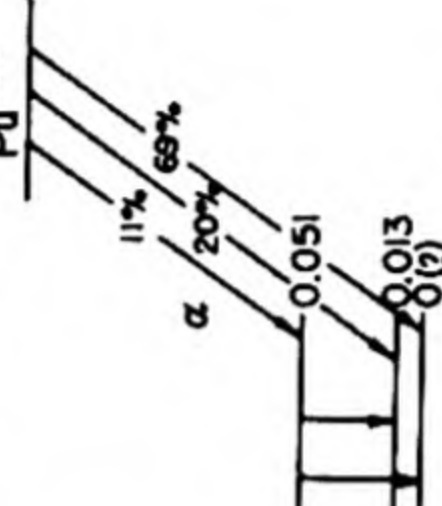
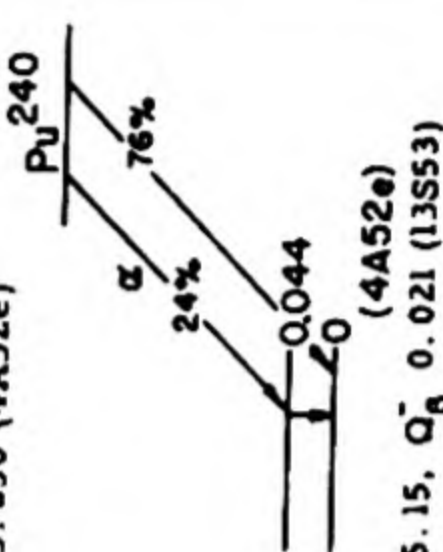
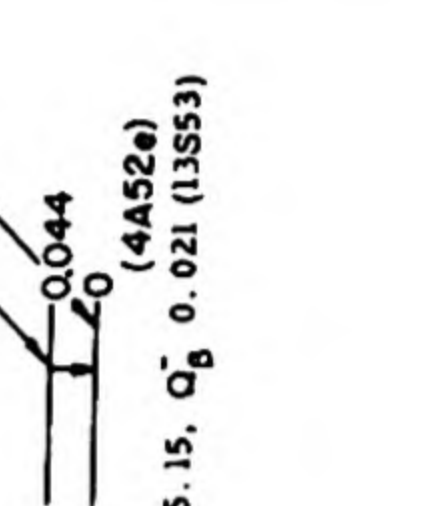
^{231}Pa	A chem, genet (IC31)	α : β stable (cons energy) (HPS)	3.43×10^4 y sp act (8W49) 3.2×10^4 y sp act (2G30)	5.042 (11%), 5.002 (47%), 4.938 (25%), 4.838 (3%), 4.720 (11%), 4.660 (1-3%) spect (4R49c, 13C51); -5.0 (85%), -4.7 (15%) ion ch (2C44, 9T46a, 13G48a)	0.034, 0.038, 0.057, 0.064, 0.082, 0.102, 0.198, 0.259, 0.301, 0.331, 0.357, 0.383 spect conv (10F52a); 0.095, 0.294, 0.323 spect conv (1M28a); 0.027 (9%), 0.087, 0.100, 0.30 (4%) abs, crit abs (3R52a); 0.044, 0.066 cl ch (4T52); 0.027 crit abs, ion ch (17S51); others (4S46, 4T49)	^{231}Pa , $I = 3/2$ (87M50) Q_α 5.131 (13S53)	natural source, daughter ^{231}Th (UY), parent ^{227}Ac (227); ^{231}Th -d-3n (4S48); daughter ^{231}U (14C50)
^{232}Pa	A chem, genet (9G49)	β^- (9G49); no EC (lim 2%) (88B52a)	1.32 d (1J50); 1.4 d (5O49); 1.6 d (9G49)	0.99 (-30%), 0.64 (-10%), 0.28 (-60%) spect (3P52); -0.28 abs (1J48b)	-0.23 (-30%), 1.05 (-100%) abs (1J48b); 0.21, 1.0 abs (5O49)	Q_α 4.70 est, Q_β 1.48, QEC 0.61 est (13S53)	^{232}Th -d-2n (9G49, 4S48, 1J50); ^{232}Th -a-p3n (4S48); ^{232}Pa -d-p (5O49); ^{232}Pa -n-y (1J50); parent ^{232}U (9G49, 5O49)
^{233}Pa	A chem, genet (1M38, 2G41, 13S41)	β^- (1M38, 2G41, 13S41)	27.4 d (2G41)	0.530, 0.430 spect (3F51); 0.5 abs (13S52); -0.2 spect, abs (21H41, 2L47, 11K50); -0.7 spect (11F44)	0.029, 0.041, 0.058, 0.076, 0.087, 0.105, 0.273, 0.302, 0.313, 0.342, 0.377, 0.400, 0.416 spect conv (11K50); 0.028, 0.040, 0.058, 0.076, 0.087, 0.105, 0.302, 0.343, 0.417 spect conv (7K51b); 0.0287, 0.0405, 0.0754, 0.0870 (rel abund 100/75/3/3) cryst spect (88B52a); 0.084, 0.298, 0.309, 0.337 spect conv (2L47); no γ > -0.4 abs (11K50)	Q_α 4.46 est, Q_β 0.53 (13S53)	daughter ^{233}Th (1M38, 2G41, 13S41, 16H41a, 13S47a); parent ^{233}U (13S47a); daughter ^{233}Np (4H47); ^{233}Th -d-n (4S48, 9G49); ^{233}Th -a-p2n (4S48); daughter ^{233}Np (15M47)
^{234}Pa (UX ₂)	A chem, genet (IC31)	β^- 99+%, IT 0.15% (4F38a, 16B45)	1.175 m (11ZB51); 1.14 m (1C31)	2.32 (80%), 1.50 (13%), 0.60 (7) (-7%) spect (19H50); 2.32 (98%) spect (16B45)	0.817 (e_K/γ 0.04) spect conv (19H50); 0.394 (with IT, 0.15%, e/γ -1), -0.9 (-2%), -1.5 (-0.2%) spect, spect conv (16B45); 0.822, 0.806, 0.782 (weak, e/γ large) spect conv (16B43a)	Q_β^- 2.32 (16B45)	natural source, daughter ^{234}Th (UX ₁), parent ^{234}U (U II)
^{234}Pa (UZ)	A chem, genet (IC31)	β^-	6.7 h (1C31)	-1.2 (10%), 0.45 (90%) spect (16B45); 1.6, 0.6 abs (4F38a)	0.85 (two γ 's) abs, β - γ coinc (16B45); -0.7 (two γ 's) abs, γ - γ coinc (4F38a, 4F38b)	Q_β^- 2.2 (?) est (13S53) Q_β^- 1.95 (4F49)	natural source, parent ^{234}U (U II); ^{234}Pa -233-n- γ (50K52)
^{235}Pa	B chem, excit, sep isotopes (11M50); genet (20H50)	β^- (11M50, 20H50)	23.7 m (11M50); 23 m (20H50)	1.4 abs (11M50)	no γ , abs (11M50)	Q_β^- 2.2 (?) est (13S53) Q_β^- 1.95 (4F49)	^{235}U -238-p-a, ^{238}U -d-an (11M50); daughter ^{235}Th (20H50)
^{227}U	B chem, genet (11M52)	α (11M52)	1.3 m (11M52)	6.8 ion ch (11M52)		Q_α 7.14 est (13S53)	^{227}Th -a-9n, parent ^{223}Th (11M52)
^{228}U	A chem, genet (11M49, 11M51)	α -80%, EC -20% (11M51)	9.3 m (11M51)	6.67 ion ch (7O50)		Q_α 6.79, QEC 0.30 calc (13S53)	^{228}Th -a-8n, parent ^{224}Th , parent ^{228}Pa (11M49, 11M51); daughter ^{228}Pu (8J48)
^{229}U	A chem, genet (11M49, 11M51)	EC -80%, α -20% (11M51)	58 m (11M51)	6.42 ion ch (11M51)		Q_α 6.53, QEC 1.29 calc (13S53)	^{229}Th -a-7n, parent ^{225}Th , parent ^{229}Pa (11M49, 11M51)

Isotope Z A	Class and identification	Percent abundance	Type of decay	Half-life	Energy of radiation in Mev		Disintegration energy and scheme	Method of production and genetic relationships
					Particles	Gamma-transitions		
^{230}U	A chem, genet (4S48)		α (4S48); β stable (cons energy) (HPS)	20.8 d (4S48)	5.85 ion ch (1J48); α_0 (77%), α_{70} (23%) spect (21S52)		Q_α 5.95 (13S53)	daughter Pa^{230} , parent Th^{226} $\text{Th}-\alpha-6n$ (4S48); daughter Pa^{230} , $\text{Pa}-d-3n$, $\text{Pa}-\alpha-p4n$ (5O49); daughter Pu^{234} (13P49); spall U (6O47)
^{231}U	A chem, sep isotopes, excit (5O49); genet (14C50)		EC 99+%, α 5.5×10^{-3} % (14C50)	4.3 d (14C50); 4.2 d (5O49)	5.45 ion ch (14C50)	0.051, 0.064, 0.076 spect conv (8O50)	Q_α 5.55, Q_{EC} 0.34 calc (13S53)	$\text{Pa}^{231}-d-2n$, $\text{Pa}^{231}-\alpha-p3n$ (5O49); $\text{Th}-\alpha-5n$ (14C50, 8O50); parent Th^{227} , parent Pa^{231} (14C50)
^{232}U	A chem, genet (9G49)		α (9G49); β stable (cons energy) (HPS)	70 y yield (8J49); -30 y yield (9G49)	5.31 range Al (1J48a); 5.27 range air (12K44); α_0 (69%), α_{58} (31%) spect (21S52)	-0.060 (coinc with 30% of α) α -conv coinc emuls (15D52)	Q_α 5.40 (13S53)	daughter Pa^{232} , parent Th^{228} (RdTh) (9G49); daughter Pu^{236} (8J49); daughter Pa^{232} , $\text{Pa}^{231}-d-n$, $\text{Pa}^{231}-\alpha-p2n$ (5O49); $\text{Th}-\alpha-4n$ (7N49)
^{233}U	A chem, genet (13S47a, 13S52)		α (13S52); β stable (cons energy) (HPS)	1.62×10^5 y sp act + mass spect (8H52a); 1.63×10^5 y sp act + mass spect (15L45); 1.2×10^5 y yield (13S52)	4.823 ion ch (5C48); α_0 (83%), α_{44} (15%), α_{94} (2%) spect (4A52a); 4.80 abs air (15C47); others (11E47)	0.0428 (0.05%), 0.0561 (0.01%) ion ch (12W52); -0.043, -0.056, 0.099 α -conv coinc emuls (11B52); 0.04, 0.08 (0.8%, $e/\gamma-8$), 0.31 (0.1%, $e/\gamma-3$) abs (4S52); 0.04, 0.09, 0.36 (all coinc with α) α - γ , α -conv coinc abs (5P51)	Q_α 4.91 (13S53)	daughter Pa^{233} (13S47a); parent Th^{229} (11E47, 4H47)
^{234}U (U_{II})	A chem, genet, mass spect (1C31)	0.0058 (1B50)	α ; β stable (cons energy) (HPS)	2.48×10^5 y sp act (12F52); 2.52×10^5 y sp act, sp act + mass spect (13K52, 13K49); 2.67×10^5 y yield (10G49); 2.35×10^5 y sp act + mass spect (15C46); spont fission: 2×10^{16} y (13G52)	4.763 ion ch (2C44); α_0 (74%), α_{47} (26%) spect (4A52a); 4.76 ion ch (13S39, 13C51); 4.78 range air (18S37), ion ch (3A47)	0.050, 0.117 scint spect (17S51a); γ_1 0.053, γ_2 0.093, γ_3 0.118 ($\gamma_1/\gamma_2/\gamma_3 = 1/-0.2/0.4$) scint spect (11B52a); 0.055 (coinc with α , e/γ large) α -conv coinc emuls (4T52); 0.065 (coinc with α , e/γ large) α - γ coinc abs, α -conv coinc abs (5P51); others (10M47, 17S51)	Q_α 4.85 (13S53)	natural source, daughter Pa^{234} (UX ₂ and UZ), parent Th^{230} (1o)
^{235}U (AcU)	A chem, mass spect (1C31)	0.715 (1B50)	α ; β stable (cons energy) (HPS)	7.13×10^8 y sp act (12F52); 7.07×10^8 y radiogenic Pb ratios (6N39); spont fission: 1.9×10^{17} y (24S52)	4.58 (10%), 4.47 (?) (-3%), 4.40 (83%), 4.20 (4%) ion ch (13G51); 4.39 ion ch (15V52)	γ_1 0.094, γ_2 0.143, γ_3 0.184, γ_4 0.289, γ_5 0.386 ($\gamma_1/\gamma_2/\gamma_3/\gamma_4/\gamma_5 = 0.9/0.2/1.0/0.1/0.05$) scint spect (11B52a); 0.187 abs (20S52); 0.167 abs (10M49)	Q_α 4.66 (13S53) U^{235} , $I = 5/2$ (102S50)	natural source, parent Th^{232} (UY)

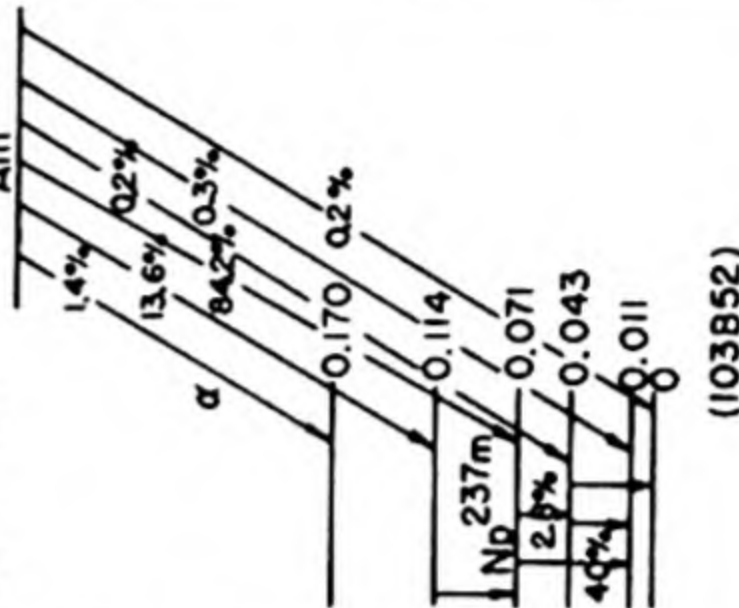
^{236}U	A chem, n-capt, mass spect (9W45, 13G51a)	α (13G51a); β stable (cons energy) (HPS)	2.39×10^7 y sp act (12F52); 2.46×10^7 y sp act (1J51a)	4.499 ion ch (1J51a); 4.5 ion ch (13G51a)	-0.050 (coinc with 27% of α) α -conv coinc emuls (15D52)	Q_α 4.58 (13S53)  (HPS)	^{235}U -n- γ (9W45, 13G51a, 1J51a)
^{237}U	A chem, excit (5N40 12M40)	β^- (5N40, 12M40)	6.75 d (81H52); 6.63 d (13M48); 6.8 d (1W48)	0.245, other β^- (weak) spect (3F53); -0.23 spect (13M48)	γ_1 0.027, γ_2 0.043, γ_3 0.059, γ_4 0.165, γ_5 0.207 (eK/ γ 1.6, K/L 5.0), γ_6 0.269, γ_7 0.334, γ_8 0.370, γ_9 0.430 ($\gamma_3/\gamma_5/\gamma_7 = 37/21/2.5$) scint spect, spect conv (3F53); 0.0598 cryst spect (88B52a); 0.032, 0.057, 0.204, 0.260 abs, spect conv (13M48); 0.14, 0.23, 0.53 abs (17B43)	Q_β^- 0.514 (3F53)	U-n-2n (12M40, 5N40, 1W48, 2A44); parent Np ²³⁷ (1W48); daughter Pu ²⁴¹ (2K45, 13S49); U-d-t (17B43, 2A44, 8J49); U- α -n (8J49)
^{238}U (U_1)	A chem, genet, mass spect (1C31)	α ; β stable (cons energy) (HPS)	4.49×10^9 y sp act (13K49); 4.51×10^9 y sp act (6N39); spont fission: 8.0×10^{15} y (24S52, 17S46)	4.18 ion ch (3A47, 2C44); 4.21 range (1S39)	-0.045 (coinc with 22% of α) α -conv coinc emuls (15D52); 0.048 (coinc with 23% of α) α -conv coinc emuls (12S52); -0.050 (coinc with 24% of α) α -conv coinc emuls (5A52a)	Q_α 4.25 (13S53)  (HPS)	natural source (18B96), parent Th ²³⁴ (UX ₁)
^{239}U	A n-capt (1M37)	β^- (12M39)	23.54 m (14M43); 23.5 m (4F47, 13M47)	1.21 spect (3F53); 1.20 abs (4F47, 4F47a); 1.2 abs (1W42, 14M42); 1.12 spect (5S47)	0.0736 spect conv, scint spect (3F53); 0.073 spect conv, abs (5S47); 0.076, >0.3 (<10%) abs (4F47, 4F47a)	Q_β^- 1.28 (3F53) Q_α 4.12 est (13S53)	U-n- γ (1M37, 2I39, 12M39, 22S42); parent Np ²³⁹ (12M40a, 22S42); U-d-p (13S49a)
^{240}U	A chem, n-capt (4S49a)	β^- (4S49a)	-- 18 h genet (4S49a)				U-n- γ (second order reaction) (4S49a); parent Np ²⁴⁰ (8H48b)
^{231}Np	A chem, genet, excit, sep isotopes (15M50)	α (15M50)	-50 m (15M50)	6.28 ion ch (15M50)		Q_α 6.39, Q_{EC} 1.92 calc (13S53)	^{238}U -d-9n, ^{233}U -d-4n, ^{235}U -d-6n, parent Pa ²²⁷ (15M50)
^{232}Np	D chem (15M50)	EC (15M50)	-13 m (15M50)		hard γ (15M50)	Q_α 6.04 est, Q_{EC} 2.7 est (13S53)	^{233}U -d-3n (15M50)
^{233}Np	A chem, excit, sep isotopes (15M50, 7O51)	EC 99+%, α -10 ⁻³ % (15M50)	35 m (15M50)	5.53 ion ch (15M50); conv: -0.3 (15M50)		Q_α 5.63, Q_{EC} 1.09 calc (13S53)	^{233}U -d-2n, ^{235}U -d-4n (15M50); ^{233}U -p-n (7O51)

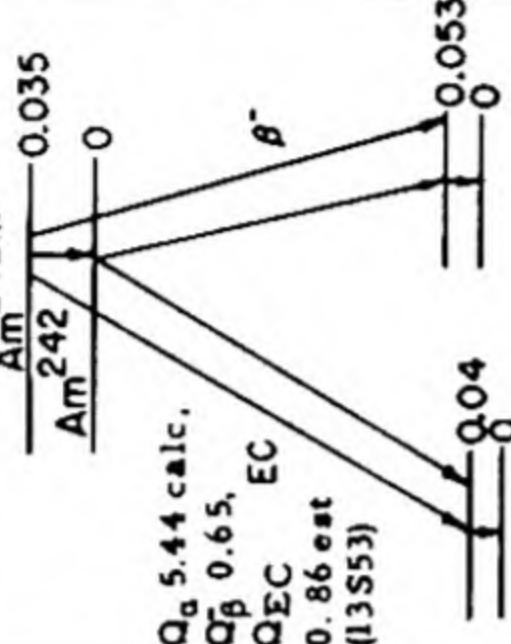

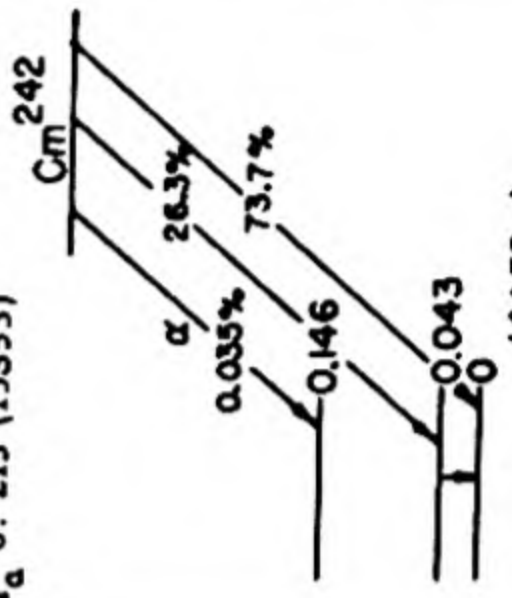
Isotope Z A	Class and identification	Percent abundance	Type of decay	Half-life	Energy of radiation in Mev		Disintegration energy and scheme	Method of production and genetic relationships
					Particles	Gamma-transitions		
${}_{93}^{234}\text{Np}$	A chem, excit, genet, sep isotopes (8J49)		EC (L/K -1) (7051a); no α (lim 0.01%) (8H49); no β^+ (8H49)	4.40 d (8H49); 4.4 d (5049)		0.177, 0.442, 0.803, 1.42 spect conv (7051a); 1.9 abs (8H49, 5049)	Q_α 5.39 est, Q_{EC} 1.8 est (13S53)	U^{235} -d-3n, U^{235} - α -p4n (8J49); U^{235} -p-2n (11G46); U^{233} -d-n (8H49); U^{233} - α -p2n (8H49, 13P49); Pa^{231} - α -n (5049); daughter Pa^{234} (13P49)
${}^{235}\text{Np}$	A chem, excit, sep isotopes (8J49)		EC (L/K >9) (8J52); α -5 x 10 ⁻³ % (8J52)	410 d (8J52)	5.06 ion ch (8J52)		Q_α 5.15, Q_{EC} 0.17 calc (13S53)	U^{235} -d-2n (8J49, 8J52); U^{233} - α -pn (8H49)
${}^{236}\text{Np}$	A chem, genet, sep isotopes, excit (8J49)		β^- -33%, EC -67% (L/K -2) (7051b)	22 h (8J49)	0.51 (-60%), 0.36 (-40%) spect (7051b)	0.150 (e/ γ large) spect conv (7051b)	Q_α 5.00 est, Q_β 0.63 est, Q_{EC} 1.03 est (13S53)	U^{235} -d-n, U^{235} - α -p2n, U -d-4n (8J49); Np^{237} -d-p2n (8J49a); U^{233} - α -p (8H49); Np^{237} -n-2n (13G45, 13F50); parent Pu^{236} (8J49, 8J49a, 8H49, 13G52)
${}^{237m}\text{Np}$	A genet (103B52)		IT (103B52)	6.3×10^{-8} s delay coinc (103B52)			see Am^{241} (7051b)	daughter Am^{241} (103B52)
${}^{237}\text{Np}$	A chem, genet, excit (1W48)		α (1W48); β stable (cons energy) (HPS)	2.20×10^6 y sp act (15M48)	4.77 ion ch (13G48c)	soft γ 's (coinc with 80% of α) α -conv coinc emuls (15D52); soft γ , spect conv (15M45)	Np^{237} , $I = 5/2$ (87M50) Q_α 4.97 est (13S53)	daughter U^{237} (1W48); parent Pa^{233} (15M47)
${}^{238}\text{Np}$	A chem, genet, n-capt, sep isotopes (13S46)		β^- (13S46, 13S49a)	2.10 d (3F50a); 2.0 d (13S49a)	1.272 (47%), 0.258 (53%) spect, spect coinc (3F50a); 1.39, 0.22 abs (1J49)	0.043, 0.047, 0.103 (L/M 1.6), 0.983, 1.03 (1.03 γ /0.98 γ = 1) spect, spect conv, β - γ , β -x coinc (3F50a); no 0.047 γ (63M52a, 4A52a); 1.1 abs (13S49a); 0.075, 1.2 abs, abs conv (1J49)	Q_α 4.83 est, Q_β 1.42, Q_{EC} 0.38 est (13S53) see Cm^{242}	U -d-2n (13S46, 13S49a, 14K49); U^{238} -d-2n (14K49); parent Pu^{238} (13S46, 14K49, 1J49, 8J49); daughter Am^{242} (13S49, 6S50a); U^{238} - α -p3n, U^{235} - α -p (8J49); Np^{237} -n- γ (1J49); Np^{237} -d-p (8J49a)

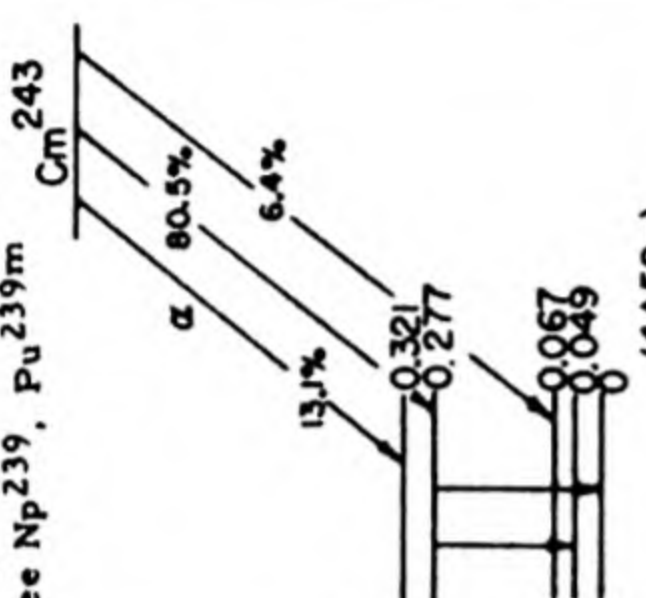
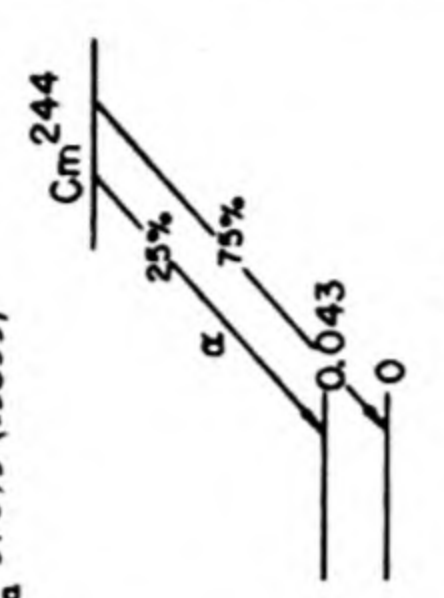
Np ²³⁹	A chem, n-capt, genet, excit (12M39, 12M40a)	β^- (12M40a)	2.33 d (1W42); 2.35 d (4F42); 2.3 d (3P46)	0.715, 0.654, 0.44, 0.33 spect (7T51); 0.718 (4.8%), 0.655 (1.7%), 0.441 (31%), 0.380 (10%), 0.329 (52%) spect (3F53); 0.705 (7%, not coinc with γ), 0.435 (46%), 0.310 (47%) spect (14G51); 1.179, 0.676, 0.403, 0.288 spect (5S47); others (22H45, 11F49)	0.049, 0.057, 0.061, 0.067 (coinc with 0.210 γ), 0.210, 0.227, 0.276 (last 3 γ 's coinc with 0.435 β^- , 0.276 γ not coinc with 0.227 γ) spect conv, β - γ , γ - γ coinc (14G51); 0.013, 0.019, 0.044, 0.049, 0.057, 0.061, 0.067, 0.077, 0.105, 0.209, 0.228, 0.254, 0.277, 0.285, 0.316, 0.334 spect conv (3F53); 0.044, 0.049, 0.057, 0.061, 0.068, 0.106, 0.209, 0.228, 0.277 spect conv (11F49); 0.0576, 0.0618 cryst spect (26J52); 0.057, 0.061, 0.067, 0.206, 0.227, 0.275 spect conv (5S47); others (4F42, 22H45, 3P46)	Q β^- 0.715 (3F53, 14G51)		daughter U ²³⁹ (12M40a, 22S42); parent Pu ²³⁹ (14K46, 13S49a); U-d-n (13S46, 13S49a, 8J49); U-a-p2n (8J49); daughter Am ²⁴³ (6S50a)
Np ²⁴⁰	A chem, genet (8H48b)	β^- (8H48b)	7.3 m (8H48b)	-1.3 abs (8H48a)				daughter U ²⁴⁰ (8H48b)
Np ²⁴¹	B chem, cross bomb (7O51a)	β^- (7O51a)	60 m (7O51a)	0.89 spect (7O51a)				U ²³⁸ -a-p (7O51a)
94Pu ²³²	B chem, sep isotopes, excit, genet (7O51a)	α >2%, EC <98% (7O51a)	36 m (7O51a)	6.58 ion ch (7O51a)				U ²³⁵ -a-7n, U ²³³ -a-5n, parent U ²²⁸ (7O51a)
Pu ²³⁴	A chem, genet, sep isotopes, excit (8H49, 13P49)	α -4%, EC -96% (7O51a, 23H52a)	9.0 h (7O51a); 8.5 h (13P49)	6.19 ion ch (7O51a); 6.2 ion ch (13P49)				U ²³³ -a-3n (8H49, 13P49, 7O51a); U ²³⁵ -a-5n (7O51a); parent U ²³⁰ , parent Np ²³⁴ (13P49, 7O51a); daughter Cm ²³⁸ (23H52a)
Pu ²³⁵	B chem, excit, sep isotopes (7O51a)	EC 99+%, α -0.002% (7O51a)	26 m (7O51a)	5.85 ion ch (7O51a)				U ²³³ -a-2n, U ²³⁵ -a-4n (7O51a)
Pu ²³⁶	A chem, excit, sep isotopes, cross bomb, genet (8J49)	α (8J49); β stable (cons energy) (HPS)	2.7 y (8J49); spont fission: 3.5 x 10 ⁹ y (13G52)	5.75 range air (8J49); 5.75 ion ch (13G53)				U ²³⁵ -a-3n, U ²³⁸ -a-6n (8J49); Np ²³⁷ -d-3n (8J49a); U ²³³ -a-n (8H49, 13P49); daughter Cm ²⁴⁰ (13S49b); daughter Np ²³⁶ (8J49, 8J49a, 8H49, 13G52)
Pu ²³⁷	B chem, sep isotopes, cross bomb (8J49)	EC (8J49)	-40 d (8J49)					U ²³⁵ -a-2n, U-a-5n (8J49); Np ²³⁷ -d-2n (8J49a)

Isotope Z A	Class and identification	Percent abundance	Type of decay	Half-life	Energy of radiation in Mev		Disintegration energy and scheme	Method of production and genetic relationships
					Particles	Gamma-transitions		
⁹⁴ Pu 238	A chem, sep isotopes, excit (13S46, 13S46a, 13S49a)		α (13S46); β stable (cons energy) (HPS)	89.6 y (13S46a); 92 y genet (13S49b); 77 y genet (13J49); spont fission: 3.8 x 10 ¹⁰ y (24S52)	5.492 (76%), 5.450 (24%) spect (4A52a); 5.47 range air (8T49); 5.51 range air (15C47)	0.045 spect conv (8O51); -0.040 (coinc with 23% of α) α -conv coinc emuls (15D52); -0.04 (e/y -700) α -y coinc, scint spect (4A52d)	Q α 5.586 (13S53)  (2+) 0.045 (0+) 0 (HPS)	U ²³⁸ -d-2n (13S46, 13S49a, 14K49, 7E42, 8J49); U ²³⁸ - α -4n, U ²³⁵ - α -n (8J49); daughter Np ²³⁸ (8J49, 1J49, 13S46a, 14K49); daughter Cm ²⁴² (13S49b)
^{239m} Pu 239	A genet (14G51)		IT (14G51)	1.1 x 10 ⁻⁹ s delay coinc (14G51)		0.049, 0.067, 0.210, 0.227, 0.276 spect conv, coinc (14G51)	see Np ²³⁹ , Cm ²⁴³  Pu ^{239m} 0.276 0.067 0.049 0 (14G51)	daughter Np ²³⁹ , parent Pu ²³⁹ (14G51)
²³⁹ Pu 239	A chem, genet, mass spect (14K46)		α (14K46); β stable (cons energy) (HPS)	24,360 y sp act (10W51); 24,400 y sp act (11W46, 14F45); 24,300 y sp act (16C49); 24,100 y calorimetric (96S47); spont fission: 5.5 x 10 ¹⁵ y (24S52)	5.150 (69%), 5.137 (20%), 5.099 (11%) spect (4A52e); 5.147 (-70%), 5.097 (-30%) spect (4R50); 5.14 ion ch (10J48); 5.15 range air (15C47); 5.13 ion ch (17C51); 5.13 range air (8T49); conv: -0.10 (weak) α -conv coinc emuls (15D52, 5A51)	γ_1 0.039, γ_2 0.0531, γ_3 0.100, γ_4 0.124, γ_5 0.384 ($\gamma_1/\gamma_2/\gamma_3/\gamma_4$; $\gamma_5 = 0.4/1.4/1.1/0.5/0.3$) spect conv, scint spect (3F52b); 0.0385 (2 x 10 ⁻³ %), 0.0520 (7 x 10 ⁻³ %) ion ch (12W51, 12W52); -0.035, 0.05 α -conv coinc emuls (15D52); 0.05 α -conv coinc emuls (5A51); others (11S2)	Q α 5.238 (13S53)  Pu ²³⁹ 3/2- 0.051 0.013 0 (14G51)	daughter Np ²³⁹ (14K46, 13S49a); U ²³⁸ - α -3n (8J49); Pu ²³⁸ -n-y (9R48, 19B48)
²⁴⁰ Pu 240	A chem, n-capt, mass spect (15C44, 14F46, 21B44)		α (8J49); β stable (cons energy) (HPS)	6580 y genet (31S1); 6240 y sp act (11W51); 6760 y sp act (10W51)	5.162 (76%), 5.118 (24%) spect (4A52e)	0.0496 spect conv, scint spect (3F52b)	Q α 5.250 (4A52e)  Pu ²⁴⁰ 0+ 0.044 0 (4A52e, HPS)	Pu ²³⁹ -n-y (15C44, 14F46, 21B44); U ²³⁸ - α -2n (8J49)
²⁴¹ Pu 241	A chem, n-capt, mass spect, excit, genet (13S49, 13S49b, 13G50)		β^- 99+%, α -10 ⁻³ % (13S49, 3T50e)	14 y genet (3T50e)	α : 4.91 ion ch (3T50e); β^- : 0.021 spect (3F52b); -0.02 abe (13S49)	γ_1 0.100, γ_2 0.145 ($\gamma_1/\gamma_2 = 5$) scint spect (3F52b)	Q α 5.15, Q β 0.021 (13S53)  Pu ²⁴¹ 0+ 0.044 0 (4A52e)	Pu ²⁴⁰ -n-y (13G50, 3T50e); U ²³⁸ - α -n (13S49); parent Am ²⁴¹ (13S49, 16C49a); parent U ²³⁷ (2K45, 13S49)

Pu^{242}	A chem, mass spect, n-capt, genet (3T50e)	α (3T50e); β stable (cons energy) (HPS)	-5×10^5 y genet (3T50e)	4.88 ion ch (3T50e)		Q_α 4.96 (13S53)	Pu^{241} -n- γ (3T50e, 3I49); daughter Am 242m (8O50a)
Pu^{243}	B chem, n-capt, cross bomb (25S51)	β^- (25S51)	4.98 h (81H52a); 5.0 h (25S51, 3T51)	0.39 spect (3T51); -0.45 abs (25S51)		Q_α 4.82 est, Q_β 0.67 est (13S53)	Pu^{242} -n- γ (25S51, 3T51); parent Am 243 (3T51)
$^{95}\text{Am}^{237}$	B chem, excit (23H52a)	EC 99+%, α 0.005% (23H52a)	-1.3 h (23H52a)	6.01 ion ch (23H52a)		Q_α 6.20 est, Q_{EC} 1.6 est (13S53)	Pu^{239} -d-4n, Pu^{239} -p-3n (23H52a)
Am^{238}	B chem, excit (6S50a)	EC (6S50a); no α (lim $3 \times 10^{-4}\%$; (23H52a)	2.1 h (23H52a)	conv (6S50a)		Q_α 5.99 est, Q_{EC} 2.22 est (13S53)	Pu^{239} -d-3n (6S50a, 23H52a)
Am^{239}	B chem, excit (13S49)	EC 99+%, α 0.003% (23H52a)	12 h (13S49)	5.75 ion ch (23H52a)		Q_α 5.85, Q_{EC} 0.78 calc (13S53)	Np^{237} - α -2n (13S49); Pu^{239} -p-n (6S50a); Pu^{239} -d-2n (13S49, 23H52a); Pu^{239} - α -p3n (23H52a)
Am^{240}	B chem, excit (13S49); chem, excit, cross bomb (6S50a)	EC (13S49); no α (lim 0.2% (23H52a)	50 h (13S49); 53 h (23H52a)			Q_α 5.76 est, Q_β 0.02 est, Q_{EC} 1.54 est (13S53)	Np^{237} - α -n (13S49); Pu^{239} -d-n (13S49, 6S50a, 23H52a); Pu^{239} - α -p2n (23H52a)
Am^{241}	A chem, n-capt, excit, mass spect (13S49)	α (13S49); β stable (cons energy) (HPS)	470 y sp act (20H52a); 475 y sp act (16C50)	5.546 (0.23%), 5.535 (0.34%), 5.503 (0.21%), 5.476 (84.2%), 5.433 (13.6%), 5.379 (1.4%) spect (4A52); 5.48 ion ch (13C48c); 5.47 range air (8T49)		Am 241, $I = 5/2$ (38F52) Q_α 5.639 (13S53)	daughter Pu^{241} (13S49, 16C49a); parent Np^{237m} (103B52)



Isotope Z A	Class and identification	Percent abundance	Type of decay	Half-life	Energy of radiation in Mev		Disintegration energy and scheme	Method of production and genetic relationships
					Particles	Gamma-transitions		
^{242m} ₉₅ Am	A chem, n-capt, genet (16M49, 13S49b)		β^- 60%, EC (L) 20%, IT 20% (8051)	16.01 h (44K52); 15.7 h (20H49a); 16 h (16M49)	0.628 spect (8050a); 0.63 abs (15G50)	0.035, 0.038, 0.053 spect conv (8051)	Q_β 0.68 (HPS) 	²⁴¹ ₉₅ Am -n-γ (16M49, 13S49); parent Cm ²⁴² (16M49, 13S49b); parent Pu ²⁴² (8050a)
²⁴² ₉₅ Am	A chem, genet, mass spect, n-capt (13S49, 6S50a)		β^- , EC, α (8051); (α/β ⁻ 0.01) (6S50a)	-100 y genet (6S50a)	β^- : 0.593 spect (8051); -0.5 abs (13S49)	0.038, 0.053 spect conv (8051)	Q_α 5.44 calc, Q_β 0.65, Q_{EC} EC 0.86 est (13S53) 	²⁴¹ ₉₅ Am -n-γ, parent Cm ²⁴² , parent Np ²³⁸ (13S49, 6S50a, 13S49b)
²⁴³ ₉₅ Am	A chem, mass spect (6S50a)		α (6S50a)	-10 ⁴ y genet (6S50a)	5.267 (-90%), 5.226 (-10%) spect (4A52a); 5.27 ion ch (13G51b)	0.075 (coinc with 90% of α) α-γ coinc, scint spect (4A52a); 0.076 scint spect (89M52a)	Q_α 5.430, Q_β 0.00 calc (13S53) (8051)	²⁴² ₉₅ Am -n-γ, parent Np ²³⁹ (6S50a); daughter Pu ²⁴³ (3T51)
²⁴⁴ ₉₅ Am	B chem, n-capt (6S50a)		β^- (6S50a)	-25 m (6S50a)				²⁴³ ₉₅ Am -n-γ (6S50a)
²³⁸ ₉₆ Cm	B chem (6S48a); chem, genet (23H52a)		EC <90%, α >10% (75C52)	2.5 h (6S48a)	6.50 ion ch (6S48a)		Q_α 6.61, Q_{EC} 0.8 est (13S53)	Pu ²³⁹ -α-5n (6S48a); parent Pu ²³⁴ (23H52a)
²³⁹ ₉₆ Cm	D chem, excit (75C52)		EC -100%, no α (lim 0.1%) (75C52)	-3 h (75C52)			Q_α 6.50 est, Q_{EC} 1.8 est (13S53)	Pu ²³⁹ -α-4n (75C52)
²⁴⁰ ₉₆ Cm	A chem, genet (13S49b)		α (13S49b); no EC (lim 0.5%) (23H52)	26.8 d (13S49b); spont fission; 7.9 × 10 ⁵ y (13G52)	6.25 ion ch (23H52); 6.3 range air (13S49b)		Q_α 6.37 (13S53)	Th-C-4n (23H52a); Pu ²³⁹ -α-3n (13S49b, 23H52)
²⁴¹ ₉₆ Cm	B chem, excit (13S49b, 23H52)		EC 99+%, α 0.2% (23H52a)	35 d (23H52)	5.90 ion ch (23H52a)		Q_α 6.3 est, Q_{EC} 0.9 est (13S53)	Pu ²³⁹ -α-2n, Am ²⁴¹ -p-n (23H52, 23H52a)
²⁴² ₉₆ Cm	A chem, genet (13S49b); mass spect (10R50)		α (13S49b); β stable (cons energy) (HPS)	162.5 d (24H50); 162 d (8J48a); spont fission; 7.2 × 10 ⁶ y (24H51)	6.110 (73.7%), 6.066 (26.3%), 5.965 (0.035%) spect (4A52, 4A52d); 6.118 ion ch (20H52); 6.08 ion ch (13G48c)	0.043 spect conv (8051); -0.04 (e/γ -600) α-γ coinc, scint spect (4A52d); -0.045 (coinc with 23% of α) α-conv coinc emuls (15D52); -0.04 (coinc with α) α-conv coinc (5P51)	see Np ²³⁸ Q_α 6.213 (13S53) 	Pu ²³⁹ -α-n (13S49b); daughter Am ²⁴² (13S49b, 13G50); Am ²⁴¹ -d-n (3T50a); daughter Cf ²⁴⁶ (25H51)

Cm^{243}	A chem, mass spect, genet (10R50)	α (10R50)	-100 y genet (3T50b)	5.985 (6.4%), 5.777 (80.5%), 5.732 (13.1%) spect (4A52d); 5.89 (15%), 5.79 (85%) ion ch (3T50b)	0.226, 0.277 (both γ 's coinc with 5.777 a) scint spect (4A52d)	Q_α 6.15 (4A52a) Q_{EC} 0.00 calc (13S53) see Np239, Pu239m 	Cm^{242} -n- γ (10R50); daughter Bk243 (3T50b)
Cm^{244}	A chem, mass spect (10R50)	α (10R50); β stable (cons energy) (HPS)	19 y (3T52); spont fission: 1.4×10^7 y (13G52)	5.798 (75%), 5.755 (25%) spect (4A52d)		Q_α 5.895 (13S53) 	daughter Am244, Cm243 -n- γ (10R50)
Cm^{245}	B chem, decay charac, genet (25H51)	α (25H51)	>500 y (25H51)	-5.6 ion ch (25H51)			daughter Bk245 (25H51)
97Bk^{243}	A chem, n-capt, genet (3T50, 3T50b)	EC 99+%, α -0.1% (3T50b)	4.6 h (3T50b)	6.72 (30%), 6.55 (53%), 6.20 (17%) ion ch (3T50b)		Q_α 6.83, Q_{EC} 1.46 calc (13S53)	Am241 - α -2n (3T50, 3T50b); Cm242-d-n (25H51); parent Cm243 (3T50b)
Bk^{244}	D chem, decay charac (3T52)	EC (3T52)	-5 h (3T52)			Q_α 6.63 est, Q_{EC} 2.27 est (13S53)	Am241 - α -n (3T52)
Bk^{245}	B chem, excit, decay charac (25H51)	EC 99+%, α -0.1% (25H51)	4.95 d (25H51)	6.33 (18%), 6.15 (48%), 5.90 (34%) ion ch (25H51)		Q_α 6.44, Q_{EC} 0.67 est (13S53)	Am243 - α -2n (3T52); Cm244 -d-n, Cm242 - α -p (25H51); parent Cm245 (25H51)
98Cf^{244}	B chem, excit, decay charac (3T50c)	α , EC (?) (3T50d)	45 m (3T50d)	7.15 ion ch (3T50d)		Q_α 7.27, Q_{EC} 0.7 est (13S53)	U-C-6n (13G51c); Cm242 - α -2n (3T50c, 3T50d)
Cf^{246}	A chem, genet (13G51c)	α (13G51c); β stable (cons energy) (HPS)	35.7 h (25H51) ~2000 y (spontaneous fission) (25H53)	6.75 ion ch (13G51c)		Q_α 6.86 (13S53)	U-C-4n (13G51c); Cm243 - α -n, Cm244 - α -2n (25H51); parent Cm242 (25H51)

RAPID METHOD FOR CALCULATING LOG (ft) VALUES

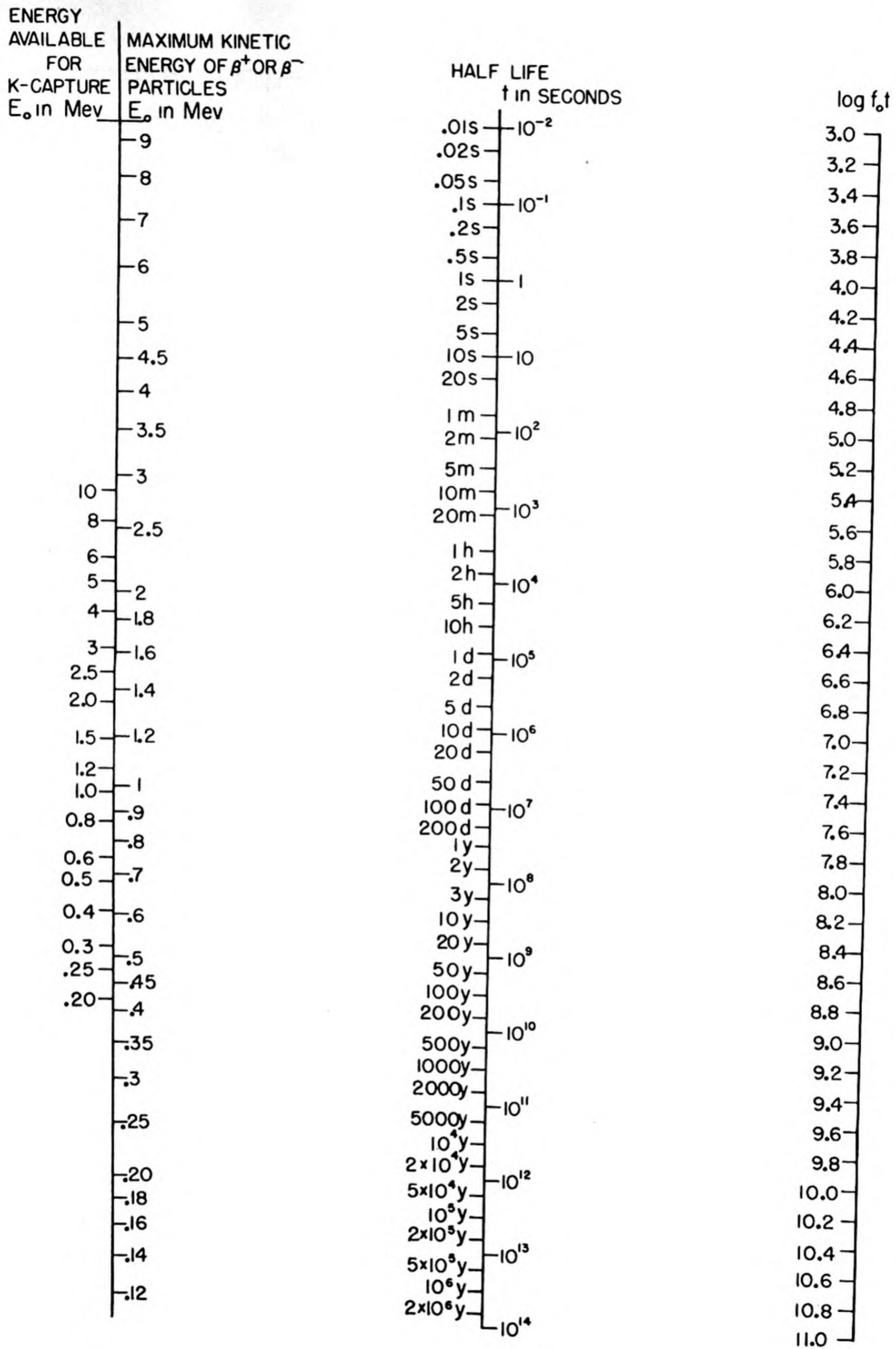
from S. A. Moszkowski, Phys. Rev. 82, 35 (1951)

The following figures permit the rapid calculation of log (ft) for a given type of decay, given energy, half-life, etc. The notation is: E_0 for β^\pm emission is the maximum kinetic energy of the particles in Mev; E_0 for K electron capture is the disintegration energy in Mev. When a β^+ emission and K electron capture go from and to the same level, E_0 for K capture = E_0 for β^+ emission + 1.02 Mev. Z is the atomic number of the initial nucleus, t is the total half-life, and p is the percentage of decay occurring in the mode under consideration. When no branching occurs, $p = 100$.

Procedure for obtaining log (ft)

- (1) First obtain $\log (f_0 t)$, using Fig. 1. E_0 is read off the left-hand side of the E_0 column for K electron capture, and off the right-hand side for β^\pm emission. Put a straight edge over the given values of E_0 and t and note where it crosses the column of $\log (f_0 t)$ values.
- (2) Then read off $\log (C)$ from Figs. 2, 3, and 4 for β^- , β^+ , and K electron capture, respectively.
- (3) Get $\Delta \log (ft)$ from Fig. 5 if $p < 100$. When $p = 100$, $\Delta \log (ft) = 0$.
- (4) $\log (ft) = \log (f_0 t) + \log (C) + \Delta \log (ft)$.

These graphs have been reproduced with the kind permission of Dr. Moszkowski. For details concerning their construction, significance, and range of usefulness, reference should be made to the original paper.

Fig. 1. $\log (f_0 t)$ as a function of E_0 and t .

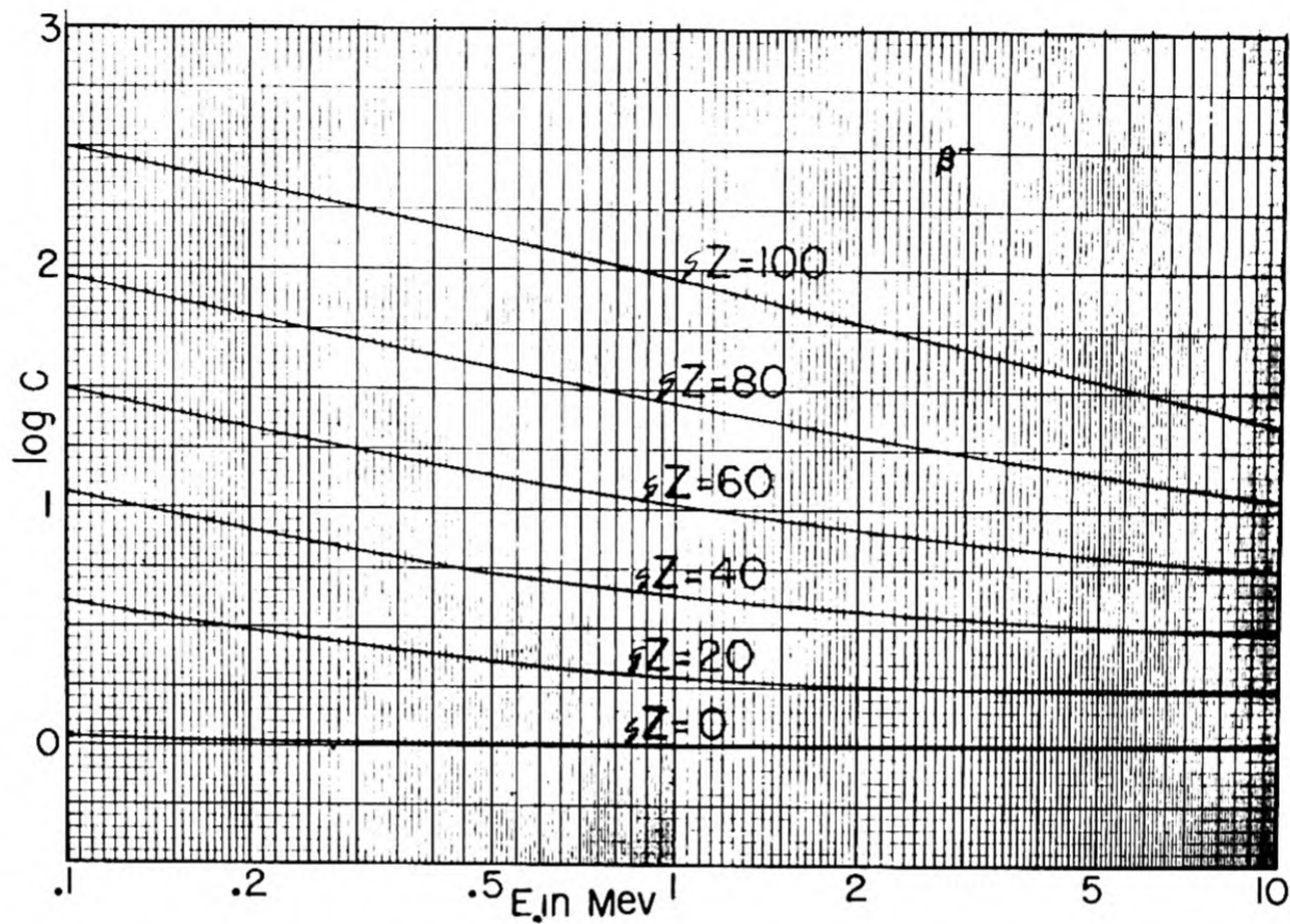


Fig. 2. $\log(C)$ as a function of E_0 and Z for β^- emission.

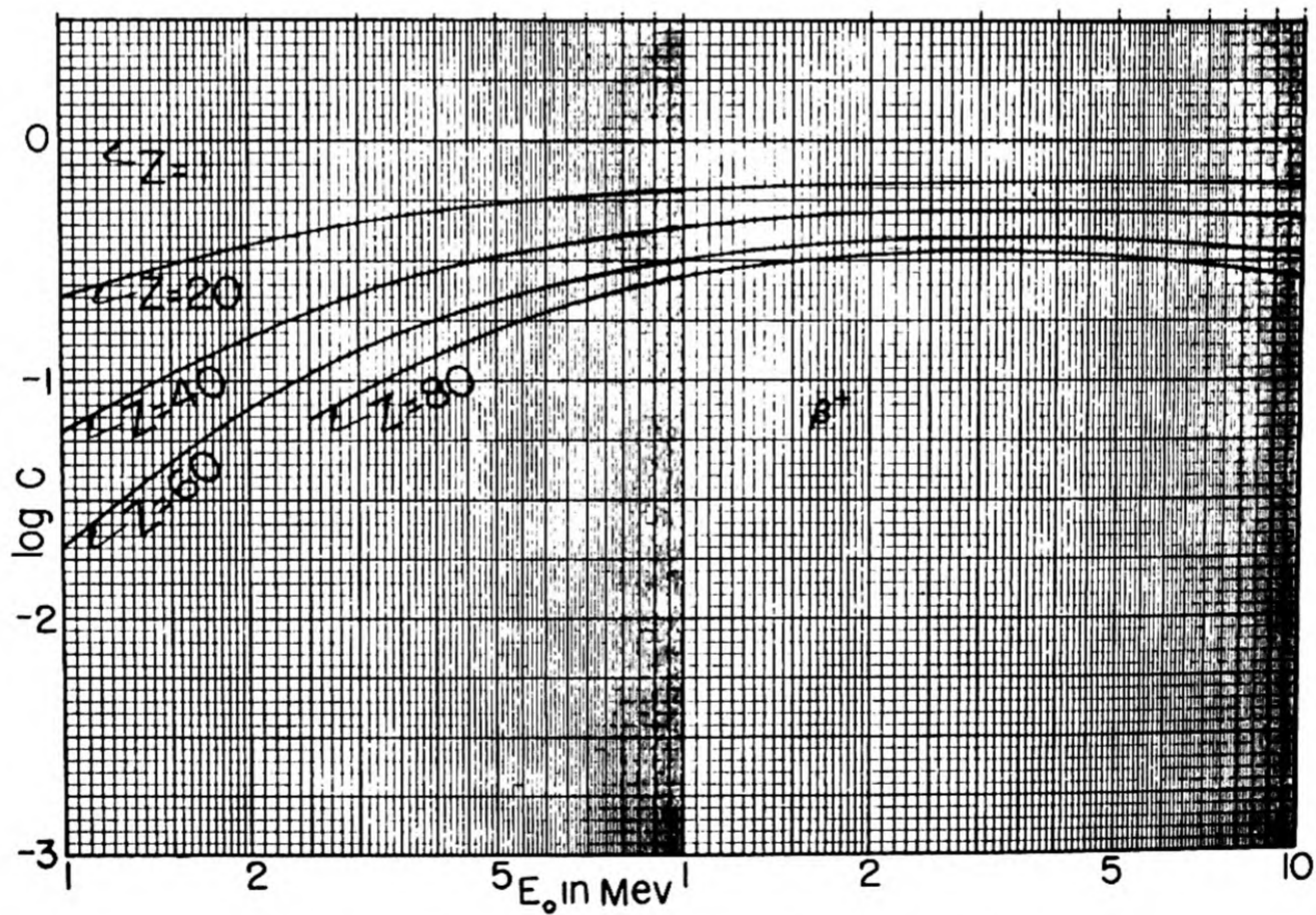


Fig. 3. $\log(C)$ as a function of E_0 and Z for β^+ emission.

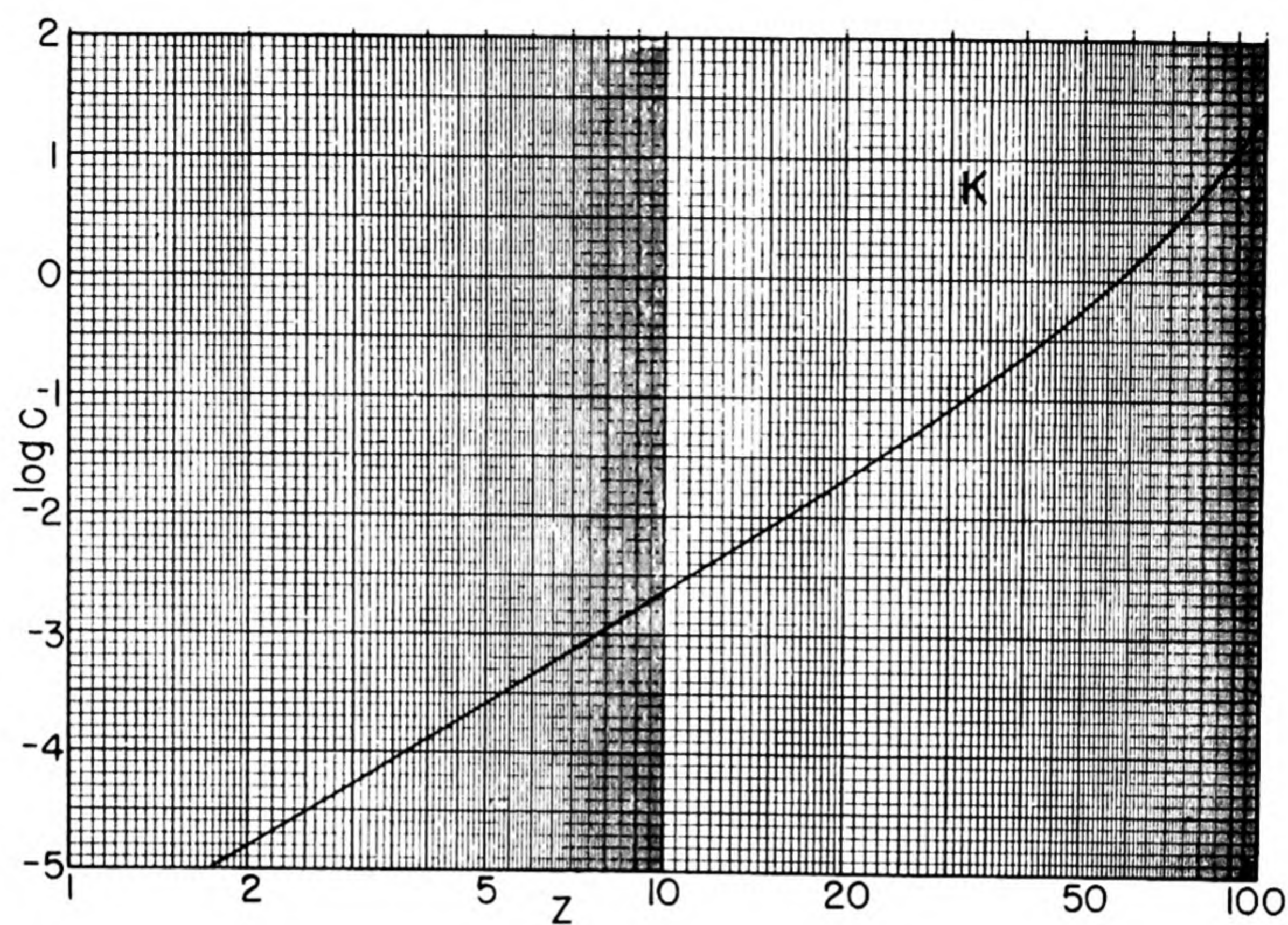


Fig. 4. $\log(C)$ as a function of Z for K electron capture.

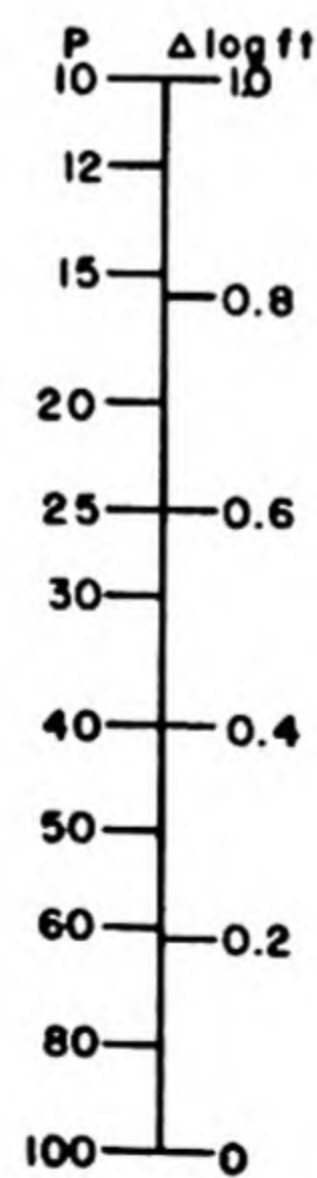


Fig. 5. $\Delta \log(ft)$ as a function of p .

- 1A20 F. W. Aston, *Phil. Mag.* **40**, 628 (1920)
- 1A35 F. W. Aston, *Proc. Roy. Soc. (London)* **149A**, 396 (1935)
- 2A44 M. B. Allen, University of California Radiation Laboratory Classified Report RL-4.6.270 (July 1944)
- 3A47 F. Alder, P. Huber, and F. Metzger, *Helv. Phys. Acta* **20**, 234 (1947)
- 3A51 F. Alder and F. C. Yu, *Phys. Rev.* **81**, 1067 (1951)
- 3A51a F. Alder and F. C. Yu, *Phys. Rev.* **82**, 105 (1951)
- 4A52 F. Asaro, F. L. Reynolds, and I. Perlman, *Phys. Rev.* **87**, 277 (1952)
- 4A52a F. Asaro and I. Perlman, private communication (Nov. 1952)
- 4A52b F. Asaro and W. J. Heiman, private communication (Aug. 1952)
- 4A52c F. Asaro and I. Perlman, *Phys. Rev.* **88**, 129 (1952)
- 4A52d F. Asaro, S. G. Thompson, and I. Perlman, private communication (Nov. 1952)
- 4A52e F. Asaro and I. Perlman, *Phys. Rev.* **88**, 828 (1952)
- 5A51 G. Albouy and J. Teillac, *Compt. rend.* **232**, 326 (1951)
- 5A52 G. Albouy, *J. phys. et radium* **13**, 309 (1952)
- 5A52a G. Albouy and J. Teillac, *Compt. rend.* **234**, 829 (1952)
- 6A38 L. W. Alvarez, *Phys. Rev.* **54**, 486 (1938)
- 6A39 L. W. Alvarez and R. Cornog, *Phys. Rev.* **56**, 613 (1939)
- 6A40 L. W. Alvarez, A. C. Helmholtz, and E. Nelson, *Phys. Rev.* **57**, 660 (1940)
- 6A40a L. W. Alvarez and R. Cornog, *Phys. Rev.* **57**, 248 (1940)(A)
- 6A49 L. W. Alvarez, *Phys. Rev.* **75**, 1815 (1949)
- 6A49a L. W. Alvarez, *Phys. Rev.* **75**, 1127 (1949)
- 6A50 L. W. Alvarez, *Phys. Rev.* **80**, 519 (1950)
- 7A46 L. T. Aldrich and A. O. Nier, *Phys. Rev.* **70**, 983 (1946)
- 8A50 P. Avignon, *J. phys. et radium* **11**, 521 (1950)
- 9A50 R. Ashapa and G. Grimm, reported in Columbia University Document CUD-53 (June 1950)
- 10A49 J. Angus, A. L. Cockroft, and S. C. Curran, *Phil. Mag.* **40**, 522 (1949)
- 11A50 R. E. Adamson, Jr., W. W. Buechner, W. M. Preston, C. Goodman, and D. M. Van Patter, *Phys. Rev.* **80**, 985 (1950)
- 12A35 E. Amaldi, O. D'Agostino, E. Fermi, B. Pontecorvo, R. Rasetti, and E. Segre, *Proc. Roy. Soc. (London)* **149A**, 522 (1935)
- 12A36 E. Amaldi and E. Fermi, *Ricerca sci.* **7**, Part I, 56 (1936)
- 13A49 D. E. Alburger, *Phys. Rev.* **76**, 435 (1949)
- 13A50 D. E. Alburger, C. Egger, and D. J. Hughes, *Phys. Rev.* **77**, 726 (1950)
- 13A50a D. E. Alburger, *Phys. Rev.* **78**, 629 (1950)
- 13A50b D. E. Alburger, E. der Mateosian, G. Friedlander, M. Goldhaber, J. W. Mihelich, G. Scharff-Goldhaber, and A. W. Sunyar, reported in Brookhaven National Laboratory Unclassified Report BNL-82 (Nov. 1950)
- 13A50c D. E. Alburger, E. der Mateosian, and M. Goldhaber, reported in Brookhaven National Laboratory Unclassified Report BNL-64 (July 1950)
- 13A51 D. E. Alburger and G. Friedlander, *Phys. Rev.* **82**, 977 (1951)
- 13A51a D. E. Alburger and G. Friedlander, *Phys. Rev.* **81**, 523 (1951)
- 13A52 D. E. Alburger, *Phys. Rev.* **88**, 339 (1952)
- 13A52a D. E. Alburger and J. Kraushaar, *Phys. Rev.* **87**, 448 (1952)
- 13A52b D. E. Alburger, *Phys. Rev.* (to be published) (1952)
- 14A48 H. R. Allan and C. A. Wilkinson, *Proc. Roy. Soc. (London)* **194A**, 131 (1948)
- 15A40 W. D. Allen and C. Hurst, *Proc. Phys. Soc. (London)* **52**, 501 (1940)
- 16A50 H. M. Agnew, *Phys. Rev.* **77**, 655 (1950)
- 17A36 E. B. Andersen, *Z. physik. Chem.* **32B**, 237 (1936)
- 17A36a E. B. Andersen, *Nature* **137**, 457 (1936)
- 18A48 R. D. Albert and C. S. Wu, *Phys. Rev.* **74**, 847 (1948)
- 19A41 H. Akabori, et al., *Proc. Phys.-Math. Soc. Japan* **23**, 599 (1941)
- 20A48 L. H. Ahrens and R. D. Evans, *Phys. Rev.* **74**, 279 (1948)
- 21A41 J. S. V. Allen, M. L. Pool, J. D. Kurbatov, and L. L. Quill, *Phys. Rev.* **60**, 425 (1941)
- 22A40 T. Amaki, T. Iimori, and A. Sugimoto, *Phys. Rev.* **57**, 751 (1940)
- 23A47 J. R. Arnold and N. Sugarman, *J. Chem. Phys.* **15**, 703 (1947)
- 24A36 A. I. Alichanian, A. I. Alichanov, and B. S. Dzheleпов, *Physik. Z. Sowjetunion* **10**, 78 (1936)
- 25A39 A. H. W. Aten, Jr., C. J. Bakker, and F. A. Heyn, *Nature* **143**, 679 (1939)
- 25A52 A. H. W. Aten, Jr. and M. Boelhouwer, *Physica* **18**, 651 (1952)
- 26A51 R. M. Adams and H. Finston, *NNES-PPR* **9**, 1791 (1951)
- 27A39 H. L. Anderson, E. Fermi, and H. B. Hanstein, *Phys. Rev.* **55**, 797 (1939)
- 28A43 M. Ageno, *Nuovo cimento* **1**, 33 (1943)
- 28A43a M. Ageno, *Nuovo cimento* **1**, 415 (1943)
- 29A52 P. Axel and R. B. Duffield, private communication (Oct. 1952)
- 30A38 K. Alexeeva, *Compt. rend. U.R.S.S.* **18**, 553 (1938)
- 31A50 N. M. Anton'eva, A. A. Bashilov, B. S. Dzheleпов, and A. V. Zolotavin, *Doklady Akad. Nauk, S.S.S.R.* **70**, 397 (1950)
- 31A50a N. M. Anton'eva, A. A. Bashilov, B. S. Dzheleпов, and A. V. Zolotavin, *Doklady Akad. Nauk, S.S.S.R.* **70**, 597 (1950); *Izv. Akad. Nauk, S.S.S.R.* **14**, 299 (1950)
- 31A51 N. M. Anton'eva, A. A. Bashilov, and B. S. Dzheleпов, *Doklady Akad. Nauk, S.S.S.R.* **77**, 41 (1951)
- 32A39 P. Abelson, *Phys. Rev.* **56**, 1 (1939)
- 33A50 D. L. Anderson and M. L. Pool, *Phys. Rev.* **77**, 142 (1950)
- 34A45 H. Atterling, E. Bohr, and T. Sigurgeirsson, *Arkiv Mat., Astron. Fysik* **32A**, No. 2 (1945)
- 35A50 K. Artemov and B. Dzheleпов, *Uspekhi Fiz. Nauk* **41**, 189 (1950)
- 36A51 H. Aeppli, A. S. Bishop, H. Frauenfelder, M. Walter, and W. Zündt, *Phys. Rev.* **82**, 550 (1951); *Helv. Phys. Acta* **24**, 355 (1951)
- 36A51a H. Aeppli, H. Albers-Schönberg, A. S. Bishop, H. Frauenfelder, and E. Heer, *Phys. Rev.* **84**, 370 (1951)
- 36A52 H. Aeppli, H. Frauenfelder, E. Heer, and R. Rüetschi, *Phys. Rev.* **87**, 379 (1952)
- 36A52a H. Aeppli, H. Albers-Schönberg, H. Frauenfelder, and P. Scherrer, *Helv. Phys. Acta* **25**, 339 (1952)
- 37A52 C. J. Avery, K. C. Kaericher, and M. L. Pool, *Phys. Rev.* **87**, 216 (1952)(A)
- 38A52 C. E. Anderson, G. W. Wheeler, and W. W. Watson, *Phys. Rev.* **87**, 668 (1952)
- 39A52 G. B. Arfken, E. D. Klema, and F. K. McGowan, *Phys. Rev.* **86**, 413 (1952)
- 40A52 D. P. Ames, M. E. Bunker, and L. M. Langer, *Phys. Rev.* (in press) (1952)

- 40A52a D. P. Ames, M. E. Bunker, and J. W. Starner, reported in Los Alamos Scientific Laboratory Classified Report WASH-75 (Jan. 1952)
- 40A52b D. P. Ames, M. E. Bunker, and B. M. Sorensen, reported in Los Alamos Scientific Laboratory Classified Report WASH-66 (March 1952)
- 1B50 K. T. Bainbridge and A. O. Nier, National Research Council Nuclear Energy Series, Preliminary Report No. 9 (Dec. 1950)
- 1B52 K. T. Bainbridge, M. Goldhaber, and E. Wilson, private communication (Oct. 1952)
- 2B50 M. E. Bunker, L. M. Langer, and R. J. D. Moffat, Phys. Rev. 80, 468 (1950)
- 2B50a M. E. Bunker and R. Canada, Phys. Rev. 80, 961 (1950)
- 2B50b M. E. Bunker, R. Canada, and A. C. G. Mitchell, Phys. Rev. 79, 610 (1950)
- 2B51 M. E. Bunker, L. M. Langer, and R. J. D. Moffat, Phys. Rev. 81, 30 (1951)
- 2B52 M. E. Bunker and J. W. Starner, reported in Los Alamos Scientific Laboratory Classified Report WASH-76 (May 1952)
- 3B44 M. Bachelet and P. Savel, Cahiers phys. No. 19, 51 (1944)
- 4B48 D. E. Bunyan, A. Lundby, A. H. Ward, and D. Walker, Proc. Phys. Soc. (London) 61, 300 (1948)
- 4B49 D. E. Bunyan, A. Lundby, and D. Walker, Proc. Phys. Soc. (London) 62A, 253 (1949)
- 5B49 W. H. Beamer and W. E. Easton, J. Chem. Phys. 17, 1298 (1949)
- 6B39 E. Bretscher and L. G. Cook, Nature 143, 559 (1939)
- 6B40 E. Bretscher and L. G. Cook, Nature 146, 430 (1940)
- 7B47 E. Broda and N. Feather, Proc. Roy. Soc. (London) 190A, 20 (1947)
- 8B48 R. E. Bell and L. G. Elliott, Can. J. Research 26A, 379 (1948)
- 8B49 R. E. Bell and H. E. Petch, Phys. Rev. 76, 1409 (1949)
- 8B50 R. E. Bell and R. L. Graham, Phys. Rev. 78, 490 (1950)
- 8B52 R. E. Bell and R. L. Graham, Phys. Rev. 86, 212 (1952)
- 8B52a R. E. Bell, R. L. Graham, and H. E. Petch, Can. J. Phys. 30, 35 (1952)
- 8B52b R. E. Bell, R. L. Graham, and L. Yaffe, Can. J. Phys. (in press) (1952)
- 9B50 G. R. Bishop, R. Wilson, and H. Halban, Phys. Rev. 77, 416 (1950)
- 10B46 G. C. Baldwin and G. S. Klaiber, Phys. Rev. 70, 259 (1946)
- 10B49 G. C. Baldwin, Phys. Rev. 76, 182 (1949)(A)
- 11B49 P. R. Bell, B. H. Ketelle, and J. M. Cassidy, Phys. Rev. 76, 574 (1949)
- 11B49a P. R. Bell and J. M. Cassidy, reported in Oak Ridge National Laboratory Unclassified Report ORNL-481 (Dec. 1949)
- 11B50 P. R. Bell, Science 112, 7 (1950)
- 11B50a P. R. Bell and J. M. Cassidy, Phys. Rev. 77, 301 (1950)
- 11B50b P. R. Bell and J. M. Cassidy, Phys. Rev. 79, 173 (1950)
- 11B50c P. R. Bell, B. Weaver, and J. M. Cassidy, Phys. Rev. 77, 399 (1950)
- 11B50d P. R. Bell, J. M. Cassidy, W. H. Jordan, and R. C. Davis, Oak Ridge National Laboratory Classified Report ORNL-782 (Oct. 1950)
- 11B50e P. R. Bell, J. M. Cassidy, and R. C. Davis, reported in Oak Ridge National Laboratory Unclassified Report ORNL-694 (June 1950)
- 11B50f P. R. Bell, J. M. Cassidy, W. H. Jordan, and R. C. Davis, reported in Oak Ridge National Laboratory Unclassified Report ORNL-782 (Oct. 1950)
- 11B51 P. R. Bell, J. M. Cassidy, and G. G. Kelley, Phys. Rev. 82, 103 (1951)
- 11B52 P. R. Bell, R. C. Davis, J. E. Francis, and J. Cassidy, reported in Oak Ridge National Laboratory Unclassified Report ORNL-1092 (Jan. 1952)
- 11B52a P. R. Bell, R. C. Davis, J. E. Francis, and J. M. Cassidy, reported in Oak Ridge National Laboratory Unclassified Report ORNL-1164 (April 1952)
- 12B51 G. W. Barton, Jr., A. Ghiorso, and I. Perlman, Phys. Rev. 82, 13 (1951)
- 13B24 D. H. Black, Proc. Roy. Soc. (London) 106A, 632 (1924)
- 14B49 D. K. Butt, unpublished data quoted in (4F49)
- 14B51 D. K. Butt and W. D. Brodie, Proc. Phys. Soc. (London) 64A, 791 (1951)
- 15B36 G. H. Briggs, Proc. Roy. Soc. (London) 157A, 183 (1936)
- 16B43 H. Bradt and P. Scherrer, Helv. Phys. Acta 16, 259 (1943)
- 16B43a H. Bradt, H. -G. Heine, and P. Scherrer, Helv. Phys. Acta 16, 455 (1943)
- 16B45 H. Bradt and P. Scherrer, Helv. Phys. Acta 18, 405 (1945); and private communication to R. W. Stoughton (Feb. 1947)
- 16B45a H. Bradt, P. C. Gugelot, O. Huber, H. Medicus, P. Preiswerk, and P. Scherrer, Helv. Phys. Acta 18, 259 (1945)
- 16B45b H. Bradt, P. C. Gugelot, O. Huber, H. Medicus, P. Preiswerk, and P. Scherrer, Helv. Phys. Acta 18, 252 (1945)
- 16B45c H. Bradt, P. C. Gugelot, O. Huber, H. Medicus, P. Preiswerk, and P. Scherrer, Helv. Phys. Acta 18, 256 (1945)
- 16B45d H. Bradt, P. C. Gugelot, O. Huber, H. Medicus, P. Preiswerk, and P. Scherrer, Phys. Rev. 68, 57 (1945)
- 16B45e H. Bradt, P. C. Gugelot, O. Huber, H. Medicus, P. Preiswerk, and P. Scherrer, Helv. Phys. Acta 18, 351 (1945)
- 16B46 H. Bradt and P. Scherrer, Helv. Phys. Acta 19, 307 (1946); Phys. Rev. 71, 141 (1947) (A)
- 16B46a H. Bradt, P. C. Gugelot, O. Huber, H. Medicus, P. Preiswerk, P. Scherrer, and R. Steffen, Helv. Phys. Acta 19, 219 (1946)
- 16B46b H. Bradt, P. C. Gugelot, O. Huber, H. Medicus, P. Preiswerk, P. Scherrer, and R. Steffen, Helv. Phys. Acta 19, 222 (1946)
- 16B46c H. Bradt, P. C. Gugelot, O. Huber, H. Medicus, P. Preiswerk, P. Scherrer, and R. Steffen, Helv. Phys. Acta 19, 218 (1946)
- 16B47 H. Bradt, P. C. Gugelot, O. Huber, H. Medicus, P. Preiswerk, P. Scherrer, and R. Steffen, Helv. Phys. Acta 20, 153 (1947)
- 16B47a H. L. Bradt and D. J. Tendam, Phys. Rev. 72, 1117 (1947)
- 17B43 E. L. Brady and W. Robinson, reported in Metallurgical Laboratory Classified Report CC-724 (June 1943)
- 17B50 E. L. Brady and M. Deutsch, Phys. Rev. 78, 558 (1950)
- 17B51 E. L. Brady and N. Sugarman, NNS-PPR 9, 613 (1950)
- 17B51a E. L. Brady, D. W. Engelkemeir, and E. P. Steinberg, NNS-PPR 9, 711 (1951)
- 18B96 H. Becquerel, Compt. rend. 122, 420, 501, 559, 609, 762, 1086 (1896)
- 19B48 R. J. Bruehlman, W. C. Bentley, and E. K. Hyde, reported in Argonne National Laboratory Classified Report ANL-4215 (Oct. 1948)

- 20B52 Berkeley Chemistry Group, unpublished results (1947-1952)
- 21B44 A. A. Bartlett, D. F. Swinehart, and R. W. Thompson, Los Alamos Scientific Laboratory Classified Reports LA-168 (Nov. 1944); LA-327 (July 1945); LA-561 (May 1946)
- 22B49 W. J. Byatt, F. T. Roger, Jr., and A. Waltner, Phys. Rev. 75, 909 (1949)
- 23B36 T. Bjerger, Nature 137, 865 (1936)
- 23B36a T. Bjerger, Nature 138, 400 (1936)
- 23B36b T. Bjerger and K. J. Broström, Nature 138, 400 (1936)
- 23B37 T. Bjerger, Nature 139, 757 (1937)
- 24B30 S. Bramson, Z. Physik 66, 721 (1930)
- 25B39 R. A. Becker and E. R. Gaerttner, Phys. Rev. 56, 854 (1939) (A)
- 25B47 R. A. Becker, A. O. Hanson, and B. C. Diven, Phys. Rev. 71, 466 (1947) (A)
- 25B49 R. A. Becker, F. S. Kirn, and W. L. Buck, Phys. Rev. 76, 1406 (1949)
- 26B37 D. S. Bayley and H. R. Crane, Phys. Rev. 52, 604 (1937)
- 27B48 T. W. Bonner, J. E. Evans, C. W. Malich, and J. R. Risser, Phys. Rev. 73, 885 (1948)
- 28B48 J. C. Bowe, M. Goldhaber, R. D. Hill, W. E. Meyerhof, and O. Sala, Phys. Rev. 73, 1219 (1948) (A)
- 28B49 J. C. Bowe and G. Scharff-Goldhaber, Phys. Rev. 76, 437 (1949)
- 28B51 J. C. Bowe and P. Axel, Phys. Rev. 84, 939 (1951)
- 28B52 J. C. Bowe and P. Axel, Phys. Rev. 85, 858 (1952)
- 29B49 J. F. Bonner, Jr., U. S. Atomic Energy Commission Unclassified Document AECU-107 (Feb. 1949)
- 30B51 J. E. Brolley, Jr., D. H. Cooper, W. S. Hall, M. S. Livingston, and L. K. Schlacks, Phys. Rev. 83, 990 (1951)
- 30B52 J. E. Brolley, Jr., J. L. Fowler, and L. K. Schlacks, Phys. Rev. 88, 618 (1952)
- 31B38 W. E. Burcham, M. Goldhaber, and R. D. Hill, Nature 141, 510 (1938)
- 32B39 H. A. Bethe and W. J. Henderson, Phys. Rev. 56, 1060 (1939)
- 33B39 W. H. Barkas, Phys. Rev. 56, 287 (1939)
- 33B40 W. H. Barkas, E. C. Creutz, L. A. Delaasso, R. A. Sutton, and M. G. White, Phys. Rev. 58, 383 (1940)
- 33B40a W. H. Barkas, E. C. Creutz, L. A. Delaasso, and R. A. Sutton, Phys. Rev. 57, 1087 (1940) (A)
- 33B52 W. H. Barkas, R. W. Deutsch, and H. Tyren, private communication (Sept. 1952)
- 34B42 L. B. Borst, Phys. Rev. 61, 106 (1942) (A)
- 35B46 E. Bleuler, P. Scherrer, M. Walter, and W. Zündt, Helv. Phys. Acta 19, 421 (1946)
- 35B46a E. Bleuler and W. Zündt, Helv. Phys. Acta 19, 375 (1946)
- 35B46b E. Bleuler and W. Zündt, Helv. Phys. Acta 19, 137 (1946)
- 35B46c E. Bleuler, W. Bollman, and W. Zündt, Helv. Phys. Acta 19, 419 (1946)
- 35B47 E. Bleuler, P. Scherrer, M. Walter, and W. Zündt, Helv. Phys. Acta 20, 96 (1947)
- 35B47a E. Bleuler and W. Zündt, Helv. Phys. Acta 20, 195 (1947)
- 35B51 E. Bleuler, J. W. Blue, and A. C. Johnson, Phys. Rev. 82, 333 (1951) (A)
- 35B52 E. Bleuler, A. K. Stebbins, and D. J. Tendam, reported in Purdue University Progress Report II (June 1952)
- 36B49 H. Brown and V. Perez-Mendez, Phys. Rev. 75, 1276 (1949)
- 36B50 H. Brown and V. Perez-Mendez, Phys. Rev. 78, 649 (1950)
- 36B50a H. Brown and V. Perez-Mendez, Phys. Rev. 78, 812 (1950)
- 37B37 W. Bothe and W. Gentner, Z. Physik 106, 236 (1937)
- 37B37a W. Bothe and W. Gentner, Naturwiss. 25, 90, 126, 191 (1937)
- 37B39 W. Bothe and W. Gentner, Z. Physik 112, 45 (1939)
- 37B41 W. Bothe and A. Flammersfeld, Naturwiss. 29, 194 (1941)
- 37B43 W. Bothe, Naturwiss. 31, 551 (1943)
- 37B46 W. Bothe, Z. Naturforsch. 1, 179 (1946)
- 37B46a W. Bothe, Z. Naturforsch. 1, 173 (1946)
- 38B40 J. C. Bower and W. E. Burcham, Proc. Roy. Soc. (London) 173A, 379 (1940)
- 39B48 H. Bradner and J. D. Gow, Phys. Rev. 74, 1559 (1948) (A)
- 40B39 K. J. Broström, J. Koch, and T. Lauritsen, Nature 144, 830 (1939)
- 40B47 K. J. Broström, T. Huus, and J. Koch, Nature 160, 498 (1947)
- 41B46 D. S. Ballantine, reported in Oak Ridge National Laboratory Classified Report Mon N-150 (Aug. 1946)
- 42B51 R. E. Batzel and G. T. Seaborg, Phys. Rev. 82, 607 (1951)
- 42B51a R. E. Batzel, D. R. Miller, and G. T. Seaborg, Phys. Rev. 84, 671 (1951)
- 43B48 J. Beneš, A. Hedgran, and N. Hole, Arkiv Mat., Astron. Fysik 35A, No. 12 (1948)
- 43B48a J. Beneš, A. Ghosh, A. Hedgran, and N. Hole, Nature 162, 261 (1948); Arkiv Mat., Astron. Fysik 35A, No. 33 (1948)
- 44B38 H. Brandt, Z. Physik 108, 726 (1938)
- 45B50 J. G. Bayly, Can. J. Research 28A, 520 (1950)
- 46B48 J. L. Berggren and R. K. Osborne, Phys. Rev. 74, 1240 (1948) (A)
- 47B49 J. P. Blaser, F. Boehm, and P. Marmier, Phys. Rev. 75, 1953 (1949)
- 47B50 J. P. Blaser, F. Boehm, and P. Marmier, Helv. Phys. Acta 23, 623 (1950)
- 47B51 J. P. Blaser, F. Boehm, P. Marmier, and H. Wäffler, Helv. Phys. Acta 24, 245 (1951)
- 47B51a J. P. Blaser, F. Boehm, P. Marmier, and P. Scherrer, Helv. Phys. Acta 24, 465 (1951)
- 47B51b J. P. Blaser, F. Boehm, P. Marmier, and D. C. Peaslee, Helv. Phys. Acta 24, 3 (1951)
- 48B46 A. R. Brosi, private communication (June 1946)
- 48B46a A. R. Brosi, reported in Oak Ridge National Laboratory Classified Reports Mon N-150 (Aug. 1946); Mon N-229 (Jan. 1947)
- 48B49 A. R. Brosi, T. W. DeWitt, and H. Zeldes, Phys. Rev. 75, 1615 (1949)
- 48B49a A. R. Brosi and P. M. Gross, Jr., reported in Oak Ridge National Laboratory Classified Report ORNL-499 (Dec. 1949)
- 48B50 A. R. Brosi, H. Zeldes, and B. H. Ketelle, Phys. Rev. 79, 902 (1950)
- 48B51 A. R. Brosi, C. J. Borkowski, E. E. Conn, and J. C. Griess, Jr., Phys. Rev. 81, 391 (1951)
- 48B51a A. R. Brosi, B. H. Ketelle, H. Zeldes, and E. Fairstein, Phys. Rev. 84, 586 (1951)
- 48B52 A. R. Brosi, B. H. Ketelle, and H. Zeldes, reported in Oak Ridge National Laboratory Classified Report ORNL-1116 (Feb. 1952)
- 48B53 A. R. Brosi, B. H. Ketelle, H. Zeldes, and F. M. Porter, Phys. Rev. (to be published) (1953)
- 49B50 J. A. Bruner and L. M. Langer, Phys. Rev. 79, 606 (1950)
- 49B50a J. Bruner, L. M. Langer, and R. D. Moffat, Phys. Rev. 77, 747 (1950) (A)

- 50B50 W. H. Burgus and J. W. Kennedy, *J. Chem. Phys.* 18, 97 (1950)
- 50B50a W. H. Burgus, J. D. Knight, and R. J. Prestwood, *Phys. Rev.* 79, 104 (1950)
- 50B51 W. H. Burgus and N. E. Ballou, *NNES-PPR* 9, 1184 (1951)
- 50B51a W. H. Burgus, L. Winsberg, J. A. Seiler, and W. Robinson, *NNES-PPR* 9, 1195 (1951)
- 50B52 W. H. Burgus, *Phys. Rev.* 88, 1129 (1952)
- 51B50 F. O. Bartell, A. C. Helmholtz, S. D. Softky, and D. B. Stewart, *Phys. Rev.* 80, 1006 (1950)
- 52B51 F. I. Boley and L. J. Laslett, *Phys. Rev.* 83, 215 (1951) (A)
- 52B51a F. I. Boley and D. J. Zaffarano, *Phys. Rev.* 84, 1059 (1951)
- 52B51b F. I. Boley and D. J. Zaffarano, Iowa State College Unclassified Report ISC-154 (July 1951)
- 53B50 G. L. Brownell and C. J. Maletskos, *Phys. Rev.* 80, 1102 (1950)
- 54B39 G. Barresi and B. N. Cacciapuoti, *Ricerca sci.* 10, 464 (1939)
- 55B47 R. Bouches, R. Daudel, P. Daudel, and R. Muxart, *J. phys. et radium* 8, 336 (1947)
- 55B49 R. Bouches and G. Kayas, *J. phys. et radium* 10, 110 (1949)
- 55B50 R. Bouches, S. R. de Groot, R. Nataf, and H. A. Tolhoek, *J. phys. et radium* 11, 105 (1950)
- 56B49 F. Boehm, O. Huber, P. Marmier, P. Preiswerk, and R. Steffen, *Helv. Phys. Acta* 22, 69 (1949)
- 56B49a F. Boehm and P. Preiswerk, *Helv. Phys. Acta* 22, 331 (1949)
- 56B50 F. Boehm, J. P. Blaser, P. Marmier, and P. Preiswerk, *Phys. Rev.* 77, 295 (1950)
- 57B47 H. S. Brown and M. G. Inghram, *Phys. Rev.* 72, 347 (1947)
- 58B38 S. W. Barnes and G. Valley, *Phys. Rev.* 53, 946 (1938) (A)
- 58B39 S. W. Barnes, *Phys. Rev.* 56, 414 (1939)
- 58B39a S. W. Barnes and P. W. Aradine, *Phys. Rev.* 55, 50 (1939)
- 59B38 J. H. Buck, *Phys. Rev.* 54, 1025 (1938)
- 60B51 F. Brown, G. C. Hanna, and L. Yaffe, *Phys. Rev.* 84, 1243 (1951)
- 60B52 F. Brown and L. Yaffe, *Can. J. Chem.* (in press) (1952)
- 60B52a F. Brown, G. C. Hanna, and L. Yaffe, private communication (Sept. 1952)
- 61B47 E. C. Barker, reported in Oak Ridge National Laboratory Classified Report Mon P-269 (March 1947)
- 62B51 J. K. Bair and F. Matenschein, *Phys. Rev.* 81, 463 (1951)
- 63B47 W. C. Barber, *Phys. Rev.* 72, 1156 (1947)
- 63B50 W. C. Barber, *Phys. Rev.* 80, 332 (1950)
- 63B52 W. C. Barber and R. H. Helm, *Phys. Rev.* 86, 275 (1952)
- 64B51 R. A. Brightsen, K. Shure, C. Fisher, and C. D. Coryell, *Phys. Rev.* 81, 298 (1951) (A)
- 65B49 F. D. S. Butement, *Phys. Rev.* 75, 1276 (1949)
- 65B50 F. D. S. Butement, *Nature* 165, 149 (1950); *Proc. Phys. Soc. (London)* 64A, 395 (1951)
- 65B50a F. D. S. Butement, *Proc. Phys. Soc. (London)* 63A, 532 (1950)
- 65B50b F. D. S. Butement, *Proc. Phys. Soc. (London)* 63A, 775 (1950)
- 65B51 F. D. S. Butement, *Nature* 167, 400 (1951)
- 65B51a F. D. S. Butement, *Proc. Phys. Soc. (London)* 64A, 428 (1951)
- 65B52 F. D. S. Butement, *Proc. Phys. Soc. (London)* 65A, 254 (1952)
- 65B52a F. D. S. Butement and R. Shillito, *Proc. Phys. Soc. (London)* (in press) (1952)
- 65B52b F. D. S. Butement and A. J. Poë, unpublished data (Oct. 1952)
- 65B52c F. D. S. Butement, private communication (Oct. 1952)
- 66B51 W. Biller, reported in University of California Radiation Laboratory Classified Report UCRL-1507 (Oct. 1951)
- 67B49 I. Bergström and S. Thulin, *Phys. Rev.* 76, 1718 (1949)
- 67B49a I. Bergström, S. Thulin, N. Svartholm, and K. Siegbahn, *Arkiv Fysik* 1, 281 (1949)
- 67B49b I. Bergström and S. Thulin, *Phys. Rev.* 76, 313 (1949)
- 67B50 I. Bergström, S. Thulin, and G. Andersson, *Phys. Rev.* 77, 851 (1950)
- 67B50a I. Bergström and S. Thulin, *Phys. Rev.* 79, 537 (1950)
- 67B50b I. Bergström, *Phys. Rev.* 80, 114 (1950)
- 67B50c I. Bergström and S. Thulin, *Phys. Rev.* 79, 538 (1950)
- 67B51 I. Bergström, *Phys. Rev.* 82, 112 (1951)
- 67B51a I. Bergström, *Phys. Rev.* 81, 638 (1951)
- 67B51b I. Bergström, *Phys. Rev.* 82, 111 (1951)
- 67B51c I. Bergström, *Nature* 167, 634 (1951)
- 67B51d I. Bergström, reported in M. Siegbahn Commemorative Volume, p 307 (Uppsala 1951); *Arkiv Fysik* 5, 191 (1952)
- 68B50 E. Berne, *Phys. Rev.* 77, 568 (1950)
- 69B44 A. Berthelot, *Ann. phys.* 19, 219 (1944)
- 70B43 H. J. Born and W. Seelmann-Eggebert, *Naturwiss.* 31, 86 (1943)
- 70B43a H. J. Born and W. Seelmann-Eggebert, *Naturwiss.* 31, 201 (1943)
- 70B43b H. J. Born and W. Seelmann-Eggebert, *Naturwiss.* 31, 420 (1943)
- 71B46 M. Burgy, L. A. Pardue, H. B. Willard, and E. O. Wollan, U. S. Atomic Energy Commission Declassified Document MDDC-16 (June 1946)
- 72B46 N. E. Ballou, reported in *J. Am. Chem. Soc.* 68, 2411 (1946)
- 72B48 N. E. Ballou, *Phys. Rev.* 73, 630 (1948)
- 72B51 N. E. Ballou, W. H. Burgus, J. B. Dial, L. E. Glendenin, H. Finston, M. F. Ravelly, B. Schloss, and N. Sugarman, *NNES-PPR* 9, 1410 (1951)
- 72B51a N. E. Ballou, T. B. Novey, D. E. Engelkemeir, E. L. Brady, and J. A. Seiler, *NNES-PPR* 9, 675 (1951)
- 72B51b N. E. Ballou, *NNES-PPR* 9, 695 (1951)
- 72B51d N. E. Ballou, W. Robinson, and L. E. Glendenin, *NNES-PPR* 9, 1115 (1951)
- 72B51e N. E. Ballou and W. H. Burgus, *NNES-PPR* 9, 1168 (1951)
- 72B51f N. E. Ballou, *NNES-PPR* 9, 1151 (1951)
- 72B51g N. E. Ballou, *NNES-PPR* 9, 1176 (1951)
- 72B51h N. E. Ballou, W. H. Burgus, and J. A. Marinsky, *NNES-PPR* 9, 1181 (1951)
- 72B51i N. E. Ballou, *NNES-PPR* 9, 1220 (1951)
- 73B50 C. Beckham and M. L. Pool, *Phys. Rev.* 80, 125 (1950) (A)
- 74B49 C. H. Braden, L. Slack, and F. B. Shull, *Phys. Rev.* 75, 1964 (1949)
- 75B49 L. J. Brown and S. Katcoff, *J. Chem. Phys.* 17, 497 (1949)

- 76B47 G. E. Boyd and Q. V. Larson, reported in Oak Ridge National Laboratory Classified Report Mon N-229 (Jan. 1947)
- 76B49 G. E. Boyd and Q. V. Larson, reported in Oak Ridge National Laboratory Classified Report ORNL-499 (Dec. 1949)
- 76B49a G. E. Boyd and Q. V. Larson, reported in Oak Ridge National Laboratory Classified Report ORNL-286 (Sept. 1949)
- 76B49b G. E. Boyd, reported in Oak Ridge National Laboratory Classified Report ORNL-229 (Feb. 1949)
- 76B50 G. E. Boyd and Q. V. Larson, reported in Oak Ridge National Laboratory Classified Report ORNL-685 (June 1950)
- 76B50a G. E. Boyd and Q. V. Larson, reported in Oak Ridge National Laboratory Classified Report ORNL-607 (March 1950)
- 76B51 G. E. Boyd and B. H. Ketelle, reported in Oak Ridge National Laboratory Classified Report ORNL-870 (March 1951)
- 76B51a G. E. Boyd and B. H. Ketelle, *Phys. Rev.* **83**, 216 (1951) (A)
- 76B51b G. E. Boyd, *Record Chem. Progress (Kresge-Hooker Sci. Lib.)* **12**, 67 (1951)
- 76B51c G. E. Boyd, reported in Oak Ridge National Laboratory Classified Report ORNL-870 (March 1951)
- 76B51d G. E. Boyd and B. H. Ketelle, reported in Oak Ridge National Laboratory Classified Report ORNL-1053 (Oct. 1951)
- 76B52 G. E. Boyd, Q. V. Larson, and G. W. Parker, *Phys. Rev.* **86**, 1051 (1952)
- 76B52a G. E. Boyd, *Phys. Rev.* **86**, 578 (1952)
- 76B52b G. E. Boyd and R. A. Charpie, *Phys. Rev.* **88**, 681 (1952)
- 76B52c G. E. Boyd, private communication (Nov. 1952)
- 77B45 E. Bohr and N. Hole, *Arkiv Mat., Astron. Fysik* **32A**, No. 15 (1945)
- 78B48 J. Beydon, *Compt. rend.* **227**, 1159 (1948)
- 79B51 W. L. Bendel, F. J. Shore, and R. A. Becker, *Phys. Rev.* **83**, 677 (1951)
- 79B52 W. L. Bendel, F. J. Shore, H. N. Brown, and R. A. Becker, *Phys. Rev.* **87**, 195 (1952) (A)
- 80B51 J. W. Barnes and A. J. Freedman, *Phys. Rev.* **84**, 365 (1951)
- 80B52 J. W. Barnes, private communication (May 1952)
- 81B46 P. T. Bittencourt and M. Goldhaber, *Phys. Rev.* **70**, 780 (1946)
- 82B46 S. B. Burson, P. T. Bittencourt, R. B. Duffield, and M. Goldhaber, *Phys. Rev.* **70**, 566 (1946)
- 82B48 S. B. Burson and C. O. Muehlhause, *Phys. Rev.* **74**, 1264 (1948) (A)
- 82B50 S. B. Burson, K. W. Blair, and D. Saxon, *Phys. Rev.* **77**, 403 (1950)
- 82B51 S. B. Burson, K. W. Blair, H. B. Keller, and S. Wexler, *Phys. Rev.* **83**, 62 (1951)
- 82B52 S. B. Burson and W. C. Rutledge, *Phys. Rev.* **86**, 633 (1952) (A)
- 83B50 C. J. Borkowski and A. R. Brosi, reported in Oak Ridge National Laboratory Classified Report ORNL-607 (March 1950)
- 84B51 H. Behrens, *Z. Naturforsch.* **6a**, 249 (1951)
- 85B50 J. R. Beyster and M. L. Wiedenbeck, *Phys. Rev.* **79**, 411 (1950)
- 85B50a J. R. Beyster and M. L. Wiedenbeck, *Phys. Rev.* **79**, 728 (1950)
- 86B49 L. A. Beach, C. L. Peacock, and R. G. Wilkinson, *Phys. Rev.* **76**, 1624 (1949)
- 86B49a L. A. Beach, C. L. Peacock, and R. G. Wilkinson, *Phys. Rev.* **76**, 1585 (1949)
- 86B49b L. A. Beach, C. L. Peacock, and R. G. Wilkinson, *Phys. Rev.* **75**, 211 (1949)
- 87B51 R. C. Bannerman, G. M. Lewis, and S. C. Curran, *Phil. Mag.* **42**, 1097 (1951)
- 87B52 R. C. Bannerman, *Proc. Phys. Soc. (London)* **65A**, 565 (1952)
- 87B52a R. C. Bannerman and S. C. Curran, *Phys. Rev.* **85**, 134 (1952)
- 88B52 C. I. Browne, J. O. Rasmussen, J. P. Surls, and D. F. Martin, *Phys. Rev.* **85**, 146 (1952)
- 88B52a C. I. Browne and I. Perlman, unpublished data (1952)
- 89B52 D. T. Baker, E. Bleuler, and R. M. Steffen, reported in Purdue University Progress Report II (June 1952)
- 90B52 D. A. Bromley and L. M. Goldman, *Phys. Rev.* **86**, 790 (1952)
- 90B52a D. A. Bromley, *Phys. Rev.* **88**, 565 (1952)
- 91B52 P. T. Barrett, *Proc. Phys. Soc. (London)* **65A**, 450 (1952)
- 92B49 E. Bestenreiner and E. Broda, *Nature* **164**, 658 (1949)
- 93B52 D. Brower, G. Hinman, G. Lang, R. Leamer, and D. Rose, *Phys. Rev.* **86**, 1054 (1952)
- 94B49 G. J. Bene, P. M. Denis, and R. C. Extermann, *Helv. Phys. Acta* **22**, 606 (1949)
- 95B51 H. N. Brown, W. L. Bendel, F. J. Shore, and R. A. Becker, *Phys. Rev.* **84**, 292 (1951)
- 96B49 J. W. Burkig and J. R. Richardson, *Phys. Rev.* **76**, 586 (1949) (A)
- 97B50 B. Bleaney and H. E. D. Scovil, *Proc. Phys. Soc. (London)* **63A**, 1369 (1950)
- 97B51 B. Bleaney and K. D. Bowers, *Proc. Phys. Soc. (London)* **64A**, 1135 (1951)
- 97B51a B. Bleaney and D. J. E. Ingram, *Proc. Roy. Soc. (London)* **205A**, 336 (1951)
- 97B51b B. Bleaney and H. E. D. Scovil, *Proc. Phys. Soc. (London)* **64A**, 204 (1951)
- 97B51c B. Bleaney, D. J. E. Ingram, and H. E. D. Scovil, *Proc. Phys. Soc. (London)* **64A**, 601 (1951)
- 97B51d B. Bleaney and D. J. E. Ingram, *Proc. Roy. Soc. (London)* **208A**, 143 (1951)
- 98B51 E. H. Bellamy, *Nature* **168**, 556 (1951)
- 99B50 P. Brix, H. Kopfermann, and W. v. Siemens, *Naturwiss.* **37**, 397 (1950)
- 99B51 P. Brix and A. Stendel, *Naturwiss.* **38**, 431 (1951)
- 100B50 D. Binder, *Phys. Rev.* **77**, 291 (1950)
- 101B51 L. E. Beghian, G. R. Bishop, and H. Halban, *Phys. Rev.* **83**, 186 (1951)
- 102B52 A. C. Birge, *Phys. Rev.* **85**, 753 (1952) (A)
- 102B52a A. C. Birge, private communication (Oct. 1952)
- 103B51 J. K. Beling, B. T. Feld, and I. Halpern, *Phys. Rev.* **84**, 155 (1951)
- 103B52 J. K. Beling, J. O. Newton, and B. Rose, *Phys. Rev.* **87**, 670 (1952); **86**, 797 (1952)
- 104B52 D. F. Bracher and A. R. Crathorn, *Nature* **169**, 364 (1952)
- 105B52 G. S. Bogle and H. E. D. Scovil, *Proc. Phys. Soc. (London)* **65A**, 360 (1952)
- 106B52 R. M. Bartholomew, F. Brown, R. C. Hawkings, W. F. Merritt, and L. Yaffe, *Can. J. Chem.* (in press) (1952)
- 106B52a R. M. Bartholomew, R. C. Hawkings, W. F. Merritt, and L. Yaffe, *Can. J. Chem.* (in press) (1952)
- 106B52b R. M. Bartholomew, F. Brown, W. D. Howell, W. Shorey, and L. Yaffe, *Can. J. Phys.* (in press) (1952)
- 107B52 J. P. Butler and B. G. Harvey, private communication (Oct. 1952)
- 108B52 S. D. Bloom, *Phys. Rev.* **88**, 312 (1952)
- 109B51 G. Bastin-Scoffier, *Compt. rend.* **233**, 945 (1951)

- 110B51 W. L. Brown, *Phys. Rev.* **83**, 271 (1951)
- 111B52 F. Begemann and F. G. Houtermans, *Z. Naturforsch.* **7a**, 143 (1952)
- 112B51 F. Barendregt and S. J. Tom, *Physica* **17**, 817 (1951)
- 113B52 K. Maack Bisgård, *Proc. Phys. Soc. (London)* **65A**, 677 (1952)
- 1C30 M. Curie and S. Cotellet, *Compt. rend.* **190**, 1289 (1930)
- 1C31 M. Curie, A. Debierne, A. S. Eve, H. Geiger, O. Hahn, S. C. Lind, St. Meyer, E. Rutherford, and E. Schweidler, *Revs. Modern Phys.* **3**, 427 (1931). Summarizes results of various investigators.
- 2C44 F. L. Clark, H. J. Spencer-Palmer, and R. N. Woodward, British Declassified Report BR-522 (Oct. 1944)
- 2C45 F. L. Clark, H. J. Spencer-Palmer, and R. N. Woodward, British Unclassified Report BR-584 (March 1945)
- 3C46 L. F. Curtiss, private communication (July 1946); value derived from average of values given in following references: Ward, Wynn-Williams, and Cave, *Proc. Roy. Soc. (London)* **125**, 713 (1929); Jedzejowski, *Ann. phys.* **9**, 128 (1928); Braddick and Cave, *Proc. Roy. Soc. (London)* **121**, 367 (1928); Gregoire, *Ann. phys.* **2**, 161 (1934); Gleditsch and Föyn, *Am. J. Sci.* **29**, 253 (1935)
- 4C34 I. Curie and F. Joliot, *Compt. rend.* **198**, 254 (1934)
- 4C34a I. Curie and F. Joliot, *J. phys. et radium* **5**, 153 (1934)
- 4C34b I. Curie, F. Joliot, and P. Preiswerk, *Compt. rend.* **198**, 2089 (1934)
- 4C39 I. Curie and P. Savitch, *Compt. rend.* **208**, 343 (1939)
- 4C44 I. Curie and G. Bouissières, *Cahiers phys.* No. 26, 1 (1944)
- 4C48 I. Curie, *Compt. rend.* **227**, 1225 (1948); *J. phys. et radium* **10**, 381 (1949)
- 5C48 T. E. Cranshaw and J. A. Harvey, *Can. J. Research* **26A**, 243 (1948)
- 6C50 L. Cranberg, *Phys. Rev.* **77**, 155 (1950)
- 7C37 W. Y. Chang, M. Goldhaber, and R. Sagane, *Nature* **139**, 962 (1937)
- 7C46 W. Y. Chang, *Phys. Rev.* **69**, 60 (1946)
- 7C48 W. Y. Chang and T. Coor, *Phys. Rev.* **74**, 1196 (1948)
- 7C48a W. Y. Chang, *Phys. Rev.* **74**, 1195 (1948)
- 8C41 A. A. Constantinov and G. D. Latyshev, *J. Phys. (U.S.S.R.)* **5**, 239 (1941)
- 9C38 S. P. Choong and J. Surugue, *J. phys. et radium* **9**, 437 (1938)
- 10C36 J. M. Cork and E. O. Lawrence, *Phys. Rev.* **49**, 788 (1936)
- 10C37 J. M. Cork and R. L. Thornton, *Phys. Rev.* **51**, 608 (1937)
- 10C38 J. M. Cork and R. L. Thornton, *Phys. Rev.* **53**, 866 (1938)
- 10C39 J. M. Cork and J. L. Lawson, *Phys. Rev.* **56**, 291 (1939)
- 10C40 J. M. Cork, J. Halpern, and H. Tatel, *Phys. Rev.* **57**, 371 (1940)
- 10C40a J. M. Cork and W. Middleton, *Phys. Rev.* **58**, 474 (1940)
- 10C41 J. M. Cork and G. P. Smith, *Phys. Rev.* **60**, 480 (1941)
- 10C42 J. M. Cork, L. N. Hadley, Jr., and C. V. Kent, *Phys. Rev.* **61**, 388 (1942) (A)
- 10C47 J. M. Cork, R. G. Shreffler, and C. M. Fowler, *Phys. Rev.* **72**, 1209 (1947)
- 10C48 J. M. Cork, R. G. Shreffler, and C. M. Fowler, *Phys. Rev.* **74**, 1657 (1948)
- 10C48a J. M. Cork, R. G. Shreffler, and C. M. Fowler, *Phys. Rev.* **73**, 1220 (1948) (A)
- 10C48b J. M. Cork, R. G. Shreffler, and C. M. Fowler, *Phys. Rev.* **74**, 240 (1948)
- 10C49 J. M. Cork, H. B. Keller, and A. E. Stoddard, *Phys. Rev.* **76**, 575 (1949)
- 10C49a J. M. Cork, H. B. Keller, and A. E. Stoddard, *Phys. Rev.* **76**, 986 (1949)
- 10C49b J. M. Cork, H. B. Keller, J. Sazynski, W. C. Rutledge, and A. E. Stoddard, *Phys. Rev.* **75**, 1778 (1949)
- 10C50 J. M. Cork, W. C. Rutledge, C. E. Branyan, A. E. Stoddard, and J. M. LeBlanc, *Phys. Rev.* **79**, 889 (1950)
- 10C50a J. M. Cork, W. C. Rutledge, C. E. Branyan, A. E. Stoddard, W. J. Childs, and J. M. LeBlanc, *Phys. Rev.* **80**, 286 (1950)
- 10C50b J. M. Cork, W. C. Rutledge, A. E. Stoddard, C. E. Branyan, and J. M. LeBlanc, *Phys. Rev.* **79**, 938 (1950)
- 10C50c J. M. Cork, H. B. Keller, W. C. Rutledge, and A. E. Stoddard, *Phys. Rev.* **77**, 848 (1950)
- 10C50d J. M. Cork, C. E. Branyan, W. C. Rutledge, A. E. Stoddard, and J. M. LeBlanc, *Phys. Rev.* **78**, 304 (1950)
- 10C50e J. M. Cork, H. B. Keller, W. C. Rutledge, and A. E. Stoddard, *Phys. Rev.* **78**, 95 (1950)
- 10C50f J. M. Cork, A. E. Stoddard, W. C. Rutledge, C. E. Branyan, and J. LeBlanc, *Phys. Rev.* **78**, 299 (1950)
- 10C50g J. M. Cork, A. E. Stoddard, W. C. Rutledge, C. E. Branyan, and J. M. LeBlanc, *Phys. Rev.* **77**, 843 (1950)
- 10C51 J. M. Cork, C. E. Branyan, A. E. Stoddard, H. B. Keller, J. M. LeBlanc, and W. J. Childs, *Phys. Rev.* **83**, 681 (1951)
- 10C51a J. M. Cork, A. E. Stoddard, C. E. Branyan, W. J. Childs, D. W. Martin, and J. M. LeBlanc, *Phys. Rev.* **84**, 596 (1951)
- 10C51b J. M. Cork, W. C. Rutledge, A. E. Stoddard, C. E. Branyan, and W. J. Childs, *Phys. Rev.* **81**, 482 (1951)
- 10C51c J. M. Cork, J. M. LeBlanc, A. E. Stoddard, D. W. Martin, C. E. Branyan, and W. J. Childs, *Phys. Rev.* **83**, 856 (1951)
- 10C51d J. M. Cork, A. E. Stoddard, J. M. LeBlanc, C. E. Branyan, D. W. Martin, and W. J. Childs, *Phys. Rev.* **83**, 856 (1951)
- 10C51e J. M. Cork, W. J. Childs, C. E. Branyan, W. C. Rutledge, and A. E. Stoddard, *Phys. Rev.* **81**, 642 (1951)
- 10C51f J. M. Cork, J. M. LeBlanc, A. E. Stoddard, W. J. Childs, C. E. Branyan, and D. W. Martin, *Phys. Rev.* **82**, 258 (1951)
- 10C52 J. M. Cork, J. M. LeBlanc, F. B. Stumpf, and W. H. Nester, *Phys. Rev.* **86**, 575 (1952)
- 10C52a J. M. Cork, J. M. LeBlanc, F. B. Stumpf, and W. H. Nester, *Phys. Rev.* **86**, 415 (1952)
- 10C52b J. M. Cork, D. W. Martin, J. M. LeBlanc, and C. E. Branyan, *Phys. Rev.* **85**, 386 (1952)
- 10C52c J. M. Cork, J. M. LeBlanc, W. H. Nester, and F. B. Stumpf, *Phys. Rev.* **88**, 685 (1952)
- 11C40 D. R. Corson, K. R. MacKenzie, and E. Segrè, *Phys. Rev.* **57**, 459, 1087 (1940)
- 11C40a D. R. Corson, K. R. MacKenzie, and E. Segrè, *Phys. Rev.* **58**, 672 (1940)
- 12C37 B. N. Cacciapuoti and E. Segrè, *Phys. Rev.* **52**, 1252 (1937)
- 12C38 B. N. Cacciapuoti, *Nuovo Cimento* **15**, 213 (1938)
- 12C39 B. N. Cacciapuoti, *Phys. Rev.* **55**, 110 (1939)
- 13C51 E. Cotton, *Ann. phys.* **6**, 481 (1951)

- 14C50 W. W. T. Crane and I. Perlman, unpublished data (1950)
- 15C44 O. Chamberlain, G. W. Farwell, and E. Segrè, Los Alamos Scientific Laboratory Classified Report LAMS-131 (Sept. 1944)
- 15C46 O. Chamberlain, D. Williams, and P. Yuster, Phys. Rev. 70, 580 (1946)
- 15C47 O. Chamberlain, J. W. Gofman, E. Segrè, and A. C. Wahl, Phys. Rev. 71, 529 (1947)
- 16C47 B. B. Cunningham and H. H. Hopkins, Jr., unpublished work (Feb. 1947)
- 16C49 B. B. Cunningham and L. B. Werner, J. Am. Chem. Soc. 71, 1521 (1949); NNES-PPR 14B, 51 (1949)
- 16C49a B. B. Cunningham, NNES-PPR 14B, 1363 (1949)
- 16C50 B. B. Cunningham, S. G. Thompson, and H. R. Lohr, unpublished data (1950)
- 17C51 M. Conjeaud and V. Naggiar, Compt. rend. 232, 499 (1951)
- 18C32 J. Chadwick, Proc. Roy. Soc. (London) 136A, 692 (1932)
- 18C35 J. Chadwick and M. Goldhaber, Proc. Roy. Soc. (London) 151A, 479 (1935)
- 19C48 J. H. Coon, M. Goldblatt, R. Nobles, and C. F. Robinson, U. S. Atomic Energy Commission Declassified Document AECD-2190 (July 1948)
- 19C49 J. H. Coon, Phys. Rev. 75, 1355 (1949)
- 20C41 R. Cornog and W. F. Libby, Phys. Rev. 59, 1046 (1941)
- 21C39 S. C. Curran and J. E. Strothers, Proc. Roy. Soc. (London) 172A, 72 (1939)
- 21C40 S. C. Curran and J. E. Strothers, Proc. Cambridge Phil. Soc. 36, 252 (1940)
- 21C40a S. C. Curran, P. I. Dee, J. E. Strothers, Proc. Roy. Soc. (London) 174A, 546 (1940)
- 21C48 S. C. Curran, J. Angus, and A. L. Cockroft, Nature 162, 302 (1948)
- 21C49 S. C. Curran, J. Angus, and A. L. Cockroft, Phys. Rev. 76, 853 (1949)
- 21C51 S. C. Curran, D. Dixon, and H. W. Wilson, Phys. Rev. 84, 151 (1951); Phil. Mag. 43, 82 (1952)
- 21C52 S. C. Curran, D. Dixon, and H. W. Wilson, private communication (Sept. 1952)
- 22C34 H. R. Crane and C. C. Lauritsen, Phys. Rev. 45, 430 (1934)
- 22C34a H. R. Crane and C. C. Lauritsen, Phys. Rev. 45, 497 (1934)
- 22C35 H. R. Crane, L. A. Delsasso, W. A. Fowler, and C. C. Lauritsen, Phys. Rev. 47, 971 (1935)
- 22C35a H. R. Crane, L. A. Delsasso, W. A. Fowler, and C. C. Lauritsen, Phys. Rev. 47, 887 (1935)
- 23C50 J. Crussard, Compt. rend. 231, 141 (1950)
- 24C49 E. C. Campbell and W. M. Good, Phys. Rev. 76, 195 (1949) (A)
- 24C50 E. C. Campbell and M. Goodrich, Phys. Rev. 78, 640 (1950) (A)
- 24C51 E. C. Campbell and M. Goodrich, private communication (Oct. 1951)
- 24C51a E. C. Campbell, J. H. Kahn, and M. Goodrich, reported in Oak Ridge National Laboratory Unclassified Report ORNL-1164 (April 1951)
- 24C52 E. C. Campbell, private communication (Oct. 1952)
- 24C52a E. C. Campbell and M. Goodrich, private communication (Oct. 1952)
- 25C50 D. Christian and D. S. Martin, Jr., Phys. Rev. 80, 1110 (1950)
- 25C52 D. Christian, R. F. Mitchell, and D. S. Martin, Jr., Phys. Rev. 86, 946 (1952)
- 26C35 J. D. Cockcroft, C. W. Gilbert, and E. T. S. Walton, Proc. Roy. Soc. (London) 148A, 225 (1935)
- 27C47 W. W. Chupp and E. M. McMillan, Phys. Rev. 72, 873 (1947)
- 27C48 W. W. Chupp and E. M. McMillan, Phys. Rev. 74, 1217 (1948) (A)
- 28C42 C. S. Cook and P. W. McDaniel, Phys. Rev. 62, 412 (1942)
- 28C46 C. S. Cook, E. T. Journey, and L. M. Langer, Phys. Rev. 70, 985 (1946)
- 28C48 C. S. Cook, L. M. Langer, and H. C. Price, Jr., Phys. Rev. 74, 548 (1948)
- 28C48a C. S. Cook, L. M. Langer, H. C. Price, Jr., and M. B. Sampson, Phys. Rev. 74, 502 (1948)
- 28C48b C. S. Cook and L. M. Langer, Phys. Rev. 74, 227 (1948)
- 28C48c C. S. Cook and L. M. Langer, Phys. Rev. 73, 601 (1948)
- 28C48d C. S. Cook and L. M. Langer, Phys. Rev. 73, 1149 (1948)
- 28C51 C. S. Cook, Phys. Rev. 83, 462 (1951)
- 29C40 E. C. Creutz, W. H. Barkas, and N. H. Furman, Phys. Rev. 58, 1008 (1940)
- 29C40a E. C. Creutz, J. G. Fox, and R. Sutton, Phys. Rev. 57, 567 (1940) (A)
- 29C40b E. C. Creutz, L. A. Delsasso, R. B. Sutton, M. G. White, and W. H. Barkas, Phys. Rev. 58, 481 (1940)
- 30C44 E. T. Clarke and J. W. Irvine, Jr., Phys. Rev. 66, 231 (1944)
- 30C46 E. T. Clarke and J. W. Irvine, Jr., Phys. Rev. 69, 680 (1946) (A)
- 30C47 E. T. Clarke, Phys. Rev. 71, 187 (1947)
- 31C50 J. W. Cobble and R. W. Atterbury, Phys. Rev. 80, 917 (1950)
- 32C39 E. C. Crittenden, Jr., Phys. Rev. 56, 709 (1939)
- 33C38 J. Cichocki and A. Soltan, Compt. rend. 207, 423 (1938)
- 34C39 R. A. Cooley, D. M. Yost, and E. M. McMillan, J. Am. Chem. Soc. 61, 2970 (1939)
- 35C52 H. Craig, Phys. Rev. 85, 688 (1952)
- 36C50 M. Ceccarelli, G. Quarenzi, and A. Rostagni, Phys. Rev. 80, 909 (1950)
- 37C51 S. A. Colgate, Phys. Rev. 81, 1063 (1951)
- 38C48 W. O. Caster and T. P. Kohman, private communication (1948)
- 39C50 W. H. Cuffey, Phys. Rev. 79, 180 (1950)
- 39C51 W. H. Cuffey, Phys. Rev. 82, 461 (1951)
- 39C51a W. H. Cuffey and R. Canada, Phys. Rev. 83, 654 (1951)
- 40C51 D. O. Caldwell and H. F. Stoddart, Phys. Rev. 81, 660 (1951) (A)
- 41C51 R. R. Carlson, Phys. Rev. 84, 749 (1951)
- 42C50 R. L. Caldwell, Phys. Rev. 78, 407 (1950)
- 43C51 R. Canada and A. C. G. Mitchell, Phys. Rev. 83, 955 (1951)
- 43C51a R. Canada and A. C. G. Mitchell, Phys. Rev. 81, 485 (1951)
- 43C51b R. Canada, W. H. Cuffey, A. E. Lessor, and A. C. G. Mitchell, Phys. Rev. 82, 750 (1951)
- 43C51c R. Canada and A. C. G. Mitchell, Phys. Rev. 83, 76 (1951)
- 44C44 M. Camac, Metallurgical Laboratory Declassified Report CC-2409 (Dec. 1944)
- 44C45 M. Camac and L. Brown, Metallurgical Laboratory Classified Report CP-2407 (Feb. 1945)
- 45C46 E. E. Conn, A. R. Brosi, J. A. Swartout, A. E. Cameron, R. L. Carter, and D. G. Hill, Phys. Rev. 70, 768 (1946)

- 46C50 A. G. W. Cameron and L. Katz, *Phys. Rev.* 80, 904 (1950)
- 47C50 R. A. Cohn and J. D. Kurbatov, *Phys. Rev.* 78, 318 (1950) (A)
- 48C38 B. R. Curtis and J. M. Cork, *Phys. Rev.* 53, 681 (1938) (A)
- 48C40 B. R. Curtis and J. R. Richardson, *Phys. Rev.* 57, 1121 (1940)
- 49C48 W. S. Cowart, M. L. Pool, D. A. McCown, and L. L. Woodward, *Phys. Rev.* 73, 1454 (1948)
- 50C48 S. D. Chatterjee and N. K. Saha, *Indian J. Phys.* 22, 515 (1948)
- 51C51 C. D. Coryell, unpublished data quoted in NNES-PPR 9, 2013 (Appendix 3) (1951)
- 51C52 C. D. Coryell, private communication (Oct. 1952)
- 51C52a C. D. Coryell, P. Leveque, and H. G. Richter, unpublished data (Oct. 1952)
- 52C41 E. P. Clancy, *Phys. Rev.* 60, 87 (1941)
- 53C50 S. V. Castner, M.S. Thesis, University of California Radiation Laboratory Unclassified Report UCRL-942 (Oct. 1950); *Phys. Rev.* 88, 1126 (1952)
- 53C51 S. V. Castner, University of California Radiation Laboratory Unclassified Report UCRL-1099 (Jan. 1951)
- 54C06 N. R. Campbell and A. Wood, *Proc. Cambridge Phil. Soc.* 14, 15 (1906); N. R. Campbell, *Proc. Cambridge Phil. Soc.* 14, 211 (1907); 557 (1908)
- 55C50 G. Charpak and F. Suzor, *J. phys. et radium* 11, 633 (1950)
- 55C51 G. Charpak and F. Suzor, *Compt. rend.* 233, 1356 (1951)
- 56C49 A. L. Cockroft and G. M. Inach, *Phil. Mag.* 40, 1014 (1949)
- 57C43 A. A. Cohen, *Phys. Rev.* 63, 219 (1943) (A)
- 58C47 P. Chudom and C. O. Muehlhause, reported in Argonne National Laboratory Classified Report CP-3801 (May 1947)
- 59C51 J. M. Cassidy, *Phys. Rev.* 83, 483 (1951) (A)
- 60C50 W. L. Carss, J. R. Gum, and M. L. Pool, *Phys. Rev.* 80, 1028 (1950)
- 61C49 S. A. Chowdary, reported in Purdue University Unclassified Report NP-943 (June 1949)
- 62C52 T. B. Cook, Jr. and S. K. Haynes, *Phys. Rev.* 86, 190 (1952)
- 63C48 S. G. Cohen, *Nature* 161, 475 (1948)
- 63C51 S. G. Cohen, *Nature* 167, 779 (1951)
- 63C52 S. G. Cohen and A. A. Jaffe, *Phys. Rev.* 86, 800 (1952)
- 64C39 G. B. Collins, B. Waldman, E. M. Stubblefield, and M. Goldhaber, *Phys. Rev.* 55, 507 (1939)
- 64C40 G. B. Collins and B. Waldman, *Phys. Rev.* 57, 1088 (1940) (A)
- 65C47 K. D. Coleman and M. L. Pool, *Phys. Rev.* 72, 1070 (1947)
- 65C47a K. D. Coleman, R. Nudenberg, and M. L. Pool, *Phys. Rev.* 72, 164 (1947) (A)
- 66C50 T. C. Chu, *Phys. Rev.* 79, 582 (1950)
- 67C51 G. W. Campbell, N. R. Sleight, and W. H. Sullivan, NNES-PPR 9, 931 (1951)
- 68C51 G. B. Cook, British Atomic Energy Report AERE C/R-729 (June 1951)
- 68C51a G. B. Cook, reported in British Classified Report AERE-PR-20 (April 1951)
- 69C51 P. E. Cavanagh, J. F. Turner, D. V. Booker, and H. J. Dunster, *Proc. Phys. Soc. (London)* 64A, 13 (1951)
- 69C51a P. E. Cavanagh, *Phys. Rev.* 82, 791 (1951)
- 69C52 P. E. Cavanagh, *Phil. Mag.* 43, 221 (1952)
- 69C52a P. E. Cavanagh, *Phil. Mag.* 43, 648 (1952)
- 70C50 L. S. Cheng and J. D. Kurbatov, *Phys. Rev.* 78, 319 (1950) (A)
- 70C52 L. S. Cheng, G. John, and J. D. Kurbatov, *Phys. Rev.* 86, 632 (1952) (A); 85, 487 (1952)
- 71C49 K. Y. Chu and M. L. Wiedenbeck, *Phys. Rev.* 75, 226 (1949)
- 72C42 A. F. Clark, *Phys. Rev.* 61, 242 (1942)
- 73C48 J. B. Chubbuck and I. Perlman, *Phys. Rev.* 74, 982 (1951)
- 74C46 P. Cuet and C. M. G. Lattes, *Nature* 158, 197 (1946)
- 75C52 R. J. Carr and G. H. Higgins, private communication (Aug. 1952)
- 76C51 J. M. Cassels, T. C. Randle, T. G. Pickavance, and A. E. Taylor, *Phil. Mag.* 42, 215 (1951)
- 77C52 R. S. Caswell, *Phys. Rev.* 86, 82 (1952)
- 78C52 A. A. Caretto and E. O. Wiig, *J. Am. Chem. Soc.* 74, 5235 (1952)
- 78C52a A. A. Caretto and S. Katcoff, private communication (Sept. 1952)
- 79C52 R. S. Caird and A. C. G. Mitchell, *Phys. Rev.* (in press) (1952)
- 80C52 P. G. Cobb, reported in Purdue University Progress Report II (June 1952)
- 81C43 K. L. Cook, *Phys. Rev.* 64, 278 (1943)
- 82C52 C. G. Campbell, W. J. Henderson, and J. Kyles, *Phil. Mag.* 43, 126 (1952); private communication (Oct. 1952)
- 83C49 R. A. Charpie, K. H. Sun, B. Jennings, and J. F. Nechaj, *Phys. Rev.* 76, 1255 (1949)
- 1D35 A. J. Dempster, *Nature* 135, 993 (1935)
- 1D35a A. J. Dempster, *Nature* 136, 65 (1935)
- 1D36 A. J. Dempster, *Nature* 138, 120 (1936)
- 1D39 A. J. Dempster, *Phys. Rev.* 55, 794 (1939)
- 1D48 A. J. Dempster, *Phys. Rev.* 73, 1125 (1948)
- 2D38 L. A. Dubridge, S. W. Barnes, J. H. Buck, and C. V. Strain, *Phys. Rev.* 53, 447 (1938)
- 2D39 L. A. Dubridge and J. Marshall, *Phys. Rev.* 56, 706 (1939)
- 2D40 L. A. Dubridge, private communication to G. T. Seaborg (1940); includes work of entire Rochester group
- 2D40a L. A. Dubridge and J. Marshall, *Phys. Rev.* 58, 7 (1940)
- 2D40b L. A. Dubridge and J. Marshall, *Phys. Rev.* 57, 348 (1940) (A)
- 3D40 W. L. Davidson, Jr., *Phys. Rev.* 57, 1086 (1940) (A)
- 3D40a W. L. Davidson, private communication (1940)
- 4D50 J. M. Dickson and T. C. Randle, *Nature* 166, 235 (1950)
- 4D51 J. M. Dickson and T. C. Randle, *Proc. Phys. Soc. (London)* 64A, 902 (1951)
- 5D35 L. A. Delsasso, W. A. Fowler, and C. C. Lauritsen, *Phys. Rev.* 48, 848 (1935)
- 5D39 L. A. Delsasso, L. N. Ridenour, R. Sherr, and M. G. White, *Phys. Rev.* 55, 113 (1939)
- 5D40 L. A. Delsasso, M. G. White, W. Barkas, and E. C. Creutz, *Phys. Rev.* 58, 586 (1940)
- 6D33 G. von Droste, *Z. Physik* 34, 17 (1933)
- 7D38 H. DeVries and J. Veldkamp, *Physica* 5, 249 (1938)
- 7D39 H. DeVries and G. Diemer, *Physica* 6, 599 (1939)

- 8D37 S. Devons and G. J. Neary, *Proc. Cambridge Phil. Soc.* 33, 154 (1937)
- 9D49 H. E. Duckworth, R. F. Black, and R. F. Woodcock, *Phys. Rev.* 75, 1616 (1949)
- 10D47 S. DeBenedetti and E. H. Kerner, *Phys. Rev.* 71, 122 (1947)
- 10D48 S. DeBenedetti and F. K. McGowan, *Phys. Rev.* 74, 728 (1948)
- 10D52 S. DeBenedetti and G. H. Minton, *Phys. Rev.* 85, 944 (1952)
- 11D39 J. V. Dunworth, *Nature* 144, 152 (1939)
- 11D47 J. V. Dunworth and B. Pontecorvo, *Proc. Cambridge Phil. Soc.* 43, 123 (1947)
- 11D47a J. V. Dunworth and B. Pontecorvo, *Proc. Cambridge Phil. Soc.* 43, 429 (1947)
- 12D42 G. Dessauer, private communication (May 1942)
- 13D50 G. von Dardel, *Phys. Rev.* 79, 734 (1950)
- 14D41 R. L. Doran and W. J. Henderson, *Phys. Rev.* 60, 411 (1941)
- 14D48 R. L. Doran and W. J. Henderson, private communication from K. Lark-Horowitz (1948)
- 15D52 D. C. Dunlavey and G. T. Seaborg, *Phys. Rev.* 87, 165 (1952)
- 15D52a D. C. Dunlavey and G. T. Seaborg, *Phys. Rev.* 85, 757 (1952) (A)
- 16D41 B. S. Dzhelepov and A. A. Konstantinov, *Compt. rend. U.S.S.R.* 30, 701 (1941)
- 16D46 B. Dzhelepov, M. Kopjova, and E. Vorbjov, *Phys. Rev.* 69, 538 (1946)
- 16D49 B. S. Dzhelepov, N. M. Anton'eva, and S. A. Shestopalova, *Doklady Akad. Nauk, S.S.S.R.* 64, 309 (1949)
- 16D51 B. Dzhelepov, N. Zhukovskii, and Yu. Kholnov, *Doklady Akad. Nauk, S.S.S.R.* 77, 233 (1951)
- 16D52 B. Dzhelepov and A. Silantov, *Doklady Akad. Nauk, S.S.S.R.* 85, 533 (1952)
- 17D51 C. F. G. Delaney, *Phys. Rev.* 81, 158 (1951)
- 17D51a C. F. G. Delaney, *Sci. Proc. Roy. Dublin Soc.* 25, 251 (1951)
- 18D40 G. Dickson, P. W. McDaniel, and E. J. Konopinski, *Phys. Rev.* 57, 351 (1940) (A)
- 19D37 B. T. Darling, B. R. Curtis, and J. M. Cork, *Phys. Rev.* 51, 1010 (1937) (A)
- 20D41 M. Deutsch and A. Roberts, *Phys. Rev.* 60, 362 (1941)
- 20D42 M. Deutsch, J. R. Downing, L. G. Elliott, J. W. Irvine, Jr., and A. Roberts, *Phys. Rev.* 62, 3 (1942)
- 20D42a M. Deutsch and L. G. Elliott, *Phys. Rev.* 62, 558 (1942) (A)
- 20D42b M. Deutsch, *Phys. Rev.* 61, 672 (1942)
- 20D42c M. Deutsch, A. Roberts, and L. G. Elliott, *Phys. Rev.* 61, 389 (1942) (A)
- 20D44 M. Deutsch and L. G. Elliott, *Phys. Rev.* 65, 211 (1944)
- 20D45 M. Deutsch, L. G. Elliott, and A. Roberts, *Phys. Rev.* 68, 193 (1945)
- 20D47 M. Deutsch, *Phys. Rev.* 72, 729 (1947)
- 20D47a M. Deutsch, *Phys. Rev.* 72, 527 (1947) (A)
- 20D49 M. Deutsch and A. Hedgran, *Phys. Rev.* 75, 1443 (1949)
- 20D49a M. Deutsch and D. T. Stevenson, *Phys. Rev.* 76, 184 (1949) (A)
- 20D50 M. Deutsch and W. E. Wright, *Phys. Rev.* 77, 139 (1950)
- 20D50a M. Deutsch and A. Hedgran, *Phys. Rev.* 79, 400 (1950)
- 20D51 M. Deutsch and G. Scharff-Goldhaber, *Phys. Rev.* 83, 1059 (1951)
- 21D40 D. DeVault and W. F. Libby, *Phys. Rev.* 58, 688 (1940)
- 22D39 R. W. Dodson and R. D. Fowler, *Phys. Rev.* 55, 880 (1939)
- 22D40 R. W. Dodson and R. D. Fowler, *Phys. Rev.* 57, 966 (1940)
- 23D48 R. B. Duffield and J. D. Knight, private communication (Oct. 1948)
- 23D49 R. B. Duffield and J. D. Knight, *Phys. Rev.* 76, 573 (1949)
- 23D49a R. B. Duffield and J. D. Knight, *Phys. Rev.* 75, 1613 (1949)
- 23D49b R. B. Duffield and J. D. Knight, *Phys. Rev.* 75, 1967 (1949)
- 23D49c R. B. Duffield and L. M. Langer, *Phys. Rev.* 76, 1272 (1949)
- 23D50 R. B. Duffield, L. Hsiao, and E. N. Sloth, *Phys. Rev.* 79, 1011 (1950)
- 23D50a R. B. Duffield and L. M. Langer, *Phys. Rev.* 77, 743 (1950) (A)
- 23D51 R. B. Duffield and L. M. Langer, *Phys. Rev.* 81, 203 (1951)
- 23D51a R. B. Duffield, reported in U. S. Atomic Energy Commission Classified Report WASH-62 (Dec. 1951)
- 23D51b R. B. Duffield and L. M. Langer, *Phys. Rev.* 84, 1065 (1951)
- 23D52 R. B. Duffield and L. M. Langer, *Phys. Rev.* (to be published) (1952)
- 24D51 C. R. Dillard, R. M. Adams, H. Finston, and A. Turkevich, *NNES-PPR* 9, 624 (1951)
- 24D51a C. R. Dillard, R. M. Adams, H. Finston, and A. Turkevich, *NNES-PPR* 9, 616 (1951)
- 24D51b C. R. Dillard, R. M. Adams, H. Finston, and A. Turkevich, *NNES-PPR* 9, 692 (1951)
- 24D51c C. R. Dillard, H. Finston, and R. M. Adams, *NNES-PPR* 9, 1101 (1951)
- 25D41 J. R. Downing, M. Deutsch, and A. Roberts, *Phys. Rev.* 60, 470 (1941)
- 25D42 J. R. Downing, M. Deutsch, and A. Roberts, *Phys. Rev.* 61, 686 (1942)
- 26D51 B. Dreyfus, J. K. Major, and P. Radvanyi, *Compt. rend.* 232, 617 (1951)
- 27D38 M. Dodé and B. Pontecorvo, *Compt. rend.* 207, 287 (1938)
- 28D50 E. B. Dale and J. D. Kurbatov, *Phys. Rev.* 80, 126 (1950) (A)
- 28D50a E. B. Dale, E. D. Richert, T. A. Redfield, and J. D. Kurbatov, *Phys. Rev.* 80, 763 (1950)
- 29D42 J. W. DeWire, M. L. Pool, and J. D. Kurbatov, *Phys. Rev.* 61, 564 (1942)
- 30D49 D. G. Douglas, *Phys. Rev.* 75, 1960 (1949)
- 30D52 D. G. Douglas, J. S. Foster, and A. L. Thompson, private communication (Oct. 1952)
- 31D50 T. Dybvig and M. L. Pool, *Phys. Rev.* 80, 126 (1950) (A)
- 32D51 S. P. Davis and F. A. Jenkins, *Phys. Rev.* 83, 1269 (1951)
- 33D46 G. Diemer and H. Groendijk, *Physica* 11, 396 (1946)
- 34D48 J. W. M. DuMond, D. A. Lind, and B. B. Watson, *Phys. Rev.* 73, 1392 (1948)
- 35D51 D. B. Duncan and J. E. Perry, *Phys. Rev.* 82, 809 (1951)
- 36D52 J. T. Dewan, T. P. Pepper, K. W. Allen, and E. Almqvist, *Phys. Rev.* 86, 416 (1952)
- 37D51 S. Das and S. K. Sen, *Indian J. Phys.* 25, 451 (1951)
- 38D52 S. S. Dharmatti and H. E. Weaver, Jr., *Phys. Rev.* 85, 927 (1952)
- 39D51 E. K. Darby and W. Opechowski, *Phys. Rev.* 83, 676 (1951)

- 39D51a E. K. Darby, *Can. J. Phys.* **29**, 569 (1951)
- 30D52 B. Dropesky and E. O. Wieg, *Phys. Rev.* **88**, 683 (1952)
- 41D52 F. Depocas and B. G. Harvey, *Phys. Rev.* **85**, 499 (1952)
- 42D52 D. Dixon, McNair, and S. C. Curran, *Physica* (in press) (1952)
- 43D52 R. M. Diamond, private communication (Nov. 1952)
- 44D52 C. Dahlstrom, J. S. Foster, and A. L. Thompson, private communication (Oct. 1952)
- 1E48 D. T. Eggen and M. L. Pool, *Phys. Rev.* **74**, 57 (1948)
- 1E49 D. T. Eggen and M. L. Pool, *Phys. Rev.* **75**, 1464 (1949) (A)
- 2E49 W. S. Emmerich and J. D. Kurbatov, *Phys. Rev.* **75**, 1446 (1949)
- 2E51 W. S. Emmerich, G. John, and J. D. Kurbatov, *Phys. Rev.* **82**, 968 (1951)
- 2E51a W. S. Emmerich and J. D. Kurbatov, *Phys. Rev.* **83**, 40 (1951)
- 2E52 W. S. Emmerich and J. D. Kurbatov, *Phys. Rev.* **85**, 149 (1952)
- 3E50 A. G. Engelkemeir and W. F. Libby, *Rev. Sci. Instr.* **21**, 550 (1950)
- 4E43 L. G. Elliott, M. Deutsch, and A. Roberts, *Phys. Rev.* **63**, 386 (1943)
- 4E43a L. G. Elliott and M. Deutsch, *Phys. Rev.* **64**, 321 (1943)
- 4E43b L. G. Elliott and M. Deutsch, *Phys. Rev.* **63**, 457 (1943) (A)
- 4E47 L. G. Elliott and R. E. Bell, *Phys. Rev.* **72**, 979 (1947)
- 4E48 L. G. Elliott and R. E. Bell, *Phys. Rev.* **74**, 1869 (1948)
- 4E49 L. G. Elliott and R. E. Bell, *Phys. Rev.* **76**, 168 (1949) (A) and private communication from R. L. Graham (Sept. 1952)
- 4E50 L. G. Elliott, R. E. Bell, et al., reported in Chalk River Laboratory Classified Report PR-P-7 (Aug. 1950)
- 4E50a L. G. Elliott et al., reported in Chalk River Laboratory Classified Report PR-P-8 (Nov. 1950)
- 4E51 L. G. Elliott and J. L. Wolfson, *Phys. Rev.* **82**, 333 (1951) (A)
- 4E51a L. G. Elliott et al., reported in Chalk River Laboratory Classified Reports PR-P-12 (Nov. 1951) and PR-P-13 (Feb. 1952)
- 4E52 L. G. Elliott, *Phys. Rev.* **85**, 942 (1952)
- 5E37 Z. V. Erchova, *J. phys. et radium* **8**, 501 (1937)
- 6E50 H. D. Evans, *Proc. Phys. Soc. (London)* **63A**, 575 (1950)
- 7E42 S. G. English and R. A. James, reported in Metallurgical Laboratory Classified Report CN-261 (Sept. 1942)
- 8E30 C. D. Ellis and G. H. Aston, *Proc. Roy. Soc. (London)* **129A**, 180 (1930)
- 8E32 C. D. Ellis, *Proc. Roy. Soc. (London)* **138A**, 318 (1932)
- 8E33 C. D. Ellis and N. F. Mott, *Proc. Roy. Soc. (London)* **141A**, 502 (1933)
- 8E34 C. D. Ellis, *Proc. Roy. Soc. (London)* **143A**, 350 (1934)
- 8E34a C. D. Ellis and W. J. Henderson, *Proc. Roy. Soc. (London)* **146A**, 206 (1934)
- 8E35 C. D. Ellis and W. J. Henderson, *Nature* **135**, 429 (1935)
- 8E36 C. D. Ellis and W. J. Henderson, *Proc. Roy. Soc. (London)* **156A**, 358 (1936)
- 9E48 C. Egger, D. J. Hughes, and C. Huddleston, *Phys. Rev.* **74**, 1239 (1948) (A)
- 10E41 S. Eklund, *Arkiv Mat., Astron. Fysik* **28A**, No. 3 (1941)
- 10E43 S. Eklund and N. Hole, *Arkiv Mat., Astron. Fysik* **29A**, No. 26 (1943)
- 10E46 S. Eklund, *Arkiv Mat., Astron. Fysik* **33A**, No. 14 (1946)
- 11E47 A. C. English, T. E. Cranshaw, P. Demers, J. A. Harvey, E. P. Hincks, J. V. Jelley, and A. N. May, *Phys. Rev.* **72**, 253 (1947)
- 12E41 D. R. Elliott and L. D. P. King, *Phys. Rev.* **60**, 489 (1941)
- 12E41a D. R. Elliott and L. D. P. King, *Phys. Rev.* **59**, 403 (1941)
- 13E46 D. W. Engelkemeir and E. L. Brady, reported in *J. Am. Chem. Soc.* **68**, 2411 (1946)
- 13E48 D. W. Engelkemeir, U. S. Atomic Energy Commission Declassified Document AECD-2125 (July 1948)
- 13E50 D. W. Engelkemeir, M. S. Freedman, and J. May, Argonne National Laboratory Unclassified Report ANL-4473 (June 1950)
- 13E51 D. W. Engelkemeir, J. A. Seiler, E. P. Steinberg, and L. Winsberg, *NNES-PPR* **9**, 1354 (1951)
- 13E51a D. W. Engelkemeir and E. L. Brady, *NNES-PPR* **9**, 746 (1951)
- 13E51b D. W. Engelkemeir, E. L. Brady, and E. P. Steinberg, *NNES-PPR* **9**, 722 (1951)
- 13E51c D. W. Engelkemeir, *Phys. Rev.* **82**, 552 (1951)
- 13E51d D. W. Engelkemeir, reported in Argonne National Laboratory Classified Report ANL-4526 (Jan. 1951)
- 13E51e D. W. Engelkemeir and N. Sugarman, *NNES-PPR* **9**, 1052 (1951)
- 13E51f D. W. Engelkemeir, M. S. Freedman, L. E. Glendenin, and R. P. Metcalf, *NNES-PPR* **9**, 1104 (1951)
- 13E51g D. W. Engelkemeir, *NNES-PPR* **9**, 1108 (1951)
- 13E52 D. W. Engelkemeir, reported in Argonne National Laboratory Classified Report ANL-4717 (April 1952)
- 14E46 J. E. Edwards and M. L. Pool, *Phys. Rev.* **69**, 253 (1946) (A)
- 14E46a J. E. Edwards and M. L. Pool, *Phys. Rev.* **69**, 140 (1946)
- 14E47 J. E. Edwards and M. L. Pool, *Phys. Rev.* **72**, 384 (1947)
- 15E39 D. Ewing, T. Perry, and R. McCreary, *Phys. Rev.* **55**, 1136 (1939) (A)
- 16E43 H. Ewald, private communication to S. Flugge and J. Mattauch, *Ber. deut. chem. Ges.* **76A**, 1 (1943); *Z. physik* **122**, 487 (1944)
- 17E39 T. Enns, *Phys. Rev.* **56**, 872 (1939)
- 18E51 N. Elliott, *NNES-PPR* **9**, 1047 (1951)
- 19E51 H. B. Evans, L. E. Glendenin, and R. P. Metcalf, *NNES-PPR* **9**, 1081 (1951)
- 20E51 R. R. Edwards, H. Gest, and T. H. Davies, *NNES-PPR* **9**, 237 (1951)
- 21E52 G. G. Eichholz and L. A. Ficko, *Phys. Rev.* **86**, 794 (1952)
- 22E52 L. S. Edwards and F. A. MacMillan, *Phys. Rev.* **87**, 377 (1952)
- 23E52 V. O. Erikson, G. Jenssen, and A. Sunde, *Physica* **18**, 91 (1952)
- 24E51 E. W. Emery, *Phys. Rev.* **83**, 679 (1951)
- 25E52 M. W. Elliott, L. S. Cheng, J. R. Haskins, and J. D. Kurbatov, *Phys. Rev.* **88**, 263 (1952)
- 26E52 G. T. Ewan and M. A. S. Ross, *Nature* **170**, 760 (1952)

- 1F36 W. A. Fowler, L. A. Delsasso, and C. C. Lauritsen, *Phys. Rev.* 49, 561 (1936)
- 1F37 W. A. Fowler and C. C. Lauritsen, *Phys. Rev.* 51, 1103 (1937)
- 2F51 M. H. Feldman, L. E. Glendenin, and R. R. Edwards, *NNES-PPR* 9, 598 (1951)
- 2F51a M. H. Feldman and L. E. Glendenin, *NNES-PPR* 9, 654 (1951)
- 3F50 M. Freedman, J. May, R. Pairs, W. Ramler, and M. Rusnak, reported in Argonne National Laboratory Classified Report ANL-4380 (March 1950)
- 3F50a M. S. Freedman, A. H. Jaffey, and F. Wagner, Jr., *Phys. Rev.* 79, 410 (1950)
- 3F50b M. S. Freedman and E. P. Steinberg, reported in Argonne National Laboratory Classified Report ANL-4427 (July 1950)
- 3F50c M. S. Freedman and D. W. Engelkemeir, *Phys. Rev.* 79, 897 (1950)
- 3F51 M. Freedman and F. Wagner, Jr., reported in Argonne National Laboratory Classified Report ANL-4526 (Jan. 1951)
- 3F52 M. S. Freedman, F. Wagner, Jr., A. H. Jaffey, and J. May, *Phys. Rev.* (in press) (1952)
- 3F52a M. Freedman, J. May, M. Rusnak, and F. Wagner, Jr., reported in Argonne National Laboratory Classified Report ANL-4717 (April 1952)
- 3F52b M. S. Freedman, F. Wagner, Jr., and D. W. Engelkemeir, *Phys. Rev.* 88, 1155 (1952)
- 3F53 M. S. Freedman, F. Wagner, Jr., D. W. Engelkemeir, J. R. Huizenga, and L. B. Magnusson, *Phys. Rev.* (to be published) (1953)
- 4F32 N. Feather, *Proc. Roy. Soc. (London)* 136, 709 (1932); 142, 689 (1933)
- 4F38 N. Feather, *Proc. Cambridge Phil. Soc.* 34, 115 (1938)
- 4F38a N. Feather and E. Bretscher, *Proc. Roy. Soc. (London)* 165A, 530 (1938)
- 4F38b N. Feather and J. V. Dunworth, *Proc. Roy. Soc. (London)* 168A, 566 (1938)
- 4F42 N. Feather, *British Classified Report CPB-83* (1942)
- 4F44 N. Feather and J. Dainty, *Proc. Cambridge Phil. Soc.* 40, 57 (1944)
- 4F47 N. Feather and R. S. Krishnan, *Proc. Cambridge Phil. Soc.* 43, 267 (1947)
- 4F47a N. Feather, *Nature* 160, 749 (1947)
- 4F48 N. Feather, J. Kyles, and R. W. Pringle, *Proc. Phys. Soc. (London)* 61, 466 (1948)
- 4F49 N. Feather, *Nucleonics* 5, No. 1, 22 (1949)
- 5F39 K. Fajans and D. W. Stewart, *Phys. Rev.* 56, 625 (1939)
- 5F40 K. Fajans and A. F. Voigt, *Phys. Rev.* 58, 177 (1940)
- 5F40a K. Fajans and W. H. Sullivan, *Phys. Rev.* 58, 276 (1940)
- 5F41 K. Fajans and A. F. Voigt, *Phys. Rev.* 60, 619 (1941)
- 5F41a K. Fajans and A. F. Voigt, *Phys. Rev.* 60, 626 (1941)
- 5F41b K. Fajans and A. F. Voigt, *Phys. Rev.* 60, 533 (1941)
- 6F50 R. L. Folger, University of California Radiation Laboratory Declassified Report UCRL-937 (Oct. 1950)
- 6F51 R. L. Folger, P. C. Stevenson, and G. T. Seaborg, University of California Radiation Laboratory Classified Report UCRL-1195 Revised (May 1951)
- 7F51 H. Faraggi and A. Berthelot, *Compt. rend.* 232, 2093 (1951)
- 7F51a H. Faraggi, *Ann. phys.* 6, 325 (1951)
- 8F40 M. Frilley, *J. phys. et radium* 1, 34 (1940)
- 8F52 M. Frilley, B. G. Gokhale, and M. Valadares, *Compt. rend.* 232, 50 (1952)
- 9F39 A. Flammersfeld, *Z. Physik* 114, 227 (1939)
- 9F39a A. Flammersfeld, *Z. Physik* 112, 727 (1939)
- 9F43 A. Flammersfeld and J. Mattauich, *Naturwiss.* 31, 66 (1943)
- 9F44 A. Flammersfeld, *Naturwiss.* 32, 36 (1944)
- 9F44a A. Flammersfeld and O. Bruna, *Naturwiss.* 32, 70 (1944)
- 9F44b A. Flammersfeld, *Naturwiss.* 32, 68 (1944)
- 9F46 A. Flammersfeld, *Z. Naturforsch.* 1, 190 (1946)
- 9F47 A. Flammersfeld and O. Bruna, *Z. Naturforsch.* 2a, 241 (1947)
- 9F47a A. Flammersfeld, *Z. Naturforsch.* 2a, 86 (1947)
- 9F50 A. Flammersfeld and C. Ythier, *Z. Naturforsch.* 5a, 401 (1950)
- 9F50a A. Flammersfeld, *Z. Naturforsch.* 5a, 687 (1950)
- 9F50b A. Flammersfeld and W. Herr, *Z. Naturforsch.* 5a, 569 (1950)
- 9F51 A. Flammersfeld, *Z. Naturforsch.* 6a, 559 (1951)
- 9F52 A. Flammersfeld, *Z. Naturforsch.* 7a, 295 (1952)
- 9F52a A. Flammersfeld, *Z. Naturforsch.* 7a, 296 (1952)
- 10F51 P. Falk-Vairant and J. Teillac, *J. phys. et radium* 12, 659 (1951)
- 10F52 P. Falk-Vairant, J. Teillac, and C. Victor, *J. phys. et radium* 13, 313 (1952)
- 10F52a P. Falk-Vairant, *Compt. rend.* 235, 796 (1952)
- 11F44 H. W. Fulbright, reported in Metallurgical Laboratory Classified Report CP-1954 (Aug. 1944)
- 11F44a H. W. Fulbright, W. Bentz, K. Booth, R. G. Gilbert, H. Huth, A. Knudson, H. Meier, H. Plew, C. A. Potter, W. Rall, A. A. Schulke, and M. Waldner, Metallurgical Laboratory Classified Report CP-1357 (Feb. 1944)
- 11F49 H. W. Fulbright, *NNES-PPR* 14B, 1011 (1949)
- 11F49a H. W. Fulbright and J. C. D. Milton, *Phys. Rev.* 76, 1271 (1949)
- 12F52 E. H. Fleming, Jr., A. Ghiorso, and B. B. Cunningham, *Phys. Rev.* 88, 642 (1952)
- 13F50 P. R. Fields, G. L. Pyle, and J. F. Mech, reported in Argonne National Laboratory Classified Report ANL-4469 (June 1950)
- 14F45 G. W. Farwell, J. E. Roberts, A. Spane, and A. C. Wahl, Los Alamos Scientific Laboratory Classified Report LAMS-293 (Oct. 1945)
- 14F46 G. W. Farwell, E. Segrè, A. Spane, and C. E. Wiegand, Los Alamos Scientific Laboratory Classified Report LA-490 (April 1946)
- 15F49 L. Feldman and C. S. Wu, *Phys. Rev.* 75, 1286 (1949) (A)
- 15F49a L. Feldman, L. Lidofsky, P. Macklin, and C. S. Wu, *Phys. Rev.* 76, 1888 (1949)
- 15F52 L. Feldman and C. S. Wu, *Phys. Rev.* 87, 1091 (1952)
- 16F34 E. Fermi, E. Amaldi, O. d'Agnostino, F. Rasetti, and E. Segrè, *Proc. Roy. Soc. (London)* 146A, 483 (1934)
- 16F41 E. Fermi and E. Segrè, *Phys. Rev.* 59, 680 (1941)
- 17F34 O. R. Frisch, *Nature* 133, 721 (1934)
- 17F35 O. R. Frisch, *Nature* 136, 220 (1935)
- 18F35 H. Fahlenbrach, *Z. Physik* 96, 503 (1935)
- 19F50 W. R. Faust, *Phys. Rev.* 78, 624 (1950)
- 20F49 J. J. Floyd and L. B. Borst, *Phys. Rev.* 75, 1106 (1949)
- 21F43 B. T. Feld, reported in Metallurgical Laboratory Classified Report CP-1016 (Oct. 1943)
- 22F47 I. Feister and L. F. Curtiss, *J. Research Natl. Bur. Standards* 38, 411 (1947)
- 22F50 I. Feister and L. F. Curtiss, *Phys. Rev.* 78, 179 (1950)

- 23F40 G. Friedlander, private communication (1940)
- 23F43 G. Friedlander and C. S. Wu, *Phys. Rev.* **63**, 227 (1943)
- 23F48 G. Friedlander, M. Goldhaber, and G. Scharff-Goldhaber, *Phys. Rev.* **74**, 981 (1948)
- 23F48a G. Friedlander and M. L. Perlman, private communication (Sept. 1948)
- 23F49 G. Friedlander, reported in Brookhaven National Laboratory Unclassified Report BNL-AS-2 (June 1949)
- 23F50 G. Friedlander, M. L. Perlman, D. Alburger, and A. W. Sunyar, *Phys. Rev.* **80**, 30 (1950)
- 23F50a G. Friedlander, M. L. Perlman, and G. Scharff-Goldhaber, *Phys. Rev.* **80**, 1103 (1950)
- 23F51 G. Friedlander and J. M. Miller, *Phys. Rev.* **84**, 588 (1951)
- 23F51a G. Friedlander and D. E. Alburger, *Phys. Rev.* **84**, 231 (1951)
- 23F51b G. Friedlander and W. C. Orr, *Phys. Rev.* **84**, 484 (1951)
- 23F52 G. Friedlander and M. L. Perlman, private communication (Aug. 1952)
- 23F52a G. Friedlander, A. Ghiorso, and I. Perlman, unpublished data (Sept. 1952)
- 23F52b G. Friedlander and J. M. Miller, private communication (Oct. 1952)
- 23F52c G. Friedlander, private communication (Dec. 1952)
- 24F51 S. E. Furberg, *Nature* **168**, 1005 (1951)
- 25F51 S. C. Fultz and M. L. Pool, *Phys. Rev.* **83**, 875 (1951) (A)
- 25F52 S. C. Fultz and M. L. Pool, *Phys. Rev.* **86**, 347 (1952)
- 26F47 H. N. Friedlander, L. Seren, and S. H. Turkel, *Phys. Rev.* **72**, 23 (1947)
- 27F50 E. W. Fuller, *Proc. Phys. Soc. (London)* **63A**, 1044 (1950)
- 27F50a E. W. Fuller, *Proc. Phys. Soc. (London)* **63A**, 1348 (1950)
- 28F47 B. J. Finkle, *Phys. Rev.* **72**, 1260 (1947)
- 28F51 B. Finkle, E. J. Hoagland, S. Katcoff, and N. Sugarman, *NNES-PPR* **9**, 1368 (1951)
- 28F51a B. Finkle, S. Katcoff, and N. Sugarman, *NNES-PPR* **9**, 663 (1951)
- 28F51b B. Finkle, D. W. Engelkemeir, and N. Sugarman, *NNES-PPR* **9**, 1083 (1951)
- 28F51c B. Finkle and N. Sugarman, *NNES-PPR* **9**, 1121 (1951)
- 29F52 C. Y. Fan, *Phys. Rev.* **87**, 252 (1952)
- 30F51 S. Fried, A. H. Jaffey, N. F. Hall, and L. E. Glendenin, *Phys. Rev.* **81**, 741 (1951)
- 31F41 J. R. Feldmeier and G. B. Collins, *Phys. Rev.* **59**, 937 (1941)
- 32F52 E. L. Fireman and D. Schwarzer, *Phys. Rev.* **86**, 451 (1952)
- 33F50 R. W. Fink, F. L. Reynolds, and D. H. Templeton, *Phys. Rev.* **77**, 614 (1950)
- 33F50a R. W. Fink and D. H. Templeton, *J. Am. Chem. Soc.* **72**, 2818 (1950)
- 33F51 R. W. Fink and E. O. Wiig, *J. Am. Chem. Soc.* **73**, 2365 (1951)
- 33F52 R. W. Fink and E. O. Wiig, *J. Am. Chem. Soc.* **74**, 2457 (1952)
- 34F52 V. Kistiakowsky Fischer, Ph.D. Thesis, University of California Radiation Laboratory Unclassified Report UCRL-1629 (Jan. 1952); *Phys. Rev.* **87**, 859 (1952)
- 35F50 C. M. Fowler and R. G. Shreffler, *Rev. Sci. Instr.* **21**, 740 (1950)
- 36F49 J. S. Fraser, *Phys. Rev.* **76**, 1540 (1949)
- 37F36 V. Fomin and F. G. Houtermans, *Physik Z. Sowjetunion* **9**, 273 (1936)
- 38F52 M. S. Fred and F. S. Tompkins, *Phys. Rev.* (in press) (1952)
- 39F52 S. C. Fung and I. Perlman, *Phys. Rev.* **87**, 623 (1952)
- 40F47 H. Frauenfelder, P. C. Gugelot, O. Huber, H. Medicus, P. Preiswerk, P. Scherrer, and R. Steffen, *Helv. Phys. Acta* **20**, 238 (1947)
- 40F50 H. Frauenfelder, O. Huber, A. de-Shalit, and W. Zündt, *Phys. Rev.* **79**, 1029 (1950)
- 40F50a H. Frauenfelder, M. Walter, and W. Zündt, *Phys. Rev.* **77**, 557 (1950)
- 41F52 A. J. Ferguson and J. H. Montague, *Phys. Rev.* **87**, 215 (1952) (A)
- 42F52 A. W. Fairhall, private communication (Dec. 1952)
- 1G22 H. Geiger, *Z. Physik* **8**, 45 (1922)
- 2G30 A. V. Grosse, *J. Am. Chem. Soc.* **52**, 1742 (1930); *Naturwiss.* **20**, 505 (1932)
- 2G39 A. V. Grosse, E. T. Booth, and J. R. Dunning, *Phys. Rev.* **56**, 382 (1939)
- 2G40 A. V. Grosse and E. T. Booth, *Phys. Rev.* **57**, 664 (1940)
- 2G41 A. V. Grosse, E. T. Booth, and J. R. Dunning, *Phys. Rev.* **59**, 322 (1941)
- 2G48 A. V. Grosse and E. T. Booth, *J. Am. Chem. Soc.* **70**, 465 (1948)
- 3G47 R. G. Grégoire and M. Perey, *Compt. rend.* **225**, 733 (1947)
- 4G49 C. H. Goddard and C. S. Cook, *Phys. Rev.* **76**, 1419 (1949)
- 5G50 L. S. Germain, *Phys. Rev.* **80**, 937 (1950)
- 6G49 L. V. Groshev and L. Y. Shavtvalov, *Doklady Akad. Nauk S.S.S.R.* **68**, 257 (1949)
- 7G51 M. A. Grace, R. A. Allen, D. West, and H. Halban, *Proc. Phys. Soc. (London)* **64A**, 493 (1951)
- 7G51a M. A. Grace and J. R. Prescott, *Phys. Rev.* **84**, 1059 (1951)
- 8G47 M. Guillot and M. Perey, *Compt. rend.* **225**, 330 (1947)
- 9G49 J. W. Gofman and G. T. Seaborg, *NNES-PPR* **14B**, 1427 (1949)
- 10G49 A. S. Goldin, G. B. Knight, P. A. Macklin, and R. L. Macklin, *Phys. Rev.* **76**, 336 (1949)
- 11G46 R. H. Goeckermann, P. R. O'Connor, and W. J. Knox, private communication (1946)
- 11G49 R. H. Goeckermann and I. Perlman, *Phys. Rev.* **76**, 628 (1949)
- 12G32 O. Gratias and C. H. Collie, *Proc. Roy. Soc. (London)* **135A**, 299 (1932)
- 13G44 A. Ghiorso, reported in Metallurgical Laboratory Classified Reports CK-1511 (April 1944); CS-1657 (May 1944)
- 13G45 A. Ghiorso, unpublished data (1945)
- 13G48 A. Ghiorso, W. W. Meinke, and G. T. Seaborg, *Phys. Rev.* **74**, 695 (1948)
- 13G48a A. Ghiorso, J. M. Hollander, and I. Perlman, U. S. Atomic Energy Commission Declassified Document AECD-2232 (July 1948)
- 13G48b A. Ghiorso, L. B. Magnusson, and G. T. Seaborg, unpublished data (July 1948)
- 13G48c A. Ghiorso, unpublished data (1948)
- 13G49 A. Ghiorso, W. W. Meinke, and G. T. Seaborg, *Phys. Rev.* **76**, 1414 (1949)

- 13G50 A. Ghiorso, R. A. James, L. O. Morgan, and G. T. Seaborg, *Phys. Rev.* **78**, 472 (1950)
- 13G51 A. Ghiorso, *Phys. Rev.* **82**, 979 (1951)
- 13G51a A. Ghiorso, J. W. Brittain, W. M. Manning, and G. T. Seaborg, *Phys. Rev.* **82**, 558 (1951)
- 13G51b A. Ghiorso, unpublished data (1951)
- 13G51c A. Ghiorso, S. G. Thompson, K. Street, Jr., and G. T. Seaborg, *Phys. Rev.* **81**, 154 (1951)
- 13G52 A. Ghiorso, G. H. Higgins, A. E. Larsh, G. T. Seaborg, and S. G. Thompson, *Phys. Rev.* **87**, 163 (1952) and private communication (Nov. 1952)
- 13G53 A. Ghiorso, unpublished rumor (1953)
- 14G49 R. L. Graham and D. H. Tomlin, *Nature* **164**, 278 (1949)
- 14G51 R. L. Graham and R. E. Bell, *Phys. Rev.* **83**, 222 (1951) (A)
- 14G51a R. L. Graham and R. E. Bell, *Phys. Rev.* **84**, 380 (1951)
- 14G52 R. L. Graham, J. L. Wolfson, and R. E. Bell, *Can. J. Phys.* **30**, 459 (1952)
- 14G53 R. L. Graham and R. E. Bell, *Can. J. Phys.* (to be published) (1953)
- 15G50 J. M. Grunlund, B. G. Harvey, N. Moss, and L. Yaffe, *Phys. Rev.* **78**, 69 (1950)
- 16G47 M. Goldblatt, E. S. Robinson, and R. W. Spence, *Phys. Rev.* **72**, 973 (1947)
- 17G49 E. R. Graves and D. I. Meyer, *Phys. Rev.* **76**, 183 (1949) (A)
- 18G38 M. Goldhaber, R. D. Hill, and L. Szilard, *Phys. Rev.* **55**, 47 (1939); *Nature* **142**, 521 (1938)
- 18G46 M. Goldhaber and R. D. O'Neal, private communication (Dec. 1946)
- 18G46a M. Goldhaber and W. J. Sturm, *Phys. Rev.* **70**, 111 (1946) (A)
- 18G46b M. Goldhaber, C. O. Muehlhause, and W. J. Sturm, reported in *Metallurgical Laboratory Classified Report CF-3574* (Oct. 1946)
- 18G46c M. Goldhaber, *Phys. Rev.* **70**, 89 (1946)
- 18G46d M. Goldhaber, L. Jacobs, and D. J. Williams, reported in *Argonne National Laboratory Classified Report CP-3647* (Nov. 1946)
- 18G47 M. Goldhaber and C. O. Muehlhause, reported in *Argonne National Laboratory Classified Report ANL-4010* (Sept. 1947)
- 18G47a M. Goldhaber, C. O. Muehlhause, and S. H. Turkel, *Phys. Rev.* **71**, 372 (1947)
- 18G48 M. Goldhaber and C. O. Muehlhause, *Phys. Rev.* **74**, 1877 (1948)
- 18G48a M. Goldhaber and C. O. Muehlhause, *Phys. Rev.* **74**, 1248 (1948) (A)
- 18G50 M. Goldhaber, private communication listed in *Natl. Bur. Standards Circular No. 499* (Sept. 1950)
- 18G51 M. Goldhaber, E. der Mateosian, G. Scharff-Goldhaber, A. W. Sunyar, M. Deutsch, and N. S. Wall, *Phys. Rev.* **83**, 661 (1951)
- 18G52 M. Goldhaber and R. D. Hill, *Revs. Modern Phys.* **24**, 179 (1952)
- 19G38 J. A. Gray, *Nature* **130**, 738 (1932)
- 19G36 J. A. Gray and J. F. Hinds, *Phys. Rev.* **49**, 477 (1936)
- 20G51 W. L. Gardner, N. Knable, and B. J. Moyer, *Phys. Rev.* **83**, 1054 (1951)
- 21G46 W. M. Good, D. Peaslee, and M. Deutsch, *Phys. Rev.* **69**, 313 (1946)
- 21G46a W. M. Good and W. C. Peacock, *Phys. Rev.* **69**, 680 (1946) (A)
- 22G49 P. J. Grant and J. M. Hill, *Nature* **163**, 524 (1949)
- 22G49a P. J. Grant and R. Richmond, *Nature* **163**, 840 (1949); *Proc. Phys. Soc. (London)* **62A**, 573 (1949)
- 22G50 P. J. Grant, *Proc. Phys. Soc. (London)* **63A**, 1298 (1950)
- 22G50a P. J. Grant, *Nature* **165**, 1018 (1950)
- 23G50 L. Gross and D. R. Hamilton, *Phys. Rev.* **80**, 484 (1950)
- 24G47 L. J. Goodman and M. L. Pool, *Phys. Rev.* **71**, 288 (1947)
- 25G51 M. L. Good, *Phys. Rev.* **83**, 1054 (1951)
- 25G51a M. L. Good, *Phys. Rev.* **81**, 891 (1951)
- 25G51b M. L. Good, *Phys. Rev.* **81**, 1058 (1951)
- 26G47 E. Gleditsch and T. Gráf, *Phys. Rev.* **72**, 640 (1947)
- 27G48 T. Gráf, *Phys. Rev.* **74**, 831 (1948)
- 27G50 T. Gráf, *Phys. Rev.* **79**, 1014 (1950)
- 27G51 T. Gráf, *Arkiv Fysik* **3**, 171 (1951)
- 28G41 A. Guthrie, *Phys. Rev.* **60**, 746 (1941)
- 28G48 A. Guthrie, private communication from K. Lark-Horowitz (1948)
- 29G43 J. Govaerts, *Bull. Soc. Roy. Sci. Liege* **12**, 555 (1943); *Chem. Zentr.* **1**, 634 (1944)
- 30G51 G. M. Griffiths, *Phys. Rev.* **83**, 852 (1951)
- 31G38 D. C. Grahame and G. T. Seaborg, *Phys. Rev.* **54**, 240 (1938) (A)
- 31G41 D. C. Grahame and H. J. Walke, *Phys. Rev.* **60**, 909 (1941)
- 32G49 D. N. Gideon, W. C. Miller, and B. Waldman, *Phys. Rev.* **75**, 329 (1949) (A)
- 33G46 L. E. Glendenin, reported in *J. Am. Chem. Soc.* **68**, 2411 (1946)
- 33G46a L. E. Glendenin and E. P. Steinberg, reported in *J. Am. Chem. Soc.* **68**, 2411 (1946)
- 33G47 L. E. Glendenin and R. R. Edwards, *Phys. Rev.* **71**, 742 (1947)
- 33G49 L. E. Glendenin, Ph.D. Thesis, Massachusetts Institute of Technology Unclassified Report NP-1242 (Dec. 1949)
- 33G51 L. E. Glendenin, *NNES-PPR* **9**, 596 (1951)
- 33G51a L. E. Glendenin, *NNES-PPR* **9**, 592 (Editor's note) (1951)
- 33G51b L. E. Glendenin, *NNES-PPR* **9**, 590 (Editor's note) (1951)
- 33G51c L. E. Glendenin and C. D. Coryell, *NNES-PPR* **9**, 687 (1951)
- 33G51e L. E. Glendenin, *NNES-PPR* **9**, 773 (1951)
- 33G51f L. E. Glendenin and E. P. Steinberg, *NNES-PPR* **9**, 793 (1951)
- 33G51g L. E. Glendenin, *NNES-PPR* **9**, 849 (1951)
- 33G51h L. E. Glendenin, *NNES-PPR* **9**, 895 (1951)
- 33G51i L. E. Glendenin, *NNES-PPR* **9**, 979 (Editor's note) (1951)
- 33G51j L. E. Glendenin and R. P. Metcalf, *NNES-PPR* **9**, 992 (1951)
- 33G51k L. E. Glendenin and J. D. Knight, *NNES-PPR* **9**, 1074 (1951)
- 33G51l L. E. Glendenin, *NNES-PPR* **9**, 1931 (1951)
- 33G51m L. E. Glendenin, *NNES-PPR* **9**, 1092 (1951)
- 33G51n L. E. Glendenin and R. P. Metcalf, *NNES-PPR* **9**, 1067 (1951)
- 33G53 L. E. Glendenin and E. P. Steinberg, *Phys. Rev.* (to be published) (1953)
- 34G46 N. Goldstein and W. Spatz, reported in *Metallurgical Laboratory Classified Report CF-3574* (Oct. 1946)
- 35G40 A. P. Grinberg and L. I. Roussinow, *Phys. Rev.* **58**, 181 (1940)
- 36G40 G. N. Glasoe and J. Steigman, *Phys. Rev.* **58**, 1 (1940)
- 37G51 K. Geiger, *Ann. Physik* **9**, 293 (1951); *Z. Naturforsch.* **6a**, 54 (1951)

- 37G52 K. Geiger, *Z. Naturforsch.* 7a, 579 (1952)
- 38G46 W. E. Grummitt and G. Wilkinson, *Nature* 158, 163 (1946)
- 38G47 W. E. Grummitt, J. Gueron, G. Wilkinson, and L. Yaffe, *Can. J. Research* 25B, 357, 364 (1947)
- 38G48 W. E. Grummitt and G. Wilkinson, *Nature* 161, 520 (1948)
- 38G51 W. E. Grummitt and G. Wilkinson, Chalk River Laboratory Declassified Report CRC-470 (March 1951)
- 39G43 B. L. Goldschmidt and F. Morgan, National Research Council of Canada, Atomic Energy Project Report MC-11 (Aug. 1943)
- 39G46 B. L. Goldschmidt and I. Perlman, reported in *J. Am. Chem. Soc.* 68, 2411 (1946)
- 39G51 B. L. Goldschmidt and I. Perlman, *NNES-PPR* 9, 709 (1951)
- 39G51a B. L. Goldschmidt and I. Perlman, *NNES-PPR* 9, 790 (1951)
- 40G40 H. Götte, *Naturwiss.* 28, 449 (1940)
- 40G41 H. Götte, *Naturwiss.* 29, 496 (1941)
- 40G42 H. Götte, *Naturwiss.* 30, 108 (1942)
- 40G43 H. Götte, reported in (16H43b)
- 40G46 H. Götte, *Z. Naturforsch.* 1, 377 (1946)
- 41G44 G. R. Gamertsfelder, *Phys. Rev.* 66, 288 (1944)
- 42G47 P. C. Gugelot, O. Huber, H. Medicus, P. Preiswerk, P. Scherrer, and R. Steffen, *Helv. Phys. Acta* 19, 418 (1947); 20, 240 (1947)
- 43G48 H. F. Gunlock and M. L. Pool, *Phys. Rev.* 74, 1264 (1948)
- 44G49 J. R. Gum, L. E. Thompson, and M. L. Pool, *Phys. Rev.* 76, 184 (1949) (A)
- 44G50 J. R. Gum and M. L. Pool, *Phys. Rev.* 80, 315 (1950)
- 45G50 M. Goodrich and E. C. Campbell, *Phys. Rev.* 79, 418 (1950) (A)
- 45G51 M. Goodrich, reported in Oak Ridge National Laboratory Unclassified Report ORNL-940 (March 1951)
- 45G51a M. Goodrich, *Phys. Rev.* 82, 759 (1951)
- 45G52 M. Goodrich and E. C. Campbell, *Phys. Rev.* 85, 742 (1952) (A) and private communication (Nov. 1952)
- 46G36 E. R. Gaerttner, J. J. Turin, and H. R. Crane, *Phys. Rev.* 49, 793 (1936)
- 47G50 P. S. Gill, C. E. Mandeville, and E. Shapiro, *Phys. Rev.* 80, 284 (1950); *Indian J. Phys.* 33, 566 (1950)
- 48G48 S. N. Ghoshal, *Phys. Rev.* 73, 417 (1948)
- 48G50 S. N. Ghoshal, *Phys. Rev.* 80, 939 (1950)
- 49G50 G. J. Goldsmith and E. Bleuler, *J. Phys. Colloid Chem.* 54, 717 (1950)
- 50G47 A. C. Graves and R. L. Walker, *Phys. Rev.* 71, 1 (1947)
- 51G52 M. J. Glaubman and F. R. Metzger, *Phys. Rev.* 87, 203 (1952) (A)
- 52G51 A. Goldstein, *NNES-PPR* 9, 1096 (1951)
- 52G51a A. Goldstein, R. P. Schuman, and W. Robinson, *NNES-PPR* 9, 1188 (1951)
- 53G51 M. M. Grandsden and W. S. Boyle, *Phys. Rev.* 82, 447 (1951)
- 54G51 H. Gest and R. R. Edwards, *NNES-PPR* 9, 1144 (1951)
- 55G50 S. Geschwind, H. Minden, and C. H. Townes, *Phys. Rev.* 78, 174 (1950)
- 56G49 R. L. Garwin, *Phys. Rev.* 76, 1876 (1949)
- 57G51 D. H. Greenberg and J. M. Miller, *Phys. Rev.* 84, 845 (1951)
- 58G51 D. Green and J. R. Richardson, *Phys. Rev.* 83, 891 (1951) (A)
- 59G52 G. A. Graves, L. M. Langer, and R. D. Moffat, *Phys. Rev.* 88, 344 (1952)
- 1H48 W. F. Hornyak, C. B. Dougherty, and T. Lauritsen, *Phys. Rev.* 74, 1727 (1948)
- 1H49 W. F. Hornyak, T. Lauritsen, and V. K. Rasmussen, *Phys. Rev.* 76, 731 (1949)
- 1H50 W. F. Hornyak and T. Lauritsen, *Phys. Rev.* 77, 160 (1950)
- 2H41 A. C. Helmholtz, *Phys. Rev.* 60, 415 (1941)
- 2H41a A. C. Helmholtz, C. Pecher, and P. R. Stout, *Phys. Rev.* 59, 902 (1941)
- 2H41b A. C. Helmholtz, *Phys. Rev.* 60, 160 (1941) (A)
- 2H42 A. C. Helmholtz, *Phys. Rev.* 62, 301 (1942) (A)
- 2H42a A. C. Helmholtz, *Phys. Rev.* 61, 204 (1942) (A)
- 2H46 A. C. Helmholtz, *Phys. Rev.* 70, 982 (1946)
- 2H48 A. C. Helmholtz and C. L. McGinnis, *Phys. Rev.* 74, 1559 (1948) (A)
- 3H50 J. A. Harvey, reported in Massachusetts Institute of Technology Progress Report NP-1586 (April 1950)
- 4H47 F. Hagemann, L. I. Katzin, M. H. Studier, A. Ghiorso, and G. T. Seaborg, *Phys. Rev.* 72, 252 (1947)
- 4H47a F. Hagemann, reported in Argonne National Laboratory Classified Report CC-3780 (March 1947)
- 4H50 F. Hagemann, *Phys. Rev.* 79, 534 (1950)
- 4H50a F. Hagemann, L. I. Katzin, M. H. Studier, G. T. Seaborg, and A. Ghiorso, *Phys. Rev.* 79, 435 (1950)
- 5H46 J. J. Howland, D. H. Templeton, and I. Perlman, University of California Radiation Laboratory Declassified Report BC-31 (Nov. 1946)
- 6H36 F. A. Heyn, *Nature* 138, 723 (1936)
- 6H37 F. A. Heyn, *Nature* 139, 842 (1937)
- 6H37a F. A. Heyn, *Physica* 4, 160 (1937)
- 6H37b F. A. Heyn, *Physica* 4, 1224 (1937)
- 6H39 F. A. Heyn, A. H. W. Aten, Jr., and C. J. Bakker, *Nature* 143, 516 (1939)
- 7H49 A. O. Hanson, R. B. Duffield, J. D. Knight, B. C. Diven, and H. Palevsky, *Phys. Rev.* 76, 578 (1949)
- 8H48 E. K. Hyde, M. H. Studier, and R. J. Bruehlman, reported in Argonne National Laboratory Classified Report ANL-4112 (March 1948)
- 8H48a E. K. Hyde and M. H. Studier, reported in Argonne National Laboratory Memorandum ANL-WMM-445 (Dec. 1948)
- 8H48b E. K. Hyde and M. H. Studier, Argonne National Laboratory Classified Report ANL-4182 (Aug. 1948)
- 8H49 E. K. Hyde, M. H. Studier, and A. Ghiorso, *NNES-PPR* 14B, 1622 (1949)
- 8H49a E. K. Hyde, M. H. Studier, H. H. Hopkins, Jr., and A. Ghiorso, *NNES-PPR* 14B, 1439 (1949)
- 8H49b E. K. Hyde, *NNES-PPR* 14B, 1435 (1949)
- 8H50 E. K. Hyde, A. Ghiorso, and G. T. Seaborg, *Phys. Rev.* 77, 765 (1950)
- 8H50a E. K. Hyde and A. Ghiorso, University of California Radiation Laboratory Unclassified Report UCRL-593 (Feb. 1950)
- 8H51 E. K. Hyde, A. Ghiorso, and G. T. Seaborg, unpublished results (Aug. 1951)
- 8H51a E. K. Hyde and A. Ghiorso, unpublished data (May 1951)
- 8H51b E. K. Hyde and G. D. O'Kelley, *Phys. Rev.* 82, 944 (1951)
- 8H52 E. K. Hyde, private communication (May 1952)

- 8H52a E. K. Hyde, NRES-PPR 17B, 46 (1952) (classified)
- 8H52b E. K. Hyde and H. B. Mathur, private communication (June 1952)
- 8H52c E. K. Hyde and F. Asaro, private communication (Dec. 1952)
- 8H53 E. K. Hyde and A. Ghiorso, Phys. Rev. (to be published) (1953); University of California Radiation Laboratory Unclassified Report UCRL-2019 (Nov. 1952)
- 9H38 M. G. Holloway and M. S. Livingston, Phys. Rev. 54, 18 (1938). Summarizes results of various investigators.
- 10H51 C. M. Huddleston and A. B. Smith, Phys. Rev. 84, 289 (1951)
- 10H52 C. M. Huddleston and A. C. G. Mitchell, Phys. Rev. (in press) (1952)
- 11H48 J. M. Hill, Proc. Cambridge Phil. Soc. 44, 440 (1948)
- 11H50 J. M. Hill and L. R. Shepherd, Proc. Phys. Soc. (London) 63A, 126 (1950)
- 12H50 A. Hedgran, K. Siegbahn, and N. Svartholm, Proc. Phys. Soc. (London) 63A, 960 (1950)
- 12H51 A. Hedgran, Phys. Rev. 82, 128 (1951)
- 12H51a A. Hedgran and S. Thulin, Phys. Rev. 81, 1072 (1951)
- 12H52 A. Hedgran and D. Lind, Arkiv Fysik 5, 177 (1952)
- 13H50 J. M. Hollander, A. Ghiorso, and I. Perlman, reported in University of California Radiation Laboratory Classified Report UCRL-923 (Sept. 1950)
- 13H50a J. M. Hollander and R. F. Leininger, Phys. Rev. 80, 915 (1950)
- 13H51 J. M. Hollander, Ph.D. Thesis, University of California Radiation Laboratory Unclassified Report UCRL-1396 (July 1951)
- 14H34 W. J. Henderson, Proc. Roy. Soc. (London) 147A, 572 (1934)
- 14H37 W. J. Henderson, L. N. Ridenour, M. G. White, and M. C. Henderson, Phys. Rev. 51, 1107 (1937)
- 14H37a W. J. Henderson and L. N. Ridenour, Phys. Rev. 52, 40 (1937)
- 14H39 W. J. Henderson and R. L. Doran, Phys. Rev. 56, 123 (1939)
- 15H45 N. Hole, Arkiv Mat., Astron. Fysik 32A, No. 3 (1945)
- 15H45a N. Hole, Arkiv Mat., Astron. Fysik 31B, No. 9 (1945)
- 15H46 N. Hole and K. Siegbahn, Arkiv Mat., Astron. Fysik 33A, No. 9 (1946)
- 15H47 N. Hole, Arkiv Mat., Astron. Fysik 34B, No. 5 (1947)
- 15H47a N. Hole, Arkiv Mat., Astron. Fysik 34B, No. 19 (1947)
- 15H48 N. Hole, Arkiv Mat., Astron. Fysik 36A, No. 2 (1948)
- 15H48a N. Hole, Arkiv Mat., Astron. Fysik 36A, No. 9 (1948)
- 15H48b N. Hole, J. Benes, and A. Hedgran, Arkiv Mat., Astron. Fysik 35A, No. 35 (1948)
- 16H24 O. Hahn and L. Meitner, Z. Physik 26, 161 (1924)
- 16H25 O. Hahn and L. Meitner, Z. Physik 34, 795 (1925)
- 16H37a O. Hahn, F. Strassmann, and E. Walling, Naturwiss. 25, 189 (1937)
- 16H39 O. Hahn and F. Strassmann, Naturwiss. 27, 11 (1939)
- 16H39a O. Hahn and F. Strassmann, Naturwiss. 27, 529 (1939)
- 16H39b O. Hahn and F. Strassmann, Physik Z. 40, 673 (1939)
- 16H39c O. Hahn and F. Strassmann, Naturwiss. 27, 89 (1939)
- 16H39d O. Hahn, F. Strassmann, and S. Flüge, Naturwiss. 27, 544 (1939)
- 16H39e O. Hahn and F. Strassmann, Naturwiss. 27, 451 (1939)
- 16H40 O. Hahn and F. Strassmann, Naturwiss. 28, 61 (1940)
- 16H40a O. Hahn and F. Strassmann, Naturwiss. 28, 54 (1940)
- 16H40b O. Hahn and F. Strassmann, Naturwiss. 28, 455 (1940)
- 16H40c O. Hahn and F. Strassmann, Naturwiss. 28, 543 (1940)
- 16H41 O. Hahn and F. Strassmann, Naturwiss. 29, 369 (1941)
- 16H41a O. Hahn and F. Strassmann, Naturwiss. 29, 285 (1941)
- 16H41b O. Hahn and F. Strassmann, Z. Physik 117, 789 (1941)
- 16H42 O. Hahn, F. Strassmann, and H. Götte, Abhandl. preuss. Akad. Wiss. Math.-naturw. Klasse, No. 3 (1942)
- 16H42a O. Hahn and F. Strassmann, Naturwiss. 30, 324 (1942)
- 16H43 O. Hahn and F. Strassmann, Naturwiss. 31, 249 (1943)
- 16H43a O. Hahn and F. Strassmann, Z. Physik 121, 729 (1943)
- 16H43b O. Hahn and F. Strassmann, Naturwiss. 31, 499 (1943)
- 17H50 K. L. Hall and D. H. Templeton, University of California Radiation Laboratory Unclassified Report UCRL-957 (Oct. 1950)
- 17H51 K. L. Hall and D. H. Templeton, unpublished data (Aug. 1951)
- 17H51a K. L. Hall, University of California Radiation Laboratory Unclassified Report UCRL-1460 (Aug. 1951)
- 18H50 W. J. Heiman and A. Voigt, Iowa State College Unclassified Report ISC-89 (June 1950)
- 18H51 W. J. Heiman and D. F. Martin, unpublished data (Aug. 1951)
- 19H50 M. Heerschap, O. P. Hok, and G. J. Sizoo, Physica 16, 767 (1950)
- 20H49a B. G. Harvey and N. Moss, reported in Chalk River Laboratory Report CRR-427 (Dec. 1949)
- 20H50 B. G. Harvey and B. I. Parsons, Phys. Rev. 80, 1098 (1950)
- 20H52 B. G. Harvey, private communication to S. G. Thompson (Feb. 1952)
- 20H52a B. G. Harvey, Phys. Rev. 85, 482 (1952)
- 21H41 E. Haggstrom, Phys. Rev. 59, 322 (1941)
- 22H45 J. Halperin and D. E. Koshland, Jr., Clinton Laboratory Classified Report CN-3422x (June 1945)
- 23H52 G. H. Higgins and K. Street, Jr., Phys. Rev. 86, 252 (1952)
- 23H52a G. H. Higgins, Ph.D. Thesis, University of California Radiation Laboratory Unclassified Report UCRL-1796 (June 1952)
- 24H49 G. C. Hanna and B. Pontecorvo, Phys. Rev. 75, 983 (1949)
- 24H50 G. C. Hanna, B. G. Harvey, and N. Moss, Phys. Rev. 78, 617 (1950)
- 24H51 G. C. Hanna, B. G. Harvey, N. Moss, and P. R. Tunnicliffe, Phys. Rev. 81, 466 (1951)
- 25H51 E. K. Hulet, S. G. Thompson, A. Ghiorso, and K. Street, Jr., Phys. Rev. 84, 366 (1951)
- 25H53 E. K. Hulet, S. G. Thompson, and A. Ghiorso, Phys. Rev. (to be published) (1953)
- 26H51 D. R. Hamilton, W. P. Alford, and L. Gross, Phys. Rev. 83, 215 (1951) (A)
- 27H49 J. E. R. Holmes, Proc. Phys. Soc. (London) 62A, 293 (1949)
- 28H46 D. J. Hughes and C. Egger, private communication (Oct. 1946)
- 28H46a D. J. Hughes and W. D. B. Spatz, private communication (Oct. 1946)
- 28H46b D. J. Hughes, J. Wallace, E. Goldfarb, C. Egger, H. Murdock, and N. Goldstein, reported in Argonne National Laboratory Classified Reports CP-3647 (Nov. 1946); CF-3574 (Oct. 1946)
- 28H47 D. J. Hughes, D. Hall, C. Egger, and E. Goldfarb, Phys. Rev. 72, 646 (1947)
- 28H47a D. J. Hughes, C. Egger, and C. M. Huddleston, Phys. Rev. 71, 269 (1947)
- 28H47b D. J. Hughes, C. Egger, and N. Goldstein, reported in Argonne National Laboratory Classified Report CP-3801 (May 1947)
- 28H48 D. J. Hughes and C. Egger, Phys. Rev. 73, 809 (1948)

- 28H48a D. J. Hughes, J. Dabbs, A. Cahn, and D. Hall, *Phys. Rev.* 73, 111 (1948)
- 28H49 D. J. Hughes, C. Egger, and C. M. Huddleston, *Phys. Rev.* 75, 515 (1949)
- 29H50 T. H. Handley, reported in Oak Ridge National Laboratory Classified Report ORNL-867 (Dec. 1950)
- 30H48 F. L. Hereford, *Phys. Rev.* 74, 574 (1948)
- 31H48 R. C. Hawkings, R. F. Hunter, W. B. Mann, and W. H. Stevens, *Phys. Rev.* 74, 696 (1948)
- 31H49 R. C. Hawkings, R. F. Hunter, W. B. Mann, and W. H. Stevens, *Can. J. Research* 27B, 545 (1949)
- 32H50 E. L. Hudspeth, C. P. Swann, and N. P. Heydenburg, *Phys. Rev.* 77, 736 (1950)
- 32H50a E. L. Hudspeth, C. P. Swann, and N. P. Heydenburg, *Phys. Rev.* 80, 643 (1950)
- 32H50b E. L. Hudspeth and C. P. Swann, *Phys. Rev.* 78, 337 (1950) (A)
- 32H52 E. L. Hudspeth, W. B. Rose, and N. P. Heydenburg, *Phys. Rev.* 85, 742 (1952) (A)
- 33H35 L. R. Hafstad and M. A. Tuve, *Phys. Rev.* 48, 306 (1935)
- 34H41 O. Huber, O. Lienhard, P. Scherrer, and H. Wäffler, *Phys. Rev.* 60, 910 (1941)
- 34H42 O. Huber, O. Lienhard, P. Scherrer, and H. Wäffler, *Helv. Phys. Acta* 15, 312 (1942)
- 34H43 O. Huber, O. Lienhard, P. Scherrer, and H. Wäffler, *Helv. Phys. Acta* 16, 33 (1943)
- 34H43a O. Huber, O. Lienhard, P. Scherrer, and H. Wäffler, *Helv. Phys. Acta* 16, 431 (1943)
- 34H43b O. Huber, O. Lienhard, and H. Wäffler, *Helv. Phys. Acta* 16, 226 (1943)
- 34H44 O. Huber, O. Lienhard, and H. Wäffler, *Helv. Phys. Acta* 17, 195 (1944)
- 34H44a O. Huber, O. Lienhard, P. Scherrer, and H. Wäffler, *Helv. Phys. Acta* 17, 139 (1944)
- 34H45 O. Huber, O. Lienhard, P. Scherrer, and H. Wäffler, *Helv. Phys. Acta* 18, 221 (1945)
- 34H47 O. Huber, H. Medicus, P. Preiswerk, and R. Steffen, *Helv. Phys. Acta* 20, 495 (1947)
- 34H48 O. Huber, P. Marmier, H. Medicus, P. Preiswerk, and R. Steffen, *Phys. Rev.* 73, 1208 (1948)
- 34H48a O. Huber, R. Steffen, and F. Humbel, *Helv. Phys. Acta* 21, 192 (1948)
- 34H49 O. Huber, R. Rütschi, and P. Scherrer, *Helv. Phys. Acta* 22, 375 (1949)
- 34H51 O. Huber, F. Humbel, H. Schneider, and A. de Shalit, *Helv. Phys. Acta* 24, 127, 629 (1951)
- 34H52 O. Huber, F. Humbel, H. Schneider, and A. de Shalit, *Helv. Phys. Acta* 25, 3 (1952)
- 34H52a O. Huber, R. Joly, P. Scherrer, and N. F. Verster, *Helv. Phys. Acta* 25, 621 (1952) and private communication (Sept. 1952)
- 35H34 M. C. Henderson, M. S. Livingston, and E. O. Lawrence, *Phys. Rev.* 45, 428 (1934)
- 35H35 M. C. Henderson, *Phys. Rev.* 48, 855 (1935)
- 36H49 E. Hayward, *Phys. Rev.* 75, 917 (1949)
- 37H35 O. Haxel, *Z. Physik* 93, 400 (1935)
- 37H48 O. Haxel, F. G. Houtermans, and M. Kemmerich, *Phys. Rev.* 74, 1886 (1948)
- 37H48a O. Haxel and F. G. Houtermans, *Z. Physik* 124, 705 (1948)
- 38H46 Zah-Wei Ho, *Phys. Rev.* 70, 782 (1946)
- 38H48 Zah-Wei Ho, *Compt. rend.* 226, 1187 (1948)
- 39H39 J. E. Hill and G. E. Valley, *Phys. Rev.* 55, 678 (1939) (A)
- 39H40 J. E. Hill, *Phys. Rev.* 57, 567 (1940) (A)
- 40H37 A. Hemmendinger and W. R. Smythe, *Phys. Rev.* 51, 1052 (1937)
- 40H40 A. Hemmendinger, *Phys. Rev.* 58, 929 (1940)
- 40H49 A. Hemmendinger, *Phys. Rev.* 75, 1267 (1949)
- 41H49 S. G. Hughes and W. E. Stephens, *Phys. Rev.* 75, 1286 (1949) (A)
- 42H46 O. Hirzel and H. Wäffler, *Helv. Phys. Acta* 19, 216 (1946)
- 42H46a O. Hirzel and H. Wäffler, *Helv. Phys. Acta* 19, 214 (1946)
- 42H47 O. Hirzel and H. Wäffler, *Helv. Phys. Acta* 20, 373 (1947)
- 42H47a O. Hirzel, P. Stoll, and H. Wäffler, *Helv. Phys. Acta* 20, 241 (1947)
- 42H48 O. Hirzel and H. Wäffler, *Phys. Rev.* 74, 1553 (1948)
- 43H47 D. C. Hess, Jr., R. J. Hayden, and M. G. Inghram, *Phys. Rev.* 72, 730 (1947)
- 43H48 D. C. Hess, Jr., *Phys. Rev.* 74, 773 (1948)
- 43H49 D. C. Hess, Jr. and M. G. Inghram, *Phys. Rev.* 76, 1717 (1949)
- 44H43 R. H. Hendricks, L. C. Bryner, M. D. Thomas, and J. O. Ivie, *J. Phys. Chem.* 47, 469 (1943)
- 45H51 R. B. Heller, E. F. Sturcken, and A. H. Weber, *Phys. Rev.* 83, 848 (1951)
- 46H40 J. B. Hoag, *Phys. Rev.* 57, 937 (1940)
- 47H37 D. G. Hurst and H. Walke, *Phys. Rev.* 51, 1033 (1937)
- 47H40 D. G. Hurst, R. Latham, and W. B. Lewis, *Proc. Roy. Soc. (London)* 174A, 126 (1940)
- 48H48 H. H. Hopkins, Jr. and B. B. Cunningham, private communication (Aug. 1948)
- 48H48a H. H. Hopkins, Jr. and B. B. Cunningham, *Phys. Rev.* 73, 1406 (1948)
- 48H49 H. H. Hopkins, Jr., Ph.D. Thesis, University of California Radiation Laboratory Report UCRL-312 (March 1949)
- 48H50 H. H. Hopkins, Jr., *Phys. Rev.* 77, 717 (1950)
- 49H49 R. N. H. Haslam, L. Katz, H. E. Johns, and H. J. Moody, *Phys. Rev.* 76, 704 (1949)
- 49H50 R. N. H. Haslam, L. Katz, H. J. Moody, and H. M. Skarsgard, *Phys. Rev.* 80, 318 (1950)
- 49H51 R. N. H. Haslam, L. A. Smith, and J. G. V. Taylor, *Phys. Rev.* 84, 840 (1951)
- 49H51a R. N. H. Haslam and H. M. Skarsgard, *Phys. Rev.* 81, 479 (1951)
- 50H51 V. Hummel and B. Hammermesh, *Phys. Rev.* 82, 67 (1951)
- 51H43 J. G. Hamilton, reported in Metallurgical Project Classified Report (work performed at Berkeley) CH-843 (Aug. 1943)
- 51H48 J. G. Hamilton, private communication (Sept. 1948)
- 52H38 M. Heyden and W. Wefelmeier, *Naturwiss.* 26, 612 (1938)
- 53H43 C. T. Hibdon, M. L. Pool, and J. D. Kurbatov, *Phys. Rev.* 63, 462 (1943) (A)
- 53H44 C. T. Hibdon, M. L. Pool, and J. D. Kurbatov, *Phys. Rev.* 65, 351 (1944) (A)
- 53H45 C. T. Hibdon, M. L. Pool, and J. D. Kurbatov, *Phys. Rev.* 67, 289 (1945)
- 53H45a C. T. Hibdon and M. L. Pool, *Phys. Rev.* 67, 313 (1945)
- 54H43 E. B. Hales and E. B. Jordan, *Phys. Rev.* 64, 202 (1943)
- 55H50 R. Hofstadter and J. A. McIntyre, *Phys. Rev.* 80, 631 (1950)
- 56H48 S. K. Haynes, *Phys. Rev.* 74, 423 (1948)
- 57H51 P. Hubert, *J. phys. et radium* 12, 823 (1951)
- 57H51a P. Hubert and J. Laberrigue-Frolow, *Compt. rend.* 232, 2420 (1951)
- 57H51b P. Hubert, *Compt. rend.* 232, 2201 (1951)
- 58H51 E. J. Hoagland and N. Sugarman, *NNES-PPR* 9, 642 (1951)

- 58H51a E. J. Hoagland and N. Sugarman, *NNES-PPR* 9, 635 (1951)
- 58H51b E. J. Hoagland and S. Katcoff, *NNES-PPR* 9, 660 (1951)
- 58H51c E. J. Hoagland and N. Sugarman, *NNES-PPR* 9, 1031 (1951)
- 59H40 J. O. Hancock and J. C. Butler, *Phys. Rev.* 57, 1088 (1940) (A)
- 60H46 R. J. Hayden and M. G. Inghram, *Phys. Rev.* 70, 89 (1946)
- 60H46a R. J. Hayden and L. G. Lewis, *Phys. Rev.* 70, 111 (1946) (A)
- 60H48 R. J. Hayden, *Phys. Rev.* 74, 650 (1948)
- 60H49 R. J. Hayden, J. H. Reynolds, and M. G. Inghram, *Phys. Rev.* 75, 1500 (1949)
- 60H50 R. J. Hayden, D. C. Hess, Jr., and M. G. Inghram, *Phys. Rev.* 77, 299 (1950)
- 61H49 R. W. Hayward and A. C. Helmholtz, *Phys. Rev.* 75, 1469 (1949) (A)
- 61H50 R. W. Hayward, *Phys. Rev.* 79, 541 (1950)
- 61H50a R. W. Hayward, *Phys. Rev.* 79, 542 (1950)
- 61H50b R. W. Hayward, *Phys. Rev.* 79, 409 (1950)
- 61H52 R. W. Hayward, *Phys. Rev.* 85, 760 (1952) (A) and private communication (Oct. 1952)
- 61H52a R. W. Hayward, *Phys. Rev.* 87, 202 (1952) (A) and private communication (Oct. 1952)
- 62H49 J. E. Hudgens, Jr. and W. S. Lyon, *Phys. Rev.* 75, 206 (1949)
- 63H48 R. E. Hein and A. F. Voigt, *Phys. Rev.* 74, 1265 (1948) (A)
- 63H50 R. E. Hein and A. F. Voigt, *Phys. Rev.* 79, 783 (1950)
- 63H52 R. E. Hein, C. M. Fowler, and R. H. McFarland, *Phys. Rev.* 85, 138 (1952)
- 64H52 R. A. House, R. L. Colligan, D. N. Kundu, and M. L. Pool, *Phys. Rev.* 86, 654 (1952) (A)
- 65H44 L. K. Hurst and M. L. Pool, *Phys. Rev.* 65, 60 (1944) (A)
- 65H44a L. K. Hurst and M. L. Pool, *Phys. Rev.* 65, 351 (1944) (A)
- 66H49 R. A. Hinshaw and M. L. Pool, *Phys. Rev.* 76, 358 (1949)
- 67H48 R. D. Hill and J. W. Mihelich, *Phys. Rev.* 74, 1874 (1948)
- 67H48a R. D. Hill, *Phys. Rev.* 74, 78 (1948)
- 67H48b R. D. Hill and W. E. Meyerhof, *Phys. Rev.* 73, 812 (1948)
- 67H49 R. D. Hill, *Phys. Rev.* 76, 333 (1949)
- 67H49a R. D. Hill, G. Scharff-Goldhaber, and G. Friedlander, *Phys. Rev.* 75, 324 (1949)
- 67H50 R. D. Hill, *Phys. Rev.* 79, 413 (1950)
- 67H50a R. D. Hill and J. W. Mihelich, *Phys. Rev.* 79, 275 (1950)
- 67H51 R. D. Hill, *Phys. Rev.* 83, 865 (1951)
- 67H51a R. D. Hill and F. R. Metzger, *Phys. Rev.* 83, 455 (1951)
- 67H51b R. D. Hill, G. Scharff-Goldhaber, and M. McKeown, *Phys. Rev.* 84, 382 (1951)
- 67H51c R. D. Hill, *Phys. Rev.* 82, 449 (1951)
- 67H51d R. D. Hill, *Phys. Rev.* 81, 470 (1951)
- 67H52 R. D. Hill, P. Axel, and A. W. Sunyar, private communication (Sept. 1952)
- 67H53 R. D. Hill and J. W. Mihelich, *Phys. Rev.* (to be published) (1953)
- 68H51 B. Hammermesh and V. Hummel, *Phys. Rev.* 84, 381 (1951)
- 68H52 B. Hammermesh, V. Hummel, L. Goodman, and D. Engelkemeir, *Phys. Rev.* 87, 528 (1952)
- 69H41 D. E. Hull and H. Seelig, *Phys. Rev.* 60, 553 (1941)
- 70H52 B. G. Hogg and H. E. Duckworth, *Phys. Rev.* 86, 567 (1952)
- 71H32 G. Hevesy and M. Pahl, *Nature* 130, 846 (1932)
- 71H35 G. Hevesy and H. Levi, *Nature* 135, 580 (1935)
- 71H36 G. Hevesy and H. Levi, *Kgl. Danske Videnskab. Selskab, Mat.-fys. Medd.* 14, No. 5 (1936); *Nature* 137, 185 (1936)
- 71H38 G. Hevesy and H. Levi, *Kgl. Danske Videnskab. Selskab, Mat.-fys. Medd.* 15, No. 11 (1938)
- 72H35 R. Hosemann, *Z. Physik* 99, 405 (1935)
- 73H49 C. Haenny, M. Najar, and M. Gailloud, *Helv. Phys. Acta* 22, 611 (1949)
- 74H51 R. W. Hoff, J. O. Rasmussen, and S. G. Thompson, *Phys. Rev.* 83, 1068 (1951)
- 74H52 R. W. Hoff, unpublished data (July 1952)
- 74H52a R. W. Hoff and F. Asaro, private communication (Aug. 1952)
- 75H49 R. F. Hibbs, U. S. Atomic Energy Commission Unclassified Report AECU-556 (Aug. 1949)
- 76H40 F. G. Houtermans, *Naturwiss.* 28, 578 (1940)
- 76H50 F. G. Houtermans, O. Haxel, and J. Heintze, *Z. Physik* 128, 657 (1950)
- 77H51 J. Hatton, B. V. Rollin, and E. F. W. Seymour, *Phys. Rev.* 83, 672 (1951)
- 78H52 R. B. Holt, R. N. Thorn, and R. W. Wanick, *Phys. Rev.* 87, 378 (1952)
- 79H52 B. C. Haldar, *Phys. Rev.* 87, 158 (1952)
- 80H52 R. L. Heath and P. R. Bell, *Phys. Rev.* 87, 176 (1952) (A)
- 80H52a R. L. Heath, *Phys. Rev.* 87, 1132 (1952)
- 81H52 J. R. Huizenga and K. F. Flynn, private communication (June 1952)
- 81H52a J. R. Huizenga, D. W. Engelkemeir, and P. R. Fields, private communication (June 1952)
- 82H52 N. M. Hintz, *Phys. Rev.* 86, 1042 (1952)
- 83H52 W. A. Hardy, G. Silvey, and C. H. Townes, *Phys. Rev.* 85, 494 (1952)
- 84H51 H. R. Haymond, W. R. Garrison, and J. G. Hamilton, *J. Chem. Phys.* 19, 382 (1951)
- 85H52 R. B. Holtzman and N. Sugarman, *Phys. Rev.* 87, 633 (1952)
- 86H52 R. J. Horsley, R. N. H. Haslam, and H. E. Johns, *Phys. Rev.* 87, 756 (1952)
- 87H33 W. D. Harkins, D. M. Gans, and H. W. Newson, *Phys. Rev.* 44, 529 (1933)
- 88H52 L. Hsiao and R. B. Duffield, private communication (Oct. 1952)
- 89H52 N. J. Hopkins, *Phys. Rev.* 88, 680 (1952)
- 91H52 E. P. Hincks and C. H. Millar, Abstract 106, June Meeting, Roy. Soc. Canada (1952)
- 92H39 H. v. Halban, Jr., F. Joliot, and L. Kowarski, *Nature* 143, 470, 680 (1939)
- 93H52 J. R. Haskins, J. E. Duval, L. S. Cheng, and J. D. Kurbatov, *Phys. Rev.* 88, 876 (1952)
- 93H52a J. R. Haskins and J. D. Kurbatov, *Phys. Rev.* 88, 884 (1952)
- 94H52 D. R. Hutchinson and M. L. Wiedenbeck, *Phys. Rev.* 88, 699 (1952)

- 1151 H. I. Israel and R. G. Wilkinson, *Phys. Rev.* **83**, 1051 (1951)
- 1152 H. I. Israel, *Phys. Rev.* **88**, 682 (1952)
- 1153 H. I. Israel, C. H. Pruett, and R. G. Wilkinson, *Phys. Rev.* (to be published) (1953)
- 2139 J. W. Irvine, Jr., *Phys. Rev.* **55**, 1105 (1939)
- 2142 J. W. Irvine, Jr., *J. Phys. Chem.* **46**, 910 (1942)
- 2146 J. W. Irvine, Jr., Oak Ridge National Laboratory Classified Report Mon C-142 (Sept. 1946)
- 3146 M. G. Inghram and R. J. Hayden, U. S. Atomic Energy Commission Declassified Document MDDC-525 (Dec. 1946)
- 3147 M. G. Inghram, D. C. Hess, Jr., and R. J. Hayden, *Phys. Rev.* **72**, 1269 (1947)
- 3147a M. G. Inghram, R. J. Hayden, and D. C. Hess, Jr., *Phys. Rev.* **72**, 349, 967 (1947)
- 3147b M. G. Inghram, D. C. Hess, Jr., R. J. Hayden, and G. W. Parker, *Phys. Rev.* **71**, 743 (1947)
- 3147c M. G. Inghram, R. J. Hayden, and D. C. Hess, Jr., *Phys. Rev.* **71**, 643 (1947)
- 3147d M. G. Inghram and R. J. Hayden, *Phys. Rev.* **71**, 130 (1947)
- 3147e M. G. Inghram, A. E. Shaw, D. C. Hess, Jr., and R. J. Hayden, *Phys. Rev.* **72**, 515 (1947)
- 3147f M. G. Inghram, R. J. Hayden, and D. C. Hess, Jr., *Phys. Rev.* **71**, 270 (1947)
- 3147g M. G. Inghram, D. C. Hess, Jr., and R. J. Hayden, reported in Argonne National Laboratory Classified Report ANL-4012 (Aug. 1947)
- 3147h M. G. Inghram, D. C. Hess, Jr., and R. J. Hayden, *Phys. Rev.* **71**, 561 (1947)
- 3148 M. G. Inghram, D. C. Hess, Jr., H. S. Brown, and E. Goldberg, *Phys. Rev.* **74**, 343 (1948)
- 3148a M. G. Inghram, D. C. Hess, Jr., and R. J. Hayden, reported in Argonne National Laboratory Classified Report ANL-4082 (Jan. 1948)
- 3148b M. G. Inghram and D. C. Hess, Jr., *Phys. Rev.* **74**, 627 (1948)
- 3148c M. G. Inghram, D. C. Hess, Jr., and R. J. Hayden, *Phys. Rev.* **74**, 98 (1948)
- 3148d M. G. Inghram, D. C. Hess, Jr., and R. J. Hayden, *Phys. Rev.* **73**, 180 (1948)
- 3149 M. G. Inghram and D. C. Hess, Jr., reported in Argonne National Laboratory Classified Report ANL-4355 (Oct. 1949)
- 3149a M. G. Inghram, D. C. Hess, Jr., and J. H. Reynolds, *Phys. Rev.* **76**, 1717 (1949)
- 3149b M. G. Inghram, R. J. Hayden, and D. C. Hess, Jr., *Phys. Rev.* **75**, 693 (1949); **74**, 1724 (1948)
- 3150 M. G. Inghram, H. S. Brown, C. Patterson, and D. C. Hess, *Phys. Rev.* **80**, 916 (1950)
- 3150a M. G. Inghram, R. J. Hayden, and D. C. Hess, Jr., *Phys. Rev.* **79**, 271 (1950)
- 3150b M. G. Inghram and J. H. Reynolds, *Phys. Rev.* **78**, 822 (1950)
- 3151 M. G. Inghram, D. C. Hess, P. R. Fields, and G. L. Pyle, *Phys. Rev.* **83**, 1250 (1951)
- 4141 J. Itoh, *Proc. Phys.-Math. Soc. Japan* **23**, 605 (1941)
- 5151 G. M. Inch and S. C. Curran, *Phil. Mag.* **42**, 892 (1951)
- 5152 G. M. Inch, J. G. Balfour, and S. C. Curran, *Phys. Rev.* **85**, 805 (1952)
- 1J48 A. H. Jaffey, quoted by M. H. Studier and E. K. Hyde, *Phys. Rev.* **74**, 591 (1948)
- 1J48a A. H. Jaffey, unpublished data (1948)
- 1J48b A. H. Jaffey and Q. Van Winkle, Argonne National Laboratory Classified Report ANL-4193 (Oct. 1948); NNES-PPR 17B, 729 (1952) (classified)
- 1J49 A. H. Jaffey and L. B. Magnusson, NNES-PPR 14B, 978 (1949)
- 1J50 A. H. Jaffey and E. K. Hyde, *Phys. Rev.* **79**, 280 (1950)
- 1J50a A. H. Jaffey and J. Lerner, reported in Argonne National Laboratory Classified Report ANL-4411 (Feb. 1950)
- 1J51 A. H. Jaffey, J. Lerner, and S. Warshaw, *Phys. Rev.* **82**, 498 (1951)
- 1J51a A. H. Jaffey, H. Diamond, A. Hirsch, and J. Mech, *Phys. Rev.* **84**, 785 (1951)
- 2J47 A. Johansson, *Arkiv Mat., Astron. Fysik* **34A**, No. 9 (1947)
- 3J48 J. V. Jelley, *Can. J. Research* **26A**, 255 (1948)
- 3J48a J. V. Jelley and E. B. Paul, *Proc. Cambridge Phil. Soc.* **44**, 133 (1948)
- 3J50 J. V. Jelley, *Proc. Phys. Soc. (London)* **63A**, 538 (1950); *Phil. Mag.* **41**, 1199 (1950)
- 4J43 J. C. Jacobsen and T. Sigurgeirsson, *Det. Kgl. Danske Vid. Sels.* **20**, No. 11 (1943)
- 4J48 J. C. Jacobsen and O. Kofoed-Hansen, *Phys. Rev.* **73**, 675 (1948)
- 5J51 W. A. Jenkins and G. D. O'Kelley, unpublished data (April 1951)
- 5J52 W. A. Jenkins and G. T. Seaborg, *Phys. Rev.* **85**, 758 (1952) (A)
- 6J51 C. J. D. Jarvis and M. A. S. Ross, *Proc. Phys. Soc. (London)* **64A**, 535 (1951)
- 7J46 S. Jnanananda, *Phys. Rev.* **69**, 570 (1946)
- 7J47 S. Jnanananda, *Phys. Rev.* **72**, 1124 (1947)
- 7J49 S. Jnanananda, *J. Sci. Ind. Research (India)* **8B**, No. 9, 147 (1949)
- 8J48 R. A. James, D. A. Orth, and G. T. Seaborg, unpublished data (July 1948)
- 8J48a R. A. James, reported in University of California Radiation Laboratory Memorandum MB-IP-247 (Jan. 1948)
- 8J49 R. A. James, A. E. Florin, H. H. Hopkins, Jr., and A. Ghiorso, NNES-PPR 14B, 1604 (1949)
- 8J49a R. A. James, S. G. Thompson, and H. H. Hopkins, Jr., NNES-PPR 14B, 1634 (1949)
- 8J52 R. A. James, A. Ghiorso, and D. A. Orth, *Phys. Rev.* **85**, 369 (1952)
- 8J52a R. A. James, private communication (Oct. 1952)
- 9J51 J. Jacquesson and A. Lataste, *Compt. rend.* **232**, 1822 (1951)
- 10J48 W. P. Jesse and H. Forstat, *Phys. Rev.* **73**, 926 (1948)
- 10L50 W. P. Jesse and J. Sadanskis, *Phys. Rev.* **78**, 1 (1950)
- 11J49 W. M. Jones, *Phys. Rev.* **76**, 885 (1949)
- 11J51 W. M. Jones, *Phys. Rev.* **83**, 537 (1951)
- 12J49 G. H. Jenks, J. A. Ghormley, and F. H. Sweeton, *Phys. Rev.* **75**, 701 (1949)
- 12J50 G. H. Jenks, F. H. Sweeton, and J. A. Ghormley, *Phys. Rev.* **80**, 990 (1950)
- 12J52 G. H. Jenks and F. H. Sweeton, *Phys. Rev.* **86**, 803 (1952)
- 13J49 E. N. Jensen, L. J. Laslett, and W. W. Pratt, *Phys. Rev.* **76**, 430 (1949)
- 13J49a E. N. Jensen, *Phys. Rev.* **76**, 958 (1949)

- 13J49b E. N. Jensen, reported in Iowa State College
Unclassified Report ISC-46 (July 1949)
- 13J50 E. N. Jensen, L. J. Laslett, and D. J. Zaffarano,
Phys. Rev. 80, 862 (1950)
- 13J51 E. N. Jensen, R. T. Nichols, and J. Clement, Phys.
Rev. 81, 143 (1951)
- 13J52 E. N. Jensen, L. J. Laslett, and D. J. Zaffarano,
Phys. Rev. 86, 1047 (1952)
- 13J52a E. N. Jensen, L. J. Laslett, D. S. Martin, Jr.,
F. J. Hughes, and W. W. Pratt, Phys. Rev.
(to be published)(1952)
- 13J52b E. N. Jensen, R. T. Nichols, J. Clement, and
A. Pohm, Phys. Rev. 85, 112 (1952)
- 14J49 F. Johnston and J. E. Willard, Phys. Rev. 75,
528 (1949)
- 15J48 E. T. Journey, Phys. Rev. 74, 1049 (1948)
- 15J49 E. T. Journey, Phys. Rev. 76, 290 (1949)
- 16J41 A. S. Jensen, Phys. Rev. 60, 430 (1941)
- 17J50 S. Johansson, Phys. Rev. 79, 896 (1950)
- 17J51 S. Johansson, Y. Cauchois, and K. Siegbahn,
Phys. Rev. 82, 275 (1951)
- 17J51a S. Johansson, reported in M. Siegbahn Commemorative
Volume, p 183 (Uppsala, 1951)
- 17J52 S. Johansson, Arkiv Fysik 4, 273 (1952)
- 17J52a S. Johansson, Arkiv Fysik 3, 533 (1952)
- 18J45 S. Jaschewski and N. Goldstein, reported in
Metallurgical Laboratory Classified Report CP-2984
(May 1945)
- 19J44 F. Joliot, Compt. rend. 218, 733 (1944)
- 20J51 L. Jacobson and R. Overstreet, NNES-PPR 9,
735 (1951)
- 21J44 P. Jensen, Z. Physik 122, 387 (1944)
- 22J50 H. E. Johns, L. Katz, R. A. Douglas, and R. N. H.
Haslam, Phys. Rev. 80, 1062 (1950)
- 23J52 W. H. Johnson, Jr., Phys. Rev. 87, 166 (1952)
- 24J38 R. Jaeckel, Z. Physik 110, 330 (1938)
- 25J52 M. W. Johns, C. D. Cox, R. J. Donnelly, and
C. C. McMullen, Phys. Rev. 87, 1134 (1952)
- 26J52 H. Jaffe and I. Perlman, unpublished data
(Aug. 1952)
- 27J51 C. M. Johnson and W. Gordy, Phys. Rev. 83, 1249
(1951)
- 28J52 J. W. Jones and T. P. Kohman, Phys. Rev. 85,
941 (1952)
- 29J52 C. D. Jeffries, H. Loeliger, and H. H. Staub,
Phys. Rev. 85, 478 (1952)
- 30J52 V. Jaccarino, B. Bederson, and H. H. Stroke,
Phys. Rev. 87, 676 (1952)
- 31J52 D. R. Jones, S. C. Fultz, and M. L. Pool,
Phys. Rev. 86, 654 (1952) (A)
- 32J52 F. A. Johnson, Abstract 76, June Meeting, Roy. Soc.
Canada (1952) and private communication (Oct. 1952)
- 33J52 A. A. Jaffe and S. G. Cohen, Phys. Rev. 86,
1041 (1952)
- 34J52 P. S. Jastram and C. E. Whittle, Phys. Rev. 87,
1133 (1952)
- 1K40 M. D. Kamen and S. Ruben, Phys. Rev. 58, 194
(1940) (A)
- 1K41 M. D. Kamen, Phys. Rev. 60, 537 (1941)
- 1K42 M. D. Kamen, Phys. Rev. 62, 303 (1942) (A)
- 1K46 M. D. Kamen, Bull. Am. Museum Nat. Hist. 87,
103 (1946)
- 2K45 T. P. Kohman, J. A. Swartout, and W. H. Sullivan,
Hanford Engineer Works Report (H)CN-3212
(Oct. 1945)
- 2K49 T. P. Kohman, private communication (1949)
- 2K49a T. P. Kohman, D. P. Ames, and J. Sedlet,
NNES-PPR 14B, 1675 (1949)
- 3K48 G. B. Knight and R. L. Macklin, Phys. Rev. 74,
1540 (1948)
- 3K49 G. B. Knight and R. L. Macklin, Phys. Rev. 75,
34 (1949)
- 4K42 C. V. Kent, J. M. Cork, and W. G. Wadey, Phys.
Rev. 61, 389 (1942) (A)
- 4K42a C. V. Kent and J. M. Cork, Phys. Rev. 62, 297
(1942) (A)
- 5K43 B. Karlik and T. Bernert, Naturwiss. 31, 492 (1943)
- 5K43a B. Karlik and T. Bernert, Naturwiss. 31, 298 (1943);
Z. Physik 123, 51 (1944)
- 5K44 B. Karlik and T. Bernert, Naturwiss. 32, 44 (1944)
- 5K46 B. Karlik and T. Bernert, Naturwiss. 33, 23 (1946)
- 6K38 A. F. Kovarik and N. I. Adams, Jr., Phys. Rev.
54, 413 (1938)
- 6K41 A. F. Kovarik and N. I. Adams, Jr., J. Appl. Phys.
12, 296 (1941) (A)
- 7K49 D. G. Karraker, F. L. Reynolds, and D. H.
Templeton, University of California Radiation
Laboratory Unclassified Report UCRL-285 (Feb. 1949)
- 7K50 D. G. Karraker and D. H. Templeton, Phys. Rev.
80, 646 (1950)
- 7K51 D. G. Karraker and D. H. Templeton, Phys. Rev.
81, 510 (1951)
- 7K51a D. G. Karraker, A. Ghiorso, and D. H. Templeton,
Phys. Rev. 83, 390 (1951)
- 7K51b D. G. Karraker, unpublished data (May 1951)
- 7K52 D. G. Karraker, R. J. Hayden, and M. G. Inghram,
Phys. Rev. 87, 901 (1952)
- 8K35 I. V. Kurtchatov, G. D. Latyshev, L. M. Nemenov,
and I. P. Selinov, Physik Z. Sowjetunion 8, 589
(1935)
- 9K39 R. S. Krishnan and D. H. T. Gant, Nature 144, 547
(1939)
- 9K40 R. S. Krishnan and E. A. Nahum, Proc. Cambridge
Phil. Soc. 36, 490 (1940)
- 9K40a R. S. Krishnan and T. E. Banks, Nature 145, 777
(1940)
- 9K40b R. S. Krishnan, Proc. Cambridge Phil. Soc. 36,
500 (1940)
- 9K41 R. S. Krishnan, Nature 148, 407 (1941)
- 9K41a R. S. Krishnan and T. E. Banks, Proc. Cambridge
Phil. Soc. 37, 317 (1941)
- 9K41b R. S. Krishnan and E. A. Nahum, Proc. Cambridge
Phil. Soc. 37, 422 (1941)
- 9K41c R. S. Krishnan, Proc. Cambridge Phil. Soc. 37,
186 (1941)
- 9K42 R. S. Krishnan and E. A. Nahum, Proc. Roy.
Soc. (London) 180A, 321, 333 (1942)
- 10K49 E. L. Kelly and E. Segrè, Phys. Rev. 75, 999
(1949)
- 10K50 E. L. Kelly, Ph.D. Thesis, University of
California Classified Report UCRL-1044 (Dec. 1950)
- 11K50 H. B. Keller and J. M. Cork, Phys. Rev. 79,
1030 (1950)
- 11K50a H. B. Keller, reported in Argonne National
Laboratory Classified Report ANL-4437 (April 1950)
- 11K51 H. B. Keller and J. M. Cork, Phys. Rev. 84, 1079
(1951)
- 12K44 M. Kahn and G. A. Linenberger, reported in
Los Alamos Scientific Laboratory Classified Report
LAMS-151 (Oct. 1944)

- 13K49 C. A. Kienberger, Phys. Rev. 76, 1561 (1949)
- 13K52 C. A. Kienberger, Phys. Rev. 87, 520 (1952)
- 14K39 J. W. Kennedy, G. T. Seaborg, and E. Segrè, Phys. Rev. 56, 1095 (1939)
- 14K40 J. W. Kennedy and G. T. Seaborg, Phys. Rev. 57, 843 (1940)
- 14K46 J. W. Kennedy, G. T. Seaborg, E. Segrè, and A. C. Wahl, Phys. Rev. 70, 555 (1946); NNES-PPR 14B, 5 (1949)
- 14K49 J. W. Kennedy, M. L. Perlman, E. Segrè, and A. C. Wahl, NNES-PPR 14B, 79 (1949)
- 15K36 K. S. Knol and J. Veldkamp, Physica 3, 145 (1936)
- 16K47 W. J. Knox, Phys. Rev. 72, 1254 (1947)
- 16K48 W. J. Knox, Phys. Rev. 74, 1192 (1948)
- 17K36 F. N. D. Kurie, J. R. Richardson, and H. C. Paxton, Phys. Rev. 49, 368 (1936)
- 17K48 F. N. D. Kurie and M. Ter-Pogossian, Phys. Rev. 74, 677 (1948)
- 17K51 F. N. D. Kurie, unpublished data quoted in (39S51a)
- 18K48 K. Knable, E. O. Lawrence, C. E. Leith, P. J. Moyer, and R. L. Thornton, Phys. Rev. 74, 1217 (1948) (A)
- 19K39 L. D. P. King, W. J. Henderson, and J. R. Risser, Phys. Rev. 55, 1118 (1939) (A)
- 19K39a L. D. P. King and W. J. Henderson, Phys. Rev. 56, 1169 (1939)
- 19K40 L. D. P. King and D. R. Elliott, Phys. Rev. 58, 846 (1940)
- 20K45 J. D. Knight, T. B. Novey, C. V. Cannon, and A. Turkevich, Metallurgical Laboratory Classified Report CC-2605 (April 1945)
- 20K49 J. D. Knight, W. H. Burgus, and R. J. Prestwood, private communication listed in NNES-PPR 9, 2063 (1951) (ref. K14)
- 20K51 J. D. Knight and G. A. Cowan, reported in Los Alamos Scientific Laboratory Classified Report WASH-58 (March 1951) and private communication (Oct. 1952)
- 20K51a J. D. Knight and D. P. Ames, reported in Los Alamos Scientific Laboratory Classified Report WASH-62 (Dec. 1951)
- 20K52 J. D. Knight and L. Baggett, private communication (April 1952)
- 21K47 B. B. Kinsey, Phys. Rev. 72, 526 (1947) (A)
- 21K50 B. B. Kinsey, G. A. Bartholomew, and W. H. Walker, Phys. Rev. 78, 481 (1950)
- 21K50a B. B. Kinsey, et al., reported in Chalk River Laboratory Classified Report PR-P-6 (March 1950)
- 22K39 G. Kuerti and S. N. Van Voorhis, Phys. Rev. 56, 614 (1939)
- 23K48 E. D. Klema and A. O. Hanson, Phys. Rev. 73, 106 (1948)
- 23K52 E. D. Klema and F. K. McGowan, Phys. Rev. 87, 524 (1952)
- 24K48 B. H. Ketelle and W. C. Peacock, Phys. Rev. 73, 1269 (1948) (A)
- 24K48a B. H. Ketelle and G. E. Boyd, reported in Oak Ridge National Laboratory Classified Report ORNL-65 (July 1948)
- 24K49 B. H. Ketelle, reported in Oak Ridge National Laboratory Classified Report ORNL-286 (Sept. 1949)
- 24K49a B. H. Ketelle, reported in Oak Ridge National Laboratory Classified Report ORNL-336 (May 1949)
- 24K49b B. H. Ketelle, reported in Oak Ridge National Laboratory Classified Report ORNL-229 (Feb. 1949)
- 24K49c B. H. Ketelle, reported in Brookhaven National Laboratory Unclassified Report BNL-C-9 (Aug. 1949)
- 24K49d B. H. Ketelle, Phys. Rev. 76, 1256 (1949)
- 24K49e B. H. Ketelle and G. W. Parker, Phys. Rev. 76, 1416 (1949)
- 24K50 B. H. Ketelle, Phys. Rev. 80, 758 (1950)
- 24K50a B. H. Ketelle and J. W. Ruch, Phys. Rev. 77, 565 (1950)
- 24K50b B. H. Ketelle, C. M. Nelson, and G. E. Boyd, Phys. Rev. 79, 242 (1950) (A)
- 24K50c B. H. Ketelle, A. R. Brosi, and H. Zeldes, Phys. Rev. 80, 485 (1950)
- 24K50d B. H. Ketelle, reported in Oak Ridge National Laboratory Classified Report ORNL-607 (March 1950)
- 24K51 B. H. Ketelle, H. Zeldes, A. R. Brosi, and R. A. Dandl, Phys. Rev. 84, 585 (1951); H. Zeldes, A. R. Brosi, and B. H. Ketelle, Phys. Rev. 81, 642 (1951)
- 24K51a B. H. Ketelle, A. R. Brosi, and H. Zeldes, reported in Oak Ridge National Laboratory Classified Report ORNL-870 (March 1951)
- 24K52 B. H. Ketelle and A. R. Brosi, private communication (Oct. 1952)
- 25K46 J. X. Khym, Oak Ridge National Laboratory Classified Report Mon C-61 (Feb. 1946)
- 26K48 N. L. Krisberg, M. L. Pool, and C. T. Hibdon, Phys. Rev. 74, 44 (1948)
- 26K49 N. L. Krisberg and M. L. Pool, Phys. Rev. 75, 1693 (1949)
- 27K50 H. E. Kubitschek, Phys. Rev. 79, 23 (1950)
- 28K48 B. D. Kern, D. J. Zaffarano, and A. C. G. Mitchell, Phys. Rev. 73, 1142 (1948)
- 28K49 B. D. Kern, A. C. G. Mitchell, and D. J. Zaffarano, Phys. Rev. 76, 94 (1949)
- 29K46 D. N. Kundu and M. L. Pool, Phys. Rev. 70, 111 (1946) (A)
- 29K47 D. N. Kundu and M. L. Pool, Phys. Rev. 71, 140 (1947) (A)
- 29K47a D. N. Kundu and M. L. Pool, Phys. Rev. 72, 101 (1947)
- 29K48 D. N. Kundu and M. L. Pool, Phys. Rev. 73, 22 (1948)
- 29K48a D. N. Kundu and M. L. Pool, Phys. Rev. 74, 1775 (1948)
- 29K49 D. N. Kundu and M. L. Pool, Phys. Rev. 76, 183 (1949) (A)
- 29K49a D. N. Kundu and M. L. Pool, Phys. Rev. 75, 1690 (1949)
- 29K50 D. N. Kundu and M. L. Pool, Phys. Rev. 78, 488 (1950)
- 29K50a D. N. Kundu, J. L. Hult, and M. L. Pool, Phys. Rev. 77, 71 (1950)
- 29K51 D. N. Kundu and M. L. Pool, Phys. Rev. 84, 481 (1951)
- 29K52 D. N. Kundu, J. D. Service, and M. L. Pool, Phys. Rev. 87, 203 (1952) (A)
- 30K50 L. Katz, A. S. Penfold, H. J. Moody, R. N. H. Haslam, and H. E. Johns, Phys. Rev. 77, 289 (1950)
- 30K51 L. Katz and A. G. W. Cameron, Phys. Rev. 84, 1115 (1951)
- 30K51a L. Katz and A. G. W. Cameron, Can. J. Phys. 29, 518 (1951)
- 31K51 J. H. Kahn, Oak Ridge National Laboratory Unclassified Report ORNL-1089 (Nov. 1951)
- 31K52 J. H. Kahn and E. C. Campbell, private communication (Oct. 1952)
- 32K46 S. Katcoff and A. Goldstein, U. S. Atomic Energy Commission Declassified Document MDDC-293 (April 1946)
- 32K47 S. Katcoff, Phys. Rev. 71, 826 (1947)
- 32K47a S. Katcoff, Phys. Rev. 72, 1160 (1947)
- 32K48 S. Katcoff, J. A. Miskel, and C. W. Stanley, Phys. Rev. 74, 631 (1948)

- 32K49 S. Katcoff, J. A. Leary, K. A. Walsh, R. A. Elmer, S. S. Goldsmith, L. D. Hall, E. G. Newbury, J. J. Povelites, and J. S. Waddell, *J. Chem. Phys.* 17, 421 (1949)
- 32K50 S. Katcoff, reported in Brookhaven National Laboratory Unclassified Report BNL-39 (Jan. 1950)
- 32K51 S. Katcoff, B. Finkle, and N. Sugarman, *NNES-PPR* 9, 587 (1951)
- 32K51a S. Katcoff and E. J. Hoagland, *NNES-PPR* 9, 659 (1951)
- 32K51b S. Katcoff and B. Finkle, *NNES-PPR* 9, 705 (1951)
- 32K51c S. Katcoff, *NNES-PPR* 9, 765 (1951)
- 32K51d S. Katcoff, *NNES-PPR* 9, 980 (1951)
- 32K51e S. Katcoff, C. R. Dillard, H. Finston, B. Finkle, J. A. Seiler, and N. Sugarman, *NNES-PPR* 9, 1005 (1951)
- 32K51f S. Katcoff, O. A. Schaeffer, and J. M. Hastings, *Phys. Rev.* 82, 688 (1951)
- 32K51g S. Katcoff, B. Finkle, N. Sugarman, L. E. Glendenin, and L. Winsberg, *NNES-PPR* 9, 1017 (1951)
- 32K51h S. Katcoff, B. Finkle, E. J. Hoagland, N. Sugarman, L. E. Glendenin, and R. P. Metcalf, *NNES-PPR* 9, 982 (1951)
- 32K51i S. Katcoff, B. Finkle, and N. Sugarman, *NNES-PPR* 9, 1097 (1951)
- 32K51j S. Katcoff, *NNES-PPR* 9, 1147 (1951)
- 32K51k S. Katcoff, *NNES-PPR* 9, 1400 (1951)
- 32K52 S. Katcoff, *Phys. Rev.* 87, 886 (1952)
- 32K52a S. Katcoff, reported in Brookhaven National Laboratory Unclassified Report BNL-149 (March 1952)
- 33K35 B. Kurtchatov, I. Kurtchatov, L. Myssowsky, and L. Roussinov, *Compt. rend.* 200, 1201 (1935)
- 34K49 J. Koch, O. Kofoed-Hansen, P. Kristensen, and W. Drost-Hansen, *Phys. Rev.* 76, 279 (1949)
- 35K51 O. Kofoed-Hansen and P. Kristensen, *Phys. Rev.* 82, 96 (1951)
- 35K51a O. Kofoed-Hansen and K. O. Nielsen, *Phys. Rev.* 82, 96 (1951); *Kgl. Danske Videnskab. Selskab, Mat. fys. Medd.* 26, No. 7 (1951)
- 35K51b O. Kofoed-Hansen, *Phil. Mag.* 42, 1448 (1951)
- 36K35 O. Klemperer, *Proc. Roy. Soc. (London)* 148A, 638 (1935)
- 37K49 M. Kemmerich, *Z. Physik* 126, 399 (1949)
- 38K50 E. Kondaiah, *Phys. Rev.* 79, 891 (1950)
- 38K50a E. Kondaiah, *Arkiv Fysik* 2, 295 (1950)
- 38K51 E. Kondaiah, *Phys. Rev.* 83, 471 (1951)
- 38K51a E. Kondaiah, *Phys. Rev.* 81, 1056 (1951)
- 38K51b E. Kondaiah, *Arkiv Fysik* 3, 47 (1951)
- 38K51c E. Kondaiah, reported in M. Siegbahn Commemorative Volume, p 411 (Uppsala, 1951)
- 38K51d E. Kondaiah, *Arkiv Fysik* 2, 295 (1951)
- 39K37 J. D. Kraus and J. M. Cork, *Phys. Rev.* 52, 763 (1937)
- 40K52 W. C. Kelly, *Phys. Rev.* 85, 101 (1952)
- 41K52 M. I. Kalkstein and W. F. Libby, *Phys. Rev.* 85, 368 (1952)
- 42K45 P. G. Kruger and W. E. Ogle, *Phys. Rev.* 67, 273 (1945)
- 42K52 P. Kruger and C. D. Coryell, private communication (Oct. 1952)
- 43K50 R. Katz, R. D. Hill, and M. Goldhaber, *Phys. Rev.* 78, 9 (1950)
- 43K52 R. Katz and M. R. Lee, *Phys. Rev.* 85, 1038 (1952)
- 44K52 T. K. Keenan, R. A. Penneman, and B. B. McInteer, *Phys. Rev.* 87, 204 (1952) (A)
- 45K40 D. C. Kalbfell and R. A. Cooley, *Phys. Rev.* 58, 91 (1940)
- 46K52 A. W. Knudsen, *Phys. Rev.* 86, 571 (1952)
- 47K42 J. D. Kurbatov, D. C. MacDonald, M. L. Pool, and L. L. Quill, *Phys. Rev.* 61, 106 (1942) (A)
- 47K43 J. D. Kurbatov and M. L. Pool, *Phys. Rev.* 63, 463 (1943) (A)
- 48K51 K. G. Kessler and W. F. Meggers, *Phys. Rev.* 80, 905 (1951)
- 49K50 H. Kuhn and K. G. Woodgate, *Nature* 166, 906 (1950); *Proc. Phys. Soc. (London)* 64A, 1090 (1951)
- 50K48 L. I. Katzin and M. Pobereskin, *Phys. Rev.* 74, 264 (1948)
- 50K52 L. I. Katzin and F. Hagemann, *NNES-PPR* 17B, 582 (1952) (classified)
- 51K51 J. Kastner, *Can. J. Phys.* 29, 480 (1951)
- 52K51 I. Kirshenbaum, J. Graff, and H. Forstat, *NNES Div. III*, 4A, 393 (1951)
- 53K43 S. Kikuchi, et al., *Proc. Phys.-Math. Soc. Japan* 25, 502 (1943)
- 54K52 P. Kofstad and G. T. Seaborg, reported in University of California Radiation Laboratory Classified Report UCRL-1770 (April 1952)
- 55K52 V. E. Krohn, Jr. and E. F. Shrader, *Phys. Rev.* 87, 685 (1952)
- 56K52 C. Kikuchi, M. H. Sirvetz, and V. W. Cohen, *Phys. Rev.* 88, 142 (1952)
- 57K51 J. D. Keys, Ph.D. Thesis, McGill University (1951)
- 58K52 J. Kraushaar, E. Wilson, and K. T. Bainbridge, private communication (Oct. 1952)
- 59K51 S. Kageyama, *J. Phys. Soc. Japan* 6, 285 (1951)
- 59K52 S. Kageyama, *J. Phys. Soc. Japan* 7, 93 (1952)
- 60K52 L. Koester, H. Maier-Leibnitz, T. Mayer-Kuckuk, K. Schmeiser, and G. Schulze-Pillot, *Z. Physik* 133, 319 (1952)
- 61K52 R. M. Kloepper, E. S. Lennox, and M. L. Wiedenbeck, *Phys. Rev.* 88, 695 (1952)
- 1L35 E. O. Lawrence, *Phys. Rev.* 47, 17 (1935)
- 2L47 P. W. Levy, *Phys. Rev.* 72, 352 (1947)
- 2L47a P. W. Levy, *Phys. Rev.* 72, 248 (1947)
- 2L48 P. W. Levy and E. Greuling, *Phys. Rev.* 73, 83 (1948)
- 2L49 P. W. Levy, reported in Oak Ridge National Laboratory Unclassified Report ORNL-312 (March 1949); U. S. Atomic Energy Commission Unclassified Document AECU-173 (March 1949)
- 2L49a P. W. Levy and E. Greuling, *Phys. Rev.* 75, 819 (1949)
- 3L33 W. F. Libby and W. M. Latimer, *J. Am. Chem. Soc.* 55, 433 (1933)
- 3L34 W. F. Libby, *Phys. Rev.* 45, 845 (1934)
- 3L39 W. F. Libby and D. D. Lee, *Phys. Rev.* 55, 245 (1939)
- 3L39a W. F. Libby, *Phys. Rev.* 56, 21 (1939)
- 3L51 W. F. Libby, private communication (Oct. 1951)
- 4L47 E. J. Lofgren, reported by (2T47a)
- 5L47 G. D. Latyshev, *Revs. Modern Phys.* 19, 132 (1947)
- 6L38 M. Lecoin, *J. phys. et radium* 9, 81 (1938)
- 6L43 M. Lecoin, M. Perey, and San-Tsiang Tsien, *Compt. rend.* 217, 146 (1943)
- 6L44 M. Lecoin, M. Perey, and San-Tsiang Tsien, *Cahiers phys.* No. 26, 10 (1944)

- 6L47 M. Lecoïn, *Compt. rend.* 224, 912 (1947)
- 6L48 M. Lecoïn, M. Perey, and J. Teillac, *Compt. rend.* 227, 121 (1948)
- 6L49 M. Lecoïn, M. Perey, and M. Riou, *J. phys. et radium* 10, 390 (1949)
- 6L49a M. Lecoïn, M. Perey, and J. Teillac, *J. phys. et radium* 10, 33 (1949)
- 6L50 M. Lecoïn, M. Perey, M. Riou, and J. Teillac, *J. phys. et radium* 11, 227 (1950)
- 7L50 C. R. Lagergren and M. E. Kettner, *Phys. Rev.* 80, 102 (1950)
- 8L39 D. D. Lee and W. F. Libby, *Phys. Rev.* 55, 252 (1939)
- 9L44 A. L. Lutz, M. L. Pool, and J. D. Kurbatov, *Phys. Rev.* 65, 61 (1944) (A)
- 10L37 L. M. Langer and M. D. Whitaker, *Phys. Rev.* 51, 713 (1937)
- 10L47 L. M. Langer, C. S. Cook, and M. B. Sampson, *Phys. Rev.* 71, 906 (1947)
- 10L49 L. M. Langer and H. C. Price, Jr., *Phys. Rev.* 76, 641 (1949)
- 10L49a L. M. Langer and H. C. Price, Jr., reported by (53M49)
- 10L50 L. M. Langer, *Phys. Rev.* 77, 50 (1950)
- 10L50a L. M. Langer and R. D. Moffat, *Phys. Rev.* 80, 651 (1950)
- 10L50b L. M. Langer, R. D. Moffat, and H. C. Price, Jr., *Phys. Rev.* 79, 808 (1950)
- 10L50c L. M. Langer, J. W. Motz, and H. C. Price, Jr., *Phys. Rev.* 77, 798 (1950)
- 10L50d L. M. Langer and R. D. Moffat, *Phys. Rev.* 78, 74 (1950)
- 10L51 L. M. Langer and R. D. Moffat, *Phys. Rev.* 82, 635 (1951)
- 10L51a L. M. Langer and G. Ford, reported in U. S. Atomic Energy Commission Classified Report WASH-62 (Dec. 1951)
- 10L52 L. M. Langer, R. D. Moffat, and G. A. Graves, *Phys. Rev.* 86, 632 (1952) (A)
- 10L52a L. M. Langer, R. B. Duffield, and C. W. Stanley, private communication (Sept. 1952)
- 10L52b L. M. Langer and R. J. D. Moffat, *Phys. Rev.* 88, 689 (1952)
- 10L52c L. M. Langer, private communication (Oct. 1952)
- 10L52d L. M. Langer and R. B. Duffield, private communication (Oct. 1952)
- 11L34 W. B. Lewis and B. V. Bowden, *Proc. Roy. Soc. (London)* 145A, 235 (1934). Summarizes the results of various investigators. Values recalculated according to (9H38)
- 11L37 W. B. Lewis, W. E. Burcham, and W. Y. Chang, *Nature* 139, 24 (1937)
- 12L36 J. J. Livingood, *Phys. Rev.* 50, 425 (1936)
- 12L37 J. J. Livingood, F. Fairbrother, and G. T. Seaborg, *Phys. Rev.* 52, 135 (1937)
- 12L37a J. J. Livingood and G. T. Seaborg, *Phys. Rev.* 52, 135 (1937)
- 12L38 J. J. Livingood and G. T. Seaborg, *Phys. Rev.* 54, 391 (1938)
- 12L38a J. J. Livingood and G. T. Seaborg, *Phys. Rev.* 54, 51 (1938)
- 12L38b J. J. Livingood and G. T. Seaborg, *Phys. Rev.* 53, 847 (1938)
- 12L38c J. J. Livingood and G. T. Seaborg, *Phys. Rev.* 53, 765 (1938)
- 12L38d J. J. Livingood and G. T. Seaborg, *Phys. Rev.* 54, 88 (1938)
- 12L38e J. J. Livingood and G. T. Seaborg, *Phys. Rev.* 54, 775 (1938)
- 12L39 J. J. Livingood and G. T. Seaborg, *Phys. Rev.* 55, 457 (1939)
- 12L39a J. J. Livingood and G. T. Seaborg, *Phys. Rev.* 55, 1268 (1939)
- 12L39b J. J. Livingood and G. T. Seaborg, unpublished data (1939)
- 12L39c J. J. Livingood and G. T. Seaborg, *Phys. Rev.* 55, 667 (1939)
- 12L39d J. J. Livingood and G. T. Seaborg, *Phys. Rev.* 55, 414 (1939)
- 12L41 J. J. Livingood and G. T. Seaborg, *Phys. Rev.* 60, 913 (1941)
- 13L51 R. F. Leininger, E. Segrè, and F. N. Spiess, *Phys. Rev.* 82, 334 (1951) (A)
- 14L47 A. Lundby, *Forsvarets Forskning Institutt, Arbok* (1947), 13
- 14L49 A. Lundby, *Phys. Rev.* 76, 1809 (1949)
- 15L45 G. A. Linenberger, reported in Los Alamos Scientific Laboratory Classified Report LAMS-256 (May 1945)
- 16L51 C. W. Li, W. Whaling, W. A. Fowler, and C. C. Lauritsen, *Phys. Rev.* 83, 512 (1951)
- 17L38 H. Lu, *Phys. Rev.* 53, 845 (1938)
- 18L39 A. M. Lawrance, *Proc. Cambridge Phil. Soc.* 35, 304 (1939)
- 19L44 J. S. Levinger, Metallurgical Laboratory Declassified Report CP-2267 (Oct. 1944)
- 19L47 J. Levinger and E. Meiners, *Phys. Rev.* 71, 586 (1947)
- 19L51 J. S. Levinger, *NNES-PPR* 9, 757 (1951)
- 19L51a J. S. Levinger, E. P. Meiners, M. B. Sampson, A. H. Snell, and R. G. Wilkinson, *NNES-PPR* 9, 603 (1951)
- 20L39 A. Langsdorf, Jr., *Phys. Rev.* 56, 205 (1939)
- 20L40 A. Langsdorf, Jr. and E. Segrè, *Phys. Rev.* 57, 105 (1940)
- 20L45 A. S. Langsdorf, Jr. and R. L. Purbrick, Metallurgical Laboratory Classified Report CP-3272 (Oct. 1945)
- 21L37 E. M. Lyman, *Phys. Rev.* 51, 1 (1937)
- 21L39 E. M. Lyman, *Phys. Rev.* 55, 1123 (1939) (A)
- 22L34 M. S. Livingston, M. C. Henderson, and E. O. Lawrence, *Phys. Rev.* 46, 325 (1934) (A)
- 22L34a M. S. Livingston and E. M. McMillan, *Phys. Rev.* 46, 437 (1934)
- 23L37 L. J. Laslett, *Phys. Rev.* 52, 529 (1937)
- 23L49 L. J. Laslett, *Phys. Rev.* 76, 858 (1949)
- 23L50 L. J. Laslett, E. N. Jensen, and A. Paskin, *Phys. Rev.* 79, 412 (1950)
- 24L37 J. L. Lawson and J. M. Cork, *Phys. Rev.* 52, 531 (1937)
- 24L39 J. L. Lawson, *Phys. Rev.* 56, 131 (1939)
- 24L40 J. L. Lawson and J. M. Cork, *Phys. Rev.* 57, 982 (1940)
- 25L46 D. C. Lincoln and W. H. Sullivan, reported in *J. Am. Chem. Soc.* 68, 2411 (1946)
- 25L51 D. C. Lincoln and W. H. Sullivan, *NNES-PPR* 9, 778 (1951)
- 26L40 H. Levi, *Nature* 145, 588 (1940)
- 27L48 R. V. Langmuir, *Phys. Rev.* 74, 1559 (1948) (A)
- 28L48 W. T. Leland and A. O. Nier, *Phys. Rev.* 73, 1206 (1948)
- 28L49 W. T. Leland, *Phys. Rev.* 76, 1722 (1949)

- 28L49a W. T. Leland, *Phys. Rev.* 76, 992 (1949)
- 28L50 W. T. Leland, *Phys. Rev.* 77, 634 (1950)
- 29L49 D. A. Lind, J. R. Brown, and J. W. M. DuMond, *Phys. Rev.* 76, 591 (1949) (A)
- 29L49a D. A. Lind, J. Brown, D. Klein, D. Muller, and J. DuMond, *Phys. Rev.* 75, 1544 (1949)
- 29L51 D. Lind and A. Hedgran, reported in M. Siegbahn Commemorative Volume, p 283 (Uppsala, 1951)
- 30L47 C. E. Leith, A. Bratenahl, and B. J. Moyer, *Phys. Rev.* 72, 732 (1947)
- 31L40 R. S. Livingston and B. T. Wright, *Phys. Rev.* 58, 656 (1940)
- 32L47 H. A. Levy and M. H. Feldman, reported in Oak Ridge National Laboratory Classified Report Mon N-432 (Dec. 1947)
- 32L48 H. A. Levy and B. Zemel, reported in Oak Ridge National Laboratory Classified Report ORNL-176 (Nov. 1948)
- 32L49 H. A. Levy and M. H. Feldman, reported in Oak Ridge National Laboratory Classified Report ORNL-286 (Sept. 1949)
- 33L49 L. Lidofsky, P. Macklin, and C. S. Wu, *Phys. Rev.* 76, 1888 (1949)
- 33L50 L. J. Lidofsky, P. A. Macklin, and C. S. Wu, *Phys. Rev.* 78, 318 (1950) (A)
- 33L51 L. Lidofsky, P. Macklin, and C. S. Wu, reported in Columbia University Report CU-97 (Nov. 1951)
- 33L52 L. Lidofsky, P. Macklin, and C. S. Wu, *Phys. Rev.* 87, 391 (1952)
- 34L51 J. Laberrigue-Frolow, *Compt. rend.* 232, 1201 (1951)
- 34L52 J. Laberrigue-Frolow, *Compt. rend.* 234, 2599 (1952)
- 35L49 W. S. Lyon, reported in Oak Ridge National Laboratory Classified Report ORNL-286 (Sept. 1949)
- 35L51 W. S. Lyon and D. J. Coombe, reported in Oak Ridge National Laboratory Classified Report ORNL-1088 (Oct. 1951)
- 35L51a W. S. Lyon, *Phys. Rev.* 82, 276 (1951)
- 35L52 W. S. Lyon, *Phys. Rev.* 87, 1126 (1952)
- 35L52a W. S. Lyon and B. Kahn, reported in Oak Ridge National Laboratory Classified Report ORNL-1276 (Oct. 1952)
- 36L39 C. Lieber, *Naturwiss.* 27, 421 (1939)
- 37L48 M. Lindner and I. Perlman, *Phys. Rev.* 73, 1202 (1948)
- 37L48a M. Lindner and I. Perlman, *Phys. Rev.* 73, 1124 (1948)
- 37L48b M. Lindner and I. Perlman, unpublished data (May 1948)
- 37L50 M. Lindner and I. Perlman, *Phys. Rev.* 78, 499 (1950)
- 37L50a M. Lindner and J. S. Coleman, *Phys. Rev.* 78, 67 (1950)
- 37L51 M. Lindner, *Phys. Rev.* 84, 240 (1951)
- 37L51a M. Lindner and J. S. Coleman, *J. Am. Chem. Soc.* 73, 1610 (1951)
- 37L52 M. Lindner and R. Osborne, private communication (July 1952)
- 37L53 M. Lindner, *Phys. Rev.* (to be published) (1953)
- 38L39 K. Lark-Horowitz, J. R. Resser, and R. N. Smith, *Phys. Rev.* 55, 878 (1939)
- 39L49 J. C. Lee and M. L. Pool, *Phys. Rev.* 76, 606 (1949)
- 40L46 G. R. Leader, reported in *J. Am. Chem. Soc.* 68, 2411 (1946)
- 40L51 G. R. Leader, *NNES-PPR* 9, 919 (1951)
- 40L51a G. R. Leader and W. H. Sullivan, *NNES-PPR* 9, 934 (1951)
- 41L51 J. S. Lawson, *Phys. Rev.* 81, 299 (1951) (A)
- 42L40 A. Langer and W. E. Stephens, *Phys. Rev.* 58, 759 (1940)
- 43L52 J. K. Long and M. L. Pool, *Phys. Rev.* 85, 137 (1952)
- 43L52a J. K. Long, M. L. Pool, and D. N. Kundu, *Phys. Rev.* 88, 171 (1952) (A)
- 44L41 H. B. Law, M. L. Pool, J. D. Kurbatov, and L. L. Quill, *Phys. Rev.* 59, 936 (1941) (A)
- 45L47 C. M. G. Lattes, E. G. Samuel, and P. Cuer, *Anais acad. brasil. cienc.* 19, 1 (1947)
- 46L51 M. J. W. Laubenstein, R. A. Laubenstein, L. J. Koester, and R. C. Mobley, *Phys. Rev.* 81, 654 (1951) (A)
- 47L50 R. M. Littauer, *Phil. Mag.* 41, 1214 (1950)
- 48L50 E. Lüscher, R. Ricamo, P. Scherrer, and W. Zündi, *Helv. Phys. Acta* 23, 561 (1950)
- 49L51 G. Lindström, *Arkiv Fysik* 4, 1 (1951); *Phys. Rev.* 83, 465 (1951)
- 49L52 G. Lindström, *Phys. Rev.* 87, 678 (1952)
- 50L52 G. M. Lewis, *Phil. Mag.* 43, 1070 (1952)
- 51L51 J. Lascoux and G. Vendryes, *Compt. rend.* 233, 858 (1951)
- 52L52 H. B. Levy and I. Perlman, *Phys. Rev.* 85, 758 (1952) (A); unpublished data (Nov. 1952)
- 53L52 D. L. Livesey and C. L. Smith, *Proc. Phys. Soc. (London)* 65A, 758 (1952)
- 54L52 L. M. Litz, S. A. Ring, and W. R. Balkwell, private communication (Nov. 1952)
- 1M23 L. Meitner, *Z. Physik* 17, 54 (1923)
- 1M28 L. Meitner, *Z. Physik* 52, 637, 645 (1928)
- 1M28a L. Meitner, *Z. Physik* 50, 15 (1928)
- 1M37 L. Meitner, O. Hahn, and F. Strassmann, *Z. Strassmann, Z. Physik* 106, 249 (1937)
- 1M38 L. Meitner, F. Strassmann, and O. Hahn, *Z. Physik* 109, 538 (1938)
- 1M40 L. Meitner, *Arkiv Mat., Astron. Fysik* 27A, No. 17 (1940)
- 1M48 L. Meitner, *Ann. Physik* 3, 115 (1948)
- 2M14 S. Meyer, V. F. Hess, and F. Paneth, *Wien. Ber.* 123, 1459 (1914)
- 3M41 W. Maurer and W. Ramm, *Naturwiss.* 29, 368 (1941); *Z. Physik* 119, 334 (1942)
- 3M42 W. Maurer and W. Ramm, *Z. Physik* 119, 602 (1942)
- 3M47 W. Maurer, *Z. Naturforsch.* 2a, 586 (1947)
- 3M49 W. Maurer, *Z. Naturforsch.* 4a, 150 (1949)
- 4M50 J. F. Miller, J. G. Hamilton, T. M. Putnam, H. R. Haymond, and G. B. Rossi, *Phys. Rev.* 80, 486 (1950)
- 5M50 M. Miwa and S. Kageyama, *J. Phys. Soc. Japan* 5, 416 (1950)
- 6M48 D. G. E. Martin, H. O. W. Richardson, and Yun-Kuei Hsü, *Proc. Phys. Soc. (London)* 60, 466 (1948)
- 6M48a D. G. E. Martin and H. O. W. Richardson, *Proc. Roy. Soc. (London)* 195A, 287 (1948)
- 6M50 D. G. E. Martin and H. O. W. Richardson, *Proc. Phys. Soc. (London)* 63A, 223 (1950)
- 7M48 K. R. MacKensie, private communication (1948)
- 8M37 J. Mattauach, *Naturwiss.* 25, 189 (1937)
- 8M39 J. Mattauach and H. Lichtblau, *Z. Physik* 111, 514 (1939)

- 9M52 F. F. Momyer, F. Asaro, and E. K. Hyde, private communication (Aug. 1952)
- 9M52a F. F. Momyer, E. K. Hyde, A. Ghiorso, and W. E. Glenn, *Phys. Rev.* **86**, 805 (1952)
- 9M52b F. F. Momyer, A. Ghiorso, and E. K. Hyde, private communication (Aug. 1952)
- 9M52c F. F. Momyer and E. K. Hyde, unpublished data (Dec. 1952)
- 10M47 R. L. Macklin and G. B. Knight, *Phys. Rev.* **72**, 435 (1947)
- 10M49 R. L. Macklin, *Phys. Rev.* **76**, 595 (1949)
- 11M48 W. W. Meinke, A. Ghiorso, and G. T. Seaborg, unpublished data (July 1948)
- 11M49 W. W. Meinke, A. Ghiorso, and G. T. Seaborg, *Phys. Rev.* **75**, 314 (1949)
- 11M50 W. W. Meinke and G. T. Seaborg, *Phys. Rev.* **78**, 475 (1950)
- 11M51 W. W. Meinke, A. Ghiorso, and G. T. Seaborg, *Phys. Rev.* **81**, 782 (1951)
- 11M52 W. W. Meinke, A. Ghiorso, and G. T. Seaborg, *Phys. Rev.* **85**, 429 (1952)
- 11M52a W. W. Meinke and K. L. Hall, private communication (Oct. 1952)
- 11M53 W. W. Meinke, *Phys. Rev.* (to be published) (1953)
- 12M35 E. M. McMillan and M. S. Livingston, *Phys. Rev.* **47**, 452 (1935)
- 12M35a E. M. McMillan and E. O. Lawrence, *Phys. Rev.* **47**, 343 (1935)
- 12M37 E. M. McMillan, M. Kamen, and S. Ruben, *Phys. Rev.* **52**, 375 (1937)
- 12M39 E. M. McMillan, *Phys. Rev.* **55**, 510 (1939)
- 12M40 E. M. McMillan, *Phys. Rev.* **58**, 178 (1940)
- 12M40a E. M. McMillan and P. H. Abelson, *Phys. Rev.* **57**, 1185 (1940)
- 12M46 E. M. McMillan, private communication (June 1946)
- 12M46a E. M. McMillan and S. Ruben, *Phys. Rev.* **70**, 123 (1946)
- 12M46b E. M. McMillan and T. M. Putnam, private communication (July 1946)
- 12M46c E. M. McMillan, W. J. Knox, and R. H. Goeckermann, private communication (June 1946)
- 12M47 E. M. McMillan, *Phys. Rev.* **72**, 591 (1947)
- 12M47a E. M. McMillan, private communication (Jan. 1947)
- 13M47 L. Melander, *Acta Chem. Scan.* **1**, 169 (1947)
- 13M48 L. Melander and H. Slatis, *Phys. Rev.* **74**, 709 (1948); *Arkiv Mat., Astron. Fysik* **36A**, No. 15 (1949)
- 14M37 A. C. G. Mitchell, *Phys. Rev.* **51**, 995 (1937)
- 14M38 A. C. G. Mitchell, *Phys. Rev.* **53**, 269 (1938)
- 14M38a A. C. G. Mitchell and L. M. Langer, *Phys. Rev.* **53**, 505 (1938)
- 14M40 A. C. G. Mitchell, L. M. Langer, and P. W. McDaniel, *Phys. Rev.* **57**, 1107 (1940)
- 14M42 A. C. G. Mitchell, L. M. Langer, and L. J. Brown, Metallurgical Project Classified Report (work performed at Indiana University) CN-409 (Dec. 1942)
- 14M43 A. C. G. Mitchell, L. Slotin, J. Marshall, V. A. Nedzel, L. J. Brown, and J. R. Pruett, Metallurgical Laboratory Classified Report CP-597 (April 1943)
- 14M47 A. C. G. Mitchell, E. T. Journey, and M. Ramsey, *Phys. Rev.* **71**, 825 (1947)
- 14M48 A. C. G. Mitchell, D. J. Zaffarano, and B. D. Kern, *Phys. Rev.* **73**, 1424 (1948)
- 14M49 A. C. G. Mitchell, J. Y. Mei, F. C. Maieschein, and C. L. Peacock, *Phys. Rev.* **76**, 1450 (1949)
- 14M49a A. C. G. Mitchell and C. L. Peacock, *Phys. Rev.* **75**, 197 (1949)
- 14M51 A. C. G. Mitchell and L. J. Brown, NNES-PPR **9**, 717 (1951)
- 14M52 A. C. G. Mitchell and A. B. Smith, *Phys. Rev.* **85**, 153 (1952)
- 14M52a A. C. G. Mitchell and R. S. Caird, *Phys. Rev.* **87**, 388 (1952)
- 15M45 L. B. Magnusson and A. Ghiorso, unpublished data (1945)
- 15M47 L. B. Magnusson and T. J. LaChapelle, unpublished data (1947)
- 15M48 L. B. Magnusson and T. J. LaChapelle, *J. Am. Chem. Soc.* **70**, 3534 (1948); NNES-PPR **14B**, 39 (1949)
- 15M50 L. B. Magnusson, S. G. Thompson, and G. T. Seaborg, *Phys. Rev.* **78**, 363 (1950)
- 16M49 W. M. Manning and L. B. Asprey, NNES-PPR **14B**, 1595 (1949)
- 17M39 H. Maier-Leibnitz, *Naturwiss.* **26**, 614 (1939)
- 18M51 C. H. Millar and A. G. W. Cameron, *Phys. Rev.* **81**, 316 (1951) (A)
- 18M51a C. H. Millar, G. A. Bartholomew, and B. B. Kinsey, *Phys. Rev.* **81**, 150 (1951)
- 18M52 C. H. Millar and A. G. W. Cameron, private communication (Oct. 1952)
- 18M52a C. H. Millar, G. A. Bartholomew, and B. B. Kinsey, private communication (Oct. 1952)
- 19M47 A. N. May and E. P. Hincks, *Can. J. Research* **25A**, 77 (1947)
- 20M51 G. G. Manov and L. F. Curtiss, *J. Research Natl. Bur. Standards* **46**, 328 (1951)
- 21M50 W. W. Miller, R. Ballentine, W. Bernstein, L. Friedman, A. O. Nier, and R. D. Evans, *Phys. Rev.* **77**, 714 (1950)
- 22M43 J. Marshall, reported in Metallurgical Laboratory Classified Report CP-718 (June 1943)
- 23M50 P. A. Macklin, L. J. Lidofsky, and C. S. Wu, *Phys. Rev.* **78**, 318 (1950) (A)
- 23M50a P. A. Macklin, L. Feldman, L. Lidofsky, and C. S. Wu, *Phys. Rev.* **77**, 137 (1950)
- 23M51 P. A. Macklin, L. I. Lidofsky, and C. S. Wu, *Phys. Rev.* **82**, 334 (1951) (A)
- 23M51a P. Macklin, L. Lidofsky, and C. S. Wu, reported in Columbia University Unclassified Report CU-96 (June 1951)
- 24M37 C. Magnan, *Compt. rend.* **205**, 1147 (1937)
- 24M41 C. Magnan, *Ann. phys.* **15**, 5 (1941)
- 25M49 K. H. Morganstern and K. P. W. Wolf, *Phys. Rev.* **76**, 1261 (1949)
- 26M42 C. E. Mandeville, *Phys. Rev.* **62**, 555 (1942)
- 26M43 C. E. Mandeville, *Phys. Rev.* **63**, 387 (1943)
- 26M43a C. E. Mandeville, *Phys. Rev.* **64**, 147 (1943)
- 26M48 C. E. Mandeville and M. V. Scherb, *Phys. Rev.* **73**, 141 (1948)
- 26M48a C. E. Mandeville and M. V. Scherb, *Phys. Rev.* **73**, 1434 (1948)
- 26M48b C. E. Mandeville, M. V. Scherb, and W. B. Keighton, *Phys. Rev.* **74**, 888 (1948)
- 26M48c C. E. Mandeville and M. V. Scherb, *Phys. Rev.* **73**, 848 (1948)
- 26M48d C. E. Mandeville and M. V. Scherb, *Phys. Rev.* **73**, 340 (1948)
- 26M48e C. E. Mandeville, M. V. Scherb, and W. B. Keighton, *Phys. Rev.* **74**, 601 (1948)
- 26M49 C. E. Mandeville, Y. H. Woo, M. V. Scherb, W. B. Keighton, and E. Shapiro, *Phys. Rev.* **75**, 1528 (1949)

- 26M49a C. E. Mandeville, M. V. Scherb, and W. B. Keighton, *Phys. Rev.* 75, 221, 329 (1949)
- 26M49b C. E. Mandeville and E. Shapiro, *Phys. Rev.* 75, 897 (1949)
- 26M49c C. E. Mandeville and E. Shapiro, *Phys. Rev.* 76, 718 (1949)
- 26M49d C. E. Mandeville, *Phys. Rev.* 75, 1017 (1949)
- 26M49e C. E. Mandeville and E. Shapiro, *Phys. Rev.* 75, 1834 (1949)
- 26M49f C. E. Mandeville and M. V. Scherb, *Phys. Rev.* 76, 186 (1949) (A)
- 26M50 C. E. Mandeville and E. Shapiro, *Phys. Rev.* 77, 439 (1950)
- 26M50a C. E. Mandeville and E. Shapiro, *Phys. Rev.* 79, 243 (1950) (A)
- 26M50b C. E. Mandeville and E. Shapiro, *Phys. Rev.* 79, 391 (1950)
- 26M51 C. E. Mandeville and E. Shapiro, *Phys. Rev.* 82, 953 (1951); *J. Franklin Inst.* 253, 145 (1952)
- 26M52 C. E. Mandeville, E. Shapiro, R. I. Mendenhall, E. R. Zucker, and G. L. Conklin, *Phys. Rev.* 86, 813 (1952)
- 26M52a C. E. Mandeville, E. Shapiro, R. I. Mendenhall, E. R. Zucker, and G. L. Conklin, *Phys. Rev.* 88, 554 (1952)
- 27M49 J. McElhinney, A. O. Hanson, R. A. Becker, R. B. Duffield, and B. C. Diven, *Phys. Rev.* 75, 542 (1949)
- 28M40 B. L. Moore, *Phys. Rev.* 57, 355 (1940) (A)
- 29M52 H. T. Motz and D. E. Alburger, *Phys. Rev.* 86, 165 (1952)
- 29M52a H. T. Motz, *Phys. Rev.* 85, 501 (1952)
- 30M40 R. L. McCreary, G. Kuerti, and S. N. Van Voorhis, *Phys. Rev.* 57, 351 (1940) (A)
- 31M40 D. Mulder, G. W. Hoeksema, and G. J. Sizoo, *Physica* 7, 849 (1940)
- 32M48 D. R. Miller, R. C. Thompson, and B. B. Cunningham, *Phys. Rev.* 74, 347 (1948)
- 32M48a D. R. Miller, Ph.D. Thesis, University of California Radiation Laboratory Declassified Report UCRL-142 (July 1948)
- 32M50 D. R. Miller, *Phys. Rev.* 78, 808 (1950)
- 33M49 V. Myers and A. Wattenberg, *Phys. Rev.* 75, 992 (1949)
- 34M47 H. A. Meyer, G. Schwachheim, and M. D. de Souza Santos, *Phys. Rev.* 71, 908 (1947)
- 35M51 P. Morrison, *Phys. Rev.* 82, 209 (1951)
- 36M47 D. E. Matthews and M. L. Pool, *Phys. Rev.* 72, 163 (1947) (A)
- 37M49 J. L. Meem, Jr. and F. Maienschein, *Phys. Rev.* 76, 328 (1949)
- 38M47 E. der Mateosian, M. Goldhaber, C. O. Muehlhause, and M. McKeown, *Phys. Rev.* 72, 1271 (1947)
- 38M49 E. der Mateosian, M. Goldhaber, and A. Smith, reported in Argonne National Laboratory Classified Report ANL-4237 (Jan. 1949)
- 38M49a E. der Mateosian and M. Goldhaber, *Phys. Rev.* 76, 187 (1949) (A)
- 38M50 E. der Mateosian and M. Goldhaber, *Phys. Rev.* 79, 192 (1950)
- 38M50a E. der Mateosian, M. Goldhaber, and D. E. Alburger, reported in Brookhaven National Laboratory Unclassified Report BNL-39 (Jan. 1950)
- 38M51 E. der Mateosian and M. Goldhaber, *Phys. Rev.* 82, 115 (1951)
- 38M51a E. der Mateosian, *Phys. Rev.* 83, 223 (1951) (A)
- 38M51b E. der Mateosian and M. Goldhaber, *Phys. Rev.* 83, 843 (1951)
- 38M51c E. der Mateosian and M. Goldhaber, unpublished data quoted in (18G52)
- 38M52 E. der Mateosian, private communication (Oct. 1952)
- 38M52a E. der Mateosian, G. Friedlander, M. Goldhaber, and A. W. Sunyar, quoted in (18G52)
- 39M50 M. L. Moon, M. A. Waggoner, and A. Roberts, *Phys. Rev.* 79, 905 (1950)
- 40M47 A. E. Miller and M. Deutsch, *Phys. Rev.* 72, 527 (1947) (A)
- 41M50 W. Mims, H. Halban, and R. Wilson, *Nature* 166, 1027 (1950)
- 41M51 W. Mims and H. Halban, *Proc. Phys. Soc. (London)* 64A, 311 (1951)
- 41M51a W. B. Mims and H. Halban, *Proc. Phys. Soc. (London)* 64A, 753 (1951)
- 42M47 J. Martelly, *Ann. phys.* 2, 555 (1947)
- 43M46 L. C. Miller and L. F. Curtiss, *Phys. Rev.* 70, 983 (1946)
- 43M47 L. C. Miller and L. F. Curtiss, *J. Research Natl. Bur. Standards* 38, 359 (1947)
- 44M48 F. Metzger and M. Deutsch, *Phys. Rev.* 74, 1640 (1948)
- 44M50 F. Metzger, *Phys. Rev.* 79, 398 (1950)
- 44M50a F. Metzger and M. Deutsch, *Phys. Rev.* 78, 551 (1950)
- 44M51 F. R. Metzger and R. D. Hill, *Phys. Rev.* 82, 646 (1951)
- 44M52 F. R. Metzger, *Phys. Rev.* 85, 727 (1952) (A)
- 44M52a F. R. Metzger, *Phys. Rev.* 86, 435 (1952)
- 44M52b F. R. Metzger and H. C. Amacher, *Phys. Rev.* 88, 147 (1952)
- 45M41 J. J. Mitchell, H. S. Brown, and R. D. Fowler, *Phys. Rev.* 60, 359 (1941)
- 46M49 F. Maienschein and J. L. Meem, Jr., *Phys. Rev.* 76, 899 (1949)
- 46M51 F. C. Maienschein, J. K. Bair, and W. B. Baker, *Phys. Rev.* 83, 477 (1951)
- 47M47 W. E. Meyerhof and G. Scharff-Goldhaber, *Phys. Rev.* 72, 273 (1947)
- 47M48 W. E. Meyerhof and M. Goldhaber, *Phys. Rev.* 74, 348 (1948)
- 47M48a W. E. Meyerhof, *Phys. Rev.* 74, 621 (1948)
- 47M52 W. E. Meyerhof, L. G. Mann, and H. I. West, Jr., private communication (Oct. 1952)
- 48M49 K. C. Mann, D. Rankin, and P. N. Daykin, *Phys. Rev.* 76, 1719 (1949)
- 48M51 K. C. Mann and G. H. Hanson, *Phys. Rev.* 83, 893 (1951) (A)
- 49M50 A. Mukerji and P. Preiswerk, *Helv. Phys. Acta* 23, 516 (1950)
- 49M52 A. Mukerji and P. Preiswerk, *Helv. Phys. Acta* 25, 387 (1952)
- 50M37 W. B. Mann, *Phys. Rev.* 52, 405 (1937)
- 50M38 W. B. Mann, *Phys. Rev.* 54, 649 (1938)
- 50M38a W. B. Mann, *Phys. Rev.* 53, 212 (1938) (A)
- 51M48 D. A. McCown, L. L. Woodward, and M. L. Pool, *Phys. Rev.* 74, 1311 (1948)
- 51M48a D. A. McCown, L. L. Woodward, and M. L. Pool, *Phys. Rev.* 74, 1315 (1948)
- 52M49 F. K. McGowan, *Phys. Rev.* 76, 1730 (1949)
- 52M50 F. K. McGowan, *Phys. Rev.* 80, 482 (1950)
- 52M50a F. K. McGowan, *Phys. Rev.* 80, 923 (1950)
- 52M50b F. K. McGowan, *Phys. Rev.* 79, 404 (1950)

- 52M50c F. K. McGowan, Phys. Rev. 77, 138 (1950)
- 52M51 F. K. McGowan, Oak Ridge National Laboratory Unclassified Report ORNL-952 (March 1951)
- 52M51a F. K. McGowan, Phys. Rev. 81, 1066 (1951)
- 52M52 F. K. McGowan, Phys. Rev. 85, 142 (1952)
- 52M52a F. K. McGowan, Phys. Rev. 85, 151 (1952)
- 52M52b F. K. McGowan and E. D. Klema, reported in Oak Ridge National Laboratory Unclassified Report ORNL-1164 (April 1952)
- 52M52c F. K. McGowan, Phys. Rev. 87, 542 (1952)
- 52M52d F. K. McGowan, E. D. Klema, and P. R. Bell, Phys. Rev. 85, 152 (1952)
- 52M52e F. K. McGowan, private communication (Oct. 1952)
- 53M49 J. Y. Mei, A. C. G. Mitchell, and D. J. Zaffarano, Phys. Rev. 76, 1883 (1949)
- 53M50 J. Y. Mei, A. C. G. Mitchell, and C. M. Huddleston, Phys. Rev. 79, 19 (1950)
- 53M50a J. Y. Mei, C. M. Huddleston, and A. C. G. Mitchell, Phys. Rev. 79, 429 (1950)
- 53M50b J. Y. Mei, C. M. Huddleston, and A. C. G. Mitchell, Phys. Rev. 79, 1010 (1950)
- 54M44 N. Marty, J. phys. et radium 5, 276 (1944)
- 54M49 N. Marty, J. Labeyrie, and H. Langevin, Compt. rend. 228, 1722 (1949)
- 54M51 N. Marty-Wollman, Ann. phys. 6, 662 (1951)
- 55M50 H. R. Muether and S. L. Ridgway, Phys. Rev. 80, 750 (1950)
- 56M50 J. Miskel, Phys. Rev. 79, 403 (1950)
- 56M50a J. Miskel and G. Friedlander, reported in Brookhaven National Laboratory Unclassified Report BNL-39 (Jan. 1950)
- 56M51 J. A. Miskel and A. C. Wahl, Phys. Rev. 84, 700 (1951)
- 56M52 J. A. Miskel and M. L. Perlman, Phys. Rev. 87, 543 (1952)
- 57M41 A. Moussa and L. Goldstein, Phys. Rev. 60, 534 (1941); Compt. rend. 212, 986 (1941)
- 58M50 L. G. Mann and P. Axel, Phys. Rev. 80, 759 (1950)
- 58M51 L. G. Mann and P. Axel, Phys. Rev. 84, 221 (1951)
- 58M52 L. G. Mann and W. E. Meyerhof, Phys. Rev. 87, 202 (1952) (A) and private communication with H. I. West, Jr. (Oct. 1952)
- 59M44 W. N. Moquin and M. L. Pool, Phys. Rev. 65, 60 (1944) (A)
- 60M48 D. L. Mock, R. C. Waddell, L. W. Fagg, and R. A. Tobin, Phys. Rev. 74, 1536 (1948)
- 61M47 E. E. Motta, Q. V. Larson, and G. E. Boyd, Phys. Rev. 72, 1270 (1947)
- 61M47a E. E. Motta, Q. V. Larson, and G. E. Boyd, reported in Oak Ridge National Laboratory Classified Report Mon N-432 (Dec. 1947)
- 61M47b E. E. Motta, G. E. Boyd, and A. R. Brosi, Phys. Rev. 71, 210 (1947)
- 61M48 E. E. Motta and G. E. Boyd, Phys. Rev. 73, 1470 (1948)
- 61M48a E. E. Motta and G. E. Boyd, Phys. Rev. 74, 220 (1948)
- 61M48b E. E. Motta and G. E. Boyd, Phys. Rev. 74, 344 (1948)
- 62M49 H. Medicus, D. Maeder, and H. Schneider, Helv. Phys. Acta 22, 603 (1949)
- 62M50 H. Medicus, P. Preiswerk, and P. Scherrer, Helv. Phys. Acta 23, 299 (1950)
- 62M50a H. Medicus and P. Preiswerk, Phys. Rev. 80, 1101 (1950)
- 62M51 H. Medicus, D. Maeder, and H. Schneider, Helv. Phys. Acta 24, 72 (1951); Phys. Rev. 81, 652 (1951) (A)
- 62M52 H. Medicus and H. T. Easterday, Phys. Rev. 85, 735 (1952) (A)
- 63M50 J. W. Mihelich and R. D. Hill, Phys. Rev. 79, 781 (1950)
- 63M51 J. W. Mihelich, M. Goldhaber, and E. Wilson, Phys. Rev. 82, 972 (1951)
- 63M51a J. W. Mihelich, reported in Brookhaven National Laboratory Unclassified Report BNL-93 (March 1951)
- 63M52 J. W. Mihelich and E. L. Church, Phys. Rev. 85, 690 (1952)
- 63M52a J. W. Mihelich, Phys. Rev. 87, 646 (1952)
- 63M52b J. W. Mihelich, private communication (Oct. 1952)
- 63M52c J. W. Mihelich and A. de Shalit, private communication (Nov. 1952)
- 63M52d J. W. Mihelich, Bull. A. P. S. 27, No. 5, Abstract V3 (1952)
- 64M40 O. Minakawa, Phys. Rev. 57, 1189 (1940)
- 64M41 O. Minakawa, Phys. Rev. 60, 689 (1941)
- 65M52 A. K. Mousuf, Phys. Rev. 88, 150 (1952)
- 66M51 C. L. McGinnis, Phys. Rev. 81, 734 (1951)
- 66M51a C. L. McGinnis, Phys. Rev. 83, 686 (1951)
- 66M52 C. L. McGinnis, Phys. Rev. 87, 202 (1952) (A) and private communication (Oct. 1952)
- 67M51 R. P. Metcalf, NNES-PPR 9, 891 (1951)
- 67M51a R. P. Metcalf, NNES-PPR 9, 898 (1951)
- 67M51b R. P. Metcalf, NNES-PPR 9, 905 (1951)
- 68M49 E. C. Mallery and M. L. Pool, Phys. Rev. 76, 1454 (1949)
- 68M50 E. C. Mallery and M. L. Pool, Phys. Rev. 77, 75 (1950)
- 69M51 M. M. Miller, C. H. Pruett, and R. G. Wilkinson, Phys. Rev. 84, 849 (1951)
- 69M51a M. M. Miller and R. G. Wilkinson, Phys. Rev. 83, 1050 (1951)
- 69M51b M. M. Miller and R. G. Wilkinson, Phys. Rev. 82, 981 (1951)
- 69M52 M. M. Miller, Phys. Rev. 88, 516 (1952)
- 70M49 W. C. Miller and B. Waldman, Phys. Rev. 75, 425 (1949)
- 71M50 E. A. Martell and W. F. Libby, Phys. Rev. 80, 977 (1950)
- 72M52 J. A. McCarthy, Phys. Rev. 87, 194 (1952) (A)
- 73M52 H. B. Mathur, M. Michel, T. O. Passell, and E. K. Hyde, private communication (Dec. 1952)
- 74M50 L. Marquez and I. Perlman, Phys. Rev. 78, 189 (1950)
- 74M51 L. Marquez and I. Perlman, Phys. Rev. 81, 953 (1951)
- 74M52 L. Marquez, Phys. Rev. 88, 225 (1952)
- 74M52a L. Marquez, Phys. Rev. 86, 406 (1952)
- 75M51 D. S. Martin, Jr. and F. J. Hughes, reported in Iowa State College Classified Report ISC-137 (May 1951)
- 75M51a D. S. Martin, Jr., E. N. Jensen, F. J. Hughes, and R. T. Nichols, Phys. Rev. 82, 579 (1951)
- 76M50 J. Macnamara, C. B. Collins, and H. G. Thode, Phys. Rev. 78, 129 (1950)
- 76M50a J. Macnamara and H. G. Thode, Phys. Rev. 78, 307 (1950)
- 77M35 J. C. McLennan, L. G. Grimmett, and J. Read, Nature 135, 505 (1935)
- 77M35a J. C. McLennan and W. H. Rann, Nature 136, 831 (1935)

- 77M35b J. C. McLennan, L. G. Grimmett, and J. Read, *Nature* 135, 147 (1935)
- 78M41 M. Melhase, unpublished data, University of California, Berkeley (Sept. 1941)
- 79M52 M. H. MacGregor and M. L. Wiedenbeck, *Phys. Rev.* 86, 420 (1952)
- 80M52 H. C. Martin and B. C. Diven, *Phys. Rev.* 86, 565 (1952)
- 81M42 K. E. Mounce, M. L. Pool, and J. D. Kurbatov, *Phys. Rev.* 61, 389 (1942) (A)
- 82M35 J. K. Marsh and S. Sugden, *Nature* 136, 102 (1935)
- 83M50 A. J. Moses and D. S. Martin, Jr., *Phys. Rev.* 79, 467 (1950)
- 83M51 A. J. Moses and D. S. Martin, Jr., *Phys. Rev.* 84, 366 (1951)
- 84M47 J. A. Marinsky, L. E. Glendenin, and C. D. Coryell, *J. Am. Chem. Soc.* 69, 2781 (1947)
- 84M49 J. A. Marinsky, reported in Massachusetts Institute of Technology Unclassified Report NP-1272 (July 1949)
- 84M49a J. A. Marinsky, L. E. Glendenin, and F. Metzger, reported in Massachusetts Institute of Technology Unclassified Report NP-1727 (July 1949)
- 84M51 J. A. Marinsky and L. E. Glendenin, *NNES-PPR* 9, 1229 (1951)
- 84M51a J. A. Marinsky and L. E. Glendenin, *NNES-PPR* 9, 1243 (1951)
- 84M51b J. A. Marinsky and L. E. Glendenin, *NNES-PPR* 9, 1264 (1951)
- 84M51c J. A. Marinsky and L. E. Glendenin, *NNES-PPR* 9, 1254 (1951)
- 84M51d J. A. Marinsky and L. E. Glendenin, *NNES-PPR* 9, 1969 (1951)
- 85M52 G. I. Mulholland and T. P. Kohman, *Phys. Rev.* 85, 144 (1952)
- 85M52a G. I. Mulholland and T. P. Kohman, *Phys. Rev.* 87, 681 (1952)
- 86M52 R. C. Mack, D. I. Prickett, and M. L. Pool, *Phys. Rev.* 86, 633 (1952) (A)
- 87M50 J. E. Mack, *Revs. Modern Phys.* 22, 64 (1950)
- 88M51 K. Murakawa and J. S. Ross, *Phys. Rev.* 82, 967 (1951)
- 89M52 D. F. Martin, unpublished data (Aug. 1952)
- 89M52a D. F. Martin, R. W. Hoff, G. H. Higgins, and S. G. Thompson, reported in University of California Radiation Laboratory Classified Report UCRL-1770 (April 1952)
- 90M52 J. H. Moon and A. L. Thompson, *Phys. Rev.* 83, 892 (1951) (A) and private communication (Oct. 1952)
- 91M51 S. L. Miller, A. Javan, and C. H. Townes, *Phys. Rev.* 82, 454 (1951)
- 92M51 J. W. Meadows and R. B. Holt, *Phys. Rev.* 83, 1257 (1951)
- 93M51 J. M. Miller and G. Friedlander, *Phys. Rev.* 84, 589 (1951)
- 94M51 D. Maeder and P. Preiswerk, *Phys. Rev.* 84, 595 (1951)
- 94M51a D. Maeder and P. Preiswerk, *Helv. Phys. Acta* 24, 625 (1951)
- 95M52 J. K. Major, *Compt. rend.* 234, 2276 (1952); *Phys. Rev.* 86, 631 (1952) (A)
- 96M52 J. Moreau and J. Perez y Jorba, *Compt. rend.* 235, 38 (1952)
- 97M52 K. C. Maclure, Ph.D. Thesis, McGill University (Sept. 1952)
- 98M51 W. M. Martin, Ph.D. Thesis, McGill University (1951)
- 98M52 W. M. Martin and S. W. Breckon, *Can. J. Phys.* (to be published) (1952)
- 99M52 M. McKeown and S. Katcoff, private communication (Oct. 1952)
- 100M52 D. E. Muller, H. C. Hoyt, D. J. Klein, and J. W. M. DuMond, *Phys. Rev.* 88, 775 (1952)
- 1N50 T. B. Novey, reported in Argonne National Laboratory Classified Report ANL-4427 (July 1950)
- 1N50a T. B. Novey, *Phys. Rev.* 78, 66 (1950)
- 1N51 T. B. Novey, D. W. Engelkeimeir, E. L. Brady, and L. E. Glendenin, *NNES-PPR* 9, 678 (1951)
- 1N51a T. B. Novey, *NNES-PPR* 9, 976 (1951)
- 1N51b T. B. Novey, W. H. Sullivan, C. D. Coryell, A. S. Newton, N. R. Sleight, and O. Johnson, *NNES-PPR* 9, 958 (1951)
- 1N51c T. B. Novey and J. D. Knight, *NNES-PPR* 9, 1043 (1951)
- 2N36 R. Naidu and R. E. Siday, *Proc. Phys. Soc. (London)* 48, 332 (1936)
- 3N36 M. E. Nahmias and R. J. Walen, *Compt. rend.* 203, 71 (1936)
- 4N50 H. M. Neumann and I. Perlman, *Phys. Rev.* 78, 191 (1950)
- 4N50a H. M. Neumann, J. J. Howland, Jr., and I. Perlman, *Phys. Rev.* 77, 720 (1950)
- 4N50b H. M. Neumann, A. Ghiorso, and I. Perlman, unpublished data (1950)
- 4N51 H. M. Neumann and I. Perlman, *Phys. Rev.* 81, 958 (1951)
- 5N38 Y. Nishina, T. Yasaki, K. Kimura, and M. Ikawa, *Nature* 142, 874 (1938)
- 5N40 Y. Nishina, T. Yasaki, H. Exoe, K. Kimura, and M. Ikawa, *Phys. Rev.* 57, 1182 (1940)
- 5N40a Y. Nishina, T. Yasaki, K. Kimura, and M. Ikawa, *Phys. Rev.* 58, 660 (1940)
- 5N40b Y. Nishina, T. Yasaki, H. Exoe, K. Kimura, and M. Ikawa, *Nature* 146, 24 (1940)
- 5N41 Y. Nishina, T. Yasaki, K. Kimura, and M. Ikawa, *Phys. Rev.* 59, 677 (1941)
- 5N42 Y. Nishina, K. Kimura, T. Yasaki, and M. Ikawa, *Z. Physik* 119, 195 (1942)
- 6N36 A. O. Nier and E. E. Hanson, *Phys. Rev.* 50, 722 (1936)
- 6N37 A. O. Nier, *Phys. Rev.* 52, 933 (1937)
- 6N37a A. O. Nier, *Phys. Rev.* 52, 885 (1937)
- 6N38 A. O. Nier, *J. Am. Chem. Soc.* 60, 1571 (1938)
- 6N38a A. O. Nier, *Phys. Rev.* 53, 282 (1938)
- 6N38b A. O. Nier, *Phys. Rev.* 54, 275 (1938)
- 6N39 A. O. Nier, *Phys. Rev.* 55, 150 (1939). Values recalculated according to 76K41
- 6N50 A. O. Nier, *Phys. Rev.* 77, 789 (1950)
- 6N50a A. O. Nier, *Phys. Rev.* 79, 450 (1950)
- 7N49 A. S. Newton, *Phys. Rev.* 75, 209 (1949)
- 7N49a A. S. Newton, *Phys. Rev.* 75, 17 (1949)
- 7N49b A. S. Newton and W. R. McDonell, University of California Radiation Laboratory Unclassified Report UCRL-395 (July 1949)
- 7N51 A. S. Newton, W. H. Sullivan, O. Johnson, and R. Nottorf, *NNES-PPR* 9, 1028 (1951)
- 7N51a A. S. Newton, A. Kant, and R. E. Hein, *NNES-PPR* 9, 1200 (1951)
- 8N47 A. Novick, *Phys. Rev.* 72, 972 (1947)

- 9N40 G. J. Neary, *Proc. Roy. Soc. (London)* **175A**, 71 (1940)
- 10N48 L. D. Norris and M. G. Inghram, *Phys. Rev.* **73**, 350 (1948)
- 11N37 S. Nishida, *Proc. Phys.-Math. Soc. Japan* **19**, 809 (1937)
- 12N35 H. W. Newson, *Phys. Rev.* **48**, 790 (1935)
- 12N35a H. W. Newson, *Phys. Rev.* **48**, 482 (1935) (A)
- 12N37 H. W. Newson, *Phys. Rev.* **51**, 624 (1937)
- 13N50 Y. A. Nemilov and L. I. Gedeonov, *Doklady Akad. Nauk S.S.S.R.* **70**, 219 (1950)
- 14N50 B. D. Nag, S. Sen, and S. Chatterjee, *Indian J. Phys.* **24**, 479 (1950)
- 15N42 M. E. Nelson, M. L. Pool, and J. D. Kurbatov, *Phys. Rev.* **62**, 1 (1942)
- 15N42a M. E. Nelson, M. L. Pool, and J. D. Kurbatov, *Phys. Rev.* **61**, 428 (1942)
- 15N50 M. E. Nelson and M. L. Pool, *Phys. Rev.* **77**, 682 (1950)
- 16N44 B. D. Nag-Chowdhury, *Proc. Nat. Inst. Sci. India* **10**, 317 (1944); *Chem. Abs.* **42**, 4452b (1948)
- 17N44 V. A. Nedzel and E. C. Barker, reported in *Metallurgical Laboratory Classified Report CP-1728* (June 1944)
- 17N51 V. A. Nedzel, *NNES-PPR* **9**, 719 (1951)
- 17N51a V. A. Nedzel, *NNES-PPR* **9**, 732 (1951)
- 17N51b V. A. Nedzel, *NNES-PPR* **9**, 1213 (1951)
- 18N51 R. W. Nottorf, *NNES-PPR* **9**, 682 (1951)
- 19N50 C. M. Nelson, B. H. Ketelle, and G. E. Boyd, *Oak Ridge National Laboratory Unclassified Report ORNL-828* (Nov. 1950)
- 20N51 G. J. Nijgh, N. F. Verster, R. H. Nussbaum, R. Van Lieshout, and C. J. Bakker, *Physica* **17**, 658 (1951)
- 21N50 R. A. Naumann, F. L. Reynolds, and I. Perlman, *Phys. Rev.* **77**, 398 (1950)
- 22N52 W. E. Nervik, reported in *University of California Radiation Laboratory Classified Report UCRL-1632* (Jan. 1952)
- 23N35 E. Neuninger and E. Rona, *Anz. Akad. Wiss. Wien, Math.-naturw. Klasse* **72**, 275 (1935)
- 23N36 E. Neuninger and E. Rona, *Anz. Akad. Wiss. Wien, Math.-naturw. Klasse* **73**, 159 (1936)
- 24N47 H. Neuert, *Z. Naturforsch.* **2a**, 432 (1947)
- 25N48 S. N. Naldrett and W. F. Libby, *Phys. Rev.* **73**, 487 (1948)
- 1046 R. K. Osborne and W. C. Peacock, *Phys. Rev.* **69**, 679 (1946) (A)
- 1047 R. K. Osborne and M. Deutsch, *Phys. Rev.* **71**, 467 (1947) (A)
- 2039 F. Oppenheimer and E. P. Tomlinson, *Phys. Rev.* **56**, 858 (1939) (A)
- 3047 W. Ogle, L. Brown, and R. Conklin, *Phys. Rev.* **71**, 378 (1947)
- 3050 W. E. Ogle, L. J. Brown, and A. N. Carson, *Phys. Rev.* **78**, 63 (1950)
- 4040 R. D. O'Neal and M. Goldhaber, *Phys. Rev.* **58**, 574 (1940)
- 4040a R. D. O'Neal and M. Goldhaber, *Phys. Rev.* **57**, 1086 (1940) (A)
- 4041 R. D. O'Neal, *Phys. Rev.* **60**, 359 (1941)
- 5049 D. W. Osborne, R. C. Thompson, and Q. Van Winkle, *NNES-PPR* **14B**, 1397 (1949)
- 6047 P. R. O'Connor and G. T. Seaborg, unpublished data (1947)
- 6048 P. R. O'Connor and G. T. Seaborg, *Phys. Rev.* **74**, 1189 (1948)
- 7049 D. A. Orth, L. Marquez, W. J. Heiman, and D. H. Templeton, *Phys. Rev.* **75**, 1100 (1949)
- 7050 D. A. Orth, A. Ghiorso, and G. T. Seaborg, unpublished data (April 1950)
- 7051 D. A. Orth and R. A. Glass, unpublished data (March 1951)
- 7051a D. A. Orth and K. Street, Jr., unpublished data (1951)
- 7051b D. A. Orth and G. D. O'Kelley, *Phys. Rev.* **82**, 758 (1951)
- 8050 G. D. O'Kelley and F. L. Reynolds, reported in *University of California Radiation Laboratory Classified Report UCRL-550* (Jan. 1950)
- 8050a G. D. O'Kelley, G. W. Barton, Jr., W. W. T. Crane, and I. Perlman, *Phys. Rev.* **80**, 293 (1950)
- 8051 G. D. O'Kelley, Ph.D. Thesis, *University of California Radiation Laboratory Unclassified Report UCRL-1243* (May 1951)
- 9049 A. Orsini, *Anais faculdade farm. odontol., Univ. São Paulo* **7**, 9 (1949)
- 10046 R. T. Overman, *U. S. Atomic Energy Commission Declassified Document MDDC-354* (Sept. 1946)
- 10047 R. T. Overman, *U. S. Atomic Energy Commission Declassified Document AECD-857* (April 1947)
- 11042 R. Overstreet, L. Jacobson, K. Scott, and J. G. Hamilton, *Metallurgical Project Declassified Report* (work performed at Berkeley) **CH-379** (Dec. 1942)
- 11043 R. Overstreet and L. Jacobson, reported in *Metallurgical Project Classified Report* (work performed at Berkeley) **CH-498** (Feb. 1943)
- 11049 R. Overstreet, L. Jacobson, and P. R. Stout, *Phys. Rev.* **75**, 231 (1949)
- 11051 R. Overstreet and L. Jacobson, *NNES-PPR* **9**, 621 (1951)
- 12042 J. J. O'Connor, M. L. Pool, and J. D. Kurbatov, *Phys. Rev.* **62**, 413 (1942)
- 13048 G. E. Owen, D. Moe, and C. S. Cook, *Phys. Rev.* **74**, 1879 (1948); **75**, 1270 (1949)
- 13049 G. E. Owen and C. S. Cook, *Phys. Rev.* **76**, 1726 (1949)
- 13050 G. E. Owen, C. S. Cook, and P. H. Owen, *Phys. Rev.* **78**, 686 (1950)
- 14040 Z. Ollano, *Ricerca sci.* **11**, 568 (1940)
- 14041 Z. Ollano, *Nuovo cimento* **18**, 11 (1941)
- 15049 J. S. Osoba, *Phys. Rev.* **76**, 345 (1949)
- 16051 J. Ovadia and P. Axel, *Phys. Rev.* **82**, 332 (1951) (A)
- 17038 O. Oldenberg, *Phys. Rev.* **53**, 35 (1938)
- 18050 F. E. O'Meara, *Phys. Rev.* **79**, 1032 (1950)
- 19052 J. Orring, *Arkiv Fysik* **4**, 469 (1952); reported in *M. Siegbahn Commemorative Volume*, p 197 (Uppsala, 1951)
- 20052 J. Owen and J. H. E. Griffiths, (to be published) (1952)
- 1P37 M. L. Pool, J. M. Cork, and R. L. Thornton, *Phys. Rev.* **52**, 239 (1937)
- 1P37a M. L. Pool and J. M. Cork, *Phys. Rev.* **51**, 1010 (1937) (A)
- 1P38 M. L. Pool, *Phys. Rev.* **53**, 116 (1938)
- 1P38a M. L. Pool and L. L. Quill, *Phys. Rev.* **53**, 437 (1938)
- 1P43 M. L. Pool and J. D. Kurbatov, *Phys. Rev.* **63**, 463 (1943) (A)
- 1P45 M. L. Pool and J. E. Edwards, *Phys. Rev.* **67**, 60 (1945) (A)

- 1P48 M. L. Pool and N. L. Krisberg, *Phys. Rev.* 73, 1035 (1948)
- 1P52 M. L. Pool and D. N. Kundu, private communication (Nov. 1952)
- 2P49 V. Perez-Mendez and H. Brown, *Phys. Rev.* 76, 689 (1949)
- 2P50 V. Perez-Mendez and H. Brown, *Phys. Rev.* 77, 404 (1950)
- 2P50a V. Perez-Mendez and H. Brown, *Phys. Rev.* 78, 812 (1950)
- 2P50b V. Perez-Mendez and P. Lindenfeld, reported in Columbia University Unclassified Document CUD-56 (Aug. 1950)
- 2P50c V. Perez-Mendez and P. Lindenfeld, *Phys. Rev.* 80, 1097 (1950)
- 2P51 V. Perez-Mendez and P. Lindenfeld, *Phys. Rev.* 83, 864 (1951)
- 3P46 K. Philipp and J. Riedhammer, *Z. Naturforsch.* 1, 372 (1946)
- 3P48 K. Philipp and F. Rehbein, *Z. Physik* 124, 225 (1948)
- 4P35 P. Preiswerk and H. von Halban, *Compt. rend.* 201, 722 (1935)
- 4P51 P. Preiswerk and P. Stahelin, *Helv. Phys. Acta* 24, 300 (1951)
- 5P51 C. A. Prohaska, Ph.D. Thesis, University of California Radiation Laboratory Unclassified Report UCRL-1395 (Aug. 1951)
- 6P46 W. C. Peacock and M. Deutsch, *Phys. Rev.* 69, 306 (1946)
- 6P46a W. C. Peacock, R. D. Evans, J. W. Irvine, W. M. Good, A. F. Kip, S. Weiss, and J. G. Gibson, *J. Clin. Invest.* 25, 605 (1946)
- 6P47 W. C. Peacock, J. W. Jones, and R. T. Overman, reported in Oak Ridge National Laboratory Classified Report Mon N-432 (Dec. 1947)
- 6P47a W. C. Peacock, *Phys. Rev.* 72, 1049 (1947)
- 6P47b W. C. Peacock, A. R. Brosi, and A. D. Bogard, reported in Oak Ridge National Laboratory Classified Reports Mon N-432 (Dec. 1947); ORNL-65 (July 1948); ORNL-176 (Nov. 1948)
- 6P48 W. C. Peacock and J. W. Jones, U. S. Atomic Energy Commission Declassified Document AECD-1812 (March 1948)
- 7P39 M. Perey, *Compt. rend.* 208, 97 (1939); *J. phys. et radium* 10, 435 (1939)
- 7P39a M. Perey and M. Lecoïn, *J. phys. et radium* 10, 439 (1939)
- 7P39b M. Perey and M. Lecoïn, *Nature* 144, 326 (1939)
- 7P41 M. Perey and M. Lecoïn, *Compt. rend.* 212, 893 (1941)
- 7P46 M. Perey, *J. chim. phys.* 43, 155, 269 (1946)
- 8P49 S. Peterson, NNS-PPR 14B, 1393 (1949)
- 8P49a S. Peterson and A. Ghiorso, NNS-PPR 14B, 1395 (1949)
- 8P49b S. Peterson and A. Ghiorso, NNS-PPR 14B, 1424 (1949)
- 9P37 A. Polessitsky, *Physik Z. Sowjetunion* 12, 339 (1937)
- 9P40 A. Polessitsky and N. Nemerovsky, *Compt. rend. U. R. S. S.* 28, 217 (1940)
- 9P40a A. Polessitsky and M. Orbeli, *Compt. rend. U. R. S. S.* 28, 215 (1940)
- 9P41 A. Polessitsky, N. Nemerovsky, M. Orbeli, and N. Baronckik, *J. Phys. (U. S. S. R.)* IV, 284 (1941)
- 10P46 M. J. Poole and E. B. Paul, *Nature* 158, 482 (1946)
- 11P46 A. K. Pierce and F. W. Brown, III, *Phys. Rev.* 70, 779 (1946)
- 12P48 M. L. Perlman and G. Friedlander, *Phys. Rev.* 74, 442 (1948)
- 12P49 M. L. Perlman, *Phys. Rev.* 75, 988 (1949)
- 12P51 M. L. Perlman and G. Friedlander, *Phys. Rev.* 82, 449 (1951)
- 12P52 M. L. Perlman and R. Schwartz, private communication (Oct. 1952)
- 13P47 I. Perlman, R. H. Goeckermann, D. H. Templeton, and J. J. Howland, Jr., *Phys. Rev.* 72, 352 (1947)
- 13P47a I. Perlman, J. J. Howland, Jr., and D. H. Templeton, unpublished data (1947)
- 13P49 I. Perlman, P. R. O'Connor, and L. O. Morgan, NNS-PPR 14B, 1651 (1949)
- 13P50 I. Perlman, A. Ghiorso, and G. T. Seaborg, *Phys. Rev.* 77, 26 (1950)
- 14P40 E. Pollard and W. W. Watson, *Phys. Rev.* 58, 12 (1940)
- 15P49 D. D. Phillips, U. S. Atomic Energy Commission Unclassified Report AECU-404 (June 1949)
- 16P52 M. Paganelli and G. Quarenzi, *Phys. Rev.* 86, 423 (1952); *Nuovo cimento* 9, 324 (1952)
- 17P38 B. Pontecorvo, *Phys. Rev.* 54, 542 (1938)
- 17P38a B. Pontecorvo and A. Lazard, *Compt. rend.* 208, 99 (1938)
- 17P49 B. Pontecorvo, D. H. W. Kirkwood, and G. C. Hanna, *Phys. Rev.* 75, 982 (1949)
- 18P50 R. W. Pringle, S. Standil, and K. I. Rouleston, *Phys. Rev.* 77, 841 (1950)
- 18P50a R. W. Pringle and S. Standil, *Phys. Rev.* 80, 762 (1950)
- 18P51 R. W. Pringle, S. Standil, H. W. Taylor, and G. Fryer, *Phys. Rev.* 84, 1066 (1951)
- 18P52 R. W. Pringle, H. W. Taylor, and S. Standil, *Phys. Rev.* 87, 384 (1952)
- 19P51 F. T. Porter and C. S. Cook, *Phys. Rev.* 81, 640 (1951)
- 19P51a F. T. Porter and C. S. Cook, *Phys. Rev.* 81, 298 (1951) (A)
- 19P52 F. T. Porter and C. S. Cook, *Phys. Rev.* 87, 464 (1952)
- 20P48 C. L. Peacock and R. G. Wilkinson, *Phys. Rev.* 74, 297 (1948)
- 20P49 C. L. Peacock and A. C. G. Mitchell, *Phys. Rev.* 75, 1272 (1949)
- 20P51 C. L. Peacock and J. L. Braud, *Phys. Rev.* 83, 484 (1951) (A)
- 21P42 E. H. Plesset, *Phys. Rev.* 62, 181 (1942)
- 22P37 C. Perrier and E. Segrè, *J. Chem. Phys.* 5, 713 (1937); 7, 155 (1939)
- 22P38 C. Perrier, M. Santangelo, and E. Segrè, *Phys. Rev.* 53, 104 (1938)
- 23P47 T. J. Parmley and B. J. Moyer, *Phys. Rev.* 72, 82 (1947)
- 23P49 T. J. Parmley, B. J. Moyer, and R. C. Lilly, *Phys. Rev.* 75, 619 (1949)
- 24P51 E. Plassmann and F. R. Scott, *Phys. Rev.* 84, 156 (1951)
- 25P52 R. M. Pearce and E. K. Darby, *Phys. Rev.* 86, 1049 (1952)
- 26P47 G. W. Parker, P. M. Lantz, M. G. Inghram, D. C. Hess, Jr., and R. J. Hayden, *Phys. Rev.* 72, 85 (1947)
- 26P49 G. W. Parker, G. E. Creek, G. M. Hebert, P. M. Lantz, and W. J. Martin, reported in Oak Ridge National Laboratory Classified Report ORNL-499 (Dec. 1949)
- 26P49a G. W. Parker, G. E. Creek, G. M. Hebert, and P. M. Lantz, reported in Oak Ridge National Laboratory Classified Report ORNL-336 (May 1949)

- 26P49b G. W. Parker, G. E. Creek, G. M. Hebert, P. M. Lantz, and W. J. Martin, reported in Oak Ridge National Laboratory Classified Report ORNL-286 (Sept. 1949)
- 26P51 G. W. Parker, reported in Oak Ridge National Laboratory Classified Report ORNL-870 (March 1951)
- 26P52 G. W. Parker and W. J. Martin, private communication (Oct. 1952)
- 27P51 J. P. Palmer and L. J. Laslett, U. S. Atomic Energy Commission Unclassified Report AECU-1220 (March 1951)
- 27P51a J. P. Palmer, *Phys. Rev.* **82**, 772 (1951) (A)
- 28P50 R. I. Powers and A. F. Voigt, *Phys. Rev.* **79**, 175 (1950)
- 29P40 C. Pecher, *Phys. Rev.* **58**, 843 (1940)
- 30P51 A. C. Pappas, *Phys. Rev.* **81**, 299 (1951) (A)
- 30P51a A. C. Pappas and C. D. Coryell, *Phys. Rev.* **81**, 329 (1951) (A)
- 30P52 A. C. Pappas, *Phys. Rev.* **87**, 162 (1952)
- 30P52a A. C. Pappas, private communication (Oct. 1952)
- 31P49 E. Picciotti, *Compt. rend.* **229**, 117 (1949)
- 32P50 W. W. Pratt, *Phys. Rev.* **80**, 289 (1950)
- 33P52 W. K. H. Panofsky and D. Reagan, *Phys. Rev.* **87**, 543 (1952)
- 34P52 I. Pullman and P. Axel, private communication (Oct. 1952)
- 35P52 T. Passel, W. A. Jenkins, and W. W. T. Crane, reported in University of California Radiation Laboratory Classified Report UCRL-1770 (April 1952)
- 1R31 E. Rutherford, C. E. Wynn-Williams, and W. B. Lewis, *Proc. Roy. Soc. (London)* **133A**, 351 (1931)
- 2R50 J. M. Robson, *Phys. Rev.* **78**, 311 (1950)
- 2R51 J. M. Robson, *Phys. Rev.* **83**, 349 (1951)
- 3R50 M. Riou, *J. phys. et radium* **11**, 185 (1950); *Compt. rend.* **228**, 678 (1949)
- 3R52 M. Riou, *J. phys. et radium* **13**, 244 (1952)
- 3R52a M. Riou, *Compt. rend.* **234**, 1157 (1952)
- 3R53 M. Riou, *Ann. phys.* (to be published) (1953)
- 4R36 S. Rosenblum, M. Guillot, and M. Perey, *Compt. rend.* **202**, 1274 (1936)
- 4R37 S. Rosenblum, M. Guillot, and M. Perey, *Compt. rend.* **204**, 175 (1937)
- 4R48 S. Rosenblum, M. Valadares, and J. Vial, *Compt. rend.* **227**, 1088 (1948)
- 4R49 S. Rosenblum, M. Valadares, M. Perey, and J. Vial, *Compt. rend.* **229**, 1009 (1949)
- 4R49a S. Rosenblum, M. Guillot, and G. Bastin-Scoffier, *Compt. rend.* **229**, 191 (1949)
- 4R49b S. Rosenblum, M. Valadares, and M. Perey, *Compt. rend.* **228**, 385 (1949)
- 4R49c S. Rosenblum, E. Cotton, and G. Bouissières, *Compt. rend.* **229**, 825 (1949)
- 4R50 S. Rosenblum, M. Valadares, and B. Goldschmidt, *Compt. rend.* **230**, 638 (1950)
- 4R51 S. Rosenblum and M. Valadares, *Compt. rend.* **232**, 501 (1951)
- 4R52 S. Rosenblum, M. Valadares, and M. Guillot, *Compt. rend.* **234**, 1767 (1952)
- 4R52a S. Rosenblum, M. Valadares, and M. Guillot, *Compt. rend.* **235**, 238 (1952)
- 4R52b S. Rosenblum, M. Perey, M. Valadares, and M. Guillot, private communication (Oct. 1952)
- 5R47 S. Rowlands, *Nature* **160**, 191 (1947)
- 6R35 J. Rotblat, *Nature* **136**, 515 (1936)
- 6R41 J. Rotblat, *Proc. Roy. Soc. (London)* **177A**, 260 (1941)
- 6R41a J. Rotblat, *Nature* **148**, 371 (1941)
- 7R36 F. Rasetti, "Elements of Nuclear Physics," Prentice-Hall, Inc., New York (1936)
- 8R40 R. Ringo, *Phys. Rev.* **58**, 942 (1940); **59**, 107 (1941). Values recalculated according to (9H38)
- 9R48 G. Reed, Jr., W. M. Manning, and W. Bentley, reported in Argonne National Laboratory Classified Report ANL-4112 (March 1948)
- 10R49 F. L. Reynolds, D. G. Karraker, and D. H. Templeton, *Phys. Rev.* **75**, 313 (1949)
- 10R50 F. L. Reynolds, E. K. Hulet, and K. Street, Jr., *Phys. Rev.* **80**, 467 (1950)
- 11R47 W. Rall and R. G. Wilkinson, *Phys. Rev.* **71**, 321 (1947)
- 11R51 W. Rall and K. G. McNeill, *Phys. Rev.* **83**, 1244 (1951)
- 12R52 P. Radvanyi, *Compt. rend.* **234**, 1275 (1952)
- 12R52a P. Radvanyi, *Compt. rend.* **235**, 289 (1952)
- 12R52b P. Radvanyi, *Compt. rend.* **235**, 428 (1952)
- 13R37 L. H. Rumbaugh, R. B. Roberts, and L. R. Hafstad, *Phys. Rev.* **51**, 1106 (1937)
- 13R38 L. H. Rumbaugh, R. B. Roberts, and L. R. Hafstad, *Phys. Rev.* **54**, 657 (1938)
- 14R38 R. B. Roberts and N. P. Heydenburg, *Phys. Rev.* **53**, 929 (1938) (A)
- 14R38a R. B. Roberts, N. P. Heydenburg, and G. L. Locher, *Phys. Rev.* **53**, 1016 (1938)
- 15R46 S. Rubin, *Phys. Rev.* **69**, 134 (1946) (A)
- 16R40 S. Ruben and M. D. Kamen, *Phys. Rev.* **57**, 549 (1940)
- 16R41 S. Ruben and M. D. Kamen, *Phys. Rev.* **59**, 349 (1941)
- 17R46 A. F. Reid, J. R. Dunning, S. Weinhouse, and A. V. Grosse, *Phys. Rev.* **70**, 431 (1946)
- 17R46a A. F. Reid and A. S. Keston, *Phys. Rev.* **70**, 987 (1946)
- 18R37 L. N. Ridenour and W. J. Henderson, *Phys. Rev.* **52**, 889 (1937)
- 18R37a L. N. Ridenour and W. J. Henderson, *Phys. Rev.* **51**, 1102 (1937)
- 19R51 L. Ruby and J. R. Richardson, *Phys. Rev.* **83**, 698 (1951)
- 20R49 J. E. Robinson, M. Ter-Pogossian, and C. S. Cook, *Phys. Rev.* **75**, 1099 (1949)
- 21R43 W. Riezler, *Naturwiss.* **31**, 326 (1943)
- 21R44 W. Riezler, *Physik Z.* **45**, 191 (1944)
- 21R46 W. Riezler, *Naturwiss.* **33**, 53 (1946)
- 22R49 S. A. Reynolds, reported in Oak Ridge National Laboratory Classified Report ORNL-286 (Sept. 1949)
- 22R50 S. A. Reynolds, reported in Oak Ridge National Laboratory Classified Report ORNL-867 (Dec. 1950)
- 23R36 J. R. Richardson and F. N. D. Kurie, *Phys. Rev.* **50**, 999 (1936)
- 23R39 J. R. Richardson, *Phys. Rev.* **55**, 609 (1939)
- 23R46 J. R. Richardson and B. T. Wright, *Phys. Rev.* **70**, 445 (1946) (A)
- 24R47 M. M. Ramsey, J. L. Meem, Jr., and A. C. G. Mitchell, *Phys. Rev.* **72**, 639 (1947)
- 25R48 G. A. Renard, *Compt. rend.* **226**, 1269 (1948)
- 25R49 G. A. Renard, *Compt. rend.* **228**, 387 (1949)
- 25R50 G. A. Renard, *Ann. phys.* **5**, 385 (1950)

- 26R50 T. R. Roberts and A. O. Nier, *Phys. Rev.* 79, 198 (1950) (A)
- 27R37 J. R. Risser, *Phys. Rev.* 52, 768 (1937)
- 27R40 J. R. Risser, K. Lark-Horowitz, and R. N. Smith, *Phys. Rev.* 57, 355 (1940) (A)
- 27R48 J. R. Risser and R. N. Smith, private communication from K. Lark-Horowitz (1948)
- 28R50 J. H. Reynolds, *Phys. Rev.* 79, 789 (1950)
- 28R50a J. H. Reynolds, *Phys. Rev.* 79, 886 (1950)
- 28R50b J. H. Reynolds, reported in Argonne National Laboratory Classified Report ANL-4515 (Oct. 1950)
- 29R50 E. Rabinowicz, *Proc. Phys. Soc. (London)* 63A, 1040 (1950)
- 30R51 H. Roderick, W. E. Meyerhof, and L. G. Mann, *Phys. Rev.* 84, 887 (1951)
- 30R52 H. Roderick, O. Lonsjo, and W. E. Meyerhof, private communication (Oct. 1952)
- 31R52 W. C. Rutledge, J. M. Cork, and S. B. Burson, *Phys. Rev.* 86, 775 (1952)
- 32R50 P. Rothwell and D. West, *Proc. Phys. Soc. (London)* 63A, 539 (1950)
- 33R41 A. Roberts, J. R. Downing, and M. Deutsch, *Phys. Rev.* 60, 544 (1941)
- 33R41a A. Roberts and J. W. Irvine, Jr., *Phys. Rev.* 59, 936 (1941)
- 33R43 A. Roberts, L. G. Elliott, J. R. Downing, W. C. Peacock, and M. Deutsch, *Phys. Rev.* 64, 268 (1943)
- 34R47 W. C. Redman and D. Saxon, *Phys. Rev.* 72, 570 (1947)
- 35R38 H. Reddemann and F. Strassmann, *Naturwiss.* 26, 187 (1938)
- 35R40 H. Reddemann, *Naturwiss.* 28, 110 (1940)
- 35R40a H. Reddemann, *Z. Physik* 116, 137 (1940)
- 36R49 B. E. Robertson, W. E. Scott, and M. L. Pool, *Phys. Rev.* 76, 1649 (1949)
- 36R50 B. E. Robertson, W. E. Scott, and M. L. Pool, *Phys. Rev.* 78, 318 (1950) (A)
- 36R50a B. E. Robertson, W. L. Carss, and M. L. Pool, *Phys. Rev.* 77, 747 (1950) (A)
- 37R46 Wilfrid Rall, *Phys. Rev.* 70, 112 (1946) (A)
- 38R50 B. Russell and A. Wattenberg, U. S. Atomic Energy Commission Declassified Document AECD-2926 (Dec. 1950)
- 39R51 B. L. Robinson and L. Madansky, *Phys. Rev.* 84, 604 (1951)
- 39R51a B. L. Robinson and L. Madansky, *Phys. Rev.* 84, 1067 (1951)
- 40R52 D. Rose, G. Hinman, and L. G. Lang, *Phys. Rev.* 86, 863 (1952)
- 41R50 E. R. Rae, *Proc. Phys. Soc. (London)* 63A, 292 (1950)
- 42R50 J. O. Rasmussen, F. L. Reynolds, S. G. Thompson, and A. Ghiorso, *Phys. Rev.* 80, 475 (1950)
- 42R52 J. O. Rasmussen, Jr., S. G. Thompson, and A. Ghiorso, *Phys. Rev.* (to be published) (1952)
- 43R52 P. L. Roggenkamp, C. H. Pruett, and R. G. Wilkinson, *Phys. Rev.* (in press) (1952)
- 43R53 P. L. Roggenkamp, C. H. Pruett, and R. G. Wilkinson, *Phys. Rev.* (to be published) (1953)
- 44R52 R. Richmond and H. Rose, *Phil. Mag.* 43, 367 (1952)
- 44R52a R. Richmond, P. J. Grant, and H. Rose, *Proc. Phys. Soc. (London)* 65A, 484 (1952)
- 45R52 G. Rudstam, P. C. Stevenson, and R. L. Folger, *Phys. Rev.* 87, 358 (1952)
- 46R52 G. W. Rodeback and J. S. Allen, *Phys. Rev.* 86, 446 (1952)
- 47R52 H. N. Ritland and F. H. Schmidt, private communication (Oct. 1952)
- 48R51 A. Rytz, *Compt. rend.* 233, 790 (1951)
- 49R52 W. Robinson and W. Bernstein, *Phys. Rev.* 86, 545 (1952)
- 50R52 K. I. Roulston and R. W. Pringle, *Phys. Rev.* 87, 930 (1952)
- 51R50 H. T. Richards, R. V. Smith, and C. P. Browne, *Phys. Rev.* 80, 524 (1950)
- 51R51 H. T. Richards, *Phys. Rev.* 83, 694 (1951)
- 52R52 H. Rose, *Phil. Mag.* 43, 1146 (1952)
- 1S37 J. Schintlmeister, *Sitzber. Akad. Wiss. Wien. Abt. IIa*, 146, 371 (1937)
- 1S39 J. Schintlmeister and K. Lintner, *Sitzber. Akad. Wiss. Wien. Abt. IIa*, 148, 279 (1939)
- 2S46 L. Seren, W. E. Moyer, and W. Sturm, *Phys. Rev.* 70, 561 (1946)
- 2S47 L. Seren, H. N. Friedlander, and S. H. Turkel, *Phys. Rev.* 72, 888 (1947)
- 2S47a L. Seren, H. N. Friedlander, and S. H. Turkel, *Phys. Rev.* 71, 454 (1947)
- 2S47b L. Seren, D. Engelkemeir, W. Sturm, H. N. Friedlander, and S. Turkel, *Phys. Rev.* 71, 409 (1947)
- 3S33 B. W. Sargent, *Proc. Roy. Soc. (London)* 139A, 659 (1933). Summarizes the results of various investigators.
- 3S39 B. W. Sargent, *Can. J. Research* 17A, 103 (1939)
- 3S39a B. W. Sargent, *Can. J. Research* 17A, 82 (1939); *Phys. Rev.* 54, 232 (1938)
- 3S52 B. W. Sargent, L. Yaffe, and A. P. Gray, *Can. J. Phys.* (in press) (1952)
- 4S46 M. H. Studier, Argonne National Laboratory Classified Report CP-3642 (Dec. 1946); NNS-PPR 17B, 634 (1952) (classified)
- 4S48 M. H. Studier and E. K. Hyde, *Phys. Rev.* 74, 591 (1948)
- 4S48a M. H. Studier and R. J. Bruehlman, private communication (Oct. 1948)
- 4S49 M. H. Studier and R. J. Bruehlman, reported in Argonne National Laboratory Classified Report ANL-4252 (Feb. 1949)
- 4S49a M. H. Studier and E. K. Hyde, unpublished data (Feb. 1949)
- 4S52 M. H. Studier, NNS-PPR 17B, 50 (1952) (classified)
- 5S45 H. Slätis, *Arkiv Mat., Astron. Fysik* 32A, No. 16 (1945)
- 5S46 H. Slätis, *Arkiv Mat., Astron. Fysik* 33A, No. 17 (1946)
- 5S47 H. Slätis, *Nature* 160, 579 (1947); *Arkiv Mat., Astron. Fysik* 35A, No. 3 (1948)
- 5S49 H. Slätis and K. Siegbahn, *Arkiv Mat., Astron. Fysik* 36A, No. 21 (1949)
- 5S49a H. Slätis and K. Siegbahn, *Phys. Rev.* 75, 318 (1949)
- 5S50 H. Slätis, S. J. du Toit, and K. Siegbahn, *Phys. Rev.* 78, 498 (1950); *Arkiv Fysik* 2, 321 (1950)
- 5S51 H. Slätis and K. Siegbahn, reported in M. Siegbahn Commemorative Volume, p 153 (Uppsala, 1951)
- 5S52 H. Slätis and L. Zappa, *Arkiv Fysik* 5, 26 (1952)
- 6S48 K. Street, Jr., R. A. James, and G. T. Seaborg, unpublished data (July 1948)
- 6S48a K. Street, Jr., A. Ghiorso, D. A. Orth, and G. T. Seaborg, unpublished data (Oct. 1948)

- 6S50 K. Street, Jr., unpublished data quoted in Phys. Rev. 78, 475 (1950)
- 6S50a K. Street, Jr., A. Ghiorso, and G. T. Seaborg, Phys. Rev. 79, 530 (1950)
- 7S44 K. Siegbahn, Arkiv Mat., Astron. Fysik 30A, No. 20 (1944)
- 7S44a K. Siegbahn and E. Bohr, Arkiv Mat., Astron. Fysik 30B, No. 3 (1944)
- 7S45 K. Siegbahn and H. Slätis, Arkiv Mat., Astron. Fysik 32A, No. 9 (1945)
- 7S46 K. Siegbahn and N. Hole, Phys. Rev. 70, 133 (1946)
- 7S46a K. Siegbahn and S. E. Petersson, Arkiv Mat., Astron. Fysik 32B, No. 5 (1946)
- 7S46b K. Siegbahn, Phys. Rev. 70, 127 (1946)
- 7S46c K. Siegbahn, Arkiv Mat., Astron. Fysik 33A, No. 10 (1946)
- 7S47 K. Siegbahn and A. Johansson, Arkiv Mat., Astron. Fysik 34A, No. 10 (1947)
- 7S47a K. Siegbahn and H. Slätis, Nature 159, 471 (1947); Arkiv Mat., Astron. Fysik 34A, No. 15 (1947)
- 7S47b K. Siegbahn, Arkiv Mat., Astron. Fysik 34B, No. 6 (1947)
- 7S47c K. Siegbahn, Arkiv Mat., Astron. Fysik 34B, No. 4 (1947)
- 7S47d K. Siegbahn, Arkiv Mat., Astron. Fysik 34A, No. 7 (1947)
- 7S47e K. Siegbahn and M. Deutsch, Phys. Rev. 71, 483 (1947) (A)
- 7S47f K. Siegbahn and H. Slätis, Arkiv Mat., Astron. Fysik 34A, No. 6 (1947)
- 7S47g K. Siegbahn, Proc. Roy. Soc. (London) 189A, 527 (1947)
- 7S48 K. Siegbahn and M. Deutsch, Phys. Rev. 73, 410 (1948); A. Hedgran, K. Siegbahn, and N. Svartholm, Proc. Phys. Soc. (London) 63A, 960 (1950)
- 7S49 K. Siegbahn and A. Ghosh, Phys. Rev. 76, 307 (1949); Arkiv Mat., Astron. Fysik 36A, No. 19 (1949)
- 7S49a K. Siegbahn, A. Hedgran, and M. Deutsch, Phys. Rev. 76, 1263 (1949)
- 7S49b K. Siegbahn, E. Kondaiah, and S. Johansson, Nature 164, 405 (1949)
- 7S49c K. Siegbahn, Phys. Rev. 75, 1277 (1949); 77, 233 (1950)
- 7S49d K. Siegbahn and W. Forsling, Arkiv Fysik 1, 505 (1949)
- 7S49e K. Siegbahn and A. Hedgran, Phys. Rev. 75, 523 (1949)
- 7S50 K. Siegbahn and M. Deutsch, Arkiv Fysik 2, 9 (1950); Phys. Rev. 77, 680 (1950)
- 7S50a K. Siegbahn and H. Slätis, Arkiv Fysik 1, 559 (1950)
- 7S50b K. Siegbahn and S. der Toit, Arkiv Fysik 2, 211 (1950)
- 7S51 K. Siegbahn, reported in M. Siegbahn Commemorative Volume, p 199 (Uppsala, 1951)
- 7S52 K. Siegbahn, Arkiv Fysik 4, 223 (1952)
- 8S31 E. Stahel, Z. Physik 68, 1 (1931); Helv. Phys. Acta 8, 651 (1935)
- 8S43 E. Stahel and W. Johnner, J. phys. et radium 5, 97 (1943)
- 9S48 D. Saxon, Phys. Rev. 73, 811 (1948)
- 9S48a D. Saxon, Phys. Rev. 74, 1264 (1948) (A)
- 9S48b D. Saxon, Phys. Rev. 74, 849 (1948)
- 9S49 D. Saxon and J. Richards, Phys. Rev. 76, 982 (1949)
- 9S49a D. Saxon and J. Richards, Phys. Rev. 76, 186 (1949) (A)
- 9S49b D. Saxon and R. Heller, Phys. Rev. 75, 909 (1949)
- 9S49c D. Saxon, reported in Argonne National Laboratory Classified Report ANL-4237 (Jan. 1949)
- 10S51 P. H. Stoker, O. P. Hok, and G. J. Sizoo, Physica 17, 164 (1951)
- 11S37 J. Surugue, Ann. phys. 8, 484 (1937)
- 11S38 J. Surugue, J. phys. et radium 9, 438 (1938)
- 11S41 J. Surugue, Compt. rend. 212, 337 (1941)
- 11S41a J. Surugue and San-Tsiang Tsien, Compt. rend. 213, 172 (1941)
- 11S42 J. Surugue, J. phys. et radium 4, 71 (1942)
- 11S46 J. Surugue, J. phys. et radium 7, 145 (1946)
- 12S46 A. K. Saha, Proc. Nat. Inst. Sci. India 12, No. 3, 159 (1946)
- 13S39 G. T. Seaborg and E. Segrè, Phys. Rev. 55, 808 (1939)
- 13S40 G. T. Seaborg, J. J. Livingood, and J. W. Kennedy, Phys. Rev. 57, 363 (1940)
- 13S41 G. T. Seaborg, J. W. Gofman, and J. W. Kennedy, Phys. Rev. 59, 321 (1941)
- 13S41a G. T. Seaborg, J. J. Livingood, and G. Friedlander, Phys. Rev. 59, 320 (1941)
- 13S41b G. T. Seaborg and G. Friedlander, Phys. Rev. 59, 400 (1941)
- 13S46 G. T. Seaborg, E. M. McMillan, J. W. Kennedy, and A. C. Wahl, Phys. Rev. 69, 366 (1946); NNES-PPR 14B, 1 (1949)
- 13S46a G. T. Seaborg, A. C. Wahl, and J. W. Kennedy, Phys. Rev. 69, 367 (1946); NNES-PPR 14B, 3 (1949)
- 13S47 G. T. Seaborg, B. B. Cunningham, H. H. Hopkins, Jr., M. Lindner, D. R. Miller, P. R. O'Connor, I. Perlman, and R. C. Thompson, Phys. Rev. 72, 740 (1947) (A)
- 13S47a G. T. Seaborg, J. W. Gofman, and R. W. Stoughton, Phys. Rev. 71, 378 (1947)
- 13S49 G. T. Seaborg, R. A. James, and L. O. Morgan, NNES-PPR 14B, 1525 (1949)
- 13S49a G. T. Seaborg, A. C. Wahl, and J. W. Kennedy, NNES-PPR 14B, 13 (1949)
- 13S49b G. T. Seaborg, R. A. James and A. Ghiorso, NNES-PPR 14B, 1554 (1949)
- 13S52 G. T. Seaborg, J. W. Gofman, and R. W. Stoughton, NNES-PPR 17B, 31 (1952) (classified)
- 13S52a G. T. Seaborg, Phys. Rev. 85, 157 (1952)
- 13S53 G. T. Seaborg, R. A. Glass, and S. G. Thompson, J. Am. Chem. Soc. (to be published) (1953)
- 14S50 A. W. Sunyar, D. Alburger, G. Friedlander, M. Goldhaber, and G. Scharff-Goldhaber, Phys. Rev. 79, 181 (1950)
- 14S50a A. W. Sunyar, D. Alburger, G. Friedlander, M. Goldhaber, and G. Scharff-Goldhaber, Phys. Rev. 78, 326 (1950) (A)
- 14S50b A. W. Sunyar, G. Friedlander, and M. Goldhaber, reported in Brookhaven National Laboratory Unclassified Report BNL-39 (Jan. 1950)
- 14S51 A. W. Sunyar, Phys. Rev. 83, 864 (1951)
- 14S51a A. W. Sunyar and J. W. Mihelich, Phys. Rev. 81, 300 (1951) (A)
- 14S52 A. W. Sunyar, J. W. Mihelich, G. Scharff-Goldhaber, M. Goldhaber, N. S. Wall, and M. Deutsch, Phys. Rev. 86, 1023 (1952)
- 14S52a A. W. Sunyar, private communication (Oct. 1952)
- 14S52b A. W. Sunyar, D. E. Alburger, G. Friedlander, M. Goldhaber, and G. Scharff-Goldhaber, unpublished data quoted in (18G52)
- 15S37 W. R. Smythe and A. Hemmendinger, Phys. Rev. 51, 178 (1937)
- 16S51 W. J. Sturm and V. Johnson, Phys. Rev. 83, 542 (1951)

- 17S41 G. Scharff-Goldhaber, Phys. Rev. 59, 937 (1941) (A)
- 17S46 G. Scharff-Goldhaber and G. S. Klaiber, Phys. Rev. 70, 229 (1946)
- 17S50 G. Scharff-Goldhaber, E. der Mateosian, M. McKeown, and A. W. Sunyar, Phys. Rev. 78, 325 (1950) (A)
- 17S51 G. Scharff-Goldhaber and M. McKeown, Phys. Rev. 82, 123 (1951)
- 17S51a G. Scharff-Goldhaber, reported in Brookhaven National Laboratory Unclassified Report BNL-103 (June 1951)
- 17S51b G. Scharff-Goldhaber, E. der Mateosian, M. Goldhaber, G. W. Johnson, and M. McKeown, Phys. Rev. 83, 480 (1951)
- 17S52 G. Scharff-Goldhaber, E. der Mateosian, and J. W. Mihelich, Phys. Rev. 85, 734 (1952) (A)
- 17S52a G. Scharff-Goldhaber, private communication (Oct. 1952)
- 18S37 G. J. Sizoo and S. A. Wytzes, Physica 4, 791 (1937)
- 18S43 G. J. Sizoo and L. F. C. Friele, Physica 10, 57 (1943)
- 19S51 G. J. Sayag, Compt. rend. 232, 2091 (1951)
- 20S52 B. F. Scott, NNES-PPR 17B, 638 (1952) (classified)
- 21S51 L. M. Slater and G. T. Seaborg, unpublished data (Aug. 1951)
- 21S52 L. M. Slater and F. Asaro, private communication (Aug. 1952)
- 22S42 K. Starke, Naturwiss. 30, 107, 577 (1942)
- 23S45a W. H. Sullivan, Phys. Rev. 68, 277 (1945)
- 23S46 W. H. Sullivan, N. R. Sleight, and E. M. Gladrow, Phys. Rev. 70, 778 (1946)
- 23S47 W. H. Sullivan, J. A. Swartout, and H. E. Wyatt, reported in Oak Ridge National Laboratory Classified Report Mon N-243 (Feb. 1947)
- 23S51 W. H. Sullivan, N. R. Sleight, and E. M. Gladrow, NNES-PPR 9, 832 (1951)
- 23S51a W. H. Sullivan, N. R. Sleight, and E. M. Gladrow, NNES-PPR 9, 820 (1951)
- 23S51b W. H. Sullivan, N. R. Sleight, and E. M. Gladrow, NNES-PPR 9, 842 (1951)
- 23S51c W. H. Sullivan, N. R. Sleight, and E. M. Gladrow, NNES-PPR 9, 817 (1951)
- 23S51d W. H. Sullivan, N. R. Sleight, and E. M. Gladrow, NNES-PPR 9, 808 (1951)
- 23S51e W. H. Sullivan, N. R. Sleight, and E. M. Gladrow, NNES-PPR 9, 1953 (1951)
- 23S51f W. H. Sullivan, N. R. Sleight, and E. M. Gladrow, NNES-PPR 9, 838 (1951)
- 23S51g W. H. Sullivan, N. R. Sleight, and E. M. Gladrow, NNES-PPR 9, 1949 (1951)
- 23S51h W. H. Sullivan, N. R. Sleight, and E. M. Gladrow, NNES-PPR 9, 1945 (1951)
- 23S51i W. H. Sullivan, N. R. Sleight, and E. M. Gladrow, NNES-PPR 9, 824 (1951)
- 23S51j W. H. Sullivan, O. Johnson, and R. Nottorf, NNES-PPR 9, 984 (1951)
- 23S51k W. H. Sullivan and S. Katcoff, NNES-PPR 9, 1015 (1951)
- 24S39 E. Segrè, R. S. Halford, and G. T. Seaborg, Phys. Rev. 55, 321 (1939)
- 24S40 E. Segrè and C. S. Wu, Phys. Rev. 57, 552 (1940)
- 24S40a E. Segrè, J. W. Kennedy, and G. T. Seaborg, unpublished work (1940)
- 24S41 E. Segrè and G. T. Seaborg, Phys. Rev. 59, 212 (1941)
- 24S49 E. Segrè and C. Wiegand, Phys. Rev. 75, 39 (1949)
- 24S49a E. Segrè, unpublished data quoted in E. Segrè and A. C. Helmholtz, Revs. Modern Phys. 21, 271 (1949)
- 24S52 E. Segrè, Phys. Rev. 86, 21 (1952); some values recalculated according to more recent half-life determinations (HPS)
- 25S51 J. C. Sullivan, G. L. Pyle, M. H. Studier, P. R. Fields, and W. M. Manning, Phys. Rev. 83, 1267 (1951)
- 26S36 A. H. Snell, Phys. Rev. 49, 555 (1936)
- 26S37 A. H. Snell, Phys. Rev. 51, 143 (1937) (A)
- 26S37a A. H. Snell, Phys. Rev. 52, 1007 (1937)
- 26S42 A. H. Snell et al., reported in Metallurgical Laboratory Classified Report CP-257 (Sept. 1942)
- 26S43 A. H. Snell, M. B. Sampson, and J. S. Levinger, Metallurgical Laboratory Classified Report CP-1176 (Dec. 1943)
- 26S47 A. H. Snell, J. S. Levinger, E. P. Meiners, Jr., M. B. Sampson, and R. G. Wilkinson, Phys. Rev. 72, 545 (1947); NNES-PPR 9, 603 (1951)
- 26S47a A. H. Snell, V. A. Nedzel, H. W. Ibaer, J. S. Levinger, R. G. Wilkinson, and M. B. Sampson, Phys. Rev. 72, 541 (1947)
- 26S50 A. H. Snell, F. Pleasonton, and R. V. McCord, Phys. Rev. 78, 310 (1950)
- 27S46 H. S. Sommers, Jr. and R. Sherr, Phys. Rev. 69, 21 (1946)
- 28S40 R. Sherr, Phys. Rev. 57, 937 (1940)
- 28S41 R. Sherr, K. T. Bainbridge, and H. H. Anderson, Phys. Rev. 60, 473 (1941)
- 28S48 R. Sherr, H. R. Muether, and M. G. White, Phys. Rev. 74, 1239 (1948) (A)
- 28S49 R. Sherr, H. R. Muether, and M. G. White, Phys. Rev. 75, 282 (1949)
- 28S52 R. Sherr and J. Gerhart, Phys. Rev. 86, 619 (1952) (A)
- 29S41 A. K. Solomon, Phys. Rev. 60, 279 (1941)
- 29S47 A. K. Solomon, R. G. Gould, and C. B. Anfinsen, Phys. Rev. 72, 1097 (1947)
- 29S48 A. K. Solomon and L. E. Glendenin, Phys. Rev. 73, 415 (1948)
- 29S50 A. K. Solomon, Phys. Rev. 79, 403 (1950)
- 30S41 J. H. C. Smith and D. B. Cowie, J. Appl. Phys. 12, 78 (1941)
- 31S50 K. H. Sun, F. A. Pecjak, R. A. Charpie, and J. F. Nichaj, Phys. Rev. 78, 338 (1950) (A)
- 31S51 K. H. Sun, B. Jennings, W. E. Shoupp, and A. J. Allen, Phys. Rev. 82, 267 (1951)
- 32S51 W. E. Stephens, J. Halpern, and R. Sher, Phys. Rev. 82, 511 (1951)
- 33S50 S. C. Snowdon, Phys. Rev. 78, 299 (1950)
- 34S52 G. Schrank and J. R. Richardson, Phys. Rev. 86, 248 (1952)
- 35S47 W. Spatz, N. Goldstein, C. Huddleston, and E. Goldfarb, reported in Argonne National Laboratory Classified Report CP-3750 (Feb. 1947)
- 36S39 N. K. Saha, Trans. Bose Res. Inst. (Calcutta) 14, 57 (1939-1941); Chem. Abstracts 42, 450i (1948)
- 36S51 N. K. Saha and K. Gopalakrishnan, Proc. Nat. Inst. Sci. India 17, 301 (1951)
- 37S36 M. B. Sampson, L. N. Ridenour, and W. Bleakney, Phys. Rev. 50, 382 (1936)
- 37S36a M. B. Sampson and W. Bleakney, Phys. Rev. 50, 732 (1936)
- 38S51 W. K. Sinclair and A. F. Holloway, Nature 167, 365 (1951)
- 39S51 J. H. Sreb, Phys. Rev. 81, 469 (1951)
- 39S51a J. H. Sreb, Phys. Rev. 81, 643 (1951)
- 40S48 A. Szalay and E. Csongor, Phys. Rev. 74, 1063 (1948)
- 41S49 L. Seidlitz, E. Bleuler, and D. J. Tendam, Phys. Rev. 76, 861 (1949)

- 42S36 R. Sagane, Phys. Rev. 50, 1141 (1936)
- 42S38 R. Sagane, S. Kojima, G. Miyamoto, and M. Ikawa, Phys. Rev. 54, 542 (1938)
- 42S38a R. Sagane, S. Kojima, G. Miyamoto, and M. Ikawa, Phys. Rev. 54, 970 (1938)
- 42S39 R. Sagane, Phys. Rev. 55, 31 (1939)
- 42S39a R. Sagane, S. Kojima, and G. Miyamoto, Proc. Phys.-Math. Soc. Japan 21, 728 (1939)
- 42S39b R. Sagane, S. Kojima, G. Miyamoto, and M. Ikawa, Proc. Phys.-Math. Soc. Japan 21, 660 (1939)
- 42S40 R. Sagane, S. Kojima, G. Miyamoto, and M. Ikawa, Phys. Rev. 57, 1179 (1940)
- 42S40a R. Sagane, S. Kojima, G. Miyamoto, and M. Ikawa, Proc. Phys.-Math. Soc. Japan 22, 174 (1940)
- 42S40b R. Sagane, S. Kojima, G. Miyamoto, and M. Ikawa, Phys. Rev. 57, 750 (1940)
- 42S41 R. Sagane, G. Miyamoto, and M. Ikawa, Phys. Rev. 59, 904 (1941)
- 42S52 R. Sagane, Phys. Rev. 85, 926 (1952)
- 44S51 R. K. Sheline, R. B. Holtzman, and C. Y. Fan, Phys. Rev. 83, 919 (1951)
- 44S51a R. K. Sheline, Phys. Rev. 82, 954 (1951)
- 44S52 R. K. Sheline and R. W. Stoughton, Phys. Rev. 87, 1 (1952)
- 44S52a R. K. Sheline, Phys. Rev. 87, 557 (1952)
- 45S48 A. D. Schelberg, M. B. Sampson, and A. C. G. Mitchell, Rev. Sci. Instr. 19, 458 (1948)
- 46S49 G. A. Sawyer and M. L. Wiedenbeck, Phys. Rev. 76, 1535 (1949)
- 46S50 G. A. Sawyer and M. L. Wiedenbeck, Phys. Rev. 79, 490 (1950)
- 47S49 R. W. Stout, Phys. Rev. 75, 1107 (1949)
- 48S50 F. W. Spiers, Nature 165, 356 (1950)
- 49S51 V. L. Sailor and J. J. Floyd, Phys. Rev. 82, 960 (1951)
- 50S50 L. Simons, Soc. Scien. Fennica Comm. Phys.-Math. 15, No. 9 (1950)
- 50S52 L. Simons, Phys. Rev. 86, 570 (1952)
- 51S42 G. P. Smith, Phys. Rev. 61, 578 (1942)
- 52S50 B. N. Sorensen, B. M. Dale, and J. D. Kurbatov, Phys. Rev. 79, 1007 (1950)
- 53S45 R. P. Schuman, reported in Metallurgical Laboratory Classified Report CN-2929 (May 1945)
- 53S45a R. P. Schuman, reported in Metallurgical Laboratory Classified Report CN-2799 (April 1945)
- 53S46 R. P. Schuman, reported in J. Am. Chem. Soc. 68, 2411 (1946)
- 53S51 R. P. Schuman and A. Camilli, Phys. Rev. 84, 158 (1951)
- 53S51a R. P. Schuman, NNES-PPR 9, 783 (1951)
- 54S46 J. A. Swartout, G. E. Boyd, A. E. Cameron, C. P. Keim, and C. E. Larson, Phys. Rev. 70, 232 (1946)
- 54S47 J. A. Swartout, reported in Oak Ridge National Laboratory Classified Report Mon N-243 (Feb. 1947)
- 55S50 K. Strauch, Phys. Rev. 79, 487 (1950)
- 55S51 K. Strauch, Phys. Rev. 81, 973 (1951)
- 56S51 L. A. Smith, R. N. H. Haslam, and J. G. V. Taylor, Phys. Rev. 84, 842 (1951)
- 57S49 L. M. Silver, Phys. Rev. 76, 589 (1949) (A); Can. J. Physics 29, 59 (1951)
- 58S38 C. V. Strain, Phys. Rev. 54, 1021 (1938)
- 59S48 L. S. Skaggs, J. S. Laughlin, A. O. Hanson, and J. J. Orlin, Phys. Rev. 73, 420 (1948)
- 60S46 J. M. Siegel and L. E. Glendenin, reported in J. Am. Chem. Soc. 68, 2411 (1946)
- 60S51 J. M. Siegel and L. E. Glendenin, NNES-PPR 9, 549 (1951)
- 61S46 E. P. Steinberg and D. W. Engelkemeir, reported in J. Am. Chem. Soc. 68, 2411 (1946)
- 61S48 E. P. Steinberg, J. A. Seiler, A. Goldstein, and A. Dudley, U. S. Atomic Energy Commission Declassified Document MDDC-1632 (Jan. 1948)
- 61S50 E. P. Steinberg and L. E. Glendenin, Phys. Rev. 78, 624 (1950)
- 61S51 E. P. Steinberg and D. W. Engelkemeir, NNES-PPR 9, 566 (1951)
- 61S51a E. P. Steinberg and M. S. Freedman, NNES-PPR 9, 1378 (1951)
- 61S51b E. P. Steinberg, NNES-PPR 9, 750 (1951)
- 61S51c E. P. Steinberg and L. E. Glendenin, NNES-PPR 9, 877 (1951)
- 62S51 F. R. Scott, Phys. Rev. 84, 659 (1951)
- 63S46 N. Sugarman and N. E. Ballou, reported in J. Am. Chem. Soc. 68, 2411 (1946)
- 63S47 N. Sugarman, private communication (April 1947)
- 63S47a N. Sugarman, J. Chem. Phys. 15, 544 (1947)
- 63S48 N. Sugarman and H. Richter, Phys. Rev. 73, 1411 (1948)
- 63S49 N. Sugarman, J. Chem. Phys. 17, 11 (1949)
- 63S49a N. Sugarman, Phys. Rev. 75, 1473 (1949)
- 63S50 N. Sugarman and H. Richter, J. Chem. Phys. 18, 174 (1950)
- 63S51 N. Sugarman, N. E. Ballou, D. W. Engelkemeir, and W. H. Burgus, NNES-PPR 9, 1163 (1951)
- 63S52 N. Sugarman, Phys. Rev. 86, 604 (1952) (A)
- 64S41 R. E. Siday, Proc. Roy. Soc. (London) 178A, 189 (1941)
- 65S38 F. Strassmann and E. Walling, Ber. deut. chem. Ges. 71B, 1 (1938)
- 65S40 F. Strassmann and O. Hahn, Naturwiss. 28, 817 (1940)
- 66S40 W. Seelmann-Eggebert, Naturwiss. 28, 451 (1940)
- 66S43 W. Seelmann-Eggebert and H. J. Born, Naturwiss. 31, 59 (1943)
- 66S43a W. Seelmann-Eggebert, Naturwiss. 31, 510 (1943)
- 66S43b W. Seelmann-Eggebert, Naturwiss. 31, 491 (1943)
- 66S46 W. Seelmann-Eggebert, Naturwiss. 33, 279 (1946)
- 66S47 W. Seelmann-Eggebert and F. Strassmann, Z. Naturforsch. 2a, 80 (1947)
- 67S51 A. F. Stehney and N. Sugarman, U. S. Atomic Energy Commission Declassified Document AECD-3047 (Jan. 1951); Phys. Rev. (in press) (1952)
- 68S48 F. B. Shull, Phys. Rev. 74, 917 (1948)
- 69S38 H. Scheichenberger, Anz. Akad. Wiss. Wien, Math.-naturw. Klasse 75, 108 (1938)
- 70S51 B. Selikson and J. M. Siegel, NNES-PPR 9, 699 (1951)
- 71S37 D. W. Stewart, J. L. Lawson, and J. M. Cork, Phys. Rev. 52, 901 (1937)
- 71S39 D. W. Stewart, Phys. Rev. 56, 629 (1939)
- 72S49 L. Slack, C. H. Braden, and F. B. Shull, Phys. Rev. 75, 1965 (1949)
- 72S49a L. Slack, G. E. Owen, and H. Primakoff, Phys. Rev. 75, 1448 (1949)
- 73S51 F. J. Shore, W. L. Bendel, and R. A. Becker, Phys. Rev. 83, 688 (1951)
- 73S52 F. J. Shore, H. N. Brown, W. L. Bendel, and R. A. Becker, Phys. Rev. 87, 202 (1952) (A)
- 74S51 K. Shure and M. Deutsch, Phys. Rev. 82, 122 (1951)
- 74S51a K. Shure, Ph.D. Thesis, Massachusetts Institute of Technology (May 1951)

- 75S49 F. Suzor, *Ann. phys.* 4, 269 (1949)
- 76S51 N. R. Sleight, *NNES-PPR* 9, 805 (1951)
- 76S51a N. R. Sleight, T. B. Novey, and L. E. Glendenin, *NNES-PPR* 9, 846 (1951)
- 76S51b N. R. Sleight and W. H. Sullivan, *NNES-PPR* 9, 928 (1951)
- 77S47 J. A. Seiler, reported in Argonne National Laboratory Classified Report ANL-4000 (Aug. 1947)
- 77S51 J. A. Seiler, *NNES-PPR* 9, 860 (1951)
- 77S51a J. A. Seiler, *NNES-PPR* 9, 910 (1951)
- 77S51b J. A. Seiler and L. Winsberg, *NNES-PPR* 9, 1206 (1951)
- 77S51c J. A. Seiler and L. Winsberg, *NNES-PPR* 9, 1225 (1951)
- 78S50 A. Storruste, *Phys. Rev.* 79, 193 (1950)
- 79S50 A. J. Saur, P. Axel, L. G. Mann, and J. Ovadia, *Phys. Rev.* 79, 237 (1950) (A)
- 80S52 P. C. Stevenson and H. G. Hicks, private communication (April 1952)
- 81S42 R. N. Smith, *Phys. Rev.* 61, 389 (1942)
- 82S48 R. Steffen, O. Huber, F. Humbel, and W. Zündt, *Helv. Phys. Acta* 21, 194 (1948)
- 82S49 R. M. Steffen, O. Huber, and F. Humbel, *Helv. Phys. Acta* 22, 167 (1949)
- 82S51 R. M. Steffen, *Phys. Rev.* 83, 166 (1951)
- 82S51a R. M. Steffen, *Phys. Rev.* 82, 827 (1951)
- 82S52 R. M. Steffen, private communication (Oct. 1952)
- 83S51 E. J. Schillinger, Jr., B. Waldman, and W. C. Miller, *Phys. Rev.* 83, 320 (1951)
- 84S49 C. W. Stanley and S. Katcoff, *J. Chem. Phys.* 17, 653 (1949)
- 84S51 C. W. Stanley and L. E. Glendenin, *NNES-PPR* 9, 947 (1951)
- 85S51 D. T. Stevenson and M. Deutsch, *Phys. Rev.* 83, 1202 (1951)
- 85S51a D. T. Stevenson and M. Deutsch, *Phys. Rev.* 84, 1071 (1951)
- 86S52 D. Schiff, *Phys. Rev.* 85, 727 (1952) (A)
- 87S52 F. H. Schmidt and G. L. Keister, *Phys. Rev.* 86, 632 (1952) (A) and private communication (Oct. 1952)
- 88S51 V. S. Shpinel, *Zhur. Eksptl. i Teoret. Fiz.* 21, 853 (1951)
- 88S51a V. S. Shpinel and N. V. Forafontov, *Zhur. Eksptl. i Teoret. Fiz.* 21, 1376 (1951)
- 88S51b V. S. Shpinel, *Zhur. Eksptl. i Teoret. Fiz.* 21, 1370 (1951)
- 89S52 R. Stump, *Phys. Rev.* 86, 249 (1952)
- 90S52 C. L. Scoville, S. C. Fulta, and M. L. Pool, *Phys. Rev.* 85, 1046 (1952)
- 91S52 A. B. Smith, *Phys. Rev.* 86, 98 (1952)
- 91S52a A. B. Smith, A. C. G. Mitchell, and R. S. Caird, *Phys. Rev.* 87, 454 (1952)
- 91S52b A. B. Smith and A. C. G. Mitchell, private communication (Oct. 1952)
- 91S52c A. B. Smith, R. S. Caird, and A. C. G. Mitchell, *Phys. Rev.* 88, 150 (1952)
- 91S52d A. B. Smith and A. C. G. Mitchell, *Phys. Rev.* 87, 1128 (1952)
- 92S48 L. R. Shepherd and J. M. Hill, *Nature* 162, 566 (1948)
- 92S48a L. R. Shepherd, *Research (London)* 1, 671 (1948)
- 93S50 B. J. Stover, *Phys. Rev.* 80, 99 (1950)
- 93S51 B. J. Stover, *Phys. Rev.* 81, 8 (1951)
- 94S50 W. Steuber, Ph.D. Thesis, University of Illinois (1950)
- 95S50 E. Shapiro and C. E. Mandeville, *Phys. Rev.* 78, 319 (1950) (A)
- 96S47 J. W. Stout and W. M. Jones, *Phys. Rev.* 71, 582 (1947)
- 97S50 G. F. Snelling and E. W. Titterton, British Atomic Energy Commission Unclassified Report AERE-G/M-55 (Sept. 1950)
- 98S48 M. V. Scherb and C. E. Mandeville, *Phys. Rev.* 73, 1401 (1948)
- 99S39 K. Sinma and F. Yamasaki, *Phys. Rev.* 55, 320 (1939)
- 100S51 N. A. Schuster and G. E. Pake, *Phys. Rev.* 81, 886 (1951)
- 101S51 K. F. Smith, *Nature* 167, 942 (1951)
- 102S50 G. L. Stukenbroeker and J. R. McNally, Jr., *J. Opt. Soc. Am.* 40, 336 (1950)
- 103S51 W. W. Schoof and R. D. Hill, *Phys. Rev.* 83, 892 (1951) (A)
- 104S52 A. de Shalit, O. Huber, and H. Schneider, *Helv. Phys. Acta* 25, 279 (1952)
- 105S52 H. Schneider, O. Huber, F. Humbel, and A. de Shalit, *Helv. Phys. Acta* 25, 259 (1952)
- 106S52 P. Stähelin, *Phys. Rev.* 87, 374 (1952)
- 107S49 L. Ya. Shavtvalov, *Zhur. Eksptl. i Teoret. Fiz.* 19, 633 (1949)
- 107S51 L. Ya. Shavtvalov, *Zhur. Eksptl. i Teoret. Fiz.* 21, 1123 (1951)
- 108S51 P. M. Sherk and R. D. Hill, *Phys. Rev.* 83, 1097 (1951)
- 109S52 R. Sher, H. J. Kouts, and K. W. Downes, *Phys. Rev.* 87, 523 (1952)
- 110S51 J. Sharpe and G. H. Stafford, *Proc. Phys. Soc. (London)* 64A, 211 (1951)
- 111S50 B. Smaller, J. May, and M. Freedman, *Phys. Rev.* 79, 940 (1950)
- 112S51 H. D. Sharma, Ph.D. Thesis, University of California Radiation Laboratory Unclassified Report UCRL-1265 (May 1951)
- 113S52 W. L. Stirling and M. Goodrich, *Phys. Rev.* 87, 176 (1952) (A)
- 114S51 F. N. Spiess, Ph.D. Thesis, University of California Unclassified Report UCRL-1494 (Oct. 1951)
- 115S52 A. Sorruate, Ph.D. Thesis, University of Oslo (1952)
- 116S52 J. B. Swan and R. D. Hill, *Phys. Rev.* 88, 831 (1952)
- 116S52a J. B. Swan, W. M. Portnoy, and R. D. Hill, *Bull. Am. Phys. Soc.* 27, No. 5, Abstract V4 (1952)
- 117S52 D. A. Silverston, *Proc. Phys. Soc. (London)* 65A, 344 (1952)
- 118S39 L. Szilard and W. H. Zinn, *Phys. Rev.* 55, 799 (1939)
- 1T05 J. J. Thomson, *Phil. Mag.* 10, 584 (1905)
- 2T47 D. H. Templeton, J. J. Howland, Jr., and I. Perlman, *Phys. Rev.* 72, 766 (1947)
- 2T47a D. H. Templeton, J. J. Howland, Jr., and I. Perlman, *Phys. Rev.* 72, 758 (1947)
- 2T47b D. H. Templeton, R. H. Goeckermann, J. J. Howland, Jr., and I. Perlman, unpublished data (Jan. 1947)
- 2T48 D. H. Templeton and I. Perlman, *Phys. Rev.* 73, 1211 (1948)
- 2T48a D. H. Templeton, A. Ghiorso, and I. Perlman, unpublished data (June 1948)
- 2T50 D. H. Templeton, *Phys. Rev.* 78, 312 (1950)

- 3T49 S. G. Thompson, A. Ghiorso, J. O. Rasmussen and G. T. Seaborg, *Phys. Rev.* 76, 1406 (1949)
- 3T50 S. G. Thompson, A. Ghiorso, and G. T. Seaborg, *Phys. Rev.* 77, 838 (1950)
- 3T50a S. G. Thompson, A. Ghiorso, and K. Street, Jr., private communication (1950)
- 3T50b S. G. Thompson, A. Ghiorso, and G. T. Seaborg, *Phys. Rev.* 80, 781 (1950)
- 3T50c S. G. Thompson, K. Street, Jr., A. Ghiorso, and G. T. Seaborg, *Phys. Rev.* 78, 298 (1950)
- 3T50d S. G. Thompson, K. Street, Jr., A. Ghiorso, and G. T. Seaborg, *Phys. Rev.* 80, 790 (1950)
- 3T50e S. G. Thompson, K. Street, Jr., A. Ghiorso, and F. L. Reynolds, *Phys. Rev.* 80, 1108 (1950)
- 3T51 S. G. Thompson, K. Street, Jr., A. Ghiorso, and F. L. Reynolds, *Phys. Rev.* 84, 165 (1951)
- 3T52 S. G. Thompson, E. K. Hulet, and A. Ghiorso, private communication (Aug. 1952)
- 4T49 J. Teillac, *Compt. rend.* 229, 650 (1949)
- 4T50 J. Teillac, *Compt. rend.* 230, 1056 (1950)
- 4T52 J. Teillac, *Ann. phys.* 7, 396 (1952)
- 4T52a J. Teillac, P. Falk-Vairant, and C. Victor, *J. phys. et radium* 13, 143 (1952); *Compt. rend.* 233, 1025 (1951)
- 4T52b J. Teillac, P. Falk-Vairant, and C. Victor, *Compt. rend.* 234, 1051 (1952)
- 5T26 J. Thibaud, *Ann. phys.* 5, 73 (1926)
- 6T36 R. L. Thornton, *Phys. Rev.* 49, 207 (1936) (A)
- 6T37 R. L. Thornton and J. M. Cork, *Phys. Rev.* 51, 383 (1937) (A)
- 6T37a R. L. Thornton, *Phys. Rev.* 51, 893 (1937)
- 6T38 R. L. Thornton, *Phys. Rev.* 53, 326 (1938) (A)
- 6T47 R. L. Thornton and R. W. Senseman, *Phys. Rev.* 72, 872 (1947)
- 7T51 E. P. Tomlinson, H. W. Fulbright, and J. J. Howland, Jr., *Phys. Rev.* 83, 223 (1951) (A)
- 7T52 E. P. Tomlinson and S. L. Ridgway, *Phys. Rev.* 88, 170 (1952) (A)
- 8T49 W. Thiel and A. H. Jaffey, reported in Argonne National Laboratory Classified Report ANL-4370 (Nov. 1949)
- 9T42 San-Tsiang Tsien, *J. phys. et radium* 3, 1 (1942); *Compt. rend.* 217, 685 (1943)
- 9T43 San-Tsiang Tsien, *Compt. rend.* 216, 765 (1943)
- 9T43a San-Tsiang Tsien, *Compt. rend.* 217, 599 (1943)
- 9T46 San-Tsiang Tsien, *Phys. Rev.* 69, 38 (1946)
- 9T46a San-Tsiang Tsien, M. Bachelet, and G. Bouissières, *Phys. Rev.* 69, 39 (1946)
- 10T49 C. M. Turner, *Phys. Rev.* 76, 148 (1949); U. S. Atomic Energy Commission Unclassified Document AECU-432 (July 1949)
- 11T48 M. Ter-Pogossian, J. E. Robinson, and C. S. Cook, *Phys. Rev.* 75, 995 (1948)
- 11T49 M. Ter-Pogossian, J. E. Robinson, and H. Goddard, *Phys. Rev.* 76, 453 (1949) (A)
- 11T49a M. Ter-Pogossian, C. S. Cook, C. H. Goddard, and J. E. Robinson, *Phys. Rev.* 76, 909 (1949)
- 11T50 M. Ter-Pogossian, C. S. Cook, F. T. Porter, K. H. Morganstern, and J. Hudis, *Phys. Rev.* 80, 360 (1950); 81, 285 (1951)
- 11T51 M. Ter-Pogossian and F. T. Porter, *Phys. Rev.* 81, 1057 (1951)
- 12T49 A. V. Tollestrup, W. A. Fowler, and C. C. Lauritsen, *Phys. Rev.* 76, 428 (1949)
- 13T47 H. G. Thode and R. L. Graham, *Can. J. Research* 25A, 1 (1947)
- 13T48 H. G. Thode, J. Macnamara, F. P. Lossing, and C. B. Collins, *J. Am. Chem. Soc.* 70, 3008 (1948)
- 13T48a H. G. Thode, *Nucleonics* 3, No. 3, 14 (1948)
- 13T49 H. G. Thode, *Research* 2, 154 (1949)
- 14T41 A. A. Townsend, *Proc. Roy. Soc. (London)* 177A, 357 (1941)
- 15T50 J. F. Turner, reported in British Atomic Energy Commission Report AERE-PR-18 (Oct. 1950)
- 15T51 J. F. Turner and P. E. Cavanagh, *Phil. Mag.* 42, 636 (1951)
- 16T46 R. Tangen, *Kgl. Norske Videnskab. Selskab. Skr.* No. 1 (1946)
- 17T47 C. A. Tobias and C. Levinthal, private communication (Jan. 1947)
- 17T48 C. A. Tobias, private communication (Sept. 1948)
- 18T51 H. K. Ticho, *Phys. Rev.* 84, 847 (1951)
- 18T52 H. K. Ticho, D. Green, and J. R. Richardson, *Phys. Rev.* 86, 422 (1952) and private communication (Oct. 1952)
- 19T47 R. C. Thompson and D. R. Miller, private communication (Jan. 1947)
- 19T48 R. C. Thompson and D. R. Miller, private communication (Jan. 1948)
- 20T39 A. W. Tyler, *Phys. Rev.* 56, 125 (1939)
- 21T47 A. Turkevich, reported in Argonne National Laboratory Classified Report ANL-4010 (Sept. 1947)
- 21T51 A. Turkevich and J. B. Niday, *Phys. Rev.* 84, 52 (1951)
- 21T51a A. Turkevich and J. B. Niday, *Phys. Rev.* 84, 1253 (1951)
- 21T51b A. Turkevich, E. P. Steinberg, B. Finkle, and N. Sugarman, *NNES-PPR* 9, 1070 (1951)
- 22T51 J. Toballem, *Compt. rend.* 233, 1360 (1951)
- 23T51 S. I. Taimuty, *Phys. Rev.* 81, 461 (1951)
- 24T45 B. Trumpy and J. J. Orlin, *Bergens Museums Årbok, Naturv. Rekke Nr.* 7 (1945)
- 25T47 D. J. Tendam and H. L. Bradt, *Phys. Rev.* 72, 527 (1947) (A)
- 25T47a D. J. Tendam and H. L. Bradt, *Phys. Rev.* 72, 1118 (1947)
- 26T51 D. A. Thomas, S. K. Haynes, C. D. Broyles, and H. C. Thomas, *Phys. Rev.* 82, 961 (1951)
- 27T49 G. M. Temmer, *Phys. Rev.* 76, 424 (1949)
- 28T38 G. F. Tape and J. M. Cork, *Phys. Rev.* 53, 676 (1938) (A)
- 29T40 L. A. Turner, *Phys. Rev.* 58, 679 (1940)
- 30T49 S. Thulin, I. Bergström, and A. Hedgran, *Phys. Rev.* 76, 871 (1949)
- 30T51 S. Thulin, *Phys. Rev.* 83, 860 (1951)
- 30T52 S. Thulin and I. Bergström, *Phys. Rev.* 85, 1055 (1952)
- 30T52a S. Thulin, *Phys. Rev.* 87, 684 (1952)
- 30T52b S. Thulin, *Arkiv Fysik* 4, 363 (1952); reported in *M. Siegbahn Commemorative Volume*, p 163 (Uppsala, 1951)
- 30T52c S. Thulin, *Arkiv Fysik* (in press) (1952)
- 31T48 J. Townsend, M. Cleland, and A. L. Hughes, *Phys. Rev.* 74, 499 (1948)
- 32T50 C. C. Thomas, Jr. and E. O. Wiig, *J. Am. Chem. Soc.* 72, 2818 (1950)
- 33T51 S. E. Turner and L. O. Morgan, *Phys. Rev.* 81, 881 (1951)
- 34T52 Y. Tomozawa, M. Umezawa, and S. Nakamura, *Phys. Rev.* 86, 791 (1952)
- 35T49 C. H. Townes, J. M. Mays, and B. P. Dailey, *Phys. Rev.* 76, 700 (1949)

- 36T51 F. S. Tompkins, M. Fred, and W. F. Meggers, *Phys. Rev.* 84, 168 (1951)
- 37T52 D. E. Tilley, Abstract 77, June Meeting, Roy. Soc. Canada (1952)
- 38T49 B. V. Thosar, *Proc. Phys. Soc. (London)* 62A, 739 (1949)
- 39T52 H. Tyren, unpublished data (March 1952)
- 40T52 B. L. Tucker and E. C. Gregg, *Phys. Rev.* 87, 907 (1952)
- 41T50 A. P. Tudge and H. G. Thode, *Can. J. Research* 28B, 567 (1950)
- 42T52 A. L. Thompson, private communication (Oct. 1952)
- 1V38 R. J. Voskuyl, Ph.D. Thesis, Harvard University (1938)
- 2V36 S. N. Van Voorhis, *Phys. Rev.* 50, 895 (1936)
- 2V36a S. N. Van Voorhis, *Phys. Rev.* 49, 889 (1936) (A)
- 2V40 S. N. Van Voorhis, private communication (1940)
- 3V45 A. F. Voigt, private communication (Jan. 1945)
- 3V48 A. F. Voigt and B. J. Thamer, *Phys. Rev.* 74, 1264 (1948) (A)
- 4V49 F. W. Van Name, Jr., *Phys. Rev.* 75, 100 (1949)
- 5V51 G. Vendryes, *Compt. rend.* 232, 1549 (1951)
- 5V51a G. Vendryes, *Compt. rend.* 233, 391 (1951)
- 6V39 G. E. Valley and R. L. McCreary, *Phys. Rev.* 56, 863 (1939)
- 6V41 G. E. Valley and H. H. Anderson, *Phys. Rev.* 59, 113 (1941) (A)
- 6V41a G. E. Valley, *Phys. Rev.* 59, 686 (1941)
- 6V41b G. E. Valley, *Phys. Rev.* 60, 167 (1941) (A)
- 7V38 O. Viktorin, *Proc. Cambridge Phil. Soc.* 34, 612 (1938)
- 8V51 N. F. Verster, G. J. Nijgh, R. Van Lieshout, and C. J. Bakker, *Physica* 17, 637 (1951)
- 9V52 D. M. Van Patter, Massachusetts Institute of Technology Unclassified Report MIT-NSE-Tech. Rep. 57 (Jan. 1952)
- 10V52 H. T. Vlaar and A. H. W. Aten, Jr., *Physica* 18, 275 (1952)
- 11V52 P. J. Van der Haack, A. E. de Vries, and A. H. W. Aten, Jr., *Physica* 18, 20 (1952)
- 12V52 A. Van der Weil and A. H. W. Aten, Jr., *Physica* 18, 356 (1952)
- 13V52 G. Vieira and L. Salgueiro, *Compt. rend.* 234, 1765 (1952)
- 14V52 C. Victor, J. Teillac, P. Falk-Vairant, and G. Bouissières, *J. phys. et radium* (to be published) (1952)
- 15V52 R. Vestergaard and E. Haeffner, *Arkiv Fysik* 3, 557 (1952)
- 1W42 A. C. Wahl and G. T. Seaborg, Metallurgical Project Classified Report (work performed at Berkeley) CN-266 (Sept. 1942)
- 1W48 A. C. Wahl and G. T. Seaborg, *Phys. Rev.* 73, 940 (1948); *NNES-PPR* 14B, 21 (1949)
- 1W52 A. C. Wahl and N. A. Bonner, *Phys. Rev.* 85, 570 (1952)
- 2W47 G. Wilkinson, *Nature* 160, 864 (1947)
- 2W48 G. Wilkinson and H. G. Hicks, *Phys. Rev.* 74, 1733 (1948)
- 2W48a G. Wilkinson, *Phys. Rev.* 73, 252 (1948)
- 2W49 G. Wilkinson and H. G. Hicks, *Phys. Rev.* 75, 1687 (1949)
- 2W49a G. Wilkinson and H. G. Hicks, *Phys. Rev.* 75, 1370 (1949)
- 2W49b G. Wilkinson and H. G. Hicks, *Phys. Rev.* 75, 696 (1949)
- 2W49c G. Wilkinson, *Phys. Rev.* 75, 1019 (1949)
- 2W50 G. Wilkinson, *Phys. Rev.* 79, 1014 (1950)
- 2W50a G. Wilkinson and H. G. Hicks, University of California Radiation Laboratory Unclassified Report UCRL-751 (June 1950)
- 2W50b G. Wilkinson and H. G. Hicks, *Phys. Rev.* 80, 491 (1950)
- 2W50c G. Wilkinson and H. G. Hicks, *Phys. Rev.* 79, 815 (1950)
- 2W50d G. Wilkinson and H. G. Hicks, University of California Radiation Laboratory Unclassified Report UCRL-744 (June 1950)
- 2W50e G. Wilkinson, *Phys. Rev.* 80, 495 (1950)
- 2W50f G. Wilkinson, reported in Massachusetts Institute of Technology Unclassified Report NP-1879 (Oct. 1950)
- 2W50g G. Wilkinson and H. G. Hicks, *Phys. Rev.* 77, 314 (1950)
- 2W51 G. Wilkinson and H. G. Hicks, *Phys. Rev.* 81, 540 (1951)
- 3W48 R. J. Walen, *Compt. rend.* 227, 1090 (1948); *J. phys. et radium* 10, 95 (1949)
- 4W43 R. Wilkinson and J. S. Levinger, reported in Metallurgical Laboratory Classified Report CP-641 (May 1943)
- 4W44 R. Wilkinson, W. Rall, and E. Meiners, reported in Metallurgical Laboratory Classified Report CP-2090 (Sept. 1944)
- 4W51 R. G. Wilkinson and W. Rall, *NNES-PPR* 9, 1124 (1951)
- 4W51a R. G. Wilkinson, W. Rall, L. C. Miller, and L. F. Curtiss, *NNES-PPR* 9, 1128 (1951)
- 4W52 R. G. Wilkinson, private communication (Oct. 1952)
- 5W39 A. G. Ward, *Proc. Cambridge Phil. Soc.* 35, 322 (1939)
- 5W39a A. G. Ward, *Proc. Cambridge Phil. Soc.* 35, 523 (1939)
- 5W42 A. G. Ward, *Proc. Roy. Soc. (London)* 181A, 183 (1942)
- 6W50 J. L. Wolfson, *Phys. Rev.* 78, 176 (1950)
- 6W52 J. L. Wolfson, private communication (Oct. 1952)
- 7W48 M. Weisabluth, T. M. Putnam, and E. Segrè, private communication (July 1948)
- 8W49 Q. Van Winkle, R. G. Larson, and L. I. Katzin, *J. Am. Chem. Soc.* 71, 2585 (1949)
- 9W45 D. Williams and P. Yuster, Los Alamos Scientific Laboratory Classified Report LAMS-195 (Jan. 1945)
- 9W46 D. Williams and P. Yuster, *Phys. Rev.* 69, 556 (1946)
- 10W51 J. C. Wallmann, Ph.D. Thesis, University of California Radiation Laboratory Classified Report UCRL-1255 (April 1951)
- 11W46 E. F. Westrum, Jr., R. W. Greenlee, and J. C. Hindman, Metallurgical Laboratory Classified Report CC-3894 (Nov. 1946)
- 11W51 E. F. Westrum, Jr., *Phys. Rev.* 83, 1249 (1951)
- 12W51 D. West and J. K. Dawson, *Proc. Phys. Soc. (London)* 64A, 586 (1951)
- 12W52 D. West, J. K. Dawson, and C. J. Mandleberg, *Phil. Mag.* 43, 875 (1952)

- 13W50 S. C. Wright, Phys. Rev. 77, 742 (1950) (A)
- 14W49 R. M. Williamson and H. T. Richards, Phys. Rev. 76, 614 (1949)
- 15W41 J. A. Wheeler, Phys. Rev. 59, 27 (1941)
- 16W40 C. S. Wu, Phys. Rev. 58, 926 (1940)
- 16W41 C. S. Wu and G. Friedlander, Phys. Rev. 60, 747 (1941)
- 16W42 C. S. Wu and E. Segrè, Phys. Rev. 61, 203 (1942) (A)
- 16W45 C. S. Wu and E. Segrè, Phys. Rev. 67, 142 (1945)
- 16W48 C. S. Wu, W. W. Havens, Jr., and L. J. Rainwater, Phys. Rev. 74, 1248 (1948) (A)
- 16W49 C. S. Wu and L. Feldman, Phys. Rev. 76, 698 (1949)
- 16W49a C. S. Wu, C. H. Townes, and L. Feldman, Phys. Rev. 76, 692 (1949)
- 16W49b C. S. Wu and L. Feldman, Phys. Rev. 76, 693 (1949)
- 16W49c C. S. Wu and L. Feldman, Phys. Rev. 76, 696 (1949)
- 16W51 C. S. Wu and L. Feldman, Phys. Rev. 82, 457 (1951)
- 16W52 C. S. Wu, B. M. Rustad, V. Perez-Mendez, and L. Lidofsky, Phys. Rev. 87, 1140 (1952)
- 17W48 A. S. Weil and J. R. Dunning, Columbia University Document CUD-9 (Feb. 1948)
- 18W50 S. D. Warshaw, Phys. Rev. 80, 111 (1950)
- 18W50a S. D. Warshaw, J. J. L. Chen, and G. L. Appleton, Phys. Rev. 80, 288 (1950)
- 19W34 L. Wertenstein, Nature 133, 564 (1934)
- 20W41 S. B. Welles, Phys. Rev. 59, 679 (1941)
- 21W39 M. G. White, L. A. Delsasso, J. G. Fox, and E. C. Creutz, Phys. Rev. 56, 512 (1939)
- 21W41 M. G. White, E. C. Creutz, L. A. Delsasso, and R. R. Wilson, Phys. Rev. 59, 63 (1941)
- 22W40 W. W. Watson and E. Pollard, Phys. Rev. 57, 1082 (1940) (A)
- 23W49 R. Wilson and G. R. Bishop, Proc. Phys. Soc. (London) 62, 457 (1949). Value recalculated in (38S51)
- 23W50 R. Wilson, Phys. Rev. 79, 1004 (1950)
- 24W48 J. R. White and A. E. Cameron, Phys. Rev. 74, 991 (1948)
- 25W48 H. Wäffler and O. Hirzel, Helv. Phys. Acta 21, 200 (1948)
- 25W50 H. Wäffler, Helv. Phys. Acta 23, 239 (1950)
- 26W51 J. J. Wilkins and F. K. Goward, Proc. Phys. Soc. (London) 64A, 849 (1951)
- 27W39 Y. Watase and J. Itoh, Proc. Phys.-Math. Soc. Japan 21, 626 (1939)
- 27W41 Y. Watase, Proc. Phys.-Math. Soc. Japan 23, 618 (1941)
- 28W41 P. K. Weimer, J. D. Kurbatov, and M. L. Pool, Phys. Rev. 60, 469 (1941)
- 28W44 P. K. Weimer, J. D. Kurbatov, and M. L. Pool, Phys. Rev. 66, 209 (1944)
- 29W52 G. Wagner and E. O. Wiig, J. Am. Chem. Soc. 74, 1101 (1952)
- 30W37 H. Walke, Phys. Rev. 52, 663 (1937)
- 30W37a H. Walke, Phys. Rev. 52, 400 (1937)
- 30W37b H. Walke, Phys. Rev. 52, 777 (1937)
- 30W37c H. Walke, Phys. Rev. 52, 669 (1937)
- 30W39 H. Walke, E. J. Williams, and G. R. Evans, Proc. Roy. Soc. (London) 171A, 360 (1939)
- 30W40 H. Walke, F. C. Thompson, and J. Holt, Phys. Rev. 57, 177 (1940)
- 30W40a H. Walke, Phys. Rev. 57, 163 (1940)
- 30W40b H. Walke, F. C. Thompson, and J. Holt, Phys. Rev. 57, 171 (1940)
- 31W50 M. A. Waggoner, M. L. Moon, and A. Roberts, Phys. Rev. 80, 420 (1950)
- 31W50a M. A. Waggoner, M. L. Moon, and A. Roberts, Phys. Rev. 78, 295 (1950)
- 31W51 M. A. Waggoner, Phys. Rev. 82, 906 (1951), 80, 489 (1950)
- 32W52 W. J. Worthington, Jr., Phys. Rev. 87, 158 (1952)
- 33W49 H. W. Wilson and S. C. Curran, Phil. Mag. 40, 631 (1949)
- 33W50 H. W. Wilson, Phys. Rev. 79, 1032 (1950)
- 33W51 H. W. Wilson, Phys. Rev. 82, 548 (1951)
- 33W51a H. W. Wilson and S. C. Curran, Phil. Mag. 42, 762 (1951)
- 33W52 H. W. Wilson and G. M. Lewis, Proc. Phys. Soc. (London) 65A, 656 (1952)
- 34W42 G. L. Weil, Phys. Rev. 62, 229 (1942)
- 35W48 L. L. Woodward, D. A. McCown, and M. L. Pool, Phys. Rev. 74, 870 (1948)
- 35W48a L. L. Woodward, D. A. McCown, and M. L. Pool, Phys. Rev. 74, 761 (1948)
- 36W51 F. P. W. Winteringham, Nature 167, 155 (1951)
- 37W45 M. L. Wiedenbeck, Phys. Rev. 68, 237 (1945)
- 37W45a M. L. Wiedenbeck, Phys. Rev. 68, 1 (1945)
- 37W45b M. L. Wiedenbeck, Phys. Rev. 67, 92 (1945)
- 37W46 M. L. Wiedenbeck, Phys. Rev. 70, 435 (1946)
- 37W47 M. L. Wiedenbeck and K. Y. Chu, Phys. Rev. 72, 1164 (1947)
- 38W52 D. R. Wiles, B. W. Smith, R. Horsley, and H. G. Thode, Chalk River Laboratory Classified Report CRC-493 (Jan. 1952)
- 39W52 F. Wagner, Jr. and M. S. Freedman, Phys. Rev. 86, 631 (1952) (A)
- 39W52a F. Wagner, Jr. and M. S. Freedman, Phys. Rev. (to be published) (1952)
- 39W52b F. Wagner, Jr., M. S. Freedman, and D. Engelkemeir, U. S. Atomic Energy Commission Declassified Document AECD-3304 (Feb. 1952)
- 39W53 F. Wagner, Jr., M. S. Freedman, D. W. Engelkemeir, and L. B. Magnusson, Phys. Rev. (to be published) (1953)
- 40W51 E. J. Wolicki, B. Waldman, and W. C. Miller, Phys. Rev. 82, 486 (1951)
- 41W43 B. Waldman and M. L. Wiedenbeck, Phys. Rev. 63, 60 (1943) (A)
- 41W49 B. Waldman, W. C. Miller, and D. Gideon, Phys. Rev. 76, 181 (1949) (A)
- 42W47 A. Wattenberg, Phys. Rev. 71, 497 (1947)
- 43W48 R. R. Williams, Jr., J. Chem. Phys. 16, 513 (1948)
- 43W51 R. R. Williams, Jr., NNES-PPR 9, 220 (1951)
- 44W51 W. E. Winsche, L. G. Stang, Jr., and W. D. Tucker, Nucleonics 8, No. 3, 14 (1951)
- 45W50 A. H. Williams and M. L. Wiedenbeck, Phys. Rev. 78, 822 (1950)
- 46W43 K. E. Weimer, M. L. Pool, and J. D. Kurbatov, Phys. Rev. 63, 59 (1943) (A)
- 46W43a K. E. Weimer, M. L. Pool, and J. D. Kurbatov, Phys. Rev. 64, 43 (1943) (A)
- 46W43b K. E. Weimer, M. L. Pool, and J. D. Kurbatov, Phys. Rev. 63, 67 (1943)
- 47W52 A. H. Wapstra, Phys. Rev. 86, 561 (1952)
- 47W52a A. H. Wapstra, Phys. Rev. 86, 562 (1952)

- 48W50 B. Weaver, *Phys. Rev.* 80, 301 (1950)
- 49W49 D. Walker, *Proc. Phys. Soc. (London)* 62A, 799 (1949)
- 49W49a D. Walker and E. W. Fuller, *Nature* 164, 226 (1949)
- 50W52 J. Walker, *Proc. Phys. Soc. (London)* 65A, 449 (1952)
- 51W51 L. Winsberg, *NNES-PPR* 9, 1273 (1951)
- 51W51a L. Winsberg, *NNES-PPR* 9, 1284 (1951)
- 51W51b L. Winsberg, *NNES-PPR* 9, 1302 (1951)
- 51W51c L. Winsberg, *NNES-PPR* 9, 1311 (1951)
- 51W51d L. Winsberg, *NNES-PPR* 9, 1292 (1951)
- 51W52 L. Winsberg, private communication (Oct. 1952)
- 52W51 W. E. Wright and M. Deutsch, *Phys. Rev.* 82, 277 (1951)
- 53W41 C. M. Witcher, *Phys. Rev.* 60, 32 (1941)
- 54W51 T. Wiedling and A. Carlsson, *Phys. Rev.* 83, 181 (1951)
- 55W51 A. Wennerblom, K. E. Zimen, and E. Ehn, *Svensk Kem. Tid.* 63, 207 (1951)
- 56W52 B. T. Wright, *Phys. Rev.* (to be published) (1952); *Bull. Am. Phys. Soc.* 27, No. 5, Abstract Q2 (1952)
- 57W52 J. Welker, A. Schardt, J. J. Howland, Jr., and G. Friedlander, private communication (Nov. 1952)
- 58W52 T. Westermark, *Phys. Rev.* 88, 573 (1952); private communication (Oct. 1952)
- 1Y47 L. Yaffe and C. E. MacKintosh, *Can. J. Research* 25B, 371 (1947)
- 1Y48 L. Yaffe and J. M. Grunlund, *Phys. Rev.* 74, 696 (1948)
- 1Y48a L. Yaffe and K. M. Justus, *Can. J. Research* 26B, 734 (1948)
- 1Y49 L. Yaffe, M. Kirsch, S. Standil, and J. M. Grunlund, *Phys. Rev.* 75, 699 (1949)
- 1Y49a L. Yaffe, B. W. Sargent, M. Kirsch, S. Standil, and J. M. Grunlund, *Phys. Rev.* 76, 617 (1949)
- 1Y50 L. Yaffe and W. H. Stevens, *Phys. Rev.* 79, 893 (1950)
- 1Y51 L. Yaffe, R. C. Hawkings, W. F. Merritt, and J. H. Craven, *Phys. Rev.* 82, 553 (1951)
- 2Y35 D. M. Yost, L. N. Ridenour, and K. Shinohara, *J. Chem. Phys.* 3, 133 (1935)
- 3Y38 T. Yasaki and S. Watanabe, *Nature* 141, 787 (1938)
- 4Y42 T. Yuasa, *Compt. rend.* 215, 414 (1942)
- 4Y52 T. Yuasa, *Compt. rend.* 235, 366 (1952)
- 5Y47 F. Yu, D. Gideon, and J. D. Kurbatov, *Phys. Rev.* 71, 382 (1947)
- 5Y48 F. Yu and J. D. Kurbatov, *Phys. Rev.* 74, 34 (1948)
- 5Y49 F. Yu, L. Cheng, and J. D. Kurbatov, *Phys. Rev.* 75, 1287 (1949) (A)
- 6Y45 R. S. Yalow and M. Goldhaber, *Phys. Rev.* 67, 59 (1945)
- 7Y51 J. N. Young, M. L. Pool, and D. N. Kundu, *Phys. Rev.* 83, 1060 (1951)
- 8Y40 H. Yamasaki and K. Sinma, *Sci. Papers Inst. Phys. Chem. Research (Tokyo)* 37, 10 (1940)
- 1Z48 B. Zajac, E. Broda, and N. Feather, *Proc. Phys. Soc. (London)* 60, 501 (1948)
- 1Z52 B. Zajac, *Phil. Mag.* 43, 264 (1952)
- 2Z49 A. S. Zavel'skii, G. Ya. Umarov, and S. K. Matushevskii, *Zhur. Eksptl' i Teoret. Fiz.* 19, 1136 (1949)
- 3Z43 W. H. Zinn, A. Wattenberg, and J. West, reported in *Metallurgical Laboratory Classified Report CP-781* (July 1943)
- 4Z42 I. Zlotowski and J. H. Williams, *Phys. Rev.* 62, 29 (1942)
- 5Z48 D. J. Zaffarano, B. D. Kern, and A. C. G. Mitchell, *Phys. Rev.* 74, 682 (1948)
- 5Z48a D. J. Zaffarano, B. D. Kern, and A. C. G. Mitchell, *Phys. Rev.* 74, 105 (1948)
- 5Z51 D. J. Zaffarano and F. I. Boley, *Phys. Rev.* 83, 223 (1951) (A)
- 6Z45 W. Zunti and E. Bleuler, *Helv. Phys. Acta* 18, 263 (1945)
- 7Z52 W. Zobel, reported in *Purdue University Progress Report II* (June 1952)
- 8Z49 H. Zeldes, A. R. Brosi, G. W. Parker, G. M. Hebert, and G. E. Creek, reported in *Oak Ridge National Laboratory Classified Report ORNL-286* (June 1949)
- 8Z50 H. Zeldes, B. H. Ketelle, and A. R. Brosi, *Phys. Rev.* 79, 901 (1950)
- 8Z51 H. Zeldes, B. H. Ketelle, and A. R. Brosi, reported in *Oak Ridge National Laboratory Classified Report ORNL-1036* (Sept. 1951)
- 8Z52 H. Zeldes, B. H. Ketelle, A. R. Brosi, C. R. Fultz, and R. F. Hibbs, *Phys. Rev.* 86, 811 (1952)
- 9Z49 K. E. Zimen, *Z. Naturforsch.* 4a, 95 (1949)
- 10Z50 E. L. Zimmerman, E. B. Dale, D. G. Thomas, and J. D. Kurbatov, *Phys. Rev.* 80, 908 (1950)
- 11Z43 R. V. Zumstein, J. D. Kurbatov, and M. L. Pool, *Phys. Rev.* 63, 59 (1943) (A)
- 12Z40 E. Zingg, *Helv. Phys. Acta* 13, 219 (1940)

Table 1.2.17—Thermal Cross Sections*
 (AECU 2040, Neutron Cross Sections, May 15, 1952;
 and Supplement 1 to AECU 2040, November 20, 1952)

Element	Isotope (%)	Reaction Cross Sections† (2200 m/sec)‡		Scattering Cross Sections§			
		σ_{abs}	σ_{act}	$\sigma_{\text{coh}}(\text{sign})$	$\sigma_{\text{la}}\left(\frac{A+1}{A}\right)^2$	$\bar{\sigma}_s$	
^1H		0.330 ± 0.007		$1.79 \pm 0.02 (-)$	81.4 ± 0.4	38 ± 4 (gas)	
	H^1 (~100)						
	H^2 (0.015)	0.46 ± 0.1 mb	12y	0.57 ± 0.01 mb	$5.4 \pm 0.3 (+)$	7.5 ± 0.1	
^2He				$1.1 \pm 0.2 (+)$	1.3 ± 0.2	0.8 ± 0.2	
	He^3 (0.00013)	np 5200 \pm 300					
	He^4 (~100)	0	0				
^3Li		70 ± 1		$0.40 \pm 0.03 (-)$	1.2 ± 0.3	1.4 ± 0.3	
	Li^6 (7.5)	(n α 910)		$6 \pm 3 (+)$			
	Li^7 (92.5)		0.9s	33 ± 5 mb	$0.80 \pm 0.05 (-)$	2.0 ± 0.5	
^4Be	Be^9 (100)	10 ± 1 mb	2.7×10^6 y	9 ± 3 mb	$7.54 \pm 0.07 (+)$	7.54 ± 0.07	7 ± 1
^5B		750 ± 10			4.4 ± 0.2	4 ± 1	
	B^{10} (18.8)	(n α 3990)			2.9 ± 0.2		
		np <0.2					
	B^{11} (81.2)		0.03s	<50 mb	4.4 ± 0.3		
^6C		4.5 mb		$5.45 \pm 0.07 (+)$	5.51 ± 0.05	4.8 ± 0.2	
	C^{12} (98.9)						
	C^{13} (1.1)		5800y	1.0 ± 0.3 mb	$4.5 \pm 0.6 (+)$	5.5 ± 1.0	
	C^{14} (5800y)	<200	2.4s	<1 μ b			
^7N		1.78 ± 0.05		$11.0 \pm 0.5 (+)$	11.4 ± 0.5	10 ± 1	
	N^{14} (99.6)	np 1.70 ± 0.05					
		n γ 0.10 ± 0.05					
	N^{15} (0.37)		7.4s	$24 \pm 8 \mu$ b			
^8O		<0.2 mb		$4.2 \pm 0.3 (+)$	4.24 ± 0.02	4.2 ± 0.3	
	O^{16} (99.76)						
	O^{17} (0.037)		5800y	C^{14} 0.5 ± 0.1			
	O^{18} (0.20)		29s	0.21 ± 0.04 mb			
^9F	F^{19} (100)	<10 mb	12s	9 ± 2 mb	$3.8 \pm 0.3 (+)$	4.0 ± 0.1	4.1 ± 0.3
^{10}Ne		<2.8			2.9 ± 0.2	2.4 ± 0.3	
	Ne^{20} (90.9)						
	Ne^{21} (0.26)						
	Ne^{22} (8.8)		40s	36 ± 15 mb			
^{11}Na	Na^{23} (100)	0.49 ± 0.02	15h	0.54 ± 0.03	$1.55 \pm 0.05 (+)$	3.6 ± 0.3	4.0 ± 0.5
^{12}Mg		59 ± 4 mb		$3.6 \pm 0.3 (+)$	3.8 ± 0.2	3.6 ± 0.4	
	Mg^{24} (78.6)	33 ± 10 mb					
	Mg^{25} (10.1)	270 ± 90 mb					
	Mg^{26} (11.3)	60 ± 60 mb	9.6m	50 ± 10 mb			
^{13}Al	Al^{27} (100)	0.215 ± 0.008	2.3m	0.21 ± 0.04	$1.5 \pm 0.1 (+)$	1.6 ± 0.1	1.4 ± 0.1
^{14}Si		0.13 ± 0.03		$2.0 \pm 0.2 (+)$	2.4 ± 0.2	1.7 ± 0.3	
	Si^{28} (92.22)	80 ± 30 mb					
	Si^{29} (4.70)	0.27 ± 0.09					
	Si^{30} (3.08)	0.41 ± 0.41	2.7h	0.12 ± 0.03			

Table 1.2.17 — (Continued)

Element	Isotope (%)	Reaction Cross Sections† (2200 m/sec)‡		Scattering Cross Sections§		
		σ_{abs}	σ_{act}	$\sigma_{\text{coh}}(\text{sign})$	$\sigma_{\text{fa}}\left(\frac{A+1}{A}\right)^2$	$\bar{\sigma}_s$
^{15}P	P^{31} (100)	0.19 ± 0.03	14.3d 0.23 ± 0.05	$3 \pm 1 (+)$	3.6 ± 0.3	10 ± 2
^{32}S	S^{32} (95.1)	0.49 ± 0.02		$1.20 \pm 0.08 (+)$	1.2 ± 0.2	1.1 ± 0.2
	S^{33} (0.74)					
	S^{34} (4.2)		87d 0.26 ± 0.05			
	S^{36} (0.016)		5m 0.14 ± 0.04			
^{35}Cl	Cl^{35} (75.4)	31.6 ± 1.0		$12.1 \pm 0.8 (+)$	15 ± 3	
		np 0.30 ± 0.10	87d $\text{S}^{35} 0.17 \pm 0.04$			
	Cl^{37} (24.6)		$4 \times 10^6 \text{y}$ 40 ± 25			
			38m 0.56 ± 0.12			
^{39}K	K^{39} (93.1)	1.97 ± 0.06	$> 3.5 \text{y}$ > 0.06	$1.5 \pm 0.1 (+)$	2.0 ± 0.2	1.5 ± 0.3
	K^{40} (0.012)	1.87 ± 0.15	$2 \times 10^6 \text{y}$ 3 ± 2			
		70 ± 20				
		np < 1				
	K^{41} (6.9)	1.19 ± 0.10	12.4h 1.0 ± 0.2			
^{40}Ca	Ca^{40} (96.9)	0.43 ± 0.02		$3.0 \pm 0.1 (+)$	3.2 ± 0.3	9 ± 2
	Ca^{42} (0.64)	0.22 ± 0.04	8.5d $< 0.1 \text{ mb}$	$3.0 \pm 0.1 (+)$	3.1 ± 0.3	
	Ca^{43} (0.14)	40 ± 3				
	Ca^{44} (2.1)		152d 0.63 ± 0.12	$0.40 \pm 0.03 (+)$		
	Ca^{46} (0.0032)					
	Ca^{48} (0.18)		8.5m 1.1 ± 0.1			
^{45}Sc	Sc^{45} (100)	23 ± 2	20s 10 ± 4	$13 \pm 1 (+)$		
			85d 12 ± 6			
			(20s \rightarrow 85d)			
^{46}Ti	Ti^{46} (8.0)	5.6 ± 0.4		$1.4 \pm 0.3 (-)$	4.0 ± 0.4	6 ± 2
	Ti^{47} (7.8)	0.6 ± 0.2				
	Ti^{48} (73.4)	1.6 ± 0.3				
	Ti^{49} (5.5)	8.0 ± 0.6				
	Ti^{50} (5.3)	1.8 ± 0.5				
		< 0.2	6m 0.14 ± 0.03			
^{51}V	V^{51} (99.8)	4.7 ± 0.2		$32 \pm 8 \text{ mb} (-)$	5 ± 1	5 ± 1
	V^{50} (0.2)		3.9m 4.5 ± 0.9			
^{52}Cr	Cr^{52} (83.7)	2.9 ± 0.1		$1.7 \pm 0.1 (+)$	4.1 ± 0.3	3.0 ± 0.5
	Cr^{54} (2.4)	16.3 ± 1.3	26.5d 11 ± 5			
	Cr^{53} (9.5)	0.73 ± 0.06				
	Cr^{55} (3.8)	17.5 ± 1.4				
	Cr^{56} (2.5)	< 0.3				

Table 1.2.17 — (Continued)

Element	Isotope (%)	Reaction Cross Sections† (2200 m/sec)‡		Scattering Cross Sections§		
		σ_{abs}	σ_{act}	$\sigma_{\text{coh}}(\text{sign})$	$\sigma_{\text{fa}}\left(\frac{A+1}{A}\right)^2$	$\bar{\sigma}_s$
$_{25}\text{Mn}$	Mn^{55} (100)	12.6 ± 0.6	2.6h 12.9 ± 0.5	1.7 ± 0.1 (—)	2.0 ± 0.1	2.3 ± 0.3
$_{26}\text{Fe}$		$\eta\alpha$ 5 ± 3 mb		11.4 ± 0.3 (+)	11.7 ± 0.3	11 ± 1
	Fe^{54} (5.9)	2.2 ± 0.2	2.9y 0.7 ± 0.3	2.20 ± 0.13 (+)	2.5 ± 0.3	
	Fe^{56} (91.6)	2.6 ± 0.2		12.6 ± 0.4 (+)	12.8 ± 0.2	
	Fe^{57} (2.20)	2.4 ± 0.2		0.64 ± 0.04 (+)	2.0 ± 0.5	
	Fe^{58} (0.33)	2.5 ± 2.0	47d 0.7 ± 0.2			
		$\eta\alpha < 1.5$ mb				
$_{27}\text{Co}$	Co^{59} (100)	34.8 ± 2.0	10.7m 14 ± 3 5.3y 20 ± 3 (99.7% of 10.7m \rightarrow 5.3y)	1.00 ± 0.06 (+)	7 ± 1	5 ± 1
$_{28}\text{Ni}$		4.5 ± 0.2		13.4 ± 0.3 (+)	17.6 ± 0.3	17.5 ± 1.0
	Ni^{58} (67.9)	4.2 ± 0.3		25.9 ± 0.3 (+)	24.4 ± 0.5	
	Ni^{60} (26.2)	2.7 ± 0.2		1.1 ± 0.1 (+)	1.0 ± 0.1	
	Ni^{61} (1.2)	1.8 ± 1.3				
	Ni^{62} (3.7)	15 ± 3		9.5 ± 0.4 (—)	9 ± 1	
	Ni^{64} (1.0)		2.6h 2.6 ± 0.4			
	Ni^{66} (2.6h)		56h 6 ± 3			
$_{29}\text{Cu}$		3.59 ± 0.12		7.0 ± 0.4 (+)	7.7 ± 0.3	7.2 ± 0.7
	Cu^{63} (69.0)	4.3 ± 0.3	12.9h 3.9 ± 0.8			
	Cu^{65} (31.0)	2.11 ± 0.17	4.3m 1.8 ± 0.4			
$_{30}\text{Zn}$		1.06 ± 0.05		4.3 ± 0.3 (+)	4.1 ± 0.2	3.6 ± 0.4
	Zn^{64} (48.9)		250d 0.5 ± 0.1 12.9h $\text{Cu}^{64} < 10^{-5}$			
	Zn^{66} (27.8)	$\eta\alpha < 20$ μb				
	Zn^{67} (4.1)	$\eta\alpha$ 6 ± 4 μb				
	Zn^{68} (18.6)	$\eta\alpha < 20$ μb	14h 0.10 ± 0.03 52m 1.0 ± 0.2			
	Zn^{70} (0.63)		2.2m 85 ± 20 mb			
$_{31}\text{Ga}$		2.71 ± 0.12			7.5 ± 0.5	4 ± 1
	Ga^{69} (60.2)	2.0 ± 0.2	20m 1.4 ± 0.3			
	Ga^{71} (39.8)	4.9 ± 0.4	14h 3.4 ± 0.7			
$_{32}\text{Ge}$		2.35 ± 0.20		8.8 ± 0.5 (+)	8.6 ± 0.5	3 ± 1
	Ge^{70} (20.4)	3.3 ± 0.3	11d 3 ± 2			
	Ge^{72} (27.4)	0.94 ± 0.09				
	Ge^{73} (7.8)	13.7 ± 1.1				
	Ge^{74} (36.6)	0.60 ± 0.06	82m 0.45 ± 0.08			
	Ge^{76} (7.8)	0.35 ± 0.07	59s 30 ± 20 mb 12h 0.2 ± 0.1 (none of 59s \rightarrow 12h)			
$_{33}\text{As}$	As^{75} (100)	4.1 ± 0.2	27h 4.2 ± 0.8	5.0 ± 0.3 (+)	7 ± 1	6 ± 1
$_{34}\text{Se}$		11.8 ± 0.4		10.0 ± 0.6 (+)	9 ± 1	13 ± 1
	Se^{74} (0.87)	48 ± 7	115d 24 ± 6			
	Se^{76} (9.0)	82 ± 7	18s 7 ± 3			
	Se^{77} (7.6)	40 ± 4				

Table 1.2.17 — (Continued)

Element	Isotope (%)	Reaction Cross Sections† (2200 m/sec)‡		Scattering Cross Sections§		
		σ_{abs}	σ_{act}	$\sigma_{\text{coh}}(\text{sign})$	$\sigma_{\text{fa}}\left(\frac{A+1}{A}\right)^2$	$\bar{\sigma}_s$
	Se ⁷⁶ (23.5)	0.4 ± 0.4				
	Se ⁸⁰ (49.8)	0.59 ± 0.06	59m 30 ± 10 mb			
			17m 0.5 ± 0.1			
	Se ⁸² (9.2)	2.0 ± 1.4	67s 50 ± 25 mb			
			25m 4 ± 2 mb			
(Order of Isomers unknown)						
35Br		6.5 ± 0.5		5.7 ± 0.4 (+)	6.1 ± 0.2	6 ± 1
	Br ⁷⁹ (50.5)	10.4 ± 1.0	4.4h 2.9 ± 0.5			
			18m 8.5 ± 1.4			
	Br ⁸¹ (49.5)	2.6 ± 0.4	36h 3.5 ± 0.5			
36Kr		28 ± 5				7.2 ± 0.7
	Kr ⁷⁸ (0.35)		34h 0.3 ± 0.1			
	Kr ⁸⁰ (2.27)	95 ± 15				
	Kr ⁸² (11.6)	45 ± 15				
	Kr ⁸³ (11.6)	205 ± 10				
	Kr ⁸⁴ (57.0)	<2	4.4h 0.10 ± 0.03			
			10y 60 ± 20 mb			
			(16% 4.4h → 10y)			
	Kr ⁸⁵ (10y)	<15				
	Kr ⁸⁶ (17.4)	<2	78m 60 ± 20 mb			
	Kr ⁸⁷ (78m)		2.3h <470			
37Rb		0.70 ± 0.07		3.8 ± 0.3 (+)	5.5 ± 0.5	12 ± 2
	Rb ⁸⁵ (72.2)		19.5d 0.72 ± 0.15			
	Rb ⁸⁷ (27.8)		17.5m 0.12 ± 0.03			
	Rb ⁸⁸ (18m)		15m <200			
38Sr		1.16 ± 0.06		4.1 ± 0.3 (+)	12.5 ± 1.0	10 ± 1
	Sr ⁸⁴ (0.55)					
	Sr ⁸⁶ (9.8)		2.7h 1.3 ± 0.4			
	Sr ⁸⁷ (7.0)					
	Sr ⁸⁸ (82.7)		53d 5 ± 1 mb			
	Sr ⁸⁹ (53d)		25y <110			
	Sr ⁹⁰ (25y)		9.7h 1.0 ± 0.6			
39Y	Y ⁹⁰ (100)	1.38 ± 0.14	61h 1.2 ± 0.3			3 ± 2
40Zr		0.18 ± 0.02		5.0 ± 0.3 (+)	7.0 ± 0.5	8 ± 1
	Zr ⁹⁰ (51.5)	0.1 ± 0.1				
	Zr ⁹¹ (11.2)	1.52 ± 0.12				
	Zr ⁹² (17.1)	0.25 ± 0.12				
	Zr ⁹⁴ (17.4)	0.08 ± 0.06	65d 0.1 ± 0.05			
	Zr ⁹⁶ (2.80)	0.1 ± 0.1	17h 0.2 ± 0.1			
41Nb	Nb ⁹³ (100)	1.1 ± 0.1	6.6m 1.0 ± 0.5	6.0 ± 0.4 (+)	6.4 ± 0.3	5 ± 1
42Mo		2.4 ± 0.2		5.7 ± 0.4 (+)	6.1 ± 0.2	7 ± 1
	Mo ⁹² (15.7)	<0.3	7h <6 mb			
	Mo ⁹⁴ (9.3)					
	Mo ⁹⁶ (15.7)	13.4 ± 1.3				

Table 1.2.17 — (Continued)

Element	Isotope (%)	Reaction Cross Sections† (2200 m/sec)‡		Scattering Cross Sections§		
		σ_{abs}	σ_{act}	$\sigma_{\text{coh}}(\text{sign})$	$\sigma_{\text{fa}}\left(\frac{A+1}{A}\right)^2$	$\bar{\sigma}_s$
44Ru	Mo ⁹⁶ (16.5)	1.2 ± 0.6				
	Mo ⁹⁷ (9.5)	2.1 ± 0.7				
	Mo ⁹⁸ (23.9)	0.4 ± 0.4	67h	0.13 ± 0.05		
	Mo ¹⁰⁰ (9.5)	0.5 ± 0.5	15m	0.20 ± 0.05		
		2.46 ± 0.12			6.2 ± 0.5	6 ± 1
	Ru ⁹⁶ (5.7)		2.8d	10 ± 4 mb		
	Ru ⁹⁸ (2.22)					
	Ru ⁹⁹ (12.8)					
46Rh	Ru ¹⁰⁰ (12.7)					
	Ru ¹⁰¹ (17.0)					
	Ru ¹⁰² (31.3)		42d	1.2 ± 0.3		
	Ru ¹⁰⁴ (18.3)		4h	0.7 ± 0.2		
	Rh ¹⁰³ (100)	150 ± 7	4.3m	12 ± 2	4.5 ± 0.5 (+)	6 ± 1
			44s	140 ± 30		
		8.0 ± 1.5			5.0 ± 0.3 (+)	4.8 ± 0.3
						3.6 ± 0.6
47Ag	Pd ¹⁰² (0.8)					
	Pd ¹⁰⁴ (9.3)					
	Pd ¹⁰⁵ (22.6)					
	Pd ¹⁰⁶ (27.1)					
	Pd ¹⁰⁸ (26.7)		13h	11 ± 3		
	Pd ¹¹⁰ (13.5)		26m	0.4 ± 0.1		
		60 ± 3			4.6 ± 0.3 (+)	7 ± 1
						6 ± 1
48Cd	Ag ¹⁰⁷ (51.9)	30 ± 2	2.3m	44 ± 9	8.7 ± 0.5 (+)	10 ± 1
	Ag ¹⁰⁹ (48.1)	84 ± 7	270d	2.8 ± 0.5	2.3 ± 0.2 (+)	6 ± 1
			24.5s	110 ± 20		
		2400 ± 200				7 ± 1
		(not 1/v, × 1.3)				
	Cd ¹⁰⁶ (1.22)		6.7h	1.0 ± 0.5		
	Cd ¹⁰⁸ (0.92)					
	Cd ¹¹⁰ (12.4)		49m	0.2 ± 0.1		
49In	Cd ¹¹¹ (12.8)					
	Cd ¹¹² (24.0)		5y	20 ± 10 mb		
	Cd ¹¹³ (12.3)	(19,500, not 1/v, × 1.3)				
	Cd ¹¹⁴ (28.8)		43d	0.14 ± 0.03		
			2.3d	1.1 ± 0.3		
	Cd ¹¹⁶ (7.6)		2.7h	1.4 ± 0.3		
		190 ± 10				2.2 ± 0.5
	In ¹¹³ (4.2)		50d	56 ± 12		
50Sn			72s	2.0 ± 0.6		
	In ¹¹⁵ (95.8)		54m	145 ± 15		
			13s	52 ± 6		
		0.65 ± 0.05			4.6 ± 0.3 (+)	4.9 ± 0.5
						4 ± 1
	Sn ¹¹² (0.95)		30m	20 ± 10 mb		
			112d	1.3 ± 0.3		
			(% of 30m → 112d unknown)			

Table 1.2.17—(Continued)

Element	Isotope (%)	Reaction Cross Sections† (2200 m/sec)‡		Scattering Cross Sections§		
		σ_{abs}	σ_{act}	$\sigma_{\text{coh}}(\text{sign})$	$\sigma_{\text{fa}}\left(\frac{A+1}{A}\right)^2$	$\bar{\sigma}_s$
⁵⁰ Sn (Com'd.)	Sn ¹¹⁴ (0.65)					
	Sn ¹¹⁵ (0.34)					
	Sn ¹¹⁶ (14.2)		14.5d	6 ± 2 mb		
	Sn ¹¹⁷ (7.6)					
	Sn ¹¹⁸ (24.0)		245d	10 ± 6 mb		
	Sn ¹¹⁹ (8.6)					
	Sn ¹²⁰ (33.0)		>400d	1 ± 1 mb		
			27h	0.14 ± 0.03		
	Sn ¹²² (4.7)		40m	0.16 ± 0.04		
			126d	1.0 ± 0.5 mb		
	Sn ¹²⁴ (6.0)		(Order of Isomers unknown)			
			10d	4 ± 2 mb		
⁵¹ Sb		5.5 ± 1.0				
	Sb ¹²¹ (57.2)	5.7 ± 0.5	2.8d	6.8 ± 1.5	3.7 ± 0.3 (+)	4.2 ± 0.3
	Sb ¹²³ (42.8)	3.9 ± 0.3	21m	30 ± 15 mb		4.3 ± 0.5
			1.3m	30 ± 15 mb		
			60d	2.5 ± 0.5		
⁵² Te		4.5 ± 0.2				
	Te ¹²⁰ (0.091)	70 ± 70			4.2 ± 0.3 (+)	4.5 ± 0.3
	Te ¹²² (2.5)	2.7 ± 0.9	100d	1.0 ± 0.5		5 ± 1
	Te ¹²³ (0.88)	390 ± 30				
	Te ¹²⁴ (4.6)	6.5 ± 1.2	58d	5 ± 3		
	Te ¹²⁵ (7.0)	1.50 ± 0.15				
	Te ¹²⁶ (18.7)	0.8 ± 0.2	90d	70 ± 20 mb		
			9.3h	0.8 ± 0.2		
	Te ¹²⁸ (31.8)	0.3 ± 0.3	32d	15 ± 5 mb		
			72m	0.13 ± 0.03		
	Te ¹³⁰ (34.4)	0.5 ± 0.3	30h	<8 mb		
			25m	0.22 ± 0.05		
⁵³ I	I ¹²⁷ (100)	6.7 ± 0.6	27m	6.3 ± 1.3	3.4 ± 0.2 (+)	3.8 ± 0.4
	I ¹²⁹ (3 × 10 ⁷ y)		12.5h	11 ± 4		3.6 ± 0.5
	I ¹³¹ (8d)		2.4h	600 ± 300		
⁵⁴ Xe		.35 ± 5				
	Xe ¹²⁴ (0.096)					4.3 ± 0.4
	Xe ¹²⁸ (0.090)					
	Xe ¹²⁹ (1.92)	<5				
	Xe ¹³⁰ (26.4)	45 ± 15				
	Xe ¹³¹ (4.08)	<5				
	Xe ¹³² (21.2)	120 ± 15				
	Xe ¹³⁴ (26.91)	<5	5.3d	0.2 ± 0.1		
	Xe ¹³⁶ (10.4)	<5	9.2h	0.2 ± 0.1		
	Xe ¹³⁸ (9.2h)	3.5 × 10 ⁶ †				
	Xe ¹³⁶ (8.93)	<5	3.9m	0.15 ± 0.08		

Table 1.2.17—(Continued)

Element	Isotope (%)	Reaction Cross Sections† (2200 m/sec)‡		Scattering Cross Sections§			
		σ_{abs}	σ_{act}	$\sigma_{\text{coh}}(\text{sign})$	$\sigma_{\text{fa}}\left(\frac{A+1}{A}\right)^2$	$\bar{\sigma}_s$	
⁵⁵ Cs	Cs ¹³³ (100)	29.0 ± 1.5	3h	16 ± 4 mb	3.0 ± 0.2 (+)	7 ± 1	20 ± 5
			2.3y	26 ± 5			
			(~100% 3h → 2.3y)				
	Cs ¹³⁵ (2 × 10 ⁶ y)	13.7d	15 ± 8				
	Cs ¹³⁷ (37y)		33m	<2			
⁵⁶ Ba		1.17 ± 0.10			3.5 ± 0.3 (+)	5 ± 1	8 ± 1
	Ba ¹³⁰ (0.101)		12.0d	30 ± 10 mb			
	Ba ¹³² (0.097)		>20y	6 ± 3			
	Ba ¹³⁴ (2.42)	2 ± 2					
	Ba ¹³⁵ (6.6)	5.6 ± 0.9					
	Ba ¹³⁶ (7.8)	0.4 ± 0.4					
	Ba ¹³⁷ (11.3)	4.9 ± 0.4					
	Ba ¹³⁸ (71.7)	0.68 ± 0.10	86m	0.5 ± 0.1			
	Ba ¹³⁹ (85m)		12.8h	4 ± 1			
	⁵⁷ La		8.9 ± 0.3			8.7 ± 0.5 (+)	9.3 ± 0.8
La ¹³⁸ (0.089)							
La ¹³⁹ (99.9)			40h	8.4 ± 1.7			
La ¹⁴⁰ (40h)			3.6h	3 ± 2			
⁵⁸ Ce		0.70 ± 0.08			2.7 ± 0.3 (+)	4 ± 1	9 ± 6
	Ce ¹³⁶ (0.19)	25 ± 25					
	Ce ¹³⁸ (0.26)	9 ± 6	140d	<0.4			
	Ce ¹⁴⁰ (88.4)	0.63 ± 0.06	28d	0.3 ± 0.1	2.8 ± 0.2 (+)	2.8 ± 0.5	
	Ce ¹⁴² (11.08)	1.8 ± 0.3	33h	1.0 ± 0.2	2.6 ± 0.3 (+)	2.6 ± 0.5	
⁵⁹ Pr	Pr ¹⁴¹ (100)	11.2 ± 0.6	19h	11 ± 3	2.4 ± 0.3 (+)	4 ± 1	
⁶⁰ Nd		44 ± 2			6.5 ± 0.4 (+)	15 ± 5	25 ± 5
	Nd ¹⁴² (27.1)	18.5 ± 2			7.5 ± 0.6 (+)		
	Nd ¹⁴³ (12.2)	290 ± 30					
	Nd ¹⁴⁴ (23.9)	4.8 ± 0.5			1.0 ± 0.2 (+)		
	Nd ¹⁴⁵ (8.3)	52 ± 4					
	Nd ¹⁴⁶ (17.2)	9.8 ± 0.8	11d	1.8 ± 0.6	9.5 ± 0.5 (+)		
	Nd ¹⁴⁸ (5.7)	3.3 ± 1.0	1.7h	3.7 ± 1.2			
	Nd ¹⁵⁰ (5.6)	2.9 ± 1.5					
	⁶¹ Pm	Pm ¹⁴⁷ (4y)		5.3d	60 ± 20		
⁶² Sm		6500 ± 1000 (not 1/v, × 1.5)					
	Sm ¹⁴⁴ (3.1)		60d	<0.25			
	Sm ¹⁴⁷ (15.0)						
	Sm ¹⁴⁸ (11.2)						
	Sm ¹⁴⁹ (13.8)	50,000 ± 20,000 †					
	Sm ¹⁵⁰ (7.4)						
	Sm ¹⁵¹ (122y)	7,000 ± 2,000 †					
	Sm ¹⁵² (26.7)		47h	150 ± 40	2.5 ± 1.0 (—)		
	Sm ¹⁵⁴ (22.5)		25m	5.5 ± 1.1			

Table 1.2.17—(Continued)

Element	Isotope (%)	Reaction Cross Sections† (2200 m/sec)‡		Scattering Cross Sections§		
		σ_{abs}	σ_{act}	$\sigma_{\text{coh}}(\text{sign})$	$\sigma_{\text{fa}}\left(\frac{A+1}{A}\right)^2$	$\bar{\sigma}_s$
${}_{63}\text{Eu}$		4500 ± 500 (not 1/v, × 0.95)				
	Eu ¹⁵¹ (47.8)	9000 ± 3000‡	9.2h		1400 ± 300‡	
	Eu ¹⁵² (5.3y)	5500 ± 1500‡				
	Eu ¹⁵³ (52.2)	420 ± 100‡				
	Eu ¹⁵⁴ (5.4y)	1500 ± 400‡				
	Eu ¹⁵⁶ (1.7y)	14,000 ± 4000‡				
${}_{64}\text{Gd}$		44,000 ± 2000 (not 1/v, × 0.85)				
	Gd ¹⁵² (0.20)		225d		<125	
	Gd ¹⁵⁴ (2.15)					
	Gd ¹⁵⁵ (14.8)	70,000 ± 20,000‡				
	Gd ¹⁵⁶ (20.6)					
	Gd ¹⁵⁷ (15.7)	160,000 ± 60,000‡				
	Gd ¹⁵⁸ (24.8)		18h		4 ± 2	
	Gd ¹⁶⁰ (21.8)		3.6m		1.5 ± 0.5	
${}_{65}\text{Tb}$	Tb ¹⁵⁹ (100)	44 ± 4	73d		>22	
${}_{66}\text{Dy}$		1100 ± 150				
	Dy ¹⁵⁴ (0.052)					
	Dy ¹⁵⁶ (0.090)					
	Dy ¹⁵⁸ (2.29)					
	Dy ¹⁶¹ (18.9)					
	Dy ¹⁶² (25.5)					
	Dy ¹⁶³ (25.0)					
	Dy ¹⁶⁴ (28.2)		1.3m		2600 ± 300‡	
			2.4h		<1000‡	
			(1.3m → 2.4h)			
${}_{67}\text{Ho}$	Ho ¹⁶⁵ (100)	64 ± 3	27h		60 ± 12	
${}_{68}\text{Er}$		166 ± 16				
	Er ¹⁶² (0.136)					
	Er ¹⁶⁴ (1.56)					
	Er ¹⁶⁶ (33.4)					
	Er ¹⁶⁷ (22.9)					
	Er ¹⁶⁸ (27.1)					
	Er ¹⁷⁰ (14.9)		7h		>7	
${}_{69}\text{Tm}$	Tm ¹⁶⁹ (100)	118 ± 6	129d		130 ± 30	
${}_{70}\text{Yb}$		36 ± 4				12 ± 5
	Yb ¹⁶⁸ (0.140)		33d		11,000 ± 3000‡	
	Yb ¹⁷⁰ (3.03)					
	Yb ¹⁷¹ (14.3)					
	Yb ¹⁷² (21.8)					
	Yb ¹⁷³ (16.1)					
	Yb ¹⁷⁴ (31.8)		4d		60 ± 40	
	Yb ¹⁷⁶ (12.7)		1.8h		7 ± 2	

Table 1.2.17 — (Continued)

Element	Isotope (%)	Reaction Cross Sections† (2200 m/sec)‡		Scattering Cross Sections§		
		σ_{abs}	σ_{act}	$\sigma_{\text{coh}}(\text{sign})$	$\sigma_{\text{la}}\left(\frac{A+1}{A}\right)^2$	$\bar{\sigma}_s$
$_{71}\text{Lu}$		108 ± 5				
	Lu ¹⁷⁵ (97.4)		3.7h 25 ± 10			
	Lu ¹⁷⁶ (2.60)		6.7d 4000 ± 800			
$_{72}\text{Hf}$		115 ± 15			8 ± 1	
	Hf ¹⁷⁴ (0.18)	1500 ± 1000				
	Hf ¹⁷⁶ (5.2)	15 ± 15				
	Hf ¹⁷⁷ (18.4)	380 ± 30				
	Hf ¹⁷⁸ (27.1)	75 ± 10				
	Hf ¹⁷⁹ (13.8)	65 ± 15				
	Hf ¹⁸⁰ (35.4)	13 ± 5	46d 10 ± 3			
$_{73}\text{Ta}$	Ta ¹⁸¹ (100)	21.3 ± 1.0	16.4m 30 ± 10 mb 122d 21 ± 7 (~100% 16.4m → 122d)	6.1 ± 0.4 (+)	6 ± 1	5 ± 1
$_{74}\text{W}$		19.2 ± 1.0		2.74 ± 0.05 (+)	5.7 ± 0.6	5 ± 1
	W ¹⁸⁰ (0.14)	60 ± 60	120d 10 ± 10			
	W ¹⁸² (26.4)	19 ± 2				
	W ¹⁸³ (14.4)	11 ± 1				
	W ¹⁸⁴ (30.6)	2.0 ± 0.3	77d 2.1 ± 0.6			
	W ¹⁸⁶ (28.4)	34 ± 3	25h 40 ± 10			
	W ¹⁸⁷ (25h)		65d 90 ± 40			
$_{75}\text{Re}$		84 ± 4				14 ± 4
	Re ¹⁸⁵ (37.1)	100 ± 8	90h 100 ± 20			
	Re ¹⁸⁷ (62.9)	63 ± 5	18h 75 ± 15			
$_{76}\text{Os}$		14.7 ± 0.7			15 ± 2	11 ± 1
	Os ¹⁸⁴ (0.018)		97d <200			
	Os ¹⁸⁶ (1.58)					
	Os ¹⁸⁷ (1.64)					
	Os ¹⁸⁸ (13.3)					
	Os ¹⁸⁹ (16.1)					
	Os ¹⁹⁰ (26.4)		15d 8 ± 3			
	Os ¹⁹² (41.0)		32h 1.6 ± 0.4			
	Os ¹⁹³ (32h)		700d 60 ± 20			
$_{77}\text{Ir}$		440 ± 20				
	Ir ¹⁹¹ (38.5)		1.4m 260 ± 100 70d 700 ± 200 (1.4m → 70d)			
	Ir ¹⁹³ (61.5)		19h 130 ± 30			
$_{78}\text{Pt}$		8.1 ± 0.4		11.2 ± 0.7 (+)	12 ± 1	10 ± 1
	Pt ¹⁹⁰ (0.012)					
	Pt ¹⁹² (0.78)		4.3d 90 ± 40			
	Pt ¹⁹⁴ (32.8)					
	Pt ¹⁹⁵ (33.7)					
	Pt ¹⁹⁶ (25.4)		18h 1.1 ± 0.3 (ground state) 82d 50 ± 20 mb			

Table 1.2.17 — (Continued)

Element	Isotope (%)	Reaction Cross Sections† (2200 m/sec)‡		Scattering Cross Sections§		
		σ_{abs}	σ_{act}	$\sigma_{\text{coh}}(\text{sign})$	$\sigma_{\text{fa}} \left(\frac{A+1}{A} \right)^2$	$\bar{\sigma}_s$
⁷⁹ Au	Pt ¹⁹⁸ (7.2)		31m	3.9 ± 0.8		
	Au ¹⁹⁷ (100)	94 ± 1	2.7d	96 ± 10	7.3 ± 0.1 (+)	9.3 ± 1.0
	Au ¹⁹⁸ (2.7d)		3.3d	16,000 ± 8,000 †		
⁸⁰ Hg		380 ± 20 (not 1/v, × 0.95)		22 ± 2 (+)		10 ± 5
	Hg ¹⁸⁶ (0.151)	3100 ± 1000 †				
	Hg ¹⁸⁸ (10.0)					
	Hg ¹⁸⁹ (16.9)	2500 ± 800 †				
	Hg ²⁰⁰ (23.1)	<60				
	Hg ²⁰¹ (13.2)	<60				
	Hg ²⁰² (29.8)		44d	3.0 ± 0.8		
	Hg ²⁰⁴ (6.8)		5.5m	0.43 ± 0.10		
⁸¹ Tl		3.3 ± 0.5		10 ± 2 (+)	10.0 ± 0.5	14 ± 2
	Tl ²⁰³ (29.5)	11.0 ± 0.9	2.7y	8 ± 3		
	Tl ²⁰⁵ (70.5)	0.77 ± 0.08	4.2m	0.10 ± 0.03		
⁸² Pb		0.17 ± 0.01		11.5 ± 0.7 (+)	11.1 ± 0.2	11 ± 1
	Pb ²⁰⁴ (1.5)	0.8 ± 0.6				
	Pb ²⁰⁶ (23.6)	26 ± 5 mb				
	Pb ²⁰⁷ (22.6)	0.69 ± 0.05				
	Pb ²⁰⁸ (52.3)	<30 mb	3.3h	0.6 ± 0.2 mb		
⁸³ Bi	Bi ²⁰⁹ (100)	32 ± 3 mb	5d	17 ± 3 mb	9.4 ± 0.1 (+)	9.4 ± 0.1
⁸⁸ Ra	Ra ²²³ (11.2d)			<100		
	Ra ²²⁶ (1620y)			15 ± 3	0.1 mb	
	Ra ²²⁸ (6.7y)		<10m	36 ± 5	<2	
⁸⁹ Ac	Ac ²²⁷ (18.6y)	500 ± 35		<2		
⁹⁰ Th	Th ²²⁷ (18.6d)			1500 ± 1000		
	Th ²²⁸ (1.90y)			<0.3		
	Th ²²⁹ (8 × 10 ³ y)			45 ± 11		
	Th ²³⁰ (8.0 × 10 ⁴ y)		25.5h	45 ± 10	<1 mb	
	Th ²³¹ (100)	7.0 ± 0.4	23.5m	7.7 ± 0.4	<0.2 mb	12.5 ± 0.2
	(1.39 × 10 ¹⁰ y)					13 ± 2
	Th ²³² (23.5m)		24.1d	1400 ± 200		
	Th ²³⁴ (24.1d)		<10m	1.8 ± 0.5	<0.01	
⁹¹ Pa	Pa ²³⁰ (17.3d)			1500 ± 250		
	Pa ²³¹ (3.4 × 10 ⁴ y)		1.3d	260 ± 50	10 ± 5 mb	
	Pa ²³² (1.3d)			700 ± 150		
	Pa ²³³ (27.4d)		1.2m	37 ± 14	<0.1	
			+ 6.7h			
	Pa ²³⁴ (UX ₂) (1.2m)			<500		
⁹² U	(UZ) (6.7h)			<5000		
				3.92**		$\sigma_t - \sigma_{\text{abs}} = 8.2^{**}$ at 2200 m/s
	U ²³⁸ (20.8d)			25 ± 10		
	U ²³⁵ (4.2d)			250 ± 100		

Table 1.2.17 — (Continued)

Element	Isotope (% $T_{1/2}$)	Reaction Cross Sections† (2200 m/sec)‡			Scattering Cross Sections§	
		σ_{abs}	σ_{act}	σ_{fission}	$\sigma_{\text{fa}} \left(\frac{A+1}{A} \right)^2$	$\bar{\sigma}_s$
$_{92}\text{U}$ (Cont'd.)	U^{232} (70y)			80 ± 20		
	U^{234} (0.0057) (2.5×10^5 y)	89 ± 7	8.8×10^5 72 ± 10	<0.65		
	U^{235} (0.714) (8.8×10^4 y)	650^{**}	2.5×10^7 101^{**}	549^{**}		
	U^{238} (99.3) (4.50×10^9 y)	2.80^{**}		$\nu = 2.5 \pm 0.1^{**}$		
	U^{239} (23.5m)		14h 22 ± 5			
	U^{240} (14.5h)					
$_{93}\text{Np}$	Np^{234} (4.4d)			900 ± 300		
	Np^{236} (22h)			10^4		
	Np^{237} (2.5×10^6 y)		2.1d 150 ± 15	19 ± 3 mb		
	Np^{238} (2.1d)			1600 ± 100		
	Np^{239} (2.3d)			3		
$_{94}\text{Pu}$	Pu^{238} (89.6y)		2.4×10^4 425 ± 75	18 ± 2		
	Pu^{239} (2.4×10^4 y)		6.6×10^3 $361^{\dagger\dagger}$	$664^{\dagger\dagger}$		
				$\nu = 3.0 \pm 0.1^{\dagger\dagger}$		
				neutrons per fission		
	Pu^{241} (~ 12 y)		$\sim 5 \times 10^4$ 400 ± 50	1080 ± 100		
$_{95}\text{Am}$	Pu^{242} ($\sim 5 \times 10^6$ y)		5h 40 ± 20			
	Am^{241} (47.5y)		16h 700 ± 200	3.2 ± 0.2		
			500y <50			
			(20% 16h — 500y)			
	$\text{Am}^{242\text{m}}$ (16h)			2000 ± 1000		
$_{96}\text{Cm}$	Am^{242} (500y)	8000 ± 1000		3500 ± 1000		
	Am^{243} ($\sim 10^4$ y)		~ 25 m 50 ± 25	<25		
	Cm^{240} (27d)			$20,000 \pm 10,000$		
	Cm^{242} (162.5d)			<5		

*This table contains the "best values" of several types of slow-neutron cross sections based on a careful consideration of all available data. Most of the cross sections have been measured several times, sometimes by different methods, and the error quoted in the table (standard error) is estimated from the consistency of the results as well as from the errors quoted for the individual measurements. The types of cross sections in the table correspond closely to methods of measurements, and the cross sections themselves are the actual measured, rather than derived quantities, as far as possible. All values given for an element refer to the natural mixtures of isotopes (that is, they are atomic cross sections), while those given for specific isotopes are isotopic cross sections. All cross sections, unless marked "mb" (millibarns), are in barns. The cross sections in this table are unclassified; those given for elements of atomic number 88 and above, and for Xe^{135} , have been declassified.

†The "reaction cross sections" refer to all cases in which the neutron is not re-emitted, that is, to (n, γ), (n,p), and (n, α) reactions. Practically all the reaction cross sections are for (n, γ)'s, and the few that are not are so marked. The absorption cross sections, σ_{abs} , are those particular reaction cross sections that are measured by observing the reaction itself in which the neutron is absorbed. The principal method used is the reactor oscillator, which measures the effect on the reactivity of a reactor caused by the absorption of the neutron. Reactor oscillator results from Argonne, Oak Ridge, and Harwell are represented in the table. In some cases, (n,p) and (n, α) reactions have been measured in cloud chambers and counters, while other absorption cross sections have been estimated from the changes in isotopic abundances after long reactor irradiations. In several instances, the principal case being boron, the absorption cross section has been obtained from the total cross section by sub-

traction of scattering. The activation cross sections, σ_{act} , are those determined from the radioactivity of the product nucleus, usually the result of an (n,γ) reaction, and in a few cases, which are specially marked, by (n,p) or (n,α) reactions. The activation cross sections always refer to particular isotopes and hence are isotopic cross sections; for monoisotopic elements, they are atomic cross sections as well. The absorption cross section, if measured for a single isotope or monoisotopic element, should agree with the activation cross section if the latter includes all activities produced. The activation cross sections for isomeric states are sometimes difficult to measure, and the results may be difficult to explain in tables. In this table, the upper (metastable) state is listed above the ground state (where the order is known), and the cross sections refer to the direct formation of each state. In those cases for which the amount of an isomeric activity would be increased indirectly by decay of another (shorter-lived) state, the percentage of the parent state that augments the activity is given. An example is cobalt for which there is a 20-b cross section for direct formation of the 5-yr activity and a 14-b cross section for the 11-min activity, practically all of which decays into its 5-yr daughter

‡ The reaction cross sections listed are those for a neutron velocity of 2200 m/sec even though the actual measurements were usually made with neutrons of wide energy spread. It should be remembered that thermal flux (nv) values are always stated for a velocity of 2200 m/sec (even though the neutrons may be above room temperature); hence, the cross section at this velocity must be used in calculations of reaction rate. In some cases, such as irradiation with well thermalized neutrons, it is quite simple to obtain the 2200-m/sec value from experimental results. In other cases, such as activation cross sections for reactor neutrons, it is difficult, and for still others, such as isotopic cross sections measured by the mass spectrometer, it is almost impossible. Each reaction cross section, unless marked "not $1/v$ " will have the same reaction rate in a Maxwell distribution as a $1/v$ absorber with the same 2200-m/sec cross section. In other words, the unmarked cross sections are either strictly $1/v$ in the thermal region or indistinguishable from $1/v$ within the accuracy quoted. The few marked "not $1/v$ " will have an effective 2200-m/sec cross section in a Maxwell distribution (at, or within about 100°C of, room temperature) obtained by multiplication of the 2200-m/sec value by the factor shown. This effective cross section when used with a thermal nv will give the correct reaction rate in a Maxwell distribution. For a few cases in which the 2200-m/sec value could not be determined, the cross sections are still included but are marked "reactor neutrons"

§ The scattering cross sections are usually constant with energy in the thermal region, except for crystal effects, and are hence not quoted for 2200 m/sec. The coherent cross section, σ_{coh} , is listed with the sign of the amplitude, where the positive sign corresponds to hard sphere scattering. The coherent scattering is that part of the total "bound-atom cross section" which contributes to such interference effects as Bragg scattering and mirror reflection. The "bound-atom cross section" is the cross section that would be observed if the atoms were completely bound (hence no thermal diffuse scattering) and yet scattered completely independently. Such a cross section, of course, is not observable experimentally but is calculated by applying the reduced mass correction, $(A + 1/A)^2$, to the free-atom cross section, σ_{fa} , which is the scattering cross section measured in the energy region (usually 10-20 ev) where the atom can be considered as a "free atom." No free-atom values are listed when the presence of resonances near thermal prevents the calculation of the bound-atom cross section. If there are no sources of incoherent scattering, such as spin dependent, isotopic, or inelastic incoherent scattering, then the measured value of σ_{coh} should be equal to $\sigma_{fa} (A + 1/A)^2$, as it is for Be as an example, compared to H in which σ_{coh} is much less than the bound-atom cross section. Sometimes the only scattering cross section that has been measured for a particular element is that averaged over the Maxwell distribution. This average scattering cross section $\bar{\sigma}_s$, will depend on the crystalline form of the sample and even upon the size of the crystal grains, but it is listed because of utility in certain practical applications

It is the purpose of the compilation to list only the actual directly measured quantities, even though it is possible in some cases to infer certain cross sections from other measurements. For instance, the calculated bound-atom cross section, which is sometimes known quite accurately, could be listed as the coherent cross section if it is assumed that there are no sources of incoherent scattering. However, only the measured value of the coherent scattering (a measurement of σ_{coh} itself, or both σ_{fa} and the incoherent cross section) is given in the column for σ_{coh} even though in some cases the value inferred from the bound-atom cross section has smaller error. An example is fluorine, where the bound-atom value is more accurate than σ_{coh} and an assumption of negligible incoherent scattering would seem justified. Nevertheless, only the measured coherent cross section is listed in the σ_{coh} column. Again, for the activation cross sections, it could be inferred that the more accurate absorption value, measured with the reactor oscillator, is correct to list for activation as well, if it is certain that only one activity is produced. Here, an example is Al^{27} where the activation agrees with the absorption but is not as accurate. The principle of listing only the directly measured quantities in the appropriate columns is again followed in this case. Some judgment is thus necessary in using the table, especially in those cases where values of different types of cross sections, which presumably should agree, do not. For instance, it would be safe to use the more accurate absorption value, 0.19 ± 0.03 b, for the production of 14.3-day P^{32} , even though the directly measured activation cross section is 0.23 ± 0.05 b. On the other hand, the cross section for production of 87-day S^{35} by the $Cl^{35}(n,p)$ reaction has been measured as 0.30 ± 0.10 b by direct observation of the reaction (in a

cloud chamber) and as 0.17 ± 0.04 b by activation. In this case, it is certainly not clear that one value is right and the other wrong, hence a weighted average probably should be used. The preparation of the cross section compilation has brought to light a number of such disagreements, and work has already begun to improve the measurements in these cases

† Reactor neutrons

** AEC Release April 7, 1952

‡ AEC Release April 7, 1952; cross sections for an approximately Maxwellian neutron spectrum with a most probable neutron velocity of 2200 m/sec

REFERENCES

1. Feshbach and Weisskopf, Phys. Rev., 76, p 1550, 1949.
2. B. T. Feld, H. Feshbach, M. L. Goldberger, H. Goldstein, and V. F. Weisskopf, Final Report of the Fast Neutron Data Project, AEC Report NYO-636.
3. Bethe, Elementary Nuclear Theory, p 6. From data on α -decay.
4. M. G. Mayer, Phys. Rev., 74, p 235, 1948.
5. K. Way, Phys. Rev., 75, p 1448, 1949.
6. R. F. Van Wye and J. S. Beckerley, Nucleonics, 9, p 17, Oct. 1951.
7. Robinson, Jour. Chem. Phys., 17, p 542, 1949.
8. Rev. Mod. Phys., 15, p 209, 1950.
9. Periman, Ghiorso, and Seaborg, Phys. Rev., 77, p 26, 1950.
10. Weisskopf and Blatt, Theoretical Nuclear Physics, John Wiley and Sons, Inc., New York, 1952.
11. Katz and Penfold, Rev. Mod. Phys., 24, p 1, 1952.
12. H. Bethe, BNL-T-7.
13. W. A. Aroux, B. G. Hoffman, and F. C. Williams, AECU-663.
14. Private Communication from M. Nelkin.
15. D. C. Brunton and G. C. Hanna, Can. Jour. Res., A28, p 190, 1950.
16. M. Deutsch and M. Ramsey, MDDC-945, 1945.
17. B. Finkle, E. Hoagland, S. Katcoff, and N. Sugarman, Report CC-2076, 1944; reproduced in Reference (18).
18. C. D. Coryell and N. Sugarman, Radiochemical Studies: The Fission Products, McGraw-Hill Book Co., Inc., New York, 1951.
19. Neutron Cross Sections, AECU-2040, May 15, 1952, and Supplement, Nov. 20, 1952.
20. BNL-170, May 15, 1952 (classified).
21. S. Untermeyer and J. T. Weills, Heat Generation in Irradiated Uranium, ANL-4790, Feb. 25, 1952.
22. KAPL-377 (classified) and KAPL-394 (classified).
23. KAPL-183 (classified).
24. K. Way and E. P. Wigner, Phys. Rev., 73, p 1318, 1948.
25. Hornyak et al, Rev. Mod. Phys., 22, p 291, 1950.
26. Ergebnisse der Exakten Wissenschaften, vol. 25, Julius Springer, Berlin, 1951.
27. D. Jackson, Nat. Res. Council of Canada, Rep. No. 2610.
28. Rev. Mod. Phys., 19, p 199, 1950.
29. Arnold, Jumez, Schafer, Swickard, and Zabel, LA-1339.
30. D. J. Hughes, Reactor Neutron Physics, Addison-Wesley Press, Inc., Cambridge (to be published).
31. Fermi, Strum, and Sachs, Phys. Rev., 71, p 589, 1947.
32. M. Lax, Rev. Mod. Phys., 23, p 287, 1951.
33. R. J. Finklestein, Phys. Rev., 72, p 907, 1947.
34. E. Meklonian, Phys. Rev., 76, p 1750, 1949.
35. D. D. Philips and R. W. Davis, AEC Report LA-740, 1949.
36. L. E. Beghiam, M. A. Grace, G. Preston, and H. Halban, Phys. Rev., 77, p 286L, 1950.
37. Byster and Carter, private communication from Los Alamos.
38. H. H. Barschall, M. E. Battat, W. C. Bright, E. R. Graves, T. Jorgensen, and J. H. Manley, Phys. Rev., 72, p 881, 1947.
39. L. Szilard, S. Bernstein, B. T. Feld, and J. Ashkin, Phys. Rev., 73, p 1307, 1948.
40. H. F. Dunlap and R. N. Little, Phys. Rev., 60, p 693, 1941.
41. Philips, LA-1142 (classified).
42. Deleted.
43. P. H. Stelson and W. M. Preston, Phys. Rev., 86, p 132, 1952.
44. C. E. Mandeville, C. P. Swann, and F. J. Seymour, Phys. Rev., 86, p 861, 1952.
45. Phys. Rev., 87, p 366, 1952.
46. Fowler and Slye, Phys. Rev., 77, p 787, 1950.
47. Martin and Diven, Phys. Rev., 86, p 565, 1952.
48. Forbes, AECU-1883.
49. Graves, LAMS-1300 (classified).
50. A. H. Snell, LA-1371.
51. Cohen, Phys. Rev., 81, p 184, 1951 and Nucleonics, 8, p 29, Feb. 1951.
52. D. J. Hughes, CF-3490, 1946 (classified).
53. Goldstein et al, CP-3574, 1946 (classified).
54. Charpie, Sun, and Jennings, Phys. Rev., 76, p 1255, 1949.

SELECTED READING LIST

NEUTRON CROSS SECTIONS, T. W. Bonner, H. Goldstein, W. W. Havens, Jr., D. J. Hughes, L. Kaplan, C. O. Muehlhause, A. H. Snell, J. R. Stehn, T. M. Snyder, R. F. Taschek, A. Wattenberg, C. W. Zobel; BNL-170 (classified) and AECU-2040.

NUCLEAR DATA, K. Way et al., National Bureau of Standards publication 499 and supplements.

FINAL REPORT OF THE FAST NEUTRON DATA PROJECT, B. T. Feld, H. Feshbach, M. L. Goldberger, H. Goldstein, V. F. Weisskopf; AEC Report NYO-636.

RADIOCHEMICAL STUDIES: THE FISSION PRODUCTS, C. D. Coryell and N. Sugarman.

K. Way, Mon-P-192 (classified).

THEORETICAL NUCLEAR PHYSICS, J. M. Blatt and V. F. Weisskopf, to be published, John Wiley and Sons, Inc., New York (1952).

INTRODUCTORY NUCLEAR PHYSICS, D. Halliday, John Wiley and Sons, Inc., New York (1950).

EXPERIMENTAL NUCLEAR PHYSICS, E. Segré et al, John Wiley and Sons, Inc., New York (to be published).

CHAPTER 1.3

Kinetic Theory of Neutrons

H. Soodak, F. Adler, and E. Greuling

The fundamental relation of neutron kinetics is the continuity equation which expresses the law of neutron conservation in the volume element, $d\mathbf{r} d\mathbf{v}$, of phase space, viz.:

Time rate of increase of neutron density = Production – Absorption – leakage

Thus, in the steady state, the Boltzmann equation is:

$$0 = S(\mathbf{r}, \mathbf{v}) + \Lambda(\mathbf{r}, \mathbf{v}, \mathbf{v}') v' n(\mathbf{r}, \mathbf{v}') - v \sigma n(\mathbf{r}, \mathbf{v}) - \text{div } \mathbf{v} n(\mathbf{r}, \mathbf{v}) \quad (1a)$$

where $n(\mathbf{r}, \mathbf{v})$ is the density of neutrons in phase space, and S is the total source, being the sum:

$$S(\mathbf{r}, \mathbf{v}) = S^{\text{ext}}(\mathbf{r}, \mathbf{v}) + \nu \Gamma(\mathbf{r}, \mathbf{v}, \mathbf{v}') v' n(\mathbf{r}, \mathbf{v}') \quad (1b)$$

of the external source S^{ext} and the fission source. The integral operators Γ and Λ refer respectively to fission and to scattering-in. To treat the time-dependent case, it is necessary to replace the left side of Eq. (1a) by $\partial/\partial t n(\mathbf{r}, \mathbf{v}, t)$ and, if desired, to correct Γ to include the delay times of the delayed neutrons.

For slowing-down without space variation, the Boltzmann equation reduces to Eq. (2)* and is treated later in this chapter. The reduction in the case of one-velocity theory leads to Eq. (17) of this chapter. Even these highly idealized problems involve integral equations of considerable complexity.

General methods are considered which are useful in attacking integral and integro-differential equations. One consists of expanding the integrands into a Taylor series or into suitable eigenfunctions (e.g., the spherical harmonics method) and results in a system of ordinary or partial differential equations. Treating Eq. (17) by the spherical harmonics expansion (in the P_1 approximation), for example, leads to the equations of elementary diffusion theory.

A second method, useful in treating Eq. (17) when scattering is isotropic, proceeds by reformulating that equation into an integral equation.

In another approach, useful in treating Eq. (2), the exact kernel is approximated by a "synthetic kernel" which is chosen such that the integral equation reduces to a differential equation. Various slowing-down theories, for example the Fermi age theory, can be represented by such synthetic kernels.

In the discussion of space and energy variation in this chapter, simultaneous approximations of diffusion and slowing-down are generally required to yield manageable equa-

*This reduction is carried out by placing $\text{div } \mathbf{v} n = 0$ and integrating over the various directions of the velocity vector.

tions such as those of the Fermi age theory. These equations are further simplified by the group-diffusion approximation and are thus reduced to a convenient form for solution by computing machines. The diffusion of thermal neutrons also is treated.

The results contained in this chapter pertain to media consisting of homogeneous regions and also of simple geometries. Although mention is made of the variational technique, the major application of this technique as well as of perturbation and iteration methods is deferred until the discussion of reactors in Chapter 1.4.

Table 1.3.1 lists definitions and notations used in this chapter.

Table 1.3.1—Table of Symbols

σ	Macroscopic cross section	$S(E) dE$	Rate of production of neutrons in dE about E per unit volume
σ_c	Capture not leading to fission	$p(E)$	"Resonance" escape probability = $q(E)$ divided by the total source strength
σ_f	Fission	f	$(\nu\sigma_f - \sigma_a)/\sigma$; $1 + f$ is the multiplication in neutron number per collision
σ_a	$\sigma_c + \sigma_f$	k	Multiplication constant: the ratio of fission neutrons produced per neutron absorbed in infinite medium. (Also the Boltzmann constant)
σ_s	Total scattering	ν	Average number of neutrons emitted per fission
σ_i	Inelastic scattering	l	Mean free path = $1/\sigma$
σ_{tr}	Transport cross section	λ	Extrapolation length (also used for mean free path and for exponent in asymptotic solution in Tables 1.3.4 and 1.3.5)
σ_t	Total cross section = $\sigma_a + \sigma_s$	D	Diffusion coefficient; constant of proportionality between neutron current and gradient ϕ
σ		L	Diffusion length
n	Neutrons per unit volume	κ	Reciprocal asymptotic attenuation distance (used as $1/L$ or in dimensionless units as $1/L\sigma$)
nv	Flux or track length per unit volume per unit time	μ	Cosine of angle between neutron velocity and the z axis; $\sigma_a/\xi(\sigma_a + \sigma_s)$ is denoted by μ in Table 1.3.6
ϕ		μ_0	Cosine of the scattering angle in the laboratory system
F_0	Directional flux	$\underline{\Omega}$	Unit vector in direction of neutron velocity
F		P_l	Legendre polynomial of degree l .
J	Current density = $\underline{\Omega} F$	K_0	Bessel functions defined as in "British Association Mathematical Tables" Vol. VI, Part I
ψ	Collision density = $\sigma_t \phi$	I_0	Used as angular frequency and as Fourier transform variable
ψ_u		ω	
\underline{v}	Neutron velocity		
$\underline{\Omega v}$			
u	$\ln E_0/E$, where E_0 is a constant energy		
τ	Fermi age variable		
q	Slowing-down density: $q(\underline{r}, E)$ is the rate per unit volume at which neutrons slow down to below energy E		
$g(E, E') dE$	Slowing-down kernel: probability of neutrons scattered at E' to land in dE about E		
$G(E, E')$	Probability of neutrons scattered at E' to land below E		
ξ	Average loss in logarithm of energy per scattering		
α	Minimum value of E/E' where E is the energy after a scattering at E		
ϵ	$\frac{1}{2\xi^2}$ times the average square of the loss in logarithm of energy per scattering		

SLOWING-DOWN WITH NO SPACE VARIATION

(Harry Soodak)

BASIC EQUATIONS

Consider the problem of slowing-down in an infinite homogeneous medium of uniform composition in the presence of a uniform source $S(E)$.* The neutron balance equation is:†

$$\psi(E) = \int_E^\infty \frac{\sigma_s(E')}{\sigma(E')} g(E, E') \psi(E') dE' + S(E) \quad (2)$$

The slowing-down density, q , is defined by:

$$q(E) = \int_E^\infty \frac{\sigma_s(E')}{\sigma(E')} G(E, E') \psi(E') dE' \quad (3)$$

where the integrated kernel, G , is:

$$G(E, E') = \int_0^E g(E'', E') dE'' \quad (4)$$

with $G(E, E) = 1$. It follows that:

$$\frac{dq(E)}{dE} = \frac{\sigma_a}{\sigma} \psi(E) - S(E) \quad (5)$$

which is a neutron balance equation equivalent to Eq. (2). If the cross sections σ_s , σ and kernel g are given, then Eq. (2) is subject to numerical analysis to obtain $\psi(E)$ for any source function $S(E)$. The slowing-down density is then obtainable by numerical integration of Eqs. (5) or (3).

The "resonance" escape probability, $p(E)$, is defined by:

$$p(E) = \frac{q(E)}{\int_E^\infty S(E) dE} \quad (6)$$

and is primarily useful when E is below the lowest energy source neutrons.

ISOTROPIC ELASTIC SCATTERING

The kernels g and G are given in Table 1.3.2 for the case of elastic scattering which is isotropic in the center-of-mass system.

GENERAL SOLUTIONS

If hydrogen ($M = 1$) is the only slowing-down element, the integral equation (2) reduces to the differential equation:

$$\frac{d\psi(E)}{dE} + \frac{\sigma_s}{\sigma} \frac{\psi(E)}{E} - \frac{dS(E)}{dE} = 0 \quad (7)$$

* All text equations are written in terms of the unambiguous variable E . The equations in terms of the logarithmic energy variables u are easily obtainable from the text equations.

† These formulas are valid also for uniform composition media of variable density with a non-uniform source as long as there is no neutron loss by leakage, where ψ , q , and S are to be interpreted as being volume integrals.

Table 1.3.2 — Elastic Kernels in Terms of E and of $u = \ln(\text{constant}/E)$

Case	$g(E, E')$	$g(u, u')$	$G(E, E')$	$G(u, u')$
Hydrogen ($M = 1$)	$\frac{1}{E'} \text{ if } E \leq E'$ $0 \text{ if } E > E'$	$e^{-(u-u')} \text{ if } u \geq u'$ $0 \text{ if } u < u'$	$\frac{E}{E'} \text{ if } E \leq E'$ $1 \text{ if } E \geq E'$	$e^{-(u-u')} \text{ if } u \geq u'$ $1 \text{ if } u \leq u'$
Single element, arbitrary mass	$\frac{1}{1-\alpha} \frac{1}{E'} \text{ if } \alpha E' \leq E \leq E'$ 0 otherwise	$\frac{1}{1-\alpha} e^{-(u-u')} \text{ if } u' \leq u \leq u' + \ln 1/\alpha$ 0 otherwise	$\frac{E - \alpha E'}{(1-\alpha) E'} \text{ if } \alpha E' \leq E \leq E'$ $0 \text{ if } E \leq \alpha E'$ $1 \text{ if } E \geq E'$	$\frac{e^{-(u-u')}}{1-\alpha} \text{ if } u' \leq u \leq u' + \ln 1/\alpha$ $0 \text{ if } u \geq u' + \ln 1/\alpha$ $1 \text{ if } u \leq u'$
Mixtures of elements, arbitrary masses	$\frac{1}{\sigma_s} \sum_i \sigma_s^{(i)} g^{(i)}$ Where $g^{(i)}$ and $G^{(i)}$ are the single element kernels for the " i "th element		$\frac{1}{\sigma_s} \sum_i \sigma_s^{(i)} G^{(i)}$	
Fermi		$\xi \delta'(u - u') + \delta(u - u')$		$\xi \delta(u - u')$
Wigner		$\frac{1}{\xi} e^{-(u-u')/\xi} \text{ if } u \geq u'$ $0 \text{ if } u < u'$		$e^{-(u-u')/\xi} \text{ if } u \geq u'$ $1 \text{ if } u \leq u'$
Greuling-Goertzel (G. G.)		$\frac{1}{\epsilon^2 \xi} e^{-(u-u')/\epsilon \xi} + \left(1 - \frac{1}{\epsilon}\right) \delta(u - u') \left\{ \begin{array}{l} \text{if } u \geq u' \\ 0 \text{ if } u < u' \end{array} \right.$		$\frac{1}{\epsilon} e^{-(u-u')/\epsilon \xi} \text{ if } u > u'$ $1 \text{ if } u \leq u'$

which in conjunction with Eq. (5) leads to:

$$q(E) = E[\psi(E) - S(E)] \quad (8)$$

and:

$$\frac{dq(E)}{dE} - \frac{\sigma_a}{\sigma} \frac{q(E)}{E} + \frac{\sigma_s}{\sigma} S(E) = 0 \quad (9)$$

Solutions of these equations are presented in Table 1.3.3.*

Table 1.3.3 — Exact Hydrogen Solutions and Solutions for Synthetic Kernels

Case	Unit point source, $S(E) = \delta(E - E_0)$	Arbitrary source, $S(E)$
Hydrogen	$q(E) = \frac{\sigma_s(E_0)}{\sigma(E_0)} e^{-\int_{E_0}^E \frac{\sigma_a}{\sigma} \frac{dE}{E}}$	$q(E) = \int_E^\infty \frac{\sigma_s(E')}{\sigma(E')} S(E') e^{-\int_E^{E'} \frac{\sigma_a}{\sigma} \frac{dE}{E}} dE'$
Exact solution	$\psi(E) = \frac{q(E)}{E} + \delta(E - E_0)$	$\psi(E) = \frac{q(E)}{E} + S(E)$
Single element	$q(E) = \frac{\sigma_s(E_0)}{\bar{\sigma}(E_0)} e^{-\frac{1}{\xi} \int_{E_0}^E \frac{\sigma_a}{\sigma} \frac{dE}{E}}$	$q(E) = \int_E^\infty \frac{\sigma_s(E')}{\bar{\sigma}(E')} S(E') e^{-\frac{1}{\xi} \int_E^{E'} \frac{\sigma_a}{\sigma} \frac{dE}{E}} dE'$
Fermi, Wigner, G. G.	$\psi(E) = \frac{\sigma(E)}{\bar{\sigma}(E)} \left[\frac{q(E)}{\xi E} + \epsilon \delta(E - E_0) \right]$ $\bar{\sigma} = \sigma_s + \epsilon \sigma_a$	$\psi(E) = \frac{\sigma(E)}{\bar{\sigma}(E)} \left[\frac{q(E)}{\xi E} + \epsilon S(E) \right]$ $\bar{\sigma} = \sigma_s + \epsilon \sigma_a$

For heavier moderators ($M > 1$), the integral equation does not reduce because of the sharp cut-off in the kernel, g . The reduction to a differential equation can be made, however, if the kernel, g , is approximated by the synthetic kernels given in Table 1.3.2.

All three approximate kernels, g , are correctly normalized and give the correct value of the average logarithmic energy loss. The G.G. kernel gives also the correct value of the average of the square of the logarithmic energy loss. These statements are referred to below as "matching of moments."

These synthetic kernels all lead to:

$$q(E) = \xi E \left[\frac{\sigma_s + \epsilon \sigma_a}{\sigma} \psi(E) - \epsilon S(E) \right] \quad (10)$$

$$\frac{dq(E)}{dE} - \frac{\sigma_a}{\xi(\sigma_s + \epsilon \sigma_a)} \frac{q(E)}{E} + \frac{\sigma_s}{\sigma_s + \epsilon \sigma_a} S(E) = 0 \quad (11)$$

$$\frac{d}{dE} \left(E \frac{\sigma_s + \epsilon \sigma_a}{\sigma} \psi \right) - \frac{\sigma_a}{\xi(\sigma_s + \epsilon \sigma_a)} \frac{\left(E \frac{\sigma_s + \epsilon \sigma_a}{\sigma} \psi \right)}{E} + S \left(\frac{1}{\xi} - \epsilon \right) - \epsilon E \frac{dS}{dE} = 0 \quad (12)$$

*Placzek¹ gives an exact solution for the case of an element of arbitrary $M > 1$ with no capture. This definitive paper contains most of the results quoted in the discussion, "Isotropic Scattering."

¹References appear at end of chapter.

where ϵ is given by:

$$\epsilon (\text{Fermi}) = 0$$

$$\epsilon (\text{Wigner}) = 1$$

$$\epsilon (\text{G. G.}) = \frac{1 - \alpha [1 + \ln 1/\alpha + \frac{1}{2} \ln^2 1/\alpha]}{(1 - \alpha) \xi^2} \quad (13)$$

$$= 1 \text{ for hydrogen}$$

$$\approx 2/3 \text{ for } M \gg 1$$

Solutions of these equations are given in Table 1.3.3. It is to be noted that the Wigner and G. G. approximations are exact for hydrogen and that all three approximations are correct asymptotically in the case of no absorption.

MIXTURES

For mixtures, the simplest procedure is to approximate the correct kernel g by the moment matched synthetic kernels,* in order to reduce Eq. (2) to a differential equation. This procedure can be expected to give poor results in a mixture of elements of significantly different masses.† A method for handling a mixture of hydrogen and a heavy element in the presence of absorption has been suggested by Goertzel³ who treats the hydrogen kernel exactly and the heavy element kernel by the Fermi approximation and thus arrives at a pair of coupled differential equations. These equations have been treated by a perturbation method.⁴

ASYMPTOTIC SOLUTIONS

For energies below those of the source neutrons, Eq. (2) reduces to the homogeneous form ($S = 0$) for which exact solutions exist for several cases. Also, an approximate solution (by Hurwitz) exists (more accurate than the Fermi, Wigner, and G. G.) for the case of a single-element moderator with slowly varying σ_a/σ . These solutions are given in Table 1.3.4.

The magnitude of the asymptotic solutions is determined by the slowing-down density just below the energy of the lowest-energy-source neutrons. In many cases of interest, absorption is negligible at the source energies, and as a result, the slowing-down density at high energies can be taken as the total source-strength.

Table 1.3.6 presents a comparison of results obtained by the Fermi, Wigner, G. G. approximations with the correct asymptotic results for the case of constant σ_a/σ (for this case, the Hurwitz method is exact); Fig. 1.3.1 presents a comparison of Fermi, G. G., Hurwitz, and exact (numerical, from Eq. 2) results for a smoothly varying σ_a/σ ($\sigma_s = \text{const.}$, $\sigma_a = \text{const.}/v$).

FLUCTUATIONS NEAR SOURCE ENERGY

For monoenergetic source neutrons (energy E_0) in a single-element moderator ($M > 1$), the collision density undergoes damped oscillations in the first few collision intervals before approaching the asymptotic form.‡ A schematic diagram of $\psi(E)$ for the case of no

*Thus for the Fermi approximation, Eqs. (10) through (13) still hold where ξ is the average logarithmic energy loss for the mixture. For the G. G. approximation, see Edlund.²

†Note the behavior of a mixture of hydrogen and a heavy element in Table 1.3.4. These transition effects do not appear in the synthetic kernel approximation.

‡The paper by Placzek¹ contains most of the results in the discussion "Slowing Down with No Space Variation."

Table 1.3.4—Asymptotic Solutions (Exact and Approximate)
 (Normalized such that $q(E_0) = 1$ where E_0 is some high energy)

Case	$\psi(E)$	$q(E)$
No absorption; single element or non-hydrogenous mixture	$\frac{1}{\xi E}$	1
No absorption; hydrogen plus a single element of mass M: $c = \frac{\sigma_s(H)}{\sigma_s(H) + \sigma_s(M)}$ $\bar{\xi} = c + (1 - c) \xi$	$\frac{1}{\xi E} + \frac{r - 1}{\left(r - \frac{1 - c}{\frac{1}{\alpha} - 1}\right) (\ln 1/\alpha) - 1} \left(\frac{E}{E_0}\right)^r \frac{1}{E}$ <p>where r is defined by:</p> $\frac{r}{1 - c} = \frac{\left(\frac{1}{\alpha}\right)^r - 1}{\frac{1}{\alpha} - 1}$	1
If $1 - c \ll \xi$	$\approx \frac{1}{E}$	1
If $M \gg 1$ and $c \ll \xi$	$\approx \frac{1}{\xi E} \left\{ 1 + \frac{c}{\xi} \left[\left(\frac{E}{E_0}\right)^{1 + \frac{c}{\xi}} - 1 \right] \right\}$	1
If $M \gg 1$ and $c \gg \xi$	$\approx \frac{1}{E} + \left(\frac{1}{\xi} - \frac{1}{c}\right) \left(\frac{E}{E_0}\right)^{1 + \frac{c}{\xi}} \frac{1}{E}$	1
Single element or non-hydrogenous mixture: $\sigma_a/\sigma \ll 1$	$\approx \frac{1}{\xi E} e^{-\int_E^{E_0} \frac{\sigma_a}{\xi \sigma_s} \frac{dE}{E}}$	$\approx e^{-\int_E^{E_0} \frac{\sigma_a}{\xi \sigma_s} \frac{dE}{E}}$
$\sigma_a/\sigma = \text{constant}$, single element	$\lambda \frac{\sigma_a}{\sigma_s} \left(\frac{E}{E_0}\right)^\lambda \frac{1}{E}$ <p>where λ is defined by:</p> $\frac{\sigma_a}{\sigma} \frac{\left(\frac{1}{\alpha}\right)^{\lambda - 1} - 1}{(1 - \alpha)(\lambda - 1)} = 1$ <p>values of λ are given in Table 1.3.5</p>	$\left(\frac{E}{E_0}\right)^\lambda$
$\sigma_a/\sigma = \text{slowly varying}$, single element; Hurwitz' solution	$\frac{1}{\sqrt{\xi}} \frac{f(\lambda)}{\sqrt{df/d\lambda}} e^{-\int_E^{E_0} \lambda \frac{dE}{E}}$ <p>where λ is defined as above, and</p> $f(\lambda) = \frac{\left(\frac{1}{\alpha}\right)^{\lambda - 1} - 1}{(1 - \alpha)(\lambda - 1)}$	$\frac{1}{\sqrt{\xi}} \frac{f(\lambda) - 1}{\lambda \sqrt{df/d\lambda}} e^{-\int_E^{E_0} \lambda \frac{dE}{E}}$ <p>the normalization assumes that</p> $\sigma_a(E_0) \approx 0$

Table 1.3.4—(Continued)

Case	$\psi(E)$	$q(E)$
Single, narrow absorption resonance at energy E_r	$\frac{1}{\xi E}$ for $E > E_r$	1 for $E > E_r$
Non-hydrogen mixture; Wigner solution is exact for this case	$\frac{1}{\xi E} e^{-\frac{1}{\xi} \int_{\text{res}} \frac{\sigma_a}{\sigma} \frac{dE}{E}}$ for $E < E_r$	$e^{-\frac{1}{\xi} \int_{\text{res}} \frac{\sigma_a}{\sigma} \frac{dE}{E}}$ for $E < E_r$
$\sigma_a/\sigma_s = \text{const}/v$; hydrogen	$\frac{1}{E} \frac{1}{\left(1 + \frac{\sigma_a}{\sigma_s}\right)^2}$	
$\sigma_a/\sigma_s = \text{const}/v$; hydrogen single element of mass M	$\frac{1}{\xi E} e^{-\left\{\left(M + \frac{1}{3}\right) \frac{\sigma_a}{\sigma_s} - \frac{1}{3} M \left(\frac{\sigma_a}{\sigma_s}\right)^2\right\}}$ where terms in $\left(\frac{\sigma_a}{\sigma_s}\right)^2$ and $M \left(\frac{\sigma_a}{\sigma_s}\right)^3$ are neglected	

Table 1.3.5—The Exponent, λ , in the Asymptotic Solution for Constant σ_a/σ
(Weinberg and Noderer, CF-51-5-98, Vol. I)

M	σ_a/σ_s	λ^*
12	0.0005	0.003168
	.005	.031588
	.05	.306496
	.1	.593757
	.2	1.118817
50	.0005	0.012663
	.005	.126248
	.05	1.225912
100	.0005	0.025162
	.005	.250831

*For $\sigma_a/\sigma_s \ll 1$ and $\lambda \ln 1/\alpha \ll 1$

$$\text{then: } \lambda \approx \frac{\sigma_a}{\xi \sigma_s + \sigma_a} \left[1 + \frac{\sigma_a/\sigma_s}{\left(\frac{\sigma_a}{\sigma_s} + \xi\right)^2} \frac{(1-\xi)^2 (1-\alpha)}{2\alpha} \right]$$

which, for a heavy element, $1 - \alpha \ll 1$, reduces to:

$$\lambda \approx \frac{\sigma_a}{\xi \sigma_s + \sigma_a} \left[1 + \frac{\xi \sigma_a/\sigma_s}{\left(\frac{\sigma_a}{\sigma_s} + \xi\right)^2} \right]$$

Table 1.3.6—Comparison of Resonance Escape Probabilities
in the Energy Range E_1 to E_2 where $\ln E_1/E_2 = 5$ and σ_a/σ_s Is Constant.

$$[p = q(E_2)/q(E_1) = (E_2/E_1)^\mu]$$

Case		Asymptotic and Hurwitz	Fermi	Wigner	G. G.
M	σ_a/σ_s	$\mu = \lambda$	$\mu = \frac{\sigma_a}{\xi\sigma_s}$	$\mu = \frac{\sigma_a}{\xi(\sigma_s + \sigma_a)}$	$\mu = \frac{\sigma_a}{\xi(\sigma_s + \epsilon\sigma_a)}$
12	0.005	0.85390	0.85346	0.85412	0.00376
	.05	.2160	.2050	.2211	
	.1	.0514	.0420	.0561	
	.2	.00372	.00177	.00508	
50	0.005	0.5319	0.5308	0.5325	
	.05	.00218	.00178	.00240	
100	0.0005	0.88178	0.88176	0.88182	
	.005	.2853	.2841	.2859	

absorption is graphed in Fig. 1.3.2 and compared to the asymptotic solution $\psi_a(E)$. The discontinuity in ψ at $E = \alpha E_0$ is a result of the sharp cut-off in the kernel $g(E, E')$. Approximate magnitudes of the deviation $D = |(\psi - \psi_a)/\psi_a|$ for large M are $D(E_0) = 50\%$, $D(\alpha E_0) = 35\%$, $D(\alpha^2 E_0) = 2\%$, and $D(\alpha^3 E_0) = 0.3\%$. The deviations decrease with M and vanish for hydrogen.

It may be noted that such oscillations are also caused by a sharp absorption resonance, since the effect is that of a negative source.

EXACT SOLUTIONS FOR SPECIAL SOURCES

From Eq. (2), a source, $S(E)$, can be readily constructed for any specified solution, $\psi(E)$. For example,⁵ if the simple asymptotic form in a non-capturing medium, $\psi = 1/\xi E$, is to hold exactly up to E_0 , and then vanish for higher energies, the required source is:

$$S = \frac{1}{\xi(1 - \alpha)} \left(\frac{1}{E_0} - \frac{\alpha}{E} \right)$$

on the interval αE_0 to E_0 ; otherwise, $S = 0$.

GENERAL SCATTERING

Although precise knowledge of the slowing-down kernels for inelastic scattering and non-isotropic elastic scattering is not available, statements may be made (Chapter 1.2) concerning their approximate forms and, in particular, about the values of ξ for these processes. Aside from the procedure of substituting these kernel forms into Eq. (2) for numerical computations, the following approximation methods are available.

For a single element with a single process such as elastic scattering, the synthetic kernel method discussed under "Isotropic Elastic Scattering—General Solutions" may be applied.

For a single element with elastic and inelastic scattering, or for a mixture, the methods of "Isotropic Elastic Scattering—Mixtures" may be applied.

A different approximation, suggested by the inelastic scattering process, is to replace the correct kernel, g , by the form:

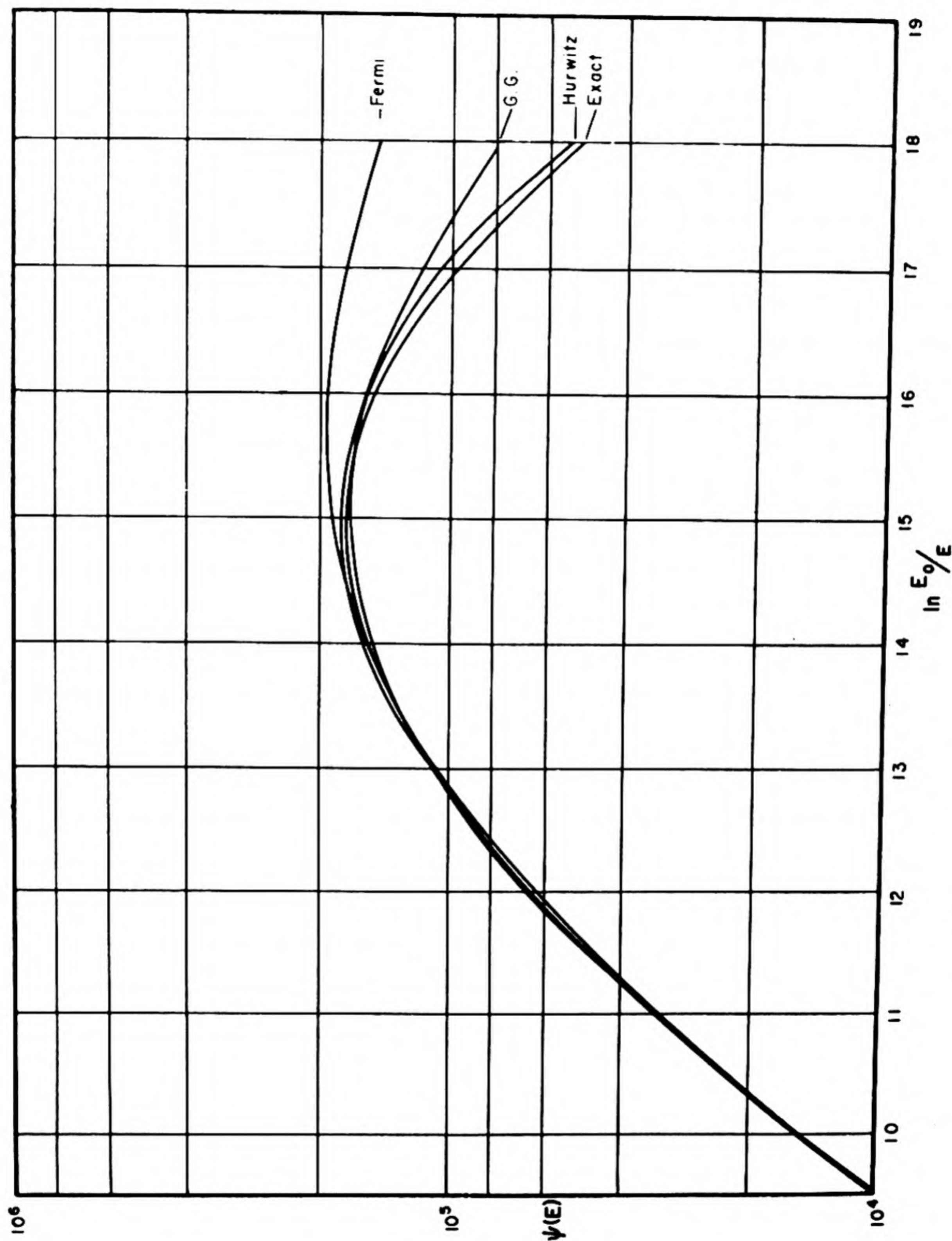


Fig. 1.3.1—Fermi, G. G., and Hurwitz, and Exact Solutions for $\psi(E)$ for Slowing-down in Deuterium. Private communication from Bell and Goad, Los Alamos. The ratio of absorption to scattering cross sections (σ_a/σ_s) was taken equal to 0.001 (E_0/E)^{1/2}.

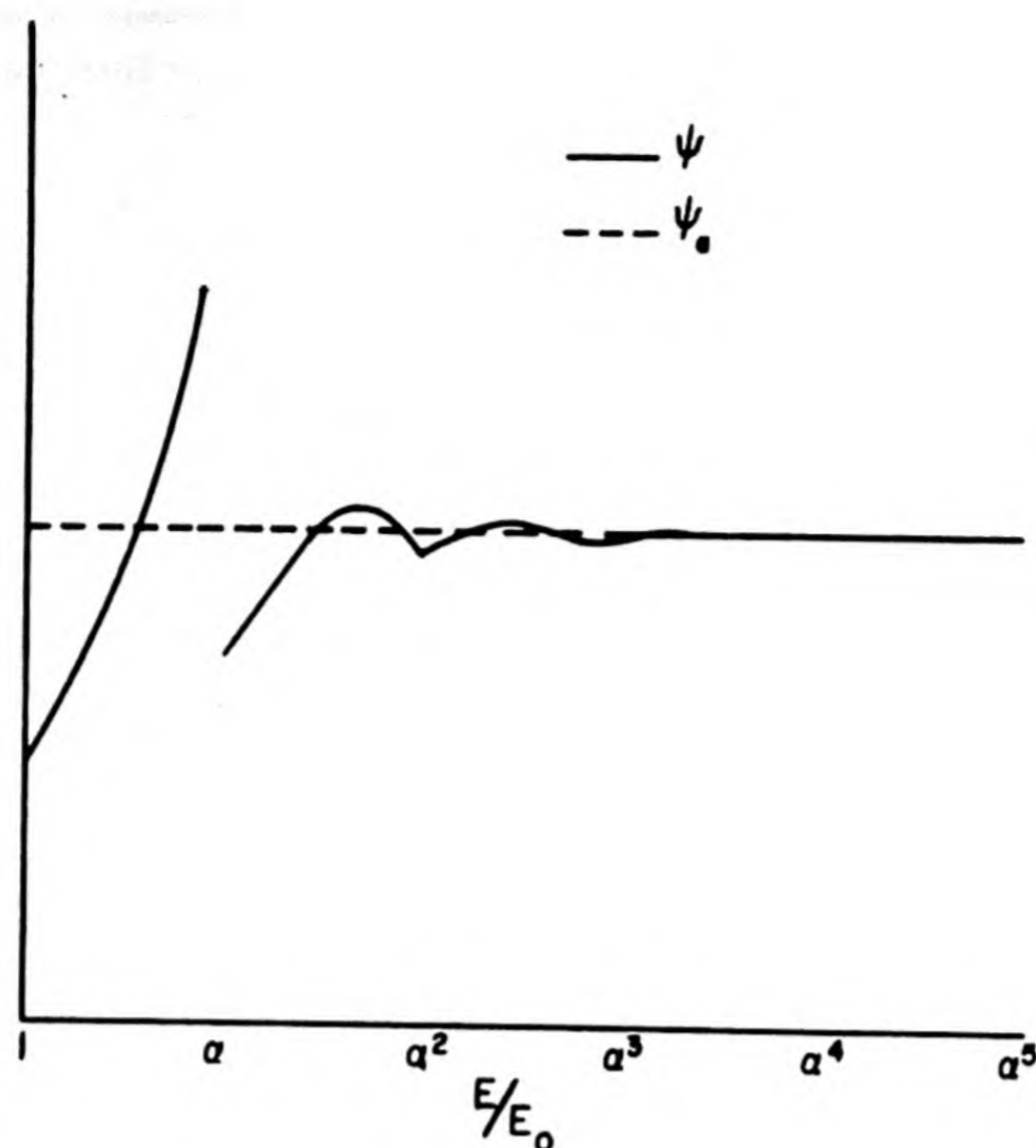


Fig. 1.3.2—Exact ψ Versus Asymptotic ψ_a for a Point Source at E_0 . Reprinted from Placzek, Phys. Rev. 69, (1946).

$$g(E', E) = \sum_i a_i \delta [E - (E' - E_i)] \quad (14)$$

which assumes the scattering to result in discrete energy jumps, E_i , with probabilities, a_i . This approximation results in a simple numerical procedure on Eq. (2).

Combination treatments are also possible; for example, computations have been made⁶ using a three-delta function kernel for inelastic scattering, with elastic scattering handled in a conventional manner.

Another type of approximation uses a sum of separable terms, $\sum_i U_i(E')v_i(E)$ for $g(E', E)$.

THERMAL DISTRIBUTIONS

In a non-capturing medium, neutrons which have been slowed down to thermal equilibrium acquire a Maxwellian velocity distribution (Table 1.3.7).

In a capturing medium, the absorption of neutrons leads to a "hardening" of their velocity distribution. This has been studied by Wigner and Wilkins⁷ for the case of atomic hydrogen with constant scattering cross-section and a $1/v$ absorber (Fig. 1.3.3). Cohen⁸ notes that the results of Wigner and Wilkins indicate an increase in the mean velocity of the neutrons by a factor of $1 + 1.2 \sigma_a(kT)/\xi\sigma_s + \dots$, and this has been compared with experiment to some extent.⁹

This hardening of the velocity spectrum may be reported by giving an effective neutron temperature such that a Maxwellian distribution at this new higher temperature would exhibit the correct average neutron velocity. In this sense, thermal neutron temperatures in reactors exceed moderator temperatures by the order of 50°C.

Table 1.3.7 — Maxwellian Distributions and Averages

Quantity	Value or formula
Normalized velocity distribution = $n(v)$	$\frac{4}{\sqrt{\pi}} \left(\frac{M}{2kT} \right)^{3/2} v^2 e^{-\frac{Mv^2}{2kT}}$
Most probable speed = α	$\sqrt{\frac{2kT}{M}}$
Normalized energy distribution = $n(E)$	$\frac{2}{\sqrt{\pi}} (kT)^{-3/2} E^{1/2} e^{-E/kT}$
Most probable energy	$\frac{1}{2} kT$
Energy at which the flux $n(E)v(E)$ is a maximum	kT
Average speed = \bar{v}	$1.128 \alpha = \frac{2}{\sqrt{\pi}} \alpha$
Root mean square speed = c	$1.225 \alpha = \sqrt{3/2} \alpha$
Average energy	$\frac{3}{2} kT = \frac{1}{2} M c^2$
Fraction of particles having speed above v	$\frac{2}{\sqrt{\pi}} \left(x e^{-x^2} + \int_x^\infty e^{-x^2} dx \right)$ where $x = v/\alpha$
$\bar{\sigma}$ for $\sigma = 1$	1
$\sigma = 1/v$	$1/\bar{v}$
$\sigma = 1/v^2$	$1/\alpha^2$
$\sigma = 1/v^n$	$\frac{1}{\alpha^n} \Gamma\left(2 - \frac{n}{2}\right)$

The average velocity \bar{v} of the distribution comes up in connection with effective neutron cross-section values:

$$\bar{\sigma} = \frac{\int \sigma n v dE}{\int n v dE} \quad (15)$$

For a $1/v$ absorber (i.e., $\sigma = b/v$), one obtains $\bar{\sigma} = b/\bar{v}$ regardless of the distribution function, n . Averages of other functions over a Maxwellian are given in Table 1.3.7.

ONE-VELOCITY THEORY

(Felix Adler)

INFINITE HOMOGENEOUS REGION

SPECIAL FORMS OF THE BOLTZMANN EQUATION

Integro-differential Formulation

In this discussion, it is assumed that the neutrons diffuse without changing their energy,

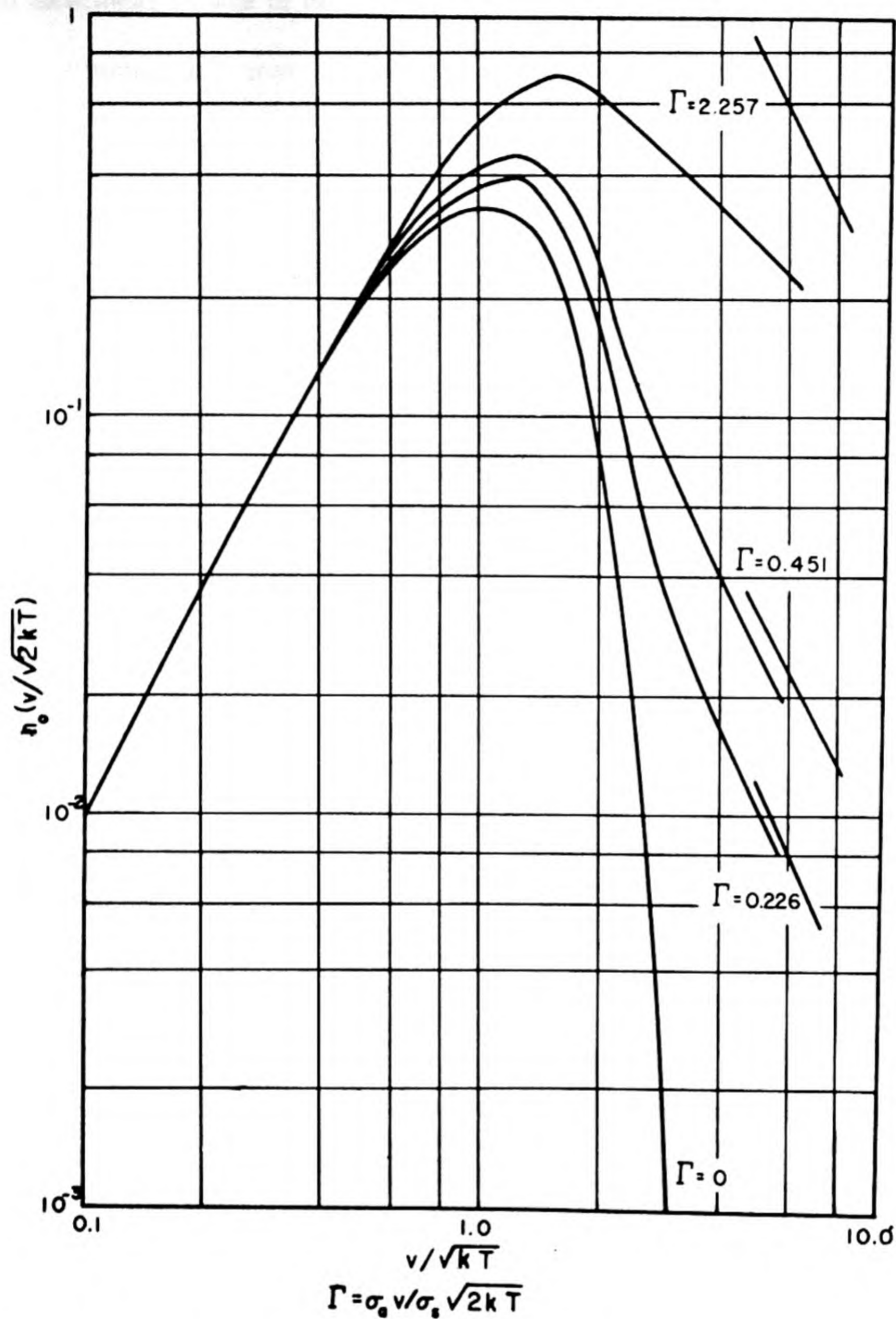


Fig. 1.3.3 — Absorption Hardening in Hydrogen Gas According to Wigner and Wilkins. Reprinted from AECD-2275.

i.e., the kernel of the Boltzmann equation reduces to:

$$\delta(v - v') \sigma_s(v, \underline{\Omega}, \underline{\Omega}')$$

In an isotropic medium, $\sigma_s(v, \underline{\Omega}, \underline{\Omega}')$ depends only on the angle between the directions of the incident and the scattered neutron and is independent of the azimuth of scattering:

$$\sigma_s(v, \underline{\Omega}, \underline{\Omega}') = \sigma_s(v, \mu_0) = \sum \frac{2l+1}{2} \sigma_{sl}(v) P_l(\mu_0) \quad (16)$$

where:

$$\mu_0 = \underline{\Omega} \cdot \underline{\Omega}'$$

and:

$$\sigma_{s1}(v) = \int_{-1}^{+1} \alpha_s(v, \mu_0) P_1(\mu_0) d\mu_0$$

The cross section for scattering, without energy loss, a neutron of speed v from the direction $\underline{\Omega}'$ into the solid angle $d\Omega$ about the direction $\underline{\Omega}$ is $\alpha_s(v, \underline{\Omega}, \underline{\Omega}') d\Omega$.

The total scattering cross-section is $\sigma_s = \sigma_{s0}$.

The Boltzmann equation is:

$$\frac{1}{v} \frac{\partial F}{\partial t} = -\text{div} \underline{\Omega} F - \sigma F(\underline{r}, \underline{\Omega}, t) + \int_{\underline{\Omega}'} F(\underline{r}, \underline{\Omega}', t) \sigma_s d\underline{\Omega}' + S(\underline{r}, \underline{\Omega}, t) \quad (17)$$

Many results have been derived for the special case where:

$$F(\underline{r}, \underline{\Omega}) = F(z, \mu)$$

i.e., slab geometry.

From the expansion of σ_s and the addition theorem of Legendre functions, one finds for steady state:

$$\mu \frac{\partial F(z, \mu)}{\partial z} + \sigma F(z, \mu) = \frac{1}{2} \sum_l (2l+1) \sigma_{s1} P_l(\mu) \int_{-1}^{+1} P_l(\mu') F(z, \mu') d\mu' + S(z, \mu) \quad (18)$$

For isotropic scattering, Eq. (17) reduces to:

$$\frac{1}{v} \frac{\partial F}{\partial t} + \mu \frac{\partial F}{\partial z} + \sigma F = \frac{1}{2} \sigma_{s0} \int_{-1}^{+1} F(z, \mu', t) d\mu' + S(z, \mu, t) \quad (19)$$

Boltzmann's equation can also be written as an integral equation; the formulation as an integral equation is particularly useful in approximation methods, e.g., the iteration method, the end-point method, and the variational method.^{10,11,12}

The Integral Equation Formulation

The integral equation for the steady-state collision density $\psi(\underline{r}, \underline{\Omega})$ is based on the first collision probability density:

$$K(|\underline{r} - \underline{r}'|) = \frac{\sigma}{4\pi |\underline{r} - \underline{r}'|^2} e^{-\sigma |\underline{r} - \underline{r}'|} \quad (20)$$

$K(|\underline{r} - \underline{r}'|)$ is the probability for a neutron starting from \underline{r}' to suffer its first collision at \underline{r} . For a distributed isotropic source, $S(\underline{r}')$, the number of neutrons per unit volume suffering their first collision at \underline{r} is:

$$\psi_1(\underline{r}) = \iiint d\underline{r}' S(\underline{r}') K(|\underline{r} - \underline{r}'|) \quad (21)$$

All collisions can be treated as first collisions by assuming that a neutron suffering any type of collision is absorbed and that $(1+f)$ new neutrons appear at the same point; i.e., for a scattering collision, $f = 0$; for real capture, $f = -1$; and for fission, $f = \nu - 1$. In this

picture, an additional source of neutrons appears in each element of volume, viz., $(1 + f)\psi_1(\underline{r})$.

Capture, scattering, and fission collisions can all occur at the same point; the number of new neutrons appearing is therefore:

$$1 + f(\underline{r}) = \frac{\sigma_s(\underline{r}) + \nu\sigma_f(\underline{r})}{\sigma(\underline{r})} \quad (22)$$

with:

$$\sigma = \sigma_s + \sigma_c + \sigma_f$$

For inhomogeneous media, $f(\underline{r})$ depends on position, e.g., is different in core and tamper of a reactor. In this picture, $\psi_1(\underline{r})$ is the collision density, and:

$$\psi(\underline{r}) = \iiint d\underline{r}' K(|\underline{r} - \underline{r}'|) [S(\underline{r}') + \{1 + f(\underline{r}')\}\psi(\underline{r}')] \quad (23)$$

Equation (23) can be generalized to include time-dependent neutron distributions; the number of first collisions occurring at time (t) at a distance (s) from the source depends on the source strength at a time $(t - s/v)$:

$$\psi(\underline{r}, t) = \iiint d\underline{r}' K(|\underline{r} - \underline{r}'|) [S(\underline{r}', t') + \{1 + f(\underline{r}')\}\psi(\underline{r}', t')] \quad (24)$$

where:

$$t' = t - |\underline{r} - \underline{r}'|/v$$

If:

$$\psi(\underline{r}, t) = \psi(\underline{r}) e^{\alpha t}$$

and:

$$S(\underline{r}, t) = S(\underline{r}) e^{\alpha t}$$

Eq. (24) reduces to Eq. (23) with the σ in the kernel replaced by $\sigma + \alpha/v$.

When S , f , and ψ in Eq. (23) are either functions only of z (slab symmetry) or of r (spherical symmetry), similar one-variable integral equations result:

$$\psi(z) = \int_{-\infty}^{+\infty} dz' K_{pl}(|z - z'|) [S(z') + \{1 + f(z')\}\psi(z')] \quad (25)$$

$$r\psi(r) = \int_{-\infty}^{+\infty} dr' K_{pl}(|r - r'|) r' [S(r') + \{1 + f(r')\}\psi(r')] \quad (26)$$

where:

$$K_{pl}(|\rho|) = \int_{|\rho|}^{\infty} dr [2\pi r K(|r|)] \quad (27)$$

is the normalized plane kernel (i.e., $\int_{-\infty}^{+\infty} d\rho K_{pl}(|\rho|) = 1$). Table 1.3.8 contains the explicit transport kernel Eq. (27). The negative values of r' encountered in Eq. (26) require one to define $S(r')$, $f(r')$, and $N(r')$ as even functions of r' .

Integral equations of the Milne type (transport kernels) for semi-infinite or infinite media are often solved by means of Fourier transforms and the use of the convolution theorem for

Table 1.3.8 — Transport Kernels

Geometry	Notation	Normalization	Kernels
Point source	$K(\underline{r} - \underline{r}')$	$\int_0^\infty 4\pi R^2 K(R) dR = 1$	$\frac{\sigma e^{-\sigma \underline{r}-\underline{r}' }}{4\pi(\underline{r} - \underline{r}')^2}$
Plane source	$K_{pl}(z - z')$	$\int_{-\infty}^\infty K_{pl}(z) dz = 1$	$\frac{\sigma}{2} E_1(\sigma z - z')$ $E_1(z) = \int_z^\infty \frac{e^{-t}}{t} dt$
Line source	$K_l(s)$	$\int_0^\infty 2\pi s K_l(s) ds = 1$	$\frac{\sigma^2}{2\pi} \int_1^\infty K_0(\sigma s t) dt$ $s = \perp$ distance from line source
Cylindrical shell source at r'	$K_c(r, r')$	$\int_0^\infty 2\pi r K_c(r, r') dr = 1$	$\frac{\sigma^2}{2\pi} \begin{cases} \int_1^\infty K_0(\sigma r t) I_0(\sigma r' t) dt, & r > r' \\ \int_1^\infty K_0(\sigma r' t) I_0(\sigma r t) dt, & r < r' \end{cases}$

Fourier transforms. Let $F\{g(x)\}$ be the Fourier transform of $g(x)$, then one obtains for an infinite medium:

$$F\{\psi(z)\} = F\{S(z)\} \frac{[\tanh^{-1}(\kappa/\sigma)]/(\kappa/\sigma)}{1 - \frac{(1+f)\tanh^{-1}(\kappa/\sigma)}{(\kappa/\sigma)}} \quad (28)$$

If the scattering is anisotropic in the laboratory system and the cross section is expanded as a series of Legendre functions, an integral equation formulation conveniently solved numerically by iteration is still possible.¹³ A trial function, e.g., a quadratic, is iterated according to Eq. (23), and the moments calculated from the iterated trial function are matched.

Variational Formulation

In the steady state when $S = 0$, the integral equation of transport theory, Eq. (23), can also be formulated as a variational principle for the eigenvalue, λ ; $\delta\lambda = 0$ where:

$$\lambda = \frac{\iiint d\underline{r} \iiint d\underline{r}' \psi(\underline{r}) \tau(\underline{r}) K(|\underline{r} - \underline{r}'|) \tau(\underline{r}') \psi(\underline{r}')}{\iiint d\underline{r} \psi^2(\underline{r}) \tau(\underline{r})} \quad (29)$$

and:

$$\tau(\underline{r}) = 1 + f(\underline{r})$$

The equivalence of Eq. (23) to $\delta\lambda = 0$ can be shown by the usual methods. For applications of Eq. (29) in general perturbation arguments, see Chapter 1.4.

The advantage of the variational method is that very simple trial functions give good results for λ .

For example, if $\tau(\underline{r})$ is constant in a sphere and zero outside, a parabolic trial function $\psi(r) = 1 - Cr^2$, where C is chosen to make λ an extremum, is often sufficient.

Sometimes (e.g., in lattice problems) it is possible to approximate $\psi(\underline{r})$ by assuming that it is piecewise constant in appropriately chosen regions (e.g., fuel or moderator).

The variational method has been very successful in problems involving complicated geometries and kernels. It can also be extended to inhomogeneous integral equations.¹⁴ In this case, the variation does not always lead to a true minimum but sometimes to a saddle point.*

THE DIFFUSION APPROXIMATION

Expansion In Spherical Harmonics

The Boltzmann equation can frequently be approximated by expansions in spherical harmonics, e.g., for anisotropic scattering, in two media problems where the media have different total mean free paths and in many cases where boundaries are not plane.^{16,17} Results and special formulae are discussed later under "Homogeneous Regions in Contact." One can obtain the elementary diffusion approximation from Eq. (18) by expanding the flux and source distributions in Legendre Polynomials:

$$S(z, \mu) = \frac{1}{2} \sum_l (2l + 1) S_l(z) P_l(\mu) \quad (30)$$

$$F(z, \mu) = \frac{1}{2} \sum_l (2l + 1) F_l(z) P_l(\mu) \quad (31)$$

and by using the orthogonality properties of the Legendre Polynomials:

$$\frac{l+1}{2l+1} \frac{dF_{l+1}}{dz} + \frac{l}{2l+1} \frac{dF_{l-1}}{dz} + \sigma F_l = \sigma_{sl} F_l + S_l \quad (32)$$

In principle, Eq. (32) constitutes an infinite system of ordinary linear differential equations. In the spherical harmonics method, the system is cut off after a certain harmonic n , and the remaining finite system of equations is solved for $F_l(z)$. This is called the P_n -approximation. Thus, the Boltzmann equation, i.e., an integro-differential equation, is replaced by a system of ordinary linear differential equations. This reduction is also possible when the cross sections depend on position.

The P_1 -Approximation

The first and simplest approximation is the ordinary diffusion approximation, where the expansion of $F(z, \mu)$ is broken off after the second term, i.e., it is assumed that $F(z, \mu)$ is almost isotropic and S is isotropic.

This approximation is valid if the following conditions are satisfied:

- (1) Sources are far away, i.e., several mean free paths from the region considered.
- (2) Boundaries of the medium are several mean free paths away from the region considered.

- (3) The probability of capture is small compared to the probability of scattering.

From Eq. (32), one obtains with $\sigma_a = \sigma_c + \sigma_f$ = the total absorption cross section:

$$\begin{aligned} \frac{dF_1}{dz} + \sigma_a \varphi &= S_0 \\ F_1 &= -\frac{1}{3(\sigma - \sigma_{sl})} \frac{d\varphi}{dz} \equiv -\frac{l^{tr}}{3} \frac{d\varphi}{dz} \end{aligned} \quad (33)$$

* For the exact conditions, compare Davison.¹⁵

where:

$$\varphi = F_0 = nv \quad (34)$$

By definition, F_1 is the net neutron current. An alternative expression for the neutron current can be found by computing the number of neutrons per second passing through an element of surface dS perpendicular to the z axis from above the xy plane, using the transport kernel [cf. Eq. (20)]:

$$J_+ dS = dS \int_0^\infty dr \int_0^{2\pi} d\psi \int_0^{\pi/2} d\theta \phi(\underline{r}) \sigma_s \frac{e^{-\sigma r} \cos\theta \sin\theta}{4\pi} \quad (35)$$

where $e^{-r\sigma}$ is the probability that neutrons leaving $d\underline{r}$ in the direction to dS are not lost on the way and $\phi(\underline{r}) \sigma_s \cos\theta dS/4\pi r^2 d\underline{r}$ is the number of neutrons being scattered in the appropriate direction at \underline{r} .

Expanding the flux in a Taylor series one obtains for $\sigma_a \ll \sigma_s$:

$$J_\pm = \left[\frac{1}{4} \phi \pm \frac{l^{tr}}{6} \frac{\partial \phi}{\partial z} + \dots \right]_{z=0} + \dots \quad (36)$$

for the number of neutrons passing into the lower (+) or upper (−) regions, and for the net current into the upper region:

$$J = J_- - J_+ = \frac{l^{tr}}{3} \frac{\partial \phi}{\partial z} \Big|_{z=0} + \dots \quad (37)$$

after making the transport correction of replacing the scattering length by the transport length l^{tr} .

The three dimensional forms* of Eq. (33) are:

$$\underline{J}(\underline{r}) = -\frac{l^{tr}}{3} \text{grad } \varphi(\underline{r}) \quad (38)$$

$$\text{div } \underline{J}(\underline{r}) + \sigma_a \varphi(\underline{r}) = S_0(\underline{r})$$

The first equation is a statement of Fick's law, viz., that the neutron current is proportional to the gradient of the flux density and through it the diffusion coefficient is defined as:

$$D \equiv l^{tr}/3 \quad (39)$$

The second equation is simply a statement of the continuity equation for the steady state. The transport mean free path is defined as:

$$l^{tr} = 1/[\sigma - \sigma_{s1}] \quad (40)$$

for weakly absorbing media:

$$l^{tr} = l_s/[1 - \mu_0] \quad (41)$$

* Eq. (38) can be derived¹⁶ from Eq. (17) by taking moments with respect to $\underline{\Omega}$ and making diffusion theory assumptions.

Useful Formulations of the Diffusion Equation

For a multiplying medium the source density in Eq. (38) is:

$$S_0(\underline{r}) = S^{\text{ext}}(\underline{r}) + \nu\sigma_f\phi(\underline{r}) \quad (42)$$

For calculations using the elementary one-group diffusion theory, Eq. (38) is most conveniently formulated as:

$$\nabla^2\phi(\underline{r}) + L_m^{-2}\phi(\underline{r}) + (3/l^{\text{tr}})S^{\text{ext}} = 0 \quad (43)$$

where:

$$L_m^{-2} = 3\sigma_a(k-1)/l^{\text{tr}} \quad (44)$$

and k , the so-called one-group multiplication constant, is defined as:

$$k \equiv \nu\sigma_f/\sigma_a$$

The solutions of problems of neutrons in a single medium have been reported in systematic form by Wallace and Le Caine.¹⁷

For solving elementary diffusion theory problems by an integral, Eq. (38) is written as:

$$\eta^{-1}\nabla^2\psi(\underline{r}) - \psi(\underline{r}) + S^{\text{ext}}(\underline{r}) + \{1 + f(\underline{r})\}\psi(\underline{r}) = 0 \quad (45)$$

where ψ is the collision density, and:

$$\eta^2 \equiv 3\sigma/l^{\text{tr}} \quad (46)$$

For generalizations to multigroup and age theory, Eq. (38) is written as an obvious continuity equation:

$$(l^{\text{tr}}/3)\nabla^2\phi(\underline{r}) - \sigma_a\phi(\underline{r}) + S^{\text{ext}}(\underline{r}) + \nu\sigma_f\phi(\underline{r}) = 0 \quad (47)$$

Integral Equations of Diffusion Theory

By the use of Green's theorem, Eq. (45) can be recast in the same form as the transport integral Eq. (23):

$$\psi(\underline{r}) = \iiint d\underline{r}' K_p^D(\eta|\underline{r} - \underline{r}'|) [S^{\text{ext}}(\underline{r}') + \{1 + f(\underline{r}')\}\psi(\underline{r}')] \quad (48)$$

where $K_p^D(\eta|\underline{r} - \underline{r}'|)$ is the solution of:

$$\eta^{-2}\nabla^2 K_p^D - K_p^D + \frac{\delta(|\underline{r} - \underline{r}'|)}{4\pi|\underline{r} - \underline{r}'|^2} = 0 \quad (49)$$

while in transport theory the kernel is given by Eq. (20). Alternatively, one can obtain from Eq. (47):

$$\sigma_a\phi(\underline{r}) = \iiint d\underline{r}' K_p^D(\kappa|\underline{r} - \underline{r}'|) [S^{\text{ext}}(\underline{r}') + \nu\sigma_f\phi(\underline{r}')] \quad (50)$$

where:

$$\kappa^2 = 3\sigma_a / l^{tr}.$$

Equation (50) can be generalized to age and multigroup formulations of the fission source term.

In the general case, too, the relations (25) to (27) between kernels for different geometries hold.

Table 1.3.9 lists useful diffusion kernels.

Table 1.3.9 — Diffusion Kernels

Geometry	Notation	Normalization	Kernels
Point source	$K_p^D(\kappa \underline{r} - \underline{r}')$	$\int_0^\infty 4\pi R^2 K_p^D(\kappa R) dR = 1$	$\frac{\kappa^2 e^{-\kappa \underline{r} - \underline{r}' }}{4\pi \underline{r} - \underline{r}' }$
Plane source	$K_{pl}^D(\kappa z - z')$	$\int_{-\infty}^{+\infty} K_{pl}^D(\kappa z) dz = 1$	$\frac{\kappa e^{-\kappa z - z' }}{2}$
Line source	$K_l^D(\kappa s)$	$\int_0^\infty 2\pi s K_l^D(\kappa s) ds = 1$	$\frac{\kappa^2}{2\pi} K_0(\kappa s)$ $s = \perp$ distance from line source
Cylindrical shell source at r'	$K_c^D(\kappa r, \kappa r')$	$\int_0^\infty 2\pi r K_c^D(\kappa r, \kappa r') dr = 1$	$\frac{\kappa^2}{2\pi} \cdot \begin{cases} K_0(\kappa r) I_0(\kappa r'), & r > r' \\ K_0(\kappa r') I_0(\kappa r), & r < r' \end{cases}$

Variational Formulation

Elementary diffusion theory for $S^{ext} = 0$ can also be formulated in terms of a variational principle; in exact analogy with Eq. (29), we obtain that λ should be minimized:

$$\lambda = \frac{\iiint d\underline{r}' \iiint d\underline{r} \psi(\underline{r}) \tau(\underline{r}) K_p^D(\eta|\underline{r} - \underline{r}'|) \tau(\underline{r}') \psi(\underline{r}')}{\iiint d\underline{r} \psi^2(\underline{r}) \tau(\underline{r})} \quad (51)$$

One-group Boltzmann and diffusion equations are self-adjoint. The generalization of Eq. (51) to non-self-adjoint problems, and the role of the adjoint are discussed in Chapter 1.4.

Time-dependent Diffusion Theory

If the neutron density is time dependent, the equation of neutron conservation is:

$$\frac{1}{v} \frac{\partial \phi(\underline{r}, t)}{\partial t} = \frac{l^{tr}}{3} \nabla^2 \phi(\underline{r}, t) - \sigma_a \phi(\underline{r}, t) + S(\underline{r}, t) \quad (52)$$

The time-dependent equation is solved, for example, by a Fourier-transform in the space coordinates and either a Fourier (steady state) or a Laplace transform (transients) in time.

An integral equation, analogous to Eq. (50) is obtained from Eq. (52) by use of the time dependent Green's function in the form:

$$\sigma_a \phi(\underline{r}, t) = \iiint d\underline{r}' dt' \kappa^2 D \frac{e^{-\left[\frac{|\underline{r}-\underline{r}'|^2}{4D(t-t')} + \kappa^2 D(t-t')\right]}}{[4\pi D(t-t')]^{3/2}} S(\underline{r}', t') \quad (53)$$

It is interesting to compare the retardation time ($t_{\text{ret}} = x/v$) entering in the integral equation and the "diffusion time" ($t_{\text{dif}} = x^2/2D$) at which the neutron intensity at x reaches its maximum:

$$\frac{t_{\text{ret}}}{t_{\text{dif}}} = \frac{2}{3} \frac{l^{\text{tr}}}{x}$$

At distances $r \gg l^{\text{tr}}$ from the source, the retardation time is negligible compared to the diffusion time. Since most experiments involve the neutron distribution far from the source, it is usually permissible to ignore the retardation and to describe the time-dependent diffusion equation by means of an equation linear in $\partial/\partial t$.

However, if retardation effects are to be considered, a new derivation of the basic diffusion equation and of Fick's law is necessary.

Proceeding as before, the result is that the neutron current is no longer proportional to the gradient of the flux but to a linear combination of time rate of change of current and gradient of flux.

Therefore the time-dependent diffusion equation will here contain $\partial^2/\partial t^2$, i.e., it is a telegrapher's equation:

$$\frac{1}{\sigma v^2} \frac{\partial^2 F_0(\underline{r}, t)}{\partial t^2} + \left[1 + \frac{\sigma_a}{\sigma}\right] \frac{1}{v} \frac{\partial F_0(\underline{r}, t)}{\partial t} = \frac{1}{3\sigma} \nabla^2 F_0(\underline{r}, t) - \sigma_a F_0(\underline{r}, t) + S(\underline{r}, t) \quad (54)$$

The solutions of Eq. (54) possess a well-defined wave front, followed by a long tail of disturbance owing to the term linear in $\partial/\partial t$. The existence of the wave front is obvious; a neutron traveling with speed v requires at least a time r/v to reach a point at a distance r from the source. As r increases, the probability of a neutron reaching r without a collision becomes smaller and smaller.

Validity of the P_1 -Approximation

The generalized Fick's Law:

$$\underline{J}(z) = -l^{\text{tr}} \frac{d}{dz} \left[\overline{\mu^2} F_0(z) \right] \quad (55)$$

where:

$$\overline{\mu^2} = \int_{-1}^{+1} d\mu \mu^2 F(z, \mu) / F_0(z) = \frac{1}{3} + \frac{2}{3} [F_2(z) / F_0(z)] \quad (56)$$

can be derived from Eq. (18) without any restrictive assumption whatsoever. Therefore, elementary diffusion theory is valid if $\overline{\mu^2}$ is independent of position.

Thus, if $F_2(z)/F_0(z)$ is independent of position, elementary diffusion theory is rigorously correct; the spatial variations of $F_2(z)/F_0(z)$ give a rough measure for the error involved in using elementary diffusion theory near a source or a boundary.

Numerical comparison of diffusion theory and exact results as well as prescriptions to extend the range of validity of results obtained from elementary diffusion theory are given in the following.

SOLUTIONS OF TRANSPORT AND DIFFUSION PROBLEMS IN INFINITE MEDIA

Exact Solutions for the Transport Equation

Isotropic Scattering ($\sigma = \nu = 1$)

The exact solutions of the transport Eq. (26) are characterized by a parameter κ , defined by:

$$\frac{\tan^{-1} \kappa}{\kappa} = \frac{1}{1+f} \quad (f > 0) \quad (57)$$

$$\frac{\tanh^{-1} \kappa}{\kappa} = \frac{1}{1+f} \quad (f < 0) \quad (58)$$

For point sources, they have (in the asymptotic region) the form:

$$n^{as}(r) = C_f \frac{e^{-\kappa r}}{4\pi r} \quad (f < 0) \quad (59)$$

$$n^{as}(r) = A \frac{e^{i\kappa r}}{4\pi r} + B \frac{e^{-i\kappa r}}{4\pi r} \quad (f > 0) \quad (60)$$

In non-multiplying media, κ is the decay or attenuation constant, and the diffusion length is defined as:

$$L = 1/\kappa\sigma \quad (\text{conventional units}) \quad (61)$$

In multiplying media, κ is essentially the inverse multiplication length, L_m .

For small f :

$$\kappa \approx \sqrt{3|f|} \sigma \quad (\text{conventional units}) \quad (62)$$

Exact solutions have been obtained for constant $f < 0$ by the Fourier transform methods for plane sources $S(z) = \delta(z)$, and point sources $S(r) = \delta(r)/4\pi r^2$, in the form:

$$n(r) = C_f \frac{e^{-\kappa r}}{4\pi r} + \epsilon_s(r) \frac{e^{-r}}{4\pi r^2} \quad (63)$$

$$n(z) = C_f \frac{e^{-\kappa|z|}}{2\kappa} + \epsilon_{p1}(|z|) \frac{E_1(|z|)}{2} \quad (64)$$

The first term represents the asymptotic solution. The non-asymptotic part of $\psi(r)$ is the product of the transport kernel $e^{-r}/4\pi r^2$ weighted by $\epsilon_s(r)$, i.e., the number of neutrons having suffered no collisions since leaving the source times $\epsilon_s(r)$. For small r , $\epsilon_s(r) \sim 1$, and C_f is:

$$C_f = \frac{2\kappa^2(1-\kappa^2)}{(1+f)(\kappa^2+f)}; f \neq 0 \quad (65)$$

C_f and $1-\kappa$ are tabulated for representative values of f in Table 1.3.10. Figure 1.3.4 shows $\epsilon_s(r)$ as a function of (r) for representative values of (f) . It is worth noting that for $r > 1$, ϵ_s and ϵ_{p1} are virtually identical.

Table 1.3.10—Characteristic Numbers for the Asymptotic Transport Solution
(M. Goldstein et al, AECD-1943)

f	$1 - \kappa^*$	C_f^*
0.0	1.00000	3.00000
-.1	0.47457	2.52237
-.2	.28959	2.05112
-.3	.17137	1.59003
-.4	.92668 (-1)	1.14595
-.5	.42496 (-1)	0.73190
-.6	.14376 (-1)	.37327
-.7	.25862 (-2)	.11620
-.8	.90878 (-4)	.90940 (-2)
-.9	.41223 (-8)	.16489 (-5)
-1.0	.00000	.00000

* The notation $x(-n)$ means $x(10)^{-n}$

Anisotropic Scattering (conventional units)

For slightly anisotropic scattering, where $\sigma_B(\mu) = \sigma_{S0} + 3\sigma_{S1}\mu/2$ and $\sigma_{S1} = \bar{\mu}_0\sigma_{S0}$, the asymptotic solution of the Boltzmann equation can be found by using a trial solution:

$$F(z, \mu) = C \frac{A + \bar{\mu}_0 \mu}{1 \pm (\kappa \mu / \sigma)} e^{\pm \kappa z} \quad (66)$$

Note that any separable solution:

$$F(z, \mu) = f(z)g(\mu)$$

must have the form of Eq. (66).

The constants κ and A are determined by the condition that the Boltzmann equation is identically satisfied by terms containing μ in the zeroth and first power:

$$(\sigma_{S0}/\kappa) \tanh^{-1}(\kappa/\sigma) = \frac{1 + 3\bar{\mu}_0(\sigma_{S0}\sigma_a/\kappa^2)}{1 + 3\bar{\mu}_0(\sigma_{S0}\sigma/\kappa^2)} \quad (67)$$

$$A = \pm (\sigma_{S0}\bar{\mu}_0/\kappa) \frac{1 - (\sigma/\kappa) \tanh^{-1}(\kappa/\sigma)}{1 - (\sigma_{S0}/\kappa) \tanh^{-1}(\kappa/\sigma)} \quad (68)$$

This approach can be extended to arbitrary scattering law, provided $F(z, \mu)$ can be factored into a product $f(z)g(\mu)$; $\bar{\mu}^2$ is then a constant, i.e., Fick's law holds [cf., Eq. (56)], and a diffusion type equation will be valid for $F_0(z)$.

For isotropic scattering, ($\bar{\mu}_0 = 0$) κ reduces to the value given previously, and:

$$F(z, \mu) = \text{constant} \frac{e^{\pm \kappa z}}{1 \pm (\kappa \mu / \sigma)} \quad (69)$$

so that:

$$\bar{\mu}^2 = \sigma \sigma_a / \kappa^2$$

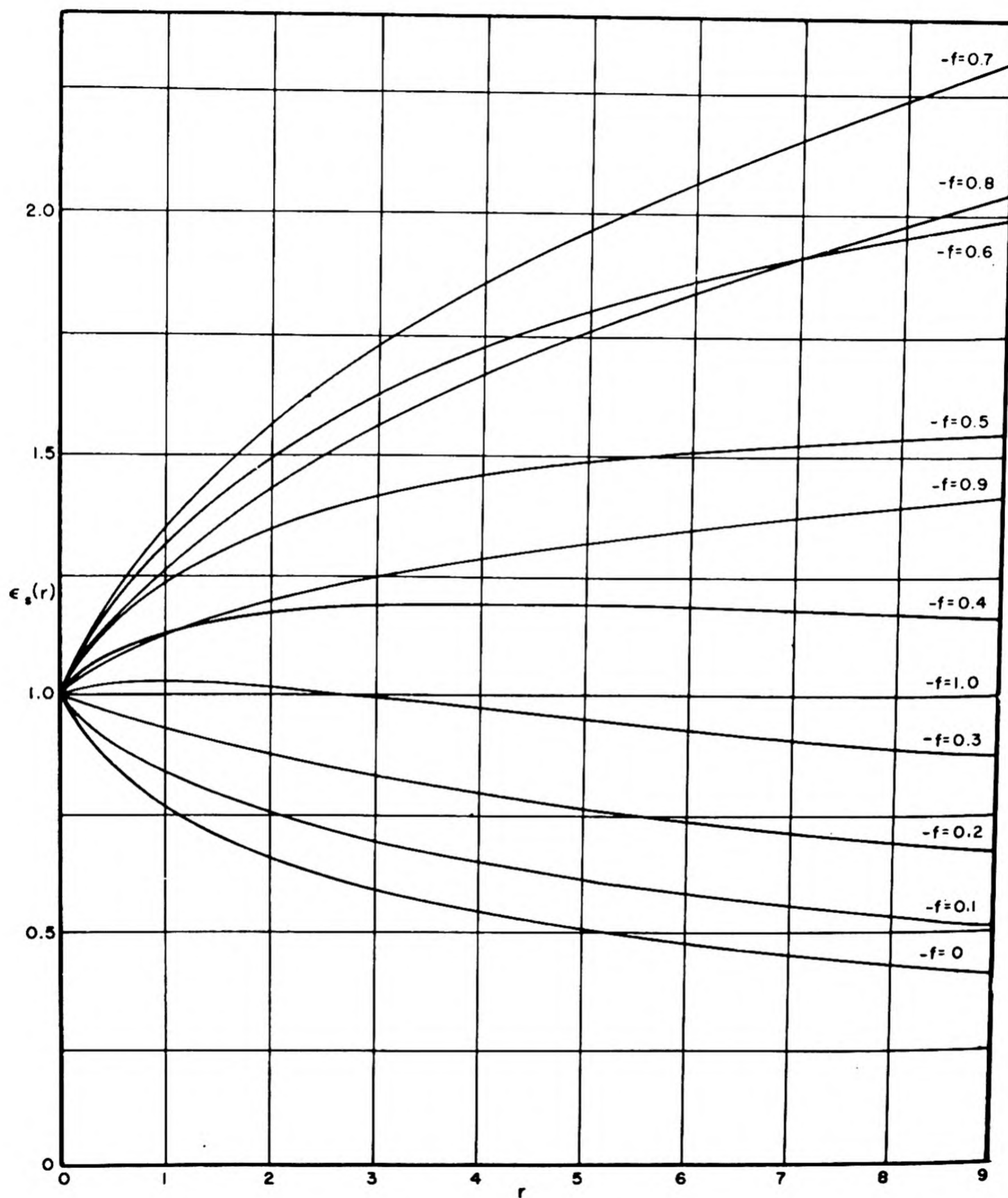


Fig. 1.3.4 — Coefficients of the Non-asymptotic Part of the Flux from a Point Source. From M. Goldstein et al, AECD-1943, LADC-506.

Applications of Results of Transport Theory in Diffusion Theory

Asymptotic Transport and Diffusion Flux

The correction to $n^{as}(r)$ given in Eq. (63) is negligible for r larger than a few mean free paths.

$n^{as}(r)$ satisfies a diffusion-type equation for an anisotropic as well as isotropic scattering law. From an expression for the angular distribution in the asymptotic region, e.g., Eq. (69), one can prove that in the asymptotic region Fick's law is valid. Redefining D of Eq. (39) as:

$$D^* \equiv \sigma_a / \kappa^2 \quad (70)$$

the equations for the asymptotic region become:

$$\underline{J}(\underline{r}) = -D^* \text{grad } n^{as}(\underline{r}) \quad (71)$$

and:

$$-\nabla^2 F_0^{as}(\underline{r}) + \kappa^2 F_0^{as}(\underline{r}) = \frac{\kappa^2}{\sigma_a} [S^{ext}(\underline{r}) + \nu \sigma_f F_0^{as}(\underline{r})] \quad (72)$$

i.e., $F_0^{as}(\underline{r})$ satisfies the basic equation of elementary diffusion theory for $\phi(\underline{r})$ given in Eq. (47).

The only effect of anisotropic scattering on the results contained in Eqs. (71) and (72) is to change the value of κ .¹⁸

The validity of the diffusion equation (72) for the asymptotic flux $F_0^{as}(\underline{r})$ is the basis for increasing the range of validity of results of elementary diffusion theory by applying suitable standard results of transport theory.

Prescriptions

The following prescriptions are frequently useful to get better approximations:

(1) Use the exact asymptotic equation (e.g., for strong absorption medium) by replacing diffusion coefficient D and diffusion length $\sqrt{l^{tr}/3\sigma_a}$ of elementary diffusion theory by D^* and L defined in Eqs. (70) and (61), respectively. If absorption is appreciable, use prescription (2).

(2) Fictitious source: For strongly absorbing media, replace the actual source term in the diffusion equation by a fictitious source $S^*(\underline{r})$:

$$S^*(\underline{r}) = 2 \frac{\sigma_a}{\sigma_s} \frac{1 - (\kappa/\sigma)^2}{(\kappa/\sigma)^2 - (\sigma_a/\sigma)} S(\underline{r}) \quad (73)$$

(3) Neutron density near a source: For a point source, replace $\delta(\underline{r})$ by the first collision density of neutrons $\psi_1 = \sigma e^{-\sigma r}/4\pi r^2$, and write a diffusion equation for the density of neutrons having experienced one or more collisions, using ψ_1 as a source.

If only prescription 1 is used and none of the others the asymptotic diffusion and transport solutions will differ by the constant factor given in Eq. (73). Actually, the distance from the source at which the diffusion theory solution becomes valid increases with increasing capture. For $f \rightarrow -1$, this distance tends to ∞ and the diffusion-theory solution is to be replaced by the first-collision density.

Time-dependent Diffusion Equation

For a source $S(z,t) = \delta(z)e^{i\omega t}$, the solution of the diffusion equation is a damped wave:

$$n(z,t) = \frac{1}{2D\sqrt{\kappa^2 + \frac{i\omega}{D}}} e^{-z\sqrt{\frac{\rho^2 + \kappa^2}{2} + i\omega}} \left(t - z\sqrt{\frac{\rho^2 - \kappa^2}{2}} \right) \quad (74)$$

where:

$$\rho^2 = \sqrt{\kappa^4 + \left(\frac{\omega}{D}\right)^2}$$

For the initial-value problem, where $F(z,t)$ at $t = 0$ is prescribed as $f_0(z)$ and where $f_0(z) \neq 0$ in a limited region, the neutron flux appears instantaneously at all points in space and persists indefinitely; there is no wavefront or retardation.

The solution $F_0^{\text{ret}}(z)$ for the generalized (telegrapher's) equation (54) in the same case contains terms $e^{-\sigma vt/2} f(z \pm vt/\sqrt{3})$ representing the waves traveling with a velocity $v/\sqrt{3}$.

The term representing the tail starts contributing at each point after the initial wavefront has reached it.

HOMOGENEOUS REGIONS IN CONTACT

BOUNDARY CONDITIONS

Boundary Conditions in Transport Theory

The boundary condition for the Boltzmann equation is: $F(x,\mu)$ must be continuous for all values of μ at a plane interface between two media.

Let $F^+(0,\mu)$ and $F^-(0,\mu)$ denote the flux at the right and left of a boundary at $z = 0$, then:

$$F^+(0,\mu) = F^-(0,\mu) \quad (75)$$

Using the spherical harmonic expansion, the boundary condition can be written as:

$$F_1^+(0) = F_1^-(0) \quad (76)$$

for all l . Corresponding boundary conditions hold at curved interfaces.

$F(x,\mu)$ does not have to be continuous if the boundary is itself a neutron source or absorber.

If one of the media, e.g., $z < 0$, is vacuum, the above boundary conditions are meaningless. There are no collisions in the vacuum and no neutron flow from vacuum into the medium, unless sources to the left of ($z = 0$) are prescribed. A vacuum acts as a perfect (black) absorber and Eq. (75) is replaced by:

$$F(0,\mu) = 0 \quad (77)$$

for $\mu > 0$ (vacuum for $z < 0$).

Boundary Conditions in Diffusion Theory

In elementary diffusion theory (P_1 approximation), $F_0(z)$ is a solution of a second-order differential obtained from Eq. (33). Both neutron flux, F_0 , and current, J , given by Fick's law, must be continuous across an interface between two media.

For a boundary between a medium and vacuum, it is postulated that the net inward flow vanishes:

$$J_-(0) = \int_0^1 \phi(0, \mu) \mu d\mu = 0 \quad (78)$$

Evaluating J_-0 by means of Eq. (36) one obtains for a plane interface the extrapolation length λ^D of elementary diffusion theory:

$$\lambda^D \equiv \left[\varphi(z) / \left(\frac{d\varphi}{dz} \right) \right]_{z=0} = \frac{2}{3} l^{tr} \quad (79)$$

λ^D is the distance beyond the boundary at which the extrapolated neutron flux would vanish according to elementary diffusion theory. In calculations, λ^D is usually replaced by the extrapolation length obtained from transport theory.*

Application of Transport Theory Results in Diffusion Theory ($\sigma = 1$)

For semiinfinite media ($z > 0$), the logarithmic derivative of F_0 at the boundary, commonly called the extrapolation length† (λ), is defined by:

$$1/\lambda = \frac{d}{dz} \log F_0^{as}(z) \Big|_{z=0} \quad (80)$$

Tables 1.3.11 and 1.3.12 give λ computed from transport theory.

For anisotropic scattering, the significant results are:

(1) For a linear scattering law ($\sigma_{S_2} = 0$) and no absorption, the emerging angular distribution, the extrapolation length measured in units of the transport mean free path, and $F_0(0)$ are the same as for the isotropic case.

(2) For a quadratic scattering law ($\sigma_{S_3} = 0$), the maximum variation in $F_0(0)$ is about 1.3 percent, and the variation in λ , measured in units of the transport mean free path, is about 0.44 percent.

For spheres and cylinders of radius (a), λ is defined by:

$$\frac{1}{\lambda} = \frac{d}{dr} \log F_0^{as}(r) \Big|_{r=a} \quad (81)$$

Graphs of λ for black spheres and cylinders imbedded in a non-absorbing medium are given in Figs. 1.3.6 and 1.3.7.

Curves II are the following approximations, good for $a > 3$:

$$\lambda_{\text{sphere}} = 0.7104 + 0.5047 a^{-1} + 0.2336 a^{-2} - 0.25 a^{-3} \log a - 0.1704 a^{-3} \quad (82)$$

$$\lambda_{\text{cylinder}} = 0.7104 + 0.2524 a^{-1} + 0.0949 a^{-2} - 0.078 a^{-3} \log a - 0.0256 a^{-3} \quad (83)$$

Curves I are good only for very small a :

$$\lambda_{\text{sphere}} = \frac{4}{3} - \frac{5}{9} a + \dots \quad (84)$$

$$\lambda_{\text{cylinder}} = \frac{4}{3} - \left(1 - \frac{16}{3\pi^2} \right) a \log a - 0.2164a + \dots \quad (85)$$

* Cf. below and Tables 1.3.11 and 1.3.12.

† In most reactor applications, this extrapolation length is but slightly different from the distance between the actual reactor boundary and the place where the analytic continuation of the interior, asymptotic solution vanishes.

Table 1.3.11 — Extrapolation Length and Related Results for Standard Cases with Plane Geometry (Milne's Problem)

(J. C. Mark, MT-26, May 1947; G. Placzek and W. Seidel, MT-5, June 1943; C. Mark, MT-50, April 1944)

Problem and restrictive assumptions	Extrapolation length, λ	Related results
No capture; scattering isotropic; normalization $J = -1$	$\sigma\lambda = z_0 = 0.7104$	$F_0(0) = \sqrt{3}$ $F_0(z) = \sqrt{3} \left\{ 1 - \frac{1}{2} z\sigma \log z\sigma \right.$ $\quad + 1.2788 z\sigma + \frac{1}{16} (\sigma z)^2 \log^2 (z\sigma)$ $\quad - 0.3822 (\sigma z)^2 \log \sigma z + 0.7068 (z\sigma)^2$ $\quad \left. + 0 [(\sigma z)^3 \log^3 \sigma z] \right\}$ (near surface)
No capture; quadratic scattering law	$\sigma\lambda = z_0 \left[1 + 0.011 \left(\frac{\sigma_{s2}}{\sigma_{s0}} \right) \right.$ $\quad \left. + 0.001 \left(\frac{\sigma_{s2}}{\sigma_{s0}} \right)^2 \right]$	$F_0(0) = \sqrt{3} \left(1 - 0.322 \frac{\sigma_{s2}}{\sigma_{s0}} \right)$
Capturing and multiplying medium; linear scattering law: $\sigma_s(\mu_0) = \frac{\sigma_{s0}}{2} (1 + 3b\mu_0)$	See Table 1.3.12 for deviations from good approximation:* $z'_0 \approx \frac{z_0}{1+f}$	$F_0^{as}(z) = \frac{1+f}{\kappa'} \sin \kappa' (z + z'_0)$ For κ' , see Table 1.3.12

* z'_0 is the distance to the plane on which the asymptotic solution vanishes, in units of the scattering length

Table 1.3.12 — Diffusion Length and Extrapolation Length for Milne's Problem for Anisotropic Scattering (Davison¹⁹)

$1 + f$	$(1 + f)z'_0$	$(\kappa')^2$
0	$1 - 3b$	-1
0.2	$0.7843 - 1.2197b$	$-0.99982 + 0.00350b$
.4	$.7300 - 0.1624b$	$-.9714 + .1660b$
.6	$.7154 + .3305b$	$-.8233 + .4009b$
.8	$.7113 + .5757b$	$-.5047 + .3902b$
1.0	$.7104 + .7104b$	0
1.2	$.7106 + .7897b$	$0.6965 - 0.8201b$
1.4	$.7117 + .8386b$	$1.5871 - 2.0921b$
1.6	$.7130 + .8693b$	$2.6732 - 3.8270b$
1.8	$.7142 + .8881b$	$3.9554 - 6.0305b$
2.0	$.7152 + .8998b$	$5.4341 - 8.7063b$
2.2	$.7162 + .9059b$	$7.1096 - 11.856b$
2.4	$.7173 + .9084b$	$8.9819 - 15.483b$
2.6	$.7184 + .9092b$	$11.051 - 19.585b$
2.8	$.7194 + .9077b$	$13.318 - 24.166b$
3.0	$.7203 + .9047b$	$15.781 - 29.224b$

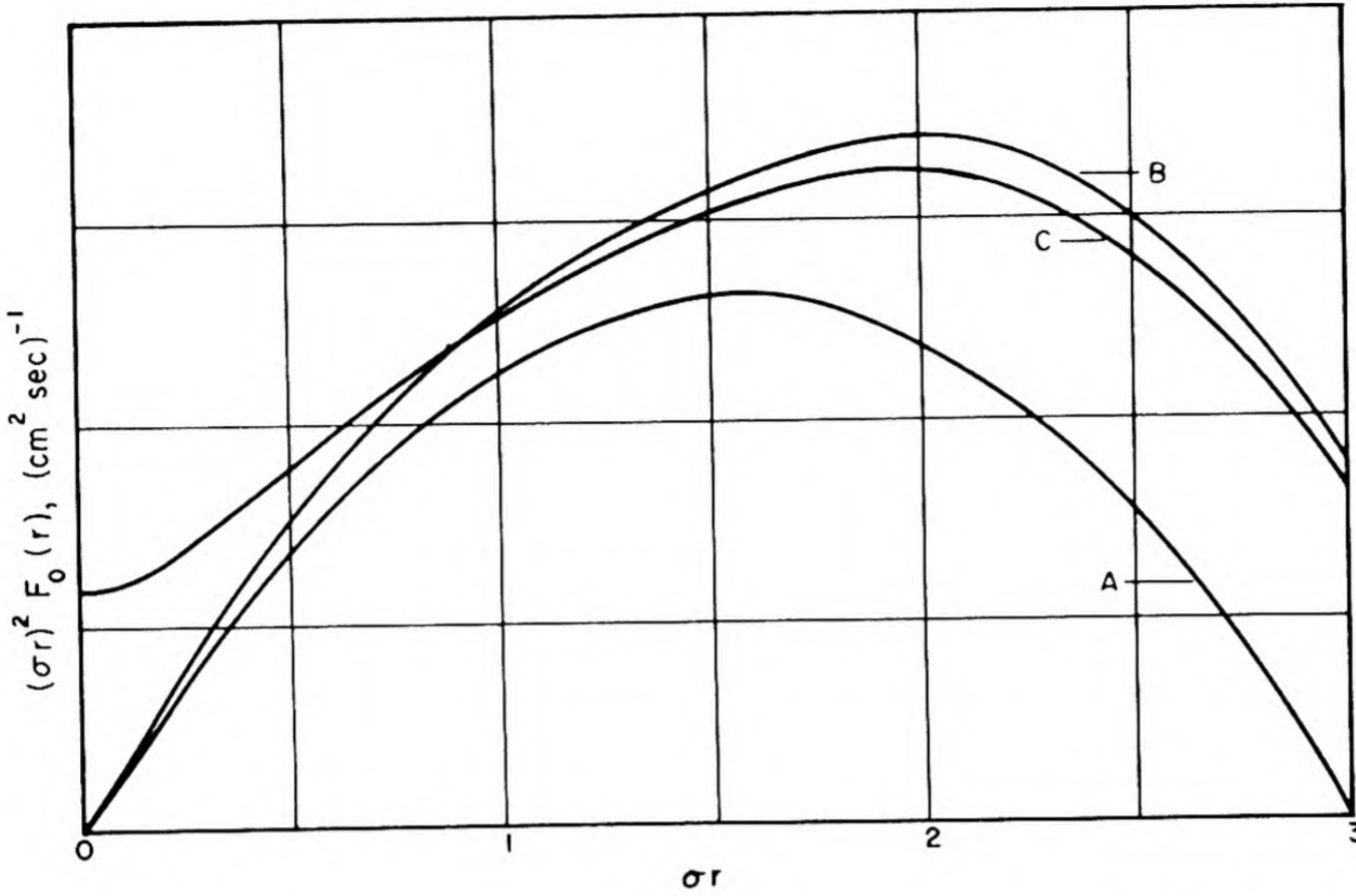


Fig. 1.3.5 — Flux from a Unit Source at the Center of a Non-absorbing Sphere of Radius Equal to Three Mean-free-paths. From R. E. Marshak, H. Brooks, And H. Hurwitz, Jr., *Nucleonics*, Vol. 4, No. 5, May 1949.

Curves III represent the probable shape of the dependence of $\lambda(a)$, indicated by spherical harmonics calculations.¹⁹⁻²⁵

The corresponding asymptotic solutions in the no-capture case as well as the plane boundary case are:

$$F_0^{as}(z) = \left(\frac{dF_0^{as}}{dz} \right)_{z=0} (z + \lambda) \quad (\text{plane}) \quad (86)$$

$$rF_0^{as}(r) = F_0^{as}(\infty) \left(r - \frac{a^2}{a + \lambda} \right) \quad (\text{sphere}) \quad (87)$$

$$F_0^{as}(r) = \left(\frac{dF_0^{as}}{dr} \right)_a [a \log(r/a) + \lambda] \quad (\text{cylinder}) \quad (88)$$

A diffusion-equation solution satisfying the boundary condition equation (80) gives the same result as transport theory does a few mean free paths away from the free boundary, since F_0^{as} satisfies the diffusion equation (72).

In many cases adequate results can be obtained by use of simple diffusion theory together with the known (from transport theory) values of λ for the given geometry.

Explicit use of transport theory is necessary, for example, to calculate the true flux and current near a strong absorber or near a free boundary.

Figure 1.3.5 plots solutions of the diffusion equation for the case of a bare sphere with a unit source at the center and $f = 0$, $R\sigma = 3$. Curve A is the solution of the straightforward diffusion equation (boundary condition $F_0(R) = 0$). Curve B is obtained by using an extrapolation prescription, and Curve C is the result of using both prescription (3) as well as an extrapolation length.

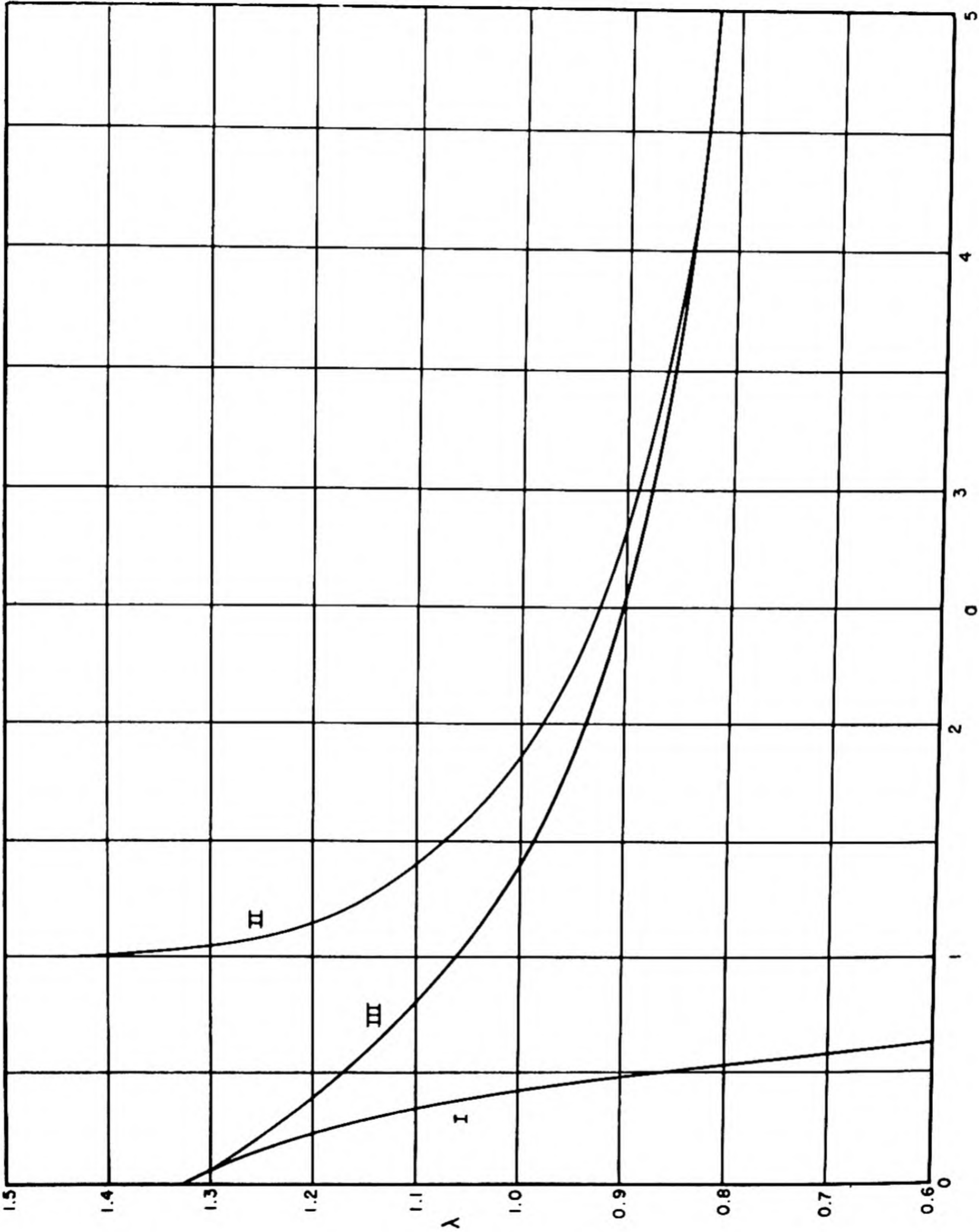


Fig. 1.3.6 — Extrapolation Distance for a Black Sphere of Radius a . From B. Davison and S. Kushneriuk, MT-214, Mar. 1946.

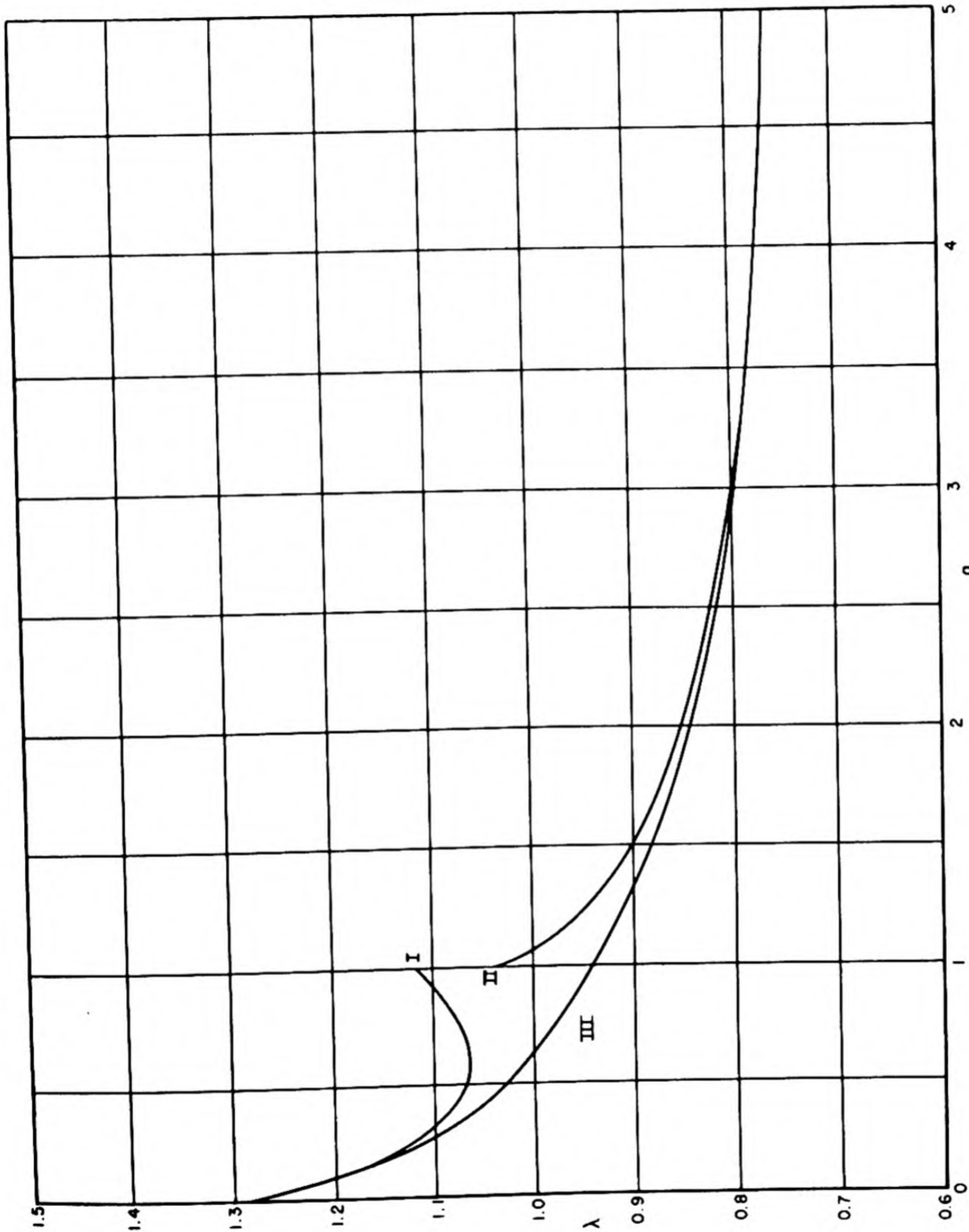


Fig. 1.3.7 — Extrapolation Distance for a Black Cylinder of Radius a . From B. Davison and S. Kushneriuk, MT-214, Mar. 1946.

In Fig. 1.3.8, $F_0(z)$ and $F_0^{as}(z)$ are shown for the no-capture case near a plane boundary to vacuum.

SOLUTIONS OF DIFFUSION AND TRANSPORT PROBLEMS IN BOUNDED REGIONS

The methods of particular interest in criticality calculations, viz., the variational method, the perturbation method, the iteration method, and the Serber-Wilson method, are discussed in Chapter 1.4.

The spherical harmonics method and its modifications²⁶⁻²⁹ summarized below are useful both in flux and reactor criticality calculations. The P_1 -approximation contains all the results of diffusion theory.

The Wiener-Hopf method and the related end-point method³⁰⁻³³ are useful in deriving the general results of transport theory.

The Spherical-harmonics Method

The basic idea of this method is to approximate the Boltzmann integrodifferential equation by a system of ordinary differential equations.

For slab geometry, the solutions to the system of linear differential equations (32) without source for the total flux F_0 and the higher angular moments are given in the P_{2n-1} -approximation for isotropic scattering by:

$$F_l(z) = \sum_{i=1}^n G_l(\nu_i) \left[A_i e^{\nu_i z} + B_i (-1)^l e^{-\nu_i z} \right] \quad (89)$$

$$l = 0, 1, \dots, 2n-1$$

For spherical geometry, the differential equations are in the P_{2n-1} -approximation:

$$\begin{aligned} (l+1) \left(\frac{d}{dr} + \frac{l+2}{r} \right) F_{l+1}(r) + l \left(\frac{d}{dr} - \frac{l-1}{r} \right) F_{l-1}(r) \\ + (2l+1) [F_l(r) - S_l(r)] - (1+f) F_0(r) \delta_{l0} = 0 \end{aligned} \quad (90)$$

The solutions $F_l(r)$ for $S_l = 0$ are given by:

$$F_l(r) = \sum_{i=1}^n G_l(\nu_i) [A_i H_l(\nu_i r) + (-1)^l B_i H_l(-\nu_i r)] \quad (91)$$

The functions $G_l(\nu)$ are defined by the recursion formula:

$$lG_l(\nu) + \frac{2l-1}{\nu} G_{l-1}(\nu) + (l-1)G_{l-2}(\nu) = 0 \quad (92)$$

and explicitly:

$$G_0 = 1$$

$$G_1 = f/\nu$$

$$G_2 = -\frac{1}{2\nu^2} (\nu^2 + 3f)$$

$$G_3 = \frac{1}{6\nu^3} [(5-4f)\nu^2 + 15f]$$

(93)

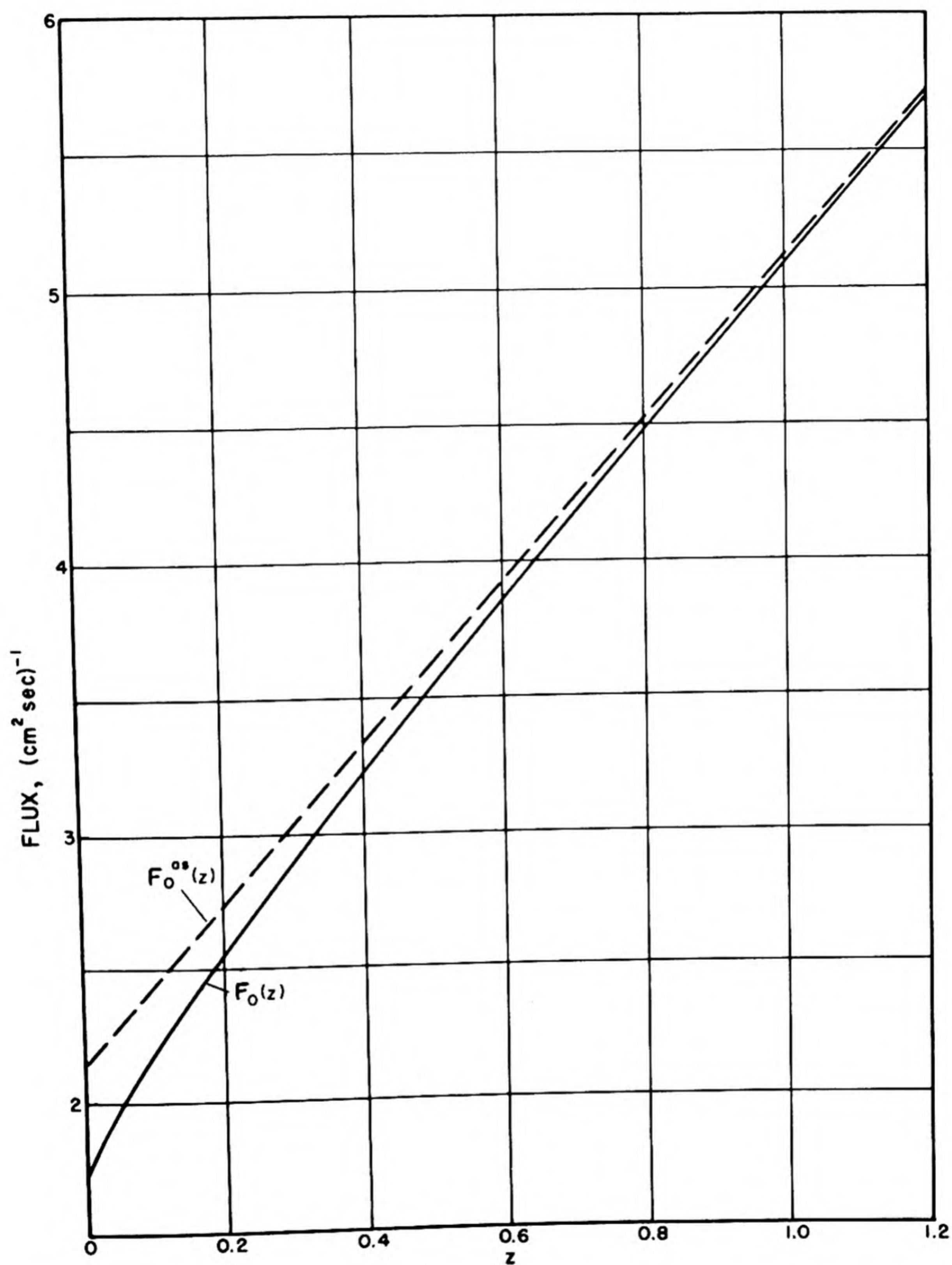


Fig. 1.3.8 — Behavior of the Asymptotic and Correct Flux near a Plane Boundary of a Semi-infinite Non-absorbing Medium. Data from C. Mark, Phys. Rev. 72, 1947.

The functions H_1 are related to the Bessel functions of purely imaginary argument of the second kind ($K_{1+1/2}$) by:

$$H_1(-x) = -\sqrt{\frac{2}{\pi x}} K_{1+1/2}(x) \quad (94)$$

Numerical values for the ν_i for use in the P_3 -approximation are given in Table 1.3.13.

Table 1.3.13 — ν_1 and ν_2 for the P_3 -approximation
(Mark⁶³)

f	$\pm\nu_1$	$\pm\nu_2$
-0	0	1.972
-0.1	0.526	2.055
-.2	.712	2.146
-.3	.835	2.242
-.4	.923	2.341
-.5	.989	2.443
-.6	1.040	2.544
-.7	1.080	2.646
-.8	1.113	2.746
-.9	1.139	2.844
-1.0	1.161	2.941

The ν_i for the P_{2n-1} -approximation are defined as roots of:

$$G_{2n}(\nu) = 0 \quad (95)$$

The smallest positive root of Eq. (95) is an approximation to κ defined by Eq. (58).
In regions containing isotropic sources (S_0), the solutions for slab geometry are:

$$F_1(z) = (F_1(z))_{\text{no source}} + p_1(z) \quad (96)$$

where:

$$p_1(z) = \sum_{i=1}^n C_i G_1(\nu_i) [e^{\nu_i z} u(\nu_i, z) + (-1)^i e^{-\nu_i z} u(-\nu_i, z)] \quad (97)$$

The c_i depend only on the ν_i ; for the P_3 -approximation:

$$c_1 = \frac{5(11\nu_1^2 - 21)}{9(\nu_1^2 - \nu_2^2)} \quad (98)$$

$$c_2 = \frac{5(11\nu_2^2 - 21)}{9(\nu_2^2 - \nu_1^2)}$$

The $u(\nu, z)$ are defined by:

$$u(\nu, z) \equiv \frac{1}{2\nu} \int_0^z S_0(t) e^{-\nu t} dt \quad (99)$$

For spherical geometry, the solutions for the $F_1(r)$ are:

$$F_1(r) = (F_1(r))_{\text{no source}} + p_1(r) \quad (100)$$

where:

$$p_1(r) = \sum_{i=1}^n c_i G_1(\nu_i) [H_1(\nu_i r) u(\nu_i, r) + (-1)^i H_1(-\nu_i r) u(-\nu_i, r)] \quad (101)$$

The c_i are defined by Eq. (98) and the $u(\nu_i r)$ are defined by:

$$u(\nu, r) = \frac{1}{2} \int_0^r S_0(t) t e^{-\nu t} dt \quad (102)$$

The arbitrary constants A_i and B_i occurring in Eqs. (89) and (91) are determined by the boundary conditions of Eq. (76).

For a semi-infinite medium only one exponentially increasing term is allowed, and $A_i = 0$ for $i = 2, 3, \dots, n$.

At a free surface ($z = a$), the following alternative boundary conditions have been used:

$$(1) \int_0^1 F(a, \mu) \mu^{2l+1} d\mu = 0, \quad l = 0, 1, \dots, n-1 \quad (103)$$

(2) The second medium is considered as a real pure absorber ($f = -1$); $F(a, \mu)$ is computed in the second medium by the spherical harmonics method and boundary-condition equation (76) is applied.

(3) $F(a, \mu)$ is required to vanish for a sufficient number of different values of μ_i to determine all constants. The values of μ_i selected are the n negative roots of $P_{2n}(\mu) = 0$.

It has been shown by Davison that conditions (2) and (3) are exactly equivalent. If media of various "greyness" are to be compared, prescription (2) may present an advantage.

A generalized spherical harmonics method applicable in principle to any geometry has been developed by Mark by using expansions in general tensor harmonics. From these expansions, angular moments for cylindrical geometry are obtained.

In any geometry, the flux F_0 satisfies in the P_{2n-1} -approximation the equation:

$$\prod_{i=1}^n (\nabla^2 - \nu_i^2) F_0(\underline{r}) = 0 \quad (104)$$

This equation factors and the constituent parts of F_0 which give its spatial dependence are solutions of Helmholtz equations:

$$(\nabla^2 - \nu_i^2) f_i(\underline{r}) = 0 \quad (105)$$

It is worth noting that the form of the solutions $f_i(\underline{r})$ depends on the geometry of the medium, but that the parameters ν_i entering the arguments of the solutions are independent of the geometry. They depend only on the order of the approximation used and on the value of f ; for any geometry, they are obtained from Eq. (95).

For slab and sphere geometries, only $2n$ F_1 's and $2n$ arbitrary constants occur in the P_{2n-1} -approximation, whereas $n(n+1)$ functions of (r) and $n(n+1)$ arbitrary constants occur in cylinder geometry.

Odd order approximations have been used more frequently; for the use of even-order approximations, see Mark.²⁶

It has been suggested²⁵ that, in the determination of extrapolation lengths, the even-order approximations converge to the exact result from above and the odd-order approximations converge from below.

Numerical work has shown that, in general, the third-order approximation leads to definite improvements over the first-order approximation and that higher approximations usually lead to smaller corrections.

Modified Spherical-harmonics Method (Wick's Method)

The basic idea of this method is to approximate the integral:

$$\int_{-1}^{+1} d\mu F(\mu, z)$$

occurring in the transport-theory equation by the use of an appropriate numerical integration formula. Wick chooses the Gauss integration formula:³⁴

$$\int_{-1}^{+1} d\mu F(\mu, z) = 2 \sum_{m=0}^n R_m F(z, \mu_m) \quad (106)$$

where the μ_m are defined as the $(n + 1)$ roots of:

$$P_{n+1}(\mu) = 0$$

and the R_m are listed through $n = 5$ in reference (35).

For $n = 1$:

$$R_0 = R_1 = 1/2$$

Equation (19) reduces to a system of ordinary differential equations:

$$\mu_i \frac{dF(z, \mu_i)}{dz} + F(z, \mu_i) = (1 + f) \sum_{m=0}^n R_m F(z, \mu_m) \quad (107)$$

n being the order of approximation. The angular dependent solution of Eq. (107) is different from that given by the spherical harmonics method. In Wick's method:

$$F(z, \mu) = \frac{1 + f}{2} \sum_{i=1}^{n+1} \frac{A_i}{1 + \nu_i \mu} e^{\nu_i z} \quad (108)$$

where the A_i are to be determined from the boundary conditions and, for n odd, the ν_i are the roots of Eq. (95).

The End-point Method

The mathematical technique used in the end-point method is to solve the integral equations of transport theory and the approximations to these equations by means of the Wiener-Hopf technique.

The basic idea of the Wiener-Hopf technique is to use the Laplace or Fourier transform of the neutron density. The transform of the neutron density can be expressed in terms of functions depending on f and the boundary conditions. It is frequently possible to determine the transforms by using Liouville's theorem and related arguments of the theory of complex variables. It is often very easy to derive simple results for the asymptotic neutron density and for the density near an interface by using the so-called Tauberian theorems.

The idea of the end-point method is to treat the behavior of the solution near each boundary as if no other boundaries existed. If the boundaries are far apart, the assumptions of the end-point method are certainly valid, and one-boundary Wiener-Hopf solutions for

different regions can be combined in such a way that the asymptotic components coincide.

It has been shown³⁶ that the method gives reasonable results if the distance between boundaries is only a few tenths of a mean attenuation distance.

The end-point method is applicable in one-dimensional problems (slab and spherical geometries) and is used in treating multiregion transport problems.

SPACE AND ENERGY VARIATIONS (Eugene Greuling and Harry Soodak)

FERMI AGE THEORY

AGING

If the diffusion approximation is made on the leakage term, there results the continuity equation:

$$\text{div } D \text{ grad } \varphi(r, E) - \sigma_a \varphi(r, E) + \frac{\partial q(r, E)}{\partial E} + S(r, E) = 0 \quad (109)$$

with:

$$D = \frac{1}{3\sigma_{tr}} \quad (110)$$

Combining this with the result of the Fermi slowing-down approximation, Eqs. (10) and (13):

$$q = \xi \sigma_s E \varphi \quad (111)$$

leads, in the case of space-independent cross sections, to:

$$\nabla^2 q(r, \tau) - 3\sigma_a \sigma_{tr} q(r, \tau) + \frac{\partial q(r, \tau)}{\partial \tau} + S(r, \tau) = 0 \quad (112)$$

where the age variable (τ) is defined* by:

$$d\tau = \frac{1}{3\xi\sigma_s\sigma_{tr}} \frac{dE}{E} \quad (113)$$

and:

$$S(r, \tau) = 3\xi\sigma_s\sigma_{tr} E S(r, E) \quad (114)$$

The age or age difference $\tau(E, E')$ between two energy values is defined by:

$$\tau(E, E') = \int_E^{E'} \frac{1}{3\xi\sigma_s\sigma_{tr}} \frac{dE''}{E''} \quad (115)$$

* τ is here defined as an increasing function of E rather than a decreasing function. If the latter alternative is chosen, the right side of Eq. (113) and the term $\partial q / \partial \tau$ of Eq. (112) should be changed in sign.

Eq. (112) may be rewritten as:

$$\nabla^2 q'(r, \tau) + \frac{\partial q'(r, \tau)}{\partial \tau} + p^{-1}(E, E_0) S(r, \tau) = 0 \quad (116)$$

with:

$$q = p(E, E_0) q' \quad (117)$$

where:

$$p(E, E_0) = e^{-\int_E^{E_0} \frac{\sigma_a}{\xi \sigma_s} \frac{dE}{E}} \quad (118)$$

and E_0 is any energy value. It is seen that, for a monoenergetic source, the solution with absorption is simply the solution without absorption multiplied by the infinite-medium resonance escape probability (as given by the Fermi slowing-down theory).

Tables 1.3.14 and 1.3.15 present some important solutions^{37,38} of the age equation in the case of single homogeneous regions. It is assumed that, for the finite regions, the extrapolated boundary (see below, "Finite Regions and Boundary Conditions") is independent of energy. It is seen that the second moment of the slowing-down distribution (the mean square distance between birth position and position of crossing a given energy value) is:

$$\overline{r^2}(E, E_0) = 6\tau(E, E_0) \quad (119)$$

Two media problems are difficult to solve because of the complicated boundary conditions (see below). Some solutions to such problems exist. Bellman, Marshak, and Wing,³⁹ have reported the solution to the problem of a monoenergetic source displaced from the plane interface between two semi-infinite non-absorbing media in which the ratio of scattering cross sections is independent of energy, and a similar problem has been reported on earlier by Friedman.⁴⁰

Table 1.3.14 — Aging in Infinite Homogeneous Medium

$[\tau = \tau(E, E_0); p = p(E, E_0)]$

Source	$q(\underline{r}, E)$	Comments
Point source At $r = 0, E = E_0$ $S = \frac{\delta(\underline{r})}{4\pi r^2} \delta(E - E_0)$	$p \frac{e^{-\frac{r^2}{4\tau}}}{(4\pi\tau)^{3/2}}$	$\overline{r^2}(E, E_0) = 6\tau$
Plane source At $x = 0, E = E_0$ $S = \delta(x) \delta(E - E_0)$	$p \frac{e^{-\frac{x^2}{4\tau}}}{(4\pi\tau)^{1/2}}$	$\overline{x^2} = \frac{1}{3} \overline{r^2} = 2\tau$
"Laplacian" source At $E = E_0$ $S = \delta(E - E_0) f(\underline{r})$ Where $\nabla^2 f(\underline{r}) = -B^2 f(\underline{r})$	$f(\underline{r}) e^{-\int_E^{E_0} \frac{\sigma_a^{eff}}{\xi \sigma_s} \frac{dE}{E}}$	$\sigma_a^{eff} = \sigma_a + DB^2$

Table 1.3.15—Aging in Finite Homogeneous Medium

$$[\tau = \tau(E, E_0); p = p(E, E_0)]$$

Case	$q(\underline{r}, E)$
Point source in sphere of extrapolated radius = a $S = \frac{\delta(\underline{r})}{4\pi r^2} \delta(E - E_0)$	$q(\underline{r}, E) = \frac{p}{2a^2 r} \sum_{m=1}^{\infty} m \sin \frac{m\pi r}{a} e^{-\frac{m^2 \pi^2}{a^2} \tau}$ $= p \frac{e^{-\frac{r^2}{4\tau}}}{(4\pi\tau)^{3/2}} \left[1 + 2 \sum_{m=1}^{\infty} \left(\cosh \frac{amr}{\tau} - \frac{2am}{r} \sinh \frac{amr}{\tau} \right) e^{-\frac{m^2 a^2}{\tau}} \right]$
Plane (non-uniform) source in infinite column of extrapolated dimensions = a, b $S = \delta(E - E_0) \delta(z) \sum_{l,m=1}^{\infty} S_{lm} \sin \frac{l\pi x}{a} \sin \frac{m\pi y}{b}$	$q(\underline{r}, E) = p \sum_{l,m=1}^{\infty} q_{lm} \sin \frac{l\pi x}{a} \sin \frac{m\pi y}{b}$ <p>where:</p> $q_{lm} = S_{lm} \frac{e^{-\frac{z^2}{4\tau}}}{(4\pi\tau)^{3/2}} e^{-\frac{1}{2}\tau \left(\frac{l^2}{a^2} + \frac{m^2}{b^2} \right)}$
Point source in infinite column of extrapolated dimensions = a, b $S = \delta(E - E_0) \delta(z) \delta(x - x_0) \delta(y - y_0)$	<p>Solution obtained from preceding one, with:</p> $S_{lm} = \frac{4}{ab} \sin \frac{l\pi x_0}{a} \sin \frac{m\pi y_0}{b}$ <p>or:</p> $q = p \frac{e^{-\frac{z^2}{4\tau}}}{(4\pi\tau)^{3/2}} \sum_{l,m=-\infty}^{+\infty} \left[e^{-\frac{(x-x_0+2al)^2}{4\tau}} - e^{-\frac{(x+x_0+2al)^2}{4\tau}} \right] \cdot \left[e^{-\frac{(y-y_0+2bm)^2}{4\tau}} - e^{-\frac{(y+y_0+2bm)^2}{4\tau}} \right]$
"Laplacian" source vanishing at extrapolated boundary: $S = \delta(E - E_0) f(\underline{r})$ $\nabla^2 f(\underline{r}) = -B^2 f(\underline{r})$ $f(\underline{r}) = 0$ at extrapolated boundary	$q(\underline{r}, E) = f(\underline{r}) e^{-\int_E^{E_0} \frac{\sigma_a^{eff}}{\xi \sigma_s} \frac{dE}{E}}$ <p>where</p> $\sigma_a^{eff} = \sigma_a + DB^2$

AGING FOLLOWED BY DIFFUSION

In thermal reactors, the aging process continues until thermal energies are reached, and the thermal neutrons then diffuse (see "Thermal Distributions," above and "Diffusion of Thermal Neutrons," below). If it is assumed that the change from aging to diffusion occurs at a definite energy (E_{th}), the thermal-neutron flux (φ_{th}), satisfies:

$$\text{div } D_{th} \text{ grad } \varphi_{th}(\underline{r}) - \sigma_{a,th} \varphi_{th}(\underline{r}) + q(\underline{r}, E_{th}) = 0 \quad (120)$$

the solution to which in the case of an infinite homogeneous medium, can be expressed, cf., Eq. (50) and Table 1.3.9, as:

$$\varphi_{th}(\underline{r}) = \int \frac{e^{-\kappa|\underline{r}-\underline{r}'|}}{4\pi D_{th} |\underline{r}-\underline{r}'|} q(\underline{r}', E_{th}) d\underline{r}' \quad (121)$$

where:

$$\kappa = \left(\frac{\sigma_{a,th}}{D_{th}} \right)^{1/2} = \frac{1}{L} \quad (122)$$

and is the reciprocal diffusion length.

Solutions^{17,37,38} of the problem of aging followed by diffusion for some interesting fast-neutron sources in simple geometries are presented in Tables 1.3.16 and 1.3.17. The extrapolated boundary is assumed to be energy-independent. It is seen that the second moment (the mean square distance between birth position and position of death by thermal absorption) is given by:

$$\overline{r^2}(E_{th}, E_0) = 6[\tau(E_{th}, E_0) + L^2] = 6M^2 \quad (123)$$

where M^2 is called the "migration area" and M is the migration length.

Figure 1.3.9 plots $r^2 \varphi_{th}$ for a point source in an infinite medium; Fig. 1.3.10 plots $4\pi \int_0^r r^2 \varphi_{th} dr$, the thermal flux within (r); and Fig. 1.3.11 plots $4\pi \int_0^a r^2 \varphi_{th} dr$ for a point source at the center of a sphere of extrapolated radius (a).

Table 1.3.16—Aging Followed by Diffusion in Infinite Homogeneous Medium

$$[\tau = \tau(E_{th}, E_0); p = p(E_{th}, E_0)]$$

Source	$\varphi_{th}(r)$	Comments
Point source at: $r = 0, E = E_0$ $S = \frac{\delta(\underline{r})}{4\pi r^2} \delta(E - E_0)$	$\varphi_{th}(\underline{r}) = \frac{p}{8\pi D_{th} r} \left\{ e^{-\kappa r} \left[1 - \operatorname{erf} \left(\kappa \sqrt{\tau} - \frac{r}{2\sqrt{\tau}} \right) \right] \right.$ $\left. - e^{\kappa r} \left[1 - \operatorname{erf} \left(\kappa \sqrt{\tau} + \frac{r}{2\sqrt{\tau}} \right) \right] \right\}$ $\varphi_{th}(\underline{r}) \approx \frac{e^{\kappa^2 \tau}}{4\pi D_{th} r} e^{-\kappa r} - \frac{\sqrt{\tau/\pi}}{2\pi D_{th} r^2} e^{-r^2/4\tau}$ <p>for $r \gg 2\kappa\tau$</p>	$r^2 = 6(\tau + L^2) = 6M^2$ $L^2 = 1/\kappa^2 = D_{th}/\sigma_{a,th}$
Plane source at: $x = 0, E = E_0$ $S = \delta(x) \delta(E - E_0)$	$\varphi_{th}(x) = p \frac{e^{\kappa^2 \tau}}{4\kappa D_{th}} \left\{ e^{-\kappa x} \left[1 + \operatorname{erf} \left(\frac{x}{2\sqrt{\tau}} - \kappa \sqrt{\tau} \right) \right] \right.$ $\left. + e^{\kappa x} \left[1 - \operatorname{erf} \left(\frac{x}{2\sqrt{\tau}} + \kappa \sqrt{\tau} \right) \right] \right\}$	$\overline{x^2} = \frac{1}{3} r^2$
"Laplacian" source at: $E = E_0$ $S = \delta(E - E_0) f(\underline{r})$ where $\nabla^2 f(\underline{r}) = -B^2 f(\underline{r})$	$\varphi_{th}(\underline{r}) = \frac{1}{\sigma_{a,th}^{eff}} q(\underline{r}, E_{th})$ $= \frac{f(\underline{r})}{\sigma_{a,th}^{eff}} e^{-\int_{E_{th}}^{E_0} \frac{\sigma_a^{eff}}{\xi \sigma_s} \frac{dE}{E}}$	$\sigma_a^{eff} = \sigma_a + DB^2$ <p>and thus</p> $\sigma_{a,th}^{eff} = D_{th} (\kappa^2 + B^2)$

Table 1.3.17 — Aging Followed by Diffusion in Finite Homogeneous Media

$$[\tau = \tau(E_{th}, E_0); p = p(E_{th}, E_0); \kappa^2 = \sigma_{a,th}/D_{th}]$$

Case	$\varphi_{th}(r)$
Point source at center of sphere of extrapolated radius = a $S = \frac{\rho(r)}{4\pi r^2} \delta(E - E_0)$	$\varphi_{th}(r) = \frac{p}{2D_{th}r} \sum_{m=1}^{\infty} \frac{m}{\kappa^2 a^2 + m^2 \pi^2} e^{-\frac{m^2 \pi^2}{a^2} \tau} \sin \frac{m\pi r}{a}$ $= \frac{p}{8\pi D_{th}r} \sum_{m=-\infty}^{\infty} \left\{ e^{-\kappa(r+2am)} \left[1 - \operatorname{erf} \left(\kappa \sqrt{\tau} - \frac{r+2am}{2\sqrt{\tau}} \right) \right] \right. \\ \left. - e^{\kappa(r+2am)} \left[1 - \operatorname{erf} \left(\kappa \sqrt{\tau} + \frac{r+2am}{2\sqrt{\tau}} \right) \right] \right\}$ $\varphi_{th}(r) \approx \frac{p e^{\kappa^2 \tau}}{4\pi D_{th}r} (e^{-\kappa r} - e^{-2a\kappa} e^{\kappa r}) \text{ for } r \gg 2\kappa\tau \text{ and } r \gg 1/\kappa$
Plane (non-uniform) source in infinite column of extrapolated dimensions = a, b $S = \delta(E - E_0) \delta(z)$ $\times \sum_{l,m=1}^{\infty} S_{lm} \sin \frac{l\pi x}{a} \sin \frac{m\pi y}{b}$	$\varphi_{th}(r) = p \sum_{l,m=1}^{\infty} \varphi_{lm} \sin \frac{l\pi x}{a} \sin \frac{m\pi y}{b}$ <p>where:</p> $\varphi_{lm} = \frac{S_{lm} e^{\kappa^2 \tau}}{4\omega D_{th} \kappa} \left\{ e^{-\omega \kappa z} \left[1 + \operatorname{erf} \left(\frac{z}{2\sqrt{\tau}} - \omega \kappa \sqrt{\tau} \right) \right] \right. \\ \left. + e^{\omega \kappa z} \left[1 - \operatorname{erf} \left(\frac{z}{2\sqrt{\tau}} + \omega \kappa \sqrt{\tau} \right) \right] \right\}$ <p>and:</p> $\omega = \sqrt{1 + \frac{\pi^2}{\kappa^2} \left(\frac{l^2}{a^2} + \frac{m^2}{b^2} \right)}$ $\varphi_{lm} \approx \frac{S_{lm} e^{\kappa^2 \tau}}{2\omega D_{th} \kappa} e^{-\omega \kappa z } \text{ for } z \gg \omega \kappa \tau$
Point source in infinite column of extrapolated dimensions = a, b $S = \delta(E - E_0) \delta(z) \delta(x - x_0) \delta(y - y_0)$	Solution obtained from preceding one, with $S_{lm} = \frac{4}{ab} \sin \frac{l\pi x_0}{a} \sin \frac{l\pi y_0}{b}$
"Laplacian" source vanishing at extrapolated boundary $S = \delta(E - E_0) f(r)$ $\nabla^2 f(r) = -B^2 f(r)$ $f(r) = 0$ at extrapolated boundary	$\varphi_{th}(r) = \frac{1}{\sigma_{a,th}^{eff}} q(r, E_{th})$ <p>where $\sigma_{a,th}^{eff} = DB^2 + \sigma_a$</p> $\varphi_{th}(r) = \frac{f(r)}{\sigma_{a,th}^{eff}} e^{-\int_{E_{th}}^{E_0} \frac{\sigma_a^{eff}}{\xi \sigma_s} dE}$ <p>where $\sigma_{a,th}^{eff} = D_{th}(B^2 + \kappa^2)$</p>

IMPROVEMENTS ON FERMI AGE THEORY

The inaccuracy of age theory is reflected in the gaussian distribution of Table 1.3.14, the moment formula, Eq. (119), the resonance escape formula, Eq. (118), and the effective escape integral in the third row of Table 1.3.14. The deviation from the gaussian distribution and the special case of hydrogenous media are considered below. The moment and escape-integral difficulties, although interrelated, are treated consecutively below.

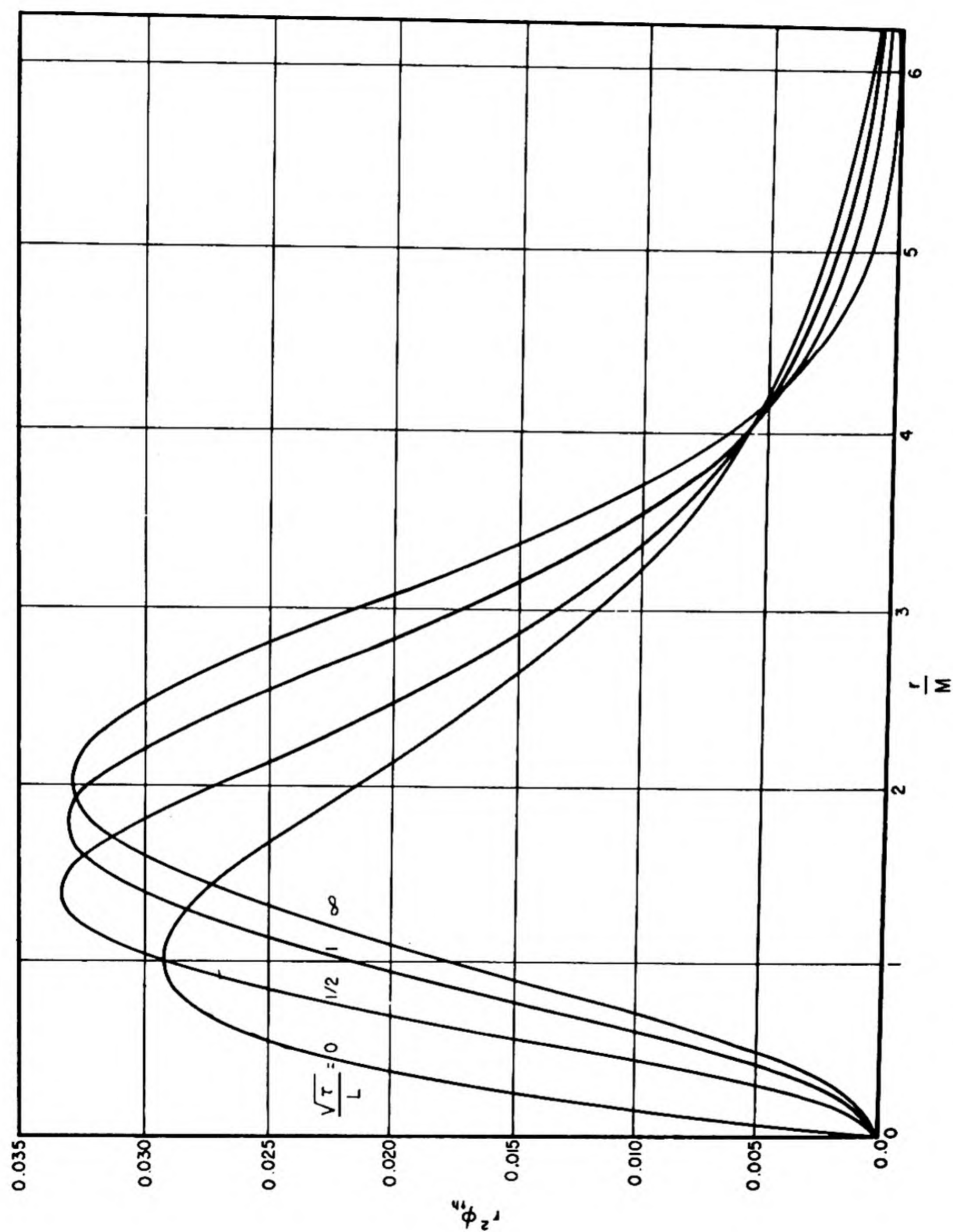


Fig. 1.3.9— Aging Followed by Diffusion in Infinite Medium Owing to Point Source of Fast Neutrons; $r^2 \phi_{th}(r)$ vs Position. Reprinted from Wallace and Le Caine, MT-12, NRC-1480.

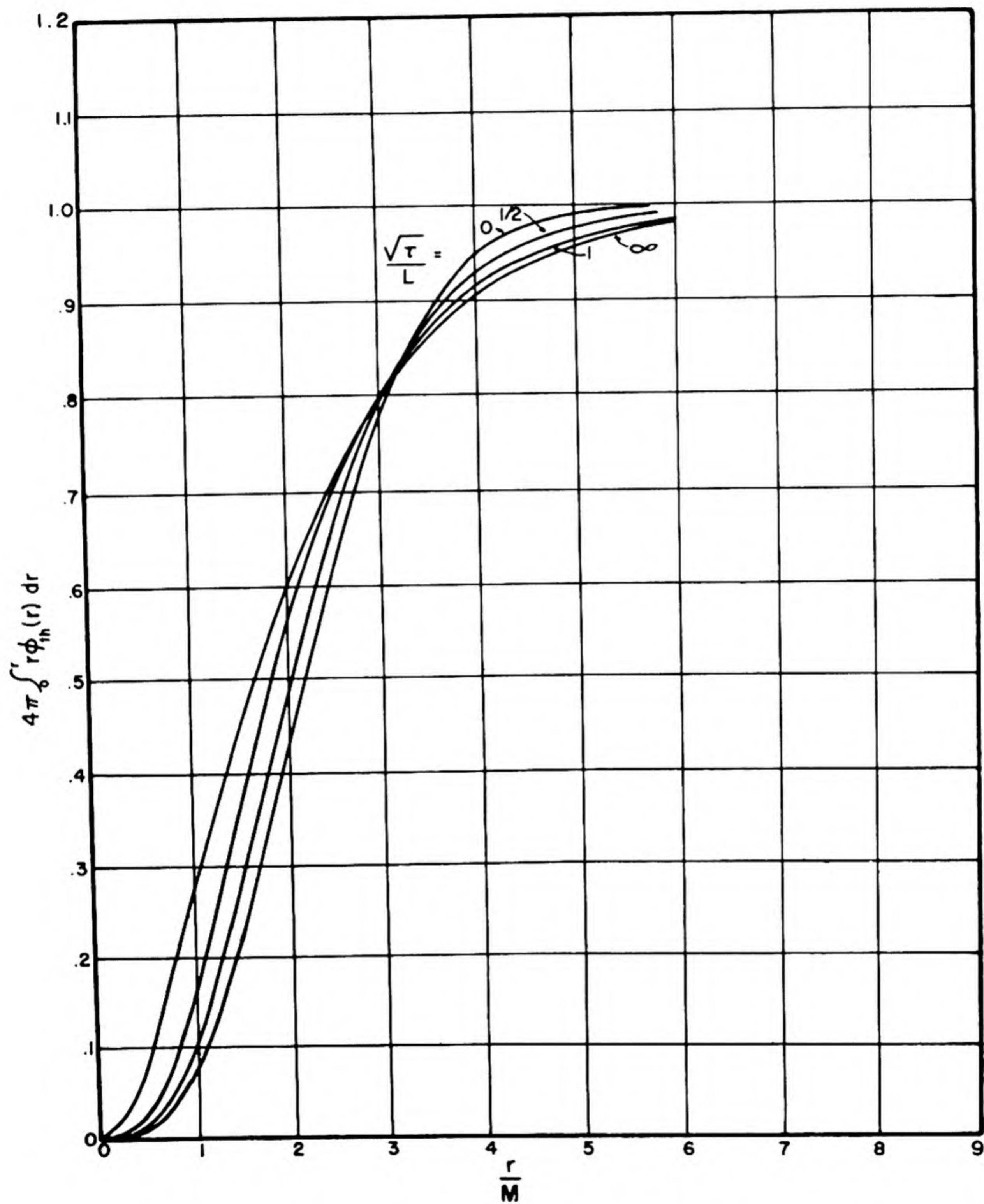


Fig. 1.3.10 — Aging Followed by Diffusion in Infinite Medium Owing to Point Source of Fast Neutrons; $4\pi \int_0^r r^2 \phi_{th}(r) dr$ vs Position. Reprinted from Wallace and Le Caine, MT-12, NRC-1480.

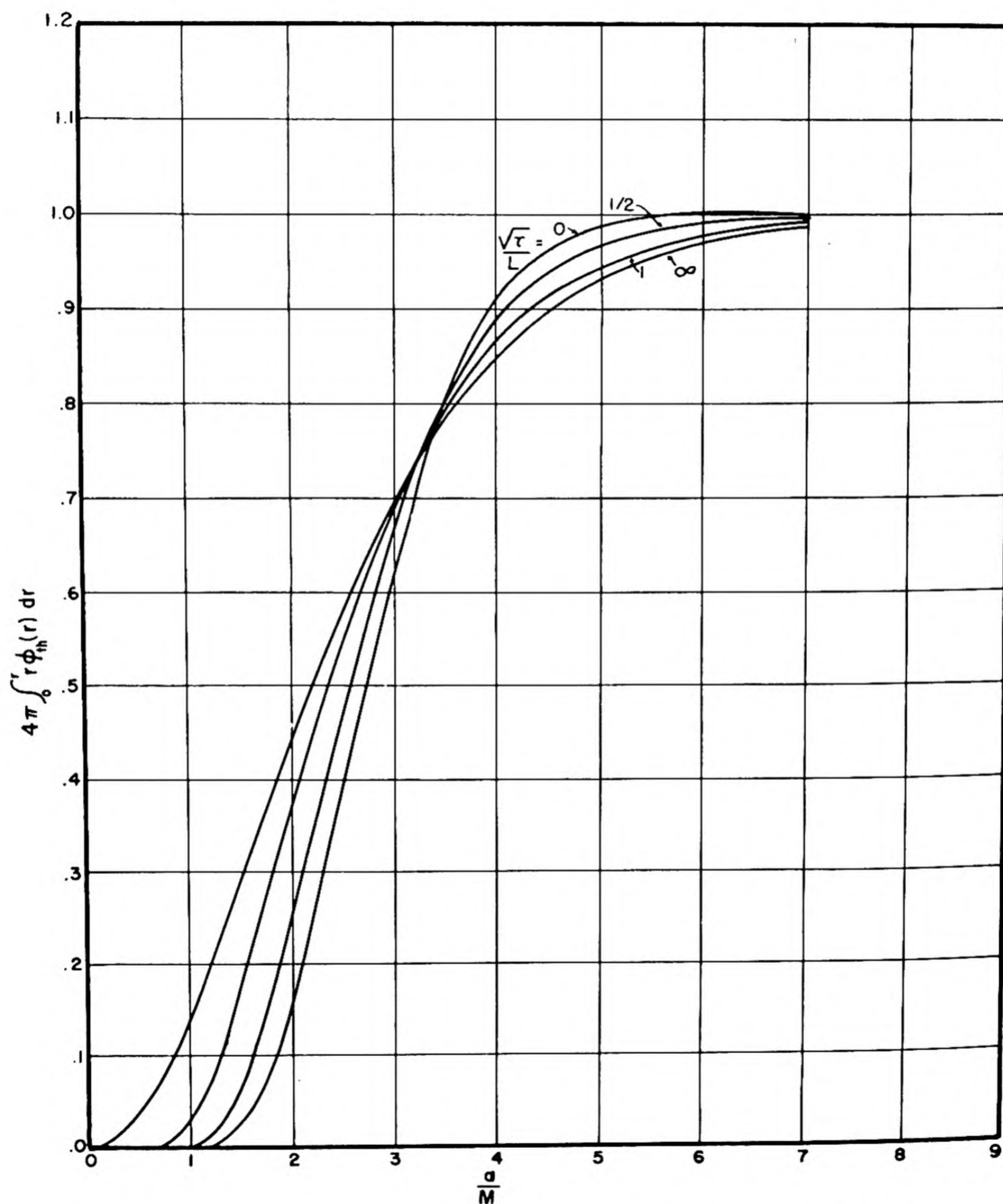


Fig. 1.3.11 — Aging Followed by Diffusion Owing to Central Point Source of Fast Neutrons in Finite Sphere of Extrapolated Radius a ; $4\pi \int_0^a r^2 \phi_x(r) dr$ vs a . Reprinted from Wallace and Le Caine, MT-12, NRC-1480.

MOMENT IMPROVEMENTS IN THE ABSENCE OF ABSORPTION

Equations (119) and (115) generally underestimate the second moment owing to a point source. As shown by Young,^{41,42} this is a result of the incorrect energy spectrum of age theory, the correct moment in the absence of absorption for an arbitrary source, $S(E)$, being given by:

$$\overline{r_q^2}(E) = 2 \int_E^\infty l \varphi(E) dE \quad (124)$$

where $\varphi(E)$, is the flux in an infinite homogeneous medium resulting from an integrated source strength of 1 per unit volume. For isotropic scattering in the laboratory system, Eq. (124) is exact with:

$$l = \frac{1}{\sigma_s(E)}$$

while for non-isotropic scattering, it is approximate with:

$$l = 1/\sigma_{tr}(E)$$

For the source:

$$S(E) = \frac{1}{\xi(1-\alpha)} \left(\frac{1}{E_0} - \frac{\alpha}{E} \right)$$

in the interval αE_0 up to E_0 , the flux (see "Exact Solutions for Special Sources" above) is given exactly by:

$$\varphi(E) = \frac{1}{\xi \sigma_s E}$$

and the resulting second moment is simply $6\tau(E, E_0)$, the age-theory result for a monoenergetic source at E_0 .

For the monoenergetic source, however, to which Eq. (119) applies, the exact spectrum $\varphi(E)$ (see "Fluctuations near Source Energy," above) differs from the asymptotic spectrum:

$$\varphi_a(E) = \frac{1}{\xi \sigma_s E}$$

in the first few collision intervals and also at the source energy E_0 , where:

$$\varphi(E_0) = \frac{1}{\sigma_s(E_0)} \delta(E - E_0)$$

Thus, Eq. (124) leads to:

$$\overline{r_q^2}(E, E_0) = \frac{2l(E_0)}{\sigma_s(E_0)} + 6\tau(E, E_0) + 2 \int_E^{E_0} l[\varphi(E) - \varphi_a(E)] dE \quad (125)$$

which gives the mean square distance between birth position at E_0 and position of crossing the energy, E .

Another second moment ($\overline{r_\varphi^2}$), the mean square distance between birth position and position of collision at energy E , is given in the Fermi, Wigner, and G. G. approximations (see "Slowing Down with No Space Variation," above) by:

$$\bar{r}_\phi^2(E) = \bar{r}_q^2(E) + \frac{2\epsilon}{\sigma_s(E) \sigma_{tr}(E)} \quad (126)$$

for energies (E) below the source energies. Equations similar to Eq. (126)* are usually written and, in the case of a monoenergetic source, used in conjunction with Eq. (125) modified by neglecting the difference between the exact and asymptotic flux. This procedure gives \bar{r}_ϕ^2 to within 1 percent of the result of an exact computation† in carbon.

ESCAPE-INTEGRAL IMPROVEMENTS

Equations (3) and (4) in the Fermi, Wigner, and G. G. approximations imply:

$$\epsilon \frac{\partial q(\underline{r}, E)}{\partial E} = \frac{q(\underline{r}, E)}{\xi E} - \sigma_s(E) \phi(\underline{r}, E) \quad (127)^\dagger$$

which for the Fermi case ($\epsilon = 0$) is identical to Eq. (111) and leads to age theory. The combination of Eq. (127) with the diffusion equation (109) gives for space-independent cross sections:

$$\nabla^2 q - 3\sigma_a \sigma_{tr} q + (1 + \epsilon \frac{\sigma_a}{\sigma_s}) \frac{\partial q}{\partial \tau} - \frac{\epsilon}{3\sigma_s \sigma_{tr}} \frac{\nabla^2 \partial q}{\partial \tau} + S(\underline{r}, \tau) = 0 \quad (128)$$

rather than Eq. (112).

The solution of Eq. (128) cannot be expressed as a product, as in Eq. (117), of the escape integral and the solution without absorption. For a monoenergetic laplacian or mode source (cf. Tables 1.3.14 and 1.3.15), the solution can be obtained by replacing ∇^2 by $-B^2$ and then using Table 1.3.3. The result is:

$$q(\underline{r}, E) = f(\underline{r}) \left[\frac{1}{1 + \epsilon \frac{\sigma_a + DB^2}{\sigma_s}} \right]_{E=E_0} e^{-\int_E^{E_0} \frac{\sigma_a^{eff}}{\xi \sigma_s} \frac{dE}{E}} \quad (129)$$

where:

$$D = \frac{1}{3\sigma_{tr}(E)}$$

and:

$$\sigma_a^{eff} = \frac{\sigma_a + DB^2}{1 + \epsilon \frac{\sigma_a + DB^2}{\sigma_s}} \quad (130)$$

For a point monoenergetic source, an ad hoc alternative⁴⁵ to the use of Eq. (128), which retains the simplicity of the age-theory result Eq. (117) (Tables 1.3.14 through 1.3.17), con-

*Weinberg and Noderer⁴³ write, in essence, the formula:

$$\bar{r}^2 = \bar{r}_q^2 + \frac{2}{[\sigma_s(E)]^2}$$

† Marshak⁴⁴ fits the scattering cross section by a sum of powers of the energy, and proceeds according to the methods described below in "Exact Space-dependence of Slowing-down Density."

‡ Eq. (127) results in Eq. (10) when Eq. (2) is valid, that is, when there is no leakage.

KINETIC THEORY OF NEUTRONS

sists of replacing Eq. (118) by a more accurate infinite-medium escape integral (Tables 1.3.3, 1.3.4, and 1.3.6) and replacing $\tau(E, E_0)$ as given by Eq. (115) by one-sixth of the measured (or more accurately computed) $\bar{r}_q^2(E, E_0)$. More general source solutions are obtainable from these ad hoc solutions by superposition.

EXACT SPACE DEPENDENCE OF SLOWING-DOWN DENSITY

DEVIATIONS FROM THE GAUSSIAN DISTRIBUTION

In an infinite nonabsorbing medium having only elastic scattering with energy-independent cross section, results more exact than those from Fermi theory have been obtained.

A Laplace transform (i.e., multiply by $e^{-\eta u}$ and integrate from 0 to ∞) of the Boltzmann equation for the collision density leads to an equation similar to Eq. (17). This "one-velocity" problem has been treated by the spherical-harmonic method.⁴⁶

An alternative method^{47,48} involves a further Fourier transform with respect to the space variable, z (i.e., multiply the equivalent one-velocity equation by e^{izy} and integrate from $-\infty$ to $+\infty$), before spherical-harmonic expansions are made. The resulting infinite sequence of equations is then solved approximately, and the Fourier and Laplace inversions are performed—the latter by the method of steepest descents. For a plane, isotropic, monoenergetic (E_0) source, with z the distance from the plane in units of the mean free path:

$$u = \ln(E_0/E)$$

$$u' = \frac{M}{2} u$$

where M is the mass of the scattering nuclei, and:

$$\tau = u/3 \xi \bar{\mu}_0$$

is the Fermi age, the resulting slowing-down density can be written (for $z < u'$) as:

$$q(z, \tau) = k(z/u') \frac{e^{-\frac{z^2}{4\tau}} \phi(z/u')}{\sqrt{4\pi\tau}} \quad (131)$$

where ϕ and K are as shown in Table 1.3.18.

The first-mentioned spherical-harmonics method, carried through the P_2 -approximation, leads to a less accurate but simpler result for $M \gg 1$, namely;

$$q(z, \tau) = [1 + (1/4)F(z^2/\tau)] \frac{e^{-\frac{z^2}{4\tau}}}{\sqrt{4\pi\tau}} \quad (132)$$

where:

$$F(z^2/\tau) = (B_1 - 2B_0) - (2B_1 - B_0)(z^2/\tau) + (B_1/4)(z^2/\tau)^2 \dots$$

$$B_0 = -\frac{4}{15M} \left(1 - \frac{7}{3M} + \dots \right)$$

$$B_1 = \frac{18}{5M} \left(1 - \frac{2}{3M} + \dots \right)$$

Equation 132 was first obtained by Placzek⁴⁹ using the method of moments.

In Fig. 1.3.12, a comparison between theory, Eq. (132), and an experimental measurement⁵⁰ in graphite is shown. An Sb^{124} -Be photoneutron source ($E_0 \approx 20$ kev) was used, and the saturated activity, A_s (which is almost proportional to q), of indium foils was measured out to about 60 cm from the source. In this energy range, the neutron mean free path is essentially constant. For comparison, the gaussian age-theory result is also shown in Fig. 1.3.12.

ASYMPTOTIC SPACE DEPENDENCE

At very large distances ($z > \frac{M}{2} u$), Wick has shown that $q \sim e^{-z}$. Numerical work done for $M = 12$ by Marshall, a student of Wick, yields the following asymptotic result:

$$q(u, z) \sim e^{-z} \left[1 - 1.44 \left(\frac{u}{z} \right)^{1/2} + 0.250 \left(\frac{u}{z} \right) + \dots \right] \quad (133)$$

for the same problem as considered previously.

Wick et al also consider energy-dependent cross sections, finding that in a nonabsorbing medium the asymptotic space variation is as $z^b e^{-z}$, where z is measured in units of the mean free path at the source energy and b depends upon how rapidly the mean free path decreases with decreasing energy.

In a multiplying medium with k (number of neutrons produced per neutron absorbed) slightly less than unity, the general asymptotic solution for the fission density at distance z from a plane source (of unit fission rate per unit area) is:⁵¹

$$f(z) = \frac{1}{2m\sqrt{1-k}} e^{-z\sqrt{1-k}/m} \quad (134)$$

where m^2 is the mean square migration distance of the neutrons, cf. Eq. (123), from fission birth to where they in turn produce fissions.

By the use of Eq. (27), point sources can be handled from the results for plane sources, e.g.:

$$q(r, \tau) = - \left[\frac{1}{2\pi z} \frac{\partial q(z, \tau)}{\partial z} \right]_{z=r} \quad (135)$$

HYDROGENOUS MEDIA

SLOWING-DOWN DISTRIBUTION

When a large fraction of the neutron energy may be lost in a single collision, as is the case for neutron-proton collisions, the Fermi age-diffusion equation (112) should be replaced by Eq. (128) with $\epsilon = 1$ for hydrogen scattering. For hydrogen, Eq. (128) is exact except for the diffusion approximation that leads to the $\nabla^2 q$ term. A solution of Eq. (128) with $\sigma_a = 0$, discussed below and shown in Fig. 1.3.13, which takes into account the energy variation of σ_s and σ_{tr} in H_2O does not give a gaussian slowing-down space distribution. If the Fermi age-diffusion equation (112) is used for hydrogen, i.e., $\epsilon = 0$ in Eq. (128), a gaussian distribution is obtained (cf. Table 1.3.14).

Despite the non-applicability of Eq. (112) for hydrogen, Wick has shown that, for constant cross section, for $M = 1$, and for non-absorbing media, the collision density of neutrons (ψ_0) slowed down through a logarithmic energy range u is very close to the gaussian distribution up to distances of u mean free paths; see Fig. 1.3.14, Table 1.3.18, and Eq. (131). The deviation from age theory (curve B of Fig. 1.3.14) becomes very large only at distances greater than u mean free paths (factor of ten at $2u$ mean free paths: curve A). Asymptotically, ψ_0 behaves as shown in curve C.

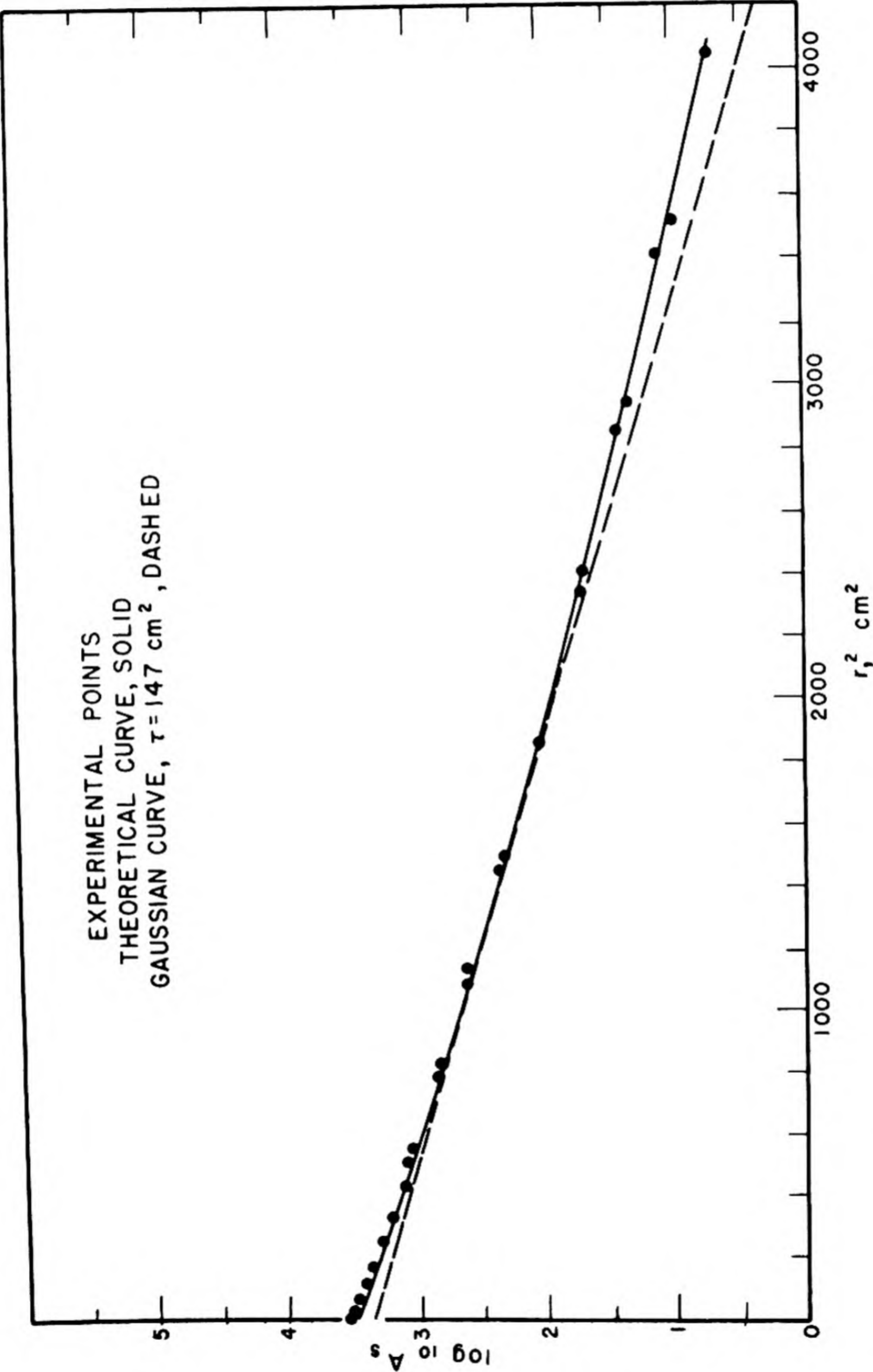


Fig. 1.3.12—Slowing-down Density to Indium Resonance in Graphite from an Sb^{124} -Be Photoneutron Source. From L. D. Roberts, J. E. Hill, and G. McCammon, ORNL-201, 1950.

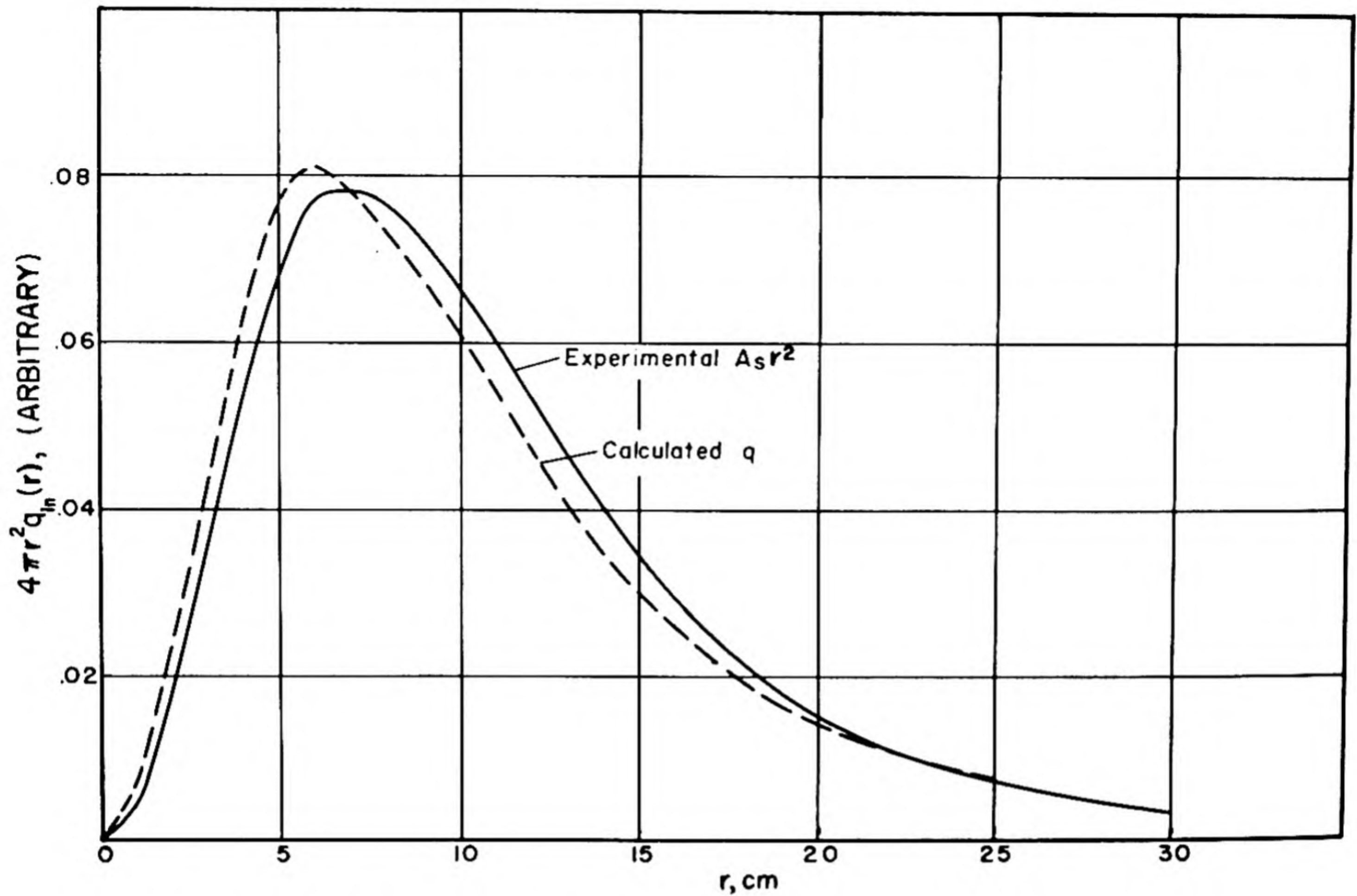


Fig. 1.3.13 — Comparison of Indium Resonance Activity with Theoretical Slowing-down Density in H_2O from a Fission Point Source. Submitted by N.D.A., Aug. 28, 1952.

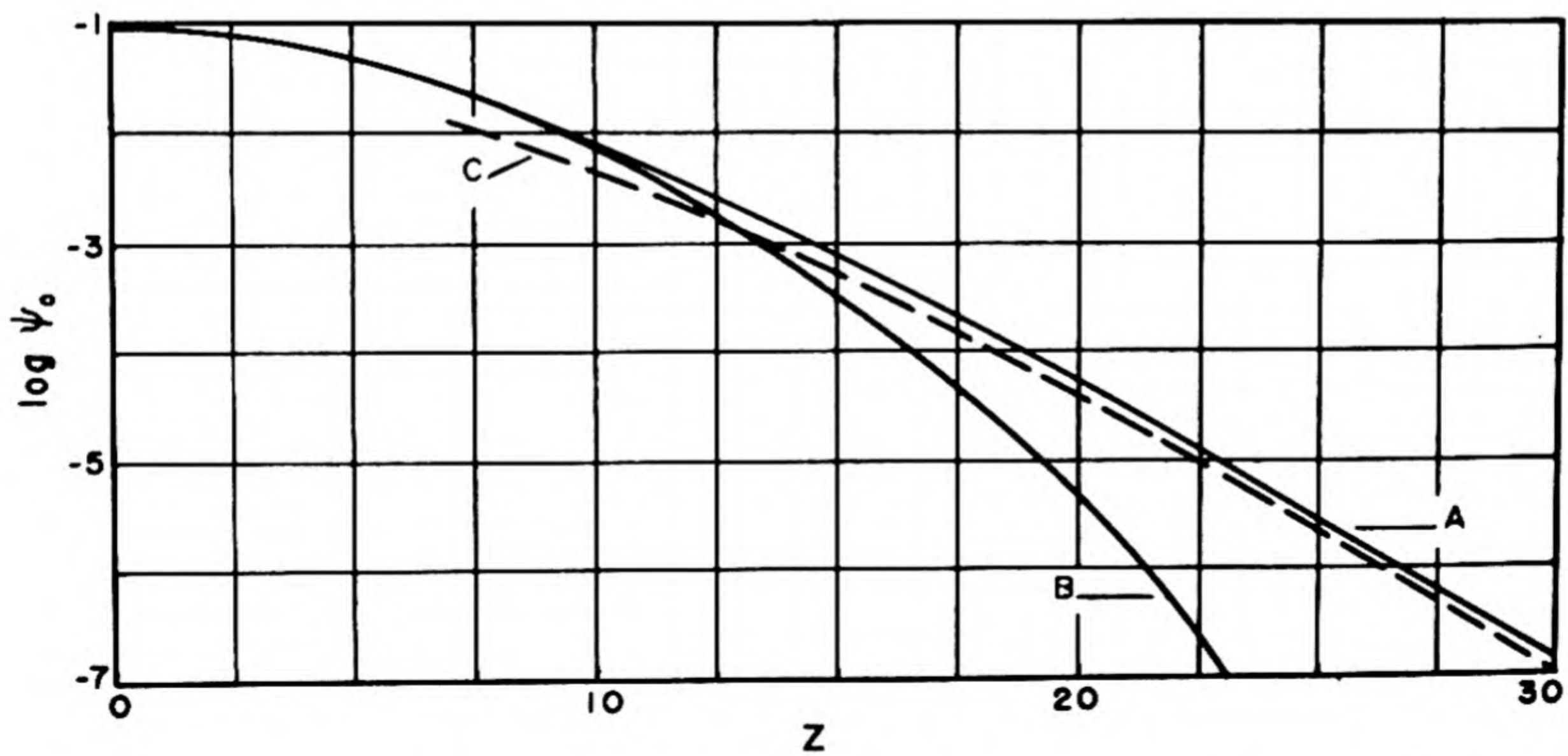


Fig. 1.3.14 — Deviation of Collision Density, $\psi_0(z)$, from the Gaussian Distribution (B) of Neutrons Slowing Down in an Infinite Medium of Constant Mean Free Path, l . From G. C. Wick, Phys. Rev. 75, 1949. Source energy = $e^{10}E$; distance from plane source = zl ; curve A is asymptotic to Curve C at very large distances.

Table 1.3.18—Coefficients Giving Deviations from the Gaussian Slowing-down Density
(Adapted from Bethe, Tonks, and Hurwitz⁴⁷)

Mass M	$K(Z/u')$	$\phi(Z/u')$
1		$1 - \frac{11}{240} \left(\frac{Z}{u'}\right)^2 + \frac{73}{32,256} \left(\frac{Z}{u'}\right)^4 \dots$
9	$1 - 2.225 \left(\frac{Z}{u'}\right)^2 + 12.39 \left(\frac{Z}{u'}\right)^4$	$1 - 1.080 \left(\frac{Z}{u'}\right)^2 + (3.169) \left(\frac{Z}{u'}\right)^4$
12		$1 - 1.142 \left(\frac{Z}{u'}\right)^2 + (3.538) \left(\frac{Z}{u'}\right)^4$
∞	$1 - 2.80 \left(\frac{Z}{u'}\right)^2 + 19.20 \left(\frac{Z}{u'}\right)^4$	$1 - 1.350 \left(\frac{Z}{u'}\right)^2 + (4.908) \left(\frac{Z}{u'}\right)^4$

The distribution of fission neutrons moderated in H_2O to In resonance energy, 1.44 ev, as measured, differs significantly from the gaussian distribution over the entire range of distances from a point source (cf. curves A and D of Fig. 1.3.15).

The solution of Eq. (128) for a point fission source in H_2O , where the presence of oxygen is taken into account by including its scattering in the transport cross section, is obtained by taking the three-dimensional Fourier transform with respect to the variable \underline{r} which is the distance from source.

The transformed function $Q(E, \omega)$ is given in Table 1.3.3 for hydrogen by the following substitution of symbols:

$$\begin{aligned} q(E) &\rightarrow Q(E, \omega) \\ \sigma(E') &\rightarrow \sigma_s(E') + \omega^2/3 \sigma_{tr} \\ \psi(E) &\rightarrow \psi(E, \omega)(1 + \omega^2/3 \sigma_s \sigma_{tr}) \end{aligned} \quad (136)$$

The solution $Q(1.44, \omega)$ was obtained by numerical integration for several ω values.⁵² The slowing-down distribution at In resonance was obtained by numerical integration of the Fourier inverse transforms after correcting⁴ Q for the small amount of slowing-down by oxygen:

$$q_{In}(r) = [1/(2\pi^2 r)] \int_0^\infty Q(1.44, \omega) \omega \sin(\omega r) d\omega \quad (137)$$

Figure 1.3.13 shows a comparison of $q_{In}(r)$ with the experimentally measured, saturated In-foil activities (A_s). This method is not suitable for obtaining the asymptotic behavior of $q(r)$. Because of the sharp resonance of In, the activity (A_s) is directly proportional to the collision density at 1.44 ev rather than to the number of neutrons crossing 1.44 ev, which is q_{In} . According to Eq. (126):

$$\overline{r_\phi^2} = \overline{r_q^2} + 2.5 \text{ cm}^2$$

Thus, the theoretical $4\pi r^2 \sigma_s \phi$ curve would appear shifted slightly towards the experimental curve.

r_ϕ^2 OF HYDROGENOUS MEDIA

Substances such as water or paraffin slow down neutrons very effectively because their hydrogen content is high. By ignoring the slowing-down effect of the heavy elements in a

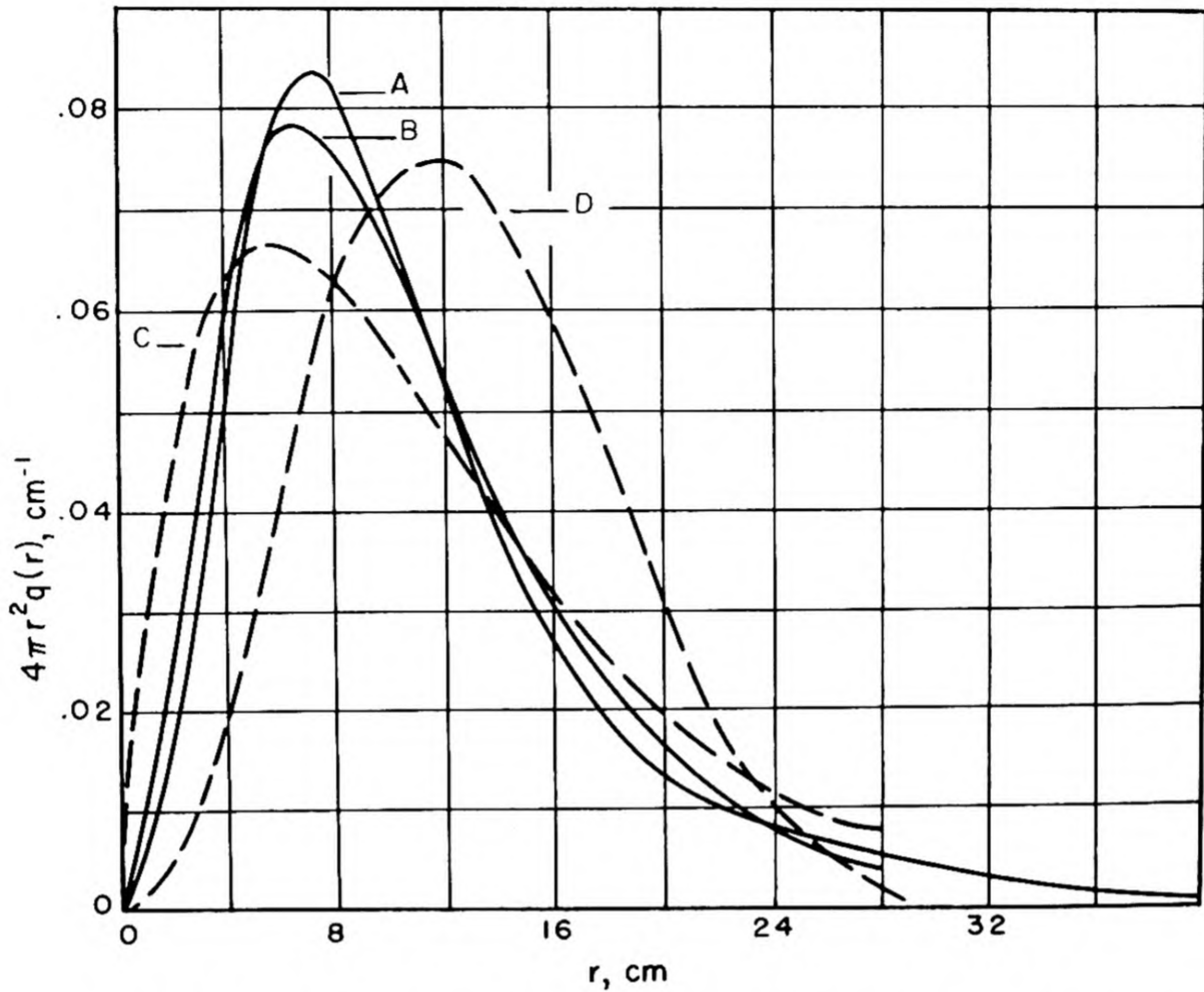


Fig. 1.3.15 — Slowing-down Distributions from a Point Fission Source in H_2O . Reprinted from S. Glasstone and M. C. Edlund, *The Elements of Nuclear Reactor Theory*, D. Van Nostrand Co., Inc., New York, 1952. (A) = experimental, to Indium resonance; (b) = convolution of three diffusion kernels; (C) = one diffusion kernel; (D) = gaussian kernel.

hydrogenous medium, very good values may be obtained for \bar{r}_ϕ^2 in terms of the behavior of the three-dimensional Fourier-transformed collision density $\psi(u, \omega)$ at $\omega = 0$, $u \neq 0$; that is:

$$\bar{r}_\phi^2 = -3 \left[\left(\frac{d^2 \psi}{d\omega^2} \right) / \psi \right]_{\omega=0} \quad (138)$$

Marshak⁵³ has indicated a method of obtaining $\psi(u, 0)$ and its second derivative as a function of u exactly. The resulting formula⁵⁴ for \bar{r}_ϕ^2 is:

$$\begin{aligned} \bar{r}_\phi^2 = 2 \left\{ \frac{l^2(0)}{C(0)} + \frac{l^2(u)}{C(u)} + \int_0^u \frac{l^2(u')}{C(u')} du' + l(0) l(u) F(0, u) \right. \\ + l(u) \int_0^u l(u') F(u', u) du' + l(0) \int_0^u l(u') F(0, u') du' \\ \left. + \int_0^u l(u') \int_0^{u'} l(u'') F(u'', u') du'' du' \right\} \quad (139) \end{aligned}$$

where:

$$F(x, y) = \exp \left[\frac{-3}{2} (y-x) + \int_x^y C(t) dt \right]$$

$l(u)$ = total mean free path at energy $E = E_0 e^{-u}$

$C(u)$ = $l(u)$ /hydrogen mean free path

THE GROUP METHOD

Although more generally applicable,* the group method is here described in terms of the diffusion equation (109).

THE FLUX EQUATIONS

Division of the energy scale into N intervals $(E_0, E_1), (E_1, E_2), \dots (E_{i-1}, E_i), \dots (E_{N-1}, E_N)$ with E_0 the highest and E_N the lowest energy, and integration of Eq. (109) over the i^{th} interval results in:

$$\text{div } D_i \text{ grad } \Phi_i(\underline{r}) - \sigma_{ai} \Phi_i(\underline{r}) + q_{i-1}(\underline{r}) - q_i(\underline{r}) + S_i(\underline{r}) = 0 \quad (140a)$$

where:

$$\Phi_i(\underline{r}) = \int_{E_i}^{E_{i-1}} \varphi_i(\underline{r}, E) dE \quad (140b)$$

and:

$$S_i(\underline{r}) = \int_{E_i}^{E_{i-1}} S(\underline{r}, E) dE \quad (140c)$$

are the integrated flux and source in the i^{th} group, and D_i and σ_{ai} are proper average quantities. The quantities q_{i-1} and q_i are the slowing-down densities, as given by Eq. (3),† at the energies E_{i-1} and E_i , and may be written as:

$$q_i(\underline{r}) = q(\underline{r}, E_i) = \sum_{j=1}^i s_{ij} \Phi_j(\underline{r}) \quad (141)$$

where the s_{ij} are defined by Eqs. (3), (140b), and (141). If the interval E_{i-1}, E_i is larger in extent than a collision interval, then s_{ii} is the only non-vanishing coefficient.

Equations (140) may be written as:

$$\text{div } D_i \text{ grad } \Phi_i(\underline{r}) - \sigma_i \Phi_i(\underline{r}) + \sum_{j=1}^{i-1} \sigma_{ij} \Phi_j(\underline{r}) + S_i(\underline{r}) = 0 \quad (142a)$$

where:

$$\sigma_i = \sigma_{ai} + s_{ii} \quad (142b)$$

*Safonov⁵⁵ treats the many-velocity transport equations. Davison⁵⁶ discusses two-group transport theory and the two-group Serber method. Feynman, Welton et al⁵⁷ use the group method in their work.

†Where $\frac{\sigma_s}{\sigma} \psi = \sigma_s \varphi$

and:

$$\sigma_{ij} = S_{i-j, j} - S_{ij} \quad (142c)$$

In Eq. (142a), the term $\sigma_i \Phi_i$ represents the total loss out of group i by absorption and slowing-down, and the terms $\sigma_{ij} \Phi_j$ in the summation represent the scattering into group i from group j . In the high-energy group, $i = 1$, the summation is to be replaced by zero. In the low-energy group, $i = N$, all the quantities S_{Nj} are taken as zero, since there is no lower group into which the neutrons can slow down.

The boundary conditions as obtained from Eqs. (157) and (158) are:

$$\text{Interface} \quad \begin{cases} \Phi_i(\underline{r}) = \text{continuous} \\ D_i \text{ grad } \Phi_i(\underline{r}) = \text{continuous} \end{cases} \quad (143a) \quad (143b)$$

$$\text{Black boundary} \quad \begin{cases} \frac{1}{\Phi_i} \frac{\partial \Phi_i(\underline{r})}{\partial \text{normal}} = \frac{1}{\lambda} \approx \frac{1}{3(0.71)D_i} \\ \text{or} \\ \Phi_i(\underline{r}) = 0 \text{ at extrapolated boundary} \end{cases} \quad (144a) \quad (144b)$$

Recipe (159) for choosing a single extrapolation length, $2.13D_{\text{eff}}$, for all energies applies to the group method as

$$D_{\text{eff}} = \frac{\sum_{i=1}^N D_i \Phi_i(\underline{r})}{\sum_{i=1}^N \Phi_i(\underline{r})} \Bigg|_{\text{at boundary}} \quad (145)$$

As an example of Eqs. (142), the two-group equations are:

$$\text{div } D_1 \text{ grad } \Phi_1(\underline{r}) - (\sigma_{a1} + s_{11}) \Phi_1(\underline{r}) + S_1(\underline{r}) = 0 \quad (146a)$$

$$\text{div } D_2 \text{ grad } \Phi_2(\underline{r}) - \sigma_{a2} \Phi_2(\underline{r}) + s_{11} \Phi_1(\underline{r}) + S_2(\underline{r}) = 0 \quad (146b)$$

where, in a thermal reactor, group 2 represents the thermal group and group 1 represents the slowing-down or fast group. For this case, the source term $S_2(\underline{r})$ is usually zero.

SLOWING-DOWN DENSITY EQUATIONS

When the Fermi approximation is used, Eq. (141) is replaced by:

$$q_i(\underline{r}) = \xi \sigma_s E_i \varphi_i(E) \quad (147)$$

which is to be inserted into Eq. (140a). In this approximation, it is possible to express the group equations in terms of q rather than ϕ . Thus Eq. (112) leads to:

$$\left(\frac{D}{\xi \sigma_s} \right)_i \nabla^2 Q_i - \left(\frac{\sigma_a}{\xi \sigma_s} \right)_i Q_i + q_{i-1} - q_i + S_i = 0 \quad (148a)$$

where:

$$Q_i = \int_{E_i}^{E_{i-1}} q(\underline{r}, E) \frac{dE}{E} \quad (148b)$$

S_i and q_i are defined as before, and $(D/\xi\sigma_s)_i$ and $(\sigma_a/\xi\sigma_s)_i$ are proper averages. Boundary conditions are obtained from Eq. (143) and Eq. (144) through the relation:

$$\Phi_i = \int_{E_i}^{E_{i-1}} \frac{q}{\xi\sigma_s} \frac{dE}{E} = \left(\frac{1}{\xi\sigma_s} \right)_i Q_i \quad (148c)$$

Similarly, Eq. (116) leads to:

$$\nabla^2 Q'_i(\underline{r}) + q'_{i-1}(\underline{r}) - q'_i(\underline{r}) + S'_i(\underline{r}) = 0 \quad (149a)$$

where:

$$Q'_i(\underline{r}) = \int_{E_i}^{E_{i-1}} q'(\underline{r}, E) \frac{dE}{E} \quad (149b)$$

and:

$$S'_i(\underline{r}) = \int_{E_i}^{E_{i-1}} \frac{s(\underline{r}, \tau)}{p(E, E_0)} \frac{d\tau}{dE} dE \quad (149c)$$

Boundary conditions are obtained through the relation:

$$\Phi_i(\underline{r}) = \int_{E_i}^{E_{i-1}} \frac{p(E, E_0)}{D} q'(\underline{r}, E) \frac{dE}{E} = \left(\frac{p}{D} \right)_i Q'_i(\underline{r}) \quad (149d)$$

where $\left(\frac{p}{D} \right)_i$ is a proper average.

Equations (148) and (149) apply only to the slowing-down process. When there is a thermal group into which neutrons slow down, the quantity q_N is not zero but is rather the source of thermal neutrons. Equations similar to Eqs. (148) and (149) may be written for the more general age equation (128).

CHOICE OF PARAMETERS

Aside from computational considerations, the major questions in applying the group method are (1) the choice of the parameters D_i , σ_{ai} , $(D/\xi\sigma_s)_i$, and the like and (2) the treatment of the q_i terms.

An answer to both questions may be obtained by assuming a form for the energy dependence of $\varphi(\underline{r}, E)$ within each group. Thus, if φ is assumed to behave as $1/E$ within each group, the parameters entering into the general group equations (142) are:

$$D_i = \frac{\int_{E_i}^{E_{i-1}} D(E) \frac{dE}{E}}{\ln E_{i-1}/E_i} \quad (150a)$$

$$\sigma_{ai} = \frac{1}{\ln E_{i-1}/E_i} \int_{E_i}^{E_{i-1}} \sigma_a(E) \frac{dE}{E} \quad (150b)$$

$$s_{ij} = \frac{1}{\ln E_{i-1}/E_i} \int_{E_i}^{E_{j-1}} \sigma_s(E') G(E_i, E') \frac{dE'}{E'} \quad (150c)$$

In Eq. (150c), any of the (exact or approximate) kernels of Table 1.3.2 may be used. Thus, in Fermi theory:

$$s_{ij} = \frac{\xi \sigma_s(E_i)}{\ln E_{i-1}/E_i}$$

and:

$$s_{ij} = 0 \text{ for } i \neq j$$

In the q equations (148) for Fermi theory, the assumption that $q(\underline{r}, E)$ depends linearly on $\ln E$ results in:

$$Q_i = \frac{1}{2} (q_{i-1} + q_i) \ln \frac{E_{i-1}}{E_i} \quad (151)$$

in terms of which, q_i may be solved for and substituted into Eq. (148a).

The solutions thus obtained may be improved by iteration.⁵⁵ Thus, for example, the $\Phi_i(\underline{r})$ resulting from the "1/E" parameters correspond to:

$$\varphi_i(\underline{r}, E) = \frac{f_i(\underline{r})}{E}$$

leading to discontinuities in $\varphi(\underline{r}, E)$ at space boundaries and group boundaries. Improvements can be made by recalculating the parameters in terms of a new spectrum (rather than $1/E$) obtained by a free-hand smoothing out of the discontinuities.

GROUP DIFFUSION KERNELS

Consider the problem of slowing-down without absorption in an infinite homogeneous medium with a point monoenergetic source at $\underline{r} = \underline{r}_0$, $E = E_0$. Assuming that each group interval is larger in extent than a collision interval ($q_i = s_{i1}\Phi_i$), the group equations may be written as:

$$\begin{aligned} l_1^2 \nabla^2 q_1 - q_1 + \delta(\underline{r} - \underline{r}_0) &= 0 \\ l_2^2 \nabla^2 q_2 - q_2 + q_1 &= 0 \\ \dots\dots\dots l_N^2 \nabla^2 q_N - q_N + q_{N-1} &= 0 \end{aligned} \quad (152a)$$

where:

$$q_i(\underline{r}) = q(\underline{r}, E_i) = s_{i1}\Phi_i(\underline{r}) \quad (152b)$$

and:

$$l_i^2 = \frac{D_i}{s_{ii}} = \frac{1}{\kappa_i^2} \quad (152c)$$

The energy E_i is, as before, at the bottom of group i .

The solutions of Eq. (152a) are:

$$q_1(\underline{r}) = k_1(\underline{r}, \underline{r}_0) \quad (153a)$$

$$\begin{aligned} q_2(\underline{r}) &= \int k_2(\underline{r}, \underline{r}^{(1)}) k_1(\underline{r}^{(1)}, \underline{r}_0) d\underline{r}^{(1)} \\ &= \frac{l_1^2}{l_1^2 - l_2^2} k_1(\underline{r}, \underline{r}_0) + \frac{l_2^2}{l_2^2 - l_1^2} k_2(\underline{r}, \underline{r}_0) \end{aligned} \quad (153b)$$

$$\begin{aligned} q_N(\underline{r}) &= \int k_N(\underline{r}, \underline{r}^{(1)}) k_{N-1}(\underline{r}^{(1)}, \underline{r}^{(2)}) \dots k_2(\underline{r}^{(N-2)}, \underline{r}^{(N-1)}) \\ &\quad \times k_1(\underline{r}^{(N-1)}, \underline{r}_0) d\underline{r}^{(1)} \dots d\underline{r}^{(N-1)} \\ &= \sum_{i=1}^N \frac{(l_i^2)^{N-1}}{\prod_{j \neq i} (l_i^2 - l_j^2)} k_i(\underline{r}, \underline{r}_0) \end{aligned} \quad (153c)$$

where, according to Table 1.3.9, the point diffusion kernel is given by:

$$k_i(\underline{r}, \underline{r}_0) = \frac{e^{-|\underline{r} - \underline{r}_0|/l_i}}{4\pi l_i^2 |\underline{r} - \underline{r}_0|} \quad (154)$$

The solution for $q_N(\underline{r})$ is thus the convolution of all N diffusion kernels. The expressions giving q_N as a super-position of the individual kernels are generally true, being valid as well for the infinite plane kernel (Table 1.3.9) and for the finite kernels,* provided the problem is spatially homogeneous, i.e., that the macroscopic cross sections are independent of position in the reactor.

In the presence of absorption, the solution $q_N^a(\underline{r})$ is related to $q_N(\underline{r})$ by:

$$q_N^a = q_N \prod_{i=1}^N \left(\frac{1}{1 + \frac{\sigma_{ai}}{s_{ii}}} \right) \quad (155)$$

The second moment:

$$\overline{r_{q_N}^2} = \overline{|\underline{r} - \underline{r}_0|^2 q_N}$$

*The finite point kernel, $k_p^f(\underline{r}, \underline{r}_0)$, for example, is defined by the equation:

$$l^2 \nabla^2 k_p^f(\underline{r}, \underline{r}_0) - k_p^f(\underline{r}, \underline{r}_0) + \delta(\underline{r} - \underline{r}_0) = 0$$

and by the boundary condition:

$$k_p^f(\underline{r}, \underline{r}_0) = 0$$

whenever \underline{r} is at the extrapolated boundary. Although not a displacement kernel, $k_p^f(\underline{r}, \underline{r}_0)$ is symmetric. Thus:

$$k_p^f(\underline{r}, \underline{r}_0) = k_p^f(\underline{r}_0, \underline{r})$$

of the point source solution is given by:

$$\overline{r_{q_N}^2} = 6 (l_1^2 + l_2^2 + \dots + l_N^2) \quad (156)$$

Fermi age theory* may be considered as the limit of group theory, as represented by Eqs. (152) as the group intervals:

$$\Delta E_i = E_{i-1} - E_i$$

approach zero and the number of groups approaches infinity. Use of Eq. (147) gives in the limit:

$$\frac{1}{s_{ii}} \rightarrow \frac{1}{\xi \sigma_s} \frac{\Delta E_i}{E_i}$$

leading to:

$$l_i^2 \rightarrow \frac{D}{\xi \sigma_s} \frac{\Delta E_i}{E_i} \rightarrow \Delta \tau_i$$

from which it follows that Eq. (152a) approaches the age Eq. (112) in the absence of absorption. Thus, Eq. (156) results in:

$$\overline{r_q^2} \rightarrow 6 \sum \Delta \tau_i = 6\tau(E, E_0)$$

and Eq. (155) leads to:

$$q^a \rightarrow q \Pi \frac{1}{1 + \frac{\sigma_a}{\xi \sigma_s} \frac{\Delta E}{E}} = qp(E, E_0)$$

A comparison of 1-group, 3-group, and age theory fits vs the measured $q_{ln}(\underline{r})$ in water is shown in Fig. 1.3.15.

FINITE REGIONS AND BOUNDARY CONDITIONS

BOUNDARY CONDITIONS

Generalizing the one-velocity results of the discussion of "Homogeneous Regions in Contact" to the many-velocity case, the boundary conditions may be approximated by the following formulas:

$$\left| \frac{1}{\varphi} \frac{\partial \varphi(\underline{r}, E)}{\partial \text{normal}} \right| = \frac{1}{\lambda} \approx \frac{1}{0.71/\sigma_{tr}(E)} = \frac{1}{0.71\lambda_{tr}} \quad (157)$$

Black boundary

or

$$\varphi(\underline{r}, E) = 0 \text{ at extrapolated boundary} \quad (158)$$

*Note that only in the Fermi approximation does the assumption (152b) remain valid as the group intervals approach zero.

where the extrapolated boundary is approximately $0.71\lambda_{tr}$ removed from the actual boundary. In regions larger in extent than a few transport paths ($\text{size} \gg \lambda_{tr}$), an accurate and enormously simplifying approximation is to choose an effective extrapolation length or extrapolated boundary as valid for all energies. A simple and physically reasonable choice* is that which correctly gives the total leakage. This leads in the case of condition (157) to a value λ_{tr}^{eff} given by:

$$\lambda_{tr}^{eff} = \frac{\int \lambda_{tr}(E) \varphi(\underline{r}, E) dE}{\int \varphi(\underline{r}, E) dE} \Bigg|_{\text{at boundary}} \quad (159)$$

The black-boundary conditions on $q(\underline{r}, E)$ and $q(\underline{r}, \tau)$ are, in Fermi age theory, Eq. (111), identical with those on $\varphi(\underline{r}, E)$. In the Wigner and G. G. approximations, Eq. (127), the q boundary conditions are more complicated, involving a combination of q and $\partial q / \partial E$:

$$\text{Interface} \quad \left\{ \begin{array}{l} \varphi(\underline{r}, E) = \text{continuous} \\ D \text{ grad } \varphi(\underline{r}, E) = \text{continuous} \end{array} \right. \quad (160)$$

$$(161)$$

These conditions also apply in age theory to $q(\underline{r}, E)$ but not directly to $q(\underline{r}, \tau)$ when τ is a different function of energy in the two media.

Improvements on Eqs. (157) and (158) are given in Tables 1.3.11 and 1.3.12 and Eqs. (81) to (88).

THE IMAGE METHOD

Finite-region problems, involving the black-boundary condition (158), may often be solved in terms of the infinite-medium solutions.

Thus, for example, the solution in Table 1.3.15 of the aging in an infinite column owing to a point source at $x_0, y_0, z = 0$ is represented as a sum of the infinite-medium solutions corresponding to the actual source and to its images at: $(x_0 + 2al, y_0 + 2bm)^+$, $(x_0 - 2al, y_0 - 2bm)^+$, $(x_0 + 2al, y_0 - 2bm)^-$, and $(x_0 - 2al, y_0 + 2bm)^-$, where (l) and (m) run from $-\infty$ to $+\infty$. The image sources all have the same strength as the actual source and have signs indicated by the superscript. The magnitudes and positions of the images are arranged so that they negate the contribution of the actual source to the solution at the boundary.

Another example is the problem of a plane source in a semi-infinite medium. The solution in this case is the sum of the infinite-medium solutions for the actual source and for its mirror image, the latter with a negative sign.

Problems involving spherical symmetry may be attacked by transforming to the equivalent plane problem, and then applying images. The solution in Table 1.3.15 of the point source at the center of a finite sphere may be obtained in this manner. The equivalent source and its images are dipoles in this case.

DIFFUSION OF THERMAL NEUTRONS

Wigner and Wilkins ("Thermal Distributions," above) have treated the problem of the energy spectrum of thermal neutrons in the absence of diffusion. The absence of similar

*A better, but more complicated choice for λ_{tr}^{eff} is the spectral average of λ_{tr} weighted with the proper adjoint function (cf. perturbation theory in 1.4 and the importance function in 1.6).

results on the more difficult problem of thermal diffusion restricts the following to simple considerations only.

DIFFUSION EQUATIONS

Assuming no low-energy-source neutrons, the diffusion equation (109) for a homogeneous medium may be written as:

$$D\nabla^2\varphi(\underline{r},E) - \sigma_a\varphi(\underline{r},E) + \frac{\partial\bar{q}(\underline{r},E)}{\partial E} = 0 \quad (162)$$

where D and σ_a depend on the neutron energy and, for energies within the thermal region ($E \sim KT$), on the temperature* of the medium. The quantity $\bar{q}(\underline{r},E)$ is still defined by Eq. (3) for E above the thermal range. For energies within the thermal range, it is defined as the net number† of neutrons crossing below the energy E and is no longer given by Eq. (3).

Integration of Eq. (162) between the limits $E = 0$ and $E = E_{th} \equiv$ an energy above which thermal effects are unimportant,‡ results in:

$$D_{th}\nabla^2\Phi_{th}(\underline{r}) - \sigma_{a,th}\Phi_{th}(\underline{r}) + q(\underline{r},E_{th}) = 0 \quad (163a)$$

where:

$$\Phi_{th}(\underline{r}) = \int_0^{E_{th}} \varphi(\underline{r},E) dE \quad (163b)$$

and is the total thermal flux:

$$D_{th} = \frac{1}{\Phi_{th}(\underline{r})} \int_0^{E_{th}} D(E) \varphi(\underline{r},E) dE \quad (163c)\S$$

$$\sigma_{a,th} = \frac{1}{\Phi_{th}(\underline{r})} \int_0^{E_{th}} \sigma_a(E) \varphi(\underline{r},E) dE \quad (163d)$$

and $q(\underline{r},E_{th})$ is obtainable by previously discussed methods.

The boundary conditions that are generally used are the group conditions (143) and (144).

ENERGY-INDEPENDENT CROSS SECTIONS

When $D(E)$ and $\sigma_a(E)$ do not depend on the energy, the thermal flux satisfies the one-velocity diffusion equation. For this case, in fact, all the one-velocity results of the discussion of "One-velocity Theory" are valid⁵⁸ for $\Phi_{th}(\underline{r})$. According to Eq. (162), the spec-

*The cross sections depend on the velocity distribution of the target nuclei, especially for light nuclei.

†A thermal neutron may increase in energy following a collision. Thus, $g(E,E')$ and $G(E,\dot{E}')$ are no longer zero for $E' < E$.

‡This ambiguity in the choice of E_{th} is a necessary consequence of any such simple considerations.

§Eq. (163c) is valid only if D_{th} is a slowly varying function of position. Note that this happens whenever the spectrum changes with position.

trum $\phi(E)$ in a Laplacian mode* is the same as the spectrum obtained without diffusion in a medium of effective cross section:

$$\sigma_a^{\text{eff}} = \sigma_a + DB^2$$

being close to Maxwellian if $\sigma_a^{\text{eff}}/\sigma_s \ll 1$.

ENERGY-DEPENDENT CROSS SECTIONS

Statements may be made concerning the case of energy-dependent cross sections if the spectrum is assumed to be uniform throughout space. This assumption leads to space-independent parameters given by Eqs. (163c and d) in terms of which the diffusion length† L is given as:

$$L^2 = D_{\text{th}}/\sigma_{a,\text{th}} \quad (164)$$

The spectrum is close to Maxwellian for $\sigma_a(E)/\sigma_s(E) \ll 1$. The above remarks concerning Laplacian modes also apply here. The stronger assumption of "complete amnesia"⁵⁹ leads to a spectrum of the form $\sigma_s/(\sigma_s + \sigma_a)$ times a Maxwellian, at positions removed from a localized source of thermal neutrons. Maxwellian averages of $1/v^n$ cross sections are listed in Table 1.3.7.

Two interesting cases in which the assumption of a uniform spectrum is very poor are (1) the diffusion in a block of high-atomic-weight material (such as uranium) in which case⁶⁰ the neutrons of each energy diffuse practically independently, resulting in a hardening effect for a $1/v$ absorber, and (2) the diffusion in a large block of crystalline matter with very small absorption cross section, (such as a graphite thermal column), in which case,^{61,62} the softening effect of the very low scattering cross section‡ may overbalance the absorption hardening and lead to the production of "cold" neutrons.

REFERENCES

1. Placzek, Phys. Rev. 69, 1946, p 428.
2. Edlund, ORNL-1154, p 63 (classified).
3. Goertzel, TAB-53, July 1950 (classified).
4. Shapiro and Preiser, ORNL-1176, Nov. 1951 (classified).
5. Young, CF-47-11-551, p 14 (classified).
6. Shapiro, unpublished.
7. Wigner and Wilkins, AECD-2275.
8. Cohen, HKF-102, pp 3.15 (classified).
9. Blehl and Cohen, TID-72, p 93 (classified).
10. Marshak, Frankel, and Nelson, LADC-79.
11. M. H. L. Pryce, MSP-2 (classified).
12. K. Fuchs, MS-85.
13. B. Carlson, AECD-2835.
14. Marshak, Phys. Rev. 71, 1947, p 688.
15. B. Davison, Phys. Rev. 71, 1947, p 694.
16. G. Placzek and G. M. Volkoff, MT-4, April 1943 (classified).
17. P. R. Wallace and J. Le Caine, NRC-1480.
18. A. M. Weinberg and L. C. Noderer, CF-51-5-98 (classified).
19. B. Davison, CRT-358, NRC-1636, June 1946.
20. B. Davison, MT-88.
21. B. Davison, MT-93.
22. B. Davison, MT-97 (classified).

* $\nabla^2\phi = -B^2\phi$, D being independent of position.

†Equation (164) is more often used to obtain D_{th} in terms of experimental values of $\sigma_{a,\text{th}}$ and L^2 .

‡At energies below which Bragg scatterings disappear.

23. B. Davison, MT-135.
24. B. Davison, MT-207.
25. B. Davison and S. Kushnerluk, MT-214.
26. C. Mark, NRC-1588.
27. C. Mark, NRC-1589.
28. G. C. Wick, Z. Physik, 121, 1943, p 702.
29. S. Chandrasekhar, Radiative Transfer, Oxford Univ. Press, New York, 1951.
30. S. Frankel and E. Nelson, LADC-76.
31. S. Frankel and E. Nelson, LADC-79.
32. S. Frankel and S. Goldberg, AECD-2056.
33. G. Placzek and W. Seidel, Phys. Rev. 72, 1947, p 550.
34. H. Margenau and G. M. Murphy, The Mathematics of Physics and Chemistry, D. Van Nostrand Co., Inc., New York, 1943, p 462.
35. H. Margenau and G. M. Murphy, The Mathematics of Physics and Chemistry, D. Van Nostrand Co., Inc., New York, 1943, p 464, Table 6.
36. Frankel and Goldberg, loc. cit., p 34.
37. P. R. Wallace and J. Le Caine, MT-12.
38. Nucleonics 4, Feb. and March 1949.
39. Bellman, Marshak, and Wing, Phil. Mag., Series 7, 40, March 1949, p 297.
40. F. L. Friedman, CP-1073, Oct. 27, 1943.
41. Young, loc. cit., p 5.
42. L. Halpern and J. G. Beckerly, Lecture Notes from Fermi, AECD-2664, p 61.
43. Weinberg and Noderer, loc. cit., vol. 1, p III-43.
44. R. E. Marshak, Rev. Mod. Phys. 19, July 1947, p 235.
45. Weinberg and Noderer, loc. cit., p III-44.
46. R. E. Marshak, H. Brooks, and H. Hurwitz, Jr., Nucleonics 5, No. 2, Aug. 1949, pp 59-68.
47. H. A. Bethe, L. Tonks, and H. Hurwitz, Jr., Phys. Rev. 80, 1950, p 11.
48. G. C. Wicks, Phys. Rev. 75, 1949, p 738.
49. G. Placzek, A-25, 1941.
50. L. D. Roberts, J. E. Hill, and G. McCammon, ORNL-201, 1950.
51. G. Placzek and Volkoff, Can. Jour. Res. A25, 1947, p 276.
52. G. Geortzel and M. Nelkin, unpublished data.
53. R. E. Marshak, Rev. Mod. Phys. 19, No. 3, 1947, p 185.
54. E. Fermi, Ricerca sci. 7, 1936, p 13.
55. Safonov, R-233 (classified).
56. B. Davison, LT-18.
57. Feynman, Welton, et al, LA-524 (classified).
58. Weinberg and Noderer, loc. cit., p I-19.
59. Weinberg and Noderer, loc. cit., p I-39.
60. Weinberg and Noderer, loc. cit., p I-36.
61. Halpern and Beckerly, loc. cit., p 48.
62. Hughes, Pile Neutron Research, Chapters 9 and 10.
63. J. C. Mark, The Spherical Harmonics Method I and II, CRT-338, NRC-1589, June 1947.

SELECTED READING LIST

THE ELEMENTS OF NUCLEAR REACTOR THEORY, S. Glasstone and M. C. Edlund, D. Van Nostrand Co., Inc.

THEORY OF NEUTRON CHAIN REACTIONS, A. M. Weinberg and L. C. Noderer, 2 volumes.

INTRODUCTION TO THE THEORY OF DIFFUSION AND SLOWING-DOWN OF NEUTRONS, R. E. Marshak, H. Brooks, and H. Hurwitz, Jr., Nucleonics 4, No. 5, 1949, pp 10-28; 4, No. 6, 1949, pp 43-49; 5, No. 1, 1949, pp 53-60; 5, No. 2, 1949, pp 59-68.

THEORY OF SLOWING-DOWN OF NEUTRONS BY ELASTIC COLLISION WITH ATOMIC NUCLEI, R. E. Marshak, Rev. Mod. Phys. 19, 1947, p 185.

TRANSPORT THEORY OF NEUTRONS, B. Davison, LT-18.

ON THE THEORY OF THE SLOWING DOWN OF NEUTRONS IN HEAVY SUBSTANCES, G. Placzek, Phys. Rev. 69, 1946, p 423.

CHAPTER 1.4

Reactor Statics; Theory and General Results

Harry Soodak

REACTORS WITHOUT SPACE VARIATION

CRITICALITY

In terms of the neutron-energy spectrum (see Chapter 1.3), the critical equation for an infinite homogeneous medium is:

$$k = \frac{\int_0^\infty \nu \sigma_f n v dE}{\int_0^\infty \sigma_a n v dE} = 1 \quad (1)$$

If the neutrons are created at a single energy which they retain until absorbed, Eq. (1) reduces to:

$$k = \nu F = 1$$

where:

$$F = \text{utilization} = \sigma_f / \sigma_a$$

if ν and F are independent of energy, this holds regardless of the fission-source spectrum and the slowing-down processes. If fissions are caused only by thermal neutrons, $k = \nu p F = 1$ applies, where p is the probability of escaping capture while slowing down. Allowing for fast-fission multiplication by a factor ϵ , the last relationship becomes:

$$k = \nu \epsilon p F = 1$$

which* is familiar in thermal reactors.

AIDS TO COMPUTATION

Determination† of systems or compositions satisfying Eq. (1) or obtaining relatively good values for k despite inaccuracies in determining the slowing-down spectrum is facilitated

*Frequently written as: $k = \eta \epsilon p f = 1$ where $\eta = \nu \left(\frac{\sigma_f}{\sigma_a} \right)_{\text{fuel}}$ and $f = \frac{\sigma_a (\text{fuel})}{\sigma_a (\text{total})}$

†In special cases, such as those noted below Eq. (1), this may follow directly; in general, it does not, and repeated trials or other procedures are needed.

by perturbation, variation, and iteration techniques (cf. the last part of this chapter).

The following illustrates the use of perturbation methods in adjusting fuel content to make a system critical. Assuming ν to be constant and splitting off the thermal group (Chapter 1.3) yields the steady-state balance equations:

$$\frac{\partial n(E)}{\partial t} = 0 = \nu \chi(E) \int_{E_{th}}^{\infty} \phi \sigma_f dE' + \nu \chi(E) \phi_{th} \sigma_{f_{th}} + \int_{E_{th}}^{\infty} g(E, E') \sigma_s \phi(E') dE' - \sigma \phi \quad (2)$$

$$\frac{\partial n_{th}}{\partial t} = 0 = \int_{E_{th}}^{\infty} G(E_{th}, E) \sigma_s \phi(E) dE - \sigma_{a_{th}} \phi_{th} = q_{th} - \sigma_{a_{th}} \phi_{th} \quad (3)$$

where:

$$\sigma = \sigma_s + \sigma_a + \sigma_f$$

$\phi(E) = \nu n(E)$ and $\chi(E)$ is the normalized fission spectrum. In this case, the criticality condition is:

$$k = p \nu \frac{\sigma_{f_{th}}}{\sigma_{a_{th}}} + (1 - p) \nu \frac{\int_{E_{th}}^{\infty} \sigma_f \phi dE}{\int_{E_{th}}^{\infty} \sigma_a \phi dE} = 1 \quad (4)$$

where:

$$p = \sigma_{a_{th}} \phi_{th} / \left(\int_{E_{th}}^{\infty} \sigma_a \phi dE + \sigma_{a_{th}} \phi_{th} \right)$$

The equations adjoint to Eqs. (2) and (3) are:

$$\frac{1}{\nu \sigma} \frac{\partial m(E)}{\partial t} = 0 = \nu \frac{\sigma_f}{\sigma} \int_{E_{th}}^{\infty} m \chi dE + \frac{\sigma_s}{\sigma} \int_{E_{th}}^E m(E') g(E', E) dE' - m + \frac{\sigma_s}{\sigma} G(E_{th}, E) m_{th} \quad (5)$$

$$\frac{1}{\nu_{th} \sigma_{a_{th}}} \frac{\partial m_{th}}{\partial t} = 0 = \nu \frac{\sigma_{f_{th}}}{\sigma_{a_{th}}} \int_{E_{th}}^{\infty} m \chi dE - m_{th} \quad (6)$$

The solution of these equations is:

$$m_{th} = \frac{\sigma_{f_{th}}}{\sigma_{a_{th}}} \nu \bar{m} \quad (7a)$$

$$m(E) = \nu \bar{m} \left\{ \int_{E_{th}}^E \sigma_f(E') \phi(E', E) dE' + q(E_{th}, E) \frac{\sigma_{f_{th}}}{\sigma_{a_{th}}} \right\} \quad (7b)$$

$$\bar{m} = \int_{E_{th}}^{\infty} m(E) \chi(E) dE \quad (7c)$$

where $\phi(E', E)$ and $q(E_{th}, E)$ are, respectively, the flux distribution at E' and thermal slowing-down density resulting from a unit source $\delta(E' - E)$ at energy E .

The first-order perturbation formula comparing two critical reactors differing only in fuel content is:

$$\delta R = 0 = \frac{\delta \nu}{\nu} + \frac{\int_{E_{th}}^{\infty} \varphi \delta \sigma_f dE + \varphi_{th} \delta \sigma_{f_{th}}}{\int_{E_{th}}^{\infty} \varphi \sigma_f dE + \varphi_{th} \sigma_{f_{th}}} - \frac{\int_{E_{th}}^{\infty} m \varphi \delta \sigma_a dE + m_{th} \varphi_{th} \delta \sigma_{a_{th}}}{\nu \bar{m} \left[\int_{E_{th}}^{\infty} \varphi \sigma_f dE + \varphi_{th} \sigma_{f_{th}} \right]} \quad (8)$$

where the $\delta \sigma$ represent the change in the labeled cross section owing to the changed fuel content, $\delta \nu$ is the change in the value of ν required to satisfy the criticality condition* Eq. (4), and φ and m correspond to the calculated case for which the obtained ν is different from its physical value. It has been assumed in Eq. (8) that the effect of the change in scattering cross section is negligible. On the basis of this assumption, Eq. (8) may also be used to estimate the change in critical mass owing to changing the fuel type. In this case, $\delta \nu$ is the change in actual ν value. If the fission spectrum is different, the term $1/\bar{m} \int m \delta \chi(E) dE$ must be added to the right side of Eq. (8). This term may also be viewed as the effect on reactivity, R , resulting from the use of a fission spectrum inaccurate by $\delta \chi(E)$.

ONE-VELOCITY REACTORS

For one-velocity reactors without any external source, Eq. (17) in Chapter 1.3 can be used with S replaced by the fission source:

$$S(\underline{r}, \underline{\Omega}, t) = \frac{1}{4\pi} \sigma_f \int F(\underline{r}, \underline{\Omega}, t) d\underline{r}$$

and the integral equation, Eq. (23) in Chapter 1.3, is true with $S(\underline{r}') = 0$ and with $1 + f$ defined as in Eq. (22), Chapter 1.3:

$$1 + f = \frac{\sigma_s + \nu \sigma_f}{\sigma}; \quad \sigma = \sigma_f + \sigma_c + \sigma_s \quad (9)$$

BARE REACTORS

THE ITERATIVE METHOD

The critical radius of a bare sphere can be computed to any degree of accuracy by an iterative method used by Placzek and reported by Carlson.¹ The method, applicable as well for anisotropic scattering, uses a polynomial trial function in Eq. (26), Chapter 1.3, and matches the moments of the trial function and its first iterate. Results obtained by use of a quadratic trial function are given in Table 1.4.1, for the case of a linear scattering law in the laboratory system. The parameter α is defined as:

$$\alpha = 3 \overline{\cos \theta} \sigma_s / \sigma \quad (10)$$

where $\overline{\cos \theta}$ is the average cosine of the angular deflection in scattering.

*The criticality condition is here regarded as the determining equation for ν even though the value thus obtained generally differs from the known physical value.

¹References appear at end of chapter.

Table 1.4.1 — Bare-sphere Critical Radius (σa) in Units of Mean Free Path ($1/\sigma$) as Computed by Quadratic Iteration (LADC-756)

f	$\alpha^* = -1.0$	$\alpha^* = -0.5$	$\alpha^* = 0.0$	$\alpha^* = 0.5$	$\alpha^* = 1.0$
0.0
.1	4.333	4.585	4.895	5.276	5.770
.2	2.846	2.997	3.178	3.396	3.678
.4	1.8081	1.8907	1.9871	2.1015	2.2408
.6	1.3593	1.4140	1.4769	1.5498	1.6364
.8	1.0993	1.1388	1.1838	1.2350	1.2946
1.0	0.9269	0.9570	0.9909	1.0290	1.0728
1.2	.8031	.8270	.8535	0.8831	0.9167
1.4	.7094	.7289	.7503	.7740	.8005
1.6	.6359	.6521	.6697	.6892	.7108
1.8	.5766	.5902	.6050	.6212	.6393
2.0	.5276	.5394	.5520	.5656	.5808
∞	.0000	.0000	.0000	.0000	.0000

$$* \alpha = \frac{3\sigma_s}{\sigma} \overline{\cos \theta}$$

THE END-POINT METHOD

The end-point method considers the asymptotic (away from boundaries) solution satisfying:

$$\nabla^2 \phi + (\kappa\sigma)^2 \phi = 0 \quad (11)$$

where, for linear anisotropy:

$$(1 + f) \frac{\tan^{-1} \kappa}{\kappa} - \frac{\alpha f}{\kappa^2} \left(1 - \frac{\tan^{-1} \kappa}{\kappa} \right) = 1 \quad (12)$$

The method then proceeds to calculate the extrapolated end point, z_0 . The shape of ϕ and the critical size for a few simple geometries* are as presented in Table 1.4.2. Values of z_0 as a function of $1 + f$ and of $b = \sigma_s \overline{\cos \theta} / (\sigma_s + \nu\sigma_f)$ are given in Table 1.3.11 where, for f significantly different from zero, terms in b^2 have been neglected.

THE SERBER-WILSON METHOD

The Serber-Wilson method is the only method mentioned that generalizes for reflected reactors and is discussed later.

COMPARATIVE ACCURACY OF THE METHODS³

The error in critical radius of a bare sphere: (a) for the end-point method, increases from 0 to ~0.2% as $1 + f$ increases from 1 to 3; (b) for the Serber-Wilson method, increases

* The method is strictly applicable only in the case of the bare sphere. Compare Ref. (2).

Table 1.4.2 — Asymptotic Flux and Critical Size for Simple Geometries

Case	Flux	Critical size
Sphere (radius a)	$\frac{\sin \kappa \sigma r}{\kappa \sigma r}$	$\sigma a = \frac{\pi}{\kappa} - z_0$
Slab (thickness $2a$)	$\cos \kappa \sigma x$	$\sigma a = \frac{\pi}{2\kappa} - z_0$
Cylinder (radius a)	$J_0(\kappa \sigma r)$	$\sigma a = \frac{2.405}{\kappa} - z_0$

rapidly from 0 to $\sim 4\%$ as $1 + f$ increases from 1 to 1.2, and then remains nearly constant at $\sim 4\%$ for higher values of $1 + f$; (c) for the iterative method with a quadratic trial function, decreases from $\sim 0.2\%$ to 0 as $1 + f$ increases from 1.2 to ∞ ; the iterative method breaks down for f near zero.

THE TRANSPORT APPROXIMATION*

The transport approximation reduces an anisotropic problem to the far simpler isotropic problem. The "isotropic equivalent" scattering cross section is chosen to be:

$$\sigma_{tr} = \sigma_s (1 - \overline{\cos \theta}) \quad (13)$$

Thus, the anisotropic case may be treated by the above methods with:

$$\begin{aligned} \sigma &= \sigma_f + \sigma_c + \sigma_{tr} \\ 1 + f &= \frac{\sigma_{tr} + \nu \sigma_f}{\sigma} \end{aligned} \quad (14)$$

$$\overline{\cos \theta} = 0$$

Results obtained in this approximation by use of quadratic iteration are compared in Fig. 1.4.1 to those of Table 1.4.1 for the case of linear scattering in a bare sphere. That the transport approximation is very accurate for f near zero (reactors greater in size than a few mean free paths) in the case of linear scattering is also exhibited by Table 1.3.11.

REFLECTED REACTORS

The end-point method can be applied to reflected reactors in the special case that core and reflectors all have the same total cross section. Derivations of equations and numerical tables are reported by Frankel and Goldberg⁴ for the case of isotropic scattering. Anisotropic scattering may be treated by the transport approximation.

The Serber-Wilson method is more general than the end-point method in that equality of total cross section in the various media is not required. The case of isotropic scattering and spherical symmetry has been extensively reported.^{5,6,7,8} Other geometries and anisotropic scattering are discussed by Davison,⁷ pp 94 and 155. Anisotropic scattering may be treated by the transport approximations.

* Compare Chapter 1.3.

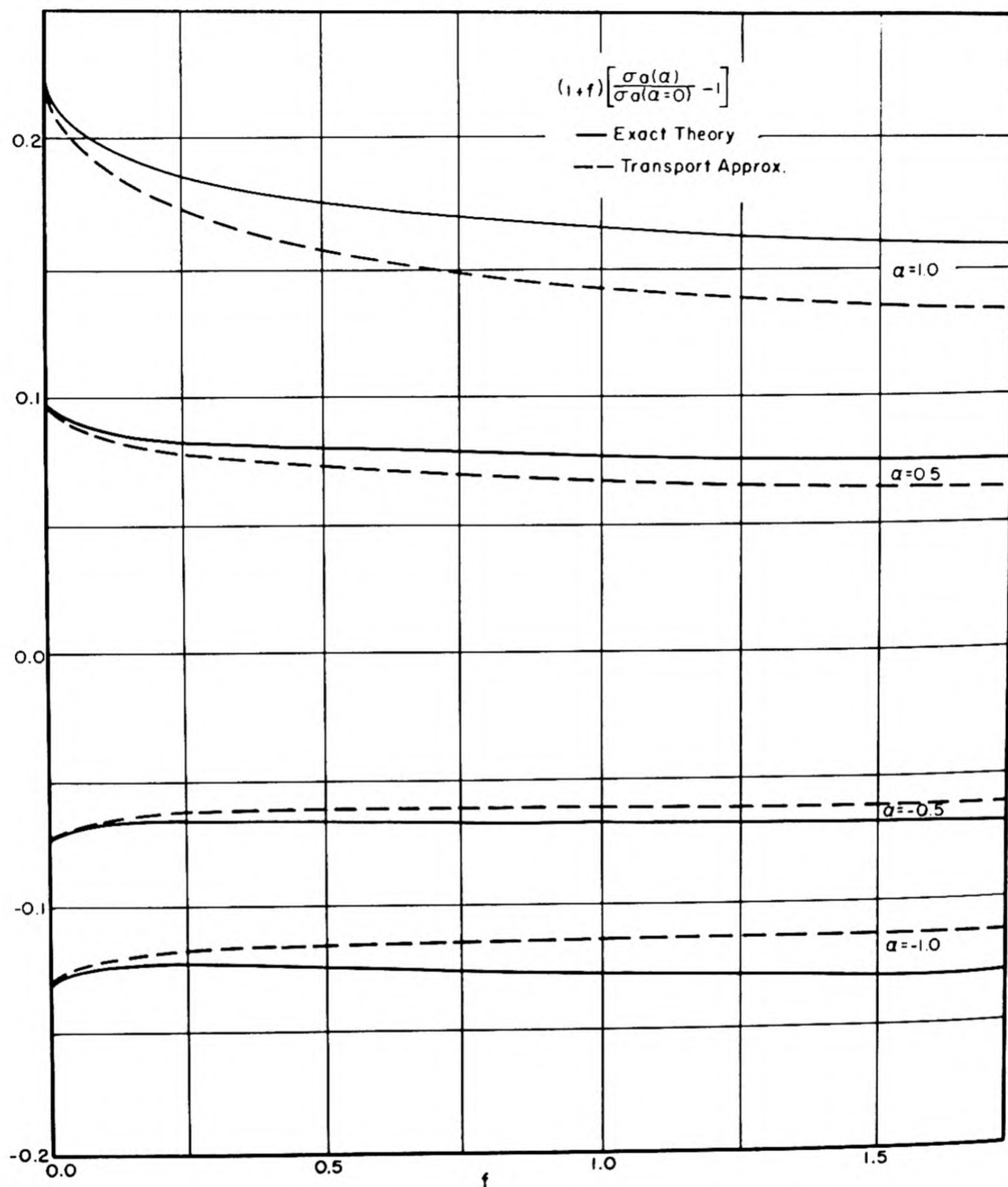


Fig. 1.4.1 — Comparison of Bare-sphere Critical Sizes with and without Transport Approximation for Linear Scattering Laws for Various Amounts of Anisotropy. Reprinted from LA-1061 (LADC-756). The quantity $1 + f = \sigma_s + \nu \sigma_f / \sigma$ times the fractional change in critical radius due to anisotropy as computed by quadratic iteration is plotted against f for various values of $\alpha = 3(\sigma_s/\sigma) \overline{\cos \theta}$, with and without the transport approximation.

The accuracy of the Serber-Wilson method is greater in the case of reflected reactors than for bare reactors. The method underestimates the critical radius, the error⁶ (less than 2 percent) being nearly the same under a wide variety of conditions.

THE SERBER-WILSON METHOD

The Serber-Wilson method deals with the asymptotic solutions in each region which, for spherical symmetry, are:

$$\varphi_c = A_c \frac{\sin \kappa_c \sigma_c r}{\kappa_c \sigma_c r} \quad (15)$$

$$\varphi_i = A_i \frac{e^{-\kappa_i \sigma_i r}}{\kappa_i \sigma_i r} + B_i \frac{e^{+\kappa_i \sigma_i r}}{\kappa_i \sigma_i r} \quad (16)$$

where $\phi = vn(r)$ is the flux, "c" denotes the core, and "i" denotes the i^{th} reflector. The cross section, σ , is the total cross section given by Eq. (14) in the transport approximation. In the same approximation, κ_c and κ_i are given by:

$$\frac{\tan^{-1} \kappa_c}{\kappa_c} = \frac{1}{1 + f_c} \quad (17)$$

$$\frac{\tanh^{-1} \kappa_i}{\kappa_i} = \frac{1}{1 + f_i} \quad (18)$$

Extension to the case of a multiplying ($f_i > 0$) reflector presents no added difficulty.

Neutron conservation implies continuity of the current density $j(r)$:

$$j(\text{normal}) = \text{continuous at boundaries} \quad (19)$$

where for any Laplacian mode, $j(r)$ is given by: *

$$j(r) = -\frac{|f|}{\kappa^2 \sigma} \text{grad } \varphi \quad (20)$$

Thus:

$$j_c(r) = A_c \frac{f}{\kappa^2 \sigma r} \left(\frac{\sin \kappa \sigma r}{\kappa \sigma r} - \cos \kappa \sigma r \right) \quad (21)$$

$$j_i(r) = \frac{|f|}{\kappa^2 \sigma r} \left[A_i e^{-\kappa \sigma r} \left(1 + \frac{1}{\kappa \sigma r} \right) - B_i e^{+\kappa \sigma r} \left(1 - \frac{1}{\kappa \sigma r} \right) \right] \quad (22)$$

where subscripts have been omitted from the right sides.

In place of the boundary conditions on the flux ϕ (cf, Chapter 1.3), the method uses the "Serber condition" which requires that the integral Eq. (23), Chapter 1.3, be satisfied at the center of symmetry. This, however, gives only one equation, and this is sufficient only in the case of a bare reactor or a single infinite reflector. In other cases, the missing

* Eq. (20) is a generalization of Eqs. (70) and (71), Chapter 1.3, being valid for $f > 0$ as well as for $f < 0$.

equations are supplied by satisfying the Serber condition "in detail."* In the spherical case under consideration, the Serber condition "in detail" reduces to the Wilson conditions that:

$$\phi(r, -1) = \text{continuous at boundaries}$$

$$\phi(r, -1) = 0 \text{ at outer boundary}$$

where $\phi(r, -1)$ is the radially inward flux at r computed as if the media to the left and right of the boundary each extended to infinity. For the asymptotic solutions, $\phi(r, -1)$ is given by:†

$$4\pi\phi_c(r, -1) = A_c \frac{(1 + f)}{\kappa} e^{\sigma r} \text{Im} E_1(\sigma r[1 - i\kappa]) \quad (23)$$

$$4\pi\phi_i(r, -1) = \frac{(1 + f)}{\kappa} e^{\sigma r} \{A_i E_1(\sigma r[1 + \kappa]) + B_i E_1(\sigma r[1 - \kappa])\} \quad (24)$$

For criticality computations, it is sufficient to apply the conditions:

$$F(\sigma r, f) = \frac{4\pi\phi(r, -1)}{j_{(\text{normal})}(r)} = \text{continuous at inner boundaries} \quad (25)$$

$$\phi(r, -1) = 0 \text{ at outer boundary.} \quad (26)$$

NUMERICAL RESULTS

Numerical results are easily obtained in the case of a single reflector, whether finite or infinite. The critical equation for this case is:

$$F_c(\sigma_c a, f_c) = F_1(\sigma_1 a, f_1, \gamma) \quad (27a)$$

where:

$$a = \text{core radius} \quad (27b)$$

$$\gamma a = \text{outer radius} \quad (27c)$$

The parameter A_c does not appear in F_c , and the parameters A_1 and B_1 are eliminated from F_1 by use of condition (26).

Figure 1.4.2 plots F_c as a function of $\sigma_c a$ for values of f_c ranging from 0.02 up to 2.0. Figure 1.4.3 plots F_1 for an infinite reflector ($\gamma = \infty$) as a function of $\sigma_1 a$ for values of f_1 ranging from 0 to -0.8. Figures 1.4.4 to 1.4.8 plot for $f_1 = 0, -0.02, -0.05, -0.1$, and -0.2 F_1 as a function of $\sigma_1 a$ for several values of γ ranging from 1.1 to ∞ .

If any of the F_1 plots is superposed‡ on Fig. 1.4.2 with the σa axes coinciding but with the origin ($\sigma_1 a = 0.1, F_1 = 0.1$) of the F_1 graph located at the point§ ($\sigma_c a = 0.1 \sigma_c / \sigma_1, F_c = 0.1$) of the F_c graph, then the solution for any given value of f_1 and for any given f_c and γ

* Davison,† p 92.

† $E_1(x) = \int_1^\infty \frac{e^{-xt}}{x} dt$, and Im signifies the imaginary part.

‡ When either curve is redrawn as a transparency.

§ This brings the two graphs into the same distance scale, the σa scales being logarithmic.

REACTOR STATICS; THEORY

is obtained from the σ_c a value or the σ_1 a value at the point of intersection of the corresponding curves. The critical radius is given by:

$$a = \frac{(\sigma_c a)}{\sigma_c} = \frac{(\sigma_1 a)}{\sigma_1}$$

Sweeney, Goldstein, and Carlson⁹ present an extensive tabulation of functions in terms of which $F(\sigma a, f)$ may be expressed.

DIFFUSION THEORY*

The one-velocity diffusion-theory equation for a homogeneous region is:

$$D\nabla^2 \varphi + (k - 1) \sigma_a \varphi = 0 \quad (28)$$

where:

$$k = \frac{\nu \sigma_f}{\sigma_a} = \frac{\nu \sigma_f}{\sigma_c + \sigma_f} \quad (29)$$

is the multiplication constant. Thus:

$$\nabla^2 \varphi + B^2 \varphi = 0 \quad (30)$$

where:

$$B^2 = \frac{(k - 1) \sigma_a}{D} = \frac{f \sigma}{D} \quad (31)$$

The buckling, B^2 , is positive in a multiplying region, in which:

$$B^2 = (k\sigma)^2 \quad (32a)$$

and negative in a non-multiplying region, in which:

$$B^2 = -(k\sigma)^2 \quad (32b)$$

It follows that Eq. (28) gives correct asymptotic solutions for a linear scattering law if κ is given by Eq. (12) or by the equivalent † equation for a non-multiplying medium. These equations lead to ‡ the following expressions for B^2 which for $0 \leq \overline{\cos \theta} \leq 0.2$ are accurate to better than 1 percent in the stated f ranges:

$$0 \leq f \leq 1.5 \quad B^2 = 3f\sigma^2 \left(1 - \frac{\sigma_s}{\sigma} \overline{\cos \theta} \right) (1 + 0.8060f) \quad (33a)$$

$$-0.6 \leq f \leq 0 \quad B^2 = 3f\sigma^2 \left(1 - \frac{\sigma_s}{\sigma} \overline{\cos \theta} \right) (1 + 0.7848f) \quad (33b)$$

* See Chapter 1.3, "One-velocity Theory."

† $(1 + f) \frac{\tanh^{-1} \kappa}{\kappa} + \frac{\alpha f}{\kappa^2} \left(1 - \frac{\tanh^{-1} \kappa}{\kappa} \right) = 1$

‡ Goldberger, unpublished. An equation usually written for $f < 0$ and $\overline{\cos \theta} = 0$ is:

$$-B^2 = 3\sigma \sigma_a \left(1 - 0.8 \frac{\sigma_a}{\sigma} \right) = -3f\sigma^2 (1 + 0.8f)$$

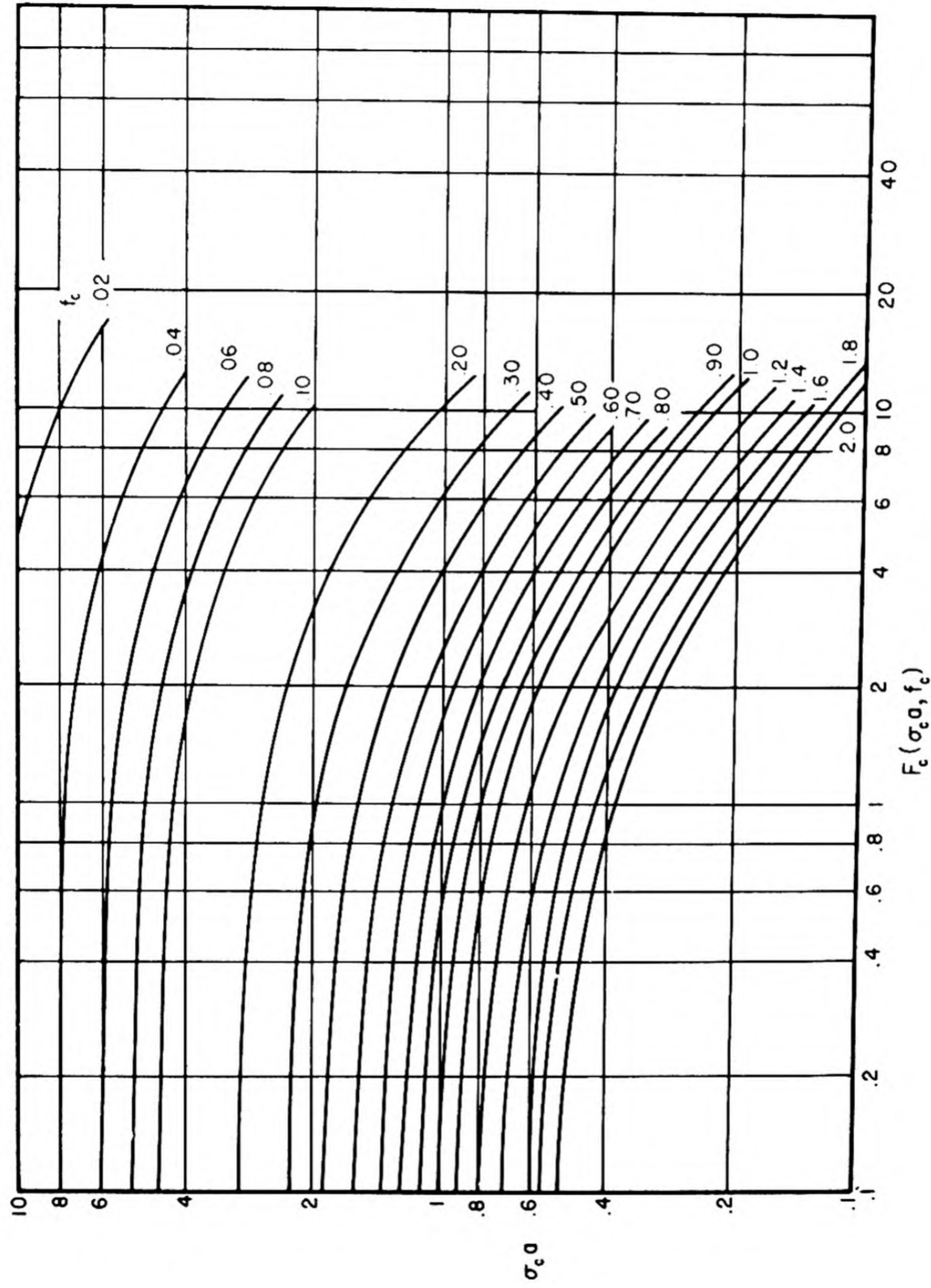


Fig. 1.4.2 — $F_c(\sigma_c a, f_c)$ as Function of $\sigma_c a$ for Various Values of f_c . From A.E.R.E. T/R-587.

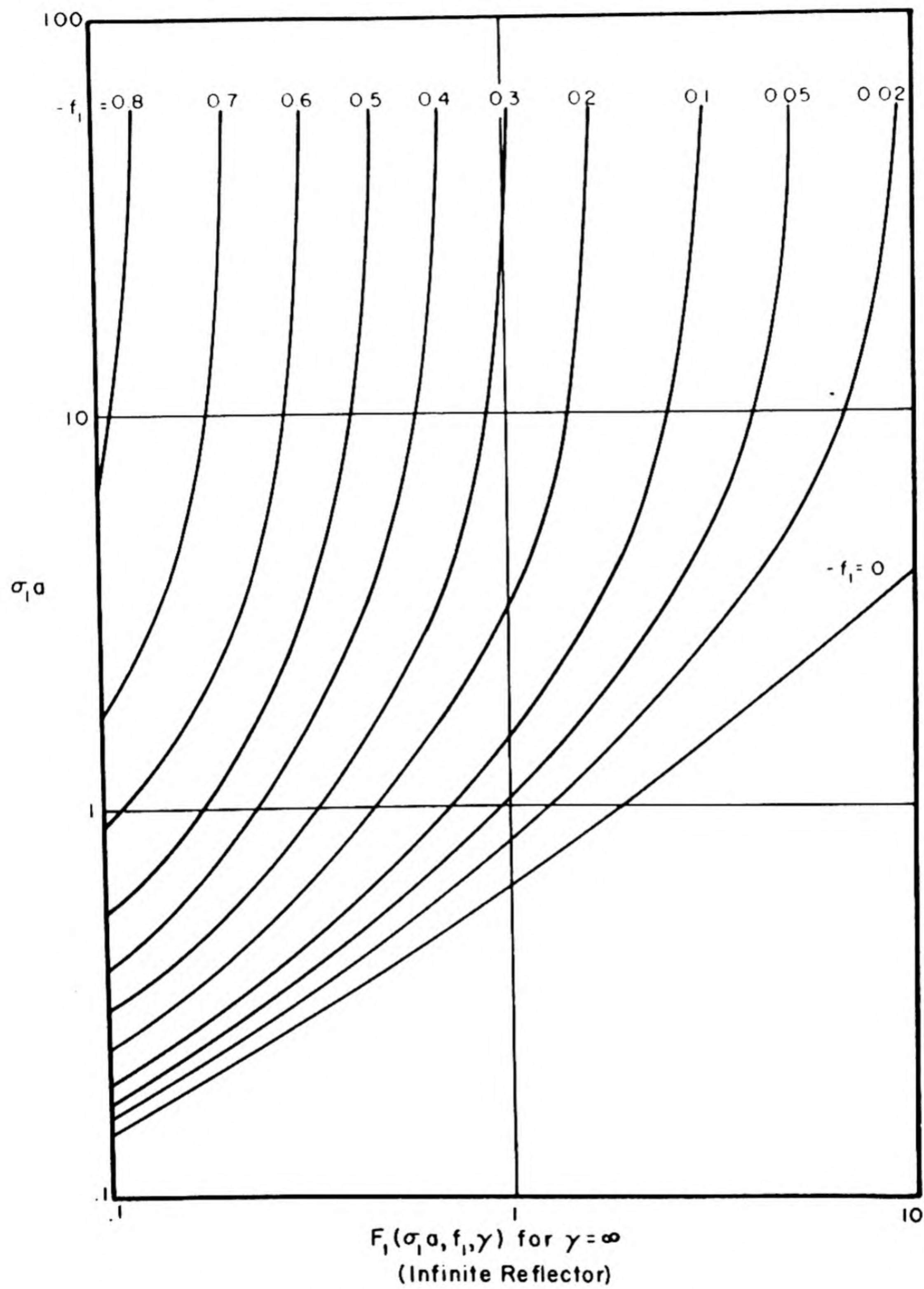


Fig. 1.4.3 — $F_1(\sigma_1 a, f_1, \gamma)$ for $\gamma = \infty$ (Infinite Reflector) as Function of $\sigma_1 a$ for Various Values of f . From A.E.R.E. T/R-586.

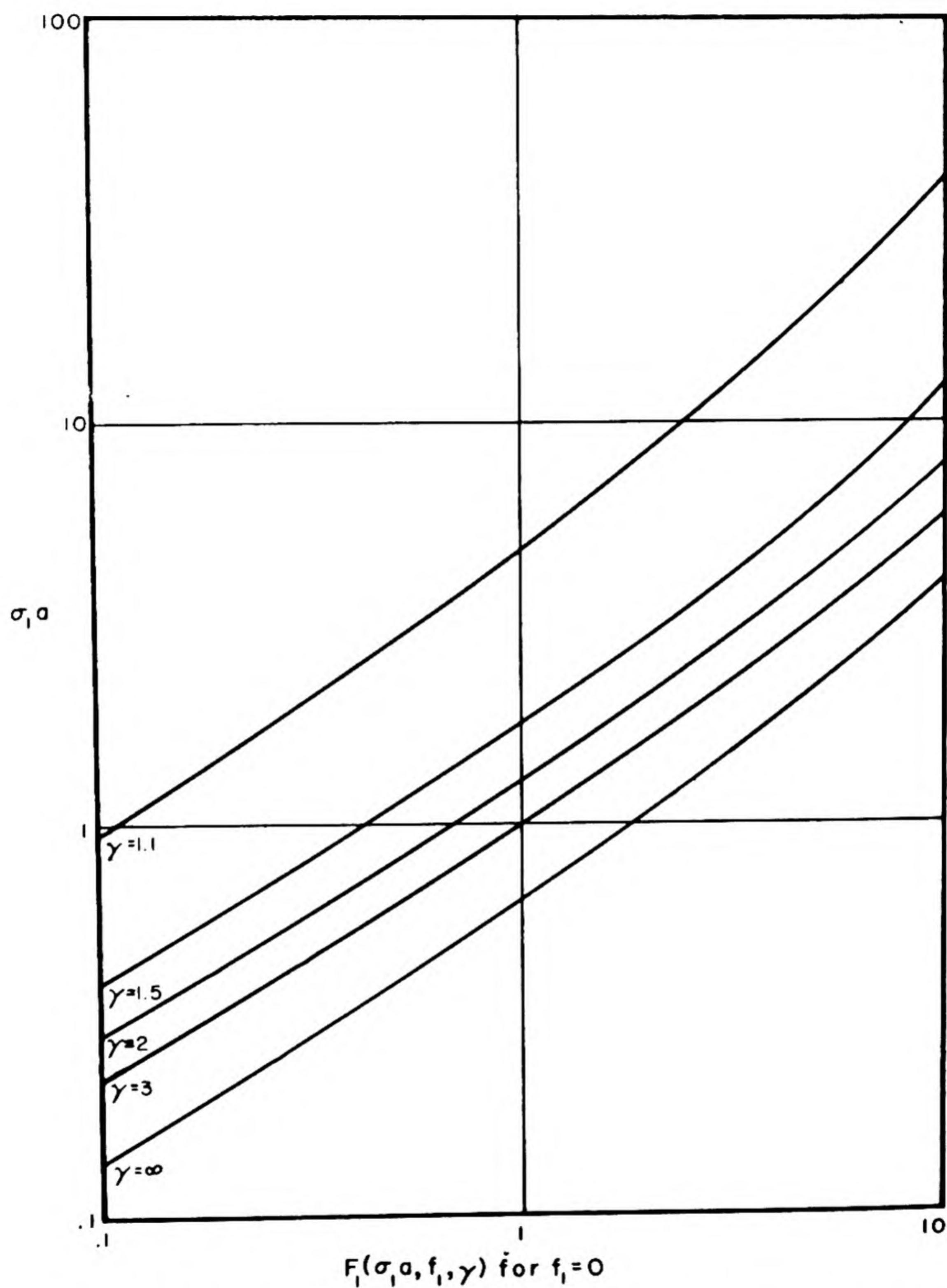


Fig. 1.4.4 — $F_1(\sigma_1 a, f_1, \gamma)$ for $f_1 = 0$ as Function of $\sigma_1 a$ for Various Values of γ .
From A.E.R.E. T/R-587.

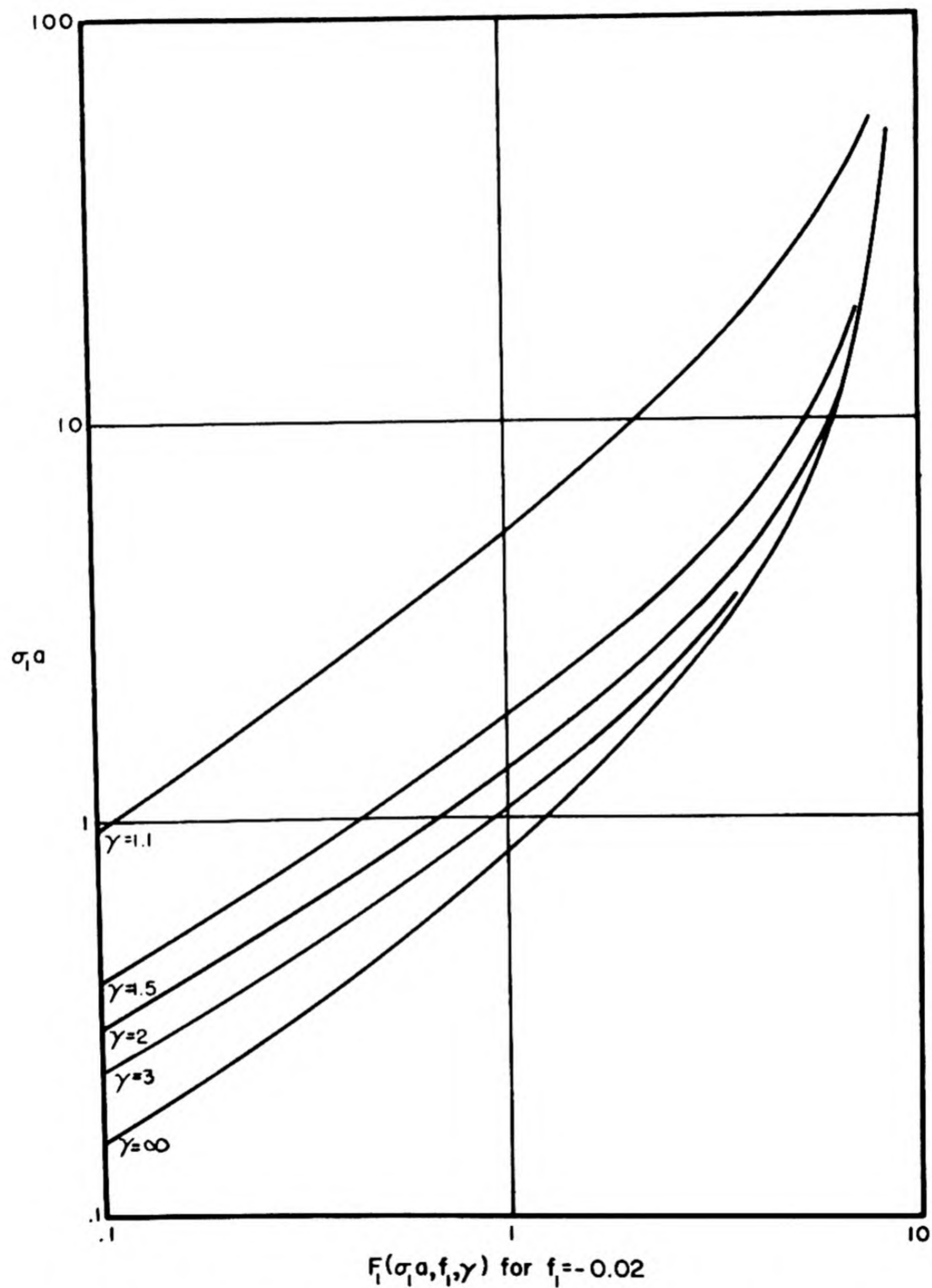


Fig. 1.4.5 — $F_1(\sigma_1 a, f_1, \gamma)$ for $f_1 = -0.02$ as Function of $\sigma_1 a$ for Various Values of γ . From A.E.R.E. T/R-587.

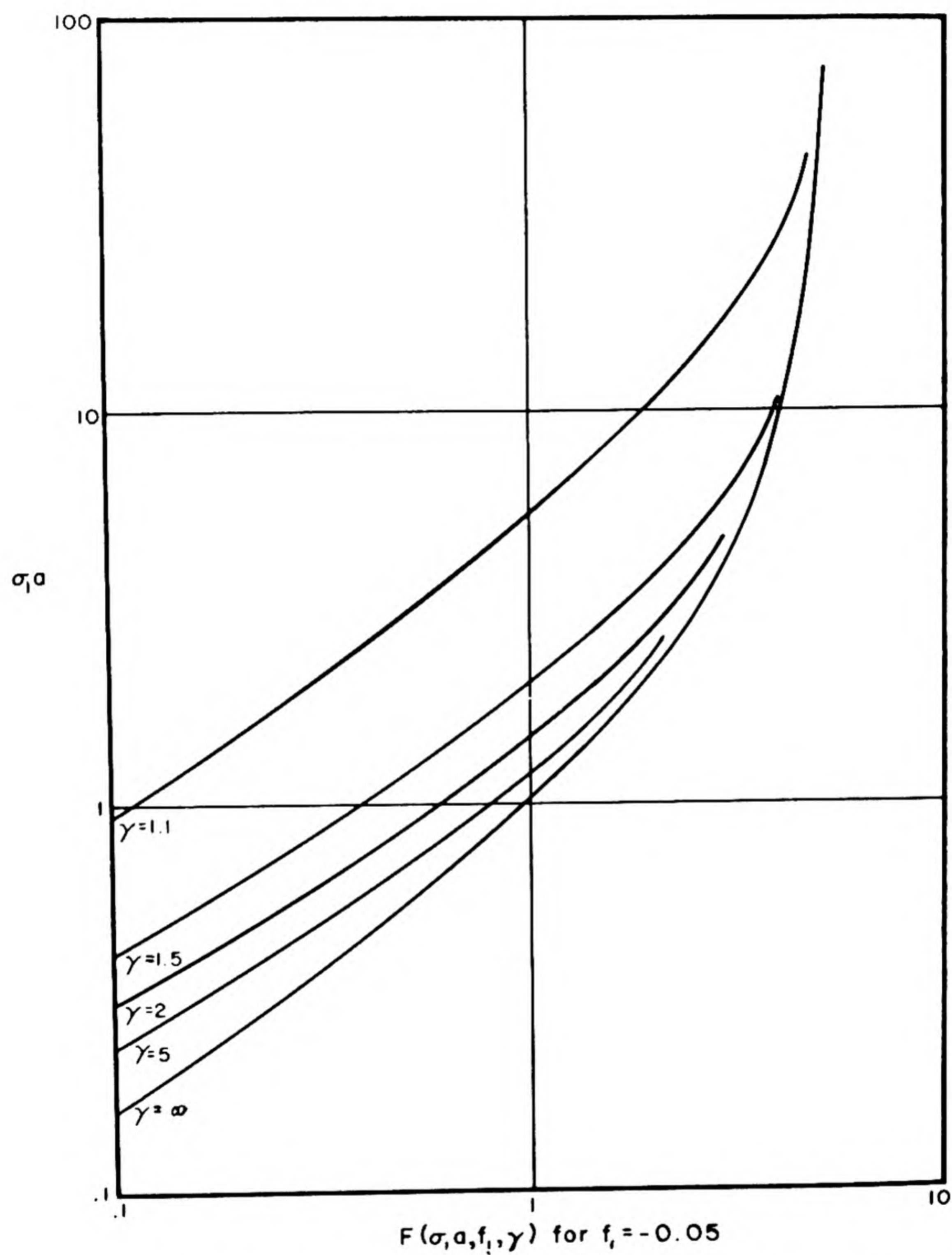


Fig. 1.4.6 — $F_1(\sigma_1 a, f_1, \gamma)$ for $f_1 = -0.05$ as Function of $\sigma_1 a$ for Various Values of γ . From A.E.R.E. T/R-587.

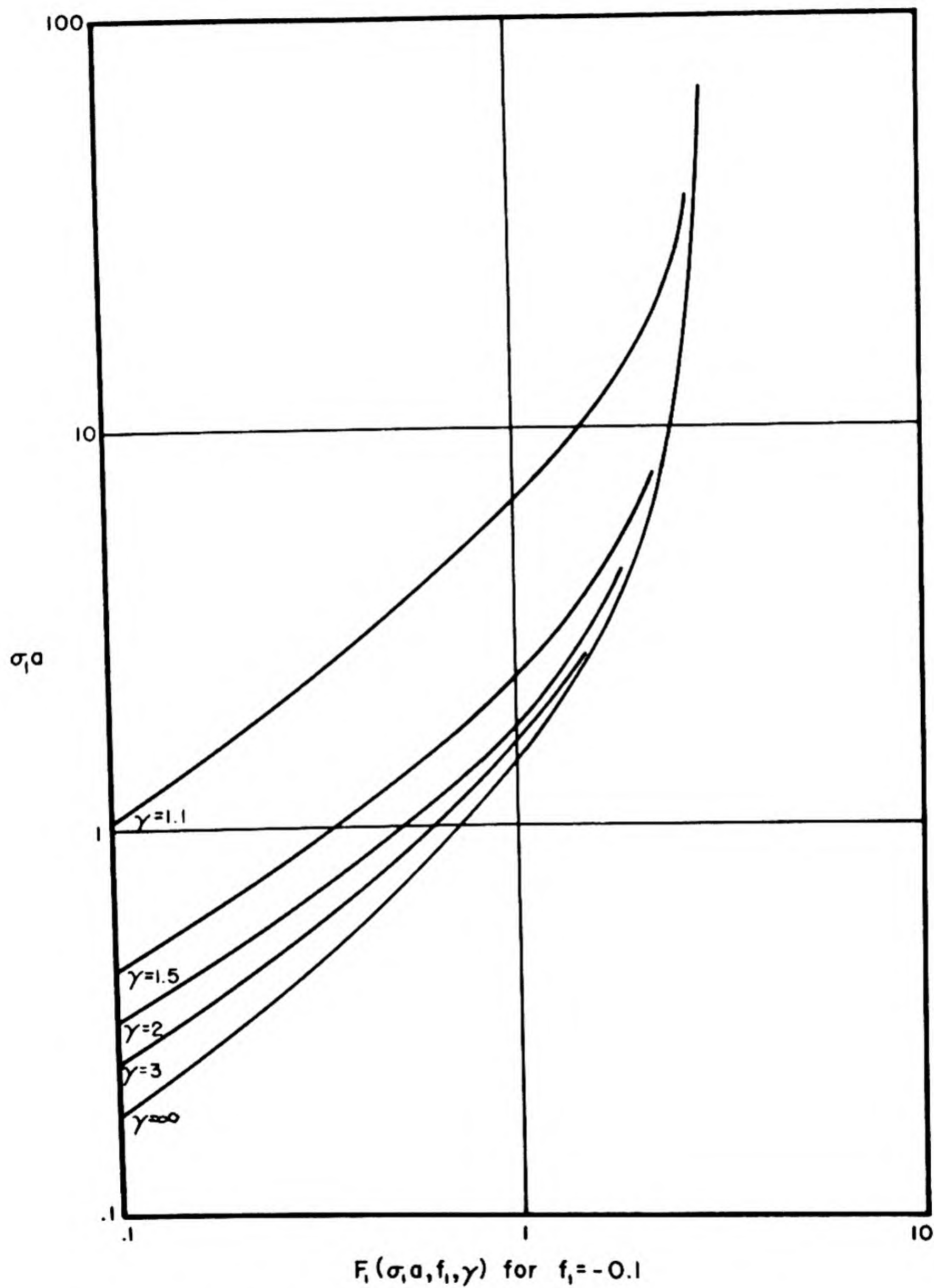


Fig. 1.4.7 — $F_1(\sigma_1 a, f_1, \gamma)$ for $f_1 = -0.1$ as Function of $\sigma_1 a$ for Various Values of γ . From A.E.R.E. T/R-587.

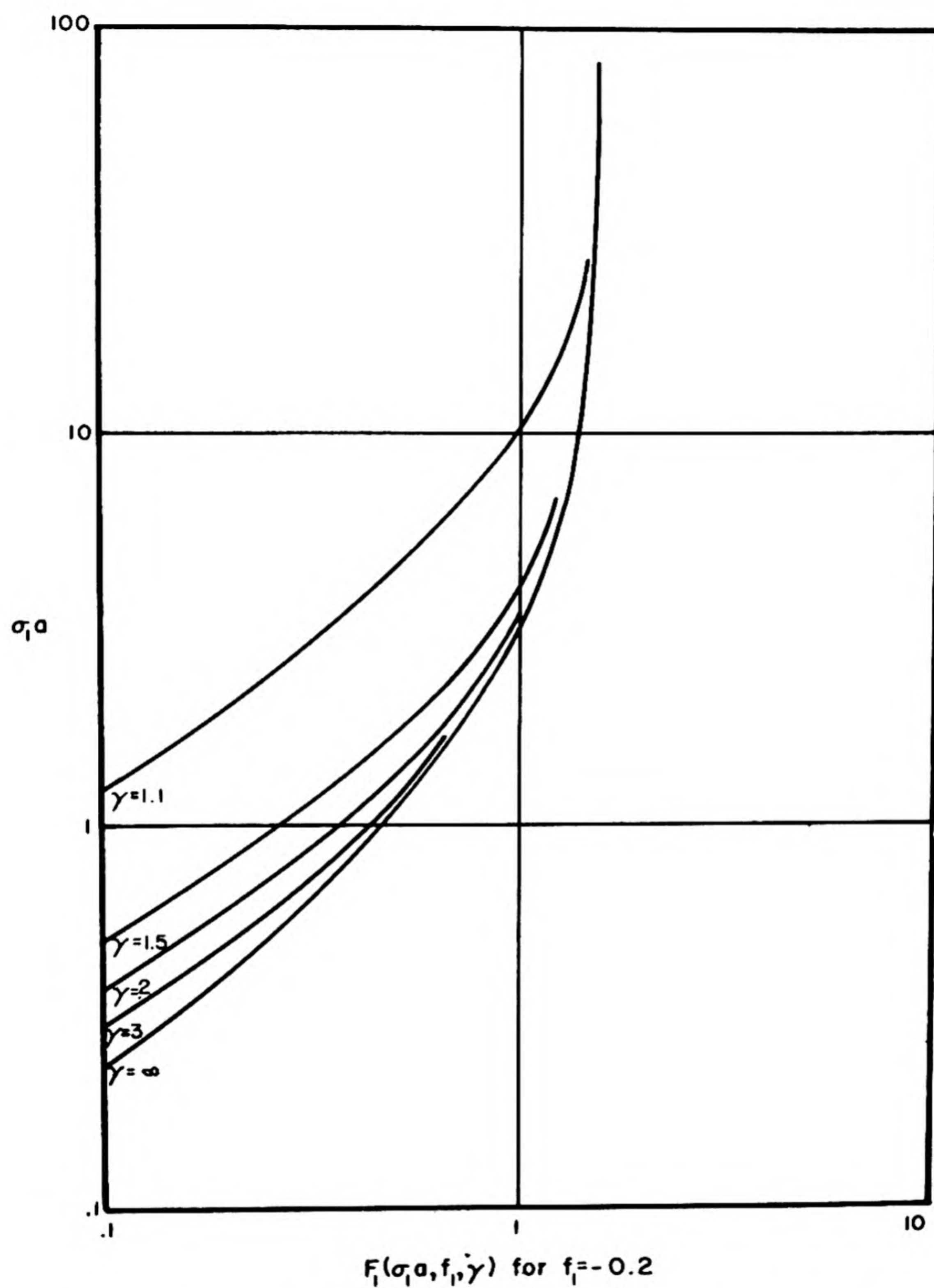


Fig. 1.4.8 — $F_1(\sigma_1 a, f_1, \gamma)$ for $f_1 = -0.2$ as Functions of $\sigma_1 a$ for Various Values of γ . From A.E.R.E. T/R-587.

The current density, j , is given by:

$$j = -D \text{ grad } \phi \quad (34)$$

and the boundary conditions are continuity of ϕ and j (normal) at interfaces, and $\phi = 0$ at an extrapolation length outside a black boundary. The diffusion constant, D , is given by: *

$$D = \frac{f\sigma}{B^2} \quad (35)$$

BARE REACTORS

In general, there are a discrete infinity of positive B^2 values for which the solutions of Eq. (30) satisfy the $\phi = 0$ boundary condition. The lowest of these B^2 values belongs to the fundamental ϕ mode and is called the geometric buckling, B_g^2 . The higher modes† cannot correspond to the steady-state solution because they call for negative neutron densities. The critical equation is:

$$B_g^2 = B_m^2 \quad (36)$$

where the material buckling, B_m^2 , is given by Eq. (31).

Table 1.4.3 presents, for some geometries, the fundamental mode along with the corresponding value of B_g^2 . The actual reactor fills the volume of the geometrical shapes considered except for an extrapolation distance from the boundaries.‡ Other geometries which have been treated are the spheroid,¹⁰ the right hexagonal cylinder;¹¹ a truncated cone,¹² and spherical segments.¹³ The spherical sector is also treated elsewhere.¹⁴

Variational Principle

The geometric buckling may be obtained by a simple variational formula:

$$\delta I = 0 \quad (37)$$

$$I = \int \phi \nabla^2 \phi d\mathbf{r} - B_g^2 \int \phi^2 d\mathbf{r} = \int (\text{grad } \phi)^2 d\mathbf{r} - B_g^2 \int \phi^2 d\mathbf{r}$$

where:

$$\phi = \phi(\alpha_1)$$

is a trial function satisfying the $\phi = 0$ boundary condition for all values of the parameters α_1 . The elimination of the α_1 from the equations:

$$\frac{\partial I}{\partial \alpha_1} = 0$$



* In the P_1 approximation (Chapter 1.3), $D = \lambda_{tr}/3$.

† Only the fundamental has no zeros inside the extrapolated boundary. The higher modes decay in time and are useful as expansion functions in dynamic considerations.

‡ This statement does not have a clear meaning for most of the considered geometries.

Table 1.4.3 — Fundamental Mode Solution and Geometric Buckling for Some Geometries; All Dimensions Are Extrapolated

(Adapted from Weinberg and Noderer, Ch. V)

Geometry	Mode, ϕ	Buckling	Comments concerning volume, V , for given buckling
Infinite slab (thickness a)	$\cos \frac{\pi x}{a}$	$B_g^2 = \pi^2/a^2$	
Infinite right circular cylinder (radius a)	$J_0(2.405 r/a)$	$B_g^2 = (2.405)^2/a^2$	
Sphere (radius a)	$\frac{\sin \pi r/a}{\pi r/a}$	$B_g^2 = \pi^2/a^2$	$V_{\text{sphere}} = \frac{4}{3} \pi a^3$
Rectangular parallelepiped (dimensions a, b, c)	$\cos \frac{\pi x}{a} \cos \frac{\pi y}{b} \cos \frac{\pi z}{c}$	$B_g^2 = \pi^2 \left(\frac{1}{a^2} + \frac{1}{b^2} + \frac{1}{c^2} \right)$	V is minimum for $a = b = c$, cube, $V_{\text{cube}} = 1.240 V_{\text{sphere}}$
Finite right circular cylinder (height H , radius a)	$\cos \frac{\pi z}{H} J_0(2.405 r/a)$	$B_g^2 = \frac{\pi^2}{H^2} + \frac{(2.405)^2}{a^2}$	V is minimum for $H = 1.85a$; $V_{\text{cyl}} = 1.142 V_{\text{sphere}}$
Sector of a sphere where α is such that it is the first root of $P_n(\cos \alpha) = 0$ for some integer n . 	$P_n(\cos \theta) \frac{J_{n+1/2}(\mu_n r/a)}{\sqrt{\mu_n r/a}}$ μ_n is first root of $J_{n+1/2}(\mu_n) = 0$	$B_g^2 = \mu_n^2/a^2$	
Hemisphere ($\alpha = \frac{\pi}{2}$, $n = 1$ from above)	$\mu_1 = 4.49$	$B_g^2 = \frac{(4.49)^2}{a^2}$	$V_{\text{hemisphere}} = 1.46 V_{\text{sphere}}$
Sector of a cylinder of height H and cross-section  where $\alpha = \frac{\pi}{2l_n}$ ($n = \text{integer}$)	$\cos \frac{\pi z}{H} \cos n\theta J_n(\mu_n r/a)$ μ_n is first root of $J_n(\mu_n) = 0$	$B_g^2 = \frac{\pi^2}{H^2} + \frac{\mu_n^2}{a^2}$	
Right elliptic cylinder height H , semi-major axis a , eccentricity ϵ	$\cos \frac{\pi z}{H} \sum_{m=0}^{\infty} A_{2m} \cos 2m\theta J_{2m}(B_g r)$	$\epsilon = \frac{B_g^2 - \pi^2/H^2}{(2.405)^2/a^2}$ 0.8 (2.51) ² / a^2 0.85 (2.63) ² / a^2 0.9 (2.84) ² / a^2 0.94 (3.12) ² / a^2	
Sphere of radius a with central black cavity of radius b	$\frac{1}{r} \sin \pi \frac{r-b}{a-b}$	$B_g^2 = \frac{\pi^2}{(a-b)^2}$	$a = \frac{\pi}{B_g} + b$

results in a value for B_g^2 as a function of the geometry.* A numerical example¹⁵ gives for a sphere of radius "a":

$$B_g^2 a^2 = 14.0$$

for a trial function:

$$\phi = \alpha_1(r - a)^2$$

and gives:

$$B_g^2 a^2 = 11.6$$

for a trial function:

$$\phi = \alpha_1(r - a)^2 + \alpha_2(r - a)^4$$

the correct result being:

$$B_g^2 a^2 = \pi^2 = 9.87$$

Effect of Density on Critical Size

In the case that the reactor undergoes a uniform compression or dilation so that the final shape is geometrically similar to the initial shape, the following theorem is valid for all cases, including multivelocity reflected reactors.

THEOREM: In any critical system, if the density of all components is reduced (increased) uniformly, then to make the system again critical, all linear dimensions must be increased (reduced) by the same factor. Thus, if ρ is the factor by which the density is multiplied, all cross sections are multiplied by ρ , linear dimensions are divided by ρ , and the mass is divided by ρ^2 .

For a reactor composed of a fluid contained in a tank of fixed shape, a uniform fluid-density change alters the geometry of the reactor. Tank shapes may be chosen¹⁶ so that the slope of the reactivity vs density curve is positive, negative, or zero.

REFLECTED REACTORS

As in the Serber-Wilson method, the flux ϕ in each homogeneous region is the solution of Eq. (30), which for spherical symmetry has the form given in Eqs. (15) and (16). The boundary conditions are simplified in that ϕ is continuous and $\phi = 0$ at extrapolated boundary replace the Serber conditions. The continuity of j (normal) is retained in order to conserve neutrons. For criticality computations, it is sufficient to use the conditions:

$$\frac{\phi}{j \text{ (normal)}} = \text{continuous at boundaries} \quad (38a)$$

$$\phi = 0 \text{ at extrapolated boundary} \quad (38b)$$

Use of the diffusion theory relations in the transport approximation:

$$j_{+n} = \frac{\phi}{4} - \frac{D}{2} \frac{\partial \phi}{\partial n} \quad (39a)$$

* Some care must be taken in order to obtain the buckling in the fundamental mode, rather than in one of the higher modes.

$$j_{-n} = \frac{\phi}{4} + \frac{D}{2} \frac{\partial \phi}{\partial n}$$

$$(j_n = j_{+n} - j_{-n})$$

(39b)

where n denotes normal, $+$ denotes outward, and $-$ denotes inward, results in rewriting Eq. (38a) as:

$a = \text{continuous}$

where the albedo, a is given by:

$$a \equiv \frac{j_{-n}}{j_{+n}} = \frac{\frac{\phi}{2j_n} - 1}{\frac{\phi}{2j_n} + 1}$$

(40a)

or:

$$\frac{\phi}{2j_n} = \frac{1+a}{1-a}$$

(40b)

Tables 1.4.4 through 1.4.6 list for plane, spherical, and cylindrical geometries, the encountered ϕ 's along with the corresponding formulas for j and ϕ/j . In these tables as in the following remarks, the symbol B is defined as:

$$B = \sqrt{|B^2|}$$

(41)

so that it is real and positive in non-multiplying as well as multiplying media.

Table 1.4.4 — Useful One-group Functions; Plane Geometry,
Coordinate x (Note: $w = Bx$)

ϕ	j	ϕ/j
$\cos w$	$DB \sin w$	$\frac{1}{DB} \cot w$
$\sin w$	$-DB \cos w$	$-\frac{1}{DB} \tan w$
$A(\cos w + \alpha \sin w)$	$ADB(\sin w - \alpha \cos w)$	$\frac{1}{DB} \frac{\cot w + \alpha}{1 - \alpha \cot w}$
e^{-w}	$DB e^{-w}$	$\frac{1}{DB}$
$A(e^{-w} + \alpha e^w)$	$ADB(e^{-w} - \alpha e^w)$	$\frac{1}{DB} \frac{1 + \alpha e^{2w}}{1 - \alpha e^{2w}}$
$\sinh B(b - x)$	$DB \cosh B(b - X)$	$\frac{1}{DB} \tanh B(b - X)$

Table 1.4.5—Useful One-group Functions; Spherical Geometry,
Coordinate r (Note: $w = Br$)

ϕ	j	ϕ/j
$\frac{\sin w}{w}$	$DB \left(\frac{\sin w}{w^2} - \frac{\cos w}{w} \right)$	$\frac{1}{DB \left(\frac{1}{w} - \cot w \right)}$
$\frac{\cos w}{w}$	$DB \left(\frac{\cos w}{w^2} + \frac{\sin w}{w} \right)$	$\frac{1}{DB \left(\frac{1}{w} + \tan w \right)}$
$A \left(\frac{\sin w}{w} + \alpha \frac{\cos w}{w} \right)$	$ADB \left[\frac{\sin w}{w} \left(\frac{1}{w} + \alpha \right) - \frac{\cos w}{w} \left(1 - \frac{\alpha}{w} \right) \right]$	$\frac{1 + \alpha \cot w}{DB \left[\left(\frac{1}{w} + \alpha \right) - \left(1 - \frac{\alpha}{w} \right) \cot w \right]}$
$\frac{e^{-w}}{w}$	$DB \frac{e^{-w}}{w} \left(1 + \frac{1}{w} \right)$	$\frac{1}{DB \left(1 + \frac{1}{w} \right)}$
$A \left(\frac{e^{-w}}{w} + \alpha \frac{e^w}{w} \right)$	$ADB \left[\frac{e^{-w}}{w} \left(1 + \frac{1}{w} \right) - \alpha \frac{e^w}{w} \left(1 - \frac{1}{w} \right) \right]$	$\frac{1 + \alpha e^{2w}}{DB \left[\left(1 + \frac{1}{w} \right) - \alpha \left(1 - \frac{1}{w} \right) e^{2w} \right]}$
$\frac{\sinh B(b-r)}{Br}$	$DB \left[\frac{\cosh B(b-r)}{Br} + \frac{\sinh B(b-r)}{B^2 r^2} \right]$	$\frac{1}{DB \left[\coth B(b-r) + \frac{1}{w} \right]}$

 Table 1.4.6—Useful One-group Functions; Cylindrical Geometry, Coordinate r
($w = Br$; notation is that of Brit. Assoc. Math. Tables)

ϕ	j	ϕ/j
$J_0(w)$	$DB J_1(w)$	$\frac{1}{DB} \frac{J_0(w)}{J_1(w)}$
$Y_0(w)$	$DB Y_1(w)$	$\frac{1}{DB} \frac{Y_0(w)}{Y_1(w)}$
$A[J_0(w) + \alpha Y_0(w)]$	$ADB [J_1(w) + \alpha Y_1(w)]$	$\frac{1}{DB} \frac{J_0(w) + \alpha Y_0(w)}{J_1(w) + \alpha Y_1(w)}$
$K_0(w)$	$DB K_1(w)$	$\frac{1}{DB} \frac{K_0(w)}{K_1(w)}$
$A[K_0(w) + \alpha I_0(w)]$	$ADB [K_1(w) - \alpha I_1(w)]$	$\frac{1}{DB} \frac{K_0(w) + \alpha I_0(w)}{K_1(w) - \alpha I_1(w)}$

Effect of the Reflector

Some general remarks may be made concerning the effect of a single reflector on the critical size. Consider the spherical case, Table 1.4.5. column 1 of the table pertains to the core, column 6 to a reflector of outside radius b and thickness $b - a = t$, and column 4 to an infinite reflector. For a thin reflector ($t \ll 1/B$), ϕ/j reduces to t/D_1 , the reflector thickness in units of the diffusion constant, D_1 . If further, $t/a \ll 1$, use of column 1 and of the critical condition:

$$\left(\frac{\phi}{j}\right)_c = \left(\frac{\phi}{j}\right)_1 \quad \begin{array}{l} c \rightarrow \text{core} \\ 1 \rightarrow \text{reflector} \end{array} \quad (42)$$

leads to a reflector saving ($\delta = a - a_0 = a - \pi/B_c$) of:

$$\delta \approx t \frac{D_c}{D_1}$$

For a thick reflector ($t \gg 1/B$), column 6 goes over into column 4 in which:

$$(\phi/j)_1 = \frac{1}{D_1(B_1 + 1/a)}$$

For a "perfect" reflector, $B_1 a \ll 1$, or $B_1 \ll B_c$:

$$(\phi/j)_1 = \frac{a}{D_1}$$

and the reflector savings in the case:

$$D_1 = D_c$$

is:

$$\delta = \frac{1}{2} a_0$$

For an "equivalent" reflector:

$$D_1 = D_c, B_1 = B_c, a = \frac{3}{4} a_0, \text{ and } \delta = \frac{1}{4} a_0$$

For a reflector in which $B_1 a \gg 1$ or $B_1 \gg B_c$:

$$(\phi/j)_1 = \frac{1}{D_1 B_1}$$

showing that the characteristic parameter is $D_1 B_1$.

Numerical

As in the Serber-Wilson method, numerical results are easily obtained for the simple geometries in the case of a single reflector, whether finite or infinite. Thus, the following graphs may be drawn:

- (1) $\frac{\phi}{j}(w_c, D_c B_c)$ for the core as a function of $w_c = B_c a$ for various values of $D_c B_c$
- (2) $\frac{\phi}{j}(w_1, D_1 B_1, \gamma)$ for the reflector as a function of $w_1 = B_1 a$ for values of $D_1 B_1$ and γ

where γ is the ratio of the outer boundary coordinate to the inner boundary coordinate, both measured from the center of symmetry. The w scales should be logarithmic, in order that superposition of the two graphs with the w axes coinciding leads to the same distance scale on the $w = Br$ axes. The w values at the point of intersection of the (1) and (2) curves give the critical coordinate a through the relations:

$$a = \frac{w_c}{B_c} = \frac{w_1}{B_1}$$

In multi-reflector problems, the value of ϕ/j at the core boundary may be computed by starting with the outermost reflector, column 6 of Table 1.4.5. Matching ϕ/j 's with the next outermost reflector, column 5, results in the value of α for that region. This process may be continued until the core radius is reached, assuming that the geometry and reflector properties are fixed in advance. The final ϕ/j may then be matched to the core, column 1 or the above-mentioned graph, to obtain allowable combinations of D_c and B_c . If all boundaries except the core boundary are fixed in advance, the above process results in a ϕ/j which is a function of the core radius. This function may then be matched to $(\phi/j)_c$ for a known core composition to yield the core radius.

A matrix method which may be used in place of the above procedure is presented below in the treatment of two-group theory.

OTHER GEOMETRIES

Geometries more complicated than the plane, spherical, and cylindrical have been treated without resort to numerical integration of the differential equations. Accurate results exist for the infinitely reflected spheroid¹⁰ and hemisphere,¹⁷ when the core and reflector have the same total cross section. The result in the hemisphere case is:

$$a_{\text{hemi}} \text{ is slightly less than } 1.3a_{\text{sphere}}$$

where the a 's are the critical radii in the infinitely tamped problem. Also, an accurate perturbation formula has been given¹⁸ for the critical volume of a nearly spherical core inside an infinite reflector of the same total cross section.

The variational method, described above, may be extended in order to obtain the critical conditions for reflected reactors. Perturbation theory¹⁹ on the diffusion equations may be used to evaluate the flux distribution in a reactor not differing overmuch in geometry from spherical symmetry, for example.

Problems such as (1) a finite cylindrical core surrounded on all sides by an infinite or finite cylindrical reflector and (2) a parallelepiped core surrounded on all sides by an infinite or finite parallelepiped reflector are often treated in the following approximation. The description given applies to a cylindrical core (radius a , height $2h$) with infinite reflector. The total volume is divided into the regions listed in Table 1.4.7 along with the assumed flux in each region and the corresponding buckling conditions. The region labeled ZR is not used in the calculation. The diffusion boundary conditions are applied to the C-Z boundary and to the C-R boundary. They are:

$$\frac{1}{D_c B_{cz}} \cot B_{cz} h = \frac{1}{D_1 B_z}$$

$$\frac{1}{D_c B_{cr}} \frac{J_0(B_{cr} a)}{J_1(B_{cr} a)} = \frac{1}{D_1 B_r} \frac{K_0(B_r a)}{K_1(B_r a)}$$

Table 1.4.7 — Approximate Method for Difficult Cylindrical Geometry

Region	ϕ	Buckling condition
Core, C $r \leq a$ $ z \leq h$	$J_0(B_{cr} r) \cos B_{cz} Z$	$B_c^2 = B_{cr}^2 + B_{cz}^2$
Core, Z $r \leq a$ $ z \geq h$	$J_0(B_{cr} r) e^{-B_z Z}$	$-B_1^2 = B_z^2 - B_{cr}^2$
Core, R $r \geq a$ $ z \leq h$	$K_0(B_r r) \cos B_{cz} Z$	$-B_1^2 = B_r^2 - B_{cz}^2$
Core, ZR $r \geq a$ $ z \geq h$	Not used	Not used

Assuming, for example, that D_c , B_c^2 , D_1 , B_1^2 , and h are fixed in advance, the two boundary conditions and the three buckling conditions enable the determination of the five unknowns, A , B_{cr} , B_{cz} , B_z , and B_r .

The method as just described is often simplified by guessing a value for B_{cz} or for B_{cr} . Such guesses may be easily related to guessed values for the reflector savings δh or δa .

MANY-VELOCITY REACTORS

THE ONE-VELOCITY OR FEYNMAN-WELTON METHOD

Reference 20 is a comprehensive report on this method and makes use of the transport approximation.* Anisotropic scattering may be treated by the spherical harmonic method. An extension of the method in the case of hydrogenous systems has been reported by Davison.²¹ The case of the bare-slab reactor with a linear scattering law has been treated by Selengut²² in an accurate approximation for not-too-thin reactors and is discussed below.

CONSTANT CROSS SECTIONS

The following two theorems are of interest for the method even though assumptions they contain are very restrictive.

THEOREM 1. If the cross sections, angular dependence of scattering, fission spectrum, and ν , are all independent of neutron energy, then the energy-integrated flux, $\int_0^\infty v n(\underline{r}, \underline{\Omega}, E) dE$, satisfies the one-velocity Boltzmann equation.

THEOREM 2. If further, the reactor consists of a bare core or of a core surrounded by reflectors which cannot alter the neutron energy,† then the direction-integrated flux:

$$\phi(\underline{r}, E) = \int v n(\underline{r}, \underline{\Omega}, E) d\Omega$$

is separable into:

$$\phi(\underline{r}, E) = F(\underline{r})G(E)$$

* See also Davison,⁷ Chapter VII.

† No fission and no slowing-down.

where $F(\underline{r})$ is the space distribution of the one-velocity problem. When scattering is isotropic, the spectrum $G(E)$ satisfies the critical condition:

$$(\sigma_s + \nu\sigma_f)G(E) = \nu\chi(E)\sigma_f \int_0^\infty G(E)dE + \sigma_s \int_0^\infty g(E,E')G(E')dE'$$

These theorems and the results below for variable cross sections illustrate the wide applicability of one-velocity theory.

VARIABLE CROSS SECTIONS (IN TRANSPORT APPROXIMATIONS)

The case of energy-dependent cross sections can be easily treated only for a bare core or a core surrounded by a reflector which cannot change the neutron energy (no slowing-down and no fission). Reflectors which do change the neutron energy may be handled by two-group theory, as discussed later.

Consider a core fission cross section, σ_f , a capture cross section, σ_c , a cross section σ_s for scattering with energy change, and a cross section σ_e for scattering with neglected energy change. The core is surrounded by a reflector in which:

$$\sigma_s = 0 \text{ and } \sigma_f = 0$$

Let:

$$\sigma_r(E) = \sigma_f(E) + \sigma_c(E) + \sigma_s(E) \quad (43)$$

be called the removal cross section.

The balance equation in terms of the removal density $A(\underline{r}, E)$ in the core:

$$A(\underline{r}, E) = \sigma_r(E)\phi(\underline{r}, E) \quad (44)$$

may be written as:

$$A(\underline{r}, E) = \int_{\text{core}} P(\underline{r}, \underline{r}', E) S(\underline{r}', E) d\underline{r}' \quad (45)$$

where the source S is given by:

$$S(\underline{r}, E) = \nu\chi(E) \int_0^\infty \frac{\sigma_f(E')}{\sigma_r(E')} A(\underline{r}, E') dE' + \int_0^\infty g(E, E') \frac{\sigma_s(E')}{\sigma_r(E')} A(\underline{r}, E') dE' \quad (46)$$

and the kernel $P(\underline{r}, \underline{r}', E)$ represents the probability that a neutron released at \underline{r}' with energy E is absorbed (with σ_a) at \underline{r} without intervening energy loss. The kernel P thus includes the effect of the "elastic" scattering σ_e in both the core and reflector.

Consider now a fictitious one-velocity problem at energy E with the reflector having the same cross sections ("elastic" and capture) as in the actual problem and with the core having the same fission and "elastic" cross sections as in the actual problem and with a capture cross section given by $\sigma_c(E) + \sigma_s(E)$. The removal cross section in this one-velocity problem is then the same as in the actual problem, given by Eq. (43), and the source density may be written as $\mu(E)A^{(1)}(\underline{r}, E)$ where $A^{(1)}$ is the one-velocity removal density and $\mu(E)$ is the number of neutrons released per neutron removed. The one-velocity balance equation is then:

$$A^{(1)}(\underline{r}, E) = \mu(E) \int_{\text{core}} P(\underline{r}, \underline{r}', E) A^{(1)}(\underline{r}', E) d\underline{r}' \quad (47)$$

with eigenfunctions $A_n(r, E)$, $n = 0, 1, 2, \dots$, and with eigenvalues:

$$\mu_n(E) = \frac{\nu_n(E)\sigma_f(E)}{\sigma_r(E)} \quad (48)$$

where $\nu_n(E)$ is the value of ν required to balance the n 'th mode of the one-velocity problem. The value of $\nu_0(E)$ and the space distribution $A_0(\underline{r}, E)$ in the fundamental mode may be obtained by the methods discussed in "One-velocity Reactors." The values in the higher modes are similarly obtainable.

The kernel $P(\underline{r}, \underline{r}', E)$ may be written as:

$$P(\underline{r}, \underline{r}', E) = \sum_{n=0}^{\infty} \frac{1}{\mu_n(E)} A_n(\underline{r}, E) A_n(\underline{r}', E) \quad (49)$$

where the modes $A_n(\underline{r}, E)$ form a normalized orthogonal* set when integrated over the core:

$$\int_{\text{core}} A_n(\underline{r}, E) A_m(\underline{r}, E) d\underline{r} = \delta_{nm} \quad (50)$$

Various approximate solutions of the many-velocity problem, Eqs. (44), (45), and (46), may be obtained by making approximations in the kernel P or by expanding $A(r, E)$ into:

$$A(r, E) = \sum_n G_n(E) A_n(r, E)$$

and keeping as many terms as desired.

Thus, in the "first upper approximation," it is assumed that:

$$\phi(r, E) = \frac{A(r, E)}{\sigma_r(E)} = G(E)A_0(\underline{r}, E) \quad (51)$$

which when substituted into Eqs. (45) and (46) leads to (after multiplication by $A_0(\underline{r}, E)$ and integration over \underline{r}) the critical equation:

$$\nu_0(E)\sigma_f(E)G(E) = \nu\chi(E) \int \sigma_f(E')G(E')A_{\infty}(E, E')dE' + \int g(E, E')\sigma_s(E')G(E')A_{\infty}(E, E')dE' \quad (52)$$

where:

$$A_{\infty}(E, E') = \int_{\text{core}} A_0(\underline{r}, E)A_0(\underline{r}, E')d\underline{r} \quad (53)$$

In the simplest, or "first lower approximation," it is further assumed that:

$$A_0(\underline{r}, E) = A_0(\underline{r}, E') = A_0(r) \quad (54)$$

from which it follows that $A_{\infty} = 1$. Equation (52) may be solved as follows, the results being written for $A_{\infty}(E, E') \approx 1$ as in the first lower approximation. Choose the normalization for $G(E)$ such that:

$$\nu \int_0^{\infty} \sigma_f(E')G(E')dE' = 1 \quad (55)$$

and solve for $G(E)$ from the integral equation:†

*A discussion of orthogonality is given by Davison,⁷ Chapter VII.

† Approximate methods for solution of such equations are discussed in Chapter 1.3.

$$\nu_0(E)\sigma_f(E)G(E) = \chi(E) + \int_0^\infty g(E,E')\sigma_s(E')G(E')dE' \quad (56)$$

The value of ν is then determined by Eq. (55).

Both these approximations are exact in the case of constant cross sections. In this case, integration over energy of Eq. (52) gives:

$$\nu_0(E)\sigma_f(E) = \nu\sigma_f(E) + \sigma_s(E)$$

thus proving Theorem 2 (above).

There are good, although not entirely rigorous, arguments leading to the statement that the upper and lower approximations lead to upper and lower estimates for ν . This statement is borne out by test calculations which further indicate that the errors owing to these approximations are less than a few percent in a variety of cases. Detailed discussions of accuracy and of procedures leading to higher approximations are discussed in the referenced reports.

INELASTIC REFLECTORS IN TWO-GROUP THEORY

Practical equations are obtained in two-group theory for the case of reflectors which slow neutrons down. The results given below may be extended to include the effects of fission in the reflector. In the following, all symbols have the same meaning as above: The subscripts 1 and 2 refer respectively to the fast and slow groups; the subscript 21 refers to inelastic scattering from group 1 to group 2; and the asterisk refers to the reflector. Thus:

$$\sigma_{r1} = \sigma_{f1} + \sigma_{c1} + \sigma_{21}$$

and:

$$\sigma_{r2} = \sigma_{f2} + \sigma_{c2}$$

In the reflector:

$$\sigma_{f1}^* = \sigma_{f2}^* = 0$$

The balance equations are:

$$A_1(\underline{r}) = \int_{\text{core}} P_1(\underline{r}, \underline{r}') S_1(\underline{r}') d\underline{r}' \quad (57)$$

$$A_2(\underline{r}) = \int_{\text{core}} P_2(\underline{r}, \underline{r}') S_2(\underline{r}') d\underline{r}' + \int_{\text{core}} P_{21}^*(\underline{r}, \underline{r}') S_1(\underline{r}') d\underline{r}' \quad (58)$$

where:

$$S_1 = \nu\chi_1 \left[\frac{\sigma_{f1}}{\sigma_{r1}} A_1 + \frac{\sigma_{f2}}{\sigma_{r2}} A_2 \right] \quad (59)$$

and:

$$S_2 = \nu\chi_2 \left[\frac{\sigma_{f1}}{\sigma_{r1}} A_1 + \frac{\sigma_{f2}}{\sigma_{r2}} A_2 \right] + \frac{\sigma_{21}}{\sigma_{r1}} A_1 \quad (60)$$

where χ_1 and χ_2 are the fraction of fission neutrons released in groups 1 and 2, and where the kernel P_{21}^* represents the probability that a group 1 neutron released at \underline{r}' in the core

is absorbed as a group 2 neutron at \underline{r} in the core after having been inelastically scattered in the reflector.

The one-velocity problems, defined as above, give for the fundamental mode:

$$A_{01}(\underline{r}) = \mu_{01} \int P_1(\underline{r}, \underline{r}') A_{01}(\underline{r}') d\underline{r}'$$

$$A_{02}(\underline{r}) = \mu_{02} \int P_2(\underline{r}, \underline{r}') A_{02}(\underline{r}') d\underline{r}'$$

In the simplest lower approximation, it is assumed that:

$$A_{01}(\underline{r}) = A_{02}(\underline{r}) = A_0(\underline{r}) \quad (61)$$

$$\phi_1(\underline{r}) = \frac{A_1(\underline{r})}{\sigma_{r1}} = G_1 A_0(\underline{r})$$

$$\phi_2(\underline{r}) = \frac{A_2(\underline{r})}{\sigma_{r2}} = G_2 A_0(\underline{r}) \quad (62)$$

$$\int_{\text{core}} P_{21}^*(\underline{r}, \underline{r}') A_0(\underline{r}') d\underline{r}' = \gamma A_0(\underline{r}) \quad (63)$$

where γ is discussed below.

These assumptions lead to a pair of homogeneous equations in G_1 and G_2 with the solubility conditions that

$$\nu = \frac{\mu_{01}\mu_{02}\sigma_{r1}\sigma_{r2}}{\chi_1(\sigma_{f2}\sigma_{21} + \sigma_{f1}\sigma_{r2}\mu_{02} + \sigma_{f2}\sigma_{r1}\mu_{01}\mu_{02}\gamma) + \chi_2\sigma_{r1}\sigma_{f2}\mu_{01}} \quad (64)$$

and with:

$$\frac{G_2}{G_1} = \frac{\mu_{01}\sigma_{r1}}{\nu\chi_1\sigma_{f2}} - \frac{\sigma_{f1}}{\sigma_{f2}} \quad (65)$$

Several approximate formulas for γ are discussed,²⁰ all having the form:

$$\gamma = \left(1 - \frac{1}{\mu_{01}}\right) \frac{\sigma_{f1}^*}{\sigma_{r1}^*} Q_2 \quad (66)$$

where Q_2 is the average probability that a neutron liberated in the tamper at velocity 2 (via inelastic scattering) is absorbed in the core. Use of the asymptotic solutions of one-velocity theory gives for Q_2 :

$$Q_2 = \frac{a^3}{3} \frac{h_1^2 h_2^2}{(h_1 + h_2)(1 + h_1 a)(1 + h_2 a)} \frac{\sigma_{r2}}{\sigma_{r2}^*} \left(1 - \frac{1}{\mu_{02}}\right) \quad (67)$$

where a is the core radius and h_1 and h_2 are determined from:

$$\frac{h_1/\sigma_1^*}{\tanh^{-1} h_2/\sigma_2^*} = \frac{\sigma_{e1}^*}{\sigma_1^*} \quad (68)$$

$$\frac{h_2/\sigma_2^*}{\tanh^{-1} h_2/\sigma_2^*} = \frac{\sigma_{e2}^*}{\sigma_2^*} \quad (69)$$

where the σ_e^* 's are the "elastic" scattering cross sections and the σ^* 's are the total cross sections being the sum of removal plus elastic cross sections. Thus, for:

$$1 - \sigma_e^*/\sigma^* = \frac{\sigma_r^*}{\sigma^*} \ll 1, \quad h \approx \sqrt{3\sigma^*\sigma_r^*}$$

NON-ISOTROPIC SCATTERING

The effect of non-isotropic scattering on the preceding results is illustrated by the case of linear anisotropy in a bare-slab reactor.²² Using the first lower approximation, the direction-dependent flux:

$$\phi(x, E, \mu) = v n(x, E, \mu)$$

may be written as:

$$\phi(x, E, \mu) = R[e^{ikx} f(E, \mu)] \quad (70)$$

where $R[x]$ denotes the real part of x . The direction-integrated flux:

$$\phi(x, E) = \int_{-1}^1 d\mu \phi(x, E, \mu)$$

has the form:

$$\phi(x, E) = H(E) \cos Kx \quad (71)$$

where:

$$K = \frac{\pi}{2a} \quad (72)$$

and a is the distance from the center of the reactor to the extrapolated boundary, assumed the same for all energies. The current density:

$$j(x, E) = \int_{-1}^1 \mu d\mu \phi(x, E, \mu)$$

has the form:

$$j(x, E) = J(E) \sin Kx. \quad (73)$$

Substitution of Eq. (70) into the Boltzmann equation results in a pair of coupled integral equations for $H(E)$ and $J(E)$ which may be written as follows:

$$H(E) = G_0(E) - G_1(E) \quad (74)$$

$$J(E) = \frac{1-\beta}{\alpha\beta} G_0(E) + \frac{1}{\alpha} G_1(E) \quad (75)$$

$$\beta(E) = \frac{\tan^{-1} \alpha(E)}{\alpha(E)} \quad (76)$$

$$\alpha(E) = K/\sigma(E) \quad (77)$$

where $\sigma(E)$ is the total cross section, and G_0 and G_1 satisfy:

$$\frac{\sigma(E)}{\beta(E)} G_0(E) = \nu \chi(E) \int_0^\infty dE' \sigma_f(E') [G_0(E') - G_1(E')] + \int_0^\infty g(E, E') dE' \sigma_s(E') [G_0(E') - G_1(E')] \quad (78)$$

$$\frac{\alpha(E)\sigma(E)}{1 - \beta(E)} G_1(E) = \int_0^\infty \frac{3\bar{\mu}_0(E')}{\alpha(E')} g(E, E') \sigma_s(E') \left[\frac{1 - \beta(E')}{\beta(E')} G_0(E') + G_1(E') \right] dE' \quad (79)$$

The equations are written in terms of G_0 and G_1 because G_1 goes to zero as $\bar{\mu}_0(E)$, the average cosine of the angle of scattering, goes to zero. Thus, G_1 is a measure of the effect of anisotropy.

The above equations correctly reduce to Eq. (52) (with $A_\infty = 1$) in the case of isotropic scattering. It is to be noted that $\sigma(E)/\beta(E) = \nu_0(E)\sigma_f(E)$, where $\nu_0(E)$ is the value of ν required to maintain criticality in a one-velocity reactor at energy E , the removal cross section being $\sigma_r = \sigma_f + \sigma_c + \sigma_s = \sigma$.

Equations (78) and (79) may be solved* for G_0 and G_1 in the normalization:

$$\nu \int_0^\infty dE' \sigma_f(E') [G_0(E') - G_1(E')] = 1 \quad (80)$$

and ν may then be obtained from Eq. (80). Using this normalization for a reactor consisting of hydrogen and an element which scatters isotropically without energy loss, Eqs. (78) and (79) reduce to:

$$\frac{\sigma(E)}{\beta(E)} G_0(E) = \chi(E) + \sigma_e(E) [G_0(E) - G_1(E)] + \int_0^\infty \frac{dE'}{E'} \sigma_{SH}(E') [G_0(E') - G_1(E')] \quad (81)$$

$$\frac{\alpha(E)\sigma(E)}{1 - \beta(E)} G_1(E) = 2 \int_0^\infty \frac{dE'}{\alpha(E')E'} \sigma_{SH}(E') \left[\frac{1 - \beta(E')}{\beta(E')} G_0(E') + G_1(E') \right] \quad (82)$$

which may be converted (by differentiation) into a pair of coupled differential equations.

UNIFORM MEDIA

Reactors in which the core and reflector have uniform scattering and moderating properties, with the fuel affecting only the absorption, afford certain simplifications in the theory and have received considerable attention. Unless specified otherwise, the fuel will be assumed to be distributed uniformly in the core; non-uniform distributions will be considered separately later.

GAUSSIAN SLOWING-DOWN

The case of a spherical thermal reactor in an infinite medium with Gaussian slowing-down has been treated by Volkoff.²³ The notation is given in Table 1.4.8.

The method starts with the equations of elementary diffusion theory:

$$\frac{d^2 f_1(r)}{dr^2} - \frac{f_1(r)}{L_1^2} = -\frac{g(r)}{D} \quad 0 \leq r \leq a \quad (83A)$$

$$\frac{d^2 f_2(r)}{dr^2} - \frac{f_2(r)}{L_2^2} = -\frac{g(r)}{D} \quad a \leq r \leq \infty \quad (83B)$$

* Approximate methods for solution of such equations are discussed in Chapter 1.3.

Table 1.4.8 — Notation for Discussion of Volkoff's Work

Symbol	Definition
r	Distance from center of symmetry
a_0	Critical radius of unreflected reactor
a	Critical radius of reflected reactor
sub 1	Indicates core
sub 2	Indicates reflector
f	r times thermal flux
g	r times slowing down density
D	Thermal diffusion constant
L	Thermal diffusion length
L_s	Slowing-down length
M	$\sqrt{L^2 + L_s^2}$, migration length
γ	L_s/L
k	Multiplication constant [$k_1 > 0$, $k_2 < 0$]
$P(x)$	Slowing-down density at position x owing to a plane source at $x = 0$
$S(r, r')$	$\frac{1}{4\pi r r'} [P(r - r') - P(r + r')]$ = slowing-down density at r owing to a unit spherical shell source at r'
$\Phi(\nu)$	Fourier transform of $P(y)$ where $y = x /L_s$

with the conditions:

$$f_1(0) = 0 = f_2(\infty)$$

$$f_1(a) = f_2(a) \quad (84)$$

$$\left. \frac{df_1(r)}{dr} \right|_{r=a} = \left. \frac{df_2(r)}{dr} \right|_{r=a}$$

where $g(r)$ is given by:

$$\frac{g(r)}{D} = \frac{rk_1}{L_1^2} \int_0^a 4\pi r' dr' f_1(r') S(r, r') + \frac{rk_2}{L_2^2} \int_a^\infty 4\pi r' dr' f_2(r') S(r, r') \quad (85)$$

which may be written in terms of the plane kernel P as:

$$\frac{g(r)}{D} = \frac{k_1}{L_1^2} \int_{-a}^{+a} f_1(r') P(|r - r'|) dr' + \frac{k_2}{L_2^2} \left\{ \int_{-\infty}^{-a} f_2(r') P(|r - r'|) dr' + \int_a^{+\infty} f_2(r') P(|r - r'|) dr' \right\} \quad (86)$$

where the range of definition of g , f_1 , and f_2 has been extended to negative values of r by regarding them as odd functions.

The actual three region (image) problem as contained in Eqs. (83), (84), and (86) is now approximated by a two-region problem formed by extending the reactor image to $-\infty$. Thus, Eq. (83A) is to hold for $-\infty \leq r \leq a$, Eq. (83B) holds for $a \leq r \leq \infty$, and Eq. (86) is replaced by:

$$\frac{g(r)}{D} = \frac{k_1}{L_1^2} \int_{-\infty}^a f_1(r') P(|r - r'|) dr' + \frac{k_2}{L_2^2} \int_a^\infty f_2(r') P(|r - r'|) dr' \quad (87)$$

This two-region problem is solved by the Wiener-Hopf method and is shown by test computation to be a very accurate approximation to the actual three-region problem. The two-region criticality* results are given below.

The critical radius is given by:

$$a = a_0[1 - \epsilon_{th} - \epsilon_f] \quad (88)$$

where a_0 is the bare critical radius, given by:

$$a_0 = \frac{\pi L_s}{\nu_1} \quad (89)$$

ϵ_{th} is the fractional reflector savings owing to thermal neutrons entering the core from the reflector:

$$\epsilon_{th} = \frac{1}{\pi} \tan^{-1} \frac{\nu_1}{\nu_2} \quad (90)$$

ϵ_f is the fractional savings owing to fast neutrons entering the core:

$$\epsilon_f = \frac{1}{\pi} [I(\nu_1, \gamma_1) - J(\nu_1, \nu_2, \gamma_2)] \quad (91)$$

and:

$$I(\nu_1, \gamma_1) = \frac{\nu_1}{\pi} P \int_0^\infty \frac{dx}{x^2 - \nu_1^2} \ln \frac{x^2 - \nu_1^2}{x^2 + \gamma_1^2(1 - k_1\Phi(x))} \quad (92)$$

$$J(\nu_1, \nu_2, \gamma_2) = \frac{\nu_1}{\pi} P \int_0^\infty \frac{dx}{x^2 - \nu_1^2} \ln \frac{x^2 + \nu_2^2}{x^2 + \gamma_2^2(1 - k_2\Phi(x))}$$

where P denotes the Cauchy principal value of the integral. The quantities ν_1 and ν_2 are the values of the infinite medium buckling (using L_s as the unit of length) and are the positive real roots of:

$$k_1 = \frac{1}{\Phi(\nu_1)} \left(1 + \frac{\nu_1^2}{\gamma_1^2} \right) \quad (93)$$

$$k_2 = \frac{1}{\Phi(i\nu_2)} \left(1 - \frac{\nu_2^2}{\gamma_2^2} \right)$$

If the reflector contains no fuel, then $k_2 = 0$ from which it follows that $\nu_2 = \gamma_2$ and $J(\nu_1, \nu_2, \gamma_2) = 0$. In this case:

$$\epsilon_{th}(k_2 = 0) = \frac{1}{\pi} \tan^{-1} \frac{\nu_1}{\gamma_2} \quad (94)$$

$$\epsilon_f(k_2 = 0) = \frac{1}{\pi} I(\nu_1, \gamma_1)$$

* Flux and slowing-down distributions are discussed in Ref. (24) where the deviations from the asymptotic solutions are investigated in the neighborhood of the core reflector interface.

For a Gaussian slowing down kernel:

$$P(|\mathbf{x}|) = \frac{1}{2\sqrt{\pi}L_s} e^{-x^2/4L_s^2} \quad (95)$$

the transform $\Phi(\nu)$ is given by:

$$\Phi(\nu) = e^{-\nu^2} \quad (96)$$

Figure 1.4.9 plots $\epsilon_{th}(k_2 = 0)$ as a function of $K = (M_1/L_s)\nu_1$ for various values of L_2/m_1 . Figure 1.4.10 plots $\epsilon_f(k_2 = 0)$ as a function of K for various values of γ_1 and also exhibits contours of constant k_1 .

For a finite reflector, the modification of the above is discussed in Ref. (25). For comparison with two-group results, see French and Hurwitz.²⁶

GENERAL KERNELS

The formal work of the preceding section applies immediately to a general displacement slowing-down kernel provided that $\Phi(\nu)$ of Eq. (96) is replaced by the appropriate transform. Applications to multigroup kernels are given by Volkoff and LeCaine.²⁷

The major simplification arising for thermal reactors from the presence of a uniform slowing-down medium in a finite or infinite region can be clearly stated: Let $S(\mathbf{x})$ be the source distribution of fission-energy neutrons. Then, the slowing-down density at thermal $q(\mathbf{x})$ may be written:

$$q(\mathbf{x}) = \int k(\mathbf{x}, \mathbf{x}') S(\mathbf{x}') d\mathbf{x}' \quad (97)$$

where $k(\mathbf{x}, \mathbf{x}')$ characterizes the medium but is independent of the fuel distribution. Then, for uniform media:

$$k(\mathbf{x}, \mathbf{x}') = k(\mathbf{x}', \mathbf{x})$$

If the medium is infinite in extent, in addition $k(\mathbf{x}, \mathbf{x}')$ depends only on $|\mathbf{x} - \mathbf{x}'|$.

If the thermal-diffusion coefficient, D , is uninfluenced by the fuel distribution, the reactor criticality equations may be written as:

$$q(\mathbf{x}) = \int k(\mathbf{x}, \mathbf{x}') \eta \sigma_{af}(\mathbf{x}') \Phi(\mathbf{x}') d\mathbf{x}' \quad (98)$$

$$(-\nabla \cdot D\nabla + \sigma_{am})\phi = q - \sigma_{af} \phi \quad (99)$$

using the Green's function, g , defined by:

$$(-\nabla \cdot D\nabla + \sigma_{am})g(\mathbf{x}, \mathbf{x}') = \sigma_{am} \delta(\mathbf{x} - \mathbf{x}') \quad (100)$$

one has:

$$\begin{aligned} \sigma_{am}\phi &= \int g(\mathbf{x}, \mathbf{x}') [q(\mathbf{x}') - \sigma_{af}(\mathbf{x}')\phi(\mathbf{x}')] d\mathbf{x}' \\ &= \int h(\mathbf{x}, \mathbf{x}') \sigma_{af}(\mathbf{x}') \phi(\mathbf{x}') d\mathbf{x}' \end{aligned} \quad (101)$$

which defines h as:

$$h(\mathbf{x}, \mathbf{x}') = \eta \int g(\mathbf{x}, \mathbf{x}'') k(\mathbf{x}'', \mathbf{x}') d\mathbf{x}'' - g(\mathbf{x}, \mathbf{x}') \quad (102)$$

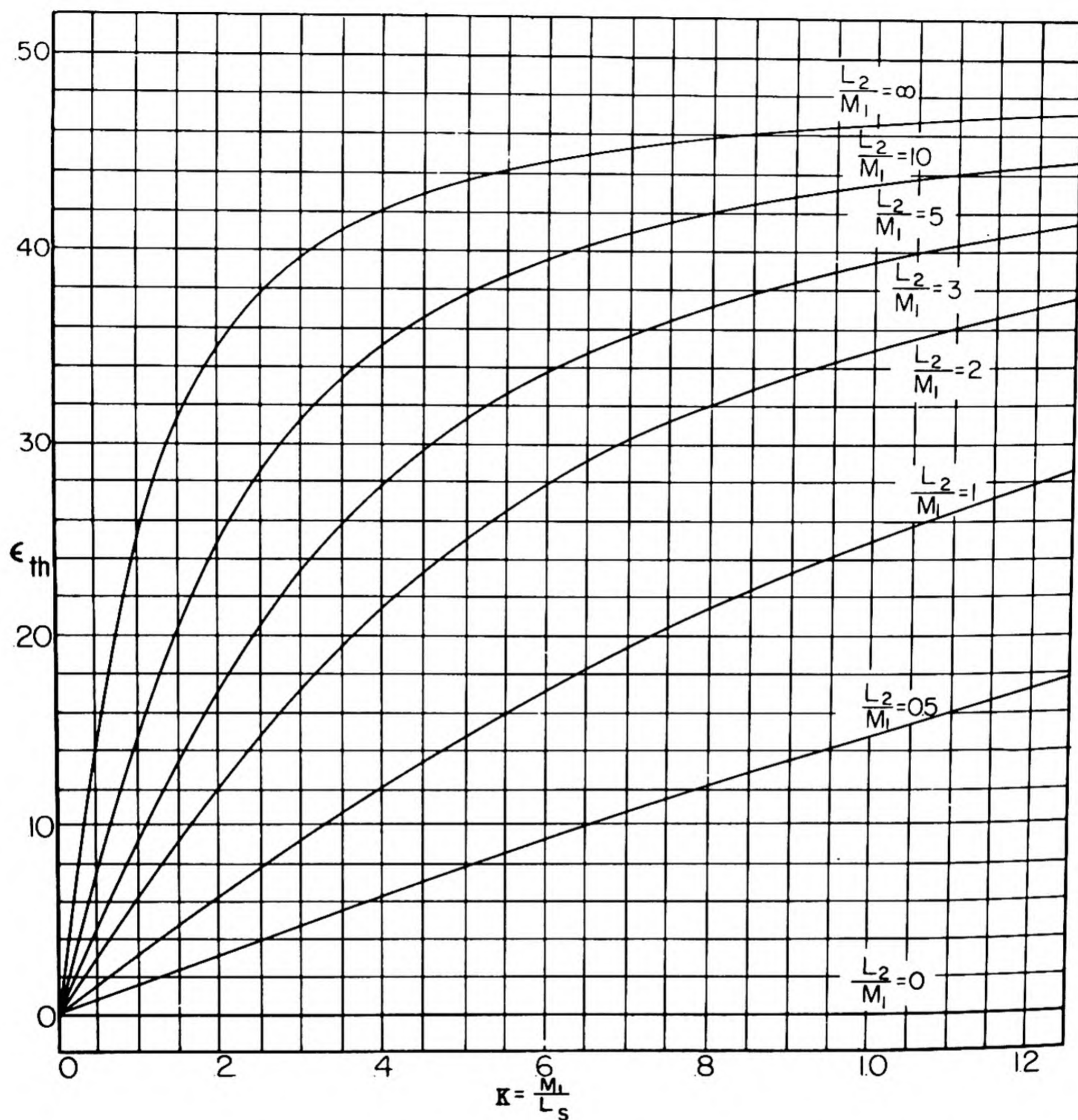


Fig. 1.4.9 — The Fractional Reflector Savings Owing to Thermal Neutrons. Reprinted from CRT-391. The curves give ϵ_{th} as a function of $K = M_1 \nu_1 / L_s$ for various values of L_2/M_1 for a non-multiplying reflector ($k_2 = 0$).

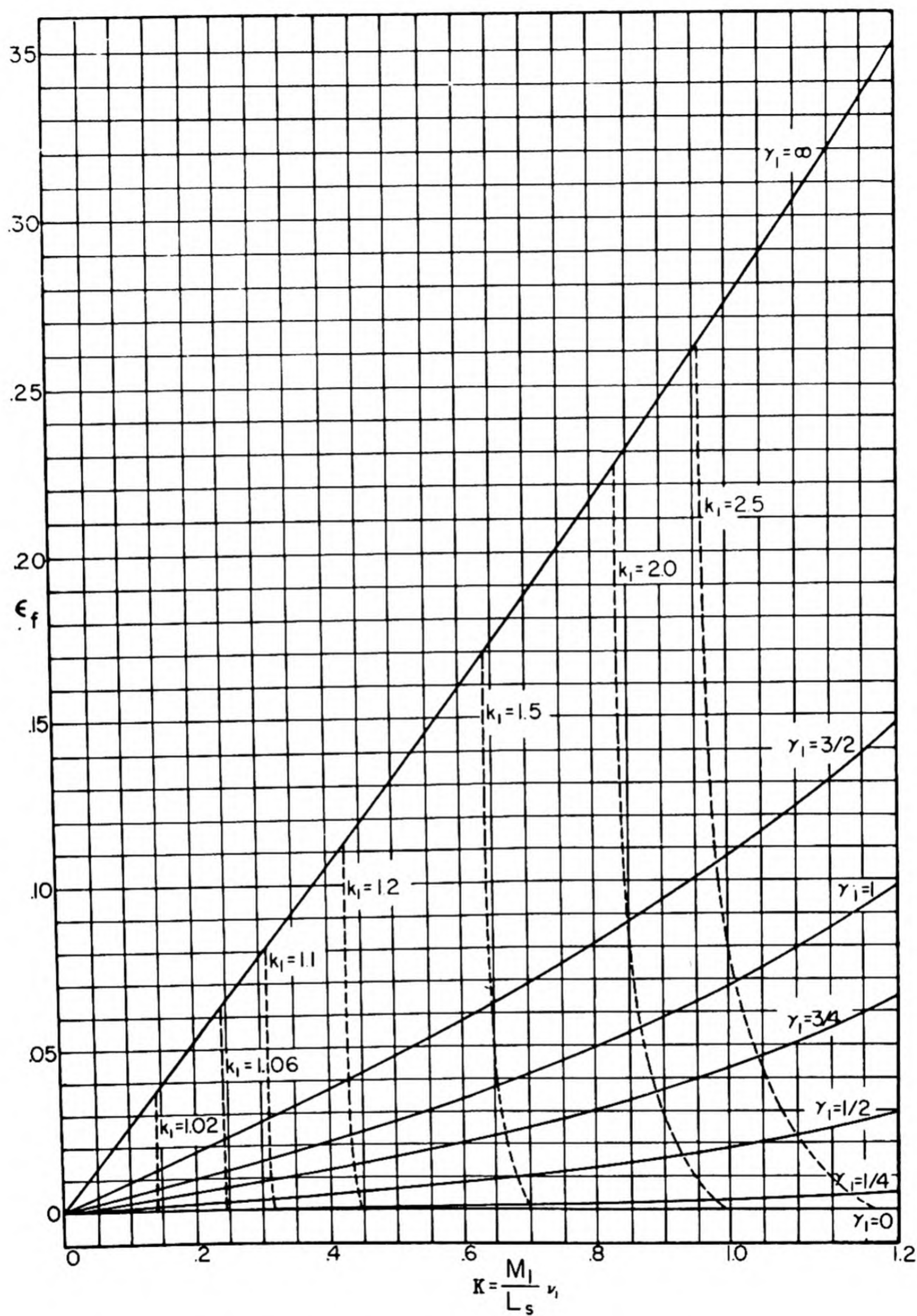


Fig. 1.4.10 — The Fractional Reflector Savings Owing to Fast Neutrons. Reprinted from CRT-91. The curves give ϵ_f as a function of $K = M_1 \nu_1 / L_s$ for various values of γ_1 for a non-multiplying reflector ($k_2 = 0$).

Owing to the uniformity of the medium, the kernel h is symmetric:

$$h(\underline{x}, \underline{x}') = h(\underline{x}', \underline{x})$$

for a wide class of kernels k in finite media. In infinite media, all k , h depends only on $|\underline{x} - \underline{x}'|$ and is clearly symmetric.

This formulation, as in Eq. (101), is a useful starting point for various considerations such as variational calculations, flat flux, and flat power.

The work of Greuling²⁸ on infinite spherical water systems illustrates variational calculations. He uses a variational principle for η obtained from Eq. (101) above by multiplication with $\sigma_{af}\phi$ and integrating:

$$\sigma_{am} \int \phi^2 \sigma_{af} d\underline{x} = \int \int \sigma_{af}(\underline{x}) \phi(\underline{x}) h(\underline{x}, \underline{x}') \sigma_{af}(\underline{x}') \phi(\underline{x}') d\underline{x}' \quad (103)$$

The value of η (as contained in h) given by this expression is stationary with respect to variations in ϕ . Greuling used a parabolic trial function for ϕ . Garabedian and Weinberg²⁹ have extended Greuling's work to finite reflectors and slab geometry.

MODE METHODS

Suppose the infinite-region slowing-down kernel $k(|\underline{x} - \underline{x}'|)$ satisfies the linear differential equation:

$$Lk(|\underline{x} - \underline{x}'|) = \delta(\underline{x} - \underline{x}') \quad (104)$$

Then, in many cases of interest, the slowing-down kernel for a finite region V , $K(\underline{x}, \underline{x}')$, satisfies the same equation and vanishes for \underline{x} or \underline{x}' on the surface $S(V)$. In such a case, $q(\underline{x})$ defined by:

$$q(\underline{x}) = \eta \int_V K(\underline{x}, \underline{x}') \sigma_{af} \phi(\underline{x}') d\underline{x}' \quad (105)$$

may be evaluated³⁰ without specific knowledge of K as follows. Let the $\psi_n(\underline{x})$ be a complete set of linearly independent solutions of:

$$(\nabla^2 + B_n^2) \psi_n = 0 \quad (106)$$

$$\psi_n(\underline{s}) = 0 \text{ if } \underline{s} \text{ on } S$$

normalized so that:

$$\int_V |\psi_n|^2 d\tau = 1$$

Then, with:

$$f_n = \int \psi_n(\underline{x}) \sigma_{af} \phi(\underline{x}) d\underline{x} \quad (107)$$

$$\bar{k}(B) = 4\pi \int_0^\infty k(r) \frac{\sin Br}{Br} r^2 dr \quad (108)$$

one has:

$$\begin{aligned}\sum_n f_n \psi_n(\underline{x}) &= \sigma_{af} \phi(\underline{x}) \\ q(\underline{x}) &= \eta \int_V K(\underline{x}, \underline{x}') \sigma_{af} \phi(\underline{x}) d\underline{x}' \\ &= \eta \sum_n f_n \bar{k}(B_n) \psi_n(\underline{x})\end{aligned}\tag{109}$$

The criticality condition may be formulated as follows. From Eqs. (99) and (109):

$$\phi(\underline{x}) = \sum_n \frac{\eta \bar{k}(B_n) - 1}{\sigma_{am} + DB_m^2} f_n \psi_n(\underline{x})$$

from which, using Eq. (107):

$$f_n = \sum_m \left(\int_V \psi_n \sigma_{af} \psi_m d\underline{x} \right) \frac{\eta \bar{k}(B_m) - 1}{\sigma_{am} + DB_m^2} f_m\tag{110}$$

This yields the critical condition in the form of the vanishing of the infinite determinant:

$$0 = \left| \left(\int_V \psi_n \sigma_{af} \psi_m d\underline{x} \right) \frac{\eta \bar{k}(B_m) - 1}{\sigma_{am} + DB_m^2} - \delta_{nm} \right|\tag{111}$$

For small reactors, only a few modes need be considered.

BARE REACTORS^{31,32,33,34}

If σ_{af} is independent of position, as in a bare homogeneous reactor:

$$\int_V \psi_n \sigma_{af} \psi_m d\underline{x} = \sigma_{af} \delta_{n,m}$$

and only the fundamental mode (smallest B^2) is of interest. The critical determinant, Eq. (111), reduced to:

$$\eta \bar{k}(B) = 1 + \frac{\sigma_{am} + DB^2}{\sigma_{af}}$$

or, with:

$$k = \frac{\sigma_{af}}{\sigma_{af} + \sigma_{am}} \cdot \eta$$

and:

$$L^2 = \frac{D}{\sigma_{af} + \sigma_{am}}$$

then:

$$k = \frac{1 + L^2 B^2}{\bar{k}(B)}\tag{112}$$

This is the usual form. For small B^2 :

$$\begin{aligned}\bar{k}(B)^* &= 4\pi \int_0^\infty k(r) \frac{\sin Br}{Br} r^2 dr \\ &= \sum_{n=0}^{\infty} \frac{(-1)^n}{(2n+1)!} \overline{r^{2n}} (B^2)^n \\ &\simeq 1 - \frac{1}{6} \overline{r^2} B^2\end{aligned}\tag{113}$$

so that:

$$k \simeq 1 + \left(L^2 + \frac{1}{6} \overline{r^2} \right) B^2 = 1 + M^2 B^2\tag{114}$$

which is the familiar expression in terms of the migration area M^2 .

$\bar{k}(B)$ may often be computed from microscopic data. Thus, the familiar Fermi theory result for a bare thermal reactor with Gaussian slowing-down may be found in most any of the standard references.³⁵ Many people have constructed nomograms from which the buckling can be readily evaluated.

Hydrogen moderated machines have been treated^{36,37} by representing the leakage as a fictitious absorption; the slowing-down then being treated correctly. The addition of heavier moderators and inelastic³⁸ slowing have been considered.

Selengut³⁹ gives a more exact transport approach for hydrogen machines, employing an approximate boundary condition. Davison²¹ considers homogeneous systems with and without reflectors.

NON-UNIFORM FUEL LOADINGS

For the general case of arbitrary fuel loading, Eq. (98) or (105) is solved with Eq. (99) by numerical methods. Often the iterative method is useful (cf. discussion at the end of this chapter).

Two special cases of non-uniform fuel loading are of special interest in thermal reactors:

- (1) Uniform volume power density in core, or $\sigma_{af}\phi = \text{constant}$ in core.
- (2) Uniform power density in core per unit fuel mass, or $\phi = \text{constant}$ in core.

For uniform power density per unit volume,⁴⁰ from Eq. (101):

$$\phi = \text{const.} \times \int_{\text{core}} h(\underline{x}, \underline{x}') d\underline{x}'\tag{115}$$

and:

$$\sigma_{af} = \frac{\sigma_{am}}{\int_{\text{core}} h(\underline{x}, \underline{x}') d\underline{x}'}\tag{116}$$

Goertzel⁴¹ has shown that in idealized thermal reactors the smallest critical mass is attained with a non-uniform loading that makes the thermal flux flat in the core. Both infinite and finite reflectors have been treated in multi-group formulation. In the case of water systems, the flat flux loading saves about 0.3 of the fuel requirement, but in a graphite system,⁴² the reduction is only a few percent.

* We assume $4\pi \int_0^\infty k(r) r^2 dr = 1$.

When the core is restricted to a smaller size, the flat-flux solution calls for a shell of fuel at the core boundary in addition to a continuous distribution in the interior. Reactors having only the shell loading have also been studied;⁴² in a two-group thermal model, such machines are possible only if $\eta - 1 > \sqrt{\tau/L}$, and hence a shell reactor of this sort is not possible in light water. In a graphite system, the fuel needed for a shell reactor is about 30 percent greater than for a uniform core reactor.

MULTIPLE REGIONS

TWO-GROUP CALCULATIONS*

When a reactor consists of several regions, each of which is homogeneous, one- or two-group models may be handled with reasonable effort. Occasionally, three-group reactors have been discussed also by the method outlined below. The present discussion, however, is restricted to two-group reactors.

The standard two-group equations in the simple geometries may be written in any region as:

$$\begin{aligned} -\frac{D_f}{r^\mu} \frac{d}{dr} r^\mu \frac{d}{dr} \phi_f + (\sigma_{sD} + \sigma_{af}) \phi_f &= \nu \sigma_{fs} \phi_s \\ -\frac{D_s}{r^\mu} \frac{d}{dr} r^\mu \frac{d}{dr} \phi_s + \sigma_{as} \phi_s &= \sigma_{sD} \phi_f \end{aligned} \quad (117)$$

The subscripts *f* and *s* refer to the fast and slow groups, respectively. Within a region the cross-sections and diffusion coefficients, are constants. $\mu = 0, 1$, or 2 for slab, cylindrical, or spherical symmetry. For cylinders of finite height, unreflected at top and bottom, the correct equations contain:

$$-\left(\frac{D}{r} \frac{d}{dr} r \frac{d}{dr} + D \frac{d^2}{dz^2} \right) \Phi$$

as the leakage term. When the form $\Phi = \phi(r) \cos \pi z/H$, where *H* is the extrapolated height, is substituted, equations of the form of Eq. (117) result, where σ_{af} and σ_{as} are the actual cross sections corrected for the longitudinal leakage. This separation may also be applied to vertically reflected cylinders where the extrapolated height involves an intelligent guess of the vertical reflector savings. Similar separations are possible for finite slabs.

The boundary and interface conditions are

(1) At center of core† ($r = 0$):

$$\frac{d\phi_f}{dr} = \frac{d\phi_s}{dr} = 0$$

(2) At outer extrapolated edge of reflector ($r = a$):

$$\phi_f = \phi_s = 0$$

(3) At interfaces between media ($r = \alpha_i, i = 1, 2, \dots, n - 1$):

* Chapter 1.3 contains some discussion of the group equations.

† In slab geometry this condition is implied by the symmetry about $r = 0$.

$$\phi_f, \phi_s, D_f \frac{d\phi_f}{dr}, D_s \frac{d\phi_s}{dr} \text{ continuous}$$

The general solution of the homogeneous equations (117) will give rise to four arbitrary constants in each of the n regions. Boundary conditions (1) and (2) yield four equations on these constants, and the interface conditions yield $4(n-1)$ so that the $4n$ arbitrary constants satisfy $4n$ conditions. Thus, the problem can be solved only in special cases. The critical equation expresses the conditions under which a solution can be found.*

Since the condition that $4n$ homogeneous equations in $4n$ variables have a solution is the vanishing of the determinant of coefficients, one could obtain a $4n$ degree determinant as the critical condition. A matrix approach⁴³ assures the vanishing of a 2×2 determinant as the critical condition ($N \times N$ determinant in N -group theory).

The matrix method will now be described. In each region, the general solution of Eq. (117) may be written as a linear superposition of solutions of the equation:

$$\left(\frac{1}{r^\mu} \frac{d}{dr} r^\mu + \kappa^2 \right) \psi_\mu(\kappa r) = 0 \quad (118)$$

where κ^2 satisfies the characteristic equation:

$$\begin{vmatrix} D_f \kappa^2 + \sigma_{SD} + \sigma_{af} & -\nu \sigma_{fs} \\ -\sigma_{SD} & D_s \kappa^2 + \sigma_{as} \end{vmatrix} = 0 \quad (119)$$

Equation (119) has two roots for κ^2 , to be written κ_1^2, κ_2^2 . For each root, Eq. (118) has two linearly independent solutions, to be written F and G . These are tabulated in Table 1.4.9 for various μ .

In the core, one may write (with ' denoting derivative with respect to argument†) for the solution of Eq. (117) subject to the central boundary conditions (and thus involving two arbitrary constants):

$$\begin{pmatrix} \phi_s \\ D_s \frac{d\phi_s}{dr} \\ \phi_f \\ D_f \frac{d\phi_f}{dr} \end{pmatrix} = \begin{pmatrix} F(\kappa_1 r) & F(\kappa_2 r) \\ D_s \kappa_1 F'(\kappa_1 r) & D_s \kappa_2 F'(\kappa_2 r) \\ R_1 F(\kappa_1 r) & R_2 F(\kappa_2 r) \\ R_1 D_f \kappa_1 F'(\kappa_1 r) & R_2 D_f \kappa_2 F'(\kappa_2 r) \end{pmatrix} \begin{pmatrix} C_1 \\ C_2 \end{pmatrix} \quad (120)$$

where:

$$\begin{aligned} R_1 &= \frac{\sigma \nu_{fs}}{D_f \kappa_1^2 + \sigma_{SD} + \sigma_{af}} \\ &= \frac{D_s \kappa_1^2 + \sigma_{as}}{\sigma_{SD}} \end{aligned} \quad (121)$$

*Form sheets and instructions for carrying out two-group calculations by hand have been published by Spinrad and Kurath, ANL-4352.

† i.e. $d/dr \psi(\kappa r) = \kappa \psi'(\kappa r)$.

Equation (120), which is a matrix equation, will be abbreviated as:

$$\psi_{\text{core}}(r) = M_{\text{core}}(r) \begin{pmatrix} C_1 \\ C_2 \end{pmatrix} \quad (122)$$

It is further possible to construct a propagation matrix $M(r, r')$ in any region which has the property:

$$\psi(r) = M(r, r') \psi(r') \quad (123)$$

This matrix is given by:

$$M(r, r') = ABC(r) C^{-1}(r') B^{-1} A^{-1} \quad (124)$$

where:

$$\begin{aligned} A &= \begin{pmatrix} 1 & 0 & 0 & 0 \\ 0 & D_s & 0 & 0 \\ 0 & 0 & 1 & 0 \\ 0 & 0 & 0 & D_f \end{pmatrix}, & A^{-1} &= \begin{pmatrix} 1 & 0 & 0 & 0 \\ 0 & D_s^{-1} & 0 & 0 \\ 0 & 0 & 1 & 0 \\ 0 & 0 & 0 & D_f^{-1} \end{pmatrix} \\ B &= \begin{pmatrix} 1 & 0 & 1 & 0 \\ 0 & 1 & 0 & 1 \\ R_1 & 0 & R_2 & 0 \\ 0 & R_1 & 0 & R_2 \end{pmatrix}, & B^{-1} &= \begin{pmatrix} R_2 & 0 & -1 & 0 \\ 0 & R_2 & 0 & -1 \\ -R_1 & 0 & 1 & 0 \\ 0 & -R_1 & 0 & 1 \end{pmatrix} \frac{1}{R_2 - R_1} \\ C(r) &= \begin{pmatrix} F(\kappa_1 r) & G(\kappa_1 r) & 0 & 0 \\ \kappa_1 F'(\kappa_1 r) & \kappa_1 G'(\kappa_1 r) & 0 & 0 \\ 0 & 0 & F(\kappa_2 r) & G(\kappa_2 r) \\ 0 & 0 & \kappa_2 F'(\kappa_2 r) & \kappa_2 G'(\kappa_2 r) \end{pmatrix} \\ C^{-1}(r) &= \begin{pmatrix} \frac{1}{\kappa_1 W(\kappa_1 r)} & 0 & 0 & 0 \\ 0 & \frac{1}{\kappa_1 W(\kappa_1 r)} & 0 & 0 \\ 0 & 0 & \frac{1}{\kappa_2 W(\kappa_2 r)} & 0 \\ 0 & 0 & 0 & \frac{1}{\kappa_2 W(\kappa_2 r)} \end{pmatrix} \\ &\times \begin{pmatrix} \kappa_1 G'(\kappa_1 r) - G(\kappa_1 r) & 0 & 0 & 0 \\ -\kappa_1 F'(\kappa_1 r) & F(\kappa_1 r) & 0 & 0 \\ 0 & 0 & \kappa_2 G'(\kappa_2 r) - G(\kappa_2 r) & 0 \\ 0 & 0 & -\kappa_2 F'(\kappa_2 r) & F(\kappa_2 r) \end{pmatrix} \end{aligned} \quad (125)$$

Table 1.4.9 — Solutions of Equation (118)

μ	Geometry	$F(\rho)$	$G(\rho)$	$W(\rho)$
0	Slab	$\cos \rho$	$\sin \rho$	1
1	Cylinder	$J_0(\rho)$	$Y_0(\rho)$	$\frac{2}{\pi\rho}$
2	Sphere	$\frac{\sin \rho}{\rho}$	$-\frac{\cos \rho}{\rho}$	$\frac{1}{\rho^2}$

where:

$$W(\rho) = F(\rho)G'(\rho) - F'(\rho)G(\rho) \quad (126)$$

and is the Wronskian of the functions F and G . It can be shown from Eq. (118) that $W(\rho) = \text{const. } \rho^{-\mu}$. In this notation:

$$\mathbf{M}_{\text{core}}(\mathbf{r}) = \mathbf{A} \mathbf{B} \begin{pmatrix} F(\kappa_1 r) & 0 \\ \kappa_1 F'(\kappa_1 r) & 0 \\ 0 & F(\kappa_2 r) \\ 0 & \kappa_2 F'(\kappa_2 r) \end{pmatrix}$$

The usual two-group diffusion treatments are given in the standard texts.^{35,44} Friedman⁴⁵ has considered two coupled Boltzman equations. Adler⁴⁶ considers the reduction of a two-group system to an equivalent one-group, with attention to boundary conditions. For additional references the reader should see the treatments of Spinrad,⁴⁷ and Wigner and Friedman.⁴⁸

In terms of the propagation matrices, one has:

$$\psi(a) = \begin{pmatrix} 0 \\ D_s \frac{d\phi_s}{dr} \\ 0 \\ D_f \frac{d\phi_f}{dr} \end{pmatrix}_{r=a} = \mathbf{M} \begin{pmatrix} C_1 \\ C_2 \end{pmatrix} \quad (127)$$

where the matrix \mathbf{M} is the product:

$$\mathbf{M} = \mathbf{M}(a_1, \alpha_{n-2}) \mathbf{M}(\alpha_{n-2}, \alpha_{n-2}) \dots \mathbf{M}(\alpha_2, \alpha_1) \mathbf{M}_{\text{core}}(\alpha_1) \quad (128)$$

and is of the form:

$$\mathbf{M} = \begin{pmatrix} \beta_1 & \gamma_1 \\ \beta_2 & \gamma_2 \\ \beta_3 & \gamma_3 \\ \beta_4 & \gamma_4 \end{pmatrix}$$

It follows that:

$$\begin{vmatrix} \beta_1 & \gamma_1 \\ \beta_3 & \gamma_3 \end{vmatrix} = 0 \text{ is the critical condition.}$$

Alternate methods reducing the $4n \times 4n$ problem are possible. Thus, for example, two sets of particular solutions ϕ_f, ϕ_g may be chosen in the outer region. Each solution is then worked inward by matching at the interfaces until the core radius (assumed known or unknown) is reached. A linear superposition of these solutions with arbitrary coefficients may then be matched to the core solutions (also involving two unknown constants) to provide four equations in the four unknowns. The problem is thus reduced to an equivalent two region problem.

Also of interest is a "back-and-forth" or trial-and-error method.⁴⁹ In this method as used for non-multiplying reflectors, the fast flux, which is known in the outermost region, is worked back to the core boundary, the position of which is guessed. From the known core composition, the slow flux can be calculated in the core and worked forward through the reflectors. It will not, in general, vanish at the extrapolated reactor boundary. The process is repeated with another guess of the location of the core boundary. Although tedious, the method has been used effectively in three-group calculations.

MULTI-GROUP CALCULATIONS*

The main method used for solution of multi-group equations with more than two-groups is a numerical iterative method.^{50,51} In a simple form, this may be described as follows. The equations are of the form:

$$-\frac{1}{r^\mu} \frac{d}{dr} D_i r^\mu \frac{d}{dr} \phi_i + \sigma_i \phi_i = \sum_{j=1}^{i-1} k_{ij} \phi_j + f_i S \quad (129)$$

where:

$$S = \nu \sum_j \sigma_{fj} \phi_j \quad (130)$$

and S/ν is the fission density. The value of ν for which Eqs. (129) and (130) have a solution may be obtained as follows. Given an $S^{(n)}(r)$, Eq. (129) is solved in sequence for $i = 1, 2, \dots$ to obtain $\phi_i^{(n)}$. Then, substitution of these $\phi_i^{(n)}$ in Eq. (130) yields $S^{(n+1)}(r)$.

This process is started by guessing $S^{(0)}(r)$ ($S^{(0)} = 1$ is good enough) and is continued until $\nu(r) = S^{(n)}(r)/S^{(n+1)}(r)$ is substantially constant (independent of r). If the ν thus obtained is not that characteristic of the fuel, the assumed composition of the reactor is varied and the computation repeated.

The $\phi_i^{(n)}$ are usually obtained by numerical integration of the differential Eq. (129) subject to the boundary conditions:

$$\begin{aligned} \frac{d\phi_i}{dr} &= 0 \quad \text{at } r = 0 \\ \phi_i &= 0 \quad \text{at } r = a \text{ (outer boundary)} \end{aligned} \quad (131)$$

Standard methods may be used for the numerical integration. However, owing to the form of the boundary conditions, a particular solution of the differential equation ϕ_{iP} and a homogeneous solution ϕ_{iH} are both obtained by integration in the direction of increasing r . Then:

$$\phi_i = \phi_{iP} + \alpha \phi_{iH}$$

* Chapter 1.3 contains some discussion of the group equations.

is again a particular solution. The value of α is so chosen that:

$$\phi_1(a) = 0$$

The calculations involved in the above iteration method are tedious. The advent of modern electronic computing machines has tended to make this method become one of the most important techniques, especially for intermediate reactors. One major advantage is that arbitrary variations of reactor properties with r do not materially add to the difficulty of solution.

ODD SHAPES

A number of references on various shape reactors are given above under "One-velocity Reactors" and in Table 1.6.8. One should note also work by Davison⁵² on extension of the spherical harmonics method to more complex shapes.

Numerous numerical approaches, such as relaxation methods, permit attack on novel geometries, especially in one-group systems, as do the electrical network or simulator analogue machines. Weinberg⁵³ mentions source-and-sink methods for handling odd shapes, corner situations, and the like; compare also the Wheeler control volume referred to in Chapter 1.6 regarding the uses of source-sink methods for bounding solutions. The following discussion of perturbation theory also indicates methods of frequent utility.

Monte Carlo methods permit attack, especially with the aid of modern computing machines, on energy-dependent reactors having odd shapes or multiple regions.

NON-UNIFORM MEDIA

Some instances of space-variable systems were mentioned above under "Non-uniform Fuel Loading."

Some solutions have been obtained for the one-group reactor equation with variable buckling;^{54,55,56,57} the quantity which satisfies that equation may involve other factors in addition to the neutron flux.⁵⁸

Goertzel⁵⁹ has investigated the conditions under which the Fermi equation for a bare reactor of variable density may be separated into space and energy equations, thus permitting solution of the problem by elementary methods. Formulae are given which apply to thermal reactors, resonance reactors, and mixed thermal-resonance reactors. He has further used a mode method⁶⁰ to study solutions of the Fermi-age equation for variable density moderator and non-uniform fuel distribution.

A transverse gap extending across a reactor has been studied theoretically and experimentally to some extent. References are given in the last part of Chapter 1.6. Empty channels such as those used for gas cooling have received considerable attention.^{61,62}

PERTURBATION THEORY

THE EIGENVALUE PROBLEM

Some of the mathematical techniques of handling eigenvalue problems are directly applicable to the reactor equations. Of specific importance are the perturbation and variation methods and the iteration methods.

The Boltzmann equation or any of its approximations may be written as:

$$\frac{\partial n}{\partial t} = Hn \tag{132}$$

where n is the neutron density,* and the operator H does not depend† on n and is therefore linear. Further, H has the form:‡

$$H = \nu J - K \quad (133)$$

where ν is the number of neutrons per fission.

Equation (132) may be transformed into an eigenvalue problem in several ways. One method considers the normal mode solutions:

$$\frac{\partial n}{\partial t} = \lambda n$$

for which the eigenvalue λ satisfies:

$$\lambda n = Hn$$

If the greatest λ value is zero, the reactor is critical. A second method considers the critical or steady-state problem:

$$\frac{\partial n}{\partial t} = 0$$

for which the eigenvalue ν_c satisfies:

$$\nu_c Jn = Kn \quad (134)$$

The lowest ν_c value is then the value of ν required to maintain a steady chain reaction.

PERTURBATION AND VARIATION METHODS

Let $d\tau$ be the volume element such that $\int n d\tau$ is the total number of neutrons§ in the reactor. Define the operator M^+ adjoint to M by the requirement that:

$$\int u M v d\tau = \int v M^+ u d\tau \quad (135)$$

for all real functions u, v that satisfy the boundary conditions on n . The operators H, J , and K are usually not self-adjoint. That is, $H = H^+$ is not usually true.

Consider, as an example, Eq. (134) and the adjoint equation:

$$\nu_c J^+ m = K^+ m \quad (136)$$

and the equation for the "perturbed" problem:¶

$$\nu_c J^+ n' = K^+ n' \quad (137)$$

* n is a function of energy, neutron velocity direction, and position.

† In power reactors, the cross sections contained in H depend on the power through temperature and density effects, thus causing H to become non-linear. This case is treated in Chapter 1.6.

‡ For the form of H, J, K , cf. Chapter 1.6, "General Equations" and "Two-group, Bare, Thermal Reactor."

§ Delayed or latent neutrons are considered in Chapter 1.6.

Multiplication of Eq. (137) by m and Eq. (136) by n' and integration of each product followed by a subtraction leads to, after use of Eq. (135):

$$\delta\nu_c = \frac{\int m(\delta K)n'd\tau - \nu'_c \int m(\delta J)n'd\tau}{\int mJn'd\tau} \quad (138)$$

where δ 's denote the primed quantity minus the unprimed quantity. This exact* result may be written in three approximate forms:

$$\delta\nu_c = \frac{\int m\delta Kn'd\tau - \nu'_c \int m\delta Jn'd\tau}{\int mJnd\tau} \quad (138a)$$

$$\delta\nu_c = \frac{\int m\delta Knd\tau - \nu'_c \int m\delta Jnd\tau}{\int mJnd\tau} \quad (138b)$$

$$\delta\nu_c = \frac{\int m\delta Knd\tau - \nu_c \int m\delta Jnd\tau}{\int mJnd\tau} \quad (138c)$$

Forms (138b) and (138c) have the advantage of not requiring knowledge of the perturbed density n' . The value of ν'_c in some applications of Eq. (138b) is simply ν . In some important cases, however, such as in the measurement of danger coefficients,⁶³ the perturbation is localized in space, and perhaps in energy, and causes an appreciable local perturbation in n . When this occurs, $\delta Kn'$ or $\delta Jn'$ may be experimentally or computationally determined and the more correct result, Eq. (138a), becomes applicable.

The variational method of arriving at form (138c) has the added advantage of leading to a method for estimating the eigenvalue ν_c . It is based on the fact that the equality:

$$\nu_c = \frac{\int mKn}{\int mJn} = \frac{\int nK^+m}{\int nJ^+m} \quad (139)$$

holds when any function is used for n so long as m satisfies Eq. (136) and when any function is employed for m provided n satisfies Eq. (137). Thus, if changed or assumed values m' and n' are used in place of m and n , the change or error, $\delta\nu_c$, is proportional to the product $(m-m')(n-n')$. Another way of stating this result is to say that expression (139) for ν_c is stationary with respect to variations of m and n about their correct values. Form (138c) is obtained from Eq. (139) by varying m , n , K , and J and neglecting terms containing the product $\delta m \delta n$.

THE REACTIVITY

THE ADOPTED DEFINITION

The reactivity, here denoted by R , generally means a quantity measuring the departure of a reactor from criticality, being unity for a critical reactor, greater than unity for a supercritical reactor, and less than unity for a subcritical reactor. In dynamic considerations, where R plays the role of an effective multiplication constant, the definition of the characteristic time is fixed by the definition adopted for reactivity.

* The approximation $\delta(\nu_c J) = \delta\nu_c J + \nu_c \delta J$ has been made.

A simple and useful definition* of reactivity is:

$$R = \frac{\nu}{\nu_c} \quad (140)$$

Thus, R is the eigenvalue of the equation:

$$RK_n = \nu J_n \quad (141)$$

which is simply a rewrite of Eq. (134). Similarly, the adjoint equation:

$$RK^+m = \nu J^+m \quad (142)$$

is a rewrite of Eq. (136). Thus, as in Eq. (139) the equality:

$$R = \frac{\nu \int m J_n d\tau}{\int m K_n d\tau} \quad (143)$$

has the stationary property. Further, the relation:

$$\frac{\delta R}{R} = \frac{\delta \nu}{\nu} - \frac{\delta \nu_c}{\nu_c} \quad (144)$$

gives the difference in reactivity between two slightly different reactors, where $\delta \nu_c$ is given by Eq. (138) or any of its approximate forms.

INTERPRETATION BY IMPORTANCE

The adjoint function m as given by Eq. (136) or Eq. (142), represents the importance† of a neutron towards maintaining the chain reaction. For any neutron distribution n , not necessarily satisfying Eq. (141), the quantity $\nu \int m J_n d\tau$ is then the creation rate of importance via fission neutrons, and $\int m K_n d\tau$ is the net destruction rate of importance owing to scattering, absorption, and leakage. Thus, Eq. (143), which is correct for any n , states that the reactivity is the multiplication constant as measured by importance (rather than by neutron number). The significance of the stationary character of Eq. (143) is that the reactivity as defined depends only on the reactor characteristics ν , J , and K and is independent of changes in the neutron distribution within the reactor.

Equation (144) may be simply interpreted when form (138c) is substituted for $\delta \nu_c$. The result may be arranged to state that the fractional increase of reactivity is equal to the fractional increase in creation rate of importance minus the fractional increase in destruction rate of importance.

The characteristic or effective generations time l is given by

$$l = \frac{I}{\int m K_n d\tau} = \frac{\int m n d\tau}{\int m K_n d\tau} \quad (145)$$

* This is the definition used by the KAPL physics group.

† See Chapter 1.6 for a physical definition of this quantity. The function m is the same as the "iterated fission probability," a term employed by the KAPL group. Cf. KAPL-98 for a comparison of this with the fission probability.

in terms of which, the dynamic equation* based on Eq. (132) may be written. The quantity I is interpreted as the total importance of neutrons, and the time l is then the average turnover time of importance, being given by the total importance divided by the destruction rate of importance.† If ν were suddenly made zero (and thus $R \rightarrow 0$), there would be no further production, and as a result, the total importance I would decay as $e^{-t/l}$.

Equation (5) states that the importance m of a neutron in a critical reactor is equal to the average importance of the neutrons emerging from the first collision. Equations (7a) and (7b) state that the importance of a neutron is given by the importance of the first generation fission neutrons resulting from the neutron in question. Equation (7c) defines \bar{m} to be the average importance of a fission neutron.

ITERATION METHODS

One useful method of solving:

$$\frac{\nu}{R} Jn = Kn$$

proceeds as follows. One guesses Jn_0 and solves the equations:

$$Kn_{k+1} = Jn_k$$

for $k = 0, 1, \dots$

Then:

$$\lim_{k \rightarrow \infty} \frac{n_k}{\int n_k d\tau} = n$$

and:

$$\lim_{k \rightarrow \infty} \frac{Jn_{k+1}}{Jn} = \frac{R}{\nu}$$

Clearly the method is useful only if the convergence is rapid, as is the case for small reactors. Also, owing to the form of the operator J , one can usually guess Jn_0 easily. This is because Jn_0 is the fission distribution multiplied by the fission spectrum. A similar approach also applies to the adjoint equations:

$$\frac{\nu}{R} J^+ m = K^+ m$$

Often it is useful to calculate in this way m_k and $n_{k'}$ (for $k = k' = 1$ possibly) and obtain R from Eq. (143). This is usually extremely accurate even with $k = k' = 1$.

* Chapter 1.6 treats the effect of delayed neutrons and further discusses Eqs. (132) and (144).

† A somewhat more physical definition by Hurwitz is that l is the weighted average of the time required by a fission neutron to produce another fission. A fission source is assumed to have a spatial distribution like the normal power distribution, and each resulting fission is weighted by the importance of the neutrons to which it gives rise.

REFERENCES

1. Carlson, AECD-2835.
2. LADC-79.
3. Carlson and Peterson, LA-1061 (also LADC-756).
4. Frankel and Goldberg, AECD-2056 (also LADC-76).
5. Wilson, Birmingham Report MS-105 (classified).
6. Serber, LA-234 (classified).
7. Davison, LT-18, Chapter III.
8. Melvin, AERE-T/R 586 and 587.
9. Sweeney, Goldstein, and Carlson, LA-1364, LA-1365, and LA-1366.
10. Fairbrother, MS-111.
11. G. Wassermann, C. R. Acad. Sci. Paris, 223, 537-539, Oct. 1946.
12. Scalletar, MonP-33, pp 16 and 17 (classified).
13. CP-1456 (classified).
14. Murray, C- and CCC-Y-12 (classified).
15. Weinberg and Noderer, p V-128 (classified).
16. Young, MonP-427 (classified).
17. Preston and Davison, MS-112.
18. Davison, CRT-361.
19. Nordheim, MonP-17 (classified).
20. Feynman, Welton, Ashkin, Ehrlich, Peshkin, and Reines, LA-524 (classified).
21. Davison, AERE T/R-826.
22. Selengut, AECD-3024.
23. Volkoff, MT-21 (classified).
24. CRT-391.
25. MT-38 (classified).
26. French and Hurwitz, KAPL-41 (classified).
27. Volkoff and Le Caine, MT-30 (classified).
28. Greuling, LA-399 (classified) and LA-493 (classified).
29. Garabedian and Weinberg, MonP-434 (classified) and MonP-435 (classified).
30. Glasstone and Edlund, The Elements of Nuclear Reactor Theory, p 352 and following pages, Van Nostrand, 1952.
31. Friedman, Nuclear Reactors, AIEE series on Nucleonics for Engineers, 1949.
32. Glasstone and Edlund, op. cit., Chapter XII.
33. Weinberg, Am. Jour. Physics, 20, p 401, 1952.
34. Weinberg and Noderer, Theory of Neutron Chain Reactions, ORNL CF-51-5-98 (2 classified volumes and 1 unclassified volume).
35. Soodak and Campbell, Elementary Pile Theory, John Wiley and Sons, New York, N. Y., 1950.
36. Goertzel, TAB-53 (classified).
37. Shapiro and Preiser, ORNL-1176 (classified).
38. Ibid., p 18 (classified).
39. Selengut, APEX-121 (classified).
40. J. E. Wilkins, Jr., unpublished.
41. Goertzel, Reactor Sci. Tech. TID-2001, April 1952 (classified).
42. Klahr, unpublished.
43. Householder and Garabedian, MonP-202 (unclassified) and MonP-246 (classified).
44. Glasstone and Edlund, op. cit., Chapter VIII.
45. Friedman, unpublished (classified).
46. Adler, CRT-395.
47. Spinrad, MonP-284 (classified).
48. Wigner and Friedman, CP-1662 (classified).
49. Nordheim, CP-2222, p 18.
50. Hurwitz and Ehrlich, Jour. Reactor Sci. Tech., to be published.
51. Safanov, RM-462 (classified), RM-570 (classified), R-233, and TID-2004 (classified).
52. Davison, AERE T/R-700; Flanders and Shortly, Jour. Applied Phys. 21, 1950, p 1326.
53. Weinberg, MonP-187 (classified).
54. Morehouse, CP-1069 (classified).
55. Chernick, BNL-126 (classified).
56. CF-3599 (classified).
57. Oak Ridge Memo CL-GY-6 (classified).
58. Chicago Handbook, Chapter IV E, p 9.
59. Goertzel, MonP-313 (classified).
60. Lexington Project Report 103 (classified).
61. Kaplan and Chernick, BNL-152, pp 29-31 (classified).
62. Davison, AERE T/R-738.
63. Brooks, KAPL-304 (classified).

CHAPTER 1.5

Reactor Statics; Experimental and Numerical Results

Mathew M. Shapiro

Classification of critical mass and related data involves numerous parameters and might be done in various ways. For example, reactors are frequently classified as fast, intermediate or resonance, semi-thermal, thermal, or mixed (i.e., fast in one part of the reactor and slow in another) according to their neutron energies. Another common classification is by moderator material. This will be employed here with energy types used as modifying or descriptive terms. Somewhat arbitrarily, "unmoderated" will be used to mean "unmoderated by carbon or lighter elements."

Ages for fission neutrons in a number of common moderators and water-metal mixtures are given in Tables 1.5.1 and 1.5.2; the spatial slowing-down distributions for some of these are shown in Figs. 1.5.1 to 1.5.6. Table 1.5.3 gives experimental ages for Ra-Be neutrons in some water-metal mixtures. Thermal diffusion lengths appear in Table 1.5.4.

HOMOGENEOUS REACTORS

MODERATED CORES

HYDROGEN MODERATORS

By fitting the measured slowing-down distribution of fission neutrons in water with a synthetic kernel, Greuling has calculated the critical mass of water-moderated, spherical reactors having an infinite water tamper. Those results which apply to highly enriched uranium appear in Fig. 1.5.7.

The water boiler reactors (LOPO, HYPO, and SUPO) are described in Table 1.5.5. Figures 1.5.8 and 1.5.9 show thermal- and fast-flux distributions for the low-powered assembly with a BeO tamper.

Tests of various tamper materials have been made by observing their effects either on the criticality of the low-powered water boiler or on its multiplication of a natural source when a small part of the BeO tamper was replaced by the specimens. BeO bricks were removed from a 3-in. \times 3-in. area extending radially from the core surface to the outside of the tamper (one foot thick) and replaced by the material to be tested. The estimated change in critical mass for the materials, when used bare and when covered by 0.030 in. of Cd, is given in Table 1.5.6 relative to bare and Cd-covered BeO.

The result of a critical experiment on the HRE is shown in Table 1.5.7.

In addition to the calculations mentioned above which are directly related to critical experiments, some additional theoretical results are of interest.

The calculated effect of varying the tamper material around a spherical core of fixed composition is shown in Table 1.5.8. The theoretical results for an infinite D₂O reflector and different fuel concentrations appear in Table 1.5.9.

Figure 1.5.10 shows the minimum critical mass of a water-tamped pure U²³⁵-H₂O spherical core as a function of core radius. The least mass (0.69 kg of U²³⁵) occurs for a radius of 16.7 cm. The shape of the fuel distribution required to minimize the mass is shown in Fig. 1.5.11. For a radius smaller than 16.7 cm, some of the fuel is lumped at the core-reflector interface. Figure 1.5.12 shows the fuel loading for a core of 13 cm radius.

D MODERATORS

Oak Ridge measurements for enriched U²³⁵ thermal D₂O systems with D₂O reflectors* appear in Table 1.5.10 and Argonne results for bare, natural-U, homogeneous systems in Table 1.5.11.

A number of computations performed by Nordheim and his group are given in Tables 1.5.12 through 1.5.16. These include bare, D₂O, and graphite reflectors and Pu and U²³⁵-U²³⁸ fuel. Table 1.5.17 gives D₂O reflector savings.

Calculated results for bare reactors with natural or slightly enriched U are shown in Fig. 1.5.13, and for natural U with perfectly pure D₂O in Table 1.5.18.

LATTICES

The term "lattice" as used herein applies to large thermal reactors usually using natural uranium.

THEORY

In the following discussion, the notation in Table 1.5.19 will be adopted.

VALUE OF η

In terms of basic constants, the number of neutrons from thermal fission per thermal neutron absorbed in U is:

$$\eta = \frac{\sigma_f(25) N_{25} \nu_{25}}{[\sigma_f(25) + \sigma_c(25)] N_{25} + \sigma_c(28) N_{28}} \quad (1)$$

With recent data^{7,8} as follows:

$$\nu_{25} = 2.5 \pm 0.1$$

$$\frac{\sigma_c(25)}{\sigma_f(25)} = 0.183 \pm 0.008$$

$$\sigma_f(25) = 549 \pm 8b$$

$$\sigma_c(28) = 2.80 \pm 0.07b$$

$$\frac{N_{28}}{N_{25}} = 137.8 \pm 1$$

* The new Argonne experimental reactor (CP-5) is to be of this type, with about 1.1 kg of U²³⁵ held in Al plates in a core 2 ft in diameter and height surrounded by about 2 ft thickness of reflector.⁶

⁶ References appear at end of chapter.

one obtains $\eta = 1.33 \pm 0.05$ for natural U. This accuracy is not adequate for low- k reactors.

Greater accuracy may be obtained with exponential and critical experiments, in which η is one of the parameters involved. The value of η usually quoted from the early Chicago graphite exponentials, using ϵ , p , f , and M^2 values calculated by the standard formulae, is 1.315.⁹

If measured thermal utilizations are used instead of the calculated values, Way¹¹ finds* $\eta = 1.340 \pm 0.7\%$ which agrees well with the value obtained from homogeneous D_2O exponential experiments.¹²

FAST EFFECT

In addition to the thermal fissions in U^{235} , there are also a few fast fissions produced in the uranium before the fast neutrons escape from the uranium lumps. The result of this effect is to increase the number of available fast neutrons by a factor ϵ given, according to a one-group theory with appropriate fast constants, by:

$$\epsilon - 1 = \frac{\left(\frac{\nu \sigma_f - \sigma_f - \sigma_c}{\sigma_t} \right) (P)}{1 - \left(\frac{\nu \sigma_f + \sigma_{cl}}{\sigma_t} \right) (P')} = \frac{GP}{1 - SP'} \quad (2)$$

Here P is the probability of a fission neutron from U^{235} colliding within the lump before escaping, and the numerator, GP , thus expresses the net neutron gain from such first-flight collisions. SP fast neutrons emerge from these first collisions within the lump, and a fraction P' of these, in turn, collide before escaping. The net gain in neutrons from these second-round collisions is thus $SPGP'$, or $SP' = x$ times the gain in the first collision. Assuming P' to be the same for all succeeding rounds of collisions, one obtains the factor $1 + x + x^2 + \dots = 1/(1-x)$, which gives the above formula.

The calculation of P and P' is a geometrical problem, with P evaluated for a source distributed like the thermal neutron flux in the lump, while for P' the source after one collision is assumed to be uniform throughout the lump. If the distribution of thermal neutrons within the lump is taken as that characteristic of diffusion into the lump, one has P as a function of κ and R (where R is the dimension of the lump and $1/\kappa$ is its thermal-diffusion length) and also of the macroscopic total fast cross section, $N\sigma_t$, as follows: $P = P(N\sigma_t R, \kappa/N\sigma_t)$, with $P' = P(N\sigma_t R, 0)$. Curves† for P are given in Fig. 1.5.14.

Table 1.5.20 gives constants for natural U; the set of numbers yields results which agree with experimental results, as shown in Table 1.5.21. Values for metal rods are given in Table 1.5.22; for smaller sizes, $\epsilon - 1$ is proportional to the radius r or, if the density be altered, to ρr . In some early calculations,¹³ the values of $\epsilon - 1$ used for U_3O_8 were about 0.8 of the values for metal of the same ρr .

In close-packed lattices (e.g., light-water moderator) fast neutrons may travel from one lump to another and give interaction effects in ϵ .^{14,15}

THERMAL UTILIZATION

In the case of a homogeneous reactor, the thermal utilization is the ratio of uranium thermal absorption cross section to total thermal absorption cross section. In a heterogeneous reactor, thermal neutrons are born in the moderator and must diffuse into the fuel, so that the average thermal flux in the fuel element is lower than that in the mod-

* This is for the entire set of 44 Chicago graphite exponentials.

† For the formulae see CP-644. For hollow cylinders see Guggenheim and Pryce, MT-199; do not use CP-644 for this case.

erator. This depression in flux decreases the thermal utilization from the value it would have in the homogeneous situation.

Most lattice calculations use a formula, Eq. (3), for f derived from simple diffusion theory. This appears¹⁶ to give values of f about 2 percent greater than measured values.

Some compensation for the errors of simple diffusion theory can be obtained by altering certain of the constants which enter. More precise calculations using the P_3 approximation are currently receiving attention.

The diffusion theory result is given here for the following configuration. A central region of radius* r_0 is filled with uranium. Following this is a sheath of absorbing but non-moderating material (e.g., steel or aluminum jacket). Following this is an air gap and finally, extending from r_1 to r_2 , moderator. r_2 is the effective outer radius of the moderator such that the volume (and mass) of moderator is that actually associated with a cell. It is assumed that the slowing-down density into thermal is uniform throughout the moderator volume and that there is no neutron current across the outer boundary r_2 . Then:

$$\frac{1}{f} - 1 = F(\kappa_0 r_0) \left(\frac{N_1 \sigma_{a1} V_1 + N_2 \sigma_{a2} V_2}{N_0 \sigma_{a0} V_0} \right) + X(\kappa_2 r_1, \kappa_2 r_2) \quad (3)$$

where V_0, V_1, V_2 are volumes; N_0, N_1, N_2 atomic densities; and $\sigma_{a0}, \sigma_{a1}, \sigma_{a2}$, absorption cross sections for fuel, sheath, and moderator, respectively. κ_0 is the reciprocal diffusion length in fuel and κ_2 that in moderator. F and X are functions as given in Table 1.5.23 and Figs. 1.5.15 through 1.5.17. Clearly $F = 1, X = 0$ corresponds to the homogeneous case. F is the ratio of the thermal neutron density at the surface of the uranium rod to the average thermal neutron density in the rod. X measures the "excess" neutron absorption in the moderator due to the excess neutron density in the moderator over that at the moderator air interface. The rise in neutron density across the jacket (blocking effect) has been neglected. It is usually a small effect for a thin jacket layer.¹⁷

Thermal constants are found in Table 1.5.4 and in Chapter 1.2. The derivation of Eq. (3) is such that Maxwell-averaged cross sections would be used, except as one alters the constants to compensate somewhat for the errors of diffusion theory. In graphite lattices, this is accomplished by increasing the value of the graphite capture cross-section σ_{a2} where it appears explicitly in Eq. (3). Thus, whereas for AGOT graphite the best value of the ratio of its capture cross-section to that of U is 0.67×10^{-3} , it is customary to employ in Eq. (3) a value of 0.78×10^{-3} ; i.e., in effect to increase the graphite capture cross section by $1/6$. This decreases f in typical graphite lattices by about⁷ 1.5%.

RESONANCE ESCAPE PROBABILITY

In the homogeneous medium with absorption and elastic moderation, the resonance escape probability according to the Wigner slowing-down theory (cf. "Slowing Down with No Space Variation," Chapter 1.3) is of the form:

$$p = \exp \left(- \int \frac{\sigma_a}{\sigma_a + \sigma_s} \frac{dE}{E} \right) \quad (4)$$

This formula is exact for (a) moderation only by hydrogen or (b) absorption only in separated sharp lines. For U resonance capture, (b) very nearly obtains and also the ab-

* In spherical or cylindrical geometry. In slab geometry, radii are to be interpreted as distances from the plane of symmetry.

sorption is confined to a fairly small energy region so that variation in ξ and σ_s may usually be neglected. Then:

$$p = \exp \left(- \frac{A}{\xi \sigma_s} \right) \quad (5)$$

where:

$$\sigma_{a \text{ eff}} = \frac{\sigma_a}{1 + \frac{\sigma_a}{\sigma_s}} = \alpha \quad (6)$$

$$\int \sigma_{a \text{ eff}} \frac{dE}{E} = \int \alpha \frac{dE}{E} = A$$

The above cross sections are macroscopic; σ_s includes the scattering of the U and all lighter atoms, and ξ is weighted over all the scatterers so that $\xi \sigma_s$ gives the total slowing-down power.

The notation of Eq. (6) is also used for microscopic cross sections. It is seen that the value of A per U atom should depend only upon the total scattering cross section per U atom (assumed independent of energy). Figures 1.5.18 and 1.5.19 give experimental results for U and Th, while Table 1.5.24 gives asymptotic values for infinite dilution with moderator. The effective absorption integral for U is increased by a factor of 26 as the dilution goes from zero to infinity; for Th, the factor is 4. Table 1.5.34 gives resonance integrals for a number of other materials.

In a system with lumped fuel elements, one has volume absorption within the lump appropriate to the homogeneous material there, plus sharp-line absorption at the lump surface of neutrons coming from the moderator outside. Thus, for lumps which are not too small, one would expect:

$$\sigma_{a \text{ eff}} = \alpha + \beta \frac{S}{M} \quad (7)$$

Here α is as before while, by a somewhat more complex argument,^{18,19,20} $4\beta = \rho(\alpha/\sigma_s)^2$; S, M, and ρ are the surface area, mass, and density of the lump, respectively. Thus, the effective absorption integral is of the form:

$$\int \sigma_{a \text{ eff}} \frac{dE}{E} = A + \mu \frac{S}{M} \quad (8)$$

For U, Figs. 1.5.18 and 1.5.20 indicate the variation in A and μ with scattering dilution; Table 1.5.25 gives values from experimental measurement on metal, and Table 1.5.26 includes values which have been used for compounds.

In addition to the above "self-protection" considerations, in lattice computations one also takes into account the depression in resonance neutron flux at the fuel rod of the same kind as discussed under thermal utilization. Thus:

$$P = e^{-1/T} \quad (9)$$

$$T = \left(\frac{N_2 V_2 (\bar{\xi} \sigma_s)_2}{N_0 V_0 \int \sigma_{a0 \text{ eff}} \frac{dE}{E}} \right) F(\kappa_0 r_0) + X(\bar{\kappa}_2 r_1; \bar{\kappa}_2 r_2) \quad (10)$$

where the bar signifies resonance neutrons, 0 and 2 refer to fuel and moderator, respectively, and the cross sections are microscopic.

Values used for $\bar{\kappa}_0$ are 0.0222ρ for U^7 and 0.025ρ for U_3O_8 ,¹³ where ρ is density in gm/cm³. Moderator constants are given in Table 1.5.27.

AGE

An approximate formula for the age of neutrons in a lattice¹⁷ is:

$$\tau = \left[\tau_{in} \frac{\sigma_{in}}{\sigma_t} P + \tau_f \left(1 - \frac{\sigma_{in}}{\sigma_t} P \right) \right] \left(\frac{V_t}{V_2 + \frac{1}{2} V_0} \right)^2 \quad (11)$$

where the total volume, V_t , is comprised of the lump volume, V_0 , the moderator volume, V_2 , and such void volume as may be present. The age to thermal of fission neutrons in the moderator, τ_f , is given in Table 1.5.1; the age τ_{in} of inelastically scattered neutrons in the moderator has been estimated⁹ at 231 cm² for graphite of density 1.6. The quantity P is the same as in Eq. (2). The above formula, in effect, supposes that the lumps contribute no elastic slowing-down but have (per unit volume) the same average scattering power as the moderator.

In the presence of empty channels, neutron streaming and anisotropic effects enter (e.g., reference 7, p. 29 ff).

THERMAL DIFFUSION AREA

If L_2^2 is the moderator thermal diffusion area, the fuel lumps absorption is taken into account by using:

$$L^2 = f_2 L_2^2 \quad (12)$$

Here f_2 is the thermal utilization of the moderator, i.e., the fraction of all thermal absorptions in the lattice which occur in the moderator. In the notation of Eq. (3) above:

$$f_2 = 1 - f \left[1 + \left(\frac{N_1 \sigma_{a1} V_1}{N_0 \sigma_{a0} V_0} \right) F(\kappa_0 r_0) \right] \quad (13)$$

Because of the higher temperature of the neutrons in a lattice, L_2^2 is somewhat greater than the values (Table 1.5.4) based on sigma-pile measurements; e.g., the neutron temperature (reference 7, p. 31) in the Oak Ridge graphite reactor is about 140°C higher than the graphite temperature, whereas in a sigma-pile, the neutron temperature is about 80°C above the graphite temperature. In materials with constant scattering cross-section, L^2 is proportional to the square root of the absolute neutron temperature.

Neutron streaming and anisotropic effects appear when there are empty channels (reference 7, p. 29 ff).

EXPERIMENTAL AND NUMERICAL RESULTS

GRAPHITE

A series of 44 graphite exponential experiments was carried out at Chicago during the war and subsequently analyzed by Way and Cashwell; their final report was never issued because* of difficulties in the cases containing water. Their last published note (reference 11, p. 24) on this study is:

"A summary of the data and calculations for the 44 graphite-uranium exponential pile experiments performed from 1941 through 1944 will be issued shortly in collaboration with E. D. Cashwell as CP-3124. In the early days there were many changes in the "best" values of the fundamental constants so that results for one group of exponential experiments would not be calculated with the same constants as those for another group. Now, however, calculations for all the experiments have been made in a uniform manner with the same values of the constants and the results are all directly comparable.

The chief purpose of the exponential experiments was to serve as a guide and check in developing theoretical methods of calculating k , the reproduction factor in a lattice, from the product $k = f p \epsilon \eta$. The symbol f denotes the thermal utilization, p the chance of escaping resonance capture, ϵ the fast effect and η the number of neutrons produced per thermal neutron captured in uranium. The theoretical methods used were so-called diffusion theory methods described in the Project Handbook Chapter IV E.

The whole group of experiments shows that 2 different values of η are needed to give agreement between the measured and calculated k 's for the experiments in which the uranium was in the form of oxide and for those in which it was used as metal. If instead of the calculated value of f , the value found directly from a measurement of the cadmium ratio is used in the product $f p \epsilon \eta$, fairly good agreement between experimental and calculated k can be found for all experiments using $\eta = 1.340$. The average deviation in the value of η needed for perfect agreement and 1.340 is only about 0.7 percent. That a large part of this deviation is due to experimental fluctuations is shown by the fact that in a group of experiments on seven almost identical lattices the deviation was ~ 0.4 percent.

This value of η , 1.340, is in good agreement with the value recently determined from the homogeneous P-9 exponential experiments, namely 1.335, and from values found by substitution of measured cross sections or cross section ratios in the definition for η .

$$\eta = \eta(25) \sigma_a(25)/\sigma_a(25 + 28) = 1.35 \text{ using } \eta(25) = 2.10,$$

$$\sigma_a(25) = 640/140, \text{ and } \sigma_c(25 + 28) = 7.13$$

$$\eta = \eta(25) \left[1 + \frac{\sigma_a(28)}{\sigma_f(25)(1 + \alpha(25))} \right]^{-1} = 1.34$$

$$\text{using } \eta(25) = 2.10, \sigma_a(28)/\sigma_f(25) = 0.66, \text{ and } 1 + \alpha(25) = 1.17$$

The conclusion seems to be that diffusion theory methods are good for determining p and ϵ but are adequate for calculating the thermal utilization only to within one or two percent. Moreover, it seems that the values of the constants now in use for the calculation of p and ϵ (see above reference in Project Handbook) must be nearly correct.

* Communication from Miss Way.

Figure 1.5.21 gives calculated multiplication factors for a considerable range of metal rod lattices; Figs. 1.5.22 through 1.5.27 give pf values for spheres and rods of full-density metal, half-density metal, and oxide.

Table 1.5.28 indicates the effect of fuel composition and density upon the best value of multiplication factor obtainable with rod lattices in graphite.

Reflector savings for graphite reflectors around graphite lattices are given approximately (reference 7, p. 46) by:

$$\text{saving} = 1.2L \tanh \frac{T}{L} \quad (14)$$

where T is the reflector thickness and L is the reflector thermal diffusion length.

BERYLLIUM

A sample of U metal in Be metal lattice was tested in a hole in the Argonne graphite pile.²² Each fuel lump contained 182 cc of U (radius of equivalent sphere = 3.52 cm), and the volume ratio of Be to U was 17.2. A buckling value of $407 \times 10^{-6} \text{ cm}^{-2}$ was obtained from what was considered to be the best of the experimental measurements made.

Theoretical calculations have been made²³ for Be metal and oxide lattices. The ages used there are now out of date.

LIGHT WATER

Six lattices of slightly enriched U metal in water have recently been measured at Brookhaven. Bucklings and water reflector savings are given in Table 1.5.29, and cadmium ratios are given in Table 1.5.30. Table 1.5.31 gives results with boron poisoning added.

Twenty-four lattices of natural U in water were operated at Oak Ridge. It was concluded²⁴ that:

(1) "The best k obtainable at room temperature with H_2O and ordinary U in a cylindrical, no-gap geometry, is probably very near 0.99.

(2) "A k larger than unity can probably be attained by going to sufficiently high temperatures or by use of a gap geometry."

Tables 1.5.32 and 1.5.33 summarize results.

Table 1.5.1 — Age of Fission Neutrons in Various Moderators

Substance	Age to indium resonance, cm ² (BNL-170)	Estimated age from indium to thermal, cm ²	Age to thermal, cm ²	Source of information*
H ₂ O	30.4 ± 0.4	1	31.4	ORNL-181, 1948 (E); ORNL-641, 1950 (E) MonP-219, 1946 (T)
D ₂ O(0.16% H ₂ O)	100 ± 5		125	CP-2796, 1945 (T); CP- 3073, 1945 (T); CP- 3453, 1946 (E); CP- 1531, 1944 (E) CP-3195, 1945 (T); MonP-269, 1947 (T)
Be ($\rho = 1.85$)	80 ± 2	17.2	97.2	ANL-4076, 1947 (E and T)
BeO ($\rho = 3.0$)			105 ± 10	MUC-WC-MLG-10, 1946 (T)
C ($\rho = 1.60$)	311 ± 3	53	364	ORNL-187, 1949 (E) BNL-152, 1952 (T)

* (E) = experimental; (T) = theoretical

Table 1.5.2 — Age of Fission Neutrons in Water—Metal Mixtures

Metal	Vol. metal Vol. H ₂ O	Experimental age to indium resonance, cm ²	Theoretical age, indium resonance to thermal, cm ²	Age to thermal, cm ²	Reference
Al	0.5	49.6	2	51.6	Experiment, ORNL-294, 1949
	1.0	76.8	3	79.8	Theory, MonP-219, 1946
Zr	0.25	35.7	Experiment ORNL-641, 1950

Table 1.5.3 — Age of Ra- α -Be Neutrons in Water—Metal Mixtures

(Munn and Pontecorvo, Canadian Jour. Res., A, 25, 157, 1947. Reference also contains spatial distribution curves for Bi-H₂O systems)

Medium, volume ratio	Concentration (C), gm-atoms/liter	Detector	Age, cm ²
H ₂ O	C _H = 111	Dy	55
H ₂ O*	C _H = 111	Rh (Cd difference)	54.5
H ₂ O	C _H = 111	In resonance	46.3
H ₂ O*	C _H = 111	Rh resonance	46.2
H ₂ O:Bi::1:1	C _H = 56 C _{Bi} = 23	Dy	93.7
H ₂ O:Bi::2:1	C _H = 74 C _{Bi} = 15	In resonance	66.3
H ₂ O:Bi::1:1	C _H = 56 C _{Bi} = 23	In resonance	79.5
H ₂ O:Bi::1:2	C _H = 37 C _{Bi} = 30	In resonance	86.2
H ₂ O:Pb::1:1	C _H = 56 C _{Pb} = 27	In resonance	72.8
H ₂ O:Fe::1.3:1	C _H = 63 C _{Fe} = 60	In resonance	53.2

* Measured with Rn- α -Be source by Amaldi and Fermi, Phys. Rev. 50, 899(1936)

Table 1.5.4 — Thermal Diffusion Length and Transport Mean-free-path of Various Materials

Substance	Thermal diffusion length (L), cm (BNL-170)	Transport mean- free-path (thermal), cm (BNL-170)	Source of information
H ₂ O	2.85 ± 0.03*	0.48 ± 0.01	L: C-55, 1942; C-63, 1942; C-82; CP-1389, 1944; CP-2601, 1945; ORNL-933, 1951
D ₂ O(0.16% H ₂ O)	116 ± 4	2.65 ± 0.15	λ_u : ORNL-933, 1951 L: CP-3364, 1945; CP-3195, 1945
Be ($\rho = 1.85$)	20.8 ± 0.5	1.43 ± .05 (using $\sigma_a(\text{th}) = 9 \text{ mb}$)	λ_u : ANL-4746; NAA Memo-236 L: ANL-4076, 1947
BeO ($\rho = 2.69$)	29 ± 2	0.90 (Calculated from original reference)	λ_u : ANL-4076, 1947 L: LA-160, 1944 λ_u : CP-3647, 1946
Graphite (corrected to $\rho = 1.60$)	54.4 ± 0.5 ($\sigma_{abs} = 4.4 \text{ mb}\dagger$)		HW-21793, 1952
GBF	52 ± 1		BNL-77, 1950
AGOT	($\sigma_{abs} = 4.8 \text{ mb}\dagger$)		
Th ($\rho = 11.2$)	2.7 ± 0.3		CL-697 (Chicago handbook)
ThO ₂ ($\rho = 6$)	4.1 ± 0.4		CL-697
U ($\rho = 18.9$)	1.55 ± 0.05		CL-697
U ₃ O ₈ ($\rho = 6.0$)	3.7 ± 0.4		CL-697

* CP-2161, 1944, gives $dL/dT = 0.0061 \text{ cm}/^\circ\text{C}$ in the temperature range 27° to 93°C

† 2200-m/sec values; obtained using a calculated value of 4.70 b for the Maxwellian average of the total cross section

Table 1.5.5—Critical Mass Data for Los Alamos Water-boilers

Model name and literature reference	Core		Tampers		Critical mass of U^{235} (M_c), gm	Maximum amount of U^{235} used (M_{max}), gm	Maximum multiplication observed
	Material	Shape	Material	Shape			
LOPO							
AECD-3059(1/25/51)	14.76% enriched uranium as	Sphere	BeO	Pseudosphere	575		
AECD-3063(9/4/44)	14.9 liters of UO_2SO_4 aqueous solution $\rho = 1.348$ (39°C) 1100 gm steel including $\frac{1}{32}$ -in. stainless-steel container	of 12-in. diameter		~1 ft thick			
AECD-3063(9/4/44)			C	Cube 4 ft side	760	?	?
LA-241(3/12/45); same as LADC-941			H ₂ O	Right cylinder, diam. = 4 ft height = 4 ft	1200 \pm 50	717	~3
HYPO							
AECD-3059(1/25/51)	14% enriched uranium as $UO_2(NO_3)_2$ aqueous solution 3000 gm steel including cooling coil and $\frac{1}{16}$ -in.-thick stainless-steel sphere container	Sphere* of 12-in. diameter	BeO	Parallelepiped 24 \times 24 \times 27 in. (against core)	808†		
			C	Parallelepiped 60 \times 48 \times 60 in.			
SUPO							
La-1301(2/7/52), same as AECD-3287	88.7% enriched uranium as 12.7 liters of $UO_2(NO_3)_2$ aqueous solution Stainless-steel sphere container‡	Sphere of 12-in. diameter	C	Cube 55 in. side	777		

* The stainless-steel sphere was filled to within 3 or 4 cm of the top. An empty 1-in.-diameter pipe passes through the core center.

† When 14.5% enrichment is used, the 1-in.-diameter hole is calculated to effect the critical mass by 30 gm.

‡ The core contains three 20-ft-long, $1/4$ -in.-OD, $3/16$ -in.-ID stainless-steel cooling coils. In addition to the 1-in. pipe in footnote (*), a $1/16$ -in.-ID hole runs completely through the reactor tangent to the sphere.

Table 1.5.6—Effect on Critical Mass of Replacing Small Portion of BeO Tamper in Water-boiler with Other Materials

(R. E. Carter et al, La-105, July 1944)

Material	Δm_0 , gm U^{235}	
	Bare	Cd covered
BeO	0	0
C	1.52	0.67
D ₂ O	1.93	.9
Pb	2.67	.5
Bi	2.74	.85
Oak	5.0	5.8
H ₂ O	5.3	4.8
Paraffin	7.0	8.7
Air	8.0	4.8
Cu	11.9	0.5
Fe	12.7	.6
WC	15.79*	3.8†
Tu	-4.54	0.6

* Density = 4.91

† Density = 5.56

Table 1.5.7—Homogeneous Reactor Critical Experiment

(Reactor dimensions and materials from TID-5022; critical fuel concentration from ORNL-1318; Sept. 19, 1952)

Core		Tamper		Fuel concentration, gm U^{235} /kg H ₂ O
Material	Shape	Material	Shape	
>90% enriched uranium as UO_2SO_4 aqueous solution	18-in.-diameter sphere, volume = 50 liters	D ₂ O	Sphere, 39 in. OD, 10 in. thick	25

Table 1.5.8 — Critical Radius and Amount of U^{235} in Spherical Core for Various Infinite Reflectors*

(CP-2182, Sept. 30, 1944)

Reflector	Critical radius (R), cm	Mass U^{235} (G), gm
Graphite ($\rho = 1.6$)	16.1	600
D ₂ O	16.3	622
H ₂ O	20.7	1273
BeO		
($\rho = 3$)	14.7	456
($\rho = 2$)	16.3	622
Be	15.5	535
None	27.3	2920

* Enrichment = 12.5%; concentration = 2.8×10^{-3} U^{235} atoms/molecule H₂O

Table 1.5.9 — Critical Radius and Amount of U^{235} in Spherical Core with Infinite D₂O Reflector for Various Concentrations of 12.5% Enriched Fuel

(CP-2185, October 1944)

Z = U^{235} atoms/ H ₂ O molecule ($\times 10^3$)	Critical radius (R), cm	Mass U^{235} (G), gm
2	18.3	668
2.4	16.1	544
2.8	14.8	794
3.2	13.8	456
3.6	13.1	438
4.0	12.6	432
5.0	11.6	421
6.0	11.2	453
10	9.5	455

Table 1.5.10—Criticality Studies on Enriched U-D₂O Systems*

(Snell, MonP-454, and Addendum)

U ²³⁵ , gm/liter	Core height, cm	Core radius, cm	Core volume, liters	Reflector thickness, cm			Critical mass, gm U ²³⁵
				Bottom	Top	Lateral	
10.35	61.8	20.8	84	20	62	50.2	869
5.17	61.8	30.4	160	20	62	40.6	930
2.58	100	40.4	512	20	24	30.6	1323

* Fuel in Al tubes of 1.5-in. diameter spaced 8.4, 11.9, or 16.9 cm. "No-hole" extrapolation of data from more complex arrangements. A few tenths percent H in the D

Table 1.5.11—Exponential Experiments with D₂O and UO₂F₂ Solutions*

(Wattenberg, CP-3364)

UO ₂ F ₂ concentration, gm/cm ³	Critical radius (R _c), cm	Volume of D ₂ O, liters	Mass of uranium, kg
0.0238	452	358,000	6,602
.7034	247	62,700	3,583
.1484	208	37,300	4,348
.2004	205	35,400	5,598
.2493	209	37,100	7,343
.2986	228	47,900	11,438
.3476	244	52,200	14,586

* For bare spherical reactors; about 0.2% H in D

Table 1.5.12 — Spherical D₂O-U Cores with Infinite D₂O Reflector

Z = U ²³⁵ atoms/D ₂ O molecule (× 10 ³)	Radius, cm		Volume, liters		Mass U ²³⁵ , gm	
	Pure U ²³⁵	12.5 U ²³⁵ : 87.5 U	Pure U ²³⁵	12.5 U ²³⁵ : 87.5 U	Pure U ²³⁵	12.5 U ²³⁵ : 87.5 U
0.1	40.4	42.2	277	315	362	411
.1	29.9	31.5	112	131	292	342
.25	27.5	28.9	87	101	284	329
.3	25.5	27.2	70	84	273	330
.5	20.7	23.4	37	54	242	350
1.0	17.4	19.3	22	30	288	393
2.0	14.6	16.9	13	20	340	527

Table 1.5.13 — Critical Radius for Bare Spherical D₂O Systems
(CP-2222)

Z = U ²³⁵ atoms/D ₂ O molecule (× 10 ³)	Critical radius, cm		
	α = 0*	α = 7*	α = 14*
0.15	...	65	...
.20	56.7	59.7	62.6
.23	54.4	57.8	60.5
.25	53.1	56.2	59.3
.27	51.8	55.3	58.3
.30	50.3	54.0	57.1

* α = atoms U²³⁸/atoms U²³⁵

Table 1.5.14—Spherical D₂O Systems with Graphite Reflectors
(CP-2813X)

Reflector thickness, cm	Core radius, cm		Volume, liters		Mass of U ²³⁵ , gm	
	Z* = 0.15 × 10 ⁻³	Z* = 0.25 × 10 ⁻³	Z* = 0.15 × 10 ⁻³	Z* = 0.25 × 10 ⁻³	Z* = 0.15 × 10 ⁻³	Z* = 0.25 × 10 ⁻³
∞	40.4	32.8	276	147	540	479
50	42.9	34.8	331	176	647	574
30	46.7	37.9	426	228	833	743
20	50.4	41.2	536	294	1048	958
0	65.3	56.0	1167	736	2283	2398

* Z = U²³⁵ atoms/D₂O molecule

Table 1.5.15—Spherical D₂O-Pu Cores with Infinite D₂O Reflector
(CP-2203X)

10 ³ Z = Pu atoms/D ₂ O molecule						
	0.1	0.2	0.25	0.3	0.5	1.0
Volume D ₂ O, liters	180	80	62	51	32	18
Mass of Pu, gm	290	210	205	205	210	240
						290

Table 1.5.16 — Laplacians for D₂O Systems
(U²³⁵ Data from XP-2813X; Pu (Data from CP-2589X)

Z = Fuel atoms/D ₂ O molecule ($\times 10^3$)	U ²³⁵ ($\times 10^3$)	Pu ($\times 10^3$)
0.08	1.43	1.91
.09	1.58	2.07
.10	1.72	2.23
.125	2.03	2.57
.150	2.31	2.86
.175	2.55	3.095
.20	2.77	3.32
.23	3.01	3.53
.25	3.15	3.65

Table 1.5.17 — D₂O Reflector Savings*
(Garabedian, CNL-36)

Reflector thickness, cm	Reflector saving, cm	
	Case I, 10.35 gm U ²³⁵ /liter	Case II, 5.17 gm U ²³⁵ /liter
0	0	0
20	15.3	15.9
30	18.8	19.5
40	20.6	21.6
50	21.6	
62	22.5	23.8
∞	24.2	26.1

* For 2-group theory; slightly larger savings obtained by other methods. The bare-core critical radius was 43.6 cm in Case I and 50 cm in Case II

Table 1.5.18 — Natural U with Pure D₂O

(Ott, MonP-374; bare unpoisoned spherical reactors at room temperature, no H impurity in the D. This report contains a criticality nomograph for D₂O-moderated machines)

D ₂ O molecules/U ²³⁸ atom	D ₂ O volume, m ³
40	34.3
60	20.4
80*	19.0
100	20.4
120	22.5

* This case calls for 0.164 gm U/cc, a total of 3120 kg U or 22 kg U²³⁵. Addition of 1.1 kg Pu reduces the volume to 13.2 m³, and the mass of U to 2140 kg. Core size reductions possible by means of a reflector were not computed

Table 1.5.19 — Notation

k = Multiplication factor = $\eta \epsilon p f$
 η = Number of neutrons produced by thermal fission for each thermal neutron absorbed in U
 ϵ = Multiplicative effect of fast fission = Total number of neutrons produced per neutron produced by thermal fission
 p = Fraction of neutrons which become thermal
 f = Thermal utilization of fuel = Thermal neutrons absorbed in U per thermal neutron captured in all materials of the lattice
 M^2 = Migration area = $\tau + L^2$
 τ = Age in lattice
 L^2 = Thermal diffusion length in lattice
 B = Buckling = $k - 1/M^2$ for k near unity

Table 1.5.20 — Data for Fast Effect in Natural Uranium

Quantity	CL-697
σ_f, b	0.29
σ_{el}, b	1.5
σ_c, b	<0.04
σ_t, b	4.3
ν	<2.55
$\frac{\kappa_0}{N_{0t}}, b$	3.5

Table 1.5.21 — Values of Fast Effect, ϵ
(BNL-152)

Shape*	Radius, cm	ϵ	
		Experimental (Hill, CP-1548)	Calculated using CL-697 constants
Cylinder	1.71	1.032 ± 0.003	1.036
Sphere	3.22	1.042 ± 0.004	1.041
Sphere	3.96	1.048 ± 0.004	1.048

* U metal ($\rho = 18.9$ gm/cc)

Table 1.5.22 — Fast Effect for U Metal Rods
(BNL-152)

Radius, cm	$\epsilon - 1$
1	0.0224
1.1	.0243
1.2	.0261
1.3	.0280
1.4	.0299
1.5	.0316
1.6	.0333
1.7	.0350

Table 1.5.23—Formulae for F and $E = X + 1$
(Science and Engineering of Nuclear Power, Vol. II)

	$F(x)$	$E(x,y)$
Plane	$x \coth x$	$(y - x) \coth (y - x)$
Cylinder*	$\frac{x}{2} \frac{I_0(x)}{I_1(x)}$	$\frac{y^2 - x^2}{2x} \frac{I_1(y)K_0(x) + I_0(x)K_1(y)}{I_1(y)K_1(x) - I_1(x)K_1(y)}$
Sphere	$\frac{x^2}{3} \frac{\tanh x}{x - \tanh x}$	$\frac{y^3 - x^3}{3x} \frac{1 - y \coth (y - x)}{1 - xy - (y - x) \coth (y - x)}$

* K_1 is here defined so as to be always positive

Table 1.5.24—Resonance Integrals for the Heavy Elements

Material	$\int \sigma_a dE/E$, barns	Remarks
Th ²³²	81.3	Measured value from CP-3093 (1945)
U	<240	Sources: CP-3580 (1946), CN-442 (1943), CP-372 (1942), CP-3202 (1945)
Hf	7700	Calculated from data in ORNL-641 (1950) on Zr containing Hf

Table 1.5.25—Resonance Integrals in Uranium

Observer	Method	Date	$A = \int \alpha(E) dE/E$, barns	$\mu = \int \beta(E) dE/E$, barns gm/cm ²	Reference
Creutz	Activation	1944	9.25	24.7	C-116

Table 1.5.26—Resonance Constants in Project Calculations

Material	A, barns	μ/A , gm/cm ²	Reference
U	9.25	$\frac{8}{3}$	CP-372
U ₃ O ₈	12	$\frac{5}{3}$	CP-372
UO ₂	11.51	1.92	CP-445
UF ₆	14.6	1.12	CN-442

Table 1.5.27—Moderator Resonance Constants
(CL-697, IV E)

Substance	$\overline{\xi\sigma_s}$, b/atom or molecule	$\bar{\kappa}_2/\rho$,* cm ² /gm
Water	38.5	0.583
Heavy water	5.28	.141
Be	1.26	.128
BeO	1.76	.0690
Graphite	0.76	.0672

* Values given are for use with U; if the fuel is oxide or hex, multiply the values of $\bar{\kappa}_2/\rho$ by 0.88

Table 1.5.28 — Effect of Fuel on Multiplication Factor

(Roughly assembled and rounded-off values based on Nucleonics, Jan. 1951; CP-372; CN-442; CP-445; CN-362)

Fuel		k_{\max}
Form	Density, gm/cc	
U	18	1.08
U	9	1.07
U	6	1.06
UO ₂	6	1.05
U ₃ O ₈	6	1.04
UF ₃	6	1.03
UF ₆	3.7	1.01
UO ₂	1	1.02

Table 1.5.29 — Water Lattices with Slightly Enriched U*

(Communication from J. Chernick, Sept. 18, 1952)

Lattice†	Buckling, ‡ cm ⁻² × 10 ³			Reflector saving, § cm		
	1st run	2d run	Average	1st run	2d run	Average
1.5:1	2.85 ± 0.06	2.94 ± 0.05	2.89 ± 0.05	7.86 ± 0.14	7.56 ± 0.11	7.71 ± 0.14
1.75:1	3.453 ± .034	3.486 ± .053	3.470 ± .033	7.16 ± .08	7.15 ± .12	7.16 ± .10
2:1	3.65 ± .09	3.86 ± .07	3.75 ± .08	7.23 ± .26	6.75 ± .20	6.94 ± .23
2.5:1	3.700 ± .055	3.647 ± .025	3.673 ± .048	6.81 ± .17	6.99 ± .09	6.90 ± .16
3:1	3.304 ± .028	3.271 ± .066	3.288 ± .018	6.82 ± .11	7.05 ± .09	6.94 ± .11
4:1	1.76 ± .10	1.88 ± .04	1.86 ± .06 [¶]	6.83 ± .52	6.37 ± .19	6.42 ± .22 [¶]

* Metal rods 0.750 in. diameter and 4 ft long, 1.027 wt-% U²³⁵, 30-mil Al cladding on rods, triangular lattice array. Values reported are results of least-squares fits

† Lattice designation is volume ratio of water + Al to U

‡ Chernick's cover letter says in part "The migration areas to be attributed to these lattices are still tentative. We get values ranging from 30–36 cm² depending on the form of the theory used to compute the thermal utilization. We hope to get better values from the analysis of intercell traverses which have just been completed. Members of the group under Karl Cohen report a value of 30 cm² if the assumption of constant reflector savings is used, 34 cm² if the variation with poison is accounted for"

§ Infinite lateral water reflector

¶ Averages for this lattice are weighted because one measurement is much poorer than the other

Table 1.5.30 — Cadmium Ratios in Slightly Enriched Water Lattices
(Communication from J. Chernick, Sept. 18, 1952)

Lattice	Gold : cadmium ratios	Indium : cadmium ratios
1.5 : 1	1.918 ± 0.052	2.576 ± 0.014
2 : 1	$2.292 \pm .038$	$3.044 \pm .16$
3 : 1	$2.884 \pm .025$	$4.30 \pm .033$
4 : 1	$3.307 \pm .045$	$5.742 \pm .092$

Table 1.5.31 — Slightly Enriched Lattices with B Poisoning
(Communication from J. Chernick, Sept. 18, 1952)

Lattice	Boron concentration, B atoms/ 10^3 H ₂ O molecules	Buckling $\times 10^3$, cm ⁻²	Reflector saving, cm
1.5 : 1	0.216	2.164 ± 0.082	7.61 ± 0.18
1.5 : 1	.563	$1.107 \pm .217$	$7.61 \pm .46$
1.5 : 1	.860	$0.243 \pm .05$	$7.75 \pm .46$
2 : 1	.359	$2.045 \pm .255$	$7.45 \pm .67$
2 : 1	.590	$1.272 \pm .314$	$7.11 \pm .78$
2 : 1	.824	$0.326 \pm .094$	$7.32 \pm .22$
3 : 1	.174	$2.086 \pm .052$	$6.79 \pm .20$
3 : 1	.345	$1.137 \pm .057$	$6.37 \pm .19$
3 : 1	.512	$0.019 \pm .049$	$6.59 \pm .17$
4 : 1	.074	$1.103 \pm .050$	$7.16 \pm .24$
4 : 1	.146	$0.596 \pm .067$	$6.60 \pm .30$
4 : 1	.218	$-.054 \pm .070$	$6.81 \pm .32$

Table 1.5.32 — Description of Natural-U Lattices in Water
(CP-2842)

Lattice	Description	Cell type	V_{H_2O}/V_U	V_{A1}/V_U	r_0 , cm
1	Vert. rods, no gap	Sq.	1.14	0	1.50
2	Vert. rods, no gap	Sq.	3.27	0	1.50
3	Horiz. stacked slugs	Sq.	0.27	0	1.40
4	Vert. rods, no gap	Hex.	1.78	0	1.50
5	Vert. rods, no gap	Hex.	3.17	0	1.50
6	Slugs in vert. tubes	Hex.	2.06	0.140	1.40
7	Vert. rods, no gap	Hex.	1.36	0	1.50
9	Slugs, cork spacer gap	Hex.	1.60	0.140	1.40
10	Slugs, cork spacer gap	Hex.	1.70	.140	1.40
11	Slugs in tubes, no gap	Hex.	1.42	.140	1.40
12	Slugs in tubes, no gap	Hex.	1.57	.140	1.40
13	Slugs in tubes, air gap	Hex.	1.92	.346	1.40
14	Slugs in tubes, air gap	Hex.	1.56	.346	1.40
16	Small rods, no gap	Hex.	1.80	0	1.00
17	Small rods, air gap	Hex.	2.01	0.247	1.00
18	Small rods, no gap	Hex.	1.50	0	1.00
19	Small rods, no gap	Hex.	2.10	0	1.00

Table 1.5.33 — Natural-U Lattices in Water
(CP-2842)

Lattice	$\delta\Delta/\delta T$	$\Delta \times 10^{16}$, cm ⁻² corrected		L^2 , cm ²		τ , cm ²		$k_{corrected}$	
		25°C	100°C	25°C	100°C	25°C	100°C	25°C	100°C
1	1.65	478	602	2.5	2.8	54.7	57.8	0.973	0.964
2	-14.6	4018	2321	3.4	3.7	39.9	42.6	.840	.898
3	23.0	6568	8293	2.2	2.4	131.0	133.0	.417	.325
4	-1.41	370	264	2.8	3.1	44.0	50.2	.983	.986
5	-8.10	3452	2844	3.4	3.7	40.1	43.0	.860	.875
6	-3.05	637	429	2.9	3.2	44.9	47.9	.970	.978
7	0.0	126	129	2.6	2.9	51.7	54.7	.993	.993
9	-2.75	84	-13	2.7	3.0	48.8	51.9	.996	1.007
10	-5.32	265	-13	2.8	2.1	47.8	51.1	.987	1.007
11	0.34	188	218	2.6	2.9	51.0	54.0	.990	0.988
12	-.46	297	268	2.7	3.0	49.2	52.2	.985	.985
13	.89	20	120	6.0	6.6	94.5	103.0	.998	.987
14		-27		6.1	6.7	112.0	121.0	1.003	
16		278		2.8	3.1	48.4	51.7	0.986	
17	-0.18	0	-8	6.8	7.5	110.0	120.0	1.000	1.001
18	2.50	660	848	2.7	3.0	51.5	54.7	0.965	0.952
19		329		2.9	3.2	46.5	49.3	.984	

Table 1.5.34—Resonance Absorption Integrals
(S. P. Harris, C. O. Muehlhause, and G. E. Thomas, Phys. Rev., 79, 1950)

Isotope	Observed cadmium ratio	Thermal- activation cross section			$\Sigma_{1/v}, \dagger$ barns	Σ_a, \ddagger barns	Source of σ_{th}	10^{-24} Nuclei per cm^2 (isotopic)	Chemical form used in experiment
		Σ_a^1/σ_{th}	(σ_{th}) , barns	$\Sigma_a^1, *$ barns					
$^{23}_{11}\text{Na}$	70.3	~0.4	0.52	~0.21	~0.21	~0	§	7.4×10^{-5}	NaF
$^{27}_{13}\text{Al}$	43.1	~.65	.22	~.14	~.09	~0.05	§	2.9×10^{-4}	Al
$^{31}_{15}\text{P}$	63.8	~.44	.23	~.10	~.09	~0.01	¶	3.1×10^{-4}	P
$^{45}_{21}\text{Sc}$	69.0	~.4	31.6	~12.6	~12.6	~0	§	2.6×10^{-5}	Sc_2O_3
$^{51}_{23}\text{V}$	70.6	~.4	4.93	~2.0	~2.0	~0	§	2.1×10^{-5}	V_2O_5
$^{55}_{25}\text{Mn}$	35	~.81	12.1	~9.8	~4.8	~5	§	6.5×10^{-5}	Mn
$^{59}_{27}\text{Co}$	23.8	1.20	34.3	41.2	13.7	27.5	§	6.1×10^{-5}	Co
$^{63}_{29}\text{Cu}$	30.8	0.92						1.4×10^{-4}	Cu
$^{65}_{29}\text{Cu}$	30.5	.93	3.62	3.35	1.45	1.90	§	6.0×10^{-5}	Cu
$^{69}_{31}\text{Ga}$	5.79	5.72	1.40	8.01	0.56	7.45	¶	3.1×10^{-5}	Ga_2O_3
$^{71}_{31}\text{Ga}$	7.96	3.94	3.36	13.2	1.3	11.9	¶	2.0×10^{-5}	Ga_2O_3
$^{75}_{33}\text{As}$	4.36	8.15	3.87	31.5	1.6	29.9	§	6.0×10^{-5}	As
$^{79}_{35}\text{Br}$	3.25	12.2	10.9	133	4	129	¶	1.0×10^{-5}	PbBr_2
$^{89}_{39}\text{Y}$	47.9	0.58	1.24	0.72	0.50	0.22	¶	4.1×10^{-5}	Y_2O_3
$^{93}_{41}\text{Nb}$	9.59	3.19	1.31	4.19	.52	3.67	§	2.5×10^{-5}	Nb_2O_5
$^{103}_{45}\text{Rh}$	7.94	3.95	149	589	60	529	¶	2.6×10^{-5}	Rh
$^{107}_{47}\text{Ag}$	13.35	2.22	44.3	98.3	17.7	80.6	¶	1.5×10^{-5}	Ag
$^{109}_{47}\text{Ag}$	3.20	12.5	97.0	1213	39	1174	¶	Zero extrapolation	Ag
$^{113}_{49}\text{In}$	2.68	16.3	56.0	913	22	891	¶		In

⁴⁹ In ¹¹⁵	3.26	12.1	196	2372	78	2294	¶	1.5 × 10 ⁻⁶	In
⁵¹ Sb ¹²¹	2.27	21.6	6.8	147	3	144	¶	1.7 × 10 ⁻⁵	Sb
⁵¹ Sb ¹²³	~1.55	~50	2.5	~125	1	~124	¶	1.3 × 10 ⁻⁵	Sb
⁵³ I ¹²⁷	2.45	19.0	6.25	119	3	116	¶	1.3 × 10 ⁻⁵	PbI ₂
⁵⁹ Pr ¹⁴¹	30.9	0.92	10.1	9.3	4.0	5.3	¶	1.8 × 10 ⁻⁵	PrO ₂
⁶² Sm ¹⁵²	3.43	11.3	138	1559	55	1504	¶	4.1 × 10 ⁻⁶	Sm ₂ O ₃
⁶³ Eu ¹⁵¹	45.7	0.61	1380	842	552	290	¶	8.3 × 10 ⁻⁶	Eu ₂ O ₃
⁷² Hf ¹⁸⁰	14.9	1.97	10.0	19.7	4.0	15.7	¶	8.0 × 10 ⁻⁶	HfO ₂
⁷² Hf ¹⁸¹	~3.0	~14	~100	~1400	40	~1360	§	2.3 × 10 ⁻⁵	HfO ₂
⁷³ Ta ¹⁸¹	25.1	25.1	20.6	517	10	507	¶	2.7 × 10 ⁻⁵	Ta
⁷⁴ W ¹⁸⁶	3.93	9.35	34.2	320	14	306	¶	3.1 × 10 ⁻⁷	W
⁷⁵ Re ¹⁸⁵	3.61	10.5	101	1061	40	1021	¶	6.6 × 10 ⁻⁶	Re
⁷⁵ Re ¹⁸⁷	8.50	3.65	75.3	275	30	245	¶	1.1 × 10 ⁻⁵	Re
⁷⁷ Ir ¹⁹¹	9.37	3.27	1000	3270	400	2870	¶	6.9 × 10 ⁻⁶	Ir
⁷⁷ Ir ¹⁹³	3.89	9.48	128	1213	51	1162	¶	1.1 × 10 ⁻⁵	Ir
⁷⁹ Au ¹⁹⁷	2.91	14.35	93	1337	37	1296	Wattenberg	5.0 × 10 ⁻⁷	Au
⁸¹ Tl ²⁰³	3.59	10.6	~12	127	~5	122	§	3.0 × 10 ⁻⁵	Tl
⁸¹ Tl ²⁰⁵	7.12	4.48	~0.17	0.76	~0.07	~0.69	§	7.3 × 10 ⁻⁵	Tl

* The sum of Σ_a and $\Sigma_{1/v}$; accurate to about 5 percent

† The cross section for absorption which takes place at energies above the Cd cut-off (~0.6 eV) in a non-resonance region is defined

as $\Sigma_{1/v} = \int_{\text{non-resonance}} \sigma_a dE/E$; accurate to 10–20 percent

‡ The resonance absorption integral, $\int \sigma_a dE/E$; the integration extends over an energy region in the neighborhood of the resonance energy; accurate to 10–20 percent

§ Unpublished work of Harnes, Muehlhause, Rasmussen, Schroeder, and Thomas

¶ Seren, Friendlander, and Turkel, Phys. Rev., 72, 1947

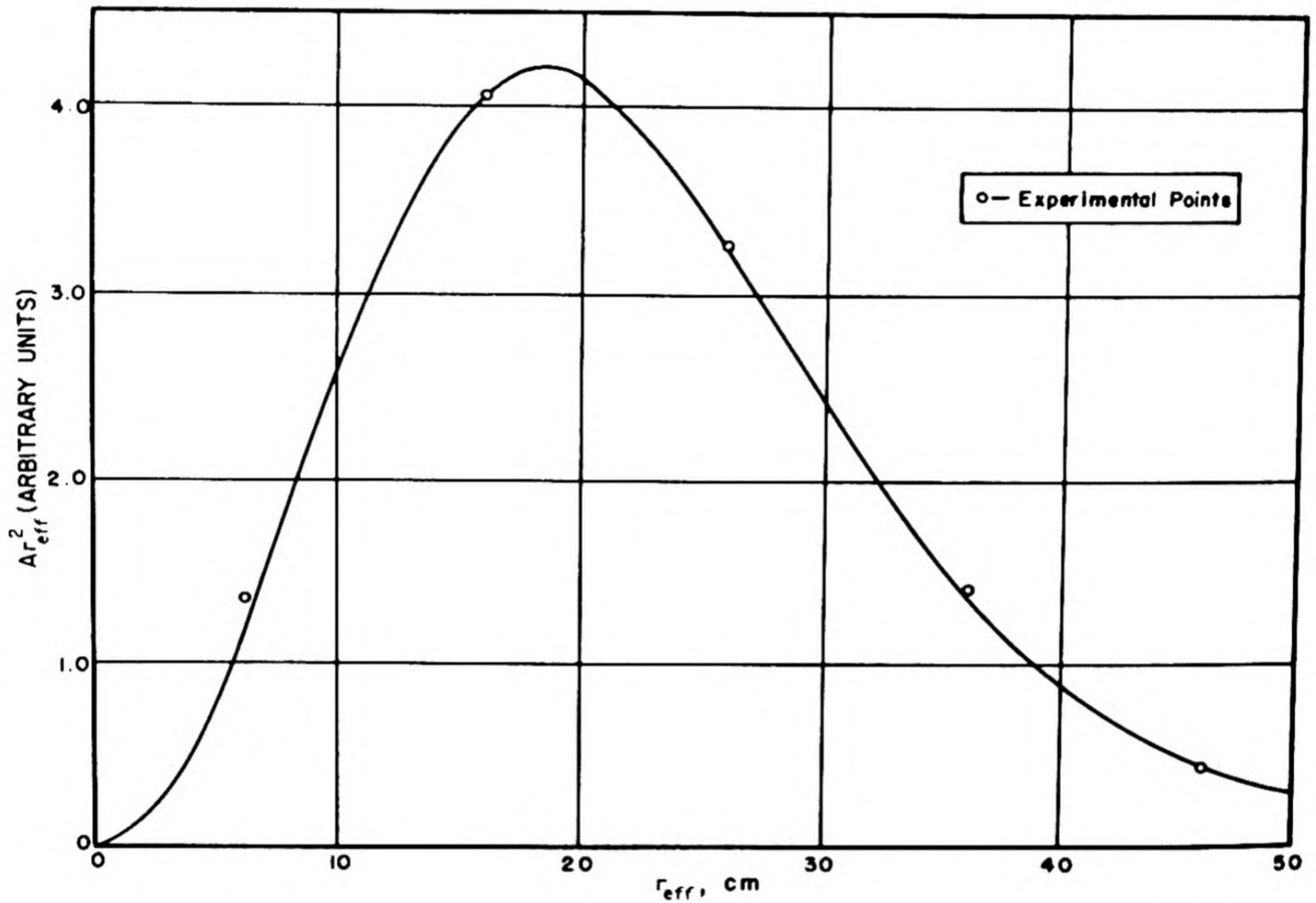


Fig. 1.5.1 — Slowing-down Distribution in D_2O . Reprinted from CP-3453, 1946. The ordinate is r^2 times the number of fission neutrons slowed to 1.4 ev (indium resonance energy). The (theoretical) curve is given by:

$$A(r) = \frac{Ae^{\tau_1/\tau_2}}{8\pi r \tau_2} \left\{ \left[1 + \phi\left(\frac{r}{2\sqrt{\tau_1}} - \sqrt{\frac{\tau_1}{\tau_2}}\right) \right] e^{-r/\sqrt{\tau_2}} - \left[1 - \phi\left(\frac{r}{2\sqrt{\tau_1}} + \sqrt{\frac{\tau_1}{\tau_2}}\right) \right] e^{+r/\sqrt{\tau_2}} \right\}$$

and is plotted for $\tau_1 = 58 \text{ cm}^2$ and $\tau_2 = 48 \text{ cm}^2$. $\phi(x) = \frac{2}{\sqrt{\pi}} \int_0^x e^{-y^2} dy$.

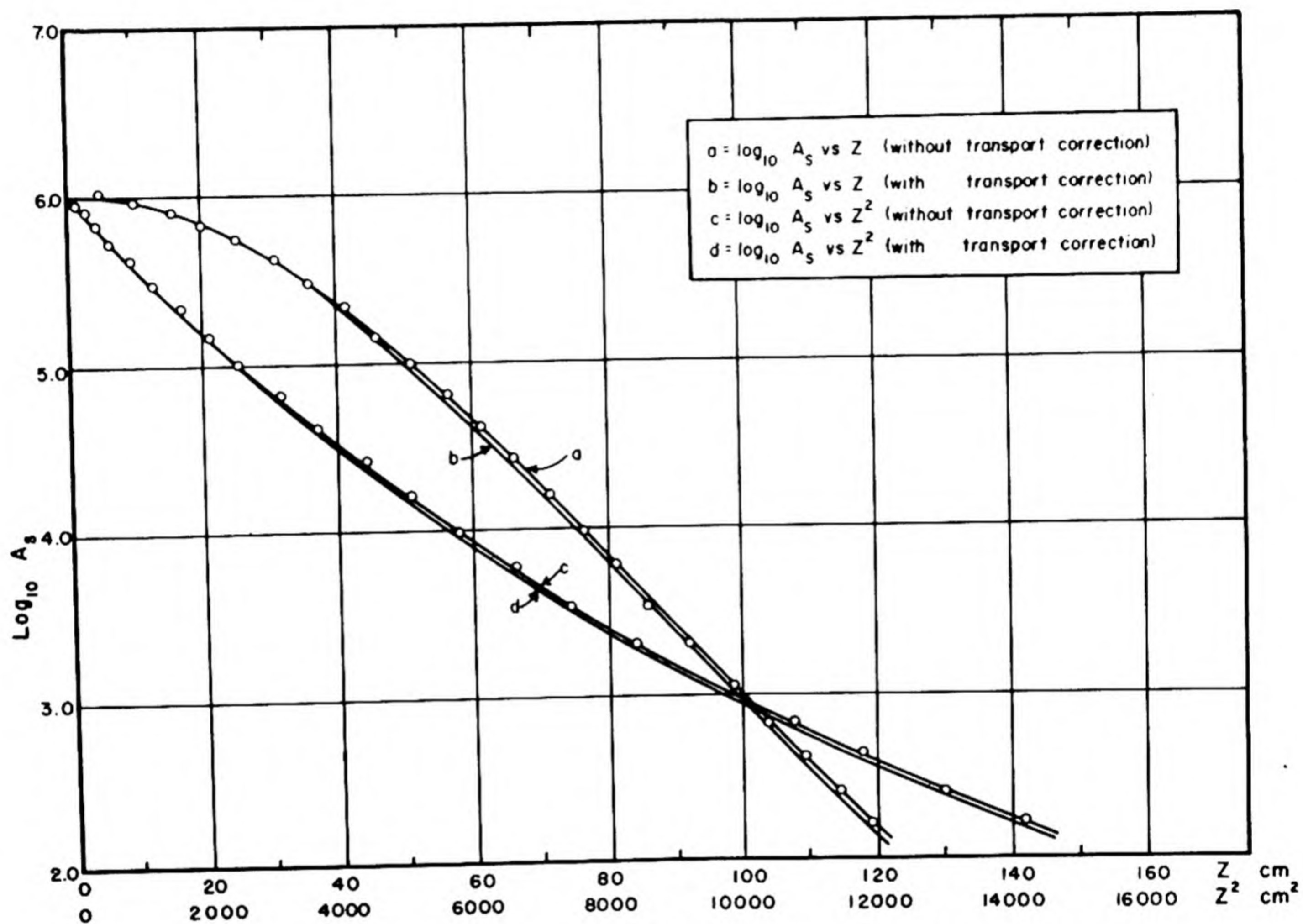


Fig. 1.5.2 — Slowing-down Distribution of Fission Neutrons from a Plane Source in Graphite. Reprinted from ORNL-187, 1949. The ordinate is the logarithm of the number of fission neutrons slowed down to 1.4 ev (indium resonance energy). If the distribution were Gaussian, curves c and d would be straight lines.

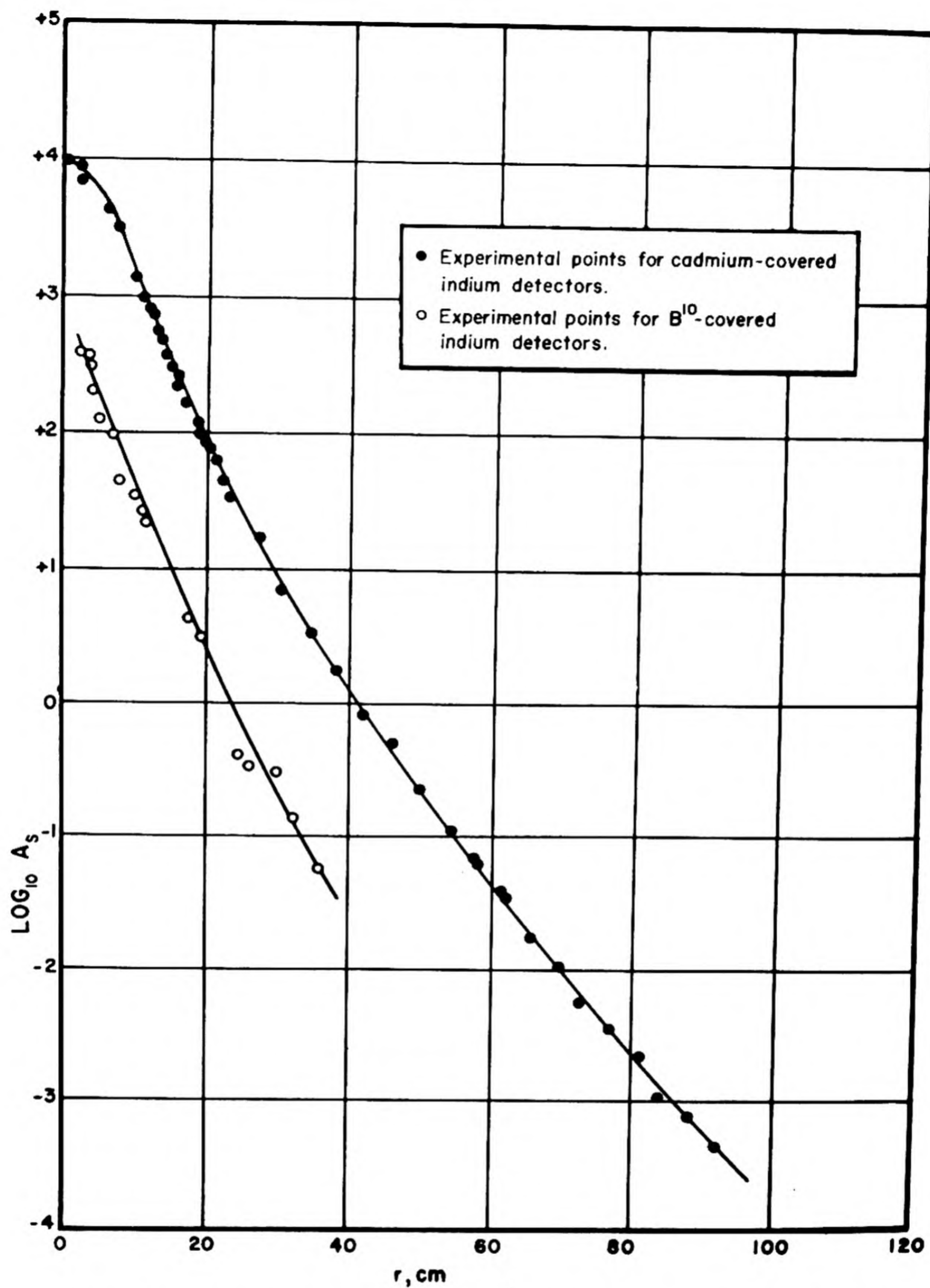


Fig. 1.5.3 — Slowing-down Distribution of Fission Neutrons in Water; Indium Resonance Activity for Point Source. Reprinted from ORNL-181, 1948.

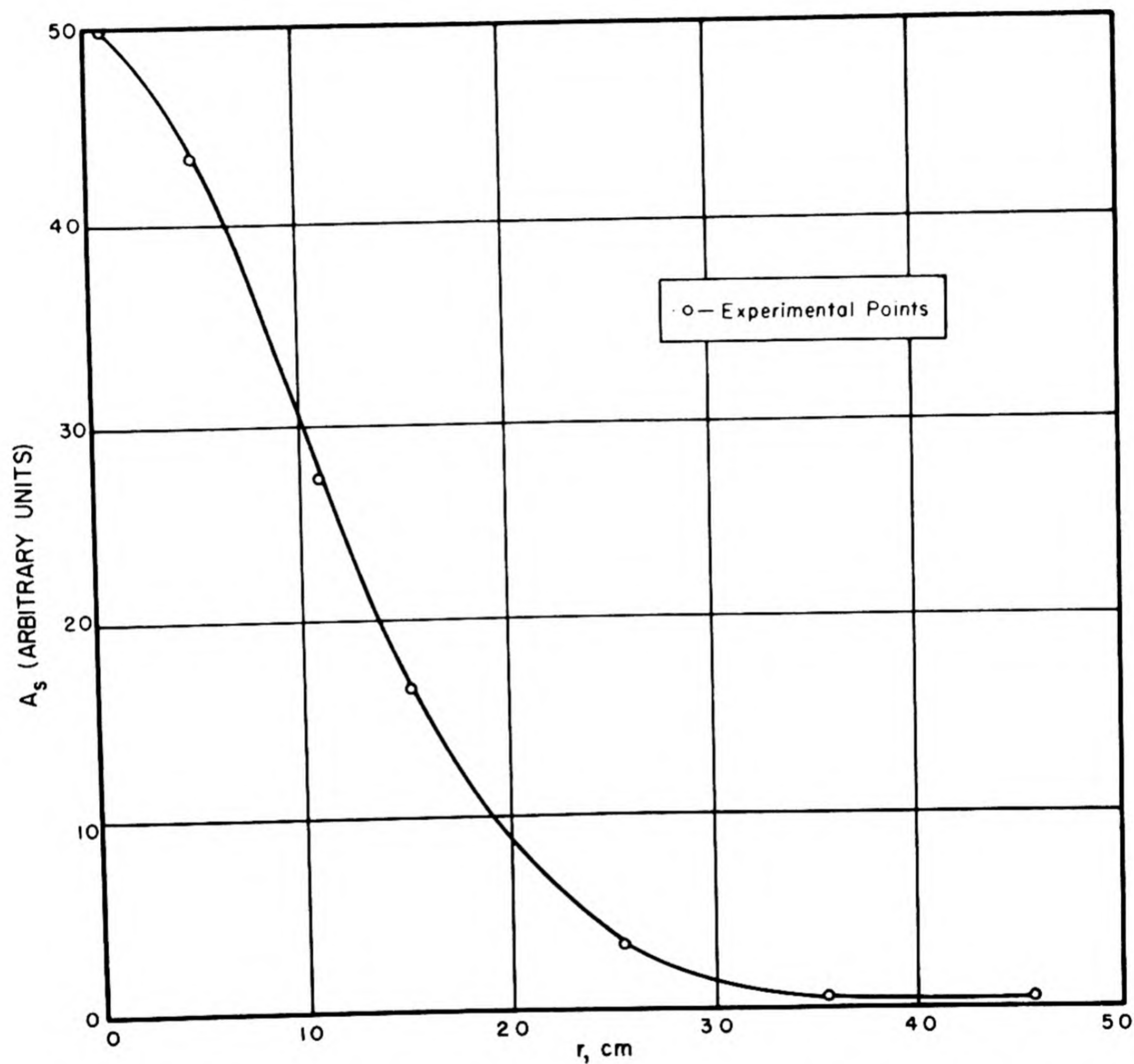


Fig. 1.5.4 — Slowing-down Distribution in Be($\xi = 1.85 \text{ gm/cc}$). Reprinted from ANL-4076, 1947. Indium resonance activity, point fission source.

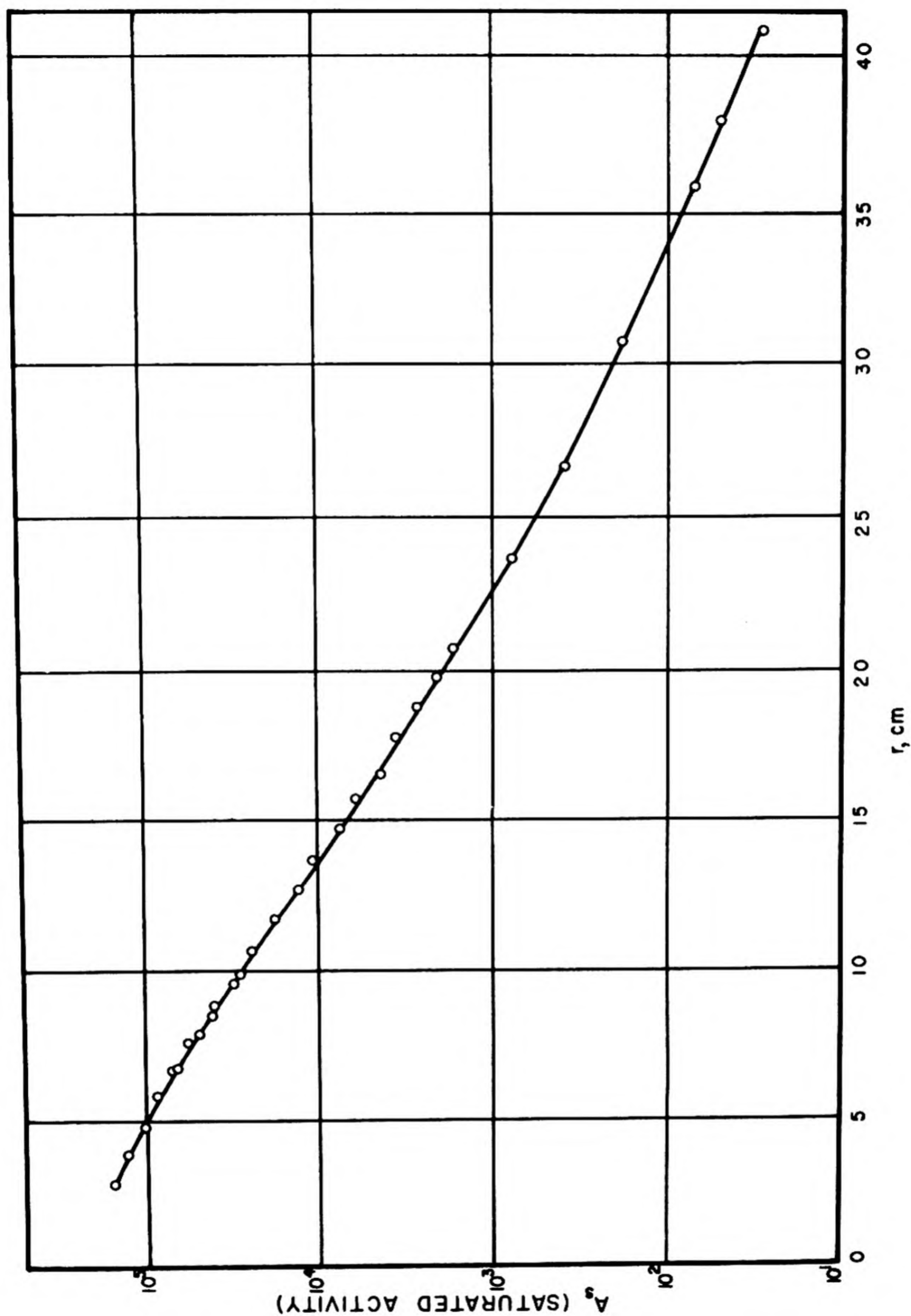


Fig. 1.5.5 — Slowing-down Distribution in Water-Zr Mixture. Reprinted from ORNL-641, 1950. Indium resonance activity, point fission source, 20% Zr by volume, 80% water. Reference also gives distributions from Ra- α -Be source in water and in water-Zr.

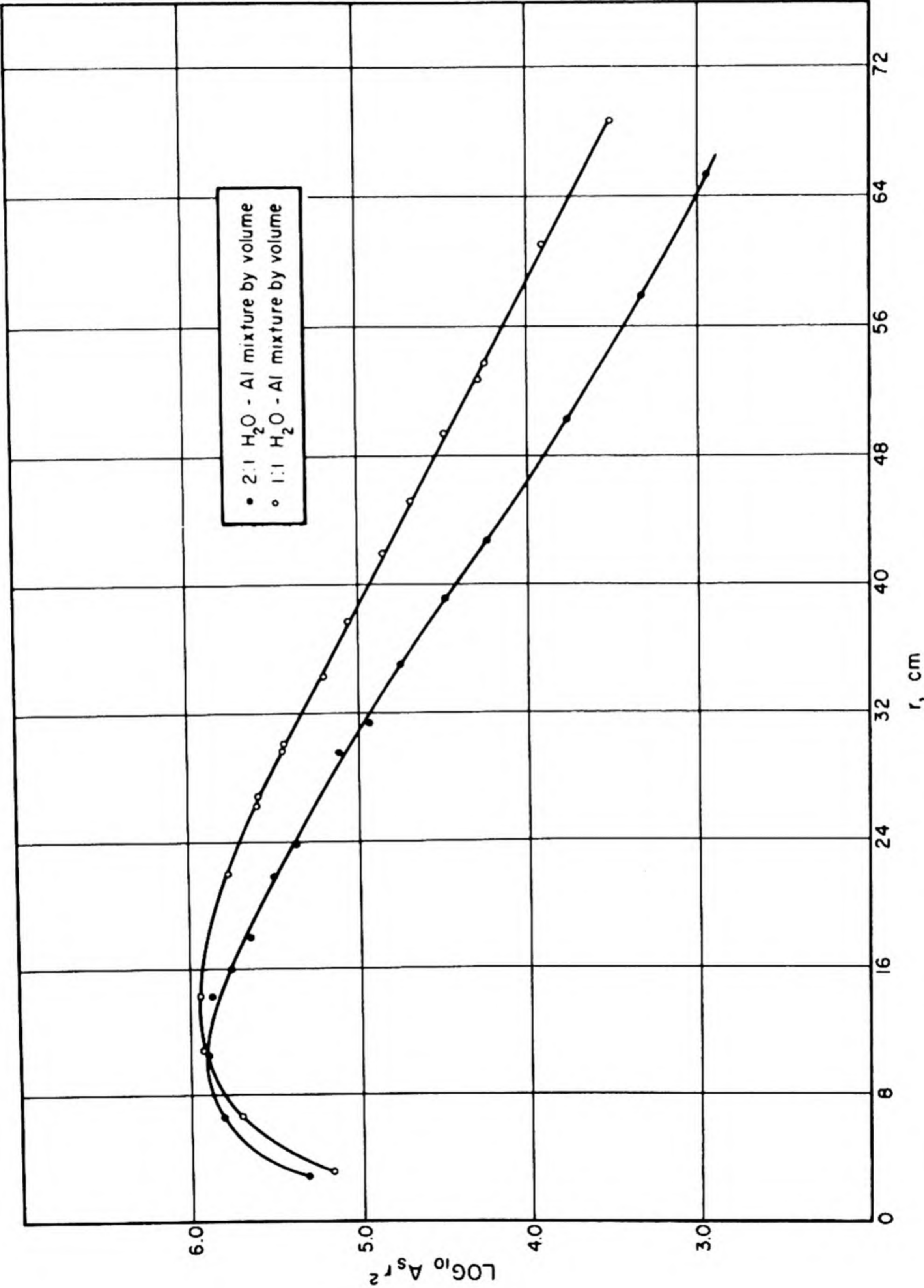


Fig. 1.5.6 — Slowing-down Distribution in Al- H_2O Mixtures. Reprinted from ORNL-294, 1949. Indium resonance activity; point fission source.

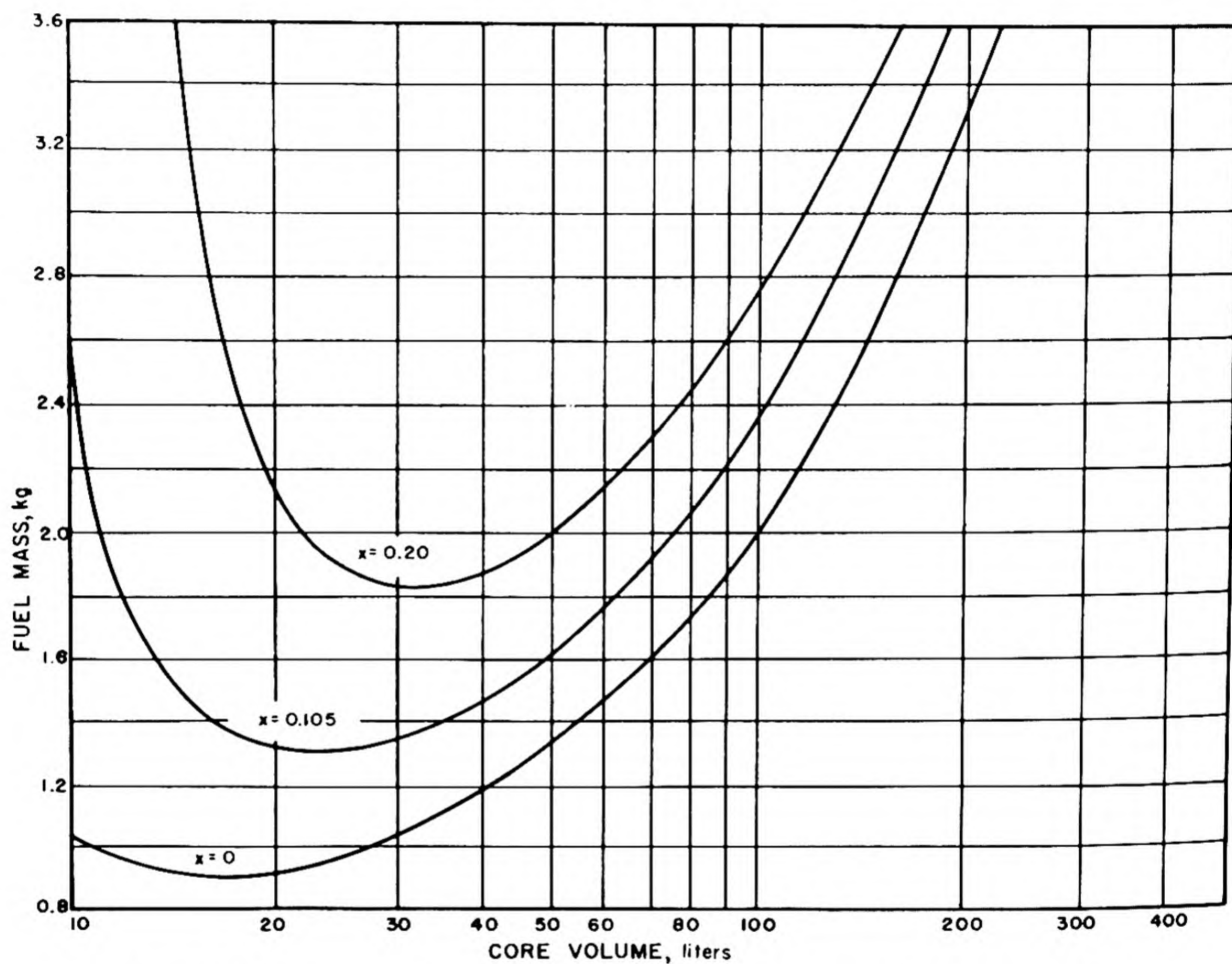
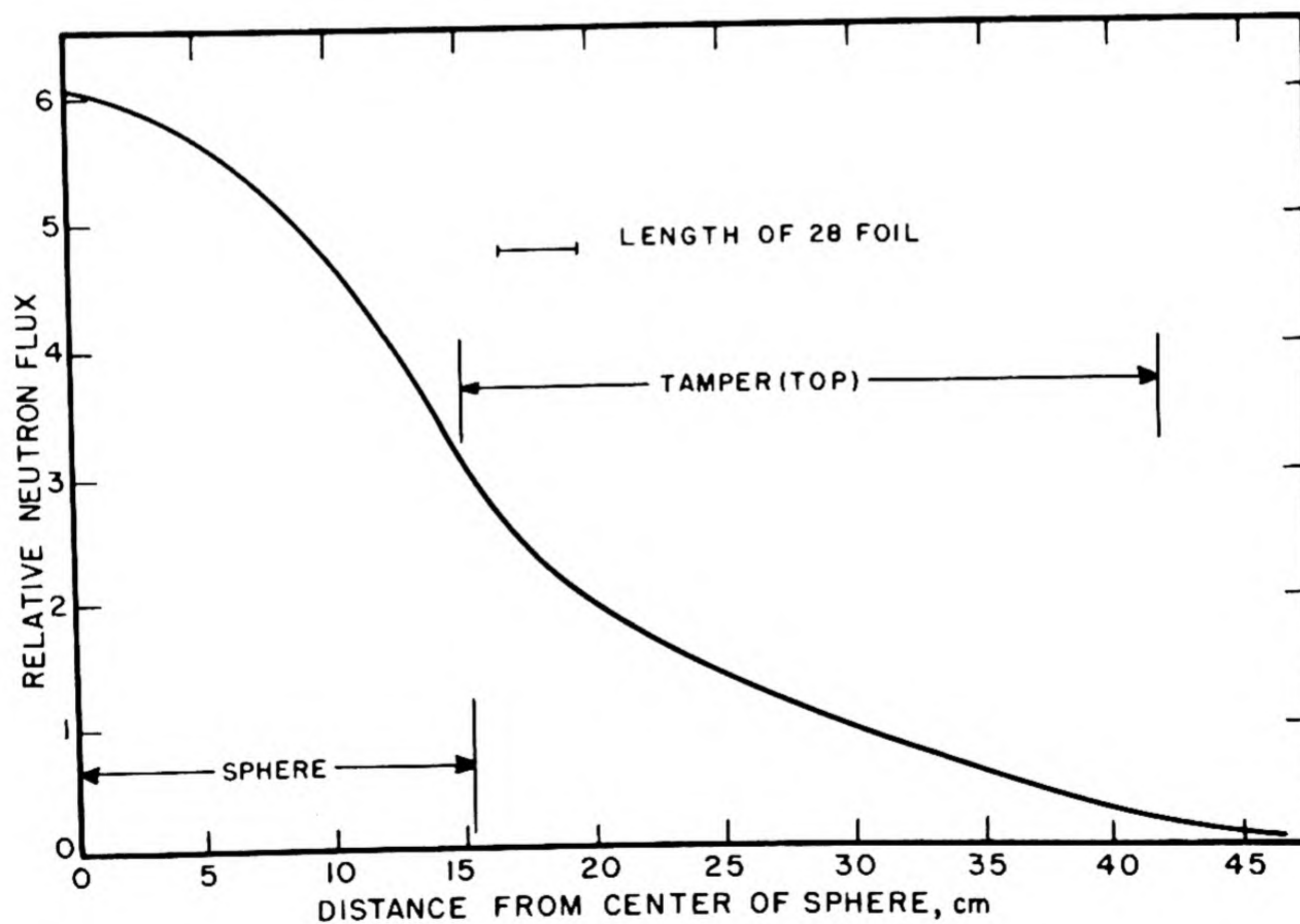
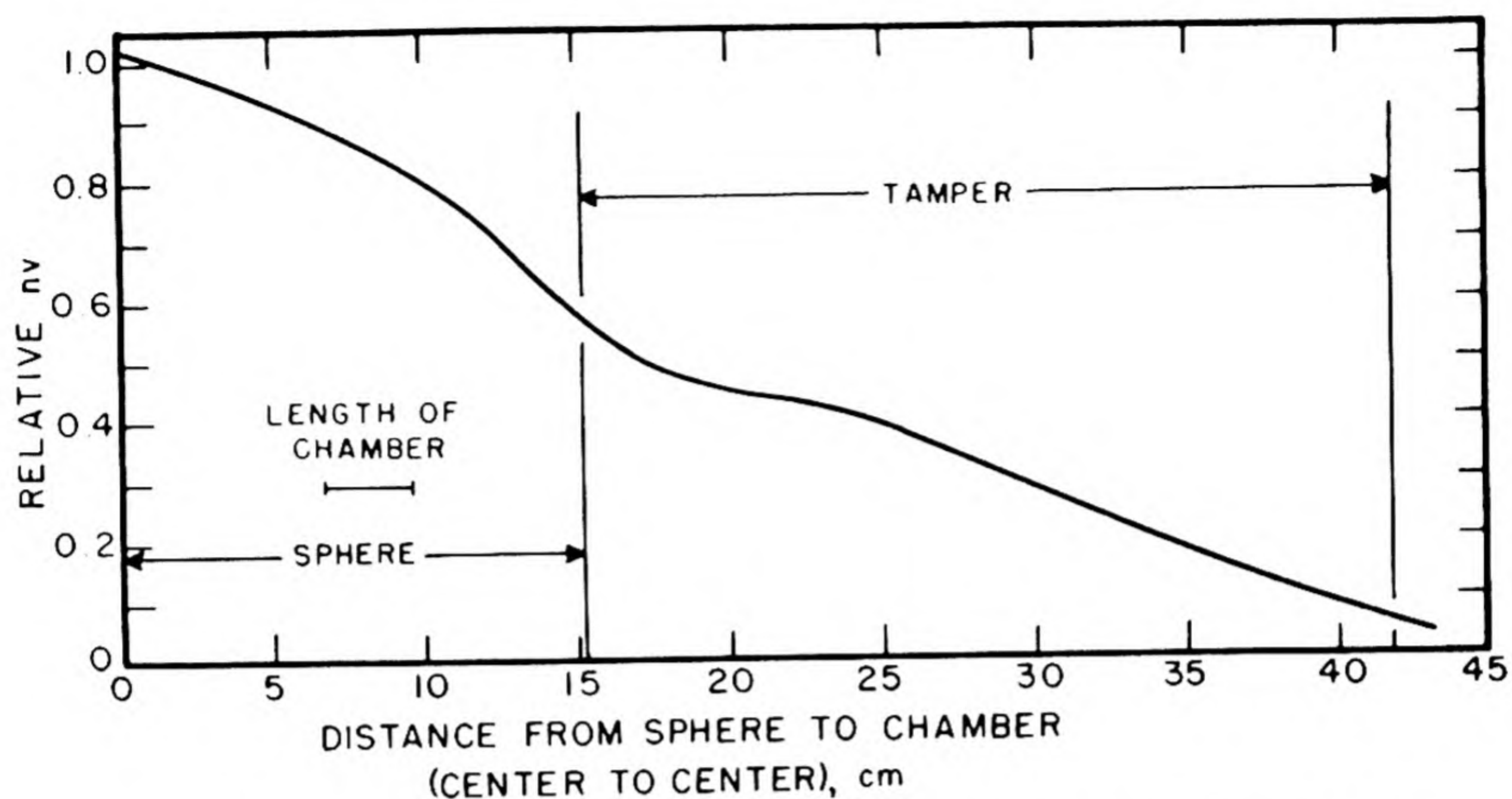


Fig. 1.5.7 — Critical Mass of Water-moderated and Tamped Spheres vs Core Volume for Highly Enriched Fuel. Reprinted from Circle Report II, Jan. 7, 1949. The quantity x is the ratio of the macroscopic poison absorption cross section to the U^{235} absorption cross sections.



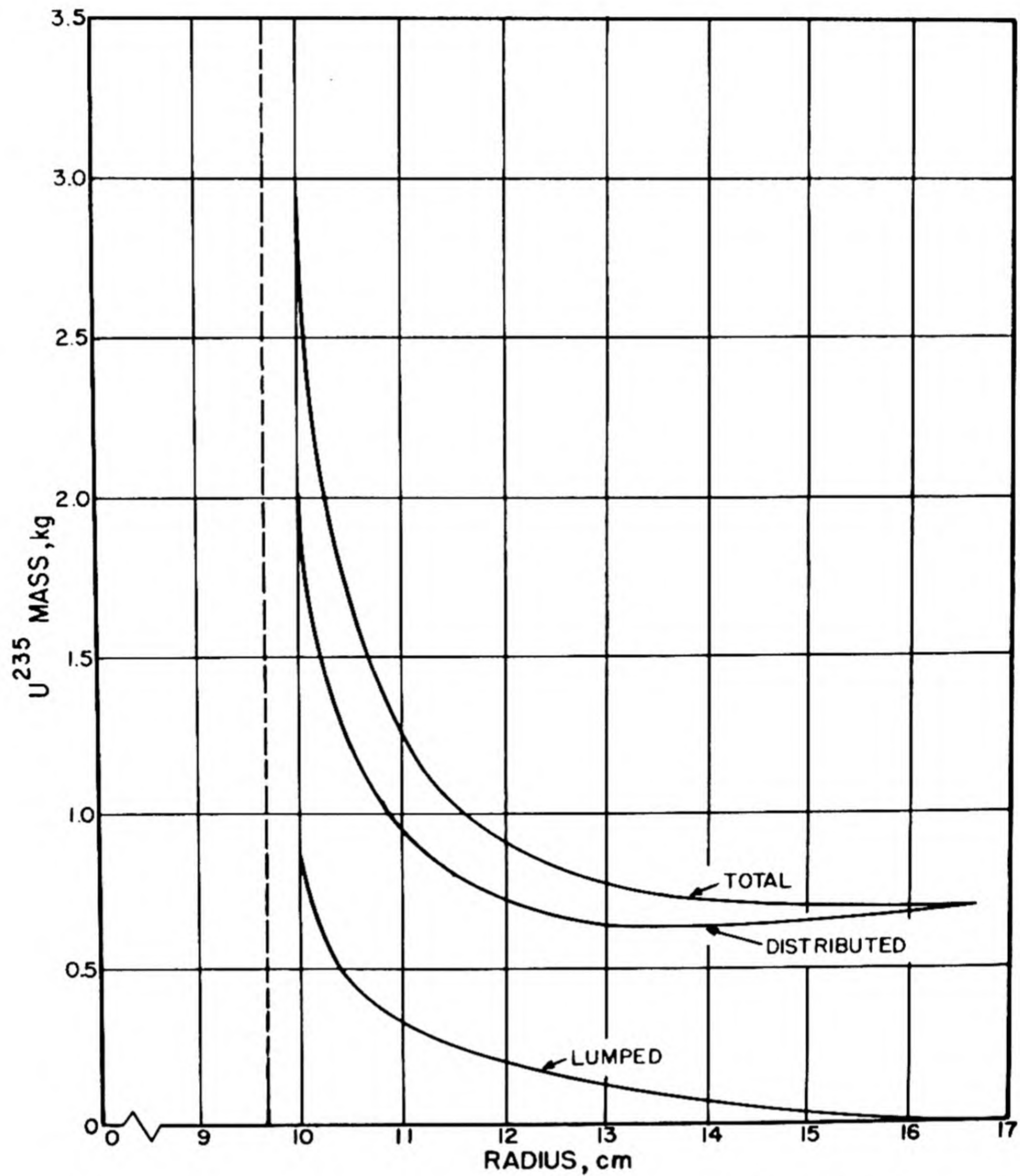


Fig. 1.5.10 — Minimum Critical Mass of a Spherical, U^{235} - H_2O Core with an Infinite Water Tamper vs Core Radius. Reprinted from Jour. Reactor Sci. Tech., April 1952. The middle curve shows the amount of fuel distributed continuously and the bottom one the amount lumped at the core-reflector interface.

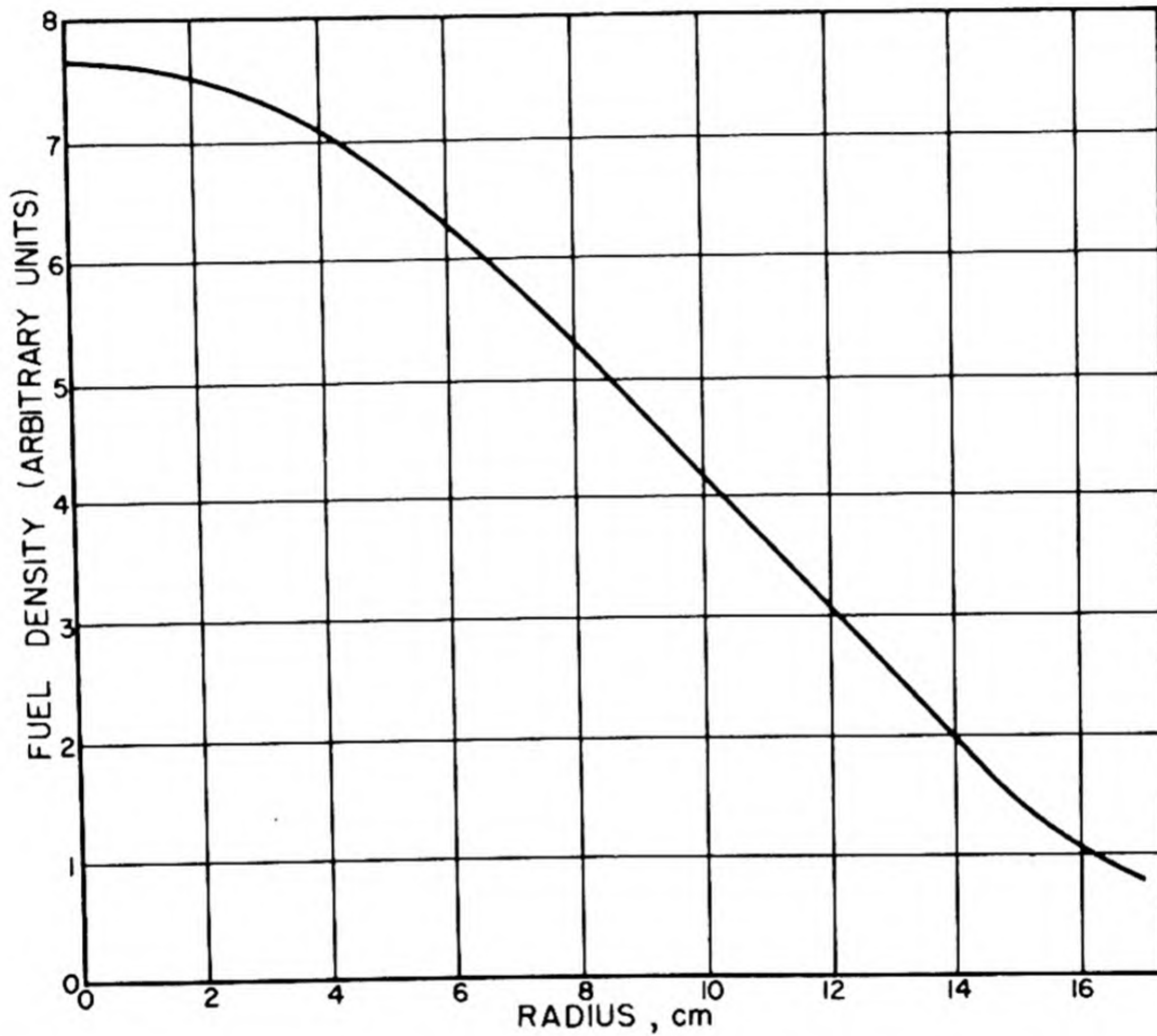


Fig. 1.5.11 — Fuel Distribution which Produces the Least Mass in a Spherical, pure U^{235} - H_2O Core with an Infinite Water Tamper. Reprinted from Jour. Reactor Sci. Tech., April 1952. The least mass occurs for a radius of 16.7 cm.

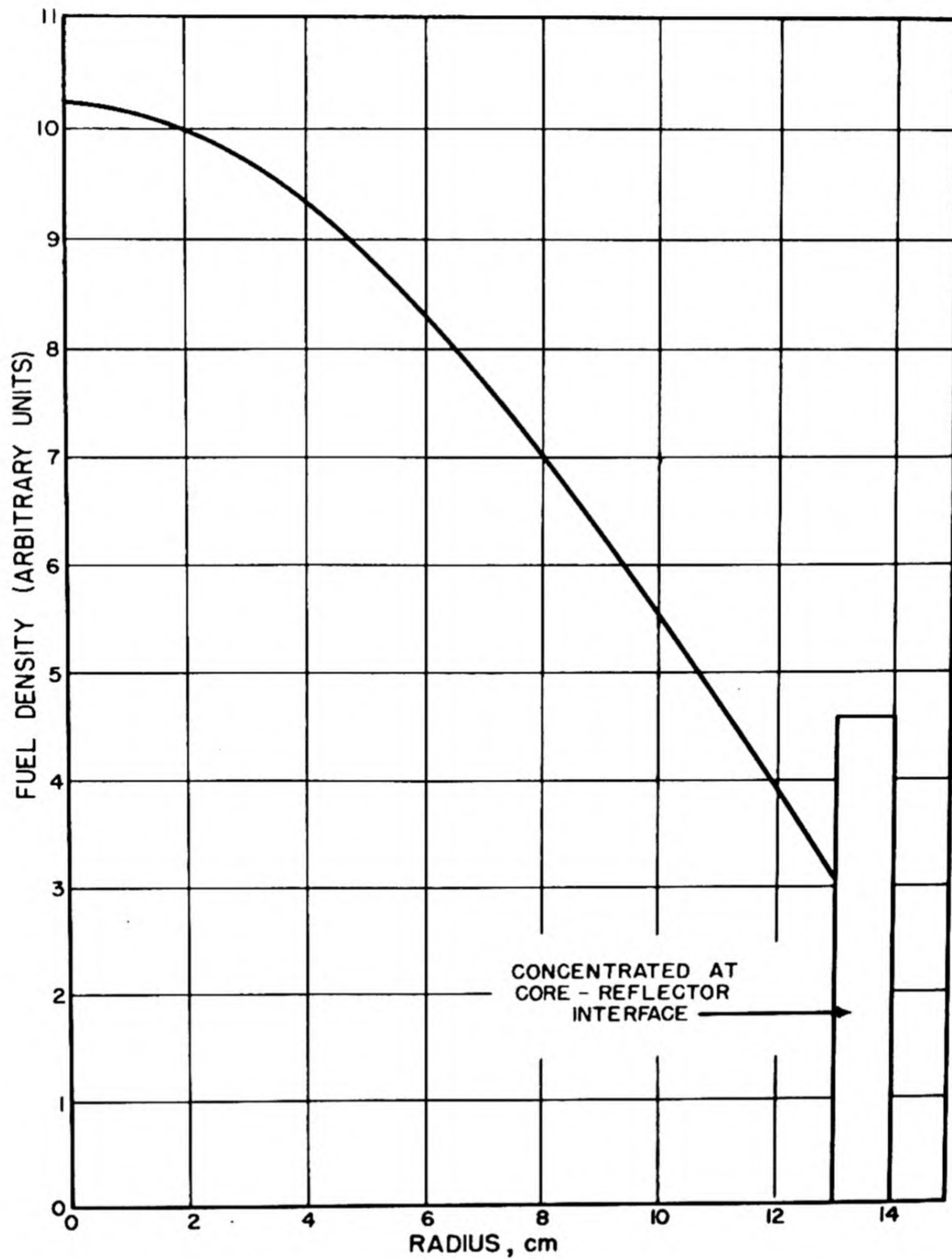


Fig. 1.5.12 — Fuel Distribution which Produces the Minimum Mass in a Spherical, Pure U^{235} - H_2O Core with an Infinite Water Tamper for a Core Radius of 13 cm. Reprinted from Jour. Reactor Sci. Tech., April 1952. This illustrates a case of smaller radius than that yielding the least mass.

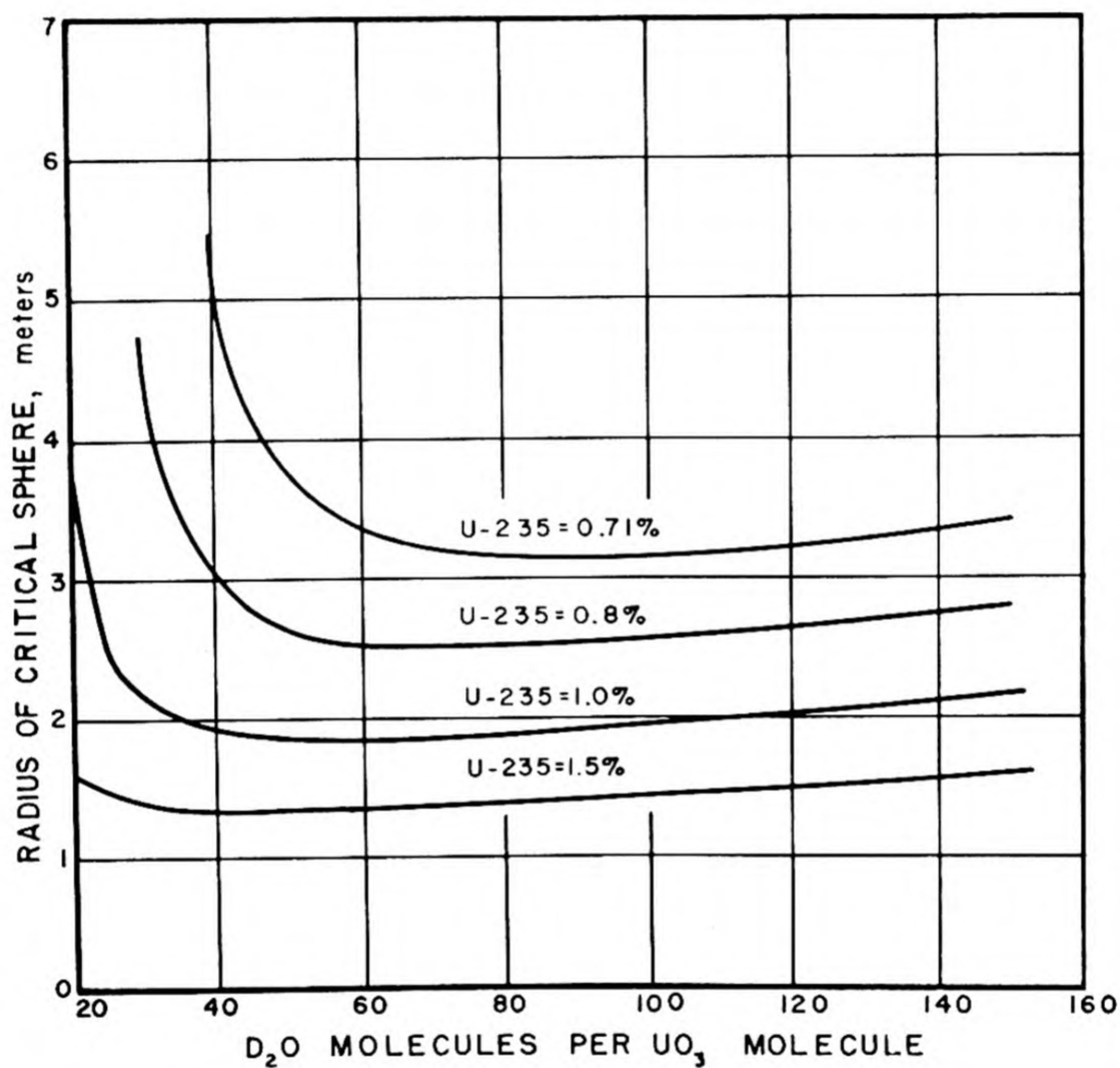


Fig. 1.5.13—Homogeneous D₂O Reactors with Natural or Slightly Enriched Uranium Fuel. Reprinted from ORNL-1096.

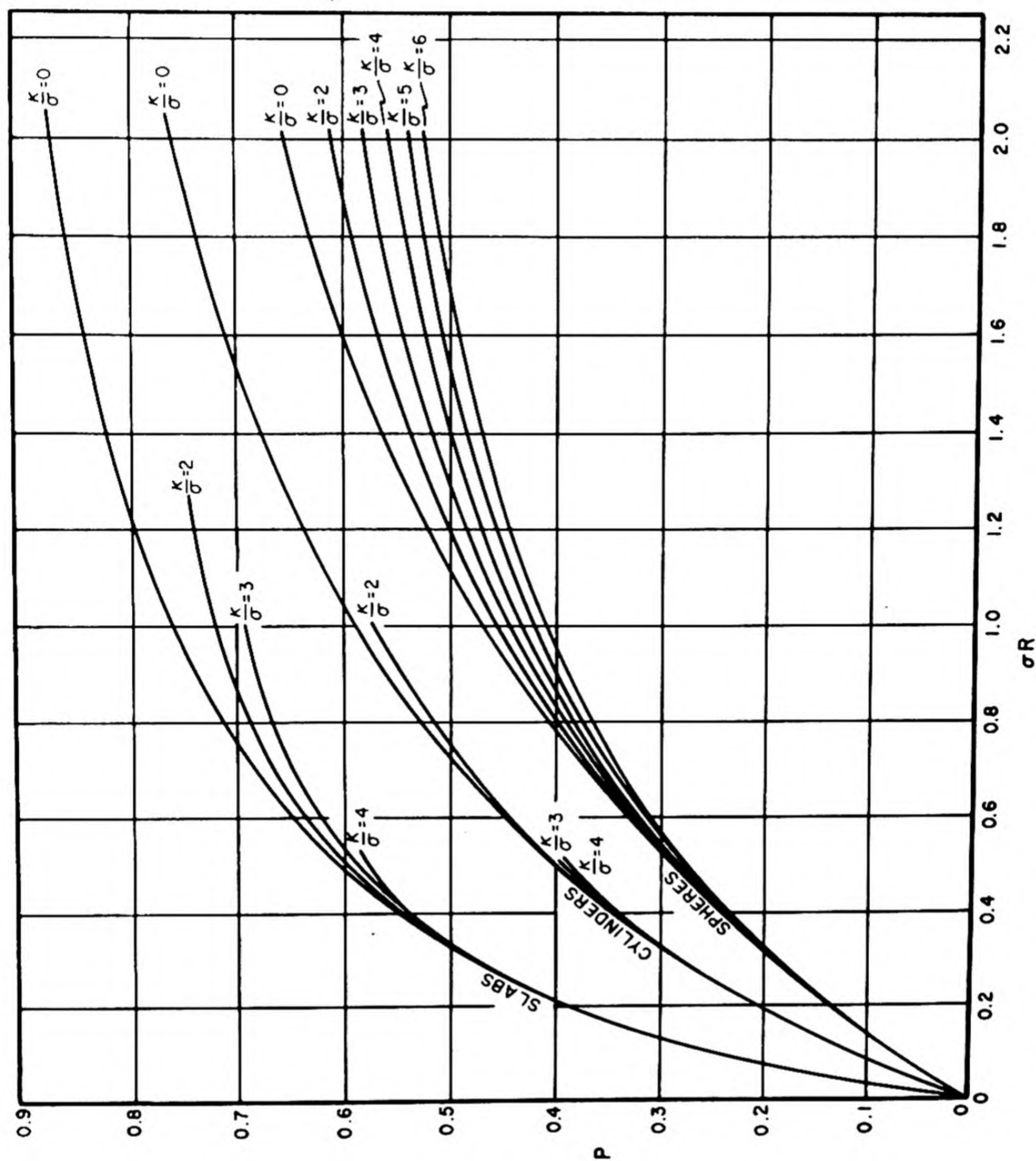


Fig. 1.5.14—Probability of First Flight Collision within a Lump. Reprinted from CP-644. On the graph, σ is the macroscopic total cross section, $N\sigma_t$ For spheres and cylinders, R is the radius; for slabs it is the half thickness.

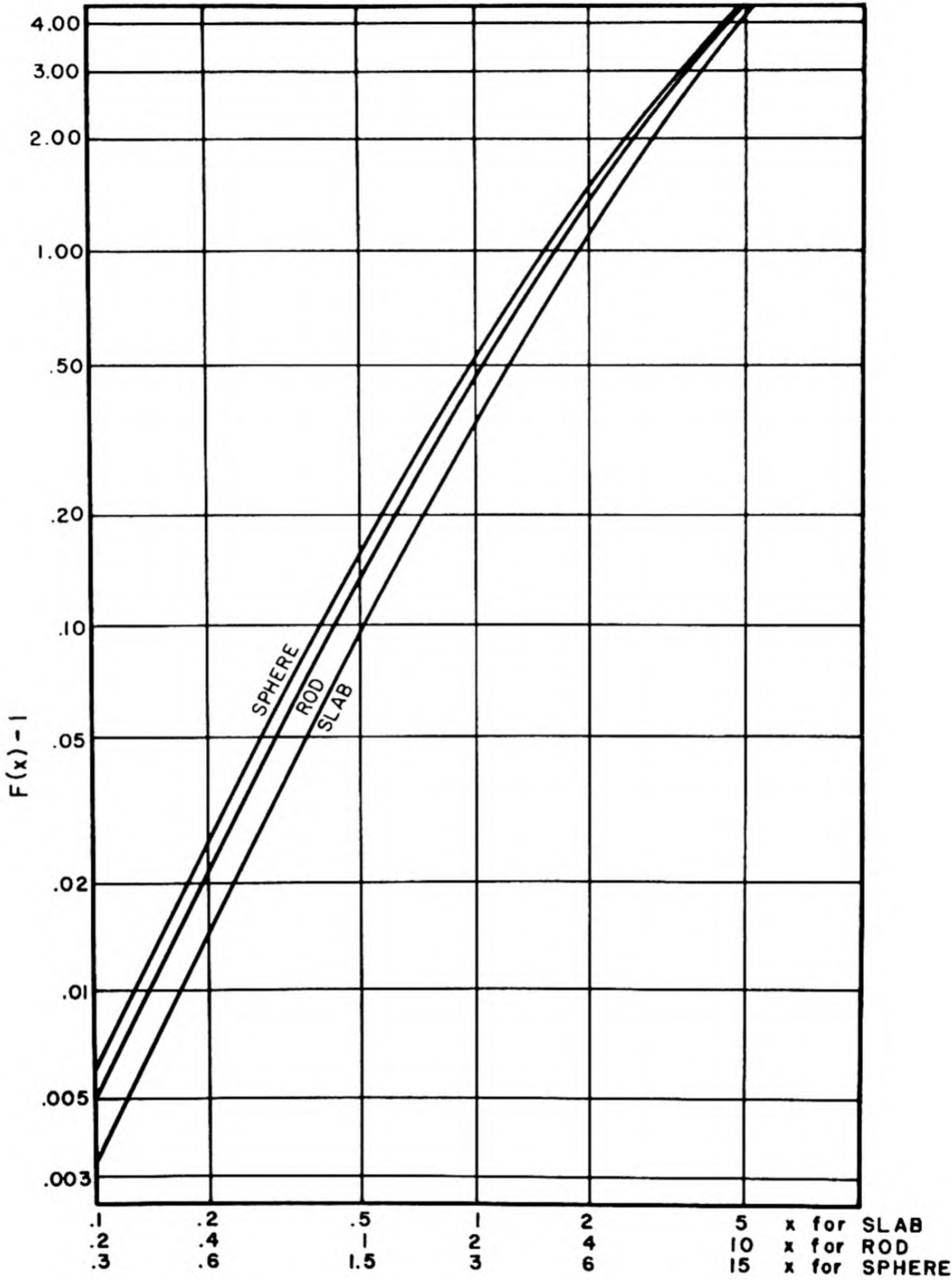


Fig. 1.5.15 — Values of F for Lattice Calculations. Reprinted from CL-697.

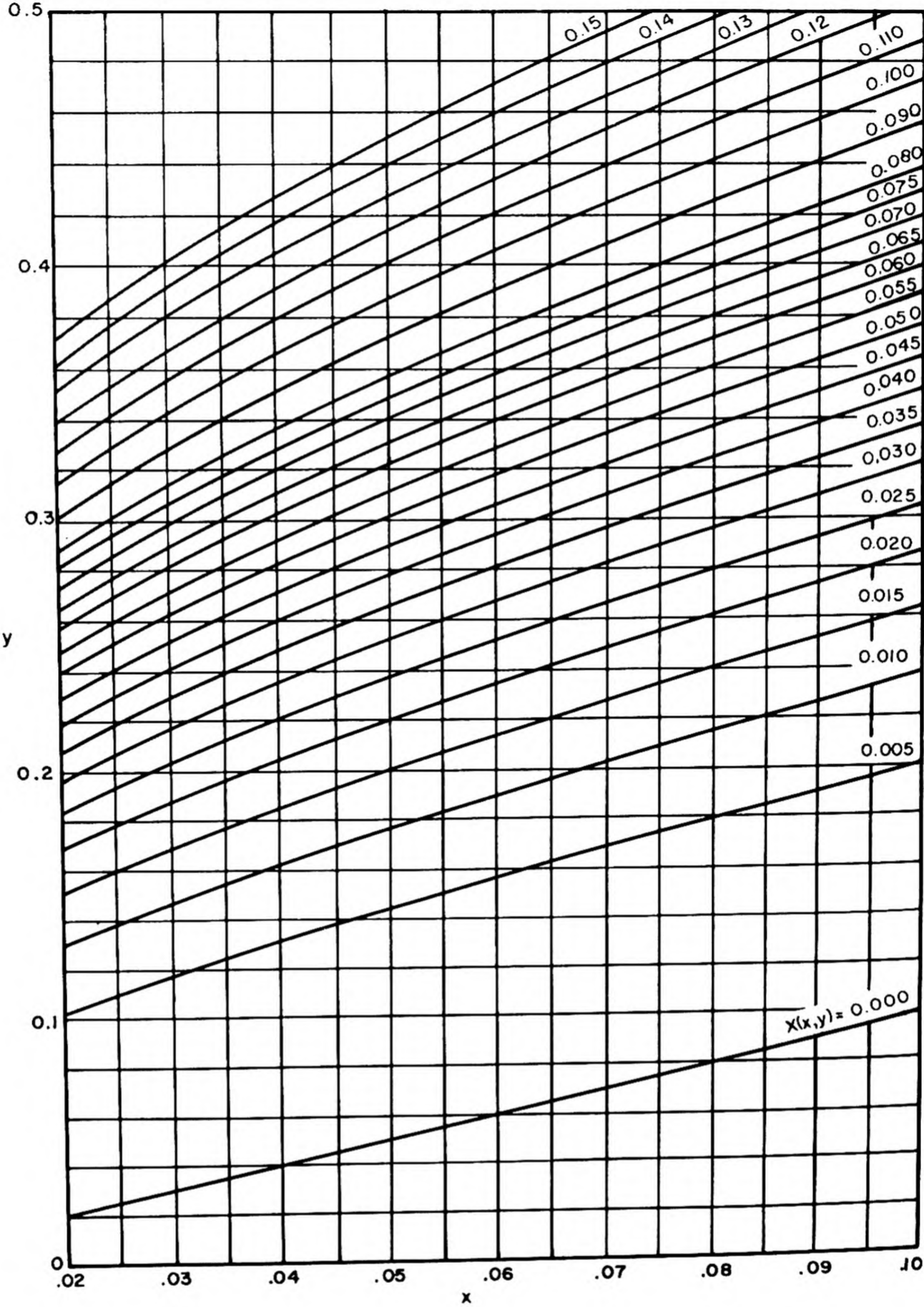


Fig. 1.5.16—Contours of $X(x,y)$ for Thermal Lattice Calculations. Reprinted from TPI-20(u).

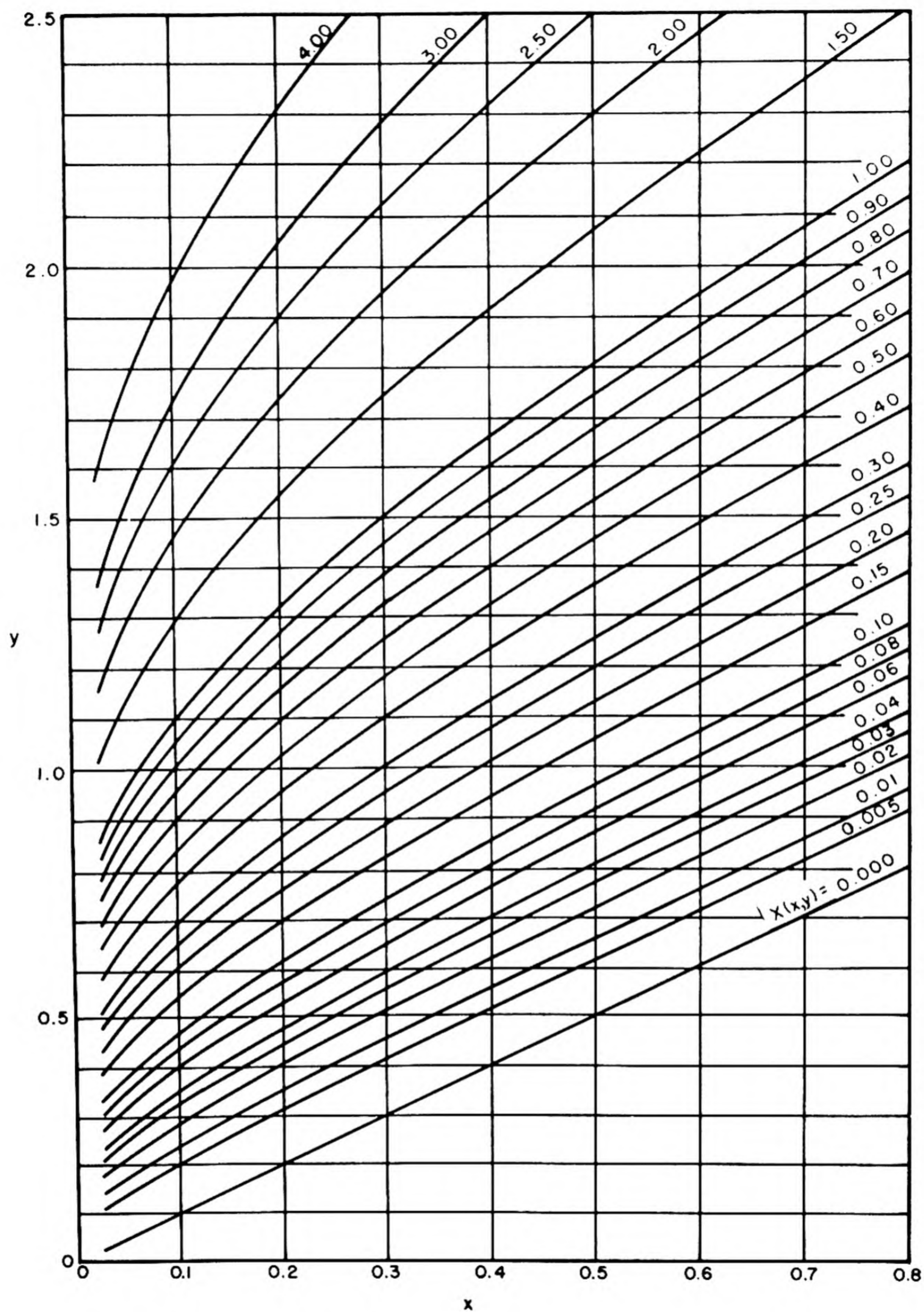


Fig. 1.5.17 — Contours of $X(x,y)$ for Resonance Lattice Calculations. Reprinted from TPI-20 (u).

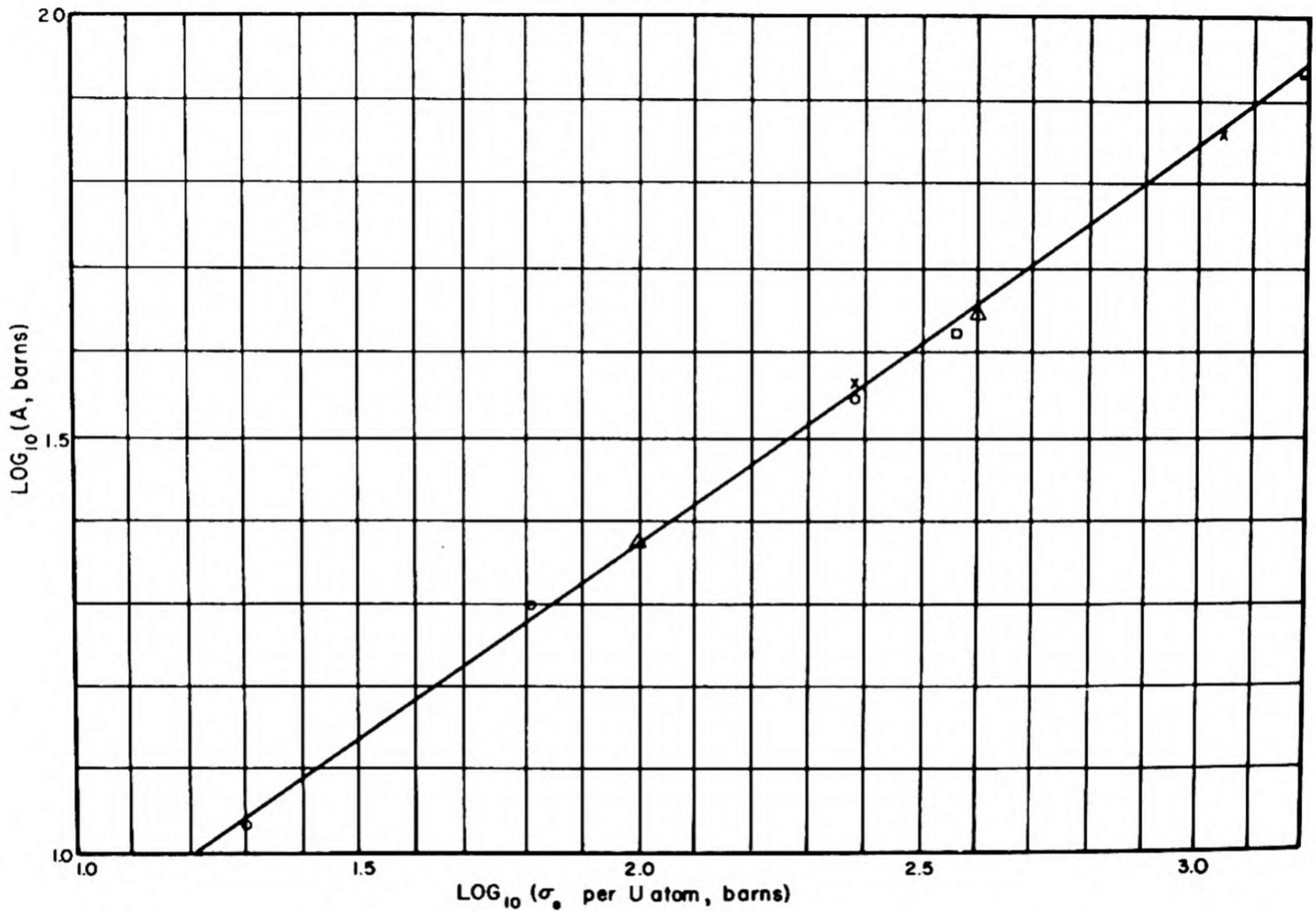


Fig. 1.5.18 — Effective Resonance Integral for U. Reprinted from Weinberg and Noderer, ORNL-51-5-98.

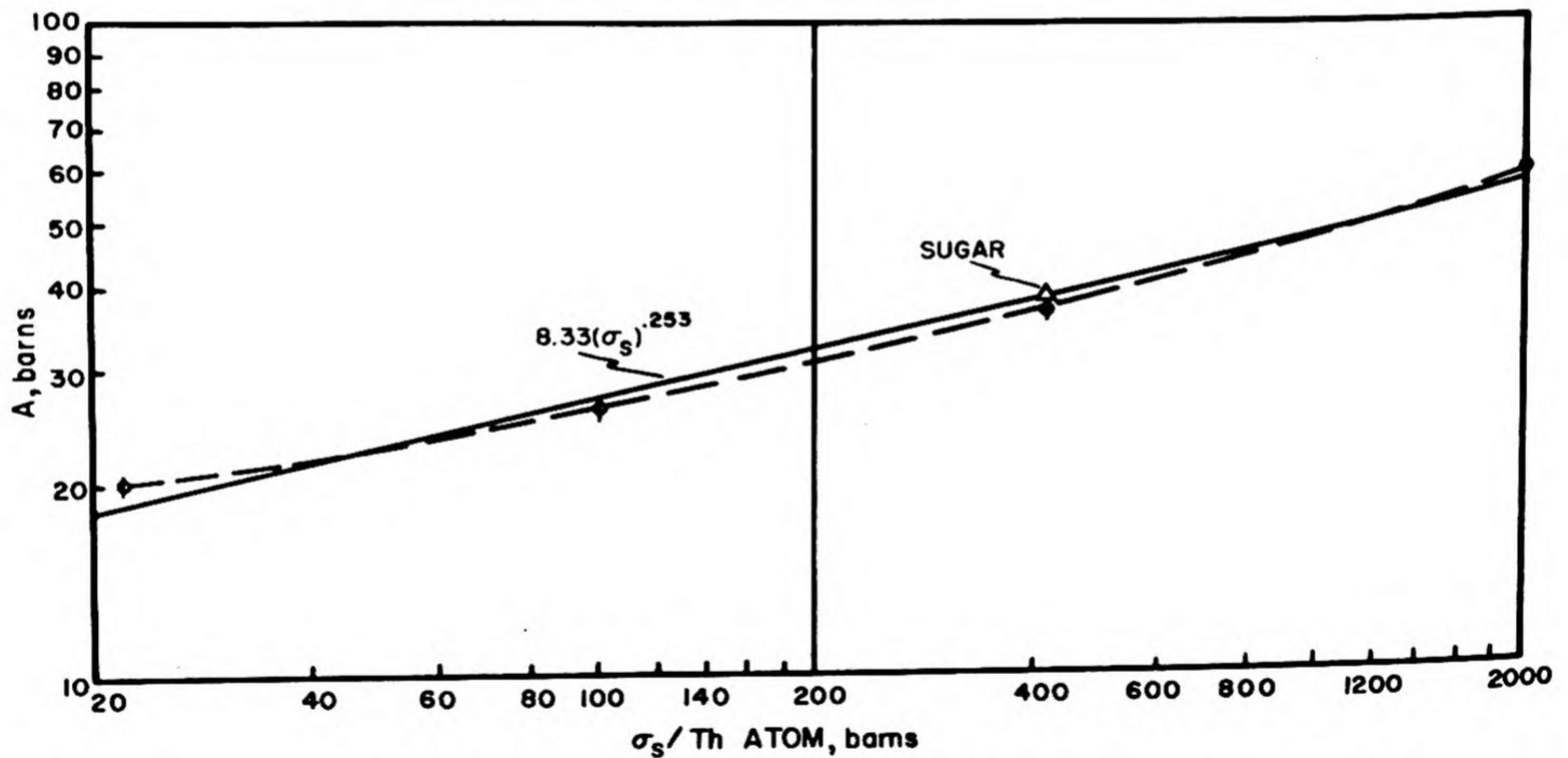


Fig. 1.5.19 — Effective Resonance Integral for Th. Reprinted from Hughes and Egger, CP-3093.

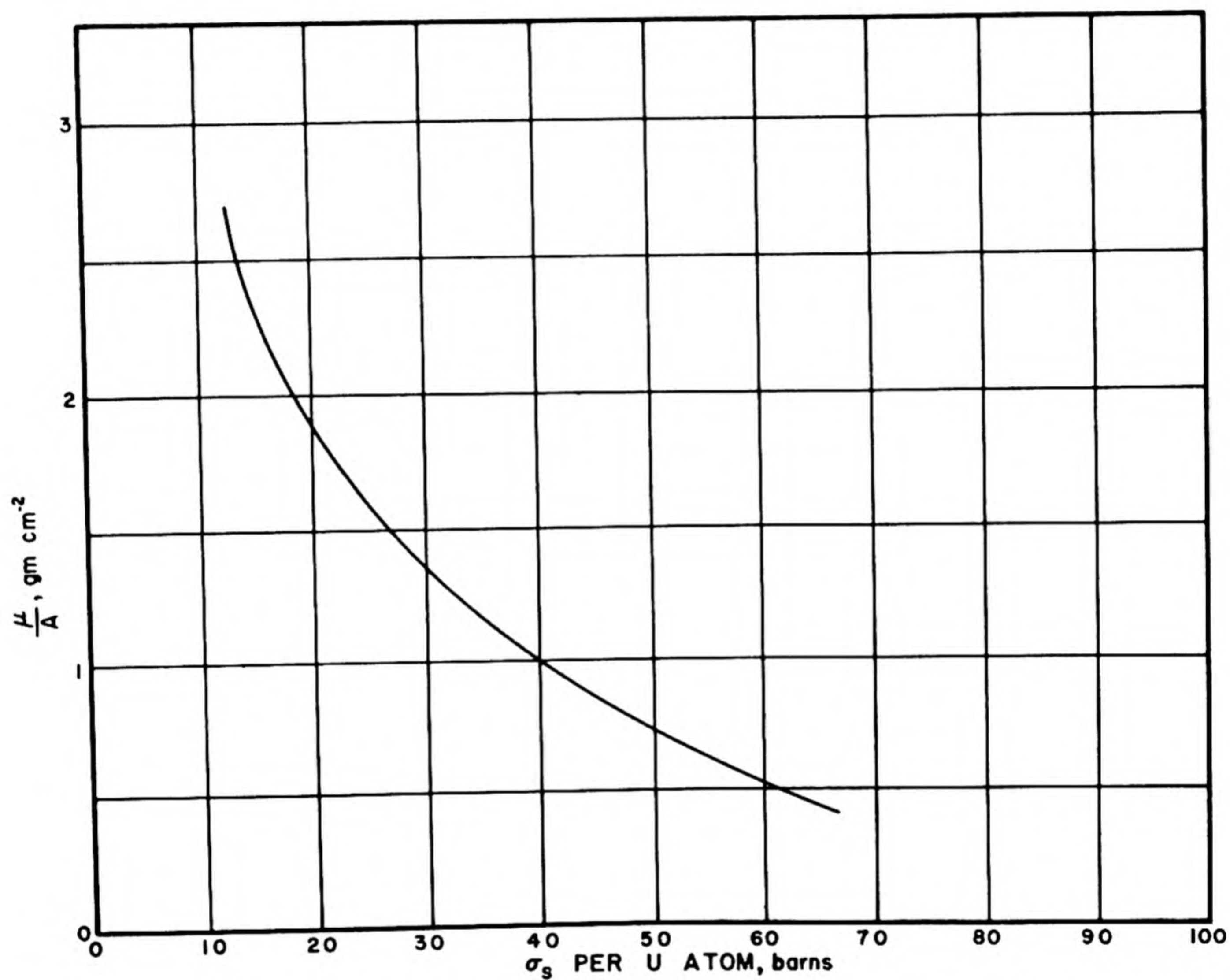


Fig. 1.5.20 — Surface Resonance Absorption in U. Reprinted from Chicago Handbook.

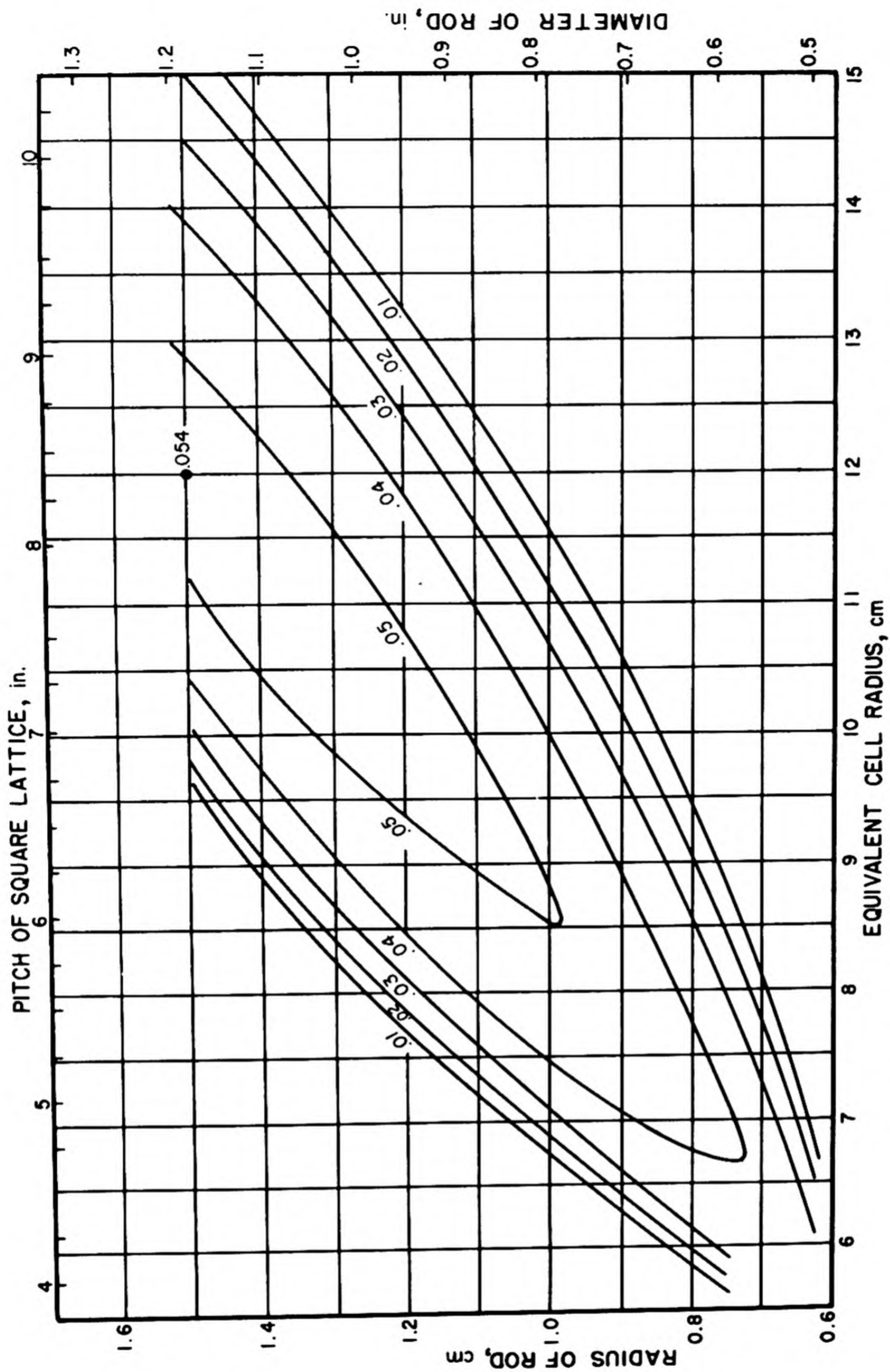


Fig. 1.5.21 — Calculated Values of $k-1$ for Uranium Metal Rods in Graphite. Reprinted from Guggenheim and Pryce, TPI-20(u), Aug. 1945. Graphite density 1.6 gm/cc; U metal 18.9 gm/cc; early project purity of materials; 1.15-mm Al sheath on rods; no air gap. The radius of the circle which has the same area as the cell is the equivalent radius. Reference report gives similar graphs for various air-gap thicknesses and other related material.

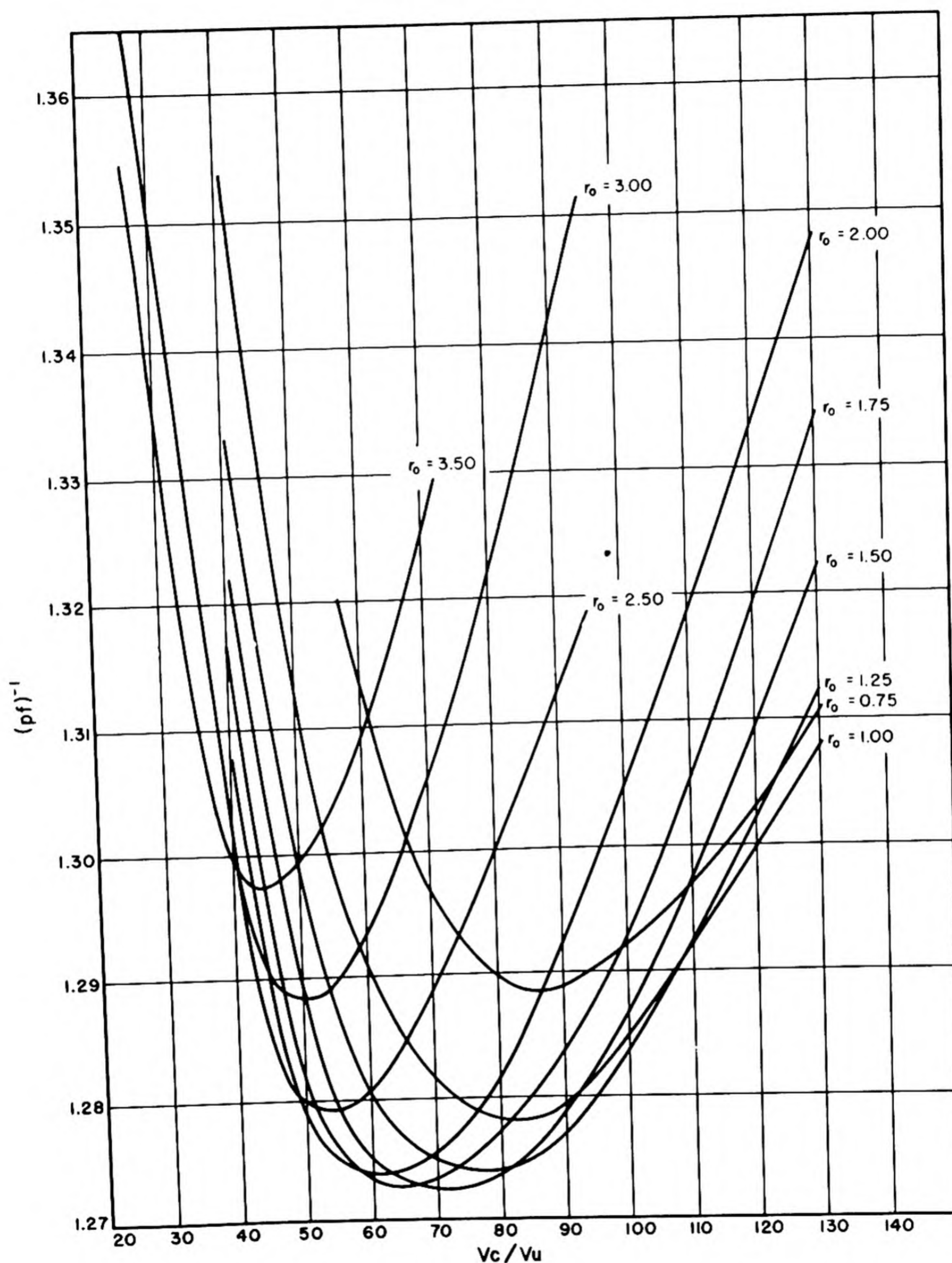


Fig. 1.5.22 — The Function pf for Uranium Metal Spheres of Density 18. Reprinted from Plass and Wigner, CP-372, Dec. 1942. Inverse of pf plotted against graphite-to-uranium volume ratio; r_0 is radius of sphere in cm. Graphite of density 1.6 gm/cc; early project purity.

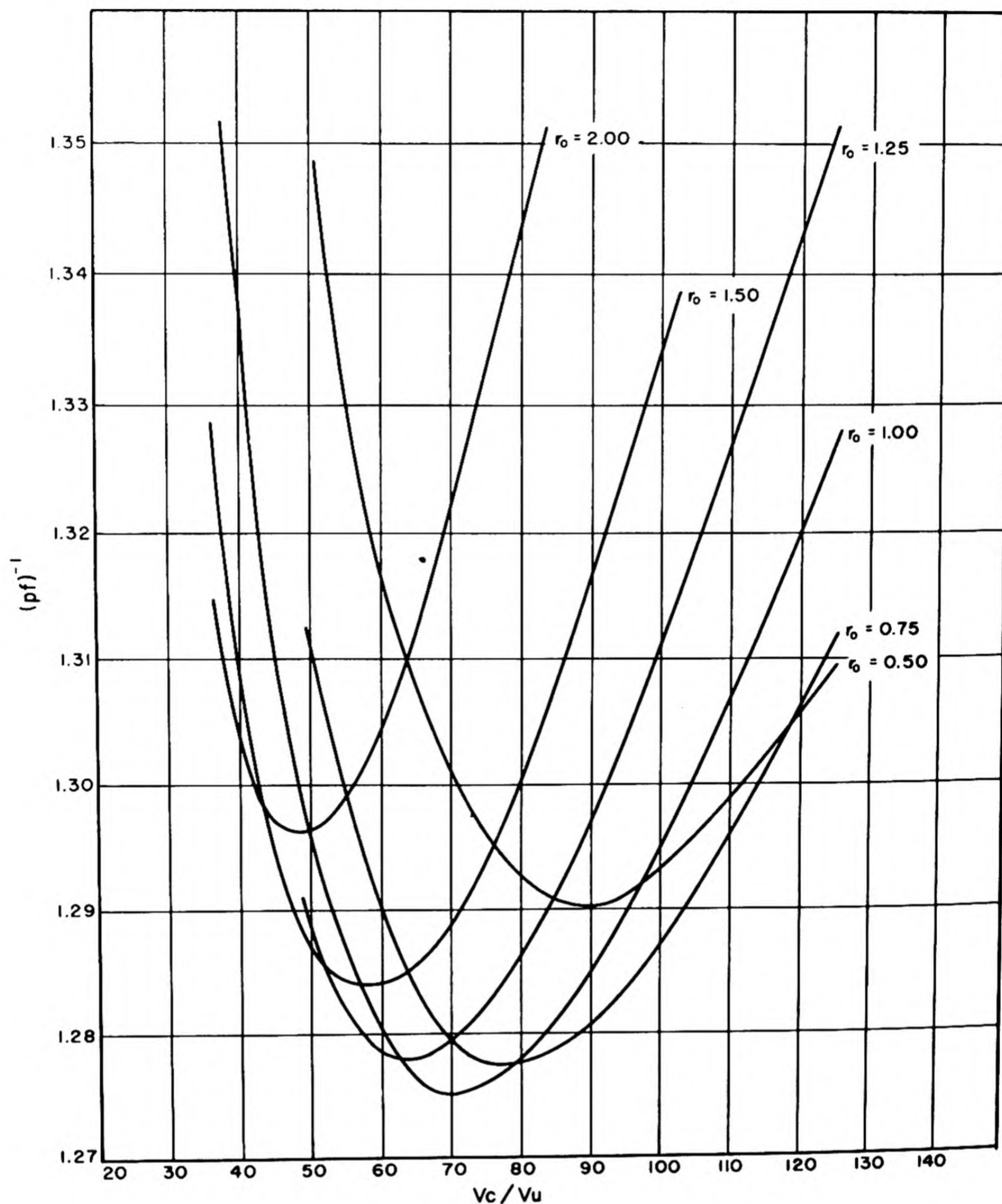


Fig. 1.5.23—The Function pf for Uranium Metal Cylinders of Density 18. Reprinted from Plass and Wigner, CP-372, Dec. 1942. Inverse of pf plotted against graphite-to-uranium volume ratio; r_0 is radius of rod in cm. Graphite of density 1.6 gm/cc; early project purity.

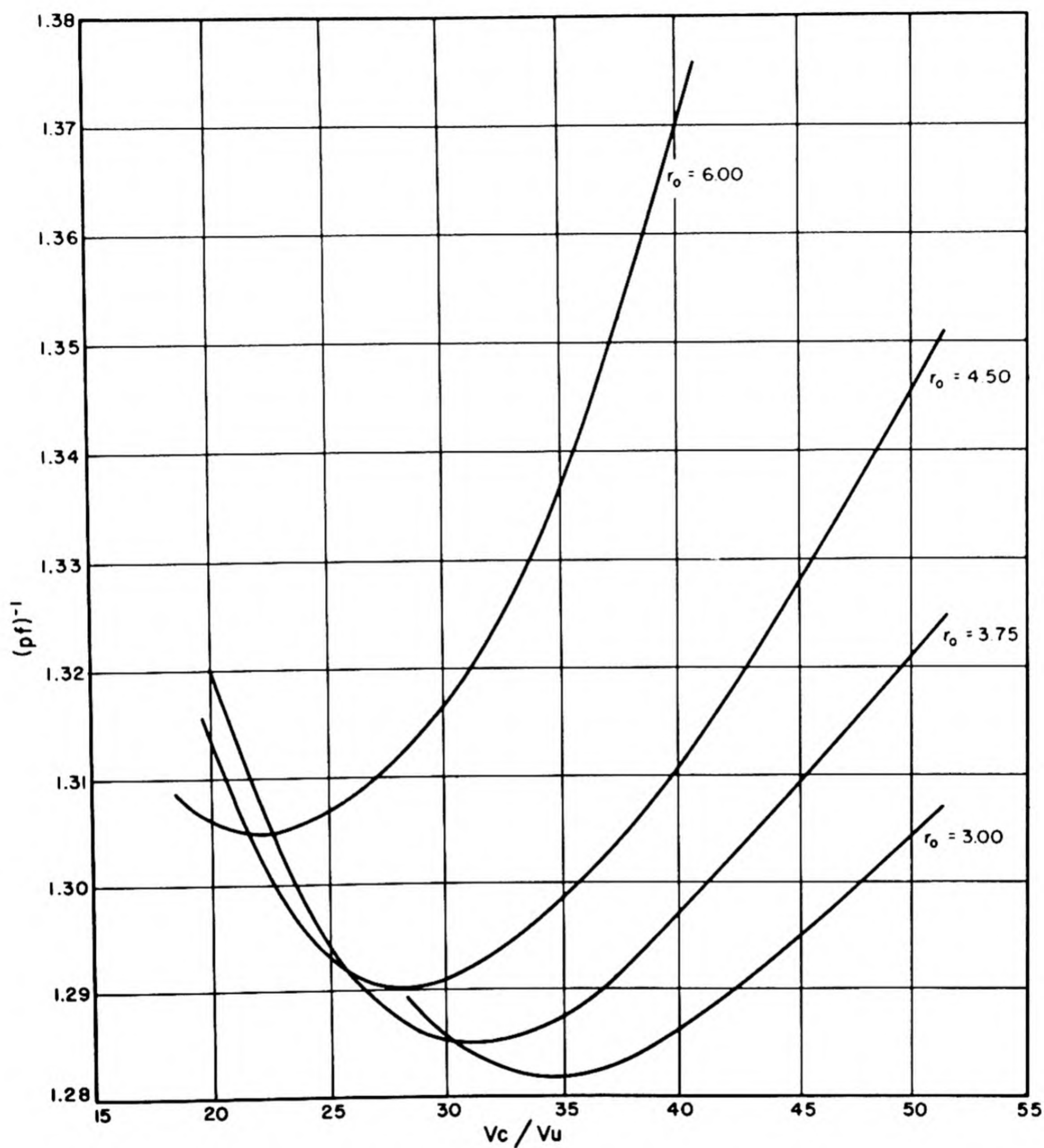


Fig. 1.5.24—The Function pf for Uranium Metal Spheres of Density 9. Reprinted from Plass and Wigner, CP-372, Dec. 1942. Inverse of pf plotted against graphite-to-uranium volume ratio; r_0 is radius of sphere in cm. Graphite of density 1.6 gm/cc; early project purity. Actually calculated for cylindrical lumps having the same volume as a sphere of the indicated radius. The difference is presumed to be very small.

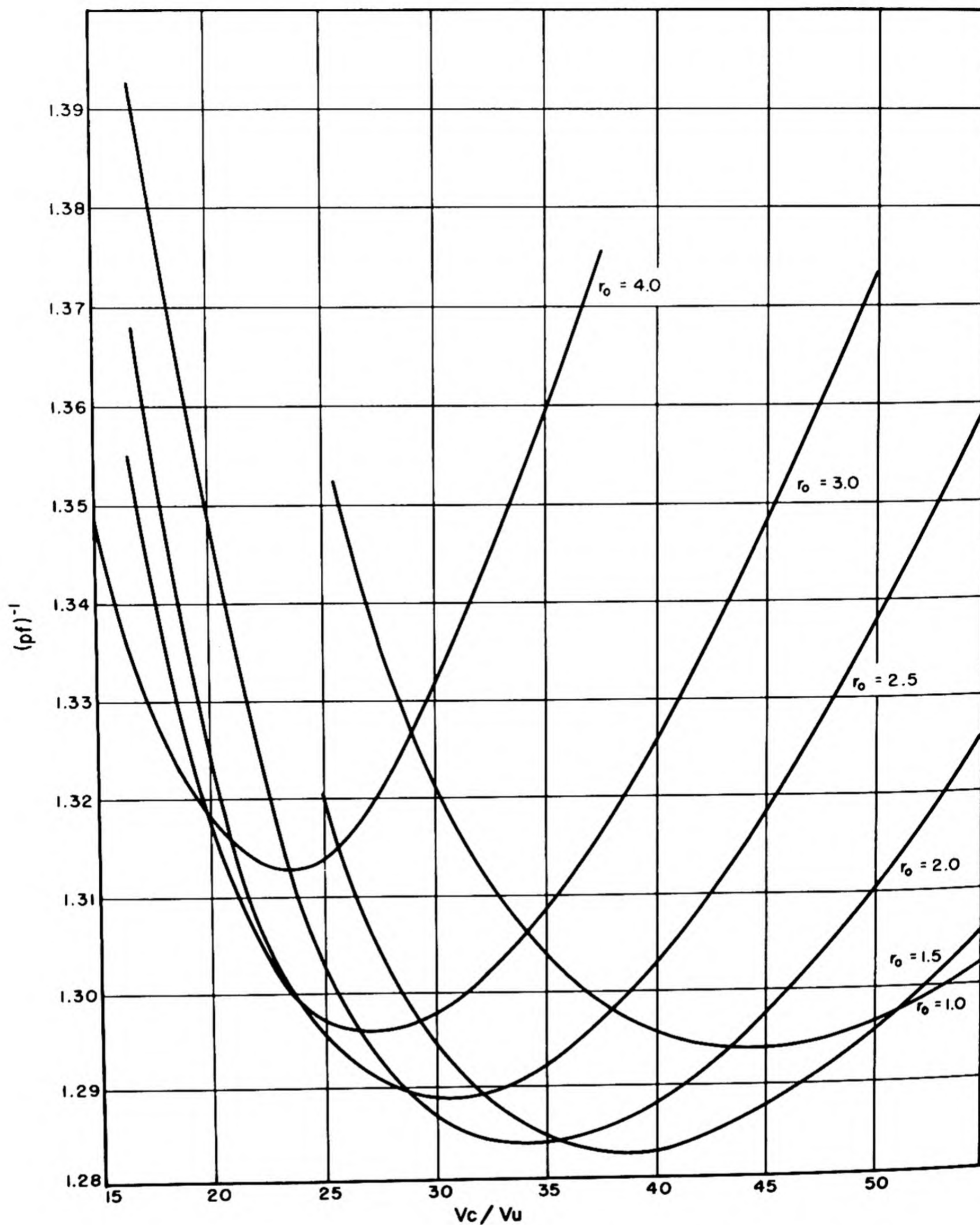


Fig. 1.5.25—The Function pf for Uranium Metal Cylinders of Density 9. Reprinted from Plass and Wigner, CP-372, Dec. 1942. Inverse of pf plotted against graphite-to-uranium volume ratio; r_0 is radius of rod in cm. Graphite of density 1.6 gm/cc; early project purity.

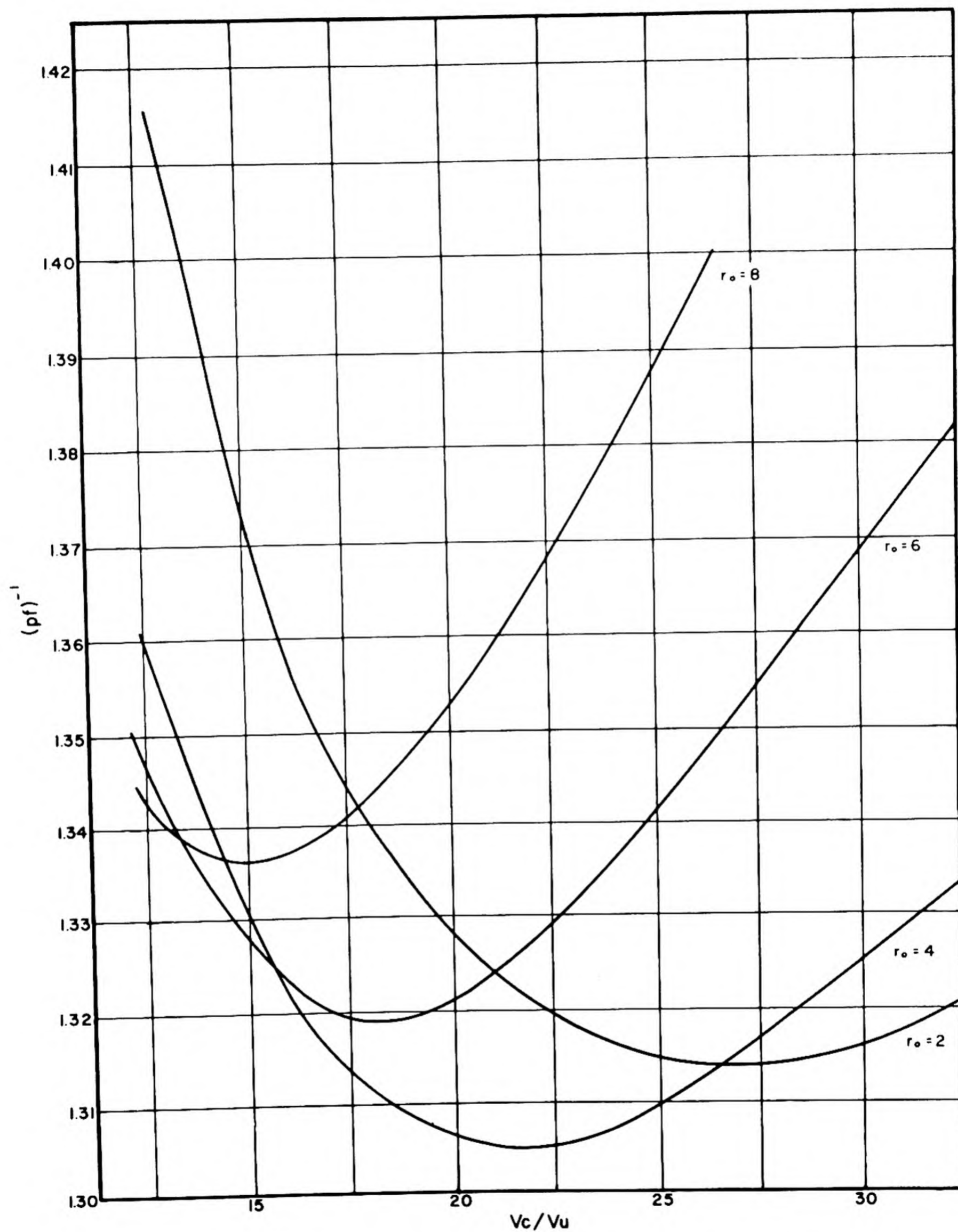


Fig. 1.5.26— The Function pf for Uranium Oxide Spheres of Density 6. Reprinted from Plass and Wigner, CP-372, Dec. 1942. Inverse of pf plotted against graphite-uranium volume ratio; r_0 is radius of sphere in cm. Graphite of density 1.6 cm/cc; early project purity. Oxide is U_3O_8 .

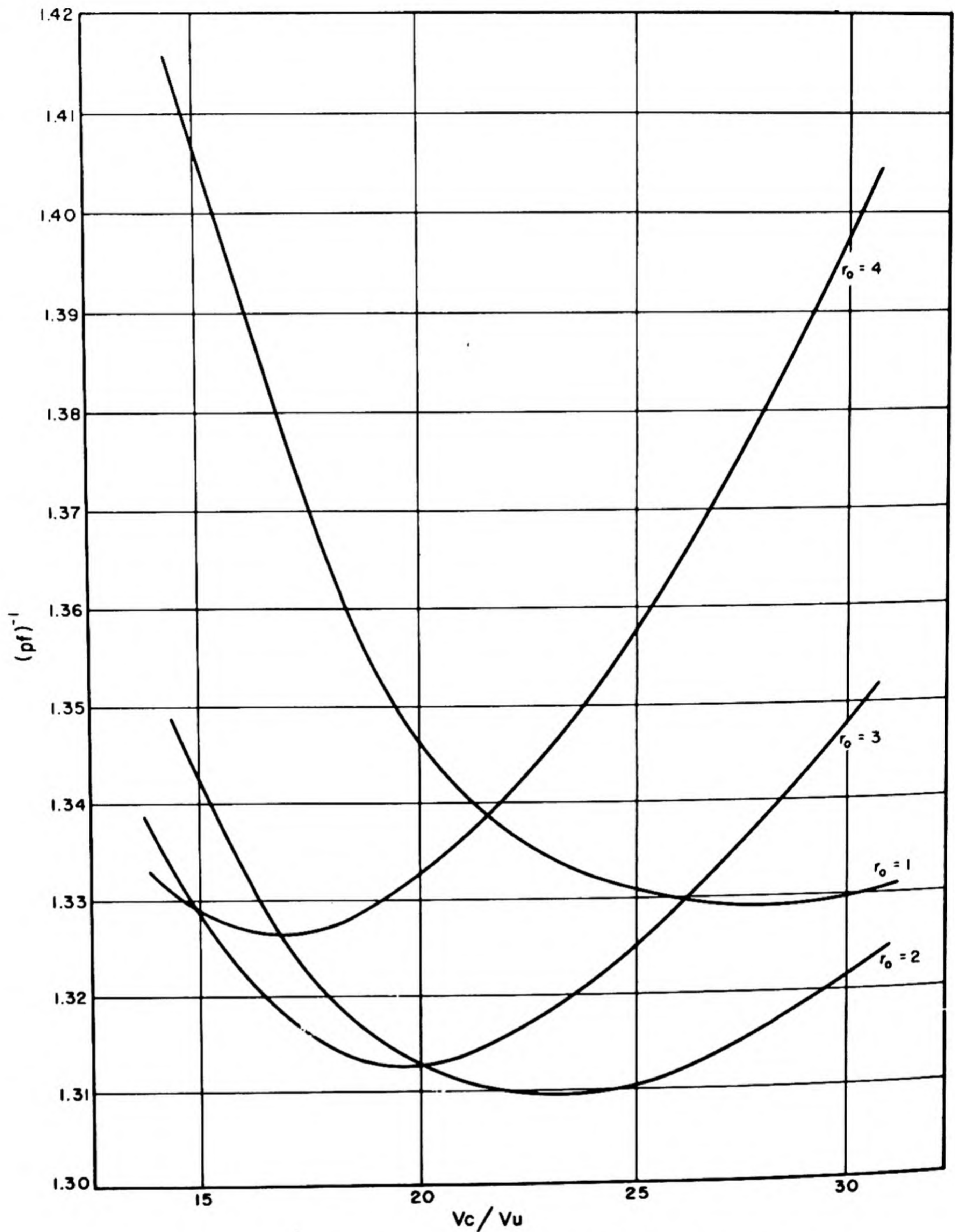


Fig. 1.5.27 — The Function pf for Uranium Oxide Cylinders of Density 6. Reprinted from Plass and Wigner, CP-372, Dec. 1942. Inverse of pf plotted against graphite-to-uranium volume ratio; r_0 is radius of rod in cm. Graphite of density 1.6 gm/cc; early project purity. Oxide is U_3O_8 .

REACTOR STATICS; EXPERIMENTAL

REFERENCES

1. Deleted.
2. Deleted.
3. Deleted.
4. Deleted.
5. Deleted.
6. TID-5022 (classified).
7. BNL-152 (classified).
8. BNL-170 (classified).
9. CL-697 (classified).
10. Deleted.
11. K. Way, CP-3209, Aug. 1945 (classified).
12. CP-3364 (classified).
13. Wigner and Plass, CP-372.
14. Clark, KAPL-743 (classified).
15. HKF-116, p 1.3 (classified).
16. K. Way, CP-3209 (classified).
17. TPI-20 (classified).
18. Weinberg and Noderer, Vol. I, Chap. IV (classified).
19. Wigner, CP-4.
20. Wigner, CP-1589 (classified).
21. Deleted.
22. CP-3407 (classified).
23. Weinberg and Williamson, CP-1231 (classified).
24. Weinberg et al, CP-2842, p 41 (classified).

CHAPTER 1.6

Reactor Dynamics

Gerald Goertzel

REACTOR KINETICS

The subject of reactor kinetics is concerned with the calculation of how the neutron density (prompt and delayed) within the reactor varies with time. Into the equations for this calculation are introduced the properties of the reactor as determined by temperature, density, motion of control rods, burn-up, and creation of poisons as known functions of time. Calculation of these properties will be discussed later in this chapter.

Most studies of reactor kinetics are based on an equivalent space-independent one-group model. Equation (1) describes this model, and the terms of these equations are interpreted for a general reactor in Eqs. (4) and (5). Problems to which the equations for the equivalent one-group space-independent model can not be adequately applied have been treated only slightly.¹

SPACE-INDEPENDENT ONE-GROUP MODEL

The equations of motion may be written as:

$$\frac{dn}{dt} = \frac{k-1}{l} n - \frac{k\beta n}{l} + \sum \lambda_i c_i + s$$

$$\frac{dc_i}{dt} = -\lambda_i c_i + \frac{k\beta_i n}{l}$$

- where:
- n = total neutrons in the reactor
 - c_i = total delayed-neutron emitters of type i
 - λ_i^{-1} = mean life of delayed-neutron emitters of type i
 - s = source strength, neutrons per unit time
 - kn/l = rate of production of neutrons (prompt and delayed) by fission
 - n/l = rate of loss of neutrons, all causes
 - $k\beta n/l$ = rate of creation of delayed-neutron emitters
 - $[(k/l) - (k\beta/l)]n$ = rate of production of prompt neutrons by fission
 - $k\beta_i n/l$ = rate of creation of delayed-neutron emitters of type i
 - $\beta = \sum_i \beta_i$

¹ References appear at end of chapter.

GENERAL EQUATIONS

The equations describing the time behavior of a nuclear reactor may be written in the form:

$$\begin{aligned}\frac{\partial N}{\partial t} &= (1 - \beta)f_0(E)JN + \sum_i f_i(E)\lambda_i C_i + S - KN \\ \frac{\partial C_i}{\partial t} &= \beta_i JN - \lambda_i C_i \\ f(E) &= (1 - \beta)f_0(E) + \sum_i \beta_i f_i(E)\end{aligned}\tag{2}$$

where: $N(\underline{x}, E, \underline{\omega})/4\pi$ = neutron density per unit volume per unit energy per unit solid angle of velocity direction

$\beta = \sum \beta_i$ = fraction of fission neutrons which are delayed (assumed independent of energy of neutron causing fission)

β_i = fraction of fission neutrons emitted by the i 'th delayed-neutron emitter

$f_0(E)$ = energy spectrum of prompt neutrons arising from fission (neutrons arising from fission are assumed to have an isotropic angular distribution), $\int_0^\infty f_0(E)dE = 1$

$f_i(E)$ = energy spectrum of neutrons emitted by the i 'th delayed-neutron emitter, $\int_0^\infty f_i(E)dE = 1$

$f(E)$ = energy spectrum of all fission neutrons

$JN = \int \int \nu(E)\sigma_f(E)vN(\underline{x}, E, \underline{\omega})dE d\omega/4\pi$ = production rate of fission neutrons per unit volume per unit time

$KN/4\pi$ = net rate at which neutrons leave the region in phase space as a result of absorption and scattering (for a one-group diffusion theory reactor model, $KN = -v \nabla \cdot D \nabla N + \sigma_a v N$)

$S/4\pi$ = source density per unit volume, energy, and solid angle

λ_i^{-1} = mean life of the i 'th-type delayed-neutron emitter

C_i = density (number per unit volume) of i 'th-type delayed-neutron emitters

THE IMPORTANCE FUNCTION

To convert Eq. (2) to the form of Eq. (1), it is useful, at least for studying the effect of small changes in J and K , to introduce the importance function, $W^*(\underline{x}, E, \underline{\omega})$. For small changes in J and K , neither W nor the shape of N will change appreciably, but the magnitude of N (and of W) may change a good deal.

The importance, W , may be defined as follows. Consider a reactor slightly below critical. A source of neutrons therein will produce an equilibrium neutron-distribution, N . As the source is moved within the reactor, the shape of N will not change much, but the magnitude may. If the equilibrium total-neutron content is a measure of the magnitude, $W(\underline{x}, E, \underline{\omega})$ may be defined as the neutron content of the reactor resulting from a unit-point, monoenergetic, unidirectional, neutron source at \underline{x} with energy E and direction $\underline{\omega}$. The absolute magnitude of W is not of interest, but its shape is.

* This function was denoted by M in Chapter 1.4.

REDUCTION OF GENERAL EQUATIONS TO EQUIVALENT ONE-GROUP SPACE-INDEPENDENT FORM

The abbreviation:

$$(f, g) = \int f g \, dE \, d\mathbf{x} \, d\omega \quad (3)$$

will be of use in the following. In terms of this notation, and the definition of W , the effect of the source term on the reactor behavior as given in Eq. (2) may be written as (W, S) . This suggests multiplying the first of Eq. (2) by W (using $\partial W / \partial t = 0$) and integrating. If one further multiplies the others of Eq. (2) by $W f_i(E)$ and integrates, there results:

$$\begin{aligned} \frac{\partial}{\partial t}(W, N) = & \left\{ W, \left[(1 - \beta) f_0(E) + \sum_i \beta_i f_i(E) \right] JN \right\} - \sum_i \beta_i (W, f_i(E) JN) \\ & + \sum_i \lambda_i (W, f_i(E) C_i) + (W, S) - (W, KN) \end{aligned} \quad (4)$$

$$\frac{\partial}{\partial t}(W, f_i C_i) = \beta_i (W, f_i JN) - \lambda_i (W, f_i C_i)$$

Equation (4) can be put into direct correspondence with Eq. (1) provided one talks of the total neutron importance (W, N) in place of the total number of neutrons n in Eq. (1). Similarly, $(W, f_i C_i)$ is the importance of type- i delayed-neutron emitters. One then defines the effective lifetime, l , so that $(W, N)/l$ is the rate of destruction of importance (W, KN) and k so that $k(W, N)/l$ is the rate of creation of importance (W, fJN) . In terms of these concepts, the following definitions change Eq. (4) formally into Eq. (1):

$$\begin{aligned} n &= (W, N) \\ c_i &= (W, f_i C_i) \\ \frac{kn}{l} &= (W, f(E) JN) \\ \frac{n}{l} &= (W, KN) \\ \frac{k\beta_i n}{l} &= \beta_i (W, f_i JN) \\ s &= (W, S) \end{aligned} \quad (5)$$

From Eq. (5), it is easily seen that:

$$k = \frac{(W, fJN)}{(W, KN)} \quad (6)$$

or, the multiplication constant, k , is the rate of creation of importance (prompt and delayed) divided by the rate of destruction of importance. Similarly:

$$l = \frac{(W, N)}{(W, KN)} \quad (7)$$

or the lifetime is the total importance divided by the rate of destruction of importance. Further discussion of the meaning of l is given in Chapter 1.4.

However, in place of β_i , one must have:

$$\beta_i \frac{(W, f_i JN)}{(W, f JN)} = \epsilon_i \beta_i \quad (8)$$

and, in place of β :

$$\epsilon \beta = \sum_i \epsilon_i \beta_i \quad (9)$$

The ϵ_i are factors giving the increased importance of delayed neutrons owing to their lower energy. The ϵ_i may often be taken as unity or, at least, as independent of i ($\epsilon_i = \epsilon$, all i).

Equation (1) may thus be applied to the general reactor provided that the definitions of Eqs. (6) and (7) are used for k , l and that β_i is replaced by $\epsilon_i \beta_i$. Since $k-1$ is a factor in the forcing term in Eq. (1), $k-1$ must be determined reasonably well. The choice of Eq. (6) as a definition for k , together with the specific choice of W as the weighting function, assures this; this is clear from the discussion of importance functions in Chapter 1.4. Methods for calculating W are discussed there.

EXAMPLE: TWO-GROUP, BARE, THERMAL REACTOR

The critical equation is:

$$-\nabla \cdot D_f \nabla v_f N_f + \sigma_{SD} v_f N_f = \nu \sigma_f v_s N_s \quad (10)$$

$$-\nabla \cdot D_s \nabla v_s N_s + \sigma_a v_s N_s = \sigma_{SD} v_f N_f$$

A comparison with Eq. (2) shows that:

$$fJN = \begin{pmatrix} 0 & \nu \sigma_f v_s \\ 0 & 0 \end{pmatrix} \begin{pmatrix} N_f \\ N_s \end{pmatrix} \quad (11)$$

$$KN = \begin{pmatrix} -\nabla \cdot D_f \nabla v_f + \sigma_{SD} v_f & 0 \\ -\sigma_{SD} v_f & -\nabla \cdot D_s \nabla v_s + \sigma_a v_s \end{pmatrix} \begin{pmatrix} N_f \\ N_s \end{pmatrix}$$

If D_f , σ_{SD} , σ_f , D_s , and σ_a are independent of position, the solution for a spherical reactor of extrapolated radius a , actual radius $a - \lambda$, is given by:

$$\begin{pmatrix} N_f \\ N_s \end{pmatrix} = \frac{\sin \pi \frac{r}{a}}{r} \begin{pmatrix} \nu \sigma_f v_s \\ L_f \end{pmatrix} \quad (12)$$

$$\begin{pmatrix} W_f \\ W_s \end{pmatrix} = \frac{\sin \frac{\pi r}{a}}{r} \begin{pmatrix} L_s \\ \nu \sigma_f v_s \end{pmatrix}$$

where:

$$L_f = \sigma_{SD} v_f + D_f v_f \left(\frac{\pi}{a} \right)^2 \quad (13)$$

$$L_s = \sigma_a v_s + D_s v_s \left(\frac{\pi}{a} \right)^2$$

provided the critical condition:

$$\nu \sigma_f v_s \sigma_{SD} v_f = L_s L_f \quad (14)$$

is satisfied. One easily calculates:

$$\begin{aligned} (W, fJN) &= L_s L_f \int \frac{\sin^2 \frac{\pi r}{a}}{r^2} \nu \sigma_f v_s dV \\ (W, KN) &= \nu \sigma_f v_s \left\{ L_s \int \frac{\sin \frac{\pi r}{a}}{r} (-\nabla \cdot D_f v_f \nabla + \sigma_{SD} v_f) \frac{\sin \frac{\pi r}{a}}{r} dV \right. \\ &\quad \left. - \nu \sigma_f v_s \int \frac{\sin^2 \frac{\pi r}{a}}{r} \sigma_{SD} v_f dV + L_f \int \frac{\sin \frac{\pi r}{a}}{r} (-\nabla \cdot D_s v_s \nabla + \sigma_a v_s) \frac{\sin \frac{\pi r}{a}}{r} dV \right\} \\ &= \nu \sigma_f v_s \left\{ \int \frac{\sin^2 \frac{\pi r}{a}}{r^2} [\sigma_{SD} v_f (L_s - \nu \sigma_f v_s) + \sigma_a v_s L_f] dV \right. \\ &\quad \left. + \int \left(\frac{d}{dr} \frac{\sin \frac{\pi r}{a}}{r} \right)^2 [L_s D_f v_f + L_f D_s v_s] dV \right\} \\ (W, N) &= \nu \sigma_f v_s (L_s + L_f) \int \frac{\sin^2 \frac{\pi r}{a}}{r^2} dV \end{aligned} \quad (15)$$

In using these equations, the underlined quantities are varied in calculating δk . Before such variation, the results simplify to:

$$(W, fJN) = L_s L_f \nu \sigma_f v_s \int \frac{\sin^2 \frac{\pi r}{a}}{r^2} dV \quad (16)$$

$$(W, KN) = \nu \sigma_f v_s \left\{ 2L_s L_f - \nu \sigma_f v_s \sigma_{SD} v_f \right\} \int \frac{\sin^2 \frac{\pi r}{a}}{r^2} dV$$

and from Eqs. (6) and (7) (the last expression in each line uses the critical condition):

$$k = \frac{L_S L_f}{2L_S L_f - \nu \sigma_f v_S \sigma_{SD} v_f} = 1 \quad (17)$$

$$1 = \frac{L_S + L_f}{2L_S L_f - \nu \sigma_f v_S \sigma_{SD} v_f} = \frac{1}{L_f} + \frac{1}{L_S}$$

From Eq. (15), one may calculate the general formula for δk arising from small changes in a critical ($k = 1$) reactor:

$$\delta k = \frac{[W, \delta(fJ-K)N]}{(W, KN)}$$

$$= \left[\int \frac{\sin^2 \frac{\pi r}{a}}{r^2} \left\{ \frac{\delta(\nu \sigma_f v_S)}{\nu \sigma_f v_S} + \frac{\delta(\sigma_{SD} v_f)}{\sigma_{SD} v_f} \left(1 - \frac{\sigma_{SD} v_f}{L_f} \right) - \frac{\delta(\sigma_a v_S)}{\sigma_a v_S} \frac{\sigma_a v_S}{L_S} \right\} dV - \int \left(\frac{d}{dr} \frac{\sin \frac{\pi r}{a}}{\frac{\pi}{a} r} \right)^2 \left\{ \frac{\pi^2}{a^2} D_f v_f \frac{\delta(D_f v_f)}{D_f v_f} + \frac{\pi^2}{a^2} D_S v_S \frac{\delta(D_S v_S)}{D_S v_S} \right\} dV \right] / \int \frac{\sin^2 \frac{\pi r}{a}}{r^2} dV \quad (18)$$

SOLUTIONS OF THE KINETIC EQUATIONS, CONSTANT k

If $s = 0$ and all coefficients are constant in Eq. (1), the general solution may be obtained in terms of n and c_i at a given time by the method of Laplace transforms. Thus, if $N(p)$ and $C_i(p)$ are the transforms of $N(t)$ and $c_i(t)$, respectively, and the initial conditions are:

$$n(0) = n_0$$

$$c_i(0) = c_{i0}$$

the transform equations are:

$$pN - n_0 = \left(\frac{k-1}{1} - \frac{k\epsilon\beta}{1} \right) N + \sum \lambda_i C_i \quad (19)$$

$$pC_i - c_{i0} = -\lambda_i C_i + \frac{k\epsilon_i \beta_i N}{1}$$

Upon solving for N , one has:

$$N = \frac{n_0 + \sum_i \frac{\lambda_i c_{i0}}{p + \lambda_i}}{p - \frac{k-1}{1} + \frac{k\epsilon\beta}{1} - \frac{k}{1} \sum \frac{\lambda_i \epsilon_i \beta_i}{p + \lambda_i}} \quad (20)$$

$$= \frac{n_0}{k} \frac{1}{\frac{1}{k\epsilon\beta} + 1 - \frac{k-1}{k\epsilon\beta} - \sum \frac{\epsilon_i \beta_i}{\epsilon\beta} \frac{\lambda_i}{p + \lambda_i}} + \sum_i \left(\frac{\lambda_i c_{i0}}{\epsilon_i \beta_i n_0} \right) \frac{\epsilon_i \beta_i}{\epsilon\beta} \frac{1}{p + \lambda_i}$$

REACTOR DYNAMICS

Upon finding the inverse transform of Eq. (20), one has:

$$n(t) = n_0 \sum A(p_i) e^{p_i t} \quad (21)$$

where the p_i are the roots of:

$$\frac{1}{k\epsilon\beta} - \frac{k-1}{\epsilon k\beta} + 1 - \sum_i \frac{\epsilon_i \beta_i}{\epsilon\beta} \frac{\lambda_i}{p + \lambda_i} = 0 \quad (22)$$

and:

$$A(p) = \frac{1}{k} \frac{\frac{1}{\epsilon\beta} + \sum_i \frac{\lambda_i c_{i0}}{\epsilon_i \beta_i n_0} \frac{\epsilon_i \beta_i}{\epsilon\beta} \frac{1}{p + \lambda_i}}{\frac{1}{k\epsilon\beta} + \sum_i \frac{\epsilon_i \beta_i}{\epsilon\beta} \frac{\lambda_i}{(p + \lambda_i)^2}} \quad (23)$$

Equations (21), (22), and (23) may be applied to a sudden increase in k at $t = 0$, where for a long time before, the reactor was operating at $k = 1$. In this case, Eq. (13) is modified by setting:

$$\frac{1}{\epsilon_i \beta_i n_0} = 1 \quad (24)$$

Solutions in this case are given in Figs. 1.6.1 and 1.6.2. If, further, $|(k-1)/(\epsilon k\beta)| \ll 1$, after using Eq. (24), the terms proportional to $1/\epsilon\beta$ in Eqs. (20), (22), and (23) may be set to zero.

Setting $1/\epsilon\beta = 0$ means that n rises suddenly at $t = 0$ to the value [using Eq. (20)]:

$$\begin{aligned} n(0_+) &= \lim_{p \rightarrow \infty} pN(p) \\ &= \frac{n_0}{k} \frac{1}{1 - \frac{k-1}{k\epsilon\beta}} \end{aligned} \quad (25)$$

This rise is known as the "prompt jump" and occurs with a mean rise time corresponding to the most negative root of Eq. (22), a period approximately given by:

$$-\frac{1}{p} = \frac{1}{k\epsilon\beta} \left/ \left(1 - \frac{k-1}{k\epsilon\beta} \right) \right. \quad (26)$$

Neglecting 1 will have negligible effects on the periods other than that of Eq. (26) for $|(k-1)/(k\epsilon\beta)| \ll 1$. For example, (assuming specifically that $\epsilon_i = \epsilon = 1$), the effect of 1 upon period is seen in Fig. 1.6.3, where the largest root of Eq. (22), $p = 1/\tau_e$, is plotted vs $k-1$ for various values of 1 .

* For $(k-1)/(\epsilon\beta k) \ll 1$, the most positive root of Eq. (22) is:

$$p \approx \frac{(k-1)/(k\epsilon\beta)}{\frac{1}{\epsilon\beta k} + \sum_i \frac{\epsilon_i \beta_i}{\epsilon\beta \lambda_i}}; \sum_i \frac{\beta_i}{\beta \lambda_i} = 12.5 \text{ sec for } U^{235}$$

$$\text{For } \frac{k-1}{\epsilon\beta k} \gg 1 + \frac{1}{\epsilon\beta}, p \approx \frac{k-1-\epsilon k\beta}{1}$$

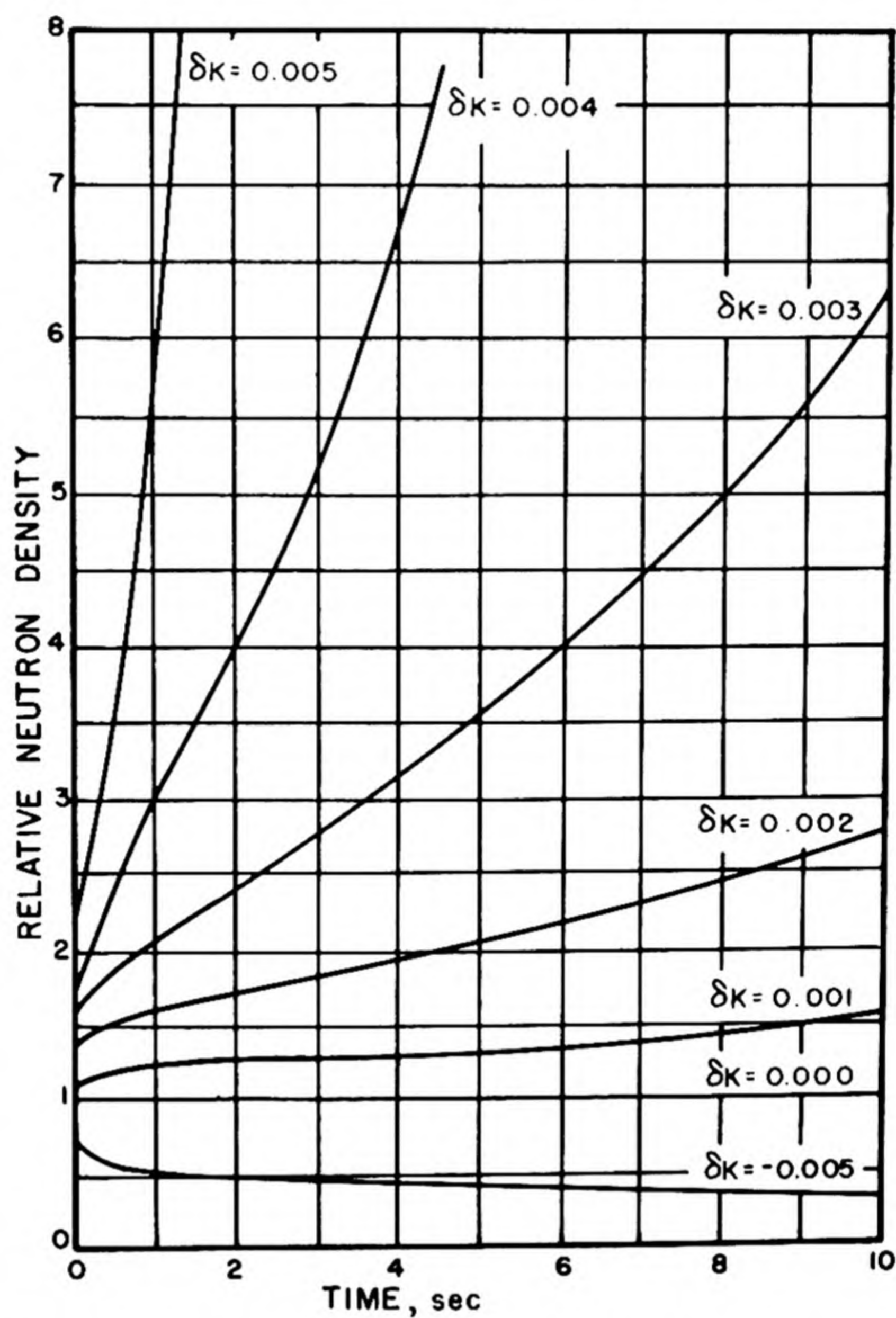


Fig. 1.6.1 — Ratio of Neutron Density Following a Sudden Change in k to the Equilibrium Value Prior to the Change. Reprinted from WAPD-34, Vol. I, RM-62.

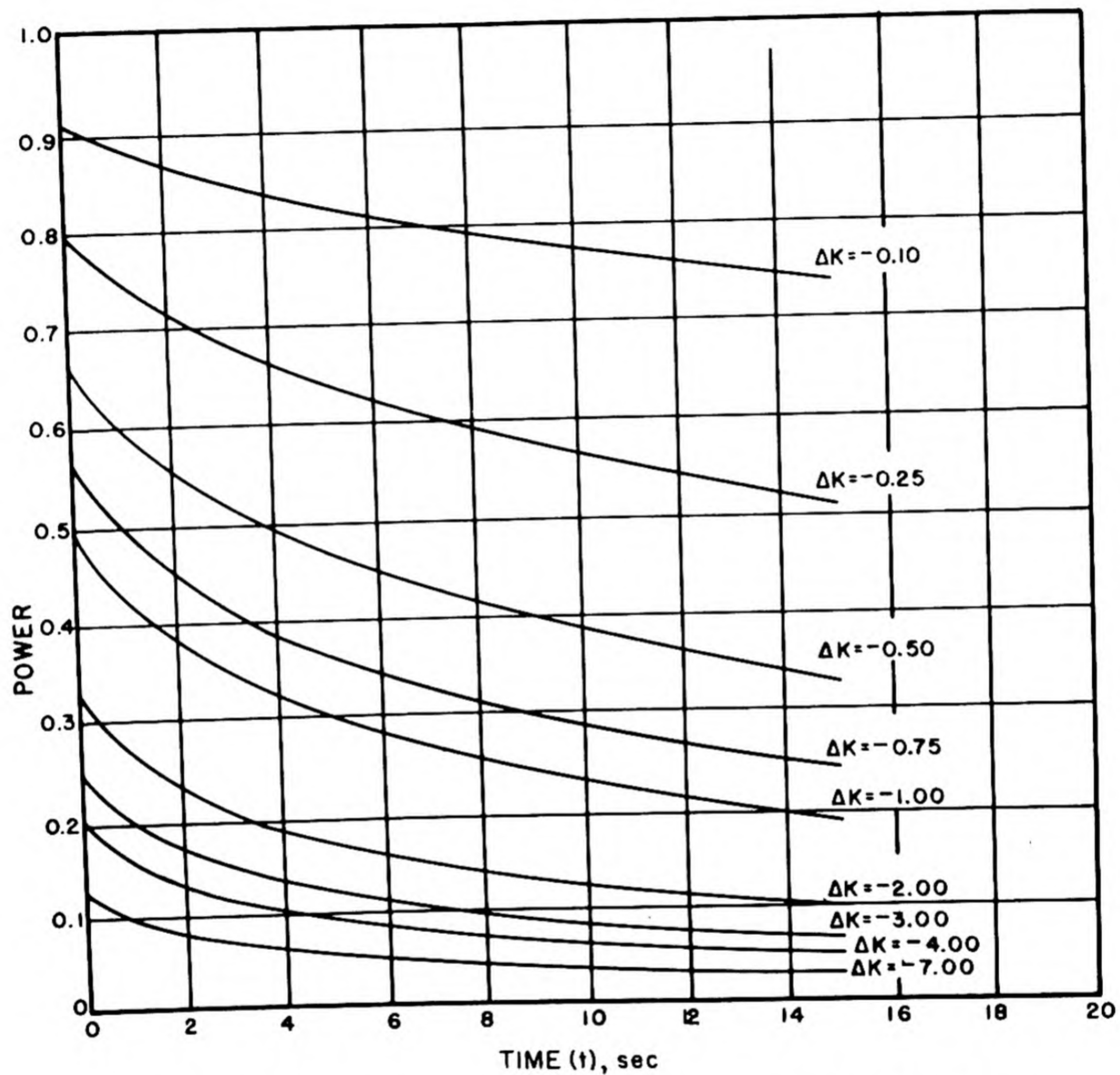


Fig. 1.6.2 — Power Following a Sudden Decrease in k . Reprinted from Reactor Physics Progress Report, KAPL-706, April 1952. Prior to changes, the power was unity.

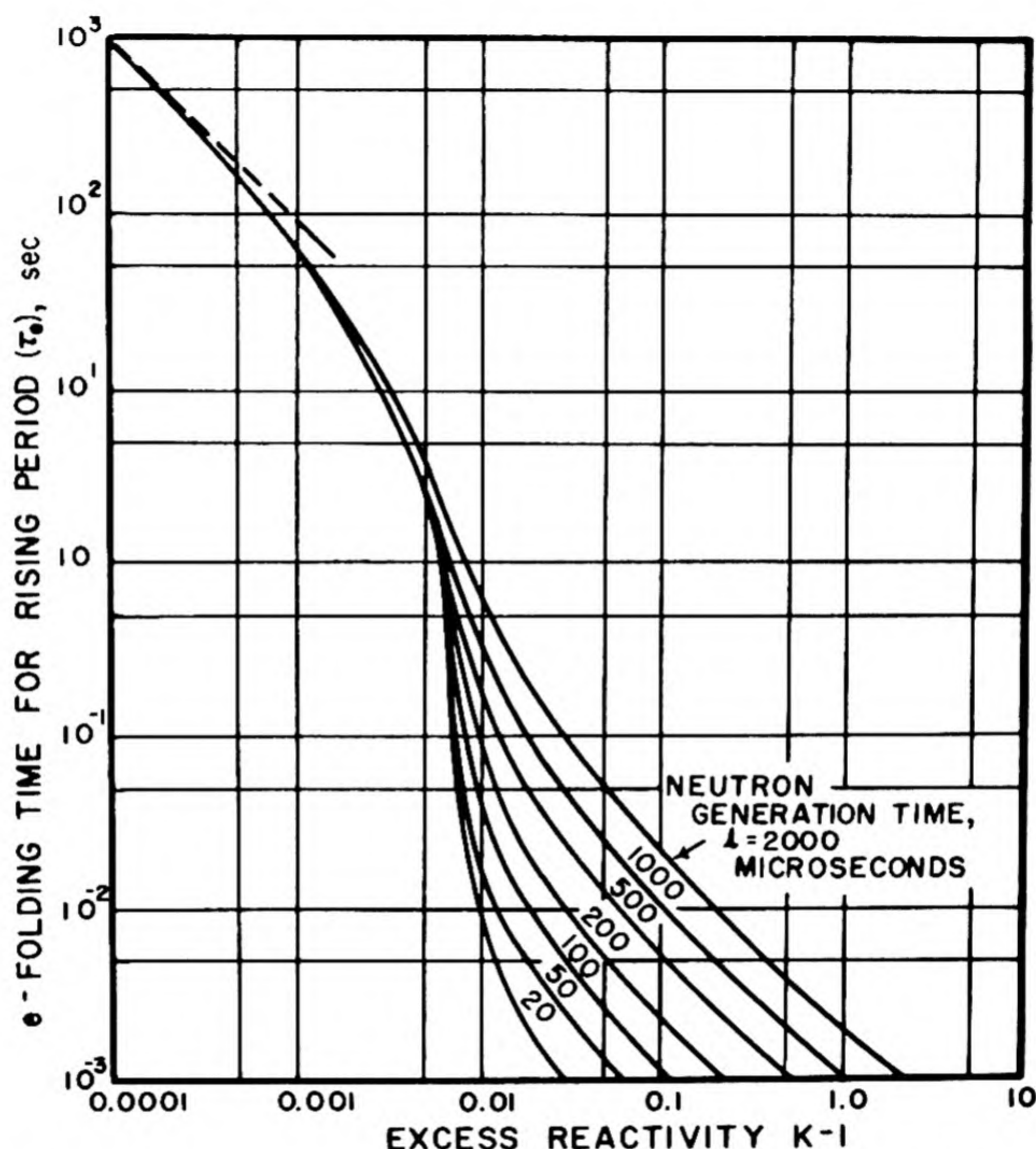


Fig. 1.6.3 — Effect of Neutron Generation Time on Reactor Period. Reprinted from M. M. Mills, *Journal of Reactor Science and Technology*, TID-71.

If one again makes the assumptions that $\epsilon_i = \epsilon$, all i , and $l = 0$, then Eqs. (22) and (23) may be solved graphically with graphs characteristic of the fissionable species involved but otherwise independent of the reactor. Thus, Figs. 1.6.4 to 1.6.10 give for U^{235} :

$$f(p) = \sum_i \frac{\beta_i}{\beta} \frac{\lambda_i}{p + \lambda_i} - 1$$

$$A(p) = \frac{\sum_i \frac{\beta_i}{\beta} \frac{1}{p + \lambda_i}}{\sum_i \frac{\beta_i}{\beta} \frac{\lambda_i}{(p + \lambda_i)^2}} \quad (27)$$

as functions of p . The line with ordinate $-(k - 1)/(\epsilon k \beta)$ intersects $f(p)$ at the p_i . The corresponding $A(p_i)$ are immediately obtainable from the graphs.

SOLUTIONS OF THE KINETIC EQUATIONS, k VARYING WITH TIME

In bringing a reactor to critical, k is increased gradually until the neutron flux is visible. To make the flux visible sooner in this process, neutron sources are usually located in the reactor.

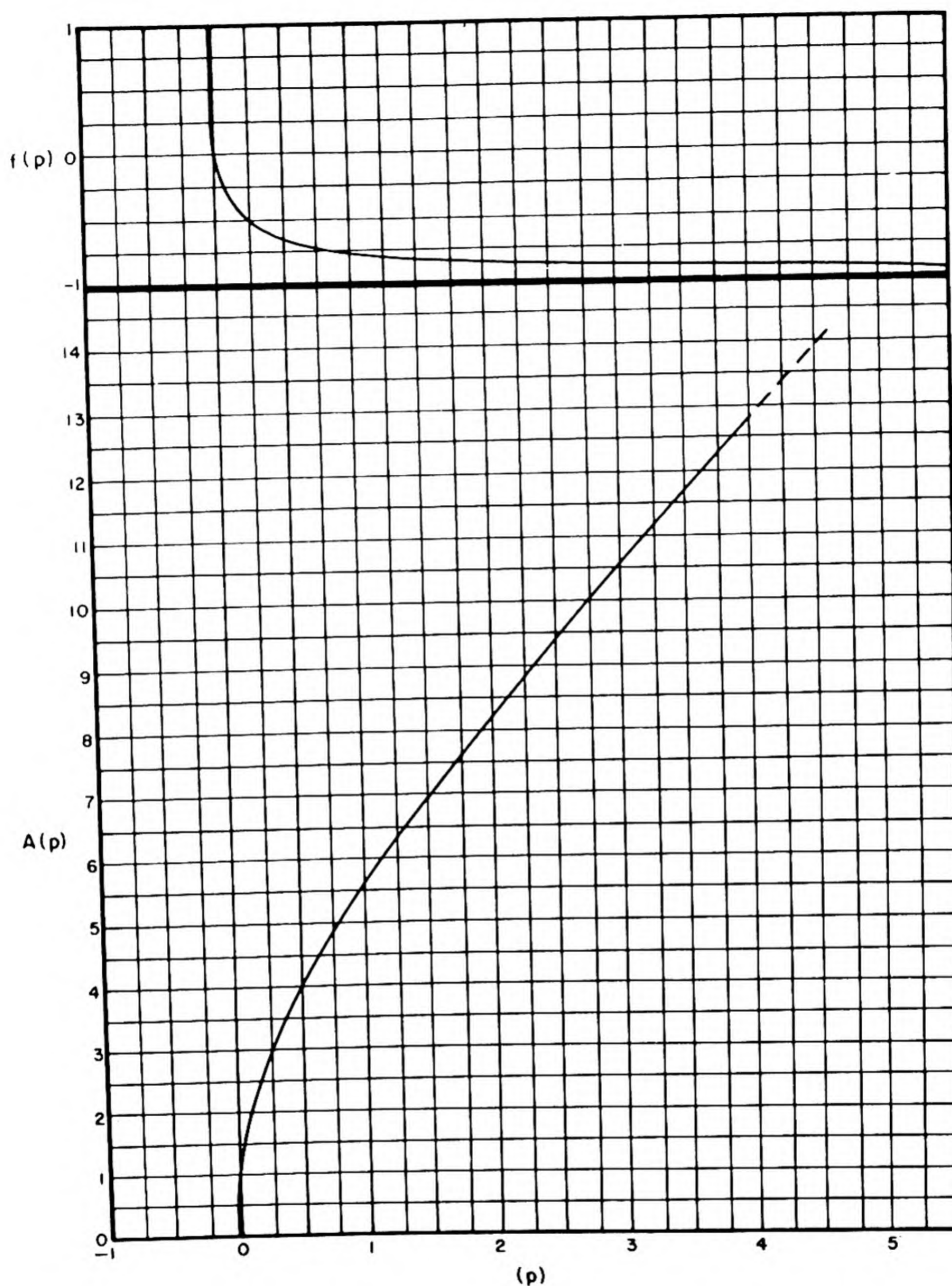


Fig. 1.6.4 — Parameters Needed to Find the Neutron Level Following a Step Change in Reactivity. Submitted by Nuclear Development Associates, Inc., Dec. 15, 1952. The figure is constructed assuming a zero neutron generation lifetime and delayed neutron characteristics for U^{235} (cf. Chapter 1.2). $n(t) = n_0 \sum_i A(p_i) e^{p_i t}$. The ordinate on the upper graph is the negative reactivity change in dollars. Go horizontally from ∂k to intersection with curve. Abscissa is p_i . The lower curve is $A(p_i)$ vs p . Use of Figs. 1.6.4 to 1.6.10 yields all six values of p_i and $A(p_i)$.

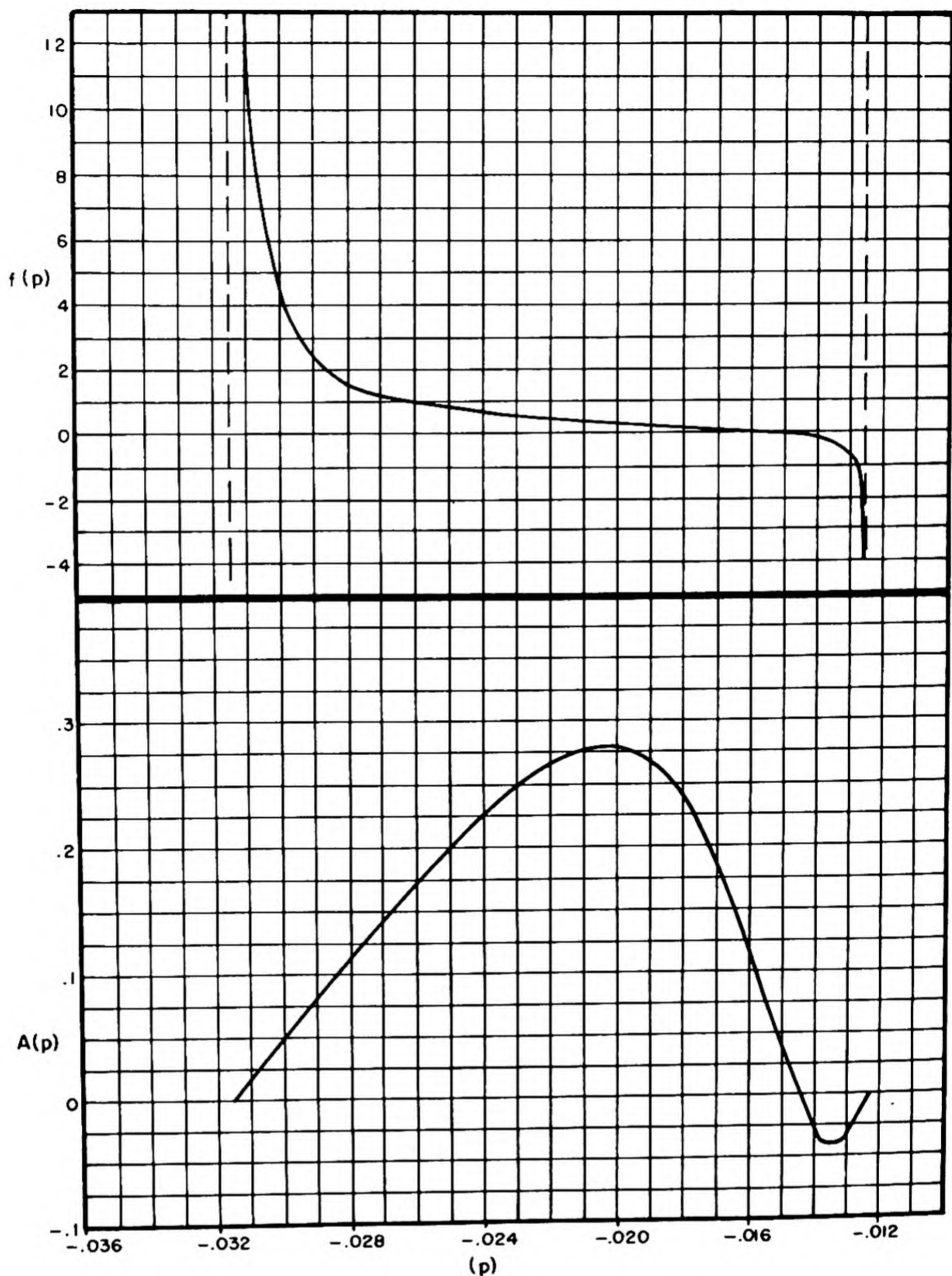


Fig. 1.6.5 — Parameters Needed to Find the Neutron Level Following a Step Change in Reactivity. Submitted by Nuclear Development Associates, Inc., Dec. 15, 1952. The figure is constructed assuming a zero neutron generation lifetime and delayed neutron characteristics for U^{235} (cf. Chapter 1.2). $n(t) = n_0 \sum A(p_i)e^{p_i t}$. The ordinate on the upper graph is the negative reactivity change in dollars. Go horizontally from ∂k to intersection with curve. Abscissa is p_i . The lower curve is $A(p_i)$ vs p . Use of Figs. 1.6.4 to 1.6.10 yields all six values of p_i and $A(p_i)$.

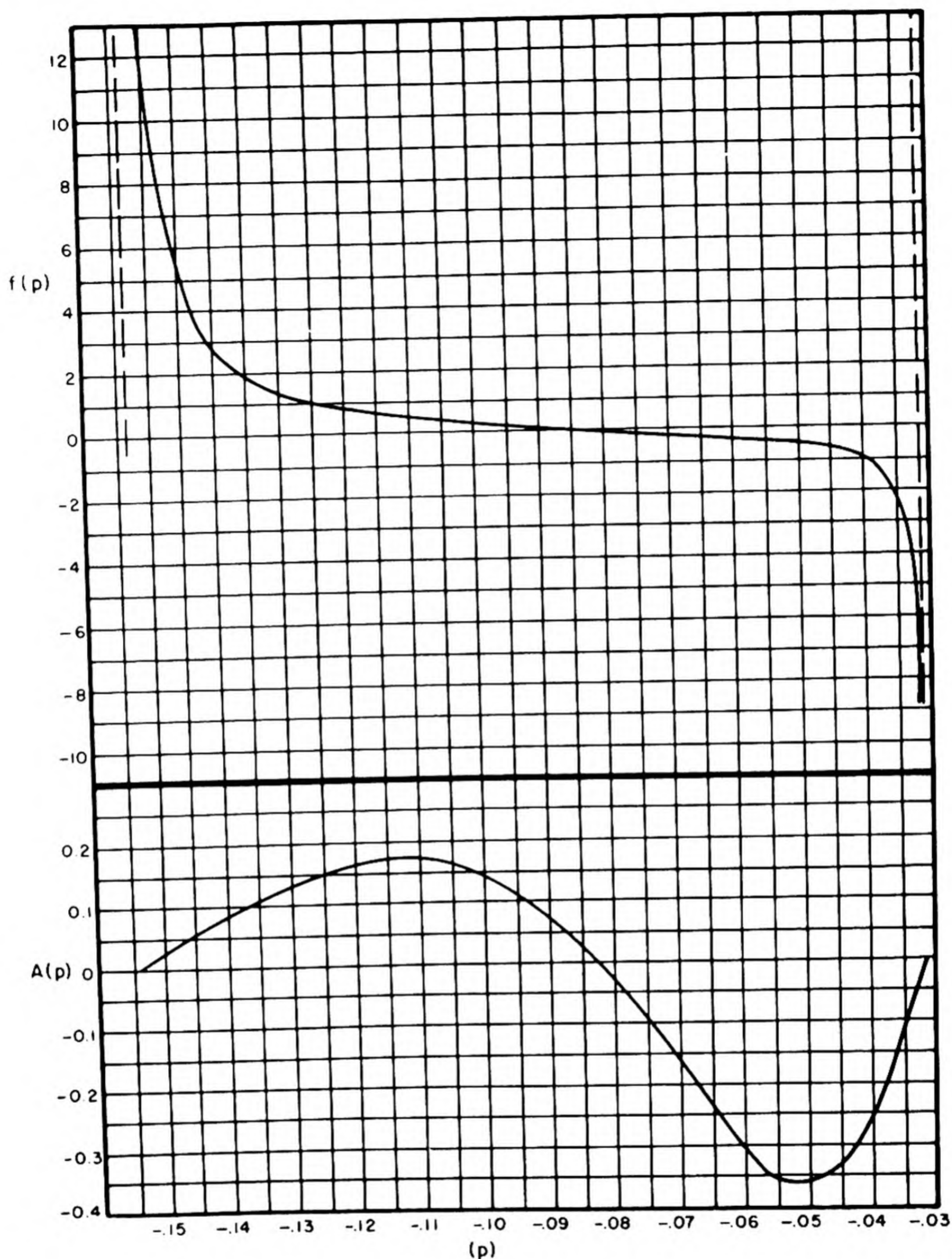


Fig. 1.6.6 — Parameters Needed to Find the Neutron Level Following a Step Change in Reactivity. Submitted by Nuclear Development Associates, Inc., Dec. 15, 1952. The figure is constructed assuming a zero neutron generation lifetime and delayed neutron characteristics for U^{235} (cf. Chapter 1.2). $n(t) = n_0 \sum A(p_i)e^{p_i t}$. The ordinate on the upper graph is the negative reactivity change in dollars. Go horizontally from ∂k to intersection with curve. Abscissa is p_i . The lower curve is $A(p_i)$ vs p . Use of Figs. 1.6.4 to 1.6.10 yields all six values of p_i and $A(p_i)$.

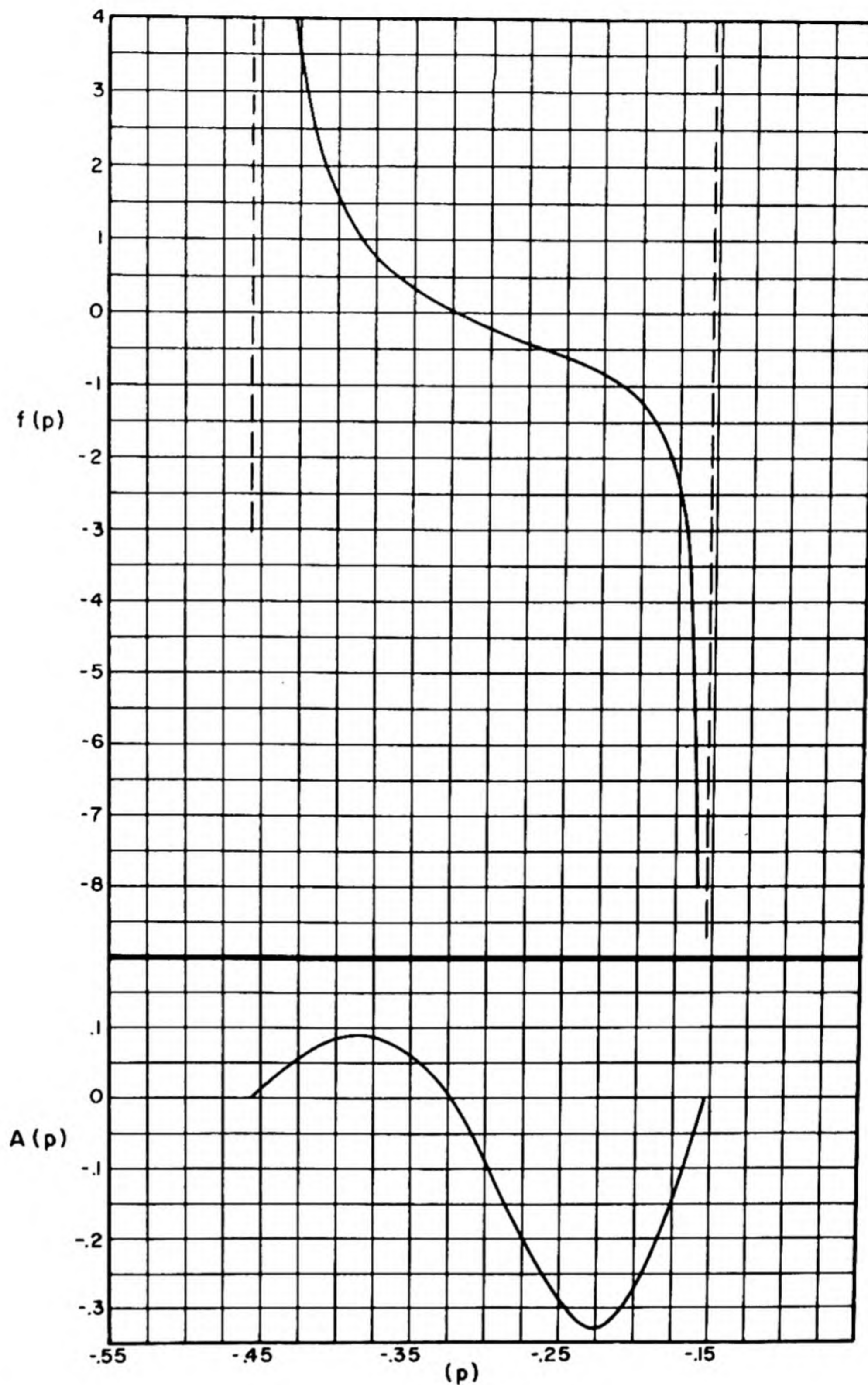


Fig. 1.6.7 — Parameters Needed to Find the Neutron Level Following a Step Change in Reactivity. Submitted by Nuclear Development Associates, Inc., Dec. 15, 1952. The figure is constructed assuming a zero neutron generation lifetime and delayed neutron characteristics for U^{235} (cf. Chapter 1.2). $n(t) = n_0 \sum_i A(p_i) e^{p_i t}$. The ordinate on the upper graph is the negative reactivity change in dollars. Go horizontally from ∂k to intersection with curve. Abscissa is p_i . The lower curve is $A(p_i)$ vs p . Use of Figs. 1.6.4 to 1.6.10 yields all six values of p_i and $A(p_i)$.

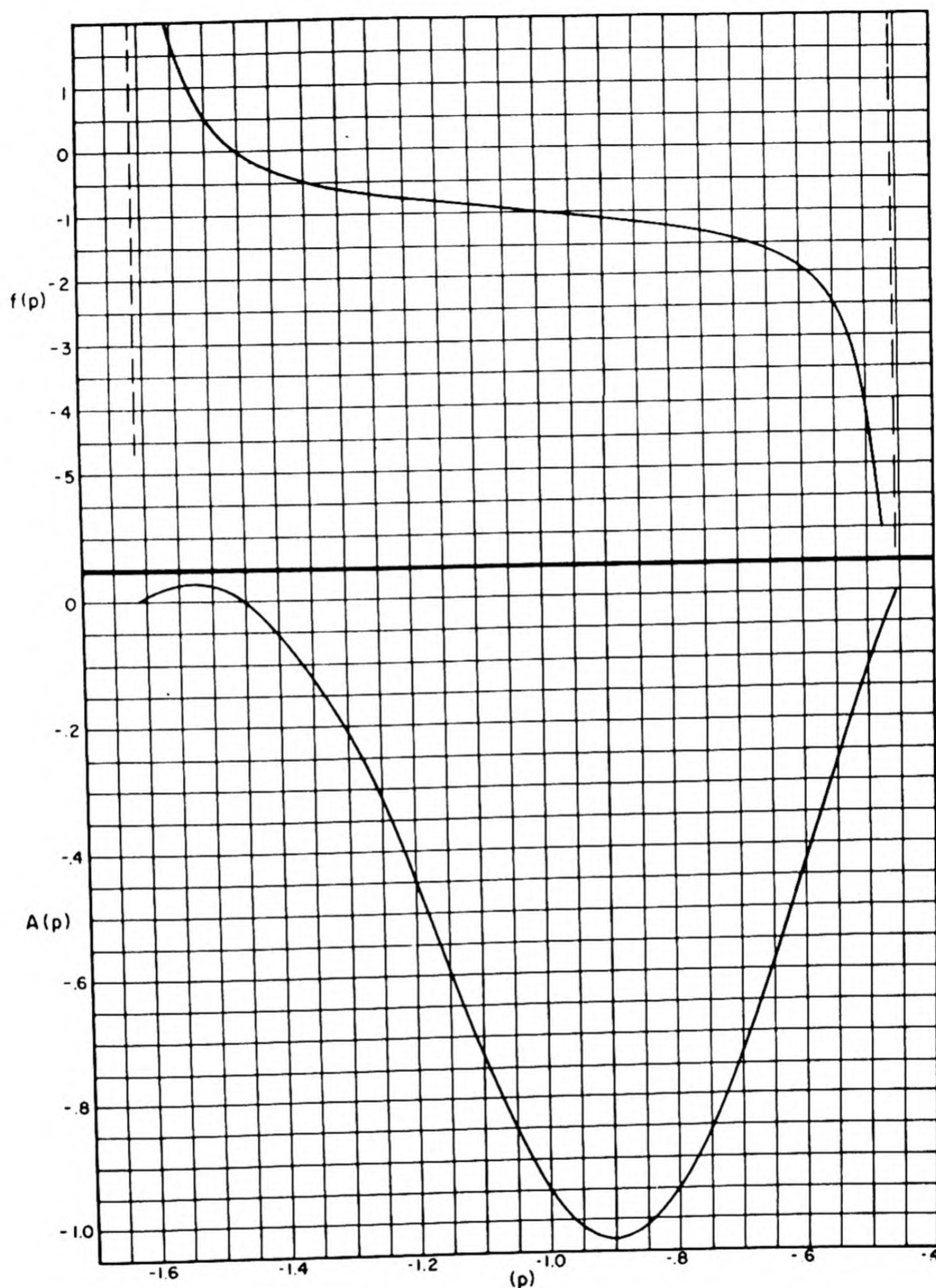


Fig. 1.6.8— Parameters Needed to Find the Neutron Level Following a Step Change in Reactivity. Submitted by Nuclear Development Associates, Inc., Dec. 15, 1952. The figure is constructed assuming a zero neutron generation lifetime and delayed neutron characteristics for U^{235} (cf. Chapter 1.2). $n(t) = n_0 \sum_i A(p_i) e^{p_i t}$. The ordinate on the upper graph is the negative reactivity change in dollars. Go horizontally from ∂k to intersection with curve. Abscissa is p_i . The lower curve is $A(p_i)$ vs p . Use of Figs. 1.6.4 to 1.6.10 yields all six values of p_i and $A(p_i)$.

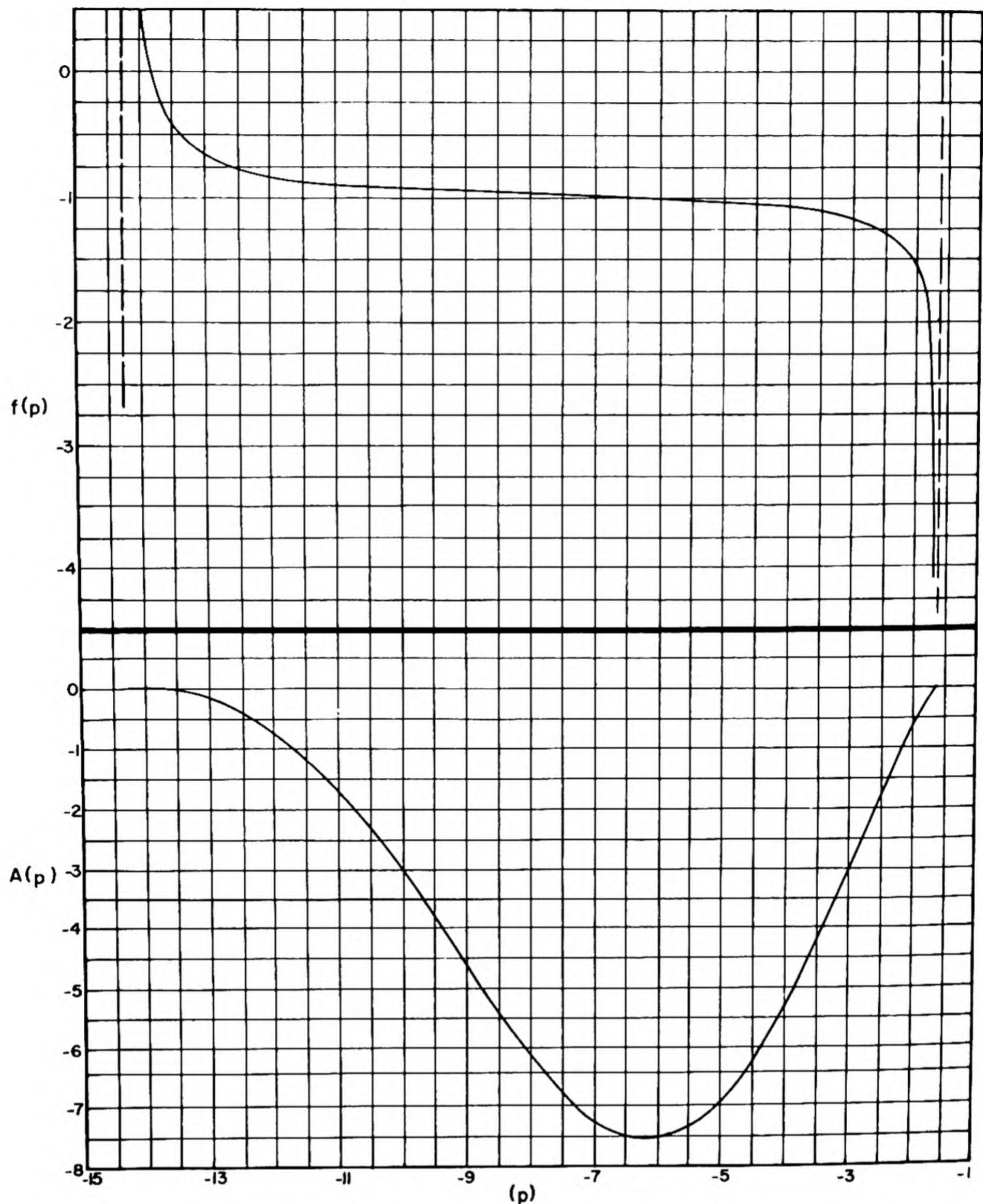


Fig. 1.6.9— Parameters Needed to Find the Neutron Level Following a Step Change in Reactivity. Submitted by Nuclear Development Associates, Inc., Dec. 15, 1952. The figure is constructed assuming a zero neutron generation lifetime and delayed neutron characteristics for U^{235} (cf. Chapter 1.2). $n(t) = n_0 \sum A(p_i)e^{p_i t}$. The ordinate on the upper graph is the negative reactivity change in dollars. Go horizontally from ∂k to intersection with curve. Abscissa is p_i . The lower curve is $A(p_i)$. The lower curve is $A(p_i)$ vs p . Use of Figs. 1.6.4 to 1.6.10 yields all six values of p_i and $A(p_i)$.

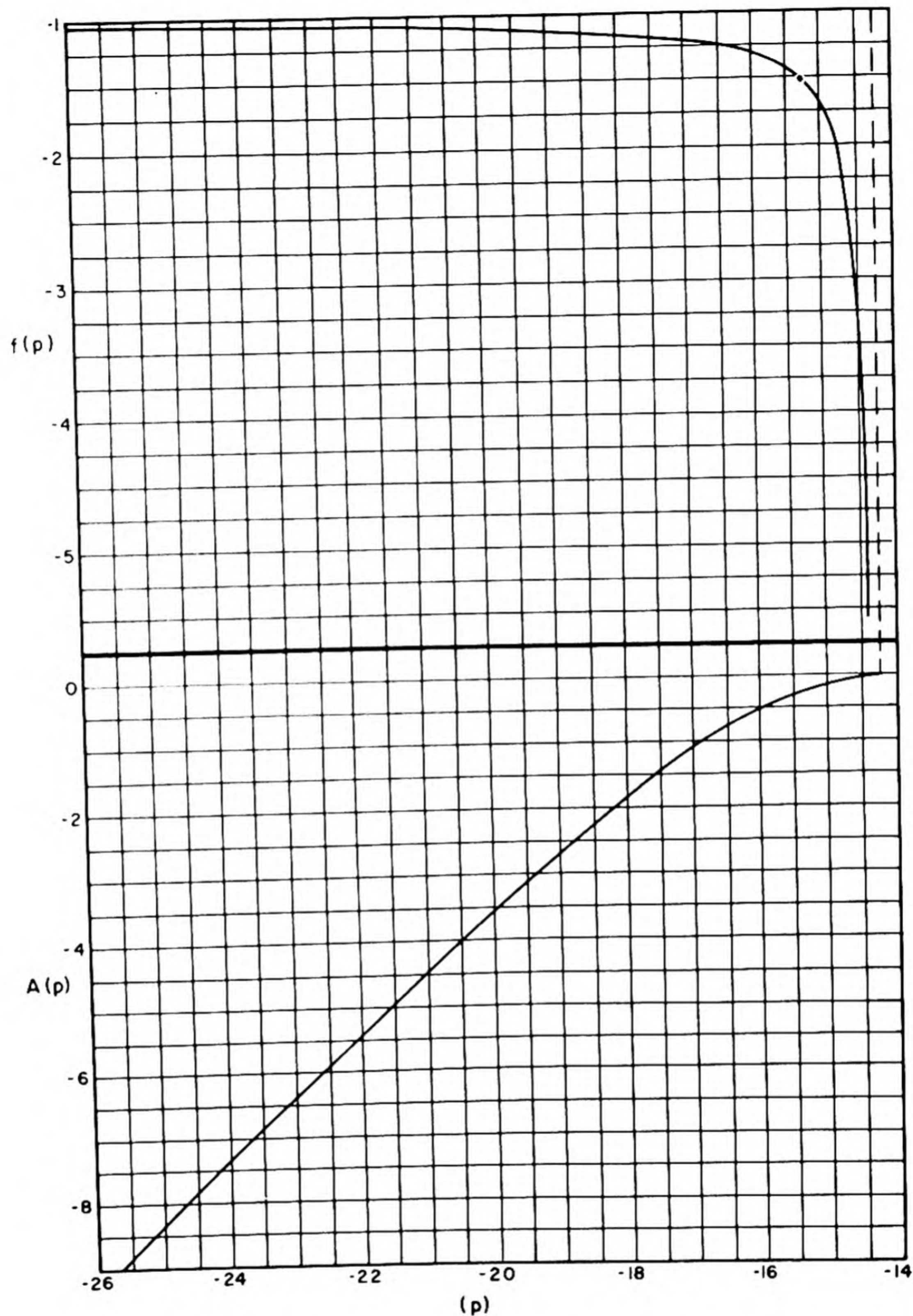


Fig. 1.6.10—Parameters Needed to Find the Neutron Level Following a Step Change in Reactivity. Submitted by Nuclear Development Associates, Inc., Dec. 15, 1952. The figure is constructed assuming a zero neutron generation lifetime and delayed neutron characteristics for U^{235} (cf. Chapter 1.2). $n(t) = n_0 \sum A(p_i)e^{p_i t}$. The ordinate on the upper graph is the negative reactivity change in dollars. Go horizontally from ∂k to intersection with curve. Abscissa is p_i . The lower curve is $A(p_i)$ vs p . Use of Figs. 1.6.4 to 1.6.10 yields all six values of p_i and $A(p_i)$.

Many people^{2,3,4} have solved the kinetic equations with $k = A + Bt$ for cases as indicated above and also for cases in which $k = 1$, $t < 0$ and $k = 1 + (dk/dt)t$ for $k > 0$. An example of this latter case is given in Fig. 1.6.11.

If $k = 1 + (dk/dt)t$ for both positive and negative times, the solution is somewhat different and depends on the source strength in the reactor.

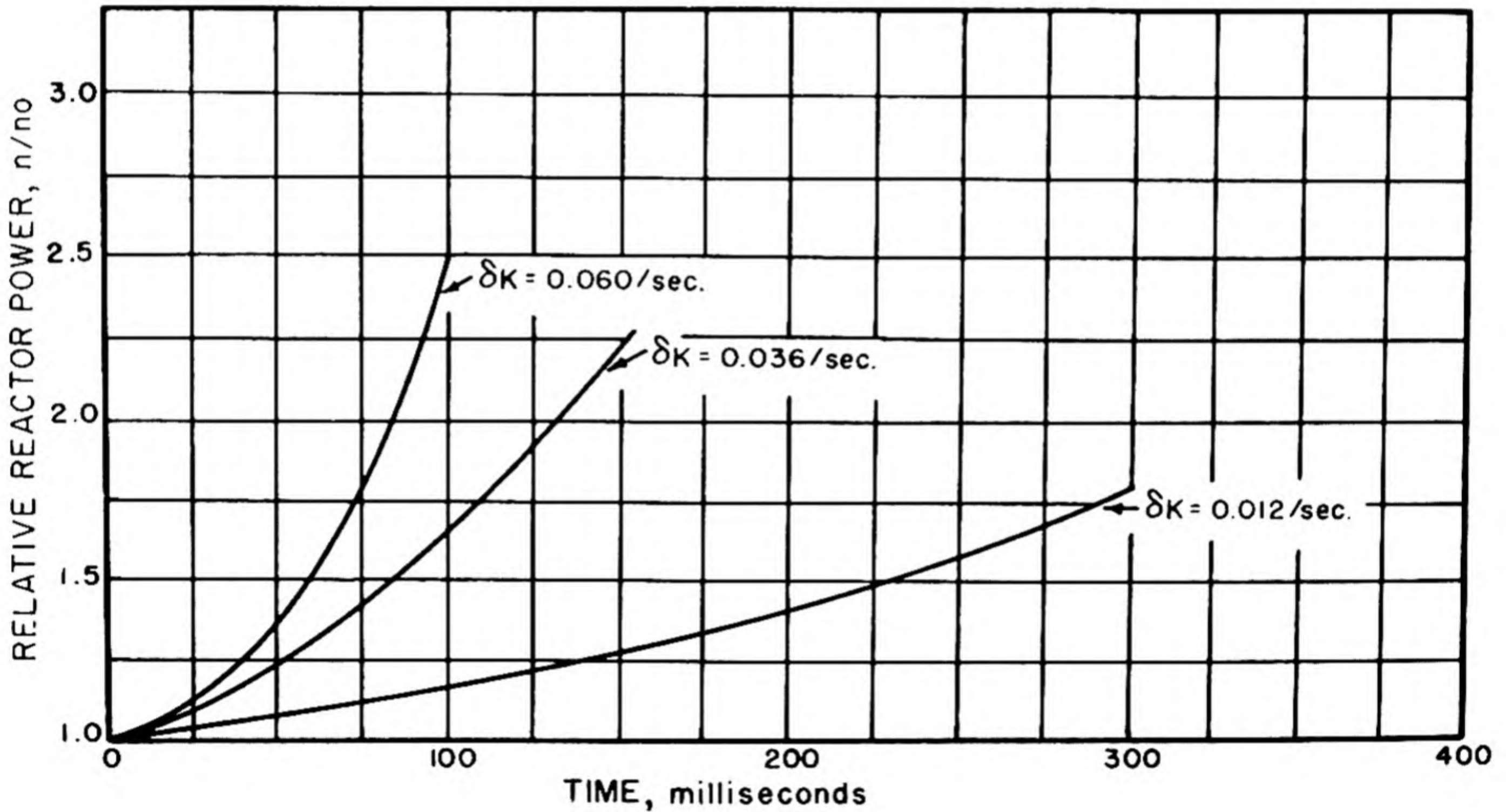


Fig. 1.6.11 — Relative Reactor Power for k Varying Linearly with Time. Reprinted from WAPD-34, Vol. I, RM-62. At time zero the reactor is critical and k commences to rise at the rate shown on each curve.

Thus, for one average neutron-delay group, neglecting the prompt lifetime, the equations for linearly varying k can be readily solved.

On the basis of the above assumptions Eq. (1) may be written:

$$0 = (k - 1)\frac{n}{l} - k\beta\frac{n}{l} + \lambda c + s \quad (28)$$

$$\frac{\partial c}{\partial t} = -\lambda c + k\beta\frac{n}{l}$$

Elimination of c gives an equation for n/l , the loss rate of neutrons. The fission rate is nearly $n/l\nu$. Thus, one has for n/l :

$$[k(1 - \beta) - 1] \frac{d}{dt} \frac{n}{ls} + (1 - \beta) \frac{n}{ls} \frac{dk}{dt} + \lambda(k - 1) \frac{n}{ls} + \lambda = 0 \quad (29)$$

which may be solved by quadrature given $k(t)$. In Fig. 1.6.12 n/l vs $(k - 1)/\beta = (t/\beta)(dk/dt)$ is plotted for $k = 1 + t dk/dt$ with various values of $\beta/(dk/dt)$ (with $\lambda = 0.05$, a value best used with $\beta = 0.004$). If at any time the change in k is stopped, the reactor period will be:

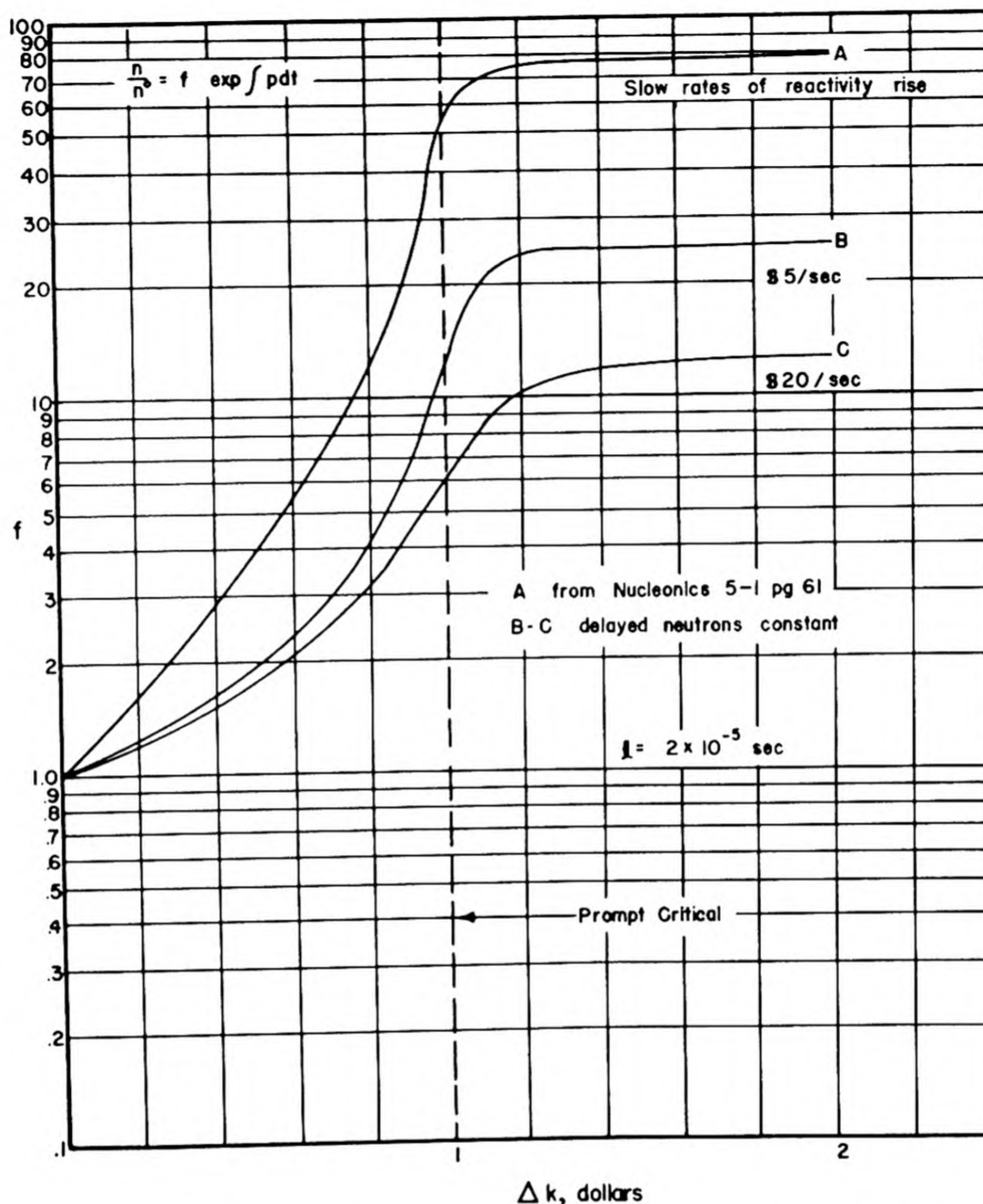


Fig. 1.6.12—Relative Reactor Power for k Varying Linearly with Time. Taken from KAPL-847 (to be published). See also, Eq. (34).

$$T = \frac{\frac{n}{n_0}}{\frac{d}{dt} \frac{n}{n_0}} = \frac{1 - k(1 - \beta)}{\lambda(k - 1)} \quad (30)$$

This period is also given in Fig. 1.6.12.

Assume the neutron flux will first be detectable after a multiplication of 10^7 . Then, if a reactor is started by increasing the reactivity at a rate of one dollar every 200 sec, the flux will become visible when the reactivity is 0.77β above delayed critical (i.e., 0.23β below prompt critical). If the reactivity is kept constant at 0.77β , the flux will continue to rise with a period of 6 sec. More accurate values of the period (calculated using six delay groups) can be obtained from Fig. 1.6.3 or 1.6.4.

The solution of Eq. (1), for k an arbitrary (specified) function of time, may be obtained numerically. The work is expedited by using:⁵

$$c_i(t) = \frac{\epsilon_i \beta_i}{1} \int_{-\infty}^t e^{-\lambda_i(t-s)} k(s)n(s)ds \quad (31)$$

to eliminate the c_i and obtain (with zero source):

$$\frac{1}{\epsilon\beta} \frac{\partial n}{\partial t} = \frac{[k(1 - \epsilon\beta) - 1]n}{\epsilon\beta} + \int_{-\infty}^t \left[\sum \lambda_i \frac{\epsilon_i \beta_i}{\epsilon\beta} e^{-\lambda_i(t-s)} \right] k(s)n(s)ds \quad (32)$$

The sum in the brackets is, for a given species of fissionable material, a universal function of $t - s$ if one uses the approximation $\epsilon_i = \epsilon$.

Plots⁶ for U^{235} of:

$$K(t) = \sum \lambda_i \frac{\beta_i}{\beta} e^{-\lambda_i t}$$

$$I(t) = \int_t^{\infty} K(s)ds \quad (33)$$

$$L(t) = \int_t^{\infty} I(s)ds$$

are given in Fig. 1.6.13.

$I(t)$ and $L(t)$ are useful in numerical integration. Thus:

$$\int_{t_1}^{t_2} K(t-s)f(s)ds = f(t_2) \left[I(t-t_2) - \frac{L(t-t_2) - L(t-t_1)}{t_2-t_1} \right]$$

$$- f(t_1) \left[I(t-t_1) - \frac{L(t-t_2) - L(t-t_1)}{t_2-t_1} \right]$$

if one may approximate $f(t)$ for t in the range t_1 to t_2 by:

$$f(t) = f(t_1) + \frac{t-t_1}{t_2-t_1} [f(t_2) - f(t_1)]$$

An approximate solution of Eq. (32) or Eq. (1) is given, for slowly varying $k(t)$, by:⁷

$$n(t) = C \sqrt{\frac{1 + \sum \frac{\epsilon_i \beta_i}{\lambda_i}}{1 + \sum \frac{\epsilon_i \beta_i / \lambda_i}{(1 + p(t) \lambda_i)^2}}} e^{\int_0^t p(t')dt'} \quad (34)$$

where $p(t)$ is the most positive root of Eq. (22) with $k = k(t)$. See Fig. 1.6.14 for applications of Eq. (34).

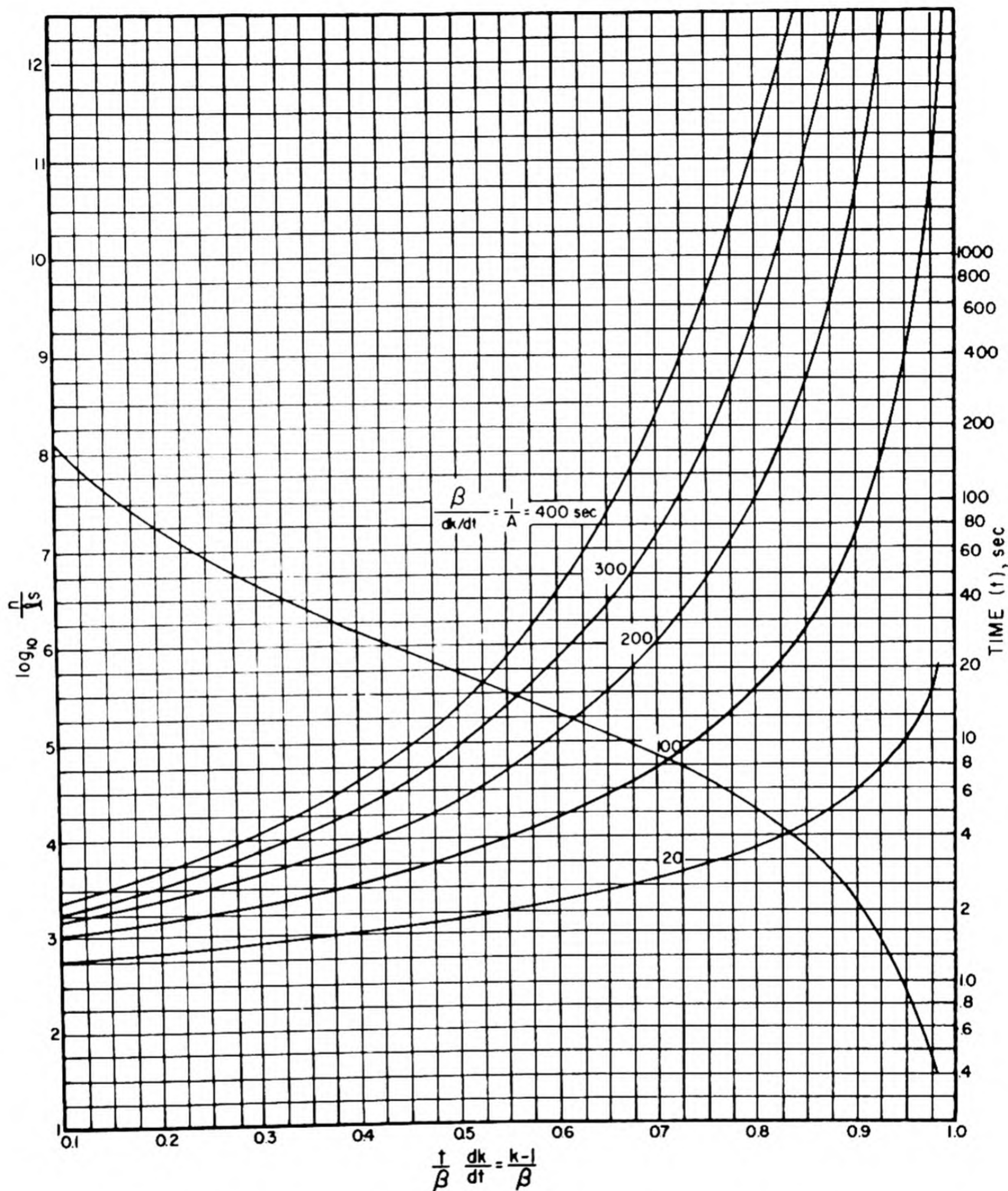


Fig. 1.6.13 — Reactor Period and Ratio of Neutron Production Rate to Source Strength for k Increasing Linearly with Time. Submitted by Nuclear Development Associates, Inc., Dec. 15, 1952. Calculations were carried out with one delay group having a mean life of 20 sec. For an example see Eq. (30) et seq in the text.

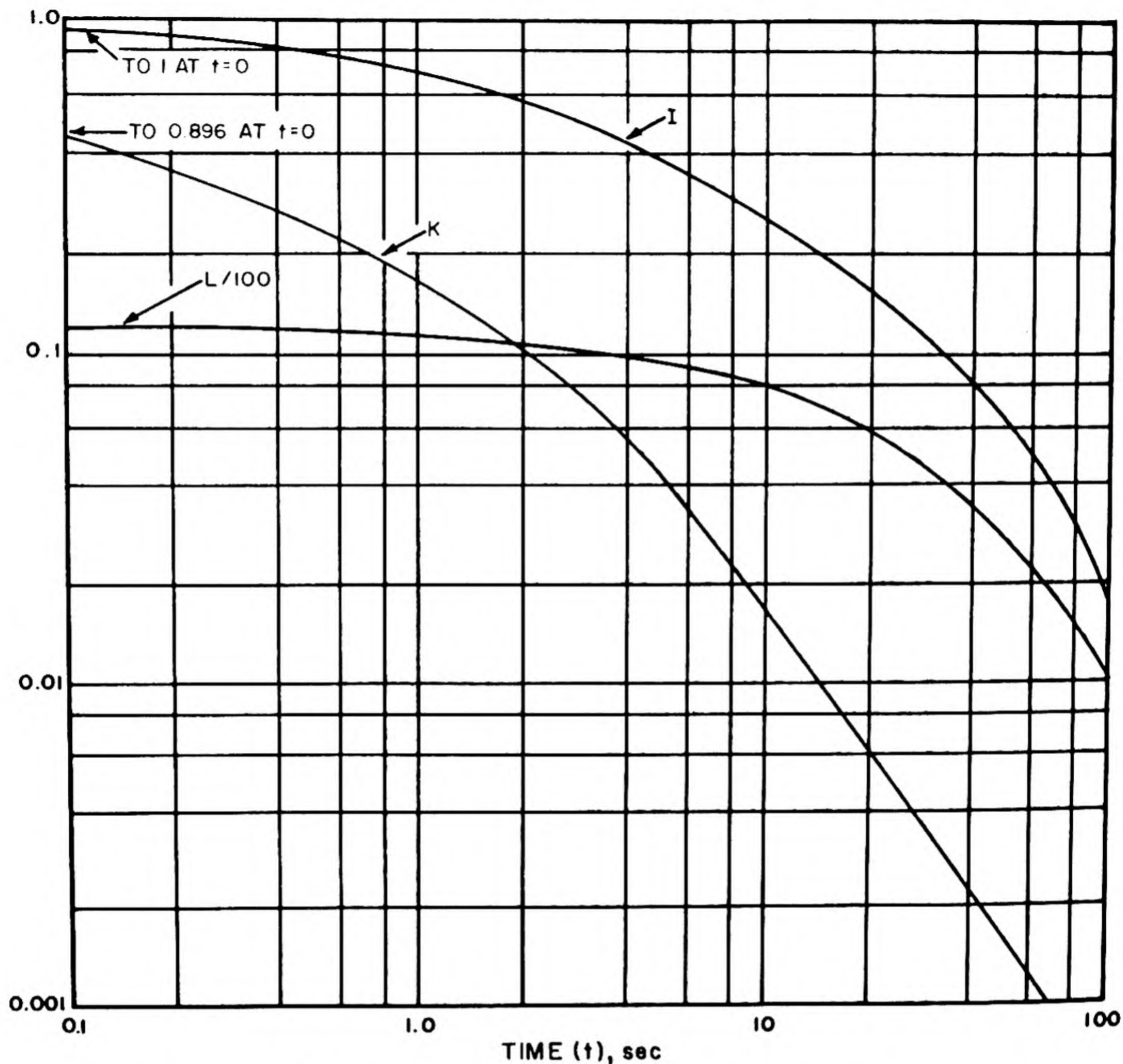


Fig. 1.6.14—Some Functions Useful when k has a Known Time Behavior. Reprinted from Reactor Physics Progress Report, KAPL-706, April 1952. See Eq. (31) et seq in the text.

INHOURS

Equation (22) may be used to determine $k - 1$ for an experimental reactor period, $T = 1/p$:

$$\begin{aligned}
 k - 1 &= \frac{1}{kT} + \epsilon\beta - \sum_i \epsilon_i \beta_i \frac{\lambda_i}{\frac{1}{T} + \lambda_i} \\
 &= \frac{1}{kT} + \sum_i \epsilon_i \beta_i \frac{\tau_i}{T + \tau_i}
 \end{aligned}
 \tag{35}$$

where $\tau_i = 1/\lambda_i$. The inhour is a unit of reactivity and is defined as a constant times the right side of Eq. (35). The definition of this constant gives for the reactivity in inhours for a period T (with τ_i, l, T in seconds):

$$I = \frac{\frac{1}{kT} + \sum_i \frac{\epsilon_i \beta_i \tau_i}{T + \tau_i}}{\frac{1}{3600k} + \sum_i \frac{\epsilon_i \beta_i \tau_i}{3600}} \quad (36)$$

Clearly, I is dimensionless and decreases as T increases. For large T , one has approximately:

$$I \approx \frac{3600}{T} \quad (37)$$

$$k - 1 \approx \frac{\sum \beta_i \tau_i}{T} \approx \frac{\sum \beta_i \tau_i}{3600} I$$

That is, the inverse of the reactor period in hours is the reactivity in units of inhours.

THE DOLLAR AS A UNIT OF REACTIVITY

The combination $(k - 1)/\beta$ occurs fairly often in the kinetic equations. This suggests the use of β as a unit of reactivity. Thus, by definition, $(k - 1)/\beta$ is the reactivity change measured in dollars (symbol \$). One one-hundredth of a dollar, as might be expected, is a cent.

REACTIVITY COEFFICIENTS AND RELATED TOPICS

Reactor dynamics is concerned with the solution of the equations of motion of a reactor system, including any external equipment with which there exists an interaction. It was indicated above that in most problems changes in the system can be represented in their effect on neutron behavior in the reactor, in terms of a single number, k , the multiplication constant.

In the following study of the changes in k arising from changes in the system, these changes are represented in terms of the thermodynamic variables of temperature and density, $T(\underline{x}, t)$, $\rho(\underline{x}, t)$, and in terms of concentrations, $z_i(\underline{x}, t)$,* of the various substances of which the reactor is constructed. Detailed consideration of control rods or other methods of obtaining control action is deferred until later in this chapter.

The starting point of these considerations is contained in Eq. (6). If one replaces k by $k + \delta k$, JN by $JN + \delta(JN)$, and KN by $KN + \delta(KN)$ in Eq. (6), where:

$$k = \frac{(w, fJN)}{(w, KN)} = 1 \quad (38)$$

there results:

$$\delta k = \frac{(w, fJN) + (w, f\delta(JN))}{(w, KN) + (w, \delta(KN))} - 1 \quad (39)$$

or, using Eq. (38):

* There is clearly one variable too many since the z_i determined ρ . It is nonetheless convenient to keep these variables.

$$\delta k = \left\{ \frac{(W, f\delta(JN))}{(W, fJN)} - \frac{(W, \delta(KN))}{(W, KN)} \right\} \left\{ \frac{1}{1 + \frac{(W, \delta(KN))}{(W, KN)}} \right\} \quad (40)$$

In Eq. (40), the second factor on the right need rarely be considered. Furthermore, unless δJ or δK are concentrated in energy or position (as in a control rod), one may replace $\delta(JN)$ and $\delta(KN)$ in Eq. (40) by $(\delta J)N$ and $(\delta K)N$, respectively. This simpler perturbation treatment yields:

$$\delta k = \frac{(W, f\delta JN)}{(W, fJN)} - \frac{(W, \delta KN)}{(W, KN)} \quad (41)$$

[It may be remarked that the two denominators on the right in Eq. (41) are equal, as follows from Eq. (38).]

In applying Eq. (41), it is often useful to write δk as an integral over the reactor volume:

$$\delta k = \int \left\{ \frac{\delta k}{\delta T} \delta T + \sum_i \frac{\delta k}{\delta z_i} \delta z_i \right\} dV \quad (42)$$

This expression defines the variational derivatives $\delta k/\delta T$, $\delta k/\delta z_i$. In Eq. (42), over-all density changes correspond to $\delta z_i/z_i = \delta\rho/\rho$, and the effect of such a density change is given by:

$$\delta k = \int \left(\sum_i z_i \frac{\delta k}{\delta z_i} \right) \frac{\delta\rho}{\rho} dV = \int \frac{\delta k}{\delta\rho} \delta\rho dV \quad (43)$$

which also defines $\delta k/\delta\rho$.

DENSITY EFFECTS

Density changes in the reactor change macroscopic cross sections and diffusion coefficients. Thus, for any macroscopic cross section, σ :

$$\frac{\delta\sigma}{\sigma} = \frac{\delta\rho}{\rho} \quad (44)$$

whereas, a diffusion coefficient, D , varies inversely as a cross section:

$$\frac{\delta D}{D} = - \frac{\delta\rho}{\rho} \quad (45)$$

In computing the effect of the density change, the motion of the boundary should not be neglected. Thus, in a slab reactor, the diffusion coefficient before and after an expansion might look like Fig. 1.6.15.

In such a case, δD may be given as in Fig. 1.6.16. It is the positive part of δD which, in a diffusion-theory reactor model, gives rise to the portion of δk coming from the change in buckling. Similar procedures apply to cross sections and the like at core-reflector interfaces.

Consider the "Two-group, Bare, Thermal Reactor" discussed previously with density changes arising only from expansion (no removal of material as in a liquid reactor).

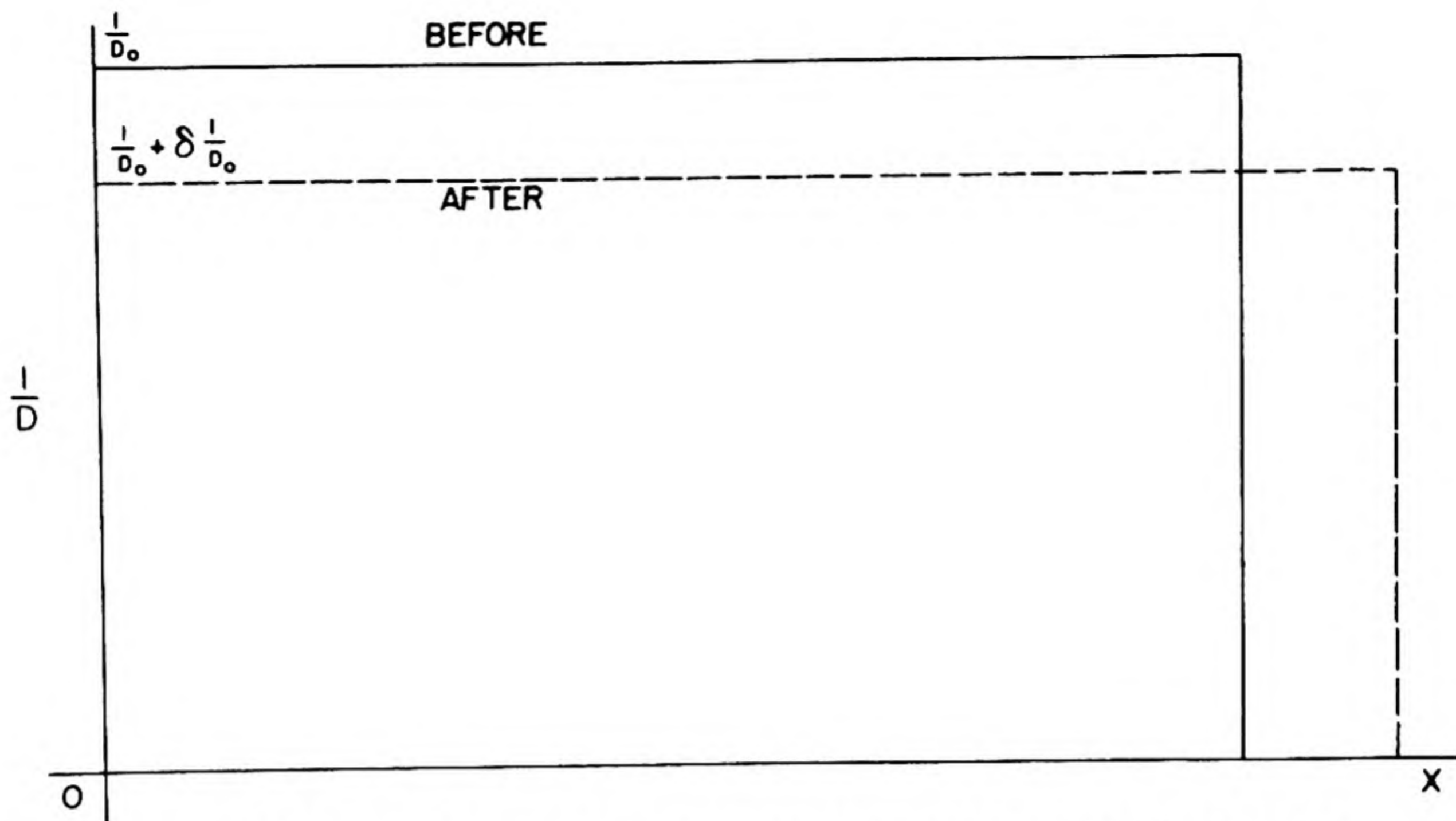


Fig. 1.6.15 — Diffusion Coefficient Before and After a Density Change. Submitted by Nuclear Development Associates, Inc. Dec. 15, 1952. The reactor is a bare slab.

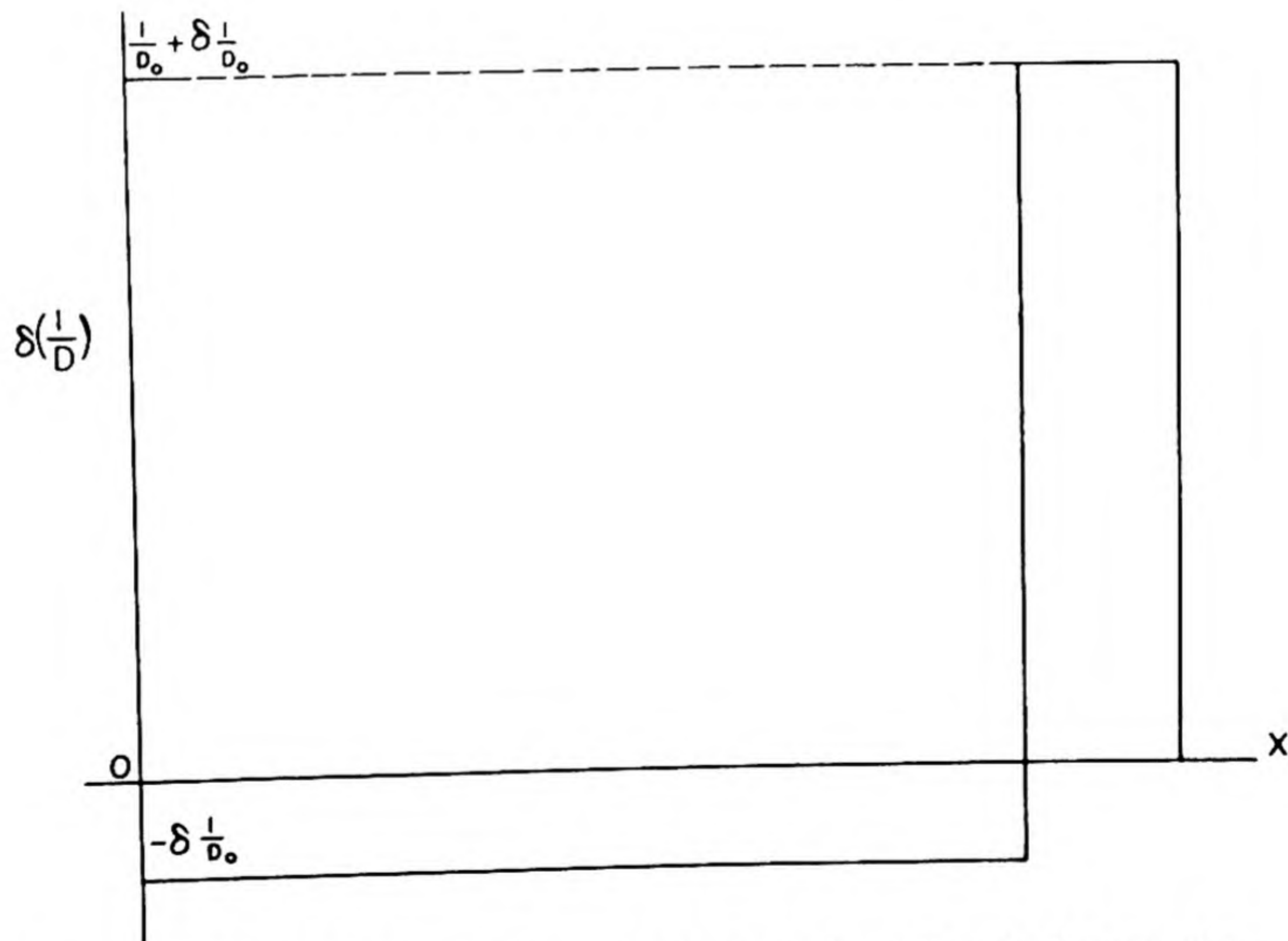


Fig. 1.6.16 — Change in Diffusion Coefficient After a Density Change. Submitted by Nuclear Development Associates, Inc. Dec. 15, 1952. The reactor is a bare slab.

Clearly, from the conservation of mass law, the motion of the boundary is given by:

$$\delta a = - \frac{\int \delta \rho \, dV}{\int \rho \, dS} = - \frac{\int \delta \rho \, dV}{4\pi \rho a^2} \quad (46)$$

On applying Eqs. (9), (41), (42), and (46), there results:

$$\left[\int \left(\frac{\sin \frac{\pi r}{a}}{r} \right)^2 dV \right] \rho \frac{\delta k}{\delta \rho} = \left\{ 2 - \frac{\sigma_{SD} v_f}{L_f} - \frac{\sigma_a v_s}{L_s} \right\} \times \left\{ \left[\left(\frac{\sin \frac{\pi r}{a}}{r} \right)^2 \right]_A + \left[\left(\frac{d}{dr} \frac{\sin \frac{\pi r}{a}}{\frac{\pi r}{a}} \right)^2 \right]_B + \left[- \left(\frac{d}{dr} \frac{\sin \frac{\pi r}{a}}{\frac{\pi r}{a}} \right)^2 \right]_{r=a} \right\} \quad (47)$$

where $[]_A$ arises from cross-section changes, $[]_B$ from diffusion-coefficient changes, and $[]_C$ from boundary motion. If $\delta \rho$ is uniform (independent of position):

$$\begin{aligned} \delta k &= \delta \rho \int \frac{\delta k}{\delta \rho} dV \\ &= \frac{\delta \rho}{\rho} \left\{ 2 - \frac{\sigma_{SD} v_f}{L_f} - \frac{\sigma_a v_s}{L_s} \right\} \times \frac{4}{3} \end{aligned} \quad (48)$$

DIRECT TEMPERATURE EFFECTS

The effect of temperature changes alone (in addition to the effect of the concomitant density changes) occurs through changes in the cross sections which are functions of the relative velocities of the neutrons and nuclei. The relative velocity changes with temperature for two reasons:

- (1) The absolute velocities of the nuclei change (Doppler effect).
- (2) The thermal-neutron velocity distribution changes.

If one considers a nuclear process with macroscopic cross section $\sigma(s)$ as a function of neutron speed, if he assumes that this cross section is a function of relative speeds of neutron and atom only, and if the number of neutrons having a speed between s and $s + ds$ is $N(s)ds$, then an effective cross section, $\sigma^*(s)$, may be so defined that:

$$\int_0^\infty \sigma^*(s) s N(s) ds \quad (49)$$

is the total number of processes under discussion that take place per unit time.

Let $Q(y) dy$ be the probability that the speed of the nuclei is between y and $y + dy$; then, if the neutron and nucleus velocity vectors are randomly oriented:⁸

$$\sigma^*(s) = \int_0^\infty \frac{x^2 \sigma(x)}{2s^2} \int_{|x-s|}^{|x+s|} \frac{Q(y)}{y} dy dx \quad (50)$$

In almost all cases of interest, the distribution of nuclear speeds can be taken as Maxwellian (cf. Chapter 1.3), and $Q(y)$ is given by:

$$Q(y) = \frac{4}{\sqrt{\pi}} \frac{1}{\alpha^3} y^2 e^{-\frac{y^2}{\alpha^2}} \quad (51)$$

where: $\alpha = (2kT/M)^{1/2}$

M = atomic mass

k = Boltzmann's constant

T = absolute temperature

In this case:

$$\sigma^*(s) = \frac{1}{\alpha s^2 \sqrt{\pi}} \int_{-\infty}^{\infty} |x| \sigma(|x|) e^{-\left(\frac{x-s}{\alpha}\right)^2} x dx \quad (52)$$

Clearly, the major contribution to the integral in Eq. (52) comes from x in the range $s \pm \alpha$. If $|x| \sigma(|x|)$ does not change much in this range, it may be removed outside as $s \sigma(s)$ with the result:

$$\sigma^*(s) \approx \sigma(s) \quad (53)$$

Note Eq. (53) is a precise result for $1/v$ cross sections.

Equation (52) is of primary interest in studying the effect on resonance capture of the spreading of sharp lines by the nuclear motion. This spread, known as "Doppler broadening," is seen clearly in Eq. (52), since $s \sigma^*(s)$ will be of appreciable size over a range 2α greater than $x \sigma(x)$. It was seen in the discussion of lattices in Chapter 1.5 that the resonance escape probability depends upon the evaluation of the integral:

$$\int \frac{\sigma_a^*}{1 + \frac{\sigma_a^*}{\sigma_s}} \frac{dE}{E}$$

When σ_a^* is varying rapidly, a factor of $1/E$ can be taken outside the integral sign with little error. For convenience in calculation, one can then investigate the quantity F , defined⁹ by:

$$F = \int \frac{\sigma_a^*}{1 + \frac{\sigma_a^*}{\sigma_s}} dE / \int \sigma_a^* dE \quad (54)$$

σ_a^* may be obtained from Eq. (52) if we use for σ_a the Breit-Wigner formula (cf. Eq. (26) of Chapter 1.2).

By introducing the reduced energy variable:

$$\xi = \frac{E - E_r}{\Gamma/2} \quad (55)$$

one may write approximately:

$$\frac{\sigma_a^*(E)}{(\sigma_a)_{\max}} = \psi(\xi) = \frac{1}{2\sqrt{\pi\theta}} \int_{-\infty}^{\infty} \frac{d\xi'}{1 + \xi'^2} e^{-\frac{(\xi - \xi')^2}{4\theta}} d\xi' \quad (56)$$

where:

$$\theta = \frac{4E_r kT}{A_m \Gamma^2} \quad (57)$$

A_m is the ratio of nuclear mass to neutron mass and E_r and Γ the energy and width of the resonance, respectively. In obtaining Eq. (56), the expansion:

$$\sqrt{\frac{2E}{\Gamma}} = \sqrt{\xi + \frac{2E_r}{\Gamma}} \simeq \sqrt{\frac{2E_r}{\Gamma}} \left(1 + \frac{\Gamma\xi}{4E_r}\right) \quad (58)$$

was used in the exponential.

For homogeneous mixtures:²

$$F \simeq \frac{2 + A(P - 1)}{P\sqrt{2(1 + P) + \gamma A^2}} \quad (59)$$

where:

$$P = \sqrt{1 + \gamma A(2 - A)}$$

$$\gamma = \frac{(\sigma_a)_{\max}}{\sigma_s}$$

and A is the root of:

$$A(5 - 4A + A^2) = 2\sqrt{\frac{\pi}{2\theta}} e^{\frac{1}{2\theta}} \operatorname{erfc}\left(\frac{1}{\sqrt{2\theta}}\right)$$

where:

$$\operatorname{erfc}(x) = 1 - \frac{2}{\sqrt{\pi}} \int_0^x e^{-\mu^2} d\mu = \frac{2}{\sqrt{\pi}} \int_x^\infty e^{-\mu^2} d\mu$$

This result is exact in the following limiting cases:

$$\left. \begin{array}{l} \theta = 0 \\ \theta = \infty \end{array} \right\} \text{any } \gamma$$

$$\left. \begin{array}{l} \gamma = 0 \\ \gamma = \infty \end{array} \right\} \text{any } \theta$$

Roe¹⁰ has treated the case of inhomogeneous mixtures, where self-absorption effects are important, in slab geometry. He considers a one-velocity problem in which the resonance absorbers are in the form of plane slabs separated by slabs of moderator. Neutrons are assumed to be produced uniformly in the moderator. In Fig. 1.6.17, F has been plotted vs $\mu\tau N(\theta)$. The auxiliary function $N(\theta)$ is given in Fig. 1.6.18. Figure 1.6.19 gives the function:

$$\frac{\theta \frac{\partial F}{\partial \theta}}{1 - N(\theta)} = \frac{T \frac{\partial F}{\partial T}}{1 - N(\theta)}$$

which is useful for calculating temperature effects. The quantities involved are defined as follows:

l_a = foil thickness

l_m = moderator thickness between foils

$\tau = \sigma_{a_{\max}} l_a$

σ_{sf} = macroscopic scattering cross section of foil

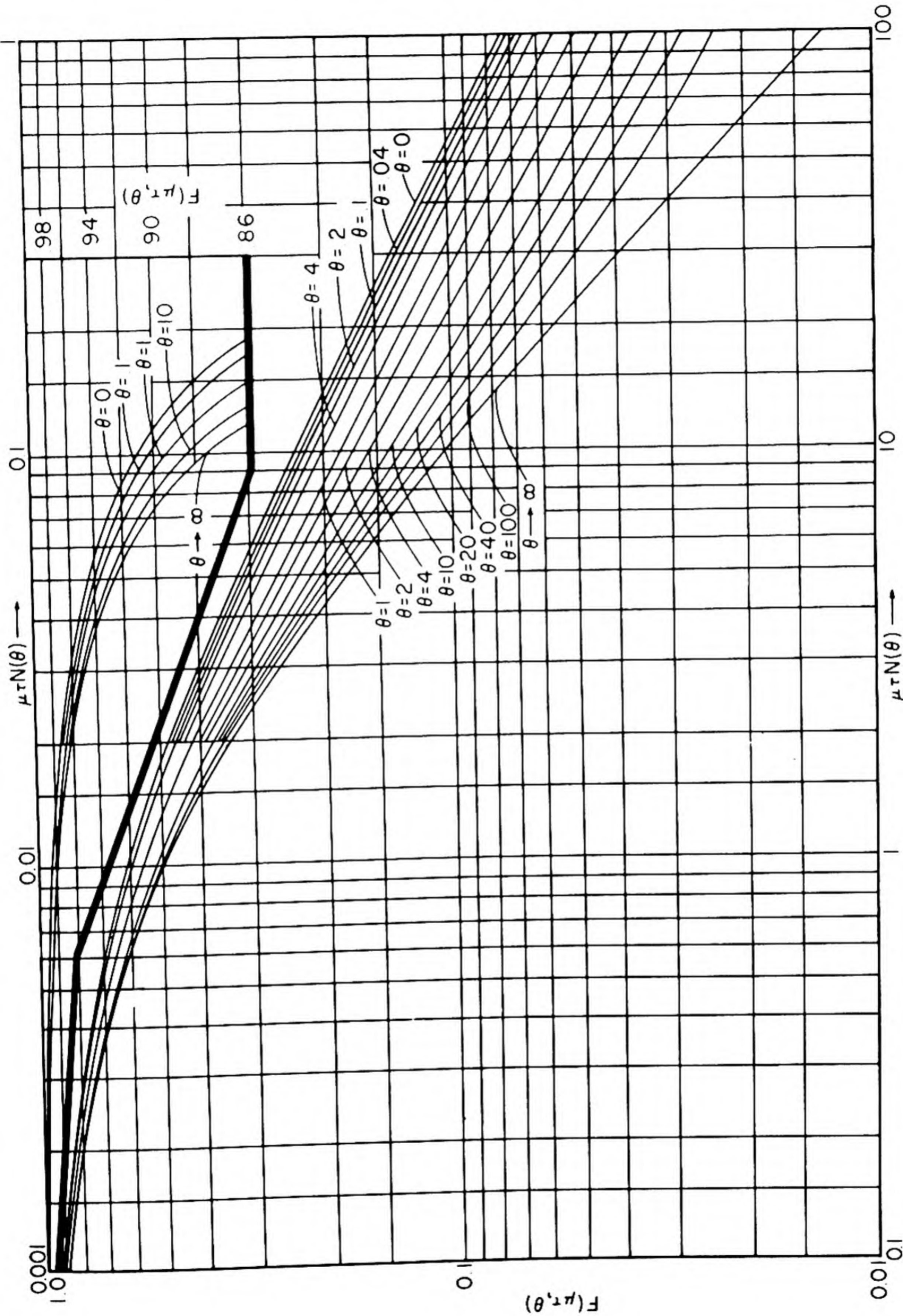


Fig. 1.6.17—Curves for Calculating the Effect of Foil Self-absorption and Doppler-broadening on Resonance Absorption. Reprinted from a personal communication from G. M. Roe at KAPL. When using curves above the heavy line, use the ordinate scale on the right. For use of these curves see text Eq. (54) et seq.

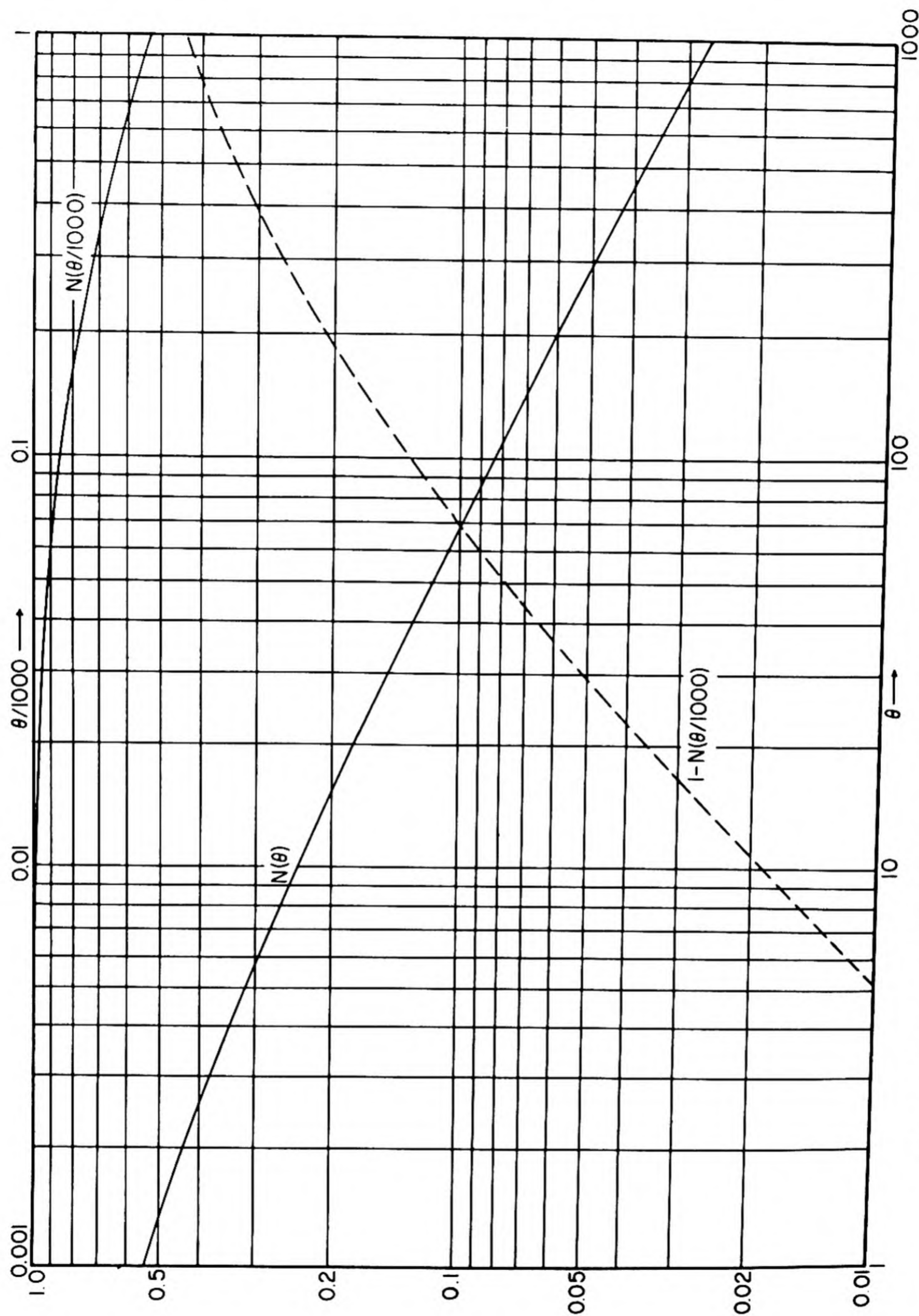


Fig. 1.6.18—Curves for Calculating the Effect of Foil Self-absorption and Doppler-broadening on Resonance Absorption. Reprinted from a personal communication from G. M. Roe at KAPL. For use of these curves see text following Eq. (54).

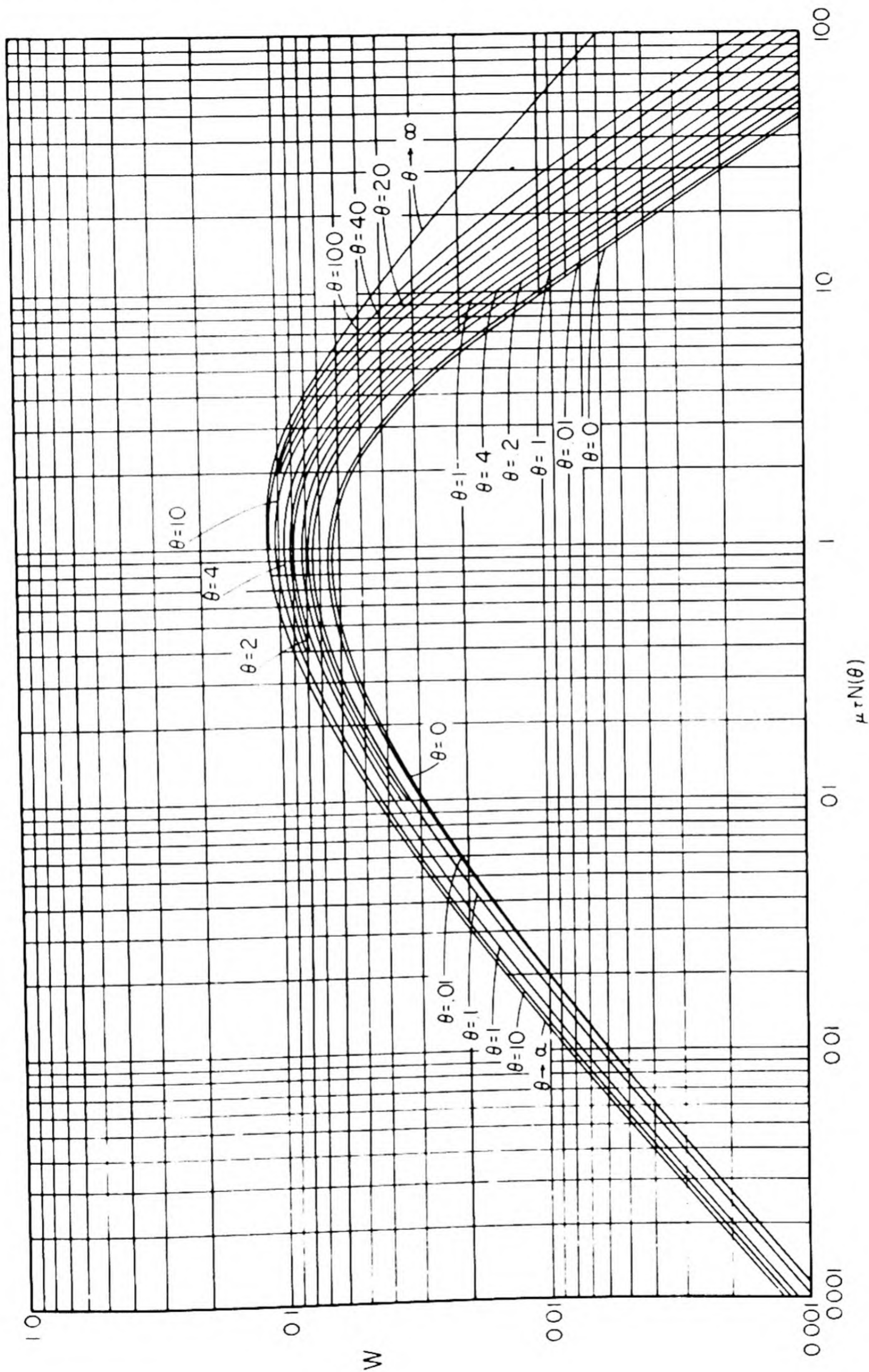


Fig. 1.6.19—Curves for Calculating the Effect of Temperature on Resonance Absorption. Reprinted from a personal communication from G. M. Roe at KAPL. $W = [\theta(\partial F/\partial \theta)/(1-N)] = [T(\partial F/\partial T)/(1-N)]$. See text following Eq. (54).

σ_{sm} = macroscopic scattering cross section of moderator

$$1/\mu = 1/\mu_0 + 2l_a\sigma_{sf}$$

$$a = (1/\epsilon)[l_m + (1 - \epsilon)l_a]\sigma_{sm}$$

ϵ = fraction of foil plane actually occupied by the foil

A plot of μ_0 vs a is given in Fig. 1.6.20.

The effect of the energy change of thermal neutrons may be calculated only on the basis of some model. The customary model assumes that the thermal neutrons are in fact represented by a density:

$$n_{th}(\underline{r}, E) = R(\underline{r})f(E, T) \quad (60)$$

where T is an appropriate mean temperature of the thermal neutrons and $f(E, T)$ is the corresponding Boltzmann distribution of neutron energies. In a weakly absorbing medium, Eq. (60) is a good approximation, with T the moderator temperature averaged over a suitable region. For absorbing media, the thermal neutrons on the average will have higher energies than those corresponding to the moderator temperature. The determination of an appropriate temperature is discussed in Chapter 1.3.

If it is assumed that T and δT are known, the value of δR may be obtained as follows:

$$f(E, T)dE = \frac{2}{\sqrt{\pi}} e^{-\frac{E}{kT}} \sqrt{\frac{E}{kT}} \frac{1}{kT} dE \quad (61)$$

The effective value of any cross section, σv , (σ in area per atom) as it appears in $n_{th}v\sigma$ is given by:

$$\overline{\sigma v}(T) = \int_0^\infty f(E, T)(\sigma v)(E)dE \quad (62)$$

so that:

$$\frac{\partial}{\partial T}(\overline{\sigma v}) = \int_0^\infty \frac{\partial f}{\partial T}(\sigma v)(E)dE \quad (63)$$

Often σv is independent of energy, in which case $\partial/\partial T(\overline{\sigma v}) = 0$. If σ is independent of energy:

$$\frac{\partial \overline{\sigma v}}{\partial T} = \sigma \frac{\partial \bar{v}}{\partial T} \quad (64)$$

where $\bar{v} = 2/\sqrt{\pi} \sqrt{2kT/m}$. Another case of interest arises in the evaluation of $\overline{D_{th}v}$. Since D_{th} is a reciprocal scattering cross section, one is interested in:

$$\left(\frac{\bar{v}}{\sigma_{sc}} \right)$$

For σ_{sc} independent of energy:

$$\frac{\frac{\partial}{\partial T} \overline{D_{th}v}}{\overline{D_{th}v}} = \frac{1}{\bar{v}} \frac{\partial \bar{v}}{\partial T} = \frac{1}{2} \frac{1}{T} \quad (65)$$

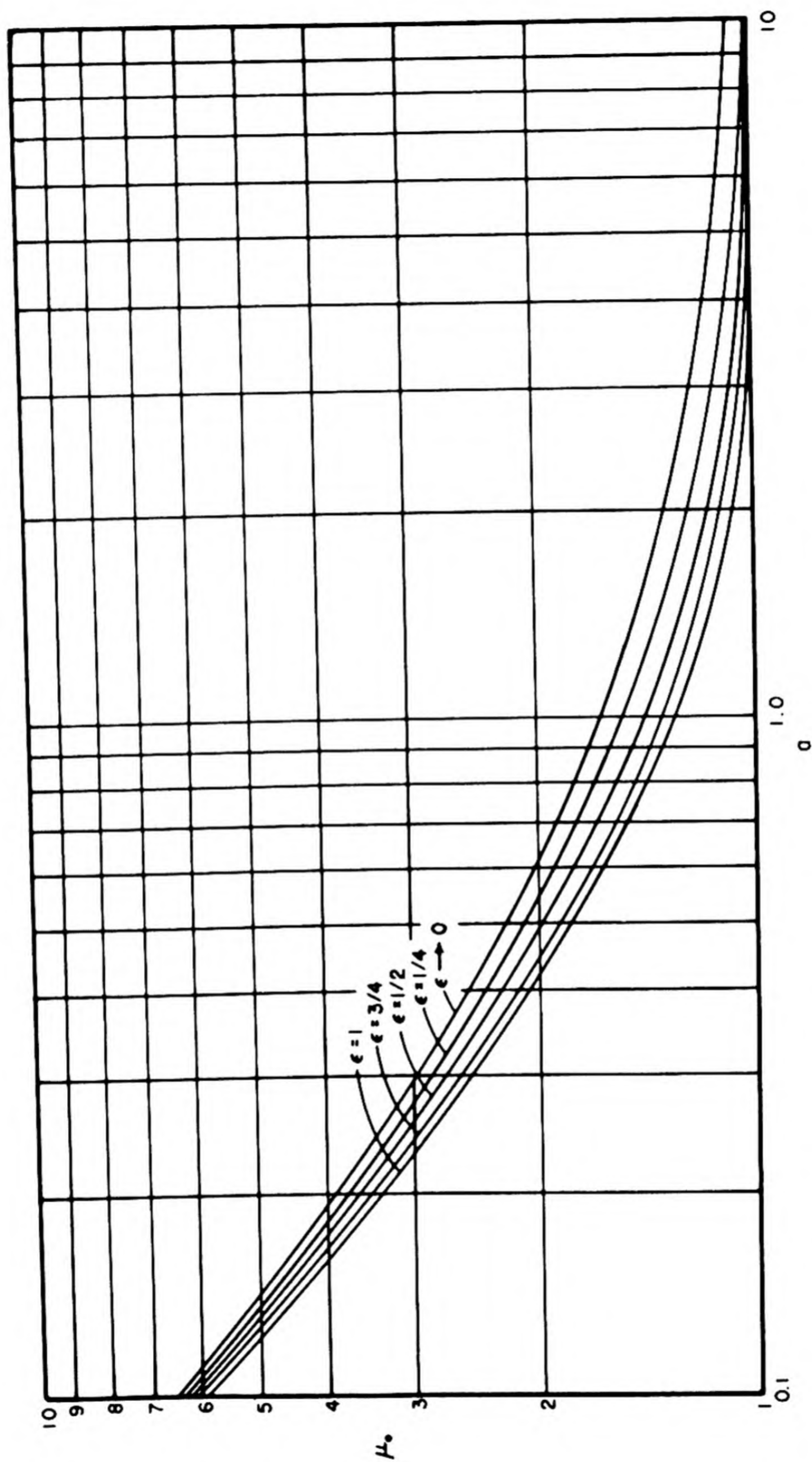


Fig. 1.6.20—Curves for Calculating the Effect of Foil Self-absorption and Doppler-broadening on Resonance Absorption. Reprinted from a personal communication from G. M. Roe at KAPL. For use of these curves see text following Eq. (54).

In terms of the bare two-group example previously considered, if one assumes that δT is independent of position, the reactivity change from these effects is given by (omitting the bar over the quantities):

$$\int \frac{\delta k}{\delta T} dV = \frac{1}{\sigma_f v_s} \frac{\partial}{\partial T} (\sigma_f v_s) - \frac{\sigma_a v_s}{L_s} \frac{\partial}{\partial T} (\sigma_a v_s) - \frac{\frac{\pi^2}{a^2} D_f v_f}{L_f} \frac{\partial (D_s v_s)}{\partial T} \quad (66)$$

In some cases, the last term on the right in Eq. (66) may be the major term. For σ_{sc} independent of energy, it contributes a negative temperature coefficient of:

$$-\int \frac{\partial k}{\partial T} dV = \frac{\frac{\pi^2}{a^2} D_s v_s}{L_s} \frac{1}{2T} \quad (67)$$

which gives a coefficient of -10^{-4} per $^{\circ}\text{C}$ at room temperature if $\frac{\frac{\pi^2}{a^2} D_s v_s}{L_s} = 0.06$.

CONCENTRATION EFFECTS

The macroscopic cross section, σ_r , for any process, r , may be written as:

$$\sigma_r = \sum_i \frac{\partial \sigma_r}{\partial z_i} z_i \quad (68)$$

where z_i is the concentration (in any units) of the i 'th nuclear species and $\partial \sigma_r / \partial z_i$ is the microscopic cross section for process r in nuclear species i (in corresponding units). From this remark, it follows that:

$$\delta \sigma_r = \sum_i \frac{\partial \sigma_r}{\partial z_i} \delta z_i \quad (69)$$

or:

$$\frac{\delta \sigma_r}{\sigma_r} = \frac{\sum_i \left(\frac{\partial \sigma_r}{\partial z_i} z_i \right) \frac{\delta z_i}{z_i}}{\sum_i \left(\frac{\partial \sigma_r}{\partial z_i} z_i \right)} \quad (70)$$

Equation (69) or Eq. (70) together with Eq. (41) permits calculation of δk in a given situation.

Concentration changes in the reactor may be purposely introduced. For example, in a liquid reactor, the fuel concentration may be varied as a means of control, or in a water-moderated reactor, a control mechanism may be the addition of a soluble neutron absorber in the water.

In addition, in reactors operating at neutron fluxes greater than approximately 10^{12} $\text{n}/(\text{cm}^2)(\text{sec})$, the neutrons themselves introduce concentration changes. For the fuel concentration decreases and the fission product concentration increases as the reactor continues in operation.

Thus, if $z_i(\underline{x}, t)$ is the concentration of any stable nuclear species i not formed in fission, then owing to burn-up:

$$\frac{1}{z_i} \frac{\partial z_i}{\partial t} = - \int \int \frac{\partial \sigma_a}{\partial z_i} v N \frac{d\omega}{4\pi} dE \quad (71)$$

so that:

$$\left[\int \int \frac{\partial \sigma_a}{\partial z_i} v N \frac{d\omega}{4\pi} dE \right]^{-1} \quad (72)$$

is the mean life of a stable nucleus of type i at position \underline{x} at time t . In particular, Eq. (71) applies to the fissionable material concentration, provided that the reactor contains no fertile material.

If z_f is fuel concentration:

$$\int \delta z_f \frac{\delta k}{\delta z_f} dV = \frac{(W, f \frac{\delta J}{\delta z_f} \delta z_f N) - (W, \frac{\delta K}{\delta z_f} \delta z_f N)}{(W, f J N)} \quad (73)$$

where:

$$z_f \frac{\delta J}{\delta z_f} N = \int \int \nu(E) \sigma_f(E) v N dE \frac{d\omega}{4\pi} = J N \quad (74)$$

and:

$$\frac{\delta K}{\delta z_f} N = \int \frac{\partial \sigma_a(E, \underline{x})}{\partial z_f} v N \frac{d\omega}{4\pi} \quad (75)$$

Early in the reactor's life, it is known that:

$$\delta z_f = A J N \quad (76)$$

where A is a constant proportional to the total energy produced by the reactor.

For the standard example introduced earlier (bare, spherical, two-group, thermal reactor), the influence of fuel burn-up may be evaluated as follows:

Define the average burn-up as:

$$\overline{\delta z_f} = \frac{\int \delta z_f dV}{V} < 0$$

Then, at least early in the reactor's life:

$$\overline{\delta z_f} = V \overline{\delta z_f} \frac{\sin \frac{\pi}{a} r}{r} / \int \frac{\sin \frac{\pi}{a} r}{r} dV \quad (77)$$

since, from Eq. (76), the concentration change has the same spatial dependence as neutron density. It is interesting to compare the reactivity change in this case with that for a uniform concentration change $(\delta z_f)_u$. From Eqs. (73), (74), and (75), it can be shown that:

$$(\delta k)_u = \frac{(\delta z_f)_u}{z_f} \left[1 - f \frac{v_s \sigma_a}{L_s} \right] = \frac{\delta M}{M} \left[1 - f \frac{v_s \sigma_a}{L_s} \right]$$

where f is the thermal utilization σ_{af}/σ_a and that if δz_f is not uniform it should be weighted with the square of the flux.* Thus:

$$\frac{\delta k}{\delta z_f} = \frac{(\delta k)_u}{(\delta z_f)_u} \frac{\sin^2 \frac{\pi r}{a} / r^2}{\int \frac{\sin^2 \pi r / a}{r^2} dV} \quad (78)$$

The reactivity change $(\delta k)_B$ resulting from the distribution of depletion given by Eq. (77) is:

$$\delta k_B = \frac{(\delta k)_u \frac{\overline{\delta z_f}}{(\delta z_f)_u} \int \left(\frac{\sin \frac{\pi r}{a}}{r} \right)^3 dV}{\int \frac{\sin \frac{\pi r}{a}}{r} dV \int \left(\frac{\sin \frac{\pi r}{a}}{r} \right)^2 dV}$$

For the same total depletion:

$$\overline{\delta z_f} = (\delta z_f)_u$$

one finds:

$$\frac{(\delta k)_B}{(\delta k)_u} = \frac{2}{3\pi} \int_0^\pi \frac{\sin^3 x}{x} dx = 2 \quad (79)$$

so that the burned fuel has twice as much effect on the reactivity as an equal amount of uniform depletion. For a bare slab reactor, the 2 in Eq. (79) becomes $4/3$.

Another concentration effect of interest is that resulting from fission-product poisons. These may be considered as consisting of the Xe^{135} chain, the Sm chain, and all the other poisons. The others may each be described approximately by the equation:†

$$\frac{\partial z_i}{\partial t} = + \gamma_i \iint \sigma_f v N \frac{d\omega}{4\pi} dE - z_i \iint \frac{\partial \sigma_a}{\partial z_i} v N \frac{d\omega}{4\pi} dE \quad (80)$$

an equation which differs from Eq. (71) only by the source term. Here γ_i is the yield (nuclei per fission) of species i . This neglects the time necessary for the nuclei formed in fission to decay into stable (or long-lived) species i . Note that the equilibrium value of z_i may be obtained from Eq. (80) by setting $\partial z_i / \partial t$ equal to zero. Further, in a ther-

* All results based on Eq. (73) in this section are valid when the changes in concentration are not large enough to produce a major distortion of the flux pattern. Morehouse and Young¹¹ and Chernick¹² have treated exactly the case of a concentration change proportional to flux for bare slab and spherical reactors. In addition, Chernick treats a slab reactor with infinite reflector and cylindrical reactors and makes some comparisons with the flux-squared weighting discussed here.

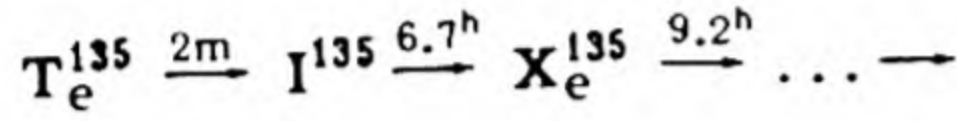
† Here z_i has the same units as $\iint N dE d\omega / 4\pi$; i.e., moles per unit volume or particles per unit volume.

mal reactor one obtains for the equilibrium (limiting) value of the ratio of poison cross-section from species z_i to fission cross section of the fuel:

$$\frac{z_i \frac{\partial \sigma_a}{\partial z_i} v}{\sigma_f v} = \gamma_i \quad (81)$$

A table of fission-product yields is given in Chapter 1.2.

Xe^{135} poison has a direct fission yield, γ_x , which is approximately 5 percent of the yield formed via the decay chain:



The half-life of the T_e^{135} is so short that negligible error is incurred in assuming the iodine to be formed immediately. The equations then are:

$$\frac{\partial z_I}{\partial t} = \gamma_I \int \sigma_f v N \frac{d\omega}{4\pi} dE - \lambda_I z_I \quad (82)$$

$$\lambda_x z_x + \frac{\partial z_x}{\partial t} = \lambda_I z_I + \gamma_x \int \sigma_f v N \frac{d\omega}{4\pi} dE - z_x \int \frac{\partial \sigma_a}{\partial z_x} v N \frac{d\omega}{4\pi} dE$$

where the loss of I by absorption of neutrons has been neglected.

As is clear from Eq. (82), the equilibrium Xe cross section is a function of the power level of the reactor. For a thermal reactor, one finds for equilibrium (or limiting) ratio of Xe cross section to the fuel thermal-absorption cross section at a given flux:

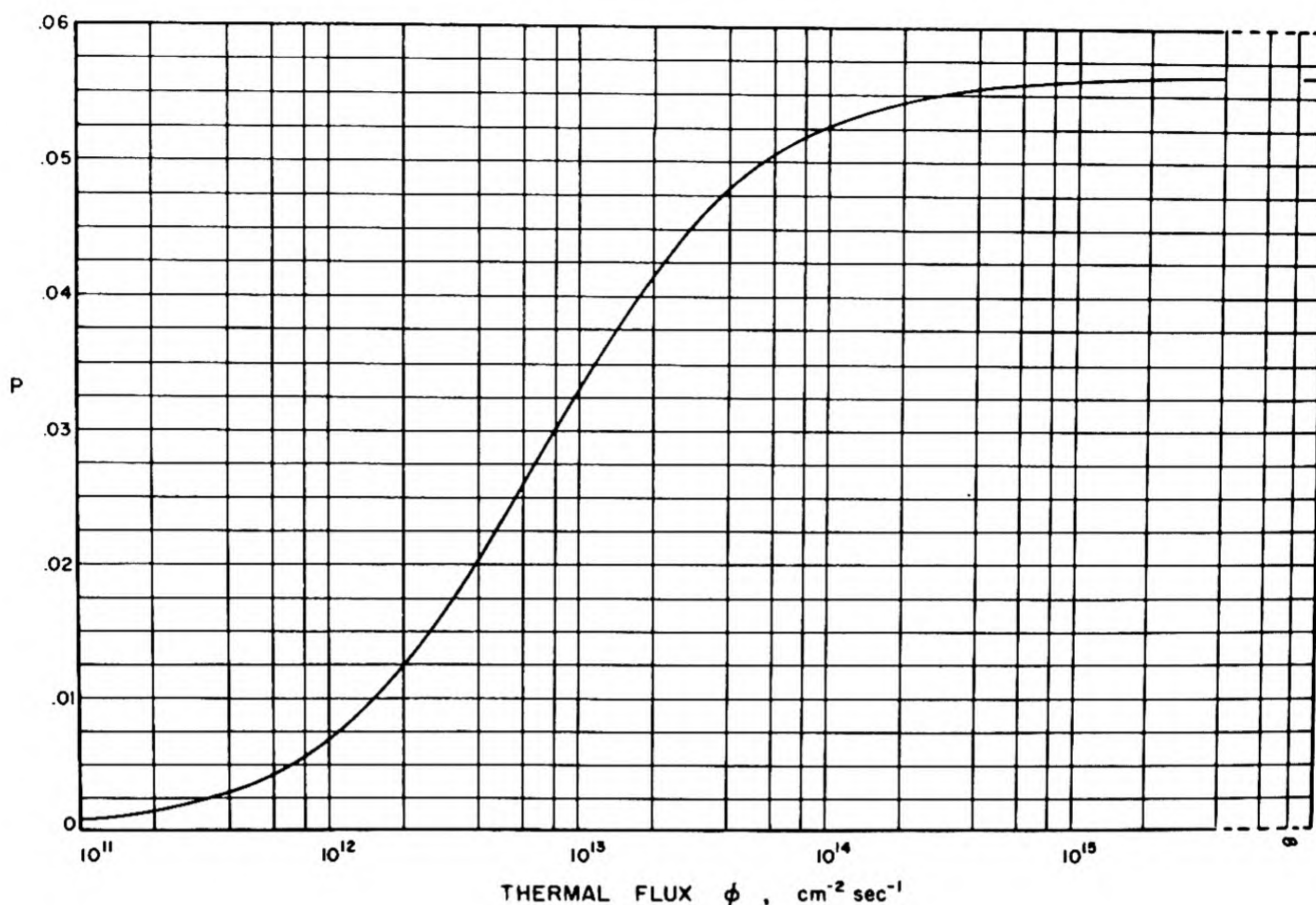
$$\begin{aligned} P \cong \frac{z_x \frac{\partial \sigma_a}{\partial z_x} v}{\sigma_a v} &= \frac{n}{\nu} (\gamma_I + \gamma_x) \frac{\frac{\partial \sigma_a}{\partial z_x} \int N_{th} \frac{d\omega}{4\pi}}{\lambda_x + \frac{\partial \sigma_a}{\partial z_x} \int N_{th} \frac{d\omega}{4\pi}} \\ &= (\eta/\nu)(\gamma_I + \gamma_x) \frac{\phi}{\phi + w} \end{aligned} \quad (83)$$

where η/ν is the ratio of the thermal-fission cross section to the thermal-absorption cross section for the fuel. $\int N_{th} d\omega/4\pi$ is the thermal-neutron density and $\phi = \int v N_{th} d\omega/4\pi$ is the thermal flux. w is defined as:

$$w = \frac{\lambda_x}{\frac{1}{v} \frac{\partial \sigma_a}{\partial z_x}} \quad (84)$$

In Fig. 1.6.21, P is plotted vs ϕ . Clearly:

$$\begin{aligned} \int \frac{\delta k}{\delta z_x} \delta z_x dV &= - \frac{(W_{th}, \overline{\sigma_a f v} P N_{th})}{(W, KN)} \\ &= - \bar{P} \frac{(W_{th}, \overline{\sigma_a f v} N_{th})}{(W, KN)} \end{aligned} \quad (85)$$

Fig. 1.6.21 — $P(\phi)$ for Xenon.

which defines \bar{P} , the uniform poison cross-section to fuel absorption-cross-section ratio which gives the same effect on reactivity as the true ratio P .

A result equivalent to Eq. (79) for Xe^{12} is more difficult to obtain. Using:

$$\phi = \phi_{\max} \frac{\sin \pi r/a}{\pi r/a} \quad (86)$$

one obtains \bar{P} for the standard reactor model introduced earlier from Eqs. (85) and (83):

$$\bar{P} = \frac{\frac{\eta}{\nu} (\gamma_I + \gamma_X) \frac{a}{\pi} \int \left(\frac{\sin \pi r/a}{r} \right)^3 \frac{1}{\frac{w}{\phi_{\max}} + \frac{\sin \pi r/a}{\pi r/a}} dV}{\int \left(\frac{\sin \pi r/a}{r} \right)^2 dV} \quad (87)$$

For a bare cylinder a good approximation to \bar{P} is:⁹

$$\bar{P} = (\eta/\nu) (\gamma_I + \gamma_X) \frac{1}{1 + 1.7 \frac{w}{\phi_{\max}}} \quad (88)$$

As before, $\bar{P} \bar{\sigma}_{af} \bar{V}$ is the cross section, $\bar{\sigma}_a \bar{V}$, of a poison uniformly distributed in the reactor which produces the same reactivity effect as the actual non-uniform poison.

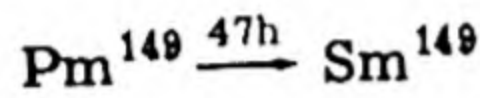
In this model, the reactivity changes caused by the addition of a uniform absorption cross section, $\delta\sigma_a$, are given by:

$$\delta k = - \frac{\delta\sigma_a}{\sigma_a} \frac{\sigma_a v_s}{L_s} = - \frac{\delta\sigma_a}{\sigma_{af}} f \frac{\sigma_a v_s}{L_s} \quad (89)$$

where $f = \sigma_{af}/\sigma_a$ is the thermal utilization and $\sigma_a v_s/L_s$ is the fraction of thermal neutrons absorbed in the reactor.

When fission products have a small enough cross section (or if it is early enough in the reactor life) so that the burn-up term (the second term on the right) in Eq. (80) can be neglected, then the poison cross section is proportional to ϕ and Eq. (79) is valid.*

The equations for samarium differ from those of xenon because the samarium isotope with the large thermal cross section (Sm^{149}) is stable. It is produced via the decay chain:†



The fission yield of Pm^{149} and the thermal cross section of Sm^{149} are given in Table 1.2.7.

Equation (80) describes the concentration of Sm^{149} and the first Eq. (82) is valid for Pm^{149} , if all quantities with the subscripts I are interpreted to refer to Pm^{149} .

FLOWING FUEL EFFECTS^{13,14}

In a circulating-fuel reactor, some delayed neutrons are born outside the reactor where they are lost. This results in an effective decrease in ν , the number of neutrons per fission, and in the β_i and λ_i . For a reactor in which the circulation time is small compared with the delayed lifetimes, one can obtain the resultant changes in the β_i . Thus, let μ be the fraction of time spent by fuel in the reactor. Then the probability that a delayed neutron will be born in the reactor is μ , so that the effective value of β_i , β_i , is given by:

$$\bar{\beta}_i = \mu\beta_i \quad (90)$$

The corresponding effective number of neutrons per fission, $\bar{\nu}$, becomes:

$$\bar{\nu} = \nu(1 - \beta) + \nu\bar{\beta} = \nu[1 - (1 - \mu)\beta] \quad (91)$$

The λ_i are not affected in this case.

For the case where the circulation time is of the order of or longer than the delayed-neutron mean lives, the detailed flow pattern of the fuel within the reactor and external loop is significant.

FORMULATION OF DYNAMIC EQUATIONS

The neutron behavior of the nuclear reactor is completely specified by Eq. (1) for which (with $s = 0$):

$$\frac{dn}{dt} = \frac{k - 1 - k\epsilon\beta}{l} n + \sum_i \lambda_i c_i \quad (92)$$

$$\frac{dc_i}{dt} = -\lambda_i c_i + \frac{k\epsilon_i\beta_i}{l} n$$

* See footnote preceding Eq. (78).

† Precursors of Pm^{149} with half-lives much less than 47 hours have been omitted.

These equations give $n(t)$ for specified $k(t)$; that is, they define the functional $n\{k(t)\}$. Complete solution of the problem requires equations which permit determination of that $k(t)$ produced by the remainder of the system for n specified over past times. That is, equations to define the functional $k\{n(t)\}$ are needed.

Part of this problem has been considered previously in the calculation of $k\{T, \rho\}$. The remainder of the problem is to find T, ρ given the heat source corresponding to $n(t)$. Clearly, it is just this part of the problem which is (1) familiar in engineering and independent of neutron physics and (2) special to the individual reactor system and intractable to detailed general discussion.

The relation between $n(t)$ and heat is discussed below where some specific, simple examples are considered. General considerations concerning the form of $k\{n\}$ are given in the discussion of linearized equations. For a linear external system, as is often the case:

$$k\{n\} = \int_{-\infty}^t K(t-s)n(s)ds + \delta k(t) + k_0 \quad (93)$$

where $\delta k(t)$ is an external forcing term. Equation (93), if valid, defines $K(t-s)$. The stability of systems where Eq. (93) holds has been discussed by Welton.¹⁶

THE REACTOR AS A HEAT SOURCE

The energy released by the fission process may be the prime purpose of the reactor, or it may be an undesired by-product. The energy distribution in kinetic energy of fission fragments and neutrons, prompt and delayed gammas, beta particles, and the like is shown in Table 1.2.11. Fission-product and beta-particle energy may be considered as a heat source at the position of the fuel. The neutron energy mainly appears as heating of the moderator, although some energy leaks out with escaping neutrons. The gamma-energy distribution is rather difficult to calculate, since the range of gamma rays is rather large. Heating by gamma rays or other particles emitted upon neutron absorption in the moderator or structure may also be important. Generally, however, for a bare homogeneous reactor, the energy production is distributed to a very good approximation as the fission source.

The presence of an energy source disturbs the temperature and density of the various parts of the reactor and produces reactivity changes as indicated in the discussion of reactivity coefficients. For a reactor with lump fuel, the major heat source is in the fuel, which will often operate at a higher temperature than the moderator. Since the moderator also has a heat source within it (gammas, neutrons slowing down, neutron capture), the power and cooling affect moderator properties and, through them, the reactivity. Furthermore, the coolant may have a marked effect on reactivity, especially in a water-cooled reactor.

The heat source density is:

$$P = Q \int \int \sigma_f v N \frac{d\omega}{4\pi} dE \quad (94)$$

where Q is the energy release per fission. Equation (94) gives the spatial distribution of that part of the fission energy appearing as kinetic energy of the fission fragments.

In the light of previous considerations [cf. Eqs. (1) and (5)], the space-independent, one-group, equivalent power may be taken as:

$$p = q \frac{kn}{l_\nu} \quad (95)$$

POWER COEFFICIENTS

A steady-state solution ($dn/dt = dc_i/dt = 0$) of Eq. (92) can exist only if $k = 1$. This implies operation at $n(t) = n^0$, where n^0 is such that:

$$k\{n^0\} = 1 \quad (96)$$

Furthermore, if various time-independent values of n are considered, $k\{n\}$ is a function in the ordinary sense of the variable n . The power coefficient of reactivity is defined as:

$$k_{n^0} = n \frac{d}{dn} k\{n\} \Big|_{n=n^0} \quad (97)$$

If $k\{n\}$ can be considered as a linear function of n , then:

$$k\{n\} = 1 + k_{n^0} \frac{n - n^0}{n^0} \quad (98)$$

Thus, in this case:

$$k\{2n^0\} - 1 = k_{n^0} \quad (99)$$

That is, the power coefficient of reactivity is the reactivity change produced by doubling the neutron level in the reactor (keeping it at the new value by control-rod motion or other means which does not affect the part of the functional $k\{n\}$ under consideration).

In any case, for the reactor system to be statically stable, it is necessary that:

$$k_{n^0} < 0 \quad (100)$$

The more negative k_{n^0} , the more stable the system. This static stability does not assure dynamic stability, but it is necessary to have dynamic stability. If Eq. (98) holds ($k\{n\}$ a linear functional), then k_{n^0} becomes more negative as n^0 increases; high-power operation leads, therefore, in a statically stable system, to greater static stability.

If Eq. (93) holds, then for constant n :

$$k\{n\} = k_0 + n \int_0^\infty K(t) dt$$

so that:

$$n^0 = \frac{1 - k_0}{\int_0^\infty K dt} \quad (101)$$

$$k_{n^0} = 1 - k_0$$

If the reactor is coupled to several independent external systems, such as a servo-operated control and the temperature-density system, the resultant partial power-coefficients may be added to obtain the resultant coefficient. A further remark is that a servo yielding integral control may be arranged to always restore the level to a pre-determined n^0 , independent of external variations. This implies that $k_{n^0} = -\infty$. Such controls are possible (cf. remarks on "Control Servomechanisms" below).

LINEARIZATION

For small departures of the various reactor-system variables from equilibrium values, it is possible to simplify the equations by considering the tangent system. This system is that of all linear systems which most closely approximates, in the neighborhood of the equilibrium point, the true system. Methods of obtaining the equations of motion of the tangent system will be discussed below under linearized equations.

The non-linearity of the equations of reactor dynamics may occur in $k\{n\}$. For the tangent system, however, one may always write $k\{n\}$ in the form of Eq. (93). This nearly always yields a good approximation for a fairly wide range of operating conditions.

Even though $k\{n\}$ is linearized, the equations are non-linear owing to the manner in which k enters Eq. (92). Specifically, the terms containing the factor kn must be approximated.

If $n = n^0 + n'$ where n^0 , the equilibrium neutron inventory, is independent of time and:

$$n' \ll n^0 \quad (102)$$

then one may linearize the kn term as follows. From Eq. (93):

$$k\{n^0 + n'\} = n^0 \int_{-\infty}^t K(t-s)ds + k_0 + \int_{-\infty}^t K(t-s) n'(s)ds$$

but:

$k\{n^0\} = 1$, since n^0 is an equilibrium value, so:

$$k\{n^0 + n'\} = 1 + \int_{-\infty}^t K(t-s)n'(s)ds \quad (103)$$

Then:

$$kn = n^0 + n^0 \int_{-\infty}^t K(t-s)n'(s)ds + n'(t) + n'(t) \int_{-\infty}^t K(t-s)n'(s)ds \quad (104)$$

The process of linearization consists in neglecting the last term on the right in Eq. (104) by assuming that it is small compared with the other terms since it contains n'^2 . This assumption becomes more valid when one notes that usually:

$$n^0 \int_{-\infty}^t K(t-s)ds \quad (105)$$

is of the order of β , which is small compared with unity.

If term (105) is sufficiently small in such terms of Eq. (92) as $(k\epsilon\beta/l)n$ and $(k\epsilon_1\beta_1/l)n$, one may write:

$$kn \approx n^0 + n'(t) = n \quad (106)$$

In the term $(k-1)n/l$, more care must be used, as is clear from Eq. (106). Thus, one uses:

$$(k-1)n \approx n^0 \int_{-\infty}^t K(t-s)n'(s)ds \quad (107)$$

From Eq. (106) and (107), with:

$$c_i(t) = c_i^0 + c_i'(t) \quad (108)$$

one obtains the steady-state equations:

$$0 = \frac{\epsilon_i \beta_i}{\lambda} n^0 + \sum \lambda_i c_i^0 \quad (109)$$

$$0 = -\lambda_i c_i^0 + \frac{\epsilon_i \beta_i}{\lambda} n^0$$

and the linearized equations:

$$\frac{dn'}{dt} = \frac{n^0}{\lambda} \int_{-\infty}^t K(t-s)n'(s)ds + \sum \lambda_i c_i' \quad (110)$$

$$\frac{dc_i'}{dt} = -\lambda_i c_i' + \frac{\epsilon_i \beta_i}{\lambda} n'$$

Further discussion of Eq. (110) is deferred until the discussion, "Form and Solution of Linearized Equations."

A SIMPLE COOLING MODEL

Consider a reactor consisting of very fine fuel rods immersed in a well stirred tank of water with water flow supplying the cooling. Then, the water temperature will satisfy an equation such as (neglecting the difference between prompt and delayed heating):

$$MC \frac{dT}{dt} = q \frac{kn}{l\nu} - g C(T - T_{in}) \quad (111)$$

where:

C is the heat capacity per unit mass of the water

M is the total mass of water in the tank

T is the water temperature

$q(kn/l\nu)$ is the power into the water (it is assumed no holdup occurs in the fuel rods)

g is the mass water flow rate through the tank.

Furthermore, the reactivity change will be of the form:

$$k - 1 = C_T(T - T_0) \quad (112)$$

where:

C_T is the temperature coefficient of reactivity, direct and through the density changes

T_0 is the temperature for which $k = 1$.

Equations (92), (111), and (112) describe the dynamic behavior of the model discussed. They further may be used to describe a solid reactor cooled via coolant channels. In such a case, T is an average reactor temperature, and the term $gC(T - T_{in})$ is interpreted as the average heat carried away by the coolant. Equation (111) is adequate in this case only if the transit time of the coolant through the reactor is small.

If the coolant is passed through a heat exchanger and back into the reactor, one may append to Eqs. (111) and (112) a further relation for the variation of T_{in} :

$$T_{in}(t) = \alpha T(t - \tau) + \beta; 0 \leq \alpha < 1 \quad (113)$$

The delay time τ due to passage through the heat exchanger loop is called a "transport delay."

SOLUTIONS OF NON-LINEAR EQUATIONS

The solution of non-linear equations is a tedious job, usually carried out numerically. Specific examples for simplified models are given below.

A SIMPLE COOLING MODEL

Consider a reactor coupled to the external system in such a way that a constant amount of power is removed. In this case, one may write, approximately:

$$C \frac{dT}{dt} = \alpha n - P_0 \quad (114)$$

$$k - 1 = C_T(T - T_0); \quad C_T < 0$$

where C is the heat capacity of the reactor and P_0 the cooling rate, whence:

$$\frac{dk}{dt} = \frac{C_T}{C} (\alpha n - P_0) \quad (115)$$

If one further neglects $(1/\epsilon\beta) dn/dt$ and considers only one delay group, Eq. (29) results for the neutron equation. Setting $s = 0$ and eliminating c , one obtains [in analogy with Eq. (29)]:

$$[k(1 - \beta) - 1] \frac{dn}{dt} + (1 - \beta)n \frac{dk}{dt} + \lambda(k - 1)n = 0 \quad (116)$$

which together with Eq. (115) completely specifies the dynamic problem. A numerical solution may be obtained if one first eliminates the time by use of:

$$\frac{d}{dt} = \frac{dk}{dt} \frac{d}{dk}$$

Numerical solutions are given in Fig. 1.6.22 for:

$$\frac{C_T P_0}{\lambda C \beta} = 0.05$$

This means that the reactivity increases owing to cooling by 0.05β in a delay period (λ^{-1}).

ACCIDENT CONSIDERATIONS

If a control rod is suddenly moved so that an excess reactivity large compared with β results, the behavior of the reactor for some time will be uninfluenced by the delayed neutrons. In this case, Eq. (1) may be written as:

$$\frac{dn}{dt} = \frac{k - 1 - \beta}{l} n \quad (117)$$

If Eq. (117) is considered in conjunction with equations describing temperature effects, one has a model to be studied for short time changes after sudden reactivity increase.^{16,17} In addition to Eq. (117), Ref. (17) considers Eq. (114) but with:

$$P_0 = \mu T \quad (118)$$

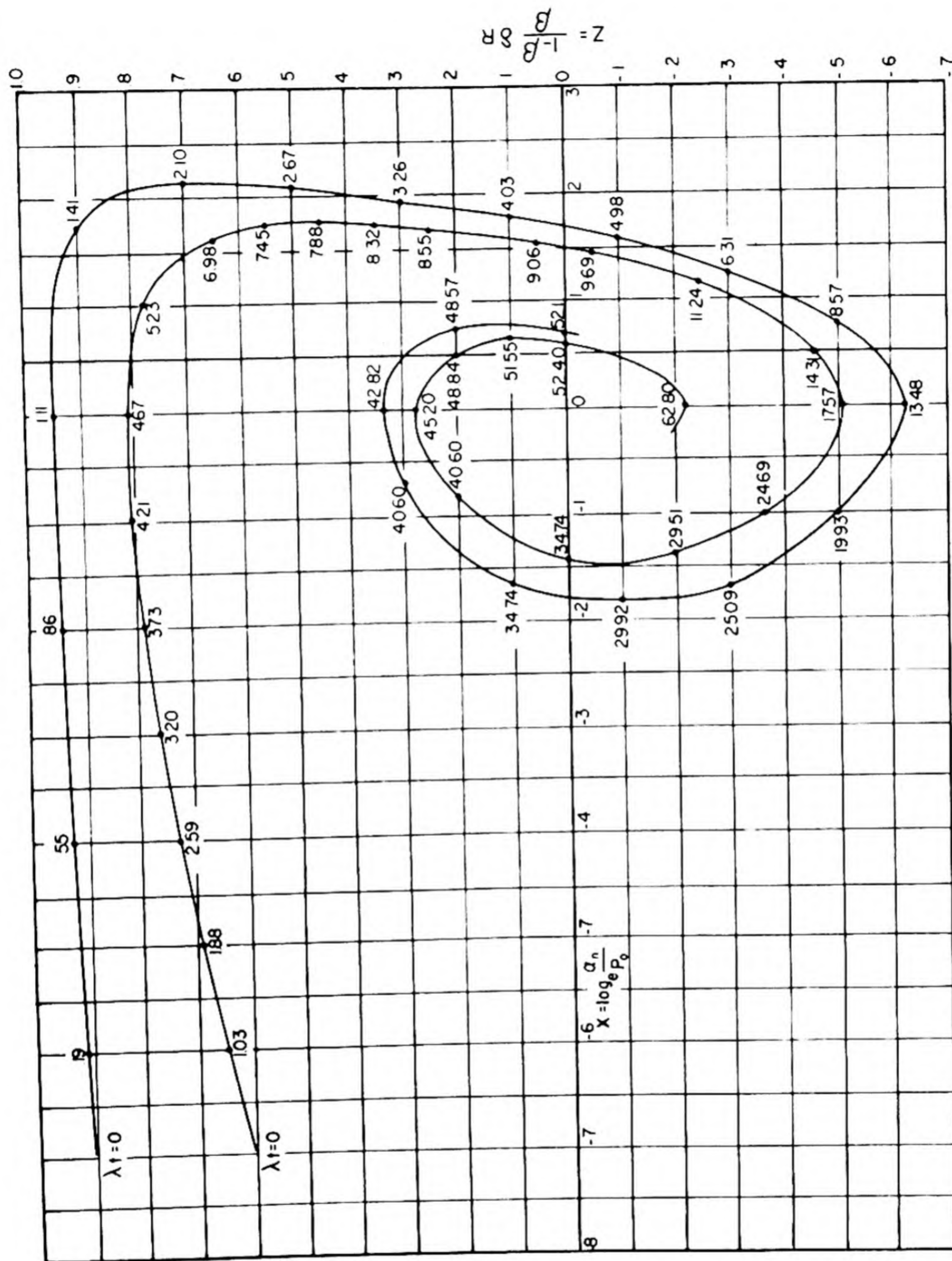


Fig. 1.6.22—Reactivity vs Reactor Power for a Simple Cooling Model. Submitted by Nuclear Development Associates, Inc., Dec. 15, 1952. The curves are labelled with the time measured in units of the mean life of delayed neutrons. The calculations assume a rate of heat removal such that the reactivity would increase by one dollar in 20 delayed neutron mean lives if there were no heating ($\alpha m = 0$).

Equations (117) and (118) together may be written in dimensionless form depending on one parameter as:

$$\frac{d^2\theta}{d\tau^2} + (c - 1) \frac{d\theta}{d\tau} - c\theta = - \left(\theta \frac{d\theta}{d\tau} + c\theta^2 \right) \quad (119)$$

where:

$$\theta = \frac{T}{T_0 + \frac{1}{-C_T}}$$

$$\tau = \frac{1 - C_T T_0}{1} t$$

$$c = \frac{\mu}{C} \frac{1}{1 - C_T T_0}$$

A solution of Eq. (119) with $c = 1$ is given in Fig. 1.6.23.

Equations (114) and (119) with $P_0 = 0$ are a special case¹⁸ of the more general system where Eq. (114) is replaced by:

$$\frac{d^n(\kappa - 1 - \beta)}{dt^n} = - \frac{\left[\int \frac{n}{n_0} dt \right]^m}{t_0^{n+m}} \quad (120)$$

which depends on one arbitrary constant, $n_0^m t_0^{n+1}$. Equation (114) corresponds to $n = 0$, $m = 1$. To discuss Eqs. (117) and (120), new variables may be introduced:

$$A = \frac{\kappa - 1 - \beta}{\kappa_0 - 1 - \beta}$$

$$\eta = \frac{n}{n_0 \left(\frac{t_0}{\tau} \right)^{1+(n/m)} (\kappa_0 - 1 - \beta)^{1+(1+n/m)}} \quad (121)$$

$$\theta = \frac{t}{1} (\kappa_0 - 1 - \beta)$$

In terms of these variables:

$$\frac{d}{d\theta} \log_e \eta = A$$

$$\frac{d^n A}{d\theta^n} = - \left(\int \eta d\theta \right)^m \quad (122)$$

with initial conditions:

$$A = 1 \text{ at } t = 0$$

$$\eta \cong 0$$

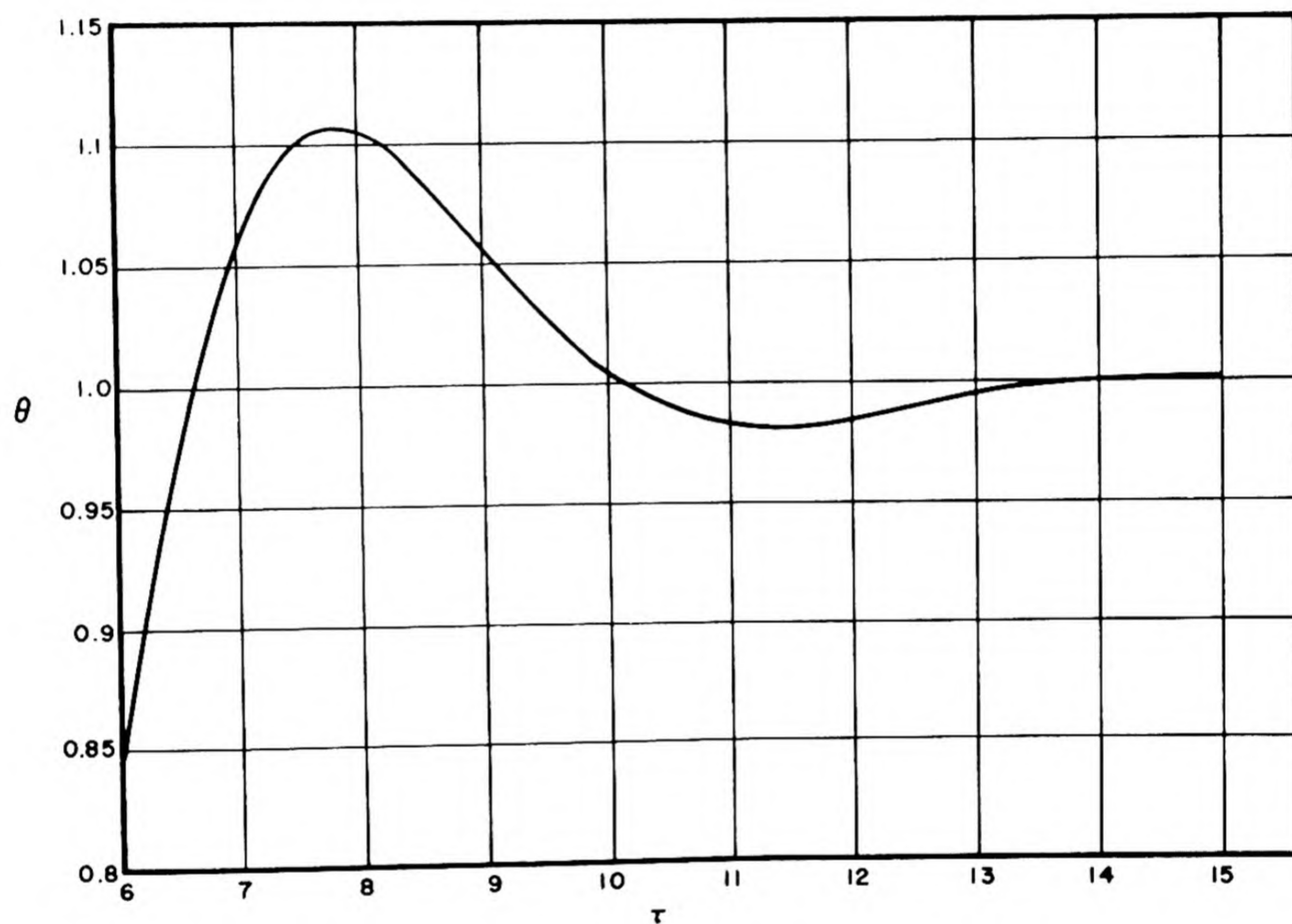


Fig. 1.6.23—Temperature vs Time for Cooling Proportional to Temperature. Reprinted from BNL-113, Aug. 1951. θ is a dimensionless temperature and τ a dimensionless time, cf. Eq. (119). The initial conditions were $\theta = 0$; $\dot{\theta} = 0.01$; initial reactor period (at $\tau = 0$) equal to the thermal relaxation time.

Total energy generated is proportional to:

$$Q = \int_0^{\infty} \eta d\theta \quad (123)$$

Plots of η vs A for various values of n and m are given in Figs. 1.6.24 and 1.6.25. Values of Q [Eq. (123)] are marked on the curves.

For the most interesting case, $n = 0$, $m = 1$, one may state an accident theorem originally given by Nordheim.¹⁹ Reference to Fig. 1.6.24 shows that, for this case, the final value of A is -1 ; i.e., the final reactivity is as much below prompt critical as the initial was above prompt critical, or the final temperature is as much above the temperature at which $k = 1 + \beta$ as the initial temperature was below this value.

An extension to this theorem which considers delayed neutrons²⁰ shows that with no cooling the final reactivity including delayed neutrons is as much below delayed critical as the initial is above delayed critical. Thus, the final reactivity is $1 - (k_0 - 1) = 2 - k_0$, and the final temperature is as much above the temperature at which $k = 1$ as the initial temperature is below this value.

Hurwitz²⁰ discusses a variation of the second of Eq. (122), which is written as follows:

$$\begin{aligned} \frac{d^n A}{d\theta^n} &= 0 & Q &\leq Q_0 \\ &= -(Q^m - Q_0^m) & Q &> Q_0 \end{aligned} \quad (124)$$

$$Q = \int_0^{\theta} \eta d\theta'$$

Curves are given in the reference.

FORM AND SOLUTION OF LINEARIZED EQUATIONS

The usefulness of studying the linearized equations, the tangent system, is a result of their much greater simplicity. The validity of such solutions is limited only by the degree of their departure from equilibrium. Stability of an equilibrium configuration means stability of the tangent system; therefore, the tangent system is most used in studying questions of stability. The process of finding the tangent system may be stated as follows.

First, an equilibrium state of the system is found by solving the non-linear equations with all time derivatives set equal to zero. The corresponding value of a dependent variable, x , is written x^0 . Thus for small oscillations about the equilibrium configuration, one may write x as a steady-state part, x^0 , plus an oscillating part, x^1 :

$$x(t) = x^0 + x^1(t) \quad (125)$$

where:*

$$|x^1(t)| \ll |x^0| \quad (126)$$

The substitution indicated in Eq. (126) is made in the equations of motion. Terms containing only quantities with superscript zero drop out because of the conditions for equilibrium. If terms containing products of first-order quantities (e.g., $x^1 y^1$) are neglected, then the resulting linear equations describe the tangent system.

* If the system is stable, $x^{(1)}$ is bounded. Then the disturbance introduced can always be made small enough so that Eq. (126) is satisfied.

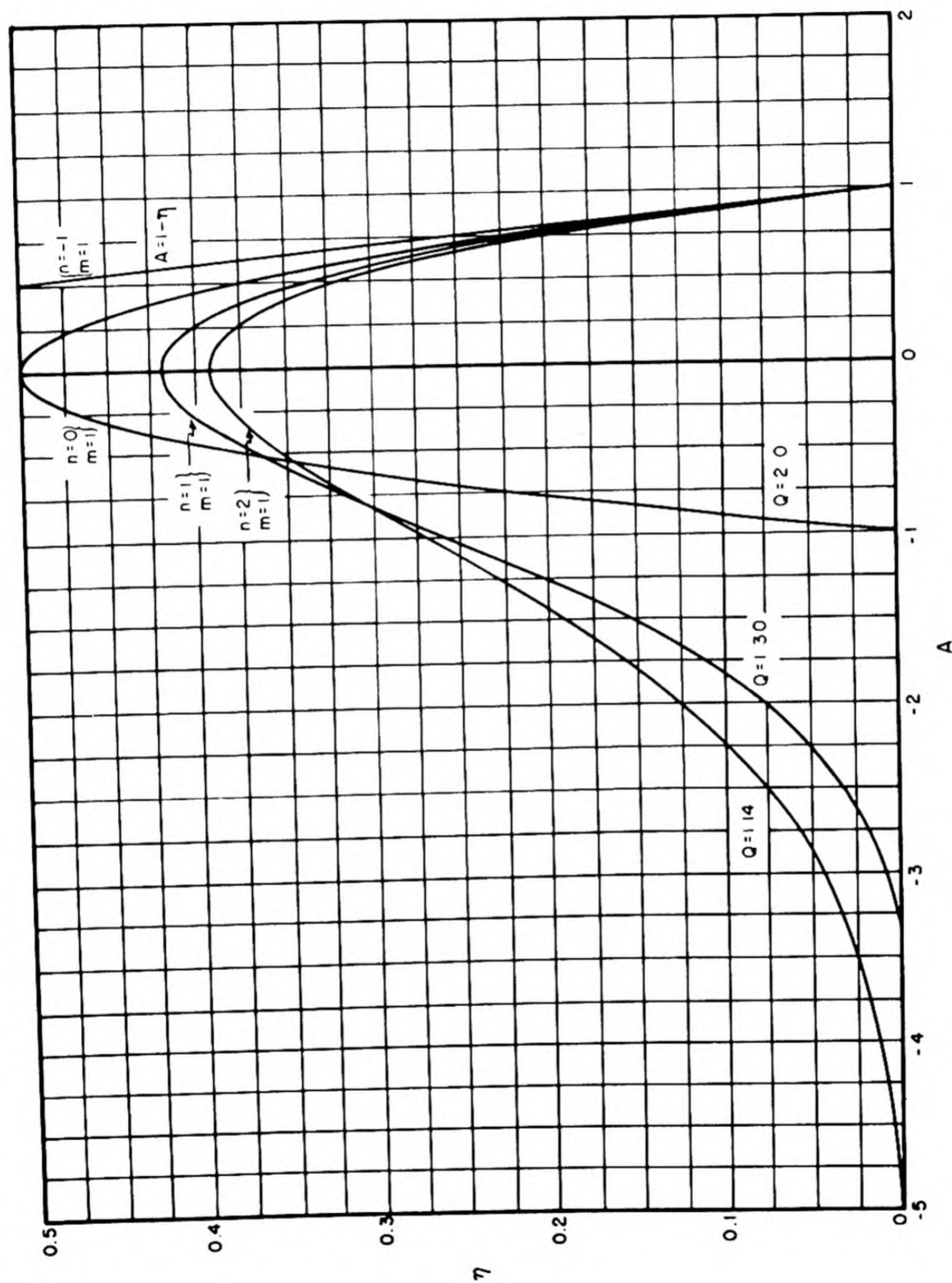


Fig. 1.6.24—Solution to an Accident Problem with No Cooling. Reprinted from KAPL-565. A is proportional to the excess reactivity, and η is proportional to the neutron density. The n^{th} derivative of the reactivity is taken proportional to the m^{th} power of the time integral of the neutron density. See Eq. (120) et seq in the text.

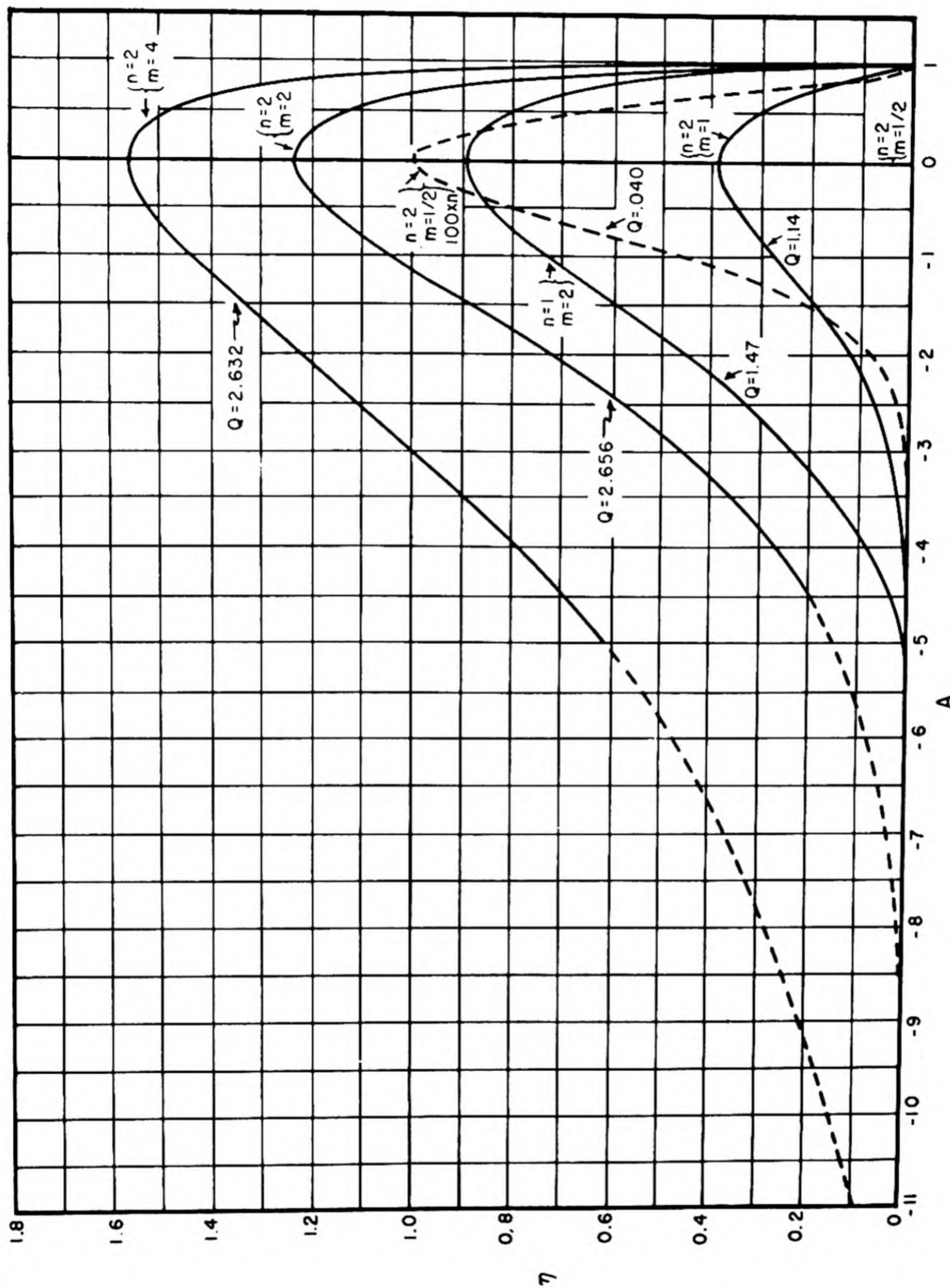


Fig. 1.6.25—Solution to an Accident Problem with No Cooling. Reprinted from KAPL-565. A is proportional to the excess reactivity, and η is proportional to the neutron density. The n^{th} derivative of the reactivity is taken proportional to the m^{th} power of the time integral of the neutron density. See Eq. (120) et seq in the text.

An example of this process was given earlier under "Formulation of the Dynamic Equations." Further examples follow:

$$\begin{aligned}
 x &= x^0 + x^1 \\
 f(x) &= f(x^0) + \left(\frac{df}{dx}\right)^0 x^1 \dagger \\
 f(x, y) &= f(x^0, y^0) + \left(\frac{\partial f}{\partial x}\right)^0 x^1 + \left(\frac{\partial f}{\partial y}\right)^0 y^1 \\
 \frac{dx}{dt} &= \frac{dx^1}{dt} \\
 xy &= x^0 y^0 + x^0 y^1 + y^0 x^1 \\
 \frac{x}{y} &= \frac{x^0}{y^0} + \frac{x^1}{y^0} - \frac{x^0}{(y^0)^2} y^1, \text{ etc.}
 \end{aligned} \tag{127}$$

LAPLACE TRANSFORMS AND TRANSFER FUNCTIONS

The linearized kinetic equations were found earlier. They are, adding a $\delta k(t)$ forcing term:

$$\begin{aligned}
 \frac{dn^1}{dt} &= \frac{n^0}{l} \int_{-\infty}^t K(t-s) n^1(s) ds + \sum \lambda_i c_i^1 - \frac{\epsilon \beta}{l} n^1 + \frac{n^0}{l} \delta k(t) \\
 \frac{dc_i^1}{dt} &= -\lambda_i c_i^1 + \frac{\epsilon_i \beta_i}{l} n^1
 \end{aligned} \tag{128}$$

Here, $K(t)$ is defined by the linearized equation:

$$k^1 = k(t) - 1 = \int_{-\infty}^t K(t-s) n^1(s) ds \tag{129}$$

Further, the power coefficient of reactivity corresponding to K is given, as before, by:

$$k_{n^0} = n^0 \int_0^\infty K(t) dt \tag{130}$$

These equations lend themselves to convenient handling with the method of Laplace transforms. The basic transform theorem is the following:

If:

$$\bar{f}(p) = \int_0^\infty e^{-pt} f(t) dt \tag{131}$$

Then, for $t > 0$:

$$f(t) = \frac{1}{2\pi i} \int_{c-i\infty}^{c+i\infty} e^{pt} \bar{f}(p) dp$$

\dagger The superscript 0 always means evaluated for the equilibrium values of the variables. Thus:

$$\left(\frac{df}{dx}\right)^0 = \left.\frac{df}{dx}\right|_{x=x_0}$$

and, for $t < 0$:

$$\frac{1}{2\pi i} \int_{c-i\infty}^{c+i\infty} e^{pt} \bar{f}(p) dp = 0$$

where the contour is such that all poles of $\bar{f}(p)$ lie to its left. $\bar{f}(p)$ is called the Laplace transform of $f(t)$.

Further results are:

$$\int_0^\infty e^{-pt} \frac{df(t)}{dt} dt = p\bar{f}(p) - f(0) \quad (132)$$

and:

$$\begin{aligned} \int_0^\infty e^{-pt} \int_0^t K(t-s) n^1(s) ds dt &= \bar{K}(p) \bar{n}^1(p) \\ \int_0^\infty K(t) dt &= \bar{K}(0) \end{aligned} \quad (133)$$

One may use these results to find a solution of Eq. (128). Thus, suppose that:

$$\left. \begin{aligned} \delta k(t) &= 0 \\ n^1(t) &= 0 \\ c_i^1(t) &= 0 \end{aligned} \right\} \text{ for } t < 0 \quad (134)$$

i.e., that the reactor was in equilibrium for negative times. The behavior of the system for $t > 0$ as forced by $\delta k(t)$ may then be found. Thus, if Eq. (128) is multiplied by e^{-pt} and integrated, one finds with the aid of Eqs. (132) and (133):

$$\bar{p} \bar{n}^1 = \sum \lambda_i \bar{c}_i^1 - \frac{\epsilon \beta}{1} \bar{n}^1 + \frac{n^0}{1} (\bar{k}^1 + \bar{\delta k})$$

$$\bar{p} \bar{c}_i^1 = -\lambda_i \bar{c}_i^1 + \frac{\epsilon_i \beta_i}{1} \bar{n}^1$$

$$\bar{k}^1 = \bar{K} \bar{n}^1$$

Elimination of the \bar{c}_i^1 yields the pair of equations:

$$\bar{n}^1 = \frac{n^0 \bar{F}(p)}{\epsilon \beta} (\bar{k}^1 + \bar{\delta k}) \quad (135)$$

$$\bar{k}^1 = \bar{K}(p) \bar{n}^1$$

where:

$$[\bar{F}(p)]^{-1} = \left\{ \frac{1p}{\epsilon \beta} + 1 - \sum \frac{\lambda_i}{\lambda_i + p} \frac{\epsilon_i \beta_i}{\epsilon \beta} \right\} \quad (136)$$

Equation (135) suggests an amplifier with feedback. This suggests calling $\bar{F}(p)$ the reactor transfer function and $\bar{K}(p)$ the external-system transfer function.

Upon eliminating \bar{k}^1 in Eq. (135), one has:

$$\bar{n}^1 = \frac{n^0/\epsilon\beta}{\bar{F}^{-1} - \frac{n^0\bar{K}}{\epsilon\beta}} \bar{\delta k} \quad (137)$$

This equation may be considered the basic formula of reactor dynamics. The properties of \bar{F}^{-1} , which are of interest in applications, are easily seen from Eq. (136) and from the plot of $\ln p/\epsilon\beta - \bar{F}^{-1}(p)$ in Figs. 1.6.4 through 1.6.10 and in Fig. 1.6.26.

Equation (137), together with the equation following Eq. (131) yields the solution to the equations of motion for $n^1(t)$. This solution will consist of the sums of residues of $\bar{n}^1 e^{pt}$ at the various zeroes of the denominator of Eq. (137) and the poles of $\bar{\delta k}$.

If the singularities of $\bar{n}^1(p)$ are all simple poles, then the solution of Eq. (128) is:

$$\begin{aligned} n^1(t) &= \frac{1}{2\pi i} \int_{c-i}^{c+i\infty} e^{pt} \bar{n}^1(p) dp \\ &= \sum_i e^{p_i t} \left. \frac{d}{dp} \left(\frac{1}{\bar{n}^1(p)} \right) \right|_{p=p_i} \end{aligned} \quad (138)$$

When $\bar{n}^1(p)$ has singularities which are not simple poles, the reader should consult a standard text on Laplace transforms.

The values of p_i for the zeroes of the denominator of Eq. (137) tell one about the stability of the system. Equation (138) shows that if any root has a positive real part the system is unstable while if all the roots have negative real parts, the system is stable.

THE FORM OF $\bar{K}(p)$

As the above considerations indicate, the characteristics of the external system are completely specified by the single function $\bar{K}(p)$, the external-loop transfer function. This function is additive for independent external loops as, for example, Xe burnup, temperature effects, flux dependent control actuation, and the like. It is thus useful to indicate the form of \bar{K} for some simple cases. In actual systems,²¹ the transfer function can become very complicated.

The cooling model discussed earlier will serve to indicate a form of temperature-coefficient contribution to the transfer function. The linearized forms of Eqs. (111), (112), and (113) are:

$$M C \frac{dT^1}{dt} = \frac{q}{l\nu} n^1 - gC(T^1 - T_{in}^1)$$

$$k^1 = C_T T^1$$

$$T_{in}^1(t) = \alpha T^1(t - \tau)$$

Taking transforms, one finds with the aid of the second of Eqs. (135):

$$\bar{K}(p) = \frac{\frac{q}{l\nu} C_T}{MCp + gC(1 - \alpha e^{-p\tau})} \quad (139)$$

The power coefficient owing to this coupling is given by:

$$\begin{aligned} k_{n^0} &= n^0 K(0) = \frac{n^0 q}{l\nu} \frac{C_T}{gC} \frac{1}{1-\alpha} \\ &= \frac{C_T (T^0 - T_{in})}{1-\alpha} \end{aligned} \quad (140)$$

In the simplest case, where T_{in} is constant and therefore $\alpha = 0$, Eq. (139) becomes:

$$n^0 \bar{K}(p) = \frac{k_{n^0}}{\frac{M}{g}p + 1} \quad (141)$$

Equation (141) may be taken as a prototype for simple external loops. It contains two parameters, the power coefficient of reactivity and a time (M/g) which in the present example is the time for the flow rate, g , to fill the tank.

The effect of Xe burnup is also, to a good approximation, described by a transfer function of the form of Eq. (141), as can be seen by referring to Eq. (153).

The transfer coefficient for a control rod may contain the analog of the transport lag, τ , of Eq. (139) due to finite time delay in the actuating mechanism. Even if this is not true, inertia effects must be considered. Thus, a possible description of a control loop might be:

$$\begin{aligned} (\ddot{x} + 2\xi\dot{x} + [\xi^2 + \omega^2]x) &= -\frac{(\xi^2 + \omega^2)}{\mu} Cn + D \\ k - 1 &= \mu x \end{aligned} \quad (142)$$

where the \ddot{x} is necessary because of inertia. ξ is the damping constant and x the position of the rod. The transfer function is then of the form:

$$\begin{aligned} n^0 \bar{K}(p) &= \frac{-C}{1 + \frac{2\xi}{\xi^2 + \omega^2}p + \frac{p^2}{\xi^2 + \omega^2}} \\ k_{n^0} &= -C \end{aligned} \quad (143)$$

More complicated control systems are often desirable. A further discussion is given below.

More generally, any $\bar{K}(p)$ may be expected to have the following characteristics:

(1) It is real for real p .

(2) $\lim_{R \rightarrow \infty} \bar{K}(Re^{i\theta}) = 0$, all θ .

(3) The singularities of $\bar{K}(p)$ are a finite or infinite number of poles.

In such a case, $\bar{K}(p)$ may be decomposed into partial fractions so that a general form is:

$$\begin{aligned} n^0 \bar{K}(p) &= \frac{A_1}{p} + \frac{A_2}{p^2} + \dots + \frac{A_m}{p^m} + \sum_i \left\{ \frac{B_1^i}{\tau_i p + 1} + \frac{B_2^i}{(\tau_i p + 1)^2} + \dots + \frac{B_{m_i}^i}{(\tau_i p + 1)^{m_i}} \right\} \\ &\quad + \sum_i \left\{ \frac{C_1^i}{\frac{p^2}{\xi_i^2 + \omega_i^2} + \frac{2\xi_i}{\xi_i^2 + \omega_i^2}p + 1} + \frac{C_2^i}{\left(\frac{p^2}{\xi_i^2 + \omega_i^2} + \frac{2\xi_i}{\xi_i^2 + \omega_i^2}p + 1 \right)^2} + \dots \right\} \end{aligned} \quad (144)$$

In interpreting $\bar{K}(p)$, it may be noted that $k_{n_0} = \infty$ unless:

$$A_1 = A_2 = \dots = A_m = 0$$

in which case:

$$k_{n_0} = B_1^i + B_2^i + \dots + C_1^i + C_2^i + \dots$$

It is instructive to discuss the meaning of the various terms of Eq. (144) by means of the differential equations which give rise to them. Each term may be thought as arising from an external-system variable. Thus, A_n/p^n arises from the system:

$$\frac{d^n}{dt^n} y^1 = n^1$$

$$k^1 = A_n y^1$$

if we recall that by definition:

$$k^1 = \int_0^t K(t-s) n^1 ds$$

Similarly, the term $B^i/(\tau_i p + 1)$ arises from:

$$\left(\tau_i \frac{d}{dt} + 1 \right) y^1 = n^1$$

$$k^1 = B^i n^1$$

A term like:

$$1 + \frac{C_1}{\xi^2 + \omega^2} p + \frac{p^2}{\xi^2 + \omega^2}$$

arises from an equation of the form of Eq. (142).

The transfer function of Eq. (139) is a simple example of one which yields an infinite-series expansion of the form of Eq. (144).

STABILITY CRITERIA

The question of whether the system under discussion is stable for small departures from equilibrium is answered in the positive if all the roots of the denominator of Eq. (137) have negative real parts. If this denominator is an algebraic equation of sufficiently small degree, all the roots are easily found. If not, other procedures may be desirable.

Real roots can be determined by plotting $\bar{F}^{-1}(p)$ and $(n^0/\epsilon\beta)\bar{K}(p)$ vs p for real p and noting the intersection. In Figs. 1.6.4 to 1.6.10, $f(p)$ is plotted for U^{235} fuel which is (for $\epsilon_i = \epsilon$):

$$f(p) = -\bar{F}^{-1}(p) + \frac{lp}{\epsilon\beta} \quad (145)$$

This may materially reduce the labor involved. Further, neglecting $lp/\epsilon\beta$ will have negligible effect on the other roots in most cases.

If all the roots are real, the above procedure is enough. If not, it is useful to use the Nyquist Stability criterion. This may be stated as follows:

If one plots any function $g(p) = u + iv$ on an argand diagram (u vs v) as $p = i\omega + \eta$ varies on the infinite contour (shown in Fig. 1.6.27), then the number of times $g(p)$ circles the origin is the number of poles of $g(p)$ with positive real parts minus the number of zeroes of $g(p)$ with positive real parts. In most applications, the location of the poles is obtained by inspection of $g(p)$.

Thus, one may determine whether the system is stable (no zeroes of g with positive real parts) without finding the roots.

In control work,²² it is conventional to plot the quantity [cf. Eq. (137)]:

$$\frac{n^0}{\epsilon\beta} \overline{F}(p) \overline{K}(p)$$

and count the number of times the locus circles -1 . It may often be more convenient to plot:

$$\overline{F}^{-1} - \frac{n^0}{\epsilon\beta} \overline{K}$$

since \overline{F}^{-1} is independent of \overline{K} and may be calculated once and for all. A plot of:

$$f(i\omega) = \overline{F}^{-1}(i\omega) - \frac{i\omega l}{\epsilon\beta} \quad (146)$$

is given in Fig. 1.6.26. An example of an application of this criterion is given in Fig. 1.6.27. This is concerned with determining in which half-plane lie the roots of:

$$W(p) = \frac{205 \frac{1 - e^{-p}}{p} - \frac{1}{2} e^{-p} - p - 0.625}{1.15p + 17.3}$$

Since the plot of the imaginary part of W vs the real part of W when p follows the contour shown in Fig. 1.6.28 does not enclose the origin, there are as many poles as zeroes in the right half-plane. One can see by inspection that W has no poles in the right half-plane, and hence no zeroes.

Other methods of determining stability without finding explicitly the roots of the denominator of Eq. (137) can be found in standard texts on servomechanisms and analysis of minimum-phase-shift electrical networks. The reactor transfer function has properties characteristic of the transfer function of a minimum-phase-shift electrical network. In such a case, a method of special interest is the use of a Bode diagram.

MEASUREMENT OF $\overline{K}(i\omega)$

The reactor transfer function $\overline{K}(p)$ can be experimentally determined in an operating reactor^{23,24} for pure imaginary p . If one oscillates a control rod at frequency ω and constant amplitude, A , then in Eq. (128):

$$\delta k(t) = RP\epsilon\beta Ae^{i\omega t} \quad (147)$$

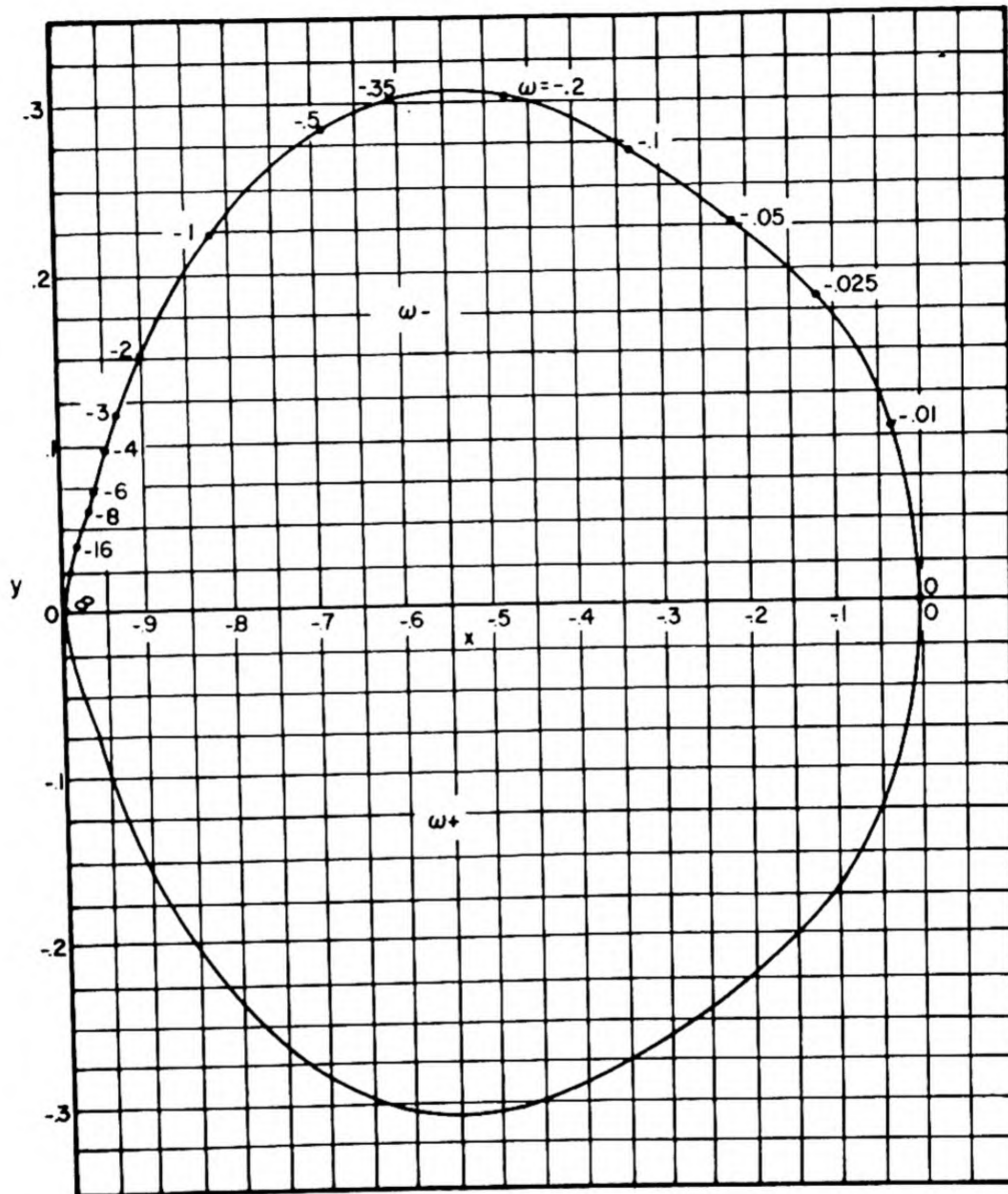


Fig. 1.6.26 — Imaginary Part of $\sum_1 (\beta_1/\beta)(\lambda_1/p + \lambda_1) - 1$ vs the Real Part for U^{235} . Submitted by Nuclear Development Associates, Inc., Dec. 15, 1952. This is plotted as p traces the contour shown in Fig. 1.6.28.

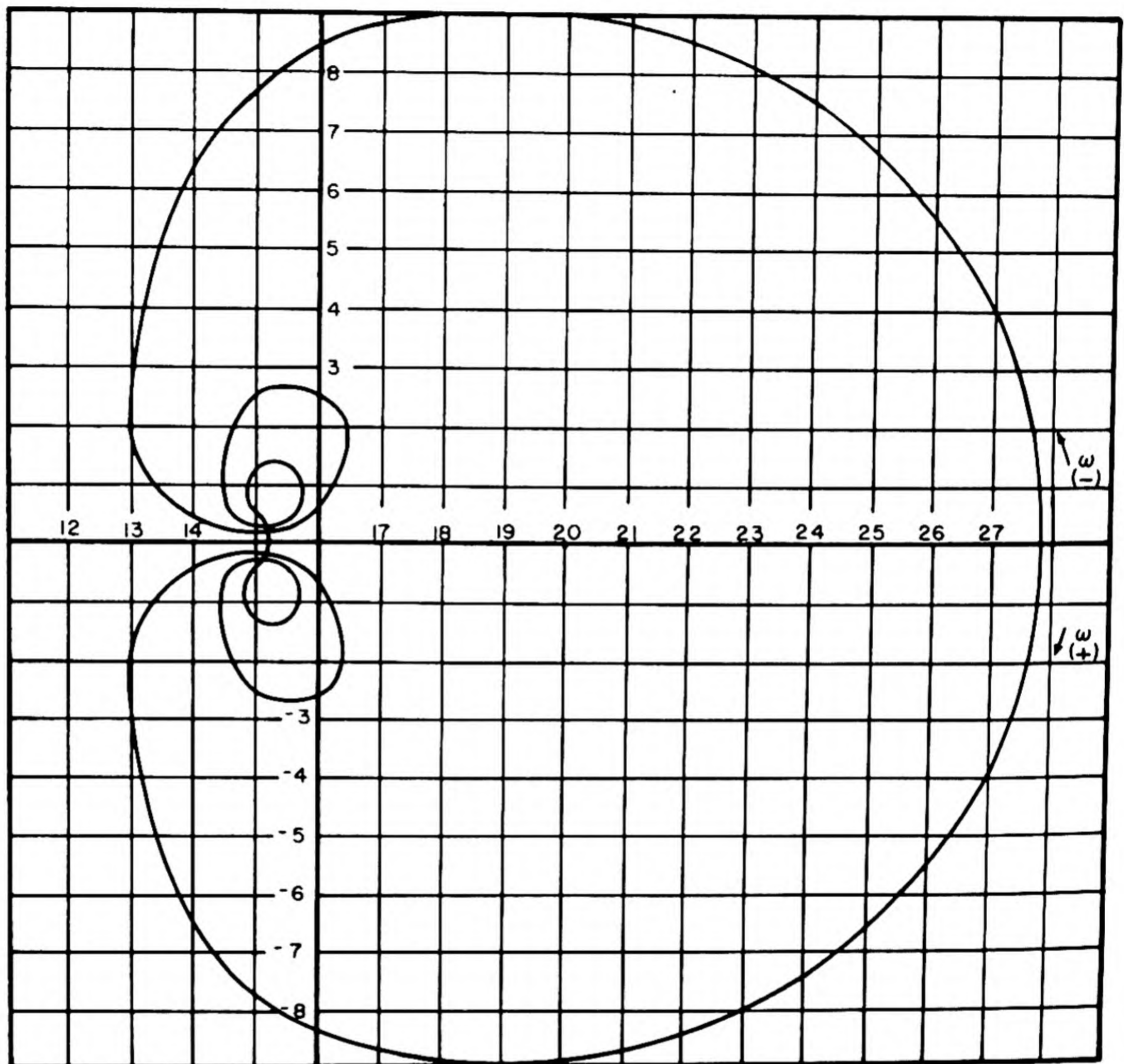


Fig. 1.6.27 — A Plot of $205[(1-e^{-P})/(p)] - [1/2 e^{-P} - 0.625]/1.15p + 17.3$ as p Traces the Contour Shown in Fig. 1.6.28. Submitted by Nuclear Development Associates, Inc., Dec. 15, 1952. Since the curve does not circle the origin and the function has no poles in the right half plane, it has no zeros in the right half plane.

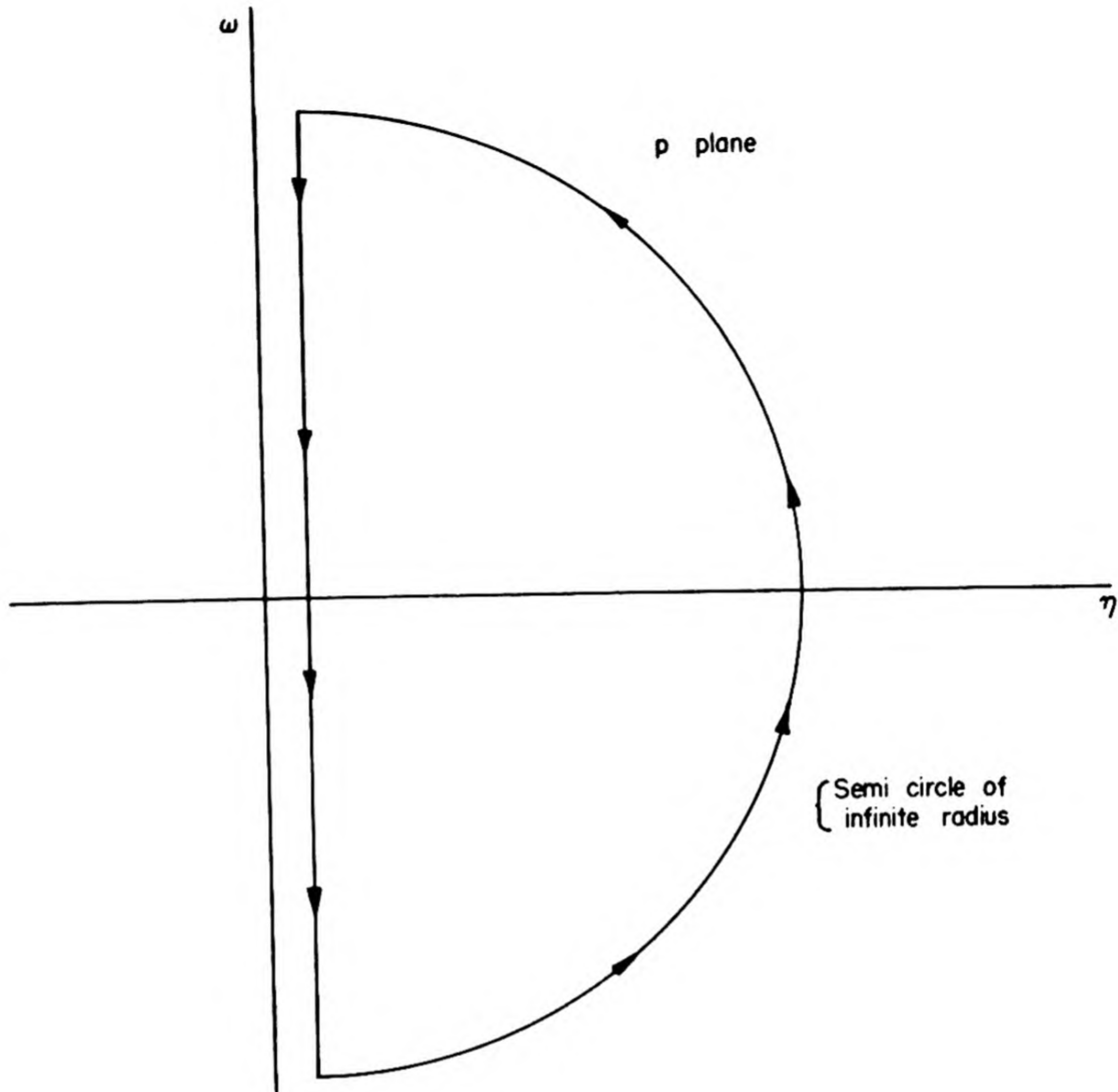


Fig. 1.6.28 — Contour of $p = \eta + i\omega$ to be Used in Applying Nyquist Criterion.
Submitted by Nuclear Development Associates, Inc., Dec. 15, 1952.

Furthermore, in such a case one will have a solution of the form:

$$\begin{aligned} \frac{n^1}{n^0} &= R p \nu e^{i\omega t} \\ c_1^1 &= R p \gamma_1 e^{i\omega t} \end{aligned} \quad (148)$$

Substituting in Eq. (128), and using:

$$\int_{-\infty}^t K(t-s) e^{i\omega s} ds = e^{i\omega t} \bar{K}(i\omega) \quad (149)$$

one finds:

$$\frac{A}{\gamma} \Big|_{n^0} = F^{-1}(i\omega) - \frac{n^0}{\epsilon\beta} K(i\omega) - 1 \quad (150)$$

In Eq. (150), A/γ is experimentally determinable as a complex number (owing to phase shift in flux response). If one measures $A/\gamma|_{n^0}$ for n^0 small (essentially $n^0 = 0$) and for a finite n^0 , there results from Eq. (150):

$$\frac{A}{\gamma}|_{n^0=0} - \frac{A}{\gamma}|_{n^0} = \frac{n^0}{\epsilon\beta} \bar{K}(i\omega) \quad (151)$$

THE XENON POWER INSTABILITY

If in Eq. (82) one neglects the variation of the iodine source (owing to its long period, this is permissible for stability studies), one has as linearized equations:

$$\begin{aligned} k^1 &= C_x z_x^1 \\ \frac{dz_x^1}{dt} &= -\lambda_x z_x^1 - n^0 v \frac{\partial \sigma_a}{\partial z_x} z_x^1 - z_x^0 \left(v \frac{\partial \sigma_a}{\partial z_x} \right) n^1 \end{aligned} \quad (152)$$

whence, using the second of Eq. (135):

$$n^0 \bar{K}(p) = - \frac{C_x n^0 z_x^0 \left(v \frac{\partial \sigma_a}{\partial z_x} \right)}{p + \lambda_e} = - \frac{1}{\lambda_e^{-1} p + 1} C_x z_x^0 \left(1 - \frac{\lambda_x}{\lambda_e} \right) \quad (153)$$

where:

$$\lambda_e = \lambda_x + n^0 \left(v \frac{\partial \sigma_a}{\partial z_x} \right) \quad (154)$$

is the reciprocal mean life of a Xe atom in the reactor at equilibrium. The time constant in Eq. (153) is (λ_e^{-1}) , and the power coefficient is:

$$k_{x^0} = -C_x z_x^0 \left(1 - \frac{\lambda_x}{\lambda_e} \right) \quad (155)$$

which is positive, since $C_x z_x^0$ is the k change due to equilibrium xenon poisoning, which is negative.

The effective value of the poison cross section is given by:

$$\sigma_{ap} = \bar{P} \sigma_{af}$$

where \bar{P} is obtained from Eqs. (83) and (85) [or Eq. (87)].

Using Eq. (89), one sees that for a bare thermal reactor:

$$\delta k = C_x z_x^0 = - \bar{P} f \frac{\sigma_a \nu_s}{L_s} \quad (156)$$

The unstable period arising from the transfer function of Eq. (153) has been calculated²⁵ as a function of ϕ under the following assumptions:

- (1) The flux and all concentrations are space independent.
- (2) One delay group with $\beta = 0.01$, and $\lambda^{-1} = 10$ sec.

Their results are given in Fig. 1.6.29.

CAVITY OSCILLATIONS

Liquid homogeneous reactors and liquid-cooled and moderated reactors admit the possibility of a particular type of relatively high frequency, unstable oscillations, which may be called cavity oscillations. This phenomena has been considered by several authors.^{26,27}

Cavity oscillations arise as follows: A tank of liquid connected to a standpipe or pressurizer will have certain resonant frequencies at which it can oscillate with relatively weak damping. Coupling of these oscillations to the reactor will often be sufficient to feed energy into the oscillations and may overcome the damping, thus leading to instability.

REMARKS ON CONTROL SERVOMECHANISMS

Suppose a control is characterized by a parameter x such that:

$$k - 1 = x \quad (157)$$

The question to be considered here is concerned with the selection of the functional $x\{n\}$ characterizing the control servomechanism. If one writes this relation in terms of:

$$\begin{aligned} x(t) &= \int_{-\infty}^t n^0 K(t-s) \left(\frac{n(s)}{n^0} - 1 \right) ds \\ \bar{x}(p) &= n^0 \bar{K}(p) \left(\frac{n(p)}{n^0} - 1 \right) \end{aligned} \quad (158)$$

it is seen that $\int_0^t K(s)ds$ is the response of x to a unit step in n/n^0 at $t = 0$. The short-time behavior of $\int_0^t K(s)ds$ may be obtained by expanding $(1/p)\bar{K}(p)$ in a power series in $1/p$:

$$\begin{aligned} \frac{1}{p} \bar{K}(p) &= \sum_{i=0}^{\infty} \frac{a_i}{p^{i+1}} \\ \int_0^t K(t)ds &= \frac{1}{2\pi i} \int_{c-i\infty}^{c+i\infty} e^{pt} \bar{K}(p)dp \\ &= \sum_{i=0}^{\infty} a_i \frac{t^i}{i!} \end{aligned} \quad (159)$$

Owing to control inertia, one sees that the initial displacement a_0 and initial velocity a_1 will vanish so that:

$$\bar{K}(p) = \sum_{i=2}^{\infty} \frac{a_i}{p^i} \quad (160)$$

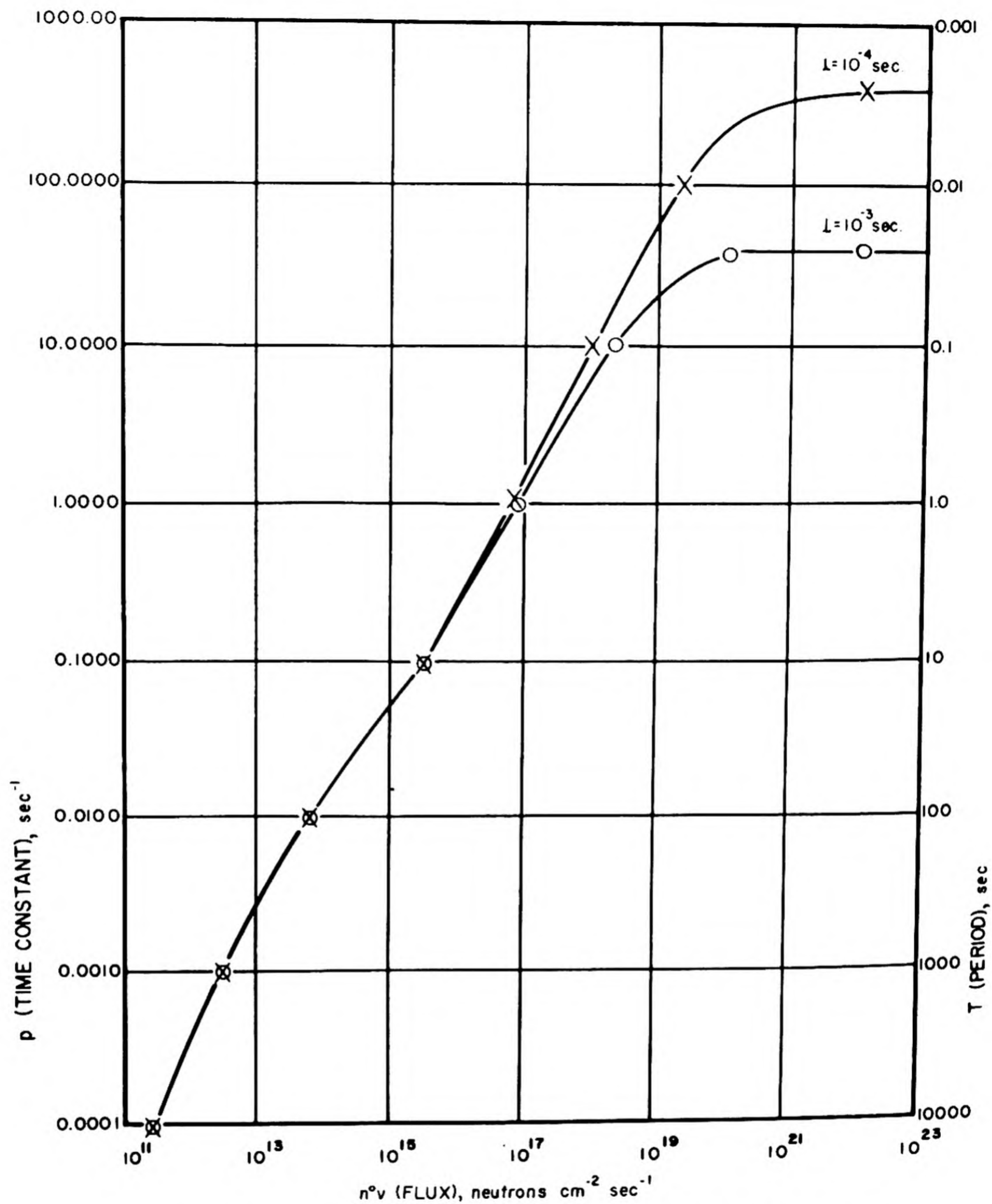


Fig. 1.6.29—Inverse Reactor Period Owing to Xenon Power Instability. Reprinted from MonP-379. The two curves are for different values of the neutron generation time.

A simple transfer function satisfying Eq. (160) is given by:

$$n^0 \bar{K}(p) = \frac{k_{n^0} (\xi^2 \pm \omega^2)}{p^2 + 2\xi p + \xi^2 \pm \omega^2} \quad (161)$$

where the plus sign means complex roots and the minus sign real roots of the denominator. In order that both roots have negative real parts (so that control is stable), one must have either the plus sign or the minus sign with $\omega^2 < \xi^2$. If Eq. (161) is expanded in powers of $1/p$, one obtains:

$$\frac{n^0}{p} \bar{K}(p) = \frac{k_{n^0} (\xi^2 \pm \omega^2)}{p^3} + \dots \quad (162)$$

The initial motion corresponding to this is:

$$n^0 \int_0^t K(s) ds = k_{n^0} (\xi^2 \pm \omega^2) \frac{t^2}{2!} + \dots \quad (163)$$

In order to make this a rapid motion, without increasing k_{n^0} , one may use large ω^2 and the plus sign.

At large times, the displacement of the power owing to a change in reactivity δk from external sources is:

$$\frac{\delta n}{n^0} = \frac{\delta k}{k_{n^0}} \quad (164)$$

as may be seen from Eq. (128) with $n' = c_1' = 0$.

This is the control error. It may be reduced to zero by having $\int_0^\infty K(t) dt$ be infinite, i.e., by having $K(\infty)$ equal a non-zero constant. This means $\bar{K}(p)$ has a pole at $p = 0$. One might try:

$$K(p) = \frac{c}{p} \frac{(\xi^2 + \omega^2)}{p^2 + 2\xi p + \omega^2 + \xi^2} \quad (165)$$

This has the disadvantage that the control motion starts as t^3 rather than as t^2 as in Eq. (163). However, a suitable transfer function is obtainable by superposition of Eq. (165) and Eq. (161).

In Ref. (28), the transfer function is written as:

$$n^0 \bar{K}(p) = \frac{\omega_n^2 B}{(p^2 + 2\xi\omega_n p + \omega_n^2)} + \frac{\omega_n^2 B}{\tau_0 p(p^2 + 2\xi\omega_n p + \omega_n^2)} \quad (166)$$

where the notation is different than in the above. Note that $k_{n^0} = B$ for the first part of the above expression, but is infinite for the second part. The reactor response, as the parameters in Eq. (166) are varied, is illustrated in Figs. 1.6.30 to 1.6.33 (note: $f_n = \omega_n/2\pi$).

In order to understand physically the meaning of Eq. (166), it may be written in terms of a differential equation:

$$\frac{d^2}{dt^2} + 2\xi\omega_n \frac{d}{dt} + \omega_n^2 x(t) = \omega_n^2 B \left\{ \frac{n(t)}{n^0} - 1 + \frac{1}{\tau_0} \int \left(\frac{n(t)}{n^0} - 1 \right) dt \right\} \quad (167)$$

It is clear that the only steady-state solution of Eq. (167) is $n = n^0$.

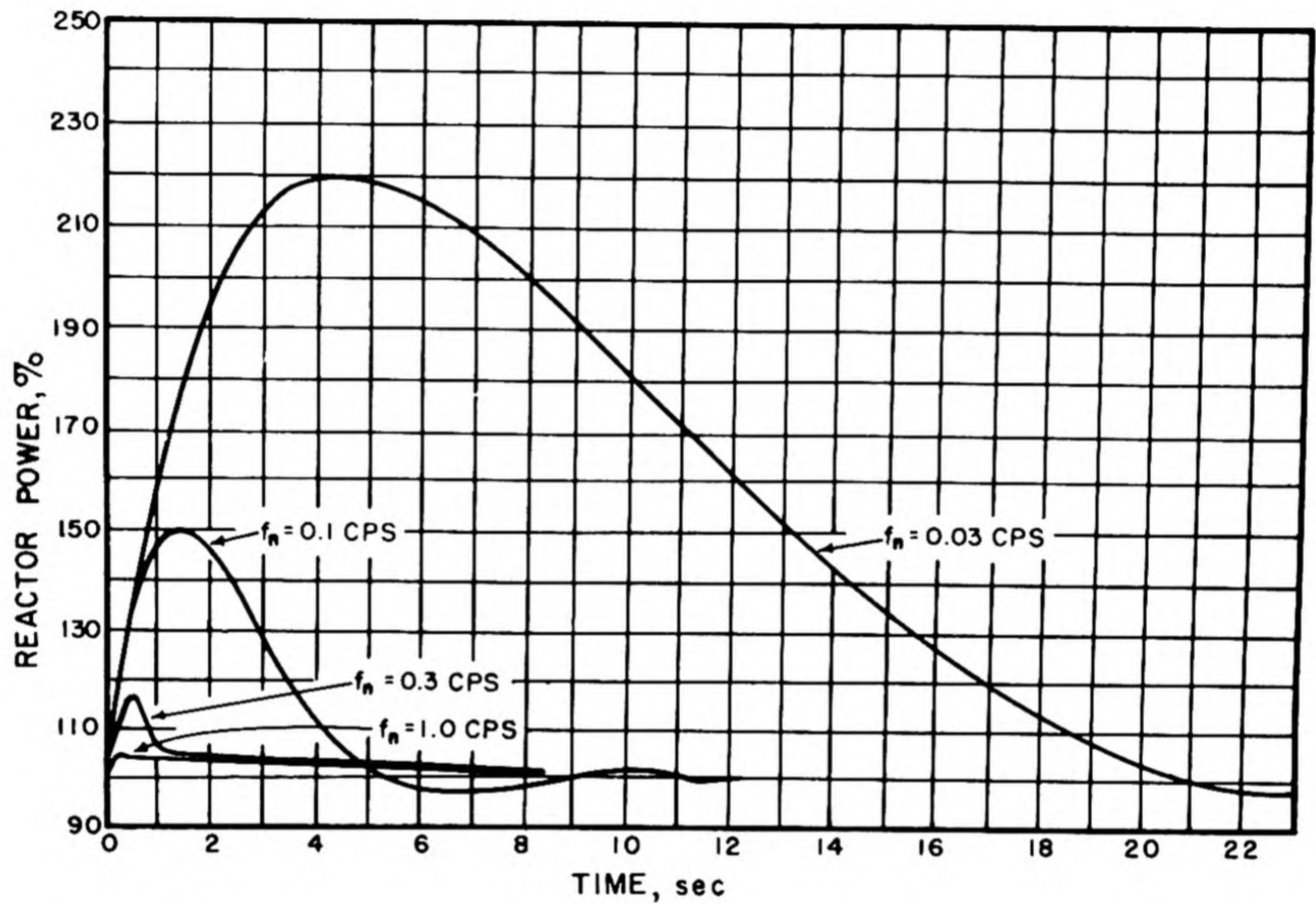


Fig. 1.6.30 — Reactor Power vs Time. Reprinted from WAPD-34, Vol. I, RM-90. The following parameters were used: Temperature coefficient = zero; disturbance = $+0.003(1 - e^{-t/0.5}) = \partial k$; regulator rod servo-parameters = optimum for each f_n .

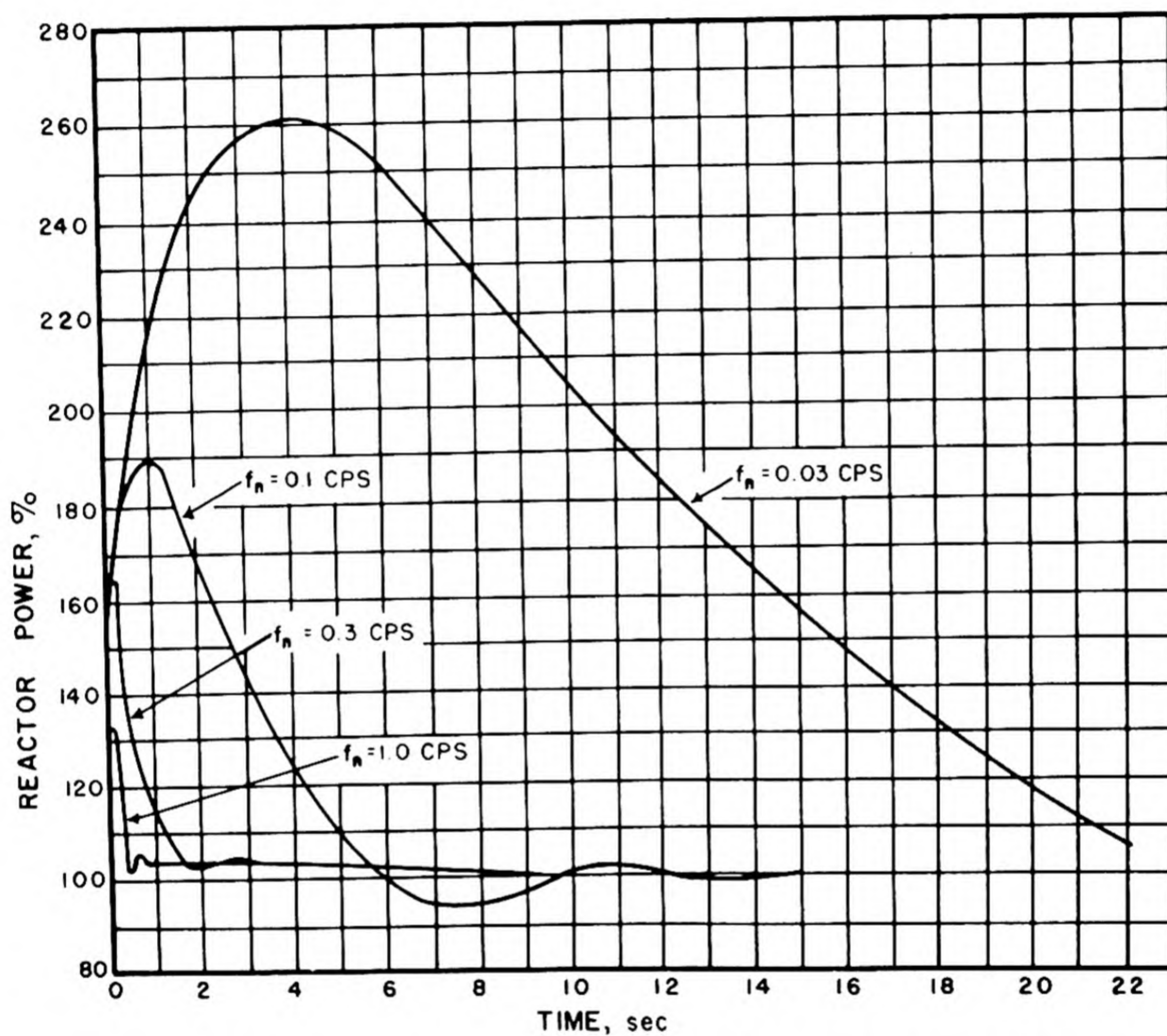


Fig. 1.6.31 — Reactor Power vs Time. Reprinted from WAPD-34, Vol. I, RM-90. The following parameters were used: Temperature coefficient = zero; disturbance = $+0.003(1 - e^{-t/0.1}) = \partial k$; regulator rod servo-parameters = optimum for each f_n .

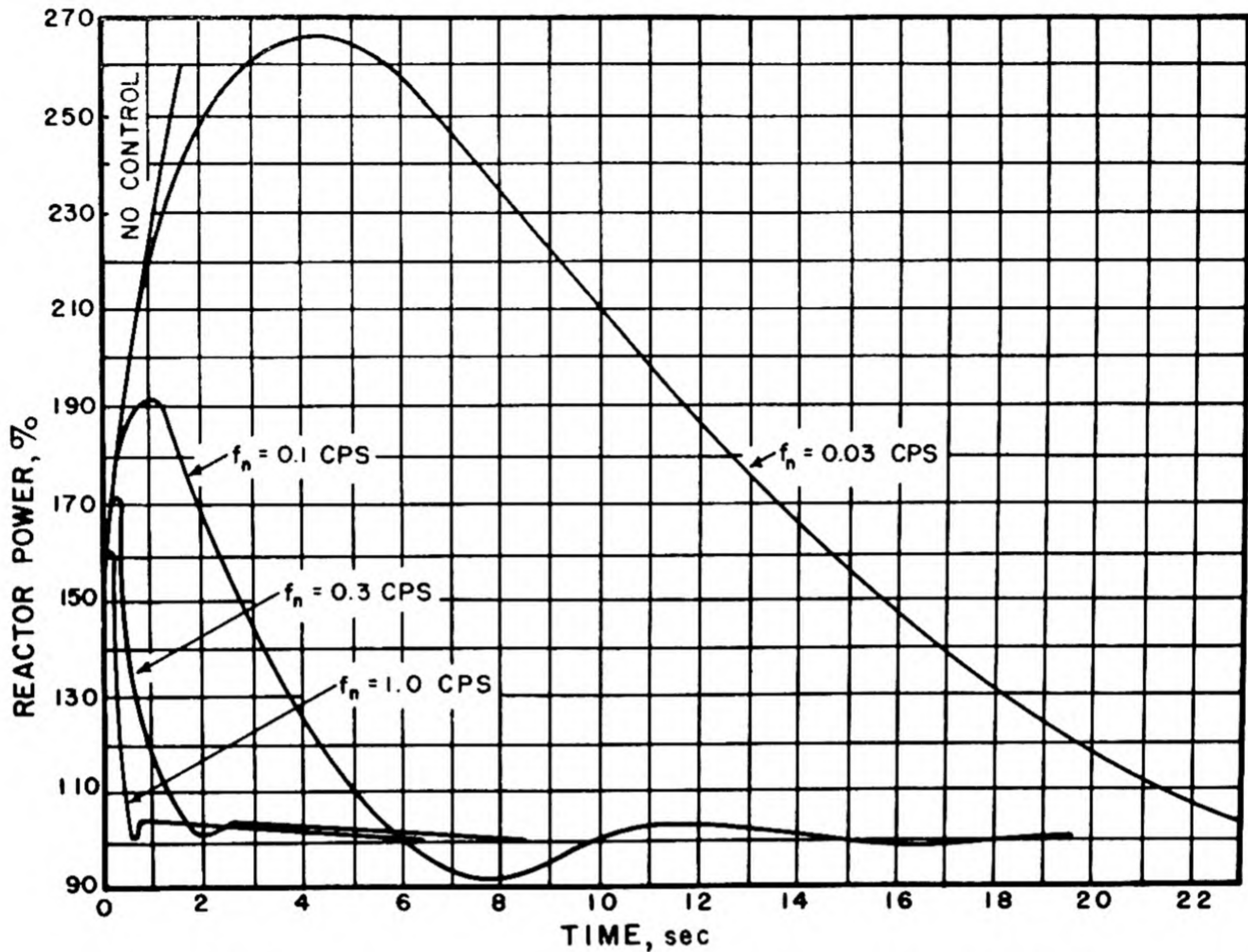


Fig. 1.6.32 — Reactor Power vs Time. Reprinted from WAPD-34, Vol. I, RM-90. The following parameters were used: Temperature coefficient = zero; disturbance = +0.003 step in δk ; regulator rod servo-parameters = optimum for each f_n .

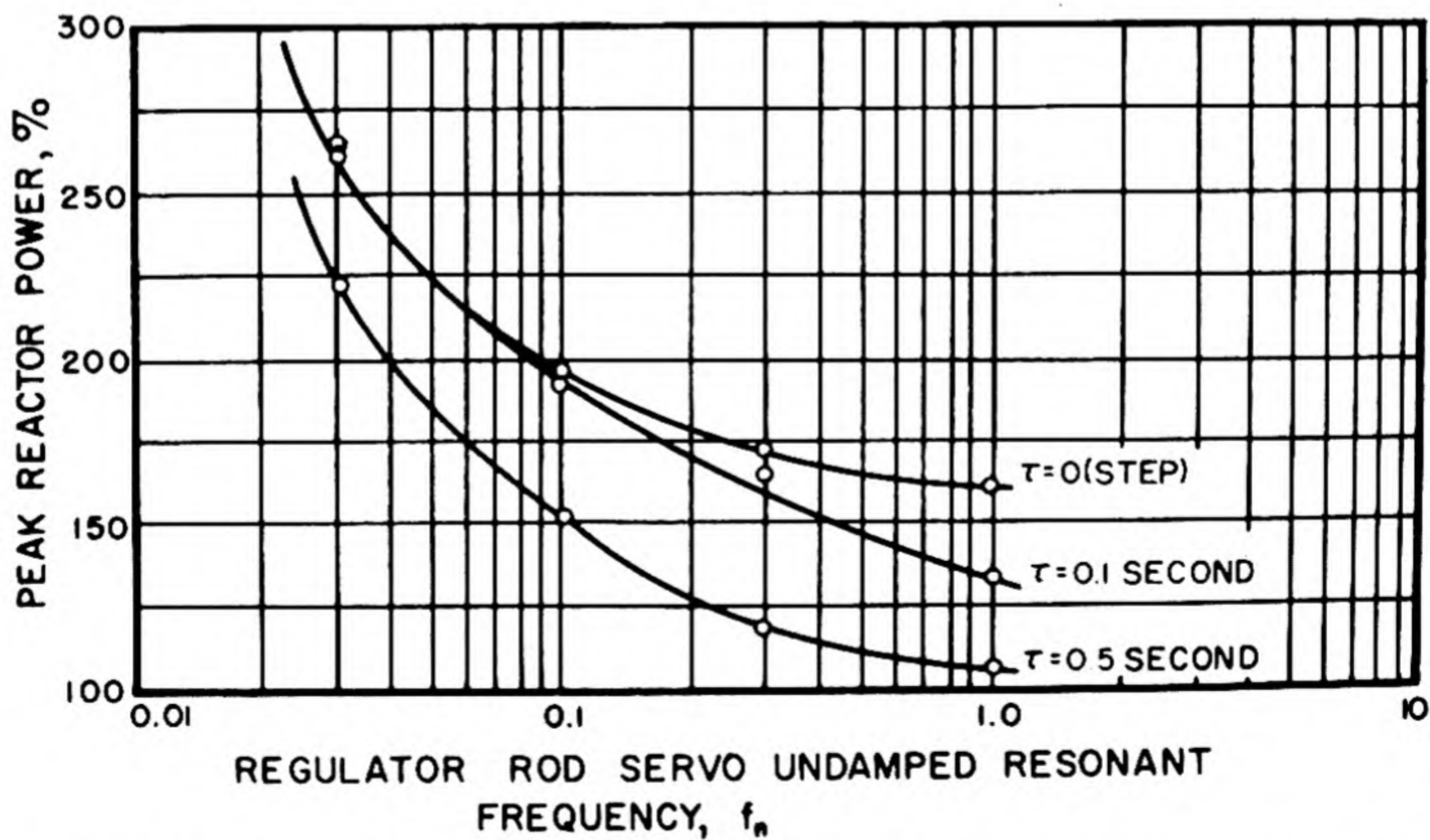


Fig. 1.6.33 — Effect of Rapidity of δk Transient on Peak Reactor Power. Reprinted from WAPD-34, Vol. I, RM-90. The following parameters were used: Temperature coefficient = zero; disturbance = $+0.003(1 - e^{-t/\tau}) = \delta k$; regulator rod servo-parameters = optimum for each f_n .

AFTER SHUTDOWN

XENON BUILDUP^{29,30}

The maximum concentration of xenon-135 after shutdown may, in a high-flux reactor, be several times the equilibrium value. This results in a large decrease in reactivity. The time variation of the xenon concentration after shutdown may be obtained from Eq. (82) with iodine source term placed equal to zero. If the reactor has been operating at constant power long enough so that the xenon and iodine concentrations have reached equilibrium values, the iodine concentration can be obtained from Eq. (82), and the ratio of xenon to fuel macroscopic thermal absorption cross sections can be obtained from Eq. (83). The general solutions of Eq. (82) are the same as for any other decay chain and were given in Chapter 1.2.

The xenon poisoning, P , for shutdown after reaching equilibrium at a given flux ϕ_0 is plotted as a function of time in Fig. 1.6.34. The peak and steady-state xenon poisoning for various reactor steady-state fluxes are given in Fig. 1.6.35. Xenon concentration trajectories for various operating maneuvers are discussed in Ref. (31).

HEATING AFTER SHUTDOWN

The heat released by radioactive decay of fission products has been treated in Chapter 1.2. In most cases, heat resulting from induced radioactivity may be neglected. Results of calculations of temperature rise (without cooling) for various reactors, as a function of time after shutdown, are given in Fig. 1.6.36.

REACTOR TEMPERATURE COEFFICIENTS

LATTICES

Experimentally obtained temperature coefficients for natural-uranium and graphite reactors are given in Table 1.6.1; barometric coefficients, arising from neutron capture in nitrogen, are also given for air-cooled units.

The theoretical situation has been recently reviewed³² with special reference to the Oak Ridge and Brookhaven reactors, as follows: Based on the notation given in Chapter 1.5 under "Lattices," one has:

$$\frac{\delta k_{\text{eff}}}{k} = \frac{\delta \epsilon}{\epsilon} + \frac{\delta \eta}{\eta} + \frac{\delta f}{f} + \frac{\delta p}{p} - B^2 \delta M^2 \quad (168)$$

This ignores graphite and metal density effects, whose contribution is only of the order of 1×10^{-6} per $^{\circ}\text{C}$, and supposes nitrogen effects to be handled separately. The term in ϵ is also only of this order and may likewise be ignored.

The remaining terms all depend upon neutron (i.e., moderator) temperature except p which depends upon metal temperature via Doppler broadening of the resonance lines. The η term will be the same for all natural-uranium reactors; the other terms will vary from one reactor to another.

Values for $-(1/\eta) d\eta/dT$ derived from experiment and calculation range from $4.5 \times 10^{-5}/^{\circ}\text{C}$ to $22 \times 10^{-5}/^{\circ}\text{C}$. This represents one of the largest terms in (168), and one of the most uncertain. From evaluation of the remaining terms and comparison with actual reactor results (Table 1.6.1), the authors conclude that the smaller values are to be preferred.

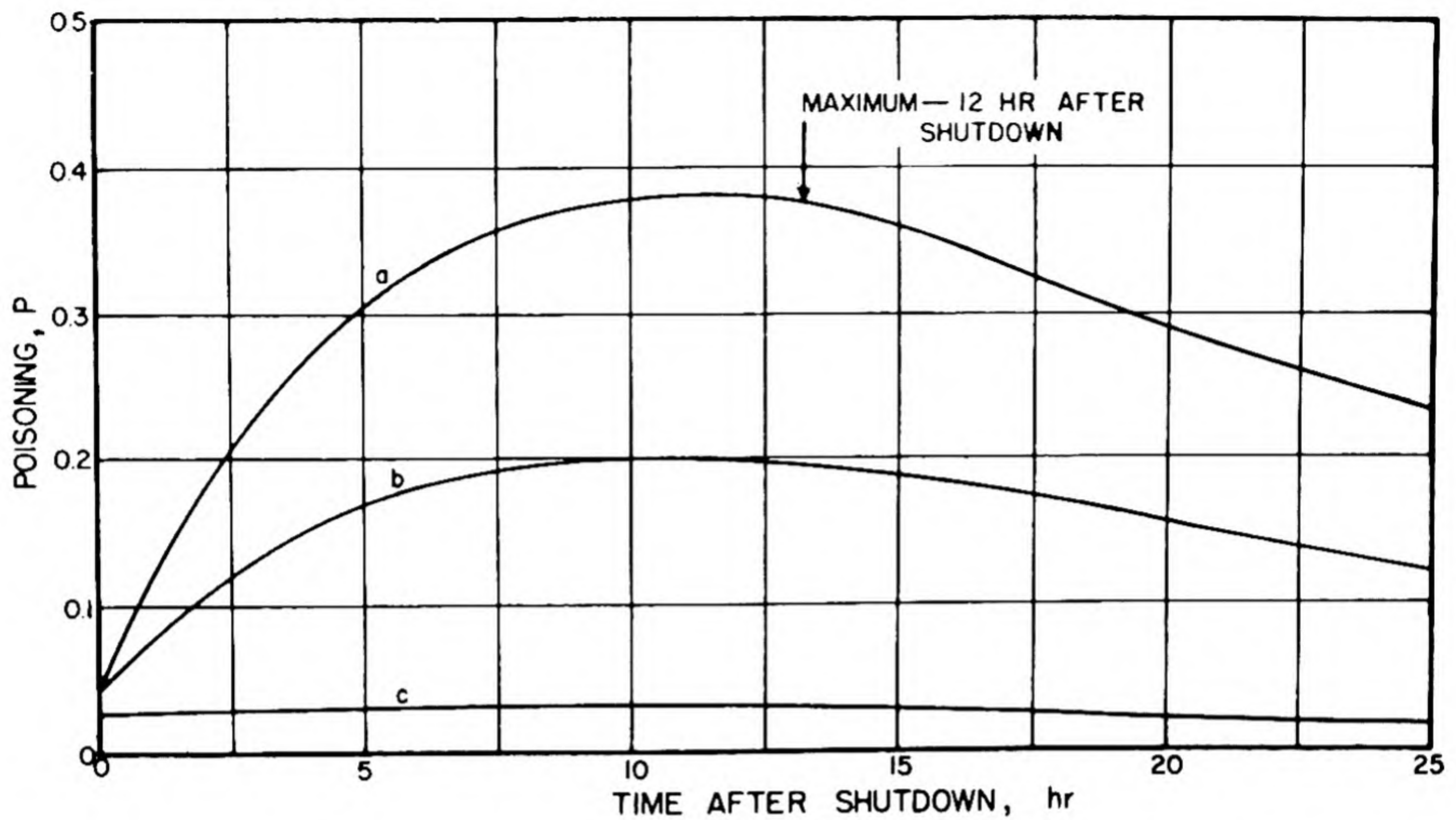


Fig. 1.6.34 — Xenon Poisoning vs Time after Shutdown. The ratio of xenon to U^{235} macroscopic thermal absorption cross sections is shown for the case where xenon and iodine are in equilibrium prior to shutdown. The curves are for different fluxes: (a) 2×10^{14} neutrons/(cm²)(sec); (b) 10^{14} neutrons/(cm²)(sec); (c) 10^{13} neutrons/(cm²)(sec). Reprinted from *The Elements of Nuclear Reactor Theory*, by S. Glasstone and M. Edlund. Copyright, 1952. By permission from D. Van Nostrand Company, Inc., New York.

The main variation in f arises from the flattening of the thermal-neutron distribution as the temperature rises, as may be found by varying the κ values in Eq. (3), Chapter 1.5. For $1/v$ absorbers, κ varies as $T^{-1/4}$ where T is the absolute temperature of the neutrons. Results calculated in this way are given in Table 1.6.2.

Variation in p with (metal) temperature involves the change in the effective volume resonance integral A as shown in Table 1.6.3. The effect of temperature on the surface term, μ , is apparently not known. In the Brookhaven and Oak Ridge machines, $\delta p/p \approx -0.12$ $\delta A/A$ [Eq. (9), Chapter 1.5] so that the contribution to Eq. (168) is some $-(1.4 \text{ to } 2) \times 10^{-5}$ per $^{\circ}\text{C}$.

The effect of (neutron) temperature on M^2 is primarily exerted through the thermal diffusion area L^2 , according to (for $1/v$ absorption, and $f_2 = 1 - f$):

$$\frac{dL^2}{dT} = L^2 \left(\frac{1}{T} - \frac{f}{f_2} \frac{1}{f} \frac{df}{dT} \right) \quad (169)$$

For the Brookhaven reactor, this amounts to about $0.35 \text{ cm}^2/^{\circ}\text{C}$, while the corresponding effect on the age is about $-0.05 \text{ cm}^2/^{\circ}\text{C}$. Thus, $dM^2/dT = 0.3 \text{ cm}^2/^{\circ}\text{C}$, and the last term in Eq. (168) is about $-2.8 \times 10^{-5}/^{\circ}\text{C}$. A similar value is obtained for the Oak Ridge reactor.

The sum of the η , f , and M^2 terms in Eq. (168) is to be compared with the "uniform graphite in vacuum" coefficient in Table 1.6.1; while the p term in Eq. (168) is to be compared with the "uniform metal" coefficient.

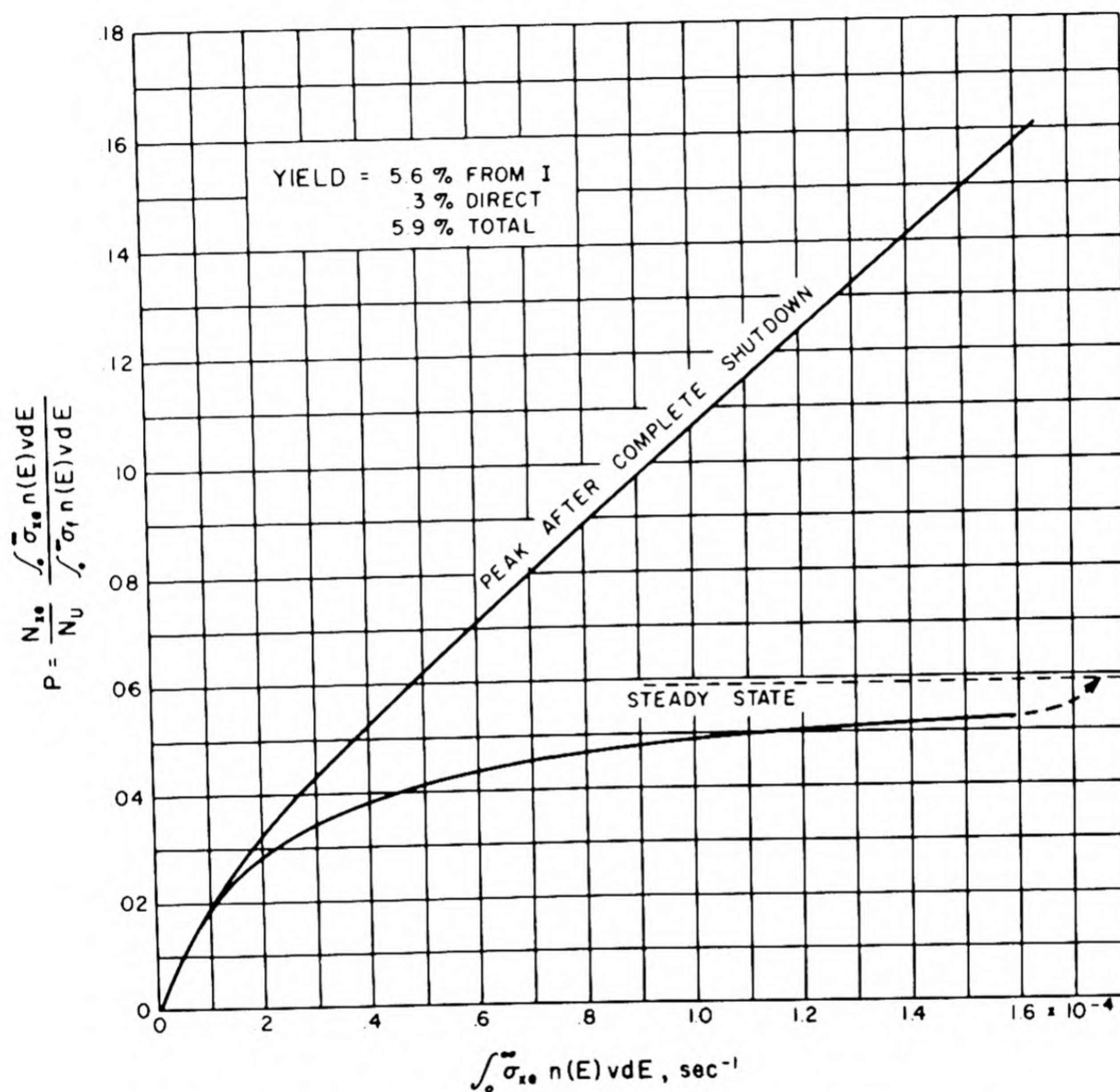


Fig. 1.6.35—Xenon Poisoning vs Flux. Taken from H. Hurwitz, private communication. Curves show peak after shutdown and steady-state poisoning as a function of steady-state flux.

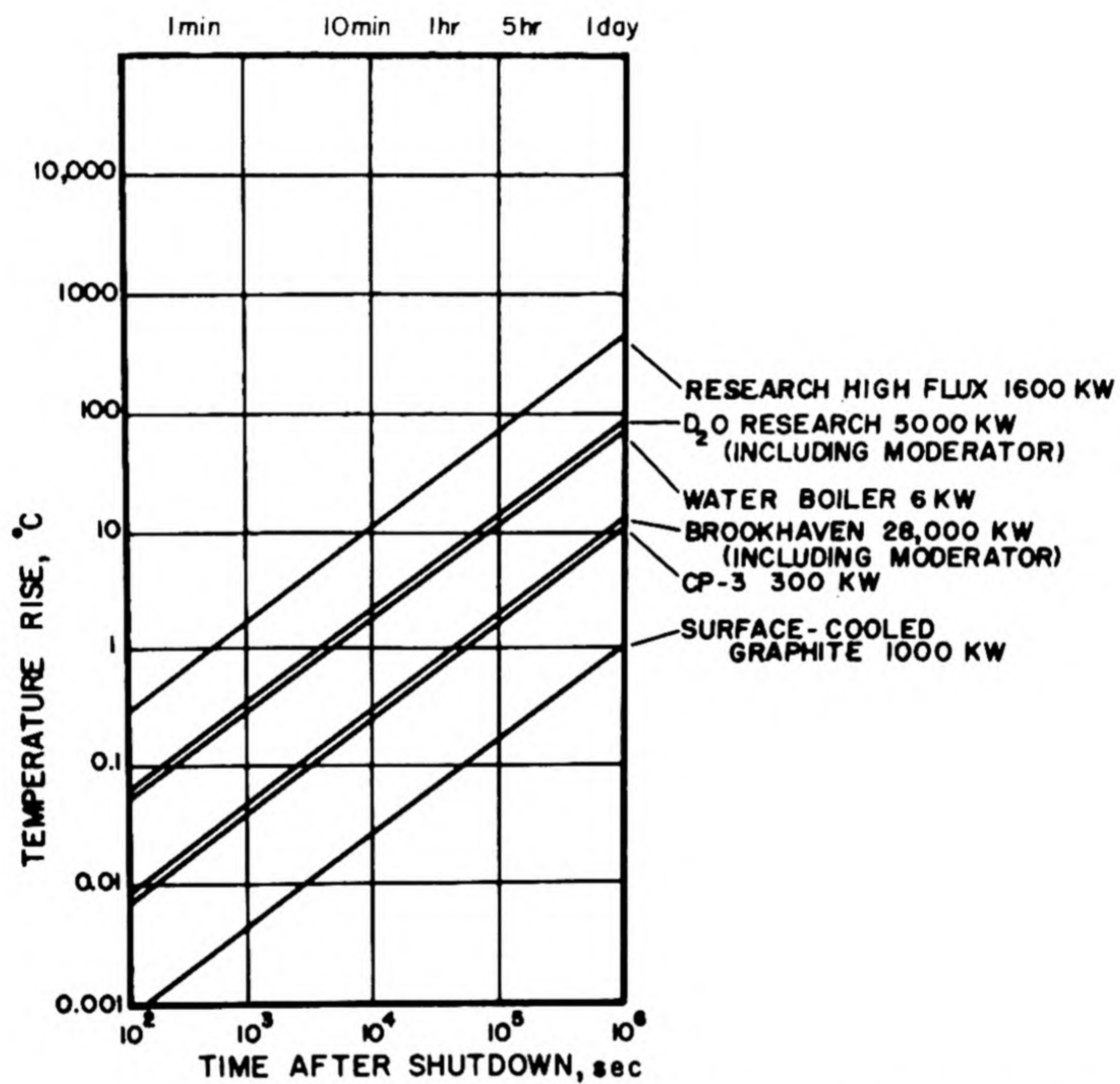


Fig. 1.6.36 — Calculated Temperature Rise After Shutdown. Reprinted from M. M. Mills, Journal of Reactor Science and Technology 58, TID-71.

Table 1.6.1 — Experimental Temperature Coefficients in Graphite Lattice Reactors

Reactor	Temperature coefficient,* $10^6 \Delta R/^{\circ}C$
Oak Ridge†	-0.78
Operating metal	-2.08
Operating graphite	-2.86
Operating total	-1.04
Uniform metal	-4.94
Uniform graphite in vacuum	-5.98
Uniform over-all in vacuum	-2.9
Uniform graphite in air	
Brookhaven,‡ 300°K	-1.82 ± 0.26§
Uniform graphite in air	-1.95 ± .13§
Uniform metal	-4.1
Uniform graphite in vacuum	

* "Operating" coefficients are referred to temperature of hottest metal in the reactor

† Kaplan and Chernick;⁵² barometric coefficient = $-1.04 \times 10^{-5} \Delta k/mm \text{ Hg}$

‡ Communication from Irving Kaplan; barometric coefficient§ = -0.91×10^{-5} in k for mm Hg

§ Data converted from inhours by using 1 inhour = 2.6×10^{-5} in k

Table 1.6.2 — Temperature Dependence of Thermal Utilization in Lattice Reactors
(Kaplan and Chernick, BNL-152)

T, °K	$1/f \partial f/\partial T (\times 10^5/^{\circ}C)$	
	Oak Ridge	Brookhaven
300-350	4.1	3.3
350-400	3.4	2.6
400-450	2.7	2.2

Table 1.6.3 — Temperature Effect on Volume Resonance Integral of U
(Kaplan and Chernick, BNL-152)

Author	$1/A \partial A/\partial T (\times 10^4/^{\circ}C)$
Creutz et al (CP-110)	1.7
Mitchell et al (CP-597)	1.1
Wigner (CP-4)	3
Dancoff (CP-1589)	1.2-1.7

REACTOR CONTROLS

ABSORBER CONTROLS

Absorbers distributed uniformly throughout the reactor change the microscopic cross sections, and the effect on reactor reactivity can be determined by methods described previously (Chapters 1.4, 1.5, and previous portions of 1.6). In practice, the absorbing material for control is frequently lumped into discrete assemblies, such as rods which move in and out of the reactor; further considerations are therefore needed.

SINGLE CONTROL RODS

A small, thermally black rod of effective radius r_0 inserted along the axis of a bare cylindrical reactor of radius R affects k by an amount approximated from 2-group theory results to be:³³

$$\Delta k = \frac{7.5}{R^2} (\tau + L^2) \left[0.116 \left(1 + \frac{\tau}{L^2} - \ln \frac{2.405 r_0}{R} \right) - \frac{\tau}{L^2} \ln K r_0 \right]^{-1} \quad (170)$$

where τ = age, L = thermal diffusion length, and $K = \sqrt{1/\tau + 1/L^2}$.

The rod affects reactivity through the neutrons it absorbs and the increase it produces in the number of neutrons escaping outward from the reactor surface. For a small axial rod, the latter effect is about 0.6 of the former.*

If the rod were black to fast neutrons as well, its effectiveness would be greater by a factor which decreases from $1 + \tau/L^2$ for very small rods to 1 for large rods.†

As the rod is displaced from the central axial position, its effectiveness decreases. Figure 1.6.37 shows the effect of radial displacement as estimated by the familiar (neutron flux)² weighting rule and also as obtained from more detailed computations. Figure 1.6.38 similarly shows the effect of longitudinal displacement, i.e., of partly withdrawing‡ the rod out the end of the reactor, as obtained from flux-squared weighting and from more elaborate calculation.

The effect of a rod is greater in reflected than in bare reactors (Fig. 1.6.39).

EFFECTIVE ROD RADIUS

As employed in the derivation of Eq. (170), r_0 is the radius at which the external diffusion solution for the neutron flux vanishes. This is somewhat less than the actual geometric radius, r , of the rod, since even with a perfectly black absorber the neutron flux merely dips downward toward the body but has not vanished by the time the surface is reached. Chapter 1.3 discusses the boundary conditions at the surface of a black body; the straight-line extrapolation distance of the external flux into the body is λl , where l is the mean-free-path. For large bodies, this gives the effective radius ($r_0 = r - \lambda l = r - 0.71l$), but for small bodies, the external diffusion solution being fitted curves downward below the straight line, and r_0 is closer to r . One may also³⁴ develop the formulae using the actual radius, r , and the surface logarithmic derivative given by λ without introducing r_0 .

* Graphs³⁴ show how these two effects vary as the rod is displaced away from the reactor axis.

† This variation is plotted³³ for different numerical cases by 2-group theory and also compared with a result obtained by Murray from more elaborate calculations.

‡ Near the tip of a partially inserted rod, its neutron absorption may be increased several fold, the so-called "lightning rod" effect. See Murray³⁸ and Wheeler.³⁹

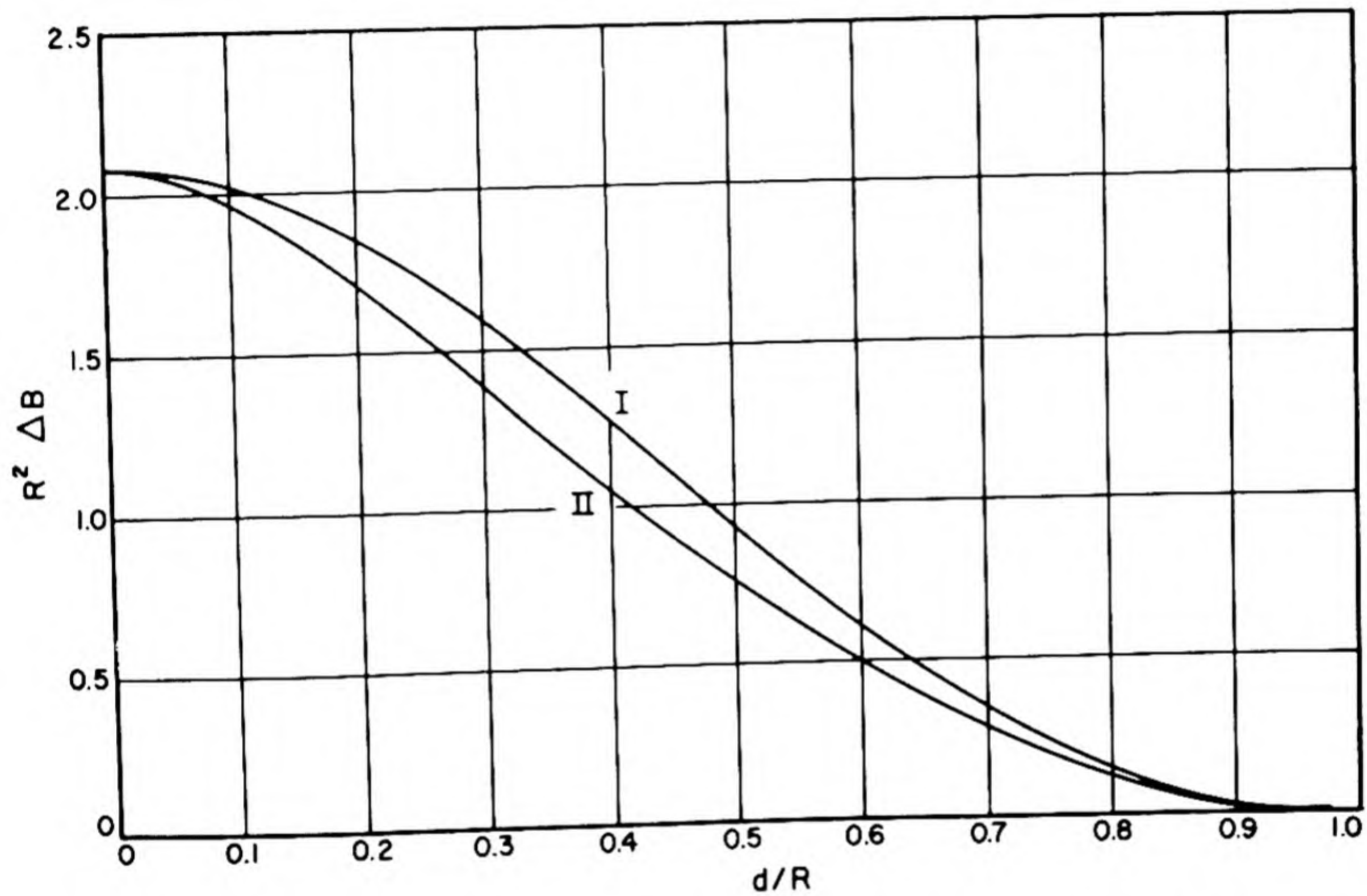


Fig. 1.6.37 — Eccentric Control Rod Effectiveness. Reprinted from Adler MT-222. Bare cylindrical reactor of radius R , rod parallel to axis and at distance d from it, effective radius of rod $= r_0 = 0.01R$. ΔB = change in buckling due to rod. (I) J_0^2 weighting; (II) superposition calculation.

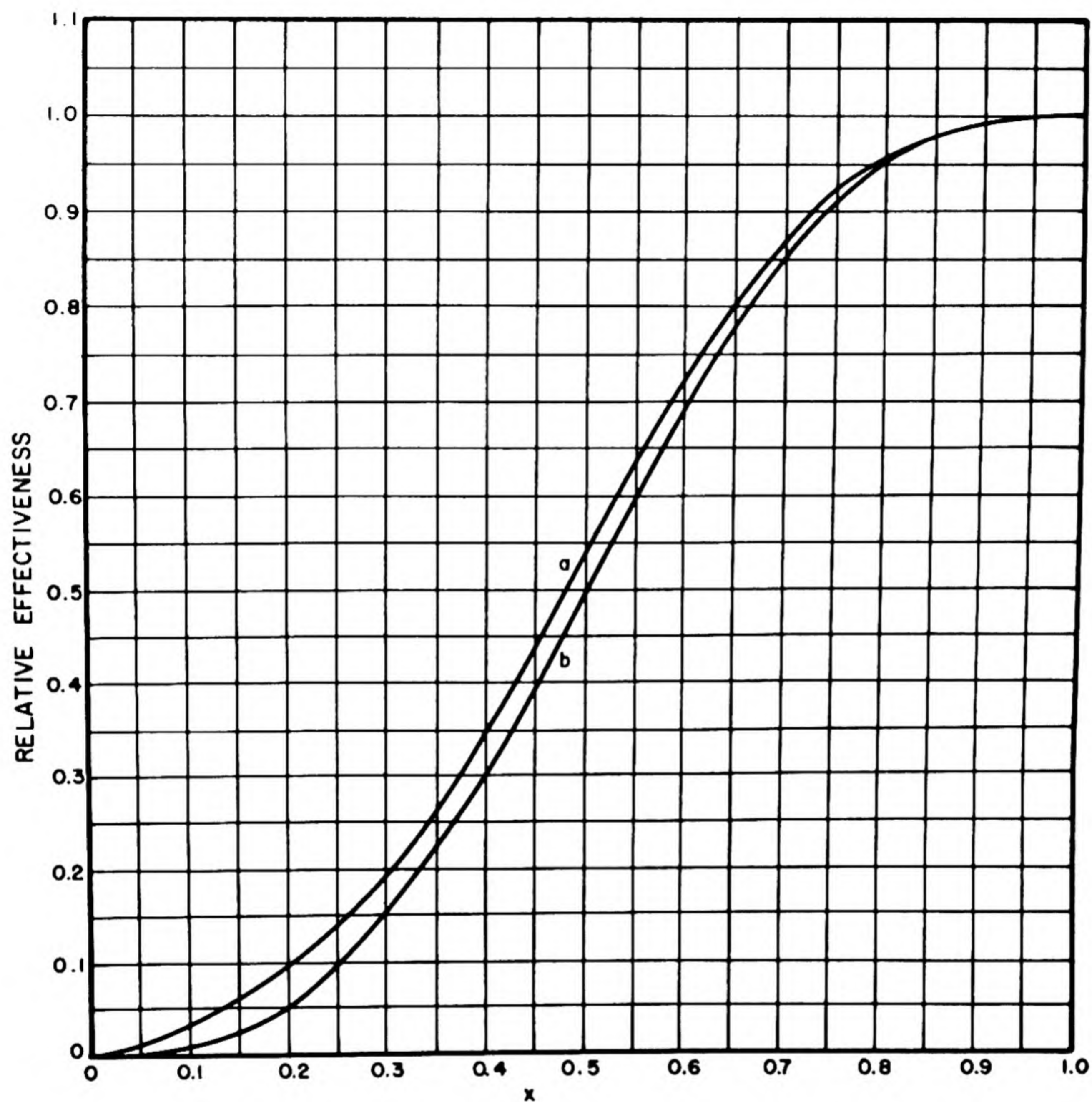


Fig. 1.6.38—Partial Withdrawal of Axial Control Rod. Reprinted from Wheeler, Principles of Nuclear Power, N-2292. Effectiveness of rod relative to effectiveness when completely inserted; x = distance of insertion + length of the cylindrical reactor. (a) Calculations by Murray for a case with reactor diameter = 90 times rod diameter = 1.77 reactor length; (b) estimate according to $2 \int_0^x \sin^2 \pi y dy = x - \sin 2\pi x / 2\pi$.

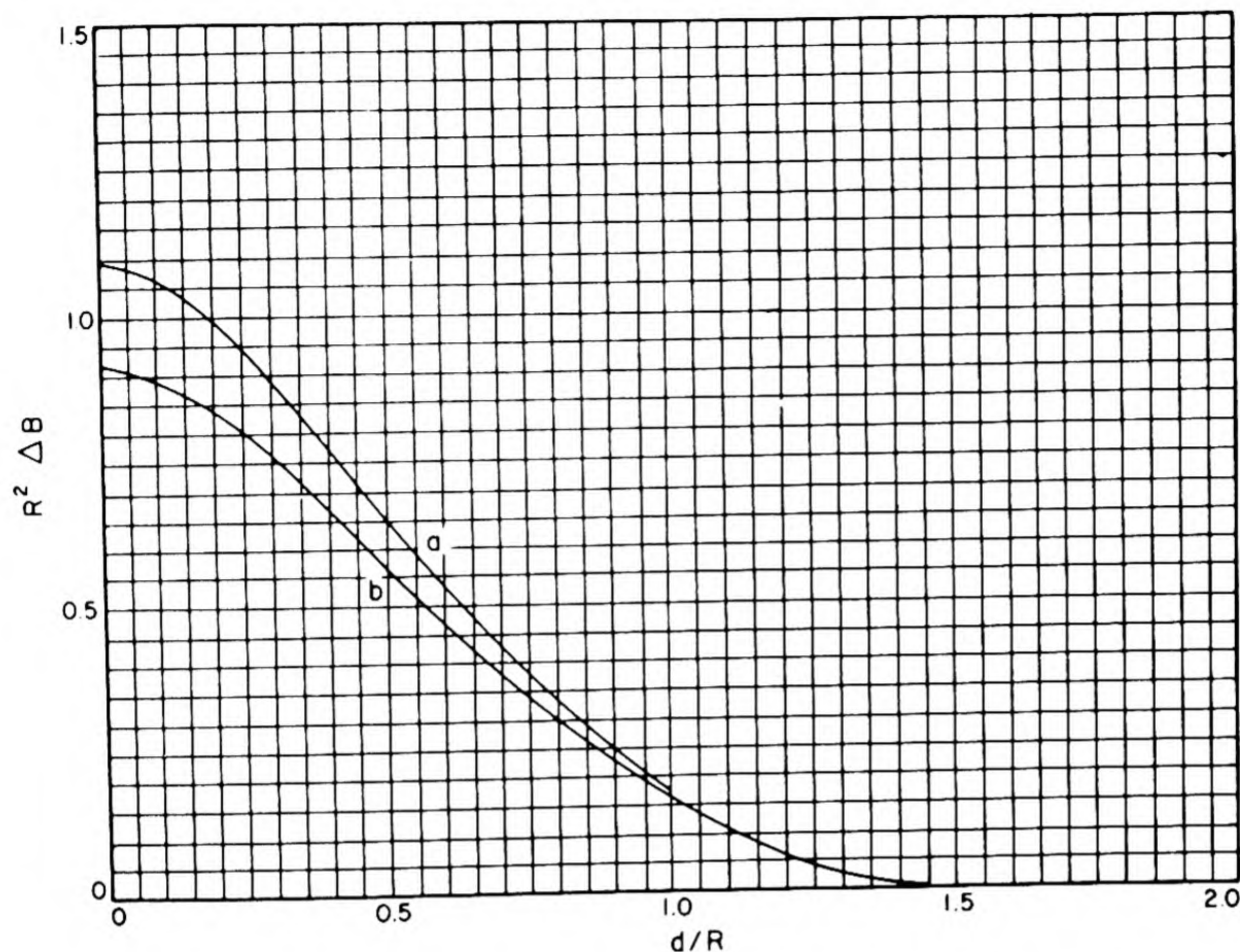


Fig. 1.6.39 — Control Rod Effectiveness in Bare vs Reflected Reactors. Reprinted from Adler, MT-222. Cylindrical core radius = R with reflector = $1.5R$ without reflector, same core buckling. Distance of rod from axis = d , effective radius of rod = $0.01R$, ΔB = change in buckling due to rod (a) in reactor with reflector (b) in bare reactor.

Wheeler³⁹ gives values for the effective radius, r_0 , for a number of cases as reported in Table 1.6.4 for black bars and in Table 1.6.5 and Fig. 1.6.40 for bars which are not black. Table 1.6.6 gives some experimental and theoretical comparison of various bar shapes.

MULTIPLE CONTROL RODS

When more than one rod is present, there are interaction effects between them. A single rod lowers the relative value of the neutron density nearby but raises it farther away. Thus, the effect of a second rod will be diminished if near the first but may be enhanced if farther away; i.e., the "shadowing" may be either negative or positive.

Table 1.6.7 gives some experimental results with two rods. In the Brookhaven reactor, the reduction in effectiveness of one bank of 8 rods owing to shadowing is estimated at 16 percent;⁴¹ for two banks crossing, the reduction is 35 percent. Figure 1.6.41 shows the effectiveness per rod of a ring of 4 rods at varying distances from the reactor axis and also the effectiveness of a single rod at the same distance; the shadowing is negative when the rods are close together and becomes positive as they separate. Figure 1.6.42 again illustrates the greater effectiveness of rods in a reflected reactor.

Table 1.6.4—Effective Radius of Black Control Bars
(Wheeler, N-2292, Principles of Nuclear Power, Chapter 22: Control)

Case	r_0
Large snugly imbedded rod*	$r e^{-0.71 l/r}$
Snugly imbedded rod†	$r e^{-\lambda l/r}$
Small (compared to l) snugly imbedded bar of perimeter‡ s	$0.46 l e^{-(8\pi l/3s)}$
Small (compared to l), snugly imbedded rod of radius r	$0.46 e^{-(4l/3r)}$
Bar in a considerably larger hole of radius r_1	$r_1 e^{-(8\pi l/3s)}$
Rod in considerably larger hole of radius r	$r_1 e^{-(4l/3r)}$
Imbedded strip of small thickness (compared to l) but with W comparable with or larger than l	$W/4 \exp -[y(1 - 0.114y + 0.048y^2)]^{-1}$ where $y = W\sqrt{3}/\pi l$
Imbedded cross formed of two thin strips each of width $W + \sqrt{2}$	Same as preceding
Large imbedded rectangular bar	See Fig. 1.6.43

* A constant in Wheeler's formula has been changed here⁵⁹

† Obtained by a slight extension of Wheeler's argument; here λ is from Chapter 1.3, "Boundary Conditions in Diffusion Theory," for a cylindrical case

‡ Perimeter determined by putting a measuring tape once about the bar and drawing it tight; in general, the tape will not touch the bar at all points

Table 1.6.5—Effective Radius of Non-black Bars

Case	r_0
Weak absorption*	
General	$r_{av} e^{-(2\pi l/3r)}$
Small (in girth compared to l) imbedded bar	$0.46 e^{-(2\pi l/3A)}$
Bar in considerably larger hole	$r_1 e^{-(2\pi l/3A)}$
Intermediate absorption†	
Rod in any size hole	$r_1 e^{-(2\pi lF/3A)}$

* Here,⁶⁰ A is the total absorption cross section ($N\sigma_a$) per unit length of bar, and r_{av} is the distance from the bar axis to the point where the average neutron absorbed in the rod may be considered to have started its last flight. Webster⁶¹ gives a formula for computing r_{av} , and also discusses the evaluation of A for fast neutrons

† Here,⁶² F is the surface-to-average neutron density for the rod a function of $x = Kr$ and plotted in Fig. 1.5.17

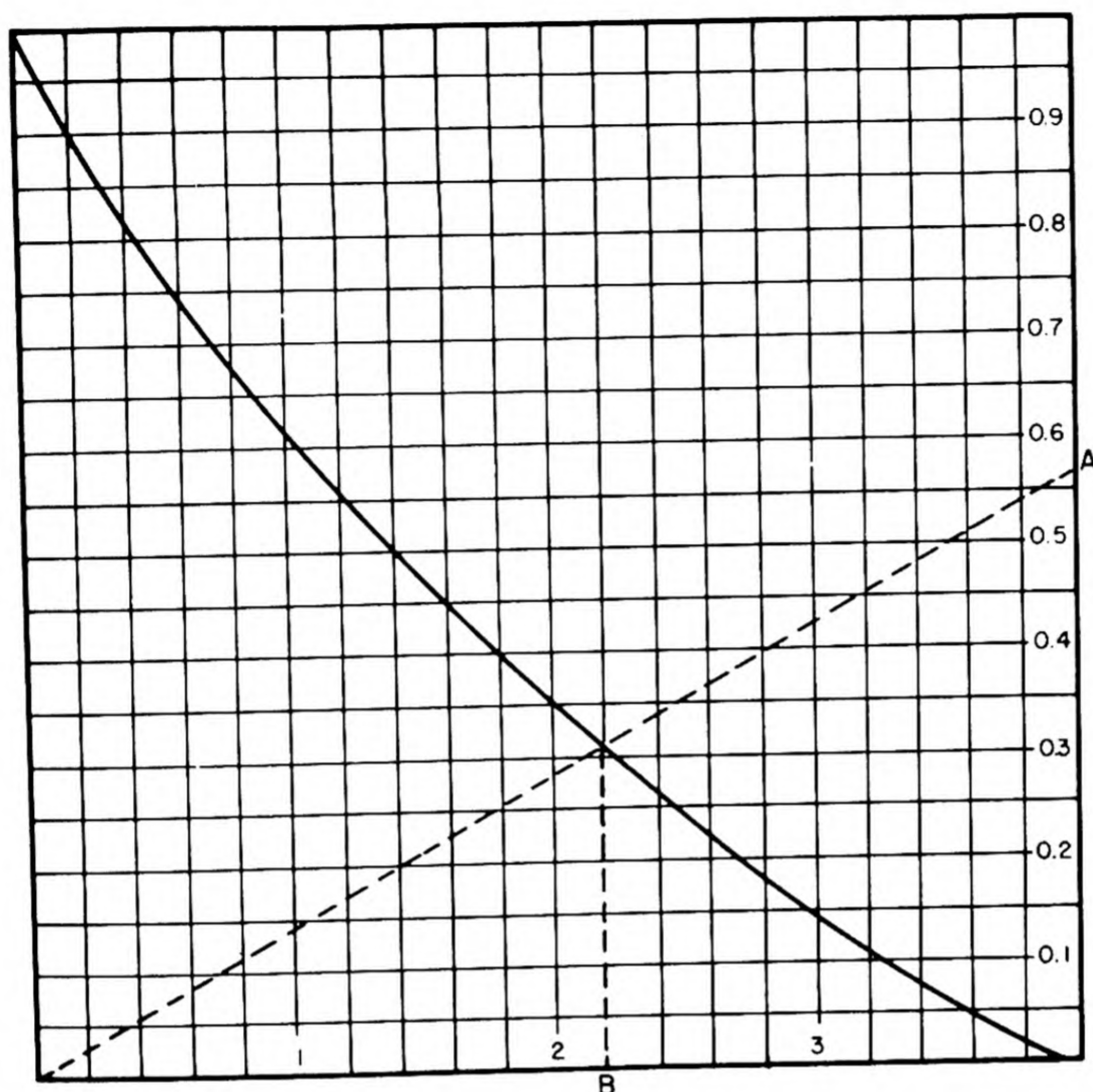


Fig. 1.6.40 — Effective Radius of Rectangular Bar. Reprinted from Wheeler, Principles of Nuclear Power, N-2292. Remove a layer of thickness 0.711 all around the bar to obtain a smaller effective rectangle of width w and thickness Aw . Plot A on right scale of graph and connect to lower left corner by a straight line intersecting curve. Below intersection, read $B = w/r_0$ on bottom scale.

Table 1.6.6 — Effect of Control Rod Shape

(Wheeler, Principles of Nuclear Power, N-2292, Sect. 22.5.30)

Shape of bar	Perimeter, cm	Observed* effectiveness relative to + bar	In-hole calculation†		Imbedded calculation‡	
			r_0 , cm	Relative effectiveness	r_0 , cm	Relative effectiveness
—	18.1	0.90	1.65	0.87	1.28	0.82
+	25.6	1.00	2.38	1.00	2.24	1.00
0	28.4	1.06	2.58	1.03	3.20	1.06

* Marshall;‡ all bars had a maximum extension of 9.05 cm and were located in a square hole equivalent in area to a circle of radius $r_1 = 5.74$ cm

† Using entry 5 of Table 1.6.4

‡ Using Table 1.6.4 entry 7 for — shape, entry 8 for + shape, and entry 1 (but with the original value 0.58 instead of 0.71) for 0 shape

Table 1.6.7—Control Rod Shadowing*

(Wheeler, Principles of Nuclear Power, N-2292, Sect. 22.3.62)

Distance between rods, in.	45	90
Effect of first rod alone	0.159	0.159
Effect of second rod alone	.211	.159
Sum of individual effects	.370	.318
Observed effect of both together	.338	.303
Decrease owing to shadowing, %	8.6	4.7

* Experiments by Zinn and Anderson⁶⁴ on first chain-reactor built at Chicago; controls were two strips of cadmium 2 in. wide and 8 ft long

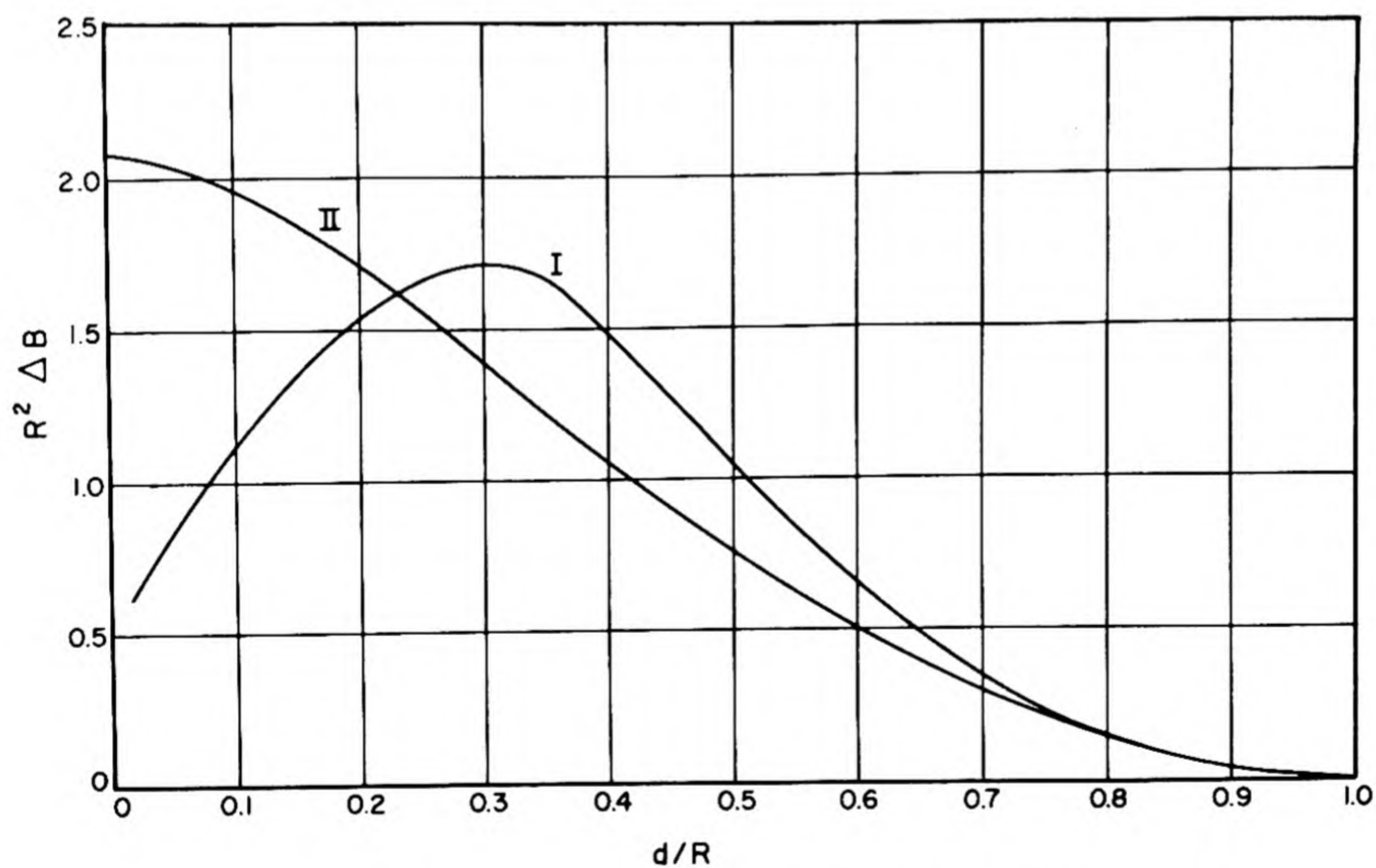


Fig. 1.6.41—Shadowing in a Ring of 4 Control Rods. Reprinted from Adler, MT-222. Bare cylindrical reactor of radius R ; effective radius of rod = $0.01R$; distance of rods from reactor axis = d ; ΔB = change in buckling. Graph shows (II) effectiveness of a single rod; (I) one-fourth the effectiveness of a ring of 4 rods.

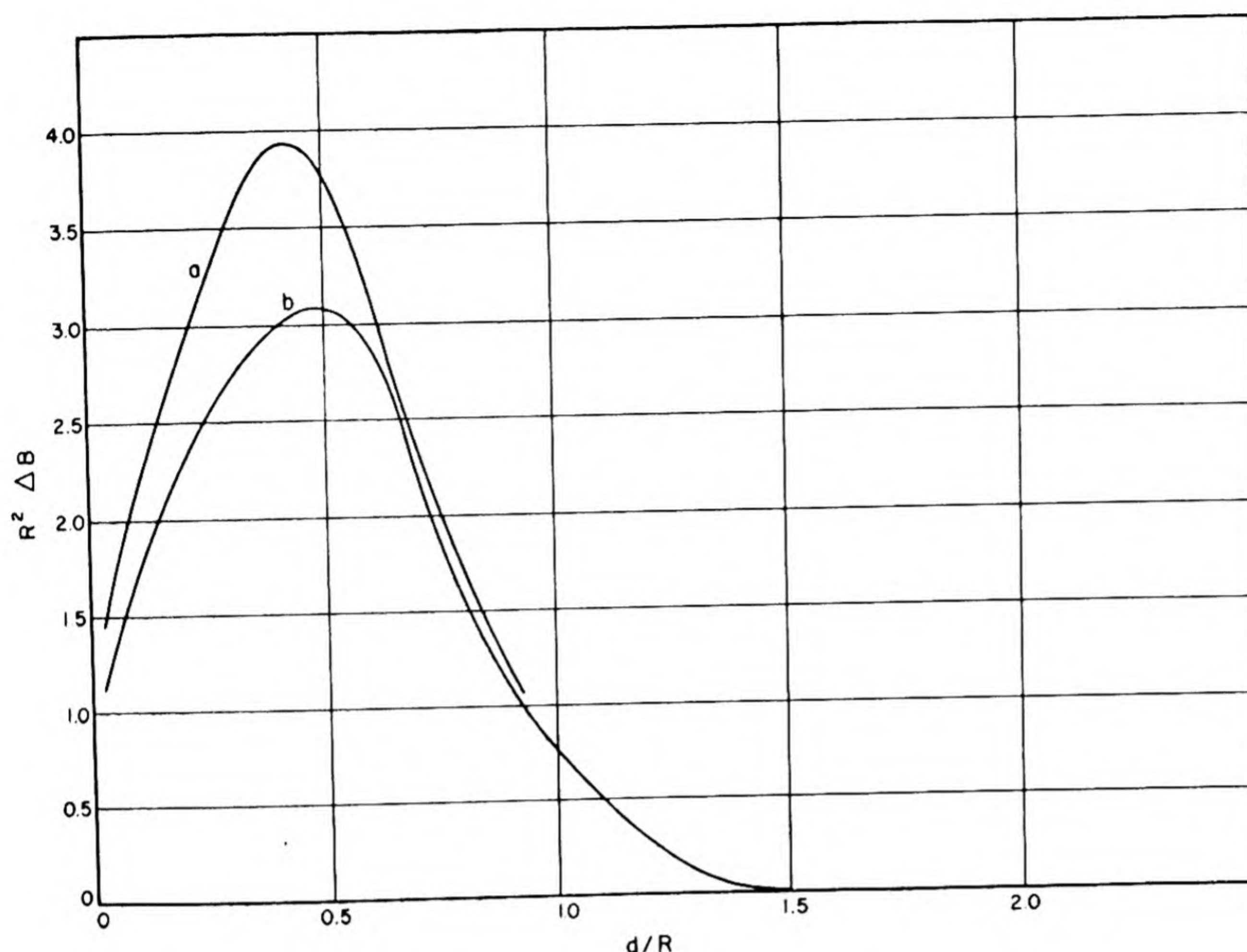


Fig. 1.6.42 — Control Rods with and without Reflector. Reprinted from Adler, MT-222. Cylindrical core of radius R with reflector, $1.5R$ without reflector; $r_0 = 0.01R$, ring of 4 rods at distance d from the core axis, ΔB = change in buckling (a) in reflected reactor (b) in bare reactor.

CONTROL REGIONS

The effect of slight spatial variations in buckling is accounted for by the flux-squared weighting rule:

$$\bar{B} = \frac{\int B \phi^2 dv}{\int \phi^2 dv} \quad (171)$$

where ϕ is the undisturbed neutron flux.* The statistical weight of a region of a reactor is the value of $\int \phi^2 dv$ for that region divided by the value of the same integral taken over the entire reactor. Evidently, the weights of different regions are additive. Figure 1.6.43 shows the weights of central regions in various shapes of bare reactors.† It is seen that the efficiency of (a small amount of) control exerted in a central region is several times what it would be if spread uniformly throughout the reactor.

* More generally,⁴² ϕ is proportional to the neutron flux multiplied by $l_{tr}(1 + \tau/L^2)$.

† Figure 1.6.44 gives some Bessel function integrals frequently encountered in cylindrical reactors.

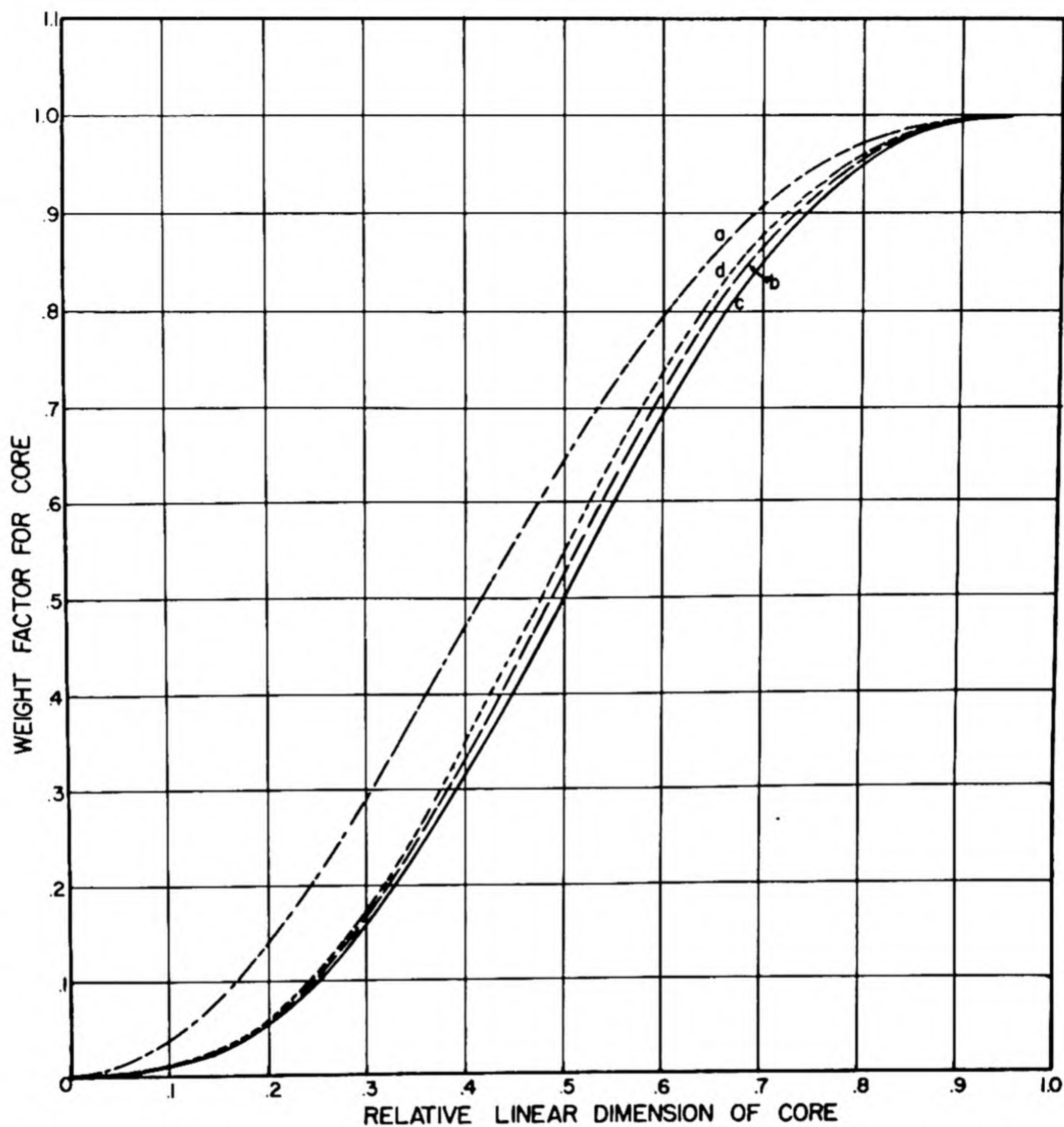


Fig. 1.6.43 — Statistical Weights for Central Regions. Reprinted from Chicago Handbook. (a) Circular cylinder with full length concentric core; (b) circular cylinder with similar concentric core, i.e., core length reduced in the same ratio as the radius; (c) sphere with concentric core; and (d) parallelepiped with similar core.

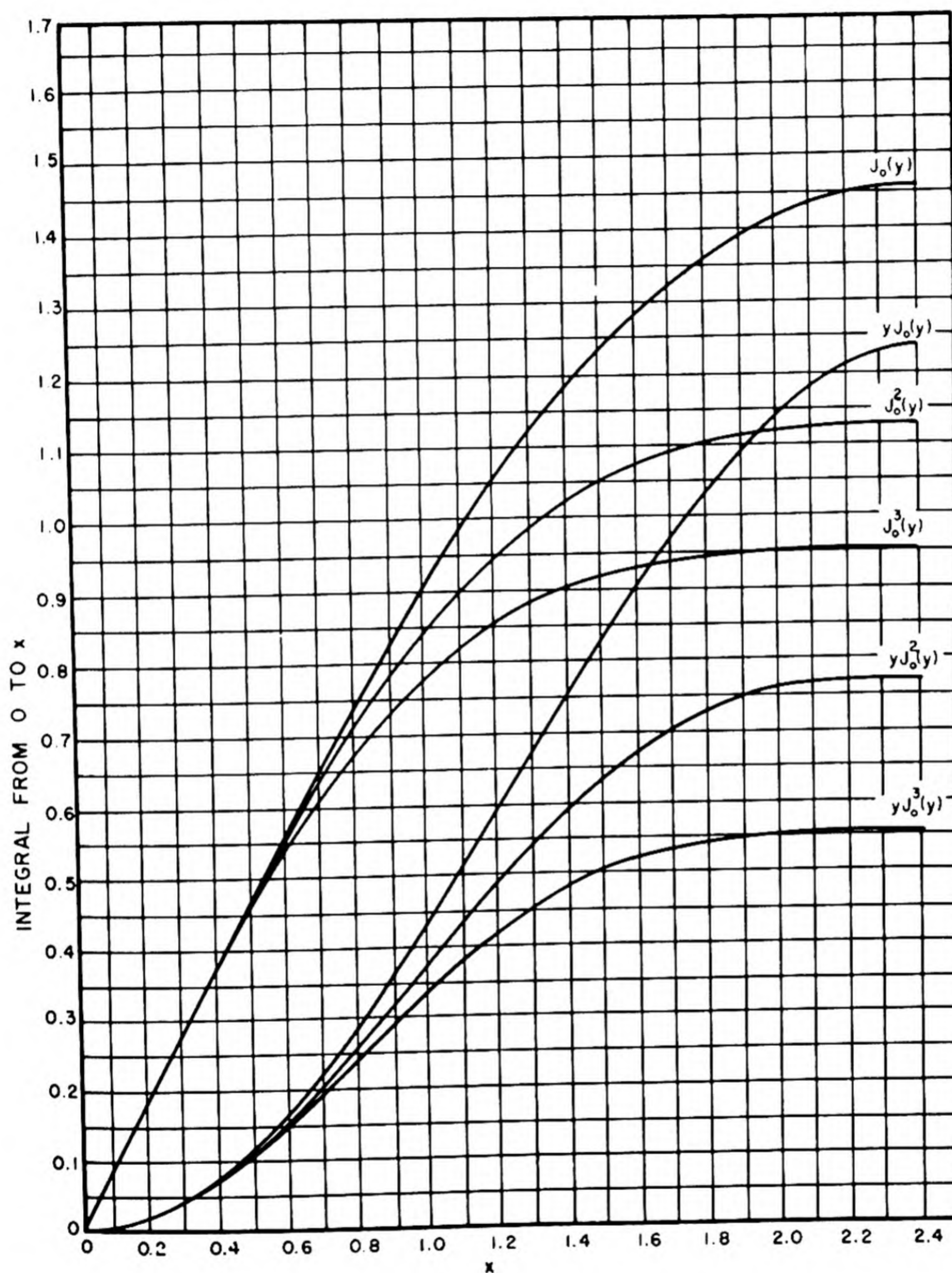


Fig. 1.6.44 — Integrals of Bessel Functions. Reprinted from Wheeler, Principles of Nuclear Power, N-2292. Shows $\int_0^x F(y)dy$, for $F(y)$ as indicated on the curves.

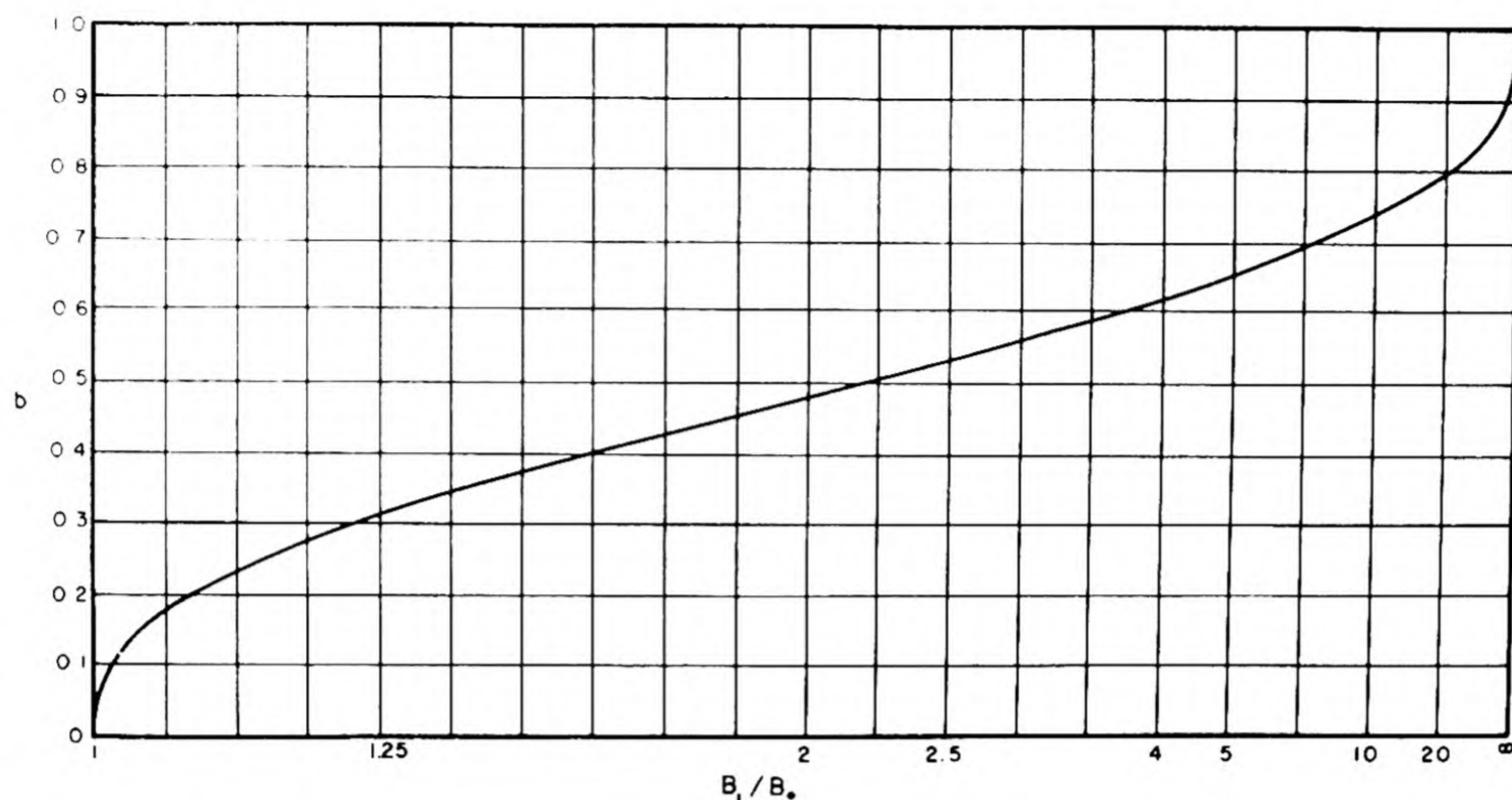


Fig. 1.6.45 — Spherical Control Region. Reprinted from Wheeler, Principles of Nuclear Power, N-2292. Concentric control region in spherical reactor; b = control region radius \div reactor radius; B = total buckling.

When large amounts of control are to be applied, the neutron flux is appreciably disturbed and the flux-squared rule no longer holds.* A principle frequently followed in large control is to apply it strongly enough in a central region of the reactor so as to flatten the flux there. The size of this central region is then adjusted so as to accomplish the desired amount of control of the reactor as a whole.

Figure 1.6.45 shows the size of the flat-flux central region needed to achieve a specified degree of control in a bare spherical reactor; Figs. 1.6.46 and 1.6.47 do the same for full-length cylindrical control regions in bare, circular and rectangular reactors. Again the efficiency† of control exerted in a central core is seen to be a few times larger than if spread throughout the reactor.

When flux flattening is to be accomplished by control rods, they are arranged in a regular lattice array throughout the control region, and their size and spacing are adjusted so as to just reduce the (radial) buckling B_1 to zero. The resulting relationship is approximately:⁴³

$$N_0(br_0) - \frac{N_1(br_2)}{J_1(br_2)} J_0(br_0) = \frac{\tau}{L^2} i H_0^{(1)}(i K r_0) \quad (172)^\ddagger$$

where r_2 = equivalent (area-wire) radius of the lattice cell associated with each rod, $b^2 = B_1$ = buckling neutralized by the rod, and the other quantities are as in Eq. (170). For small arguments in the Bessel functions, this becomes:^{33,44}

*The corresponding weighting factor would now be the product of the disturbed and undisturbed fluxes.

† Described by $\frac{B_1 - B_0}{B_1} \frac{\text{total volume}}{\text{core volume}}$

‡ Wheeler's Figure 22.5.23 is a nomograph for solving this equation.

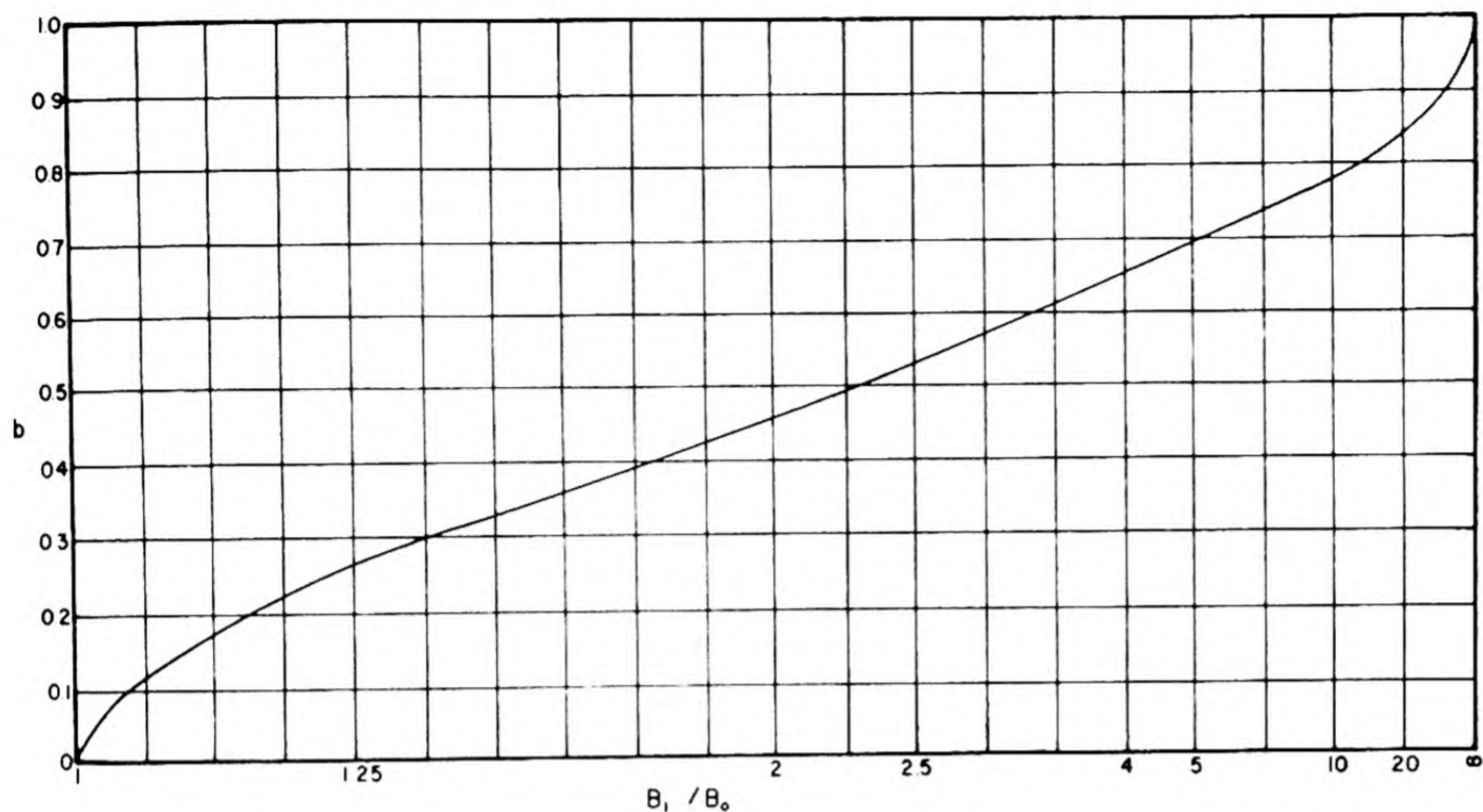


Fig. 1.6.46 — Cylindrical Control Region. Reprinted from Wheeler, Principles of Nuclear Power, N-2292. Full length concentric control region in a cylindrical reactor. Radius of control region + radius of reactor = b ; B = radial buckling.

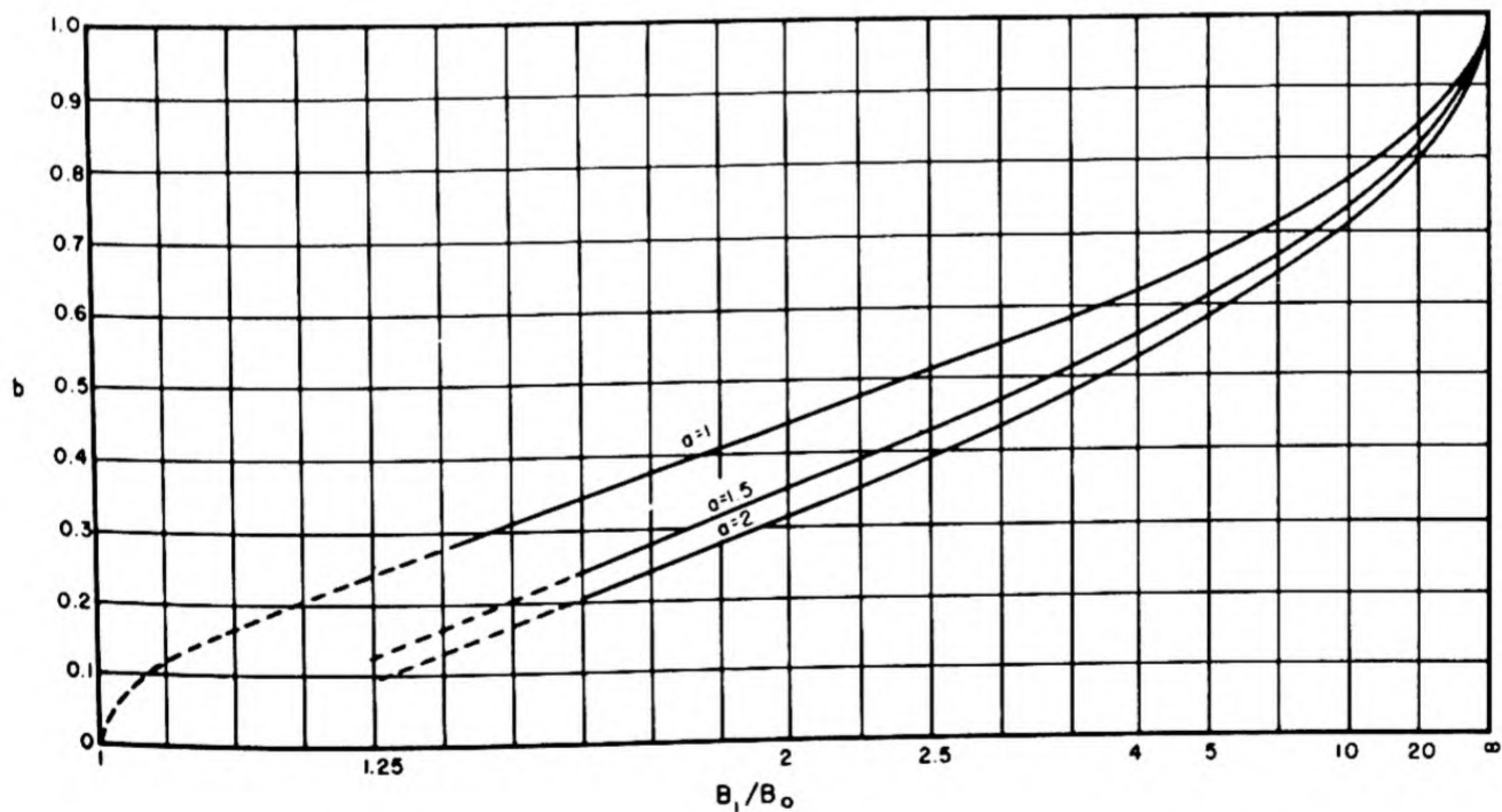


Fig. 1.6.47 — Rectangular Control Region. Reprinted from Wheeler, Principles of Nuclear Power, N-2292. Full-length rectangular control region in rectangular prism reactor. Length of reactor rectangle + width of reactor rectangle = a . Between reactor rectangle and the control rectangle within it, is a constant thickness border all around. Width of control rectangle + width of reactor rectangle = b . B_1 = transverse (after longitudinal cosine component is removed) buckling outside the control region; B_0 = critical uniform transverse buckling for entire reactor rectangle. Calculations approximate and less reliable where lines are dashed. The reference report also gives upper bounds to b .

$$b^2 = \frac{2}{r_0^2} \left(\ln \frac{1.123}{br_0} + \frac{\tau}{L^2} \ln \frac{1.123}{Kr_0} \right)^{-1} \quad (173)$$

The effective change in multiplication factor within the control region thus brought about by the rod bank is $\Delta k = b^2(\tau + L^2)$.

CONTROL BOUNDARIES

The action of a control rod as considered above is, in effect, to insert into the reactor a boundary (e.g., of radius r_0) at which the thermal (or both thermal and fast) flux vanishes. Such black boundaries can be imagined in various shapes and arrangements, and (when considered to cause all neutron fluxes to vanish) hence create different shapes or volumes for the reactor. In certain geometrically simple cases,* the resulting control effect can be readily found. For example, a black sheet passing through the center of a bare spherical reactor converts it into two bare hemispheres, and the resulting effect on the buckling required can be obtained from Table 1.4.3. Table 1.6.8 gives buckling values for some additional cylindrical shapes.

Table 1.6.8 — Buckling Values for Cylindrical Shapes*

Cross section of cylinder	Buckling	Buckling relative to circle for same area
Circle of radius a	$(2.405/a)^2$	1
Square of side a	$2(\pi/a)^2$	1.0865
Equilateral triangle of altitude a	$4(\pi/a)^2$	1.2546
Semi-circle of radius a	$(3.832/a)^2$	1.2694
45°–45°–90° triangle of leg a	$5(\pi/a)^2$	1.3581
30°–60°–90° triangle of hypotenuse a	$112/9 (\pi/a)^2$	1.4637

* From a preliminary and incomplete ORNL table by Sangren. The values given are for the transverse buckling only; for finite height H of the cylinder there is an additive term $(\pi/H)^2$ in the total buckling

GAPS

Separation of the reactor core into halves with an adjustable gap between them for control purposes has been envisaged (sometimes with the aim of not disturbing the power pattern in planes parallel to the gap). The BNL reactor has a transverse gap (though not for control purposes) and a comprehensive review of gap theory is in preparation.†

Figure 1.6.48 gives experimental results on the reactivity effect of gaps of variable thickness and shows calculated results for comparison.

* Wheeler⁴⁶ illustrates a number of these and, for μ_1 of cylindrical sectors in Table 1.4.3, gives the approximate expression $1 + 1.861^{1/2}$.

† Chernick and Kaplan⁴⁹ include comparison of theory with experimental results of Callihan et al.,⁵⁰ on a split water-moderated machine. Reference (51) gives some discussion of gap theory.

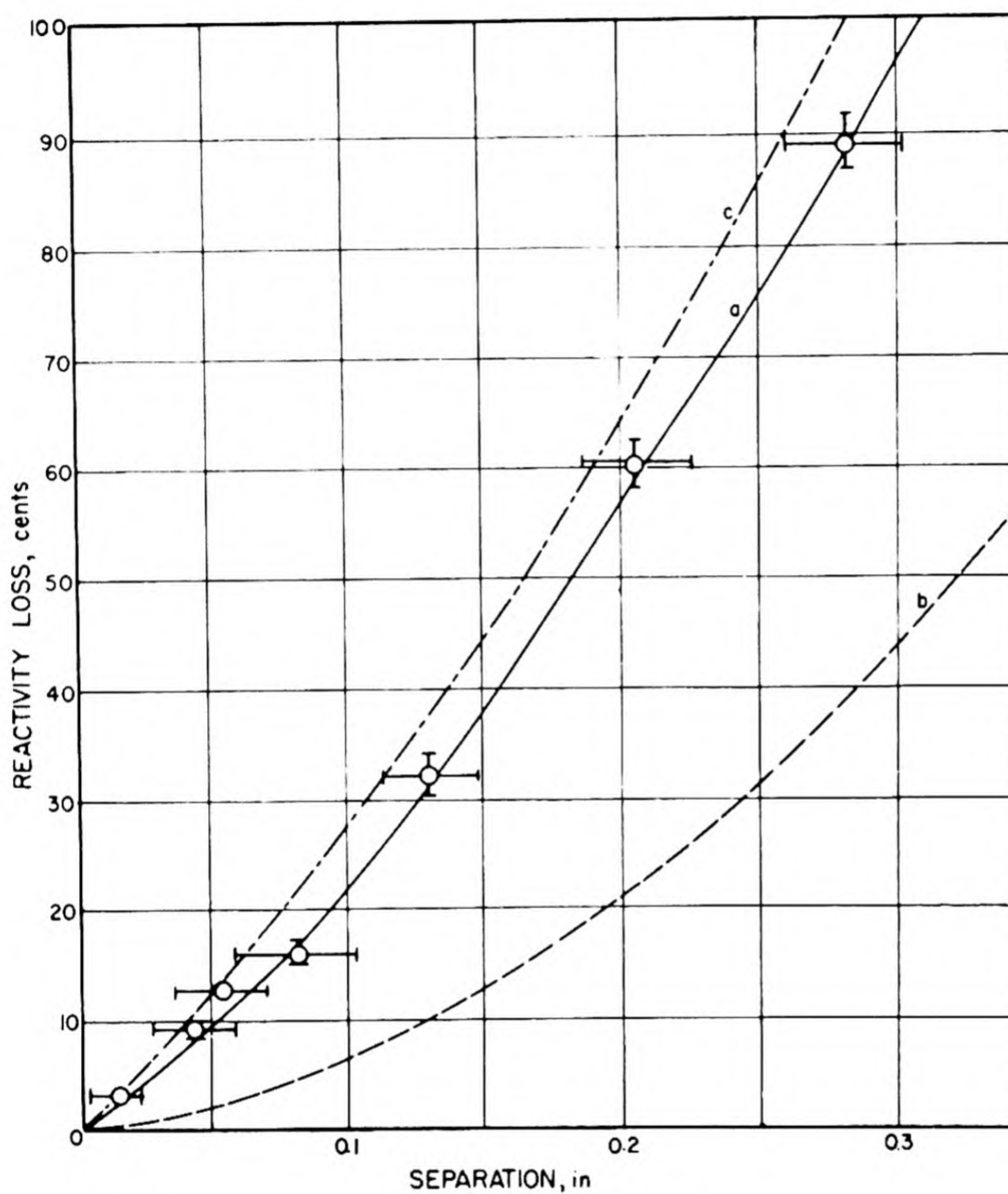


Fig. 1.6.48 — Reactivity Effect of Transverse Gap. Reprinted from Tamor, ORNL-1320. (a) Experimental results in a homogeneous 25-graphite critical experiment; (b) calculated from the theory of Goldberger and Wilkins (CP-3443); and (c) calculated from an extension of that theory.

REFERENCES

1. A. M. Weinberg, Theory of Oscillating Absorber in a Chain Reactor, AECD-2044, June 7, 1948.
2. Sylvan Wallach, Solutions of the Pile Kinetic Equation When the Reactivity is a Linear Function of the Time, WAPD-13.
3. Coveyou and Mulliken, AECD-2407.
4. Reactor Physics Progress Report, KAPL-706, April 1952, p 22 (classified).
5. Reactor Physics Progress Report, KAPL-706, April 1952 (classified).
6. Reactor Physics Progress Report, KAPL-706, April 1952, p 25 (classified).
7. H. Hurwitz, Nucleonics, July 1949, p 61.
8. R. R. Coveyou, YF-10-74.
9. Reactor Phys. Prog. Rep., loc cit, p 28.
10. G. M. Roe, KAPL, personal communication (classified).
11. Morehouse and Young, CP-1069 (A-1460) (classified).
12. Chernick, BNL-126 (classified).
13. HKF-109, p 3.19 (classified).
14. ORNL-730, July 6, 1950, p 64 (classified).
15. T. Welton, CF-52-10-107, Oct. 17, 1952 (classified).
16. BNL-173.
17. BNL-113, Aug. 1951 (classified).
18. KAPL-565 (classified).
19. Nordheim, CP-2589 (classified).
20. H. Hurwitz, KAPL-646, Dec. 20, 1951, p 23 (classified).
21. WAPD-34, Vol. I (classified).
22. Brown and Campbell Servomechanisms, John Wiley and Sons, New York.
23. Reactor Phys. Prog. Rep., loc cit, p 21.
24. Transfer Function of Argonne CP-2, Nucleonics 10, No. 8, Aug. 1952.
25. K. Donelian and J. Menke, MonP-379 (classified).
26. HKF-109, Chapter III (classified).
27. Welton, ORNL-1121 (classified).
28. WAPD-34 (RM-90) (classified).
29. Glasstone and Edlund, The Elements of Nuclear Reactor Theory, D. Van Nostrand Co., Inc., New York, 1952.
30. Gale Young, MonP-457 (classified).
31. KAPL-847, to be published (classified).
32. Kaplan and Chernick, BNL-152, pp 50-59 (classified).
33. Wigner et al, CP-1461 (classified).
34. Adler, MT-222.
35. Webster, NEPA-650 (classified).
36. Deleted.
37. CP-3581 (classified).
38. Murray, CP-1235.
39. Wheeler, N-2292 (classified), Sect. 22.6.10 to 22.6.12.
40. Wheeler, N-2292 (classified), Sect. 22.3.63.
41. Kaplan and Chernick, loc cit, p 70f.
42. Chicago Handbook, IVE, p 25 (classified).
43. Wheeler, loc cit, Sect. 22.5.22.
44. Chicago Handbook IVE, p 28 (classified).
45. Wheeler, loc cit, Fig. 22.3.69.
46. Wash-24 (classified).
47. ORNL-1177 (classified).
48. Bendt, MonP-385 (classified).
49. Chernick and Kaplan, BNL-182 (in draft form as BNL log C-6150) (classified).
50. Callihan et al, K-126, Fig. 14 (classified).
51. Kaplan and Chernick, loc cit, p 37ff.
52. Kaplan and Chernick, loc cit, p 58f.
53. Deleted.
54. Visner, ORNL-CF-52-9-9 (classified).
55. Miles et al, TID-2001, p 10 (classified).
56. Callihan et al, ORNL-1227 (classified).
57. Callihan et al, ORNL-1294 (classified).
58. Lichtenberger, ORNL Reactor Physics Conference, Sept. 10-12, 1952 (classified).
59. Kaplan and Chernick, loc cit, p 68.
60. Wheeler, loc cit, Sect. 22.4.18.
61. Webster, loc cit, p 27.
62. Wheeler, loc cit, Sect. 22.4.20.
63. Marshall, CP-718 (classified).
64. Zinn and Anderson, CP-510 (classified).

Section 2

RADIATION SHIELDING

Prepared by
OAK RIDGE NATIONAL LABORATORY
with parts by
NUCLEAR DEVELOPMENT ASSOCIATES
and
NATIONAL BUREAU OF STANDARDS

Acknowledgments

This section could not have been completed without the devoted efforts of Mrs. Lorraine Swift Abbott, the section editor. In addition to attending to the myriad details of submitting so many documents for publication, she has made real contributions to the subject matter by extensive use of the ORNL library. Her clarification of the presentations, in particular the tables of data, has materially enhanced the utility of the work.

Similar credit should be accorded to Mrs. May King Hullings; whose contributions have been catholic and competent. Much of the computing, preparation of some of the tables and graphs, some of the editing, and part of the expediting comprise her notable contributions.

For assistance in preparation of Chapter 2.2, thanks are due to Karl Z. Morgan. In Chapter 2.3, Gladys White contributed many of the tables and undertook a major share of the editorial work. Ann T. Nelms did a considerable share of the early editorial work, and Ida E. Hornstein had some part in the latter stages of the editorial work. Lewis V. Spencer and John Doggett contributed the tables of asymptotic constants so indicated, which are previously unpublished.

Permission of H. L. F. Enlund is gratefully acknowledged for the inclusion in Chapter 2.7 of his treatment of shield heating from capture-gamma rays.

The chapter on materials has been prepared with considerable assistance from Mrs. Abbott and Mrs. Hullings, aforementioned, as well as A. S. Kitzes, who reviewed the treatment of cements, concretes, and boral. H. L. F. Enlund helped by reviewing the chapter in its early stages.

The appendix on constants and conversion factors was prepared by Philip Mittelman of NDA.

Finally, the Information and Reports Division of ORNL is to be thanked for its competent work in publishing the drafts and particularly for the art work in which much effort was expended toward satisfying the needs of the individual authors.

E. P. Blizard

April 24, 1953

Author's Preface

In spite of some five years of research, exact calculational methods of shield design are still hopelessly complicated, and it appears likely that simpler approximations may never be adequate in many cases. As a consequence, the approach to the problem has turned to a cataloguing of solutions which have been obtained by experiment or machine calculation and to developing methods of tailoring these solutions to new problems.

In the case of gamma-ray attenuation through homogeneous media of a single element, the polynomial method of Spencer and Fano is being exploited in a joint program by the National Bureau of Standards and Nuclear Development Associates, and the early results of this program are presented in this section. Solution to more complicated gamma-ray attenuation problems for several regions or for mixtures of materials has no more than begun, and cataloguing of these results will be a much more extensive effort. Experiments such as those of Hayward and Hubbell on back-scattering and of Kirn, Kennedy, and Wyckoff¹ on oblique penetration are examples of the experiments required to solve many shielding problems which become extremely complicated in the analytical approach. It has been suggested that the Monte Carlo method lends itself well to such problems, but this has not yet been demonstrated.

The neutron attenuation problems of most interest in reactor shielding are those of the penetration of hard neutrons through large thicknesses of hydrogenous material (usually water). Enough experimental information has been gathered to check simple theories of this attenuation so that for most cases an adequate solution can be had either from basic calculations using shielding-experiment ("effective removal") cross sections or from direct geometrical transformation of an experimental result. This class of problems can include appreciable quantities of other materials (e.g., iron, lead, beryllium), provided they are located close to the source and followed by at least 50 cm of water or its equivalent.

The fast-neutron attenuation of thick nonhydrogenous shields is but poorly understood and almost unexplored experimentally. Concretes, which are intermediate in hydrogen content (~1 percent by weight), have been measured to some extent.

The compound problem of neutron and gamma attenuation in which neutron-induced gamma rays dominate has not been essayed analytically with any simple success. The very few calculations which have been tried have succumbed to hopeless complications and have been dropped. The experimental approach, on the other hand, has been quite adequate, especially since the development of optimization techniques. No relief seems to be in the offing, however, from the continued need for an experiment for each new situation. Eventually, perhaps enough data will be available to warrant an ordered catalogue of results from which new problems can be solved by interpolation between old experiments.

Basic information, such as cross sections and fission yields, although much of it is now available, is not by any means completely at hand, so that some of the shield designs must rest on conjecture. Although quite some effort has been spent on refining these conjectures, such as the calculations of cross sections carried out by NDA², the results are, of course, not quite as reliable as experimental results, and the latter are therefore much needed.³

¹References appear at end of Preface.

AUTHOR'S PREFACE

In view of the unsettled state of the shielding art, this section does not offer recipes for every situation, although probably enough information is given to permit a fairly respectable reactor-shield design. In most cases, however, it will be necessary to refer to other works, in particular to experimental results too voluminous to include in a handbook.

In Chapter 2.1, the known information regarding the fission sources of neutrons and gamma rays is given. Although fission-product radiations are treated, no compilation is made of the radiations from other nuclides with the exception of capture-gamma radiations.

Chapter 2.2 treats the current opinions on radiation tolerances as used at ORNL.

For Chapter 2.3, on gamma-ray attenuation, we were most fortunate in being able to enlist the services of the National Bureau of Standards and Nuclear Development Associates, which organizations have had most to do with developing a useful method and its exploitation.

Chapter 2.4 on neutron attenuation treats a much less satisfactory art, giving a correspondingly less analytical treatment, which nevertheless is as complete as we were able to make it at the time of writing (1952).

Chapter 2.5 on geometry is essentially an introduction to the art of applying the results of experiments to new source-receiver configurations. Since this chapter was prepared (early 1952), another treatment has appeared which will also be useful.⁴

Chapter 2.6, which treats ducts through shields, gives the phenomenological treatment of this problem, taking parameters from mockup experiments rather than relying on the complicated analysis which evolves from a start with cross sections.

Chapter 2.7 on heating in shields treats a problem which must depend to some extent on the basic attenuation calculations themselves, although the region of interest for heating is generally that of much smaller attenuations for which different methods are applicable.

Chapter 2.8 shows how standard treatments of extremum problems are applied to shield design.

Chapter 2.9 on shield materials treats a very voluminous subject with an attempt at brevity. This chapter is one which is sure to grow with the nuclear energy business.

REFERENCES

1. S. Kirn, R. J. Kennedy, and H. O. Wyckoff, Oblique Attenuation of Gamma-rays from Cobalt-60 and Cesium-137 in Polyethylene, Concrete, and Lead, NBS-2125, Dec. 23, 1952.
2. B. T. Feld, H. Feshbach, M. L. Goldberger, H. Goldstein, and V. F. Weisskopf, Final Report of the Fast Neutron Data Project, NYO-636, Jan. 31, 1951.
3. H. Goldstein, Some Fast-neutron Measurements Needed for Shielding Studies, NYO-640, Aug. 24, 1951 (classified).
4. M. L. Storm, H. Hurwitz, Jr., and G. M. Roe, Gamma-ray Absorption Distributions for Plane, Spherical, and Cylindrical Geometries, KAPL-783, July 24, 1953 (classified).

NOTE TO THE DECLASSIFIED EDITION

This declassified section has been prepared by deleting classified information from the original version. No effort has been made to revise or bring up to date the remaining material, which was based upon information available up to about April 1952.

As one might expect, considerable advances have been made since this section was originally written. As a guide to the literature up to October 1, 1954, the reader is referred to "Radiation Shields and Shielding; A Bibliography of Unclassified AEC Report Literature," TID-3032 and TID-3032 (Suppl. 1).

CHAPTER 2.1

Sources of Radiation

E. P. Blizard and F. C. Maienschein

RADIOACTIVE NUCLEI

The radiations from radioactive nuclei are given in a number of unclassified reference charts¹⁻³ which are not reproduced here.

RADIATIONS FROM FISSION

PROMPT NEUTRONS

The distribution of neutrons from the thermal fission of U^{235} is well approximated by Watt's^{4,5} empirical formula:

$$N(E) dE = \sqrt{\frac{2}{\pi e}} \sinh \sqrt{2E} e^{-E} dE \quad (1)$$

where $N(E) dE$ is the number of neutrons of energies E to $E + dE$ per neutron emitted, and E is the neutron energy in millions of electron volts. The fission spectrum of the neutrons from Pu^{239} is about the same.⁶ Watt's expression (1) is given in Table 2.1.1 and Fig. 2.1.1.

Table 2.1.1 — Watt's Fission Spectrum

E, mev	N(E), mev ⁻¹	E, mev	N(E), mev ⁻¹	E, mev	N(E), mev ⁻¹
0	0	1.3	3.180×10^{-1}	5.0	3.849×10^{-2}
0.1	2.027×10^{-1}	1.4	3.073×10^{-1}	6.0	1.808×10^{-2}
.2	2.678×10^{-1}	1.5	2.955×10^{-1}	7.0	9.314×10^{-3}
.3	3.060×10^{-1}	1.6	2.842×10^{-1}	8.0	4.424×10^{-3}
.4	3.303×10^{-1}	1.7	2.729×10^{-1}	9.0	2.074×10^{-3}
.5	3.454×10^{-1}	1.8	2.602×10^{-1}	10.0	9.538×10^{-4}
.6	3.525×10^{-1}	1.9	2.498×10^{-1}	11.0	4.400×10^{-4}
.7	3.559×10^{-1}	2.0	2.369×10^{-1}	12.0	1.995×10^{-4}
.8	3.543×10^{-1}	2.5	1.839×10^{-1}	13.0	8.969×10^{-5}
.9	3.512×10^{-1}	3.0	1.387×10^{-1}	14.0	3.997×10^{-5}
1.0	3.444×10^{-1}	3.5	1.026×10^{-1}	15.0	1.772×10^{-5}
1.1	3.366×10^{-1}	4.0	7.470×10^{-2}		
1.2	3.272×10^{-1}	4.5	5.381×10^{-2}		

¹References appear at end of chapter.

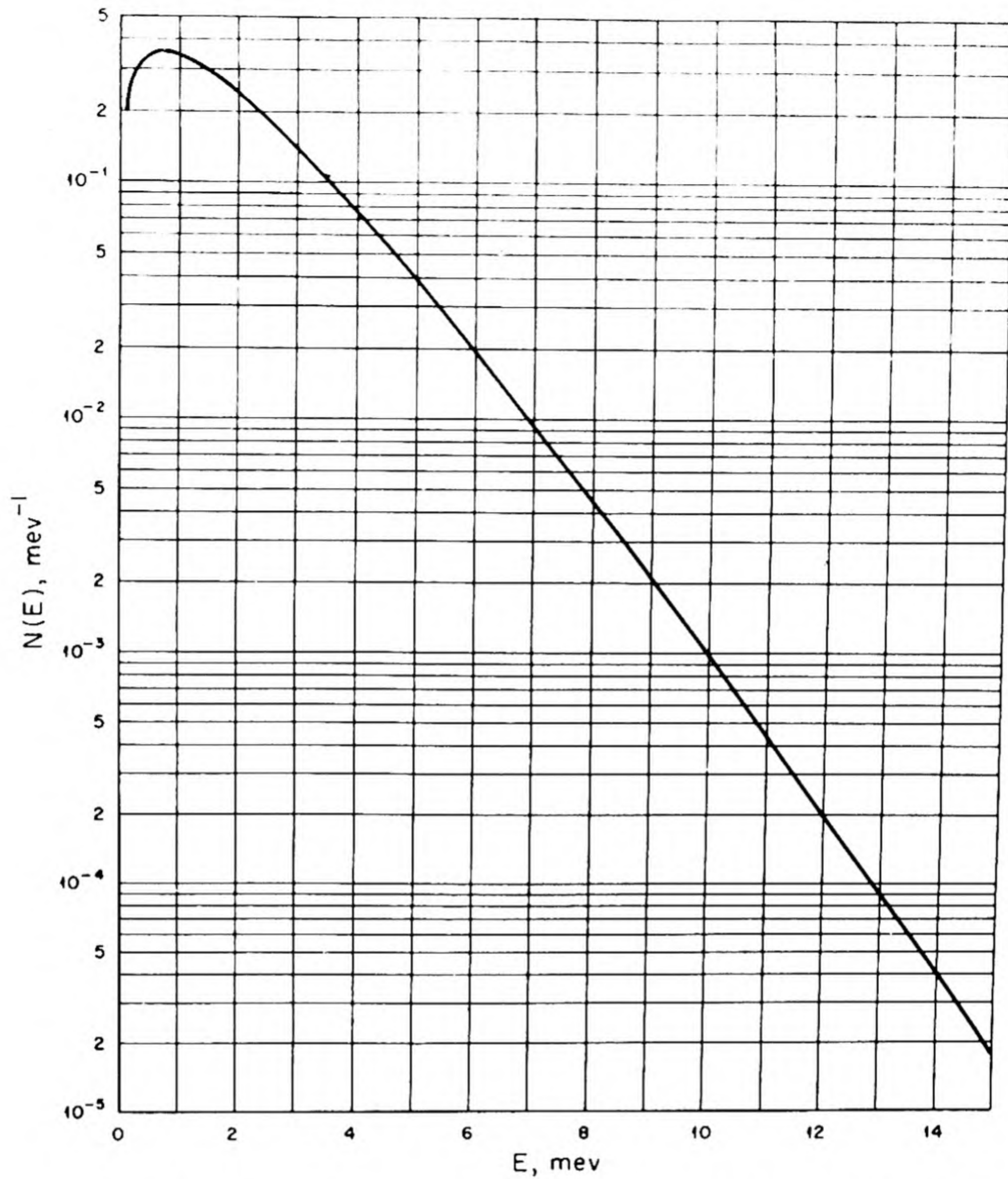


Fig. 2.1.1 — Watt's Spectrum of Fission Neutrons. Submitted by Oak Ridge National Laboratory, Sept. 10, 1952.

An approximate form for the fission spectrum for large E is:

$$N(E) dE = \frac{1}{\sqrt{2\pi e}} e^{-(E - \sqrt{2E})} dE \quad (2)$$

For a fit in slope and magnitude at any energy E_0 , the following form can be used for $E_0 > 3$ mev:

$$N(E) dE = \frac{1}{\sqrt{2\pi e}} e^{\sqrt{E_0/2} - (1 - 1/\sqrt{2E_0})E} dE \quad (3)$$

If this form is fit at 8 mev, the result is:

$$N(E) dE \approx 1.8e^{-0.75E} dE \quad (4)$$

The data which the above formulas fit include measurements of energies up to 17 mev.

PROMPT GAMMA RAYS

The two measurements of prompt gamma rays of fission agree in total energy but not in average energy per photon. Neither of the two experiments is very precise, but that of Deutsch and Rotblat is usually used, although the justification for this is not convincing. Any calculation should allow for the possibility that either is correct. The data are given in Table 2.1.2.

Table 2.1.2 — Gamma-radiation Energies from Fission

Total energy per fission, mev	Average energy per photon, mev	Reference
5.1 ± 0.3	1	7
4.6 ± 0.1	2.5	8

FISSION PRODUCTS

GAMMA RAYS

The data on the relative yields of the various fission products have been summarized elsewhere.^{9,10}

The gross gamma activity of fission products can be estimated by use of the expressions listed in Table 2.1.3. Although the data are not complete for either Pu^{239} or U^{235} fission products, there is probably not much difference in the gamma-activities of their fission products.

Table 2.1.3 — Delayed Gammas from Fission Products

Rate		Validity	Fissioning isotope	Reference
Mev/(sec)(fission)*	C/fission			
	$4 \times 10^{-11}\dagger$	0–1.7 msec	Pu^{239}	12
	$2 \times 10^{-11}\dagger$	1.7–3.4 msec	Pu^{239}	12
	1×10^{-11}	40–140 msec	U^{235}	13
	(constant)			
$0.90t^{-1.20}$		10 sec–1 day	U^{235}	14, 15
$4.2t^{-1.28}$		20 min–3 days	U^{235}	14, 16
$49.0t^{-1.41}$		50–100 days	U^{235}	14, 16

*Gamma source strength, mev/sec, at t sec after one fission

†Activity relative to radium source in equilibrium with its decay products

For times after irradiation longer than about 3 hr, the hard gamma rays can be identified with relatively few individual emitters¹¹ shown in Table 2.1.4.

DELAYED NEUTRONS

Delayed neutrons are defined as those emitted at measurable times after fission. The delayed neutrons that are important from the shielding viewpoint are listed in Table 2.1.5.

Table 2.1.4 — Fission-fragment Hard-gamma Emitters

Nuclides†	Half-life†	U ²³⁵ fission yield, %‡	Yield per decay, %‡	Energy, mev
Ru ¹⁰⁶ , Rh ¹⁰⁶	1 yr, 30 sec	0.48	2	2.9 ¹⁷
Ce ¹⁴⁴ , Pr ¹⁴⁴	275 days, 17.5 min	5.3	Weak	>D ¹⁷
			2	2.185 ¹⁷
			2	2.6 ¹⁸
Eu ¹⁵⁶	15.4 days	0.013	60	2 ¹⁹
Ba ¹⁴⁰ , La ¹⁴⁰	12.8 days, 40 hr	6.1	3.2	2.5 ²⁰
Te ¹³² , I ¹³²	77.7 hr, ²¹ 2.4 hr	4.5 ²¹	2.7	2.0 ^{22,23}
Te ^{131*} , Te ¹³¹	30 hr, 25 min	0.45 ²¹	21.6	>D ²³
I ¹³⁵	6.7 hr	5.6	1.95	2.4 ²⁴
			4	1.8 ²⁵
Kr ⁸⁸ , Rb ⁸⁸	2.77 hr, 17.8 min	3.1§	<15	2.8 ²⁶
			19–34	1.85 ²⁶

†If two entries occur, they refer to parent and daughter, and the latter is the hard-gamma emitter

‡Multiply third and fourth columns to obtain gamma photons per 10⁴ fissions

§Interpolated value

Table 2.1.5 — Delayed Neutrons

(D. J. Hughes, Delayed Neutrons, CF-3596, Feb. 1946)

Half-life, sec	Energy, kev	Absolute yields per 10 ⁴ neutrons emitted (prompt and delayed)		
		U ²³⁵	U ²³³	Pu ²³⁹
55.6	250	2.5	1.8	1.4
22.0	570	16.6	5.8	10.5
4.51	412	21.3	8.6	12.6
1.52	670	24.1	6.2	...
0.43	400	8.5	1.8	11.9
	Total	73.0	24.2	36.4

SECONDARY SOURCES OF RADIATION

Secondary gamma radiation, produced by neutron reactions, consists of two important types: (1) capture-gamma radiation and (2) gamma rays from inelastic scattering. Secondary neutrons are produced by the photoneutron process. Secondary radiations are of considerable importance since it is because of these that a single type of shielding (e.g., water for neutrons) is often inadequate, being relatively transparent for the secondary radiation.

CAPTURE GAMMAS

When a neutron is captured by a nucleus, a new nucleus is formed in an excited state. The excitation energy, or binding energy of the neutron in the new nucleus, may be dissipated almost at once ($\sim 10^{-13}$ sec) by the emission of one or more gamma rays (for ex-

Table 2.1.6 — Light Isotopes Useful for Suppression of Capture Gamma Radiation

Isotope	Charged particle reaction	Percent of radiative captures	Total absorption cross section, barns	Total energy of gamma rays, mev
Li ⁶	(n, α)	0	910	...
B ¹⁰	(n, α)	93	3800	0.48
N ¹⁴	(n, p)	6	1.7	10.8*

*B. B. Kinsey (Ref.²⁹, Table 2.1.7) gives the spectral distribution of the harder nitrogen captive gamma rays as follows

Line	Energy, mev	Intensity relative to A
A	10.816 \pm 0.015	1.00
B	9.156 \pm .030	0.09
C	8.278 \pm .016	.19
D	7.356 \pm .012	.56
E	7.164 \pm .010	.19
F	6.318 \pm .010	.9
G	5.554 \pm .010	1.5
H	5.287 \pm .010	2.3
I	4.485 \pm .010	0.8

ceptions see Table 2.1.6). For the light elements and magic* nuclei only a single gamma ray may be emitted with an energy corresponding to the binding energy. For other nuclei many gamma rays are emitted in competition with the ground-state transition. Table 2.1.7 presents a summary of capture-gamma-ray spectra that have been investigated.

The following instruments have been used for measuring capture-gamma-ray spectra:

(1) A pair spectrometer, which utilizes magnetic deflection of electron pairs in order to determine their energies. This instrument permits high resolution and has thus shown the presence of lines in capture-gamma-ray spectra. Determination of the energy dependence of the sensitivity for this spectrometer is rather difficult.

(2) Deuterium-loaded nuclear plates in which photoproton tracks are observed. This technique yields less resolution than the pair-spectrometer method and requires a considerable investment of time in reading the plates.

(3) Scintillation spectrometers, which have been adapted only recently to the study of capture-gamma-ray spectra. This method may yield considerable information in the future with somewhat poorer resolution than the pair spectrometer method. The resolution would be quite adequate for shielding purposes, however, and the sensitivity should be higher.

INELASTIC SCATTERING GAMMAS

The capture-gamma-ray process described above is the most important reaction for neutrons of low energy. For higher neutron energies, however, it is possible that the compound nucleus formed upon neutron capture may re-emit a neutron, leaving the residual nucleus in an excited state which subsequently decays by the emission of one or more gamma rays. In contrast to capture gamma rays, inelastic-scattering gamma rays will have a total energy less than that of the incident neutron.

*Magic nuclei are those having closed, or nearly closed, shells of nucleons so that they behave much as light nuclei. Notable examples are lead and bismuth, which although they are heavy nuclei, nevertheless give a single capture gamma photon per capture, a property usually characteristic of the lighter nuclei.

Table 2.1.7 — Capture-gamma-ray Data

Target nucleus	Spectral type*	Binding energy,† mev	References
H ¹	1	2.23	27
Li ⁶	3	...	28
Be ⁹	1	6.797 ± 0.008	29
B ¹⁰	3	...	28
C ¹²	1	4.948 ± 0.008	29
N ¹⁴	2	10.823 ± .012	29
F ¹⁹	1	6.60 ± .03	30
Na ²³	2	6.961 ± .012	30, 31
Mg ^{24, 25, 26}	2	7.334 ± .012 (24)	30
Al ²⁷	1	7.724 ± .10	30, 32, 33
Si ^{28, 29, 30}	2	8.476 ± .13 (28)	30
P ³¹	2	7.94 ± .03	34
S ³²	2	8.64 ± .02	34
Cl ³⁵	2	8.56 ± .03	34
K ³⁹	2	7.77 ± .03	31, 35, 36
Ca ⁴⁰	2	...	36
Mn ⁵⁵	1	7.25 ± 0.03	33, 35, 37, 38
Fe ⁵⁶	1	7.63 ± .01	33, 35, 37
Co ⁵⁹	2	7.73 ± .04	35, 37
Ni ⁵⁸	1	9.01 ± .03	35
Ni ⁶⁰	1	8.55 ± .03	35
Cu ^{63, 65}	1	7.91 ± .01 (63)	35
Br ^{79, 81}	2	8.5–9.0	32
Ag ^{107, 109}	2	~ 8.0	37
Cd ¹¹³	2	~ 7.5	31, 32
In ¹¹⁵	2	7.0–7.5	37
La ¹³⁹	2	7.5–8.0	32
W	2	7.4	39
Au ¹⁹⁷	2	9.0–9.5	32
Hg	2	8.0–8.5	32
Pb ²⁰⁶	1	6.734 ± 0.008	36
Pb ²⁰⁷	1	7.380 ± .008	36
Bi ²⁰⁹	1	4.170 ± .015	36
U ²³⁵	2	~ 5†	

*1, ground-state transition predominates; 2, ground-state transition does not predominate; 3, charged-particle reaction

†Isotope assignment, if any, is indicated in parentheses

‡E. P. Blizard, estimate only, based on calculation of gamma intensity near to an MTR-type reactor. This is gamma-ray emission on thermal neutron nonfission capture, which constitutes 15.5% of all capture processes

Only a very few measurements have been made of gamma-ray spectra from inelastic scattering. Data on gamma-ray energies and inelastic cross sections are available for 2.5-mev neutrons for several light nuclei.⁴⁰ In recent experiments with 15-mev neutrons, determinations of the energies of inelastically scattered neutrons from light and magic nuclei showed a reduction in neutron energy to about 2 mev.^{41, 42} The gamma-ray energies were not experimentally determined, but by analogy with the neutron-capture process it may be presumed that light and magic nuclei will give rise to gamma rays which are harder than those of other nuclei.

PHOTONEUTRONS

Photoneutron production, which may be considered the reverse of the neutron-capture process, comprises a secondary source of neutrons. In neutron capture, the neutron binding energy was made available to the gamma radiation. Consequently, in order for photoneutron production to take place, the incident gamma ray must have an energy at least equal to the neutron binding energy. For only two nuclei, D^2 (2.23 mev) and Be^9 (1.67 mev), are these threshold energies low enough to allow an appreciable production of photoneutrons in shield materials.

Other threshold energies are listed in an extensive table published by Sher et al.⁴³ Figure 2.1.2 shows the photoneutron cross sections for D^2 and Be^9 , together with the curve for Al^{27} , which is included to show the general shape of photoneutron cross-section curves for other nuclei. The curves shown in Fig. 2.1.2 are not theoretical but are merely an attempt to give a best fit to the experimental points. As may be seen from the scale used for the cross section, photoneutron cross sections are, in general, much smaller than neutron-capture or inelastic-scattering cross sections.

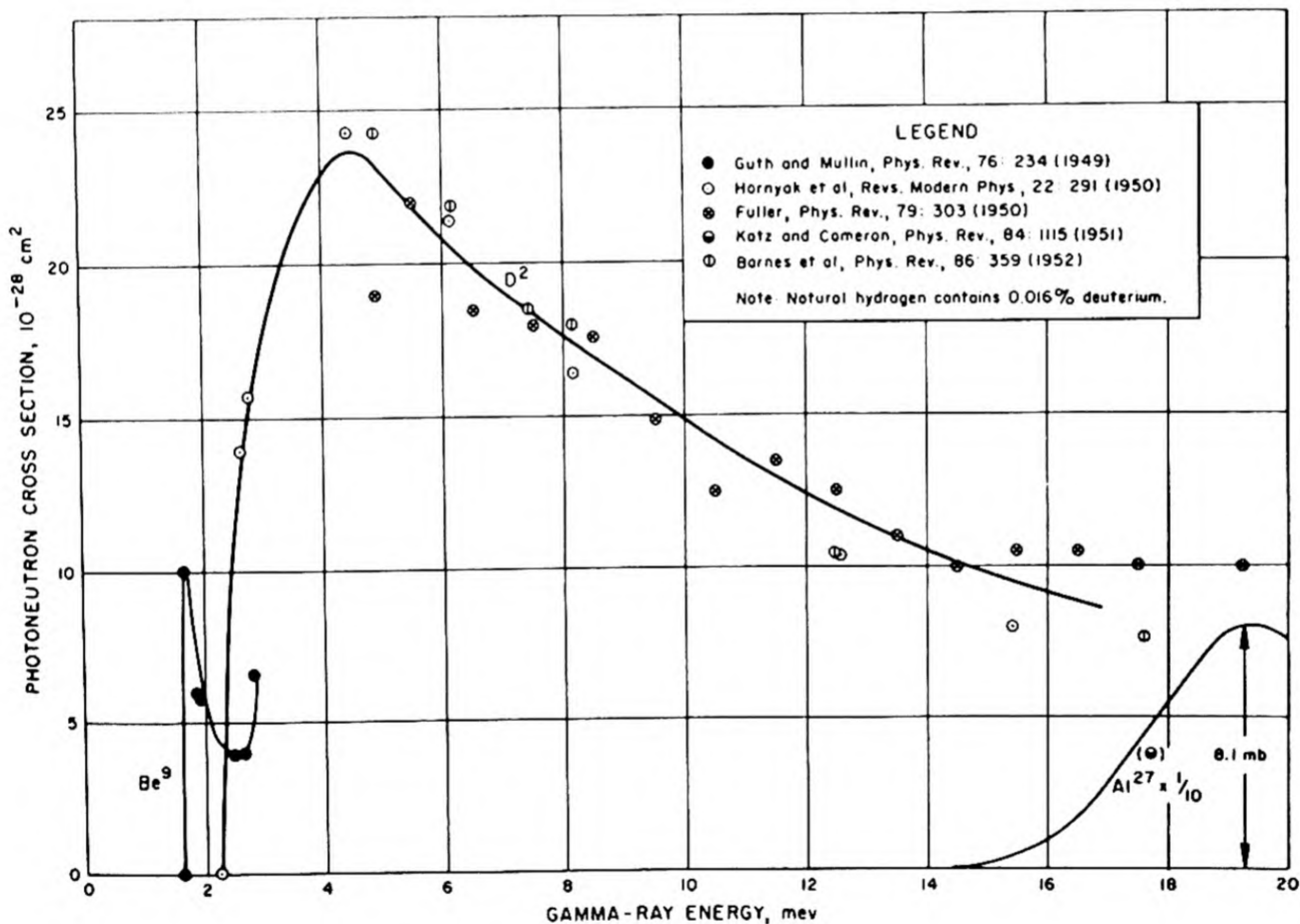


Fig. 2.1.2 — Photoneutron Cross Sections for Be^9 , Al^{27} , and D^2 . Submitted by Oak Ridge National Laboratory, June 23, 1952.

REFERENCES

1. Chart of the Nuclides, prepared by Knolls Atomic Power Laboratory, General Electric Research Laboratory, 1950 edition.
2. W. H. Sullivan, "Trilinear Chart of Nuclear Species," John Wiley & Sons, Inc., New York, 1949.
3. E. Segre, Segre Isotope Chart, AECD-2111, April 1948; declassified July 21, 1948.
4. B. E. Watt, Energy Spectrum of Neutrons from Fissions Induced by Thermal Neutrons, LA-718, 52 pp, Dec. 17, 1948.
5. N. Nereson, Fission Neutron Spectrum of U^{235} , Phys. Rev., 85, 600, 1952.
6. N. Nereson, The Fission Neutron Spectrum of Plutonium, LA-1078, 22 pp, Mar. 8, 1950; declassified July 16, 1952 (AECD-3428; LADC-1215).
7. M. Deutsch and J. Rotblat, Investigation of Fission Gamma Rays, LA-170, 22 pp, Nov. 13, 1944, declassified May 25, 1951.
8. B. B. Kinsey, R. C. Hanna, and D. Van Patter, Gamma Rays Produced in the Fission of U^{235} , Can. J. Research, 26A: 79-98 (1948).
9. K. Way and N. Dismuke, Fission Product Yields, Oak Ridge National Laboratory, ORNL-280, 50 pp, May 18, 1950.
10. C. D. Coryell and N. Sugarman, editors, "Radiochemical Studies: The Fission Products," pp 1381-1382 and 2018-2055, McGraw-Hill Book Company, Inc., New York, 1951.
11. W. K. Ergen, Hard Gamma Emitters among Fission Fragments, Aircraft Nuclear Propulsion Project, ANP-59, 25 pp, May 3, 1951.
12. I. Halpern and P. B. Moon, Short-Period Delayed Gammas from Fission of 25 and 49, LA-253-A, Dec. 7, 1945.
13. L. D. P. King and E. Fermi, quoted in reference 12.
14. K. Way and E. P. Wigner, The Rate of Decay of Fission Products, Phys. Rev., 73: 1318-1330 (1948); also appears as Paper 43, pp 436-458 in Coryell and Sugarman, op. cit. (10).
15. N. Sugarman, S. Katcoff, B. Finkle, N. Elliott, and J. D. Knight, Decay of Gross Fission Products after Short Irradiations. III. Counter Studies of γ Activity and Energy, Paper 37, pp 371-386 in Coryell and Sugarman, op. cit. (10).
16. L. B. Borst, Estimates of Amount of Radiation and of Accompanying Energy Liberation from Fission Products, Paper 34, pp 344-350 in Coryell and Sugarman, op. cit. (10).
17. D. E. Alburger, E. der Mateosian, M. Goldhaber, and S. Katcoff, Gamma-Rays in the Decay of Rh^{46} and Pr^{41} , Phys. Rev., 82: 332 (1951).
18. C. E. Mandeville and E. Shapiro, Radiations from Cerium (144) $\xrightarrow{\beta}$ Praseodymium (144) $\xrightarrow{\beta}$ Neodymium (144), Phys. Rev., 79: 243 (1950).
19. L. Winsberg, Study of the Fission Chain $10h\ Sm^{(156)}-15.4d\ Eu^{(156)}$, Paper 198, pp 1302-1310 in Coryell and Sugarman, op. cit. (10).
20. B. Russell, D. Sachs, A. Wattenberg, and R. Fields, Yields of Neutrons from Photo-Neutron Sources, Phys. Rev., 73: 545-549 (1948).
21. A. C. Pappas and C. D. Coryell, Activities and Fission Yields in Chains of Masses 129 to 134, Phys. Rev., 81: 329 (1951).
22. F. C. Maienschein, J. K. Bair, and W. B. Baker, private communication with W. K. Ergen.
23. G. W. Parker, private communication with W. K. Ergen.
24. H. A. Levy and M. H. Feldman, Hard Gamma Emitters in Fission, pp. 71-83 (especially p 80) in J. A. Swartout, Chemistry Division Quarterly Progress Report for Period Ending June 30, 1949, Oak Ridge National Laboratory, ORNL-286, 236 pp, Sept. 14, 1949.
25. A. D. Bogard, A. R. Brosi, et al, Calibration of Assay Equipment, pp 59-65 in E. H. Taylor, Report of the Chemistry Division for the Months March, April, May, 1948, Oak Ridge National Laboratory, ORNL-65, 187 pp, July 9, 1948.
26. M. E. Bunker, L. M. Langer, and R. J. D. Moffat, The Disintegration of Rb^{88} , Phys. Rev., 81: 30-32 (1951).
27. R. E. Bell and L. G. Elliott, Gamma-Rays from the Reaction $H^1(n,\gamma)D^2$ and the Binding Energy of the Deuteron, Phys. Rev., 79: 282-285 (1950).
28. W. F. Hornyak, T. Lauritsen, P. Morrison, and W. A. Fowler, Energy Levels of Light Nuclei. III, Revs. Mod. Phys., 22: 291 (especially p 321) (1950).
29. B. B. Kinsey, G. A. Bartholomew, and W. H. Walker, γ -rays Produced by Slow Neutron Capture in Beryllium, Carbon, and Nitrogen, Can. J. Phys., 29: 1-13 (1951).
30. B. B. Kinsey, G. A. Bartholomew, and W. H. Walker, Neutron Capture γ -Rays from Fluorine, Sodium, Magnesium, Aluminum, and Silicon, Phys. Rev., 83: 519-534 (1951).
31. C. H. Millar, A. G. W. Cameron, and M. Glicksman, Gamma-ray Studies Using Deuterium-loaded Photographic Plates, Can. J. Res., 28A: 475-487 (1950).
32. B. Hamermesh, Neutron Capture Gamma-Ray Spectra, Phys. Rev., 80: 415-419 (1950).
33. B. Hamermesh and V. Hummel, Scintillation Counter Studies of Neutron Capture Gamma-Ray Spectra, Phys. Rev., 83: 663-664 (1951).
34. B. B. Kinsey, G. A. Bartholomew, and W. H. Walker, Neutron Capture γ -Rays from Phosphorus, Sulfur, Chlorine, Potassium, and Calcium, Phys. Rev., 85: 1012-1023 (1952).
35. B. B. Kinsey, G. A. Bartholomew, and W. H. Walker, Transitions to the Ground States in Nuclei Excited by Slow Neutron Capture, Phys. Rev., 78: 481-482 (1950).
36. B. B. Kinsey, G. A. Bartholomew, and W. H. Walker, Neutron Capture γ -Rays from Lead and Bismuth, Phys. Rev., 82: 380-388 (1951).
37. B. Hamermesh, Odd-Even Effect in Neutron Capture Gamma-Ray Spectra, Phys. Rev., 81: 487 (1951).
38. R. W. Pringle and G. Isford, Scintillation Spectroscopy of the Gamma-Rays from Slow Neutron Capture in Manganese, Phys. Rev., 83: 467-468 (1951).
39. B. B. Kinsey, letter of Feb. 22, 1950, to E. P. Blizard.
40. M. A. Grace, L. E. Beghian, G. Preston, and H. Halban, The Inelastic Scattering of Fast Neutrons, Phys. Rev., 82: 969 (1951).
41. P. H. Stelson and C. Goodman, The Inelastic Scattering of 15-mev Neutrons by Lead, Iron, and Aluminum, Phys. Rev., 82: 69-71 (1951).
42. B. G. Whitmore and G. E. Dennis, The Inelastic Scattering of Fast Neutrons in Lead and Bismuth, Phys. Rev., 84: 296-297 (1951).
43. R. Sher, J. Halpern, and A. K. Mann, Photoneutron Thresholds, Phys. Rev., 84: 387-394 (1951).

CHAPTER 2.2

Permissible Levels of Radiation

M. S. Fair

ROENTGEN

The roentgen is defined as "that quantity of X- or gamma-radiation such that the associated corpuscular emission per 0.001293 gm of air produces, in air, ions carrying one electrostatic unit (esu) of quantity of electricity of either sign."

The roentgen is a unit of X- or gamma-ray energy loss in 1 cc of dry air under standard conditions (0°C and 760 mm Hg). As defined, the roentgen is a unit of dose without reference to time or the energy of the ionizing radiation. Air was chosen as the absorption medium because it is convenient and because body tissue, water, and air all have approximately the same absorption value per gram for a wide range of radiation wavelength.

Within the 0.001293 gm of air, photoelectrons and Compton electrons will be formed by interaction of X- or gamma-rays with electrons of the atoms contained in the volume of air; pair electrons will be produced if the photon energy is more than twice the mass energy of the electron ($> 2 mc^2 \doteq 1 \text{ mev}$). The definition demands that all "associated corpuscular emission" be absorbed in air. Many of the particles will leave the volume (1 cc) in which they were formed, but they must remain in air until all their energy is dissipated. The 1-cc volume is the volume from which the secondaries originate and is not the volume from which the ions are collected.

Every ion produced by the secondaries must be measured. This means collecting all the ions formed in a volume that will be larger than the original volume of 1 cc.* This new volume will be determined by the energy of the X- or gamma-rays, which will determine the range of the secondaries. It is very important that the ions be collected before any of them have a chance to recombine. For each ionization event, two particles are produced, a positive and a negative; they are called an "ion pair." Either the positive or the negative charges may be collected and measured. Thus, it is seen that actually there are 2 esu of charge, 1 esu of positive and 1 esu of negative charge per cubic centimeter of air corresponding to a roentgen.

Since the charge on the electron is 4.8×10^{-10} esu, then the number of electrons per electrostatic unit is:

$$1/4.8 \times 10^{-10} = 2.083 \times 10^9$$

This then is also the number of ion pairs (i.p.) per electrostatic unit, because only one partner of the ion pair is measured.

* In practice, because of experimental convenience, the volume in which the secondary electrons are produced is probably many cubic centimeters of air. The resulting ions collected are divided by this volume in calculating the roentgens.

The mass of air referred to (0.001293 gm) is 1 cc of dry air at 0°C and 760 mm Hg. There are 2.083×10^9 ion pairs per cubic centimeter per roentgen (by definition 1 r = 1 esu/cc) or:

$$1 \text{ r} = \frac{2.083 \times 10^9 \text{ i.p./cc}}{0.001293 \text{ gm/cc}} = 1.61 \times 10^{12} \left(\frac{\text{i.p.}}{\text{gm air}} \right)$$

If an average of 32.5 ev is expended by secondary electrons to form each ion pair in air, then:

$$1 \text{ r} = 1.61 \times 10^{12} \frac{\text{i.p.}}{\text{gm air}} \times 32.5 \frac{\text{ev}}{\text{i.p.}} = 5.24 \times 10^{13} \frac{\text{ev}}{\text{gm air}}$$

Since 1 ev is equal to 1.6×10^{-12} erg:

$$1 \text{ r} = 5.24 \times 10^{13} \frac{\text{ev}}{\text{gm air}} \times 1.6 \times 10^{-12} \frac{\text{ergs}}{\text{ev}} = 83.8 \frac{\text{ergs}}{\text{gm air}}$$

To summarize:

$$\begin{aligned} 1 \text{ r} &= 1 \text{ esu/cc (standard air)} \\ &= 2.083 \times 10^9 \text{ i.p./cc} \\ &= 1.61 \times 10^{12} \text{ i.p./gm} \\ &= 5.24 \times 10^7 \text{ mev/gm} \\ &= 83.8 \text{ ergs/gm} \\ &= 6.77 \times 10^4 \text{ mev/cc} \end{aligned}$$

The roentgen is independent of the time required for ionization. A "dosage rate" given as roentgens per hour is commonly used. The product of the dosage rate (r/hr) and time (hr) gives the total dose.

The unit of dosage rate measured in roentgens per unit time must not be confused with gamma-ray intensity. Gamma-ray intensity is measured in energy units per unit area per unit time, such as ergs per square centimeter per second. Ionization intensity is measured in roentgens per unit time, in air.

The roentgen measures electrostatic units per cubic centimeter of air; therefore, a dose of 500 r given to a small part of the body will not have serious consequences, and as the volume exposed approaches zero, the energy absorption also approaches zero. A dose of 500 r over the entire body would represent a large absorption of ionizing energy and would probably result in death.

CURIE

The curie was originally defined as that quantity of radon in radioactive equilibrium with 1 gm of radium. Since 1 gm of radium has about 3.7×10^{10} atoms disintegrating per second, this fact is a basis for the definition of the curie and is the unit applied to radioactive materials other than radium. Thus, 1 curie of P^{32} , Na^{24} , or C^{14} means "the amount of the isotope necessary to provide disintegrations at the rate of 3.700×10^{10} atoms/sec." A useful formula for computing the activity of a given mass of a radioisotope is:

$$M = \frac{130,000 \text{ G}}{A \text{ T}}$$

where:

T is the half-life in days,
 M is the activity in millicuries,
 A is the atomic mass of the radioactive isotope,
 G is the weight in micrograms.

For example, 1 μg of Ca^{45} ($T = 180$ days) has an activity of:

$$M = \frac{130,000}{45 \times 180}$$

$$= 16 \text{ mC}$$

It may be noted that the definition says 3.700×10^{10} disintegrations/sec and not 3.700×10^{10} particles emitted per second.* The number of particles emitted per second can only be obtained from a knowledge of the decay scheme. For example, Mn^{52} has a half-life of 6.5 days. It decays by positron emission in 35 percent of the transitions and by electron capture in 65 percent of the transitions. Therefore, 1 mC of Mn^{52} emits only $0.35 \times 3.700 \times 10^7 = 1.3 \times 10^7 \beta^+$ particles/sec, even though there are 3.700×10^7 d/sec.

The curie is not to be used as a measure of radiation dose delivered.

ROENTGEN EQUIVALENT PHYSICAL (rep)

When dealing with radiations other than photons or energy dissipation in tissue rather than in air, it is incorrect in the strict sense to use the roentgen, and a new unit of ionizing radiation dose is needed. In 1942, H. M. Parker defined a unit called the roentgen equivalent physical (rep) as that quantity of ionizing radiation that dissipates 83 ergs per gram of tissue.

Recently (since 1948), it has been common practice to use a slightly larger unit with the above definition but corresponding approximately to the energy loss in water or tissue (between 90 and 100 ergs/gm, depending upon the energy of the radiation and the specific ionization of the ionizing particle) when 83.8 ergs is dissipated in a small air cavity in the medium. The roentgen equivalent physical is "that quantity of any ionizing radiation (such as X-rays, gamma-rays, electrons, protons, neutrons) which is absorbed in tissue to the extent of 93 ergs per gram of tissue."

ROENTGEN EQUIVALENT MAN (rem)

The roentgen equivalent man is defined as "that amount of radiation absorbed in tissue which has the relative biological equivalence in man of 1 r of X- or gamma-rays."

It has been determined experimentally that the secondary ionization from recoil protons produced by fast neutrons (2 mev) is about ten times ($\text{RBE} = 10$) as damaging as the same amount of energy absorbed from secondary electrons produced by X-rays.

For fast neutrons:

$$1 \text{ rem} = \frac{93}{10} \frac{\text{ergs}}{\text{gm tissue}} = 0.1 \text{ rep}$$

* Distinction must be made between disintegrations per second (d/sec) and counts per second (c/sec). The latter term is frequently used in connection with radioisotope counting. The relationship is $c/\text{sec} = f \text{ d/sec}$ in which f is a correction factor for scattering, absorption, geometry, and counter efficiency.

The "additivity" of different types of radiation may be illustrated as follows:

$$\begin{aligned} 30 \text{ mr/hr gamma} &= 30 \text{ mrem/hr} \\ 1.5 \text{ mrep/hr fast neutron} &= 15 \text{ mrem/hr} \\ 3500 \text{ slow neutrons/(cm}^2\text{)(sec)} &= 15 \text{ mrem/hr} \\ \text{Total} &= 60 \text{ mrem/hr} \end{aligned}$$

Table 2.2.1 gives the values of RBE, rep, rem, and the corresponding approximate flux values for the maximum permissible exposure to various types of radiation. These values correspond to those recommended by the United States Radiation Protection Committee and the values recommended by the United States, Great Britain, and Canada at the Chalk River conference September 29, 1949. It should be noted that these maximum permissible exposure rates are considered to be safe for a life-time exposure. In the emergency of atomic warfare, there would be justification in permitting exposures 100 times these values. Tables 2.2.2 and 2.2.3 give the maximum permissible operating levels used to control radioactive hazards at ORNL.

ROENTGENS PER HOUR AT UNIT DISTANCE

Source strength can be expressed conveniently in terms of roentgens per hour at a distance of 1 meter or 1 cm. The roentgens per hour at 1 meter is sometimes called an "rh.m." This unit does not require a knowledge of the decay scheme of the source. Thus, 1 rhm of Co^{60} is that amount of Co^{60} whose unshielded gamma-rays produce 1 r/hr (in air) at a distance of 1 meter from the source. If this source is enclosed in a spherical shield so that at 1 meter 0.1 r/hr is measured, then the source strength is 0.1 rhm.

Many radium sources are enclosed in platinum tubes of either 0.5 or 1 mm thickness.

$$\text{For 0.5-mm Pt:} \quad S = 8.4 M$$

$$\text{For 1-mm Pt:} \quad S = 7.8 M$$

where:

S is the source strength in roentgens per hour at 1 cm

and:

M is the mass of radium in milligrams

For example, suppose we are given a 10-mg radium source enclosed in a 1-mm platinum filter. To find the roentgens per hour received at 2 meters from this source, we have:

$$7.8 \times 10 = 78 \text{ r/hr at 1 cm}$$

Using the inverse square law, at 200 cm:

$$\frac{78}{(200)^2} = \frac{78}{40,000} = 1.95 \times 10^{-3} \text{ r/hr} = 1.95 \text{ mr/hr}$$

The wall of a gamma-measuring chamber should be made of material with an effective atomic number equal to that of air, and the chamber should be filled with air. This chamber may be as large as desired if sufficient voltage is applied across the chamber. If the wall is of material having an effective atomic number different from that of air, the inner wall should be lined with graphite or other similar material. The thickness of the wall should be equal to or greater than the maximum range of the secondary electron radiation. Since the effective atomic number of live tissue is about the same as that of air, an air wall chamber gives a good measurement of body exposure for X- and gamma-radiation.

Table 2.2.1 — Maximum Permissible Exposure in Terms of Flux Corresponding to 60 mrem per Day (300 mrem/wk on a 5-day work-week basis)*

Type of radiation	RBE	Approximate flux to give 1 MPE in 24-hr day†	
		General equation‡	Example
X- or gamma-ray	1	1500/CE photons/(cm ²)(sec)	1300 photons/(cm ²)(sec) of 1 mev
Beta	1	1600/SP beta rays/(cm ²)(sec)	17 betas/(cm ²)(sec) of 1 mev max. or 32 electrons/(cm ²)(sec) of 1 mev
Fast neutrons	10	20/D fast neutrons/(cm ²)(sec)	22 fast neutrons/(cm ²)(sec) of 2 mev
Thermal neutrons	5	...	600 thermal neutrons/(cm ²)(sec) of 0.02 ev
Alpha (internal effects only)	20	80/SP alpha rays/(cm ²)(sec)	0.003 alpha rays/(cm ²)(sec) of 5 mev§

* Table by K. Z. Morgan

† These values of flux correspond to $60 \times 0.093/\text{RBE}$ ergs per gram of tissue and apply to the normal flux incident to body tissue. Backscattering is taken into account only in the case of thermal neutrons

‡ $C = 1 \pm 0.2$ from 70 kev to 4 mev; it is given more exactly by the equation: $C = 0.32(\mu - \sigma_s)10^5$

where: $(\mu - \sigma_s)$ = total minus Compton scattering coefficient of absorption, cm⁻¹

E = energy, mev

S = specific ionization in air

P = mass stopping power in tissue relative to air

D = constant given approximately by the equation, $D \doteq 1.2 - e^{-0.5E}$

§ Average value over the short range of alpha in tissue is 0.0016 alphas/(cm²)(sec) for 5 mev

Table 2.2.2 — Maximum Permissible Exposures to Personnel from External Sources

Type of radiation	Permissible exposure
Gamma	60 mr/day or 300 mr/week*
Beta	60 mrep/day or 300 mep/week*
Slow neutron	1750 neutrons/(cm ²)(sec)(8-hr day)
Fast neutron	66 neutrons/(cm ²)(sec)(8-hr day)

Emergency exposure

In case of fire or other emergency, "AEC Contract Policy and Operations," Jan., 1951, stipulates the following:

The permissible limit for AEC emergency radiation monitoring teams, who normally would be exposed to some radiation in the course of regular duties, was placed at 10 r. The permissible emergency exposure for persons not exposed to radiation in the normal course of their occupations was set at 25 r

* Permissible exposure to the hands and forearms only 1.5 rep/week

Table 2.2.3 — Maximum Permissible Values for Beta-Gamma and Alpha Contamination at ORNL

Type of contamination	Indication of magnitude			
	$\mu\text{c/cc}$	$\beta\text{-}\gamma^*$	Smear†	
			$\beta\gamma$, counts/min	γ , counts/min
Air concentration				
Without masks	$C_{LL}, \dagger 3 \times 10^{-11}, \alpha$ 1st count, $10^{-8}, \beta, \gamma$			
With filter-type masks	$C_{LL}, \dagger 10^{-8}, \alpha$ 1st count, $10^{-5}, \beta, \gamma$			
With positive air-supply masks	$C_{LL}, \dagger > 10^{-8}, \gamma$ 1st count, $> 10^{-5}, \beta, \gamma \S$			
Water concentration				
Leaving settling basin	$1.5 \times 10^{-3}, \beta, \gamma$			
Leaving White Oak Lake	$10^{-5}, \alpha, \beta, \gamma$			
In Clinch River	$10^{-7}, \alpha, \beta, \gamma$			
Thyroid count for iodine content		400 counts/min (Bi GM)		
Surface or material				
Hand count (palm or back)		700 counts/min		
Protective clothing leaving laundry		1000 counts/min		
Personal clothing to be released from impoundment		500 counts/min		
Shoes, inside		1000 counts/min		< 10
Shoes, outside		10,000 counts/min		< 10
Hot laboratories (tables, floors, etc.)		Post area > 7.5 mr/hr	< 200	< 10
Acid bottles, acid carboys, gas cylinders		None detectable	< 20	< 10
Material to X-10 shops		< 1 mr/hr	< 50	< 10
Equipment leaving X-10		< 0.5 mr/hr	< 50	< 10
Commercial carriers leaving X-10		< 1 mr/hr	< 50	< 10
AEC controlled carriers		Safe handling	< 200	< 10
Isotope containers leaving X-10		Up to 200 mr/hr	< 50	< 10
Burial ground (at ground level)		< 7.5 mr/hr		
Salvage materials		< 0.2 mr/hr	< 20	< 10
Material to stores, glass shop, etc.		None detectable	< 20	< 10
Lunchrooms and offices used as such		None detectable	< 20	< 10
Floors in hallways, storage rooms, cold laboratories; table tops, janitors' closets, furniture		< 0.2 mr/hr	< 50	< 10
Instruments for Health Physics calibration		1000 counts/min	< 50	< 10

* There must be no detectable alphas with such instruments as Poppy, Zeuto, or Juno

† Beta smears counted at approximately 10% geometry; alpha smears counted at approximately 50% geometry

‡ Long-lived count; see George Koval, Determination of Particulate Air-borne Long-lived Activity, MDDC-1503, June 22, 1945

§ Exposure to contaminated air while wearing positive air-supply masks is governed by external exposure levels

SELECTED READING LIST

- RADIOACTIVITY UNITS AND STANDARDS, R. D. Evans, *Nucleonics* 1: 32, Oct. 1947.
- TENTATIVE DOSE UNITS FOR MIXED RADIATIONS, H. M. Parker, *Radiology* 54: 257, Feb. 1950.
- NATIONAL BUREAU OF STANDARDS HANDBOOKS: H23, H27, H41, H42, H47, H48, H49, H50, H51.
- DETERMINATION OF PARTICULATE AIR-BORNE LONG-LIVED ACTIVITY, George Koval, MDDC-1503, 8 p, June 22, 1945, declassified Dec. 1, 1947.
- NUCLEAR SCIENCE IN ENGINEERING EDUCATION: A SELECTED LIST OF REFERENCES FOR INSTRUCTORS, TID-3011, 17 pp.
- MAXIMUM PERMISSIBLE DOSE, K. Z. Morgan, *AIHA Quarterly*, Mar. 1953.
- K. Z. Morgan, *National Bureau of Standards Handbook*, H52 (classified).
- "Standards of Radiological Protection and Control" in THE ROLE OF ENGINEERING IN NUCLEAR ENERGY DEVELOPMENT, K. Z. Morgan, Third Annual Oak Ridge Summer Symposium; Aug. 27 to Sept. 7, 1951, TID-5031, Dec. 1951, p 176.

CHAPTER 2.3

Gamma-ray Attenuation

U. Fano

EXTENT OF SURVEY

SOURCES OF RADIATION

Electromagnetic radiation of high photon energy (high frequency) usually originates from excited atomic nuclei, from excited atoms, or from electrons traversing matter and is called X-rays or gamma rays. In this chapter, "gamma rays" indicate high-energy electromagnetic radiation from any source, even though this term usually refers to radiation from nuclear sources only.

ENERGY OF RADIATION

This chapter deals primarily with gamma rays having photon energies between 0.1 and 10 mev. Some information will apply to radiation with energies extending roughly one order of magnitude above or below this range.

ELEMENTARY PROCESSES AND MULTIPLE PROCESSES

Gamma rays traversing matter interact with it through separate "elementary" processes. Present information on elementary processes is generally adequate for shielding applications. Each photon may experience a succession of elementary processes. The combined effect of a succession of processes upon the over-all propagation of gamma rays has been under study in recent years.

ELEMENTARY INTERACTION PROCESSES

BRIEF DESCRIPTION OF PROCESSES¹

KINDS OF INTERACTION

Basic Interaction with Atomic Electrons – (I)

The electromagnetic field of gamma rays exerts an oscillating electric force on the charge of the atomic electrons within any material and a (smaller) magnetic torque on

¹References appear at end of chapter.

their spin. Each electron reacts as an elementary particle endowed with mass and spin angular momentum and subject to forces from other constituents of the material.

Basic Interaction with Nuclear Particles (Nucleons) – (II)

The electromagnetic field of gamma rays exerts an oscillating electric force on the charge of the nuclear protons within any material and a (smaller) magnetic torque on the spins of protons and neutrons. Each nucleon reacts as an elementary particle endowed with mass and spin angular momentum and subject to forces from other nucleons.

Interaction with the Electric Field Surrounding Charged Particles (Nuclei and Electrons) – (III)

The electromagnetic field of gamma rays can induce electric currents in space in which there is also an electrostatic field. These currents are associated with the generation of electron-positron pairs.

Interaction with the Meson Field Surrounding Nucleons – (IV)

The electromagnetic field of gamma rays can induce electric currents in the space surrounding a proton or a neutron, in which there is also a meson field. These currents are associated with the generation of mesons.

EFFECT OF INTERACTION UPON A PHOTON

Outright Absorption – (a)

A photon may disappear as a result of interaction within a material. Its energy is then taken up by the interacting system within the material.

Elastic (Coherent) Scattering – (b)

A photon may be deflected (scattered) owing to interaction with an atomic system (such as an atom or nucleus). The possibility of scattering is necessarily associated with, and quantitatively related to, the possibility of absorption. If the atomic system recoils as a whole under the impact of the photon, its internal energy is not increased, and the scattering is elastic. The effects of elastic gamma-ray interaction with different parts of the system combine “coherently” (i.e., by addition of amplitudes).

Inelastic (Incoherent) Scattering – (c)

If the scattering of a photon causes an atomic particle to recoil with respect to the others, the internal energy of the atomic system is increased and the photon energy correspondingly depleted. The effects of inelastic gamma-ray interactions with different parts of the system combine “incoherently” (i.e., by addition of intensities).

TYPES OF PROCESSES

Different types of processes may arise from each kind of interaction (I, II, III, or IV) leading to each of the end results (a, b, or c) – i.e., 12 types of processes in all.^{2,3} Many of these processes are quite infrequent; some have not yet been observed. The following processes, whose symbol indicates mechanism and end-effect, are most important.

Photoelectric Effect (Ia)

A photon disappears, and an atomic electron (usually from the proximity of the nucleus) leaves its atom at high speed, having absorbed the photon energy. This effect predominates for lower-energy gamma rays especially for high- Z materials. Its cross section attains 1,000-10,000 barns/atom for 0.1-mev gammas. The cross section decreases rapidly with increasing gamma energy, E , very roughly like E^{-3} for $E < 0.5$ mev and like E^{-1} for $E > 0.5$ mev. The cross section for atoms of different elements is roughly proportional to Z^5 for $E \geq 0.1$ mev. The ejected electron flies off prevalently sideways to the photon beam for $E \ll 0.5$ mev, prevalently forward otherwise as a result of the high photon momentum.

Compton Scattering (Ic)⁴

A photon is scattered inelastically and an atomic electron recoils out of an atom, much as though it had been initially free.* The energy taken up by the electron depends primarily on its recoil momentum. This effect predominates for gammas of 1-5 mev in high- Z materials and even more greatly and over a much wider energy range in low- Z materials. Its cross section approaches 1 barn per electron for 0.05-mev gammas and decreases to less than 0.1 barn at 10 mev. The recoil electron flies off prevalently in the direction of the incident photon, the more nearly so the higher the fraction of photon energy it carries away and the higher the photon energy. It never recoils backwards, of course.

Pair Production (IIa)

A photon of more than 1 mev disappears, and its energy transfers to an electron-positron pair which springs out of the space around an atomic nucleus or (less frequently) around an atomic electron. This effect predominates for high photon energies, especially in high- Z materials. The cross section is zero at 1 mev but rises monotonically above this energy until it levels off near 50 mev for high- Z materials and at a higher energy for low- Z . The largest cross sections approach 100 barns/atom. In the region where the cross section is rising, it varies from element to element approximately in proportion to Z^2 . The electron and positron are projected prevalently in the direction of the incident photon, especially when the photon energy, E , and hence its momentum, are very large. Most of the electrons and positrons are confined to directions within $(0.5 \text{ mev}/E)$ radians from the photon direction.

Rayleigh Scattering (Ib)

Gamma rays scattered by small angles impart only a small recoil, especially when their energy is low. The recoil is then often absorbed by a whole atom or molecule so that the scattering action of different atomic electrons combines coherently. The probability of this effect is thereby enhanced and prevails greatly at low energies. Even for photon energies above 0.1 mev, Rayleigh scattering is less probable than Compton scattering by only one or two orders of magnitude. This scattering is more likely for high- Z than for low- Z materials.

Minor Effects

Nuclear photoelectric effect (IIa) has a small cross section which approaches 1 barn/atom only for high Z and for 15- to 20-mev photons. However, this effect results most

* This scattering is actually classed as elastic as long as one considers the electron as an isolated particle; on the contrary, it is classed as inelastic if the electron is considered as a part of the whole material.

frequently in the ejection of one or more neutrons and is made conspicuous by the high penetrating power of the neutrons. Nuclear scattering (IIb) and Delbruck scattering (IIIb) are at present barely detectable. Meson effects (IV) become appreciable only near or above 150 mev and then only with cross sections of the order of millibarns.*

PROBABILITY OF PROCESSES⁶

'NARROW-BEAM' ATTENUATION OF MONOCHROMATIC GAMMAS

The total probability that a photon of given energy suffers some interaction process while traversing a layer of matter is studied experimentally with the schematic arrangement of Fig. 2.3.1. A well collimated ("narrow") beam of homogeneous (monochromatic)

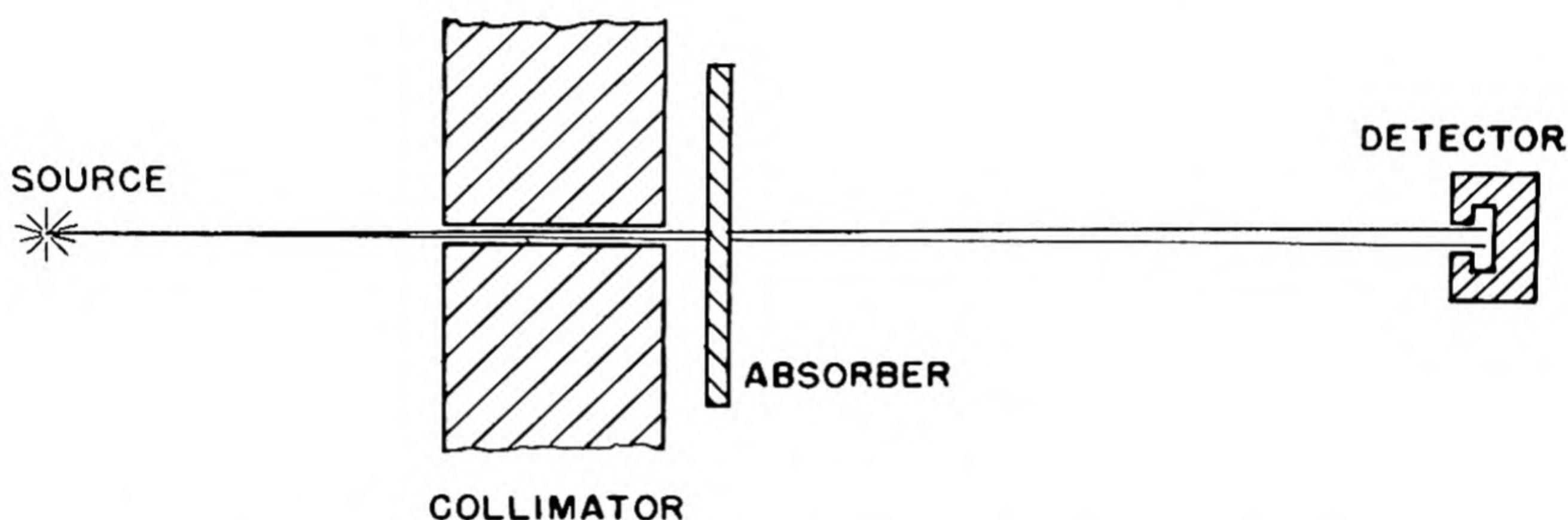


Fig. 2.3.1— Schematic Diagram for Measurement of Narrow-beam Attenuation Coefficient.

gamma rays penetrates a layer of matter (absorber) and then reaches a detector. Absorption or appreciable deflection of a photon prevents it from reaching the detector. The attenuation of the intensity received by the detector, as the absorber thickness increases, measures the combined probabilities of outright absorption and of deflection.

EXPONENTIAL LAW OF ATTENUATION

If a photon has a probability (p) of traversing an absorber of thickness (x) without suffering absorption or deflection, the probability on no process through a thickness $2x$ must be p^2 . This condition implies that p depends on x according to:

$$p = e^{-\mu x} \quad (1)$$

where μ represents the "absorption coefficient" (probability of a process per unit thickness). If x is expressed in cm, μ is expressed in cm^{-1} . "Narrow-beam" attenuation experiments verify Eq. (1) and measure μ (see Fig. 2.3.2).

COMPONENTS OF THE ABSORPTION COEFFICIENT

The total probability, μ , that any process takes place per unit thickness of absorber is the sum of the probabilities of occurrence of the various kinds of processes. "Narrow-

*See Rossi⁵ for a discussion of these processes.

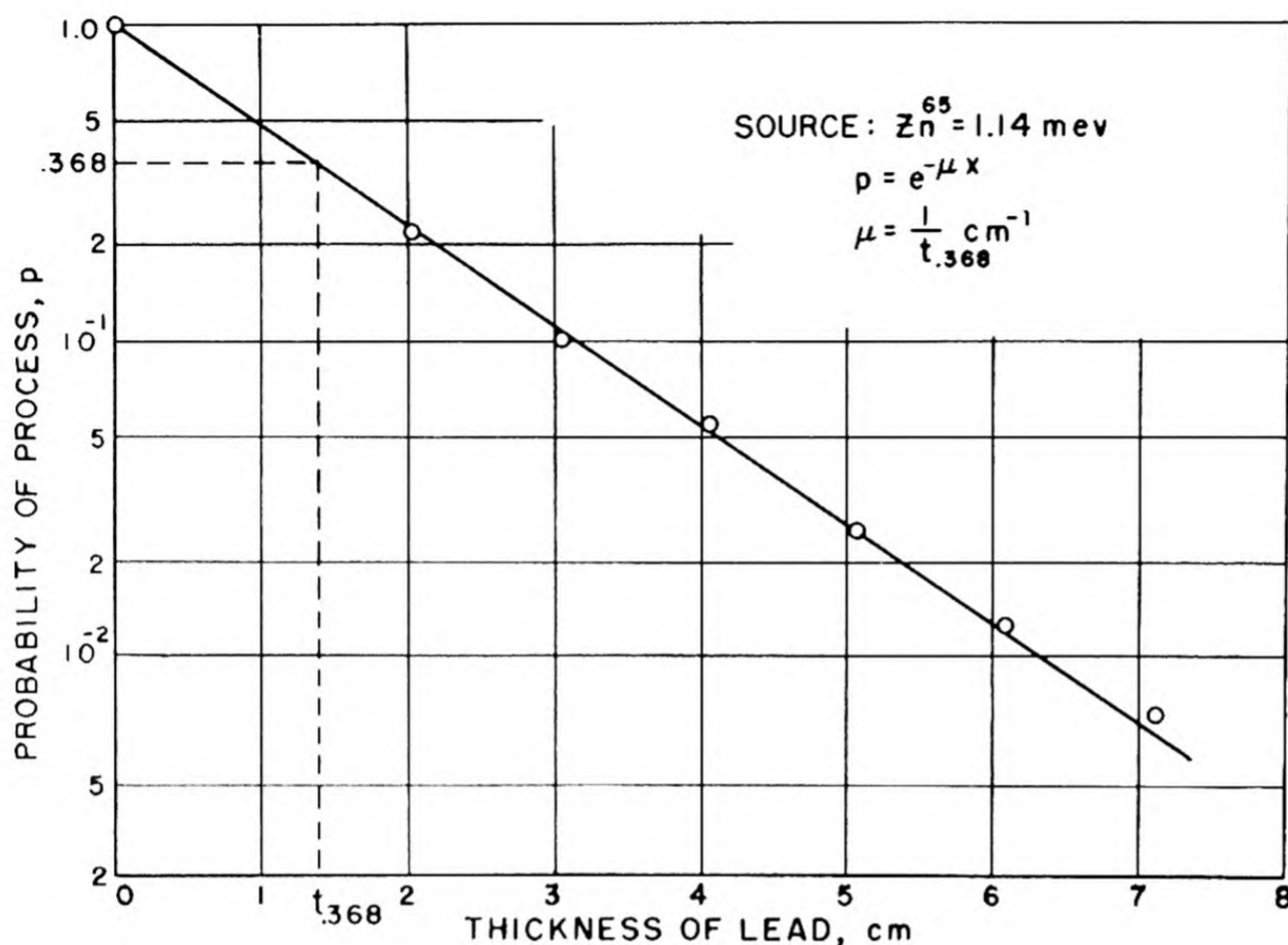


Fig. 2.3.2 — An Illustration of the Experimental Verification and Measurement of Narrow-beam Attenuation Coefficients for Monoenergetic Sources. Data from C. M. Davisson and R. D. Evans, Phys. Rev. 81, 1951.

beam" experiments yield only the total μ , but the μ 's for the various processes are generally provided by the theory or by special experiments. The formula:

$$\mu = \mu_{\text{photo}} + \mu_{\text{scatt}} + \mu_{\text{pair}} \quad (2)$$

is often encountered, where μ_{photo} pertains to process Ia, μ_{scatt} to Ic and Ib combined (or to Ic alone), μ_{pair} to IIIa, and other processes are disregarded.

MASS ABSORPTION COEFFICIENT

A layer of matter absorbs according to the quantity of matter it contains which is the thickness traversed, x in Eq. (1), times the density of the material. Therefore, absorber "thicknesses" are conveniently expressed on a mass basis (gm/cm^2). Accordingly, μ is often expressed in $(\text{gm}/\text{cm}^2)^{-1}$ or cm^2/gm (square centimeters per gram) and called "mass absorption coefficient."

COMBINATION OF MASS ABSORPTION COEFFICIENTS

The probabilities that a photon suffer an interaction process with atoms of different elements in an absorber add without mutual disturbance.* Therefore, the mass absorption

* Exception must be made for the effect of chemical binding upon the contribution of valence electrons to Rayleigh scattering and for the coherent combination of Rayleigh scattering by different atoms which matters only under special circumstances, particularly in crystals.

coefficient of a chemical compound or mixture is an average of the mass absorption coefficients of the constituent elements, weighted in proportion to the abundance of each element by weight. For example, for water (1 part H, 8 parts O):

$$\mu_{\text{H}_2\text{O}} = \frac{1}{9} \mu_{\text{H}} + \frac{8}{9} \mu_{\text{O}} \quad (3)$$

provided the μ 's are expressed as mass absorption coefficients.

HALF-VALUE LAYER

The absorber thickness $t_{1/2}$ which has a probability $1/2$ of letting through a photon undisturbed (i.e., which reduces the intensity of a "narrow beam" to $1/2$) is called the "half-value layer" of the given absorber material for the given energy of monochromatic gammas. It follows from Eq. (1) that:

$$t_{1/2} = (\ln 2)/\mu = 0.693/\mu \quad (4)$$

since $e^{-\mu t_{1/2}} = 1/2$.

TABLES OF MASS ABSORPTION COEFFICIENTS⁶

Data for certain important substances are given in Table 2.3.1. The same data diminished by the contribution of Rayleigh scattering (process 1b) are given in Table 2.3.2 for convenience in applications where the small-angle Rayleigh process is disregarded.

Table 2.3.1—Mass Absorption Coefficients for Various Materials

(G. R. White, X-ray Attenuation Coefficients from 10 to 100 mev, Nat. Bu. Standards, NBS Report-1003, May 13, 1952)

Photon energy, mev	Mass absorption coefficient, cm ² /gm			
	H ₂ O	Al	Fe	Pb
0.1	0.171	0.169	0.370	5.46
.15	.151	.138	.196	1.92
.2	.137	.122	.146	0.942
.3	.119	.104	.110	.378
.4	.106	.0927	.0939	.220
.5	.0967	.0844	.0840	.152
.6	.0894	.0779	.0769	.119
.8	.0786	.0683	.0668	.0866
1.0	.0706	.0614	.0598	.0703
1.5	.0576	.0500	.0484	.0523
2.0	.0493	.0431	.0422	.0456
3.0	.0396	.0353	.0359	.0413
4.0	.0339	.0310	.0330	.0416
5.0	.0302	.0284	.0314	.0430
6.0	.0277	.0266	.0305	.0445
8.0	.0242	.0243	.0298	.0471
10.0	.0221	.0232	.0300	.0503

Table 2.3.2—Mass Absorption Coefficients, cm^2/gm , Disregarding Rayleigh Scattering Contribution
(Prepared by G. R. White)

Photon energy, mev	Mass absorption coefficient, cm^2/gm			
	H ₂ O	Al	Fe	Pb
0.1	0.167	0.160	0.342	5.29
.15	.149	.133	.182	1.84
.2	.136	.120	.138	0.895
.3	.118	.103	.106	.355
.4	.106	.0922	.0918	.208
.5	.0967	.0840	.0828	.145
.6	.0894	.0777	.0761	.114
.8	.0786	.0682	.0668	.0837
1.0	.0706	.0614	.0595	.0683
1.5	.0576	.0500	.0484	.0514
2.0	.0493	.0431	.0422	.0451
3.0	.0396	.0353	.0359	.0410
4.0	.0339	.0310	.0330	.0416
5.0	.0302	.0284	.0314	.0430
6.0	.0277	.0266	.0305	.0445
8.0	.0242	.0243	.0298	.0471
10.0	.0221	.0232	.0300	.0503

ENERGY DISSIPATION OWING TO INTERACTIONS ALONG A "NARROW BEAM"

GAMMA-RAY ESCAPE SIDEWISE FROM A BEAM

The energy of photons which experience an interaction process in a material need not be entirely dissipated very near the point of interaction. The atomic particles to which the energy is transferred may travel some distance (see below). More important, part of the energy of the incident photons is carried away in various directions by photons of lower energy as a result of processes among which the following are most important.

Fluorescence

When an "inner-orbit" atomic electron is ejected by photoelectric effect (process Ia), one of the outer atomic electrons will take its place and thereby become more tightly bound. The excess binding energy may be released in the form of an X-ray photon (fluorescence). The probability of fluorescence⁷ (as opposed to a second electron-ejection) and the energy of the radiated photon are increasing functions of the atomic number of the material. See data in Table 2.3.3.

Scattering

Scattered photons carry away a fraction of the incident-photon energy, in the event of a Compton process (Ic), or all of it in the event of coherent scattering (Ib). Data on the average energy fraction removed are shown in Table 2.3.4.

Table 2.3.3 — Fluorescent Yield in the K Series*

(From C. D. Broyles et al, Phys. Rev. 89, 1953)

Element	Yield	Element	Yield
8 O	0.00	34 Se	0.60
10 Ne	.01	35 Br	.63
12 Mg	.02	38 Sr	.71
14 Si	.05	42 Mo	.77
16 S	.09	47 Ag	.83
17 Cl	.11	50 Sn	.85
18 A	.13	54 Xe	.87
20 Ca	.17	60 Nd	.89
24 Cr	.27	70 Yb	.92
26 Fe	.34	78 Pt	.94
28 Ni	.42	80 Hg	.95
29 Cu	.46	82 Pb	.95
30 Zn	.49	84 Po	.96

* Fluorescent yield in the K series is the probability that an atom which has been ionized in the K shell will emit a photon of a frequency in the K series

Table 2.3.4 — Fraction of Incident-photon Energy Retained After Compton Scattering, Averaged Over All Angles of Scattering

(Prepared by A. T. Nelms)

Initial photon energy, mev	Fraction retained by photon
0.1	0.861
.15	.817
.2	.782
.3	.729
.4	.690
.5	.659
.6	.632
.8	.592
1.0	.560
1.5	.505
2.0	.469
3.0	.423
4.0	.394
5.0	.373
6.0	.357
8.0	.333
10.0	.316

Annihilation

When a photon disappears as a result of pair production (process IIIa), the positron of the pair eventually combines with an atomic electron releasing 1 mev of energy (and sometimes more) in the form of two photons (occasionally one only).

Bremsstrahlung

The gamma-ray energy transferred to electrons (or positrons) within a material may be re-radiated in the form of X rays (bremsstrahlung). For particles of energy above 10 mev and for high Z, this effect accounts for removal of most of the energy. At lower energies, the average energy fraction radiated by an electron (or positron) of energy E (mev) is of the order of:

$$Z E / 1,000 \quad (5)$$

where Z is the atomic number of the material.

ENERGY TRANSPORT BY ATOMIC PARTICLES

Electrons and Positrons

Most of the energy transferred from gamma rays to a material is taken up by electrons (or positrons) and then dissipated along the path of these particles. The distance traveled by electrons (or positrons) is very small compared to the mean free path of gamma rays at energies up to a few mev but not at higher energies (see Table 2.3.5). Furthermore, the path of electrons and positrons is very tortuous, especially for high Z and at energies below 10 mev.

Table 2.3.5 — "Relative Range" of Electrons and Photons of Equal Energy in Water

[Principles of Radiological Physics, Nat. Bu. Standards, U. Fano, NBS Report-1002, May 1951 (to be published as a contribution to Biological Effect of Radiations, edited by A. Hollaender, McGraw-Hill, New York)].

Energy, mev	μR^*
0.1	0.004
1.0	.04
10.0	.2
100.0	.6

* μR = Product of narrow-beam absorption coefficient of the X-rays (which may be regarded as the reciprocal of a range) and of the "true" range of electrons (measured along the track)

Neutrons and Other Particles

Neutron generation absorbs only a small fraction of the incident gamma energy even under optimum conditions (see above), but the ejected neutrons travel quite far (see

Chapter 2.4). Protons and other charged fragments ejected from nuclei carry a very minor fraction of the total gamma energy and do not travel far.

ENERGY-ABSORPTION COEFFICIENT ("TRUE ABSORPTION" COEFFICIENT)

To characterize the fraction of its energy dissipated by a narrow beam of gamma rays in traversing an absorber, the probability of each interaction process must be multiplied by the probable fraction, f , of the photon energy which is actually dissipated in the absorber as a result of the process. In the event of a photoelectric effect, the value of f discounts the fluorescence radiation; in the event of scattering, it discounts the scattered radiation; in the event of pair production, it discounts the annihilation radiation; and in all events, it discounts the (usually small) bremsstrahlung loss. Accordingly, the "energy absorption coefficient," μ_{En} , is defined by modifying Eq. (2) in the following manner:

$$\mu_{En} = f_{photo} \mu_{photo} + f_{scatt} \mu_{scatt} + f_{pair} \mu_{pair} \quad (6)$$

The values of the f fractions can be estimated from theoretical and experimental data.

TABLES OF ENERGY-ABSORPTION COEFFICIENTS

Data on $f_{scatt} \mu_{scatt}$ (for Compton processes only, $f_{scatt} \mu_{scatt}$ being often indicated by σ_a) are often given in the literature. Data on μ_{En} are often based on the assumption $f_{photo} = f_{pair} = 1$ ($f_{photo} \sim 1$ for low- Z materials, the choice of f_{pair} is not critical as long as μ_{pair} is small). More accurate data are given for certain materials in Table 2.3.6.

GENERAL PROBLEM OF PENETRATION

A gamma-ray photon often experiences as many as 5 or 10 scattering processes before its eventual absorption. The direction of propagation thereby becomes increasingly random, and the initial straight penetration tends to go over into a diffusion process.

The penetration of gamma rays through a homogeneous medium of infinite extension is rather well understood. Much detailed information is available on this subject. However, the solution of specific problems involves some adaptation of published data. In addition, there is only meager understanding of the effects of inhomogeneities in a material and of boundaries between materials (these effects are not always large).*

The information given in the rest of this chapter pertains to gamma-ray propagation through homogeneous media of infinite extension, except where otherwise noted.

PERTINENT PHYSICAL EFFECTS

PRIMARY AND SECONDARY RADIATION

The interaction processes experienced by gamma rays give rise to a variety of "secondary radiations," such as scattered gammas and electrons ejected by photoelectric effect (see "Types of Process" above). The gammas emitted directly from a source are called "primaries." For primary gammas up to 10 mev, the secondaries which contribute much to penetration are themselves gammas (of lower energies), since secondary electrons do not travel far and secondary neutrons are few in number. Therefore, the study of gamma-ray attenuation deals with photons of various energies even where the primaries are monoenergetic.

* See "Other Studies" discussed later in this chapter.

Table 2.3.6 — Energy-absorption Coefficients for Various Materials*

(Prepared by G. R. White and I. E. Hornstein)

Energy, mev	Energy-absorption coefficient, cm ² /gm			
	H ₂ O	Al	Fe	Pb
0.088	0.0252	0.0445	0.312	2.46
.10	.0253	.0371	.219	2.16
.125	.0266	.0307	.123	1.55
.15	.0278	.0282	.0801	1.08
.175	.0289	.0276	.0595	.779
.20	.0299	.0275	.0485	.586
.25	.0312	.0279	.0390	.358
.30	.0320	.0283	.0340	.241
.40	.0328	.0287	.0306	.136
.50	.0330	.0287	.0293	.0904 (.0901)†
.60	.0329	.0286	.0287 (.0286)†	.0689 (.0684)
.70	.0326	.0283	.0280 (.0278)	.0566 (.0560)
.80	.0321	.0278	.0274 (.0272)	.0483 (.0477)
.90	.0316	.0274	.0268 (.0266)	.0431 (.0424)
1.0	.0311 (.0310)†	.0270 (.0269)	.0264 (.0261)	.0391 (.0384)
1.25	.0297 (.0296)	.0258 (.0257)	.0252 (.0248)	.0325 (.0317)
1.5	.0284 (.0283)	.0247 (.0246)	.0241 (.0237)	.0290 (.0280)
1.75	.0272 (.0271)	.0237 (.0236)	.0232 (.0227)	.0275 (.0260)
2.0	.0261 (.0260)	.0229 (.0227)	.0224 (.0219)	.0265 (.0248)
2.5	.0243 (.0241)	.0216 (.0213)	.0215 (.0209)	.0260 (.0238)
3.0	.0229 (.0227)	.0205 (.0201)	.0210 (.0203)	.0264 (.0238)
4.0	.0208 (.0204)	.0192 (.0188)	.0208 (.0198)	.0290 (.0253)
5.0	.0194 (.0189)	.0185 (.0180)	.0211 (.0198)	.0317 (.0272)
6.0	.0184 (.0178)	.0180 (.0174)	.0214 (.0200)	.0344 (.0287)
7.0	.0176 (.0170)	.0177 (.0171)	.0219 (.0203)	.0368 (.0298)
8.0	.0170 (.0163)	.0176 (.0169)	.0225 (.0206)	.0391 (.0309)
9.0	.0165 (.0158)	.0175 (.0168)	.0232 (.0209)	.0410 (.0319)
10.0	.0161 (.0154)	.0176 (.0167)	.0238 (.0213)	.0428 (.0328)

* Values of the fractions f were estimated as follows:

$$f_{\text{photo}} = 1 - F_K K_\alpha / h\nu$$

$$f_{\text{scatt}} = 1 - R_C - 1/h\nu \int_0^{T_{\text{max}}} p_C(h\nu, T) T G_{\text{Brem}}(T) dT$$

$$f_{\text{pair}} = 1 - 2mc^2/h\nu - 1/h\nu \int_0^{h\nu-2mc^2} p_p(h\nu, T^+, T^-) \{T^+ G_{\text{Brem}}(T^+) + T^- G_{\text{Brem}}(T^-)\} dT^+$$

where: K_α = energy of radiation in the K series
 I_K = binding energy of electron in K shell
 R_C = average fraction of incident-photon energy retained by photon after Compton scattering (see Table 2.3.4)

$p_C(h\nu, T)$ = probability that Compton scattering yields recoil electron of energy T

$p_p(h\nu, T^+, T^-)$ = probability that pair production yields positron of energy T^+ and electron of energy T^-

$G_{\text{Brem}}(T)$ = fraction of electron energy radiated as Bremsstrahlung (from NBS Report No. 2364)

† Energy-absorption coefficients with corrections for Bremsstrahlung loss are given in parentheses. The simple law of combination of absorption coefficients for a mixture of elements, according to Eq. (3), does not hold exactly when the effect of $G_{\text{Brem}}(T)$ is appreciable

FILTRATION

Photons of different energies traveling together through an absorber, e.g., in a "narrow-beam" attenuation experiment (Fig. 2.3.1) with a non-monoenergetic source, have different probabilities of experiencing interaction processes. The gammas with higher interaction probability (i.e., the less penetrating, or "softer," ones—which usually are those of lower energy) are removed from the beam in the course of penetration faster than those with

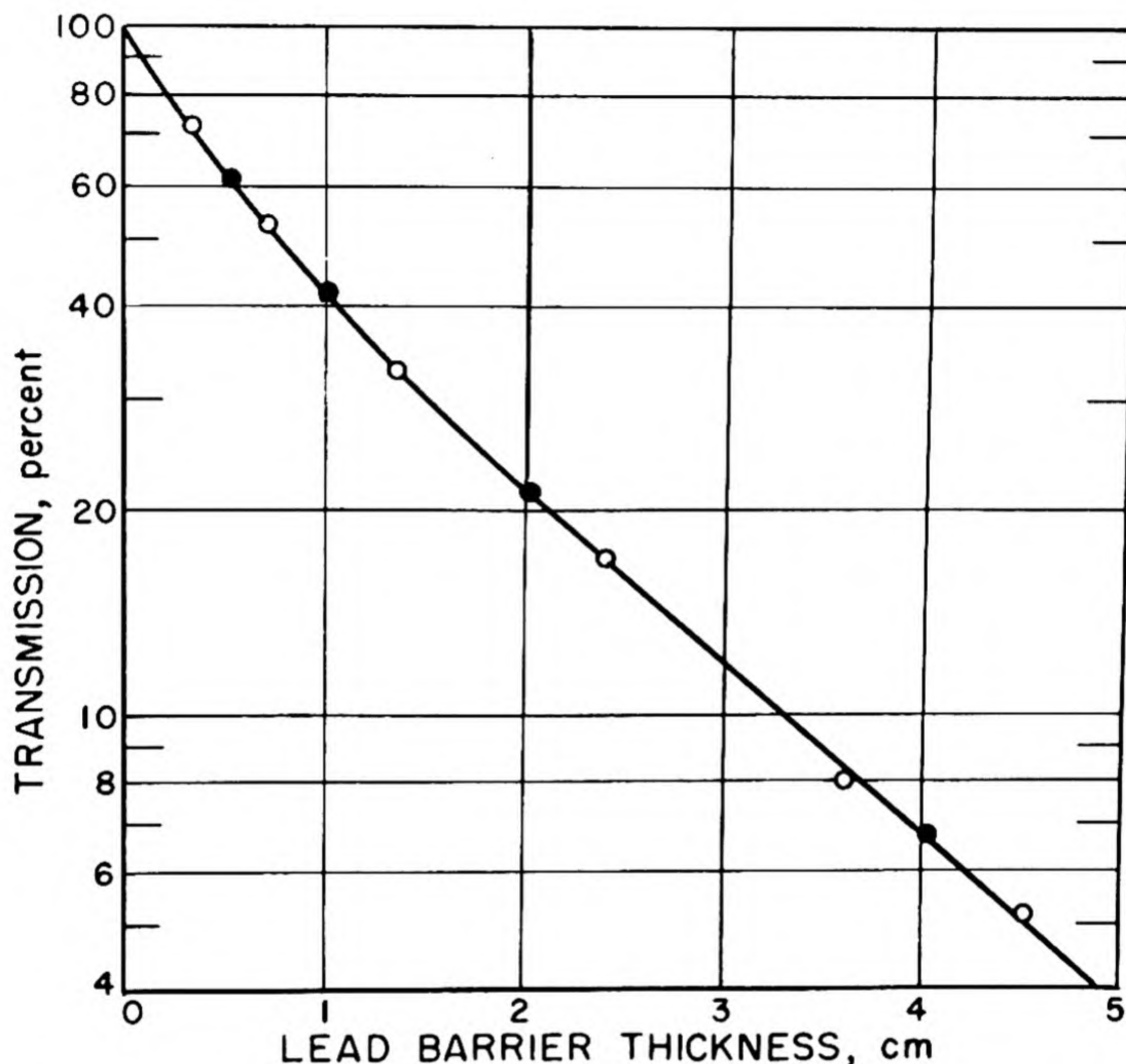


Fig. 2.3.3— Illustration of the Experimental Measurement of Attenuation Coefficients for a Non-monoenergetic (Radium) Source. Narrow-beam conditions: ●—Kaye, Binks, and Bell; ○— H. O. Wyckoff and R. J. Kennedy, Jour. Res. Nat. Bu. Standards 42, 1949.

lower interaction probability. Thus, penetration to deep layers of the absorber has an effect of "filtration" which selects gammas with low probability of interaction (i.e., the "harder" component of the initial beam). Accordingly, the successive layers of an absorber attenuate the beam by smaller and smaller fractions. The semi-logarithmic plot of intensity vs thickness, which is a straight line for monoenergetic gammas in Fig. 2.3.2, has a decreasing slope (corresponding to a decreasing average value of the absorption coefficient μ) for a non-monoenergetic beam in Fig. 2.3.3.

BROAD-BEAM ATTENUATION

In an attenuation experiment free from the "narrow beam" limitation (see Fig. 2.3.4, in which the aperture of the collimator of Fig. 2.3.1 has been greatly increased), the loss by scattering of some gammas initially aimed at the detector is compensated in part by the

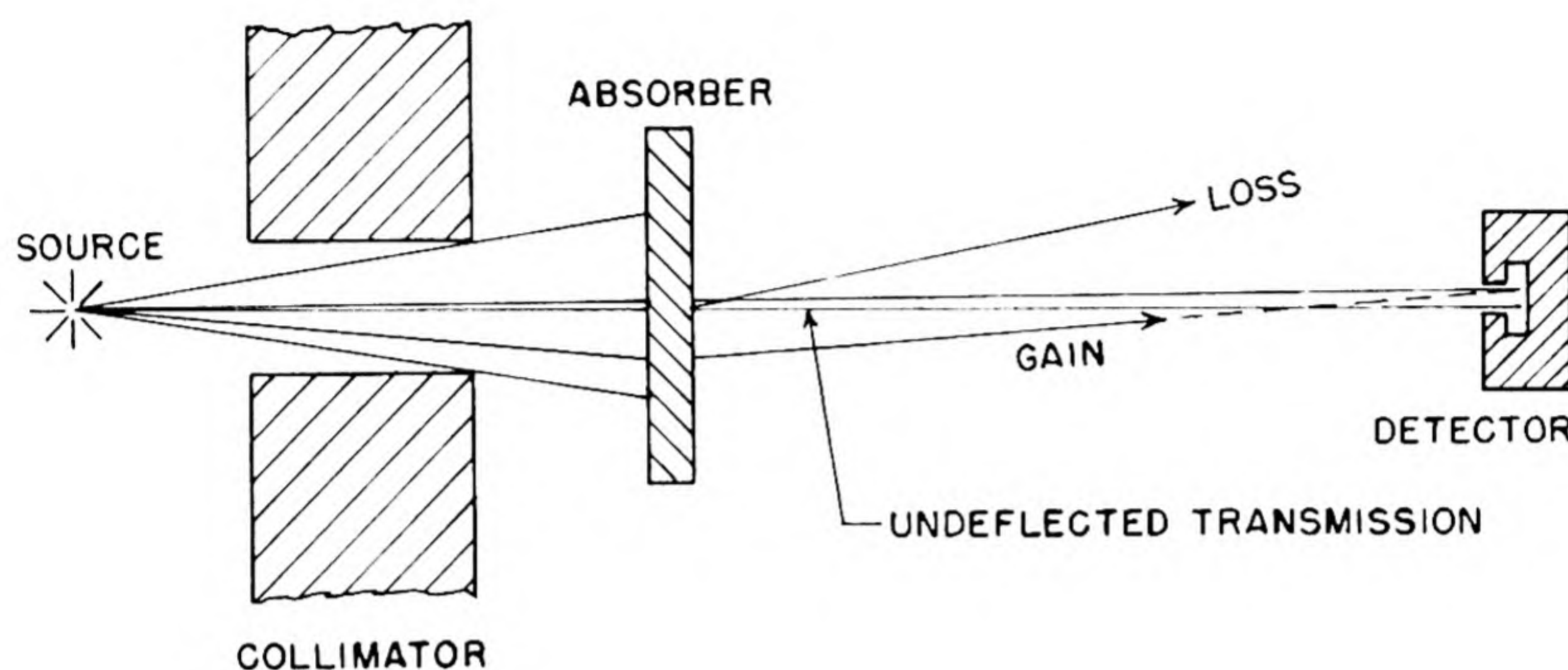


Fig. 2.3.4 — Schematic Diagram Showing "Loss" of Radiation Aimed at the Detector but Scattered Away from It, and Compensating "Gain" of Radiation Aimed in Other Directions but Scattered toward the Detector.

deflection toward the detector of gammas initially directed otherwise.* Therefore, one finds a lower attenuation under "broad-beam" than under "narrow beam" conditions, i.e., a spuriously low apparent value of the absorption coefficient. As the absorber thickness increases, the "gain" derived from the "broad-beam" condition becomes comparatively smaller (owing to the increased chance of multiple interaction processes). Therefore, the apparent value of the absorption coefficient goes up with increasing absorber thickness, as witnessed by the increasing slope of the plot in Fig. 2.3.5.† It approaches the value of the "narrow-beam" coefficient, without ever attaining it.‡

ACCUMULATION OF SECONDARIES

Not only in the "broad-beam" experiment but also generally the presence of secondary scattered gammas influences heavily the whole process of gamma-ray penetration. Compton scattering is, on the whole, the most frequent process for medium-energy gammas in

*See Davisson and Evans.⁸ An estimate of this effect, valid for rather thin absorbers and moderate beam apertures has been given, though incorrectly, by Tarrant. This remark refers mainly to the number of photons scattered toward the detector or away from its direction, rather than to the energy retained by these photons after scattering.

†This may not hold when the initial energy exceeds the minimum point of the absorption coefficient curve.

‡Notice that the "broad-beam" effect yields downward curvature, whereas the curvature of Fig. 2.3.3 is upward owing to the filtration effect. Concurrent departures from a monoenergetic source and from "narrow-beam" condition tend to compensate and may fail to be observed.

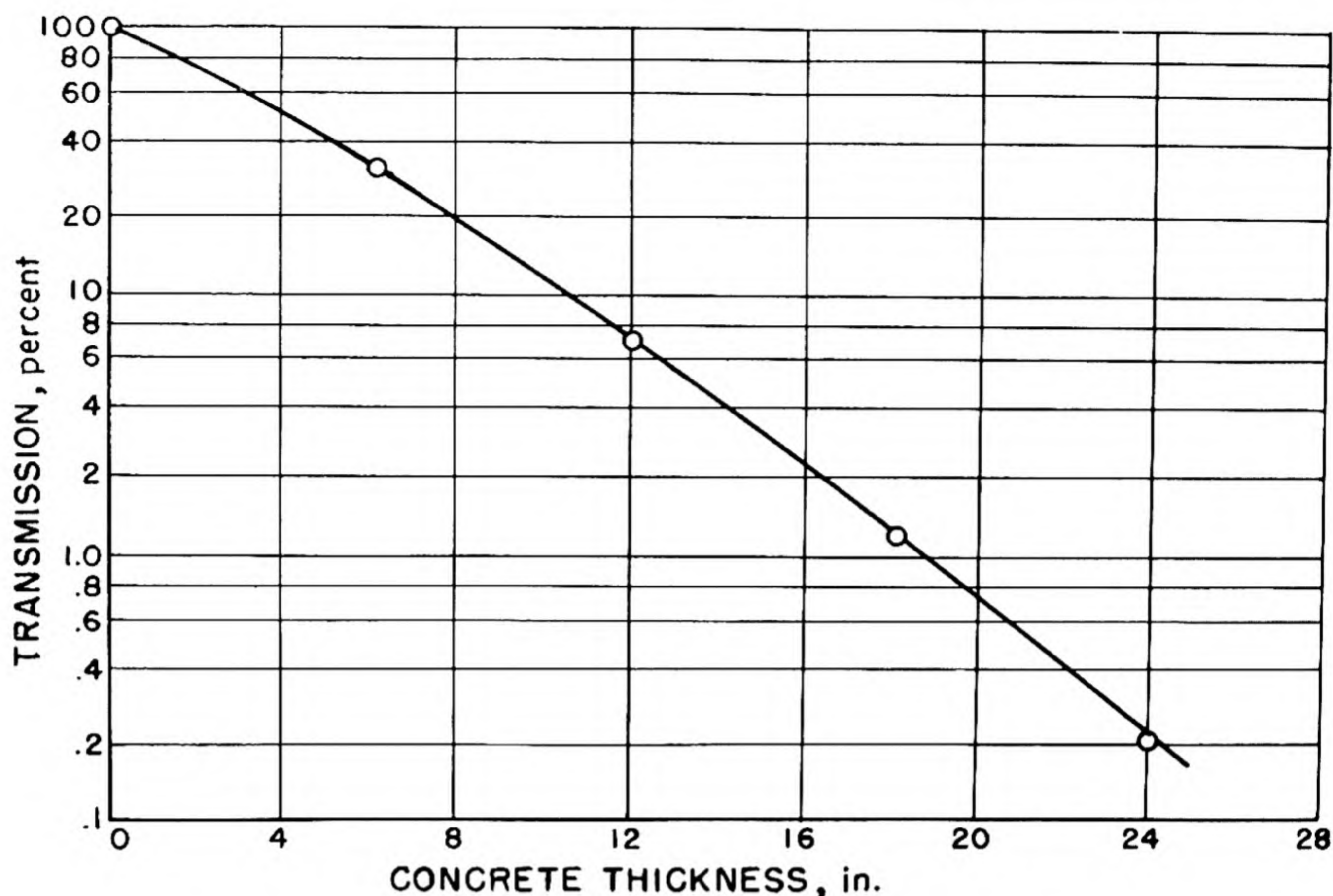


Fig. 2.3.5 — Broad-beam Attenuation Curve for Gamma Rays from Co^{60} . R. J. Kennedy, H. O. Wyckoff, and W. A. Snyder, Jour. Res. Nat. Bu. Standards 44, 1950.

the energy range of 0.1-10 mev, especially in low-Z materials. A photon may easily experience 5 to 10 successive Compton processes before its eventual outright absorption, which most frequently occurs in a photoelectric process. The photon energy decreases in each process. The gamma-ray energy suffers thereby a progressive degradation. The average fractional energy loss in a Compton process⁴ decreases in the course of degradation.* Therefore, the gamma photons tend to accumulate in the lower portion of the spectrum down to the energy range where outright photoelectric absorption becomes predominant.⁶

POLARIZATION EFFECT

Gamma-ray sources usually generate unpolarized radiation, but the radiation becomes partially polarized in the course of repeated scattering. As a result, any three successive paths of a photon separated by scattering processes have a slight tendency to be coplanar. This effect tends to increase the over-all penetration but only by a few percent.⁹

FORMULATION OF THE COMPLETE PROBLEM

MAPPING THE GAMMA-RAY FLUX

Given a distribution of gamma-ray sources within a material, the general problem of penetration consists of determining the intensity and spectrum of the gammas (primaries and secondaries) which flow in each direction at each point of the medium.

*See also Table 2.3.3.

MONOENERGETIC SOURCES

It is adequate to solve the problem separately for sources of monoenergetic gammas of different energies, because any source may be regarded as the superposition of monoenergetic sources whose gammas penetrate independently.

PENETRATION OF THE PRIMARIES

Despite the large accumulation of secondary gammas, the exponential attenuation of the primaries (as observed under "narrow-beam" conditions) usually constitutes the single most important factor affecting the gamma-ray penetration, especially since the primaries usually* have a lower μ than any of their secondaries. At any point of a medium, the flux of the primary gammas alone can be easily calculated, since the primaries penetrate according to the simple "narrow-beam" exponential law (Fig. 2.3.2). For a point at a distance x from a gamma-ray source, the product μx in the exponent of $e^{-\mu x}$ in Eq. (2) (with the value of μ corresponding to the medium and the source energy under consideration) represents the depth of penetration expressed in "relaxation lengths." This number serves as a crude initial index of the attenuation of the gammas from the source to the point.

BUILD-UP FACTOR

Since the main problem arises from the accumulation of secondaries, it is often convenient to focus on the ratio of the total amount of gammas at any one point to the amount of primaries only. For any specific instrument of gamma-ray detection and measurement at a given location, its actual response may be considered a result of all gammas and its ideal response a result of the primaries only. The ratio of these two responses is the "build-up factor" pertaining to the given instrument and to its location (see Fig. 2.3.6). The results of gamma-ray attenuation studies are often expressed as build-up factors.

PARTIAL AND SIMPLIFIED PROBLEMS

Much understanding and useful information on gamma-ray attenuation is gained from the study of problems schematized so as to involve a reduced number of variables.

ENERGY DEGRADATION ONLY ("NRL" PROBLEM†)

If a source is distributed uniformly throughout a medium, the secondaries are distributed uniformly also, and the only question concerns the accumulation of secondaries of various energies. The same problem arises with respect to the spectrum of secondaries integrated over the whole medium without reference to the source position. The solution of this problem is straightforward.‡ The spectrum of secondaries is cut off on the low-energy side

*Except for high-Z materials and primary energies above a few mev.

†From an experiment by Faust and Johnson.¹⁰

‡The number of photons of energy E , $N(E)$, is determined by the number of all photons $N(E')$ with energies E' higher than E up to the source energy E_0 , multiplied by the probability $p(E, E')$ that the next interaction process changes the energy from E' to E :

$$N(E) = \int_E^{E_0} p(E, E') N(E') dE' \quad (7)$$

The number of photons of energy E_0 is given by the source strength; thereafter, the equation can be solved stepwise by carrying out the integration to lower and lower values of E . This procedure lends itself well to automatic computer operation. For exploratory numerical solutions, see Karr and Lamkin.¹¹ Extensive calculations have been made incidental to more complex problems (see "Calculation of the Parameters" later in this chapter).

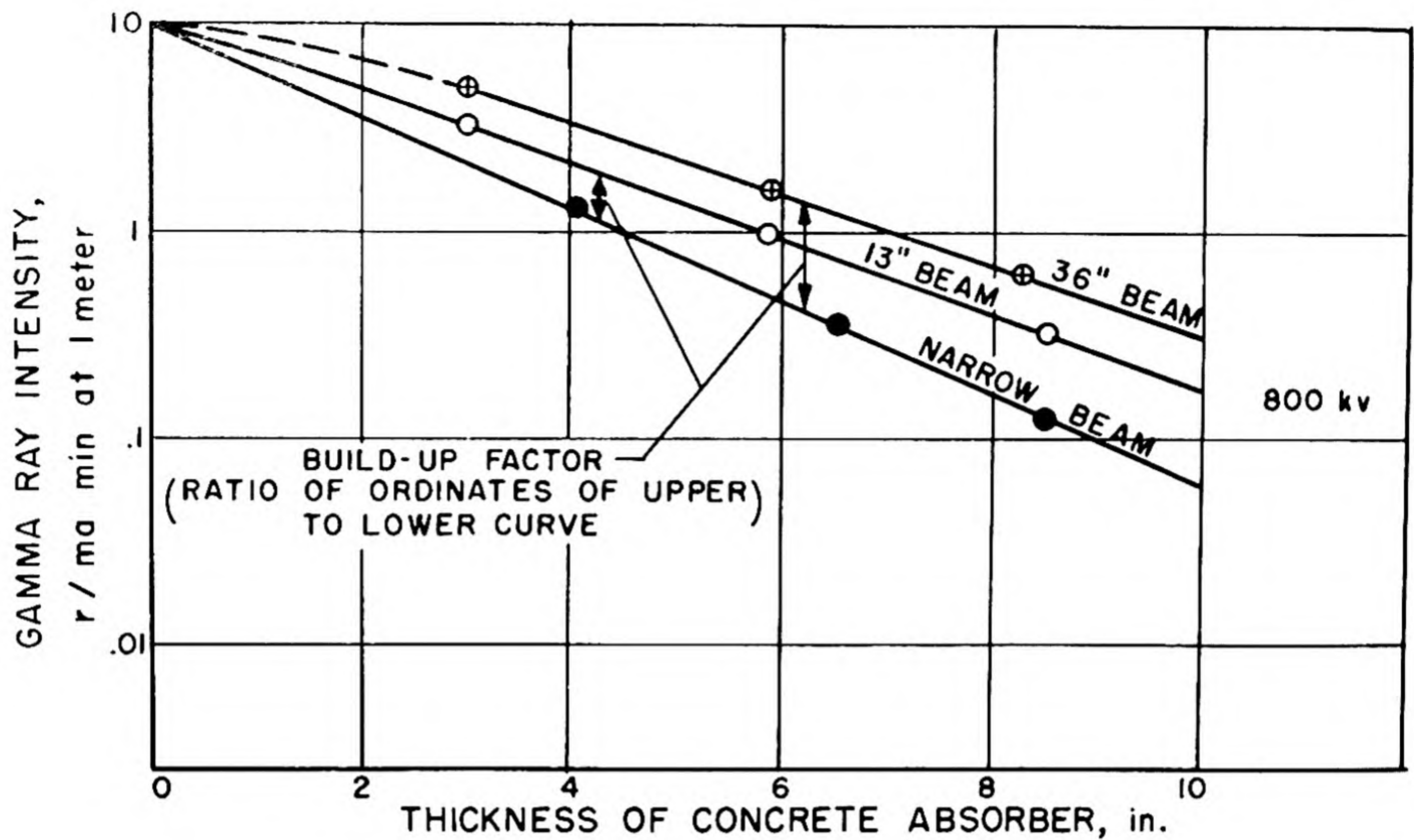


Fig. 2.3.6 — Illustration of the Build-up of Secondary X-rays Under Broad-beam Conditions. from H. O. Wyckoff, R. J. Kennedy, and W. R. Bradford, *Nucleonics* 3, No. 11, 1948.

where the probability of the photoelectric effect rises sharply and peaks above the cut-off except for high- Z materials.

DEGRADATION AND DEFLECTION

Photons tend to lose track of their initial direction as a result of successive scattering processes. One may inquire about the distribution-in-direction of the gammas degraded to a certain energy, regardless of their position with respect to the source. Certain obliquity parameters of the distribution-in-direction (such as the mean obliquity of penetration) remain independent of one another in the course of successive scattering processes. Their termination reduces to a number of separate "NRL" problems.*

* If the number of photons of energy E traveling at an angle ϑ with respect to the initial direction is $N(E, \vartheta)$, the "obliquity parameters" are the values of the Legendre polynomials $P_1(\cos \vartheta)$ integrated over the distribution $N(E, \vartheta)$:

$$N_1(E) = \int_0^\pi P_1(\cos \vartheta) N(E, \vartheta) 2\pi \sin \vartheta d\vartheta$$

These parameters obey the equations:

$$N_1(E) = \int_E^{E_0} p(E, E') P_1 \left(1 - \frac{mc^2}{E} + \frac{mc^2}{E'} \right) N_1(E') dE' \quad (8)$$

where p is the same as in Eq. (1). Since $P_0 = 1$, N_0 is the $N(E)$ above and Eq. (8) reduces to Eq. (7) for $1 = 0$; since $P_1 = \cos \vartheta$, N_1 is essentially the mean obliquity $\langle \cos \vartheta \rangle$. For exploratory numerical solutions see Spencer and Jenkins.¹² Extensive calculations have been made, incidental to more complex problems (see "Calculation of Parameters" later in this chapter).

SCHEMATIC GEOMETRIES*

Gamma-ray sources distributed in space with particular symmetries lead to distributions of secondaries with corresponding symmetries. Often the gamma distribution depends on a single space coordinate, the distance from the source. (The same simplification can be attained, regardless of source symmetry, by inquiring only about the gamma-ray distribution along one space coordinate integrated over the remaining coordinates.)

Plane Sources

A source distributed uniformly over a plane yields a gamma-ray distribution uniform over any plane parallel to the source plane, which depends only on the distance from the source. Further simplification (without further elimination of variables) arises when the source radiation flows either perpendicularly to the source plane ("plane-collimated source" or "plane monodirectional source") or evenly in all directions ("plane isotropic source").

Point Isotropic Source

A source concentrated at one point, which radiates evenly in all directions, yields a gamma-ray distribution uniform over every spherical surface centered in the source and dependent only on the distance from the source.

Point-collimated Source

A source concentrated at one point which radiates in a single direction has only a cylindrical symmetry which is preserved in the distribution of secondaries. The gamma-ray flux depends on two position coordinates (axial and radial distances). Any source can be regarded as an aggregate of point-collimated sources.

DEEP PENETRATION

The study of extremely deep gamma-ray penetrations serves (1) to treat unusually severe shielding problems and (2) to increase confidence in methods of calculation whose reliability tends to decrease as the depth of penetration increases. Deep-penetration studies have led to the establishment of certain mathematical laws and to the development of workable methods of calculation. Most practical problems can be handled by methods suited for moderate penetration (see "Moderate Penetration" below).

QUALITATIVE ANALYSIS¹³

THE MOST PENETRATING SPECTRAL COMPONENT

Usually the primary gammas are more penetrating than any of their secondaries. However, if the energy, E , of the primaries exceeds the energy, E_m , at which the "narrow-beam" absorption coefficient attains its minimum value, secondaries degraded to energy E_m constitute the most penetrating component of the whole spectrum in the medium and play the leading part in determining the deepest penetration. The value of E_m for various materials is given in Table 2.3.7.

* For fuller discussion, see Chapter 2.5.

Table 2.3.7—Energy at Which Narrow-beam Absorption Coefficients
Attain Minimum Values, E_m
(Prepared by G. R. White)

Z	E_m , mev	Z	E_m , mev
4 Be	94	20 Ca	13
5 B	70	26 Fe	9
6 C	55	30 Zn	7.6
7 N	45	40 Zr	5.4
8 O	40	48 Cd	4.4
9 F	34	56 Ba	3.9
10 Ne	30	74 W	3.5
13 Al	21	82 Pb	3.4
		92 U	3.3

LIMITED EQUILIBRIUM OF SOFTER SECONDARIES

At great depths of penetration, secondaries of energy substantially lower than that of the most penetrating component tend to attain a steady state, namely to become distributed in energy and in direction in a manner which no longer varies with depth and which is essentially the same as the distribution considered above under "Degradation and Deflection."

CRITICAL SPECTRAL RANGE

The dynamics of deep penetration are governed by an ever-increasing accumulation of secondaries with energies just below that of the most penetrating component and which are, therefore, only barely less penetrating. The spectral range which is critical in this respect narrows progressively in the course of penetration, while the spectral range in a steady state (see above) spreads to higher energies. The accumulation of secondaries follows a different trend depending on whether the most penetrating component has the energy E_m or is the primary itself, i.e., whether or not the absorption coefficient, μ , has a minimum in the critical range.

CONCLUSION

Since the lower-energy secondaries in a steady state include more and more of the spectrum as the penetration progresses and thus carry nearly the whole energy flux, the main characteristic of deep penetration is the variation of the intensity level of these secondaries as a function of depth. However, this variation is controlled by the secondaries in the critical range.

TREND OF PENETRATION FOR SOURCE ENERGIES BELOW THE "MINIMUM" E_m

LIMITATIONS

The following applies only to plane-collimated, plane-isotropic, and point-isotropic sources (or combinations thereof); it also applies in principle, but hardly in practice,¹⁴ to any plane source.

MATHEMATICAL LAW

The intensity of the gamma-ray flux at great depths for source energies below E_m follows the trend:

$$e^{-\mu_0 x} x^K \quad (9)$$

where x is the distance from the source, μ_0 is the absorption coefficient of the primary gammas in the medium under consideration (expressed in units reciprocal to those of x), and K is a constant. For a plane-collimated source, x^K represents the variation of the "build-up" factors.*

VALUES OF THE CONSTANT K

The constant K depends on the source geometry and on certain functions, A and B , of the probabilities of interaction processes for primary gammas in the medium under consideration. The values of A and B for various materials and primary energies are given in Table 2.3.8. The value of K for a plane-collimated source, as a function of A and B , is

Table 2.3.8—Constants A and B on Which the Exponent of the Build-up Factor Depends

(Prepared by John Doggett and L. V. Spencer)

Source energy, mev	H ₂ O		Al		Fe		Sn		Pb		U	
	A	B	A	B	A	B	A	B	A	B	A	B
10	7.5	7.54	4.1	6.21								
8	6.6	6.87	4.0	5.91	0.48	4.64						
6	5.5	5.96	3.8	5.43	1.2	4.56						
4	4.0	4.91	3.3	4.68	2.0	4.25	0.40	3.61				
3	3.1	4.22	2.7	4.10	2.1	3.89	.86	3.49	0.33	2.88	0.22	2.72
2	2.1	3.38	2.0	3.33	1.8	3.30	1.4	3.13	1.7	2.65	2.0	2.48
1	0.96	2.37	0.96	2.37	0.89	2.36	1.1	2.22	1.7	1.75	1.9	1.53
0.8	.73	2.12	.73	2.12	.72	2.11	0.92	1.95	1.6	1.43	1.8	1.21
.6	.52	1.86	.52	1.86	.54	1.84	.83	1.63	1.5	1.033	1.6	0.852
.4	.32	1.58	.32	1.57	.37	1.52	.77	1.17	1.35	0.579	1.4	.449
.3	.22	1.41	.22	1.40	.32	1.32	.74	0.798	1.2	.333	1.2	.260
.2	.13	1.23	.155	1.21	.31	1.01	.72	.417	0.95	.133	0.97	.100
.15	.086	1.12	.145	1.09	.33	0.767	.70	.223	.77	.0647	.82	.0485

given in Table 2.3.9. The tabulated value of K must be reduced by 1 for a plane-isotropic source and by 2 (inverse square distance effect) for a point-isotropic source.

* Notice that x^K is merely proportional to the "build-up" factor but is not numerically equal to this factor. The results of calculations (see Tables 2.3.11 to 2.3.14) and of an experiment show that Eq. (9) holds adequately, in some cases at least, for depths upwards of 10–15 relaxation lengths. Inspection of Tables 2.3.11 to 2.3.14 disproves the frequent notion that the build-up factor varies linearly with x at low depths.

Table 2.3.9 — The Exponent K of the Build-up Factor as a Function of Constants A and B
(Prepared by L. V. Spencer and John Doggett)

A	B									
	0.02	0.05	0.1	0.25	0.5	1	2	4	6	8
0.02	0.0200	0.0516	0.1095	0.374	2.63	13.00	42.3	113.0	189.5	272
.05	.01939	.0494	.1052	.332	1.328	5.49	17.21	45.5	76.5	108.9
.1	.01846	.0473	.0988	.293	0.871	2.98	8.84	23.0	38.5	54.7
.25	.01617	.0411	.0844	.231	.547	1.439	3.81	9.48	15.69	22.2
.5	.01341	.0338	.0687	.1798	.388	0.887	2.11	4.96	8.16	11.32
1	.01003	.0252	.0506	.1289	.265	.559	1.211	2.67	4.24	5.87
2			.0335	.0841	.1696	.345	0.709	1.477	2.28	3.11
4								0.821	1.173	1.674
6								.577	0.870	1.165
8								.447	.671	0.897

TREND OF PENETRATION FOR SOURCE ENERGIES ABOVE THE "MINIMUM" E_m

LIMITATIONS

The following information applies to all plane sources and to point-isotropic sources (or combinations thereof).

MATHEMATICAL LAW

The intensity of the gamma-ray flux at great depths, for source energies above E_m , follows the trend:

$$e^{-\mu_m x + H(\mu_m x)^{1/3}} x^{-5/6} \quad (10)$$

for plane sources and:

$$e^{-\mu_m x + H(\mu_m x)^{1/3}} x^{-11/6} \quad (11)$$

for point-isotropic sources, where x is the distance from the source, μ_m is the minimum value of the absorption coefficient in the medium under consideration, i.e., the value of μ for gammas of energy E_m expressed in units reciprocal to those of x , and H is a constant which depends on the probabilities of interaction processes for gammas of energies near E_m .*

VALUES OF THE CONSTANTS

The values of μ_m and H for certain materials are given in Table 2.3.10.

SEMI-ASYMPTOTIC CALCULATIONS

A method for the detailed numerical calculation of gamma-ray fluxes from plane sources or point-isotropic sources, which makes use of the mathematical laws and in which the

* See the footnote following Eq. (9). The laws (10) and (11) become effective at greater depths than Eq. (9).

Table 2.3.10— The Values of H and μ_m for Various Materials
(Prepared by L. V. Spencer)

Material	$\mu_m, *$ cm ² /gm	H
H ₂ O	0.0167	2.0
Al	.0216	2.1
Fe	.0300	2.8
Sn	.0351	2.6
W	.0391	2.5
Pb	.0410	2.3
U	.0425	2.1

*Values of μ_m without Rayleigh scattering as in Table 2.3.2 were used in all calculations of broad-beam attenuation

effort required does not increase rapidly with increasing depth of penetration, has been developed through the pilot stage. Results are available for plane-collimated sources of 10.2 mev in Pb and of 5.1 mev in Fe.¹⁵

MODERATE PENETRATION

Most of the detailed information available on gamma-ray penetration derives from calculations which are based, directly or indirectly, on the "polynomial method."¹⁶ The labor required by this method is roughly constant up to penetration depths of the order of 10–15 "relaxation lengths" and thereafter increases roughly in proportion to the cube of the penetration, which makes the method unsuitable for extreme depths. Some of the calculations have been checked by experiments, very satisfactorily.^{17,18,19} The following paragraphs provide some information on the method, which is intended as background for the flexible utilization of its results (see "Calculation of Parameters" below).

An alternate method (successive calculation of the distributions of photons that have been scattered 1,2,3... times) has received considerable application^{20,21} especially to Pb, a high-Z material where the sequence of Compton processes ends early owing to high photoelectric absorption.

PRINCIPLES OF THE POLYNOMIAL METHOD

DEFINING THE GAMMA-RAY DISTRIBUTION BY SUITABLE PARAMETERS

Great labor saving, as well as additional insight, result if the gamma-ray distribution in a medium can be characterized by a few parameters only, which in turn can be calculated directly. (This should be possible, since the relevant features of any physical phenomenon are seldom very numerous.) To this end, one may seek an analytical expression for the gamma-ray distribution, which contains in principle an infinity of parameters (sufficient to describe the distribution in infinite detail) but such that in practice the values of all but a few parameters have a negligible influence on the distribution in the range of interest and may be safely disregarded.

CHOICE OF THE ANALYTICAL EXPRESSION

At a distance of $\mu_0 x$ "relaxation lengths" (see "Penetration of the Primaries" above) from a plane source or point-isotropic source, the flux $N(x, E, \vartheta)$ of photons of energy E traveling at an angle ϑ with respect to the direction of the source has been usually represented as a sum of terms of the following type:

$$N(x, E, \vartheta) = e^{-\mu_0 x} \sum_{nl} N_{nl}(E) L_n(\mu_0 x) P_l(\cos \vartheta) \quad (11)$$

Here, $e^{-\mu_0 x}$ represents the exponential attenuation of the primaries, $L_n(\mu_0 x)$ is a polynomial of the Laguerre (or related) type, $P_l(\cos \vartheta)$ is a Legendre polynomial, and $N_{nl}(E)$ are the coefficients to be calculated from theory (see below). The gamma-ray flux at x , irrespective of direction,* is represented by the terms with $l = 0$ only [$e^{-\mu_0 x} \sum_n N_{n0}(E) L_n(\mu_0 x)$] because the $P_l(\cos \vartheta)$ for $l \neq 0$ have average value zero. Calculation of the coefficients with $n = 0, 1, 2, 3$ only, setting those with $n > 3$ equal to zero, may yield an adequate approximation for $\mu_0 x$ as large as 10 or even 15,† in the sense that the terms with $n > 3$ would yield no substantial correction in this range. Any other analytical expression which can be fitted by a calculation equivalent to the calculation of the N_{nl} 's would be equally acceptable, provided it converges adequately.

CALCULATION OF THE PARAMETERS

The parameter N_{00} is essentially the same as the number of photons $N(E)$ of Eq. (7), and the parameters N_{0l} are essentially the same as the "obliquity parameters" N_l of Eq. (8). They depend on the number of photons of certain energies and directions irrespective of their distance from the source. The parameters $N_{nl}(E)$ depend on the same numbers of photons but weighted in proportion to certain functions of their distance from the source (polynomials of grade n). Each N_{nl} is determined by an "NRL" equation, similar to Eq. (8) but with a correction which requires previous knowledge of parameters with lower values of n .‡ Thus, the N_{nl} 's can be calculated in succession for higher and higher values of n .

AVAILABLE RESULTS OF CALCULATIONS

The raw results of calculations have the form of "weighted obliquity parameters," as indicated above, calculated separately for various materials, source geometries, and source energies and tabulated for a series of secondary-photon energies. These data usually get processed and published in part, in the form of answers to specific questions, such as plots of the build-up factor for a specific instrument vs distance from the source. However, processed and published data may not answer just the type of question required for a specific application (e.g., they may not give the build-up factor for a desired type of instrument, or they may fail to give indications regarding the distribution-in-direction). In this event, the desired application may be achieved by procuring the original raw data (see below) and by reprocessing them according to need.

* Notice the difference between the total flux through a point irrespective of direction and the net transport through a plane perpendicular to the source direction.

† The reason for the success of the representation (11) is discussed by Spencer and Fano.¹⁶

‡ Each $N_{nl}(E)$ depends on the value of the same parameter for photons of energy E' , which subsequently drop to the energy E , as in Eq. (8). However, the value $\int_E^{E_0} P_l(E, E') N_{nl}(E') dE'$ would yield a number of photons of energy E weighted according to the distance from the source at which they are generated. The correction takes into account the average travel of photons before the next interaction process.

EXPLORATORY CALCULATIONS

Pilot calculations have been made in sizable numbers^{9,19,22-24} and, in part, checked by experiments.¹⁷⁻¹⁹ These results serve primarily, at present, to provide a quantitative illustration of certain specific features of the gamma-ray flux.

NDA-NBS PROGRAM (H. GOLDSTEIN, NDA)²⁵

A comprehensive program of calculations by the polynomial method is being carried out by Nuclear Development Associates in conjunction with the Bureau of Standards. The aim of the program is directed at producing answers on gamma-ray penetration for materials, source geometries, and initial energies of interest in the shielding of reactors. Accordingly, the initial energies chosen generally cover the range from 0.5 to 10 mev. The materials involved extend over the complete periodic table, including pure Compton scatterer, H₂O, Al, Fe, Sn, W, Pb, U. For almost all of the materials and source energies, computations have been made for point-isotropic sources and, in most cases, also for plane monodirectional source geometry. In addition, for Compton scatterer, iron, and lead (the most important class of materials in practice), calculations have also been made for infinite plane sources in which the distribution of the source photons in the angle θ from the normal to the plane is given by the Legendre polynomials $P_n(\cos \theta)$, $n = 1, 2, 3$. Since the P_0 case (plane isotropic) is directly related to the point-isotropic solution, the results cover the first four Legendre polynomials which, it is hoped, will permit approximating the answer for any arbitrary plane source, symmetric about the normal, which does not vary too rapidly with θ .

The range of penetrations which these calculations are designed to cover is from 1 to 20 "relaxation lengths" (see "Penetration of the Primaries" above) from the source. The number of moments needed for such penetrations, and the number of cases considered, is so extensive as to preclude hand computations. Instead, the Bureau of Standards automatic computer, SEAC, has been used in all problems.

Certain simplifications in the nature of the gamma-ray interaction have been made which greatly reduce the complexity of the calculations without affecting the accuracy of the results significantly. Only three processes have been considered. Two of these, photoelectric effect and pair-production, have been assumed completely absorptive, thus neglecting such secondary effects as fluorescence, bremsstrahlung, and annihilation radiation. The third process, incoherent Compton scattering, is the only scattering treated. For the energies and materials discussed, coherent scattering is at such small angles as to be no scattering at all and has therefore been omitted from both the total absorption coefficient and the scattering kernel. Polarization effects in the incoherent scattering have also been neglected.

It is difficult to state the expected accuracy of the results, as it varies with the number of moments calculated, the type of material, the penetration, and the energy region of the scattered spectrum being considered. In general, the error in integrated quantities, such as build-up factors, will have less effect on the final calculated intensity than the normal uncertainties in the value of the absorption coefficient.

It is expected that full details of the calculation will be published in 1953 as an Atomic Energy Commission report. Complete tables of build-up factors and differential spectra will be included in the report along with illustrative examples of angular distributions. These results will not exhaust the calculations which can be made from the raw output of the machine, however. To make these more generally available, it is therefore intended to place annotated microfilm copies of the SEAC output at each of the AEC deposit libraries.

TABLES OF BUILD-UP FACTORS (H. GOLDSTEIN, NDA)

To illustrate the type of results obtained from this program, Tables 2.3.11 to 2.3.14 present the calculated dose build-up factors with a point-isotropic source in an infinite medium composed of H_2O , Al, Fe, and Pb, respectively. The designation "dose" indicates the gamma-ray flux is to be measured in terms of roentgens per unit time, i.e., with the energy spectrum weighted in proportion to the energy absorption coefficient of air (see "General Problem of Penetration" above). Table 2.3.15 lists the values used here in computing the build-up factors given in the tables.

The accuracy of the results for Pb and Fe is estimated roughly at 5 percent, except at the greatest penetration, where the errors may be as large as 15 percent. The low-energy portion of the spectrum (which is the most difficult to calculate) contributes disproportionately to the dose build-up factor for water and aluminum. Hence, the limit of error for these materials is undoubtedly greater, probably being around 10 percent for medium penetrations, rising to 25–30 percent for the deepest penetration.

Table 2.3.11 — Dose Build-up Factor, B_r , for Pb, Point-isotropic Source

E_0 , mev	$\mu_0 r$				
	2	4	7	10	15
0.5	1.42	1.69	2.00	2.27	2.65
1	1.69	2.26	3.02	3.74	4.81
2	1.76	2.51	3.66	4.84	6.86
3	1.68	2.43	3.75	5.30	8.44
4	1.56	2.25	3.61	5.44	9.80
5.11	1.46	2.08	3.44	5.55	11.74
6	1.40	1.97	3.34	5.69	13.80
8	1.30	1.74	2.89	5.07	14.05
10	1.23	1.58	2.52	4.34	12.54

Table 2.3.12 — Dose Build-up Factor, B_r , for Fe, Point-isotropic Source

E_0 , mev	$\mu_0 r$					
	2	4	7	10	15	20
0.5	3.09	5.98	11.73	19.23	35.42	55.6
1	2.88	5.39	10.21	16.18	28.31	42.7
2	2.38	4.08	6.99	10.47	16.83	24.0
3	2.12	3.44	5.74	8.35	13.25	18.8
4	1.94	3.03	4.91	7.11	11.23	16.0
6	1.72	2.58	4.14	6.02	9.89	14.7
8	1.56	2.23	3.49	5.07	8.50	13.0
10	1.42	1.95	2.98	4.35	7.54	12.4

EXPERIMENTAL SOURCES OF DATA

Considerable amounts of experimental data have been taken regarding various phases of gamma-ray penetration. However, most of the effort was directed to the solution of specific

Table 2.3.13 — Dose Build-up Factor, B_r , for Al, Point-isotropic Source

E_0 , mev	μ_0 r					
	2	4	7	10	15	20
0.5	4.24	9.47	21.5	38.9	80.8	141
1	3.31	6.57	13.1	21.2	37.9	58.5
2	2.61	4.62	8.05	11.9	18.7	26.3
3	2.32	3.78	6.15	8.65	13.0	17.7
4	2.08	3.22	5.01	6.88	10.1	13.4
6	1.85	2.70	4.06	5.49	7.96	10.4
8	1.68	2.37	3.45	4.58	6.56	8.52
10	1.55	2.12	3.01	3.96	5.63	7.32

Table 2.3.14 — Dose Build-up Factor, B_r , for H_2O , Point-isotropic Source

E_0 , mev	μ_0 r					
	1	2	4	7	10	15
0.256	3.09	7.14	23.0	72.9	166	455
.5	2.52	5.14	14.3	38.8	77.6	178
1	2.08	3.50	7.21	14.6	24.0	44.7
2	1.83	2.77	4.88	8.46	12.4	19.5
3	1.69	2.42	3.91	6.23	8.63	12.8
4	1.58	2.17	3.34	5.12	6.94	9.97
6	1.46	1.91	2.80	4.08	5.33	7.34
8	1.39	1.77	2.49	3.51	4.50	6.05
10	1.32	1.63	2.22	3.04	3.82	5.07

Table 2.3.15 — Energy Absorption-coefficient for Air in Thomson Units Per Electron Utilized in the Preparation of Tables 2.3.11 Through 2.3.14

E , mev	μ_A	E , mev	μ_A
0.03	0.694	0.6	0.146
.04	.308	.8	.145
.05	.188	1	.138
.06	.143	1.5	.127
.08	.118	2	.118
.1	.116	3	.105
.15	.125	4	.0965
.2	.134	5	.0912
.3	.144	6	.0866
.4	.147	8	.0808
.5	.144	10	.0777

problems and therefore had a limited usefulness for the purpose of general penetration study or of reactor shielding. Other recent experiments had more general aims but represent thus far only initial stabs. Some pertinent references will be given here, grouped according to their line of endeavor.

DATA ON GAMMA-RAY DISTRIBUTION IN "PHANTOMS"

Radiologists need estimates of the "dose" received by various portions of a body which is exposed to a radiation beam of given area and given characteristics. Many experiments were made, mostly using mock-ups of human bodies ("phantoms"), with X-ray beams up to the million-volt range, some also with betatrons.*

RADIOLOGICAL SHIELDING DATA

The design of safe radiological installations³¹⁻³⁵ is related, though not too closely, to the design of reactor shielding. Until recent times, radiological shielding studies constituted nearly the sole source of information on high-energy gamma penetration.

OTHER STUDIES

BACKSCATTERING

A systematic analysis of the backscattering of a collimated beam of Co^{60} gammas by the surface of a semi-infinite medium of various materials has been conducted.³⁶ Typical spectra of radiation backscattered through 150° are shown in Figs. 2.3.7 to 2.3.9. The peaks above 200 kev result from single scattering. The lower-energy peak from the lead target results from fluorescence. Studies of the influence of a nearby wall upon the response of a detector have also been made.^{37,38} For example, Kennedy et al found when an ionization chamber was brought near a concrete barrier, remaining at a fixed distance from a Co^{60} source, its reading was subject to increases of the order of 10 percent.

SIDESCATTERING

Data on the radiation scattered sidewise by a phantom exposed to an X-ray beam are given in the radiological literature.^{31,39,40}

ANALYSIS OF RADIATION TRANSMITTED THROUGH A BARRIER

Little experimental information seems to be available on this subject. Spectral analysis by scintillation is in progress.⁴¹

RADIATION INTENSITY IN THE PROXIMITY OF A BOUNDARY

Measurements have been made of the transition effect at the surface of a water tank as the source and/or the detector pass from air to water.⁴²

EFFECTS OF INHOMOGENEITIES OF A MEDIUM

A study on the effect of voids in a water tank is reported in the classified literature.

* For the lower-energy range see particularly Glasser, Quimby, Taylor, and Weatherwax,²⁶ Mayneord and Lamerton,²⁷ and the data of the British Hospital Physicist Assoc.,²⁸ for the higher energies, see Adams et al,²⁹ and Charleton and Breed.³⁰

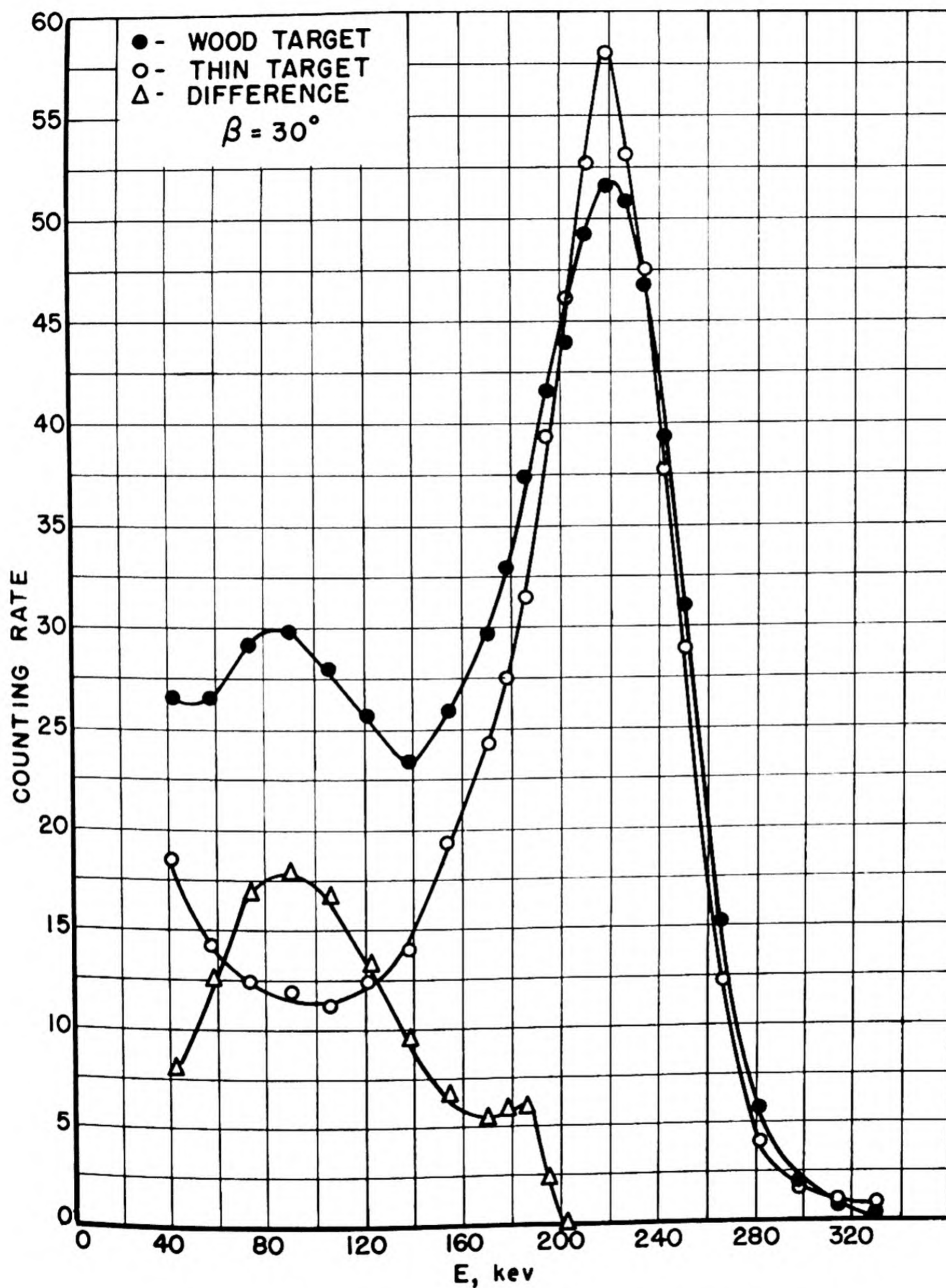


Fig. 2.3.7— Spectrum of Gammas Backscattered from Wood.

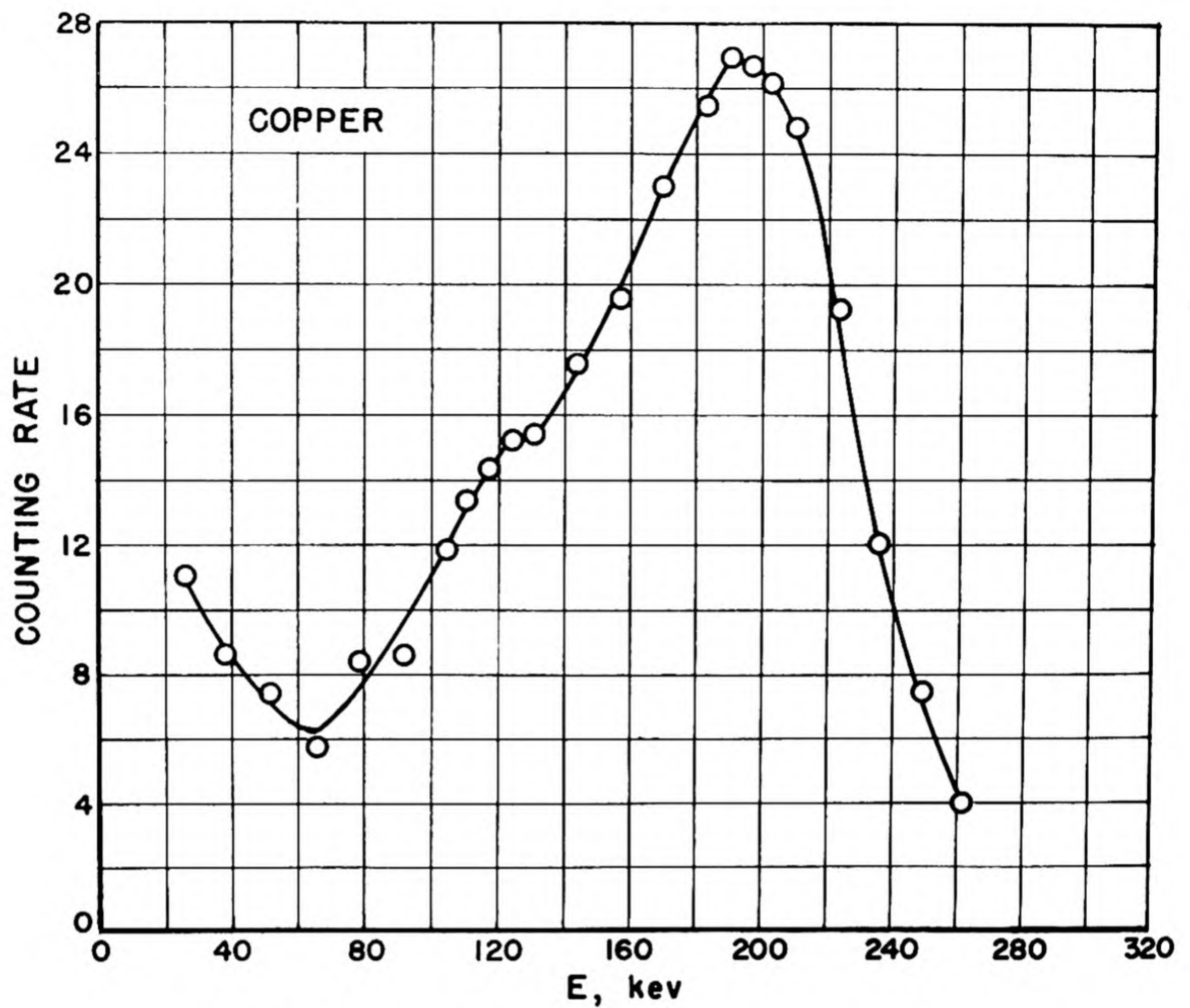


Fig. 2.3.8— Spectrum of Gammas Backscattered from Copper.

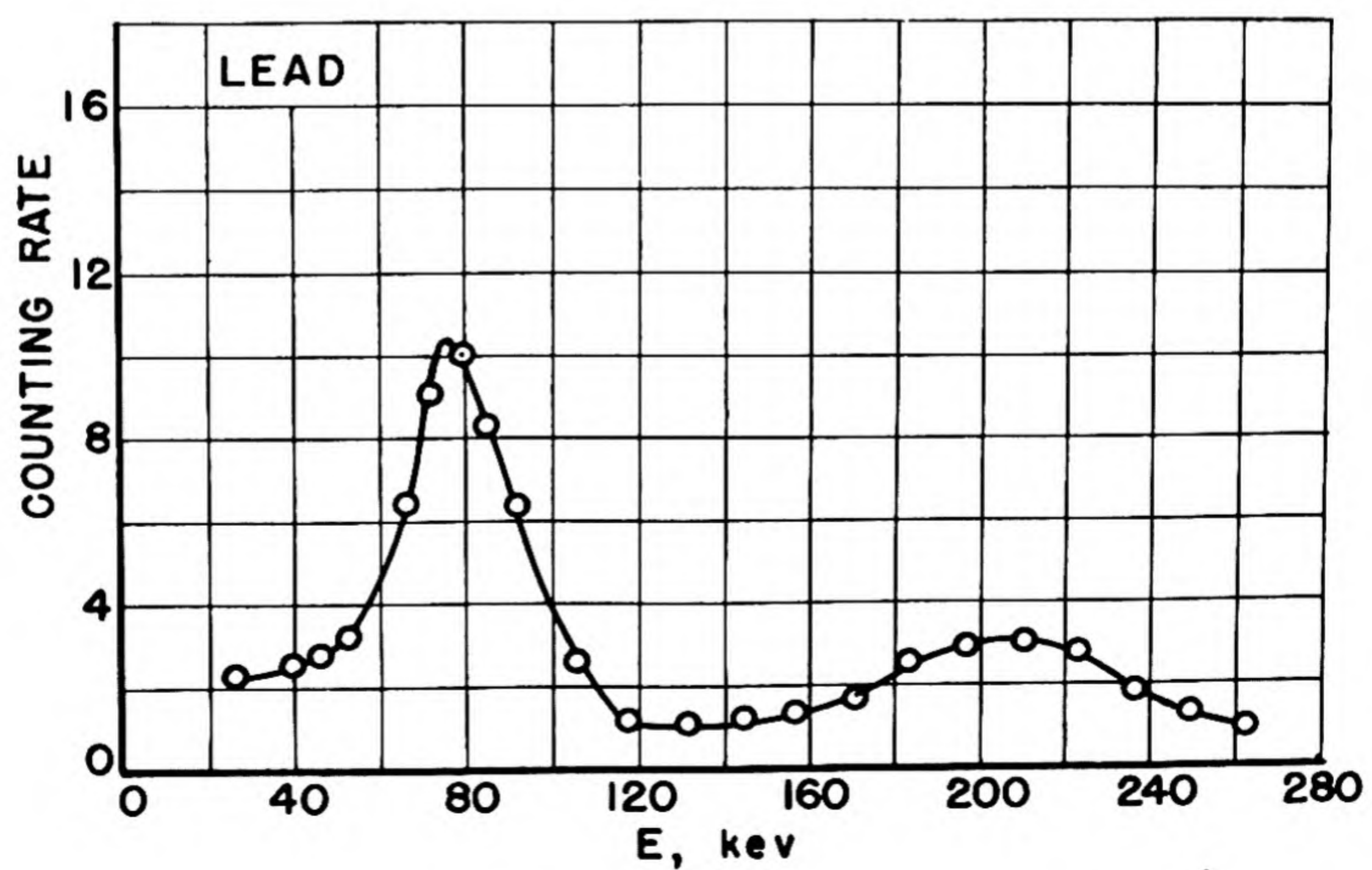


Fig. 2.3.9— Spectrum of Gammas Backscattered from Lead.

REFERENCES

1. U. Fano, Principles of Radiological Physics, Nat. Bu. Standards, NBS Report-1002, May 1951, 231 pp.
2. F. K. Richtmyer and E. H. Kennard, Introduction to Modern Physics, McGraw-Hill Book Co., Inc., New York, 1947, pp 501-530.
3. F. Rasetti, Elements of Nuclear Physics, Prentice-Hall, Inc., New York, 1948, pp 76-98.
4. A. T. Nelms, Graphs of the Compton Energy-angle Relationship and the Klein-Nishina Formula from 10 kev to 500 mev, Nat. Bu. Standards, to be published.
5. B. Rossi, High-energy Particles, Prentice-Hall, Inc., New York, 1952.
6. G. R. White, X-ray Attenuation Coefficients from 10 to 100 mev, Nat. Bu. Standards, NBS Report-1003, May 13, 1952, 93 pp.
7. E. H. S. Burhop, Auger Effect and Other Radiationless Transitions, Cambridge Monographs on Physics, Cambridge Press, 1952.
8. C. M. Davisson and R. D. Evans, Gamma-ray Absorption Coefficients, Rev. Mod. Phys. 24, 1952, p 79.
9. L. V. Spencer and C. Wolff, Penetration and Diffusion of Hard X-rays: Polarization Effects, Phys. Rev., to be published.
10. W. R. Faust and M. H. Johnson, Phys. Rev. 75, 1949, p 467.
11. P. R. Karr and J. C. Lamkin, Phys. Rev. 76, 1949, p 1843.
12. L. V. Spencer and F. A. Jenkins, Phys. Rev. 76, 1949, p 1885.
13. U. Fano, Penetration of K and Gamma Rays to Extremely Great Depths, Nat. Bu. Standards, Jour. Res. Nat. Bu. Standards, to be published.
14. Ibid, Sections 2f and B.
15. L. V. Spencer, Phys. Rev. 88, 1952, p 793.
16. L. V. Spencer and U. Fano, Penetration and Diffusion of X-rays; Calculation of Spatial Distributions by Polynomial Expansion, Jour. Res. Nat. Bu. Standards 46, 1951, p 446.
17. G. R. White, Phys. Rev. 80, 1950, p 154.
18. E. Hayward, Phys. Rev. 86, 1952, p 493.
19. J. O. Elliot et al, Phys. Rev. 85, 1952, p 1048.
20. G. H. Peebles, Phys. Rev. 83, 1951, p 237.
21. G. H. Peebles and M. S. Plesset, Phys. Rev. 81, 1951, p 430.
22. L. V. Spencer and U. Fano, Phys. Rev. 81, 1951, p 464.
23. L. V. Spencer and F. A. Stinson, Phys. Rev. 85, 1952, p 662.
24. M. J. Berger and J. Doggett, Nat. Bu. Standards Rep. No. 2224.
25. H. Goldstein, J. E. Wilkins, Jr., and L. V. Spencer, Phys. Rev., in press.
26. O. Glasser, E. H. Quimby, L. S. Taylor, and J. L. Weatherwax, Physical Foundations of Radiology, Haeber, New York, 1944.
27. W. V. Mayneord and L. F. Lamerton, Atlas of X-ray Dose Distribution, Royal Cancer Hospital, London.
28. Brit. Jour. Radiology 25, 1952, p 88.
29. G. D. Adams et al, Amer. Jour. Roentgen 60, 1948, p 153.
30. E. D. Charleton and H. E. Breed, Amer. Jour. Roentgen 60, 1948, p 158.
31. H. O. Wyckoff and L. S. Taylor, X-ray Protection Design, Nat. Bu. Standards Handbook 50, May 9, 1952, 36 pp.
32. H. O. Wyckoff and C. B. Braestrup, X-ray and Radium Protection, Charles C. Thomas, Springfield, Ill., to be published.
33. H. O. Wyckoff and C. B. Braestrup, Radiology 51, 1948, p 840.
34. H. O. Wyckoff, R. J. Kennedy, and W. R. Bradford, Nucleonics 3, 1948, p 62.
35. F. S. Kirm et al, in preparation, NBS-2125.
36. E. Hayward and J. Hubbell, Nat. Bu. Standards Rep. No. 2264.
37. R. J. Kennedy, F. S. Kirm, and H. O. Wyckoff, to be published.
38. G. J. Hine, to be published.
39. C. W. Wilson and B. J. Perry, Brit. Jour. Radiology 25, 1952, p 210.
40. E. S. Jetter and H. Blatz, Nucleonics 10, 1952, p 43.
41. P. R. Bell, J. E. Richardson, and R. L. Heath, ORNL-1365.
42. M. A. Van Dilla and G. J. Hine, Nucleonics 10, 1952, p 54.

SELECTED READING LIST

- X-RAY ATTENUATION COEFFICIENTS FROM 10 TO 100 MEV, Nat. Bu. Standards, G. R. White, NBS Report-1003, May 13, 1952, 93 pp.
- PRINCIPLES OF RADIOLOGICAL PHYSICS, Nat. Bu. Standards, U. Fano, NBS Report-1002, May, 1951, 231 pp. (to be published as a contribution to Biological Effect of Radiations, edited by A. Hollaender, McGraw-Hill, New York).
- GAMMA-RAY ABSORPTION COEFFICIENTS, C. M. Davisson and R. D. Evans, Rev. Mod. Phys. 24, 1952, p 79.
- GRAPHS OF THE COMPTON ENERGY-ANGLE RELATIONSHIP AND THE KLEIN-NISHINA FORMULA FROM 10 KEV TO 500 MEV, Nat. Bu. Standards, A. T. Nelms (to be published as a NBS Circular).
- SOME APPLICATIONS OF NUCLEAR PHYSICS TO MEDICINE, W. V. Mayneord, Brit. Jour. Radiology, Supplement 2, 1952.
- DETERMINATION OF THE ENERGY OF BETA PARTICLES AND PHOTONS BY ABSORPTION, L. E. Glendenin, Nucleonics, 2, No. 1, 1948, p 12.

X-RAYS IN THEORY AND EXPERIMENT, A. H. Compton and S. K. Allison, Van Nostrand, N. Y., 1948, Chaps. III and VII.

THE QUANTUM THEORY OF RADIATION, W. Heitler, Oxford, London, 2nd edition, 1944.

STATUS REPORT ON CALCULATIONS OF GAMMA RAY PENETRATION, Nuclear Development Associates, R. Aronson and H. Goldstein, NDA-15C-1, Nov. 6, 1952, 31 pp.

PENETRATION OF X AND GAMMA RAYS TO EXTREMELY GREAT DEPTHS, Nat. Bu. Standards, U. Fano (to be published in Jour. Res. Nat. Bu. Standards).

PENETRATION AND DIFFUSION OF X-RAYS. CALCULATION OF SPATIAL DISTRIBUTIONS BY POLYNOMIAL EXPANSION, Nat. Bu. Standards, L. V. Spencer and U. Fano, Jour. Res. Nat. Bu. Standards 46, 1951, p 446.

X-RAY PROTECTION DESIGN, Nat. Bu. Standards, H. O. Wyckoff and L. S. Taylor, Nat. Bu. Standards Handbook 50, May 9, 1952, 36 pp.

X-RAY AND RADIUM PROTECTION, H. O. Wyckoff and C. B. Braestrup (to be published by Charles C. Thomas, Springfield, Illinois).

CHAPTER 2.4

Neutron Attenuation

A. Simon

INTERACTION PROCESSES*

In passing through matter, a neutron will lose energy or be removed only by collisions with nuclei. If the total kinetic energy is conserved in collision with nucleus X , the reaction may be written as $X(n,n)X$ and is called elastic scattering. However, if the re-emitted neutron leaves the target nucleus in an excited state X' , the process is called inelastic scattering and may be written $X(n,n)X'$. Finally, the neutron may induce a nuclear reaction which leads to a different residual nucleus, Y , and new end products. If the end product is a capture gamma ray, the reaction $X(n,\gamma)Y$ is called radiative absorption, and if a particle (or particles) emerges, a particle reaction [$X(n,p)Y$, $X(n,\alpha)Z$, etc.] has occurred.

A table of neutron cross sections has been prepared by the AEC Cross Sections Committee and issued as AECU-2040. The data listed are for total cross sections (the sum of elastic scattering and reaction processes).

ABSORPTION $X(n,\gamma)Y$

For low-energy neutrons (less than about 1 kev), the only reactions that occur with appreciable cross section in nuclear collisions are elastic scattering and radiative absorption. Exceptions to this are some particle reactions in very light nuclei and fission in the very heavy nuclei. Elastic scattering serves only to alter the direction and degrade the energy of the neutrons. Ultimately, except for the cases just mentioned, the neutrons are captured with the emission of one or more gamma rays.

Upon capturing a slow neutron, the resultant compound nucleus has an excitation approximately equal to the binding energy of the neutron (~ 8 mev). The nucleus may release this energy with the emission of a single gamma ray and go to its ground state. However, if the nucleus has some intermediate energy levels between 8 mev and its ground state, it may instead emit several lower-energy gamma rays in cascade while going to the lowest state. In light nuclei or in the so-called "magic" nuclei, the average level spacing is large, and gamma transitions are often directly to the ground state. Table 2.1.7 summarizes the current capture gamma-ray data.

The existence of capture gamma rays greatly complicates the shielding problem since it is no longer sufficient merely to slow down and capture the neutrons. Owing to the (n,γ) reaction, these neutrons now give rise to new sources of energetic gamma rays at the point

*See also Section 1 this volume.

of capture. One means of suppressing these capture gamma rays is to include small quantities of a material, such as boron, which has a very high cross section for thermal neutron capture via an (n, α) reaction (see "Particle Reactions $X(n, p)Y$ and $X(n, \alpha)Z$," below). It should be noted that there is another source of secondary gamma radiation. These are gamma rays that may accompany inelastic neutron scattering (see "Inelastic Scattering $X(n, n)X'$," below). At higher energies of the order of 1 mev, elastic and inelastic scattering and particle reactions become dominant.

ELASTIC SCATTERING $X(n, n)X$

Elastic neutron scattering may occur in two ways: (1) By actual formation of a compound nucleus followed by re-emission of the neutron leaving the nucleus in its ground state. The cross section for this type of scattering shows the usual resonance structure at neutron energies below about 10 mev. (2) By so-called "potential" scattering in which the neutron does not appreciably penetrate the nuclear surface. The cross section for this process shows no resonance structure and decreases monotonically with increasing neutron energy. It should be clearly noted that the "resonance" elastic scattering and the "potential" scattering contributions are coherent. Hence, the resultant cross section is not simply the sum of the two.

For low-energy neutrons (less than about 1 mev), the angular distribution of scattering is isotropic in the center-of-mass system. As the energy increases, asymmetries appear. (The exception to this is scattering in hydrogen where spherical symmetry is observed up to 13 mev.) The angular distribution owing to the "resonance" elastic scattering is characteristic of the spins of the levels of the compound nucleus involved and is more or less isotropic. The "potential" scattering shows a strong forward peak (owing to shadow scattering or diffraction around the nucleus) which becomes more pronounced with increasing energy.

At energies of a few mev, the elastic scattering often approaches the conditions appropriate to the continuum approximation (see Chapter 1.2). That is, the compound nucleus, once formed, has so many different available modes of breakup that "resonance" elastic scattering occurs with essentially zero probability. In this case, the elastic scattering is entirely "potential," and a strong forward peak is seen. The elastic scattering cross section, then, approaches the limit of πR^2 (where R is the nuclear radius) for high energies while the total cross section approaches the limit $2\pi R^2$. Experimental verification of the shadow peak has been demonstrated by Journey et al.¹

Owing to the fact that total kinetic energy is conserved in elastic scattering, it is possible to write a simple relation connecting neutron scattering-angle and energy (this is given in Chapter 1.2).

INELASTIC SCATTERING $X(n, n)X'$

Inelastic scattering is the result of the decay of the compound nucleus to an excited state of the target nucleus. The process is not energetically possible until the incident neutron has enough energy to raise the target nucleus to its first excited state. As a result, thresholds for this process will be generally higher in both the light and magic nuclei where level spacings are larger. Little experimental information is available on inelastic scattering. Cross sections are available for 2.5-mev neutrons for several light nuclei^{2,3} as well as for 15-mev neutrons.^{4,5,6} A compilation of inelastic scattering cross sections is being made by the AEC Cross Sections Committee.

In most cases, the excess energy of the residual nucleus is removed by the emission of one or more gamma rays. Some data on inelastic gamma rays are available.¹⁻⁶

¹References appear at end of chapter.

Inelastic scattering can be useful in shields since this process will degrade neutrons to an energy below the inelastic threshold. However, light materials must still be used to further degrade the neutrons, and in addition, the secondary inelastic gamma rays may constitute a problem.

PARTICLE REACTIONS $X(n,p)Y$ AND $X(n,\alpha)Z$

A part of the neutron cross section above about 1 mev will be made up of various particle reactions. Below this energy, these reactions are inhibited either by the energetics of the process or by the necessity of barrier penetration by the charged particles which are the reaction products.

Of particular interest in shielding are some light-particle reactions which occur with thermal neutrons. These reactions can be used to avoid gamma rays and are listed in Table 2.1.6.

HYDROGEN CROSS SECTION

The neutron-proton scattering cross section is isotropic up to 13 mev and has been put in a convenient form by several authors. From the work of Blatt and Jackson,⁷ the cross section σ can be written as:

$$\sigma = \frac{3}{4} \sigma_t + \frac{1}{4} \sigma_s$$

where:

$$\sigma_t = \frac{4\pi}{k^2} \sin^2 \delta_t$$

$$\sigma_s = \frac{4\pi}{k^2} \sin^2 \delta_s$$

$$k \cot \delta_t = -\frac{1}{a_t} + b_t k^2$$

$$k \cot \delta_s = -\frac{1}{a_s} + b_s k^2$$

k being the neutron wave number, and:

$$k^2 = 1.21 \times 10^{24} E \text{ cm}^{-2}$$

if E is in mev. Adequate agreement with experimental results is obtained by taking:

$$a_t = 0.54 \times 10^{-12} \text{ cm} \quad a_s = -2.37 \times 10^{-12} \text{ cm}$$

$$b_t = 0.89 \times 10^{-13} \text{ cm} \quad b_s = 0.135 \times 10^{-12} \text{ cm}$$

A very convenient approximation to σ is given by:

$$\sigma = \frac{10.97}{E + 1.66}$$

where σ is in barns and E is in mev. Table 2.4.1 compares the exact and approximate ex-

pressions for hydrogen cross section. This expression is good from 3 mev to the maximum energies of interest. Of particular interest to shielding is the steep monotonic increase of the hydrogen cross section with decreasing neutron energy. This effect makes hydrogen a very desirable component of a shield as is discussed more fully in the next chapter.

Table 2.4.1 — Comparison of Exact and Approximate Hydrogen Cross Sections

E, mev	Hydrogen cross section (σ), barns	
	Exact	Approximate
0	20.3	6.6
2	2.91	3.00
4	1.94	1.94
6	1.43	1.43
8	1.14	1.14
10	0.94	0.94
12	.79	.80

EFFECTIVE REMOVAL CROSS SECTION

If neutron reactions in matter consisted solely of particle reactions and capture, the problem of neutron attenuation would be very simple. A neutron source of a given energy E_0 , in a plane geometry, would be attenuated according to a simple exponential law:

$$I \sim e^{-\Sigma(E_0)t} \quad (1)$$

where $\Sigma(E_0)$ is the macroscopic total neutron cross section and t is the thickness of material traversed. In an actual material, however, elastic and inelastic scattering is occurring, and as a result, there are large numbers of degraded neutrons being attenuated as well. The resultant observed attenuation is no longer purely exponential. Instead, it has the general form of an exponential, corresponding to the source attenuation, times a buildup factor. Thus:

$$I \sim B(t, E_0)e^{-\Sigma(E_0)t} \quad (2)$$

where B depends on the initial source energy, E_0 , as well as on the depth of penetration. At large distances of penetration, the buildup factor might be expected to be very large since only a small fraction of the neutrons will be uncollided. For example, a total thickness of 20 mean-free-paths is not uncommon in shielding work.

The situation is changed, however, if the shield is made up partly of hydrogenous material. It has been noted (Table 2.4.1) that the hydrogen cross section increases steeply with decreasing neutron energy. As a result, once a neutron suffers a hydrogen collision, it is essentially removed from the beam. This effect is caused by: (1) the large energy loss that usually occurs in such a collision, which makes subsequent collisions much more probable, and (2) altering of the direction of travel of the neutron, which usually increases the path length necessary for the neutron to move from the source to a detector, again increasing the probability of subsequent hydrogen collisions. It is this second effect which makes even an elastic collision with the heavy nuclei more effective since there is more probability of a subsequent hydrogen collision.

It is now clear from the previous description of elastic scattering that "resonance" elastic scattering, which tends to have a nearly isotropic angular distribution, is approximately equivalent to absorption. On the other hand, not all of the "potential" elastic scattering is equivalent to absorption since the neutrons in the large forward diffraction peak (shadow scattering) are essentially undeflected. It is to be expected, therefore, that the attenuation in a shield composed of heavy material as well as hydrogen will behave very much like an exponential with an "effective removal cross section"⁸ which is somewhat smaller than the total cross section. Qualitatively, this cross section, σ_r , is the sum of the actual reaction and capture cross sections, the inelastic cross section, and that part of the elastic scattering which is not in the "shadow" peak. Employing this definition, one obtains:

$$I \sim B(E_0, t) e^{-\Sigma_r t} \quad (3)$$

Now, the buildup factor is expected to remain reasonably small.

The precise value of the removal cross section could not be calculated from the qualitative definitions which have been given, even if the neutron cross sections were known. Instead, it is obtained experimentally by bulk shielding measurements at a facility such as the ORNL Lid Tank.^{9,10} Specific analyses are indicated later in this chapter. The use of the removal cross section in calculating the attenuation of neutron dose in a shield is discussed below under "Use of Removal Cross Section."

ATTENUATION OF FISSION NEUTRONS IN WATER (REMOVAL CROSS SECTION FOR OXYGEN)

The most convenient hydrogenous shielding material is water. Here the oxygen plays the role of a heavy element, and it should be possible to define a removal cross section. Figure 2.4.1 illustrates the results of neutron-attenuation measurements in the Bulk Shielding Facility and Lid Tank Facility at ORNL.^{9,10} All data are transformed to the case of a plane-collimated fission source of 1 watt/cm² strength. The solid curve shows the result of a calculation⁹ of the attenuation in water assuming no oxygen attenuation but properly taking into account the hydrogen cross section and buildup. The other two curves indicate attempted fits including an oxygen-removal cross section of 0.6 and 0.7 barns. It is seen that 0.7 barns gives the best fit to the BSF data. This disagreed somewhat with a determination based on thermal-neutron attenuation in the Lid Tank⁸ which gave $\sigma_r = 0.91$ barns. The uncertainty in the oxygen measurement is a result of the particular geometry of the experiment. An ideal way to measure a removal cross section of solids is to insert a slab of the material to be tested into the water of the Lid Tank. The resulting attenuation curve at long distances behind this slab is then compared with the same curve for pure water, and a removal cross section is easily determined. This procedure was used for iron and lead. Oxygen, however, is distributed throughout the medium, and the entire water curve must be fitted by an exponential times the hydrogen attenuation. The uncertainty in this fitting leads to the uncertainty in the oxygen removal cross section.

ATTENUATION IN LEAD

Measurements have been made in the ORNL Lid Tank of the attenuation of neutrons in water behind a series of alternating layers of Pb and H₂O.¹¹ Thermal measurements were made at distances varying from 90 to 150 cm from the source plate and for a varying number of lead slabs. These data were analyzed by Podgor,¹² and a removal cross section of 3.4 barns was found for lead. This agrees very well with an earlier determination by Albert and Welton.⁸

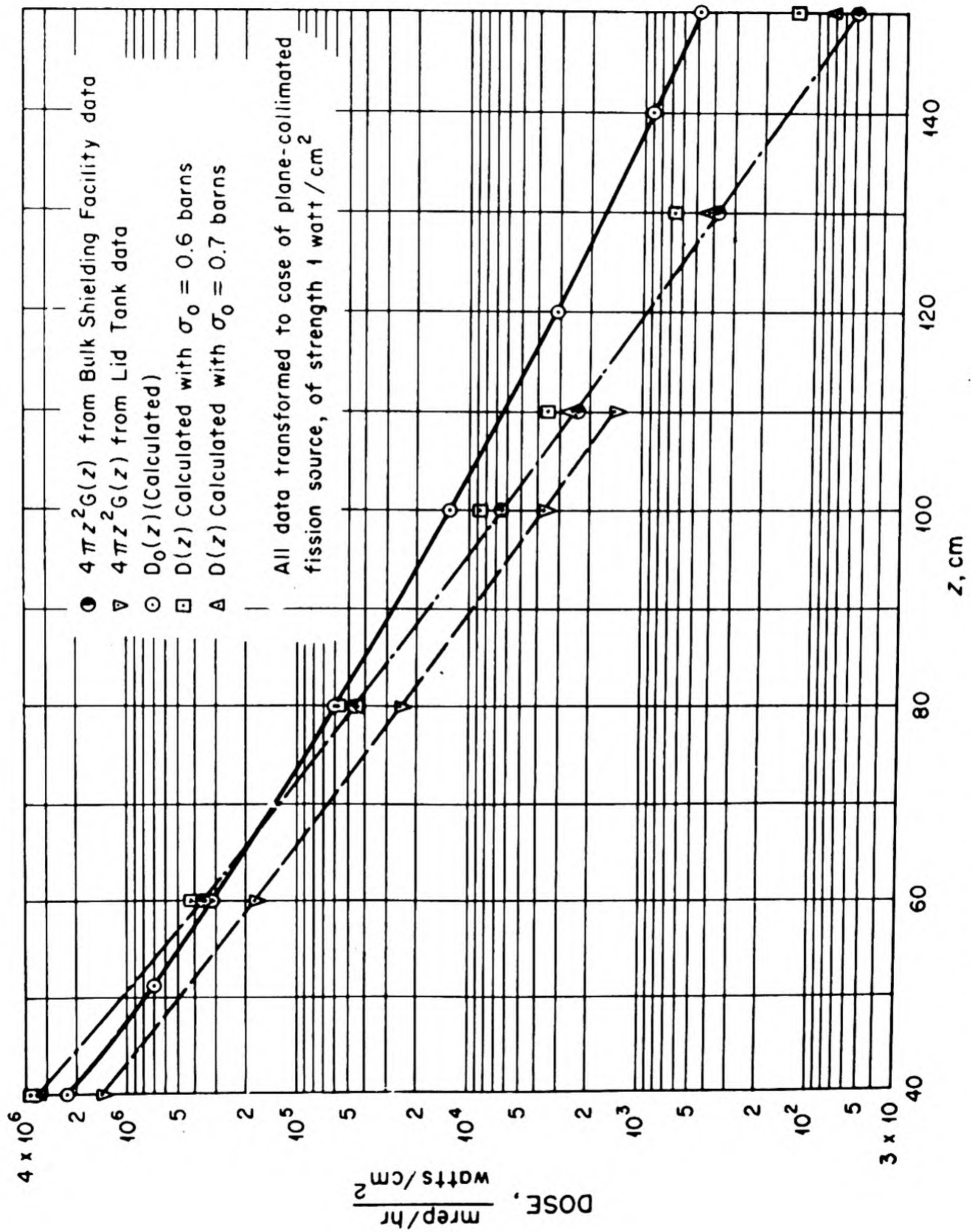


Fig. 2.4.1 — Comparison of Neutron-dose Calculations with Experimental Values for a Water Shield. Submitted by Oak Ridge National Laboratory, Nov. 7, 1952.

ATTENUATION IN IRON

Lid Tank measurements of neutron attenuation in borated water behind a series of iron slabs has been reported.¹³ Analysis of these data¹² yields a removal cross section of 2.0 barns for iron. This also in agreement with an earlier determination.⁸

USE OF REMOVAL CROSS SECTION

A number of removal cross sections are tabulated in Table 2.4.2. The results for Pb and Fe are probably good for the listed significant figures.

The attenuation for a mixture of a heavy material and water is now simply:

$$I = I_0 e^{-\Sigma_r t_h} D(t_w)$$

where:

I_0 = effective source strength (taken to be a plane-collimated source)

Σ_r = removal cross section of heavy materials

t_h = total thickness of heavy materials

t_w = total thickness of water

$D(t_w)$ = attenuation in water taken from the experimental curves in Fig. 2.4.1

Table 2.4.2 — Removal Cross Sections

Substance	σ_r , barns/atom
Al	1.2
C	0.84
Cu	2.0
Fe	2.0
Pb	3.4

The use of these removal cross sections, together with the measured water attenuation (Fig. 2.4.1), in calculating the attenuation of neutron dose in a shield is valid as long as large thicknesses of heavy material do not occur. Large thicknesses of heavy material (i.e., with no interposition of hydrogenous material) will allow streaming-through of neutrons in the energy region below about 1 mev because heavy materials attenuate neutrons by inelastic scattering only down to the threshold for this process (around 1 mev).

Below this energy only elastic scattering occurs, and this effect is very inefficient. As a result, the attenuation of dose will be much smaller than the calculated value. The fast neutron flux, of course, is still correctly accounted for.

ATTENUATION IN CONCRETE

Experiments on the neutron attenuation of ordinary concretes have been made at the "core hole" shielding facility^{9,10} at Oak Ridge. The results of these experiments have been summarized.¹⁶ Of particular interest in shielding are Portland concrete, boron cement, Brookhaven concrete, and W-1 concrete. Portland concrete was composed of four parts Tennessee limestone gravel, two parts river sand, and one part Portland cement. Boron

cement consists of equal weights of MgO and colemanite, gauged with saturated MgCl_2 solution. Brookhaven and W-1 concretes are mixtures of Portland cement and iron aggregate. Barytes concrete, a mixture of BaSO_4 aggregate and Portland cement, is also of great use in shielding today.

Table 2.4.3 lists the approximate atomic compositions of the various concretes. The water content, which is the most variable quantity in concrete mixes, is that found in the cured state. The fast-neutron attenuation lengths observed in the various shields are summarized in Table 2.4.4. An extensive bibliography of concrete shielding literature may be found in a recent Hanford report.¹⁸

Table 2.4.3 — Approximate Atomic Composition of the Various Concretes and Cements

Material	Elemental components, atoms/cc or moles/liter													
	Fe	H	B	O	Mg	Cl	Ca	Ba	Si	Al	Mn	S	C	Total
Portland concrete	0.13	4.8	...	71.8	0.2	...	14.5	...	15.6	0.44	...	0.06	10.8	118.3
Boron cement	...	79.1	7.98	68.2	16.42	6.93	2.66	181.3
Brookhaven concrete	54.7	21.1	...	47.7	0.35	...	6.45	...	2.10	0.79	1.22	0.11	...	134.5
W-1 concrete	40.5	20.1	3.28	38.8	.62	...	12.15	...	3.65	1.36	0.21	.18	...	120.8
Barytes concrete	0.11	5.17	...	63.5	.2	...	3.4	11.9	4.1	0.4	...	12.0	...	100.8

Table 2.4.4 — Measured Relaxation Lengths
in Various Concretes and Cements

Shield	Density	Relaxation length, cm
Portland concrete	2.3	11.1
Boron cement	2.0	7.6
Brookhaven concrete	4.3	6.3
W-1 concrete	3.6	6.6
Barytes concrete	3.5	8.0

REFERENCES

1. E. T. Journey et al, Inelastic Collision and Transport Cross Sections for Some Light Elements, Los Alamos Scientific Lab., LA-1339, Dec., 1951, 14 pp.
2. M. A. Grace, L. E. Beghian, G. Preston, and H. Halban, The Inelastic Scattering of Fast Neutrons, Phys. Rev. 82, 1951, p 969.
3. H. H. Barschall et al, Measurement of Transport and Inelastic Scattering Cross Sections for Fast Neutrons, II. Experimental Results, Phys. Rev. 72, 1947, p 881.
4. P. H. Stelson and C. Goodman, The Inelastic Scattering of 15-mev Neutrons By Lead, Iron, and Aluminum, Phys. Rev. 82, 1951, p 69.
5. B. G. Whitmore and G. E. Dennis, The Inelastic Scattering of Fast Neutrons in Lead and Bismuth, Phys. Rev. 84, 1951, p 296.
6. P. H. Stelson and W. M. Preston, The Inelastic Scattering of Fast Neutrons from Iron, Phys. Rev. 86, 1952, p 132.
7. J. M. Blatt and J. D. Jackson, On the Interpretation of Neutron-Proton Scattering Data by the Schwinger Variational Method, Phys. Rev. 76, 1949, p 18.
8. R. D. Albert and T. A. Welton, WAPD-15, Nov. 30, 1950, 39 pp (classified).
9. T. A. Welton and E. P. Blizard, TID-2002, Aug. 1952, p 73 (classified).
10. E. P. Blizard, Part II, ORNL-51-10-70 Revised, Mar. 7, 1952, 42 pp (classified).
11. ORNL-858, Nov. 29, 1950, p 19 (classified).
12. S. Podgor, ORNL-895, Jan. 23, 1951, 16 pp (classified).
13. ORNL-919, Feb. 26, 1951, p 105 (classified).
14. Deleted.
15. Deleted.
16. H. P. Sleeper, Jr., ORNL-436, Dec. 21, 1949, 48 pp (classified).
17. Deleted.
18. T. A. Linxweiler, HW-24071, April 9, 1952, 153 pp (classified).

CHAPTER 2.5

Geometry

E. P. Blizzard

Most shields are designed by comparison with others which have been measured. Since the geometries differ from one situation to another, transformations are required which will predict the radiation to be expected in one situation on the basis of an observation in another. A discussion of these transformations is based on the following fundamentals.

Flux, probably the most basic type of measurement, is variously described as "particle density times average speed," or "rate of events divided by the macroscopic cross section." It is probably described most graphically in terms of the radiation incident on a small totally absorbing sphere. For this non-directional detector, the flux is the incident radiation divided by its projected area. In case the detector is not totally absorbing, the reading will be somewhat less and can therefore be associated with a smaller effective cross-sectional area. This is the case with nuclear cross sections, the areas being so chosen that they will correctly describe the rate of occurrence of a particular event (e.g., absorption).

Biological dose is usually assumed to be proportional to the flux, and this will be exactly true if no self-shielding occurs in the receptor (e.g., man). Since it is conservative to assume no receptor self-shielding, this is usually done. The dose with no self-shielding is often referred to as the "milligoat" reading, this being the dose to be expected in a very small sphere of flesh.

Current is simply the radiation passing through a surface per unit surface area. This radiation is recorded on a flat detector oriented normal to some preferred direction, so that in effect the response of the detector is proportional to the cosine of the direction of arrival with the preferred direction. Current is thus a vector quantity as opposed to flux which is a scalar.

The difference between flux and current is illustrated by the response of foil detectors. Thin foils, for which self-absorption is negligible, appear to be an array of widely spaced spheres (nuclei) and hence record the flux. On the other hand a thick foil, being essentially black to the radiation, records current normal to the foil.

In shielding, the flux is of most interest, since this is usually more conservative as an estimate of the dose. Since "flux" has been used in other fields in the same connotation as "current," the term "dose" has been adopted for shielding work and unless otherwise specified is assumed to be the dose with no receptor self-shielding.

"Attenuation function" or "attenuation kernel" is defined in terms of the response of a detector to radiation from a nearby source. This function is therefore dependent on the medium, the source, the detector, and the distance between source and detector if flux is to be measured. If current is to be measured, an additional variable specifying direction is necessary.

For a dose detector a distance R from an isotropic source of unit strength, the reading would be:

$$D_{Pt}(R) = G(R) \quad (1)$$

This equation is then adequate to define the dose attenuation kernel $G(R)$. It is of course assumed throughout that dose will vary linearly with source strength. The applicability of Eq. (1) to actual cases should be carefully considered before the transformations discussed below are used; the following conditions in particular should be noted:

- (1) The detector and source(s) must be isotropic.
- (2) The medium must attenuate equally in all directions and in all regions.
- (3) Boundaries must be far removed or unimportant.

The first condition is easily met. The second often is not met, especially for the case of gamma rays in, for example, a laminated lead-water shield. The third condition is almost never met, but fortunately the boundaries usually have a constant effect so that the transformations are nevertheless not much affected.

TRANSFORMATIONS FOR UNSPECIFIED ATTENUATION FUNCTIONS

The first and most general class of transformations to be considered is that in which the attenuation function is totally unspecified. For this case, the attenuation function must be independent of angle, as indicated by Eq. (1).

POINT TO INFINITE PLANE

For an infinite plane of isotropic sources of unit strength per unit plane area embedded in an infinite medium, the dose to be expected at a distance z from the plane is:

$$D_{Pl}(z, \infty) = 2\pi \int_z^\infty G(R) R dR \quad (2)$$

This equation is useful when $G(R)$ is known, either from measurement or calculation. On the other hand, the measurement may have given the dose from the plane-distributed source, in which case the differentiated form of Eq. (2) is useful:

$$G(z) = -\frac{1}{2\pi z} \frac{d}{dz} D_{Pl}(z, \infty) \quad (3)$$

POINT TO PLANE DISK

In case the plane isotropic source of unit surface strength is limited to a disk of radius a , the dose at a point on the axis a distance z from the disk (see Fig. 2.5.1) is:

$$D_{Pl}(z, a) = 2\pi \int_z^{\sqrt{z^2 + a^2}} G(R) R dR \quad (4)$$

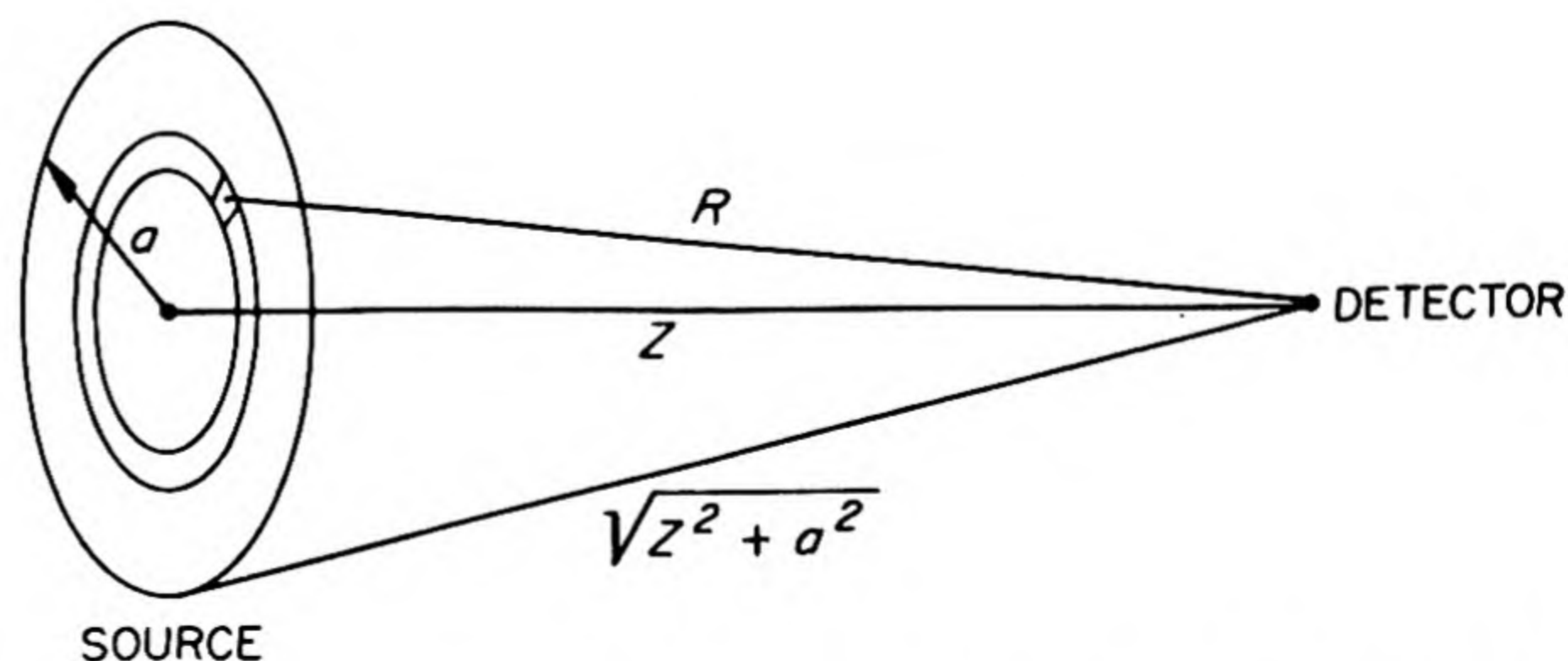


Fig. 2.5.1—Disk Source and Dose Detector. Submitted by Oak Ridge National Laboratory, Oct. 28, 1952.

PLANE DISK TO POINT

The inverse of the previous transformation is obtained by differentiating Eq. (4) with respect to z . This then leads¹ to the following series:

$$G(z) = \sum_{\nu=0}^{\infty} B(\sqrt{z^2 + \nu a^2}) \quad (5)$$

where:

$$B(z) = -\frac{1}{2\pi z} \frac{d}{dz} D_{Pl}(z, a)$$

The use of this transformation is illustrated in Fig. 2.5.2.

PLANE DISK TO INFINITE PLANE (HURWITZ TRANSFORMATION)

By quite similar manipulation,² the dose to be expected with an infinite plane source can be found in terms of measurements on the axis of a finite disk source. Both sources are assumed to have unit strength per unit area and to be isotropic:

$$D_{Pl}(z, \infty) = \sum_{\nu=0}^{\infty} D_{Pl}(\sqrt{z^2 + \nu a^2}, a) \quad (6)$$

Thus, the dose at a distance " z " away from an infinite plane source is just equal to the sum of readings on the axis of a disk of radius " a " taken at z , $\sqrt{z^2 + a^2}$, $\sqrt{z^2 + 2a^2}$, etc. In case " a " is large compared with the apparent attenuation length of the disk measurements, this will converge quickly, although not as quickly as the series represented by Eq. (5).

If the dose on the disk axis can be well represented in the region beyond some distance z_0 by:

$$D_{Pl}(z, a) = D_{Pl}(z_0, a) e^{-(z-z_0)/\lambda} \quad (7)$$

then the exact expression, Eq. (6), can be approximated for $z \simeq z_0$ by the inequality:

$$1 + \alpha > \frac{D_{Pl}(z, \infty)}{D_{Pl}(z, a)} \simeq \frac{1}{2} + \alpha \quad (8)$$

where:

$$\alpha = \frac{2\lambda^2}{a^2} \left(\frac{z}{\lambda} + 1 \right)$$

Note that in Eq. (8) the upper limit $(1/2 + \alpha)$ is a closer approximation to the true value of the ratio of doses. Furthermore, most experimental data vary from the condition expressed by Eq. (7) in such a way that the ratio in Eq. (8) is increased; that is, the left hand side of Eq. (7) becomes greater than the right at large values of $z - z_0$. Equation (8), therefore, may not give a genuine upper limit.

PLANE TO SPHERE

If an isotropic source of unit strength per unit area is spread on a spherical surface which is wholly within an attenuating medium, it is possible to predict the dose as a function of distance from this surface if the dose is known for the case of an infinite-plane

¹References appear at end of chapter.

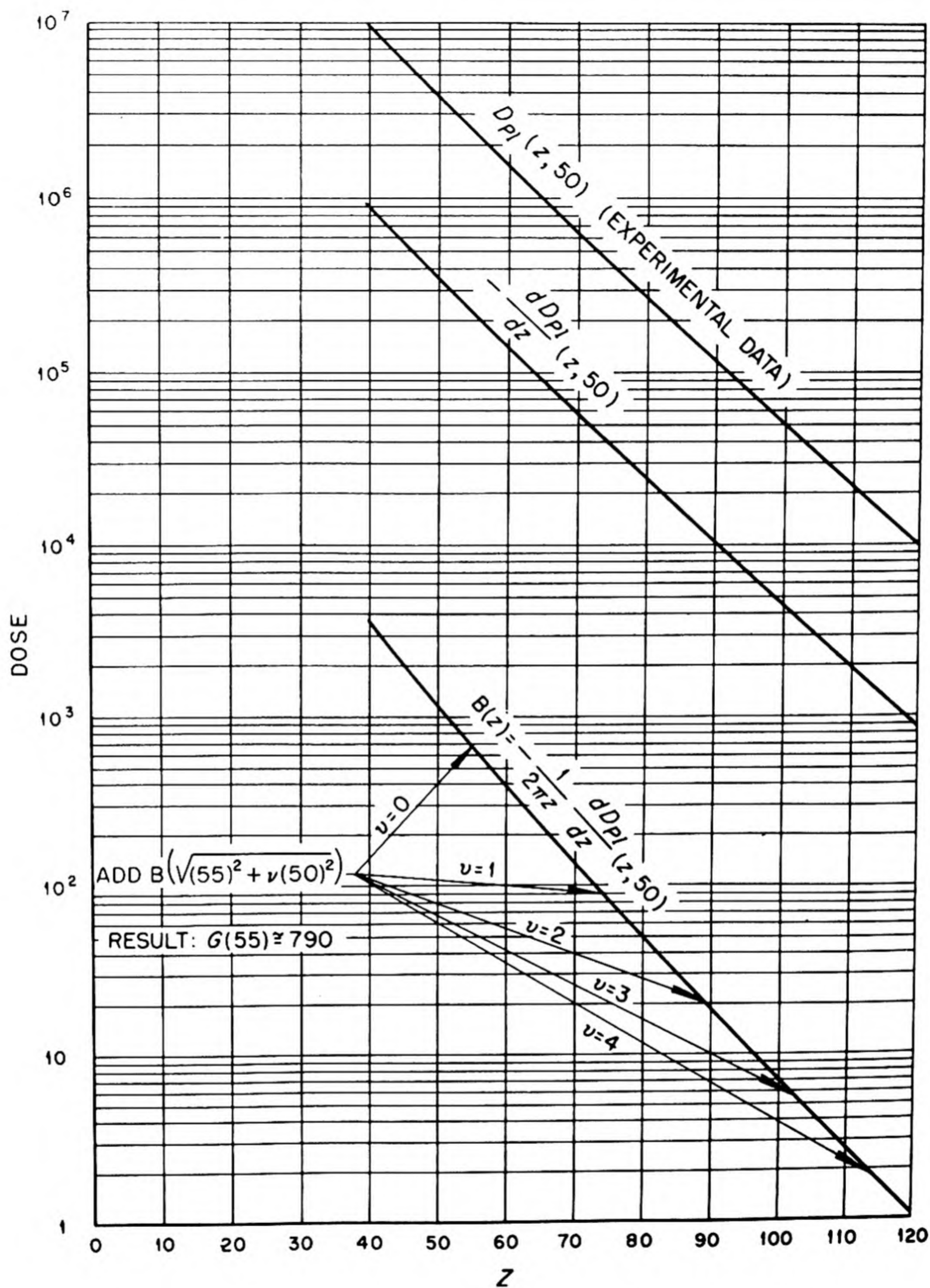


Fig. 2.5.2— Illustration of Plane Disk to Point Transformation. Submitted by Oak Ridge National Laboratory, Oct. 28, 1952.

isotropic source. Strictly, the material inside the sphere must be the same as that outside, and the source must be so thin as not to affect the attenuation. Actually, however, neither of these conditions need be very closely met, since most of the observed dose comes from radiation which travels more or less directly through the shield from the nearest source region. The dose at a distance r_0 from the center of the sphere whose radius is r ($r_0 > r$) is:

$$D_s(r_0, r) = \frac{r}{r_0} \left[D_{Pl}(r_0 - r, \infty) - D_{Pl}(r_0 + r, \infty) \right] \quad (9)$$

where the quantities in the brackets are the doses to be expected at distances of $r_0 - r$ and $r_0 + r$ from infinite-plane sources of the same surface source strength.

If the attenuation length for the plane data is sufficiently small, then the second term in the square brackets can be ignored:

$$D_s(r_0, r) \approx \frac{r}{r_0} D_{Pl}(r_0 - r, \infty) \quad (10)$$

when $\lambda \ll 2r$.

PLANE TO CYLINDER

There is no simple and general transformation for this case, but it can be shown that for most attenuation functions the following expression is approximately correct for the dose at a distance r from the axis of an infinitely long cylinder of radius r_0 with uniform isotropic surface source strength:

$$D_c(r_0, r) \approx \sqrt{\frac{r}{r_0}} D_{Pl}(r_0 - r, \infty) \quad (11)$$

Strictly, the material inside the cylinder should match that outside in attenuation, but in most applications, this will make little difference.

TRANSFORMATIONS FOR PARTIALLY SPECIFIED ATTENUATION FUNCTIONS

SOURCE ON A QUADRIC SURFACE

For the purposes of this derivation, the form of the attenuation function is unspecified for the distance z from the detector to the nearest source point. For other points of the source, the increased attenuation is assumed to be a pure exponential, that is:

$$G(R) \approx G(z) e^{-(R-z)/\lambda} \quad (12)$$

The geometry is shown in Fig. 2.5.3.

The detector is on the Z axis, a distance z from origin; the unit strength isotropic source is assumed to be spread uniformly on a quadric surface tangent to X, Y plane. The equation of the surface near the origin is:

$$z_1 \approx -\frac{1}{2} \left(\frac{(x_1)^2}{a} + \frac{(y_1)^2}{b} \right) \quad (13)$$

where z_1 = distance from source surface to X, Y plane; a = radius of curvature in Y, Z plane; and b = radius of curvature in X, Z plane. The dose at $(z, 0, 0)$ is then given by:

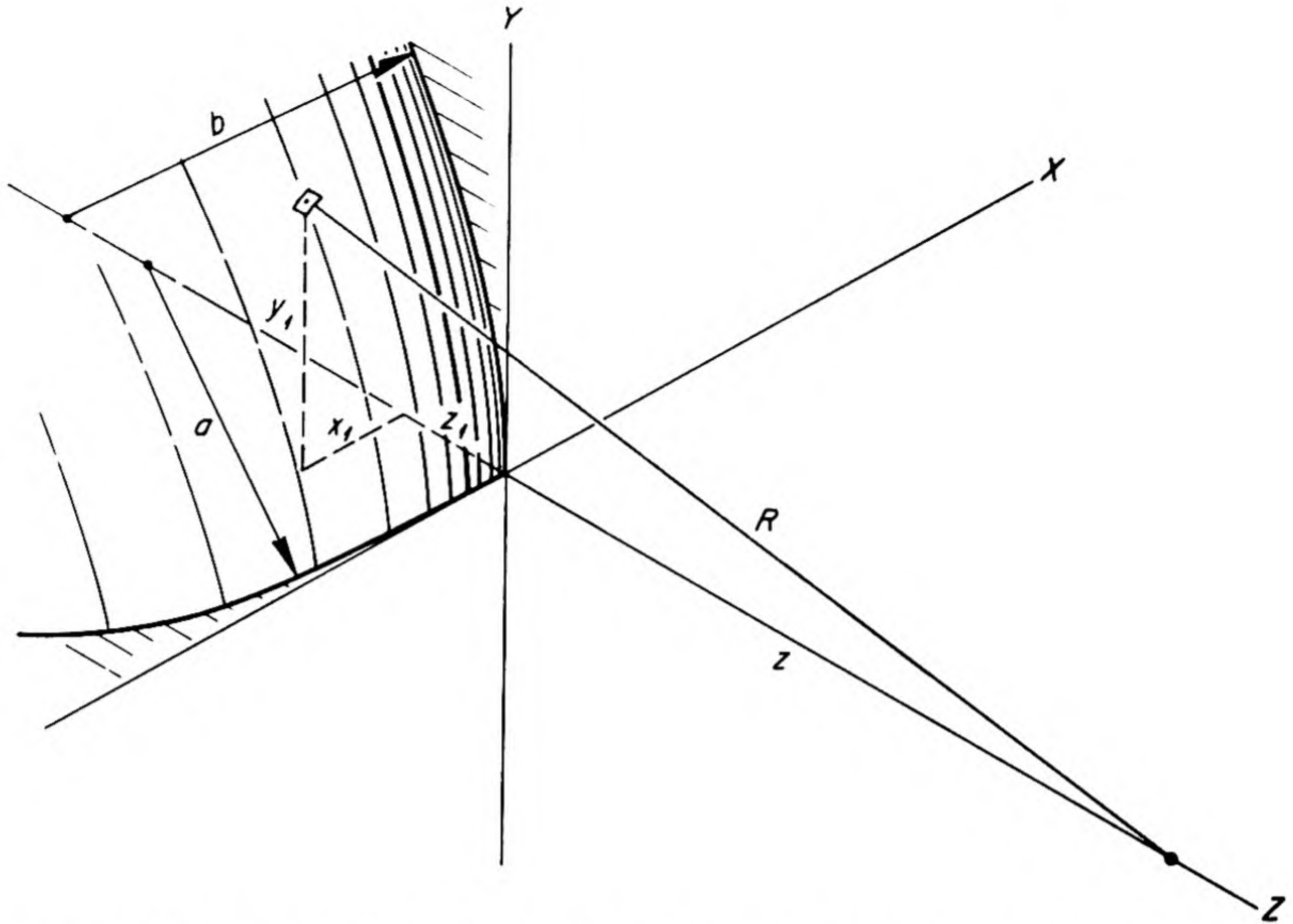


Fig. 2.5.3 — Geometry for Quadric Surface Source. Submitted by Oak Ridge National Laboratory, Oct. 29, 1952. Only one quadrant shown.

$$D_q(z, a, b) \approx 2\pi G(z) \left[\frac{1}{\left(\frac{1}{\lambda z} + \frac{1}{\lambda a}\right)^{1/2} \left(\frac{1}{\lambda z} + \frac{1}{\lambda b}\right)^{1/2}} + \frac{1}{2a^2 \left(\frac{1}{\lambda z} + \frac{1}{\lambda a}\right)^{3/2} \left(\frac{1}{\lambda z} + \frac{1}{\lambda b}\right)^{1/2}} + \frac{1}{2b^2 \left(\frac{1}{\lambda z} + \frac{1}{\lambda a}\right)^{1/2} \left(\frac{1}{\lambda z} + \frac{1}{\lambda b}\right)^{3/2}} \right] \quad (14)$$

For $a, b \gg \lambda$:

$$D_q(z, a, b) = 2\pi G(z) \left[\frac{1}{\left(\frac{1}{\lambda z} + \frac{1}{\lambda a}\right)^{1/2} \left(\frac{1}{\lambda z} + \frac{1}{\lambda b}\right)^{1/2}} \right]$$

For a derivation of this expression, see Welton and Blizzard.³

SPECIAL CASES

For a plane surface, $a, b \rightarrow \infty$, and:

$$D_{pl}(z, \infty) = 2\pi z \lambda G(z) \quad (15)$$

This is directly comparable to Eq. (3).

For a spherical surface, $a = b = r$, and for these, which are much larger than λ :

$$D(z, r) \cong 2\pi \lambda G(z) \frac{zr}{z + r} \quad (15a)$$

The same result can be found from combination of Eqs. (3) and (10).

SOURCE ON A PLANE SURFACE—THE EFFECTIVE SOURCE AREA

It has been pointed out by Tonks that it is possible to define an "effective source area," an "effective cone of radiation," and an "effective solid angle of radiation" for the case of a uniform isotropic source on a plane surface (see Fig. 2.5.4).

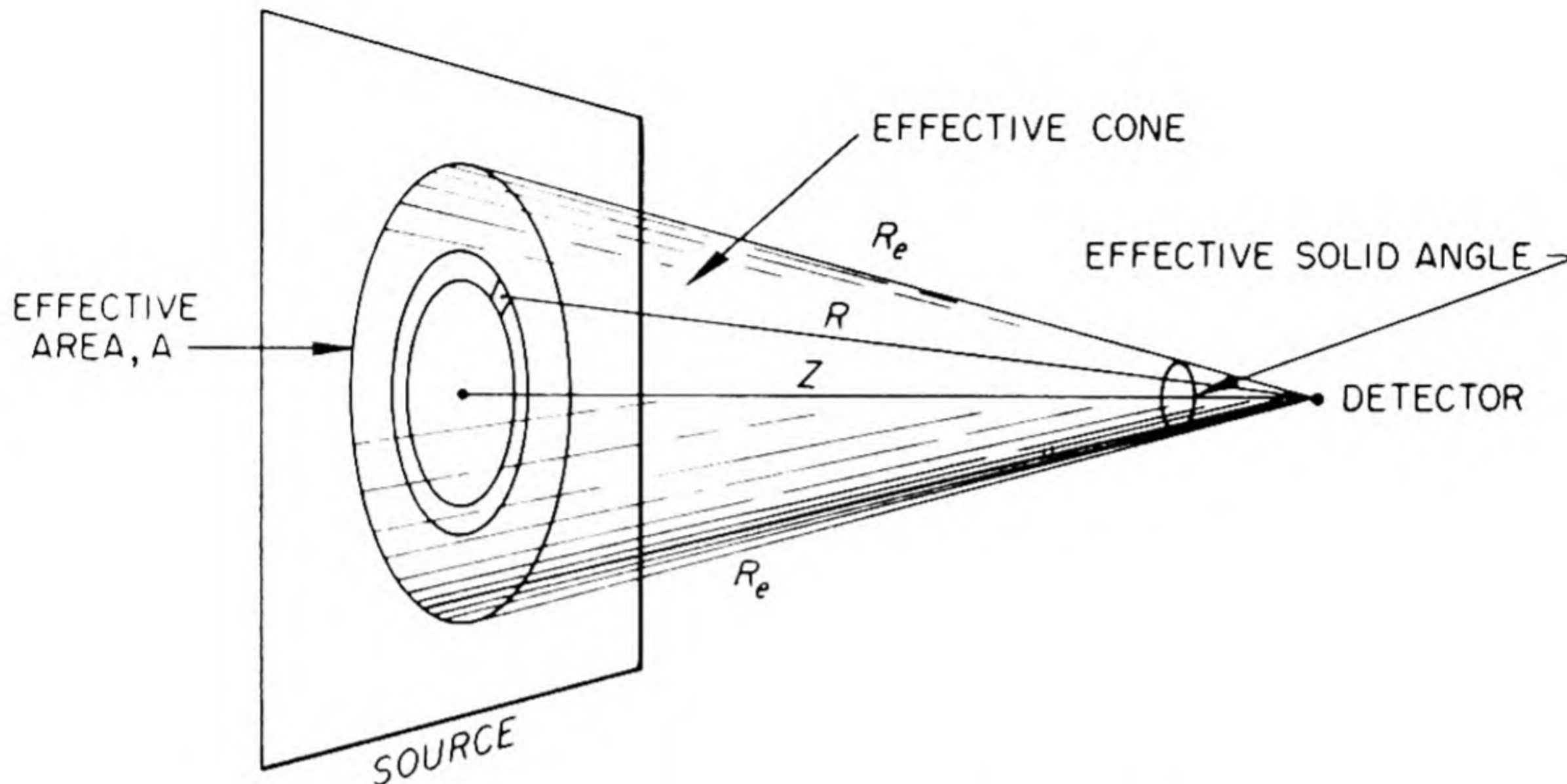


Fig. 2.5.4—Geometry of Effective Source Area. Submitted by Oak Ridge National Laboratory, Oct. 30, 1952. Cone of radiation, and solid angle of radiation.

The effective source area A is defined as that part of the plane source contained within a circle centered at the base of the perpendicular from detector to source of such size that:

$$D_{p1}(z, \infty) = A D_{pt}(z) \quad (16)$$

In other words, if all the sources on A were located at a point a distance z from the detector, the dose would just equal the dose from the original whole plane of sources.

Using the approximation characteristic of this section, Eq. (12), for substitution in Eq. (2), it is seen by simple integration that:

$$D_{p1}(z, \infty) = 2\pi(\lambda z + \lambda^2)G(z) \quad (17)$$

Or, in the light of Eqs. (1) and (16):

$$A = 2\pi(\lambda z + \lambda^2) \quad (18)$$

and the distance from the edge of the effective source to the detector is:

$$R_e = \sqrt{(z + \lambda)^2 + \lambda^2} \approx z + \lambda \quad \lambda \ll z \quad (19)$$

In other words, the effective source area is just that circle of source which is within a distance greater by one relaxation length than the nearest point. The effective cone of radiation is thus that cone defined by A and the detector. The effective solid angle is:

$$\Omega_e = 2\pi \left(\frac{R_e - z}{R_e} \right) \quad (20)$$

$$\approx 2\pi \frac{\lambda}{R_e} \quad \lambda \ll z \quad (20a)$$

The effective source area concept is often quite useful in estimating the intensity to be expected from unusual source shapes. Tonks' method consists simply in using the part of the actual source which lies within the effective source area as if it were the only source. Thus, if A is the source area which is within A , then the dose is taken to be:

$$D_{A_1}(z) = \frac{A_1}{A} D_{Pl}(z, \infty) = A_1 D_{Pt}(z) \quad (21)$$

This formula must of course be used with caution, paying attention to the possibility that other sources outside the effective source area might contribute significantly by virtue of a large source density. In the computation of the effects of variations in the shield, these can be expected to be most effective when they occur within the effective cone of radiation.

TRANSFORMATIONS FOR THE SIMPLE ATTENUATION FUNCTIONS

For many shielding calculations, a simple form is chosen for the basic attenuation function, and with this, the geometric manipulations then become more or less straightforward. The more common situations are illustrated below.

THE ATTENUATION FUNCTIONS, ONE REGION

The basic attenuation function is of course the simple exponential on which is superimposed the inverse-square-law attenuation. For this assumption, the dose at a distance R from a unit strength (one per unit time) source is simply:

$$G_1(R) = \frac{e^{-\mu R}}{4\pi R^2} \quad (22)$$

where μ is called the attenuation coefficient, a characteristic of the medium, of the source, and (in most cases) of the detector. This expression applies rigorously only to unscattered radiation. Allowance is made for scattered radiation by inclusion of a so-called "buildup factor," which is a function not only of source, medium, and detector, but also of the distance from the source. This is usually expressed as follows:

$$G(R) = \frac{B(\mu R)e^{-\mu R}}{4\pi R^2} \quad (23)$$

It is clear that Eq. (22) expresses a special case of Eq. (23), namely, that for which $B = 1$. This is referred to as a unitary buildup factor.

BUILDUP FACTORS

While a more complete discussion of the computation of a buildup factor is not given here, a simple approximation is described. For gamma-ray attenuation in which the Compton process is dominant for the source energy, a linear buildup factor gives a reasonable approximation for large attenuations of the total energy flux. Specifically, for thick shields:

$$B \approx \mu R \quad (24)$$

This approximation does not fit the situation for thin shields [note that for $\mu R < 1$, $G(R) < G_1(R)$]. As a consequence, for shields of intermediate thicknesses, the buildup factor is taken as a sum of unitary and linear buildup factors. Most generally:

$$B \approx 1 + k\mu R \quad (25)$$

where k is a constant best chosen to fit the situation. For the case of gamma rays of about 1 mev on lead, k is about unity. It has been demonstrated by Goldstein⁴ that it is possible to normalize the buildup factor to ensure a proper accounting of all the energy absorption. This would result in fixing k if Eq. (25) is chosen for the form of B .

Thus, if a source of unit strength of photons of energy E_0 is embedded in a material and the detector reads simply heat release, then the heating due to previously uncollided photons is:

$$H_0(R) = \frac{\tau(E_0) E_0 e^{-\mu(E_0)R}}{4\pi R^2} \quad (26)$$

where $\tau(E_0)$ is the energy absorption coefficient, referred to by Heitler⁵ as $\mu - \sigma_s$, and $\mu(E_0)$ is the total interaction coefficient. The buildup factor for heat generation is then defined by the following equation for the heat absorption from virgin as well as scattered flux:

$$H(R) = B(\mu R) H_0(R) \quad (27)$$

From the conservation of energy, the source must in equilibrium emit as much as is absorbed, i.e.:

$$E_0 = 4\pi \int_{R=0}^{\infty} R^2 H(R) dR$$

or:

$$\frac{1}{\tau(E_0)} = \int_{R=0}^{\infty} B(\mu R) e^{-\mu R} dR \quad (28)$$

The latter equation can thus be used to determine " k " for a variety of photon energies and materials, but it is necessary to caution that the method is not applicable to large shield thicknesses.

ATTENUATION FUNCTIONS, MANY REGIONS

For many regions, the problem becomes much more difficult, but a first estimate is obtained by simply extending the basic attenuation function on the basis of the ray lengths in the several regions:

$$G(R) = B(\mu_1 R_1 + \mu_2 R_2 + \mu_3 R_3 + \dots) \frac{e^{-(\mu_1 R_1 + \mu_2 R_2 + \dots)}}{4\pi R^2} \quad (29)$$

where μ_1, μ_2, μ_3 , etc., are the attenuation coefficients; R_1, R_2, R_3 , etc., are the ray lengths for the several media; and $R = R_1 + R_2 + R_3 + \dots$

DEFINITIONS FOR TABLES

In the tables of intensities (Tables 2.5.2 through 2.5.4) the following terms are used:

(1) Unit Sources:

- (a) Isotropic surface:* Emitting unit per second per square centimeter of surface, equally in all directions (both sides).
- (b) Cosine Surface:* Emitting $(\cos\theta)/4\pi$ per second per square centimeter of surface per steradian for $0 < \theta < \pi/2$, and emitting 0 for $\pi/2 < \theta < \pi$, where θ is the angle between the outward-drawn normal to the surface and the direction of emission.
- (c) Volume: Emitting unity per cubic centimeter per second isotropically from a region (herein referred to as region 1 and assigned an attenuation coefficient μ_1). A simple integration shows that this source in a plane-limited region is identical in radiation emitted with a cosine surface source on the plane emitting $(\cos\theta)/4\pi\mu_1$ per second per sterad per square centimeter of surface.
- (d) Filament: Non-self-absorbing straight-line source, emitting unity per centimeter per second isotropically.

(2) Detectors:

- (a) Non-directional (milligoat): Described earlier in this chapter.
- (b) Cosine: Response proportional to cosine of angle between preferred direction and direction of arrival of radiation. (As described in the preceding text, of these two detector types, the non-directional detector indicates microscopic dose, ionization in a non-absorbing region, etc., whereas the cosine detector indicates total current through a plane, leakage, the source available for production of secondary radiation such as capture gamma rays, the rate of arrival on a completely absorbing surface, etc.)

(3) Buildup Factors:

- (a) Unitary: $B(\mu R) = 1$ (no built-up radiation, as in a nonscattering medium).
- (b) Linear: $B(\mu r) = \mu_1 R_1 + \mu_2 R_2 + \dots$ (Combinations of these two can be had by linear addition, which is left to the reader).

(4) Distance:

- (a) z is always used as the distance from the detector to the nearest element of source, and the preferred direction is that of this ray.

(5) Exponential Integral Functions:† (Table 2.5.1 and Figs. 2.5.6, 2.5.7, and 2.5.8)

$$E_n(x) = \int_x^\infty \frac{e^{-p}}{p^n} dp \quad (30)$$

$$= \frac{e^{-x}}{x^n} - n E_{n+1}(x) \quad (31)$$

$$\approx \frac{e^{-x}}{x^n} (x \gg 1) \quad (31a)$$

(6) Intensity:

This term refers to the response of the detector, either nondirectional, in which case flux is meant, or cosine, in which case current is implied. The use of the term "flux" in the table is avoided in order to circumvent the ambiguity arising from its occasional

* Isotropic and cosine surface sources are chosen so that both radiate equally in the outward normal direction. This is illustrated in Fig. 2.5.5.

† Tabulated in "Tables of Sine, Cosine, and Exponential Integrals," prepared by the Federal Works Agency, Work Projects Administration, for the City of New York, A. N. Lowan, technical director, sponsored by the National Bureau of Standards, New York, 1940; also see tables of $-Ei(-x) = E_1(x)$ in E. Jahnke, "Jahnke-Emde Tafeln hoheren Funktionen," B. G. Teubner Co., Leipzig, 1948.

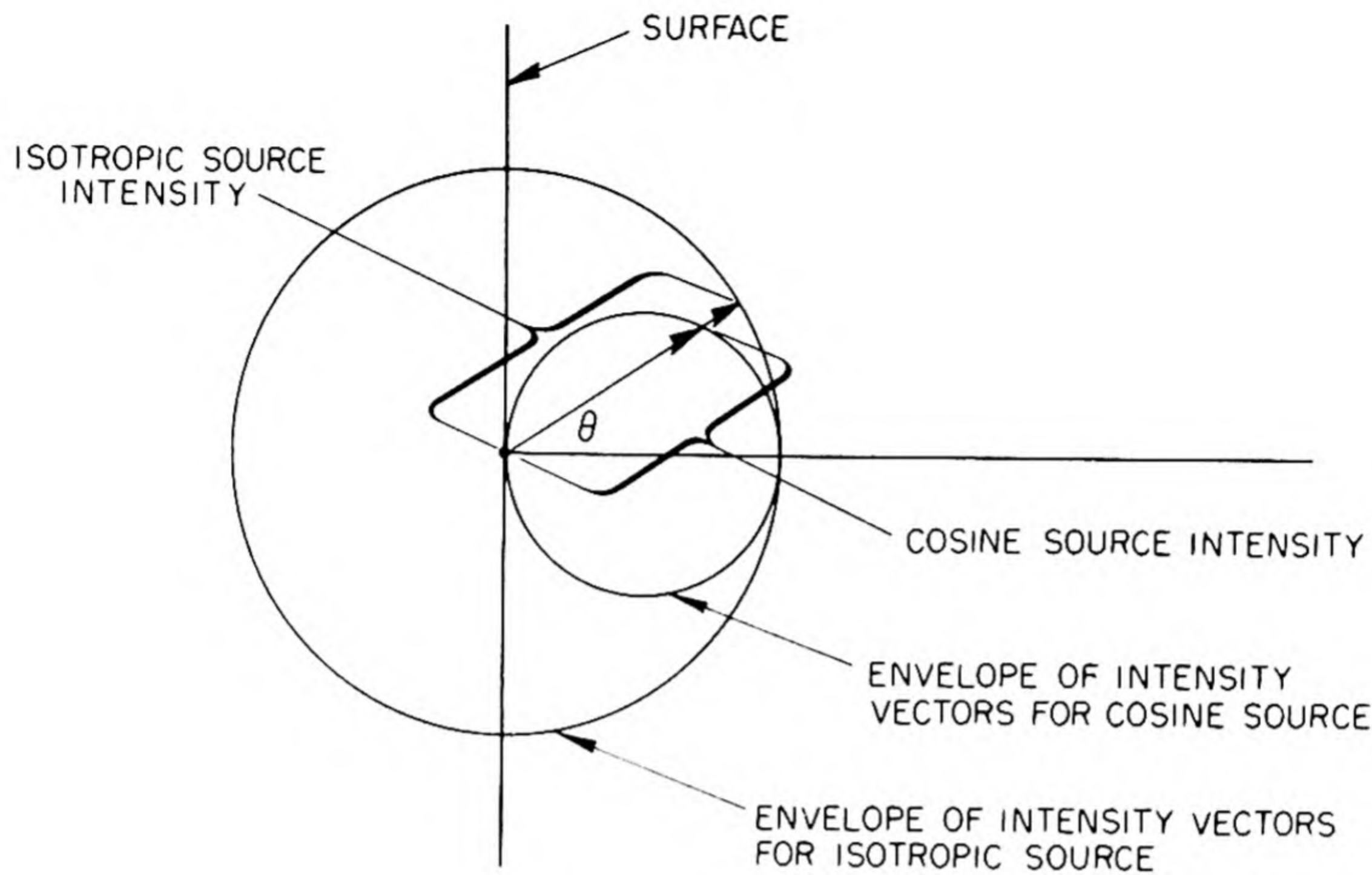


Fig. 2.5.5— Illustration of the Relative Strengths of the Isotropic Surface and Cosine Surface Sources as Used in This Chapter. Submitted by Oak Ridge National Laboratory, Oct. 28, 1952.

connotation of current. Whether number or energy (or other) flux or current is implied depends on the definition of the buildup factor and is not properly a subject for discussion under "geometry."

POINT TO LINE

Isotropic source distributed along a straight line, of strength unity per centimeter per second; nondirectional detector; linear build-up factor:

$$D(z) = \frac{\mu}{2\pi} K_0(\mu z) \approx \frac{\mu}{2\pi} \sqrt{\frac{\pi}{2\mu z}} e^{-\mu z} \quad (\mu z \gg 1) \quad (32)$$

SELF-ABSORBING SMALL CYLINDER

For the case of a source distributed in a cylinder for which self-absorption is important but for radius not large compared with relaxation lengths, see the referenced work.^{6,7,8}

REFERENCES FOR OTHER TRANSFORMATIONS

The foregoing transformations have been the most useful for general shield design. Occasionally, however, unusual configurations are of interest, and for these, reference is made to two project handbooks^{9,10} and to the comprehensive treatment of Wende.¹¹

Table 2.5.1 — Exponential Integral Functions

x	$E_1(x)$	$E_2(x)$	$E_3(x)$	x	$E_1(x)$	$E_2(x)$	$E_3(x)$
1.0	2.19×10^{-1}	1.485×10^{-1}	1.097×10^{-1}	11.0	1.400×10^{-6}	1.180×10^{-7}	1.000×10^{-8}
.2	1.584×10^{-1}	9.26×10^{-2}	5.83×10^{-2}	.2	1.127×10^{-6}	9.35×10^{-8}	7.78×10^{-9}
.4	1.162×10^{-1}	5.99×10^{-2}	3.29×10^{-2}	.4	9.08×10^{-7}	7.40×10^{-8}	6.06×10^{-9}
.6	8.63×10^{-2}	3.99×10^{-2}	1.949×10^{-2}	.6	7.31×10^{-7}	5.87×10^{-8}	4.72×10^{-9}
.8	6.47×10^{-2}	2.71×10^{-2}	1.195×10^{-2}	.8	5.89×10^{-7}	4.65×10^{-8}	3.69×10^{-9}
2.0	4.89×10^{-2}	1.877×10^{-2}	7.53×10^{-3}	12.0	4.75×10^{-7}	3.69×10^{-8}	2.89×10^{-9}
.2	3.72×10^{-2}	1.317×10^{-2}	4.86×10^{-3}	.2	3.83×10^{-7}	2.93×10^{-8}	2.25×10^{-9}
.4	2.84×10^{-2}	9.36×10^{-3}	3.20×10^{-3}	.4	3.08×10^{-7}	1.848×10^{-8}	1.376×10^{-9}
.6	2.19×10^{-2}	6.72×10^{-3}	2.14×10^{-3}	.6	2.49×10^{-7}	1.469×10^{-8}	1.078×10^{-9}
.8	1.686×10^{-2}	4.86×10^{-3}	1.447×10^{-3}	.8	2.01×10^{-7}	1.165×10^{-8}	8.61×10^{-10}
3.0	1.305×10^{-2}	3.55×10^{-3}	9.92×10^{-4}	13.0	1.622×10^{-7}	1.168×10^{-8}	8.45×10^{-9}
.2	1.013×10^{-2}	2.60×10^{-3}	6.88×10^{-4}	.2	1.309×10^{-7}	9.30×10^{-9}	6.63×10^{-10}
.4	7.89×10^{-3}	1.925×10^{-3}	4.81×10^{-4}	.4	1.057×10^{-7}	7.40×10^{-9}	5.20×10^{-10}
.6	6.16×10^{-3}	1.430×10^{-3}	3.39×10^{-4}	.6	8.53×10^{-8}	5.89×10^{-9}	4.08×10^{-10}
.8	4.82×10^{-3}	1.067×10^{-3}	2.41×10^{-4}	.8	6.89×10^{-8}	4.69×10^{-9}	3.21×10^{-10}
4.0	3.78×10^{-3}	8.00×10^{-4}	1.726×10^{-4}	14.0	5.57×10^{-8}	3.74×10^{-9}	2.54×10^{-10}
.2	2.97×10^{-3}	6.02×10^{-4}	1.242×10^{-4}	.2	4.50×10^{-8}	2.98×10^{-9}	1.982×10^{-10}
.4	2.34×10^{-3}	4.54×10^{-4}	8.99×10^{-5}	.4	3.63×10^{-8}	2.38×10^{-9}	1.559×10^{-10}
.6	1.841×10^{-3}	3.44×10^{-4}	6.54×10^{-5}	.6	2.94×10^{-8}	1.896×10^{-9}	1.226×10^{-10}
.8	1.453×10^{-3}	2.62×10^{-4}	4.78×10^{-5}	.8	2.37×10^{-8}	1.513×10^{-9}	9.66×10^{-11}
5.0	1.148×10^{-3}	1.993×10^{-4}	3.51×10^{-5}	15.0	1.919×10^{-8}	1.207×10^{-9}	7.62×10^{-11}
.2	9.09×10^{-4}	1.523×10^{-4}	2.59×10^{-5}	.2	1.551×10^{-8}	9.64×10^{-10}	6.01×10^{-11}
.4	7.20×10^{-4}	1.166×10^{-4}	1.914×10^{-5}	.4	1.255×10^{-8}	7.70×10^{-10}	4.73×10^{-11}
.6	5.71×10^{-4}	8.95×10^{-5}	1.421×10^{-5}	.6	1.015×10^{-8}	6.15×10^{-10}	3.74×10^{-11}
.8	4.53×10^{-4}	6.88×10^{-5}	1.058×10^{-5}	.8	8.21×10^{-9}	4.92×10^{-10}	2.95×10^{-11}
6.0	3.60×10^{-4}	5.30×10^{-5}	7.91×10^{-6}	16.0	6.64×10^{-9}	3.93×10^{-10}	2.33×10^{-11}
.2	2.86×10^{-4}	4.10×10^{-5}	5.92×10^{-6}	.2	5.37×10^{-9}	3.14×10^{-10}	1.842×10^{-11}
.4	2.28×10^{-4}	3.17×10^{-5}	4.45×10^{-6}	.4	4.35×10^{-9}	2.51×10^{-10}	1.455×10^{-11}
.6	1.816×10^{-4}	2.45×10^{-5}	3.35×10^{-6}	.6	3.52×10^{-9}	2.01×10^{-10}	1.152×10^{-11}
.8	1.448×10^{-4}	1.903×10^{-5}	2.53×10^{-6}	.8	2.85×10^{-9}	1.609×10^{-10}	9.11×10^{-12}
7.0	1.155×10^{-4}	1.479×10^{-5}	1.911×10^{-6}	17.0	2.31×10^{-9}	1.288×10^{-10}	7.21×10^{-12}
.2	9.22×10^{-5}	1.150×10^{-5}	1.449×10^{-6}	.2	1.867×10^{-9}	1.032×10^{-10}	5.70×10^{-12}
.4	7.36×10^{-5}	8.96×10^{-6}	1.100×10^{-6}	.4	1.512×10^{-9}	8.26×10^{-11}	4.52×10^{-12}
.6	5.89×10^{-5}	6.99×10^{-6}	8.37×10^{-7}	.6	1.225×10^{-9}	6.62×10^{-11}	3.58×10^{-12}
.8	4.71×10^{-5}	5.46×10^{-6}	6.38×10^{-7}	.8	9.92×10^{-10}	5.30×10^{-11}	2.84×10^{-12}
8.0	3.77×10^{-5}	4.27×10^{-6}	4.87×10^{-7}	18.0	8.04×10^{-10}	4.25×10^{-11}	2.25×10^{-12}
.2	3.02×10^{-5}	3.34×10^{-6}	3.72×10^{-7}	.2	6.51×10^{-10}	3.41×10^{-11}	1.786×10^{-12}
.4	2.42×10^{-5}	2.62×10^{-6}	2.86×10^{-7}	.4	5.28×10^{-10}	2.73×10^{-11}	1.417×10^{-12}
.6	1.936×10^{-5}	2.05×10^{-6}	2.19×10^{-7}	.6	4.27×10^{-10}	2.19×10^{-11}	1.124×10^{-12}
.8	1.552×10^{-5}	1.610×10^{-6}	1.683×10^{-7}	.8	3.46×10^{-10}	1.758×10^{-11}	8.93×10^{-13}
9.0	1.245×10^{-5}	1.265×10^{-6}	1.294×10^{-7}	19.0	2.81×10^{-10}	1.41×10^{-11}	7.09×10^{-13}
.2	9.99×10^{-6}	9.95×10^{-7}	9.96×10^{-8}	.2	2.28×10^{-10}	1.132×10^{-11}	5.63×10^{-13}
.4	8.02×10^{-6}	7.82×10^{-7}	7.69×10^{-8}	.4	1.845×10^{-10}	9.08×10^{-12}	4.48×10^{-13}
.6	6.44×10^{-6}	6.16×10^{-7}	5.94×10^{-8}	.6	1.496×10^{-10}	7.29×10^{-12}	3.56×10^{-13}
.8	5.17×10^{-6}	4.85×10^{-7}	4.60×10^{-8}	.8	1.213×10^{-10}	5.86×10^{-12}	2.83×10^{-13}
10.0	4.16×10^{-6}	3.83×10^{-7}	3.55×10^{-8}	20.0	9.84×10^{-11}	4.70×10^{-12}	2.25×10^{-13}
.2	3.34×10^{-6}	3.02×10^{-7}	2.75×10^{-8}				
.4	2.69×10^{-6}	2.39×10^{-7}	2.13×10^{-8}				
.6	2.16×10^{-6}	1.887×10^{-7}	1.654×10^{-8}				
.8	1.740×10^{-6}	1.492×10^{-7}	1.286×10^{-8}				

Table 2.5.2 — Unshielded Infinite-plane Surface Sources

Source	Detector	Intensity
Isotropic	Non-directional	Infinite
	Cosine	$\frac{1}{2}$
Cosine	Non-directional	$\frac{1}{2}$
	Cosine	$\frac{1}{4}$

Table 2.5.3 — Unshielded Volume-distributed Plane-limited Source

Source	Detector	Buildup $B(\mu, R)$	Intensity
Volume	Non-directional	1	$1/(2\mu_1)$
	Cosine	1	$1/(4\mu_1)$

Table 2.5.4 — Infinite Slab Shield of Thickness z and Attenuation Coefficient μ : Infinite Surface or Volume Source

Source	Detector	Buildup $B(\mu, R)$	Intensity	
			Exact	Approximate for $\mu z \gg 1$
Isotropic surface, $1/(\text{sec})(\text{cm}^2)$	Non-directional	Unitary	$\frac{1}{2} E_1(\mu z)$	$\frac{1}{2} \frac{e^{-\mu z}}{\mu z}$
		Linear	$\frac{1}{2} e^{-\mu z}$	$\frac{1}{2} e^{-\mu z}$
	Cosine	Unitary	$\frac{1}{2} \mu z E_2(\mu z)$	$\frac{1}{2} \frac{e^{-\mu z}}{\mu z}$
		Linear	$\frac{1}{2} \mu z E_1(\mu z)$	$\frac{1}{2} e^{-\mu z}$
Cosine surface, $\cos\theta/4\pi/(\text{sec})(\text{cm}^2)(\text{sterad})$	Non-directional	Unitary	$\frac{1}{2} \mu z E_2(\mu z)$	$\frac{1}{2} \frac{e^{-\mu z}}{\mu z}$
		Linear	$\frac{1}{2} \mu z E_1(\mu z)$	$\frac{1}{2} e^{-\mu z}$
	Cosine	Unitary	$\frac{1}{2} (\mu z)^2 E_3(\mu z)$	$\frac{1}{2} \frac{e^{-\mu z}}{\mu z}$
		Linear	$\frac{1}{2} (\mu z)^2 E_2(\mu z)$	$\frac{1}{2} e^{-\mu z}$
Volume, attenuation coefficient in source = μ_1	Non-directional	Unitary	$\frac{1}{2\mu_1} \mu z E_2(\mu z)$	$\frac{1}{2\mu_1} \frac{e^{-\mu z}}{\mu z}$
		Linear	$\frac{1}{2\mu_1} e^{-\mu z}$	$\frac{1}{2\mu_1} e^{-\mu z}$
	Cosine	Unitary	$\frac{1}{2\mu_1} (\mu z)^2 E_3(\mu z)$	$\frac{1}{2\mu_1} \frac{e^{-\mu z}}{\mu z}$
		Linear	$\frac{1}{2\mu_1} [e^{-\mu z} - (\mu z)^2 E_3(\mu z)]$	$\frac{1}{2\mu_1} e^{-\mu z}$

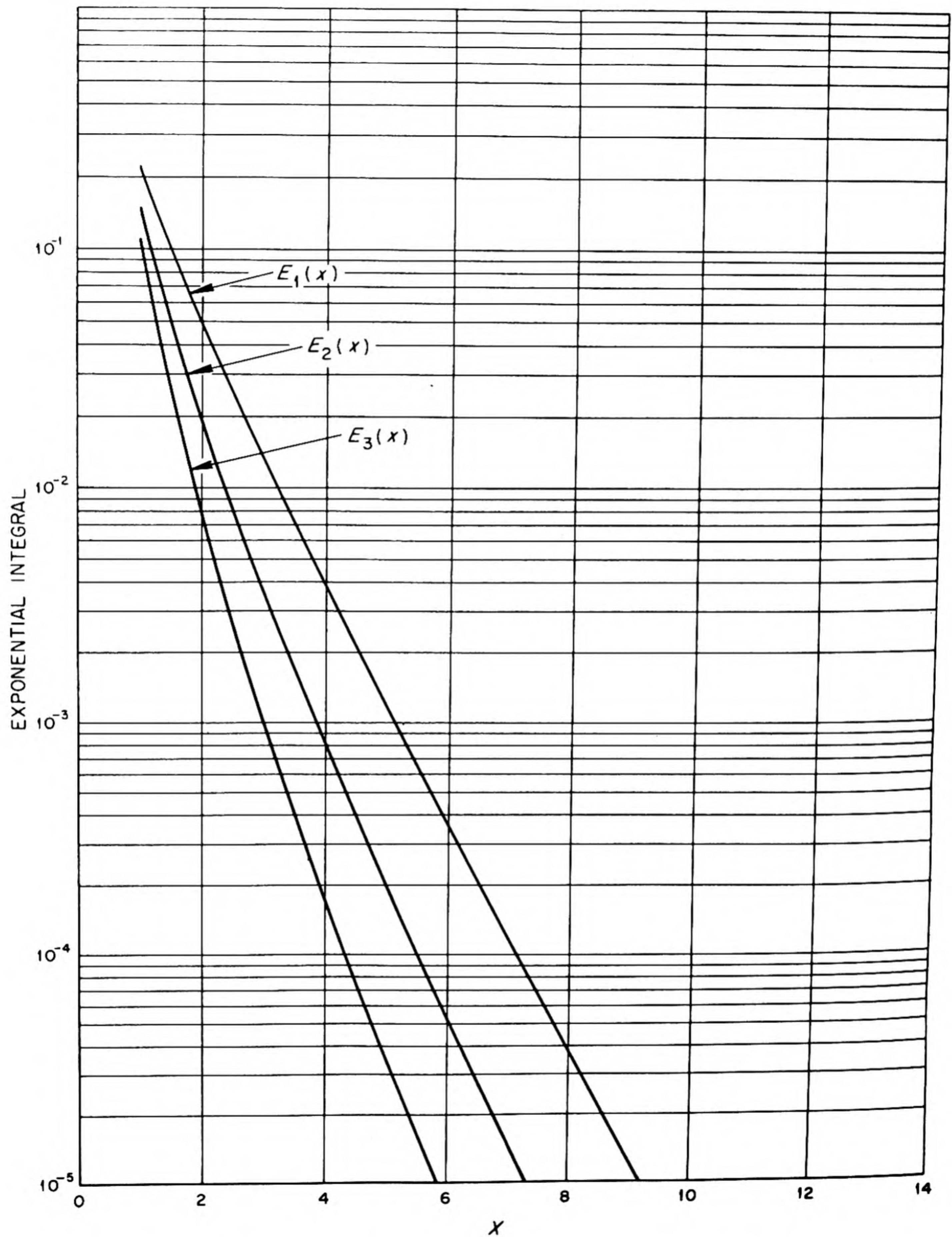


Fig. 2.5.6—The Exponential Integral Functions $E_1(x)$, $E_2(x)$, and $E_3(x)$, where

$$E_n(x) = \int_x^\infty \frac{e^{-p}}{p^n} dp.$$

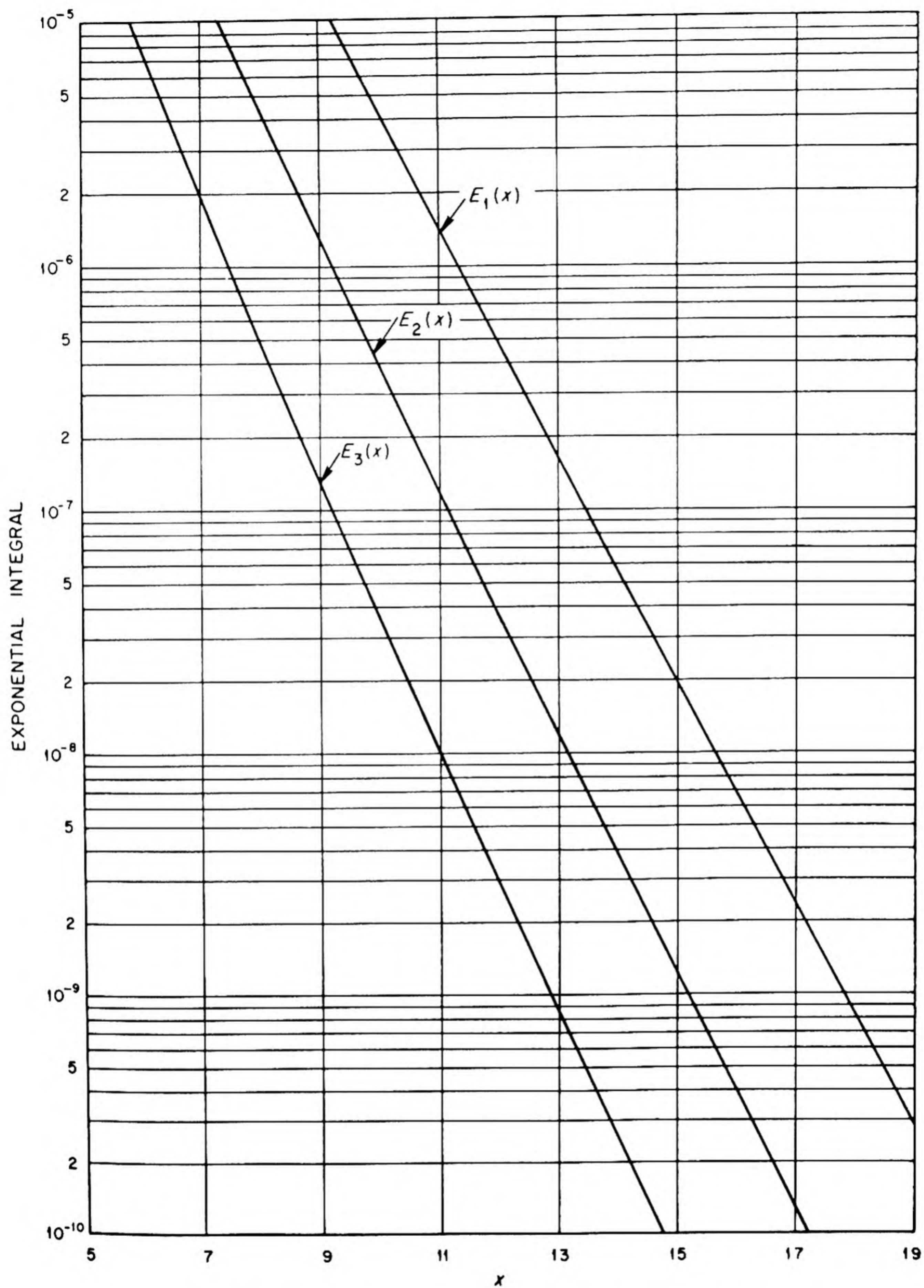


Fig. 2.5.7—The Exponential Integral Functions $E_1(x)$, $E_2(x)$, and $E_3(x)$, where

$$E_n(x) = \int_x^\infty \frac{e^{-p}}{p^n} dp.$$

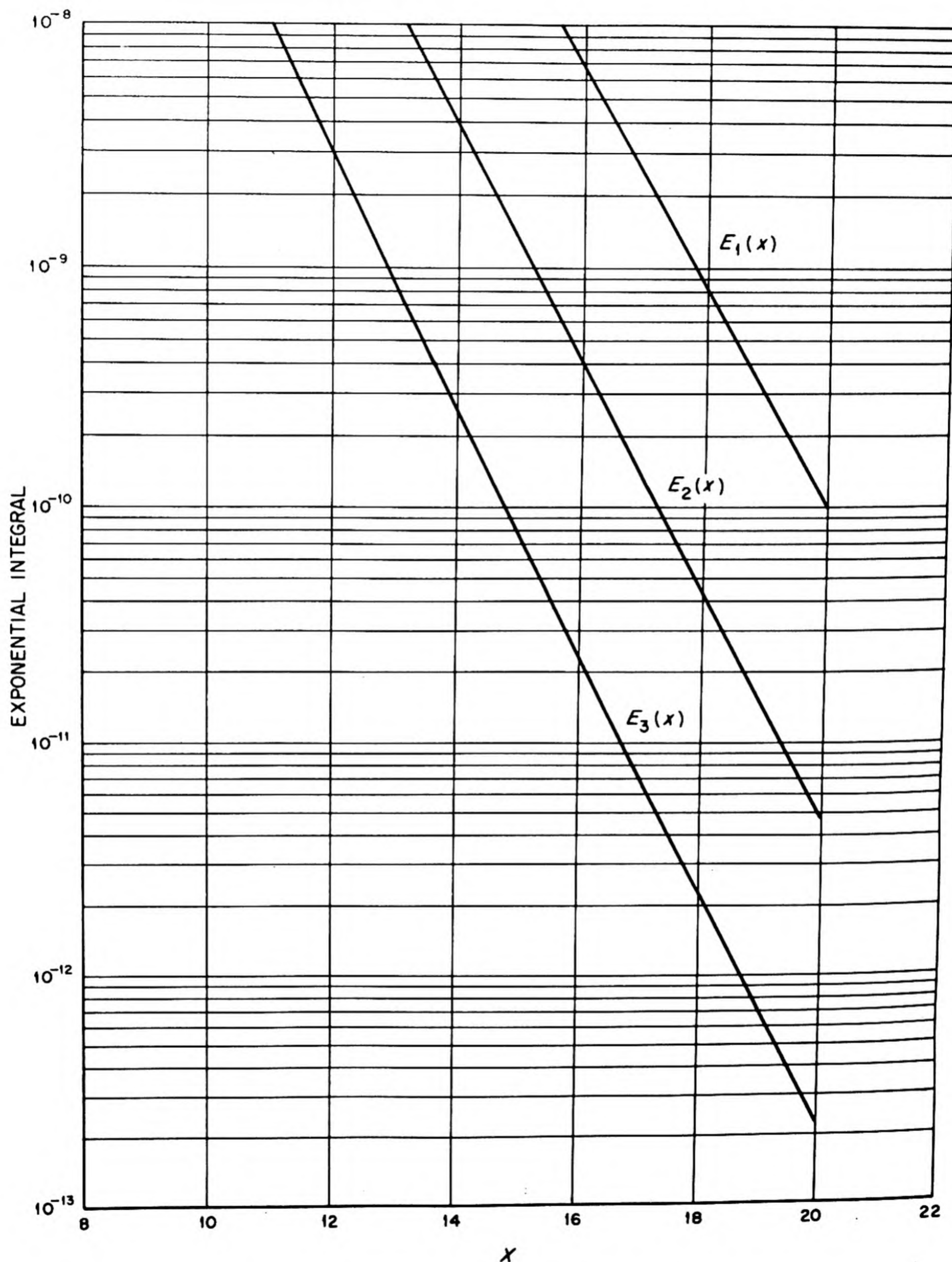


Fig. 2.5.8—The Exponential Integral Functions $E_1(x)$, $E_2(x)$, and $E_3(x)$, where

$$E_n(x) = \int_x^\infty \frac{e^{-p}}{p^n} dp.$$

REACTOR LEAKAGE

Often it is possible to express the distribution of source strength (usually proportional to reactor power) in the region near its surface by a simple linear equation:

$$\alpha(z_1) = \alpha_0 + \alpha_1 z_1 \quad (33)$$

where z_1 is the distance into the core from the surface, and α_0 and α_1 are constants. In this case, the equivalent isotropic surface source (in the sense of the previous section) as recorded by a nondirectional detector (milligoat) is:

$$\sigma = \frac{\alpha_0}{\mu_1} + \frac{\alpha_1}{\mu_1} \quad (34)$$

where μ_1 is the core attenuation coefficient.

REFERENCES

1. E. P. Blizard, "Transformation from Disc to Point Source Geometry," ORNL, C. F. 52-3-219, Mar. 27, 1952.
2. E. P. Blizard, Part I, Oak Ridge National Laboratory, C. F. 51-10-70, p 54, 72 pp, Jan. 30, 1952 (classified).
3. T. A. Welton and E. P. Blizard, Reactor Sci. Tech, 2, No. 2, Aug. 1952 (classified).
4. H. Goldstein, Phys. Rev., in press.
5. Heitler "Quantum Theory of Radiation," Oxford press.
6. H. Castle, H. Ibser, G. Sacher, and A. M. Weinberg, CP-644, May 4, 1943 (classified).
7. F. H. Murray, Fast Effects, Self-Absorption, Fluctuation of Ion Chamber Readings, and the Statistical Distribution of Chord Lengths in Finite Bodies, CP-G-2922, April 6, 1945.
8. S. Kushneriuk, Atomic Energy Project (Canada), 7 pp, May 6, 1947 (classified).
9. Chap. V, Sec. F, in Project Handbook, ed. by R. S. Mulliken, P. Morrison, et al, CL-697, Vol. II (classified).
10. Appendix 8 in Materials Testing Reactor Project Handbook, ed. by J. H. Buck and C. F. Levse, Argonne National Laboratory and Oak Ridge National Laboratory, ORNL-963, 584 pp, May 7, 1951 (classified).
11. C. W. J. Wende, E. I. duPont de Nemours and Company, Inc., M-1324 (N-609, TNX-7) 66 pp, Jan. 11, 1944 (classified).

CHAPTER 2.6

Ducts Through Shields

A. Simon

The principal experimental investigations of ducts up to this time have been concerned with the effects of air ducts and voids on gamma-ray and neutron transmission in water. Many experiments on the attenuation of fast neutrons by long thin air ducts in water* can be understood on the basis of a phenomenological theory. This theory is presented below and is followed by a brief summary of the effect of internal voids on neutron attenuations. The effect of ducts and voids on the attenuation of gamma rays is considered in a latter part of this chapter.

ATTENUATION OF NEUTRONS BY AIR DUCTS IN SHIELDS (THEORY)

The attenuation of neutrons by a long, thin, circular duct can be calculated by an albedo approach. It is assumed that the walls of the duct reradiate neutrons with an intensity proportional to the flux incident upon the wall. The constant of proportionality is the albedo, and it is assumed that the reradiation is partly isotropic and partly cosine distribution about the normal to the wall. If the reradiated flux into a unit solid angle $d\Omega$ is written:

$$\frac{dF}{d\Omega} = \frac{A + 2B \cos\theta}{2\pi} \alpha' F_{\text{inc}}$$

where:

F_{inc} = flux incident on wall

α' = albedo of wall

and since by conservation of neutrons there follows:

$$A + B = 1$$

it can be shown¹ that the total flux at the end of a long, thin duct of length l and radius δ is given by:

$$F = \frac{N_0}{2\pi l^2} \left(1 + \frac{A \alpha'}{1 - \alpha'} + \frac{4B\delta\alpha'}{l(1 - \alpha')} \right) \quad (2)$$

*These experiments have not yet been published in a single report; most, however, have been reported in various ORNL and ANP (classified) quarterly reports over the period from 1949 to 1952.

¹References appear at end of chapter.

Here, N_0 is the total (isotropic) source strength at the mouth of the duct. The first term represents the uncollided (non wall-scattered) flux.

The fast-neutron albedos for water and concrete have been measured at the Bulk Shielding Facility at ORNL.² It was found that the albedos for both were of the order of 0.1. This result, coupled with the fact that A and B are less than or equal to unity, allows one to neglect all but the first term to a reasonable approximation. Hence, the flux at the mouth of a straight duct is caused by just the uncollided neutrons to within a few percent:

$$F = \frac{N_0}{2\pi l^2} \quad (3)$$

An interesting by-product of this result is the prediction that one should be able to collimate a source of fast neutrons without greatly distorting the spectrum.

The effect of a single bend in a duct can be calculated by making a simple assumption. The flux entering the region of the bend, as shown in the previous paragraph, is just the uncollided flux arriving from the source. This dose of neutrons is completely absorbed in the walls of the bend, and as a result, a reradiated flux leaves the walls with a source strength proportional to the albedo of the medium. The exact effect of the complicated scatterings at the corner is unknown; however, it will be assumed that the reradiated flux is emitted uniformly from a region of area A_t in the vicinity of the bend and with an angular distribution given by:

$$\frac{dF}{d\Omega} = \frac{\alpha' D}{A_t} \frac{A + 2B \cos\theta}{2\pi} \quad (4)$$

where: D = total uncollided neutron dose entering the region of the bend
 α' = albedo of the walls

By conservation of neutrons:

$$A + B = 1$$

On the basis of this assumption, the total dose at the end of a duct consisting of two long, thin, straight sections of length l_1 and l_2 (both of radius δ) joined at an angle θ can be shown¹ to be:

$$F = N_0 \left(\frac{\delta^2}{2l_1^2} \right) \left(\frac{\alpha \delta^2}{2l_2^2 \sin\theta} \right) (A + 2B \sin\theta) \quad (5)$$

Here:

N_0 = total (isotropic) source strength at the mouth of the duct

α = "effective albedo," a constant which is proportional to the actual albedo of the walls

The factor $1/\sin\theta$ arises from the fact that the region of wall at the bend which is visible from the end of the duct is approximately proportional to this quantity. Figure 2.6.1 illustrates this point.

Equation (5) may be generalized to cover the broad case of $n + 1$ straight sections of length l_i ($i = 1, 2, \dots, n + 1$) joined at angles given by $\theta_{i, i+1}$ where the subscripts denote the angle between the appropriate straight sections. The result is:

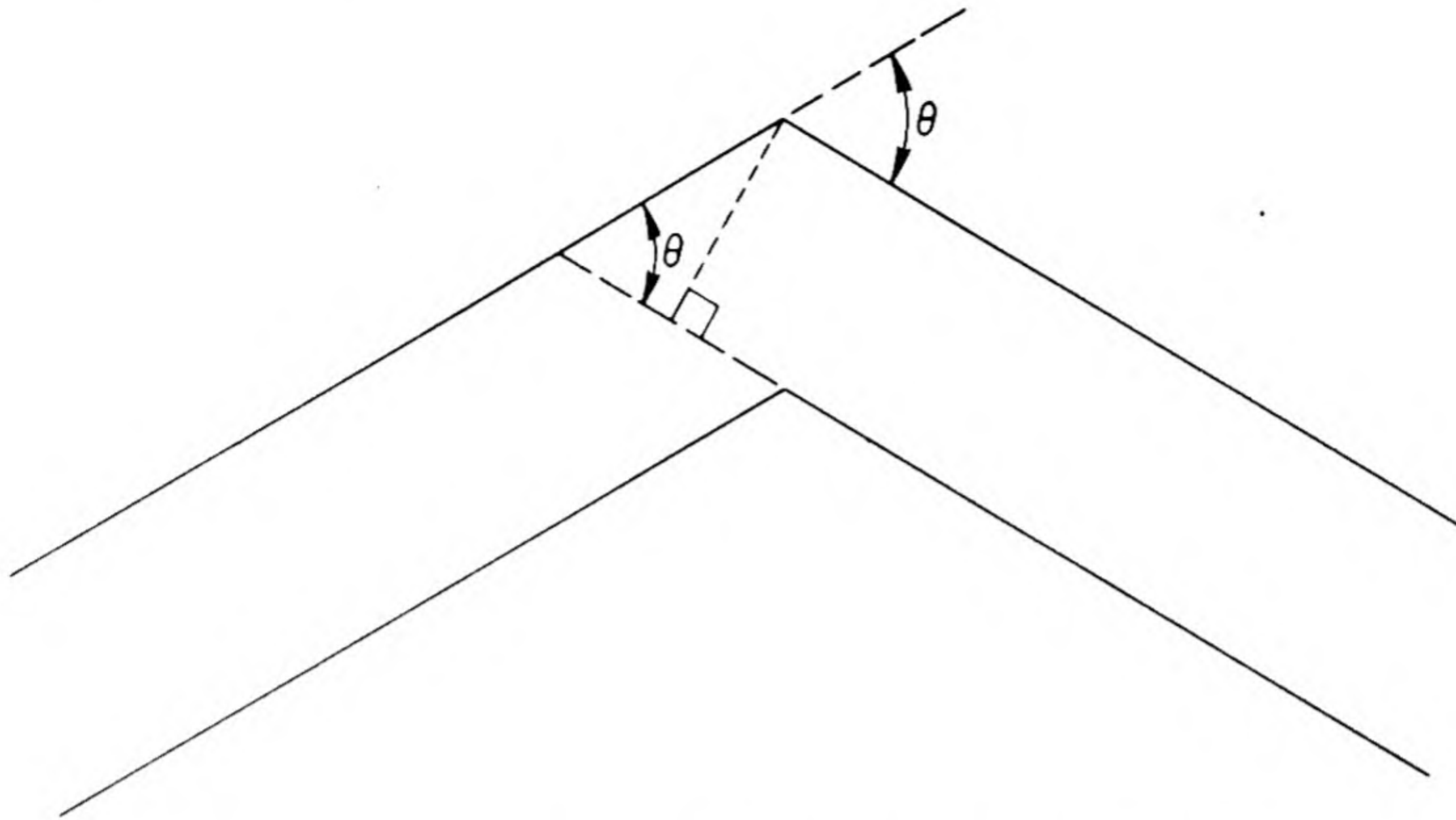


Fig. 2.6.1 — Dependence of Visible Wall Region at a Bend on the Angle of Bend.
Submitted by Oak Ridge National Laboratory, Nov. 7, 1952.

$$D = N_0 \left(\frac{\delta^2}{2l_1^2} \right) \left[\frac{\alpha \delta^2 (A + 2B \sin \theta_{1,2})}{2l_2^2 \sin \theta_{1,2}} \right] \dots \left[\frac{\alpha \delta^2 (A + 2B \sin \theta_{n,n+1})}{2l_{n+1}^2 \sin \theta_{n,n+1}} \right] \quad (6)$$

In the special case of equal lengths of straight sections with equal bends, this becomes:

$$D = N_0 \left(\frac{\delta^2}{2l^2} \right) \left(\frac{\alpha \delta^2}{2l^2 \sin \theta} \right)^n (A + 2B \sin \theta)^n \quad (7)$$

or, since $A + B = 1$:

$$D = N_0 \left(\frac{\delta^2}{2l^2} \right) \left(\frac{\alpha \delta^2}{2l^2 \sin \theta} \right)^n [1 - B(1 - 2 \sin \theta)]^n \quad (8)$$

It should be noted that Eq. (8) is not valid for angles that are so small that neutrons can go directly from one mouth of the duct to the other. In addition, the formula breaks down at angles small enough so that a large section of the wall of the bend ($>A_1$) can be seen from the end of the next leg. In this region of θ , the predicted dose should be an overestimate of the measured effect.

The constant α and B in Eq. (8) are to be determined from experiment. Their values depend on the nature of the source spectrum used as well as the type of detector. The present experiments at the Lid Tank and Thermal Column at ORNL use a fission source and detect the neutrons by means of a BF_3 counter positioned at a water-equivalent of 10, 20 or 30 cm behind the mouth of the duct. These results can be fitted by taking $B \cong 0$ (i.e., pure isotropic reradiation by the walls of the duct). The value of α depends on the counter position and is listed in Table 2.6.1.

The large values of α that are needed are undoubtedly the result of using a BF_3 detector. Such a detector heavily weights the contribution of those neutrons which can be thermalized in 10, 20, or 30 cm of water. On the other hand, the measured albedos of water and concrete² were obtained by use of a dosimeter. It is quite probable that the wall albedos

Table 2.6.1 — "Effective Albedo" Determined by BF_3 Measurements

Water-equivalent distance between counter and duct, cm	α
10	2.4
20	1.0
30	0.56

for lower-energy neutrons are considerably higher than those for the fast flux. The decrease in the value of α as the water-equivalent distance increases is in line with this picture.

It is to be expected that future experiments on duct attenuation using a dosimeter as a detector will give lower values of α .

INTERNAL VOIDS

A simplified analysis of the effect of internal voids in shields on neutron transmission has been given by Tonks.³ A method of estimating the effect of areas of weaker shielding is developed which is applicable to voids of many shapes. The result is given in terms of the excess attenuation over that which would be attained with a uniform shield having the minimum thickness found in the neighborhood of the void. This "minimal ray" technique should not be used if streaming through ducts exists. However, if the duct has been made sufficiently tortuous so that direct streaming is negligible compared to the general void effect (sometimes called "reduced density" effect), then this technique may prove to be of value.

The design of patches to compensate for internal voids has been considered by Bourieus.⁴

A diffusion theoretical treatment of the propagation of neutrons in an empty duct has been given by Whitcombe⁵ and later by Roe.⁶ It is not clear to what extent these treatments are applicable to fast neutrons.

ATTENUATION OF GAMMA RAYS BY AIR DUCTS AND VOIDS

The albedos for the reflection of Co^{60} gamma rays (~ 1.3 mev) by concrete have been measured at ORNL Bulk Shielding Facility.² By using a 50-cc standard 10^{12} ion chamber, the albedo was found to be 0.04. As a result, it may be expected that the neutron attenuation theory is applicable to gamma rays insofar as the effect of a long, thin, straight duct is concerned; that is, the attenuation should be geometrical. The effect of a bend on gamma attenuation is likely to be quite different from that for neutrons.

Large-scale measurements on the effect of voids on gamma-ray attenuation in water have been performed at Brookhaven.⁷ The experiments have been interpreted by Kouts⁸ on the basis of a two-group perturbation treatment using the integral form of the transport theory.

REFERENCES

1. A. Simon and C. E. Clifford, ORNL-1217, Nov. 28, 1952, 24 pp (classified).
2. H. E. Hungerford, ORNL-CF-52-4-99, April 16, 1952, 21 pp (classified).
3. L. Tonks, KAPL-107, Jan. 17, 1949, 12 pp (classified).
4. W. G. Bourieus, NEPA-1536, Aug. 24, 1950, 15 pp (classified).
5. D. W. Whitcombe, A Diffusion Solution for the Cylindrical Ducting Problem of Infinite Geometry, Oak Ridge Nat. Lab., ORNL-668, April 19, 1950, 14 pp.
6. G. M. Roe, The Penetration of Neutrons Through an Empty Cylindrical Duct in a Shield, Knolls Atomic Power Lab., KAPL-712, Mar. 29, 1952, 20 pp.
7. W. W. Pratt and H. J. Kouts, BNL Log No. C-6456, Aug. 25, 1952, 78 pp (classified).
8. H. J. Kouts, BNL Log No. C-6459, Sept. 15, 1952, 19 pp (classified).

CHAPTER 2.7

Heat Generation in Shields

F. H. Murray

GAMMA SOURCES

The primary gamma sources (see "Sources of Radiation," Chapter 2.1) in the reactor core have a spatial density proportional to the thermal-neutron density except for modifications resulting from motion of the fuel which changes the position of fission products that emit gammas. For calculation purposes, the primary sources of fixed fuels are often assumed to be uniformly distributed throughout the core. The calculations made in the design of the reactor may furnish more detailed information concerning source distributions.¹

For uniform source distribution, the number of fissions per second per cubic centimeter is:

$$A = 3 \times 10^{13} P/V$$

where:

P = power, kw

V = volume, cc

assuming 3×10^{10} fissions per joule.

If $\Gamma(E) dE$ is the number of photons per fission of energy E to E + dE (E measured in millions of electron volts), then $A \Gamma(E) dE$ is the corresponding source-density in the core. Owing to the uncertainty concerning the energy distribution for very-short-period gamma emitters in the fission products, $\Gamma(E)$ is less well-known than is the total gamma energy released per fission.

Secondary sources in the core or reflector may be comprised of capture gammas or inelastic scattering gammas, and the densities of these sources may be estimated when the neutron flux pattern in the core is known. Since part of the neutron flux results from (γ, n) processes, especially in Be or D, its calculation may require successive approximations in which the initial fluxes are the primary fluxes.

GAMMA-RAY ABSORPTION

BUILD-UP FACTOR FOR A HOMOGENEOUS MEDIUM

The build-up factor for energy absorption of gammas may be approximated by a method* proposed by H. Goldstein, which proceeds as follows:

* For other treatments, cf. refs. (2), (3), (4), and (5).

¹ References appear at end of chapter.

Let $I(r, E, \vec{\Omega})$ be the energy flux at a distance r of energy E and a direction $\vec{\Omega}$ from a point source, and let:

$$I_0(r, E) = \int_{4\pi} I(r, E, \vec{\Omega}) d\Omega$$

be the total flux in all directions. The total absorption cross section (see "Gamma Attenuation," Chapter 2.3) is very nearly:

$$\mu_{En} = \mu_{\text{pair}} + \mu_{\text{photo}} + \int \frac{d\sigma}{d\Omega} \left(\frac{E \text{ electron}}{E} \right) d\Omega$$

The total energy absorbed per unit volume at r , from a source of Q photons of energy E_0 per second, is:

$$W(r, E_0) = \int_0^{E_0} \mu_{En} I_0 dE$$

The uncollided flux at r is:

$$I_0^0(r, E_0) = \frac{QE_0 e^{-\mu(E_0)r}}{4\pi r^2}$$

where $\mu(E_0)$ is the narrow-beam absorption coefficient for energy E_0 , and the build-up factor, B , which is a function of the initial energy and the distance, is given by:

$$B_{En}(\mu_0 r, E_0) = \frac{\int_0^{E_0} \mu_{En} I_0(r, E) dE}{\mu_{En}(E_0) I_0^0(r, E_0)}$$

The energy absorbed at r is then:

$$w(r, E_0) = B_{En}(\mu_0 r, E_0) \mu_{En}(E_0) I_0^0(r, E_0)$$

We must have from the conservation of energy:

$$\int_{\text{All space}} w(r, E_0) dV = QE_0$$

hence:

$$\int_0^\infty B_{En}(x, E_0) e^{-x} dx = \frac{\mu_0}{\mu_{En}(E_0)}$$

For some problems, the build-up factor, B , may be represented by a linear function:

$$1 + k\mu_0 r$$

from which:

$$k = \frac{\mu_0}{\mu_{En}(E_0)} - 1$$

HEATING OF A REGION

If the build-up factor, B , is known, as from the method of the previous paragraph, then it is possible to calculate the total heat absorbed in a region V with a uniform source throughout by evaluation of the following double integral (see Fig. 2.7.1):

$$W_V = \int_V dV_1 \int_V w(r_{12}) dV_2$$

or:

$$W_V = \int_A dA_1 \cos \nu_1 \int_A \frac{dA_2 \cos \nu_2}{(r_{A_1 A_2})^2} \psi(r_{A_1 A_2})$$

where:

$$\psi(r) = \int_0^r (r-y)y^2 w(y) dy$$

For two regions, one inside the other, such as might be encountered with a core and reflector, the total heat absorbed in core and reflector (if they can be assigned about the same absorption coefficients) is:

$$W_{\text{core+refl.}} = \int_{\text{core}} dV_1 \int_{\text{core+refl.}} w(r_{12}) dV_2$$

or (see Fig. 2.7.2):*

$$W_{\text{core+refl.}} = \int_{A_2} dA_2 \cos \nu_2 \left[\int_{A'_1} \frac{dA'_1 \cos \nu'_1 \psi(r_{A_2 A'_1})}{(r_{A_2 A'_1})^2} + \int_{A''_1} \frac{dA''_1 \cos \nu''_1 \psi(r_{A_2 A''_1})}{(r_{A_2 A''_1})^2} \right]$$

Thus, the energy transmitted to the shield is just the difference between the total emitted and $W_{\text{core+refl.}}$. For spherical core and reflector with radii R_2 and R_1 and $R_2 > R_1$:

$$W = \int_{R_2-R_1}^{R_2+R_1} \phi(r) \psi(r) dr$$

where:

$$\phi(l)dl = \iint_{l \leq r_{A_1 A_2} \leq l+dl} \frac{dA_1 \cos \nu_1 dA_2 \cos \nu_2}{(r_{A_1 A_2})^2}$$

or:

$$\phi(l)dl = \frac{2\pi^2}{l^3} [l^4 - (R_2^2 - R_1^2)^2] dl$$

* The direction cosines ν_1 and ν_2 are those made by the line from dA_2 to dA_1 , with the exterior normal at dA_1 and the interior normal at dA_2 , respectively. At dA''_1 , $\cos \nu''_1$ is negative; $\cos \nu_2$ is positive or zero; the curve on which the line from dA_2 is tangent to the core separates the areas A'_1 , A''_1 .

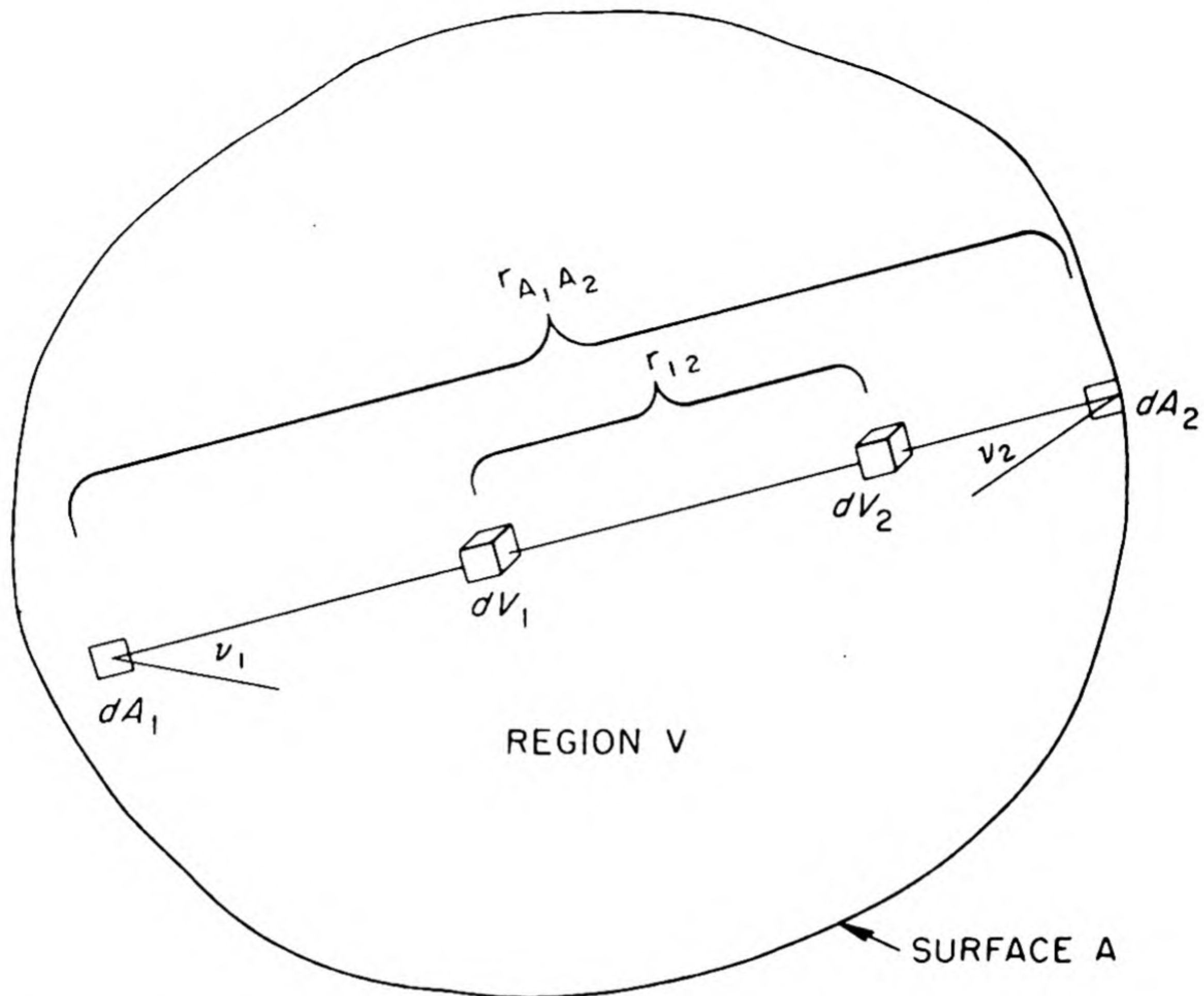


Fig. 2.7.1 — Illustration of Integration for Heating in a Region in Which Sources Are Uniformly Distributed. Submitted by Oak Ridge National Laboratory, April 1, 1953.

SPECIAL CASES

LOS ALAMOS REACTORS

Los Alamos measurements on the photon flux spectrum from the core of the fast reactor and the flux from a U^{235} slug in the glory hole of the water boiler were found to be of almost identical exponential type as functions of the energy E . The number of photons per thousand electron volts interval at 8 mev was less than the value at 0.5 mev by a factor of 10^4 for each. The average energy was nearly 1 mev in each case. Prompt fission gammas and delayed gammas from fission products each contributed about 45 percent of the total energy of the gamma radiation; capture gammas from U^{235} contributed about 10 percent.⁶

BULK SHIELDING FACILITY REACTOR

The Bulk Shielding Facility Reactor at Oak Ridge National Laboratory includes about 3 kg U^{235} , is water moderated, and has aluminum structural members; the Al/ H_2O volume ratio is about 0.7. The gamma fluxes in the surrounding pool of water at various distances from the reactor face as functions of energy are available in four Oak Ridge National Laboratory reports.⁷⁻¹⁰

OTHER REACTORS

Heat generation in several other reactors is described in Chapter 1.6.

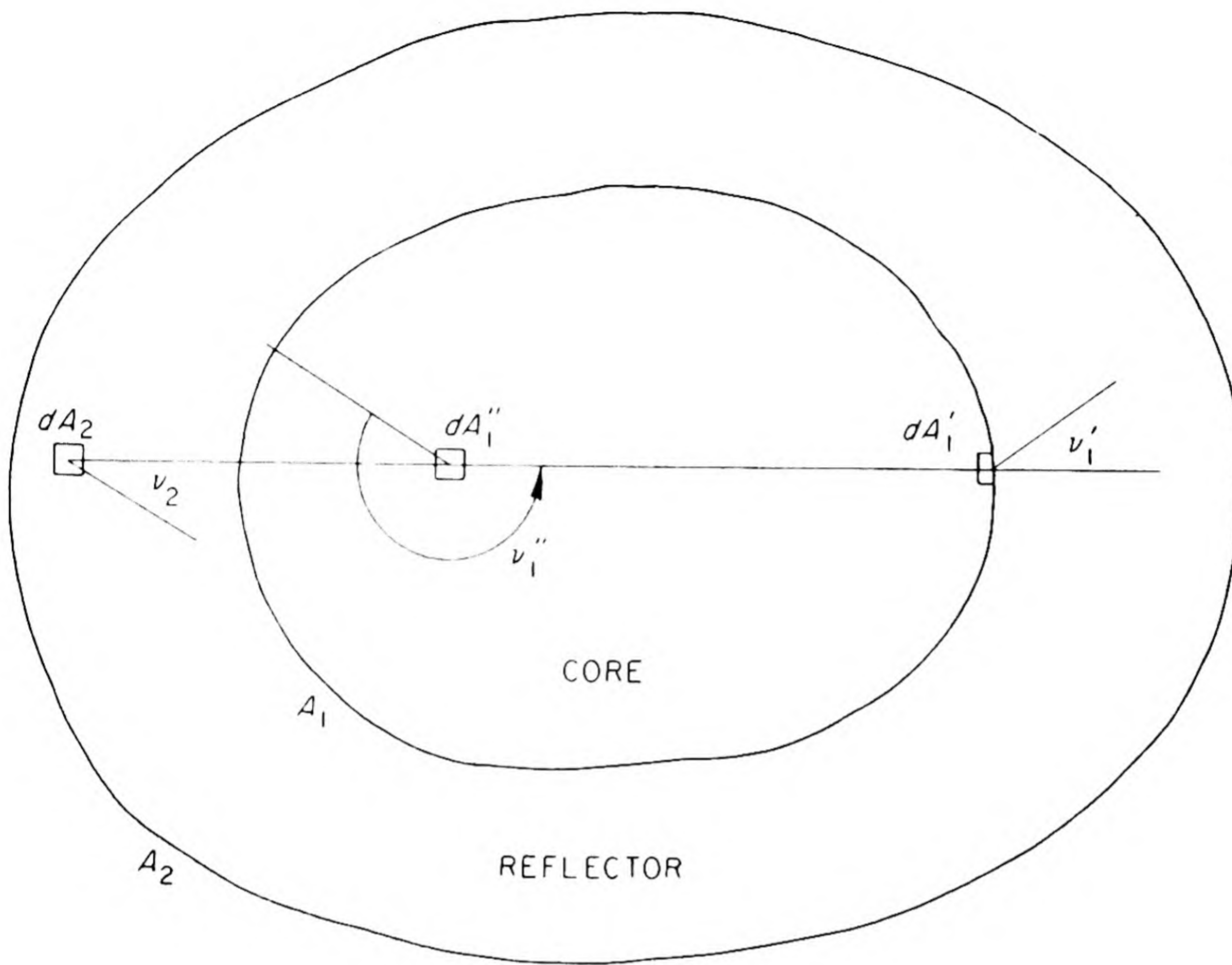


Fig. 2.7.2 — Illustration of Integration for Heating in Two Regions Owing to Sources in One Region. Submitted by Oak Ridge National Laboratory, April 1, 1953.

ENERGY ABSORPTION OF CAPTURE GAMMAS

If the gamma mean-free-path is short as in heavy materials, the method of Enlund¹¹ may be used. An infinite plane source of neutrons emitting a current I_0 of slow neutrons into an infinite plane-limited slab produces a flux, ϕ , in the material, with:

$$\phi = \frac{I_0 e^{-Kz}}{KD}$$

where:

- I = neutron current, $-Dd\phi/dz$ at $z = 0$, $\text{cm}^{-2} \text{sec}^{-1}$
- $K = \sqrt{3\Sigma_a\Sigma_t}$, cm^{-1}
- Σ_a = neutron absorption coefficient, cm^{-1}
- Σ_t = neutron transport coefficient, cm^{-1}
- D = diffusion coefficient
- z = distance to point of neutron absorption, cm

Then:

$$\Sigma_a \phi(z) = \frac{\Sigma_a I_0 e^{-Kz}}{DK} = KI_0 e^{-Kz} = \text{number of neutrons absorbed at } z$$

$n(E)$ = fraction of neutron captures which yield a gamma ray of energy E , mev

$\mu_{En}(E)$ = energy absorption coefficient, cm^{-1}

$\mu(E)$ = linear absorption coefficient, cm^{-1}

$\alpha = K/\mu$

b = distance to point of gamma energy absorption, cm

CASE I: $K > \mu$

$$\Gamma(E) = n(E) \frac{EI_0}{2} \mu_{En}(E) F(\mu b, \alpha)$$

where:

$$F(\mu b, \alpha) = e^{-\alpha \mu b} \left\{ e^{\alpha \mu b} [-\text{Ei}(-\mu b)] + \text{Ei} [\mu b(\alpha - 1)] + \ln \frac{\alpha + 1}{\alpha - 1} \right\}$$

Then the heating in the material is:

$$H(E) = \frac{\Gamma(E)}{6.25 \times 10^{12}} \text{ watts/cm}^3$$

CASE II: $K = \mu$

$$\Gamma(E) = n(E) \frac{EI_0}{2} \mu_{En}(E) F(\mu b, 1)$$

where:

$$F(\mu b, 1) = e^{-\mu b} \{ e^{\mu b} [-\text{Ei}(-\mu b)] + \ln \mu b + \ln 2\gamma \}, \ln \gamma = 0.5772$$

CASE III: $K < \mu$

$$\Gamma(E) = n(E) \frac{EI_0}{2} \mu_{En}(E) F(\mu b, \alpha)$$

where:

$$F(\mu b, \alpha) = e^{-\alpha \mu b} \left\{ e^{\alpha \mu b} [-\text{Ei}(-\mu b)] + \text{Ei} [-\mu b(1 - \alpha)] + \ln \frac{1 + \alpha}{1 - \alpha} \right\}$$

Curves showing $F(\mu b, \alpha)$ as functions of μb for various values of α are given in Fig. 2.7.3.

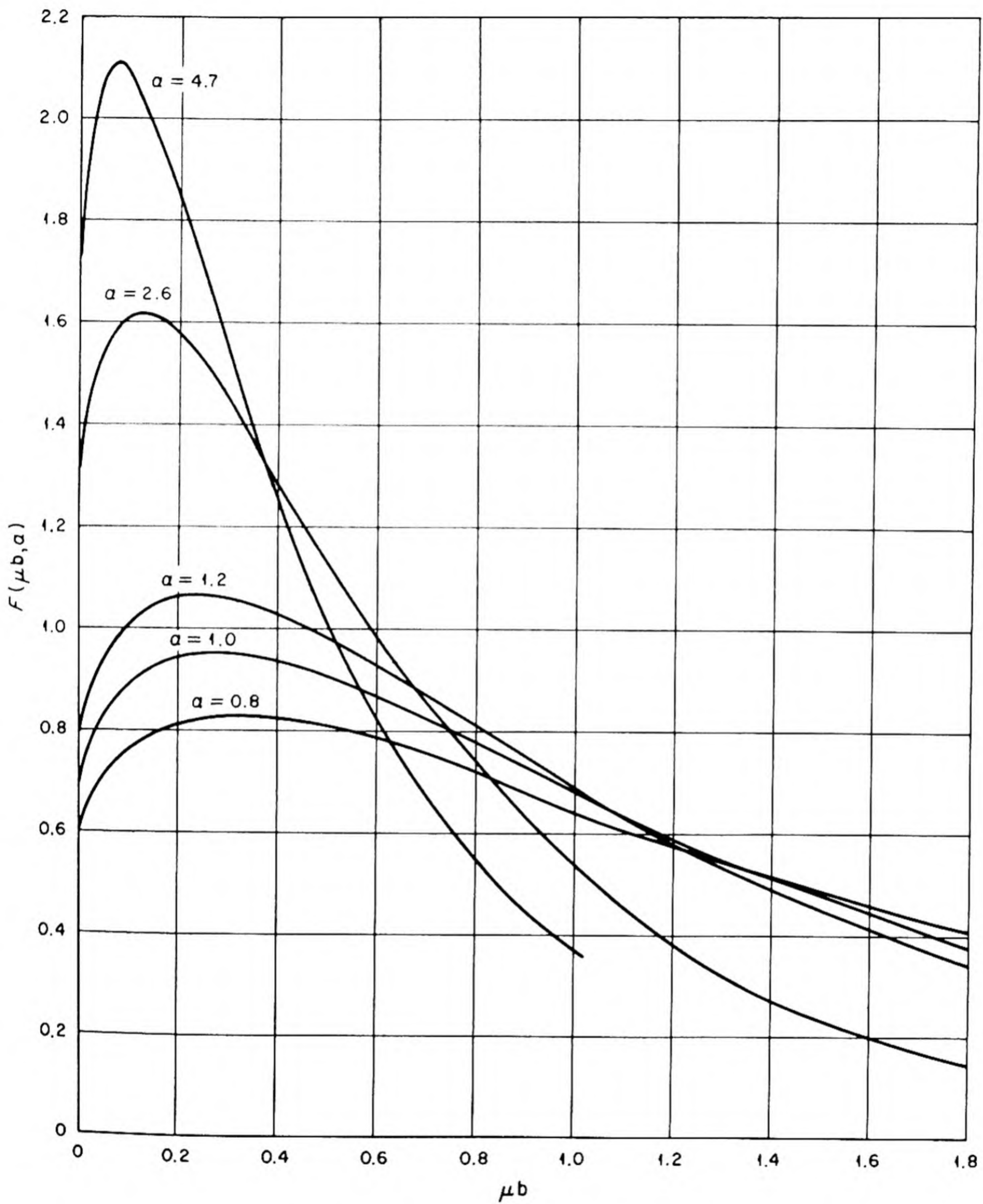


Fig. 2.7.3 — Energy Absorption of Capture Gammas Produced within a Plane-limited Infinite Medium. Submitted by Oak Ridge National Laboratory, April 1, 1953.

REFERENCES

1. D. K. Holmes, ANP-58, Feb. 15, 1951, 38 pp (classified).
2. H. Hurwitz, J. B. Nims, and M. L. Storm, KAPL-753, July 14, 1952, 75 pp (classified).
3. M. L. Storm, H. Hurwitz, and G. M. Roe, KAPL-783, July 24, 1952, 92 pp (classified).
4. H. Hurwitz, J. B. Nims, and M. L. Storm, KAPL-800, Oct. 7, 1952, 65 pp (classified).
5. J. A. Rich and R. E. Slovacek, KAPL-866, Jan. 7, 1953 (classified).
6. J. W. Motz, Gamma-ray Spectra of the Los Alamos Reactors, Phys. Rev. 86, 1952, pp 753-754.
7. F. C. Maienschein, Oak Ridge Nat. Lab., CF-52-3-1, March 3, 1952, 7 pp (classified).
8. Ibid., CF-52-7-71, July 8, 1952, 16 pp (classified).
9. Ibid., CF-52-8-38, Aug. 8, 1952, 7 pp (classified).
10. F. C. Maienschein and T. A. Love, Oak Ridge Nat. Lab., CF-52-11-124, Nov. 17, 1952, 6 pp (classified).
11. H. L. F. Enlund, Energy Absorption of Capture Gammas, Oak Ridge Nat. Lab., CF-52-6-99 Supplement, Oct. 16, 1952, 4 pp.

CHAPTER 2.8

Shield Optimization with Respect to Weight

E. P. Blizzard

GENERAL THEORY

The optimization of a shield with respect to weight is here assumed to be limited simply to choosing that configuration of available materials which reduces the radiation to a tolerable level and has minimum weight. Broader considerations, such as a reduction in reactor power for the purpose of reducing shield weight with a possible concomitant increase in performance, will not be considered.

The most general expression for shield weight is taken to be an integral of the density of the shield over the whole shield:

$$W = \int_{\text{shield}} \rho(x,y,z) dV \quad (1)$$

where $\rho(x,y,z)$ is the density, dV is a volume element, and x,y,z represent coordinates to specify location within the shield.

While Eq. (1) is the most general expression of the weight, the integration may often be carried out at once, leaving the weight W as a function of relatively few parameters which defined the integration limits in Eq. (1).

Another expression, analogous to Eq. (1), for the biological dose would be excessively complicated and involve unknown cross sections. It is possible, however, to write an expression for the variation in the dose which is caused by a variation in the configuration. The most general expression allows variation both within the shield and on its surface. Although all parameters which specify the configuration should be examined in an optimization, the method is demonstrated here for a variation of one function within the shield (e.g., volume fraction of lead in a lead-water region) and another on the surface (e.g., shield thickness):

$$\delta D = \int_{\text{shield volume}} D'_{\alpha}(x,y,z) \delta \alpha(x,y,z) dV + \int_{\text{shield surface}} D'_t(x,y,z) \delta t(x,y,z) dS \quad (2)$$

where $\alpha(x,y,z)$ is a point function describing the shield composition, for example, the volume fraction of heavy component; $t(x,y,z)$ is a function describing the surfaces of the shield; $\delta t(x,y,z)$, the variation in $t(x,y,z)$, is taken to be normal to the shield surface at (x,y,z) and positive for increase of shield thickness; dV and dS are volume and surface elements, respectively, the latter being taken at the variable (usually outer) surface; and D'_t and D'_{α} are functional derivatives defined in the subsequent paragraphs.

Consider a small element of shield volume $\delta V(x,y,z)$ in which the value of $\alpha(x,y,z)$ is changed by an amount $\delta\alpha(x,y,z)$. If this change causes a change in the dose, D , (at the position outside the shield occupied by personnel) by an amount $\delta_\alpha D$, then the functional derivative is defined* as:

$$D'_\alpha = \lim_{\delta V \delta \alpha \rightarrow 0} \frac{\delta_\alpha D}{\delta V \delta \alpha} \quad (3)$$

D'_α is thus a true observable of an experiment. Thus, if α is the volume-fraction of lead in a spherically symmetrical lead-water shield, a measurement to determine $D'_\alpha(r)$ would consist of inserting a spherical lead shell of thickness $\tau = \delta V / 4\pi r^2$ in the water at r , and observing the change in the dose rate, D . The total thickness is presumed fixed. Then, since $\delta\alpha = 1$:

$$D'_\alpha(r) \cong \frac{\delta_\alpha D}{4\pi r^2 \tau} \quad (4)$$

The quantity usually measured in this connection is the "replacement length," l , which is much like a relaxation length, to describe the effect of replacing water with lead. Thus:

$$l(r) = - \lim_{\tau \rightarrow 0} \frac{\tau D}{\delta_\alpha D} \approx \frac{\tau D}{\delta_\alpha D} \quad (5)$$

or:

$$D'_\alpha(r) = - \frac{D}{4\pi r^2 l(r)} \quad (6)$$

That " l " is a function of r follows from the fact that in a reactor shield the lead would be subjected to a neutron flux which would produce capture and inelastic scattering gamma rays. Clearly, the closer to the core (the smaller the radius), the greater is this secondary production. The optimization procedure will be seen to balance this disadvantage against the savings in weight for a given lead thickness.

Next, if increasing the shield thickness by δt over a small surface element δS produces a change $\delta_t D$ in the dose, then the definition follows that:

$$D'_t = \lim_{\delta S \delta t \rightarrow 0} \frac{\delta_t D}{\delta S \delta t} \quad (7)$$

Thus, if a spherical shell is added to the spherically symmetrical shield of the illustration, then:

$$D'_t(r) = \frac{1}{4\pi r_0^2} \left(\frac{\partial D}{\partial r} \right)_{r=r_0} \quad (8)$$

$$= - \frac{D}{4\pi r_0^2 \lambda(r_0)} \quad (9)$$

where $\lambda(r_0)$ is the dose relaxation length for addition of shield material at r_0 , the outer radius.

*Strictly, $\int_V \delta\alpha dV$ should be used instead of $\delta V \delta\alpha$ in Eq. (3).

By standard methods,* the optimization is shown to require that for all points within the shield:

$$\frac{\partial \rho}{\partial \alpha} + \frac{\Lambda}{D_0} D'_\alpha = 0 \quad (10)$$

and for all points on the surface:

$$\rho + \frac{\Lambda}{D_0} D'_t = 0 \quad (11)$$

where Λ is a LaGrange multiplier and D_0 is the specified tolerance dose.

SPHERICALLY-SYMMETRICAL TWO-COMPONENT SHIELD

For a shield which is spherically symmetrical and consists of two components, the conditions on $l(r)$ and $\lambda(r)$ which will prevail when the shield is optimized are, from Eqs. (10) and (11):

$$\frac{\partial \rho}{\partial \alpha} = \frac{\Lambda}{4\pi r^2 l(r)} \quad (12)$$

$$\rho(r_0) = \frac{\Lambda}{4\pi r_0^2 \lambda(r_0)} \quad (13)$$

or, since $\partial \rho / \partial \alpha = \rho_1 - \rho_2$, the difference in densities of the two components:

$$r^2 l(r) = \frac{\rho(r_0) r_0 \lambda(r_0)}{\rho_1 - \rho_2} = \text{constant} \quad (14)$$

It has been shown³ that this result is equivalent to that of Tonks and Hurwitz,⁴ which was derived with more specific assumptions regarding the actual attenuation functions.

Equation (14) gives the condition which will prevail when a two-component shield is optimized. Although this method gives only a criterion for recognizing an optimized shield, it is always possible to use the criteria of Eqs. (10) and (11) to indicate the direction in which to change a near-optimum shield to approach the optimum.

PARAMETER OPTIMIZATION

In case the shield configuration can be expressed simply in terms of a finite number of parameters, integration of Eqs. (10) and (11) over the shield give the simple result:

$$\frac{\partial W}{\partial \alpha} + \frac{\Lambda}{D_0} \frac{\partial D}{\partial \alpha} = 0 \quad (15)$$

*Reference (1) gives the method in detail; ref. (2) gives the general method.

¹References appear at end of chapter.

$$\frac{\partial W}{\partial t} + \frac{\Lambda}{D_0} \frac{\partial D}{\partial T} = 0 \quad (16)$$

where α is now simply a parameter, and these equations apply for all parameters. Essentially, they say that for any shield parameter, α :

$$\left(\frac{\partial W}{\partial \alpha} \right) / \left(\frac{\partial D}{\partial \alpha} \right) = \text{constant} \quad (15a)$$

and this is the basic criterion to use in simple optimizations.

Example – Consider a box shield about a box source, to be shielded from a person some distance off on one of the prime axes: Clearly, the radiation leaving the near face is more effective than that leaving the sides (which is assumed not negligible because of air scattering). Furthermore, the radiation leaving the sides is more important than that leaving the far (left) face. From Eq. (15), the criterion is that:

$$\frac{\partial W}{\partial \alpha} / \frac{\partial D}{\partial \alpha} = \frac{\partial W}{\partial \beta} / \frac{\partial D}{\partial \beta} = \frac{\partial W}{\partial \gamma} / \frac{\partial D}{\partial \gamma} = \text{constant} \quad (15a,b,c)$$

where α , β , and γ are the three parameters as shown in Fig. 2.8.1, and $\partial D / \partial \alpha$ is the change in the dose at the sensitive location (human figure in the sketch) with a change in

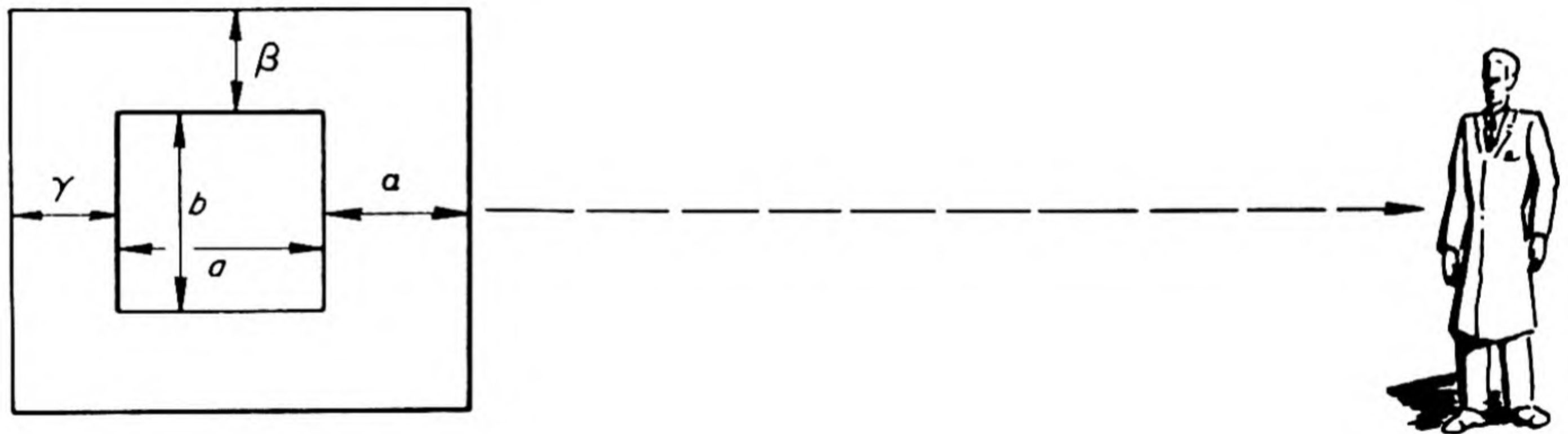


Fig. 2.8.1 — Box-shaped Shield. Submitted by Oak Ridge National Laboratory, Mar. 6, 1953.

the thickness parameter α . In the simple case of exponential attenuation in the shield, with relaxation length λ , the derivatives would simply be:

$$\frac{\partial D}{\partial \alpha} = - \frac{D_n}{\lambda} \quad (17a)$$

$$\frac{\partial D}{\partial \beta} = - \frac{D_s}{\lambda} \quad (17b)$$

$$\frac{\partial D}{\partial \gamma} = \frac{D_f}{\lambda} \quad (17c)$$

where D_n , D_s , and D_f are the dose contributions of radiation from the near, side, and far periphery of the shield, respectively.

Of course, $\partial W/\partial \alpha$ is simply the shield density, ρ , multiplied by the near face area, $(b + 2\beta)^2$.

The equations which will be satisfied for an optimized shield are thus:

$$\frac{\rho(b + 2\beta)^2}{D_n/\lambda} = \frac{4\rho(a + \alpha + \gamma)(b + 2\beta)}{D_s/\lambda} = \frac{\rho(b + 2\beta)^2}{D_f/\lambda} \quad (18)$$

The adjunct condition that the total dose be equal to some specified limit D_0 is expressed by:

$$D_0 = D_n + D_s + D_f \quad (19)$$

REFERENCES

1. E. P. Blizard, ORNL-1471, Secret.
2. Paul Lévy, *Problèmes Concrets d'Analyse Fonctionnelle*, Gauthiers-Villars, Paris, 1951.
3. H. Goldstein and E. P. Blizard, *Reactor Sci. Tech.* 1, No. 2, Aug. 1951, 3 pp (classified).
4. L. Tonks and H. Hurwitz, Jr., KAPL-76, June 8, 1948, 23 pp (classified).
5. Deleted.
6. Deleted.

CHAPTER 2.9

Shield Materials

H. E. Hungerford

SELECTION OF MATERIALS FOR SHIELDS

The selection of materials for shielding nuclear reactors depends upon such factors as the type of reactor, its designated power level, the physical and nuclear characteristics of the shield material under consideration, use and position of the material in the shield, and availability and cost of the material.

Shields for stationary reactors are usually made from inexpensive and easily available materials, and the shield thicknesses are governed primarily by radiation tolerances for personnel or by low background requirements for radiation experiments. Shields for mobile reactors must generally be small and light, and materials are therefore selected for special attenuation properties and placed at positions where these properties will be most effectively employed; such shields may necessarily contain uncommon and expensive materials. Reflectors, coolants, and structural materials must also be considered in shield designs.

TYPES OF SHIELD MATERIALS

NEUTRON SHIELDS

The lightest neutron shields contain a high percentage of hydrogen. Ordinary water makes a cheap but effective hydrogenous shield. Many organic hydrogenous compounds and some metal hydrides make thinner shields than water does for the same amount of neutron attenuation but these materials may be heavier or more susceptible to radiation damage. Useful hydrogenous substances for shields include plastics, petroleum products, rubbers, hydrides, and wood.

Other light elements such as lithium and beryllium have high removal cross sections and therefore may be attractive as shield materials.

Good neutron-attenuation characteristics are exhibited by elements of high atomic density, such as iron, copper, tungsten and lead, but this advantage is offset by their high weight. Such substances are usually employed in a shield for other reasons and are present in conjunction with hydrogenous materials.

GAMMA SHIELDS

Metals of high atomic number and high density make the most effective gamma shields, the most effective being uranium, thorium, lead, gold, and tungsten. Other fairly effective gamma-shielding metals in the medium-weight range include iron, copper, nickel, chromium, and their alloys.

MATERIALS FOR SUPPRESSION OF CAPTURE GAMMA RAYS

Boron and lithium are often used within shields to suppress secondary gamma radiation arising from neutron capture by the shield material (see Table 2.1.6). Boron-containing substances include metallic boron, boron carbide, boron oxide, solutions of boron salts in water and other solvents, plastics and rubber impregnated with boron compounds, sprays and paints containing boron, and a large number of organic compounds containing boron. Lithium-bearing substances are metallic lithium, lithia, lithium hydride, and various vehicles, solvents, and other agents containing lithium compounds.

STRUCTURAL MATERIALS

Materials necessary for structure and support may or may not have good shielding characteristics but must be accounted for in the over-all shield design. These materials include metals, such as steel and aluminum, and non-metallic building materials, such as brick, rock, concrete, and wood.

MISCELLANEOUS MATERIALS

These materials include (1) moderators, such as beryllium and graphite, (2) coolants, such as air and other gases, liquid metals, water, and other fluids, and (3) component and auxiliary equipment, such as control mechanisms, pumps, heat exchangers, piping and ducting, and electronic equipment. The shielding effects of air voids must also be taken into consideration.

POSITION OF MATERIALS WITHIN A SHIELD

The performance of a shield depends to a large extent upon the location of its various components. Most construction materials, such as high-melting metals and alloys, concretes, and bricks, may be used with precaution in all parts of the shield. Shields constructed entirely from these materials are usually safe but also thick and bulky. Most organic substances cannot be used at all in high-flux regions of the inner (primary) shield because of radiation damage and deterioration. Likewise, many metals cannot be used in this region because of warpage, creep, fatigue, changes in crystalline structure, and similar damage resulting from the generation of high temperatures and other radiation effects. While most substances may be used in the outer (secondary) shield where less heat is generated and lower fluxes are encountered, it is important, especially in the design of light-weight shields, to employ the correct materials in their most efficient arrangement. Lamination (the use of layers of different materials) often achieves the most effective shields.

PROPERTIES OF SHIELD MATERIALS

The following information is designed to provide physicists and engineers with a useful source of reference for the physical and nuclear properties of important shield materials. In general, only those materials not dealt with elsewhere in this Handbook are included here. Basic nuclear data are presented elsewhere in this volume, and materials of general interest in the field of reactor design are described in Volume 3. An attempt has been made in the presentation of the following tables to be clear, concise, and uniform throughout. The tables have all been carefully referenced to provide access to the sources of information.

NUCLEAR PROPERTIES

The nuclear properties presented in Tables 2.9.1 through 2.9.6 were selected on the basis of their usefulness to shield design. Included in these tables is information not only for complete materials, but also for compounds found in shield materials. Basic data on cross sections and the like are given elsewhere in this volume.

Table 2.9.1 — Atomic Numbers, Atomic Weights, Densities, and Atomic Densities of the Elements

Element	Atomic number	Atomic weight	Density, * gm/cc	Atomic density† (N), atoms/cc $\times 10^{22}$
H	1	1.008	8.987×10^{-5} (gas at STP) 0.0808 (solid at -252.7°C)	0.00541 4.24
Li	3	6.940	0.53	4.60
Be	4	9.02	1.8	12.0
B	5	10.82	2.5	13.9
C	6	12.01	3.51 (diamond) 2.26 (graphite)	17.6 11.3
N	7	14.008	1.25×10^{-3} (gas at STP) 1.026 (solid at -196.8°C)	0.00537 3.47
O	8	16.000	1.429×10^{-3} (gas at STP) 1.426 (solid at -183°C)	0.00538 4.29
Na	11	22.997	0.97	2.54
Mg	12	24.32	1.74	4.31
Al	13	26.97	2.702	6.03
Si	14	28.06	2.4	5.15
P	15	30.98	1.82 (yellow) 2.20 (red)	3.54 4.28
S	16	32.066	2.07 (rhombic) 1.96 (monoclinic)	3.89 3.68
Cl	17	35.457	3.24×10^{-3} (gas at STP) 1.56 (solid at -33.6°C)	0.0055 2.64
K	19	39.096	0.86	1.32
Ca	20	40.08	1.55	2.33
Ti	22	47.90	4.5	5.64
Cr	24	52.01	7.1	8.22
Mn	25	54.93	7.2	7.89
Fe	26	55.85	7.86	8.48
Co	27	58.94	8.9	9.09
Ni	28	58.69	8.90	9.13
Cu	29	63.54	8.92	8.46
Zn	30	65.38	7.140	6.58
As	33	74.91	5.7	4.58
Zr	40	91.22	6.4	4.23
Ag	47	107.88	10.5	5.67
Cd	48	112.41	8.6	4.61
Sn	50	118.70	7.31 (white)	2.92
Ba	56	137.36	3.5	1.53
W	74	183.92	19.3	6.31
Au	79	197.2	19.3	5.89
Hg	80	200.61	13.546	4.07
Pb	82	207.21	11.34	3.30
Bi	83	209.00	9.8	2.82
Th	90	232.12	11.4	2.90
U	92	238.07	18.90	4.73

* At 20°C , unless otherwise specified

† Normal state, unless otherwise specified; all values calculated

Table 2.9.2 — Calculated Mass Absorption Coefficients of Gamma Rays for the Elements

Atomic number, Z	Element*	Symbol*	Atomic weight, A	μ/ρ , cm ² /gm				
				0.5 mev	1 mev	2 mev	3 mev	6 mev
1†	Hydrogen	H	1.008	0.173	0.126	0.0878	0.0693	0.0449
2	Helium	He	4.003	.0874	.0625	.0425	.0337	.0247
3	Lithium	Li	6.940	.0756	.0540	.0360	.0288	.0216
4†	Beryllium	Be	9.02	.0772	.0564	.0394	.0313	.0212
5	Boron	B	10.82	.0809	.0587	.0437	.0323	.0277
6†	Carbon	C	12.01	.0870	.0635	.0443	.0356	.0246
7†	Nitrogen	N	14.008	.0870	.0636	.0443	.0357	.0251
8†	Oxygen	O	16.0000	.0871	.0636	.0444	.0359	.0255
9	Fluorine	F	19.0000	.0826	.0600	.0421	.0342	.0245
10	Neon	Ne	20.183	.0867	.0627	.0443	.0357	.0260
11†	Sodium	Na	22.997	.0835	.0608	.0427	.0348	.0255
12	Magnesium	Mg	24.32	.0863	.0625	.0440	.0362	.0267
13†	Aluminum	Al	26.97	.0844	.0614	.0431	.0353	.0266
14†	Silicon	Si	28.06	.0873	.0635	.0448	.0367	.0279
15	Phosphorus	P	30.98	.0854	.0617	.0434	.0358	.0274
16	Sulphur	S	32.066	.0879	.0636	.0448	.0368	.0287
17	Chlorine	Cl	35.457	.0846	.0611	.0430	.0357	.0278
18†	Argon	A	39.944	.0795	.0574	.0406	.0336	.0267
19	Potassium	K	39.096	.0859	.0620	.0437	.0366	.0289
20†	Calcium	Ca	40.08	.0885	.0637	.0451	.0378	.0302
21	Scandium	Sc	45.10	.0826	.0593	.0418	.0350	.0284
22	Titanium	Ti	47.90	.0818	.0588	.0413	.0347	.0285
23	Vanadium	V	50.95	.0805	.0577	.0406	.0342	.0283
24	Chromium	Cr	52.01	.0827	.0589	.0417	.0351	.0293
25	Manganese	Mn	54.93	.0817	.0583	.0411	.0348	.0294
26†	Iron	Fe	55.85	.0840	.0598	.0422	.0359	.0305
27	Cobalt	Co	58.94	.0828	.0598	.0416	.0353	.0472
28	Nickel	Ni	58.69	.0866	.0613	.0434	.0369	.0319
29†	Copper	Cu	63.54	.0834	.0588	.0416	.0356	.0309
30	Zinc	Zn	65.38	.0841	.0585	.0418	.0357	.0314
31	Gallium	Ga	69.72	.0820	.0575	.0406	.0349	.0307
32	Germanium	Ge	72.60	.0820	.0572	.0403	.0347	.0308
33	Arsenic	As	74.91	.0824	.0573	.0403	.0350	.0311
34	Selenium	Se	78.96	.0811	.0561	.0395	.0343	.0308
35	Bromine	Br	79.916	.0830	.0572	.0402	.0350	.0318
36	Krypton	Kr	83.70	.0817	.0563	.0397	.0346	.0315
37	Rubidium	Rb	85.48	.0835	.0567	.0400	.0349	.0322
38	Strontium	Sr	87.63	.0842	.0569	.0402	.0351	.0327
39	Yttrium	Y	88.92	.0859	.0577	.0408	.0358	.0335
40	Zirconium	Zr	91.22	.0864	.0578	.0409	.0360	.0338
41	Columblum	Cb	92.91	.0864	.0584	.0414	.0363	.0343
42†	Molybdenum	Mo	95.95	.0879	.0581	.0412	.0362	.0343
43	Masurium	Ma
44	Ruthenium	Ru	101.7	.0883	.0577	.0410	.0361	.0344
45	Rhodium	Rh	102.91	.0902	.0584	.0415	.0367	.0353
46	Palladium	Pd	106.7	.0901	.0577	.0410	.0363	.0351
47	Silver	Ag	107.88	.0920	.0586	.0416	.0369	.0358
48	Cadmium	Cd	112.41	.0912	.0576	.0409	.0363	.0354

Table 2.9.2 — (Continued)

Atomic number, Z	Element*	Symbol*	Atomic weight, A	μ/ρ , cm ² /gm				
				0.5 mev	1 mev	2 mev	3 mev	6 mev
49	Indium	In	114.76	0.0922	0.0578	0.0411	0.0364	0.0357
50†	Tin	Sn	118.70	.0923	.0573	.0407	.0361	.0356
51	Antimony	Sb	121.76	.0928	.0573	.0406	.0361	.0357
52	Tellurium	Te	127.61	.0915	.0560	.0396	.0354	.0351
53†	Iodine	I	126.92	.0954	.0579	.0408	.0364	.0364
54	Xenon	Xe	131.3	.0954	.0571	.0402	.0361	.0363
55	Cesium	Cs	132.91	.0978	.0578	.0406	.0367	.0369
56	Barium	Ba	137.36	.0978	.0572	.0402	.0363	.0367
57	Lanthanum	La	138.92	.100	.0581	.0406	.0368	.0373
58	Cerium	Ce	140.13	.103	.0591	.0411	.0373	.0380
59	Praseodymium	Pr	140.92	.106	.0601	.0417	.0380	.0388
60	Neodymium	Nd	144.27	.107	.0601	.0416	.0379	.0389
61	Promethium	Pm	~146	.109	.0607	.0419	.0385	.0395
62	Samarium	Sm	150.43	.110	.0606	.0415	.0382	.0394
63	Europium	Eu	152	.112	.0613	.0420	.0387	.0400
64	Gadolinium	Gd	156.9	.113	.0608	.0416	.0383	.0397
65	Terbium	Tb	159.2	.115	.0613	.0417	.0386	.0401
66	Dysprosium	Dy	162.46	.116	.0616	.0417	.0386	.0403
67	Holmium	Ho	164.94	.118	.0620	.0419	.0388	.0406
68	Erbium	Er	167.2	.120	.0626	.0422	.0391	.0411
69	Thulium	Tm	169.4	.122	.0632	.0424	.0394	.0415
70	Ytterbium	Yb	173.04	.123	.0633	.0423	.0393	.0415
71	Lutecium	Lu	174.99	.125	.0641	.0427	.0396	.0420
72	Hafnium	Hf	178.6	.126	.0643	.0427	.0396	.0420
73	Tantalum	Ta	180.88	.128	.0650	.0430	.0399	.0424
74†	Tungsten	W	183.92	.131	.0655	.0432	.0400	.0426
75	Rhenium	Re	186.31	.134	.0662	.0436	.0402	.0429
76	Osmium	Os	190.2	.136	.0663	.0436	.0402	.0429
77	Iridium	Ir	193.1	.138	.0670	.0437	.0403	.0431
78†	Platinum	Pt	195.23	.142	.0676	.0444	.0407	.0435
79	Gold	Au	197.2	.145	.0687	.0449	.0409	.0440
80	Mercury	Hg	200.61	.147	.0692	.0451	.0411	.0441
81	Thallium	Tl	204.39	.149	.0695	.0452	.0410	.0442
82†	Lead	Pb	207.21	.152	.0703	.0456	.0413	.0445
83	Bismuth	Bi	209	.156	.0714	.0461	.0417	.0449
84	Polonium	Po	~210	.160	.0728	.0468	.0420	.0456
85	Astatine	At	~221	.157	.0709	.0454	.0409	.0442
86	Radon	Rn	222	.161	.0723	.0462	.0415	.0449
87	Francium	Fr	~224	.164	.0735	.0467	.0419	.0453
88	Radium	Ra	226.05	.168	.0746	.0472	.0423	.0458
89	Actinium	Ac	~227	.173	.0760	.0479	.0429	.0465
90	Thorium	Th	232.12	.175	.0762	.0477	.0428	.0463
91.	Protactinium	Pa	231	.183	.0784	.0489	.0443	.0475
92†	Uranium	U	238.07	.185	.0779	.0483	.0435	.0471

* Names and symbols of elements listed in accordance with International Atomic Weights of 1952

† G. R. White²; all other values are interpolated by M. K. Hullings³

Table 2.9.3 — Molecular Densities of Compounds Found in Shielding Materials and Atomic Densities of Hydrogen in the Compounds

Compound	Chemical formula	Molecular weight	Density, gm/cc	Molecular density (N), molecules/cc ($\times 10^{22}$)	Atomic density of hydrogen in compound (N_H), hydrogen atoms/cc $\times 10^{22}$
Acetic acid	$C_2H_4O_2$	60.05	1.05	1.05	4.21
Aluminum oxide	Al_2O_3	101.94	4.00	2.36	...
Ammonia*	NH_3	17.03	0.771	2.73	8.18
Arsenous oxide	As_2O_3	197.82	3.85	1.17	...
Barium sulfate	$BaSO_4$	233.42	4.50	1.16	...
Beryllium carbide	Be_2C	30.05	1.9	3.81	...
Beryllium oxide	BeO	25.02	3.02	7.27	...
Boron carbide	B_4C	55.29	2.54	2.77	...
Boron oxide	B_2O_3	69.64	1.85	1.60	...
Calcium carbonate	$CaCO_3$	100.09	2.71	1.62	...
Calcium oxide	CaO	56.08	3.32	3.57	...
Cellulose	$(C_6H_{10}O_5)_n$	162.14	1.35	0.502	5.02
Chromic oxide	Cr_2O_3	152.02	5.21	2.06	...
Dodecane	$C_{12}H_{26}$	170.33	0.75	0.302	6.76
Ferric oxide	Fe_2O_3	159.70	5.12	1.93	...
Ferrous oxide	FeO	71.85	5.7	4.78	...
Glycerin	$C_3H_8O_3$	92.09	1.26	0.824	6.59
Heavy water	D_2O	20.028	1.1076	3.32	6.64†
Lead oxide	PbO	223.21	9.2	2.48	...
Limonite	$2Fe_2O_3 \cdot 3H_2O$	373.44	3.8 (ave)	0.61	...
Lithium borohydride	$LiBH_4$	21.79	0.686	1.90	7.58
Lithium hydride	LiH	7.95	.820	6.21	6.21
Lucite	$(C_5H_8O_2)_n$	100.11	1.2	0.722	5.78
Magnesium chloride	$MgCl_2$	95.23	2.32	1.14	...
Magnesium oxide	MgO	40.32	3.65	5.45	...
Neoprene	$(C_4H_5Cl)_n$	88.54	1.23	0.84	4.20
Octane (n)	C_8H_{18}	114.22	0.703	.371	6.68
Pentane (n)	C_5H_{12}	72.15	.626	.523	6.28
Polyisoprene	$(C_5H_8)_n$	68.11	.92	.81	6.51
Polymethyl methacrylate	$(C_5H_8O_2)_n$	100.11	1.2	.722	5.78
Potassium hydroxide	KOH	56.10	2.044	2.62	2.62
Potassium oxide	K_2O	94.19	2.32	1.48	...
Silicon carbide	SiC	40.07	3.17	4.76	...
Silicon oxide	SiO_2	60.06	2.32	2.33	...
Sodium hydroxide	$NaOH$	40.00	2.13	3.20	3.20
Sodium oxide	Na_2O	61.99	2.27	2.21	...
Tetramethyl ammonium borohydride	$(CH_3)_4NBH_4$	89.00	0.813	0.550	8.80
Thorium borohydride	$Th(BH_4)_4$	291.53	2.59	.535	8.56
Titanium hydride	TiH_2	49.92	3.78	4.56	9.12
Titanium hydride (commercial)	TiH_2	49.92	3.25	3.92	7.84
Titanium oxide	TiO_2	79.90	4.26	3.21	...
Uranium hydride	UH_3	241.09	10.86	2.71	8.14
Water	H_2O	18.016	1.00	3.35	6.69

* Values given for the liquid state

† Deuterium atoms/cc

Table 2.9.4 — Densities of Some Additional Shielding Materials and Approximate Atomic Densities of Hydrogen in the Materials

Material	Density, gm/cc	Atomic density of hydrogen in compound (N_H), hydrogen atoms/cc $\times 10^{22}$ (approx.)
Fuel oil	0.89	6.4
Gasoline	0.70–0.74	6.7
Natural rubber	0.92	6.51
Paraffin	0.87–0.91	7.82–8.01
Synthetic rubber	.9–1.2	4.2–8.0
Masonite	1.3	4.7
Woods		
Ash	0.64	2.5
Balsa	.16	0.61
Hickory	.81	3.2
Oak, white	.71	2.75
Pine, white	.67	2.5
Spruce	.47	1.8
Hydrocarbons		
Aliphatic	0.77–0.80	6.6–7.14
With aromatic ring	.85–1.05	4.69–6.85
With 1 alicyclic ring	.823–0.938	6.65–7.40
Petroleum	.8–1.0	7.0–7.7
Other hydrocarbon fuels		7.0–7.2
Esters	.81–1.38	3.4–6.4
Amines, amides, and other nitrogen compounds	.83–1.34	2.85–8.38
Carbonyl compounds*	.85–1.27	2.99–6.45
Silicon compounds	.85–0.89	4.74–6.95
Miscellaneous compounds with boiling point $\sim 200^\circ\text{C}$.74–1.57	

* Includes organic acids, aldehydes, ketones, diketones, acid anhydrides, and the like

Table 2.9.5 — Calculated Mass Absorption Coefficients of Gamma Rays for Various Materials Used in Shielding

Material	Density (ρ), gm/cc	Mass absorption coefficient (μ), cm^{-1}		
		1 mev	3 mev	6 mev
Air*	0.001294	0.0000336	0.0000254	0.0000209
Aluminum	2.7	.166	.0953	.0718
Ammonia (liquid)	0.771	.0612	.0322	.0221
Beryllium	1.85	.104	.0579	.0392
Beryllium carbide	1.9	.112	.0627	.0429
Beryllium oxide (hot-pressed blocks)	2.3	.140	.0789	.0552
Bismuth	9.80	.700	.409	.440
Boral	2.53	.153	.0865	.0678
Boron (amorphous)	2.45	.144	.0791	.0679
Born carbide (hot-pressed)	2.5	.150	.0825	.0675
Bricks				
Fire clay	2.05	.129	.0738	.0543
Kaolin	2.1	.132	.0750	.0552
Silica	1.78	.113	.0646	.0473
Carbon	2.25†	.143	.0801	.0554

Table 2.9.5 — (Continued)

Material	Density (ρ), gm/cc	Mass absorption coefficient (μ), cm ⁻¹		
		1 mev	3 mev	6 mev
Clay	2.2	0.130	0.0801	0.0590
Cements				
Colemanite borated	1.95	.128	.0725	.0528
Plain (1 Portland cement: 3 sand mixture)	2.07	.133	.0760	.0559
Concretes				
Barytes†	3.5	.213	.127	.110
Barytes-boron frits†	3.25	.199	.119	.101
Barytes-limonite†	3.25	.200	.119	.0991
Barytes-lumite-colemanite†	3.1	.189	.112	.0939
Iron-Portland†	6.0	.364	.215	.181
MO (ORNL mixture)	5.8	.374	.222	.184
Portland§ (1 cement: 2 sand: 4 gravel mixture)	2.2	.141	.0805	.0592
	2.4	.154	.0878	.0646
Flesh¶	1	.0699	.0393	.0274
Fuel oil (medium weight)	0.89	.0716	.0350	.0239
Gasoline	.739	.0537	.0299	.0203
Glass				
Boro-silicate	2.23	.141	.0805	.0591
Lead (Hi-D)	6.4	.439	.257	.257
Plate (ave)	2.4	.152	.0862	.0629
Iron	7.86	.470	.282	.240
Lead	11.34	.797	.468	.505
Lithium hydride (pressed powder)	0.70	.0444	.0239	.0172
Lucite (polymethyl methacrylate)	1.19	.0816	.0457	.0317
Paraffin	0.89	.0646	.0360	.0246
Rocks				
Granite	2.45	.155	.0887	.0654
Limestone	2.91	.187	.109	.0824
Sandstone	2.40	.152	.0871	.0641
Rubber				
Butenediene copolymer	0.915	.0662	.0370	.0254
Natural	.92	.0652	.0364	.0248
Neoprene	1.23	.0813	.0462	.0333
Sand	2.2	.140	.0825	.0587
Stainless steel, type 347	7.8	.462	.279	.236
Steel (1% carbon)	7.83	.460	.276	.234
Uranium	18.7	1.46	.813	.881
Uranium hydride	11.5	0.903	.504	.542
Water*	1.0	.0706	.0396	.0277
Wood				
Ash	0.51	.0345	.0193	.0134
Oak	.77	.0521	.0293	.0203
White pine	.67	.0452	.0253	.0175

* G. R. White²

† Graphite theoretical density

‡ Latest concrete mixtures for shielding reported by Gallaher and Kitzes.⁴

§ Elemental composition, wt-%: H, 1.0; O, 52.9; Si, 33.7; Al, 3.4; Fe, 1.4; Ca, 4.4; Mg, 0.2;

C, 0.1; Na, 1.6; K, 1.3

¶ Composition, wt-%: O, 65.99; C, 18.27; H, 10.15; N, 3.05; Ca, 1.52; P, 1.02

Table 2.9.6 — Measured Effective Removal Cross Sections
(ORNL Lid Tank Measurements, corrected to Jan. 1, 1953)

Material	Symbol	Removal cross section, barns
Aluminum	Al	1.2
Copper	Cu	2.0
Graphite	C	0.84
Iron	Fe	2.0
Lead	Pb	3.4

COMPOSITIONS AND PHYSICAL PROPERTIES

In the following tables, an attempt was made to give the latest and most authoritative data compiled from many sources. All information on a given material is grouped as closely together as possible. Much new and heretofore unavailable information on special materials recently developed, or now being developed, is included. The data are grouped as follows: (1) cements and concretes (Tables 2.9.7 through 2.9.24); (2) hydrogenous materials (Tables 2.9.25 through 2.9.38); and (3) miscellaneous materials (Tables 2.9.39 through 2.9.52). The last category includes metals and structural materials other than cements and concretes.

Table 2.9.7 — Compositions of Cements

Material	Portland cement*		Colemanite borated cement†,‡		Plain cement§			
	Wt-% (approx.)	Vol-% (approx.)	Wt-%	Vol-%	1 cement: 3 sand mixture		1 cement: 2 sand mixture	
					Wt-%	Vol-%	Wt-%	Vol-%
MgO	2	2.6	28.1	13.5				
SiO ₂	23	29.6						
Al ₂ O ₃	8	6.2						
Fe ₂ O ₃	4	2.4						
CaO	63	59.2						
Colemanite¶			28.1	20.3				
MgCl ₂			13.4	13.0				
H ₂ O			30.4	53.2	7.5	16.0	10.1	20.3
Portland cement					15.0	21.4	19.8	26.5
Sand**					77.5	62.6	70.1	53.2

* Hool and Johnson⁵

† Rockwell and Roehrenbeck⁶

‡ Elemental composition, wt-%: B, 4.44; H, 4.06; Mg, 20.21; Cl, 10.01; O, 55.8; Ca, 5.47

§ Plain cement percentages calculated from volume ratios of sand plus allowed water content per bag of cement⁷

¶ Ca₂B₆O₁₁·5H₂O

** For composition of sand see Table 2.9.8

Table 2.9.8 — Composition of Sand*

Material	Wt-%	Vol-%
SiO ₂	78.1	73.7
Al ₂ O ₃	6.5	3.83
Fe ₂ O ₃	1.9	0.85
CaCO ₃	2.8	2.43
Na ₂ O	2.3	2.41
K ₂ O	1.4	1.42
H ₂ O	7.0	15.3

* Average of dry compositions (corrected for water content) given by Pirsson⁸

Table 2.9.9 — Physical Properties of Cements

Property	Value or description		
	Colemanite borated cement*		Plain cement 1 cement : 3 sand mixture
	Plain	With 5% Al turnings	
Density, gm/cc	1.95	1.99	2–2.15 (ave)†
Specific heat, gm-cal/gm			0.20‡
Thermal conductivity, Btu/(hr)(ft)(°F)	0.51	0.63	
Tensile strength, lb/sq in.			150–600§
Compressive strength, lb/sq in.	1,500	3,540	500–5600§,¶
Coefficient of expansion, per °F			~6 × 10 ⁻⁶ **
Modulus of elasticity, lb/sq in.	70,000	178,000	~3,000,000**

* Rockwell and Roehrenbeck⁶

† Derived from Portland cement and sand densities as follows:

Portland cement	3.15 gm/cc for solid material
	~1.5 gm/cc for loose powder
Sand	2.65 gm/cc with 7% moisture content

‡ Handbook of Chemistry and Physics⁹

§ Varies according to mechanical analysis (sieve sizes) of sand. The above values are quoted from Mechanical Engineers' Handbook⁷

¶ Varies according to water content. A cement mix using 5½ gal water per 94-lb bag of cement has a compressive strength of approximately 3500 lb/sq in.¹⁰

** From Concrete Engineers' Handbook, 1st edition, by G. A. Hool and N. C. Johnson.⁵ Copyright, 1918. By permission from McGraw-Hill Book Company, Inc., New York

Table 2.9.10—Composition of Ordinary Concrete (Portland Concrete)*

Material	Vol-%	Wt-%
Portland cement†	12.1	8.2
Sand‡	24.3	28.7
Gravel	48.6	56.4
Water	15.0	6.7

* Concrete varies widely according to the mix and raw materials used. This table lists a typical composition§ for a high-strength concrete with mixer's proportions of 1 cement: 2 sand: 4 gravel plus 15% water^{5,7,11}

† For composition of Portland cement, see Table 2.9.7

‡ For composition of sand, see Table 2.9.8

§ Elemental composition, wt-%: H, 1.0; O, 52.9; Si, 33.7; Al, 3.4; Fe, 1.4; Ca, 4.4; Mg, 0.2; C, 0.1; Na, 1.6; and K, 1.3

Table 2.9.11—Physical Properties of Ordinary Concrete (Portland Concrete)*

Property	Value or description
Density, gm/cc	2.3
Specific heat, Btu/(lb)(°F)	0.156
Thermal conductivity, Btu/(hr)(ft)(°F)	1 at 200°F
Tensile strength, lb/sq in.	~350†
Compressive strength, lb/sq in.	3500† after 28 days
Cost	~\$6.50/cu yd

* Gallaher and Kitzes⁴ unless specified otherwise

† General Engineering Handbook¹⁰

Table 2.9.12—Composition of MO Concrete*

Material	Density = 5.2 gm/cc†		Density = 5.8 gm/cc‡
	Wt-%	Vol-%	Wt-%
MgO	7.8	12.5	5.00
Steel punchings ($\frac{3}{4}$ in.)	47.8	62.4	51.4
Steel shot ($\frac{1}{8}$ in.)	21.6		23.1
Steel shot ($\frac{1}{20}$ in.)	14.4		15.4
MgCl ₂	2.4	7.7	1.4
H ₂ O	6.0	17.4	3.7

* This concrete has been found not to stand up under weathering. A new concrete has been developed to replace MO concrete for use in shields (see Iron-Portland concrete, Table 2.9.20)

† Rockwell and Roehrenbeck⁶ reported that this MO mixture had a density of 5.8. Rockwell¹² stated that the original density was probably in error.¹³ Kitzes, Rockwell, and Gallaher¹⁴ give a density of 5.2 from an experimental determination for the mix originally reported⁶ to have a density of 5.8

‡ T. Rockwell^{12,13}

Table 2.9.13 — Physical Properties of MO Concrete

Property	Value or description	
	Density = 5.2 gm/cc*	Density = 5.8 gm/cc†
Specific heat, gm-cal/gm	0.144	
Thermal conductivity, Btu/(hr)(ft)(°F)	2.4	
At 122°F		5.17
At 527°F		3.42
Thermal expansion coefficient, per °C	$\sim 1.0 \times 10^{-5}$	1.1×10^{-5}
Compressive strength, lb/sq in.		4000–5000‡
At room temperature	4000–6000	
At 300°C	1200–3300	
At 500°C	700–1000	
Modulus of elasticity, lb/sq in.	2.5×10^5	
Modulus of rupture, lb/sq in.	1380	
Heat evolved upon setting, watts/lb	<0.224	

* Rockwell and Roehrenbeck⁶ reported this MO mix to have a density of 5.8; the density was experimentally determined to be 5.2 by Kitzes et al¹⁴

† Kitzes et al¹⁴

‡ Developed strength after aging for 3 to 7 days; drops off rapidly because of poor aging characteristics

Table 2.9.14 — Composition of Barytes Concrete

(Gallaher and Kitzes⁴)

Material	Concrete for pouring		Concrete blocks	
	Amount for 1 cu yd, lb	Wt-%	Amount for 1 cu yd, lb	Wt-%
Barytes aggregate, coarse (1 in.)	2660	45.15
Barytes aggregate fine ($\frac{3}{8}$ in.)	2320	39.23
Barytes aggregate, medium ($\frac{1}{2}$ in.)	5270	87.9
Portland cement	550	9.37	500	8.3
Water	370 (44.5 gal)	6.25	230 (27.5 gal)	3.8

Table 2.9.15 — Composition of Barytes Aggregate*
(Gallaher and Kitzes⁴)

Material	Coarse† (1 in.), wt-%	Fine‡ (3/8 in.), wt-%
BaSO ₄	95.9	81.6
Fe	1.0	9.8§
Ca	0.5	0.9
O ₂	1.3	6.2

* Supplied by L. A. Woods and Sons, Sweetwater, Tennessee, at \$18/ton

† Specific gravity = 4.2

‡ Specific gravity = 4.0

§ The increase in Fe content of fine aggregate results from concentration of Fe₂O₃ during crushing

Table 2.9.16 — Physical Properties of Barytes Concrete
(Gallaher and Kitzes⁴)

Property	Value or description
Density, gm/cc	3.5
Specific heat, gm-cal/gm	
At 122°F	0.123
At 392°F	.150
Thermal conductivity, Btu/(hr)(ft)(°F)	
At 122°F	.926
At 212°F	.997
At 392°F	.866
At 482°F	.745
Compressive strength, lb/sq in.	
Age 28 days	3600
Age 112 days	4200
Shear strength, lb/sq in.	845
Expansion upon setting, in./in.	
After 2 to 3 days	8×10^{-4}
After 28 days	5×10^{-4}

Table 2.9.17 — Composition of Barytes-Limonite Concrete*
(Gallaher and Kitzes⁴)

Material	Amount for 1 cu yd, lb	Wt-%	Vol-%
Barytes aggregate, coarse ($\frac{3}{4}$ in.)	2210	40.4	} 44.5
Barytes aggregate, fine ($\frac{3}{8}$ in.)	1050	19.2	
Limonite, crushed ($2\text{Fe}_2\text{O}_3 \cdot 2\text{H}_2\text{O}$)	1220	22.3	19.8
Portland cement, Type I	610	11.1	12.0
Water	384 (46 gal)	7.0	23.7

* Density, 3.25; 7-day compressive strength, 3750 lb/sq in.; other physical properties similar to barytes concrete

Table 2.9.18 — Elemental Compositions of Barytes and Barytes-Limonite Concretes
(Gallaher and Kitzes⁴)

Element	Barytes (blocks), wt-%	Barytes-Limonite, wt-%
Fe	8.78	13.66
H	0.43	1.02
O	31.03	37.70
Mg	0.38	0.23
Ca	4.53	5.37
Ba	41.93	31.97
Na	0.13	0.09
Si	1.74	1.35
Al	0.57	0.50
Mn	.07	.14
S	9.94	7.58

Table 2.9.19 — Description of Several Concretes Recently Developed for Shielding Use
(Gallaher and Kitzes⁴)

Material	Description
Iron-Portland	Dense Portland-cement concrete developed to replace MO concrete; good workability; high density (~6 gm/cc), low water content (~3%)
Colemanite-Barytes	Boron in colemanite ($2\text{CaO} \cdot 3\text{B}_2\text{O}_3 \cdot 5\text{H}_2\text{O}$) acts as gamma suppressor, but high solubility of colemanite retards initial set of Portland cement; this concrete has higher density (3.1 gm/cc) than ordinary concrete, high water content (6–8%), and 1% boron content
Boron Frits-Barytes*	Boron in boron frits acts as gamma suppressor, and boron frit is less soluble than colemanite; thus, detrimental effect on initial set of Portland cement is not so great; this concrete has higher density (3.1 gm/cc) than ordinary concrete, medium water content (5%), and 1% boron content
Lumnite-Colemanite-Barytes†	As an alternate to using Portland cement in barytes-colemanite concrete, lumnite was used and found to retard initial set of cement only slightly; this concrete has higher density (3.1 gm/cc) than ordinary concrete, high water content (~9.3%), and 1% boron content; curing methods were unsatisfactory
Lumnite-Portland-Colemanite Barytes†	Portland cement usually accelerates initial set of lumnite, but addition of colemanite counterbalanced this effect; this concrete has higher density (3.1 gm/cc) than ordinary concrete, high water content (8–10%), and 1% boron content

*For composition of boron frits, see Table 2.9.21

†For composition of lumnite, see Table 2.9.22

Table 2.9.20 — Compositions of Several Concretes Recently Developed for Shielding Use

(Gallaher and Kitizes⁴)

Material	Iron-Portland		Colemanite-barytes		Boron frits-barytes		Lumnite- colemanite-barytes		Lumnite-Portland- colemanite-barytes	
	Amount for 1 cu yd, lb	Wt-%	Amount for 1 cu yd, lb	Wt-%	Amount for 1 cu yd, lb	Wt-%	Amount for 1 cu yd, lb	Wt-%	Amount for 1 cu yd, lb	Wt-%
Iron punchings*	5070	50.4								
SAE shot†										
No. 1110	2280	22.8								
No. 330	1520	15.2								
Portland cement										
Type I	890	8.9	830	14.96	660	12.0				
Type III										
Water	260	2.7	310	5.6	280	5.0	413	7.9	460	8.5
	(31 gal)		(37.5 gal)		(33 gal)		(49.5 gal)		(55 gal)	
Barytes aggregate, ‡ specially graded§			3920	72.22						
Barytes aggregate, ‡ coarse (3/4 in.)										
Barytes aggregate, ‡ fine (3/8 in.)										
Colemanite, specially graded¶			400	7.14						
Colemanite, dust										
Boron frits**					670	12.2	334	6.4	350	6.45
Lumnite††							795	15.2	460	8.5

* Slugs ranging from 1/4 to 1 in. in diameter; rust not removed prior to use

† SAE 1110 and SAE 330 shot were 1/8 and 1/32 in. in diameter, respectively

‡ For composition of barytes aggregate, see Table 2.9.15

§ 95–100% passing through No. 4 sieve size

¶ 100% passing through No. 16 sieve size

** For composition of boron frits, see Table 2.9.21

†† For composition of lumnite, see Table 2.9.22

Table 2.9.21 — Analysis of Boron Frits*
(Gallaher and Kitzes⁴)

Material	Wt-%
SiO ₂	31.00
Al ₂ O ₃	1.70
B ₂ O ₃	27.40
CaO	5.20
BaO	12.90
ZnO	6.70
Na ₂ O	12.20
K ₂ O	1.00
F	1.90

* Boron frit is formed by fritting borax with silica and is obtained from the Chicago Vitreous Enamel Products Co., Cicero, Illinois

Table 2.9.22 — Analysis of Lumnite*
(Gallaher and Kitzes⁴)

Material	Wt-%
SiO ₂	9.1
FeO	5.9
Fe ₂ O ₃	4.7
Al ₂ O ₃ + TiO ₂	41.6
CaO	36.8
MgO	1.0
SO ₃	0.17
Insoluble residue	.70

* A calcium aluminate hydraulic cement manufactured by Universal Atlas Cement Co., New York, N. Y.

Table 2.9.23 — Elemental Compositions of Several Concretes Recently Developed for Shielding Use
(Gallaher and Kitzes⁴)

Element	Iron-Portland, wt-%	Colemanite- Barytes, wt-%	Boron Frits- Barytes, wt-%	Lumnite- Colemanite- Barytes, wt-%	Lumnite-Portland- Colemanite- Barytes, wt-%
Fe	87.50	1.03	2.19	3.07	1.87
H	0.33	0.85	0.56	1.09	1.10
B		.98	1.04	0.88	1.02
O	5.82	34.89	33.80	36.95	36.98
Mg	0.13	0.22	0.23	0.14	0.20
Ca	3.96	8.46	6.26	5.48	7.67
Ba		40.70	40.13	38.59	38.03
Na		0.11	1.21	0.11	0.11
Si	0.91	1.76	3.31	.96	1.49
Al	.33	0.61	0.64	1.76	1.32
Mn	.35	.01	.02	0.12	0.04
S	.05	9.63	9.15	9.06	8.97
Zn			0.66		
K			.10		
F			.23		
Ti				1.27	0.071

Table 2.9.24 — Densities and Compressive Strengths of Several Concretes Recently Developed for Shielding Use
(Gallaher and Kitzes⁴)

Concrete	Density, gm/cc	Compressive strength, lb/sq in.
Iron-Portland	5.8–6.0	3663 (age–32 days) 5288 (age–91 days) 2500 (after 6-day cure)
Colemanite-barytes	3.1–3.2	
Boron frits-barytes	3.1	
Lumnite-colemanite-barytes	3.1	~3500
Lumnite-Portland-colemanite-barytes	3.1	3000 (after 6-day cure)

Table 2.9.25 — Physical Properties of Ammonia (Liquid), NH_3

Property	Value or description*
Appearance	Pungent colorless liquid
Density, gm/cc	
Of solid (-79°C)	0.817
Of liquid (-77.7°C)	.771
Specific heat of liquid, gm-cal/gm	
At -60°C	1.047
At 0°C	1.098
At 20°C	1.125
At 100°C	1.48
Heat of vaporization, gm-cal/gm	
At -33.35°C	327.1
At -20°C	317.6
At -10°C	309.7
At 0°C	301.6
Heat of fusion (m.p., -77.7°C),	94.15
Heat of formation, kg-cal/mol	-11.00 (heat evolved)
Free energy of formation, kg-cal/mol	-3.94 (heat evolved)
Thermal conductivity, Btu/(hr)(ft)($^\circ\text{F}$)	0.29
Melting point, $^\circ\text{C}$	-77.7
Boiling point, $^\circ\text{C}$	-33.35
Solubility in water (0°C), parts per 100	89.9
Critical constants	
Temperature, $^\circ\text{C}$	132.9
Pressure, lb/sq in.	1651 (112.3 atm)
Density, gm/cc	0.235

* Handbook of Chemistry,¹⁵ Handbook of Chemistry and Physics,⁹ and Chemical Engineers' Handbook¹⁶

Table 2.9.26 — Composition of Fuel Oil*†

Density (ave), gm/cc	Composition, wt-%				
	C	H	S	N	O
0.89	85.62	11.98	0.35	0.50	0.60

* Fuel oil is comprised of the crude-oil fractions distilling between 200° and 370°C ; its chemical composition and specific gravity vary with the type of crude oil. Mid-Continent crude oils yield a fuel oil (specific gravity, 0.89) which is a mixture predominantly of saturated hydrocarbons with a small percentage of unsaturated chains and aromatics

† Reprinted from Mechanical Engineers' Handbook,[†] 5th edition, edited by L. S. Marks. Copyright, 1951. By permission from McGraw-Hill Book Company, Inc., New York

Table 2.9.27 — Physical Properties of Fuel Oil

Property	Value or description*
Density (ave), gm/cc	0.89
Specific heat (21°–58°C), gm-cal/gm	.51
Thermal conductivity (13°C), cal/(sec)(cm)(°C)	0.355×10^{-3}
Thermal expansion coefficient (24°–120°C), per °C	$.955 \times 10^{-3}$
Boiling point range, °C	210–360
Flash point, °C	
Open cup	250
Closed cup	100–200
Viscosity (15.6°C), cp	660
Susceptibility to spontaneous heating	None

* Handbook of Chemistry,¹⁵ Handbook of Chemistry and Physics,⁹ and Chemical Engineers' Handbook¹⁶

Table 2.9.28 — Composition of Gasoline*†

Density at 60°F, gm/cc	Composition, wt-%		
	C	H	S
0.713	84.3	15.7	...
.739	84.9	14.76	0.08

* The composition^{†,17} of gasoline varies with the method of production and the type of crude oil from which it is obtained; in general it is made up of saturated aliphatic compounds ranging from C_5H_{12} to $C_{12}H_{26}$, with an average composition corresponding to C_8H_{18} (octane)

† Reprinted from Mechanical Engineers' Handbook,⁷ 5th edition, edited by L. S. Marks. Copyright, 1951. By permission from McGraw-Hill Book Company, Inc., New York

Table 2.9.29 — Physical Properties of Gasoline

Property	Value or description*
Density, gm/cc	0.70–0.74
Specific heat (20°C), gm-cal/gm	0.5
Thermal conductivity (4°C), cal/(sec)(cm)(°C)	0.45×10^{-3}
Boiling point, °C	38–205
Flash point (closed cup), °C	–45
Vapor pressure (room temp.), mm Hg	2.0
Explosive limits, % by vol. in air	
Upper	6
Lower	1.3
Susceptibility to spontaneous heating	None

* Handbook of Chemistry,¹⁵ Mechanical Engineers' Handbook,⁷ and Collier's Encyclopedia¹⁷

Table 2.9.30 — Composition and Physical Properties of Lucite (Plexiglass)*

Property	Value or description
Chemical formula	Polymethyl methacrylate, $(C_5H_8O_2)_n$
Appearance	Transparent colorless or whitish thermoplastic; hard
Density, gm/cc	1.18–1.2
Specific heat, gm-cal/gm	0.35
Thermal conductivity, cal/(sec)(cm)(°C)	$4-6 \times 10^{-4}$
Thermal expansion coefficient, per °C	$7-9 \times 10^{-5}$
Elongation at yield, %	1–10
Tensile strength, lb/sq in.	4,000–6,000
Flexural strength, lb/sq in.	10,000–20,000
Compressive strength, lb/sq in.	9,000–15,000
Heat distortion point, °C	58–93
Decomposition (thermal) temperature, °C	170–250
Water absorption, %	0.3–0.6
Flammability, in./min	$\frac{1}{2}$ –1 (slight)

* Reprinted from Handbook of Chemistry,¹⁵ 7th edition, edited by N. A. Lange. Copyright, 1949. By permission from Handbook of Publishers, Inc., Sandusky, Ohio

Table 2.9.31 — Composition and Physical Properties of Rubber*

Property	Value or description		
	Natural rubber	Neoprene	Butenediene copolymer
Chemical formula	Polyisoprene, $(C_5H_8)_n$	$(C_4H_5Cl)_n$	$C_{365}H_{727}$
Density, gm/cc	0.92	1.23	0.915
Specific heat, gm-cal/gm	.45	~0.45	.464
Thermal conductivity, Btu/(hr)(ft)(°F)	1.07	1.07	...
Elongation (gum stock), %	775	600	800
Resilience, %	90	75	50
Tensile strength (gum stock), lb/sq in.	3100	2800	2000
Tear resistance, lb/sq in.	1640	1100	1000
Creep (70°C)	26	62	...
Maximum usable temperature, °C	80	65	65
Brittle point, °C	–56	–40	–45

* Reprinted from Handbook of Chemistry,¹⁵ 7th edition, edited by N. A. Lange. Copyright, 1949. By permission from Handbook of Publishers, Inc., Sandusky, Ohio

Table 2.9.32 — Composition and Physical Properties of Paraffin*

Property	Value or description†
Density range, gm/cc	0.87–0.91
Specific heat (0°–20°C), gm-cal/gm	0.694
Thermal conductivity (0°C), cal/(sec)(cm)(°C)	0.688×10^{-3}
Thermal expansion coefficient (20°C), per °C	5.88×10^{-4}
Melting point, ‡ °C	48–56
Boiling point, °C	>370
Flash point, °C	
Open cup	199
Closed cup	221

* Paraffin is composed of the heavy waxy components of crude-oil distillate, which are solid at room temperature. They are mainly saturated compounds with a formula ranging from $C_{18}H_{38}$ to $C_{35}H_{72}$ (average composition near $C_{25}H_{52}$)^{15,17}

† Handbook of Chemistry and Physics,⁹ Handbook of Chemistry,¹⁵ and Collier's Encyclopedia¹⁷

‡ Commercial types of paraffin wax are usually designated by their melting point range, three of which are: (1) 118°–120°F; (2) 122°–124°F, and (3) 130°–132°F

Table 2.9.33 — Typical Analyses of Surface and Ground Waters in the United States*

Material	Analyses of various types of water, † ppm				
	Type A	Type B	Type C	Type D	Type E
Silica (SiO ₂)	2.4	12	10	9.4	22
Iron (Fe)	0.14	0.02	0.09	0.2	0.08
Calcium (Ca)	5.8	36	92	96	3.0
Magnesium (Mg)	1.4	8.1	34	27	2.4
Sodium (Na)	1.7	6.5	8.2	183	215
Potassium (K)	0.7	1.2	1.4	18	9.8
Bicarbonate (HCO ₃)	14	119	339	334	549
Sulfate (SO ₄)	9.7	22	84	121	11
Chloride (Cl)	2.0	13	9.6	280	22
Nitrate (NO ₃)	0.54	0.1	13	0.2	0.52
Total dissolved solids	31	165	434	983	564
Total hardness as CaCO ₃	20	123	369	351	17

* Reprinted from Handbook of Chemistry,¹⁵ 7th edition, edited by N. A. Lange. Copyright, 1949. By permission from Handbook Publishers, Inc., Sandusky, Ohio

† Type A: Natural soft water; contains around 30 ppm of dissolved solids; found in rivers and lakes of New England, New York, and mountainous regions of U. S.; high corrosive action

Type B: Intermediate-hard water; contains well over 100 ppm of dissolved solids; typical of Great Lakes and St. Lawrence waterway; may need to be softened for industrial use

Type C: Hard water from wells 30 to 60 ft deep; contains well over 300 ppm of dissolved solids; commonly used in heart of U.S. for public supplies; must be softened for domestic and industrial uses

Type D: Hard water from wells 2,000 ft deep; contains more chloride than Type C and high number of dissolved solids; not common; must be softened for industrial use

Type E: Naturally softened water from wells 300 ft deep or more; high totality of dissolved solids but hardness very low; may be highly colored; common in Atlantic and Gulf coastal plain

Table 2.9.34 — Physical Properties of Water at Various Temperatures*
(Handbook of Chemistry¹⁵)

Temperature, °C	Density, † gm/cc	Specific heat, gm-cal/gm	Heat of vaporization, gm-cal/gm	Thermal conductivity, cal/(sec)(cm)(°C)	Cubical expansion, ‡ per °C	Viscosity, cp
0	0.99984	1.00874	595.9			1.7921
4	0.99997§					
4.1				1.29×10^{-3}		
12				1.36×10^{-3}		
15		1.0000				
20	0.99820	0.99859	584.9		8.18×10^{-5}	1.0050
40.8				1.555×10^{-3}		
50	0.98804	0.99829	568.5			
80		1.00239	551.5		2.81×10^{-4}	0.3565
100	0.95835	1.00645	539.55			

* Critical constants: Temperature, 0°C; pressure, 217.72 atm; density, 0.4 gm/cc

† Absolute values

‡ Approximate values

§ Greatest density

Table 2.9.35 — Composition of Various Types of Wood*

Type of wood	Composition, wt-%					
	Cellulose	Lignin	Resins and polyoses†	Acetic acid	Inorganic ash‡	Moisture
Balsa	54.2	26.5	4.93	5.80	2.12	6.47
Hickory	56.2	23.4	8.71	2.51	0.69	8.49
Spruce	41.5	28.0	25.9	1.39	.31	2.90
White ash	53.4	28.4	8.80	2.66	.34	6.40
White oak	48.7	32.7	8.25	2.57	.43	7.35
White pine	54.2	26.5	14.5	1.43	.43	2.94
						87.7
						37.7
						66.1
						50.8
						45.3
						49.4

* From E. Hägglund¹⁸ and Handbook of Chemistry,¹⁵ 7th edition, edited by N. A. Lange. Copyright, 1949. By permission from Handbook Publishers, Inc., Sandusky, Ohio

† Polyoses include pentosan, hexosan, mannan, xylan, and saccharides; resins include proteins, fats, and terpenes

‡ Ash content varies; contains small amounts of K₂O, CaO, MgO, P₂O₅, Fe₂O₃, SO₃, SiO₂, and Na₂O. First three compounds are the most abundant

Table 2.9.36 — Physical Properties of Various Types of Wood

Property	Balsa	Hickory	Spruce	White ash	White oak	White pine
Average density, * gm/cc	0.16	0.81	0.47	0.64	0.71	0.67
Density range, † gm/cc	0.11–0.20	0.60–0.93	0.31–0.55	0.51–0.85	0.46–0.85	0.31–0.70
Specific heat, ‡ gm-cal/gm	Between 0.45 and 0.65 for most woods§					
Thermal conductivity, ** cal/(sec)(cm)(°C)						
Parallel to grain						
Perpendicular to grain	0.000115				.00083	.00083
Thermal expansion coefficient, per °C	$2-5 \times 10^{-6}$ for most woods§					
Tensile strength, ** lb/sq in.						
Bending stress at proportional limit, †† lb/sq in.		10,900	6,500		4,400	5,100
Maximum crushing strength (parallel to grain), †† lb/sq in.		8,970	5,590		7,900	6,000
Maximum shearing strength, †† lb/sq in.		2,140	1,070		7,040	4,840
Hardness, ††, †† lb						860
End			630	1,680	1,420	500
Side			490	1,260	1,330	400

* Air-dried wood¹⁵† Hägglund¹⁸

‡ The specific heat of practically all woods when oven-dry is 0.327 gm-cal/gm

§ Chemical Engineers' Handbook¹⁶¶ Mechanical Engineers' Handbook⁷** From Handbook of Chemistry,¹⁵ 7th edition, edited by N. A. Lange. Copyright, 1949. By permission from Handbook Publishers, Inc., Sandusky, Ohio†† Handbook of Engineering Fundamentals¹⁹‡‡ Load required to embed an 0.444-in. ball to $\frac{1}{2}$ its diameter in the wood

Table 2.9.37 — Relationship Between Density of Wood and Volume Composition
(E. Hägglund¹⁸)

Density, gm/cc	Composition, vol-%	
	Cell walls	Pores
0.1	6.7	93.3
.2	13	87
.3	20	80
.4	27	73
.5	34	66
.6	40	60
.7	47	53
.8	53	47
.9	60	40

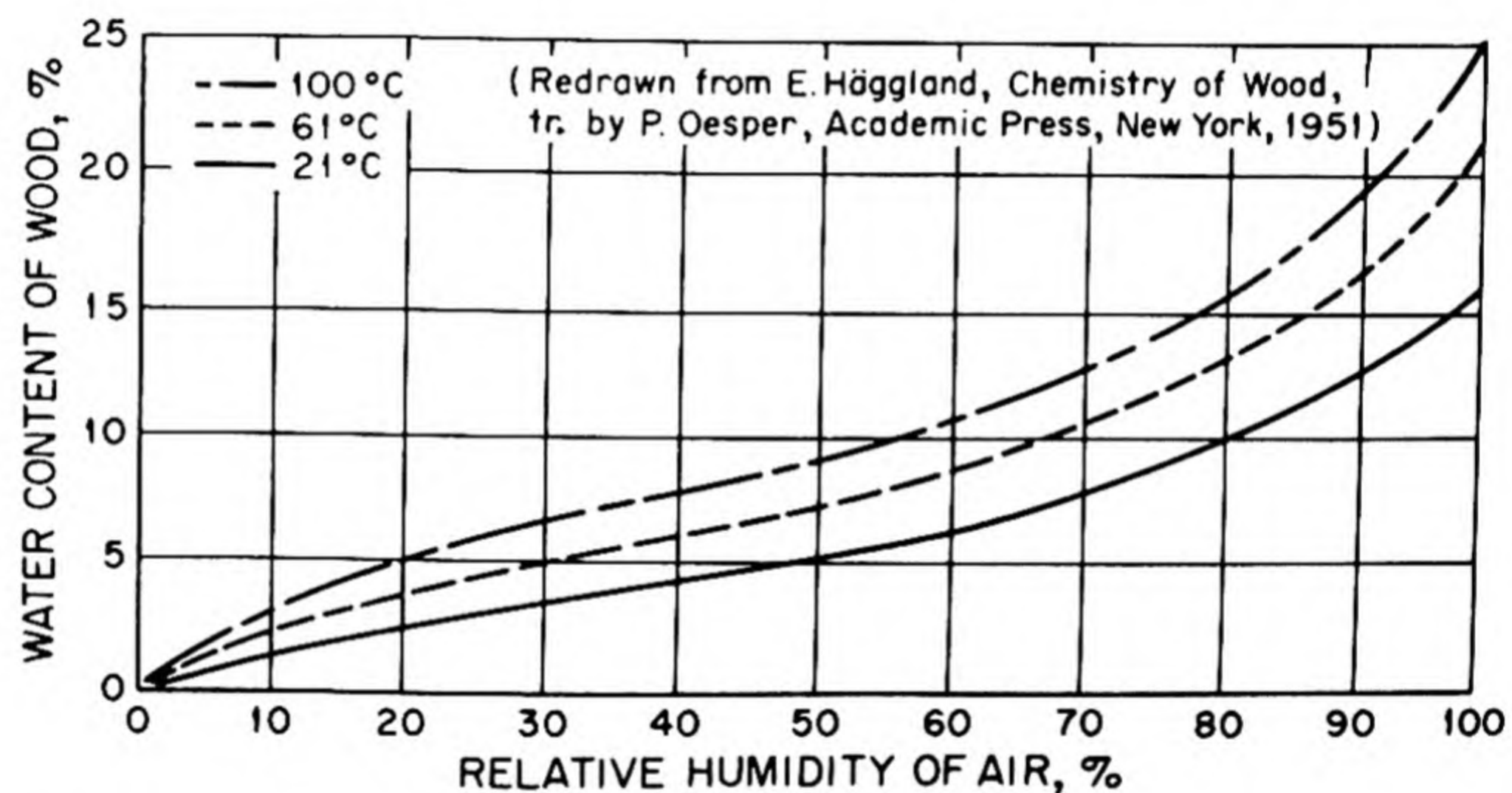


Fig. 2.9.1 — Relationship Between Water Content of Air-dried Wood and Relative Humidity of the Air at Various Temperatures. Submitted by Oak Ridge National Laboratory, Mar. 16, 1953; redrawn from Hägglund¹⁸

Table 2.9.38 — Composition and Physical Properties of Masonite

Property	Value or description
Composition*,†	Wood-fiber board of the Masonite Corp. produced from by-product wood chips reduced to cellulose fibers by high-pressure steam; contains ~6% hydrogen
Density,† gm/cc	1.3
Tensile strength,‡ lb/sq in.	7,000–8,000
Flexural strength,‡ lb/sq in.	12,000–13,000
Modulus of rupture,* lb/sq in.	5,000–15,000
Usefulness in shields§	Slows down fast neutrons; absorbs some thermal neutrons; has little effect on gamma rays

* Brady²⁰

† Quinn and Thompson²¹

‡ Simonds, Weith, and Bigelow²²

§ Hanford Works Technical Manual²³

Table 2.9.39 — Densities and Boiling-point Ranges of Various Organic Compounds
(NEPA-1381²⁴)

Type of compound	Formula range	Density range, gm/cc	Boiling point, °C
Hydrocarbons			
Aliphatic	C ₁₆ H ₃₄ to C ₂₆ H ₅₄	0.77–0.80	136–242*
With aromatic ring	C ₁₄ H ₂₀ to C ₃₃ H ₇₂	.85–1.05	133–334*
With 1 alicyclic ring	C ₁₄ H ₂₈ to C ₃₁ H ₆₀	.823–0.938	123–208*
Petroleum		.8–1.0	700–1000
Esters		.81–1.38	146–370
Amines, amides, and other nitrogen compounds		.83–1.34	180–350
Carbonyl compounds†		.85–1.27	180–350
Silicon compounds		.85–0.89	165–450
Miscellaneous compounds with boiling point 200°C		.74–1.57	187–215

* Temperatures at 10-mm-Hg pressure

† Includes organic acids, aldehydes, ketones, diketones, acid anhydrides, and the like

Table 2.9.40 — Composition of Dry Air*

Component	Symbol	Composition	
		Wt-%	Vol-%
Nitrogen	N ₂	75.50	78.06
Oxygen	O ₂	23.15	20.99
Argon	A	1.292	0.9323
Carbon dioxide	CO ₂	0.05	.03
Hydrogen	H ₂	.0007	.01
Neon	Ne	.0014	.0018
Helium	He	.000065	.0005
Krypton	Kr	.0003	.0001
Ozone	O ₃	.0001	.00006
Xenon	Xe	.00004	.000009

* Reprinted from Handbook of Chemistry,¹⁵ 7th edition, edited by N. A. Lange. Copyright, 1949. By permission from Handbook Publishers, Inc., Sandusky, Ohio

Table 2.9.41 — Density of Air at Various Temperatures

Temperature, °C	Density of dry air at 760 mm Hg,* gm/liter	Moist air†		
		Relative humidity, %	Vapor pressure, mm Hg	Density, gm/liter
-147	0.92‡			
-20	1.396			
0	1.293	45	2.090	1.292
		81	3.732	1.291
20	1.205	44	7.72	1.192
		74	13.05	1.183
50	1.092	45	41.63	1.070
		75	69.38	1.055
100	0.9458			
200	.7457			
300	.6166			
400	.5248			

* From Handbook of Chemistry,¹⁵ 7th edition, edited by N. A. Lange. Copyright, 1949.
By permission from Handbook Publishers, Inc., Sandusky, Ohio

† Handbook of Chemistry and Physics⁸

‡ Liquid, value given in gm/cc

Table 2.9.42 — Compositions of Various Types of Bricks*

Type of brick	Composition, wt-% (ave)					
	SiO ₂	Al ₂ O ₃	Fe ₂ O ₃	TiO ₂	MgO	CaO
Fire clay (high-heat duty)	50-57	36-42	1.5-2.5	1.5-2.5
Kaolin (white)	52	45.4	0.6	1.7	0.2	0.1
Silica	96	1	1	2

* Reprinted from Mechanical Engineers' Handbook,[†] 5th edition, edited by L. S. Marks.
Copyright, 1951. By permission from McGraw-Hill Book Company, Inc., New York

Table 2.9.43 — Physical Properties of Various Types of Bricks*

Property	Fire clay (high-heat duty)	Kaolin (white)	Silica
Density, † gm/cc	2.1	2.1	1.8
Specific heat, gm-cal/gm	0.23	0.22	0.23
Thermal conductivity, Btu/(hr)(ft ² /in.)(°F)			
At 400°F	6		8
At 800°F	7	11	10
At 1200°F	8	12	12
At 2400°F	12	14	15
Mean thermal expansion coefficient, per °F	0.27×10^{-5}	0.23×10^{-5}	$0.46 \times 10^{-5} \ddagger$
Weight of $9 \times 4\frac{1}{2} \times 2\frac{1}{2}$ in. brick, lb.	7.5	7.7	6.5
Porosity, %	20 (ave)	18	25 (ave)
Reheat shrinkage, %	0 to ± 1.5 at 2550°F	-0.7 to 1.0 at 2910°F	0.5 to 0.8 at 2640°F
Deformation under load, %	2.5 to 10 at 2460°F and 25 lb/sq in.	0.5 at 2640°F and 25 lb/sq in.	Shears at 2900°F and 25 lb/sq in.
Fusion point, °F	3130 (approx.)	3200	3075 (approx.)
Spalling resistance	Good	Excellent	Poor §

* Reprinted from Mechanical Engineers' Handbook,[†] 5th edition, edited by L. S. Marks. Copyright, 1951. By permission from McGraw-Hill Book Company, Inc., New York

† Approximate; calculated

‡ Up to 0.56 at red heat

§ Excellent if left above 1200°F

Table 2.9.44 — Compositions of Lead and Silica Glasses

Material	Lead glass*, †		Silica glass, ‡ wt-%	
	Wt-%	Vol-%	Plate glass§	Boro-silicate glass
PbO	81.0	53.1		
SiO ₂	17.3	44.5	72	80.6
TiO ₂	1.35	1.9		
As ₂ O ₃	0.35	0.5		
CaO			15	0.8
Na ₂ O			13	3.8
K ₂ O				0.2
Al ₂ O ₃				2.0
B ₂ O ₃				11.9

* "Hi-D" glass made especially for radiation shielding by Penberthy Instrument Co., Inc., Seattle, Washington. Elemental composition, wt-%: Pb, 75.19; O, 15.65; Si, 8.08; Ti, 0.81; As, 0.27

† Kernohan and McCammon²⁵

‡ From Van Nostrand's Scientific Encyclopedia,²⁶ 2d edition. Copyright, 1947. By permission from D. Van Nostrand Company, New York

§ Average values for several glasses

Table 2.9.45 — Physical Properties of Lead and Silica Glasses

Property	Lead glass* (Hi-D glass)	Silica glass	
		Plate glass†	Boro-silicate glass‡
Appearance	Light yellow tint; colorless in thin sections		
Density, gm/cc	6.4	2.4	2.23
Specific heat, gm-cal/gm		0.25	0.20
Thermal conductivity, cal/(sec)(cm)(°C)		2.37×10^{-3}	2.8×10^{-3}
Thermal expansion coefficient, per °C		0.49×10^{-6}	0.325×10^{-5}
Tensile strength, lb/sq in.		4,000	4,000–10,000
Strain point, °F		890	960
Softening point, °F		2,600	1,510
Index of refraction	1.96	1.47	1.47
Gamma shielding characteristic	Approximately equivalent of steel; 55% as effective as lead§		

* Kernohan and McCammon²⁵† From Handbook of Chemistry,¹⁵ 7th edition, edited by N. A. Lange. Copyright, 1949. By permission from Handbook Publishers, Inc., Sandusky, Ohio‡ Values for Corning No. 7740 glass¹¹

§ Manufacturer's claim

Table 2.9.46 — Composition of Various Types of Commercial Iron
(Metals Handbook²⁷)

Component	Composition, wt-%			
	Armco ingot iron	Wrought iron (Byers No. 1)	Cast iron (gray)	Steel (SAE-1095)
Fe	99.83	98.475	92.95	97.13
O	0.11	In slag
S	.025	0.01	0.10	0.014
Mn	.017	.015	.65	.36
C	.012	.08	3.4	1.02
P	.005	.062	0.3	0.013
Si	Trace	.158	2.6	.08
Slag	...	1.20
Cu	0.05

Table 2.9.47 — Physical Properties of Various Types of Commercial Iron
(Metals Handbook²⁷)

Property	Ingot iron	Wrought iron (Byers No. 1)	Cast iron (gray)	Carbon steel (SAE-1095)
Appearance	Pure iron is bright lustrous metal; impurities change appearance (to gray or black) and physical properties			
Density, gm/cc	7.86	7.70	6.95–7.35	7.83
Specific heat, gm-cal/gm	0.133*	0.1152* (15°–100°C)	0.1189* (20°–100°C)	0.116 (50°–100°C)
Thermal conductivity, cal/(sec)(cm)(°C)	(18°–100°C) ~0.175 (18°C) ~.15 (200°C)	0.144 (18°C)	0.11	0.113 (0°C) .106 (200°C)
Thermal expansion, per °C	$11.7 \times 10^{-6} \dagger$ (20°C) $12.7 \times 10^{-6} \dagger$ (100°C)	11.4×10^{-6} (18°–100°C)	10.5×10^{-6} (0°–100°C)	11.5×10^{-6} (15°–75°C)
Elongation, %	45 (16°C) 26.5 (200°C)	25–40†	25–30†	22*
Tensile strength, lb/sq in.	49,500 (16°C) 65,600 (200°C)	42,000–52,000	25,000–50,000	70,000
Compression strength, lb/sq in.	19,400‡		65,000–160,000	
Melting point, °C	1,539 ± 1	1,510*	1,230*	1,430*
Brinell hardness	82–100¶	105	150–220	402**

* Handbook of Chemistry¹⁵

† Alpha iron

‡ Percent in 8 in.

§ Percent in 2 in.

¶ Hot-rolled rods or plates

** Quenched⁹

Table 2.9.48 — Composition and Physical Properties of Commercial Lead
(Handbook of Chemistry¹⁵ and Handbook of Chemistry and Physics⁹)

Property	Value or description
Composition of commercial lead	99.8% Pb, 0.2% As
Appearance	Soft heavy metal, malleable and ductile. Color, gray
Density (20°C) gm/cc	11.34
Specific heat (0°–100°C), gm-cal/gm	0.0305
Thermal conductivity (18°C), cal/(sec)(cm)(°C)	0.0827
Thermal expansion coefficient (20°C), per °C	29.1×10^{-6}
Tensile strength, lb/sq in.	1600
Yield strength, lb/sq in.	710
Ultimate strength, lb/sq in.	2000–3000
Melting point, °C	327.5
Brinell hardness	~4.2 (commercial); 2.9–3.0 (pure)

Table 2.9.49 — Composition of Various Types of Natural Rock*

Material	Composition, wt-%		
	Granite	Sandstone	Limestone
SiO_2	70	85	2
Al_2O_3	14	17	0.2
Fe_2O_3	2	2	.4
FeO	1
MgO	1	...	5.0
CaO	3	1	45
CaCO_3	46
Na_2O	3.5	2.5	...
K_2O	5	2	...
H_2O plus organic	1.5	0.5	1.4

* Natural rock varies in composition from locality to locality.
The above values are averages derived from Pirsson⁸

Table 2.9.50 — Physical Properties of Various Types of Natural Rock*

Property	Granite	Sandstone	Limestone
Appearance	Evenly granular; color varying from white to dark gray, depending on amount of feldspar in it	Grains of quartz held together by cementing agent; yellow, red, or brown color most common	Fine-grained rock, varying from whitish color to yellow, brown, or gray
Average density, gm/cc	2.65	2.4	2.7
Density range, gm/cc	2.5–3.1	2.24–2.4	2.3–2.9
Mean specific heat, gm-cal/gm	0.195	0.22	0.217
Thermal conductivity, Btu/(hr)(ft)(°F)	1.0–2.32	1.1	0.3–0.75
Coefficient of thermal expansion, per °C	8.3×10^{-6}	$7-12 \times 10^{-6}$	9×10^{-6}
Crushing strength, lb/sq in.	15,000–40,000	1,500–15,000†	3,000–40,000†
Pore vol, % of total	0.15	5–30	0–15

* Handbook of Chemistry and Physics,⁹ Kent's Mechanical Engineers' Handbook,¹¹ Mechanical Engineers' Handbook,⁷ and Pirsson⁸

† Great range owing to variations in the porosity of the rock

Table 2.9.51 — Composition of Stainless Steel, Type-347* (High-chromium steel)

Material	Composition	
	Wt-%	Vol-%
Fe	68.35	66.06
Cr	18.0	19.29
Ni	10.5	8.96
Mn	2.00	2.13
Si	1.00	3.19
C	0.08	0.15
P	.04	.15
S	.03	.07

* Handbook of Chemistry¹⁵ and Handbook of Chemistry and Physics⁹

Table 2.9.52 — Physical Properties of Stainless Steel, Type-347*

Property	Value or description*
Density, gm/cc	7.8
Specific heat, gm-cal/gm	0.113
Thermal conductivity, cal/(sec)(cm)(°C)	.042
Thermal expansion coefficient, per °C	17.3×10^{-6}
Elongation, %	40
Tensile strength, lb/sq in.	85,000
Yield strength, lb/sq in.	33,000
Ultimate strength, lb/sq in.	85,000
Melting point, °C	1430–1470
Brinell hardness	150

* Handbook of Chemistry¹⁵ and Handbook of Chemistry and Physics⁹

BORON-CONTAINING MATERIALS

It is convenient to group the boron-containing substances separately, not only because of their importance to shield design, but also to clearly demonstrate the diversified manner in which boron may be incorporated into a shield. Data on boral, an alloy of boron and aluminum, are given in Tables 2.9.53 and 2.9.54; data on boron-bearing concretes are given in Tables 2.9.19 through 2.9.24; and data on boron, boron oxide, and boron carbide will be found in Volume 3 of this Handbook.

BORATION OF WATER

Capture gamma-ray production within water shields may be suppressed by the addition of small amounts of boron to the water, which is accomplished by virtue of the large thermal capture cross section of boron. The relatively soft gamma ray ($\frac{1}{2}$ mev) subsequently emitted is more easily absorbed within the shield than the harder gammas which are characteristic of capture in most other materials (Table 2.1.7).

Table 2.9.55 lists the solubilities of several boron-containing substances in water and the present boron concentrations of saturated solutions.

BORON COATINGS FOR METALS

Recent experiments by the ceramics group at Y-12 plant, Carbide & Carbon Chemical Company, Oak Ridge, Tennessee have indicated that it is possible to coat iron to a thickness of 0.020 in. with a boron-containing glass.¹ The method, developed for small samples, is: The sample to be coated is first cleaned and sandblasted, and a boron glass (a chemical analog of silica glass with borates replacing silicates) is prepared and ground to size (150–200 mesh). The sample is then heated to a dull red heat far above the melting range of the glass ($\sim 800^\circ\text{C}$), and the ground boron glass is flame-sprayed onto the surface.

The final product has a smooth glaze-like appearance much like a porcelanized coating. The color ranges from black or chalk gray for very thin coatings (1 mil) to whitish gray

¹ References appear at end of chapter.

or yellowish for coatings 20 mils thick and over. The coating is very brittle and will chip off under bending or deformation of the metal.

So far no coatings above about 25 mils thickness have been successful. Thicker coatings tend to peel and crack. Not much work has been done in multiple layer coatings. It is White's opinion that multiple-layer coatings would not be successful but that it may be possible to prepare sandwich-type samples built up of alternate layers of metal and coating.

This type of coating has been tried only on iron and aluminum. The coating is not successful on aluminum but may possibly be made to work on copper and on stainless steel. The coating will not withstand temperatures above the melting range of the glass (600°C).

The glass used in the sample-coating was made from the following percentages of raw materials by weight:

H_3BO_3 - 42.83%
 Pb_3O_4 - 54.55%
 ZnO - 2.61%

An analysis of the finished glass had the following composition by weight:

B_2O_3 - 35%
 PbO - 62.5%
 ZnO - 2.5%

The flame-spraying technique works best on small samples. For large samples, a different procedure is necessary to produce even coatings. A 5- by 5-ft slab of iron is now being coated for test in the ORNL Bulk Shielding Facility. The coating is put on in a furnace.

Table 2.9.53 — Composition of Boral*

(Kitzes and Hullings;²⁸ original boral composition reported by McKinney and Rockwell²⁹)

Component	Without Al cladding, wt-%	With Al cladding ($\frac{1}{4}$ in. sheet), wt-%
Molecular composition		
Aluminum (2S)	65.0	80.0
Boron carbide	35.0	20.0
Elemental composition		
Aluminum (2S)	65.0	80.0
Boron	27.5	15.7
Carbon	7.5	4.5

* Boral, an engineering material for absorption of thermal neutrons, is a mixture of B_4C and Al. The alloy is held in an aluminum cladding $\frac{20}{1000}$ in. thick, without which the material is brittle and difficult to handle. The standard boral composition, supplied by Carbide and Carbon Chemicals Company, Y-12 Plant, Oak Ridge, Tenn., shown above is available in $\frac{1}{4}$ and $\frac{1}{8}$ in. thick sheets. The B_4C content in the alloy can be as high as 50%; impurities less than 1%; major impurity is iron

Table 2.9.54 — Physical Properties of Boral

Property	Value or description†
Appearance	Aluminum-like alloy; can be rolled, sheared, sawed, drilled, tapped, hot-formed, die-cast, welded
Density, gm/cc	2.53
Specific heat, gm-cal/gm	0.175
Thermal conductivity, Btu/(hr)(ft)(°F)	25 at 200°F 19 at 500°F
Elongation, %	0.4
Tensile strength,* lb/sq in.	5500
Shear strength,* lb/sq in.	8240
Heat generation from (n, α) reaction, watts/(ft ²)(nv)	7.4×10^{-10}
Cost (1953)‡	\$18 per sq ft for $\frac{1}{4}$ -in.-thick sheets; \$15 per sq ft for $\frac{1}{8}$ -in.-thick sheets;

* The strength of the sheets of boral lies in the aluminum cladding and does not vary with the composition of the B_4C -Al alloy

† McKinney²⁸ and Kitzes and Hullings²⁹

‡ Rinderer³⁰

Table 2.9.55—Solubility of Boron-containing Substances in Water at Various Temperatures
(Handbook of Chemistry¹⁵ and Handbook of Chemistry and Physics⁹)

Compound	Solubility in water, gm/100 ml H ₂ O										Boron concentration, wt-% in H ₂ O		
	0°C	10°C	20°C	30°C	40°C	50°C	60°C	70°C	80°C	90°C	100°C	0°C	100°C
NH ₄ HB ₄ O ₇ ·3H ₂ O	10 in cold water; soluble in hot water												
HBO ₃ *	2.66	3.57	5.04	6.60	8.72	11.54	14.81	18.62	23.75	30.38	40.25	0.45	5.0
B ₂ O ₃ †	1.1	1.5	2.2		4.0	6.2			9.5		15.7		4.2
(CH ₃) ₃ B†	Slightly soluble in water												
LiBO ₂	0.9	16 at 45°C											
Li ₂ B ₄ O ₇ ·5H ₂ O	Very soluble												
KBF ₄ ‡		0.44											
K ₂ B ₂ O ₄	14.7	71											
K ₂ B ₄ O ₇ ·5H ₂ O		Very soluble in hot water											
AgBO ₂		26.7											
NaBF ₄ ¶		40 at 35°C; very soluble in hot water											
Na ₂ B ₂ O ₄		9.05 at 25°C											
Na ₂ B ₄ O ₇		108 at 26.5°C											
Na ₂ B ₂ O ₄ ·4H ₂ O		26											
Na ₂ B ₄ O ₇ ·10H ₂ O†		36 at 35°C											
NaBO ₂ ·3H ₂ O·H ₂ O**		Soluble in cold water; very soluble in hot water											
	1.3	8.79											
		24.4											
		31.5											
		41											
		52.5											
	1.3	1.6	2.7	3.9		10.5	20.3					0.28	5.1
		0.30 at 20°C											
		0.26 at 15°C											

* Solubility in glycerin, 22.2 parts per hundred at 20°C; in ether, 0.25 parts per hundred at 25°C

† Soluble in glycerin

‡ Very soluble in alcohol and ether

§ Soluble in alkalis

¶ Slightly soluble in alcohol

** Decomposes above 60°C

REFERENCES

1. G. D. White, Y-12 Plant, private communication.
2. G. R. White, X-ray Attenuation Coefficients from 10 Kev to 100 Mev, Nat. Bur. Stand., NBS-1003, May 13, 1952, 93 pp.
3. M. K. Hullings, Gamma-ray Total Mass Absorption Coefficients, Oak Ridge Nat. Lab., ORNL-CF-53-2-266, Feb. 12, 1953, 5 pp.
4. R. B. Gallaher and A. S. Kitzes, Summary Report on Portland Cement Concretes for Shielding, Oak Ridge Nat. Lab., ORNL-1414, Feb. 7, 1953, 30 pp.
5. G. A. Hool and N. C. Johnson, Concrete Engineers' Handbook, 1st ed., McGraw-Hill Book Co., Inc., New York, 1947.
6. T. Rockwell and F. J. Roehrenbeck, ORNL-17, Mar. 24, 1948, 24 pp.
7. Mechanical Engineers' Handbook, 5th ed., L. S. Marks, editor, McGraw-Hill Book Co., Inc., New York, 1950.
8. L. V. Pirsson, Rocks and Rock Minerals, 2nd ed., revised by A. Knopf, John Wiley and Sons, Inc., New York, 1926.
9. Handbook of Chemistry and Physics, 34th ed., C. D. Hodgman, editor, Chemical Rubber Publishing Co., Cleveland, Ohio, 1952.
10. General Engineering Handbook, 2nd ed., C. E. O'Rourke, editor, McGraw-Hill Book Co., Inc., New York, 1940.
11. Kent's Mechanical Engineers' Handbook, Design and Production Volume, 12th ed., C. Carmichael, editor, John Wiley and Sons, Inc., New York, 1950.
12. T. Rockwell to E. P. Blizzard, Memo Y-EI-1 (classified).
13. ORNL-653 (classified).
14. A. S. Kitzes, T. Rockwell, and R. B. Gallaher, Summaries of Studies on Oxychloride Cement and Concrete, ORNL-709, to be published.
15. Handbook of Chemistry, 7th ed., N. A. Lange, editor, Handbook Publishers, Sandusky, Ohio, 1949.
16. Chemical Engineers' Handbook, 2nd ed., J. H. Perry, editor, McGraw-Hill Book Co., Inc., New York, 1941.
17. Collier's Encyclopedia, C. P. Barry, editor, P. F. Collier and Son Corp., New York, 1950.
18. E. Hägglund, Chemistry of Wood, trans. by P. Oesper, Academic Press, New York, 1951.
19. Handbook of Engineering Fundamentals, 2nd ed., O. W. Eshbach, editor, John Wiley and Sons, Inc., New York, 1952.
20. G. S. Brady, Materials Handbook, 7th ed., McGraw-Hill Book Co., Inc., New York, 1951.
21. G. F. Quinn and L. B. Thompson, CE-1125, Dec. 9, 1943 (classified).
22. H. R. Simonds, A. J. Weith, and M. H. Bigelow, Handbook of Plastics, 2nd ed., D. Van Nostrand Co., Inc., New York, 1949.
23. Hanford Works Technical Manual, HW-10475, Sept. 15, 1951 (classified).
24. C. D. Newman, R. O. Bolt, J. G. Carroll, G. A. Christiansen, B. A. Fries, J. W. Kent, and E. G. Lindstrom, NEPA-1381, April 18, 1950, 31 pp (classified).
25. R. H. Kernohan and G. M. McCammon, Fading Characteristics of Gamma-induced Coloration in High-density Glass, Oak Ridge Nat. Lab., ORNL-975, Mar. 20, 1951, 19 pp.
26. Van Nostrand's Scientific Encyclopedia, 2nd ed., D. Van Nostrand Co., Inc., New York, 1947.
27. Metals Handbook, 1948 ed., T. Lyman, editor, The American Society for Metals, Cleveland, Ohio, 1948.
28. A. S. Kitzes and W. O. Hullings, Borai: A New Thermal Neutron Shield, Supplement 1, Oak Ridge Nat. Lab., ORNL-981, July 3, 1951, 18 pp.
29. V. L. McKinney and T. Rockwell, III, ORNL-242, Aug. 31, 1949 (classified).
30. C. Rinderer, Y-12 Plant, Carbide and Carbon Chem. Corp., Oak Ridge, Tenn., private communication.

Appendix 1

Conversion Factors and Miscellaneous Data

Table A.1.1 — Constants

(CF-51-8-10)

Velocity of light (C):	$(2.99776 \pm 0.00004) \times 10^{10}$ cm/sec = $(9.8356 \pm 0.00013) \times 10^8$ ft/sec
"Absolute" zero (T_0):	$-273.16 \pm 0.01^\circ\text{C} = -459.69 \pm 0.02^\circ\text{F}$
Faraday constant (F):	96514.0 ± 10 abs coulombs/phys. gm equiv.
Avogadro's number (N_0):	$(6.02283 \pm 0.0011) \times 10^{23}$ molecules/chem-mole
Chemical/physical mass unit:	1.000272 ± 0.000005
Plank's constant (h):	6.6242×10^{-27} erg-sec = 4.1349×10^{-15} ev-sec
Charge of electron (e):	4.8025×10^{-10} abs esu = 1.60203×10^{-20} abs emu = 1.60203×10^{-19} abs coulombs
Compton wavelength (λ_0):	2.4265×10^{-10} cm
Fine structure constant ($\frac{e^2}{hc} = a$):	$0.0072977 = \frac{1}{137.030}$
Boltzman constant (k):	1.38047×10^{-16} erg/deg = 3.2982×10^{-24} cal/deg = 8.6170×10^{-5} ev/deg
Stefan-Boltzmann constant (σ):	5.6728×10^{-5} erg/(cm ²)(deg ⁴)(sec)
Bohr nuclear magneton ($\frac{e\hbar}{2M_{\text{pc}}} = \mu_{\text{p}}$):	5.049×10^{-24} erg/gauss

Table A.1.2 — Conversion Factors

Multiply	By	To obtain
	Energy	
Btu	6.59×10^{15}	mev
Btu	1054.8	joules
Btu	2.930×10^{-4}	kw-hr
Btu	3.929×10^{-4}	hp-hr
Btu	252	gm-cal
cal (15°)	2.6126×10^{19}	ev
cal (15°)	4.1855×10^7	ergs
cal (15°)	4.1855	joules
ergs	6.2421×10^{11}	ev
ergs	10^{-7}	joules
ergs	2.3892×10^{-8}	cal (15°)
ev	1.60203×10^{-12}	ergs
ev	1.60203×10^{-19}	joules
ev	3.8276×10^{-20}	cal (15°)
gm	5.6095×10^{32}	ev
gm	8.9866×10^{20}	ergs
gm	8.9866×10^{13}	joules
gm	2.1471×10^{13}	cal (15°)
gm-cal	2.616×10^{13}	mev
gm-cal	4.186	joules
gm-cal	1.163×10^{-6}	kw-hr
gm-cal	1.559×10^{-6}	hp-hr
gm-cal	3.969×10^{-3}	Btu
hp-hr	1.677×10^{19}	mev
hp-hr	2.684×10^6	joules
hp-hr	0.7457	kw-hr
hp-hr	6.413×10^5	gm-cal

APPENDIX 1

Table A.1.2 — (Continued)

Multiply	By	To obtain
Energy		
hp-hr	2545	Btu
joules	6.25×10^{12}	mev
joules	2.778×10^{-7}	kw-hr
joules	3.722×10^{-7}	hp-hr
joules	0.2389	gm-cal
joules	9.480×10^{-4}	Btu
joules	6.2421×10^{18}	ev
joules	1×10^7	ergs
joules	0.23892	cal (15°)
kw-hr	2.25×10^{19}	mev
kw-hr	3.6×10^6	joules
kw-hr	1.341	hp-hr
kw-hr	8.60×10^5	gm-cal
kw-hr	3.413×10^3	Btu
mev	1.6×10^{-13}	joules
mev	4.44×10^{-20}	kw-hr
mev	5.95×10^{-20}	hp-hr
mev	3.82×10^{-14}	gm-cal
mev	1.517×10^{-16}	Btu
Time		
days	2.738×10^{-3}	yr
days	24	hr
days	1440	min
days	8.640×10^4	sec
hr	1.141×10^{-4}	yr
hr	0.04167	days
hr	60	min
hr	3600	sec
min	1.901×10^{-6}	yr
min	6.944×10^{-4}	days
min	1.667×10^{-2}	hr
min	60	sec
sec	3.169×10^{-8}	yr
sec	1.157×10^{-5}	days
sec	2.778×10^{-4}	hr
sec	1.667×10^{-2}	min
yr	365.26	days
yr	8766	hr
yr	5.260×10^5	min
yr	3.156×10^7	sec
Length		
cm	0.01	m
cm	.3937	in.
cm	.03281	ft
ft	.3048	m
ft	30.48	cm
ft	12	in.
in.	0.0254	m
in.	2.54	cm
in.	0.0833	ft

PHYSICS

Table A.1.2—(Continued)

Multiply	By	To obtain
Length		
meters	100	cm
meters	39.37	in.
meters	3.281	ft.
microns	10^{-6}	meters
microns	10^{-4}	cm
microns	3.937×10^{-5}	in.
microns	3.281×10^{-6}	ft
Volume		
cu cm	10^{-6}	m ³
cu cm	6.102×10^{-2}	in. ³
cu cm	2.642×10^{-4}	gal
cu cm	3.531×10^{-5}	ft ³
cu cm	1.308×10^{-6}	yd ³
cu ft	2.832×10^{-2}	m ³
cu ft	2.832×10^4	cm ³
cu ft	1728	in. ³
cu ft	28.32	liters
cu ft	3.704×10^{-2}	yd ³
cu ft	7.481	gal
cu in.	1.639×10^{-5}	m ³
cu in.	16.39	cm ³
cu in.	5.787×10^{-4}	ft ³
cu meter	1×10^6	cm ³
cu meter	6.102×10^4	in. ³
cu yd	7.646×10^5	cm ³
cu yd	27	ft ³
cu yd	764.6	liters
cu yd	202	gal
gal	3785	cm ³
gal	0.1337	ft ³
gal	3.785	liters
gal	4.951×10^{-3}	yd ³
liters	1000	cm ³
liters	3.531×10^{-2}	ft ³
liters	1.308×10^{-3}	yd ³
liters	0.2642	gal
Angular displacement		
deg	1.745×10^{-2}	rad
deg	2.778×10^{-3}	rev
rad	57.3	deg
rad	0.1592	rev
rev	360	deg
rev	6.283	rad
Pressure		
atm	76	cm Hg
atm	1033	gm/cm ²

APPENDIX 1

Table A.1.2—(Continued)

Multiply	By	To obtain
Pressure		
atm	2177	lb/ft ²
atm	14.70	lb/in. ²
cm Hg	1.316×10^{-2}	atm
cm Hg	13.6	gm/cm ²
cm Hg	27.85	lb/ft ²
cm Hg	0.1934	lb/in. ²
gm/cm ²	9.678×10^{-4}	atm
gm/cm ²	7.356×10^{-2}	cm Hg
gm/cm ²	2.048	lb/ft ²
gm/cm ²	1.422×10^{-2}	lb/in. ²
lb/ft ²	4.725×10^{-4}	atm
lb/ft ²	3.591×10^{-2}	cm Hg
lb/ft ²	0.4882	gm/cm ²
lb/ft ²	6.944×10^{-3}	lb/in. ²
lb/in. ²	6.804×10^{-2}	atm
lb/in. ²	5.171	cm Hg
lb/in. ²	70.3	gm/cm ²
lb/in. ²	144	lb/ft ²
Density		
gm/cm ³	1×10^3	gm/liter
gm/cm ³	62.43	lb/ft ³
gm/liter	1×10^{-3}	gm/cm ³
gm/liter	6.243×10^{-2}	lb/ft ³
lb/ft ³	1.602×10^{-2}	gm/cm ³
lb/ft ³	16.02	gm/liter
Thermal conductivity		
Btu/(hr)(°F)(ft)	4.134×10^{-3}	gm-cal/(sec)(°C)(cm)
Btu/(hr)(°F)(ft)	12	Btu/(hr)(°F)(ft ² /in.)
Btu/(hr)(°F)(ft ² /in.)	3.44×10^{-4}	gm-cal/(sec)(°C)(cm)
Btu/(hr)(°F)(ft ² /in.)	8.33×10^{-2}	Btu/(hr)(°F)(ft)
gm-cal/(sec)(°C)(cm)	241.9	Btu/(hr)(°F)(ft)
gm-cal/(sec)(°C)(cm)	2903	Btu/(hr)(°F)(ft ² /in.)

Table A.1.3—Radiation Dose Units

Radiation	Roentgen	Energy absorbed, roentgen equivalent physical (rep)	Biological damage, roentgen equivalent man (rem)	Relative biological effectiveness (rbe)
X-ray	1	1	1	...
Gamma	1	1	1	1
Beta	...	1	1	1
Thermal-neutron	...	1	5	5
Fast-neutron	...	1	10	10
Proton	...	1	10	10
Alpha-particle	...	1	20	20

Table A.1.4—Gamma Energy Flux to Dose Rate

Gamma energy, mev	To produce 1 r/hr, 10^5 mev/(cm ²)(sec)	To produce 0.3 r/40-hr wk, 10^3 mev/(cm ²)(sec)
0.5	5	3.75
1	5.5	4.125
2	6	4.5
5	8	6.0
10	10	7.5

Table A.1.5—Neutron Flux to Dose Rate

(W. S. Snyder and J. Neufeld, Maximum Permissible Neutron Flux for Fast and Thermal Neutrons, Symposium on the Biophysical and Biological Effects of Neutrons, Mar. 17-18, 1952)

Neutron energy	To produce 1 rem/hr, 10^3 r/(cm ²)(sec)	To produce 0.3 rem/40 hr, r/(cm ²)(sec)
Thermal	240	1800
5 kev	220	1650
0.5 mev	11	82.5
2.5 mev	5.2	39
5.0 mev	3.2	24
10 mev	3.33	25

Table A.1.6 — Neutron Wavelengths for Various Energies

Energy	KT _{20°}	1 ev	1 mev
Neutron,* Å	0.28635×10^{-8}	0.045512×10^{-8}	4.5501×10^{-13}
Photon,† Å	0.0049068	12.395×10^{-8}	0.012395×10^{-8}

*Entries are $\lambda = \frac{h}{p} = \frac{h}{mv}$
 †Entries are λ

Table A.1.7—Neutron Energy, Wavelength, Velocity, and Time of Flight*

($\lambda = 2\pi\lambda =$ wavelength, Å (10^{-8} cm); $E =$ energy, ev; $v =$ velocity, cm/sec; $t =$ time of flight, μ sec/m)

$\lambda = \dots$	6.2832λ	$0.28696/\sqrt{E}$	$3.9554 \times 10^5/v$	$0.0039554t$
$\lambda = 0.159155-\lambda$	\dots	$0.045512/\sqrt{E}$	$62,452/v$	$0.00062952t$
$E = 0.081774 \lambda^2$	$0.0020714/\lambda^2$	\dots	$5.2269 \times 10^{-13}v^2$	$5226.9/t^2$
$v = 3.9554 \times 10^5/\lambda$	$62,952/\lambda$	$1.3832 \times 10^6\sqrt{E}$	\dots	$10^8/t$
$t = 252.82\lambda$	$1588.5 + \lambda$	$72.297/\sqrt{E}$	$10^8/v$	\dots

*This table is valid to $1\frac{1}{2}$ percent for $E < 10$ mev

Table A.1.8—Low-energy Neutrons

Energy, ev	Wavelength, Å	Velocity, cm/sec
0.001	9.0430	4.3740×10^4
.01	2.8596	1.3832×10^5
.02	2.0221	1.9561×10^5
.0259*	1.7786	2.2239×10^5
.03	1.6510	2.3957×10^5
.04	1.4298	2.7664×10^5
.05	1.2789	3.0929×10^5
.06	1.1674	3.3881×10^5
.07	1.0808	3.6596×10^5
.08	1.0110	3.9122×10^5
.09	0.95321	4.1495×10^5
.1	.90430	4.3740×10^5
.2	.63944	6.1858×10^5
.4	.45215—	8.7480×10^5
.6	.36918	1.0714×10^6
.8	.31972	1.2372×10^6
1	.28596	1.3832×10^6

* $0.025851 \text{ ev} = kT_{300^\circ\text{K}}$

Table A.1.9 — Miscellaneous Factors and Definitions

- (1) 1 atomic mass unit (amu) = 1.65990×10^{-24} gm = 931.12 mev
- (2) 1 barn = nuclear unit of cross section = 10^{-24} cm²
- (3) 1 curie = 3.68×10^{10} disintegrations/sec
- (4) 1 rutherford = 1.00×10^6 disintegrations/sec
- (5) Width of level having lifetime of 1 sec = 4.1349×10^{-15} ev
- (6) Lifetime of state with width of 1 ev = 4.1349×10^{-15} sec
- (7) $kT_{0^\circ\text{C}} = 0.02354$ ev; $kT_{15^\circ\text{C}} = 0.02483$ ev; $kT_{20^\circ\text{C}} = 0.02526$ ev; $kT_{300^\circ\text{K}} = 0.02585$ ev
- (8) Relaxation length (τ) is the thickness of absorber which will reduce the radiation intensity to $1/e$ times its initial value

2.3τ = distance to reduce radiation to 0.1 times its initial value

τ cm to fall to $1/e$ $I_0 = >0.906 \tau$ in. to fall to $0.10 I_0$

- (9) In a reactor operating at a power level of P watts, $P \times 3.1 \times 10^{10}$ fissions/sec occur
- (10) Conversion Factors for Gamma-ray Cross Section

σ_T = microscopic cross section in Thompson units per electron

σ_b = microscopic cross section in barns (10^{-24} cm²)

μ = linear absorption coefficient in cm⁻¹

μ_m = mass absorption coefficient in cm²/gm

r_0 = classical electron radius

1 Thompson unit = $0.665 \text{ b} = \frac{8}{3} \pi r_0^2 \text{ cm}^2$

In a medium of Z electrons/molecule and molecular weight A :

$$\sigma_b = 0.665 Z \sigma_T$$

$$\mu_m = \frac{0.6023}{A} \sigma_b = \frac{0.6023Z}{A} \times 0.665 \sigma_T$$

$$\mu = \rho_{\mu_m} = \frac{0.6023\rho}{A} \sigma_b = \rho_{el} \frac{\sigma_b}{Z} \times 10^{-24}$$

where: ρ = mass density in gm/cm³

ρ_{el} = electron density per cm³

1 gm/cm³ = 0.4882 lb/ft³

Appendix 2

Reactor Summary Tables
(North American Aviation, Inc.)

Table A.2.1—Chicago Pile No. 1 (CP-1)

LOCATION	University of Chicago Chicago, Illinois
RESPONSIBLE ORGANIZATION	Design Metallurgical Laboratory, University of Chicago Construction Metallurgical Laboratory, University of Chicago Operation Metallurgical Laboratory, University of Chicago
PURPOSE	Research
STATUS	In operation from Dec., 1942 to Feb., 1943
MATERIALS	Fuel Natural uranium; 5.6 metric tons as metal 32.9 metric tons as UO ₂ 3.7 metric tons as U ₃ O ₈ Moderator Graphite; 266 metric tons Reflector Graphite; 84 metric tons Structural material Graphite Reactor atmosphere Air Shield None
LATTICE TYPE	Pseudospheres in 8 1/4 in. and 8 in. cubical arrays
DIMENSIONS	Core (effective) Polar radius; 10 ft 2 in. Equatorial radius; 12 ft 9 in. Reflector Over-all 24 1/2 x 24 1/2 x 19 1/2 ft high
STRATEGIC MATERIAL	Fissionable Material U ₂₃₅ ; 296 kg Consumption Negligible Burn-up Negligible Average cycle time None COOLING SYSTEM None AUXILIARY FACILITIES None OPERATING CONDITIONS None
CONTROLS	Total heat power 200 watts Useful power output 0 Innage Indefinite Heat flux Negligible Power density (average) 10.7 x 10 ⁻⁶ kw/l Specific power (average) 6.8 x 10 ⁻⁴ kw/kg 25 Maximum fuel temperature Negligible rise Maximum moderator temperature Negligible rise
PHYSICS	Shim 1 horizontal 1/8 x 3 1/2 in. cadmium strip on steel rod Regulating 1 horizontal 1/4 x 3 1/2 in. steel clad boron steel rod Safety 1 horizontal cadmium on steel rod Reactivity change Cell radius 13 cm (8 1/4 in. spacing) 12.6 cm (8 in. spacing) Resonance escape (clean and cold) 0.896 d Thermal utilization (clean and cold) 0.866 b 0.869 c 0.871 d

Diffusion length squared (clean and cold) ^a	342 b cm ² 296 c cm ² 330 d cm ²
Age (clean and cold) ^a	370 cm ²
Buckling (clean and cold)	45 b x 10 ⁻⁶ cm ⁻² 58.9 c x 10 ⁻⁶ cm ⁻² 101.2 d x 10 ⁻⁶ cm ⁻²
Prompt neutron lifetime	About 1 x 10 ⁻³ sec
k _∞ (clean and cold)	1.055 (average) 1.032 b 1.039 c 1.07 d
k _{eff} (clean and cold)	1.0005 a
δ k (temperature)	-0.0001/°C
δ k (poisons)	Negligible
δ k (pressure)	About -6.4 x 10 ⁻⁶ /mb
NEUTRON FLUX DENSITY	Fast Thermal
EXPERIMENTAL FACILITIES. 1 - 4 1/8 x 4 1/8 in. removable stringer	7 - foil slots
CAPITAL INVESTMENT ^a	\$2.7 x 10 ⁶
REFERENCES	E. Fermi, AECD-3269, 47 pp, January 4, 1952
a. Estimated	
b. Uranium oxide in Speer graphite	
c. Uranium oxide in AGOT graphite	
d. Uranium metal in AGOT graphite	

Table A.2.2—Chicago Pile No. 2 (CP-2)

LOCATION	Argonne National Laboratory Chicago, Illinois	Diffusion length squared (clean and cold)	342 ^b cm ² 296 ^c cm ² 330 ^d cm ²
RESPONSIBLE ORGANIZATIONS			
Design	Metallurgical Laboratory, University of Chicago	Age (clean and cold) ^a	370 cm ²
Construction	Metallurgical Laboratory, University of Chicago	Buckling (clean and cold)	45.6 x 10 ⁻⁶ cm ⁻²
Operation	Argonne National Laboratory	58.9 c x 10 ⁻⁶ cm ⁻²	
PURPOSE	Research	101.2 d x 10 ⁻⁶ cm ⁻²	
STATUS	In operation since Mar., 1943	Prompt neutron lifetime	About 1 x 10 ⁻³ sec
MATERIALS			
Fuel	Natural uranium; 9.1 metric tons as metal ^a 29.5 metric tons as UO ₂ ^a 1.3 metric tons as U ₃ O ₈ ^a	k _∞ (clean and cold)	1.055 (average) 1.032 ^b 1.039 ^c 1.07 ^d
Moderator	Graphite; 314 metric tons	k _{eff} (clean and cold)	1.004
Reflector	Graphite; 115 metric tons	δk (temperature)	-0.0001/°C
Structural material	Graphite	δk (poisons)	Negligible
Reactor atmosphere	Air	δk (pressure)	-6.4 x 10 ⁻⁶ /mb
Shield	Ordinary concrete, wood, and lead	NEUTRON FLUX DENSITY	
LATTICE TYPE	Pseudospheres in 8 1/4 in. and 8 in. cubical arrays	Fast	4.5 x 10 ⁵ n/(cm ²)(sec)(watt) ^a
DIMENSIONS			
Core	20 x 18 x 17 ft high	Thermal: maximum	1.5 x 10 ⁵ n/(cm ²)(sec)(watt) ^a
Reflector	1 ft thick	average	34 x 34 in. x 20 ft long removable
Shield	5 ft of ordinary concrete on sides 6 in. lead plus 40 in. wood on top	EXPERIMENTAL FACILITIES	
Over-all	32 x 30 x 23 ft high (excluding thermal column)	5 x 5 ft thermal column	
STRATEGIC MATERIAL			
Fissionable material	U ²³⁵ ; 280 kg ^a	9 - 4 1/4 x 4 1/4 in. removable stringers	
Consumption	2.7 x 10 ⁻³ gm/day ^a	1 - 2 5/8 in. x 15 ft long vertical slot	
Burn-up	Indefinite	Various monitoring slots	
Average cycle time	Indefinite	REFERENCES . . . Experimental Production of a Divergent Chain Reaction	
COOLING SYSTEM	None	E. Fermi, AEC-D-3269, 47 pp, January 4, 1952	
AUXILIARY FACILITIES			
Reactor atmosphere	Ventilating system	A Brief General Description of the Argonne Uranium-	
OPERATING CONDITIONS			
Total heat power	10 kw (nominal)	Graphite Pile (CP-2), H.E. Metcalf, CP-2459,	
Useful power output	0	11 pp, Secret, Dec. 20, 1944	
Innage	Approx. 0.1	a. Estimated	
Heat flux	Negligible	b. Uranium oxide in Speer graphite	
Power density (average)	6.4 x 10 ⁻⁴ kw/l	c. Uranium oxide in AGOT graphite	
Specific power (average)	3.6 x 10 ⁻² kw/kg 25	d. Uranium metal in AGOT graphite	
Average fuel temperature	About 25°F rise		
Average moderator temperature	About 15°F rise		
CONTROLS			
Shim	1 horizontal, steel supported, cadmium strip		
Regulating	2 horizontal, strip supported, cadmium strips		
Safety	3 horizontal, steel supported, cadmium strips		
Reactivity Change	0.005		
PHYSICS			
Cell radius	13 cm (8 1/4 in. spacing) 12.6 cm (8 in. spacing)		
Resonance escape (clean and cold)	0.896 ^d		
Thermal utilization (clean and cold)	0.866 ^b 0.869 ^c 0.871 ^d		

Table A.2.3—ORNL Graphite Reactor (X-10)

LOCATION	Oak Ridge National Laboratory Oak Ridge, Tennessee	Coolant pressure	Sub-atmosphere
RESPONSIBLE ORGANIZATIONS		Coolant pressure drop through reactor	19.25 in. of H ₂ O
Design	DuPont	Pumping rate	7,200 lb/min
Construction	DuPont	Pumping power required	800 hp
Operation	ORNL	CONTROLS	
PURPOSE	Research and radioisotope production	Shim	4 - 1 3/4 x 1 3/4 in. x 19 ft horizontal boron-steel rods
STATUS	In operation since Nov., 1943	Regulator	2 - 1 3/4 x 1 3/4 in. x 19 ft horizontal boron-steel rods
MATERIALS		Safety	4 - 1 1/2 in. dia. x 8 ft vertical boron-steel rods
Fuel	Natural uranium; 47.63 metric tons (typical)		2 - 1 3/4 in. dia. x 17 ft 2 in. vertical tubes for 3/8 in. boron-steel shot
Fuel cladding	Aluminum; 0.035 in. wall, 0.060 in. end cap	Reactivity change (late 1944 loading)	0.0389
Moderator (and reflector)	Graphite; 612.5 metric tons	FUEL HANDLING	
Coolant	Air	Charging	Hand charging, straight push through of slugs
Fertile material	Varied	Discharging	Slugs drop into canal
Structural material	Graphite	PHYSICS	
Reactor atmosphere	Air	Cell radius	11.46 cm
Shield	Ordinary and berytes-haydite concrete, plus waterproofing pitch	Resonance escape (clean and cold)	0.886
	1.1 in. dia. rods in 8 in. square array	Thermal utilization (clean and cold)	0.890
LATTICE TYPE	24 x 24 x 24 1/3 ft (including reflector)	Diffusion length squared (clean and cold)	297 cm ²
DIMENSIONS		Age (clean and cold); axial	398 cm ²
Core	24 x 24 x 24 1/3 ft (including reflector)	radial	386 cm ²
Reflector	Depends upon loading	Buckling (clean and cold)(experimental)	92 x 10 ⁻⁶ cm ⁻²
Shield	2 ft of ordinary concrete retaining walls (waterproofed with pitch), 5 ft of berytes-haydite concrete	Prompt neutron lifetime	About 1 x 10 ⁻³ sec
Over-all	47 x 38 x 35 ft	k _∞ (clean and cold)	1.067
STRATEGIC MATERIAL		k _{eff} (clean and cold)(typical)	1.021
Fissionable material	U235; 343 kg (typical)	δ k (temperature)(graphite plus fuel)	-2.86 x 10 ⁻⁵ /C°
Consumption	About 4.5 gms/day	δ k (poisons)(typical)	6.5 x 10 ⁻³
Burn-up	Indefinite	δ k (pressure)	-7.8 x 10 ⁻⁶ /mb
Average cycle time	Indefinite	k _{eff} (hot and poisoned)(typical)	1.004
COOLING SYSTEM		NEUTRON FLUX DENSITY	
Type	Air: Once through	Fast	
Coolant treatment	Filtered	Thermal: maximum	3.2 x 10 ⁵ n/(cm ²)(sec)(watt)
Blowers	1 - 275 lb/min steam driven fan (stand-by) 2 - 3300 lb/min centrifugal blowers	average	1.4 x 10 ⁵ n/(cm ²)(sec)(watt)
OPERATING CONDITIONS (typical)		EXPERIMENTAL FACILITIES	20 x 24 in. x 24 ft removable axial core
Total heat power	3800 kw	4 - 1.684 in. dia. x 24 ft axial experimental holes	
Useful power output	0	1 - 3 1/8 x 2 15/32 in. x 24 ft axial doughnut hole	
Innage	0.9	10 - 4 x 4 in. x 24 ft experimental holes	
Rod power	Indefinite	2 - 14 1/2 x 14 in. animal tunnels in top shield	
Heat flux: maximum	7300 BTU/(sq ft)(hr) a	6 - observation and experimental holes into discharge air plenum	
average	3300 BTU/(sq ft)(hr) a	1 - drainable water filled core plug to accommodate additional thermal column or bulk material testing tank	
Power density: maximum	4.4 kw/l	REFERENCES	Graphite Uranium Production Piles, AEC Technical Information Service, L.B. Borst, NNES-IV-5a, 457 pp, Secret, 1951
average	1.9 kw/l	An Experimental and Theoretical Study of the Subcritical BNL Reactor, Brookhaven National Laboratory, J. Cherrick, et al, BNL-60, 109 pp Secret, June 15, 1950	
Specific power: maximum	24.8 kw/kg 25 a		
average	11.1 kw/kg 25 a		
Maximum fuel temperature	660°F		
Maximum sheath temperature	473°F		
Maximum moderator temperature	292°F		
Coolant inlet temperature	77°F		
Coolant outlet temperature	194°F		
Coolant velocity			

a. Estimated

Table A.2.4—Brookhaven Graphite Research Reactor (BGRR)

LOCATION	Brookhaven National Laboratory Upton, New York	Coolant pressure (inlet, i.e. across inlet filter).	-1.7 in. H ₂ O
RESPONSIBLE ORGANIZATIONS		Coolant pressure drop through reactor	50.2 in. H ₂ O
Design	H. K. Ferguson Company	Pumping rate	24,000 lbs/min
Construction	H. K. Ferguson Company	Pumping power required (air and water)	About 5700 kw
Operation	Brookhaven National Laboratory	CONTROLS	
PURPOSE	Research and radioisotope production	Regulator	2 - 2 x 2 in. x 25 1/2 ft, horizontal 1 3/4% boron steel rods
STATUS	In operation since Aug., 1950	Shim and safety	14 - 2 x 2 in. x 25 1/2 ft, horizontal 1 3/4% boron steel rods
MATERIALS		2 - 3 1/2 in. dia. diagonal shot wells in gap 2 - 3 1/2 in. dia. x 25 ft shot wells	
Fuel	Natural uranium; 52.5 metric tons (typical)	Reactivity change	0.505
Fuel cladding	Aluminum; 0.030 in. wall, 6 - 0.6 in. fins; 0.232 lbs/ft	FUEL HANDLING	
Moderator	Graphite; 350 metric tons	Charging	By hand and remote grappeling equipment
Reflector	Graphite; 382 metric tons	Discharging	By hand and remote grappeling equipment
Coolant	Air	PHYSICS	
Fertile material	Varies	Cell radius	11.46 cm
Structural material	Graphite	Resonance escape (clean and cold)	0.884
Reactor atmosphere	Air	Thermal utilization (clean and cold)	0.896
Shield	Steel and limonite concrete	Diffusion length squared (clean and cold)(axial)	334 cm ²
LATTICE TYPE	1.1 in. dia. rods in 8 in. square array	(radial)	316 cm ²
DIMENSIONS		Age (clean and cold)(axial)	407 cm ²
Core	7 ft dia. by 22 ft (typical)	(radial)	385 cm ²
Reflector	About 9 ft on sides, 1 1/2 ft on ends	Buckling (experimental)	92.4 x 10 ⁻⁶ cm ⁻²
Shield	9 in. steel; 4 ft 3 in. limonite concrete with iron aggregate	Prompt neutron lifetime	About 1 x 10 ⁻³ sec
Over-all	37 1/2 x 55 x 33 1/2 ft high	k _∞ (clean and cold)	1.074
STRATEGIC MATERIAL		k _{eff} (clean and cold)(typical)	1.032
Fissionable material	U ²³⁵ ; 370 kg	δ k (temperature)(total)	-4 x 10 ⁻⁵ /°C
Consumption	22.5 gm/day (average)	δ k (poisons)(typical)	-0.017
Average cycle time	Indefinite	k _{eff} (hot and poisoned)(typical)	1.005
COOLING SYSTEM		NEUTRON FLUX DENSITY	
Type	Once through	Fast	2.59 x 10 ⁵ n/(cm ²)(sec)(watt)
Coolant source	Atmosphere	Thermal (maximum)	29 - 4 x 4 in. x 25 ft experimental holes
Coolant treatment	Inlet filter Outlet filter	EXPERIMENTAL FACILITIES	
Blowers	5 - 1,500 hp motor driven centrifugal fans 1 - 15 hp gasoline driven emergency blower	1 - 12 x 12 in. x 25 ft removable axial core 1 - 2 channel, 25 ft sample conveyor system 11 - 12 1/2 ft pneumatic tubes 1 - 20 x 20 ft section of removable shield blocks on top of reactor 30 - intercell 12 1/2 ft fuel channels 2 - openings into central gap 2 - exposure tunnels under the reactor	
Pumps	3 - 4,500 gpm, motor driven centrifugal water pumps	CAPITAL INVESTMENT	\$19 x 10 ⁶
AUXILIARY FACILITIES		REFERENCES	Report on the Brookhaven Nuclear Reactor Brookhaven National Laboratory, BNL-18, 180 pp, Secret, June 22, 1948
Reactor services	Slug canning facility		
OPERATING CONDITIONS (typical)			
Total heat power	26,000 kw (28,000 kw design point)		
Useful power output	0		
Innage	0.9		
Rod power (average)	38 kw		
Heat flux (average)	20,730 BTU/(sq ft)(hr)		
Power density (average)	1.07 kw/l		
Specific power (average)	70 kw/kg 25		
Maximum moderator temperature	41°F		
Coolant inlet temperature	265°F		
Coolant outlet temperature (at reactor exit plenum)			

The Brookhaven Nuclear Reactor:
Theory and Nuclear Design Calculations,
Brookhaven National Laboratory,
I. Kaplan and J. Chernick, BNL-152
80 pp, Secret, January, 1952

Table A.2.5—Materials Testing Reactor (MTR)

LOCATION	National Reactor Testing Station	Heat flux (average)	294,000 BTU/(sq ft)(hr)
RESPONSIBLE ORGANIZATIONS	Arco, Idaho	Power density (average)	291 kw/l
Design	Oak Ridge National Laboratory, Argonne National Laboratory, and Blaw-Knox Construction Company	Specific power (average)	10,000 kw/kg 25
Construction	Phillips Petroleum Company	Maximum moderator temperature	125°F
Operation	Fluor Corporation	Coolant inlet temperature	100°F
PURPOSE	Research	Coolant outlet temperature	115°F
STATUS	In operation since April, 1952	Coolant velocity	30 ft/sec
MATERIALS		Coolant inlet pressure	73 psia
Fuel	U235 as uranium-aluminum alloy	Coolant pressure drop through reactor	40 psi
Fuel Cladding	Aluminum	Pumping rate	20,000 gpm
Moderator	H ₂ O; 0.117 in. film	Pumping power required	
Reflector	Beryllium; 2.61 metric tons Graphite; 68.7 metric tons	CONTROLS	
Coolant	H ₂ O; 0.117 in. film	Shim	4 - combination aluminum-cadmium box and fuel element rods
Fertile material		Regulator	2 - 1 1/2 in. dia. aluminum-cadmium rods and beryllium rods
Structural material	Aluminum, stainless steel, and concrete	Safety	4 - combination aluminum-cadmium box and beryllium rods
Shield	H ₂ O, iron, and beryllium concrete	Reactivity change	Effected by all rods
LATTICE TYPE	Slab type	FUEL HANDLING	
DIMENSIONS		Charging	Remote grappling devices from top of tank
Core	Up to 15 x 27 x 24 5/8 in.	Discharging	Remote grappling devices from top of tank. Spent fuel lowered through discharge chute to canal beneath reactor
Reflector	Beryllium; extends from core to 54 1/4 in. dia. cylinder Graphite; pebble zone out to 7 1/3 ft sq x 9 ft high blocks out to 12 x 14 x 9 1/4 ft high	PHYSICS ^a	
Shield	8 in. iron; 9 ft beryllium concrete; or 17 1/2 ft of H ₂ O plus top plug	Resonance escape (clean and cold)	1.0
Over-all	32 1/2 x 34 x 40 2/3 ft high	Thermal utilization (clean and cold)	0.76
STRATEGIC MATERIAL		Diffusion length squared (clean and cold)	3.5 cm ²
Fissionable material	U235; 2.98 kg	Age (clean and cold)	64.2 cm ²
Consumption (at full power)	3.6 g/day	Buckling (clean and cold)	0.01 cm ⁻²
Burn-up	Indefinite	Prompt neutron lifetime	2.63 x 10 ⁻⁴ sec
Average cycle time	Indefinite	k _{eff} (clean and cold)	1.61
COOLING SYSTEM		Conversion ratio	None
Type	Recirculated H ₂ O	NEUTRON FLUX DENSITIES ^a	
Coolant source	Wells	Fast (maximum)	1.2 x 10 ¹⁴ n/(cm ²)(sec)
Coolant treatment		Epithermal (maximum)	6 x 10 ¹⁴ n/(cm ²)(sec)
Pumps	3 (1 standby) - 10,000 gpm (97.5 psi), 700 hp horizontal, electrically driven, centrifugal pumps	Thermal (maximum)	2 x 10 ¹⁴ n/(cm ²)(sec)
Safety	2 - 850 gpm, electrically driven, centrifugal pumps 1 - 1000 gpm, gasoline driven, centrifugal pump 1 - 400 lb/min, electrically driven, blower 1 - 400 lb/min, gasoline driven, blower 1 - 150,000 gal, 170 ft head, working reservoir 1 - 150,000 gal, 150 ft head storage tank	EXPERIMENTAL FACILITIES	See text
		CAPITAL INVESTMENT	\$18 x 10 ⁶
		REFERENCES	Materials Testing Reactor Project Handbook, Oak Ridge National Laboratory, J.H. Buck and C.F. Leyse, ORNL-963, 584 pp. Secret, May 7, 1951
Retention basin	750 kva Diesel-electric generator	a. Preliminary calculations	
AUXILIARY FACILITIES			
Standby equipment			
OPERATING CONDITIONS			
Total heat power	30,000 kw		
Useful power output	0		

Table A.2.6—Low-Intensity Training Reactor (LITR)

LOCATION	Oak Ridge National Laboratory	CONTROLS	Shim3 - combination fuel and cadmium box rods
RESPONSIBLE ORGANIZATIONS	Oak Ridge, Tennessee	Regulator	1 - 1 1/2 in. vertical aluminum rod with 20 in. cadmium tube insert	
Design	Oak Ridge National Laboratory	Safety	Effectuated by shim rods	
Construction	Oak Ridge National Laboratory	Reactivity change	0.18 a	
Operation	Oak Ridge National Laboratory	FUEL HANDLING		
PURPOSE	Experimental and research	Charging	Remote grappling devices	
STATUS	In operation since Feb., 1950	Discharging	Remote grappling devices. Depleted elements stored in top tank	
MATERIALS		PHYSICS ^b		
Fuel	U235 as uranium-aluminum alloy	Resonance escape (clean and cold)	1.0	
Fuel Cladding	Aluminum; 0.020 in. thickness	Thermal utilization (clean and cold)	0.76	
Moderator	H ₂ O; 0.117 in. film	Diffusion length squared (clean and cold)	3.65 cm ²	
Reflector	Beryllium; 1.5 metric tons	Age (clean and cold)	64.2 cm ²	
Coolant	H ₂ O; 0.117 in. film	Buckling (clean and cold)	10 ⁻² cm ⁻²	
Fertile material	None	Prompt neutron lifetime	2.63 x 10 ⁻⁴ sec	
Structural material	Aluminum	k _∞ (clean and cold)	1.61	
Shield	Concrete blocks, sand and borated plastic	k _{eff} (clean and cold)	1.05	
LATTICE TYPE	Slab geometry	NEUTRON FLUX DENSITIES		
DIMENSIONS		Fast (maximum)	9.5 x 10 ¹² n/(cm ²)(sec)	
Core	up to 15 x 27 in. x 24 5/8 in. long	Epithermal (maximum)	4.8 x 10 ¹³ n/(cm ²)(sec)	
Reflector	8 in. thick (minimum)	Thermal: maximum (in lattice)	1.6 x 10 ¹³ n/(cm ²)(sec)	
Shield	12 ft thick (minimum)	maximum (in reflector)	2 x 10 ¹³ n/(cm ²)(sec)	
Over-all	28 1/2 x 28 1/2 x 34 ft high	EXPERIMENTAL FACILITIES.	2 - 3/4 in. ID pneumatic rabbit systems	
STRATEGIC MATERIAL		6 - 6 in. dia. horizontal test holes	4 - 3 in. dia. vertical test holes (outside of tank)	
Fissionable material	U235; 2.8 kg	CAPITAL INVESTMENT	\$1 x 10 ⁶ a	
Consumption	1.5 g/day	REFERENCES	Mock-up Design Report, Oak Ridge National Laboratory, W.R. Call and D.J. Mallon, ORNL-701, 138 pp, Secret October 27, 1949	
Burn-up	Indefinite	Materials Testing Reactor Project Handbook Oak Ridge National Laboratory, J.H. Buck and C.F. Leyse, ORNL-963, 584 pp, Secret, May 7, 1951		
Average cycle time	Indefinite			
COOLING SYSTEM				
Type	Recirculated water			
Coolant treatment	Deminerzalization and deaeration (batchwise)			
Pumps	2 - 1000 gpm (at 78 psi) electrically driven centrifugal pumps (1 as standby)			
Safety	Natural convection Gravity-fed water-spray system			
OPERATING CONDITIONS				
Total heat power	1500 kw			
Useful power output	0			
Heat flux (average)	1.31 x 10 ⁴ BTU/(sq ft)(hr)			
Power density (average)	15.7 kw/l			
Specific power (average)	530 kw/kg 25			
Maximum moderator temperature				
Coolant inlet temperature	103.5°F			
Coolant outlet temperature	112°F			
Coolant velocity				
Coolant inlet pressure				
Coolant pressure drop through reactor	2 1/2 psi a			
Pumping rate	1200 gpm			
Pumping power required	55 kw			

a. Estimated
b. Preliminary calculations

a. Estimated
b. Preliminary calculations

Table A.2.7 — Bulk Shielding Reactor (BSR)

LOCATION	Oak Ridge National Laboratory	CONTROLS	Shim	2 - 1 1/4 x 2 1/2 in. vertical, cadmium-lead rods
RESPONSIBLE ORGANIZATIONS	Design Oak Ridge, Tennessee	Regulator	1 - 1 1/4 x 2 1/2 in. vertical, cadmium-lead rod	
Construction	Oak Ridge National Laboratory	Safety	Reactivity change All rods	
Operation	Oak Ridge National Laboratory	FUEL HANDLING	Charging Long handled grappling device	
PURPOSE	Oak Ridge National Laboratory	Discharging	Long handled grappling device; depleted elements stored in pool	
STATUS	In operation since Dec., 1950	PHYSICS ^a	Resonance escape (clean and cold) 1.0	
MATERIALS	Fuel U ²³⁵ as uranium-aluminum alloy	Thermal utilization (clean and cold) 0.76	Diffusion length squared (clean and cold) 3.5 cm ²	
Fuel Cladding	Aluminum	Age (clean and cold) 64.2 cm ²	Buckling (clean and cold) 0.01 cm ⁻²	
Moderator	H ₂ O; 0.117 in. film	Prompt neutron lifetime	k _∞ (clean and cold) 1.61	
Reflector	Beryllium oxide and/or H ₂ O	k _{eff} (clean and cold) 1.003	δk (temperature)	
Coolant	H ₂ O; 0.117 in. film	δk (poisons)	k _{eff} (hot and poisoned) 1.003	
Fertile material	None	NEUTRON FLUX DENSITIES ^a	Fast (average) 1 x 10 ¹¹ n/(cm ²)(sec)	
Structural material	Aluminum	Epithermal (average) 3 x 10 ¹¹ n/(cm ²)(sec)	Thermal: maximum 2 x 10 ¹² n/(cm ²)(sec)	
Shield	H ₂ O	average 1 x 10 ¹² n/(cm ²)(sec)	EXPERIMENTAL FACILITIES	
LATTICE TYPE	Slab geometry	CAPITAL INVESTMENT \$217,000	REFERENCES The New Bulk Shielding Facility at Oak Ridge National Laboratory, Oak Ridge National Laboratory, W.M. Breazeale, ORNL-991, 55 pp, Secret, May 8, 1951	
DIMENSIONS	Core up to 15 x 27 in. x 24 in. high			
Reflector	Depends upon loading			
Shield	16 ft of H ₂ O, or equivalent			
Over-all (pool)	40 x 20 x 20 ft			
STRATEGIC MATERIAL	Fissionable material U ²³⁵ ; 2.4 to 4 kg			
Consumption	Indefinite			
Burn-up	Indefinite			
Average cycle time	Indefinite			
COOLING SYSTEM	Type Water; natural convection			
Coolant source	Sodium chromate as corrosion inhibitor			
Coolant treatment	OPERATING CONDITIONS			
Total heat power.	Useful power output 100 kw			
Innage	Heat flux (maximum) Indefinite			
Power density (average)	1800 BTU/(sq ft)(hr)			
Specific power (average)	1.1 kw/l			
Maximum fuel temperature	30 kw/kg 25			
Maximum sheath temperature				
Maximum moderator temperature				
Pumping power required	0			

a. Preliminary calculations

Table A.2.8 — Argonne Heavy Water Reactor (CP-3')

LOCATION	Argonne National Laboratory, Chicago, Illinois	
RESPONSIBLE ORGANIZATIONS		
Design	Argonne National Laboratory	
Construction	Argonne National Laboratory	
Operation	Argonne National Laboratory	
PURPOSE	Research	
STATUS	In operation from June, 1944 to Jan., 1950 with natural uranium as CP-3. Began operation with enriched fuel in July, 1950 as CP-3'	
MATERIALS		
Fuel	^{235}U ; 4.2 kg as 2% uranium-aluminum alloy	
Fuel Cladding	Aluminum	
Coolant tubes	None	
Moderator	D_2O ; 4.78 metric tons	
Reflector	Top; D_2O	
	Sides and bottom; graphite	
Coolant	D_2O	
Total D_2O requirement	5.72 metric tons	
Fertile material	None	
Structural material	Aluminum	
Reactor atmosphere	Helium	
Shield	Lead and ordinary concrete	
LATTICE TYPE	0.850 in. dia. rods in 5 3/8 in. square array	
DIMENSIONS		
Core	6 ft dia. x 5 1/2 ft	
Reflector	2 ft thick on sides and bottom; 1 ft thick on top	
Shield	4 in. of lead and 8 ft of concrete on sides; 1 ft of lead and 4 ft of laminated steel and masonite on top (modified right octagonal prism)	
Over-all	26 ft across flats by 14 ft high	
STRATEGIC MATERIAL		
Fissionable material	^{235}U	
Consumption	0.29 g/day	
Burn-up	Indefinite	
Average cycle time	Indefinite	
COOLING SYSTEM		
Type	D_2O , recirculated	
Coolant treatment	Filtering	
	Ion exchange purification	
Pumps	1 - canned rotor, sealed, electrically driven, 200 gpm centrifugal pump	
	1 - standby, sealed, centrifugal pump	
AUXILIARY FACILITIES		
Reactor atmosphere	Helium, recirculated	
OPERATING CONDITIONS		
Total heat power	275 kw	
Useful power output	0	
Innage	Indefinite	
Rod power (average)	2.25 kw	
Heat flux: maximum	13,300 BTU/(sq ft)(hr)	
average	5,600 BTU/(sq ft)(hr)	
Power density: maximum	0.12 kw/l	
average	0.05 kw/l	
Specific power: maximum	168 kw/kg	
Maximum fuel temperature	About 120°F	
Maximum sheath temperature	About 110°F	
Maximum moderator temperature	105°F	
Coolant inlet temperature	91°F	
Coolant outlet temperature	104°F	
Coolant velocity	Indefinite	
Coolant inlet pressure	Negligible	
Coolant pressure drop through reactor	Negligible	
Pumping rate	About 150 gpm	
Pumping power required	Negligible	
CONTROLS		
Shim	2 - 4 1/8 x 2 1/2 x 61 in., aluminum-jacketed cadmium, signal-arm-type rods	
Regulator	1 - 7/8 in. OD x 45 in., aluminum-jacketed cadmium, vertical rod	
Safety	2 - 4 1/8 x 2 1/2 x 64 3/4 in. aluminum-jacketed cadmium, signal-arm-type rods	
	2 - 1 1/4 in. OD x 36 in. aluminum-jacketed cadmium, vertical rods	
Reactivity change	0.102	
FUEL HANDLING		
Charging	Manually charged initially	
Discharging	Spent rods withdrawn into a lead coffin	
PHYSICS		
Cell radius	4.35 cm	
Resonance escape (clean and cold)	1.0	
Thermal utilization (clean and cold)	0.8	
Diffusion length squared (clean and cold)	465 cm ²	
Age (clean and cold)	125 cm ²	
Buckling (clean and cold)	882 x 10 ⁻⁶ cm ⁻²	
Prompt neutron lifetime	2.3 x 10 ⁻³ sec	
k_{∞} (clean and cold)	1.6	
k_{eff} (clean and cold)	About 1.016	
δk (temperature)	-5 x 10 ⁻⁴ /°C	
δk (poisons)(equilibrium xenon)	About -0.005	
k_{eff} (hot and poisoned)	About 1.006	
Conversion ratio	None	
NEUTRON FLUX DENSITIES		
Fast	3.5 x 10 ¹¹ n/(cm ²)(sec)	
Thermal: maximum	3.4 x 10 ¹² n/(cm ²)(sec)	
average	1.7 x 10 ¹² n/(cm ²)(sec)	
EXPERIMENTAL FACILITIES	4 - off-axis, 1 3/8 in. ID vertical thimbles in reactor tank	
	1 - axial, 1 3/4 in. ID vertical thimble in reactor tank	
	7 - horizontal, 3 7/8 in. to 10 13/16 in. square test holes	
	1 - horizontal, 29 11/16 x 21 7/8 in. hole, filled with graphite, with 10 thimbles	
	1 - horizontal 5 x 5 ft thermal column with beam hole	
CAPITAL INVESTMENT	A Report to the Atomic Energy Commission on the Proposed CP-3' Reactor, Argonne National Laboratory, ANL-WHZ-250, 96 pp, Secret, June 15, 1950	
REFERENCES		

a. To be replaced by CP-5 in late 1953

Table A.2.9 — Argonne Research Reactor (CP-5)

LOCATION	Argonne National Laboratory, Lemont, Illinois	
RESPONSIBLE ORGANIZATIONS		
Design	Argonne National Laboratory	
Construction	Argonne National Laboratory	
Operation	Argonne National Laboratory	
PURPOSE	Scheduled to replace CP-3 ^a late in 1953	
STATUS	Research	
MATERIALS		
Fuel	U ²³⁵ as uranium-aluminum alloy	
Fuel Cladding	Aluminum; box type, 2 - 0.122 in. side plates and 2 - 0.051 in. side plates, about 2.4 x 3 in. over-all	
Coolant tubes	D ₂ O; 2 to 2 1/2 ft thick	
Moderator	Graphite; 29.5 metric tons	
Reflector: primary	D ₂ O; 2 to 2 1/2 ft thick	
secondary	D ₂ O	
Coolant	D ₂ O	
Total D ₂ O requirement	6.8 metric tons	
Fertile material	None	
Structural material	Aluminum and steel	
Reactor atmosphere	Helium	
Shield	Boral, lead, and limonite-iron-aggregate concrete	
LATTICE TYPE	Grid box elements in 6 in. square array b	
DIMENSIONS		
Core (equivalent)	2 ft dia. x 2 ft	
Reflector: primary	2 to 2 1/2 ft of D ₂ O	
secondary (sides and bottom)	2 ft of graphite	
Shield	3 1/2 in. of lead and 4 ft 8 1/2 in. of heavy concrete	
Over-all	20 1/3 ft across flats by 13 ft 6 1/2 in.	
STRATEGIC MATERIAL		
Fissionable material	U ²³⁵ ; 1.15 kg	
Consumption (average)	0.84 g/day	
COOLING SYSTEM		
Type	D ₂ O, recirculated	
Coolant treatment	Ion exchange columns (continuous)	
Pumps	2 - paralleled (1 standby), 1000 gpm, mechanical seals, electrically driven, centrifugal pumps	
AUXILIARY FACILITIES		
Reactor atmosphere	Helium, recirculated	
OPERATING CONDITIONS (Uniform loading)		
Total heat power	1000 kw	
Useful power output	0	
Rod power (average)	About 80 kw	
Heat flux (average)	34,000 BTU/(sq ft)(hr)	
Power density (average)	6 kw/l	
Specific power (average)	870 kw/kg 25	
Maximum fuel temperature	148°F	
Maximum sheath temperature	146°F	
Coolant inlet temperature	117°F	
Coolant outlet temperature	124°F	
Coolant velocity	5.4 ft/sec	
Coolant inlet pressure	About 5 psi	
Coolant pressure drop through reactor	About 2 psi	
Pumping rate	1000 gal/min	
Pumping power required	10 hp primary 30 hp secondary	
CONTROLS		
Shim	4 - 1 x 5 1/2 x 60 in. aluminum-jacketed, cadmium, signal-arm type rods	
Regulator	1 - 1 1/2 in. OD, aluminum-jacketed cadmium, vertical rod	
Safety	Effectuated by shim rods	
Reactivity change (by safety rods)	Quick drain of D ₂ O to core level	
FUEL HANDLING		
Charging	Lowered through individual access holes in tank plug	
Discharging	Drawn up into shielded coffin	
PHYSICS		
Resonance escape (clean and cold)	1.0	
Thermal utilization (clean and cold)	0.9 a	
Diffusion length squared (clean and cold)	87.5 cm ² a	
Age (clean and cold)(two groups)	128 cm ²	
Buckling (clean and cold)	3 x 10 ⁻³ cm ⁻² a	
Prompt neutron lifetime	About 1 x 10 ⁻³ sec	
k _∞ (clean and cold)	1.85	
k _{eff} (clean and cold)	1.125 a	
δ k (temperature)(total)	-0.015 a	
δ k (poisons)(typical)	-0.083 a	
k _{eff} (hot and poisoned)	1.027 a	
Conversion ratio	None	
NEUTRON FLUX DENSITIES ^a		
Fast (average)	About 10 ¹² n/(cm ²)(sec)	
Epithermal (average)	About 10 ¹³ n/(cm ²)(sec)	
Thermal: maximum	2.8 x 10 ¹³ n/(cm ²)(sec)	
average	2.3 x 10 ¹³ n/(cm ²)(sec)	
EXPERIMENTAL FACILITIES		
1 - 6 in. dia., horizontal test holes in reactor tank: 6 - 1 in. dia., 13 - 3 in. dia., and 3 - 4 in. dia.		
20 - vertical thimbles in graphite reflector: 13 - 3 in. dia., and 7 - 6 in. dia.		
2 - 12 in. dia., horizontal beam holes		
2 - 4 in. dia., horizontal beam holes		
2 - 6 in. dia., horizontal test holes tangent to core		
2 - 8 x 12 in., horizontal test holes in bottom graphite reflector		
1 - 1 in. dia. horizontal pneumatic tube below lattice		
1 - 2 in. dia. horizontal pneumatic tube below lattice		
2 - 5 x 5 ft thermal columns with 16 3/4 in. sq axial test holes		
CAPITAL INVESTMENT	\$1.8 x 10 ⁶ a	
REFERENCES	Feasibility Report for the Argonne Research Reactor (CP-5), Argonne National Laboratory, J.M. West and J.T. Weills, ANL-4779, 23 pp, Secret May 7, 1951	

a. Estimated
b. See text

Table A.2.10—Thermal Test Reactor (TTR)

LOCATION	Knolls Atomic Power Laboratory Schenectady, New York	FUEL HANDLING Charging	Manually operated tongs
RESPONSIBLE ORGANIZATIONS		Discharging	Manually operated tongs
Design	Knolls Atomic Power Laboratory	PHYSICS	
Construction	Knolls Atomic Power Laboratory	Resonance escape (clean and cold)	1.0
Operation	Knolls Atomic Power Laboratory	Thermal utilization (clean and cold)	
PURPOSE	Research	Diffusion length squared (clean and cold)	
STATUS	In operation since Jan., 1951	Age (clean and cold)	5 x 10 ⁻⁴ sec
MATERIALS		Prompt neutron lifetime	
Fuel	U ²³⁵ as uranium-aluminum alloy	Buckling (clean and cold)	
Fuel Cladding	None	k _∞ (clean and cold)	
Fuel tubes	Aluminum	k _{eff} (clean and cold)	Limited to about 1.002
Moderator	Paraffin base oil between fuel discs	δk (temperature)	About 8 x 10 ⁻⁵ /°C
	H ₂ O between fuel assemblies	δk (poisons)	Negligible
Reflector	Graphite	k _{eff} (hot and poisoned)	Limited to about 1.002
Coolant	None	Conversion ratio	None
Fertile material	None	NEUTRON FLUX DENSITIES	
Structural material	Aluminum	Fast	
Reactor atmosphere	None	Thermal: maximum (central column)	3.6 x 10 ⁹ n/(cm ²)(sec)
Shield	Ordinary and high density concrete	average (in active section)	1.6 x 10 ⁹ n/(cm ²)(sec)
LATTICE TYPE	Cylindrical slab	EXPERIMENTAL FACILITIES	1 - 12 in. dia. internal, vertical, thermal column
DIMENSIONS			1 - external, horizontal thermal column
Core	18 in. dia. x 18 in.	CAPITAL INVESTMENT	Feasibility Report for the KAPL Thermal Test Reactor, Knolls
Reflector	About 2 1/3 ft thick	REFERENCES	Atomic Power Laboratory, H.B. Stewart, et al, KAPL-436, 32 pp, Secret, Nov. 9, 1950
Shield	6 ft thick		Supplement No. 1, Feasibility Report for the KAPL Thermal Test Reactor, Knolls Atomic Power Laboratory, H.B. Stewart, et al, KAPL-436, 25 pp, Secret, April 3, 1951
Over-all	22 x 27 x 14 ft high		
STRATEGIC MATERIAL			
Fissionable material	U ²³⁵ ; more than 2.6 kg		
Consumption	Negligible		
Burn-up	Negligible		
Average cycle time	Indefinite		
COOLING SYSTEM			
AUXILIARY FACILITIES			
OPERATING CONDITIONS			
Total heat power	100 watts		
Useful power output	0		
Innage	Indefinite		
Rod power (average)	5 watts		
Heat flux			
Power density (average)	2.4 watts		
Specific power (average)	0.04 kw/kg 25		
Maximum fuel temperature	Negligible		
Maximum moderator temperature	Negligible		
CONTROLS			
Shim	Provided by loading variation		
Regulator	2 - 1/2 in. dia., vertical, aluminum-clad cadmium rods		
Safety	4 - 1/2 in. dia., vertical, aluminum-clad cadmium rods		
	6 - 4 in. wide, 1/32 in. thick, iron-clad cadmium sheets		
Reactivity change	About 0.08		

Table A.2.11—Low Power Research Reactor (LPRR)

LOCATION	RESPONSIBLE ORGANIZATIONS	CONTROLS
Design	North American Aviation, Inc.	Shim 4 - 2 in. dia. vertical rod of boron carbide filled stainless steel tubing plus a moderator section
Construction		
Operation		Regulator 1 - 1 in. dia. vertical rod of boron carbide filled stainless steel tubing
PURPOSE	Research	Safety 2 - 2 x 4 in. vertical rods of boron carbide filled stainless steel cans
STATUS	Design study	Reactivity change 0.275
MATERIALS		FUEL HANDLING
Fuel	U235 in graphite	Charging } Core tank with all fuel handled as a unit
Fuel Cladding	None	Discharging }
Coolant tubes	Aluminum; 1/8 in. wall	
Moderator	Graphite; 1/3 metric tons	PHYSICS ^a
Reflector	Graphite; 20 metric tons	Resonance escape (clean and cold) b 0.8666
Coolant	D ₂ O	Thermal utilization (clean and cold) 0.8903
Total D ₂ O requirement	270 kg	Diffusion length squared (clean and cold) 129 cm ²
Fertile material	None	Age (clean and cold) 383 cm ²
Structural material	Aluminum and graphite	Buckling (clean and cold) 1.15 x 10 ⁻³ sec
Reactor atmosphere	Helium (low pressure)	Prompt neutron lifetime 1.9
Shield	Steel and iron-ore-colemanite concrete	k _∞ (clean and cold) 1.095
LATTICE TYPE	Homogeneous	δ k (temperature) -4 x 10 ⁻⁴ /°C
DIMENSIONS		δ k (poisons) -0.0175
Core	46 in. dia. x 42 in. high	k _{eff} (hot and poisoned) 1.035
Reflector	28 in. on sides; 24 in. on top and bottom	Conversion ratio None
Shield	Steel; 1 in. Concrete; 72 in.	NEUTRON FLUX DENSITIES
Over-all	Octagonal prism; 20 2/3 ft across flats x 14 1/3 ft high	Fast: maximum 3.5 x 10 ¹² n/(cm ²)(sec)
STRATEGIC MATERIAL		average 1.2 x 10 ¹² n/(cm ²)(sec)
Fissionable material	U235; 4 kg	Thermal (average) 1.2 x 10 ¹² n/(cm ²)(sec)
Consumption	6.3 x 10 ⁻² gm/day	EXPERIMENTAL FACILITIES: 2 - 3 in. dia. horizontal holes tangential to core tank
COOLING SYSTEM		6 - 3 1/2 in. dia. horizontal holes extending to core tank
Type	Recirculated D ₂ O	2 - 2 in. dia. horizontal pneumatic tubes tangential to core tank
Coolant treatment	Ion exchange demineralization	6 - 3 in. dia. vertical tubes in reflector for multiple specimen irradiations
Pumps	Not specified	1 - 4 1/2 x 4 1/2 ft horizontal thermal column
AUXILIARY FACILITIES		CAPITAL INVESTMENT \$6 x 10 ⁵
OPERATING CONDITIONS		REFERENCES A Low Power Research Reactor Engineering Design Report, North American Aviation, Inc., In preparation
Total heat power	150 kw	a. Preliminary calculations
Useful power output	0	b. Escape from capture in epithermal region
Heat flux (average)	4100 BTU/(sq ft)(hr)	
Power density (average)	0.18 kw/l	
Specific power (average)	37.5 kw/kg 25	
Coolant inlet temperature	140°F	
Coolant outlet temperature	158°F	
Coolant velocity	0.657 ft/sec	
Coolant inlet pressure	About 5 psig	
Coolant pressure drop through reactor	Negligible	
Pumping rate (D ₂ O)	50 gpm	
Pumping power required (total)	4 3/4 hp	

Table A.2.12—Los Alamos Water Boiler (SUPO)

LOCATION	Los Alamos Scientific Laboratory	Coolant pressure drop through reactor	About 60 psi
RESPONSIBLE ORGANIZATIONS		Pumping rate	3 1/4 gpm
Design	Los Alamos Scientific Laboratory	Pumping power required	None
Construction	Los Alamos Scientific Laboratory	CONTROLS	
Operation	Los Alamos Scientific Laboratory	Shim	Solution concentration and regulator rods
PURPOSE	Research	Regulator	2 - 9/16 in. dia. x 18 in., vertical boron10 steel jacketed (cadmium plated) rods extending into core
STATUS	In operation, with design variations, since May, 1944		
MATERIALS			
Fuel	Uranium (88.7% U ²³⁵); 980 gm as uranyl nitrate solution	Safety	2 - 1/32 x 3 x 30 in., vertical, aluminum clad 1 - 1/32 x 3 x 30 in., vertical, aluminum clad, cadmium sheets cadmium sheet 0.08
Coolant tubes	Stainless steel, 1/4 in. OD x 1/32 in. wall	Reactivity change	
Moderator	H ₂ O	FUEL HANDLING	
Reflector	Graphite	Charging	Transfer flask with fluid
Coolant	H ₂ O	Discharging	control by air pressure variation
Fertile material	None	PHYSICS	
Structural material	Stainless steel	Resonance escape (clean and cold)	
Reactor atmosphere	Air	Thermal utilization (clean and cold) ^a	0.71
Shield	Boron carbide, paraffin, steel, lead and concrete	Diffusion length squared (clean and cold) ^a	1.47 cm ²
LATTICE TYPE	Homogeneous	Age (clean and cold) ^a	33 cm ²
DIMENSIONS		Prompt neutron lifetime	
Core	12 in. dia	Buckling (clean and cold)	1.44
Reflector	21 1/2 in. thick or greater	k _∞ (clean and cold)	
Shield	Boron carbide plus paraffin; 1/2 in. Steel; 2 in. Lead; 4 in. Concrete; 5 ft	k _{eff} (clean and cold)	-2.4 x 10 ⁻⁴ /°C
Over-all	15 x 15 x 11 ft high	Δk (temperature)(true)	-3.5 x 10 ⁻⁴ /°C
STRATEGIC MATERIAL		Δk (poisons)	
Fissionable material	U ²³⁵ , 895 gms	k _{eff} (hot and poisoned)	
Consumption	About 5 x 10 ⁻³ gm/day	Conversion ratio	None
Burn-up	Indefinite	NEUTRON FLUX DENSITIES ^a	
Average cycle time	Indefinite	Fast (maximum)	4.2 x 10 ² n/(cm ²)(sec)(watt)
COOLING SYSTEM		Epithermal (maximum)	6.2 x 10 ² n/(cm ²)(sec)(watt)
Type	H ₂ O	Thermal (maximum)	3.8 x 10 ⁷ n/(cm ²)(sec)(watt)
Coolant source	Well water	EXPERIMENTAL FACILITIES	
Coolant treatment	Filtered	1 - 1 in. dia., horizontal test hole through reactor core	
Pumps	None	1 - 1 7/16 in. dia. horizontal test hole tangent to reactor core	
Retention basin	None	2 - horizontal, graphite thermal columns (1 - 4 x 4 ft and 1 - 5 x 5 ft), with several removable stringers	
AUXILIARY FACILITIES		CAPITAL INVESTMENT	The Los Alamos Homogeneous Reactor,
Reactor atmosphere	Recirculated air system	REFERENCES	Supo Model, Los Alamos Scientific Laboratory, L.D.P. King, LA-1301, October, 1951
OPERATING CONDITIONS (typical)			
Total heat power	35 kw		
Useful power output	0		
Innage	0.3 to 0.4		
Heat flux (average)	28,000 BTU/(sq ft)(hr)		
Power density (average)	2.8 kw/l		
Specific power (average)	39 kw/kg		
Average fuel solution temperature	180°F		
Coolant inlet temperature	60°F		
Coolant outlet temperature	130°F		
Coolant velocity			
Coolant inlet pressure	60 psi		

a. Estimated

Table A.2.13 — Homogeneous Reactor Experiment (HRE)

LOCATION	Oak Ridge National Laboratory Oak Ridge, Tennessee	Innage	Indefinite
RESPONSIBLE ORGANIZATIONS			
Design	Oak Ridge National Laboratory	Power density (average)	20 kw/l
Construction	Oak Ridge National Laboratory	Specific power (average)	About 600 kw/kg 25 in core
Operation	Oak Ridge National Laboratory	Fuel solution inlet temperature	407°F
PURPOSE	Experimental	Fuel solution outlet temperature	482°F
STATUS	In operation since April, 1952	Fuel solution inlet pressure	1000 psia
MATERIALS			
Fuel	U ²³⁵ , 1.6 to 2.1 kg as UO ₂ SO ₄ in water	Fuel solution pressure drop through reactor	Negligible
Coolant tubes	None	Pumping rate	100 gpm
Moderator	H ₂ O	Pumping power required (total)	25 kw
Reflector	D ₂ O	CONTROLS	
Total D ₂ O requirement	About 0.5 metric ton	Shim	1 - assembly of stainless steel clad, boron sheets in the form of cylindrical segments, tangential to core in reflector, Variation of fuel concentration
Coolant	Circulating fuel	Regulator	1 - stainless steel clad, boron sheet in the form of a cylindrical segment, tangential to core in reflector
Fertile material	None	Safety	1 - assembly of stainless steel clad, boron sheets in the form of cylindrical segments, tangential to core in reflector
Structural material	Stainless steel	FUEL HANDLING	
Reactor atmosphere	Decomposition and fission product gases	Charging	Pump injection into circulating system
Shield	Steel and barytes concrete	Discharging	Drain to dump tanks
LATTICE TYPE			
DIMENSIONS			
Core	18 in. ID sphere	NEUTRON FLUX DENSITIES ^a	
Reflector	10 in. thick	Thermal: average	2 x 10 ¹³ n/(cm ²)(sec)
Shield	7 ft thick or more	EXPERIMENTAL FACILITIES	
Over-all	22 x 26 x 18 2/3 ft high	CAPITAL INVESTMENT	
STRATEGIC MATERIAL			
Fissionable material (total)	U ²³⁵	REFERENCES	
Consumption	About 1 gm/day	Homogeneous Reactor Experiment Feasibility Report, Oak Ridge National Laboratory, ORNL-730, 108 pp, Secret, July 6, 1950	
Burn-up	Indefinite	Homogeneous Reactor Project Quarterly Progress Report, Oak Ridge National Laboratory, ORNL-1318, 184 pp, Secret, Sept. 19, 1952	
Average cycle time	Indefinite	a. Estimated	
COOLING SYSTEM			
Type	Recirculated liquid fuel		
Coolant treatment	Batch processing		
Pumps	1 - 100 gpm, Westinghouse Model 100A sealed armature, centrifugal pump 2 - 1 gpm, Pulsafeeder pumps		
AUXILIARY FACILITIES			
Safety	Natural convection cooling system		
OPERATING CONDITIONS			
Moderator cooling	Circulation of D ₂ O through heat exchangers		
Power production	1 - 250 kw steam turbo-generator		
Total heat power	1000 kw		
Useful power output	About 120 kw (design)		

INDEX

INDEX

A

Absorption coefficients, narrow-beam, combinations
for mixtures of elements, 641-642
components of, 640-641
definition for monochromatic gammas, 640
filtration effect, 648
(See also Energy-absorption coefficients and Mass
absorption coefficients)

Absorption of capture gammas, 705-707

Activity-mass formula, 630-631

Adjoint equation for infinite homogeneous medium,
428

Adjoint operator, 471

Age, definition of, 401
of fission neutrons, in moderators, 485
in water-metal mixtures, 486
for lattice reactors, 482, 485
measurement of, 49-51
of Ra- α -Be neutrons in water-metal mixtures,
486
and slowing-down length, 402
of water lattices, 501

Age equation, with absorption, 402
solutions for homogeneous regions, 402-403
for variable-density medium, 470

Age theory, 401-405
continuity equation in, 401
deviation from, 412
group method for, 418-419
and group theory, 422
migration area in, 404
moment improvements without absorption,
409-410
slowing-down distance in, 409
two media problems in, 402

Aging, in finite homogeneous medium, 403
followed by diffusion, 403-408
in finite homogeneous media, 405
in infinite homogeneous medium, 404
in infinite homogeneous medium, 402

Air, composition of, 741
density of, 742
mass absorption coefficient of, 721

Albedo, 446
approach to neutron attenuation, 695
effective, 696-698
table, 698
fast-neutron, for concrete, 696, 697
for water, 696, 697
gamma-ray for concrete, 698

Albedo, wall, in single-bend duct, 696
in straight duct, 695

Alpha (see Cross sections, capture-to-fission ratio
of)

Alpha particles, emission in fission, 67
range of, 66-67

Aluminum, $\sigma_c(1 - \overline{\cos \theta})$ value for, 110

Ammonia, atomic density of, 720
mass absorption coefficient of, 721
molecular density of, 721
molecular weight of, 721
physical properties of, 733

Amu (see Atomic mass unit)

Analysis of U. S. waters, 736

Argonne Heavy Water Reactor, 769

Argonne Research Reactor, 770

Ash, atomic density of hydrogen in, 721
mass absorption coefficient of, 722
white, composition of, 738
physical properties of, 739

Atomic density, of elements, 717
of hydrogen, in compounds, 720
in organic compounds, 720

Atomic mass unit, definition of, 61
energy equivalent of, 61

Atomic numbers of elements, 717-719

Atomic weights of elements, 717-719

Attenuation, gamma, by air ducts and voids, 698
by single straight duct, 698
neutron, dependence of visible wall region at
bend on angle of bend, 696, 697
by multiple-bend duct, 696-697
by single-bend duct, 696
by single straight duct, 695, 696
by voids, 698

Attenuation constant, for linear anisotropy, 430
(See also Diffusion length and Transport theory)

Attenuation function, definition of, 677-678

Attenuation kernel (see Attenuation function)

B

Balsa, atomic density of hydrogen in, 721
composition of, 738
physical properties of, 739

Barytes aggregate, composition of, 727

Beryllium, lattices moderated by, 484
(n, 2n) reaction in, 82-83
 $\sigma_c(1 - \overline{\cos \theta})$ value for, 110
slowing-down density in, 507

- Beryllium, total cross section of, 78-79, 142
 use of, for neutron monochromator, 22
 in neutron sources, 1
 Beta decay (see Radioactive decay)
 Binding energy, 61, 626
 of additional neutron, 62, 86-105
 and packing fraction, 62
 Biological dose, 677
 Boiling points of organic compounds, 741
 Boltzmann equation, 365
 for anisotropic scattering, 380
 solutions, 455
 spherical harmonics in, 381
 for energy-independent cross sections, 450
 integral equation formulation for one-velocity theory, 378-380
 integro-differential formulation for infinite homogeneous region, 376-378
 for isotropic scattering, 378
 kernel for, 378
 plane kernel for, 379
 for slab geometry, 378
 time-dependent treatment of, 379
 variational formulation of, 380-381
 (See also Transport equation)
 Boral, composition of, 750
 mass absorption coefficient of, 721
 physical properties of, 750
 Boration of water, 748
 Boron, use in neutron detectors, 23-24, 29
 Boron coatings for metals, 748-749
 Boron-containing materials, 748-751
 solubility of, 748, 751
 Boron frits, composition of, 731
 Boundary conditions for black medium, 423
 Boundary equations, in diffusion theory, across
 interface between two media, 390
 between medium and vacuum, 390-391
 in group-diffusion method, 418
 for group method, 465
 for slowing down with absorption in finite regions, 422-423
 for slowing-down density, for Greuling-Goertzel approximation, 423
 for Wigner approximation, 423
 in spherical-harmonic method, 390
 in transport theory, 390
 Breit-Wigner formula, for capture cross section, 71
 for scattering cross section, 72
 Bricks, composition of, 742
 mass absorption coefficient of, 721
 physical properties of, 743
 Broad-beam attenuation, 649, 650
 apparent absorption coefficient, 649
 gamma deflection, 649
 Brookhaven Graphite Research Reactor, 765
 Buckling, 435
 effective value of, 608
 geometric, 443, 444
 stationary formula for, 443
 material, approximations for, 435
 for heavy-water system, 494
 measurement of, 55
 for water lattices, 501
 values for cylindrical shapes, 614
 for water lattices, 499, 500
 Build-up factors, 651-652, 684-685
 for gamma-ray absorptions, 701-702
 linear, definition of, 686
 NDA-NBS calculation, tables, 660, 661
 trend at great depths, 655
 data, 656
 unitary, definition of, 686
 Bulk Shielding Reactor, 768
 spectral distributions of, 704
- ## C
- Cadmium ratio, 18, 51
 for water lattices, 500
 Capture gammas, absorption of, 705-707
 Carbon, total cross section of, 78-79, 143
 (See also Graphite)
 Cements, colemanite borated, composition of, 723
 physical properties of, 724
 composition of, 723
 mass absorption coefficient of, 722
 physical properties of, 724
 plain, composition of, 723
 physical properties of, 724
 portland, composition of, 723
 Chemical binding, 78-80, 144-145
 Chicago Pile No. 1, 762
 Chicago Pile No. 2, 763
 Chopper, neutron, 19
 Chromium, $\sigma_c (1 - \cos \theta)$ value for, 110
 Collision mechanics, 75-78, 110, 134
 Collision reactions, 11, 70-84, 110-114, 128-157, 351-363
 laboratory and center-of-mass coordinates for, 70
 Composition, of air, 741
 of barytes aggregate, 727
 of barytes concrete, 726
 of barytes-limonite concrete, 728
 of boral, 750
 of boron frits, 731
 of bricks, 742
 of cements, 723
 of concretes, 730
 of fuel oil, 733
 of gasoline, 734
 of glass, 743
 of iron, 744
 of lucite, 735
 of lumnite, 731
 of masonite, 740
 of MO concrete, 725
 of ordinary concrete, 725
 of paraffin, 736
 of rocks, 746
 of rubber, 735
 of sand, 724
 of shield materials, 723-748
 of stainless steel type 347, 747
 of woods, 738
 Compound nucleus, excitation of, 62
 fission of, 68
 formation of, 71, 75
 cross section for, 80-81
 Compounds in shield materials, 720
 atomic densities of hydrogen in, 720

- Compounds in shield materials, densities of, 720
 molecular densities of, 720
 removal cross sections of, 723
- Compressive strength of concretes, 732
- Compton scattering, 639
 probability of, 639
 removal of incident photon energy, 643, 644
- Concretes, barytes, composition of, 726
 elemental composition of, 728
 physical properties of, 727
 barytes-limonite, composition of, 728
 compressive strength of, 728
 density of, 728
 elemental composition of, 728
 boron frits-barytes, composition of, 730
 compressive strength of, 732
 density of, 732
 description of, 729
 elemental composition of, 732
 colemanite-barytes, composition of, 730
 compressive strength of, 732
 density of, 732
 description of, 729
 elemental composition of, 732
 composition of, 674, 730
 compressive strength of, 732
 density of, 732
 elemental composition of, 732
 iron-portland, composition of, 730
 compressive strength of, 732
 density of, 732
 description of, 729
 elemental composition of, 732
 lumnite-colemanite-barytes, composition of, 730
 compressive strength of, 732
 density of, 732
 description of, 729
 elemental composition of, 732
 lumnite-portland-colemanite-barytes, composition of, 730
 compressive strength of, 732
 density of, 732
 description of, 729
 elemental composition of, 732
 mass absorption coefficient of, 722
- MO, composition of, 725
 physical properties of, 726
- ordinary, composition of, 725
 physical properties of, 725
- Cone of radiation, 683, 684
- Constants, 754
- Continuity equation, 365, 382
 for slowing-down density, 367
- Control (see Reactor dynamics)
- Control boundaries, 614
- Control gaps, 614-615
- Control regions, 609-614
- Control rods, effective radius of, 602, 605-607
 for black bars, 606
 for non-black bars, 605-607
 flux flattening by, 612
 multiple, shadowing effect for, 605, 608
 shape of, relative effectiveness for, 605, 607
 single, 602-605
 effective radius of, 602
 longitudinal displacement of, 602, 604
- Control rods, single, radial displacement of, 602, 603
 transfer function of, 583-584, 593
- Conversion factors, angular displacement, 756
 density, 757
 energy, 754-755
 gamma-ray cross section, 760
 length, 755-756
 pressure, 756-757
 thermal conductivity, 757
 time, 755
 volume, 756
- Copper, $\sigma_e (1 - \cos \theta)$ value for, 110
- Counters (see Neutron detectors)
- Critical equation, for bare thermal reactor,
 in terms of migration area, 464
 eigenvalue formulation of, 471
 for infinite homogeneous medium, 427
 for thermal reactor, by mode method, 463
 for two-group theory, 466
- Critical mass, 477-478, 485-495
 data for water boilers, 488
 minimum, for water reactor, 478, 512
 of reactors, deuterium-moderated, 478, 491-495, 515
 heavy-water-moderated, with graphite reflectors, 493
 with heavy-water reflector, 491-493
 without reflector, 492
 homogeneous, with moderated cores, 477-478, 488-495, 510-515
 hydrogen-moderated, 477-478, 488-490, 510-514
 water-moderated, 477
 effect of reflector on, 478, 490
- Critical size, of bare spheres, 430
 effect of density on, 445
 for odd-shaped reflected reactors, 449
 for simple geometries, 431
 for thermal reactor, with Gaussian slowing down, 458
- Cross sections, absorption, 42-45
 measurement of, by activation method, 44
 by change in reactor reactivity, 43-44
 by depletion method, 44
 by diffusion length, 45
 by substitution method, 42-43
 by transmission method, 42
 average values for, 376
 capture, 73
 Breit-Wigner formula for, 71
 measurement of, 47-48
 capture-to-fission ratio of, 69
 measurement of, 48-49
 definition of, 41
 differential, in center-of-mass and laboratory systems, 70
 effect of density on, 554
 effective value of, 562
 elastic scattering, value of, 78, 110-111, 129, 135-141, 351-363
 fission, 68, 117-126
 measurement of, 47
 free-atom, 80
 inelastic, data for, 80, 112-114
 of iron, 47
 for inverse process, 74
 measurement of, 41-49

Cross sections, neutron, 71-74, 128-132
 radiative capture, 62, 130
 Breit-Wigner fit for cadmium, 83, 152
 for 1-mev neutrons, 84, 130
 removal, 451
 scattering, 45-46, 71-72
 Breit-Wigner formula for, 72
 differential, measurement of, 45
 for large angles, 46
 by poor-geometry experiment, 46
 by recoil counters, 45-46
 inelastic, 47
 measurement of, by direct spectrum method, 47
 by gamma-ray method, 47
 by transmission method, 47
 total, 46
 measurement by transmission, 46
 thermal values of, 351-363
 total, 41-42
 of beryllium, 79, 142
 of carbon, 79, 143
 of deuterium, 145
 of hydrogen, 144
 measurement by transmission experiment, 41
 for total transport reaction, 74, 131
 transport, 78, 111
 definition of, 78
 values of, 111, 487
 Crystal effects, 78-80, 142-145
 Crystal monochromator, 21-22
 resolution of, 21
 Curie, 630-631
 Current, definition of, 677
 neutron (see Neutron current)

D

Danger coefficients, and absorption cross-section
 measurement, 43
 for measurement of capture-to-fission ratio,
 48-49
 Density, of air, 742
 of compounds in shield materials, 720
 of concretes, 732
 of elements, 717
 of organic compounds, 741
 of wood, and volume composition, 740
 Deuterium, reactors moderated by, critical mass of,
 478, 491-495, 515
 slowing down in, 370, 374
 total cross section of, 145
 Diffusion, in crystalline matter, 425
 of gamma rays, 646
 hardening effect in, 425
 in high-atomic-weight material, 425
 softening effect in, 425
 of thermal neutrons, 423-425
 with energy-independent cross sections, 424-425
 Diffusion coefficient, 382, 389
 correction to, 389
 effect of density on, 554
 thermal, effect of temperature on, 562
 Diffusion constant, 443
 Diffusion equation, for homogeneous multiplying
 region, 435

Diffusion equation, solutions of, 466, 468
 asymptotic, 393
 for bare reactors, 443-445
 for cylindrical geometries, 446, 447
 near free boundary, 393
 for plane geometries, 446
 for spherical geometries, 446, 447
 time-dependent, 389-390
 useful formulations of, 383
 validity of, 389
 Diffusion kernel (see Kernel)
 Diffusion length, 386, 389
 for anisotropic scattering, 392
 measurement of, 52-54, 56
 thermal, 425
 for lattice reactors, 482, 487
 values of, 487
 for water lattices, 501
 Diffusion theory, boundary conditions in, across
 interface between two media, 390
 between medium and vacuum, 390-391
 effect of anisotropic scattering in, 389
 extrapolation length in, 391
 for homogeneous reactors, 435, 443-450
 integral equations of, 383-384
 prescriptions for improving, 389
 near source, 389
 for strongly absorbing media, 389
 results of transport theory in, 389
 for linear scattering law, 391
 for quadratic scattering law, 391
 retardation time in, 385
 time-dependent, 384-385
 Green's function for, 384-385
 telegrapher's equation in, 385
 transport correction to, 382
 validity of, 385
 variational formulation of, 384
 Diffusion time, 385
 Doppler effect, 73, 597
 and reactivity, 556
 Dosage rate, 630
 Ducts, air, 695
 albedo approach, 695
 multiple-bend, 696
 principal investigations of, 695
 single-bend, 696
 straight, 695
 Dynamics (see Reactor dynamics)

E

Effective removal cross section, 670-671
 definition of, 671
 of iron, 723
 of lead, 723
 specific values for, iron, 673
 lead, 671
 oxygen, 671, 672
 table, 673
 use in calculating shields, 673
 (See also Removal cross section)
 Effective source area, 683-684
 Einstein energy-mass formula, 61
 Elastic scattering, 668

Elastic scattering, angular distribution of, 668
 definition of, 667
 "potential," 668, 671
 "resonance," 668, 671
 Electrons, range of, 66
 Elemental composition, of concretes, 732
 barytes, 728
 barytes-limonite, 728
 Elementary interaction processes, 637-647
 classification by effect on photons, 638
 classification by mechanism, 637-638
 probability, 640-643
 Elements, atomic densities of, 717
 atomic numbers of, 717-719
 atomic weights of, 717-719
 densities of, 717
 mass absorption coefficients of, 718-719
 removal cross sections of, 723
 Energy absorption, of core, 703
 of core and reflector, 703
 of shield, 703
 of spherical core and reflector, 703
 Energy-absorption coefficients, 702
 narrow-beam, 646
 table, 647, 661
 Energy dissipation, 643-647
 energy transport, 645-646
 by electrons, 645
 distance traveled, 645
 by neutrons, 645
 distance traveled, 645
 by positrons, 645
 distance traveled, 645
 by protons, 646
 distance traveled, 646
 sidewise gamma escape, 643-645
 annihilation, 645
 bremsstrahlung, 645
 fluorescence, 643, 644
 fluorescent yield, 644
 scattering, 643, 644
 energy fraction scattered, 644
 Energy range, 637
 Exponential integral functions, definition of, 686
 figures, 690-692
 table, 688
 Exponential law of attenuation, 640, 641
 importance for penetration problem, 651
 Exponential pile, 55-56
 Extrapolation distance, 399
 for anisotropic scattering, 392
 for black cylinders, 391, 395
 for black spheres, 391, 394
 in diffusion theory, 391
 effective, 423
 in group method, 418
 measurement of, 54-55
 for plane geometry, 392
 in transport theory, 391
 Extrapolation length (see Extrapolation distance)

F

Fermi age theory, 370, 401-405
 (See also Age theory and Slowing down)

Feynman-Welton method, 450-456
 Fick's law, 382, 387
 validity of, 385
 in asymptotic region, 389
 Fission, 67-70, 106-110, 117-127
 alpha-particle emission in, 68
 cross sections for, 68, 117-126
 energy release in, 70, 110
 gamma-ray spectrum, 69
 neutron spectrum, 69
 neutron yield, delayed, 67
 spontaneous, 68
 decay constant, 106
 thresholds, 68, 106
 of uranium 235, energy distribution in, 110
 Fission products, 68-69, 106-108, 109, 127
 delayed neutrons, 623, 624
 gamma rays, 623, 624
 gross activity of, 623
 hard emitters, 623, 624
 half-lives of, 106-108
 kinetic energy of, 67, 68, 70, 108, 110
 radiation from, time dependence of, 68-69, 110
 range of, 67, 105
 thermal absorption cross sections of, 106-108
 yields of, 68, 106-108, 127
 Fission sources, 621-624
 Flux, definition of, 677
 Flux distribution, in sigma pile, 53, 54
 for water boiler, 477, 511
 Foils, thick, 677
 thin, 677
 Fuel oil, atomic density of hydrogen in, 721
 composition of, 733
 mass absorption coefficient of, 722
 physical properties of, 734

G

Gamma rays, attenuation of, 637-666
 capture, 624-626
 materials for suppression of, 716
 emission probability, 66
 experimental information on, 660, 662-664
 backscattering, 662-664
 distribution near boundary, 662
 distribution in "phantoms," 662
 effect of inhomogeneities, 662
 radiation emerging from barrier, 662
 radiological shielding, 662
 sidescattering, 662
 fission, 623, 624
 spectrum of, 69
 flux-dose conversion factor, 758
 inelastic scattering, 625-626
 instruments for measuring, 625
 prompt, 623
 Gamma sources, (γ, n), 701
 inelastic-scattering, 701
 primary, 701
 Gaps, effect on multiplication, 56
 Gasoline, atomic density of hydrogen in, 721
 composition of, 734
 mass absorption coefficient of, 722
 physical properties of, 734

Geometry, shielding, 677-693
 Glass, composition of, 743
 mass absorption coefficient of, 722
 physical properties of, 744
 Granite, composition of, 746
 mass absorption coefficient of, 722
 physical properties of, 747
 Graphite, lattices moderated by, 483-484, 499, 522-528
 reactors moderated by, flat flux for, 465
 $\sigma_c(1 - \overline{\cos \theta})$ value for, 110
 slowing down in, 412, 413
 slowing-down density in, 412, 505
 Group-diffusion method, 417-422
 boundary conditions in, 418
 choice of parameters in, 419-420
 flux equations for, 417-418
 iteration technique in, 420
 kernels for, 420-422
 slowing-down density in, equations for, 418-419

H

Half-value layer of absorber, 642
 Heat generation in shields, 701-708
 Heavy-water system, material buckling for, 494
 Hickory, atomic density of hydrogen in, 721
 composition of, 738
 physical properties of, 739
 Homogeneous Reactor Experiment, 774
 Homogeneous reactors, bare, 463-464
 comparative accuracy of methods for, 430-431
 end-point method for, 430, 431
 flux in, 444
 iterative method for, 429-430
 critical mass of, 477-478, 485-495
 diffusion theory for, 435, 443-450
 hydrogen-moderated, 464
 multiregion, two-group treatment of, 465-469
 multivelocity, anisotropic scattering in, 455-456
 approximate solutions for, 452-453
 Feynman-Welton method for, 450-456
 one-velocity treatment of, 450-456
 with nonuniform moderator, 470
 odd shapes of, 470
 one-velocity treatment of, 429-450
 reflected, 445-449
 and cylindrical geometry, 449-450
 approximate solutions for, 450
 end-point method for, 431
 solutions for odd shapes, 449-450
 two-group theory for, 453-455
 Serber-Wilson method for, 431, 433-434
 thermal, mode methods for, 462-463
 treatment of, for Gaussian slowing down, 456-461
 for symmetric slowing-down kernel, 459
 transport approximation for, 431, 432
 treatment for energy-dependent cross sections, 451-453
 with uniform moderator, 456-465
 with flat thermal flux, 464
 with minimum mass, 464
 with nonuniform fuel loading, 464-465
 with uniform power density, 464

Homogeneous reactors, with variable-density moderator, 470
 with variable fuel distribution, 470
 water-moderated, 462
 (See also Critical mass and Critical size)
 Hydrogen, atomic density of, in compounds, 720
 in organic compounds, 720
 cross section, 669-670
 total, 144
 exact solutions for slowing down, 369
 and heavy element, slowing down in, 370
 reactors moderated by, 464
 critical mass of, 477-478, 488-490, 510-514
 scattering by, energy distribution from, 76-77
 slowing down in, 367, 369
 slowing-down density in, 412, 414-416
 slowing-down length in, 415
 use in neutron detector, 32
 (See also Water)

I

Image method, 423
 Importance, 473-474
 definition of, 532
 of delayed neutron emitters, 533
 and generation time, 473-474
 and reactivity, 473
 Indium, use as neutron detector, 25
 Inelastic scattering, 668-669
 cross sections, 668
 definition of, 667
 gamma rays in, 668-669
 Intensity of radiation, 630
 Interaction processes, elementary (see Elementary interaction processes)
 Ion pairs, 629
 Iron, atomic density of, 717
 composition of, 744
 effective removal cross section of, 723
 inelastic cross section of, 47
 mass absorption coefficient of, 718, 722
 physical properties of, 745
 $\sigma_c(1 - \overline{\cos \theta})$ value for, 110
 Isotopes, table of, 158-350

K

Kernel, for Boltzmann equation, 378
 convolution of, 421
 diffusion, 383, 384
 group-diffusion, 420-422
 plane, for Boltzmann equation, 379
 point diffusion, 421
 for slowing down, 368
 symmetric, slowing down by, 459
 synthetic, for slowing down, 368-370, 373
 solutions for, 369
 use for critical mass of water reactors, 477
 transport, 380
 solution by Fourier transforms, 379-380
 Kinetic theory of neutrons, 365-426

L

- Lattice reactors, 478-485, 487, 495-503, 516-528
 - age for, 482, 485
 - diffusion length for, thermal, 482, 487
 - effective resonance integral for, 481-482
 - experimental and numerical results for, 483-484, 499-501, 522-528
 - fast-fission effect for, 479, 483, 495-496, 516
 - data for, 495
 - interaction effects for, 479
 - uranium metal rods, 496
 - values of, 496
 - multiplication factor for, 484
 - resonance escape probability for, 480-483, 497-498, 502-503, 520-521
 - surface and volume absorption in, 481
 - thermal utilization for, 479-480, 483, 487, 497, 517-519
- Lead, atomic density of, 717
 - effective removal cross section of, 723
 - mass absorption coefficient of, 719, 722
 - physical properties of, 746
- Leakage, reactor, for shielding calculations, 693
- Limestone, composition of, 746
 - mass absorption coefficient of, 722
 - physical properties of, 747
- Los Alamos Water Boiler, 773
- Low-intensity Training Reactor, 767
- Low Power Research Reactor, 772
- Lucite, atomic density of, 720
 - composition of, 735
 - mass absorption coefficient of, 722
 - molecular density of, 720
 - molecular weight of, 720
 - physical properties of, 735
- Lumnite, composition of, 731

M

- Masonite, atomic density of hydrogen in, 721
 - composition of, 740
 - physical properties of, 740
- Mass absorption coefficients, of elements, 718-719
 - narrow-beam, 641
 - table, 642
 - of shield materials, 721-722
- Materials Testing Reactor, 766
- Maximum permissible contamination, 633-634
- Maximum permissible exposure, 633
- Maxwell-Boltzmann distribution, 425, 556-557
 - and averages, 376
 - for thermal neutrons, 375, 376
- Metals, boron coatings for, 748-749
- Migration area, 464
 - effect of temperature on, 598
 - measurement of, 56
- Milligoat, 677
- Moderation (see Slowing down)
- Molecular densities, of compounds in shield materials, 720
- Molecular weights, of organic compounds in shield materials, 720
- Multigroup diffusion theory, calculation techniques for, 469

- Multigroup diffusion theory, iteration method for, 469
 - (See also Two-group theory)
- Multiplication, interpretation of, 57
 - measurement of, 56-57
- Multiplication factor, 56
 - effect of fuel on, 499
 - effective change by control rods, 614
 - for homogeneous region, 435
 - for lattice reactors, 484
 - for lattices, effect of fuel composition on, 484, 499
 - metal-rod, 484, 522
 - one-group, 383
 - stationary expression for, 533
 - for uranium rods in graphite, 522
 - for water lattices, 501
- Multiplication length, 386

N

- Neutron attenuation, 667-675
 - build-up factor in, 670
 - in concrete, 673-674
 - relaxation lengths for, 674
 - in iron, 673
 - in large thickness of heavy material, 673
 - in lead, 671
 - in water, 671, 672
- Neutron balance (see Continuity equation)
- Neutron current, definition of, 382
- Neutron detection, of fast neutrons, 40-41
 - by fission chambers, 33
 - of slow neutrons, by activation, 25-29
 - standardization of activation foils, 40
 - by threshold detectors, 33-35
 - (See also Neutron detectors)
- Neutron detectors, 23-36
 - for fast neutrons, 32-36
 - "long" counter as, 32
 - photographic emulsions as, 35
 - proton recoil counters as, 32-33
 - scintillation counters as, 35-36
 - isotopes useful for, 25
 - and photographic emulsions, 30-32
 - and resonance scatterers, 29-30
 - for slow neutrons, 23-32
 - fission counters as, 24
 - ionization chambers as, 23-24
 - proportional counters as, 23-24
 - scintillation counters as, 32
 - threshold, isotopes for, 34
 - use of indium as, 25
 - (See also Neutron detection)
- Neutron energy, 759
- Neutron flux, conversion to dose rate, 758
 - thermal, standardization of, 39
- Neutron reactions, 71-84, 110-114, 128-157, 351-363
 - cross sections for, hydrogen, angular distribution of, 669
 - total, 669
 - approximate formula for, 669
 - total, 667
 - (n, α), 84, 155-157
 - (n,p), 84, 114
 - (n,2n), approximate formulas for, 83

Neutron reactions, (n,2n), approximate formulas for,
 in beryllium, 82
 in copper, 82, 114
 in nickel, 82
 in thallium, 82
 in photographic emulsions, 30
 radiative capture, 83-84, 130, 152-154
 (See also Cross sections and Scattering)
 Neutron sources, 1-23
 gamma-ray intensity of, for Po-Be, 3-4
 for Ra-Be, 3
 mock fission, 19
 production of monoenergetic neutrons, 19-23
 by crystal monochromator, 21-22
 by filters, 22-23
 by pulsed cyclotron, 21
 by time-of-flight spectrometer, 19-21
 from reactors, 16-18
 and fission plate, 16
 and thermal column, 16
 spectrum of, for Po-B, 5, 6
 for Po-Be, 4
 for Ra-Be, 3
 use of beryllium in, 1
 use of polonium in, 1, 2
 use of radium in, 1
 using alpha particles, from polonium, 3-5
 from radium, 1, 5
 from radon, 4-5
 using gamma-ray bombardment, of beryllium, 5-6
 of deuterium, 5-6
 manufacture of, 10-13
 neutron energy from, 6
 properties of, 8-9
 spectrum of, 7
 yield of, 8-10
 using particle accelerators, 11, 14-15
 and D-D reaction, 14
 and (d,n) reactions, 15
 and (p,n) reactions, 15
 yields of, measurement of, absolute, 36-37
 relative, 37-39
 use of reactor for, 37-39
 for Ra-B, 5
 from thick targets, 1, 2
 time dependence for, 1
 Neutron temperature, 375
 measurement of, 49
 in various reactors, 49
 Neutron time of flight, 759
 Neutron velocity, 759
 average value of, 376
 Neutron wavelength, 758, 759
 Neutron width, for capture, 73
 for decay of nucleus, 75
 for scattering, 73
 Neutrons, "cold," production of, 425
 delayed, 69-70, 109, 623, 624
 and circulating fuel, 569
 energy of, 109
 mean life of, 109
 parents of, 109
 yields of, 109
 fission, 621-622
 spectrum of, 69
 low-energy, 759

Neutrons, prompt, 621-622
 thermal (see Thermal neutrons)
 Nickel, $\alpha_e (1 - \cos \theta)$ value for, 110
 Nuclear physics, 61-364
 nomenclature in, 61, 84
 Nuclear plates, deuterium-loaded, 625
 Nuclear reactions, kinetic energy available for, 70
 momentum conservation in, 70
 reciprocity theorem for, 74-75
 schematic theory of, reaction cross section from,
 74, 132
 total cross section from, 74, 129
 transport cross section from, 74, 131
 Nucleus, binding energy of (see Binding energy)
 compound (see Compound nucleus)
 cross sections of (see Cross sections)
 level density of, 75, 80-81, 133
 level spacings of, 62, 130
 level width of, 71
 "magic," 62
 mass of, 61-62, 86-105, 115-116, 130
 empirical formula for, 62
 packing fraction of, 86-105
 radioactive, 621
 radius of, 61, 85
 spin of, 63, 158-350
 stability plot of, 62, 115
 stable, properties of, 61-63, 85-105, 115-116,
 130, 158-350
 unstable (see Radioactive decay)

O

Oak, mass absorption coefficient of, 722
 white, atomic density of hydrogen in, 721
 composition of, 738
 physical properties of, 739
 One-group methods (see One-velocity theory)
 One-velocity theory, 376-401
 diffusion approximation in, 381-385
 for homogeneous regions in contact, 390-401
 in infinite homogeneous region, 376-390
 integral equation formulation for, 378-380
 for multivelocity reactors, 450-456
 spherical harmonics, expansion in, 381
 (See also Boltzmann equation)
 Organic compounds, boiling points of, 741
 densities of, 741
 mass absorption coefficients of, 721-722
 in shield materials, atomic densities of hydrogen
 in, 720
 molecular weights of, 720
 ORNL Graphite Reactor, 764

P

Packing fraction, 62
 and binding energy, 62
 experimental values of, 62, 116
 Pair production, 639
 probability of, 639
 Paraffin, atomic density of hydrogen in, 721
 composition of, 736
 mass absorption coefficient of, 722
 physical properties of, 736

Particle reactions, 669
 Penetration in homogeneous media, 646
 deep, 653-657
 critical spectral range, 654
 limited equilibrium, 654
 most penetrating spectral component, 653-654
 primary gammas, 653
 secondaries degraded to E_m , 653, 654
 trends of penetration, 654-657
 factors affecting, 646, 648-650
 accumulation of secondaries, 649-650
 broad-beam effect, 649, 650
 degradation and deflection, 652
 energy degradation only, 651-652
 filtration effect, 648
 penetration of primaries, 651
 moderate, 657-661
 polynomial method, 657-658
 calculation of parameters, 658
 choice of analytical expression, 658
 distribution defined by parameters, 657
 exploratory calculations, 659
 NDA-NBS calculations, 659
 Perturbation theory, 470-474
 and reactivity, 554
 for reactivity change, 429
 Photoelectric effect, atomic, 639
 probability of, 639
 nuclear, 639-640
 probability of, 639
 Photoneutrons, 627
 Physical properties, of ammonia, 733
 of barytes concrete, 727
 of boron, 750
 of bricks, 743
 of cements, 724
 of fuel oil, 734
 of gasoline, 734
 of glass, 744
 of iron, 745
 of lead, 746
 of lucite, 735
 of masonite, 740
 of MO concrete, 726
 of ordinary concrete, 725
 of paraffin, 736
 of rocks, 747
 of rubber, 735
 of shield materials, 723-748
 of stainless steel type 347, 748
 of water, 737
 of woods, 739
 Pine, white, atomic density of hydrogen in, 721
 composition of, 738
 mass absorption coefficient of, 722
 physical properties of, 739
 Platinum filters, 632
 Plutonium 239, delayed-neutron data for, 109
 Poison, concentration of, time-dependent equation
 for, 564-565
 cross section, effective value of, 567-568
 fission-product, time-dependent equations for,
 566-567
 (See also Xenon)
 Poisson distribution law, 63
 Polonium, use in neutron sources, 1, 2

Polymethyl methacrylate (see Lucite)
 Potential scattering, 72
 Protons, range of, 67

R

Radiation, dose units, 757
 permissible levels of, 629-635
 sources of, 621-628
 Radiative capture, definition of, 667
 gamma-ray energies in, 667
 suppression of gamma rays in, 668
 Radioactive decay, 63-66, 158-350
 by alpha-particle emission, 65
 Geiger-Nuttall law for, 65
 by beta-particle emission, 65
 and delayed neutrons 69-70, 109
 disintegration constant for, 63
 by gamma-ray emission, 65-66
 half-life for, 63
 isotopic properties of, 66, 158-350
 law of, 63
 mean life for, 63
 statistics of, 63
 Radioactive decay chain, equations for, 63-65
 Radium, sources, 632
 use in neutron sources, 1
 Range, of alpha particles, 66-67
 of charged particles, 67
 of electrons, 66
 energy relations for, 66-67, 105
 of fission products, 67, 105
 of protons, 67
 Reaction cross sections, (n,p) for oxygen, values of,
 114
 (n,2n) values of, 114
 Reactivity, change of, perturbation calculation of,
 536
 coefficients of, 553-569
 definition of, 472-473
 direct temperature effect on, 556-564
 Doppler effect on, 556
 effect of burn-up on, 565
 effect of concentration on, 564-569
 effect of density on, 554-555
 effect of fission products on, 566
 effect of flowing fuel on, 569
 effect of fuel content on, 429
 effect of gaps on, 614-615
 effect of pile boundary movement on, 556
 and importance, 473
 iterative method for finding, 474
 and period, effect of generation time on, 540
 and poisoning, effective value of, 567-568
 power coefficient of, 571, 581
 stationary expression for, 473
 temperature of, experimental values for lattices,
 601
 temperature coefficients of, for lattice piles,
 597-598, 601
 unit of, dollar, 553
 in hour, 552-553
 upper and lower estimates for, 453
 Reactor dynamics, 531-616
 and accidents, 574, 576-580

- Reactor dynamics, and control servomechanisms, 591, 593-596
 - and coupling to external system, 569-580
 - and delayed neutrons, 531
 - equations for, equivalent one-group space-independent form of, 533-534
 - equations of motion for, 532
 - space-independent one-group model, 531
 - and generation time, 473-474, 533
 - and heat sources, 570
 - after shutdown, 597, 600
 - and instability caused by xenon, 590-592
 - Laplace transform method for, 536, 581-583
 - linearization of equations for, 572-573
 - solutions of, 578, 581-592
 - and periods, 537, 548-549, 583
 - and prompt rise, 537
 - solutions of equations with constant k , 536-547
 - solutions of non-linear equations for, 574-580
 - solutions for step change in k , 540-547
 - solutions for time-dependent k , 540, 548-552
 - and stability, 571
 - Nyquist criterion for, 586
 - and transfer functions, 581-583
 - of external system, 582-585
 - measurement of, 586, 589-590
 - roots of, 585-586
 - and transport delay, 573
 - and two-group bare thermal reactor, 534-536
(See also Reactivity)
 - Reactor oscillator, and absorption cross-section measurement, 43
 - and resonance absorption integral, 52
 - Reactor period (see Reactor dynamics)
 - Reactor statics, theory and general results of, 427-475
 - Reactors, exponential (see Exponential pile)
 - heterogeneous (see Lattice reactors)
 - as neutron source, 16-18
 - summary tables, 761-774
(See also Homogeneous reactors)
 - Reduced mass, 70
 - Reflector savings, due to fast neutrons, 461
 - due to thermal neutrons, 460
 - for graphite lattices, 484
 - for heavy-water-moderated reactors, 494
 - for water lattices, 499, 500
 - Reflectors, control by, 614
 - effect of, 448
 - elastic, 450-451
 - inelastic, 453-455
 - Relative biological equivalence, 631
 - Removal cross section, of elements, 723
 - effective (see Effective removal cross section)
 - Resonance absorption integral, measurement of, 51-52
 - Resonance escape probability, 367, 480-482, 498, 502-503, 520-521
 - comparison of theories for, 373
 - effect of temperature on, 557
 - Fermi theory for, 402
 - in finite homogeneous medium, 403
 - improvements in, 410-411
 - in infinite homogeneous medium, 402
 - Resonance integral, 481
 - effect of temperature on, 598, 601
 - Resonance integral, effective, for thorium, 520
 - for uranium, 497
 - of uranium, effect of temperature on, 601
 - values of, 497, 502-503
 - Resonance neutron flux, 481-482
 - Resonance scattering, 72-73
 - Rocks, composition of, 746
 - mass absorption coefficient of, 722
 - physical properties of, 747
 - Roentgen, 629-630
 - Roentgen equivalent man, 631-633
 - Roentgen equivalent physical, 631
 - Roentgen-hour-meter, 632
 - Rubber, composition of, 735
 - mass absorption coefficients of, 722
 - natural, atomic density of hydrogen in, 721
 - physical properties of, 735
- ## S
- Samarium, production in fission, 569
 - Sand, composition of, 724
 - mass absorption coefficient of, 722
 - Sandstone, composition of, 746
 - mass absorption coefficient of, 722
 - physical properties of, 747
 - Scattering, angle of, 75
 - angular distribution of, 78, 110, 135-141
 - anisotropic, 77-78
 - mean logarithmic energy loss for, 77
 - slowing down by, 373, 375
 - in center-of-mass and laboratory coordinate systems, 75, 134
 - coherent, 79
 - cross section for, 71-72
 - Breit-Wigner formula for, 72
 - elastic, 75-80, 110-111, 129, 134-145, 351-363
 - average cosine of angle, 110
 - capture, 82
 - cross-section values for, 78, 110-111, 129, 135-141, 351-363
 - of gamma rays, 638
 - isotropic, slowing down in, 367-375
 - asymptotic solutions for, 370-374
 - mean logarithmic energy loss for, 75
 - values of, 110
 - number of collisions to thermalize 2-mev neutrons by, 110
 - Rayleigh, of gamma rays, 639
 - probability of, 639
 - Incoherent, 79
 - Inelastic, 80-82, 112-114, 132-133, 146-151
 - approximate formulas for, 81-82, 132-133, 146-151
 - neutron energy distribution, 80-81, 132-133, 146-150
 - total cross section, 81, 132, 151
 - Compton, of gamma rays (see Compton scattering)
 - effect on transport cross section, 79
 - of gamma rays, 638
 - slowing down by, 373, 375
 - isotropic, 76-77, 110
 - energy distribution from, 76
 - mean logarithmic energy loss for, 76

INDEX

- Scattering, isotropic, mean scattering angle for, 76
 - linear law of, effect on diffusion theory, 391
 - quadratic law of, effect on diffusion theory, 391
- Scattering angle, mean square of, 387
- Schematic geometries, 653
 - plane sources, 653
 - flux calculations, 656-657
 - point-collimated source, 653
 - point-isotropic source, 653
 - flux calculations, 656-657
- Secondary radiation, 646
 - electrons, 646
 - gammas, 646
 - accumulation in lower portion of spectrum, 650
 - critical spectral range, 654
 - limited equilibrium of softer secondaries, 654
- Self-adjoint equations, 384
- Self-shielding, from resonance absorption, effect of temperature on, 558
- Serber-Wilson method, boundary conditions for, 434
 - for homogeneous reactors, 431, 433-434
 - numerical results for, 434-442
- Shield materials, 715-752
 - air, composition of, 741
 - density of, 742
 - mass absorption coefficient of, 721
 - ammonia, atomic density of, 720
 - mass absorption coefficient of, 721
 - molecular density of, 720
 - molecular weight of, 720
 - physical properties of, 733
 - barytes aggregate, composition of, 727
 - barytes concrete, composition of, 726
 - elemental composition of, 728
 - physical properties of, 727
 - barytes-limonite concrete, composition of, 728
 - compressive strength of, 728
 - density of, 728
 - elemental composition of, 728
 - boral, composition of, 750
 - mass absorption coefficient of, 721
 - physical properties of, 750
 - boron coatings for metals, 748-749
 - boron-containing, 748-751
 - solubility of, 748, 751
 - boron frits, composition of, 731
 - boron frits-barytes concrete, composition of, 730
 - compressive strength of, 732
 - density of, 732
 - description of, 729
 - elemental composition of, 732
 - bricks, composition of, 742
 - mass absorption coefficient of, 721
 - physical properties of, 743
 - cement, mass absorption coefficients of, 722
 - colemanite-barytes concrete, composition of, 730
 - compressive strength of, 732
 - density of, 732
 - description of, 729
 - elemental composition of, 732
 - colemanite borated cement, composition of, 723
 - physical properties of, 724
 - composition of, 723-748
 - compounds in, 720
 - atomic densities of hydrogen in, 720
 - densities of, 720
 - Shield materials, compounds in, molecular densities of, 720
 - concrete, descriptions of, 729
 - mass absorption coefficients of, 722
 - fuel oil, atomic density of hydrogen in, 721
 - composition of, 733
 - mass absorption coefficient of, 722
 - physical properties of, 734
 - gasoline, atomic density of hydrogen in, 721
 - composition of, 734
 - mass absorption coefficient of, 722
 - physical properties of, 734
 - glass, composition of, 743
 - mass absorption coefficient of, 722
 - physical properties of, 744
 - granite, composition of, 746
 - mass absorption coefficient of, 722
 - physical properties of, 747
 - iron, atomic density of, 717
 - composition of, 744
 - effective removal cross section of, 723
 - mass absorption coefficient of, 718, 722
 - physical properties of, 745
 - iron-portland concrete, composition of, 730
 - compressive strength of, 732
 - density of, 732
 - description of, 729
 - elemental composition of, 732
 - lead, atomic density of, 717
 - effective removal cross section, 723
 - mass absorption coefficient of, 719, 722
 - physical properties of, 746
 - limestone, composition of, 746
 - mass absorption coefficient of, 722
 - physical properties of, 747
 - lucite, atomic density of, 720
 - composition of, 735
 - mass absorption coefficient of, 722
 - molecular density of, 720
 - molecular weight of, 720
 - physical properties of, 735
 - lunite, composition of, 731
 - lunite-colemanite-barytes concrete, composition of, 730
 - compressive strength of, 732
 - density of, 732
 - description of, 729
 - elemental composition of, 732
 - lunite-portland-colemanite-barytes concrete, composition of, 730
 - compressive strength of, 732
 - density of, 732
 - description of, 729
 - elemental composition of, 732
 - masonite, atomic density of hydrogen in, 721
 - composition of, 740
 - physical properties of, 740
 - mass absorption coefficients of, 721-722
 - MO concrete, composition of, 725
 - physical properties of, 726
 - natural rubber, atomic density of hydrogen in, 721
 - nuclear properties of, 716-722
 - ordinary concrete, composition of, 725
 - physical properties of, 725
 - organic compounds in, atomic densities of hydrogen in, 720

- Shield materials, organic compounds in, boiling points of, 741
- densities of, 741
- mass absorption coefficients of, 721-722
- molecular weights of, 720
- paraffin, atomic density of hydrogen in, 721
- composition of, 736
- mass absorption coefficient of, 722
- physical properties of, 736
- physical properties of, 723-748
- plain cement, composition of, 723
- physical properties of, 724
- portland cement, composition of, 723
- position of, 716
- properties of, 716-751
- rocks, composition of, 746
- mass absorption coefficient of, 722
- physical properties of, 747
- rubber, composition of, 735
- mass absorption coefficients of, 722
- physical properties of, 735
- sand, composition of, 724
- mass absorption coefficient of, 722
- sandstone, composition of, 746
- mass absorption coefficient of, 722
- physical properties of, 747
- selection of, 715
- stainless steel type 347, composition of, 747
- mass absorption coefficient of, 722
- physical properties of, 748
- structural, 716
- for suppression of capture gamma rays, 716
- types of, 715-716
- water, analyses of, 736
- atomic density of, 720
- molecular density of, 720
- molecular weight of, 720
- physical properties of, 737
- woods, atomic densities of hydrogen in, 721
- composition of, 738
- density of, and volume composition, 740
- mass absorption coefficients of, 722
- physical properties of, 739
- water content of, and relative humidity, 740
- Shields, gamma, 715
- heat generation in, 701-708
- neutron, 715
- optimization of, 709-713
- replacement length in, 710
- two-component, optimization of, 711
- Sigma pile, 52
- Slowing down, with absorption, boundary conditions for, in finite regions, 422-423
- Fermi approximation for, 409-410
- Greuling-Goertzel approximation for, 370, 409-410
- Hurwitz approximation for, 370
- improvements in resonance escape probability, 410-411
- Wigner approximation for, 370, 409-410
- by anisotropic scattering, 373, 375, 455-456
- approximation methods, for, 373, 375
- asymptotic solutions for, 371-372
- in deuterium, 370, 374
- for energy-dependent cross sections, 412
- for energy-independent cross sections, 450
- Slowing down, exact hydrogen solutions for, 369
- exact solutions for special sources, 373
- fluctuations near source energy in, 370, 373, 375
- Gaussian, for uniform media, 456-461
- in graphite, 412, 413
- in heavy moderators, 369
- in hydrogen, 367, 369
- by inelastic scattering, 373, 375
- by isotropic elastic scattering, 367-375
- asymptotic solutions for, 370-374
- kernels for, 368
- Gaussian, 459
- synthetic, 368-370
- solutions for, 369
- mean length for measurement of, 50
- in mixtures, 370
- of hydrogen and heavy element, 370
- in multiplying medium, 412
- of neutrons, in crystal, 79
- with no space variation, 367-376
- basic equations for, 367
- in media of variable density, 367
- with space variation, 401-425
- treatment by symmetric kernel, 459
- in uniform media, 456-465
- (See also Group-diffusion method)
- Slowing-down density, in Al-H₂O, 509
- asymptotic space dependence of, 412
- in beryllium, 507
- comparison of point and plane source solutions for, 412
- continuity equation for, 367
- deviations from Gaussian, 415
- equations for, in group-diffusion method, 418-419
- exact space dependence of, deviations from Gaussian distribution, 411-413, 415
- Fermi approximation for, 401
- in finite homogeneous medium, 403
- in graphite, 412, 505
- in heavy water, 504
- in H₂O-Zr, 508
- in hydrogen, 412, 414-416
- moments of, 51
- without space variation, 367
- in water, 415, 422, 506
- Slowing-down length, and age theory, 402
- in group-diffusion method, for point source, 421-422
- in hydrogen, 415
- Solid angle of radiation, 683-684
- Solubility of boron-containing materials, 748, 751
- Source strength, 632
- calculation of, inverse-square law for, 632
- platinum filter, 632
- radium source, 632
- Sources, anisotropic, 381
- of gamma rays, 637
- special, for exact solutions in slowing down, 373
- Spectral distribution, of Bulk Shielding Facility Reactor, 704
- of Los Alamos reactors, 704
- Spectrometer, gamma-ray, pair, 625
- scintillation, 625
- Spherical-harmonics methods, 396, 398-400
- boundary conditions at free surface, 399

Spherical-harmonics methods, expansion of cross section in, 377
 modified, 400
 P_1 -approximation in, 381-382
 validity of, 385
 P_2 -approximation in, 411
 P_3 -approximation in, 398
 P_n -approximation in, 381
 P_{2n-1} -approximation in, 398
 solutions for isotropic source, in slab geometry, 398
 in spherical geometry, 399
 solutions for slab geometry, 396
 solutions for spherical geometry, 396
 use in one-velocity theory, 381
 Wick's method, 400
 Spin, nuclear, values for ground state of stable nuclei, 63, 158-350
 Spruce, atomic density of hydrogen in, 721
 composition of, 738
 physical properties of, 739
 Stainless steel, type 347, composition of, 747
 mass absorption coefficient of, 722
 physical properties of, 748
 SUPO (see Los Alamos Water Boiler)
 Symbols, kinetic-theory, 366

T

Telegrapher's equation, 390
 in time-dependent diffusion theory, 385
 Thermal column, neutron distribution in, 18
 Thermal neutrons, in capturing medium, 375
 diffusion of, 423-425
 with energy-dependent cross sections, 425
 with energy-independent cross sections, 424-425
 hardening of, 49
 "hardening" of velocity distribution, 375
 Maxwell-Boltzmann distribution for, 375, 376
 in noncapturing medium, 375, 376
 (See also Neutron flux, thermal)
 Thermal Test Reactor, 771
 Thermal utilization, temperature dependence in lattice piles, 601
 Thorium, effective resonance integral for, 520
 Thorium 232, delayed-neutron data for, 109
 Threshold detectors, 33-35
 Time-of-flight spectrometer, 19-21
 properties of, 20
 resolution of, 19
 Transformations, shielding, for exponential attenuation with unitary or linear build-up, point to line, 687
 slab shields, 689
 for partly specified attenuation functions, 681-684
 source on plane surface, 683-684
 source on quadric surface, 681-682
 for simple attenuation functions, 684-692
 for unspecified attenuation functions, 678-681
 infinite plane to point, 678
 plane to cylinder, 681

Transformations, shielding, for unspecified attenuation functions, plane disk to infinite plane, 679
 plane disk to point, 679, 680
 plane to sphere, 679, 681
 point to infinite plane, 678
 point to plane disk, 678
 Transport equation, asymptotic solution of, 386
 for anisotropic scattering, 387
 exact solutions of, by Fourier transform, 386
 for isotropic scattering, 386-388
 plane sources, 386
 point sources, 386
 separable solution of, for anisotropic scattering, 387
 Transport kernel (see Kernel, transport)
 Transport mean free path for weakly absorbing media, 382
 Transport theory, attenuation constant of, 386, 387
 for anisotropic scattering, 387
 approximation for, 398
 boundary conditions in, 390
 correction to diffusion theory, 382
 end-point method in, 400-401
 extrapolation length in, 391
 Fourier transform in, 400
 kernels for, 380
 results applied in diffusion theory, 389
 (See also Boltzmann equation)
 Two-group theory, 465-469
 critical equation for, 466
 matrix method for, 466

U

Unshielded sources, cosine, 689
 isotropic, 689
 volume, plane-limited, 689
 Uranium, resonance integral of, effect of temperature on, 601
 thermal data for, 478-485, 487, 495-503, 516-528
 Uranium 233, delayed-neutron data for, 109
 Uranium 235, delayed-neutron data for, 109
 fission of, energy distribution in, 110
 Uranium 238, delayed-neutron data for, 109

V

Variational methods, for Boltzmann equation, 380-381
 for buckling, 443, 445
 for diffusion theory, 384
 for water-moderated reactor, 462
 Voids, gamma-ray attenuation by, 698
 neutron attenuation by, 698

W

Water, analyses of, 736
 atomic density of, 720
 boration of, 748
 comparison of slowing-down theories for, 422
 heavy, reactors moderated by, reflector savings
 494

PHYSICS

Water, heavy, reactors moderated by, slowing-down density in, 504

(See also Deuterium and Heavy-water system)

lattices moderated by, 484, 499-501

metal mixtures in, age for, 486

molecular density of, 720

molecular weight of, 720

physical properties of, 737

reactors moderated by, critical mass of (see Critical mass)

slowing-down density in, 415, 506, 508, 509

Water boiler reactors, 477, 488

critical-mass data for, 488

Water lattices, age of, 501

buckling for, 499, 500

cadmium ratio for, 500

diffusion length for, 501

material buckling for, 501

multiplication factor for, 501

Water lattices, reflector savings for, 499, 500

Watt's formula for fission neutrons, 621-622

Woods, composition of, 738

density of, and volume composition, 740

mass absorption coefficients of, 722

physical properties of, 739

water content of, and relative humidity, 740

X

Xenon, build-up after shutdown, 597-599

concentration in reactors, 566-567

formation in fission, 567

poisoning, effective value of, 568

equilibrium value of, 566-567

power coefficient for, 590

power instability of, 590-592

